Heinrich Heine Universität Düsseldorf

JÜLICH Forschungszentrum

Biaryl-based natural products as structural motif for pharmaceutically relevant compounds

Moritz Kornelius Theodor Klischan

Bioorganische Chemie an der Heinrich-Heine-Universität im Forschungszentrum Jülich

Forschungszentrum Jülich GmbH
Institut für Bio- und Geowissenschaften
IBOC – Bioorganische Chemie

Biaryl-based natural products as structural motif for pharmaceutically relevant compounds

Moritz Kornelius Theodor Klischan

Bioorganische Chemie an der Heinrich-Heine-Universität im Forschungszentrum Jülich

Band 49

ISBN 978-3-95806-801-8

Bioorganische Chemie an der Heinrich-Heine-Universität im Forschungszentrum Jülich

Band 49

Herausgegeben von Jörg Pietruszka

Heinrich Heine
Universität
Düsseldorf

Biaryl-based natural products as structural motif for pharmaceutically relevant compounds

Inaugural-Dissertation

zur Erlangung des Doktorgrades
der Mathematisch-Naturwissenschaftlichen Fakultät
der Heinrich-Heine-Universität Düsseldorf

vorgelegt von

Moritz Kornelius Theodor Klischan
aus Düsseldorf

Düsseldorf, September 2024

Bibliografische Information der Deutschen Nationalbibliothek.
Die Deutsche Nationalbibliothek verzeichnet diese Publikation in der
Deutschen Nationalbibliografie; detaillierte Bibliografische Daten
sind im Internet über http://dnb.d-nb.de abrufbar.

Gedruckt mit der Genehmigung der
Mathematisch-Naturwissenschaftlichen Fakultät
der Heinrich-Heine-Universität Düsseldorf

Referent:	Prof. Dr. Jörg Pietruszka
Korreferent:	Prof. Dr. Thomas J.J. Müller
Tag der mdl. Prüfung:	27.09.2024
Herausgeber:	Prof. Jörg Pietruszka
Umschlaggestaltung:	Grafische Medien, Forschungszentrum Jülich GmbH
Druck:	Grafische Medien, Forschungszentrum Jülich GmbH
Copyright:	Forschungszentrum Jülich 2025

Bioorganische Chemie an der Heinrich-Heine-Universität Düsseldorf
im Forschungszentrum Jülich, Band 49

D 61 (Diss. Düsseldorf, Univ., 2024)

ISBN 978-3-95806-801-8

Aus dem Institut für Bioorganische Chemie
der Heinrich-Heine-Universität Düsseldorf

Gedruckt mit Genehmigung der
Mathematisch-Naturwissenschaftlichen Fakultät
der Heinrich-Heine-Universität Düsseldorf

Berichterstatter:

1. Prof. Dr. Jörg Pietruszka

2. Prof. Dr. Thomas J. J. Müller

Tag der mündlichen Prüfung: 27.09.2024

Publications

Parts of this work have been published, chapters containing such passages are clearly indicated.

- Moritz K. T. Klischan, Flaminia Mazzone, Lena Berning, Julian Greb, Max Schlamkow, Mona Haase, Wolfgang Frey, Björn Stork, Klaus Pfeffer, Jörg Pietruszka
  ACS Omega, **2023**, 8, 44, 41816 – 41834. 10.1021/acsomega.3c06503
  'Modular Approach for the Synthesis and Bioactivity Profiling of 8,8'-Biflavones'.
  First draft of manuscript; compilation of biological and chemical results; Synthesis of most flavonoids; Development of chemical methodology; Idea and conceptualization.
- Moritz K. T. Klischan, Céline David, Daniel Grudzinski, Wolfgang Frey, Björn Stork, Jörg Pietruszka
  Org. Lett. **2024**, 26, 25, 5258–5262. 10.1021/acs.orglett.4c01308
  'Application of Cyclic Diaryliodonium Salts in the Synthesis of Axially Chiral Natural Product Analogues'. First draft of manuscript; compilation of biological and chemical results; Synthesis of most compounds; Development of chemical methodology; Idea and conceptualization.
- Flaminia Mazzone, Moritz K. T. Klischan, Julian Greb, Sander H. J. Smits, Jörg Pietruszka and Klaus Pfeffer
  Front. Chem. **2024***, 12, 1406307*. 10.3389/fchem.2024.1406307
  'Synthesis and In vitro evaluation of bichalcones as novel anti-toxoplasma agents'.
  Synthesis of most flavonoids; Development of part of the chemical methodology; Idea and conceptualization.
- Julian Greb, Till Drennhaus, Moritz K. T. Klischan, Zachary W. Schroeder, Wolfgang Frey, Jörg Pietruszka
  Chem. Eur. J. **2023**, 29, e202300941. 10.1002/chem.202300941
  'A Common C_2-Symmetric 2,2'-Biphenol Building Block and its Application in the Synthesis of (+)-di-*epi*-Gonytolide A'
  Contributions towards scalable synthesis of chromones and scalable synthesis of biphenol. Separation of the brominated key intermediates by distillation and recycling of biquinone.

Publications not discussed in this thesis

- Diana Amariei, Mona Haase, Moritz K. T. Klischan, Martin Wäscher, Jörg Pietruszka *ChemCatChem*, **2024**, e202400052. 10.1002/cctc.202400052
  'High-Throughput Colorimetric Detection and Quantification of Indoles and Pyrroloindoles for Enzymatic Activity Determination.'
  Electrochemical investigations of the oxidation potential of indoles.

Conference attendances

Hannover, Germany – GDCh-Wissenschaftsforum Chemie 2021 – University of Hannover - participation only

Online – Irsee Conference 2021 – participation only

Bayreuth, Germany – BNPDS 2022- University of Bayreuth – Poster presentation: 8,8'-Biflavone analogues: Scalable Synthesis of a Library of *Toxoplasma Gondii* Inhibitors, Moritz K. T. Klischan, Julian Greb, Flaminia Mazzone, Lena Berning, Max Schlamkow, Jörg Pietruszka

Bonn, Germany – ACS Publications Symposium: Biological and Medicinal Chemistry 2023 – University of Bonn - Poster presentation: 8,8′-Biflavone Analogues -Bioactivity Comparison of Dimers with Monomers, Moritz K. T. Klischan, Julian Greb, Flaminia Mazzone, Lena Berning, Max Schlamkow, Björn Stork, Klaus Pfeffer, Jörg Pietruszka

Gothenburg, Sweden – 23rd Tetrahedron Symposium2023 – Svenska Mässan - Poster presentation: Chiral acetylene – surprising regio- and diastereoselectivity in the Pd-catalyzed construction of quaternary chiral centers, Moritz K. T. Klischan, Xavier Abel-Snape, Jörg Pietruszka, Mark Lautens

Final Theses

The present dissertation also contains results of the following final theses:

B.Sc. Max Schlamkow (Fachhochschule Aachen, Bachelor's Thesis **2021**) 'Palladium-katalysierte Catellani-Reaktionen: Funktionalisierung von Aromaten für die Synthese Biaryl-basierter Naturstoffe'

B.Sc. Daniel Grudzinski (Heinrich Heine University Düsseldorf, Bachelor's Thesis **2023**) 'Auf dem Weg zu neuartigen, enantiomerenreinen 8,8'-Biflavonen'

Chapters and sections containing results generated by the corresponding authors are clearly indicated. The corresponding work was carried out under the current author's direction.

Table of Contents

“Oh no, not again. Many people have speculated that if we knew exactly why the bowl of petunias had thought that we would know a lot more about the nature of the Universe than we do now.”

― Douglas Adams, The Hitchhiker's Guide to the Galaxy

“Also auch Du bist so müde, so chemiemüde. Es ist mir dies ein ordentlicher Trost. Du glaubst nicht, wie müde ich bin, wie satt ich die Chemie habe, wie namentlich gewisse Theile mich ordentlich anekeln, mir wenigstens so langweilig sind, daß ich gähnen muß, wenn ich daran denke. Sind wir denn schon so alt oder was ist es? Diese nervenschwächende Wirkung muß wirklich der Chemie eigenthümlich sein. Ich glaube, die materiellen Influenzen, die Dämpfe, Gerüche und all die Teufelstinkereien haben großen Antheil daran. Besonders ist es das Prakticum, was Einen so herunterbringt.”

― Friedrich Wöhler, Aus einem Brief an Justus von Liebig (22.07.1847)[1]

“The great tragedy of science—the slaying of a beautiful hypothesis by an ugly fact.”

― Thomas Huxley 1870

[1] The contents of this quote do not represent the present authors personal views and is only meant to show this interesting historical correspondence between Friedrich Wöhler and Justus von Liebig.

Abbreviations

ABTS	2,2'-azino-bis(3-ethylbenzothiazoline-6-sulfonicacid	EDTA	Ethylenediaminetetraacetic acid
AnFreq	Analytical Frequency	*ee*	Enatiomeric excess
BIDIME	Biaryl dimethoxy	*et al.*	*et alia/alii/aliae* (latin: and others)
BINAM	1,1′-Binaphthyl-2,2′-diamine	GRK	Graduiertenkolleg
BINAP	1,1′-Binaphthyl-2,2′-diphosphine	KR	Kinetic resolution
BINOL	1,1′-Binaphthyl-2,2′-diol	MOM	Methylene methoxy
BINSA	1,1′-Binaphthyl-2,2′-disulfonic acid	MOP	Biaryl monophosphine
BIPOL	biphenol	NBE	Norbornene
BOX	Bis oxazoline	NOBIN	2-amino-2'-hydroxy-1,1'-binaphthyl
Bz	Benzyol	NOESY	Nuclear Overhauser Enhancement Spectroscopy
CFF	Condensed Fukui function	OBC	oxabicycle
CUF	Cupressuflavone	Ox. add.	Oxidative Addition
dba	dibenzylidene acetone	Pd-cycle	Palladacycle
d.r.	Diastereomeric ratio	prDA	Pre-retro-*Diels-Alder*
DBQ	Dibenzoquinone	QUINAP	Quinoline-naphthalene
DFT	Densitiy functional theory	r.r.	Regioisomeric ratio
DKR	Dynamic kinetic resolution	Red. elim.	Reductive Elimination
DMAc	Dimethylacetamide	SE_{Ar}	Electrophilic aromatic substitution
DMF	Dimethylformamide	smNBE	Structurally modified norbornene
DOSY	Diffusion-Ordered Spectroscopy	*T. gondii*	*Toxoplasma gondii*
dr.	Dram	Tf	Triflate
d.r.	Diastereomeric ratio	THF	Tetrahydrofuran
DYKAT	Dynamic kinetic asymmetric transformation	VANOL	3,3′-diphenyl-[2,2′-binaphthalene]-1,1′-diol
e.r.	Enantiomeric ratio	VAPOL	2,2′-diphenyl-[3,3′-biphenanthrene]-4,4′-diol

1 Abstract

Biaryls are important structural motifs for both pharmaceutically relevant compounds as well as ligands, and catalysts in chemical transformations. With the aim of contributing to the ever-expanding methodology towards biaryls, different synthesis strategies were devised and implemented to obtain synthetically relevant biaryls. Moreover, stereoselective palladium catalyzed transformations were investigated for the synthesis of bicyclic compounds.

8,8″-Biflavones, a class of biaryl-based natural products, were investigated for their bioactivity against various human pathogens. A synthesis route for the construction of highly functionalized racemic biaryl building blocks in three steps was established in a scalable fashion. Enabled by this method, the first extensive library of 8,8″-biflavone analogues was synthesized. This dedicated library was then evaluated regarding its pharmaceutical potential in cooperation with M.Sc. *Lena Berning* and M.Sc. *Flaminia Mazzone* (Heinrich Heine University Düsseldorf). In addition to promising results for these biflavones, bichalcones obtained as key intermediates were identified as novel drug scaffolds. Based on these first hits, further amino-8,8″-biflavones including the first non-C_2-symmetrical 8,8″-biflavone were synthesized. In cooperation with M.Sc. *Céline David* (Heinrich Heine University Düsseldorf) the structure activity relationship was probed, and bioactivities obtained. Next a strategy involving cyclic diaryliodonium salts towards an enantiopure building block was implemented. Extensive investigations were undertaken, and ultimately a scalable protocol successfully established. These prochiral building blocks were then applied to construct enantiopure dimeric flavonoids and thus the usefulness of the established methodology shown.

In addition to these investigations, palladium-catalyzed methods were investigated to overcome advanced synthetic challenges. For one, the *Catellani* reaction was used to obtain biaryls inaccessible by state-of-the-art methods. Factors critical for this transformation were identified, and a protocol for the synthesis of tri-*ortho*-substituted biaryls established. Moreover, first investigations into stereodynamic biaryl-based palladacycles were conducted. The proposed stereodynamics of these palladium complexes were supported by preliminary computational calculations (DFT).

Finally, in collaboration with the working group of Prof. *Mark Lautens* (University of Toronto), the use of chiral oxabicycles as acetylene analogues was thoroughly investigated. A mechanism to explain the observed stereoselectivity of the reaction was proposed and supported by experimental findings. Finally, DFT calculations were conducted to rationalize the observed selectivities.

2 Zusammenfassung

Biaryle sind wichtige Strukturmotive für sowohl Pharmazeutika als auch Liganden und Katalysatoren in chemischen Transformationen. Verschiedene Synthesestrategien wurden untersucht und implementiert, mit dem Ziel, zu dem Repertoire der Biarylsynthesen beizutragen. Weiterhin wurden stereoselektive, palladiumkatalysierte Transformationen zur Synthese von bicyclischen Systemen mit Hilfe von chiralen Auxiliaren untersucht.

Die Bioaktivtäten von 8,8″-Biflavonen wurden gegen verschiedene Humanpathogene untersucht. Eine skalierbare Syntheseroute zur Konstruktion hochfunktionalisierter racemischer Biaryl-Bausteine über drei Schritte konnte etabliert werden. So konnte die erste umfassende 8,8″-Biflavon-Bibliothek synthetisiert werden. Das pharmakologische Potenzial dieser Bibliothek wurde durch die Kooperationspartnerinnen M.Sc. *Lena Berning* und M.Sc. *Flaminia Mazzone* (HHU Düsseldorf) evaluiert. Zusätzlich zu Biflavonen wurden bioaktive Bichalkone als neuartige Leitstrukturen für weitere biologische Untersuchungen identifiziert. Basierend auf diesen ersten Untersuchungen wurden weitere Amino-8,8″-biflavone, inklusive des ersten nicht-C_2-symmetrischen 8,8″-Biflavons, synthetisiert. In Kooperation mit M.Sc. *Céline David* (HHU Düsseldorf) wurde die Struktur-Aktivitätsbeziehung dieser Verbindungen untersucht. Daraufhin wurde eine Synthesestrategie implementiert, bei der prochirale cyclische Diaryliodonium-Salze verwendet wurden, um enantiomerenreine Bausteine zu synthetisieren. Schlussendlich konnte ein skalierbares Syntheseprotokoll etabliert wurde. Basierend auf diesen Ergebnissen konnten enatiomerenreine, dimere Flavonoide hergestellt werden.

Zusätzlich zu diesen Untersuchungen wurden palladiumkatalysierte Strategien angewandt, um moderne synthetische Problemstellungen zu adressieren. So wurde die *Catellani*-Reaktion zur Synthese von ansonsten unzugänglichen Biarylen untersucht. Für diese Reaktion kritische Faktoren wurden identifiziert und ein Protokoll für die Synthese von tri-*ortho*-substituierten Biarylen etabliert. Weiterhin wurden Untersuchungen zu stereodynamischen biarylischen Palladacyclen unternommen und Ergebnisse durch *in silico* Studien (DFT) unterstützt.

Schlussendlich konnte die erhaltene Expertise genutzt werden um in einer Kollaboration mit der Arbeitsgruppe von Prof. *Mark Lautens* (University of Toronto), eine neuartige, palladiumkatalysierte Methode zu etablieren. Ein Reaktionsmechanismus, der die Stereoselektivität erklären kann, wurde vorgeschlagen und mit experimentellen Funden belegt. Ferner wurden DFT-Berechnungen durchgeführt, um die beobachteten Selektivitäten zu erklären.

3 Introduction and Objectives

3.1 Flavonoids and Biaryls

Humanity has unknowingly benefited from the ingestion of flavonoid containing plants throughout its history. Be it as the drink Xocolātl[2][1] or cocoa[2] in Mesoamerica and the Aztec empire for hundreds of years,[3] or as traditional herbal medicinal plants such as *Ginkgo biloba* since at least the Yuan dynasty (1280–1368 C.E.)[4]. Flavonoids are the most abundant group of polyphenols found in the human diet[5] and have been associated with a plethora of beneficial biological effects[6] including anti-cancer, cardiovascular modulating, and even neuromodulating effects.[7] The mode of action is often attributed to anti-oxidant properties or by modulating signalling pathways[8] though results need to carefully be considered to not overestimate the potential of this ubiquitous compound class.[9] The biosynthesis and metabolic function of flavonoids has been evaluated thoroughly.[10] In particular, biflavones, naturally occurring flavone dimers found among various *gymnosperms*,[11] have emerged as a valuable subclass with relevant biological activities.[12] Research into the reduction of disease-related mortality benefits greatly from the accessibility of such diverse compound classes. Infectious disease and cancer are among the most prevalent causes of death globally.[13] In recent years new challenges have arisen that amplify the urgent need for suitable treatments. In particular, drug resistance continues to be the primary limiting factor in overcoming cancer and microbial diseases,[14] and has even been named the most pressing issue for human health[15] with "[…] significant global economic and security implications".[13] To combat this global crisis, the identification of new drug scaffolds is of ever greater importance.[16] This relentless demand for therapeutical agents highlights the need for scalable and diversifiable chemical methods to identify and obtain novel drug candidates. Natural product inspired drugs are of particular interest.[17] Biaryl based secondary metabolites may constitute one such high-potential class of compounds.[18] In 2018, 15% of FDA approved small molecules contained at least one atropisomeric axis, which makes this compound class of particular interest for medicinal chemists.[19] The conformational stability of such drug candidates is of great importance.[20] For these reasons, biaryl-based natural product inspired drugs may help overcome challenges of drug-resistance. Phytochemicals have been shown to address *cis*-platin resistance[21] including recent examples of biflavone ginkgetin (**1**) (Figure 1).[22] Additional biaryl based natural products such as phomoxanthone A (**2**),[23] gonytolide A (**3**),[24] rugulotrosin A (**4**),[25] and viriditoxin (**5**)[26] just to name a few have proven to be of great pharmaceutical interest (Figure 1). Methodologies towards such biaryl-based compounds are well established, yet there are still

[2] The word chocolate is derived from this. Classical Nahuatl: A combination of xocolia ("to make sour") + ātl ("water")

challenging synthetic hurdles that need to be overcome.[18, 27] The establishment of new methods providing access to an ever-greater variety of natural product inspired compounds must be addressed for years to come. Particularly enantiopurity of such axially chiral natural products needs to be achieved.[28]

A di-/tri-ortho biaryl-based natural products

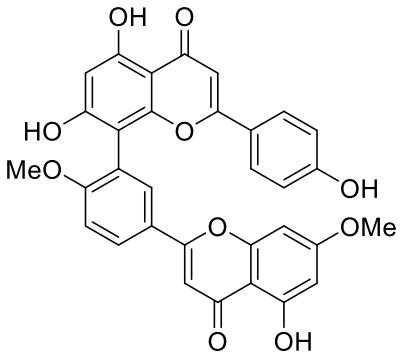

ginkgetin (**1**)

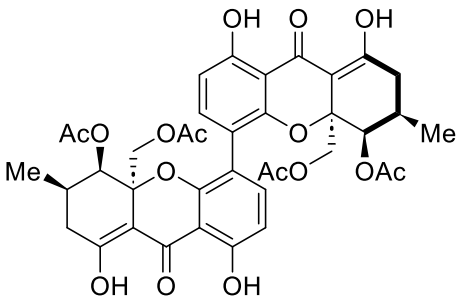

phomoxanthone A (**2**)

B tetra-ortho biaryl-based natural products

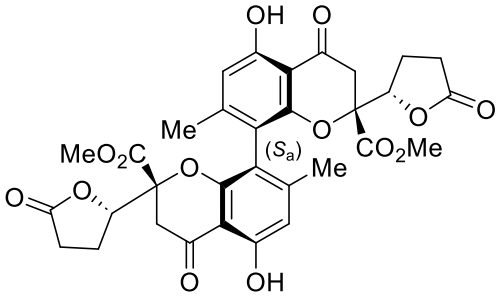

gonytolide A (**3**)

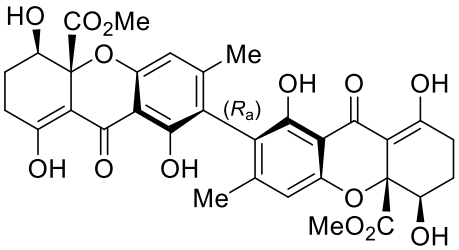

rugulotrosin A (**4**)

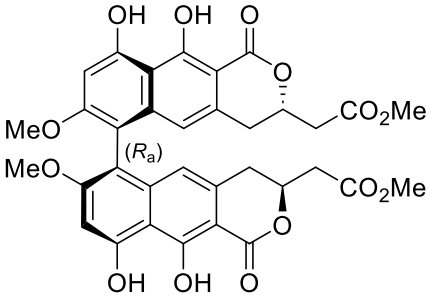

viriditoxin (**5**)

Figure 1: Biaryl based natural products.

3.2 Thesis objective

As outlined in the previous section, there is an urgent need to establish reliable methodologies to obtain novel drug candidates. As part of this work, new synthetic strategies towards the construction of biaryl key intermediates shall be investigated. The scalability of these synthetic methods is of great importance to synthesize adequate amounts of potentially bioactive molecules for *in vitro* trials. Particularly, the stereoselective synthesis and resolution of biaryls will be investigated. After establishing such protocols, racemic 8,8″-biflavones as an underexplored category of the broader class of flavonoids shall be synthesized and their biological activity against microbes and human cancer cell lines evaluated (Chapter 5.1.1). This biological profiling is to be done in cooperation with the research training group 2158 (GRK 2158) '*Natural products and natural product analogues against therapy-resistant tumors and microorganisms: new lead structures and modes of action*'. Initial biological hits that are obtained by this study will subsequently be synthesized in an enantioenriched fashion to identify eutomer and distomer (Chapter 5.2). The transformative power of palladium catalysis is to be leveraged to establish new methods towards the desired biaryl motif. In particular, the *Catellani*-reaction will be used to shorten established synthetic routes (Chapter 5.3). Moreover, the synthetic value of palladacyclic biaryl intermediates towards enantioenrichment of synthetically useful biaryls will be assessed (Chapter 5.4). The methodological knowledge gathered from these investigations shall be applied to the stereoselective multicomponent synthesis of indenes (Chapter 5.5).

Chapter 5.1.1

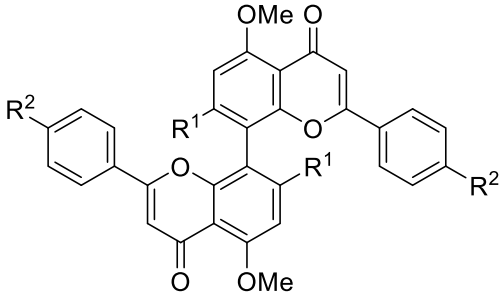

Racemic biflavonoids

Chapter 5.2

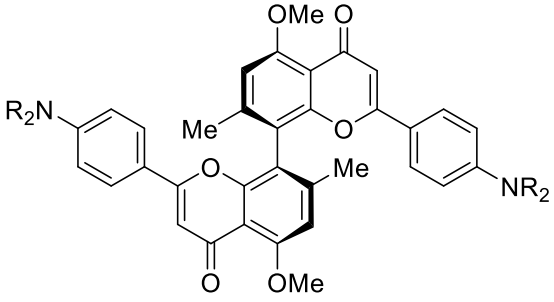

Synthesis of enantiopure biflavonoids

Chapter 5.3

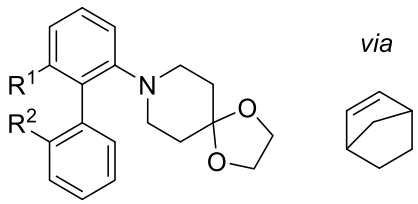

Catellani reaction

Chapter 5.4

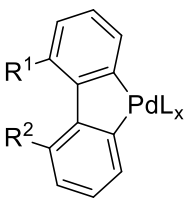

Palladacycles

Chapter 5.5

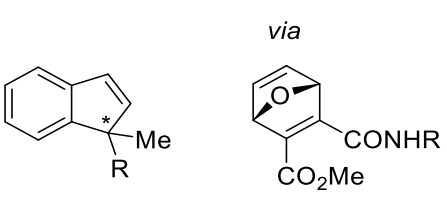

Oxabicycles as chiral acetylene

4 State of Knowledge

Biaryl-based structural motifs are found throughout nature. While the biosynthesis of such natural products involves specialized oxidases and laccases to achieve C–C bond formation,[29] for the most part synthetic chemists have had to make due with transition metal catalysis.[30] Only recently new methods making use of enzymes have been explored,[31] and few general enzymatic approaches reported to date.[32] Nevertheless, chemists have been interested in obtaining these biarylic structures since at least the 1890s.[33] Of particular interest is the phenomenon of axial chirality observed for sterically hindered biaryls. In 1922 the first optically active biaryl was reported and the mode of chirality proposed.[34] Axially chiral compounds are commonly referred to as atropisomers (historically: atropoisomers). Atropisomers are defined as containing distinct rotational isomers with a somewhat arbitrary half-life of 1000 seconds which corresponds to an energetic barrier $\Delta G_e^{\ddagger}$ of 90 – 100 kJ·mol^{-1} (22 – 24 kcal·mol^{-1}).[35] IUPAC recommends the use of S_a and R_a as the stereodescriptors to assign the absolute configuration[36] though *P* (plus) and *M* (minus) can still commonly be found in literature (Scheme 1).[27, 37] Biaryls, containing such rotationally stable isomers are often tri-*ortho*- or even tetra-*ortho*-substituted (*ortho* relative to the biaryl bond). Such enantioenriched biaryls are ubiquitous structures found in nature.[18] Organisms exist that are capable of producing axially chiral natural products with both (R_a) or (S_a) configuration selectively[38] often relying on dirigent proteins to achieve stereoselectivity.[39] Enzyme catalyzed approaches for the resolution and desymmetrization of biaryls have been compiled in a recent review.[40] The atropisomers of such chiral biaryl based natural products can possess selectivity towards enzyme and receptor targets[41] making the resolution of such compounds of great importance in addition to best-practices and regulations in drug development.[28]

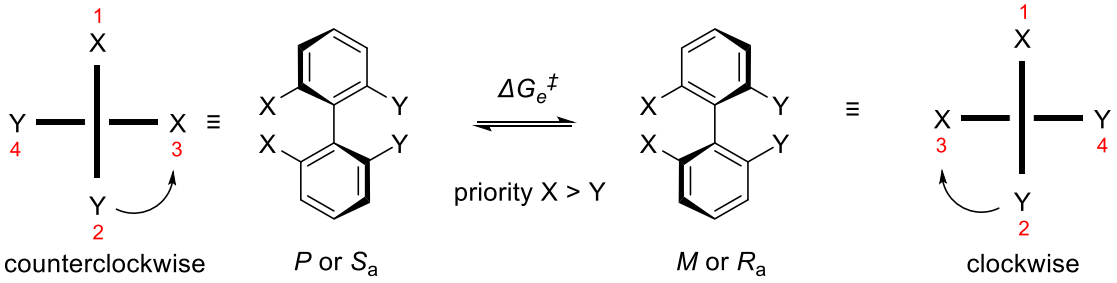

Scheme 1: Stereodescriptors for axially chiral biaryls. Based on *Bringmann et al.*[27]

4.1 Biaryl construction

Generally, the construction of biaryls can be classified into the following categories: oxidative couplings (Scheme 2A), homo/cross-couplings (Scheme 2B) and de-novo synthesis (Scheme 2C). These coupling strategies have historically been employed to obtain both racemic mixtures as well as enantioenriched products.[42] Complementary to these biaryl construction strategies, forming the biaryl in a racemic or achiral fashion can also be leveraged to then subsequently resolve this mixture by various methods (Scheme 2D). In addition to classic aryl-aryl atropisomers, C–N atropisomers in form of amides and polycyclic system have gathered considerable interest in literature but will not be discussed in detail as part of this dissertation.[43] Over the following section, a brief rundown of definitions and contemporary reviews on the topic will be given for each of these various strategies.

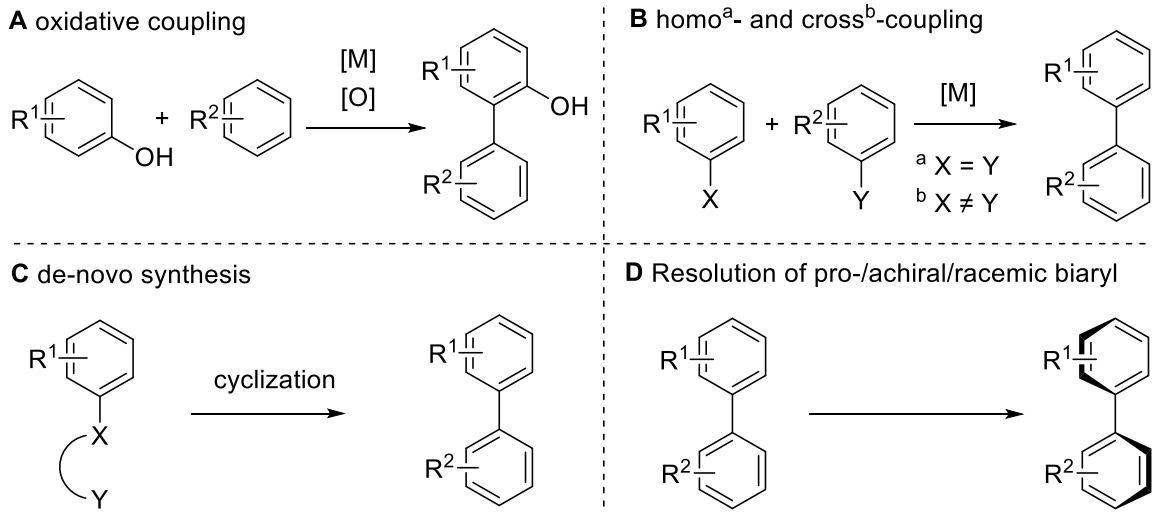

Scheme 2: Illustrative examples of various biaryl construction strategies.

Oxidative couplings (Scheme 2A) rely on the C–H activation of the monomeric units and have been named 'the most widespread pathway in the biosynthesis of biaryl natural products'[44] attested by many literature known examples.[45] The repertoire of this biomimetic approach[46] has since been expanded by contemporary methods. Most notably the groups of *Kozlowski*,[47] and *Pappo*[48] in addition to others have worked on establishing and applying new methods using Fe-[48a, 48c, 48d, 49], Cu-[50] and V-[51]catalysts just to name a few. The ultimate goal of these methods is to achieve selective and efficient C–C bond formation.[52] Especially the field of oxidative coupling to form heterodimers enabled by chemo- and regioselectivities[48a, 49c] has been explored in recent years.[47a, 47b, 48c, 48d, 53] Though attempts have been made to explain observed selectivities,[47b] the mechanisms of such radical based reactions are still under scrutiny. Substrates employed often contain hydroxy groups as mechanisms often proceed *via* phenoxy radicals.[47a, 47b, 48c, 48d, 53] Generally, oxidative couplings tend to suffer from low

selectivities. While naphthol is known to form well-localized radicals under oxidative conditions in *ortho* position to the hydroxy group,[54] phenol derived phenoxy radicals are less localized. To avoid rampant side product formation or polymerization, artificial substrates that—as of date—serve little use in natural product synthesis are often used. The *Müller* group exploited such low regioselectivity to achieve diversity oriented total synthesis of various racemic biaryl based natural products.[49b] Most recently oxygen-mediated catalyst-free dimerization and trimerization of flavones have been investigated highlighting the advance in transition metal free couplings.[55]

Homocoupling and cross-coupling reactions (Scheme 2B) are an essential class of various C–C bond forming methods. Historically, homocouplings such as the *Ullmann*-coupling first reported in 1901, have played a major role in biaryl synthesis.[33b] Even though the applicability of such methods for unsymmetrical biaryls is inherently low due to the nature of symmetrically functionalized substrates, contemporary synthesis strategies are still able to make use of this robust method employing stochiometric amounts of relatively inexpensive copper.[56] Since the late 1970s various cross coupling methods have been developed to mitigate the drawbacks associated with homocouplings in addition to the use of sub-stoichiometric amounts of metal catalyst.[57] Palladium-catalyzed reactions to obtain biaryls involve the use of an aryl (pseudo)halide (X = Cl, Br, I, OTf) in combination with various nucleophiles such as aryl boronates (Y = $B(OH)_2$) (*Suzuki-Miyaura* coupling) (Scheme 2B).[58] Other palladium-catalyzed cross-coupling reactions such as *Stille*-, *Kumada*-, *Negishi*-, *Heck*-couplings,[59] and—more recently—*Buchwald-Hartwig*-aminations[60] have also found widespread application in synthesis of pharmaceutically relevant molecules.[61] Since the advent of these methods in the 1980s and 1990s, nickel has gathered considerable attention as a replacement for palladium in cross-coupling protocols[62] but has yet failed to replace the 'Jack of all Trades' palladium. The 2010 Nobel Prize in chemistry was awarded to Prof. *Akira Suzuki* as a co-recipient for his efforts in the field of palladium-catalyzed cross-coupling reactions.[63] In drug discovery and medicinal chemistry, biaryls and the *Suzuki-Miyaura*-coupling in particular are over-proportionally represented among drug candidates again emphasizing the importance of this class of aryl-aryl bond formation.[61b]

In relation to these first two strategies, de-novo syntheses (Scheme 2C) have as of date been less explored but have still gained considerable attention most notably among these atroposelective de-novo syntheses.[64]

4.2 Enantiomeric enrichment of biaryls

The enantioselective construction of biaryls is synthetically challenging.[18, 27] A narrow substrate scope or tailor made solutions are often the concessions made to accommodate complex target structures.[25, 65] Diastereoselective couplings by the utilization of chiral auxiliaries are some of the earliest examples of stereoselective biaryl formation but still find application in modern syntheses.[66] Moreover, the use of chiral ligands has been applied to many coupling strategies, in particular *Suzuki-Miyaura*-couplings.[67] As mentioned in the previous section, in addition to the stereoselective construction of the biaryl bond, various methods of enantioenrichment of racemic, stereodynamic or prochiral biaryls exist (Scheme 2D, Scheme 3). These atroposelective transformation of biaryls have recently been compiled in an illustrative overview article by the *Lassaletta* group and will only be concisely summarized here.[68] In addition to more modern approaches, chiral auxiliaries as resolving agents played a historically important role especially in natural product synthesis.[49b, 56a, 56b, 69] As a 'spiritual successor' to this approach, kinetic resolution (KR) (Scheme 3A) is a classic method wherein both atropisomers are separated by the selective transformation of one of the enantiomers.[70] Similar to resolutions using auxiliaries, the maximum obtainable yield for each enantiomer is capped at 50%. Dynamic kinetic resolution (DKR) (Scheme 3B) is a more contemporary method that involves racemization of the starting material and subsequent selective transformation of one enantiomer in the same fashion as KR.[71] The theoretical maximum possible yield of enantiopure (>99%*ee*) product in this and all following methods is >99%. Examples of kinetic dynamic resolutions include selective ring opening of stereodynamic lactones or cyclic diaryliodonium salts.[72] Dynamic kinetic asymmetric transformation (DYKAT) (Scheme 3C) exploits prochiral intermediates. The definition of a DYKAT is discussed in extraordinary detail in literature.[73] Desymmetrization (Scheme 3D) transforms enantiotopic substituents of achiral starting materials that contain an already rotationally hindered biaryl bond. Finally, deracemization has gained renewed interest over the last decade (Scheme 3E). This method proceeds by selectively transforming one enantiomer into the other, making it the most straightforward of these processes.[74]

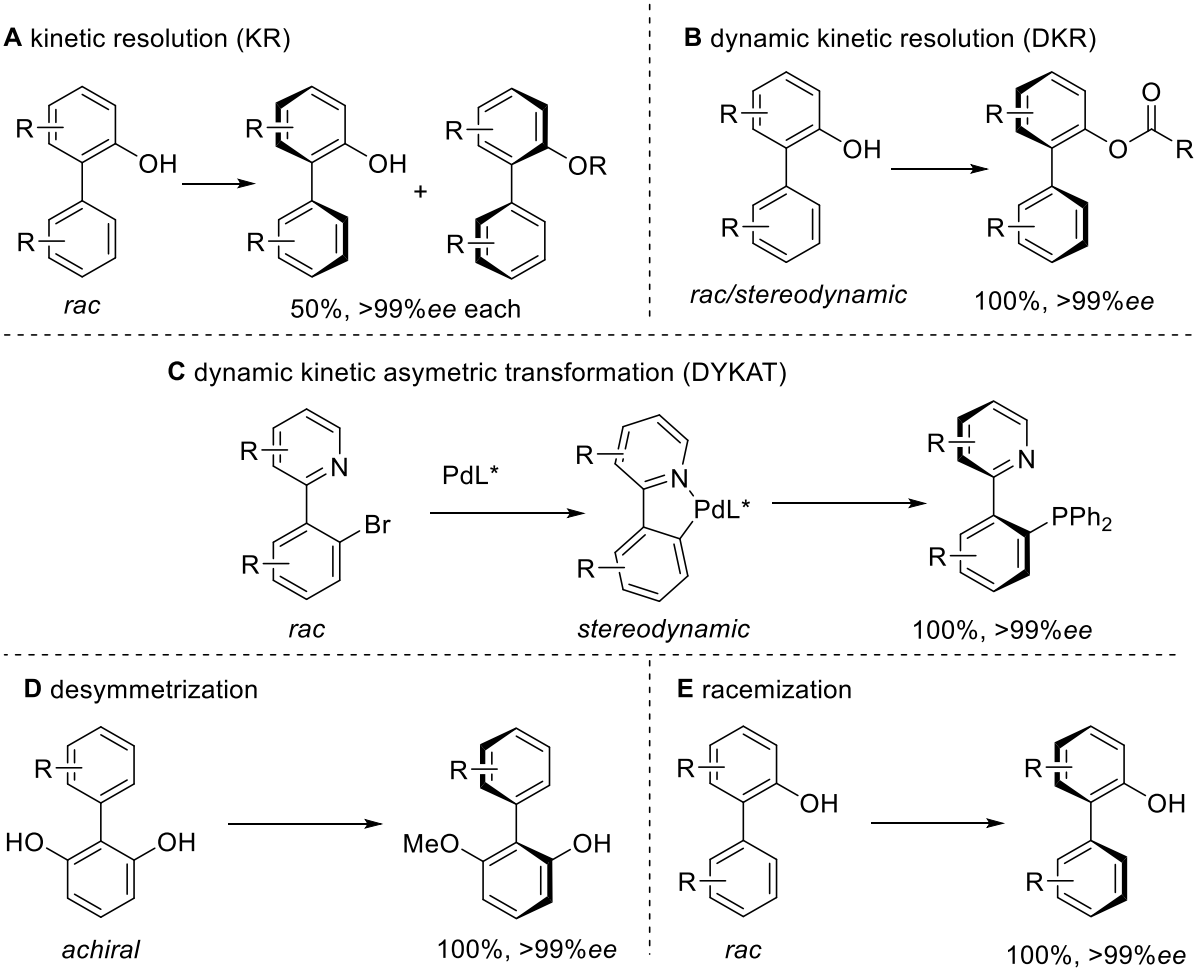

Scheme 3: Illustrative examples of various strategies employed to resolve and/or enantioenrich achiral/prochiral or racemic starting materials with maximum possible yield and enantiomeric excess.

4.2.1 Resolution of stereodynamic cyclic diaryliodonium salts

As outlined in the previous section, one of the strategies to obtain enantioenriched biaryls, is to leverage stereodynamic key-intermediates or starting materials (Chapter 4.2, Scheme 3B). For the context of this thesis, this method will be elucidated in more detail. In the following section, some of the newest trends in this field of research will be presented.

Cyclic diaryliodonium salts **6** have emerged as a useful class of stereodynamic prochiral compounds. The conformers of this compound class readily interconvert and thus no stable atropisomers ($\Delta G < 22$ kcal·mol^{-1}) exist at room temperature.[75] In recent years many applications for iodonium salts have been reported. *Heinen et al.* used cyclic diaryliodonium salts **6** as halogen-bonding organocatalysts in the amination of benzyl chlorides.[76] Applications of iodonium salts—synthetically useful building blocks—were compiled in a review on the topic in 2017,[72c] but have since greatly been expanded resulting from the inception of stereoselective catalytic ring opening reactions to form axially chiral biaryls **7**, first reported by *Zhao et al*. in 2018.[75] A variety of nucleophiles have thus far been reported for

this stereoselective ring opening reaction. Among these are primary amines,[75] thioesters,[77] *O*-alkyl hydroxylamines,[78] carboxylates,[79] triazoles,[80] halides,[81] and bulky anilines (using chiral cobalt cations).[82] These advances were compiled in a recent review on the topic.[83] This stereoselective ring opening, akin to a dynamic kinetic resolution (DKR), is able to produce enantiopure (>99%*ee*) product often with yields >90% (Scheme 4B). Tetra-*ortho*-substituted biaryls are thus constructed very cleanly, circumventing the issues otherwise associated with sterically congested biaryls.[18, 27] The synthesis of cyclic diaryliodonium salts generally proceeds *via* oxidation of 2-iodobiaryls **8** synthesized from nitro- **9** or amino arenes **10** (Scheme 4A). A limitation of this otherwise ubiquitous compound class is the incompatibility of electron-rich substrates with the oxidative cyclization conditions.[84] It could be shown that while the oxidation of the aryl iodide proceeds smoothly, the subsequent triflic acid (TfOH) induced electrophilic aromatic substitution (S_EAr) results in side reactions.[85]

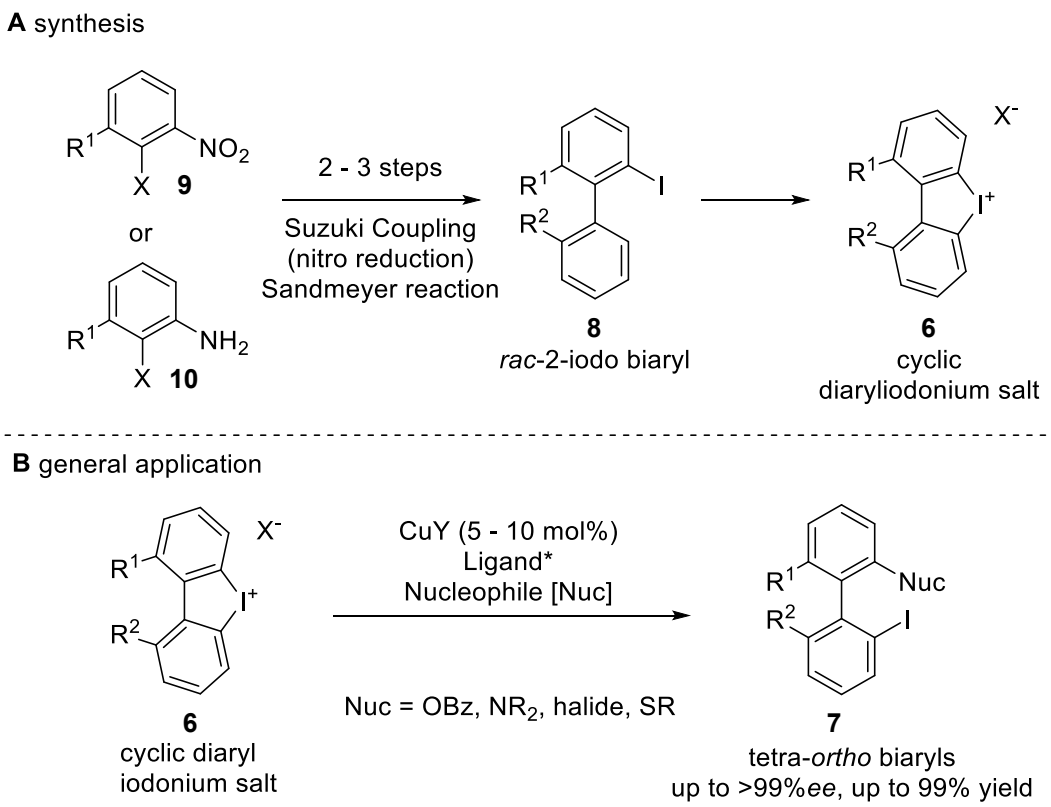

Scheme 4: (A) Synthesis and (B) application of cyclic diaryliodonium salts.

In addition to iodonium salts, cyclic diaryl λ^3-bromane ('cyclic diarylbromonium salts') **11** are also literature known but exhibit different reactivities and selectivities.[86] The synthesis proceeds *via* denitrogenative cyclization of 2-amino-2′-bromo biaryls **12** (Scheme 5A). Ring opening using carboxylic acids or amines generates different possible regioisomeric products (**13** and **14**) depending on the substitution pattern as was shown by *Lanzi et al.* (Scheme 5B).[87] Compared to cyclic diaryliodonium salts **6**, the mechanism is believed to proceed *via* an aryne

intermediate **15** explaining this reactivity (Scheme 5C). In addition to this application in the generation of biaryl scaffolds, cyclic diaryl λ^3-bromane **11** can also be employed as chiral organocatalysts as was shown by *Yoshida et al.*[88] *Lanzi et al.* also recently expanded the collection of cyclic hypervalent halogen containing compounds by synthesizing and utilizing the first cyclic diaryl-λ^3-chloranes.[89] No efforts have been undertaken into making use of the stereodynamic properties of such system.

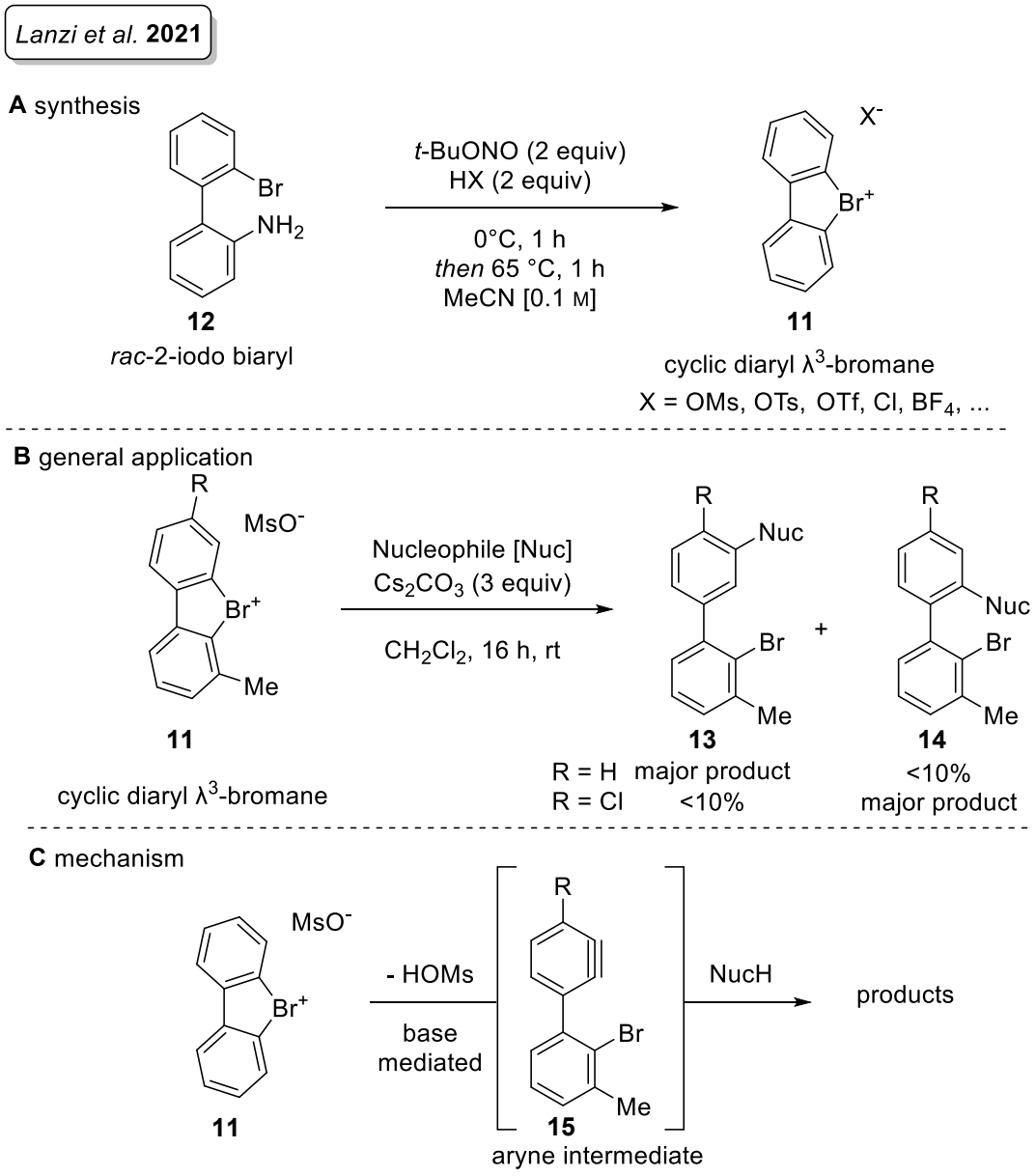

Scheme 5: (A) Synthesis, (B) regioselective ring opening and (C) proposed mechanism of the ring opening of cyclic diaryl λ^3-bromanes. In accordance with *Lanzi et al.*[87]

4.3 Biaryl based natural product synthesis

As stated in the introduction, biaryl-based compounds have emerged as exciting drug scaffolds. Bioactive biaryl-based natural products as an inspiration for new pharmaceutically relevant compounds have therefore thoroughly been investigated. *Bringmann et al.*[18, 37, 44, 90] and *Kozlowski et al.*[91] compiled exceptionally important review articles on the topic of axially chiral biaryl-based natural product synthesis with the most recent being published in 2019 in addition to further important overviews by other groups on the topic.[27, 68, 92] In the following section an illustrative overview of various biaryl based natural products, their bioactivity, and the total synthesis strategies will be discussed. Strategies employed since the early 2010s will be highlighted. In particular, C_2-symmetrical biaryls will be conferred to highlight historical and contemporary strategies towards enantioenriched products.

4.3.1 Polyketides

Oxidative coupling strategies are common among polyketide based natural product synthesis. In particular, vanadium-based catalysts originally developed by *Hwang et al.*,[51a] have found application in natural product synthesis[65a] as well as oxidative hetero-couplings both compiled in a recent review.[53] Modern vanadium coupling methodology involve the use of chiral mono-metallic complexes most recently expanded by the *Kozlowski* group.[93] In 2011 *Park et al.* highlighted the vanadium catalyzed oxidative coupling of a semiviriditoxin analogue **16** to construct the biaryl axis in an atropodiastereoselective manner (Scheme 6A).[26] The substrate-dependent diastereomeric ratio (d.r.) could be improved from 76:24 to 89:11 by utilizing a bimetallic vanadium catalyst originally developed by *Guo et al* ((S_a,*R*)-cat) (**17**)[51b] Subsequently, the anti-bacterial agent viriditoxin (**5**) was obtained over five steps starting from their highly functionalized coupling product **18** and in an overall yield of 4% over 12 steps (Scheme 6B).

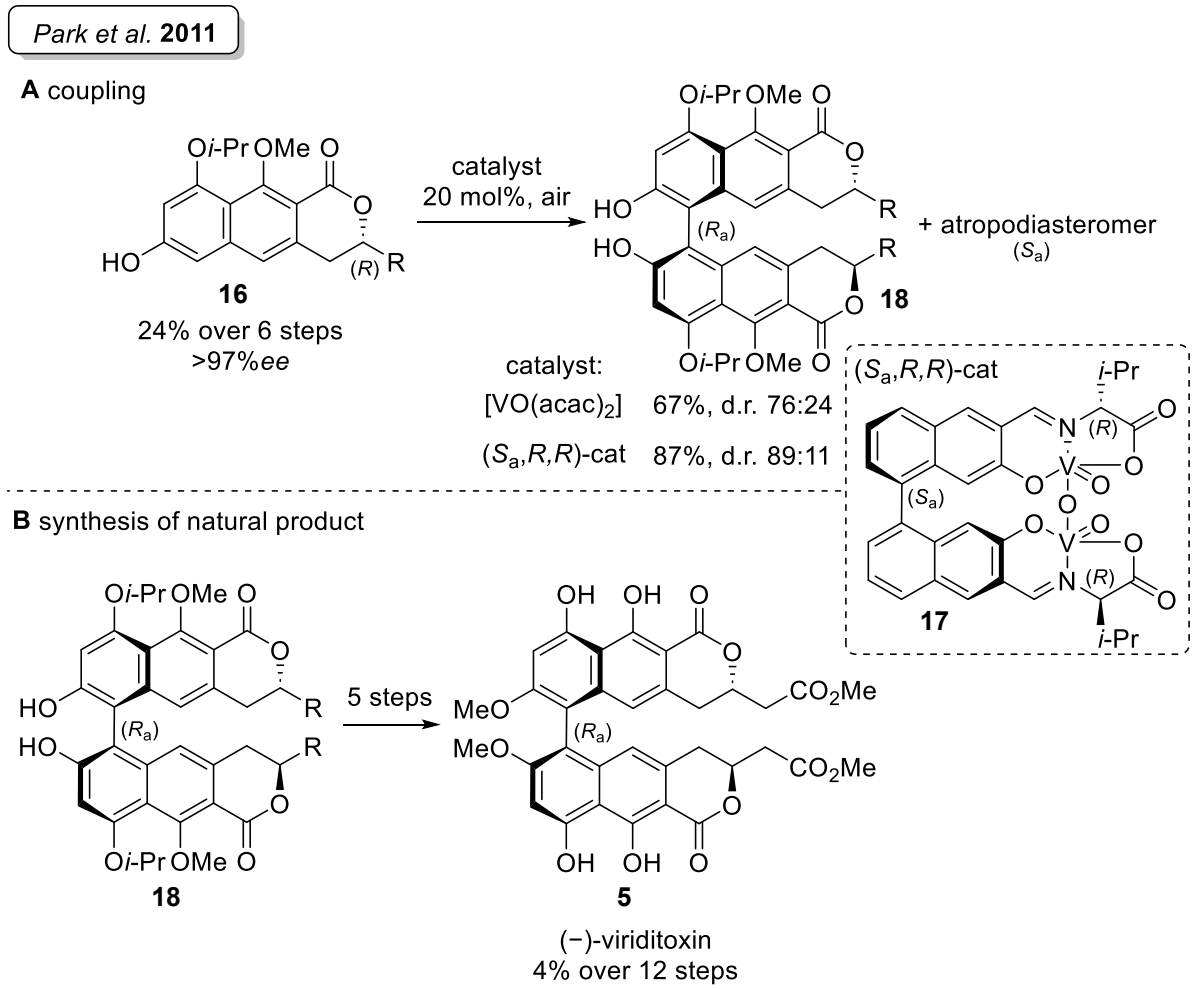

Scheme 6: Total synthesis of Viriditoxin. In accordance with *Park et al.*[26]

Purely substrate-dependent atropodiasteroselective couplings have been used to a lesser degree in the total synthesis of a variety of natural products. *Qin et al.* obtained rugulotrosin A (**4**) from intermediate **19** in addition to the atropodiastereomers of either enantiomer with opposite selectivity to the desired enantiomer (d.r. 1:3) (Scheme 7A) and subsequently showed the antibacterial activity of these compounds.[25] The biaryl bond was forged using a *Suzuki-Miyaura*-type one-pot synthesis to couple the monomeric precursor **20**. *Xiao et al.* obtained ascherxanthone A (**21**), an antimalarial agent,[94] as the major isomer (d.r. 2.2:1) using the previously mentioned coupling strategy by *Qin et al. via* the highly functionalized monomer **22** (Scheme 7B).[95] *Wu et al.* synthesized gonytolide A (**3**),[65a] an immunostimulant,[24] by oxidative coupling utilizing a halide blocking group crucial for the regioselectivity of the coupling. The diastereoselectivity of this reaction could be tuned (d.r. 1:2.9 to 1:1.2) by the variation of the employed halide blocking group of the monomer **23** (Scheme 7C). It is important to note that the number of expected diastereomers was incorrectly assessed, as the C_2-symmetry lowers the number of expected diastereomers. The foremost and the latter of these investigations were conducted by the *Porco Jr.* group.

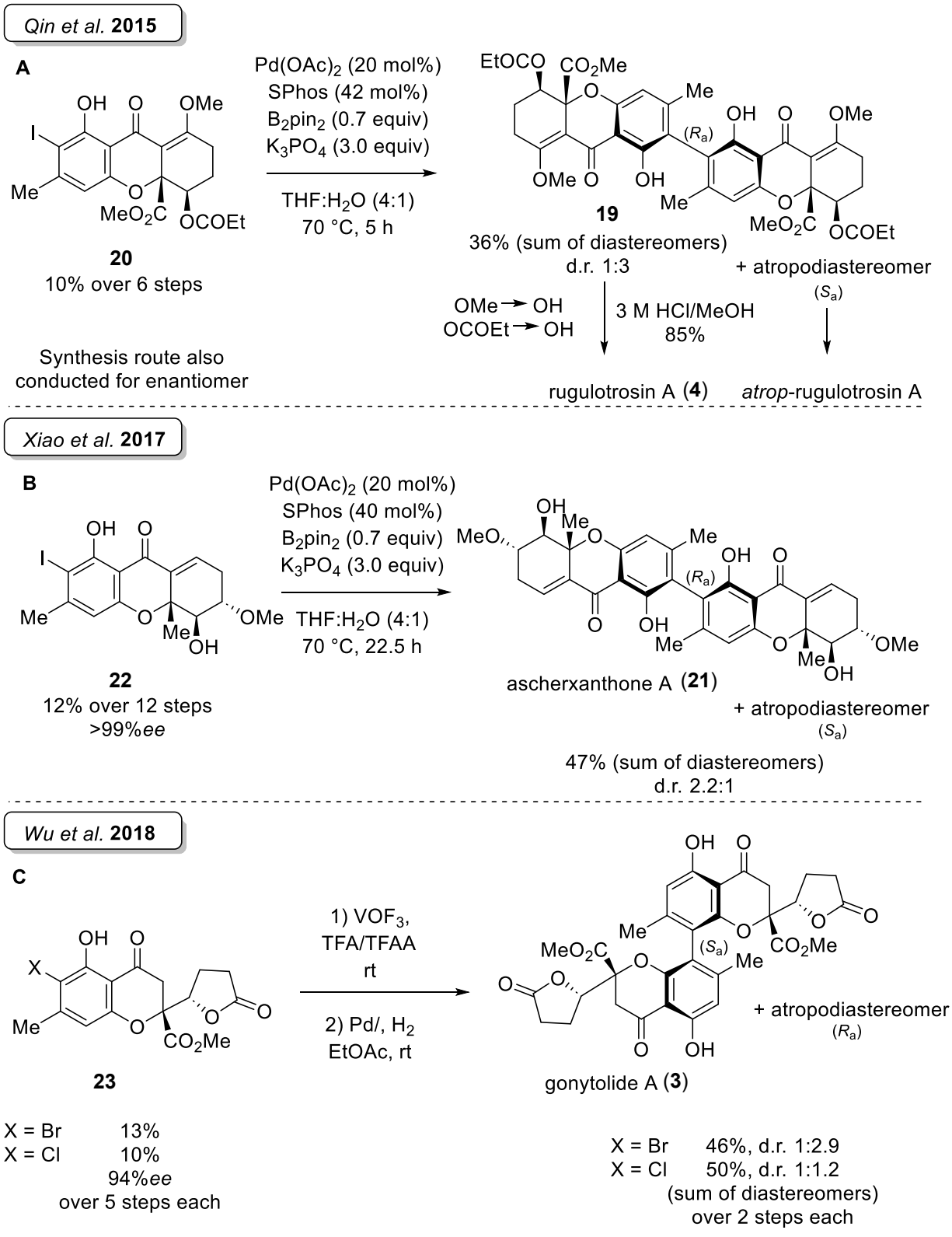

Scheme 7: Various atropodiastereoselective coupling strategies. (A) Total synthesis of rugulotrosin A in accordance with *Xiao et al.*[95] (B) Total synthesis of ascherxanthone A in accordance with *Qin et al.*[25] (C) Total synthesis of gonytolide A in accordance with *Wu et al.*[65a]

The group of *Porco Jr.* has utilized additional strategies to access naturally occurring dimeric polyketides. In their total synthesis of aurofusarin (**24**), *Qi et al.* used oxidative palladium-catalyzed couplings of monomeric key intermediate **25** in combination with

deracemization of the racemic coupling product **26**.[96] The deracemization strategy was based on earlier investigations of 2,2′-bi-1-naphthol (VANOL) deracemization,[97] which were based on even earlier 1,1′-bi-2-naphthol (BINOL) deracemizations[98] and asymmetric couplings by *Smrcina et al.*[99] *Qi et al.* were able to show that the oxidation of the enantiopure intermediate **26** to obtain aurofusarin (**24**) only gave a racemic mixture. Using density functional theory (DFT)[100] calculations they showed that these tetra-*ortho* congested bichinones **24** were configurationally unstable possessing a rotational barrier of 22 kcal·mol^{-1}, barely scratching the atropisomerism threshold.[35]

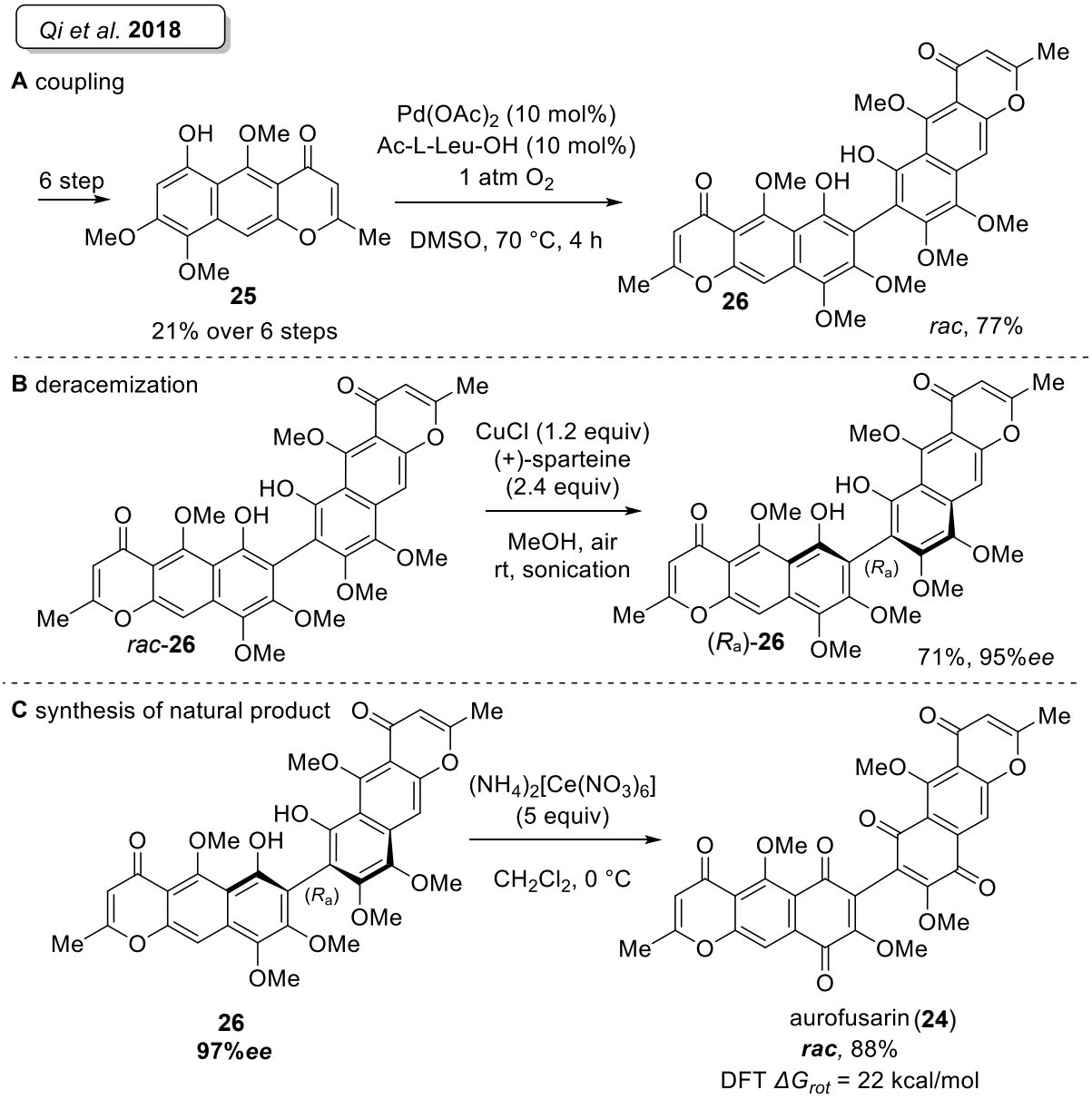

Scheme 8: Total synthesis of aurofusarin with deracemization of axially chiral intermediate. In accordance with *Qi et al.*[96]

More recently the *Pietruszka* group has developed several strategies for the synthesis of axially chiral biaryls and shown their application in the synthesis of natural products. In particular a common building block biphenol (BIPOL) **27** was used to show the wide application of these approaches. In 2023 *Greb et al.* synthesized the MOM-protected biphenol (MOM_2-BIPOL) **28** starting from the brominated monomer **29**[96] by the use of copper mediated coupling originally developed by the *Lipshutz* group[101] and improved the use of biquinone (DBQ) (**30**) (Scheme 9A). The resolution was performed using a deracemization approach with yields of up to 30% over the nine-step sequence with an enantiomeric excess of >99%*ee* (Scheme 9B).[96] In the end di-*epi*-gonytolide A (**31**) could be obtained *via* this approach in a diastereoselective manner (Scheme 9C).[102]

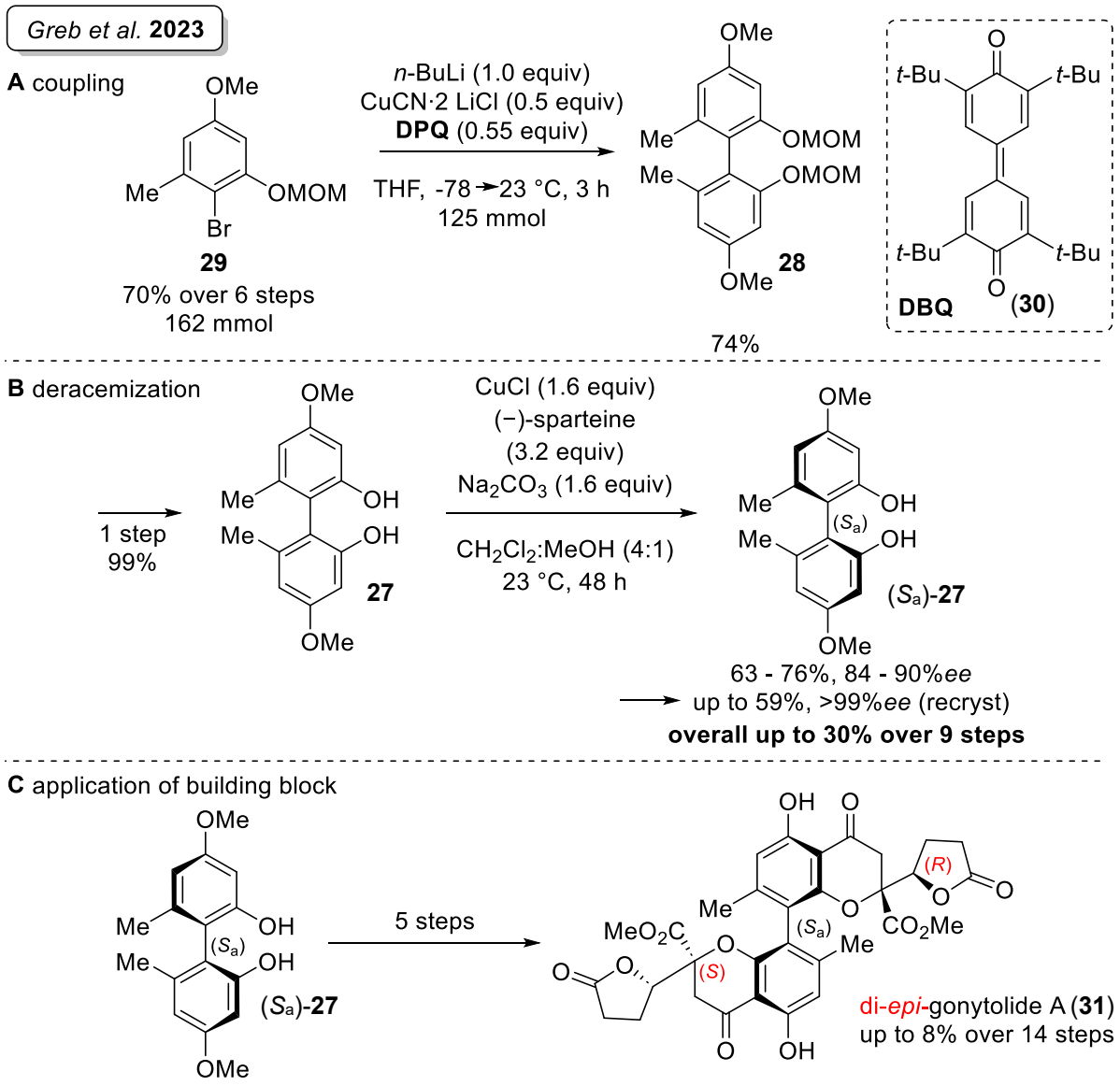

Scheme 9: Synthesis if di-*epi*-gonytolide A (**31**) (stereogenic centers which are inverted compared to gonytolide A (**3**) are highlighted). In accordance with *Greb et al.*[102]

Also in 2023 *Ganardi et al.* reported the synthesis of isokotanin A (**32**), an antifeedant agent against fungivorous beetles, utilizing the same biphenol building block **27**.[103] The construction of MOM-biphenol **28** was performed by *Suzuki-Miyaura* coupling akin to conditions by *Qin et al.* (Scheme 10A),[25] using the same previously synthesized brominated building block **29**.[102] Kinetic resolution of diester **33** was conducted by the use of a lipase (*Candida rugosa* lipase) to obtain the enantiopure building blocks **34** and **27** in yields of 20 – 21% over ten steps (Scheme 10B). Finally, isokotanin A (**32**) was synthesized to accentuate the usefulness of building block **27** and the method overall (Scheme 10C).

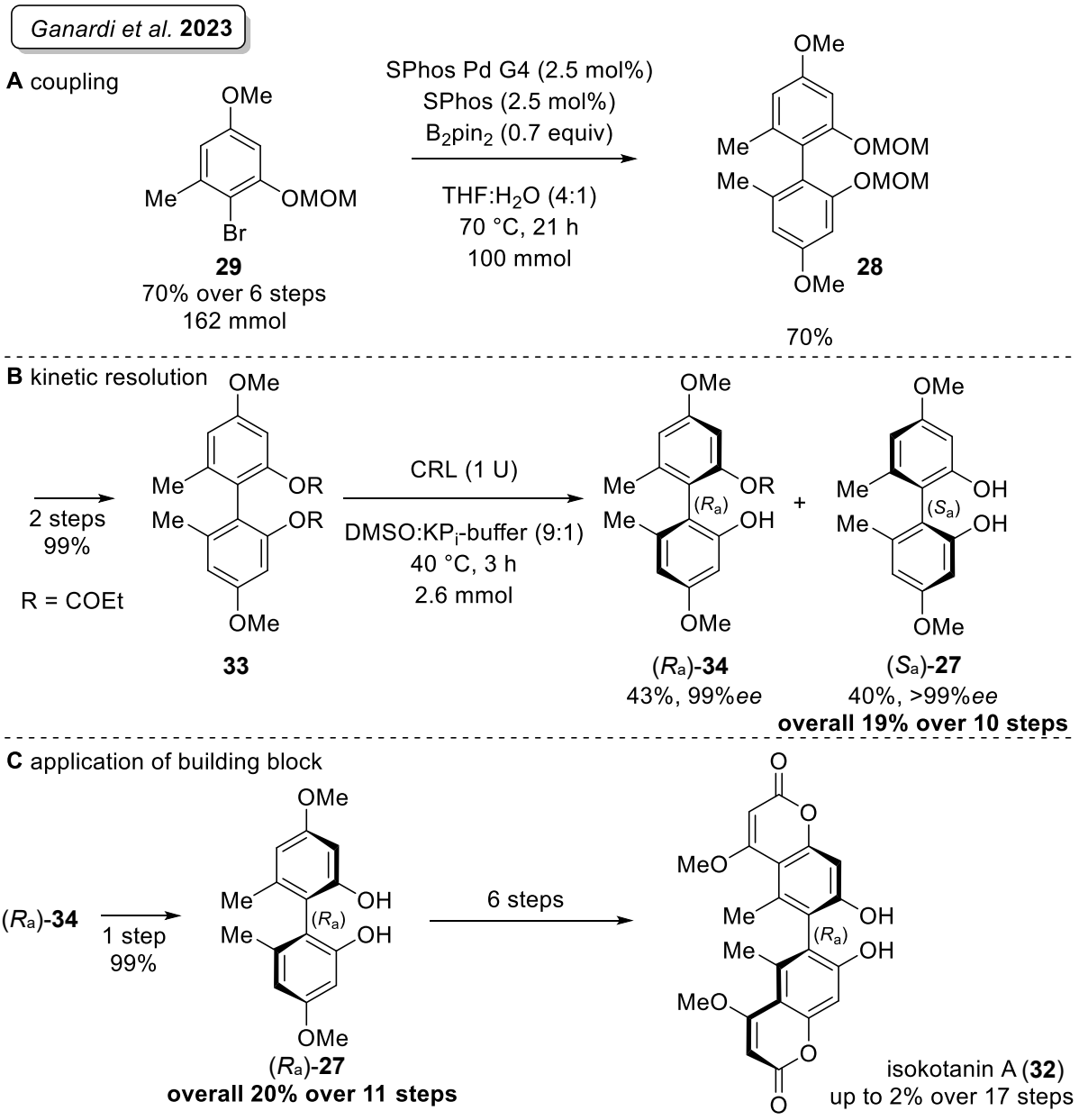

Scheme 10: Total synthesis of isokotanin A. In accordance with *Ganardi et al.*[103]

4.3.2 Biflavones

As outlined in the introduction, flavones are naturally occurring phenylpropanoids. Biflavones are a more elusive subclass of dimers found among various *gymnosperms*.[11] Often, these dimers are derived from the flavone monomer apigenin (**35**) (Figure 2). Few naturally occurring structural modifications besides glycosylations have been reported.[104] As the dimerization of the monomeric units is proposed to proceed *via* oxidative phenolic coupling,[40] a wide variety of connectivities are observed in nature. Ether-linked biflavones such as hinikoflavone (**36**) and delicaflavone (**37**) support the proposed phenoxy-radical based coupling (Figure 2A). These compounds display various anti-cancer related activities.[105] Another biologically relevant subclass are non-C_2-symmetrical C–C linked biflavones such as 3′,8″-biflavones amentoflavone (**38**) and ginkgetin (**1**) (Figure 2B),[12] the former exerting activity against kinetoplastid parasites among others.[12g] Overall, the structure-activity relationship of these compounds has hardly been investigated.[106] C_2-symmetrical biflavones include 6,6″-biflavones **39** and 8,8″-biflavone cupressuflavone (CUF) (**40**) first isolated from *Cupressus torulosa* (Figure 2C).[11a] These structures have hardly been evaluated for their pharmacological potential,[106-107] and few reports on non-natural analogues exist.[108] Representatives of all classes of biflavones, namely amentoflavone (**38**), CUF (**40**), and hinokiflavones (**36**) appear in some, but not all *Cupressus* species.[109] Very few examples of enantioenriched biflavones have been reported to date. Enantiopure CUF (Figure 2C) was first isolated in 1968 by *Ilyas et al.*[110] Non-C_2-symmetrical 6,8″-biflavone agathisflavone (**41**) (Figure 2B) was first isolated in 2016 from the *angiosperm*, *Schinus terebinthifolius* (Brazilian peppertree) by *Covington et al.* and the absolute configuration assigned.[111] In comparison with polyketide-based natural products, biflavones are comparably simple structures only containing a single stereogenic element, a feature exploited by *Kikuchi et al.* in the synthesis of simplified gonytolide A (**3**) analogues.[108a] This strategy leveraged the ease of synthesis of a single stereogenic axis in combination with the retention of bioactivity.[112]

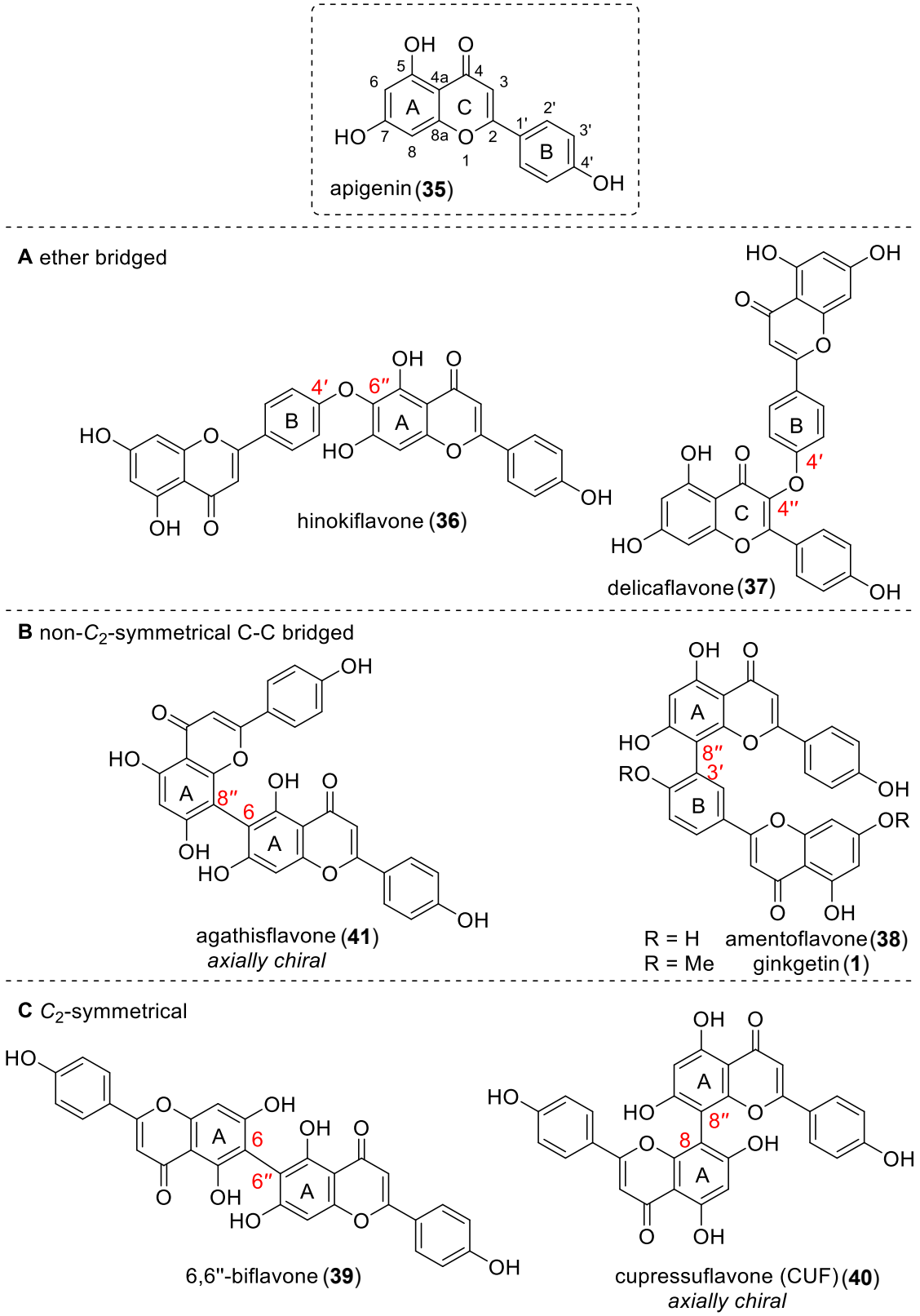

Figure 2: Various connectivites of naturally occurring biflavones as bioactive natural products. Axially chiral occurring biflavones are indicated.

4.3.2.1 8,8″-biflavones

In the context of this dissertation, 8,8′′-biflavones will be discussed in detail. In the following, an overview of the history of CUF (**40**) isolation, synthesis, and assessment of bioactivity will be given. CUF (**40**) was first isolated in 1966 from *Cupressus torulosa* where its name is derived from,[11a] with various total synthesis strategies of *rac*-CUF established in the early 1970s.[113] The absolute stereochemistry remained unresolved for over 20 years until the absolute configuration of a natural analogue of 4',4''',7,7''-tetra-O-methyl-cupressuflavone (tetramethyl-CUF) (**42**) was first assigned in 1992 by Harada *et al* using theoretical CD spectra.[114] Subsequently several protocols were developed in the 1990s to synthesize enantiopure biflavones. These synthetic routes mostly relied on the use of chiral auxiliaries to enantioenrich the final product by resolution or enantioselectively construct the biaryl bond.

The bioactivity of CUF has been assessed to some degree. CUF has been shown to exert little to no cyctotoxicity while possessing significant anti-inflammatory, antinociceptive and analgestic properties.[107a] Moreover, while antiviral activity was observed, no direct inhibition of Herpes Simplex Virus type 1 (HSV-1) could be detected.[107b] A correlation between degree of methylation and Aβ aggregation inhibitory activity, relevant in the development of Alzheimer's disease, was also reported.[106] While dimethylether derivatives showed significant activity, tri- and tetramethyl ethers of CUF were inactive. Another study by *Takahashi et al.* found non-methoxylated CUF to be a poor β-secretase (BACE-1) inhibitor, a protein relevant in the Aβ aggregation process.[115] Additionally, only moderate cytoprotective effects regarding amyloid-β peptide Aβ42 were observed resulting in a low cell viability.[107e] In contrast to other biflavones, CUF showed no significant activity towards Dengue virus NS5 RNA-dependent RNA polymerase.[116] Beneficial properties towards oxidative stress suppression were discovered by a study investigating CCl_4 induced toxicity in mice. While untreated mice displayed a significant increase in alanine aminotransferase, aspartate aminotransferase and alkaline phosphatase expression, mice pre-treated with CUF showed a decrease throughout, confirming a hepatoprotective function.[107d] CUF was also found to not only inhibit bone loss caused by osteoporosis, but also stimulate bone formation.[107c] CUF showed no activity towards leishmaniasis, a protozoal disease.[117]

In 1995 *Zhang et al.* were able to confirm the previously assigned (R_a)-configuration by synthesis of both enantiomers of hexamethyl-CUF (**43**). This synthesis strategy uses Ullmann-coupling of halogenated flavone monomer **44** to form the biaryl bond in a yield of 55% (Scheme 11A).[56a] While diastereoselective *Ullman*-type couplings using chiral auxiliaries

were first reported in 1993 by *Nelson et al.*,[118] the authors opted for the use of chiral auxiliaries as resolving agents (Scheme 11B). The resulting diastereomers **45** and **46** were separated by recrystallization. In 1997 a synthesis strategy based on this original protocol was established for the synthesis of the first enantioenriched non-natural 8,8″-biflavone **43b** (Ar = Ph).[56b] Overall a yield of 13% over 7 steps was reported (Scheme 11C). The limitation of this protocol by using highly functionalized monomers is apparent.

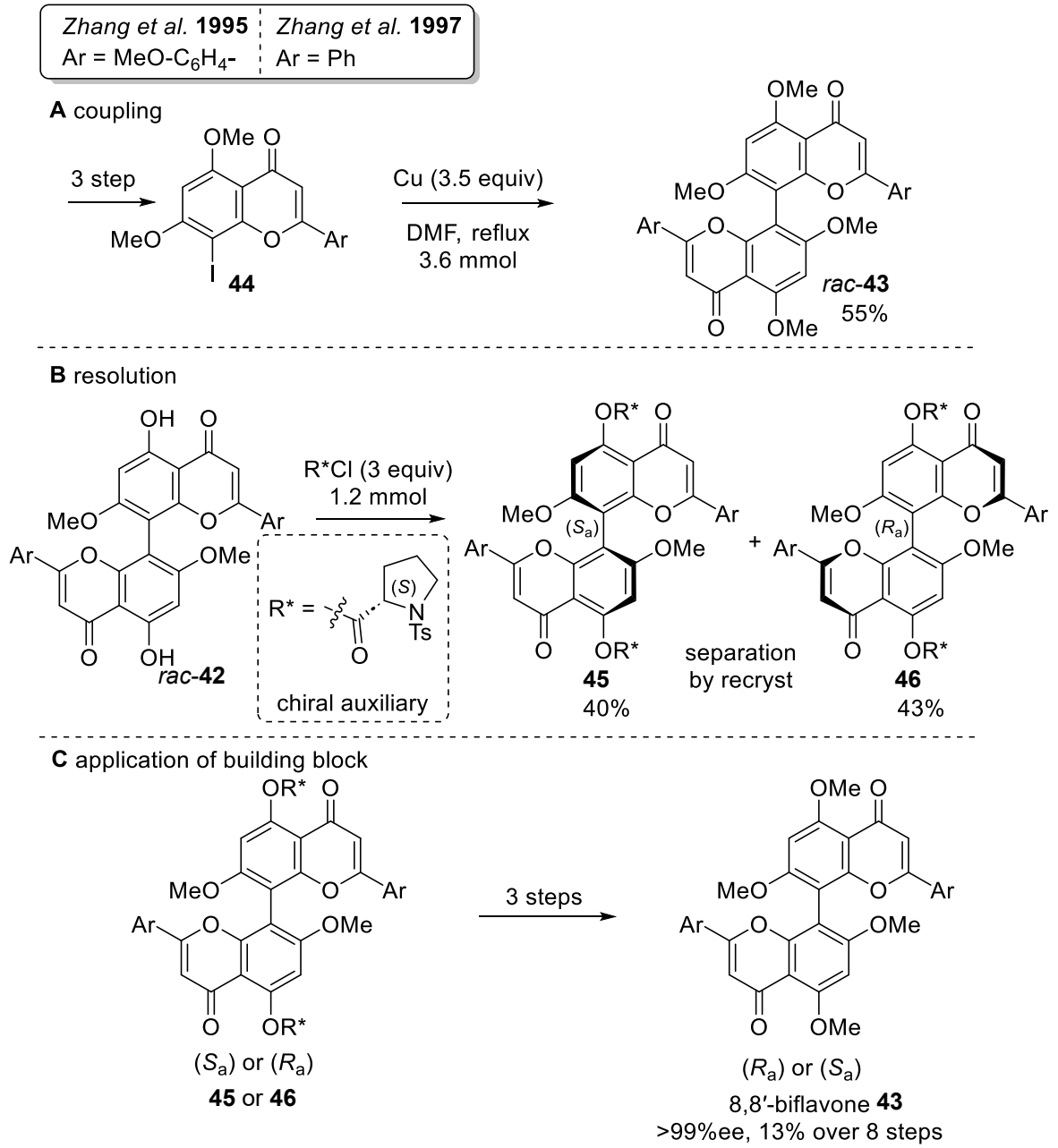

Scheme 11: Enantiomeric excess inferred from diastereomeric ratios. In accordance with *Zhang et al.*[56a, 56b] Yields reported for Ar = Ph.

Li et al. of the *Harada* group, who originally assigned the absolute configuration by CD-spectroscopy, independently also published the total synthesis of tetramethyl-CUF (**42**) in 1997.[69] The biaryl bond was constructed *via* an iron-mediated oxidative coupling of acetophenone **47** (Scheme 12A). Oxidative couplings using $FeCl_3$ were developed as early as the 1870s to obtain BINOL.[119] This early protocol was then improved by the utilization of immobilization of the iron and subsequent solid phase synthesis.[54] The substrate scope was expanded by *Jempty et al.* using phenols instead of naphthols.[120] Since then a variety of natural products were successfully synthesized using this method.[49a, 49b, 65c, 108a] During the coupling, *Li et al.* observed a chlorinated side product **48** that was able to be suppressed after screening and performing the reaction over 6 days.[69] The resolution of both enantiomers of the racemic coupling product **49** was conducted by the use of a chiral auxiliary. The forming diastereomers **50** and **51** were separated by preparative HPLC (Scheme 12B). In their protocol, partial racemization occurred during the auxiliary cleavage step of (R_a)-atropodiastereomer **51** (d.r. 99:1 to e.r. 89:11). The enantiopure product **42** was obtained in a yield of 5% over seven total steps with 78%*ee* (Scheme 12C). The enantiomeric excess was able to be increased to >99%*ee* by recrystallization.

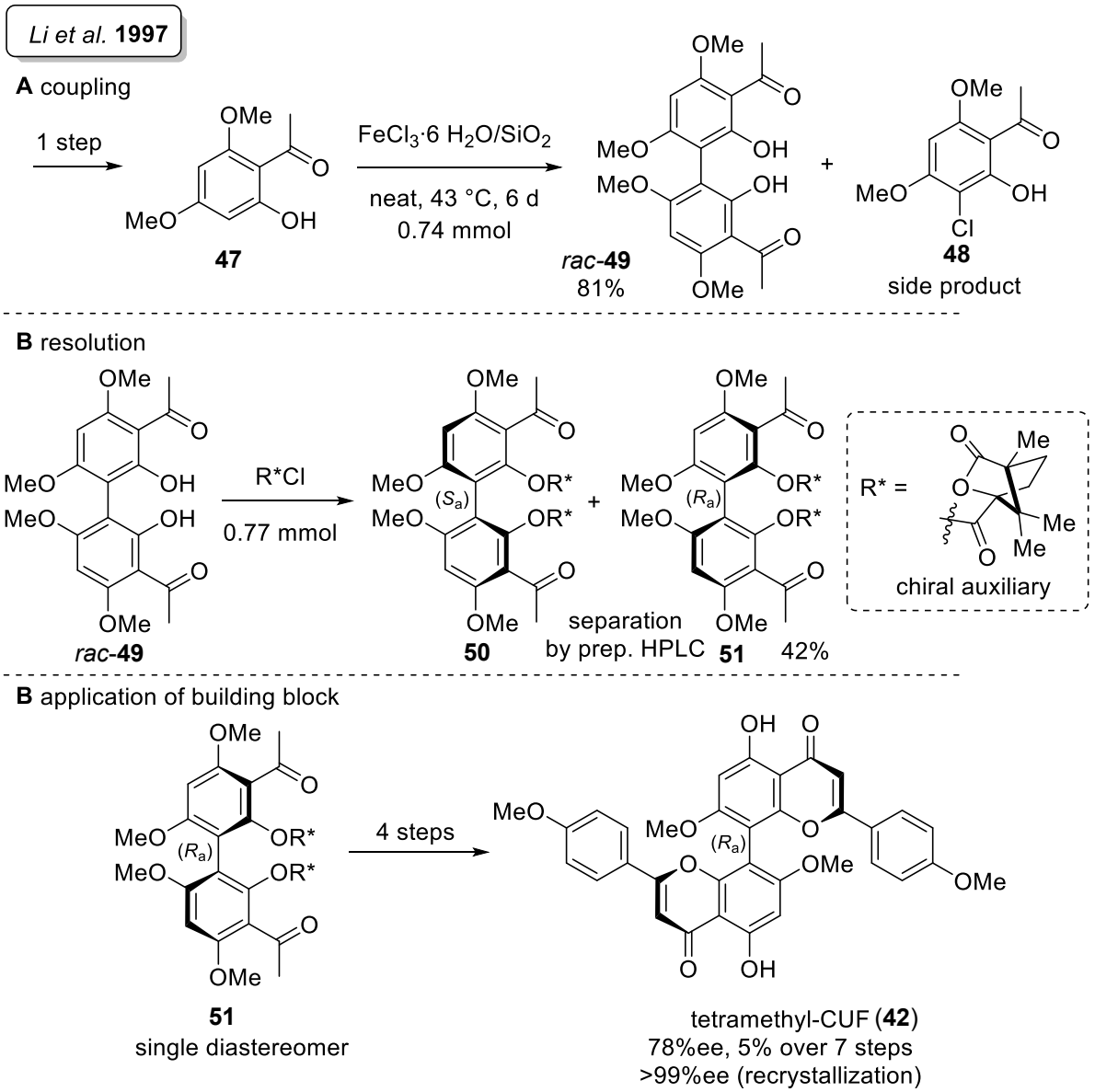

Scheme 12: Synthesis of enantiopure tetramethyl-CUF (**42**). In accordance with *Li et al.*[69]

In the same year (1997) an alternative coupling strategy was independently reported by *Lin et al.*[121] In their synthesis, the biaryl bond was forged in a diastereoselective manner by the use of *Lipshutz*-type cuprates with a chiral linker connecting the monomeric units **52** (Scheme 13A).[101] Enantiomeric excess was not reported by *Lin et al.* though implied to be >99%*ee* in accordance with optical rotation, obtained by enantiopure samples and inferred from the diastereomeric purity of the coupling product **53**. The final product tetramethyl-CUF (**42**) was obtained in a yield of 6% over 15 steps (Scheme 13B).

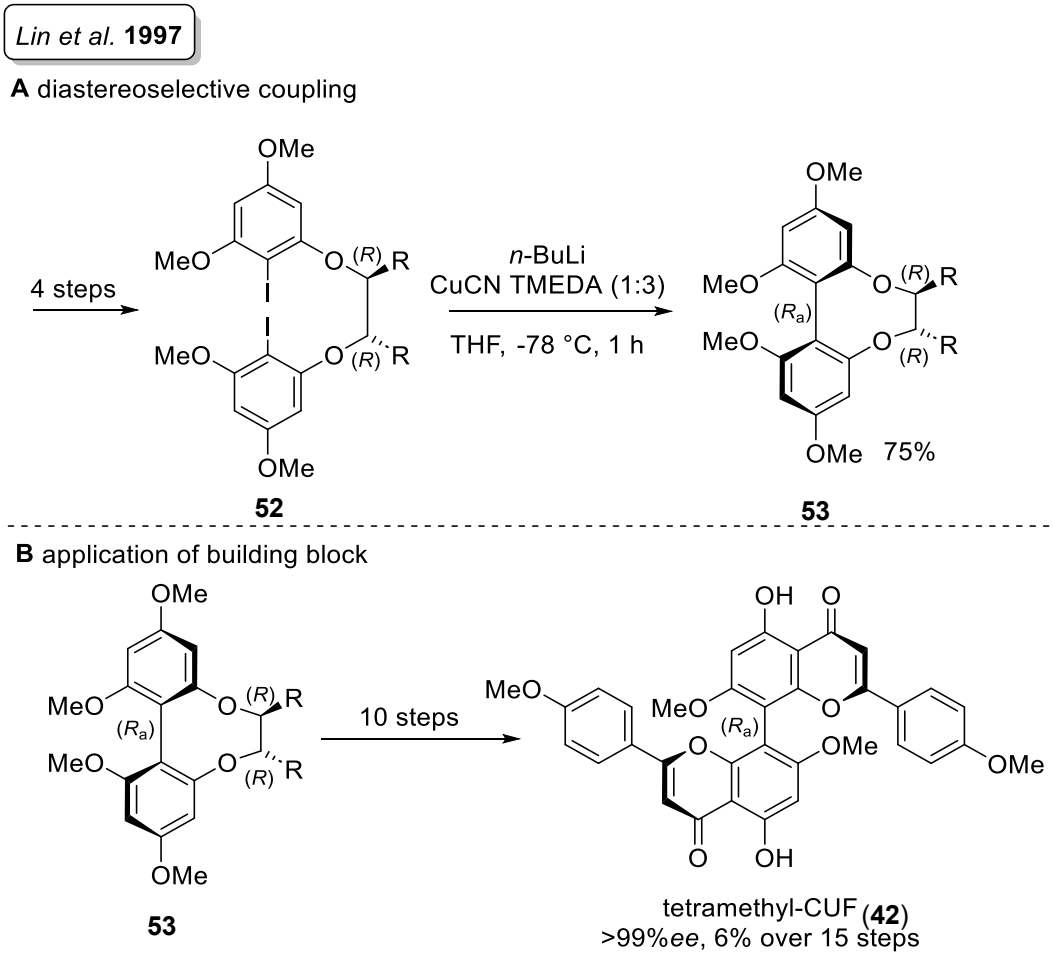

Scheme 13: Total synthesis of tetramethyl-CUF (**42**). Unknown scales. Enantiomeric excess inferred from comparison. In accordance with *Lin et al.*[121]

Since these investigations in the late 1990s only singular attempts at the synthesis of 8,8″-biflavones have been undertaken, such as the synthesis of the racemic non-natural derivative Me,Me′-tetramethyl-CUF (**56**) by *Kikuchi et al.* in 2016 (Scheme 14B).[108a] The oxidative coupling of the benzoate monomer **54** proceeded with relatively low yields of 32% in providing the coupling product **55** (Scheme 14A). Hitherto, these investigations are the only efforts into synthesizing A-ring analogues of 8,8″-biflavones.

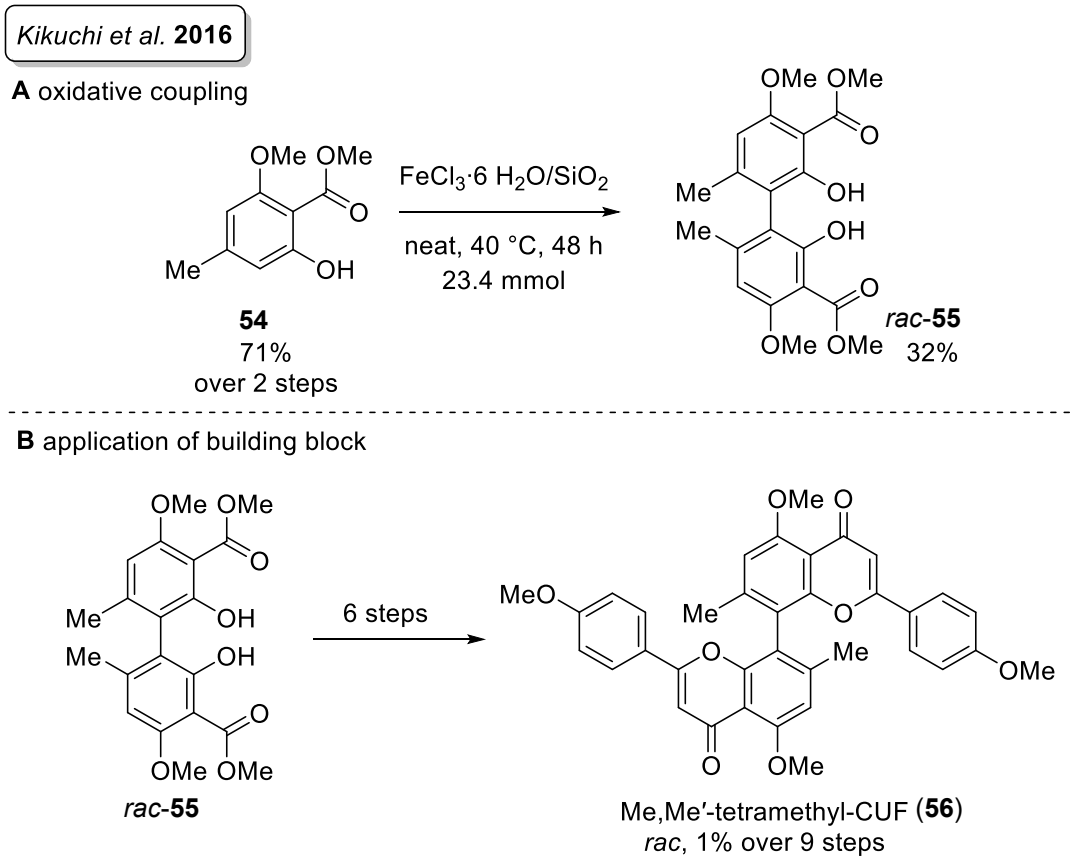

Scheme 14: Racemic synthesis of Me,Me′-tetramethyl-CUF (**56**). In accordance with *Kikuchi et al.*[108a]

4.4 Biaryl based ligands

In addition to being a useful scaffold in natural product inspired synthesis and drug discovery, biaryls have generated considerable interest in catalysis. One of the first examples of the use of axially chiral ligands in asymmetric transition metal catalysis constitutes the investigations by the *Noyori* group.[122] In 1980, BINAP (**57**) was successfully synthesized in an enantioenriched fashion by *Miyashita et al.* based on resolution of the enantiomers by formation of diastereomeric palladium complexes (Scheme 15A).[123] This bidentate ligand could subsequently be used in the rhodium-catalyzed asymmetric hydrogenation of alkenes **58** to obtain chiral amino acids **59** (Scheme 15B).[124] This achievement was recognized by awarding the Nobel Prize in chemistry to Prof. *Ryoji Noyori* as a co-recipient in 2001.[125]

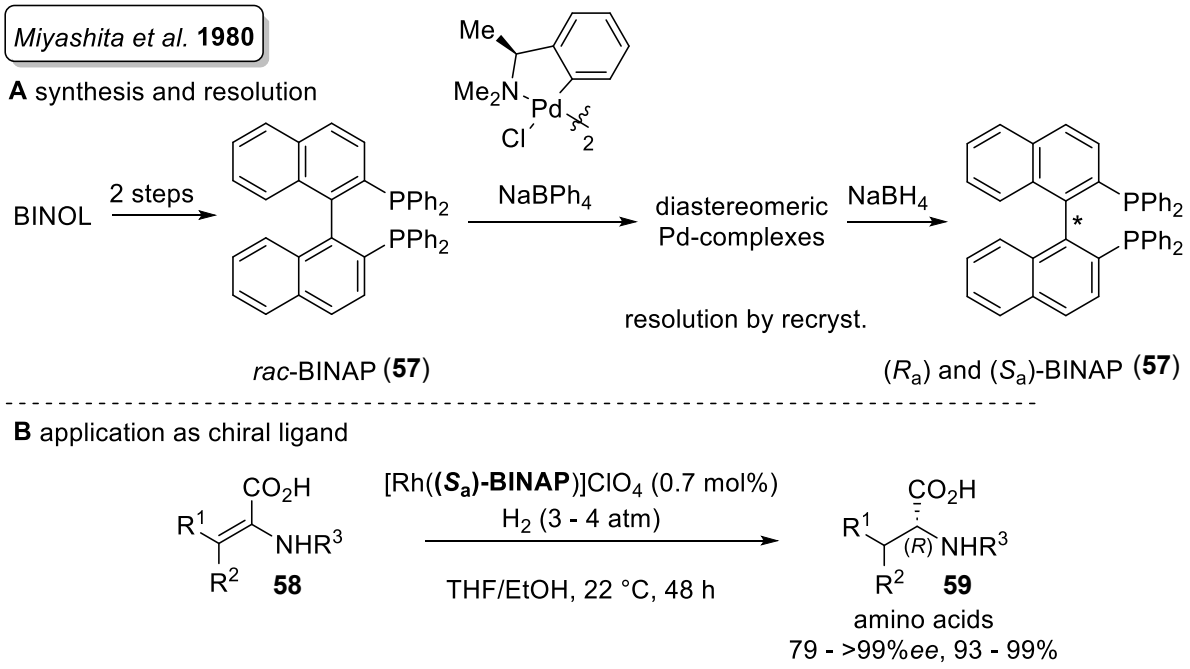

Scheme 15: Synthesis of enantioenriched BINAP (**57**) and subsequent use in the asymmetric rhodium-catalyzed hydrogenation of olefins. In accordance with *Miyashita et al.*[124]

After this first investigation, the use of axially chiral ligands became more widespread. Since the first report of an asymmetric *Suzuki-Miyaura* coupling using axially chiral phosphine ligands in 2000 by *Yin et al.* (*Buchwald* group),[126] many such asymmetric couplings towards axially chiral biaryls involve the use of axially chiral ligands.[42b, 67] A comprehensive overview of various types of axially chiral ligands has been compiled by *Lassaletta et al.*[92c] A brief overview of these ligands will be presented (Figure 3). BINAP (**57**) based axially chiral phosphine ligands received considerable attention in the late 1990s.[127] *Nishida et al.* reported the two-fold-de-novo synthesis of C_2-symmetrical heterobiaryls using axially chiral phosphine ligands with excellent enantiomeric excess.[64b] Since then, achiral biaryl monophosphines **60**

(MOP) (commonly referred to as *Buchwald*-type ligands) emerged as a class of useful ligands in *Suzuki-Miyaura* type couplings,[128] as well as *Buchwald-Hartwig* type aminations (Figure 3A).[129] BIDIME (**61**) is an example of a 'next-generation' monophosphine ligand that was originally developed by *Tang et al.* as a rigid ligand for *Suzuki-Miyaura* couplings.[130] As a *P*-chiral analogue, it expands the range of available chiral biaryl monophosphine ligands since 2010.[131] Chiral phosphoramidite ligands **62** have been used in various transition metal catalyzed reactions and have been attributed "a meteoric rise"[132] since their inception in 1996 by the *Feringa* group with the first BINOL based example.[133] Non-phosphorous ligands include BINAM-type ligands (**63**). Another important class of ligands are multi-donor-atom biaryls (Figure 3B). These include *P,N*-ligands like QUINAP (**64**), bearing a phosphorous atom and a nitrogen atom that can individually be modified regarding steric and electronic properties[134] or *N,O*-type ligand NOBIN (**65**). Axially chiral phosphoric acid esters **66** have successfully been employed as organocatalysts for various transformations including, but not limited to, atroposelective arylations and kinetic resolutions (Figure 3C).[135] The application and synthesis of these and other strong axially chiral *Brønsted* acid catalysts such as BINSA (**67**) is covered in a review by *Akiyama et al.*[136]

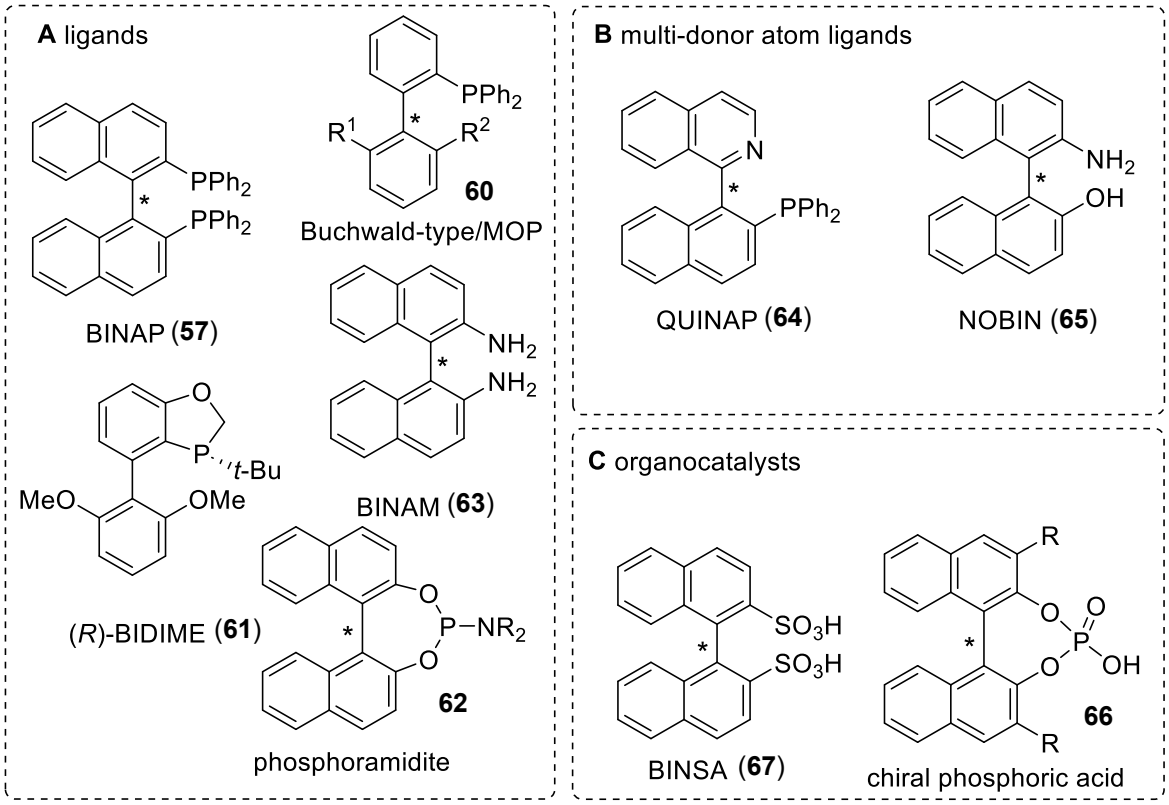

Figure 3: Selection of biaryl-based chiral ligands.

4.5 Palladium catalysis

As mentioned in the introduction of this chapter, palladium catalysis has been detrimental in the synthesis of complex molecules. Be it the *Suzuki-Miyaura* cross coupling developed in 1981,[58a] or the *Buchwald-Hartwig* amination reported in 1994.[137] Attempts at overcoming palladium by organocatalysis[138] have thus far been debunked and attributed to palladium impurities.[139] Nickel promises to exert similar reactivity though this metal is still less explored and appears less universally applicable.[62] As of date, palladium-catalyzed reactions remain some of the most important tools for C–C bond formation. In the following sections an overview of relevant resources will be given to gain in-depth knowledge on palladium catalysis. Additionally, advances in the field, especially towards the synthesis of biaryl scaffolds and functionalization of such biaryl-based structures will be discussed.

4.5.1 General considerations

Palladium-catalyzed reactions generally follow the same elementary steps found in most transition metal-catalyzed reactions.[140] The *Catellani* reaction—a multicomponent reaction—[141] marvelously displays a plethora of the most important elementary steps commonly found in many palladium-catalyzed reactions. To truly rationalize observed reactivities, the mechanism and catalytic cycle of a reaction must be thoroughly understood. A short overview of these steps will be given in this section (Scheme 16). A more detailed account on the catalytic cycle of *Catellani* type reactions was compiled by *Wang et al.*[140b] The common starting point for most palladium catalyzed reactions is a mono- or di-ligated Pd^0-species (**I**). This species can undergo oxidative addition (**a**) of an electrophilic organic compound such as aryl iodides **68** to form the oxidative addition (ox. add.) complex (**II**). Next, a coordination (not depicted) and migratory insertion (**b**) of norbornene (**69**) (transient directing group) takes place to form both a new C–C and a Pd–C bond (**III**). Vicinal C–H activation (**c**) forms a palladacycle (Pd-cycle) (**IV**) *via* the (formal) extrusion of hydrogen iodide. A second oxidative addition step (**d**) of an electrophile EX proceeds due to the electron-rich nature of the double-carbide-ligated palladacycle to form a Pd^{IV}-cycle (**V**). Reductive elimination (**e**) in the *Catellani* reaction generally proceeds chemoselectively to provide palladium complex **VI**. Steric bulk of the system favors norbornene extrusion (**f**) (*β*-carbide elimination) to form the less bulky palladium complex **VII**. Transmetallation (or more broadly X-type ligand exchange) (**g**) with a nucleophile NucY forms complex **VIII**, followed by a final reductive elimination (**h**). This regenerates the initial Pd^0-species (**I**) under extrusion of the desired product **70**. Steps such as ligand coordination and decoordination and competing mechanisms may alter the details and order of steps in the catalytic cycle but are not depicted for the sake of clarity.

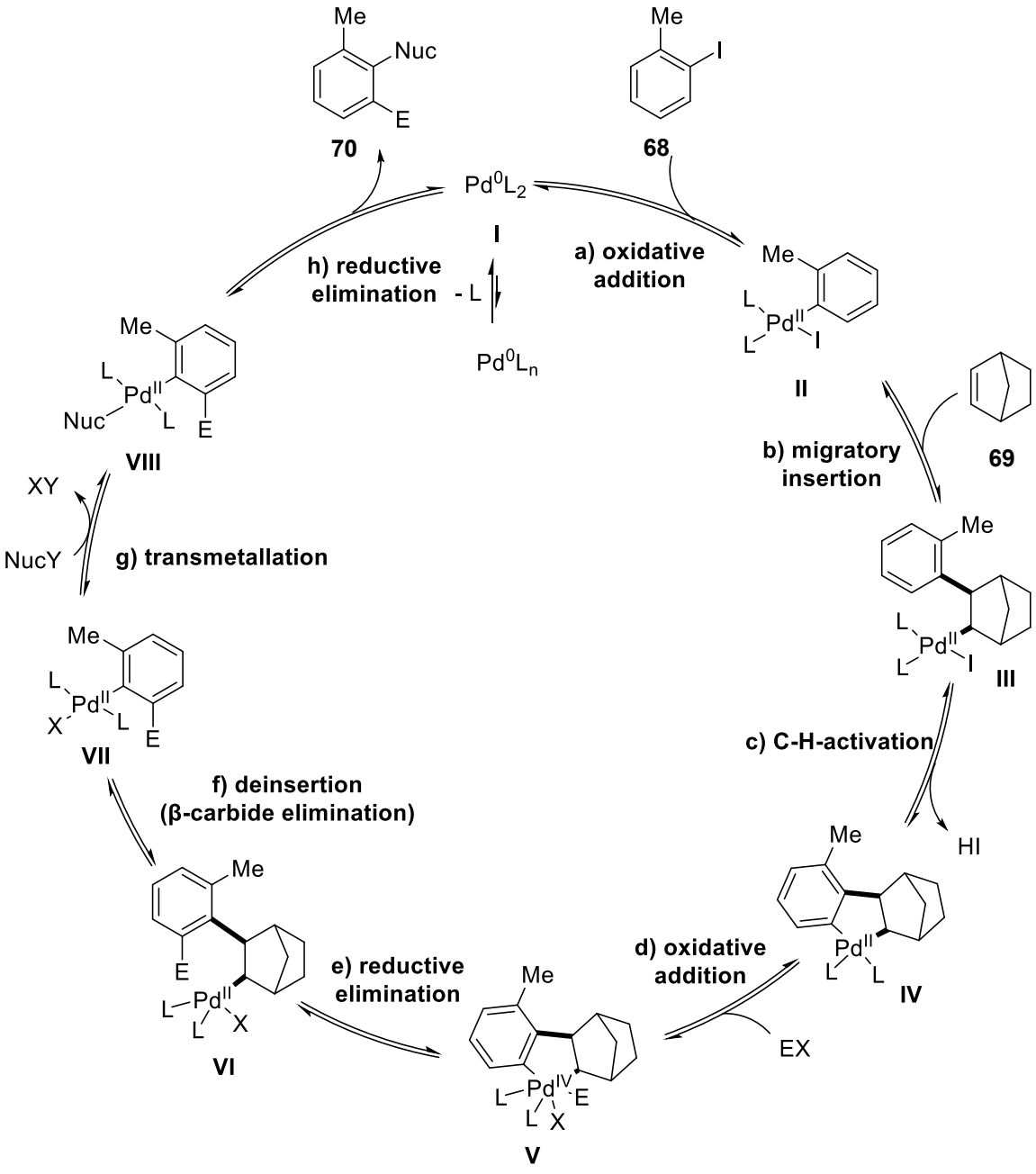

Scheme 16: Simplified proposed catalytic cycle of a palladium catalyzed *Catellani*-type reaction. *Cis-trans* isomerization and ligand exchanges omitted for clarity. Based on *Wang et al.*[140b]

The first consideration in establishing a new palladium-catalyzed reaction is the palladium source. Even though experimental screening is required to actually deduce optimal conditions, general considerations should be made. One should be aware of common side reactions and causes of catalyst inhibition. Palladium catalysts are generally employed as either Pd^0- or Pd^{II}-sources (Figure 4). Readily available and common Pd^0-sources include the ubiquitous tetrakis triphenylphosphine ($Pd(PPh_3)_4$) palladium-ligand system as well as the Fu-catalyst ($Pd(t\text{-}Bu_3P)_2$)[142]. These preformed palladium complexes suffer from the presence of defined ligands and thus are not universally applicable. In addition, handling of electron-rich $(t\text{-}Bu)_3P$

can be especially troublesome. The [(*t*-Bu)$_3$PH]BF$_4$ acid-phosphine adduct is typically used instead.[143] The sterically bulky Fu-catalyst was historically used for applications such as the solvent-tuned orthogonal transformation of aryl chlorides and triflates.[144] Additional common Pd^0-sources include Pd(dba)$_2$ and Pd$_2$(dba)$_3$. Reactions involving these catalysts can suffer from the presence of liberated dibenzylideneacetone (dba) as a competing ligand. Pd$_2$(dba)$_3$ has also been shown to consist of up to 40% palladium nanoparticles[145] according to DOSY-NMR[146] analysis. The aforementioned Pd^{II}-catalysts are useful in Pd^0/Pd^{II}-catalyst systems as well as Pd^{II}/Pd^{IV} catalysis.[147] The most common Pd^{II} precursor is Pd(OAc)$_2$. Even though universally applicable under many reaction conditions, reaction rates and conversion heavily depend on the purity of the Pd(OAc)$_2$ attributed to nitrite-impurities (Pd$_3$(OAc)$_{6-n}$(NO2)$_n$) and polymeric palladium lattices.[148] The mode of Pd(OAc)$_2$ reduction to Pd^0 has also been under scrutiny. Using ^{31}P-NMR studies it was deduced that phosphine oxidation is pivotal for the reduction.[149] Additionally, coupling reagents may act as the reductant depending on the reaction conditions.[150] To overcome these issues of palladium activation, modern catalysts are designed to include a ligand that serves the sole function of reducing the Pd^{II} in-situ. This group of pre-catalysts includes the (η^3-allyl)Pd(L)(Cl) type complexes[151] as well as the Pd GX pre-catalysts developed by the *Buchwald*-group.[152] One of the latest generations of the latter (G4) was developed in 2014[153] and has since found widespread application in literature.[154]

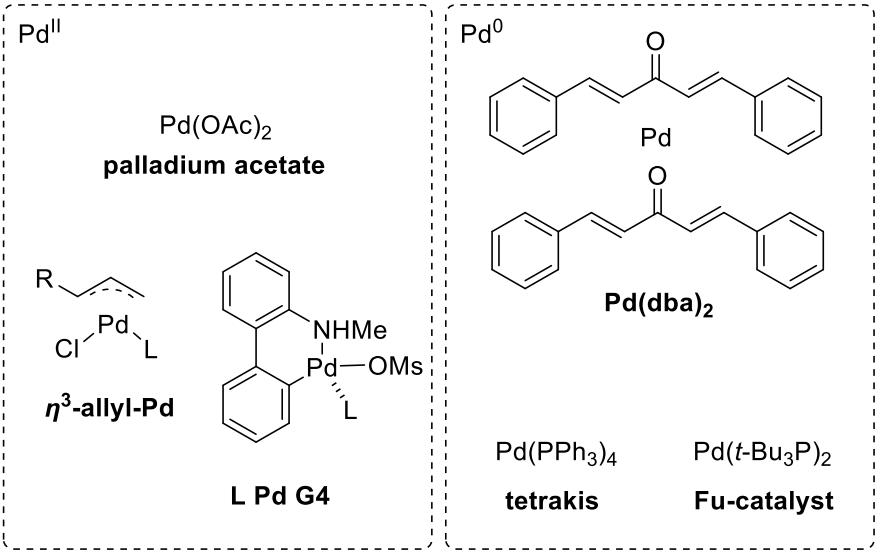

Figure 4: palladium precatalysts commonly found in synthesis.

In addition to ensuring proper Pd-activation, all other parameters need to be chosen to fit the reaction and cannot be generalized. The choice of supporting ligand is extensively discussed in literature.[128, 154-155] Stereoelectronic effects have to be taken into consideration and a proper

screening must be conducted to identify the right choice of ligand. Even the choice of halide starting material can have a detrimental effect on the reactivity of a system.[156] Kinetic investigations of elementary steps in Pd-catalyzed reaction mechanisms are crucial in understanding the relevant factors during optimizations.[157]

4.5.2 C–H-activation

C–H activation is a common reaction type encountered in palladium catalysis.[158] Especially the *Catellani* group[141a, 159] and *Lautens* group[156, 160] among many others have investigated such reactions and elucidated their modes of action.[161] Modern transition metal catalyzed reactions are slowly but surely encroaching on biomimetic levels of transformative power.[162] Highly chemoselective palladium-catalyzed distal aliphatic C–H activations of alkyl side chains **71** highlight the usefulness of such transformations to synthesize otherwise unobtainable products **73** (Scheme 17).[163] The applications of C–H activations are manifold and often proceed *via* palladacyclic intermediates **72**. Many such reactions also contain a Pd^{IV}-intermediate.[147]

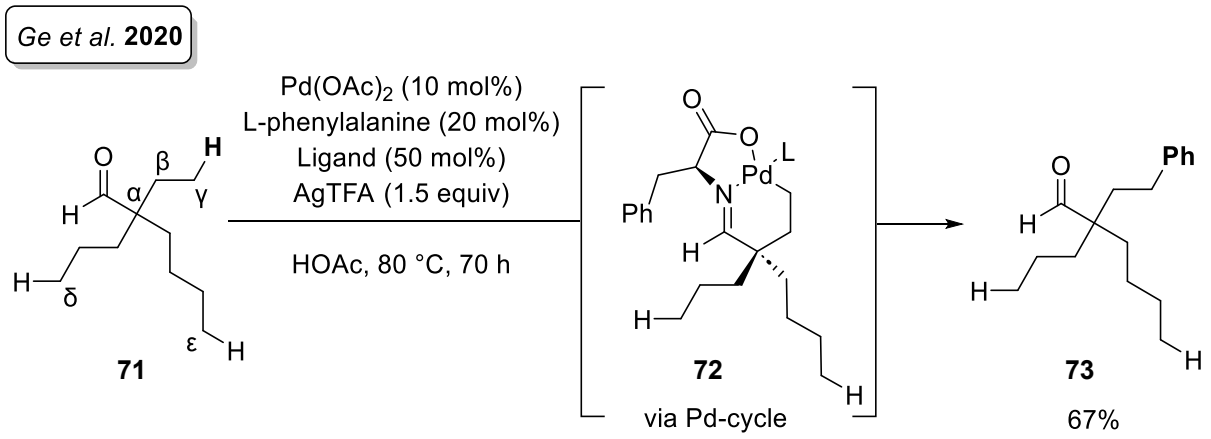

Scheme 17: Pd-catalyzed selective γ-functionalization. In accordance with *Ge at al.*[163a]

Carboxylates and carbonates have been shown to play a crucial role in the C–H activation step.[164] In particular, the *Fagnou* group has elucidated many aspects like the mechanistic proceeding *via* a concerted metalation-deprotonation (CMD) mechanism,[165] which was substantiated by DFT calculations.[166] Carboxylates were shown to be crucial in this inner sphere mechanism. It could experimentally be shown that the addition of substoichiometric amounts of pivalic acid (*t*-$BuCO_2H$) in combination with a carbonate base accelerates the C–H activation in the coupling reaction of arenes **74** with aryl halides **75** to form biaryls **76** (Figure 16A).[167] In their protocol *Lafrance et al.* successfully employed the MOP-type ligand DavePhos (**77**),[167] which was later shown to be inconsequential for this reaction.[168] Solvents may serve as ligands in these types of transformations.[169] DFT calculations of the carboxylate coordination complex supported a lower transition barrier between ground state **GS-1** and transition state **TS-1** compared to carbonate coordination (Figure 16B).[167] Comprehensive reviews exist on the topics of carboxylate assisted C–H activation in palladium complexes[170] or general transition metals[171] using DFT calculations. In addition to the aforementioned

importance of carboxylate mediated C–H activation, it is important to mention the so called ‘cesium-effect’, meaning the observed effect of cesium cations being a privileged counterion in these reactions.[172] The right choice of base in these transformations is thus imperative.[173]

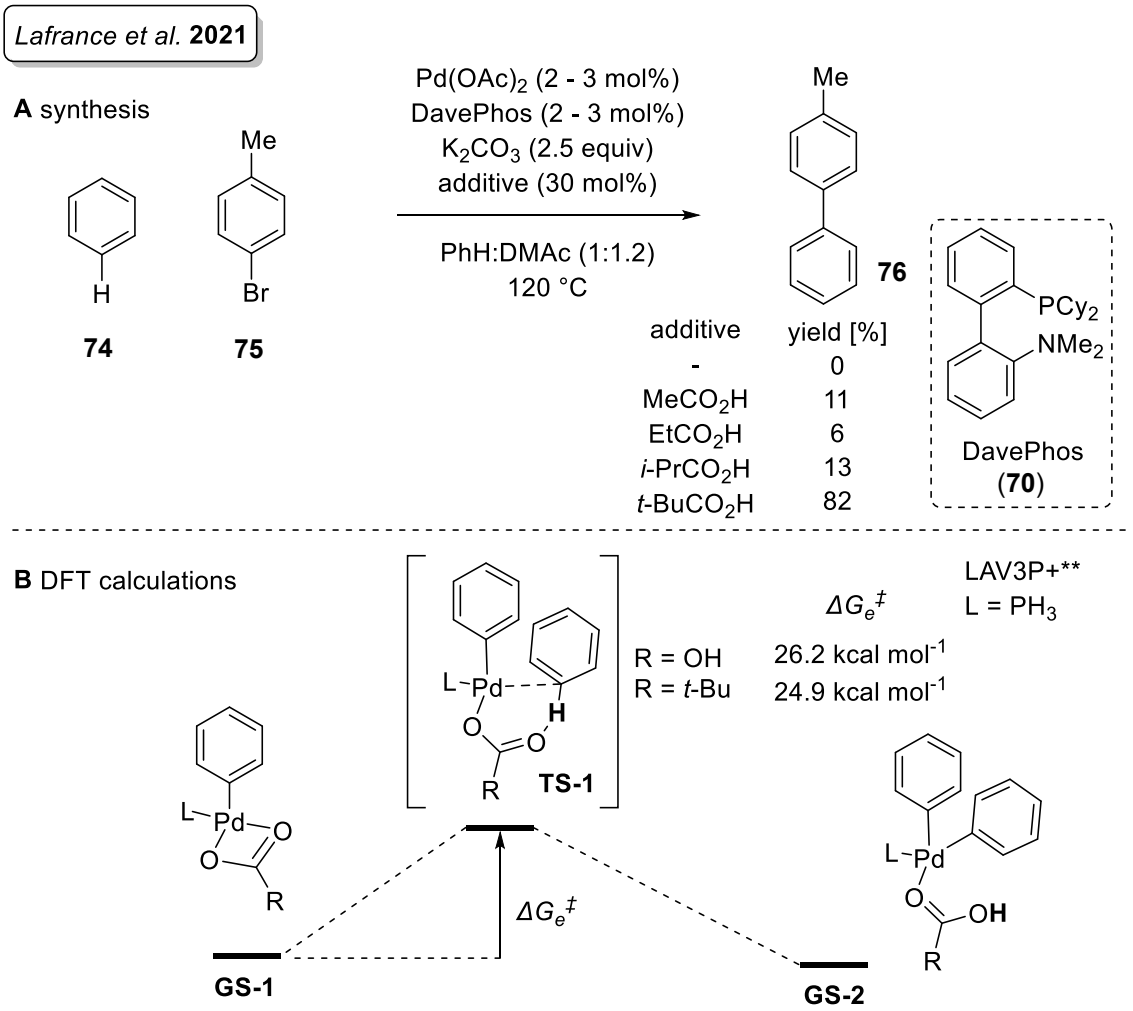

Scheme 18: (A) Carboxylate mediated C–H activation to form biaryls. (B) DFT calculations to rationalize observed effect. In accordance with *Lefrance et al.*[167]

4.5.3 Biaryl Palladacycle

As mentioned in the previous section, palladacycles (Pd-cycles) are crucial in many palladium-catalyzed reactions. Using achiral or racemic biaryls, these cyclic complexes have been leveraged in many transformations to form stereodynamic intermediates. These can then further be functionalized and transformed into useful biaryl products. In the following section, a concise summary of efforts in this field of research will be presented including Pd^{II}- and Pd^{IV}-based palladacycles.

The *Lassaletta* group has investigated various methods towards the generation of axially chiral heterobiaryls *via* DYKAT using palladium catalysis (Chapter 4.2, Scheme 3D).[68, 92c, 174] The enantioselective synthesis of heterobiarylic structures **78** was first reported in 2013 by *Mosquera et al* using aryl iodide **79** and tri-organoindium reagent **80** in combination with chiral ligand **81** (Scheme 19A).[175] Stereoselectivity of this coupling strategy was low (20%*ee*). In the same year, *Ros et al.* reported the synthesis of enantioenriched heterobiaryls **82** *via* stereodynamic palladacyclic intermediates using racemic triflates **83** (Scheme 19B).[174a] Phosphoramidite ligand **84** was employed and enantioselectivities of up to 93%*ee* achieved. In the same year *Bhat et al.* reported the use of DKR to also access QUINAP (**64**) *via* palladium catalysis, starting from the corresponding racemic triflate **85** (Scheme 19C).[176] Ferrocene-based (R,S_{Fc})-Josiphos (**86**) was used to achieve a stereoselectivity of up to 90%*ee* (>99%*ee* after recrystallization) using this strategy. It is worth noting that in their approach, a step is involved that is akin to the classification of a DYKAT.[68]

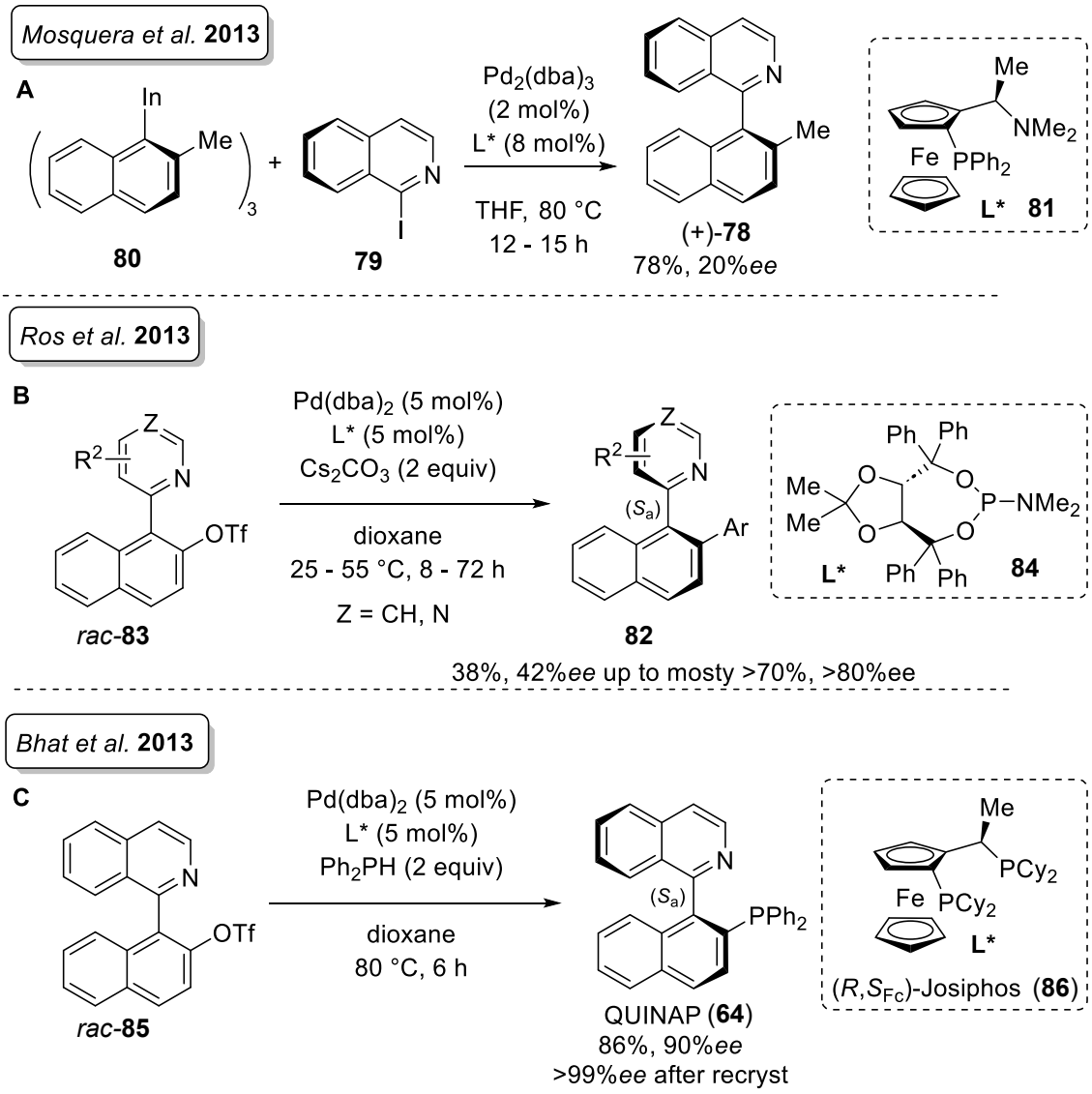

Scheme 19: (A) Investigations towards the enantioselective construction of heterobiaryls. In accordance with *Mosquera et al.*[175] (B) DYKAT of racemic heterobiaryls *via* Pd^{II}-cyclic intermediate. In accordance with *Ros et al.*[174a] (C) DYKAT/DKR of racemic heterobiaryl **85** to obtain QUINAP (). In accordance with *Bhat et al.*[176]

The scope of QUINAP-type structural motifs **87** accessible by this method using triflates **88** was expanded in 2016 (Scheme 20A).[174b] DFT calculations showed, that the starting material **85** is configurationally stable ($\Delta G^{\ddagger}_{e}$ = 29.3 kcal·mol^{-1}) and the oxidative addition product forms a palladacyclic intermediate **89** that interconverts readily at 40 °C on the time scale of seconds ($\Delta G^{\ddagger}_{e}$ = 18.7 kcal·mol^{-1}) (Scheme 20B). This supports the proposed DYKAT mechanism.

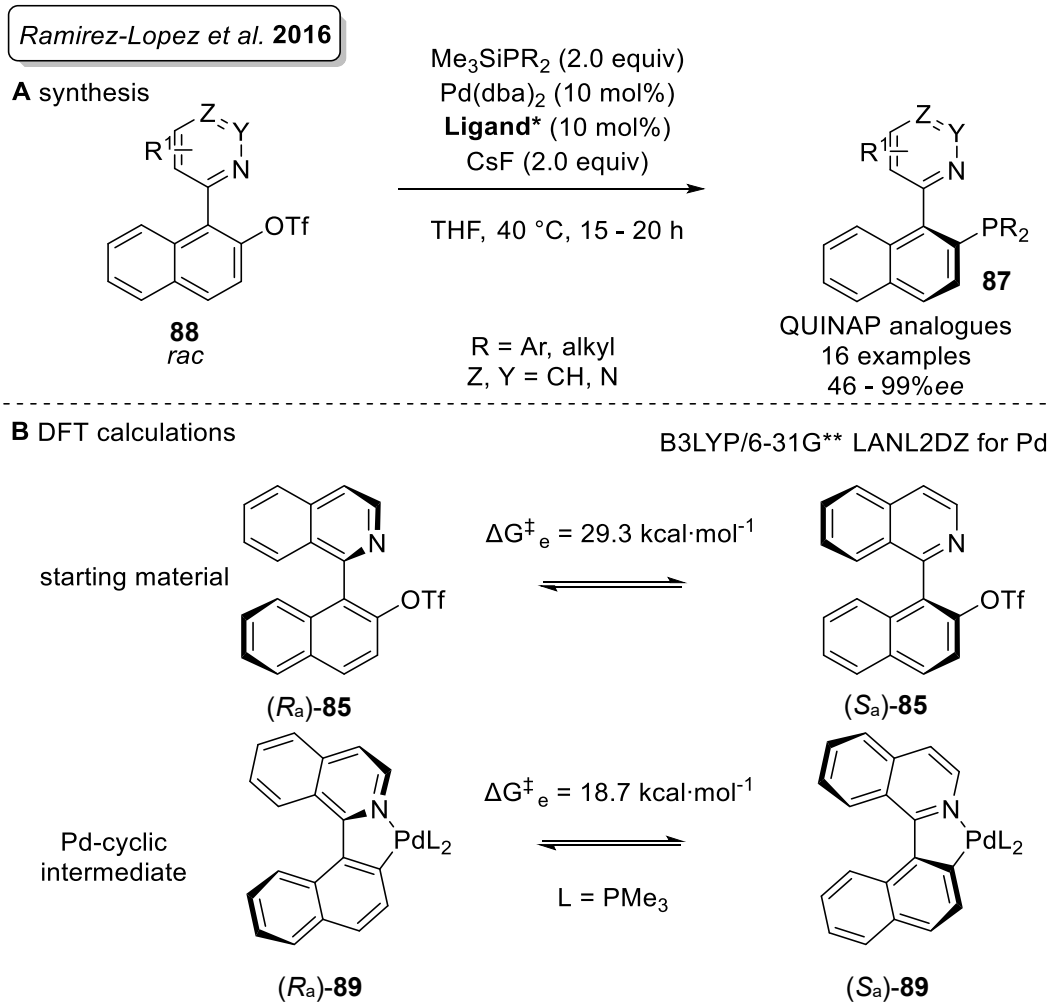

Scheme 20: (A) Synthesis of QUINAP analogues *via* DYKAT. (B) Mechanistic rational of stereodynamization through palladacycle formation. In accordance with *Ramirez-Lopez et al.*[174b]

In addition to these Pd^{II}-cycles with intramolecular nitrogen-coordination, Pd^{IV}-cycles have found applications in the synthesis of non-hetero-biaryls **90** (Scheme 21). In 2001 *Retbøll et al.* were the first to describe these 5-membered palladacycles **91**, supported by an obtained x-ray structure.[177] The selective functionalization of 2-halobiaryl **92** involving palladacyclic intermediates **91** is literature known and often involve proceeding *via* a C–H activation step. In particular, the *Zhang* group has investigated many such systems.[178]

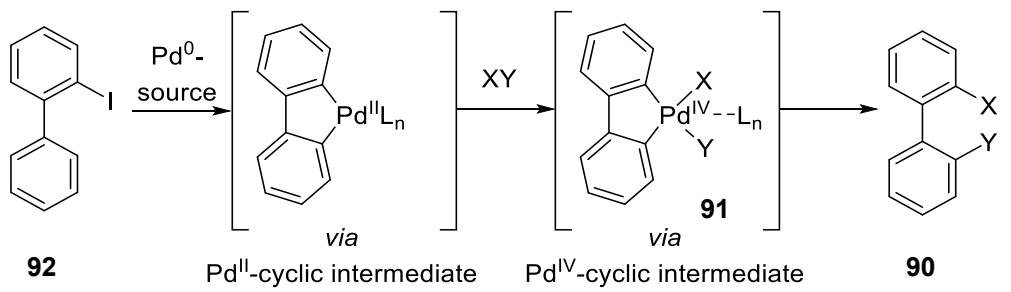

Scheme 21: Palladacyclic intermediates in the synthesis of *ortho*-functionalized biaryls.

Lu et al. described the palladium-catalyzed double silylation of 2-iodo biaryls **92** in polar solvents (Scheme 22A).[179] To probe the mechanism, an isolated palladacycle was subjected to the reaction conditions. The desired product **93** was obtained, supporting the proposed mechanism of the dibenzometallacyclopentadiene (metal 2,2′-biphenyl complex) **91**[180] intermediate being a plausible productive species in the catalytic cycle. In 2021 the diastereoselective amination *via* palladacycles using chiral amino acids **94** was reported by *Cheng et al*. (Scheme 22B).[181] The obtained tetraphenylene-analogous products **95** were obtained in a diastereopure fashion. This constitutes the first—and so far only—stereoselective synthesis involving such palladacycles. The inversion barrier of this saddle-shaped aza-analogue of tetraphenylene **96** was shown to be configurational stabile ($\Delta G^{\ddagger}_{e}$ = 31.5 kcal·mol^{-1}).[182] The scope has since been expanded by *Luo et al.* (Scheme 22C).[182]

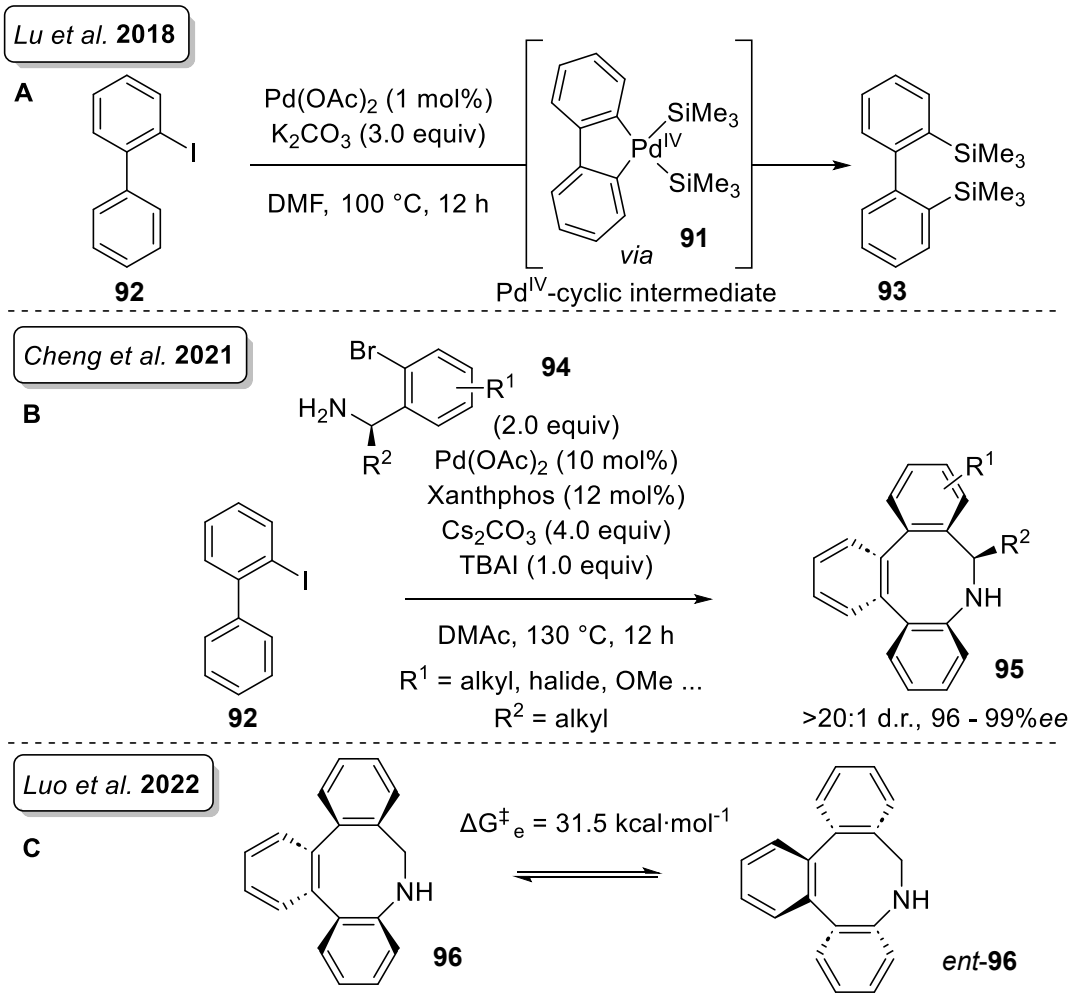

Scheme 22: (A) palladium catalyzed silylation of 2-iodo biaryls *via* C–H activation and formation of a palladacyclic intermediate. In accordance with *Lu et al.*[179] (B) Diastereoselective formation of saddle-shaped *N*-heterocycle analogous to tetraphenylene. In accordance with *Cheng et al.*[181] (C) DFT calculation for the inversion barrier saddle shaped 8-membered heterocycles. In accordance with *Luo et al.*[182]

Such palladacyclic intermediates have found applications in various further transformations including but not limited to formation of large ring systems,[183] or *Catellani*-type one pot reactions.[184] Formation of C–H activation products (fluorenes) **97** using biarylic starting materials **98** with vicinal sp^3-centers should be mentioned as a potential competing reaction pathway. Such protocols involving the formation of the relevant 6-membered-palladcycle **99** have been described in literature (Scheme 23B).[185] Moreover, scrambling of the Pd-nucleus relevant for non-C_2-symmetrical starting materials **100** and thus formation of regioisomeric Pd-complexes **101** and **102** are literature known (Scheme 23A).[186] Though the electron-rich nature of these double carbide-ligated Pd^{II} complex may be the reason for the second oxidative addition, C–H activation of Pd^{IV}-biaryl complexes *via* acetate ions was investigated in detail by *Maleckis et al.* and may present and alternative pathway.[187]

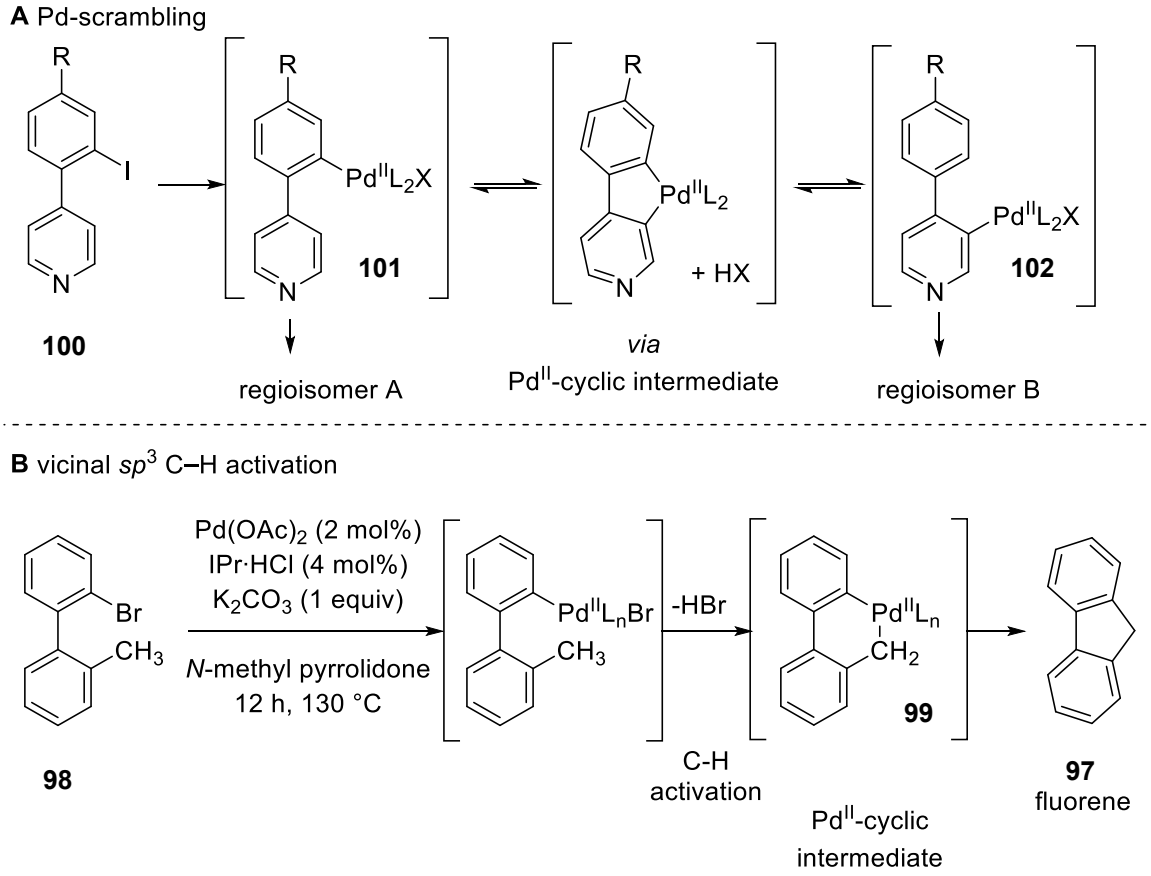

Scheme 23: (A) Formation of regioisomeric products *via* Pd^{II}-cycle in accordance with *Karig et al.*[186] (B) Formation of fluorene products *via* vicinal sp^3 C–H activation in accordance with *Hsiao et al*.[185]

4.5.4 The *Catellani* reaction

Domino reactions are defined by the stepwise formation of multiple bonds over multiple steps. The formation of a first functionality successively enables the formation of subsequent bonds, proceeding in this fashion until the final product is formed. This definition was coined in 1996 by *Lutz Tietze*.[188] Fewer steps, less waste, less labor and lower costs are the advantages of such an approach. One such method is the *Catellani* reaction developed in the 1990s[3], which utilizes norbornene (**69**), a strained bicycle, as a privileged transient directing group.[141a, 159a] The reaction is typically defined as an *ortho* C–H activation of aryl iodides **103** and—to a lesser extend—aryl bromides[189] and aryl triflates.[190] Functionalization of an intermediate palladacycle **104** with a second electrophile (EX) and finally termination with a nucleophile (NucY) generates the desired product **70** (Scheme 24). The mechanism of this reaction was discussed in a previous section (Chapter 4.5.1). Additionally, termination *via* C–H activation or further functionalization *via* a cascade instead of a nucleophile has also been reported.[160d] Since the first reports, a plethora of publications have focused on elucidating the mechanism of the reaction.[156, 159a, 160c, 191] In 2019 *Wang et al.* published a review covering all relevant nucleophile-electrophile combinations up until that point.[140b] It also gives a descriptive overview on the mechanism and possible pitfalls of this reaction. The *Catellani* reaction continues to be explored for the synthesis of ever-more complex molecules.[160d, 192]

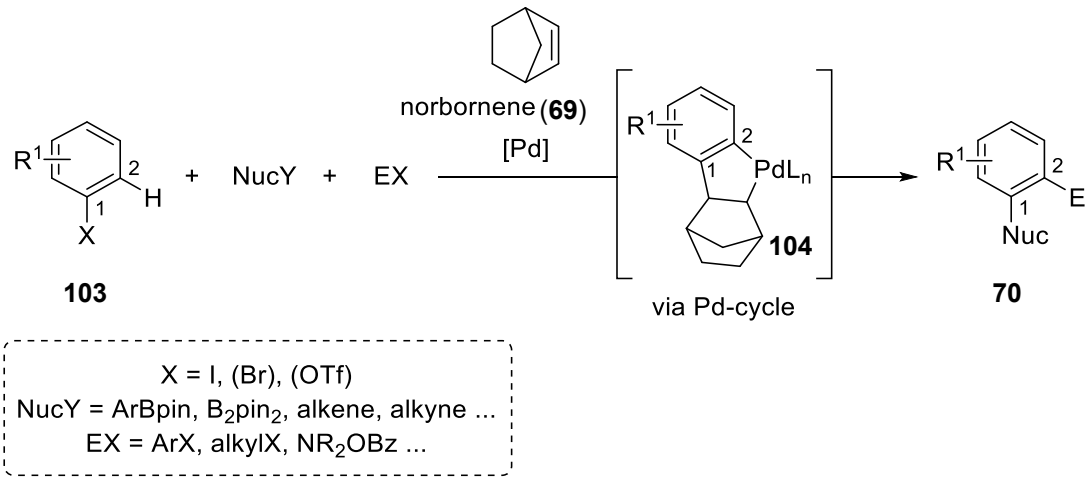

Scheme 24: General *Catellani*-type reaction using norbornene (**69**) as a directing group *via ortho*-C–H activation complex **104**.

[3] By the namesake, the *Catellani* group

The *Catellani* reaction is able to demonstrate that complex biaryls can be synthesized in a straightforward manner. Contemporary developments in the field of palladium catalysis, such as Pd-source and ligand design, have also successfully been applied to the *Catellani* reaction. *Buchwald*-type precatalysts (Pd G4)[193] and biaryl-monophosphine ligands[192, 194] have successfully been employed in various transformations. Even sterically bulky tri-*ortho*-substituted biarylic systems have successfully been synthesized, as was demonstrated by *Motti et al.* in the synthesis of terphenyls.[159b] Electron-rich aryl halides as well as electron-rich aryl boronic acid ester are also accepted in the construction of biaryls.[195]

Ortho-selective amination reactions using electrophilic *O*-benzoylhydroxylamines (BHA) **105** were first demonstrated by *Dong et al.* in 2013 (Scheme 25A).[196] The use of BHA **105** allowed for the synthesis of *meta*-aminated arenes **106**—electronically inverse compared to a classic *Buchwald-Hartwig* aminations.[137] An overview on the applications of these aminating reagents was published in 2017 by *Dong et al.*[197] Aryl iodides **103** were universally accepted while aryl bromides were accepted with the addition of Ag_2CO_3.[196] Using BHA **105**, the desired proto-depalladation product **106** could be observed even in the absence of a hydride source (29% even without any *i*-PrOH).[196] This was thought to occur due to elimination of benzoic acid from BHAs which is known to occur under basic conditions. Deuterium labelling studies by *Lautens et al.* demonstrated that the ipso hydrogenation can result from the *ortho*-abstracted hydrogen atom.[160a] Expanding this methodology of *ortho*-selective aminations, di-*ortho*-substituted 2-aminobiaryls **107**, relevant in the synthesis of iodonium salts (Chapter 4.2.1), were synthesized by *Ye et al.* in 2014, using boronic acid esters **108** as the terminating agent (Scheme 25B).[195] $BzONBn_2$ as a BHA ammonia surrogate was incompatible with the reaction conditions attributed to steric bulk.[195] The first use of a true ammonia surrogate BHA **109** was demonstrated by *Shi et al.* in 2015 (Scheme 25C).[194] Aryl iodide **110** was selectively transformed using B_2pin_2 as the terminating nucleophile. The authors were able to demonstrate, that HBpin was the cause for *ipso*-hydrogenation and not caused by BzOH present in the reaction mixture.[194] Deprotection of the amine protected coupling product **111** was performed to obtain amine **112**·HCl *via* double retro-aza-1,4-Michael-addition based on a protocol by *Renaud et al.,*[198] later improved upon by *Aschwanden et al.*[199]

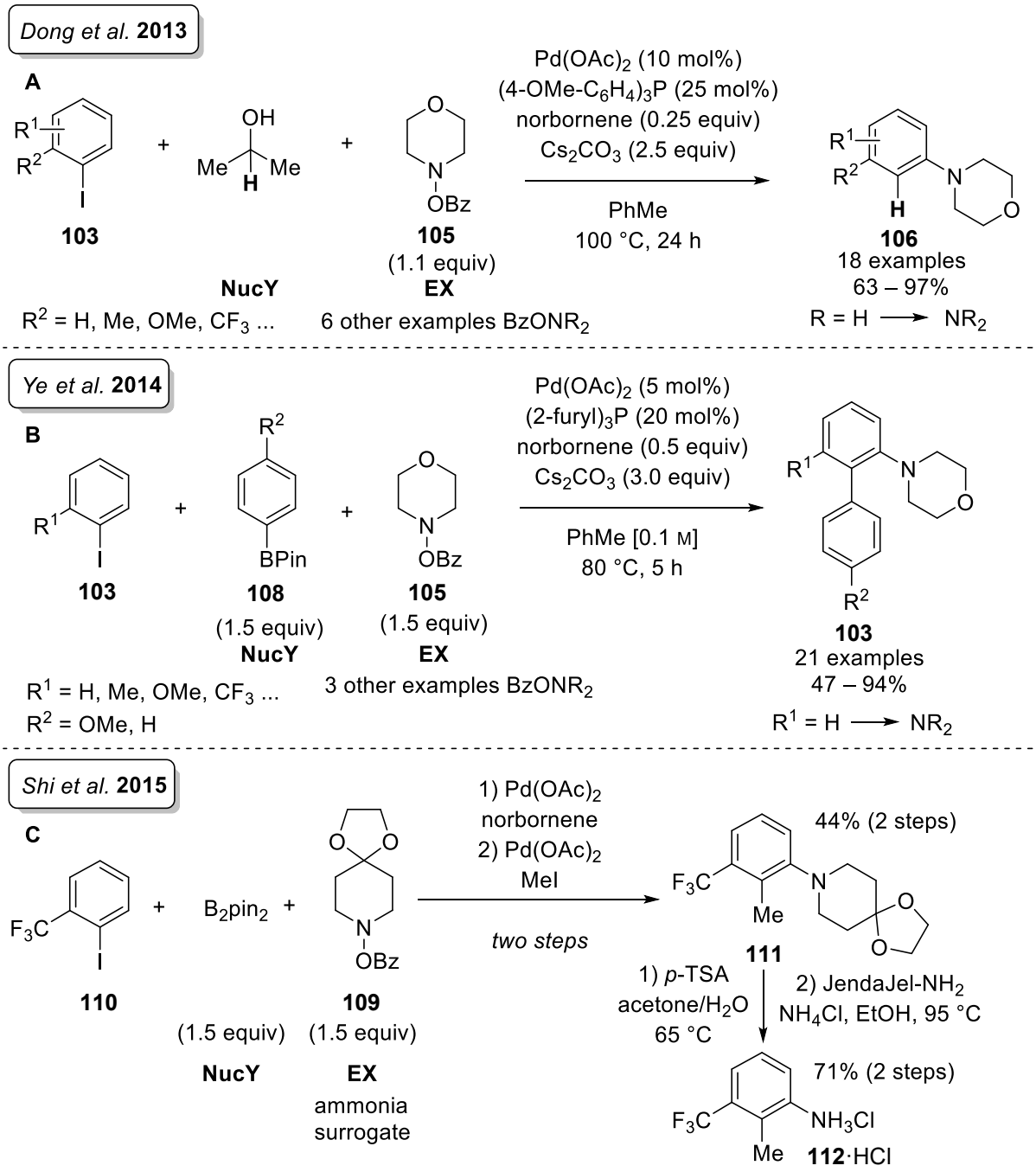

Scheme 25: *Ortho*-selective aminations using palladium-catalyzed *Catellani* reactions. (A) Synthesis of 1,3-subsituted-anilines **106**. In accordance with *Dong et al.*[196] (B) Synthesis of di-*ortho* 2-amino biaryls **103**. In accordance with *Ye et al.*[195] (C) Synthesis and deprotection of aniline **112**. In accordance with *Shi et al.*[194]

Enantioselective *Catellani* reactions for the construction of axially chiral biaryls have also been reported. *Ding et al.* demonstrated the use of axially chiral ligand **113** to obtain enantioenriched biaryl benzaldehydes **114**, starting from 2-naphthyliodides **115** (Scheme 26A).[200] The BINAM (**63**)-based chiral ligand contains both a stereogenic axis as well as a *P*-chiral stereogenic center (Scheme 26B). The second electrophile consisted of alkyl chloride **116** and the terminating nucleophile of aryl boronic acids **117**. Moreover, *Catellani*-type reactions have also been conducted using further bicycles other than norbornene and norbornadiene[201]. The

use of structurally modified norbornene analogues (smNBEs) are discussed in a 2020 review by *Li et al*.[202] Building on these developments, various strategies towards the synthesis of axially chiral biaryls using smNBE in a point-to-axial chirality transfer have been demonstrated in recent years. In 2020 Liu et al. were able to demonstrate the use of chiral norbornene mono-ester **118** in combination with various terminating nucleophiles starting from 2-naphthyliodide **119** with electrophile **120** to obtain products **121** in an enantiomeric excess of mostly >96%*ee* (Scheme 26C).[203] Based on this protocol further enantioselective *Catellani*-reactions have since been investigated using the same smNBE **118**,[204] as well as a scope of analogous smNBEs for the synthesis of axially chiral biaryl monophospine ligands.[205]

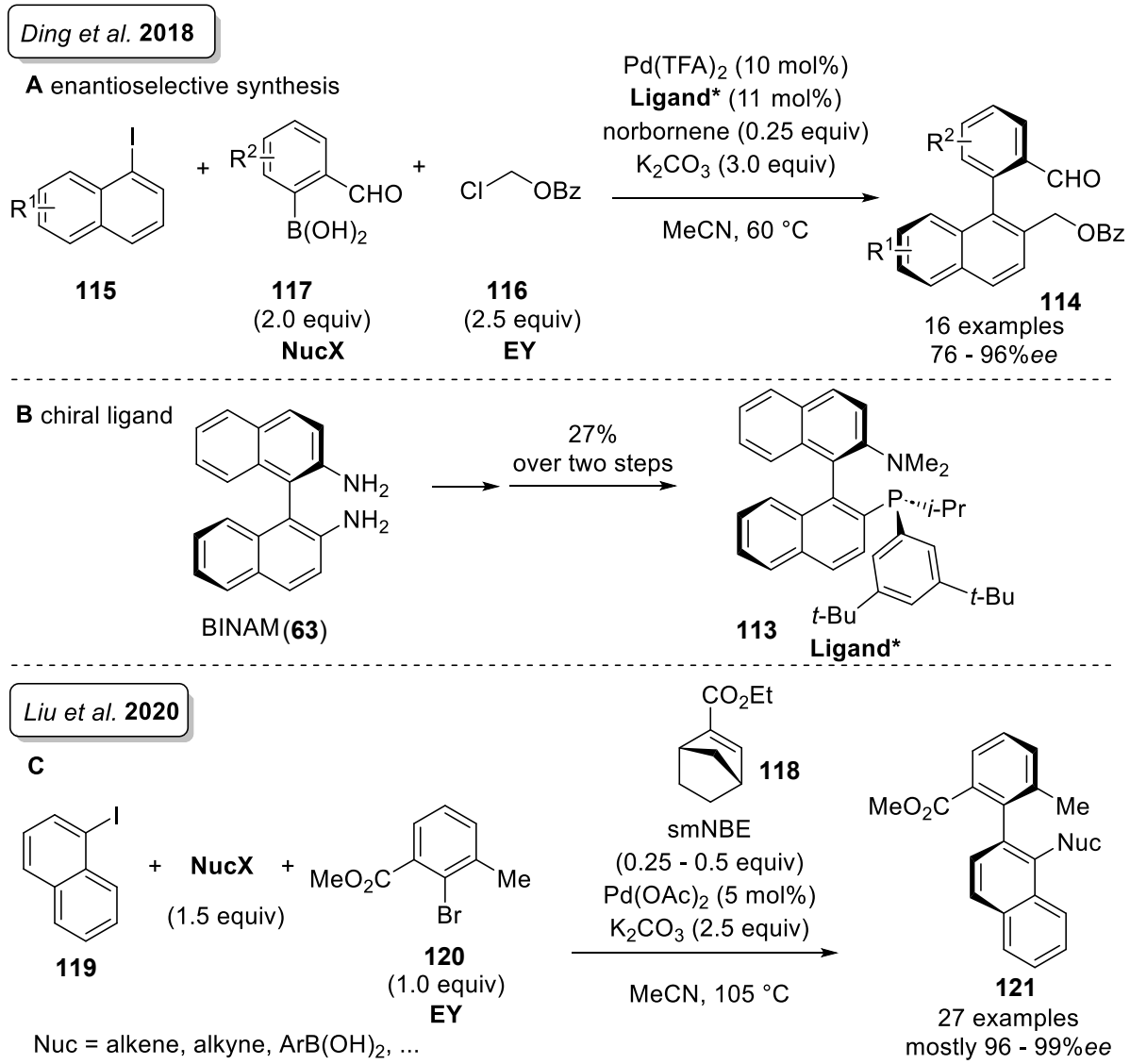

Scheme 26: (A) Stereoselective synthesis of axially chiral biaryls **114** using chiral ligand **113**. (B) Synthesis pf chiral ligand **113** employed, in accordance with *Ding et al*.[200] (C) Stereoselective synthesis of axially chiral biaryls using structurally modified norbornene **118**, in accordance with *Liu et al*.[203]

5 Results and Discussion

The contents of the following chapters explore various methods towards biaryls both racemic as well as enantioselective (Chapters 5.1.1, 5.2). Additionally, exciting new reactions were explored leveraging palladium catalysis (Chapters 5.3, 5.4, 5.5). The bioactivity of the relatively underexplored class of 8,8″-biflavones was investigated. To accomplish this, a robust method had to be established to easily diversify the desired library. Bichalcones and 8,8″-biflavones were synthesized racemically, making use of key intermediate biaryls (5.1.1). Next, a new method for the synthesis of enantiopure biphenols was established. This method utilizing cyclic diaryliodonium salts was benchmarked against established synthesis routes. To emphasize the usefulness of the biphenol building block both enantiomers of the most bioactive biflavone and bichalcone were synthesized (Chapter 5.2). Moreover, new methods towards otherwise inaccessible biaryls *via* palladium catalysis were investigated. The *Catellani* reaction was applied for the synthesis of sterically hindered 2-aminobiaryls (Chapter 5.3). Furthermore, the application of stereodynamic palladacycles as linchpins in the enantioselective synthesis of biaryls was investigated (Chapter 5.4). Finally, the use of oxabicycles as chiral acetylene analogues in multicomponent palladium-catalyzed reactions was examined. Stereochemical implications of intermediates identified in this reaction were explored. The mechanism of the reaction was elucidated, and data supported by DFT calculations (Chapter 5.5).

Chapter 5.1.1

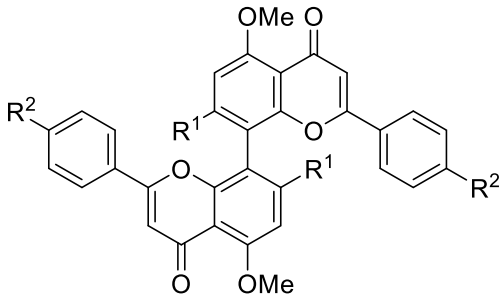

Racemic biflavonoids

Chapter 5.2

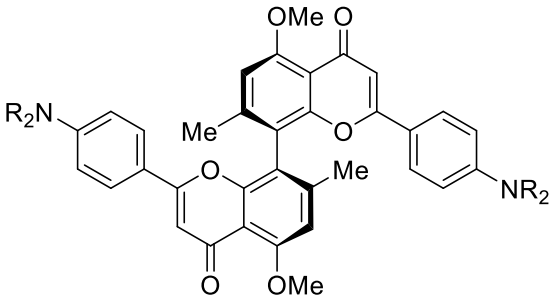

Synthesis of enantiopure biflavonoids

Chapter 5.3

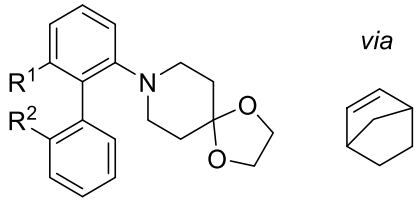

Synthesis of 2-aminobiaryls *via* the *Catellani* reaction

Chapter 5.4

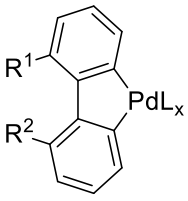

Investigation of palladacycles

Chapter 5.5

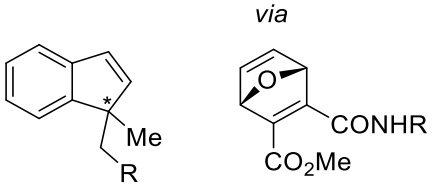

Oxabicycles as chiral acetylene

5.1.1 Racemic biflavones and bichalcones

The following chapter is a revised version of results published in Klischan et al. ACS Omega ***2023****,*[108b] *and contains results published in Greb et al. Chem. Eur. J.* ***2023****,*[102] *and generated by Daniel Grudzinski as part of a bachelor thesis.*[206]

In this chapter the scalable and modular synthesis of a library of 65 monomeric and racemic dimeric flavonoids including twenty-two 8,8″-biflavones is discussed. Generally, the biflavone library included common A-ring scaffolds. Permuting the B-ring would allow for easy diversification of the library. After careful consideration of alternative synthesis strategies (Chapter 5.1.2) the sterically demanding tetra-*ortho*-substituted axis was constructed racemically by regioselective iron-mediated oxidative coupling (Chapter 5.1.3). The robustness of this step was validated, and the usefulness of this transformation shown by the library of synthesized bioflavonoids. The biological activities of this compound library were evaluated by *Flaminia Mazzone* (Institute of Medical Microbiology and Hospital Hygiene, Heinrich Heine University Düsseldorf, *Pfeffer* group), *Lena Berning* (Institute of Molecular Medicine I, Heinrich Heine University Düsseldorf, *Stork* group), *Céline David* (Institute of Molecular Medicine I, Heinrich Heine University Düsseldorf, *Stork* group) and in collaboration with *Mona Haase* (Institute of Bioorganic Chemistry, Heinrich Heine University Düsseldorf, *Pietruszka* group) but will not be discussed in detail as part of this thesis.[4] Additionally, the bioactivity of the biflavones was compared to the corresponding monomeric flavones. Both, similar activities,[107f] as well as vastly different activities,[106] and often much higher activities of natural product dimers have been reported in literature.[23a, 24, 207] Such effect would thus be accounted for. Finally, based on a biflavone from this initial library with high bioactivity, a subset of amino 8,8″-biflavones was synthesized (Chapter 5.1.4).

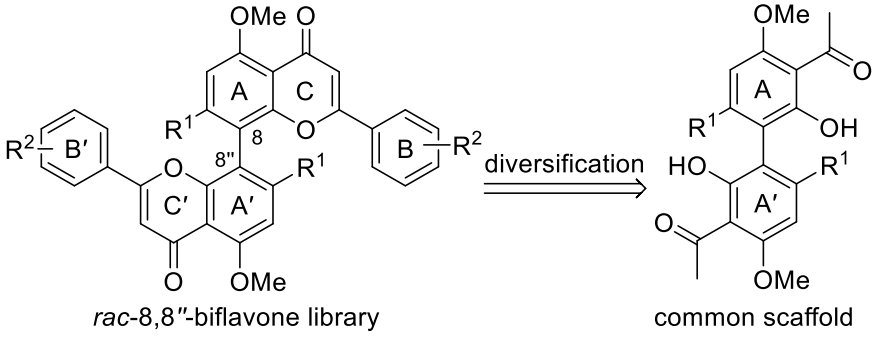

Scheme 27: Synthesis towards 8,8″-biflavones starting from a common scaffold starting material.

[4] Biological activities will be discussed in their respective theses in addition to the corresponding journal article.

5.1.2 Synthesis of *rac*-BIPOL

Parts of the following chapter were published in Greb et al. Chem. Eur. J. ***2023****.*[102]

The rational of synthesizing 8,8″-biflavones was to close the literature gap on non-natural analogues of this compound family (Chapter 4.3.2.1). A well-known overview by *Newman et al.* highlights the general trend of focused compound libraries in natural product inspired drug discovery.[17] With a diversity-oriented synthesis strategy, it should be possible to determine the potential of this compound class beyond literature known bioactivities of the naturally occurring cupressuflavone (**40**) (Chapter 4.3.2). The following synthesis route was conceptualized by *Julian Greb*.[102] Contributions and modifications of the established route are described herein.

The initial plan towards a library of racemic 8,8″-biflavones involved the use of biphenol **27** (BIPOL) as a key-building block *via* a synthetic route established by *Greb et al.* (Scheme 28).[102] Following literature known procedures, the sequence towards BIPOL (**27**) was conducted on decagram scale.[102] The application of this building block has been shown in the syntheses of di-*epi*-gonytolide A (**31**) by *Greb et al.*[102] and isokotanine A (**32**) by *Ganardi et al.*[103] The substitution pattern enabled by this route mirrors the non-natural and highly bioactive 8,8″-biflavone derivative identified by *Kikuchi et al.*[108a]

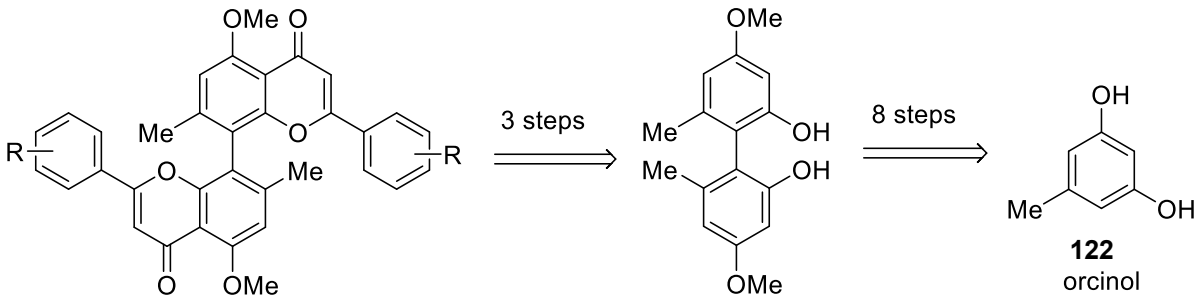

Scheme 28: Retrosynthetic considerations towards 8,8″-biflavones with biphenol **27** as a key-intermediate.

Commencement of the synthesis route proceeded smoothly and according to literature protocols.[102] Methyl protection of commercially available orcinol (**122**) was performed in a scale of 75 mmol (Scheme 29). Subsequent methyl mono-deprotection of arene **123** gave the desired product **124** in a selective and straightforward manner. Acetylation—crucial for the regioselectivity of the following bromination—also proceeded smoothly with an overall yield of 84% for arene **125** over three steps.

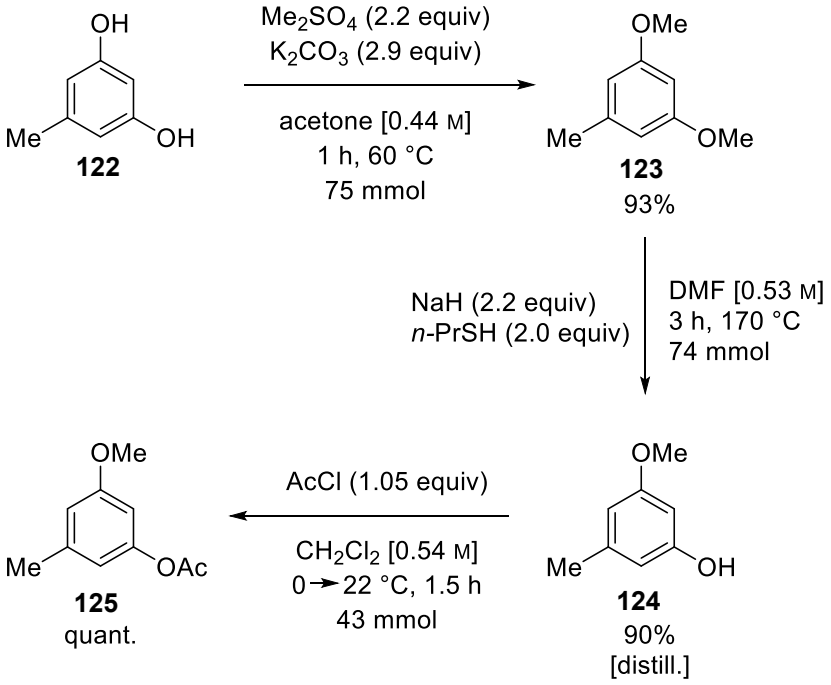

Scheme 29: Synthesis sequence towards acetylated arene **125**.

With ample acetylated arene **125** at hand, the bromination was investigated (Scheme 30). Following the previously established protocol by *Greb et al.* brominated product was obtained as a mixture of regioisomers (86:14, **126**:**127**).[102] Subsequent acetyl deprotection to obtain the phenol proceeded smoothly. Separation of the regioisomers at the present scales was possible by recrystallization yet tedious and low yielding. Therefore, alternative separation strategies were investigated. A comparison of literature values revealed that *ortho*-halogenated phenol **128** has a lower melting point (lit.: 73 °C) compared to the *para*-substituted regioisomer **129** (lit.: 122 °C).[208] To exploit this property, separation by Kugelrohr® distillation was attempted. Indeed, isolation of the desired regioisomer **128** was successful at 100 °C *in vacuo* in a yield of 73% with phenol **129** being obtained with minor impurities of **128** in a yield of 20% over two steps respectively. Thus, scalability of this step could be assured.

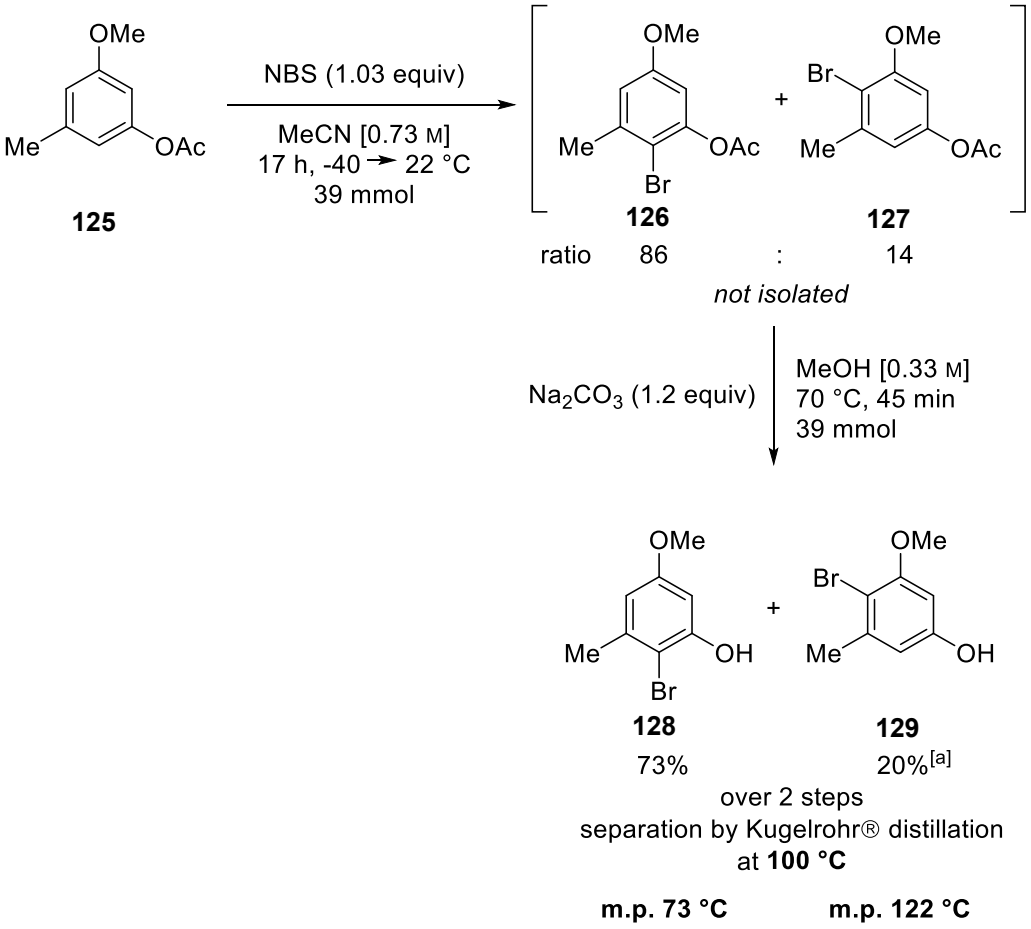

Scheme 30: Selective bromination of arene **125** resulting in a mixture of regioisomers able to be separated by Kugelrohr® distillation. [a] Obtained as a 94:6 mixture of **129**:**128**.

With isolation and scalable synthesis of the brominated phenols at hand, MOM protection of **128** (99% yield) and oxidative coupling of the resulting product **29** following conditions by *Greb et al.* was conducted (Scheme 31).[102] The product $(MOM)_2$-BIPOL (**28**) was obtained in a yield of 86% in accordance with literature (83%[102]). The use of stochiometric amounts of readily oxidizable tetra-*tert*-butyl diquinone (DBQ) (**30**)—a quinoid type oxidant—prompted the investigation into its reusability. Fortunately, by exploiting the low solubility of DBQ (**30**) in methanol, removal of bulk amounts was enabled by simple filtration. Recycling the thus obtained oxidant was facile. Oxidation of the reduced form DBQ-H_2 proceeded quantitatively over night by leaving the filter cake at ambient conditions.[5] Thus, not only could the workup be improved by easy removal of the strongly staining DBQ (**30**) but scalability by recycling of the same oxidant was enabled. With ample starting material at hand, the deprotection of $(MOM)_2$-BIPOL (**28**), progressed without issue to obtain BIPOL (**27**) in a yield of 52% over the entire sequence of eight steps.

[5] The oxidant was suspected to be the O_2 in the air.

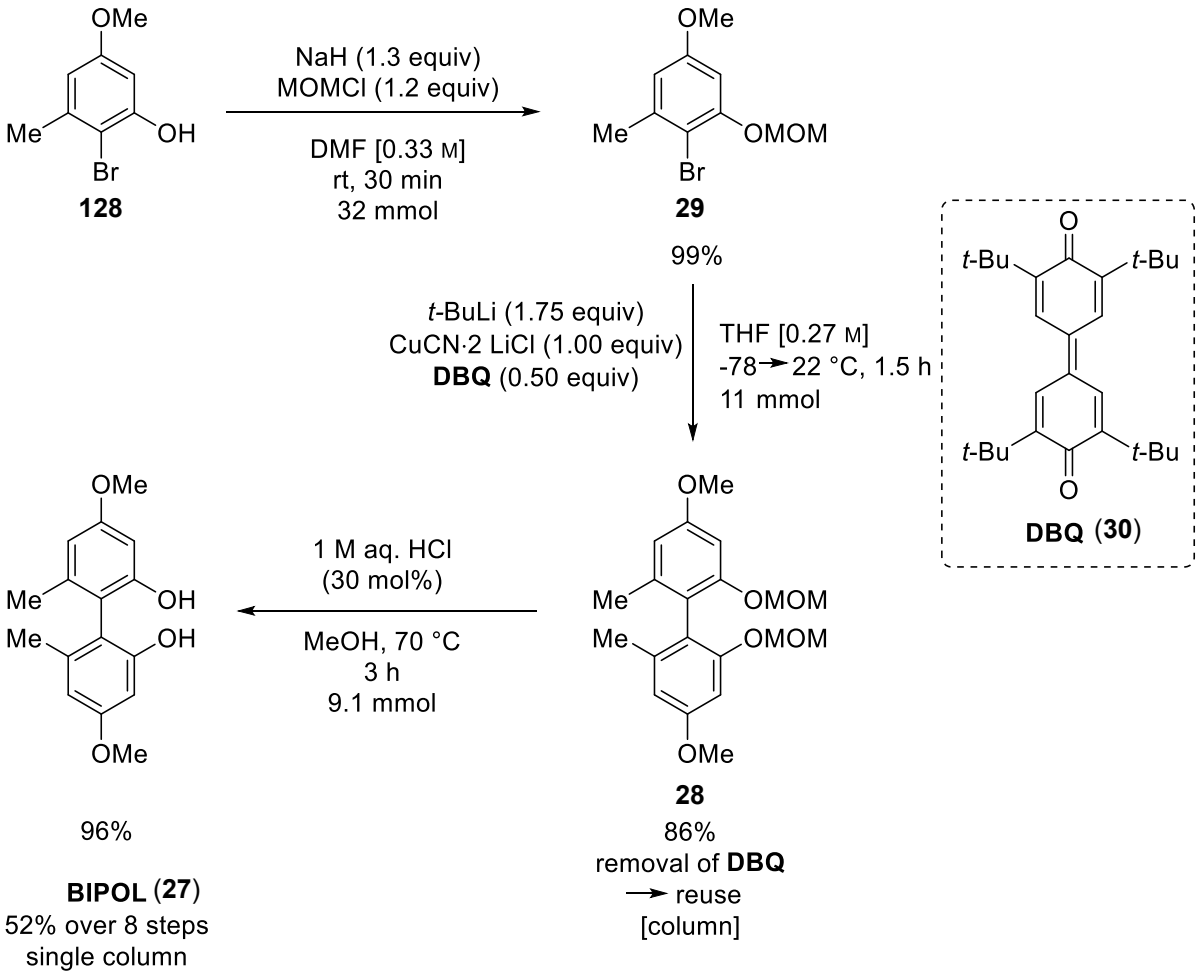

Scheme 31: Synthesis of BIPOL (**27**) by oxidative coupling developed by *Lipshutz et al.*[101] and improved by *Greb et al.*[102]

Overall, the synthesis route towards *rac*-BIPOL (**27**) *via* this large scale and high yielding process could successfully be improved. Separation of the brominated regioisomers **128** and **129** was enabled by Kugelrohr® distillation. Additionally, recycling of DBQ (**30**) was successful, improving the scalability of this approach. The brominated arene regioisomers **128** and the MOM protected **29** were used as common starting materials in subsequent chapters (Chapter 5.2.1).

5.1.3 Biflavonoid library

The following chapter is a revised version of Klischan et al. ACS Omega ***2023****.*[108b]

Even though the approach described in the previous section (Chapter 5.1.2) is valuable for the synthesis of polyketide-based natural products and biflavone analogues (Chapter 4.3), an alternative method towards the synthesis of biflavones was investigated. To account for the substitution pattern found in naturally occurring cupressuflavone (CUF) (**40**) (Chapter 4.3.2), a strategy towards both flavones with methyl- and methoxy-groups at C7 and C7′ was required. Literature known selective iron-mediated oxidative couplings of electron-deficient phenols were considered.[69, 108a] This strategy would allow access to biacetophenone key-intermediates in three steps without requiring column chromatographic purification to access the racemic biflavones (compared to eight steps as described in Chapter 5.1.2 with column chromatographic isolation). Following this strategy, biflavones would be obtained as racemic mixtures. This relied on the hypothesis, that the eutomer (meaning bioactive enantiomer)[209] would be active while the distomer (complementary enantiomer) would be inactive rather than antagonistic towards the same bioactivity.[210] It is acknowledged that pharmacokinetics and -dynamics also depend on whether a racemic mixture or enantiopure compounds are used.[211] Thus, a more general insight into feasibility of the synthesis method and potential of this compound class would be asserted using the racemic mixtures. The cost-benefit of establishing an enantiopure synthesis method would therefore rely on the bioactivities of the racemic library. Potential drug candidates for *in vivo* trials[212] would subsequently be synthesized in an enantiopure fashion based on the obtained best hits (Chapter 5.2).

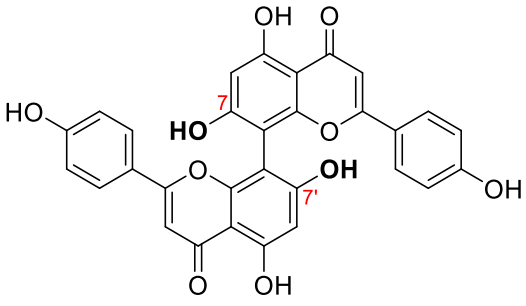

Cupressuflavone (40)

Scheme 32: Cupressuflavone (CUF) (**40**), the naturally occurring 8,8″-biflavone.

The starting point of this iron-mediated synthesis strategy was a protocol developed by *Li et al.*[69] Scalability was of great concern for the viability of this approach.[213] Commercially available phenols **122** and **130** were transformed *via* acetophenones **131** and **132** to methyl protected acetophenones **133** and **47** by literature known methods (Scheme 33).[69, 214] These served as common starting materials to access all monomeric as well as dimeric flavonoids.

The synthesis of biacetophenones **134** and **49** would be conducted by oxidative coupling. With these valuable building blocks (three steps, gram-scale without column chromatographic isolation) in hand, *Claisen-Schmidt* condensation using aldehydes to obtain chalcones **135 – 148** and bichalcones **165 – 178** was conducted. These served as useful intermediates as they could be investigated as simplified analogues compared to the corresponding flavones and biflavones, effectively doubling the pool of potentially bioactive compounds. Flavones **150 – 163** and biflavones **179 – 192** would then be accessed by subsequent oxidative cyclization. The permutation of the B-ring (R^2) was chosen to reflect a variety of electronic and steric effects. Among these, various CUF methyl ethers were synthesized.

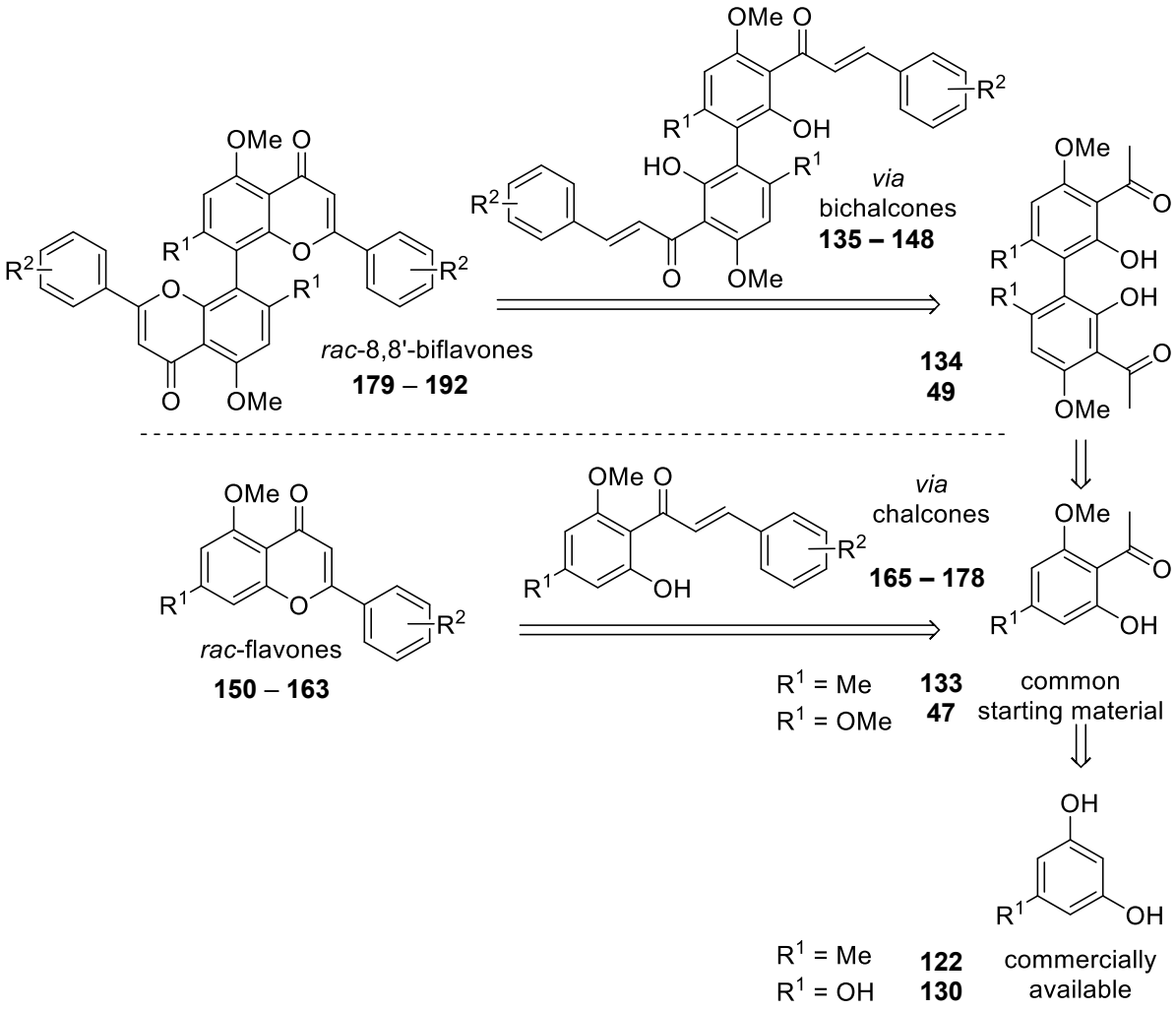

Scheme 33: Retrosynthesis of flavones and biflavones starting from commercially available phenols **122** and **130**.

5.1.3.1 Flavones

First, a robust synthesis of the acetophenone key-intermediates **133** and **47** was required. Literature known protocols for a Friedel-Crafts acetylation followed by a methyl protection proceeded smoothly.[215] The desired products were synthesized over two steps on deca-gram-scale in yields of 74% (**133**) and 70% (**47**) respectively (Scheme 34).

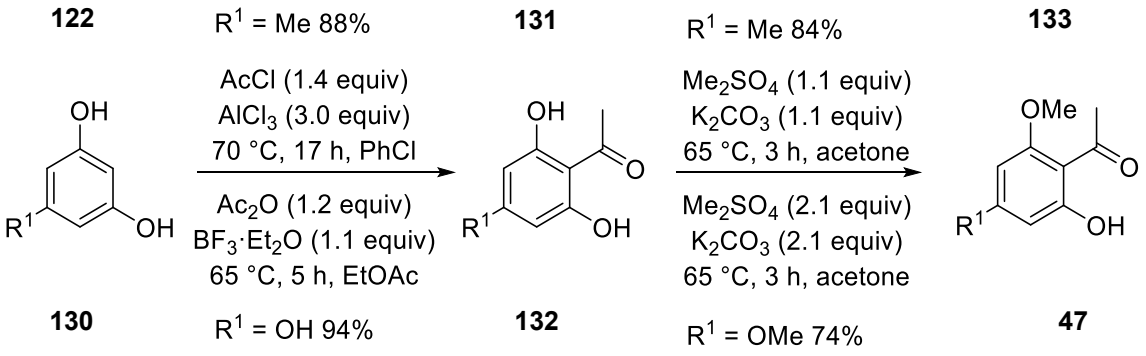

Scheme 34: Synthesis sequence towards methyl protected acetophenones **133** and **47**.

Starting from these acetophenones, the monomeric chalcones and flavones were synthesized next. Before settling on a two-step process, a literature known one-pot strategy towards the desired flavone scaffold was investigated (Scheme 35).[216] Using commercially available acetophenone **193** an aldol condensation with benzaldehyde followed by an oxidative cyclization with catalytical amounts of iodine was conducted. Flavone **194** was isolated in low yields (8%). Due to this unselective product formation, this approach was thus not further investigated.

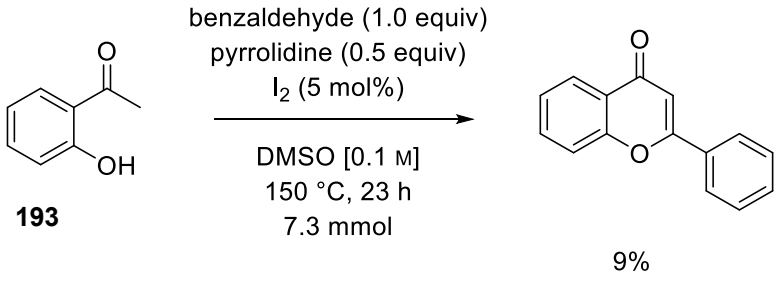

Scheme 35: Synthesis of flavone **194** starting from acetophenone **193**.

Even though one more step was required to synthesize biflavones via bichalcones, the latter could serve as potentially bioactive natural product intermediates. Acetophenones **133** and **47** were transformed to the corresponding chalcones monomers **135 – 148** by *Claisen-Schmidt* condensation (Scheme 36). For some reactions, incomplete conversions were observed. These were addressed by addition of further 0.6 equivalents of the corresponding aldehyde after 6 h which then gave full conversion overnight. In addition to these arene-based chalcones, the synthesis of heteroarene (2-pyridyl) chalcone **149** was conducted. Unfortunately, conversion to

product was very low (36%) with suspected flavanone being the main observed side product. This issue would only amplify with the synthesis of the corresponding bichalcones due to twice the amount of potential cyclizations. Generally speaking, the monomeric chalcones obtained exhibited low solubility in common organic solvents, thus purification by column chromatography was avoided. Recrystallization from methanol removed most flavanone and aldehyde impurities.

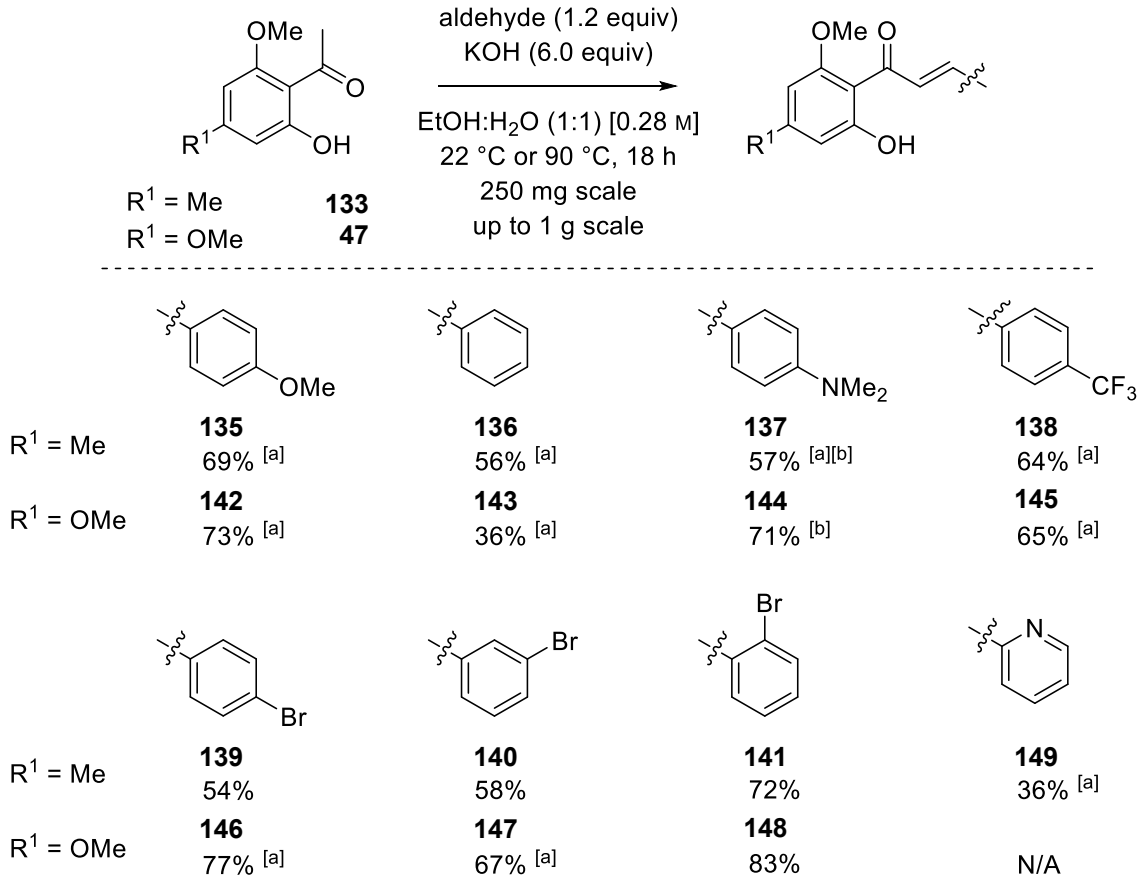

Scheme 36: Synthesis of chalcones starting from acetophenones **133** and **47**. Isolated yields. [a] 1.8 equiv aldehyde instead. [b] 90 °C.

To probe the observed formation of flavanones, acetophenone **131** was subjected to comparable reaction conditions to form chalcone **195** (Scheme 37A). The main product observed by ^{1}H-NMR was suspected to be flavanone **196** indicated by characteristic geminal peak sets (Scheme 37B). This implied, that the ring closure of the *Michael*-system and thus formation of flavanone vs chalcone occurred preferentially with a vicinal phenol hydroxy group. In case of methyl protected chalcones, the hydroxy group is trapped by the vicinal carbonyl leaving the *Michael*-system with a methoxy group unable to cyclize (compare Chapter 5.2.3.2).

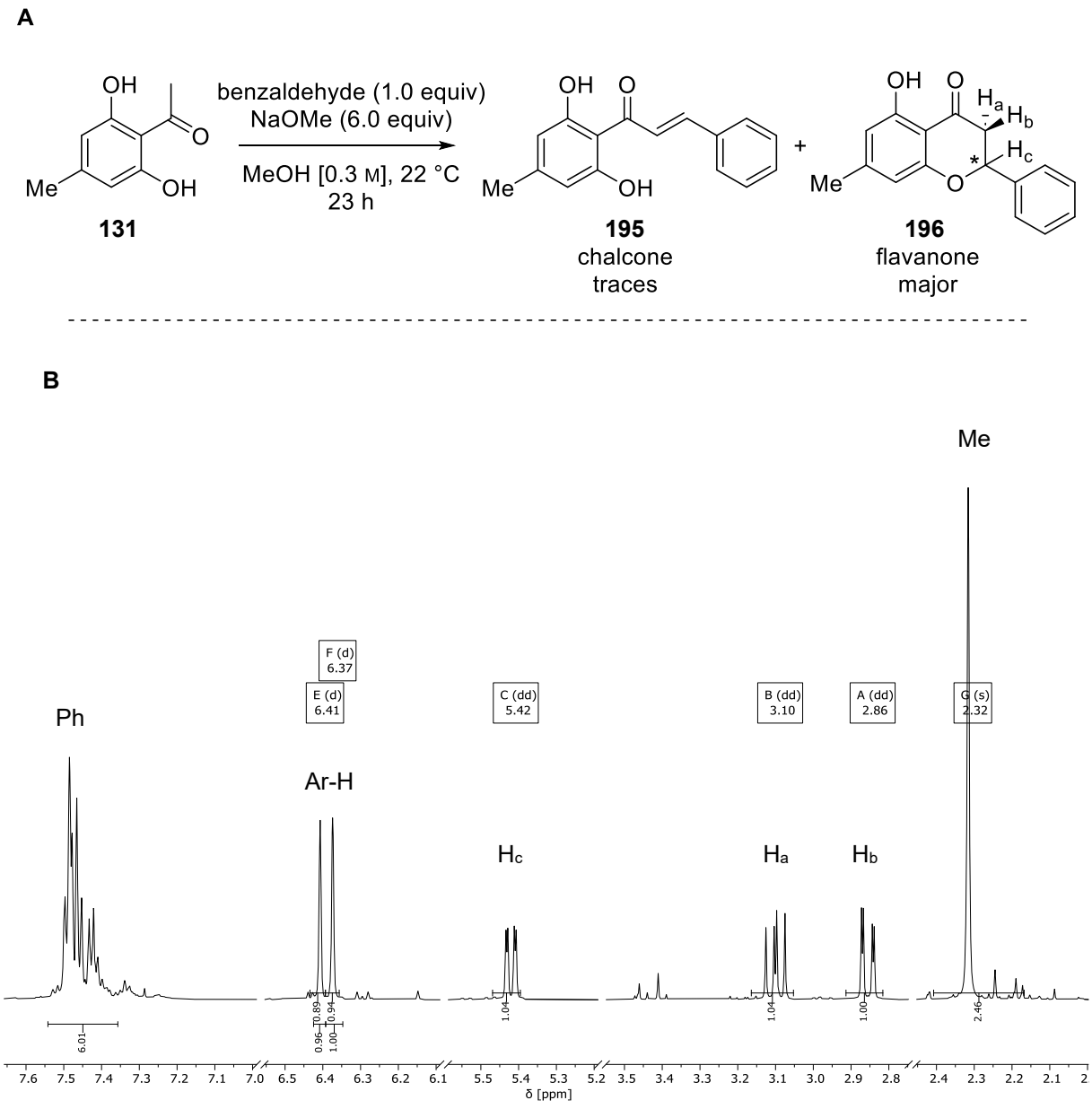

Scheme 37: (A) Chalcone synthesis using acetophenone **131** with the formation of major amounts of flavanone side product. (B) ^{1}H-NMR signals observed, corresponding to flavanone.

With a protocol for the synthesis of chalcones **135 – 148** established, the oxidative cyclization towards flavones **150 – 163** following literature known procedures was investigated next.[217] This method involved the use of catalytic amounts of I_2 in DMSO with the latter serving a dual role as both solvent and oxidant for the regeneration of I_2.[218] All desired flavones except for one could be obtained in yields of 36 – 93%. In case of the cyclization of 2-pyridyl chalcone **149** to flavone **164** mostly signals akin to flavanone side product **197** were observed (Scheme 37B). Thus, for the subsequent biflavone library, heteroarene substituents were not included. Overall, the desired flavones could be isolated in four steps from commercially available bulk starting materials requiring only one final column chromatographic purification over this sequence.

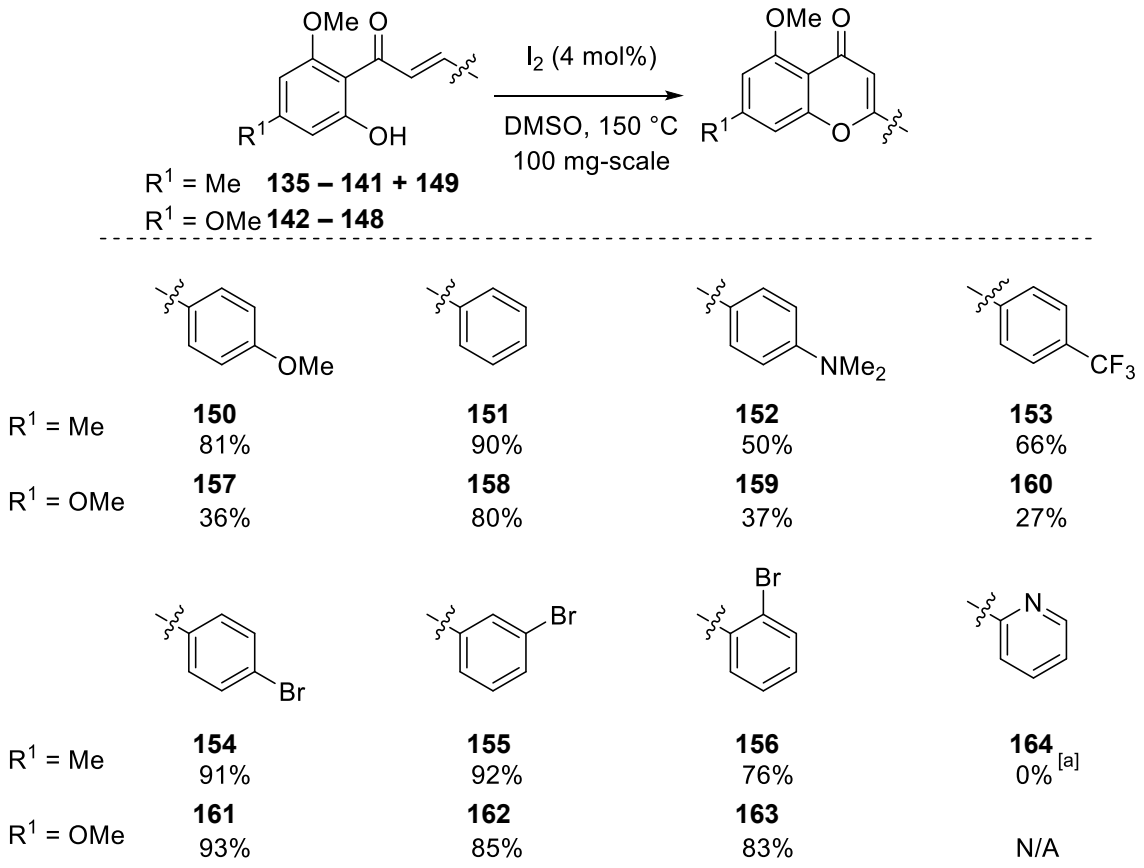

Scheme 38: Oxidative cyclization of chalcones to flavanones. [a] Only flavanone side product observed according to ^{1}H-NMR.

5.1.3.2 Biflavones

To obtain the analogous bichalcones and by extension biflavones, the next task was the synthesis of biacetophenones **134** and **49**. After extensive screening conducted by *Julian Greb* regarding a variety of recent catalytic methods for the synthesis of **134**[108b] the oxidative coupling using stochiometric amounts of $FeCl_3$ proved the most promising for this transformation. The method was originally established by *Li et al.* using silica bound $FeCl_3$ *via* solid phase synthesis.[69] This method has since been applied to the synthesis of a variety of natural products.[49a, 49b, 65c, 108a] It is important to mention, that trace amounts of paramagnetic Fe^{III} impeded evaluation of crude reaction products. Thus, a washing step using Na_2EDTA, able to coordinate trivalent cations, was required.[219] Initial results using this strategy showed low selectivities. Using acetophenone **133** as the starting material, product **134** formation was miniscule (Table 1, entry 1). Instead, a major side product was observed that was identified as chlorinated acetophenone **198**. This highly regioselective chlorination was in line with a side product observed by *Li et al*.[69] To increase conversion to product, the conditions of the $FeCl_3/SiO_2$ preparation were investigated. Generally, $FeCl_3$ was first dissolved in the mentioned solvent or solvent mixture, then a defined amount of silica was added, the mixture sonicated for 15 minutes and solvents then removed under vacuum at elevated temperatures using a rotational evaporator until a dry powder remained (1 mbar). The initial preparation conditions used Et_2O as the solvent at 40 °C. The use of a solvent mixture of Et_2O:MeOH as described in the original protocol[69] did not result in a significant increase in selectivity (Table 1, entry 2). An increase in temperature during $FeCl_3/SiO_2$ preparation as well as freshly purchased $FeCl_3 \cdot 6\ H_2O$ helped in achieving a higher selectivity but again resulted in significant formation of side product **198** (Table 1, entry 10). Delightfully, using anhydrous $FeCl_3$ instead of $FeCl_3 \cdot 6\ H_2O$ in combination with anhydrous solvents resulted in a marked increase in selectivity (Table 1, entry 8). These optimal conditions were scaled up to 8 g-scale. High selectivity and conversion were retained during scale up, and a fair yield of 58% for biacetophenone **134** with a reaction time of 2.5 h was achieved. Interestingly, the synthesis of biacetophenone **49** did not suffer from the same issues of side product formation in line with the original protocol,[69] resulting in a yield of biacetophenone **49** of 52%. Significantly, the reaction time of the original protocol was decreased from 6 days to 6.5 h. The constitution of biacetophenone **134** was confirmed by x-ray analysis provided by *Julian Greb*[102, 108b] as well as by 2D-NMR data.

Table 1: Oxidative coupling of acetophenones under different conditions. Entries for different conditions of acetophenone coupling.

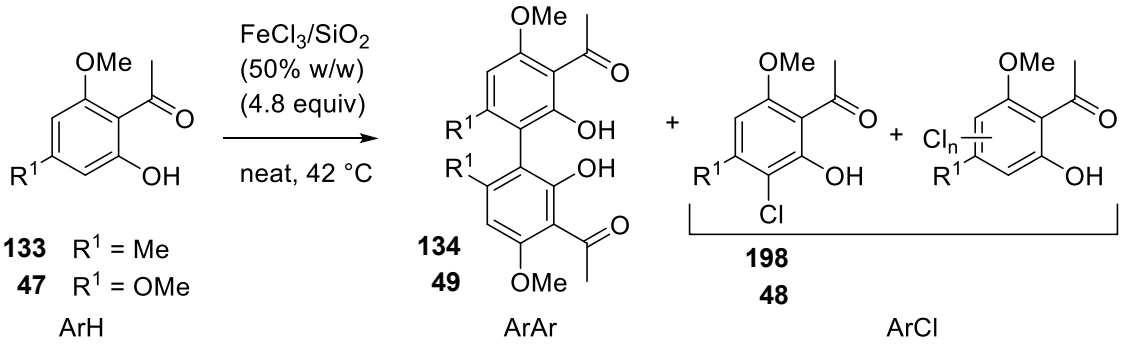

133 R^1 = Me
47 R^1 = OMe
ArH

134
49
ArAr

198
48
ArCl

#	[Fe]	Scale [g]	reaction time [h]	$FeCl_3$ [equiv]	$FeCl_3/SiO_2$ preparation	ArH [%]	ArCl [%]	ArAr[e] [%]
				R^1 = Me				
1	$FeCl_3 \cdot 6\ H_2O$[a]	1	6.0	4.6	I	34	45	21
2	$FeCl_3 \cdot 6\ H_2O$[a]	1	5.0	4.6	II	0	94	6
3	$FeCl_3 \cdot 6\ H_2O$[a]	1	3.2	2.8	II	18	71	11
4	$FeCl_3 \cdot 6\ H_2O$[a]	0.5	4.0	4.6	II	11	66	23
5	$FeCl_3 \cdot 6\ H_2O$[b]	0.5	3.0	4.6	II	58	20	22
6	$FeCl_3 \cdot 6\ H_2O$	4	16	4.6	II	37	56	7
7	$FeCl_3 \cdot 6\ H_2O$	2	5.0	2.8	II	62	24	13
8	$FeCl_3$	0.5	4.5	4.8	III	6	16	78 (36)
9	$FeCl_3$	1.4	4.5	4.8	III	16	19	65 (30)
10	$FeCl_3 \cdot 6\ H_2O$[c]	4	5.5	4.8	IV	6	43	51
11[f]	$FeCl_3$	4	5.5	4.8	III	38	12	49
12	$FeCl_3$	4	3.5	4.8	III	6	18	76 (39)
13	$FeCl_3$	4	8.5	4.8	IV	43	7	50 (23)
14	$FeCl_3$[d]	8	2.5	4.8	III	3	9	**88 (58)**
				R^1 = OMe				
15	$FeCl_3 \cdot 6\ H_2O$	8	6.5	4.6	I	15	4	**81 (52)**

Reactions were stopped if no more conversion to product was observed after taking aliquots as reaction controls; [a] significant amount of additional side products, complex NMR; [b] Dissolved $FeCl_3/SiO_2$ thrice in Et_2O and MeOH removing the solvent in between each dissolution step; [c] newly purchased; [d] workup with aq. HCl (1 M) instead of H_2O. [e] Conversion of starting material 3a according to ^{1}H-NMR; Isolated yield in parentheses. [f] 37.5 % w/w $FeCl_3/SiO_2$. Conditions: I: $FeCl_3/SiO_2$ prepared at 40 °C in Et_2O; II: $FeCl_3/SiO_2$ prepared at 40 °C in Et_2O:MeOH (9:1); III: $FeCl_3/SiO_2$ prepared at 40 °C then 60 °C in anhydr. Et_2O:MeOH (9:1); IV: $FeCl_3/SiO_2$ prepared at 40 °C then 60 °C in (non-anhydr.) Et_2O:MeOH (9:1).

To unambiguously assign the correct connectivity of the forming side product, chlorination of the acetophenone starting material was conducted. Both regioisomers **198** and **199** could be isolated in addition to the double chlorinated product **201** (Scheme 39).

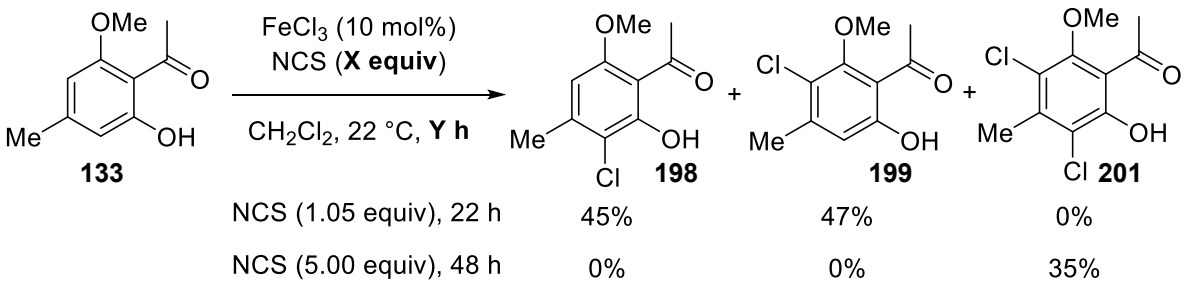

Scheme 39: Chlorination of acetophenone **133** to obtain references for the oxidative coupling.

With these chlorinated acetophenones in hand, the oxidative coupling under the same conditions as the optimized protocol was investigated (Scheme 40). This was done to determine if chlorinated acetophenone dimers **202** and **203** could be obtained this way. This, in turn, would enable access to additional biaryl structural motifs as halides have been shown to serve as useful protecting groups.[65a, 220] Particularly, the coupling of *ortho*-OH obstructed main side product **198**, would give insights into side product formation during the oxidative coupling. Under the previously optimized conditions, no conversion to product was observed. Instead, only low conversion to the double chlorination product **201** was observed by ^{1}H-NMR with mostly unreacted acetophenone starting materials. This may be the results of unfavorable stereo-electronic modification by the chlorine substituent.

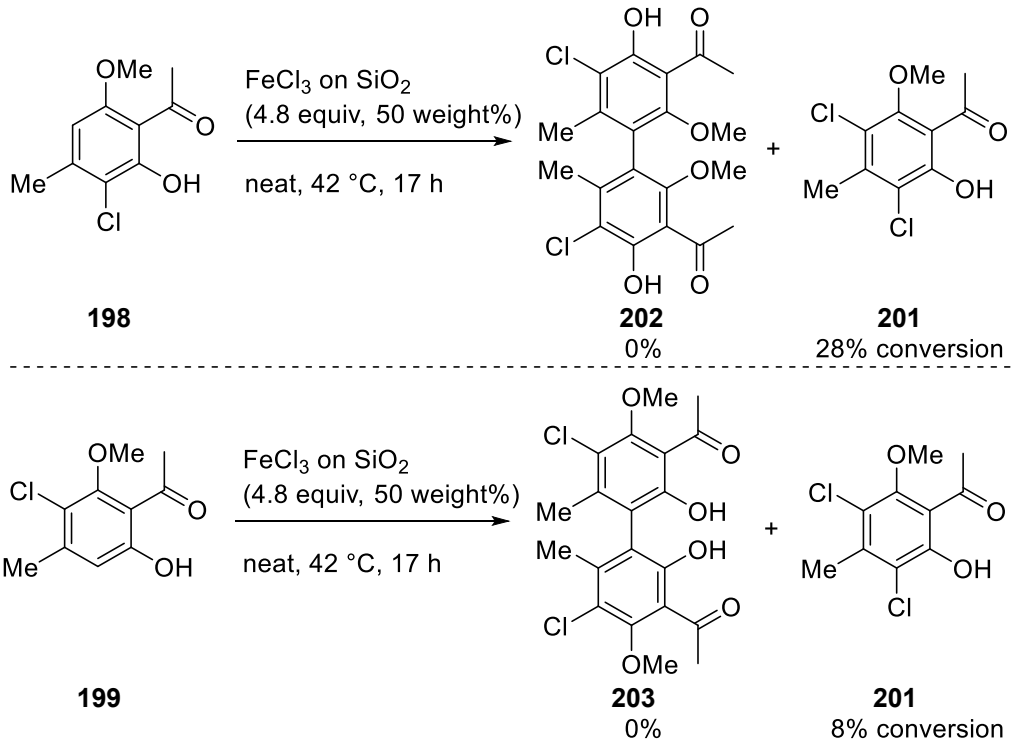

Scheme 40: Oxidative coupling attempt of chlorinated acetophenones **198** and **199**.

With a protocol for the synthesis of biacetophenones **134** and **49** established, the synthesis of bichalcones was addressed. Applying the conditions of the chalcone monomer protocol gave most bichalcones **165 – 176** in acceptable yields (23 – 94%) and purity (Scheme 41). Isolation of these highly insoluble compounds was achieved by scale up and recrystallization using methanol. Only **177** and **178** were not obtained in sufficient purity. Flavanone side products and insufficient conversion of starting material were attributed to the low solubility of these chalcone dimers. A complex mixture of isomers, side products and unconverted biacetophenone **49** resulted in complex crude ^{1}H-NMRs. Flavanone type side products were particularly problematic due to the axially chiral biaryl bond resulting in a range of diastereomeric side products (Chapter 5.2.3.1). Overall, 14 bichalcones could be obtained in a yield of up to 94% (**183**) on a 200 mg scale. Singular examples could be scaled up to 1.5 g (4.0 mmol) scale using this protocol.

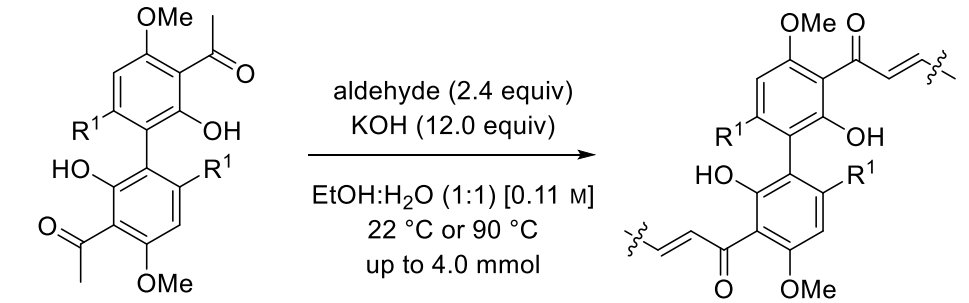

R^1 = Me **134**
R^1 = OMe **49**

	165 83% [a]	**166** 88% [a]	**167** 50% [b]
R^1 = Me			
R^1 = OMe	**172** 45%	**173** 23% [a]	**174** 24% [b]

R^1 = Me	**168** 94% [a]	**169** 94% (97%)[c]	**170** 86%	**171** 65%
R^1 = OMe	**175** 27%	**176** 55%	**177** 34% [d]	**178** 23% [d][e]

Scheme 41: Synthesis of bichalcones starting from biacetophenones **49** and **134**. Isolated yields. [a] 3.6 equiv aldehyde. [b] at 90 °C. [c] 4.0 mmol scale. [d] presumed mixture of chalcone and flavanones and mono addition product. [e] 1 h reaction time

To account for the low solubility of the bichalcones, an alternative protocol using an ionic liquid as dual solvent-catalyst-system was investigated. Pyrrolidine was chosen to fit this role of organocatalyst[216] as well as forming a liquid with acetic acid. Bichalcone **181** could be obtained in yields comparable with the previously discussed method (47% vs 50%). The approach appeared less generally applicable as other bichalcones (**168** and **169**) could not be isolated (Table 2). Additionally, isolation by precipitation, filtration, and subsequent methanol wash was complicated due to the high solubility in and low volatility of these ionic liquids.

Table 2: Synthesis of chalcone dimers using ionic liquids with various (but equimolar) equivalents of pyrrolidine and AcOH.

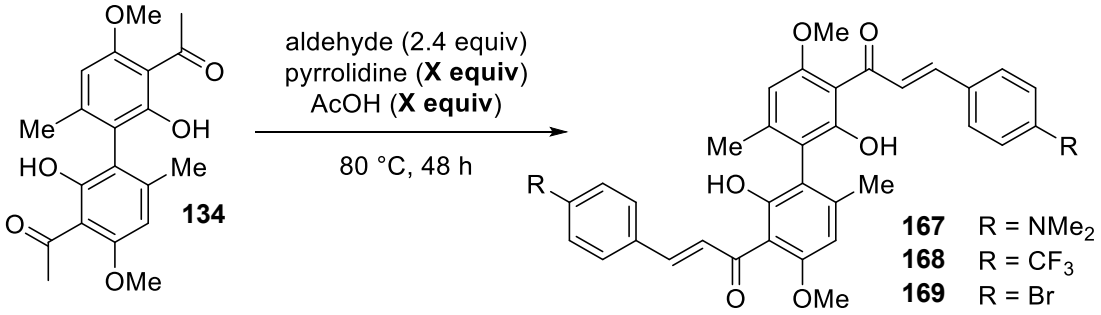

#	AcOH [equiv]	pyrrolidine [equiv]	Product	Isolated Yield [%]
1	1.0	1.0	**167**	47
2	5.0	5.0	**167**	41
3	50.0	50.0	**167**	–[a]
4	5.0	5.0	**168**	–[a]
5	5.0	5.0	**169**	–[a]

[a] complex mixture according to ^{1}H NMR.

In addition to the aforementioned flavanone side products, additional peak sets could be observed in the ^{1}H-NMR spectra of crude bichalcones. The peaks observed did not correspond to flavanone peak sets bearing vastly different signals in ^{1}H-NMR. Flavanone side products were additionally not detectable by HPLC (purity >99% according to normal phase HPLC and 96% according to reversed phase HPLC). Full interconversion of this additional peak set in $CDCl_3$ at ambient temperature over 72 h to the major peak set associated with product **166** was observed by ^{1}H-NMR (Figure 5A). The regression followed a linear trend with $R^2 > 0.99$, though more data points are necessary to reinforce this observation (Figure 5C). Purification by washing in hot methanol also resulted in full conversion. Thus, an in solution configurationally unstable conformer is a likely explanation for this additional peak set.

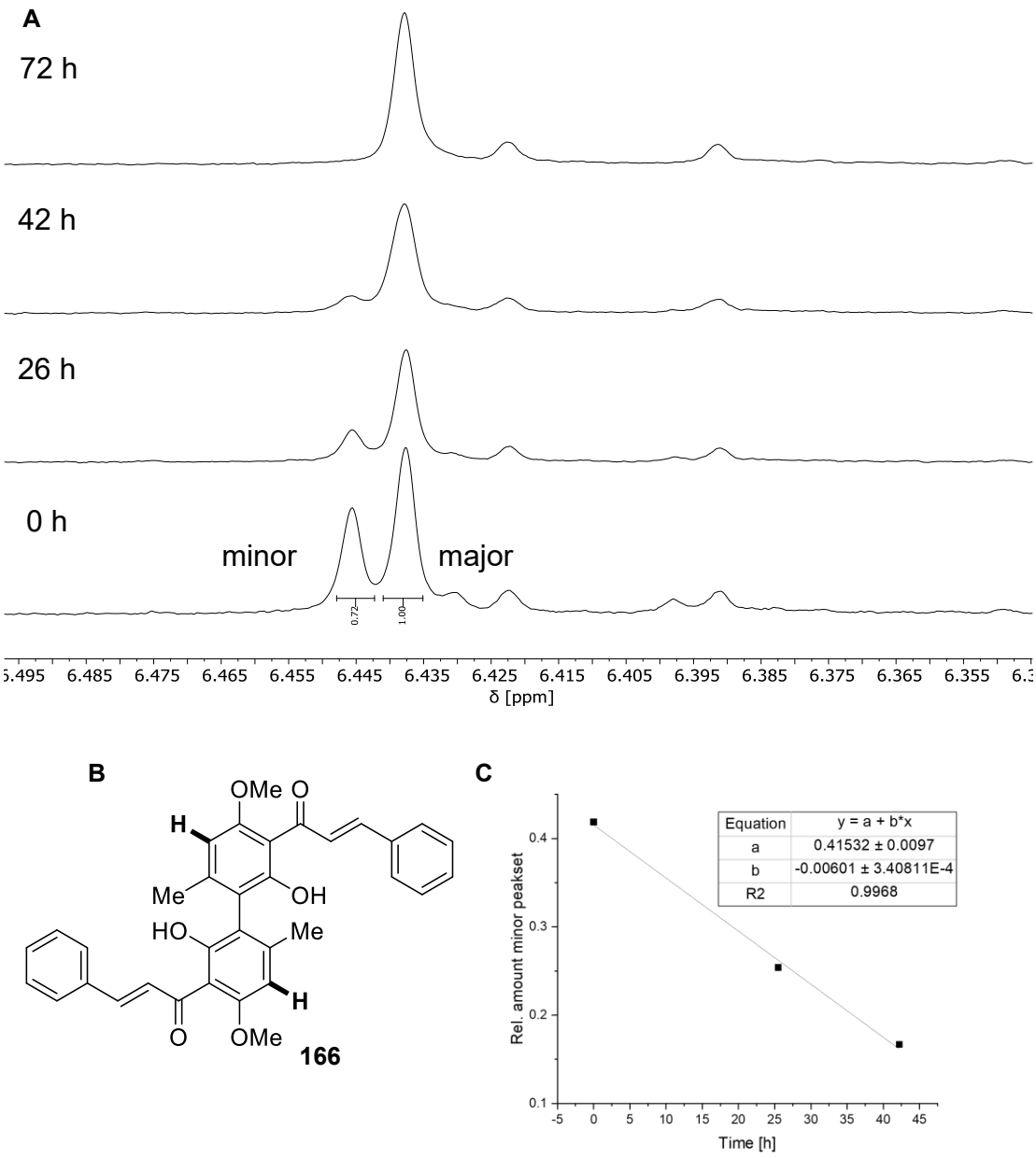

Figure 5: (A) ^{1}H-NMR spectra of the same mixture over time measured at indicated times since preparation of NMR sample with minor peak set vanishing over time. Quantification by integration over same area at different times. (B) Aromatic protons integrated in **A** indicated in bold font (C) Linear Regression of suspected bichalcone **166** isomer interconversion over time.

With these assessments of bichalcone side products in place and a suitable protocol for the synthesis of bichalcones established, the library of corresponding biflavones was synthesized next. Conditions of the flavone monomer synthesis were modified and successfully applied to the dimers (Scheme 42). The reaction was scaled up to 0.93 mmol scale for biflavone **181** and 1.9 mmol scale for **183**. All biflavones lest *meta*-Br-biflavone **191** could be obtained under these conditions. The low purity of bichalcone starting material **177** and its low solubility even in DMSO were thought to be responsible. In total, thirteen 8,8″-biflavones were obtained. Yields up to 39% (**183**) over five steps were achieved highlighting the synthetic usefulness of

this route. A very select number of biflavones were synthesized and provided by *Max Schlamkow*.

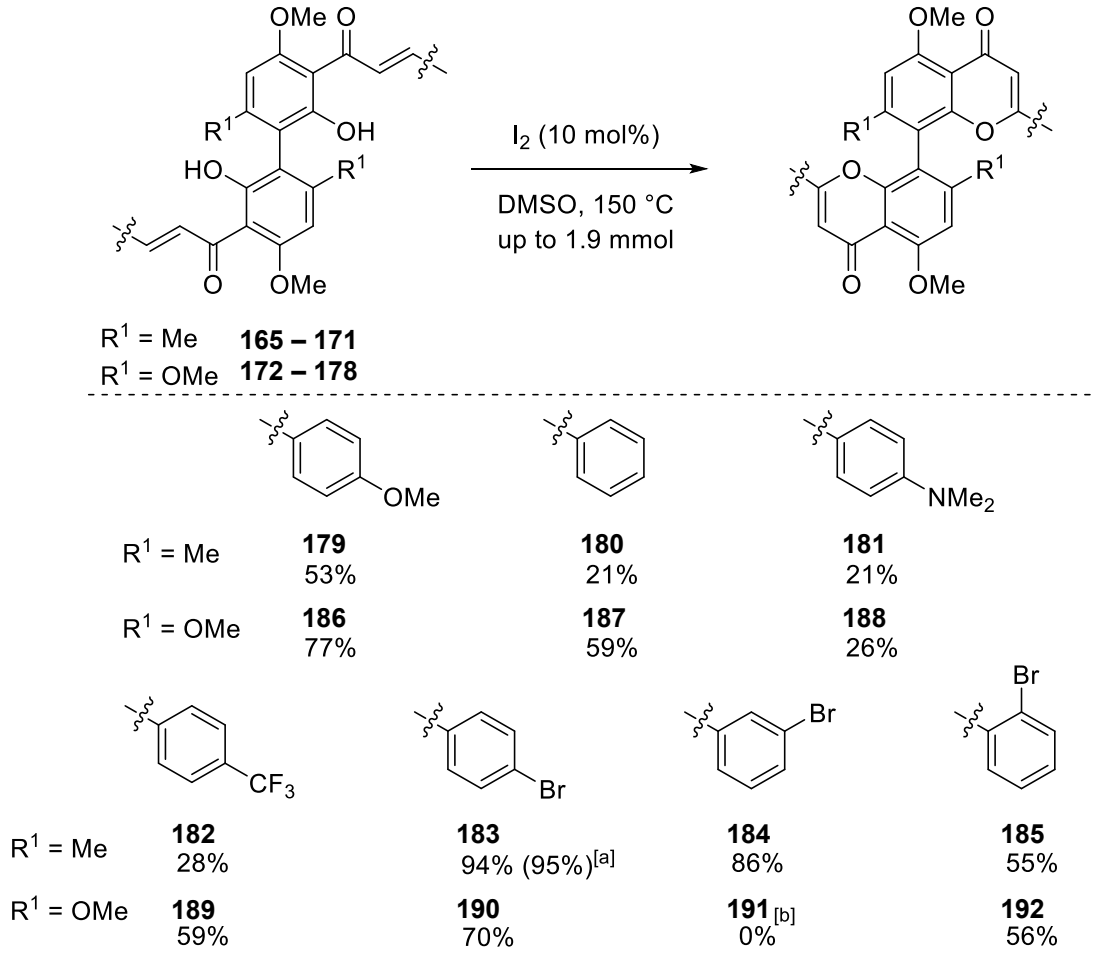

Scheme 42: Oxidative cyclization of bichalcones to biflavones. Isolated yields. [a] 1.9 mmol scale. [b] Complex ^{1}H-NMR.

The obtained flavones, biflavones, chalcones and bichalcones were evaluated regarding their bioactivity. The cytotoxicity (IC_{50}, inhibitory concentration[6]) against malignant human cell lines (HeLa cells) and against protozoal parasite *Toxoplasma gondii* (*T. gondii*)[221] were assessed.[7] The latter is an especially abundant and successful human parasite[222] with a dire need for new therapeutic agents.[223] Biflavones have been shown to exert anti-microbial activity in literature.[12g] Overall, biflavones generally exhibited higher bioactivity (lower IC_{50}) than the corresponding flavone monomer counterpart (Figure 6).[108b] Additionally, selectivity indices (SI) were calculated for *T. gondii* by dividing the cytotoxicity against the fibroblast host cells $IC_{50\,Hs27}$ by the cytotoxicity against *T. gondii* $IC_{50\,T.\,gondii}$. A large SI implies a high inhibition of parasite proliferation but low cytotoxicity against the healthy human host cells.

[6] IC_{50} represents the concentration of substrate at which 50% of the cells are viable.

[7] By *Lena Berning* and *Flaminia Mazzone*

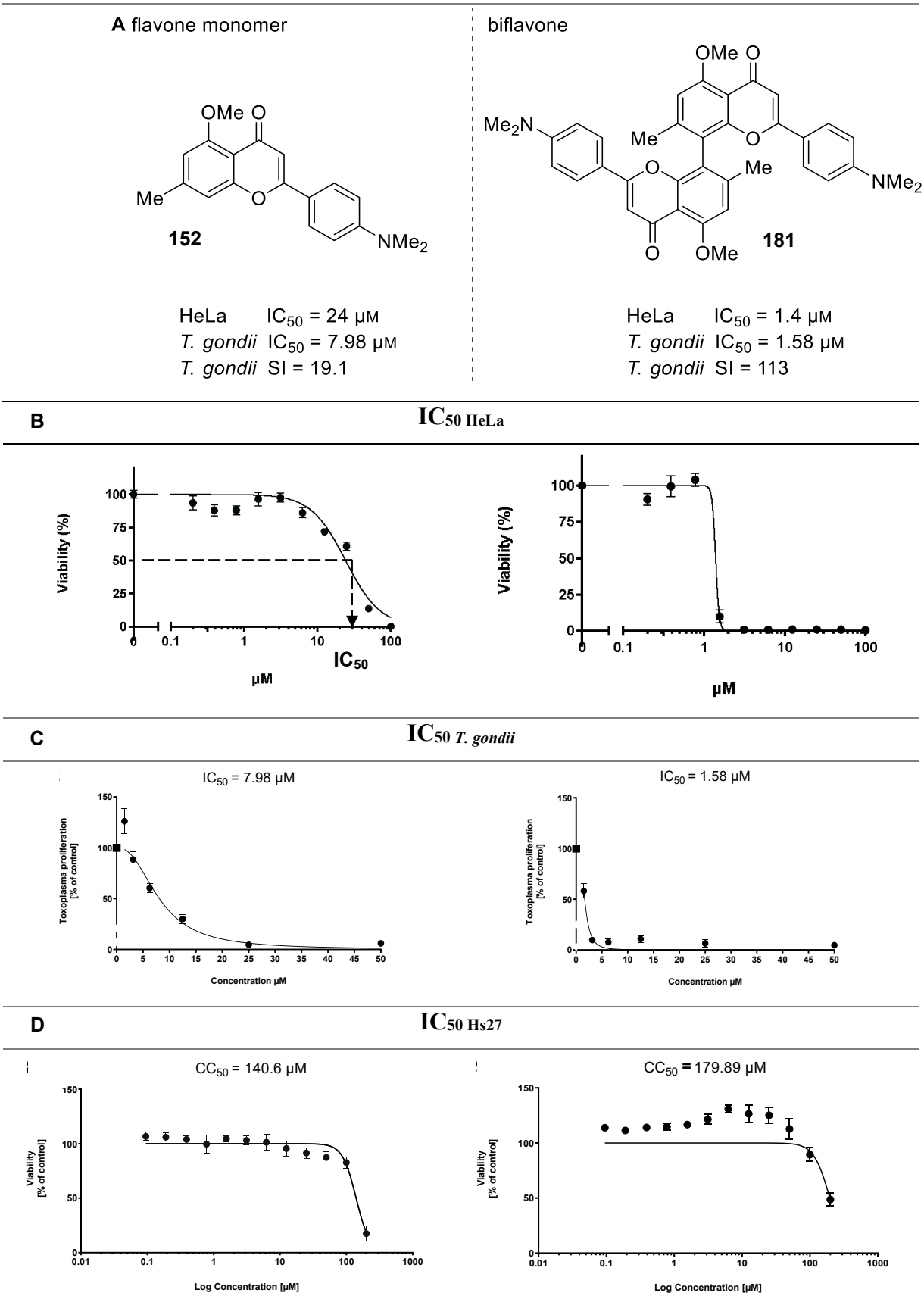

Figure 6: (A) Bioactivity of flavone **152** and biflavone **183** (B) $IC_{50\ HeLa}$ with visual cue (C) $IC_{50\ T.\ gondii.}$. (D) $IC_{50\ Hs27}$ (also referred to as cytotoxicity concentration CC_{50}).

In summary the highly bioactive bichalcone **166**[224] and biflavone **181**[108b] were identified. While both structures exhibited bioactivity against *T. gondii* proliferation, biflavone **181** showed high activity against malignant human HeLa cells. These compounds would serve as lead structures for following investigations (Chapter 5.1.4 and Chapter 5.2.3) (Figure 7). Especially bichalcone **166** ($IC_{50\ T.\ gondii}$ 0.114 µM, SI > 1750) showed an overall activity and selectivity index greater than pyrimethamine (lit.: $IC_{50\ T.\ gondii}$ 0.4 µM, SI > 202)[225], the current gold-standard treatment for toxoplasmosis.[226]

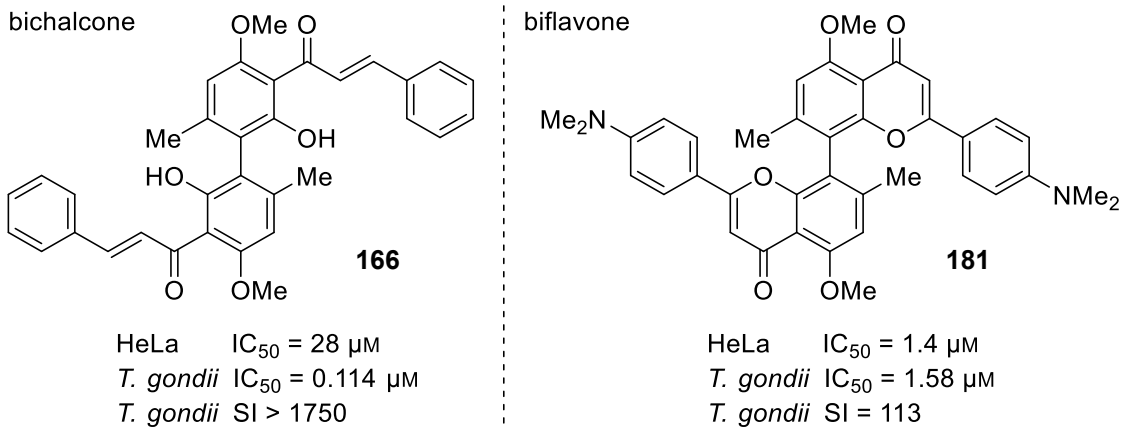

Figure 7: Most overall active racemic compounds bichalcone **166**[224] and biflavone **181**.[108b]

Further modification of biflavone **181** by methoxy deprotection (**204**) resulted in full loss of biological activity (Scheme 43). The cause of this loss of activity could be related to the carbonyl-hydroxy H-bridge suspected to be present between these functional groups. A change in pharmacokinetics or -dynamics may strongly influence the activity of this compound. Additionally, the yet unidentified molecular target may exert stronger binding due to the lipophilic nature of a methoxy group. A further probing of the structure activity relationship would be required to identify the narrowness of the target.

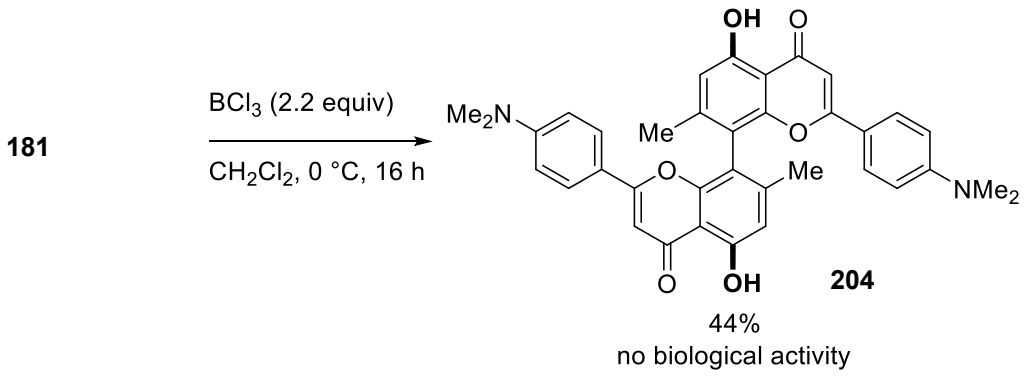

Scheme 43: Selective deprotection of the methoxy groups of biflavone **181** for the synthesis of biflavone **204**. Yield of isolated product.

In addition to activity against various cell lines, the antioxidant capacity of the flavones was assessed *in chemico* relative to ascorbic acid using a literature known ABTS (2,2′-azino-bis(3-ethylbenzothiazoline-6-sulfonicacid) protocol.[227] An $ABTS^{\bullet+}$ radical cation is reduced in the presence of the screened compounds resulting in the disappearance of the absorption maximum of $ABTS^{\bullet+}$ at 734 nm. A better reductant will result in faster reduction and thus a higher antioxidant capacity. All measurements were performed as triplicates. The calibration curve exhibited good linearity (Figure 8). Overall, electron-rich flavones and biflavones exhibited a high ascorbic acid equivalent antioxidant capacity (AEAC) (Table 3).

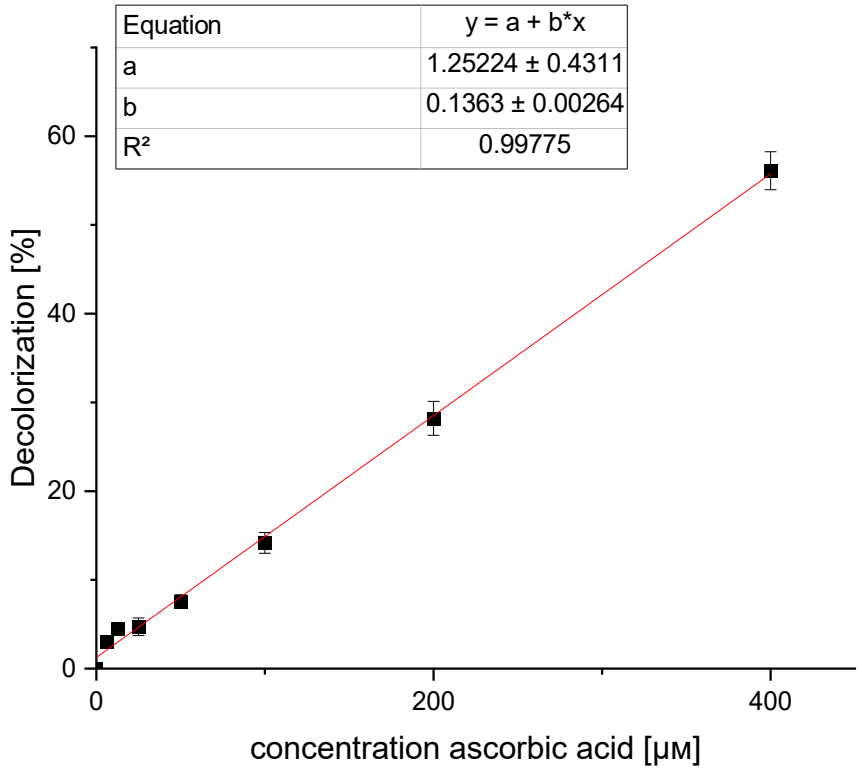

Figure 8: Calibration curve of ascorbic acid at the concentration range of 0 – 400 µM with linear fit.

Table 3: Ascorbic acid equivalents antioxidant capacity (AEAC) of flavones and biflavones and corresponding standard deviation (SD).

R^1	Ar	flavone	AEAC [mmol $mmol^{-1}$]	SD	biflavone	AEAC [mmol $mmol^{-1}$]	SD
Me	**4-OMe**	**150**	0.084	0.007	**179**	0.237	0.001
OMe	**4-OMe**	**157**	0.075	0.008	**186**	0.129	0.007
Me	**H**	**151**	0.013	0.007	**180**	0.048	0.001
OMe	**H**	**158**	0.014	0.006	**187**	0.070	0.005
Me	**4-NMe_2**	**152**	0.110	0.002	**181**	0.197	0.003
OMe	**4-NMe_2**	**159**	0.081	0.001	**188**	0.215	0.000
Me	**4-CF_3**	**153**	0.055	0.007	**182**	0.098	0.001
OMe	**4-CF_3**	**160**	0.048	0.006	**189**	0.050	0.005
Me	**4-Br**	**154**	0.036	0.000	**183**	0.026	0.007
OMe	**4-Br**	**161**	0.018	0.006	**190**	0.037	0.005
Me	**3-Br**	**155**	0.032	0.008	**184**	0.028	0.002
OMe	**3-Br**	**162**	0.056	0.001	**191**	–	–
Me	**2-Br**	**156**	0.017	0.006	**185**	0.025	0.007
OMe	**2-Br**	**163**	0.020	0.004	**192**	0.069	0.008
Me[a]	**4-NMe_2**				**204**	0.037	0.009

[a].Methyl deprotected biflavone **204**.

In summary, various methods were explored to obtain a library of flavonoids. In particular, a sequence towards biphenol **27** was optimized and chalcone and flavone synthesis conditions were successfully established. Moreover, oxidative iron-mediated coupling was successfully transferred to a new acetophenone substrate. Side products obtained over this sequence were identified and suppression of such side product successfully enabled. In the end, bioactivities were obtained so that lead structures for further investigations could be identified. First, non-natural biflavone **181** showed promising selective activity against protozoal parasite *T. gondii* and malignant human cell lines while exhibiting little cytotoxicity against healthy human cell lines (fibroblasts) in addition to antioxidant properties. Additionally, bichalcones (particularly **166**) could be identified as a novel scaffold for further evaluations. These types of bichalcones as non-natural analogues not found in the natural biosynthesis are of particular interest due to the unexploredness of this high-potential compound class.

5.1.4 Amino 8,8″-biflavones

The following chapter contains results obtained by Daniel Grudzinski as part of a bachelor's thesis[206] and is a revised version of Klischan et al. Org. Lett. ***2024****.[228]*

As discussed in the previous section, the biflavone exerting the highest bioactivity was identified as **181**. Bearing two dimethyl amino functionalities, a strategy was devised that allowed for diversification of this substitution pattern. By probing if variation of the amine substituent modulates the activity against malignant human cell lines, the structure activity relationship would be investigated. This would be done by the synthesis of a focused library of amino biflavones. First the low yields obtained for amino biflavone **181** *via* the previously established synthesis route (11% over two steps starting from biacetophenone **134**) needed to be addressed. A strategy capitalizing on readily available brominated biflavone **183** (88% over two steps starting from **134**) as a platform for diversification was conceived (Figure 9). Palladium-catalyzed *Buchwald-Hartwig* amination using various readily available amines would give access to a scope of racemic amino-biflavones in a single step.

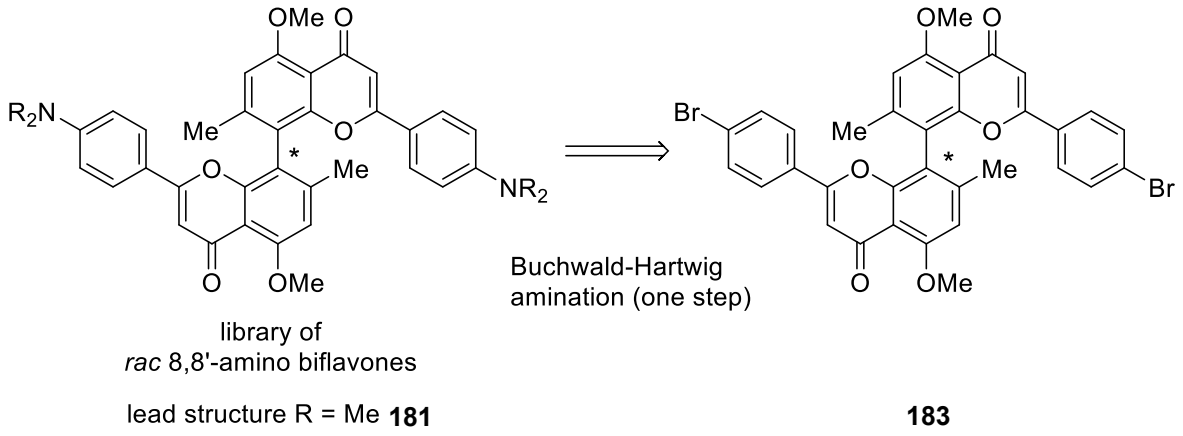

Figure 9: Synthesis strategy of amino biflavones starting from brominated biflavone **183**.

Investigations were initiated by choosing promising starting conditions. To ensure adequate palladium-activation, a *Buchwald*-type precatalyst was chosen as the Pd-source (Chapter 4.5.1).[153] The palladium precatalyst (Pd G4)$_2$ (**205**) was obtained following a literature known procedure over two steps starting from 2-aminobiphenyl (**206**) *via* methyl protected **207** (Scheme 44A).[153] Base mediated activation of (Pd G4)$_2$ (**205**) to obtain a catalytically active Pd^0 species results in the formation of carbazole **208** as a side product (Scheme 44B).

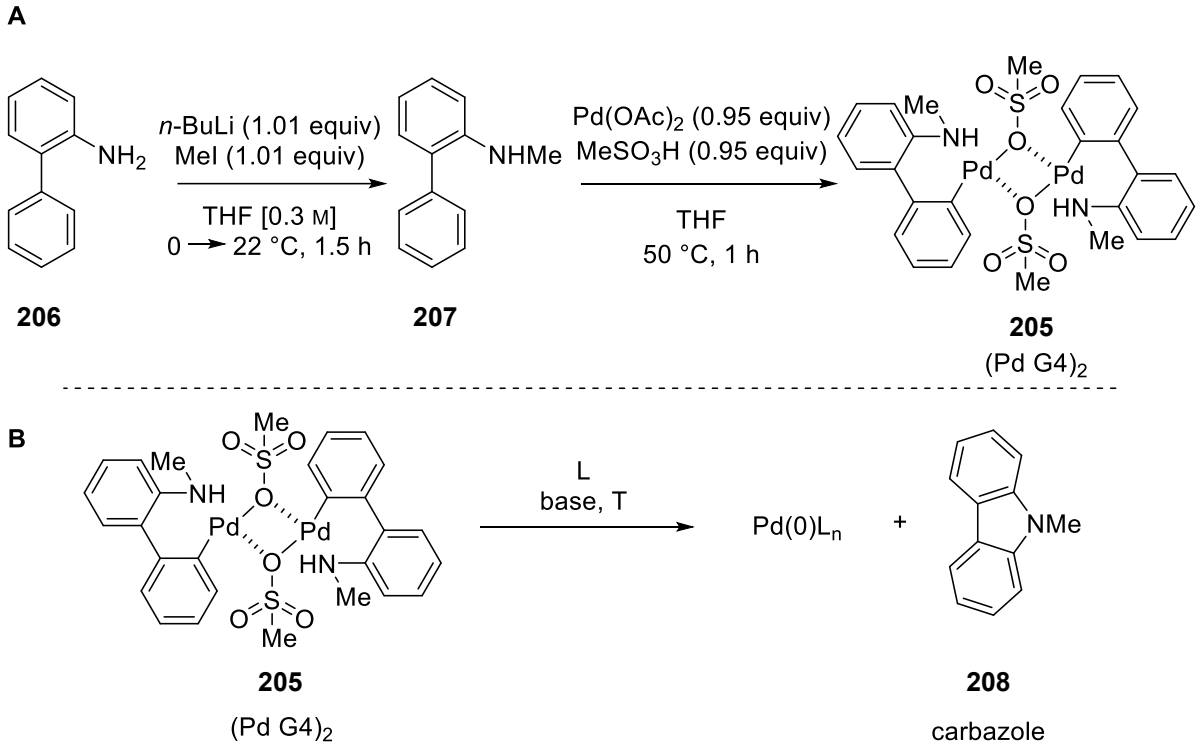

Scheme 44: (A) Synthesis of $(Pd\ G4)_2$ (**205**). (B) Base mediated carbazole formation.

First, the *Buchwald-Hartwig* amination was performed using flavone monomer **154** as a test substrate. Incomplete conversion of C_2-symmetrical biflavone **183** would result in a mixture of mono-amination and double-amination products hardly distinguishable by ^{1}H-NMR. Thus, determining the optimal reaction conditions by NMR would be cumbersome. Cs_2CO_3 was chosen as the base to allow for more sensitive functional group tolerance in addition to $(Pd\ G4)_2$ (**205**) as the Pd-source. Reactions were set up in 2 dram (2 dr.)[8] vials (see Chapter 7.1, Figure 29). After a short optimization by *Daniel Grudzinski*,[206] a protocol could be established for secondary (2°) amines. The low initial conversions were attributed to substantial evaporation of the amine during the setup of the reaction (Table 4, entry 1 – 2). An increase in amine equivalents did result in higher conversion to product. Yet, it was of even greater importance for full conversion to not purge the amine with an argon balloon (Table 4, entry 3 vs. 4). This was again attributed to the volatility of the amine. A subsequent investigation of purging morpholine with argon for 1 h in triplicates revealed full evaporation (0±0% according to ^{1}H-NMR in triplicates with 1,3,5-trimethoxylbenzene as internal standard). Additionally, the equivalents of RuPhos (**209**)—a typical MOP-type ligand for *Buchwald-Hartwig* couplings of secondary amines[152, 229]—greatly influenced the conversion to product due to suspected competitive binding of the amine (Table 4, entry 5 – 6).[230] The desired product **210** could be

[8] dram: unit of measure, 1 dram roughly equivalent to 3.7 mL

obtained in a yield of 89% with an effective Pd-loading of 5 mol% (2.5 mol% $(Pd\ G4)_2$, dinuclear Pd-precatalyst) (Table 4, entry 6).

Table 4: Palladium catalyzed *Buchwald-Hartwig* amination screening using **154**.

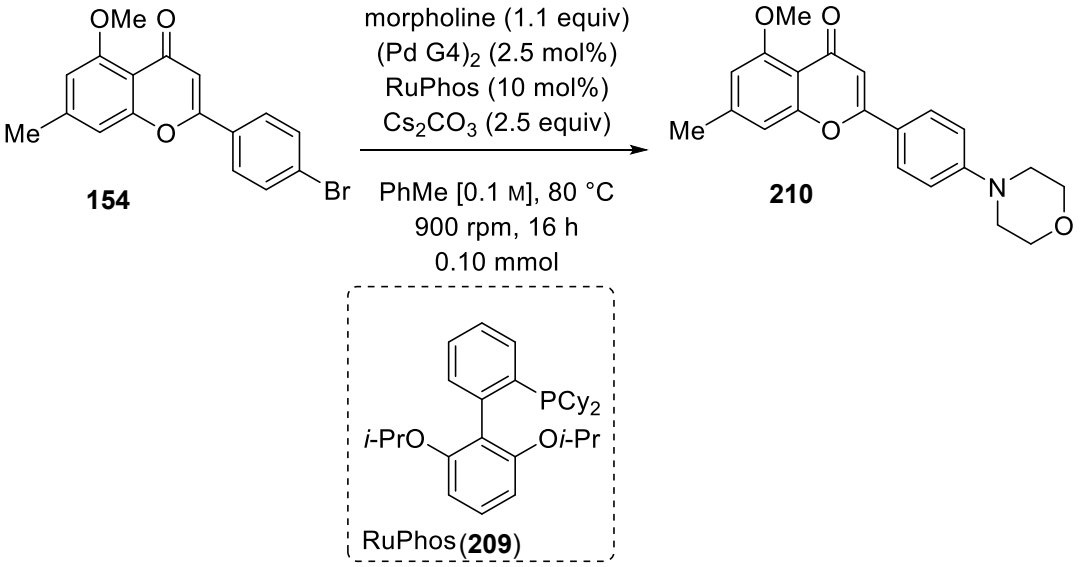

#	Variation	Conversion of 154 [%]	Product [%][a]
1	None	0	0
2	BINAP (10 mol%)	5	0
3	Morpholine (2.2 equiv)	42±2	6±1
4	No amine purging, Morpholine (2.2 equiv)	72	59
5	No amine purging, Morpholine (2.2 equiv), RuPhos (20 mol%)	100	89±5
6	No amine purging, Morpholine (2.2 equiv), RuPhos (40 mol%)	100	94±1 (89)[b]

Reactions were performed on a 0.10 mmol scale. Entries with standard deviation performed as duplicates. [a] Conversion to product according to ^{1}H-NMR in parentheses using 1,3,5-trimethoxybenzene as an internal standard. [b] Isolated yield.

In addition to the use of morpholine, the use of benzylamine as a primary (1°) amine was investigated. Full conversion of starting material **154** was observed yet lower conversion to product **211** (56%) detected (Scheme 45). This was attributed to RuPhos being particularly suited for secondary amines,[152, 229] making multi-additions and oligomer formation more likely.

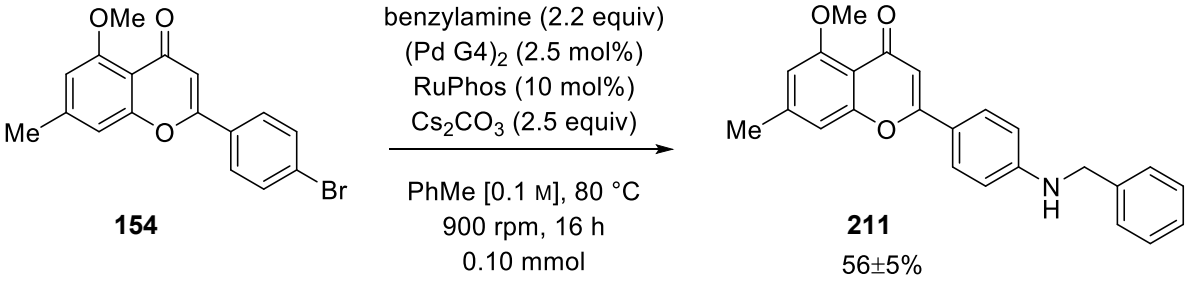

Scheme 45: Palladium-catalyzed synthesis of amino flavone monomer **211**. Reaction performed as duplicate.

With the monomer synthesis established and notably full conversions of starting material achieved, the conditions were translated to the dimer synthesis. The scope of biflavones was chosen to test the influence of amines with increasing steric bulk. Acyclic 2° amines (**181**, **212**), cyclic 2° amines (**213**, **214**, **215**, **216**) as well as acyclic 1° amines (**217**, **218**) were chosen to obtain a diverse scope of substitution patterns (Figure 10).

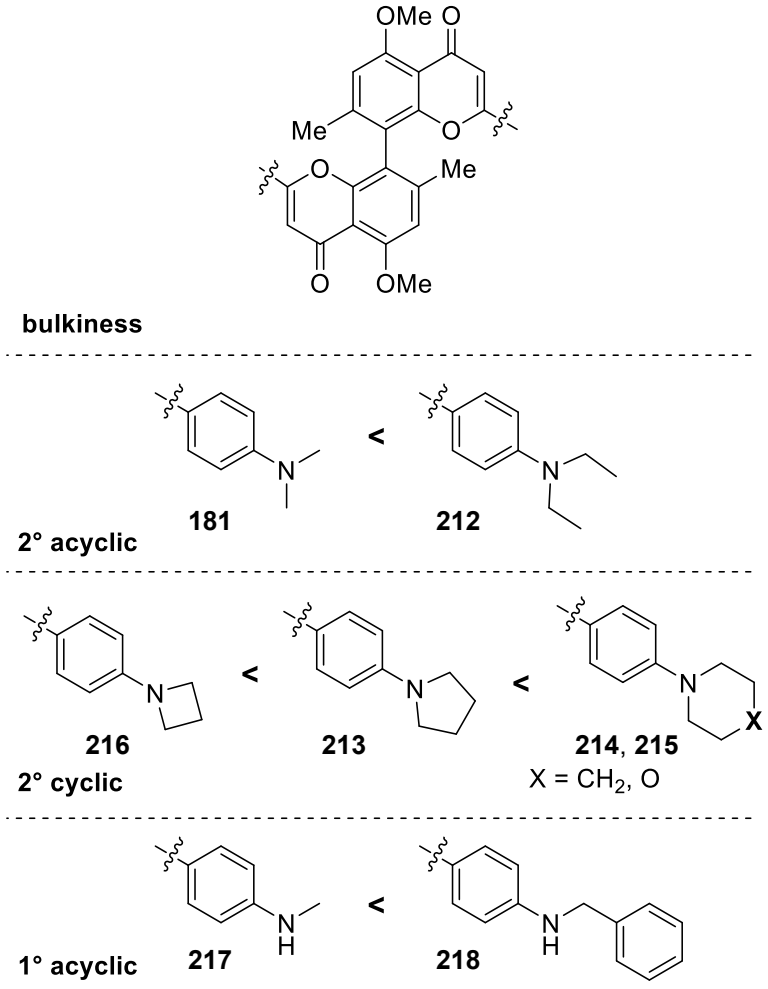

Figure 10: Scope of target amino 8,8″-biflavones with amines with various degrees of bulkiness.

Translating the reaction conditions established for the monomers to the biflavones, the dedicated library could be obtained. Even a catalyst-loading of 2.5 mol% gave full conversion to product for select substrates (Scheme 46). In other cases, increasing the 5 mol% to match the flavone monomer amination was required to achieve full conversion. In addition to the use of commercially available cyclic and acyclic amines, the hydrochloride salts of dimethylamine and methylamine were employed. When doing so, additional base was added to compensate for the ammonium deprotonation (1.0 equivalents base per equivalent amine). Yields ranged from 75 – 94% for the six examples of secondary amines **181** – **216** (Scheme 46). Biflavone **181** was included in the scope so that the influence of potentially biologically relevant palladium could be investigated and compared to the results using the previous method.[231] Benzylamine-derived product **218** could also be obtained in a yield of 34%. When using the hydrochloride of methylamine, no formation of product **217** was observed. Instead, the use of BrettPhos as the ligand gave some yet still low conversion of starting material to the desired product **217** (8% yield). Additionally, a non-C_2-symmetrical biflavone could be isolated that turned out to bear a methoxy/methylamine substitution pattern (**219**) in a yield of 7%. Overall, a library of nine 8,8″-biflavones was obtained with reaction conditions especially suited for the synthesis of secondary amines including hydrochlorides. A number of these biflavones were synthesized and provided by *Daniel Grudzinski*.[206]

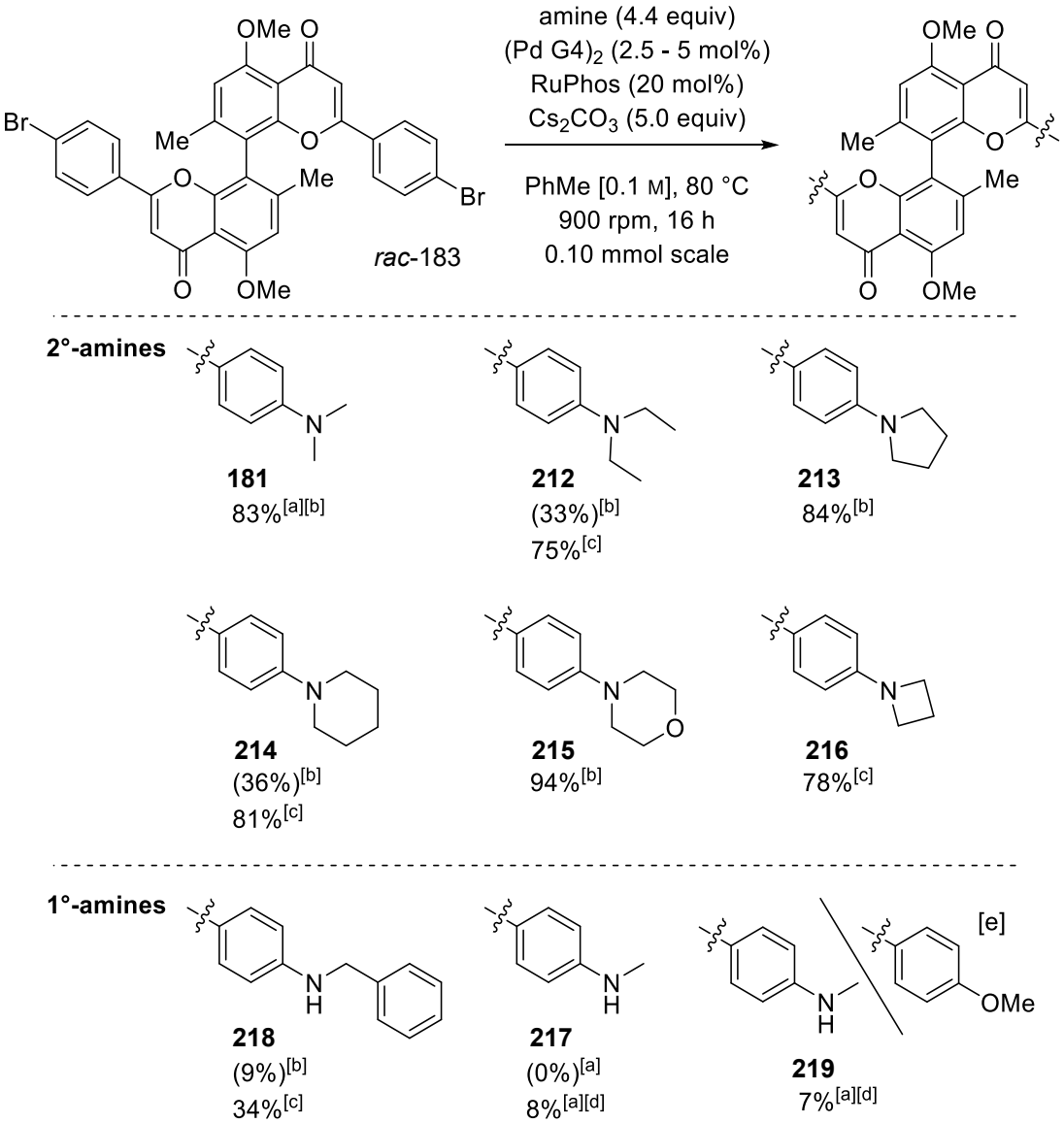

Scheme 46: Synthesis of a library of 8,8″-amino biflavones by palladium-catalyzed *Buchwald-Hartwig* amination. Reactions were performed on a 0.10 mmol scale. Isolated yields. [a] HCl salt of amine used, HCl Cs_2CO_3 (9.4 equiv). [b] $(Pd\ G4)_2$ (2.5 mol%). [c] $(Pd\ G4)_2$ (5.0 mol%). [d] $(Pd\ G4)_2$ (5.0 mol%), BrettPhos (20 mol%). [e] non-C_2-symmetrical methylamine/methoxy biflavone side product using NH_3MeCl. Conversion to product according to ^{1}H-NMR with 1,3,5-trimethoxybenzene as internal standard in parentheses.

The activity of these compounds against HeLa cells ($IC_{50\ HeLa}$) was assessed by *Céline David*.[228] The IC_{50} values clearly indicated that the Pd-catalyzed synthesis route did not influence the bioactivity of the compounds (Figure 11). While the biflavones with pyrrolidine **216** and dimethylamine **214** substituents were active, similarly small azetidine **219** and slightly bulkier diethylamine **215** were entirely inactive ($IC_{50\ HeLa} > 50\ \mu M$) (Figure 11). Interestingly, non-C_2-symmetrical biflavone **219** was more active than the corresponding methyl amine derived biflavone **217**. These results may imply that the biological target prefers small substituents. The discrepancy in size between biflavone with azetidine **219** versus pyrrolidine **216** substituent may be the result of unfavorable bond angles, again supporting a

rather tight binding affinity. Non-C_2-symmetrical biflavone **219** may support this hypothesis by showing that a sterically small substituent on one side of the biflavone may be favored. Further investigations at identifying a target by proteome analysis should elucidate these findings.

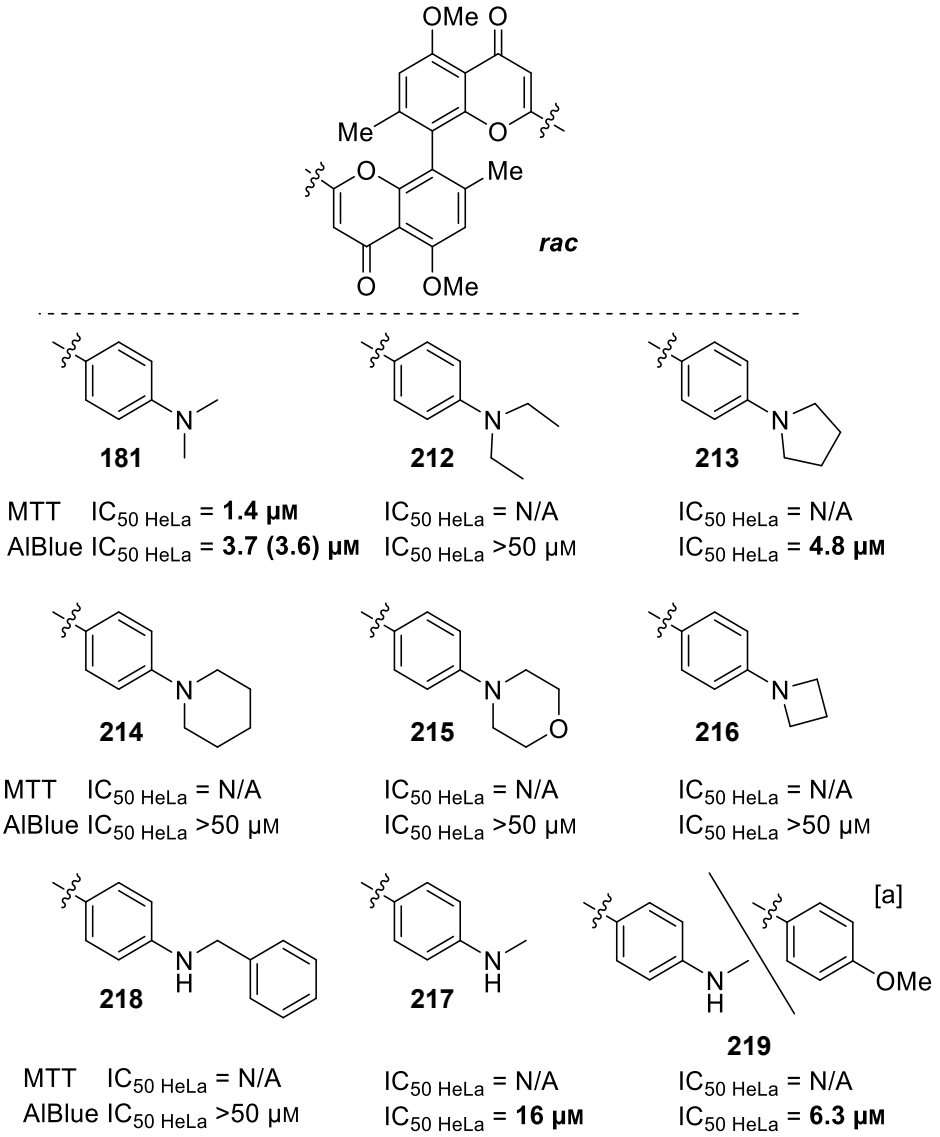

Figure 11: $IC_{50\ HeLa}$ of 8,8″-amino biflavones.[228] Values of MTT assay and value in brackets via Alamar Blue assay from compounds used in previous study[108b] [a] non-C_2-symmetrical methylamine/methoxy biflavone.

Thus, a reliable method for the amination of flavones was established. A dedicated library of nine amino biflavones could be obtained. While the protocol was suited for secondary amines, primary amines were still accepted as well as the hydrochlorides of either. The most active biflavone was identified as the previously synthesized dimethyl amine derived **181**. The first-ever reported non-C_2-symmetrical 8,8″-biflavone was synthesized. A correlation between steric bulk of the substituents and activity could be observed. Moreover, it could be shown that palladium content did not influence the observed bioactivity.

5.2 Cyclic diaryliodonium salts towards enantiopure BIPOL

The following chapter contains results obtained by Daniel Grudzinski as part of a bachelor's thesis,[206] additionally containing results published in Klischan et al. Org. Lett. ***2024***[228] *as well as in Mazzone et al. Front. Chem.* ***2024***.[224]

As was discussed in a previous chapter (5.1.2) and was shown in literature,[102-103] biphenol **27** (BIPOL) can be used as a building block for various polyketide based natural products. A strategy towards enantiopure BIPOL **27** was conceived involving the use of cyclic diaryliodonium salts as stereodynamic key intermediates (Scheme 47). This strategy would bear the advantage of being able to introduce nucleophiles other than oxygen to generate a more diverse range of valuable intermediates than the previously used methods (Chapter 4.3).[102] This would constitute the first use of cyclic diaryliodonium salts in natural product synthesis. To show the usefulness of the method, both enantiomers of the most bioactive bichalcones and biflavones identified by the previous investigations on racemic biflavones (5.1.1) were to be synthesized.

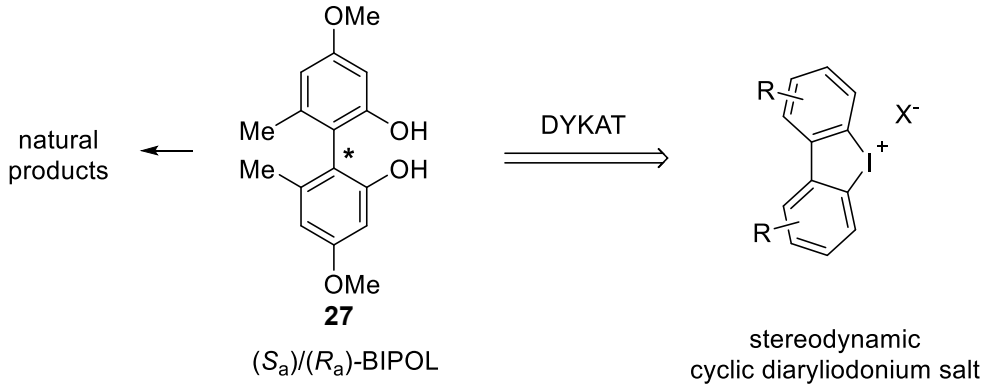

Scheme 47: Strategy towards biphenol **27** involving cyclic diaryliodonium salts.

5.2.1 Electron-rich cyclic diaryliodonium salts

To obtain the substitution pattern found in polyketide based natural products (Chapter 4.3.1), electron-rich cyclic diaryliodonium salt **220** would need to be constructed. Starting from the previously synthesized—and readily available—brominated arene **128** (Chapter 5.1.2) would eliminate the requirement for optimization of starting material synthesis. The 2-iodobiaryl **221** required for the subsequent oxidative cyclization to the cyclic diaryliodonium salt **220** would be synthesized over five steps (Scheme 48). To provide adequate amounts of starting material over the six-step sequence, scalability was of great importance.

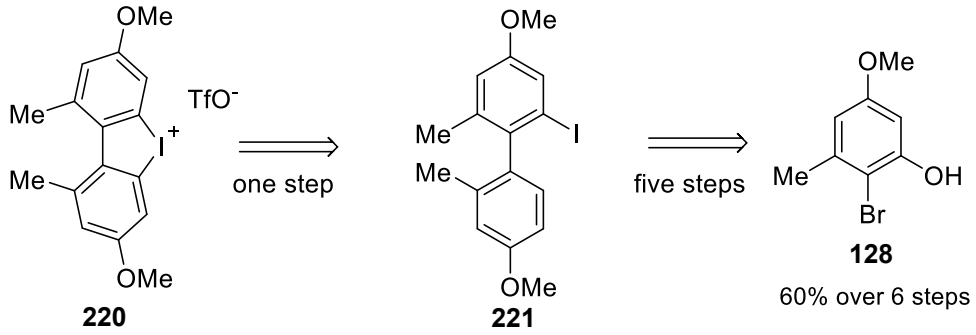

Scheme 48: Cyclic diaryliodonium salt **220** as a key intermediate towards the synthesis of enantiopure BIPOL **27**.

5.2.1.1 Borylation

The first step involved the scalable synthesis of boronic acid ester **222**. Biaryl monophospohine ligands have successfully been employed in borylations.[232] The influence of borylating agent equivalents as well as the palladium-loading were investigated to establish the most economically viable protocol for an adequate scale up. After screening for various conditions (Table 5, entries 1 – 12), palladium-catalyzed borylation using HBpin, commonly referred to as *Masuda*-borylation (**A**),[233] provided a robust method to provide *ortho*-borylated arenes. Similar conditions using B_2pin_2, referred to as *Miyaura*-borylation (**B**), also gave acceptable yields though with a lower selectivity (compare Table 5, entries 13 and 14).[234] Additionally, 1,4-dioxane was able to be replaced with THF (Table 5, entry 17). Thus, anhydrous solvent provided by the solvent purification system available at the institute could be leveraged. This would remove the need for costly commercially available anhydrous 1,4-dioxane or labor-intensive drying procedures. The main impurities in the crude product consisted of pinacol, phosphine ligands and carbazole **208**, a side product during the activation of Pd G4-type precatalysts (Scheme 44) and proto-dehalogenated side product **223**. A protocol for the isolation of boronic acid ester **222** by Kugelrohr®-distillation and following base-wash was established. Thus, a convenient protocol for the synthesis of large quantities of boronic acid

esters is presented, avoiding column chromatographic purification. The reaction could be scaled up to 29 mmol scale and the product isolated in a yield of 85% using 1 mol% Pd.

Table 5: Screening conditions for the synthesis of aryl boronic acid ester **222**.

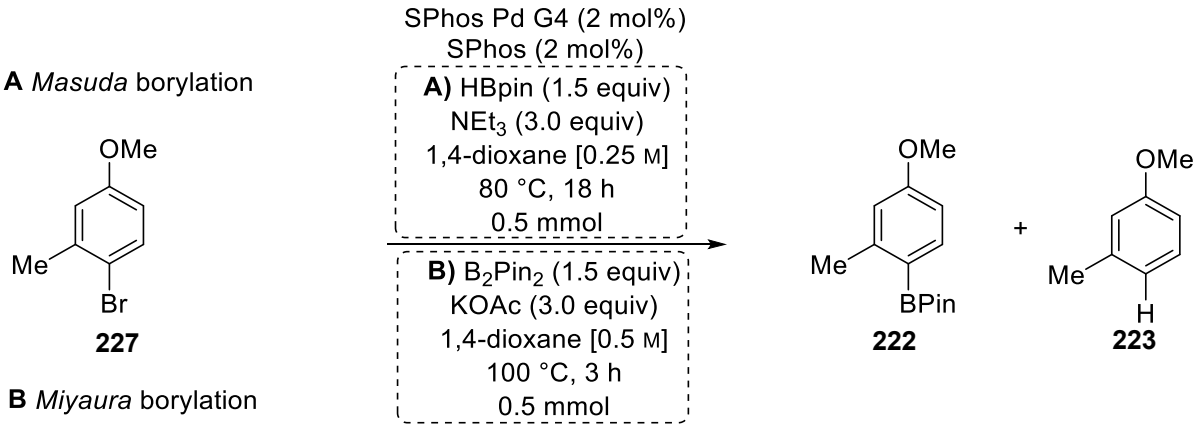

#	Method	Variations	Product [%][a]	Yield [%][b]
1	**B**	None	53	44
2	**B**	B_2pin_2 (1.2 equiv)	72	–
3	**B**	[Pd]/L (1 mol%)	73	–
4	**B**	B_2pin_2 (2.0 equiv)	83	–
5	**B**	B_2pin_2 (2.0 equiv) [Pd]/L (1 mol%)	73	–
6	**B**	B_2pin_2 (3.0 equiv)	75	–
7	**B**	80 °C	96	–
8	**B**	B_2pin_2 (3.0 equiv), 80 °C	93	–
9	**B**	18 h	96	–
10	**A**	2 h	90	78
11	**A**	22 °C	74[c]	–
12	**A**	Pd (1 mol%)	83[c]	–
13	**B**	2.0 mmol, [Pd]/L (1 mol%)	77	64
14	**A**	2.0 mmol, [Pd]/L (1 mol%)	84	80
15	**A**	7.2 mmol, [Pd]/L (1 mol%)	92	78
16	**A**	14 mmol, [Pd]/L (1 mol%)	94	**84**
17	**A**	29 mmol, [Pd]/L (1 mol%) THF, 65 °C	93	**85**

Reactions on a 0.5 mmol scale. [a] Borylated product **222** against total integrals (proto dehalogenated side product **223** + borylated product **222**) according to ^{1}H-NMR. [b] isolated yield. [c] incomplete conversion.

5.2.1.2 *Suzuki-Miyaura* cross-coupling

With a scalable method for the synthesis of aryl boronic acid ester **222** in hand, the *Suzuki-Miyaura* cross-coupling was investigated next. The initial conditions were based on literature known conditions by *Ganardi et al.* employing SPhos (**224**) as the supporting ligand (Table 6).[103] The construction of the biaryl bond in tetra-*ortho* substituted systems—as found in axially chiral natural products—is sterically demanding, often requiring tailor-made solutions.[25, 65] The present synthesis strategy would only be concerned with the less sterically demanding tri-*ortho* substitution pattern. After a short screening, the amount of palladium catalyst used could be decreased significantly from 2.5 mol% to 0.5 mol% to form biaryl **225** in a yield of 94% using MOM-protected **29** (Chapter 5.1.2). Using boronic acid ester **226** and aryl bromide **227** resulted in lower yields (Figure 12). This was done to probe the steric effect of the palladium complex and indicated, that the transmetalation step was inherently more sterically hindered. Overall, though a useful protocol, a direct coupling of unprotected phenol **128** to the biaryl **228** would remove both a protection and a deprotection step in the total synthesis of diaryliodonium salt **220**. Decreasing the temperature to 22 °C still gave the product in lower yet acceptable yield (Table 6, entry 8). In the end, biaryl phenol **228** could be obtained in a yield of 81% on a 3.9 mmol scale using 1 mol% palladium (Table 6, entry 10). The *Suzuki* reaction without MOM-protecting group gave larger amounts of proto-dehalogenation side product. Decreasing the equivalents of boronic acid ester resulted in a lower yield due to an increase in proto dehalogenation side product **124** and oxidative coupling product **229** (Table 6, entry 11).

Table 6: Screening conditions for the synthesis of biaryl **225** and biaryl **228** *via Suzuki* cross-coupling.

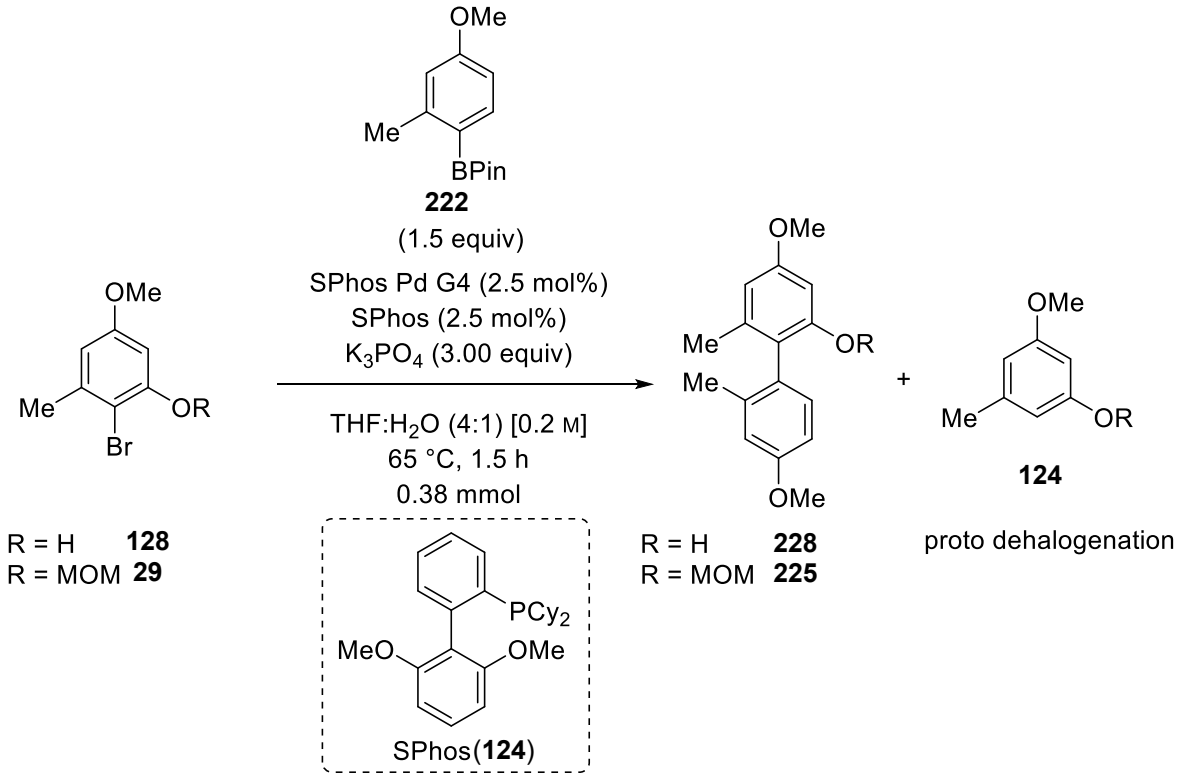

#	Variations	Yield[a] [%]
	R = MOM	
1	None	87
2	22 °C, 18 h	–[b]
3	ArBr **227** and ArBpin **226**[c]	79
4	0.76 mmol, [Pd]/L (1 mol%)	94
5	0.76 mmol, [Pd]/L (0.5 mol%)	94
	R = H	
6	None	89
7	22 °C, 4.5 h	96[d]
8	22 °C, 18 h, [Pd]/L (1 mol%)	67
9	22 °C, 18 h, 0.72 mmol, [Pd]/L (1 mol%)	83
10	22 °C, 18 h, 3.9 mmol, ArBpin (1.3 equiv), [Pd]/L (1 mol%)	81
11	22 °C, 18 h, 18 mmol, ArBpin (1.1 equiv), [Pd]/L (1 mol%)	56[e]

[a] isolated yields. [b] incomplete conversion.[c] instead of aryl bromide **29** and aryl boronic acid ester **222**, aryl bromide **227** and arylboronic acid ester **226** were employed (the latter provided by *Julian Greb*[103]). [d] inseparable phenol impurity, according to quantitative ^{1}H-NMR. [e] significant amounts of proto-dehalogenation side product.

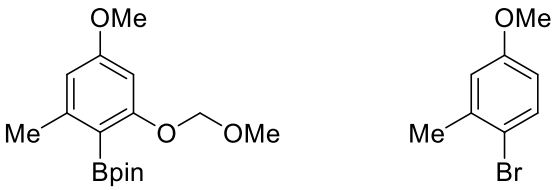

226 **227**

Figure 12: Aryl boronic acid ester **226** provided by *Julian Greb*[103] and aryl bromide **227**.

MOM-deprotection of biaryl **225** proceeded smoothly in a yield of 99% to obtain biaryl phenol **228**.[102]

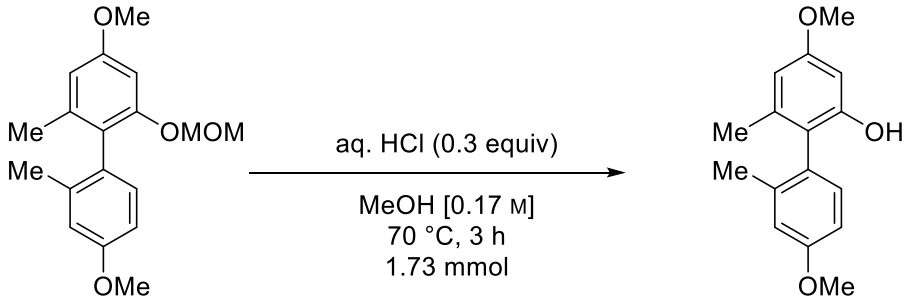

225 **228**
99%

Scheme 49: MOM-deprotection of biaryl **225**.

Overall, a borylation-*Suzuki* cross-coupling sequence involving 2 mol% palladium over two steps starting from phenol **128** could be established. Alternatively, a sequence using MOM-protected arene **29** using 1.5 mol% palladium over three steps was also viable. The former reaction was scaled up to 18 mmol scale.

5.2.1.3 Triflation and amination experiments

With the construction of the tri-*ortho*-substituted axis of biaryl **228** established, transformation of the phenol to an aryl iodide was performed. Unfortunately, no such direct functional group interconversion exists.[235] Instead, introducing an amine as a linchpin for a *Sandmeyer* type reaction was chosen as the most direct route (Scheme 50). The necessary steps involved the synthesis of triflate **230** (Scheme 50 a) with subsequent palladium-catalyzed amination using an ammonia surrogate to obtain 2-aminobiaryl **221** (Scheme 50 b) and finally, a *Sandmeyer* reaction to access 2-iodobiaryl **231** (Scheme 50 c).

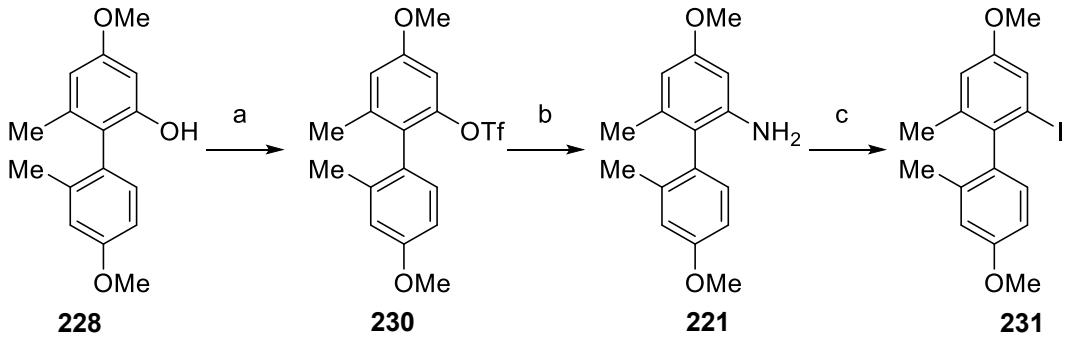

Scheme 50: Functional group interconversion sequence to obtain aryl iodide **231**. [a] Triflation. [b] Amination (potentially with an additional step for the deprotection of the ammonia surrogate). [c] *Sandmeyer*-reaction.

To conduct initial investigations, the triflation amination sequence was investigated with readily available phenol **124** (Chapter 5.1.1). Following a literature known procedure by *Lee at al.*,[236] the desired triflation product **232** was obtained in a yield of 92% by Kugelrohr® distillation (Scheme 51).

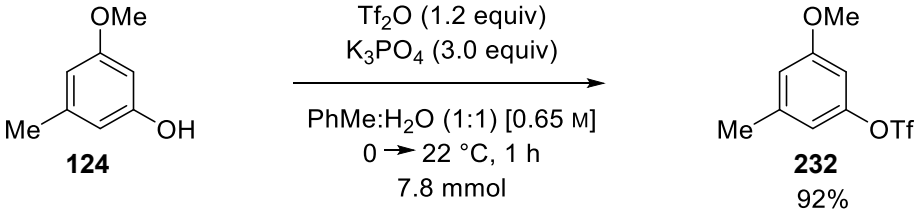

Scheme 51: Triflation of phenol **124**.

Next, the transformation to the aryl amine by *Buchwald-Hartwig* reaction was explored. Freshly distilled benzophenone imine was chosen as a literature known ammonia surrogates to generate primary (1°) aryl amines[60] (other contenders included $(NH_4)_2SO_4$ known for aryl bromides or chlorides[237] and $Zn(HMDS)_2$[236]). Starting conditions were based on a similar, literature know transformation by *Xin et al.*[238] Unfortunately, initial reactions were sluggish and conversions incomplete (Table 7, entries 1 – 5). Activation of the palladium catalyst was suspected to be inadequate (Table 7, entries 5 – 6). In *Buchwald-Hartwig* type aminations, the amine may coordinate competitively and may thus be responsible for Pd^0 deactivation.[230] Additionally, activation of the Pd^{II} species by means of oxidation of the phosphine ligand as reported in literature[149] is not trivial and relies heavily on regents employed.[148, 150] Efforts towards the generation of an active Pd^0-species by pre-activation of the Pd^{II}-source were unsuccessful (Table 7, entries 5-6). The use of a Pd G4 precatalyst[153] was key in the conversion of starting material indicating that Pd^0-activation was indeed responsible. Activation of the Pd G4 catalyst before the addition of benzophenone imine was crucial in complete conversion of starting

material again underscoring the competitive amine/imine coordination. The coupling product **233** could be obtained in a yield of 88%.

Table 7: *Buchwald-Hartwig* amination of model substrate **232** using benzophenone imine.

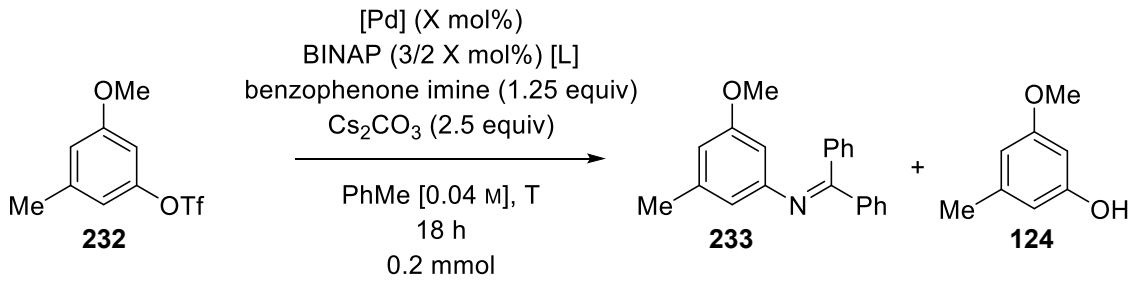

#	Pd-source	Pd [mol%]	Ligand	solvent	T [°C]	Ar-OH [%]	Product [%][a]
1	$Pd(OAc)_2$	6.7	BINAP	THF	70	24	0
2[b]	$Pd(OAc)_2$	2	BINAP	glyme	85	100	0
3[b]	$Pd(OAc)_2$	2	BINAP	PhMe	100	4	46
4	$Pd(OAc)_2$	2	BINAP	1,4-dioxane	100	82	18
5	$Pd(OAc)_2$[c]	5	BINAP	PhMe	100	2	5
6	$Pd(OAc)_2$[c]	10	BINAP	PhMe	100	3	13
7	$Pd(OAc)_2$[c]	20	BINAP	PhMe	100	0	100 (46)
8	SPhos Pd G4	2.5	-	PhMe	110	3	3
9	SPhos Pd G4	2.5	SPhos	PhMe	110	0	20
10	BINAP PdG4[d]	5	BINAP	PhMe [0.2 M]	22	0	0
11	BINAP Pd G4[d]	5	BINAP	PhMe [0.2 M]	80	0	100
12	BINAP Pd G4[d]	5	BINAP	PhMe [0.2 M]	110	0	100 (**88**)

[a] relative conversion of aryl triflate **232** according to ^{1}H-NMR. Isolated yield in parentheses. [b] After 2 days. [c] preactivation by stirring Pd and ligand with $PhB(OH)_2$ for 20 min at rt. [d] prepared by stirring BINAP and $(Pd\ G4)_2$ (**205**) in PhMe for 5 min and then adding Cs_2CO_3 and stirring for a further 30 min at 22 °C.

With an understanding of the handling of *Buchwald-Hartwig* aminations of electron-rich triflates established, the sequence towards 2-iodobiaryl **231** was continued. First the triflation of biaryl **228** was conducted following the same protocol as before. Unfortunately, incomplete conversion (<10%) was observed. Insufficient stirring and therefore background-hydrolysis of the triflic anhydride was suspected to be the cause of this. Thus, a different protocol[239] was

employed avoiding the use of an aqueous solution of base. Indeed, triflate **230** could be obtained by this method in a yield of 87% (Scheme 52).

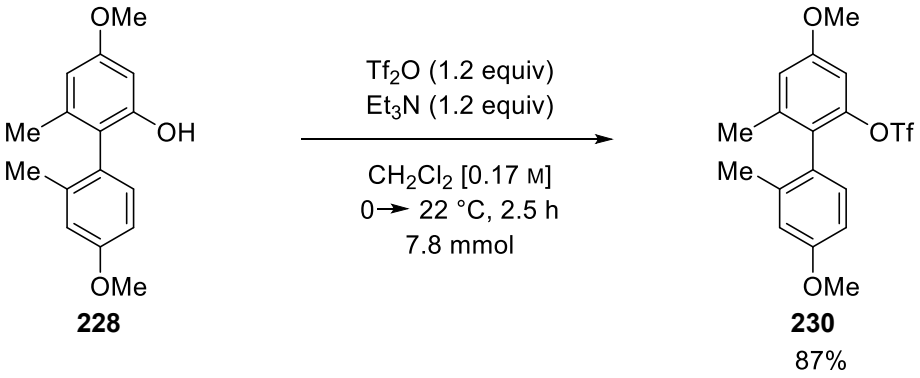

Scheme 52: Triflation of biaryl phenol **228**.

With adequate quantities of triflate **230** in hand, the *Buchwald-Hartwig* amination of the biaryl could be conducted using the previously established conditions (Scheme 53A). In parallel, freshly distilled benzylamine was used as an alternative ammonia surrogate. Using benzophenone imine conversions of starting material and to product **234** were incomplete, while the use of benzylamine resulted in clean and full conversion to the desired product (Scheme 53B). After a scale up to 3.6 mmol, product **235** was isolated in a yield of 95%.

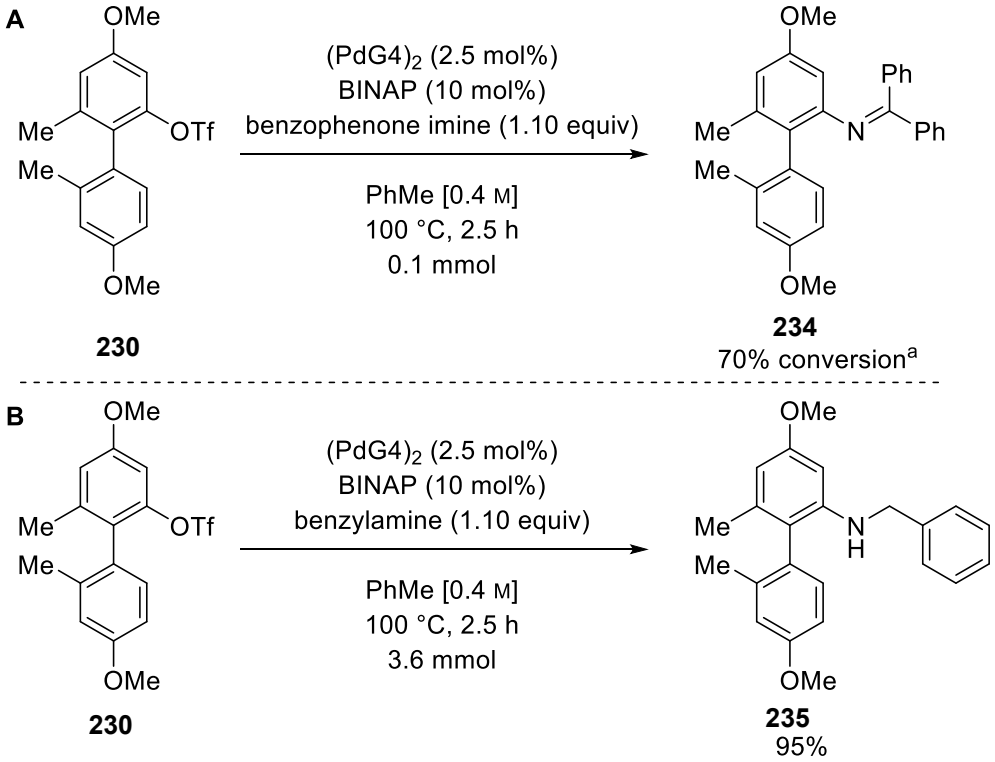

Scheme 53: Palladium-catalyzed *Buchwald-Hartwig* amination of triflate **230** [a] relative ratio according to ^{1}H-NMR.

Deprotection was conducted by hydrogenation and delivered 2-aminobiaryl **221** in a yield of 93% (Scheme 54) in a straightforward manner.

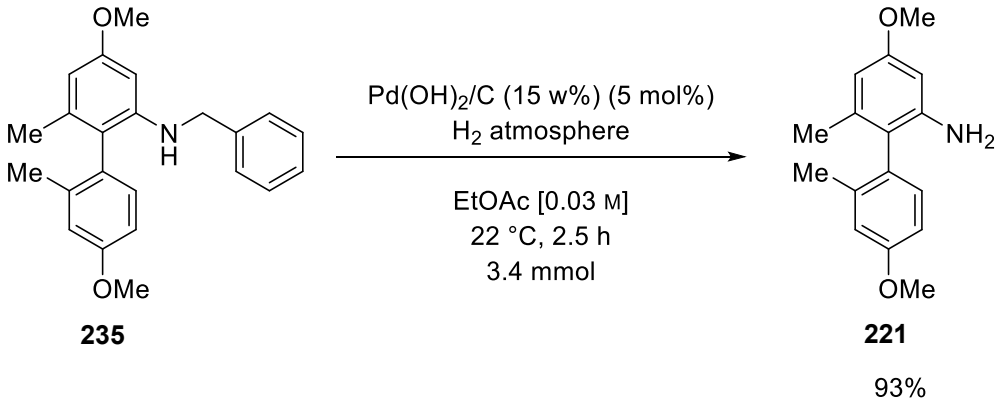

235 **221**

93%

Scheme 54: Palladium-catalyzed hydrogenation to remove the benzyl protecting group to obtain 2-aminobiaryl **221**.

Therefore, a *Buchwald-Hartwig* amination protocol using primary benzylamine with a subsequent deprotection was established.

5.2.1.4 *Sandmeyer* reaction

Next, transformation of the amine to the iodide was investigated. Initial reaction conditions were based on a protocol by *Zhao et al.*[75] Acetone was able to dissolve the starting material amine and thus chosen as the solvent. Initially, large amounts of proto dehalogenated side product **229** were observed (Table 8, entry 2). A high selectivity towards product was especially necessary due to poor separability of product **231** from side product **229** (R_f = 0.51 vs. 0.48 petroleum ether:PhMe 7:3 v/v). Even though ^{1}H-NMR of the red-colored crude product showed no major side products and implied yields >90%, filtration over silica resulted in yields of 70 – 80%. The discrepancy in yield is explained by high-molecular and colorful impurities not detectable by NMR and removed during column chromatographic isolation. In the end, the desired product could be obtained in a yield of 75%.

Table 8: *Sandmeyer* reaction to transform 2-aminobiaryl **221** to 2-iodobiaryl **231**

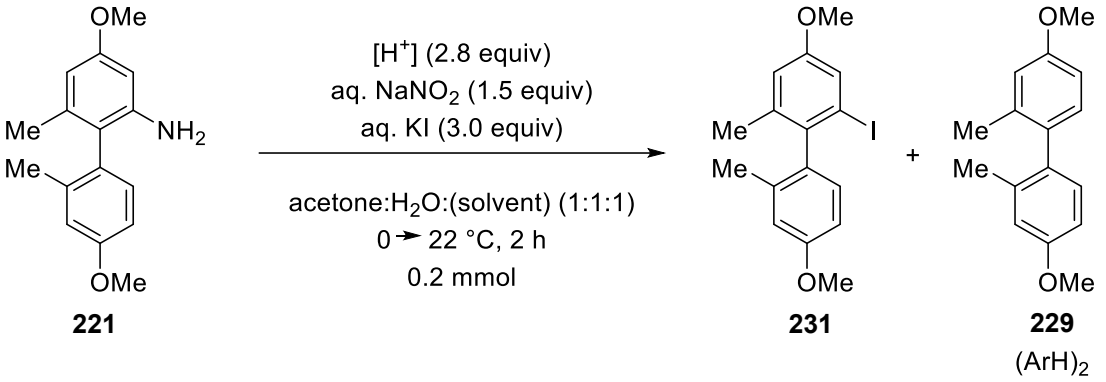

#	Variations	Solvent	[H+]	Product [%][a]	(ArH)2 [%][a]
1	None	Et_2O	H_2SO_4	76	24
2	0.1 mmol, no acetone	Et_2O	H_2SO_4	58	42
3	None[b]	Et_2O	H_2SO_4	80	20
4	None[b]	EtOAc	H_2SO_4	81	18
5	$NaNO_2$ (1.0 equiv)[b]	EtOAc	H_2SO_4	84	16
6	EtOAc[b]	EtOAc	HCl	92	8
7	$NaNO_2$ (1.3 equiv)[b]	EtOAc	HCl	93	7
8	$NaNO_2$ (1.5 equiv)[b]	EtOAc	HCl	93	7
9	$NaNO_2$ (1.5 equiv)[b] 0.8 mmol	EtOAc	HCl	88 (**75**)	12

[a] relative conversion of aryl triflate **232** according to ^{1}H-NMR. Isolated yield in parentheses. [b] Slow addition: aqueous solutions of $NaNO_2$ (0.5 mL/h) and KI (0.2 mL/h) were added *via* syringe pump.

With 2-iodobiaryl **231** in hand, the synthesis of electron-rich cyclic iodonium salts could be investigated. Unfortunately, transformation of 2-iodobiaryl **231** under literature known conditions was unsuccessful (Scheme 55A).[240] Reaction controls were performed 5 mins after the addition of acid. Only complex ^{1}H-NMR spectra were obtained. Even conditions developed for electron-rich diaryliodonium salts using toluene sulfonic acid (TsOH) were incompatible with the employed biarylic system (Scheme 55A).[84, 241] A brown tar with unidentifiable signals and complex ^{1}H-NMR spectra was obtained. The synthesis strategy had to be reevaluated after this setback.

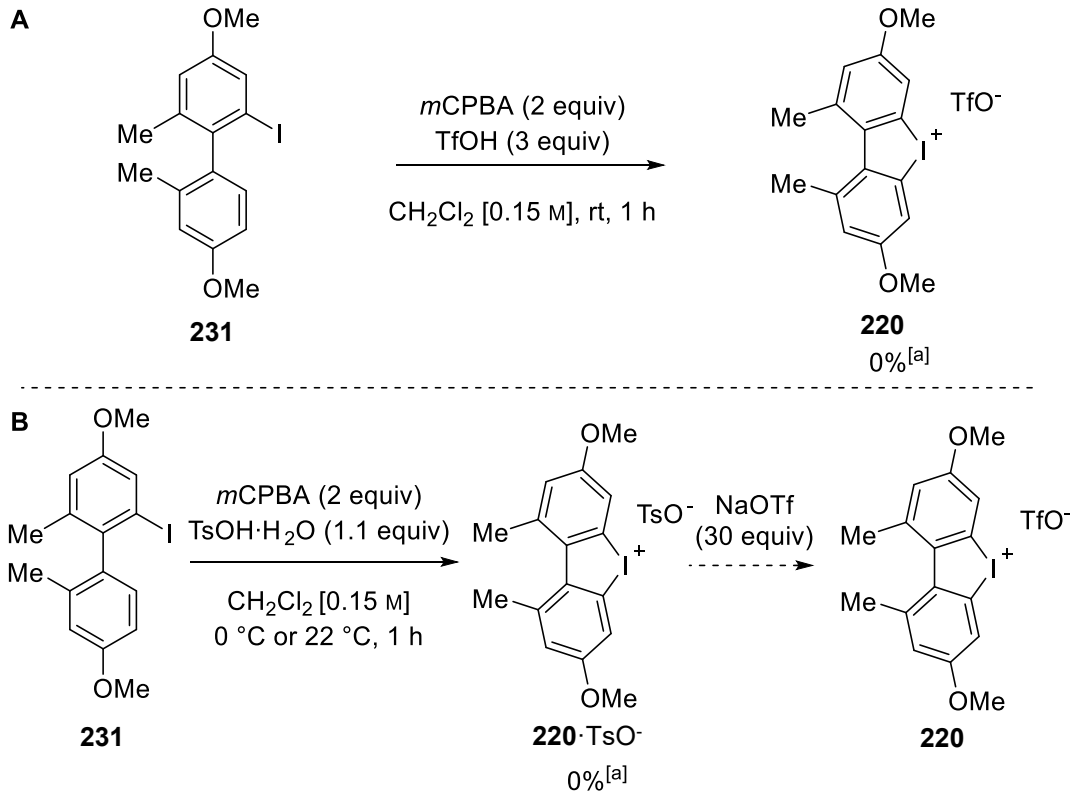

Scheme 55: Oxidative acid catalyzed cyclization of 2-iodobiaryl **231** to form the desired cyclic diaryliodonium triflate salt **220**. [a] complex ^{1}H-NMR.

Overall, protocols for the *Masuda* (and *Miyaura*) borylation, *Suzuki-Miyaura* cross-coupling, *Buchwald-Hartwig* amination and *Sandmeyer* reaction could successfully be established. These procedures will serve as the basis for future investigations in following chapters. Additionally, knowledge gathered from these optimizations would play a pivotal role in following studies.

5.2.2 Non-electron-rich cyclic diaryliodonium salt

The following chapter contains results obtained by Daniel Grudzinski as part of a bachelor's thesis,[206] additionally containing results published in Klischan et al. Org. Lett. ***2024***[228] *as well as in Mazzone et al. Front. Chem.* ***2024***.[224]

The synthesis strategy was reevaluated so that an alternative approach would benefit from a lot of the knowledge and protocols obtained thus far. This strategy revolved around the synthesis of less electron-rich 2-iodobiaryl **236** to then form literature known cyclic diaryliodonium salt **237**. Enantiopure 2,2′-diiodobiaryl **238** would be obtained *via* enantioselective ring opening (akin to a dynamic kinetic resolution) (Figure 9). Introduction of the methoxy groups would proceed by Ir-catalyzed *meta*-selective borylations to access the 1,3,5 substitution pattern (**239**). Critically, this synthesis strategy allows for the use of the boronic acid esters as synthetic handles for further functionalization. Overall, both enantiomers of biphenol **27** could be obtained *via* this strategy in eight steps, a step-count unmatched by the previous synthetic strategy (5.2.1).

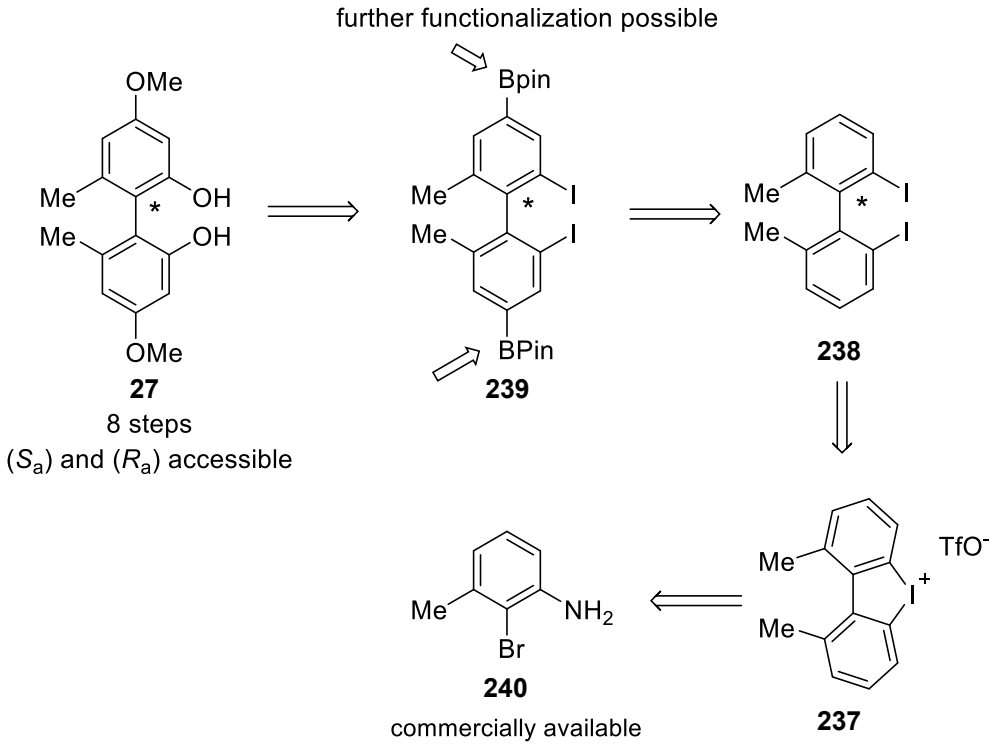

Scheme 56: Synthesis strategy avoiding electron-rich cyclic diaryliodonium salts *via* cyclic diaryliodonium salt **237**.

5.2.2.1 Synthesis of Starting material

First, cyclic diaryliodonium salt **237** was to be synthesized on decagram scale. Starting from commercially available **240**, quantitative conversion to product was observed following the conditions of the previously established *Suzuki* cross-coupling protocol (Chapter 5.2.1.2). Addition of HCl to the crude mixture precipitated the 2-aminobiaryl **241·HCl** which was isolated in a yield of 91%. The subsequent *Sandmeyer* reaction again proceeded smoothly providing the corresponding 2-iodobiaryl **236** in a yield of 81% (Scheme 57A). Finally, *via* the literature known oxidative ring closure,[77] iodonium salt **237** was obtained in a yield of 78% (Scheme 57B). No column chromatographic isolation was required over this three-step sequence, simple filtration over silica or Celite® was sufficient which greatly highlights the scalability of this approach.

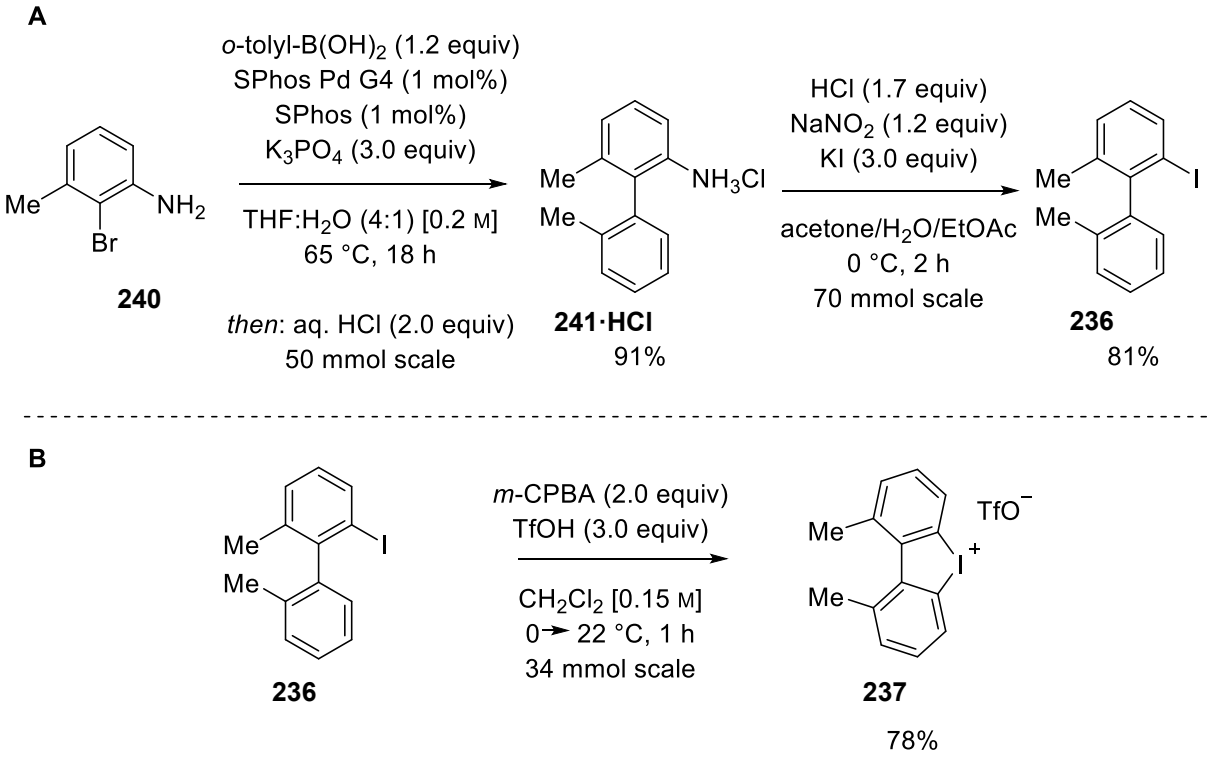

Scheme 57: Synthesis route towards cyclic diaryliodonium salt **237**.

5.2.2.2 Cyclic diaryliodonium enantioselective ring opening

To carry out enantioselective ring opening of cyclic diaryliodonium salt **237**, bisoxazoline (BOX) ligand **L1** was synthesized following literature known procedures using dinitrile **242** and aminoindanol **243**.[242] The product was isolated in a yield of 23% (lit.: 100%[242a], 71%[242b]) with the mono addition product **244** as a major side product (27%) (Scheme 58). In general, literature known conditions contained major discrepancies regarding equivalents $Zn(OTf)_2$ used in the reaction (reported 1.0 equivalents to be optimal, mass of experimental procedure

corresponds to 0.1 equivalents).[242] Ultimately, affordable and commercially available BOX ligand **L2** was purchased to avoid lengthy optimizations of said conditions.[9][243]

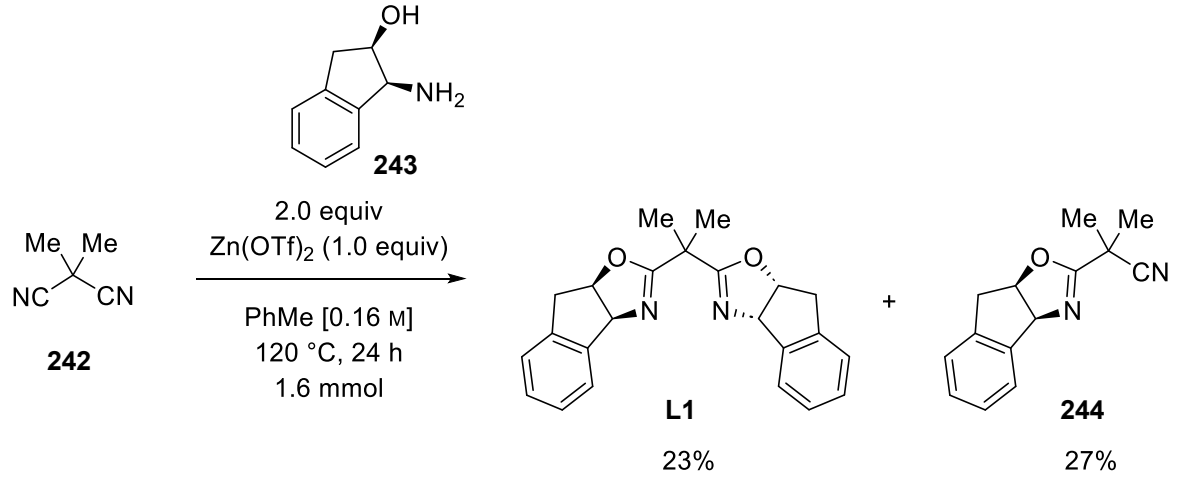

Scheme 58: Synthesis of BOX ligand **L1**.

Next, the ring opening using iodide sources was investigated in collaboration with *Daniel Grudzinski*. The enantioselective ring opening of iodonium salts using halides is literature known with protocols by *Zhu et al.*[81b] (cond. A, Table 9) and *Ke et al.*[81a] (cond. B, Table 9). The viability of their approaches was investigated and showed similar enantiomeric excess only differing in conversion to product (Table 9, entries 6 and 7). Ultimately, the protocol by *Zhu et al.*[81b] was chosen to avoid the use of HFIP due to concerns regarding polyfluorinated compounds even though conversions to product were higher.[244] From this point onward anhydrous CH_2Cl_2 in combination with dried NaI were used to improve yields as hydrolysis of **237** was reported as the major side product in this reaction.[81b] Ring opening in the absence of both ligand (entry 1) and Cu with ligand (entry 2) were investigated. This would effectively constitute the racemic background ring opening. Indeed, a conversion to product of 5% by ^{1}H-NMR was observed. This is in agreement with the experimentally observed e.r. of 97:3 (94%*ee*). Enantiomeric excess was difficult to assess for the (S_a)-**238** enantiomer due to the poor baseline separation and thus is reported with 91%*ee* (Table 9, entry 11) even though indirect assessment of the following steps indicated 94%*ee*, the same enantiomeric excess as (R_a)-**238** (Table 9, entry 12). After successful scale up to 18.0 mmol, both enantiomers of 2,2′-iodo biaryl **238** were obtained in yields of 82 – 94% by filtration. Synthesized BOX ligands **L1** and commercially purchased **L2** gave comparable *ee* values (Table 9, entry 4 and 6).

[9] (*S,S*)-**L2** 89€/g, (*R,R*)-**L2** 107€/g, 11/11/2023 BLDPharm

Table 9: Optimization of the enantioselective ring opening of cyclic biaryl iodonium salt **237**.

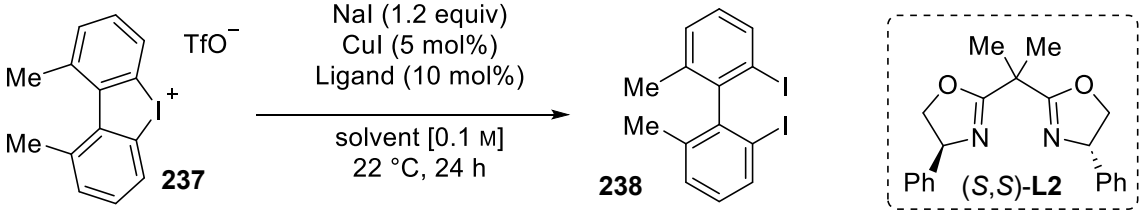

#	Cu [mol%]	Scale [mmol]	Conditions	Ligand [mol%]	Product [%][a]	ee [%][c]
1	5	0.05	A	–	(5)	–
2	–	0.05	A	–	(5)	–
3	5	1.50	TBAI (1.0 equiv), CH_2Cl_2	–	93	*rac*
4	5	0.33	A	(*S*,*S*)-**L1**	90	88
5	5	1.32	A	(*S*,*S*)-**L1**	88	88
6	5	0.10	A	(*S*,*S*)-**L2**	(100)	92
7	5	0.10	B	(*S*,*S*)-**L2**	(73)	88
8	5	1.50	A	(*S*,*S*)-**L2**	96	94
9[b]	5	1.50	B	(*S*,*S*)-**L2**	82	84
10[b]	5	12.0	B	(*S*,*S*)-**L2**	94	91
11	5	18.0	B	(*S*,*S*)-**L2**	86	91
12	5	18.0	B	(*R*,*R*)-**L2**	82	−94

Condition A: **L2** 10 mol%, TBAI (1.0 equiv), HFIP. Condition B: **L2** 7.5 mol%, NaI (1.2 equiv), CH_2Cl_2. [a] Isolated yield; conversion to product according to ^{1}H-NMR in parentheses using 1,3,5-trimethoxybenzene as an internal standard. [b] **L2** 10 mol%. [c] enantiomers not base line separated by HPLC, thus *ee* reported may vary.

5.2.2.3 Borylation

With key-intermediate **238** in hand introduction of the methoxy groups in *meta*-position was tackled to obtain biaryl **239**. Ir-catalyzed borylations have been established since the early 2000s by *Ishiyama et al.* of the Miyaura group.[245] The selectivity of these C–H activation reactions is sterically controlled. In particular the Hartwig-group has investigated the mechanism of this reaction.[246] Plenty of review articles highlight the wide application and usefulness of this transformation.[247] Additionally, biarylic systems have been subjected to similar transformations albeit only achiral phosphines.[248] As outlined in the introduction to this chapter, the boronic acid ester moieties introduced in this step would serve as linchpins for further functionalization, such as the oxidation to the desired phenol. Initial conditions using 6 mol% iridium (3 mol% dinuclear Ir-source) gave a selective turnover to product. Separation of the mono-borylated side product **245** proved not possible by column chromatography in addition to low solubility of the borylated product **239**. Thus, full conversion of starting material and intermediate products was of major importance for full characterization. First, the catalyst loading was investigated. Lowering the catalyst loading on this scale below 1.5 mol% $[Ir(COD)OMe]_2$ only gave trace amounts product **239** (Table 10, entries 1 – 4). A scale up in the same reaction vessel (2 dram vials, see Chapter 7) with 1.5 mol% $[Ir(COD)OMe]_2$ instead gave conversion to product analogous to 3 mol% (Table 10, entries 9 and 10). Reactions were continued to be carried out with 3 mol% $[Ir(COD)OMe]_2$ for any scale ups for the sake of robustness. A reaction time of 1 h gave high conversion to product yet incomplete conversion of intermediate **245** (Table 10, entry 5). A reaction at 22 °C gave incomplete conversion mostly to intermediate product **245** (Table 10, entry 6). The use of 2.2 equivalents B_2pin_2 were required to achieve near-quantitative yields (Table 10, entry 8). In the end, a catalyst loading of 3 mol% $[Ir(COD)OMe]_2$ gave excellent yields of 98% on 10 mmol scale (Table 10, entry 11 and 12). Purification by filtration over a plug of silica in combination with a subsequent base wash resulted in full removal of trace impurities of catalyst and pinacol. Thus, a very high yielding protocol could be established. Enantiomeric excess remained high over this sequence.

Table 10: Optimization of the double *meta*-selective borylation.

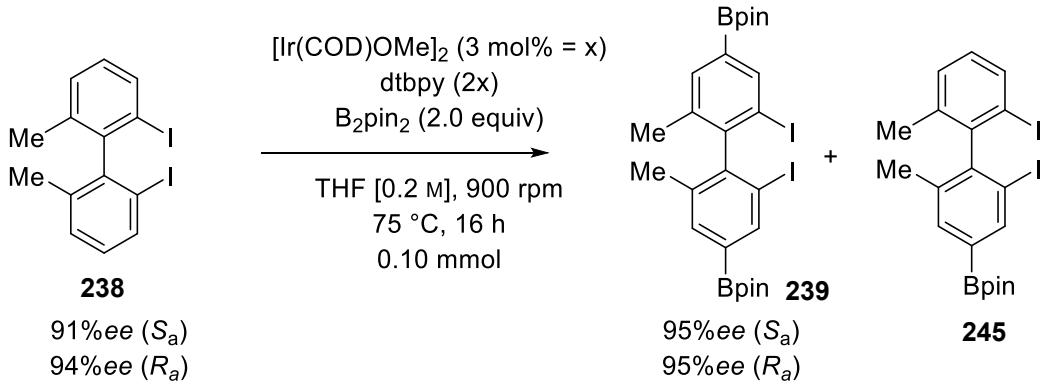

238
91%*ee* (S_a)
94%*ee* (R_a)

239
95%*ee* (S_a)
95%*ee* (R_a)

245

#	Variations	Product [%][a]	Intermediate [%]
1	None	(89±3)	5±1
2	$[Ir(COD)OMe]_2$ (0.38 mol%)	(1±1)	(1±1)
3	$[Ir(COD)OMe]_2$ (0.75 mol%)	(0±0)	(2±1)
4	$[Ir(COD)OMe]_2$ (1.5 mol%)	(7)	(43)
5	1 h reaction time	(78±0)	(28±5)[b]
6	22 °C	(33±5)	(50±4)[b]
7	Anhydr B_2pin_2	(90)	traces
8	B_2pin_2 (2.2 equiv)	(99)	traces
9	0.5 mmol scale, B_2pin_2 (2.2 equiv)	96[b]	traces
10	0.5 mmol scale, $[Ir(COD)OMe]_2$ (1.5 mol%), B_2pin_2 (2.2 equiv)	93[b]	traces
11	(S_a), 10.0 mmol scale, B_2pin_2 (2.2 equiv)	98[b]	traces
12	(R_a), 10.0 mmol scale, B_2pin_2 (2.2 equiv)	98[b]	traces

Reactions were performed on 0.10 mmol scale. Entries with standard deviation performed as duplicates. [a] Conversion to product according to ^{1}H-NMR in parentheses using 1,3,5-trimethoxybenzene as an internal standard. [b] Isolated yield.

An x-ray structure was obtained (Dr. *Wolfgang Frey,* University of Stuttgart) for the (S_a)-enantiomer that confirmed the absolute configuration (Figure 13).

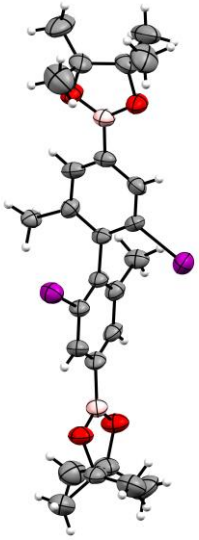

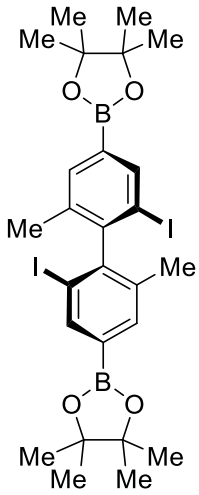

(S_a)-**239**

Figure 13: Left: X-ray structure of **239**. ORTEP at 50% probability. Right: Lewis structure interpretation.

5.2.2.4 Oxidation boronic acid ester and methylation

With the borylation established, the functional group interconversion to the phenol was tackled. There are a variety of methods for the oxidation of boronic acids to phenols using different oxidizing agents. Oxone®, a mixture of potassium persulfate and potassium sulfate is a cheap, non-toxic and comparably benign option.[249] Initial conditions were based on a protocol by Maleczka *et al.*[250] After a short screening, a reaction time of 24 h in combination with 4.0 equivalents Oxone® (effectively 2.0 equivalents potassium peroxomonosulfate) gave the desired product **246** in yields of 82 – 85% with little observed intermediate **247** (Table 11). The remaining mass-balance could be explained by over-oxidation of the aryl-iodide as is reported in literature.[251]

Table 11: Optimization of the double oxidation of aryl boronic acid esters.

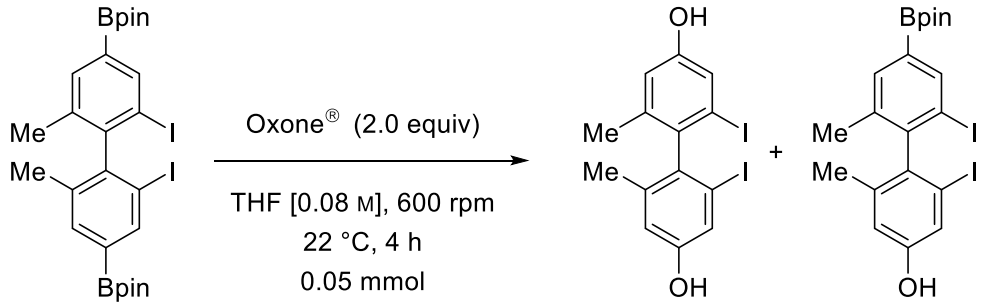

239 **246** **247**

95%*ee* (S_a)
95%*ee* (R_a)

92%*ee* (S_a)
94%*ee* (R_a)

#	Variations	(ArBpin)$_2$ [%][a]	(ArOH)$_2$ [%][a]	ArBpin-ArOH [%][a]
1	None	3	68	24
2	Acetone	73	22	0
3	24 h	4	75	15
4	24 h, Oxone® (4.0 equiv)	0	77	5
5	24 h, Oxone® (4.0 equiv), 0.40 mmol scale	–	**85**[b]	–
6	(S_a), 24 h, Oxone® (4.0 equiv), 4.00 mmol scale	–	**85**[b]	–
7	(R_a), 24 h, Oxone® (4.0 equiv), 4.00 mmol scale	–	**82**[b]	–

Reactions performed on a 0.05 mmol scale. [a] Conversion to product according to ^{1}H-NMR using 1,3,5-trimethoxybenzene as an internal standard. [b] isolated yield.

Subsequent methyl protection proceeded smoothly to provide 2,2′-diiodobiaryl **249** yields of 89% – 95%. Enantiomeric excess was retained over the oxidation-methylation sequence.

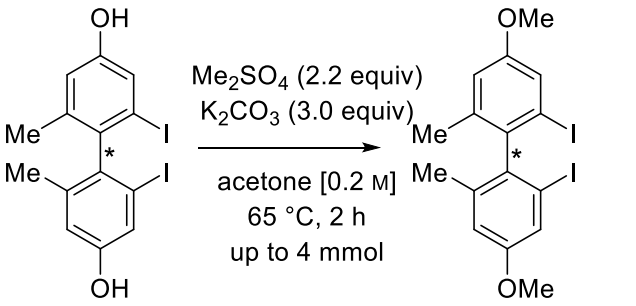

246
92%*ee* (S_a)
94%*ee* (R_a)

249
89%, 92%*ee* (S_a)
95%, 95%*ee* (R_a)

Scheme 59: Methylation of biphenol **246**.

Thus, a reliable and high yielding sequence towards meta-methoxylated biaryls could be established with yields of 74% (S_a) and 76% (R_a) over three steps. Furthermore, the absolute configuration and proposed structure of key-intermediate **239** were supported by an x-ray structure (measured by Dr. *Wolfgang Frey*).

5.2.2.5 Dehalo-Oxygenation

The final step towards biphenol **27** involved the transformation of the aryl iodide into a phenol. Initial investigations for this transformation were based on the literature known protocol by *Ke et al.*[81a] The reaction follows a metal-halogen exchange with subsequent addition of freshly distilled nitro benzene (lit.: 63% yield for **253**). The efficacy of this first step was probed by deuteration experiments (Table 12). Deuterium incorporation was high for both **249** and **238** (Table 12, entries 1 and 5, Figure 14, Figure 15). Curiously, when using THF as the solvent, quantitative conversion to mono-butylation side product **251** with deuteration >95% was observed (Table 12, entry 2). The formation of this product was investigated in more detail to also identify potential sources of protonation. First, the reaction was stirred at 22 °C for 1 h in THF before quenching with D_2O (Table 12, entry 3). Little double protonation/deuteration product **238** was observed. Instead, previously observed mono-butylation product **251** as well as suspected double-butylation product **252** were detected. Deuteration of **238** <10% indicated that protonation occurs at ambient temperatures under these conditions. The use of 4.4 equivalents of *n*-BuLi was investigated (Table 12, entry 4). The additional equivalents of base would eliminate excess *n*-BuI. Indeed, little butylation was observed supporting the notion of *n*-BuI serving as the butyl source *via* nucleophilic substitution. The *n*-BuI could also be the proton source by elimination of HI. While little butylation was observed when using 4.4 equivalents of *n*-BuLi, little deuteration was also observed indicating that background protonation at 22 °C still occurs. Still, the use of 4.4 equivalents *n*-BuLi additionally served the

purpose of eliminating excess *n*-BuI that could also lower yields of the phenol products by forming butyl ether side products.

Table 12: Optimization of the deuteration experiments to show the efficacy of the metal-halogen exchange.

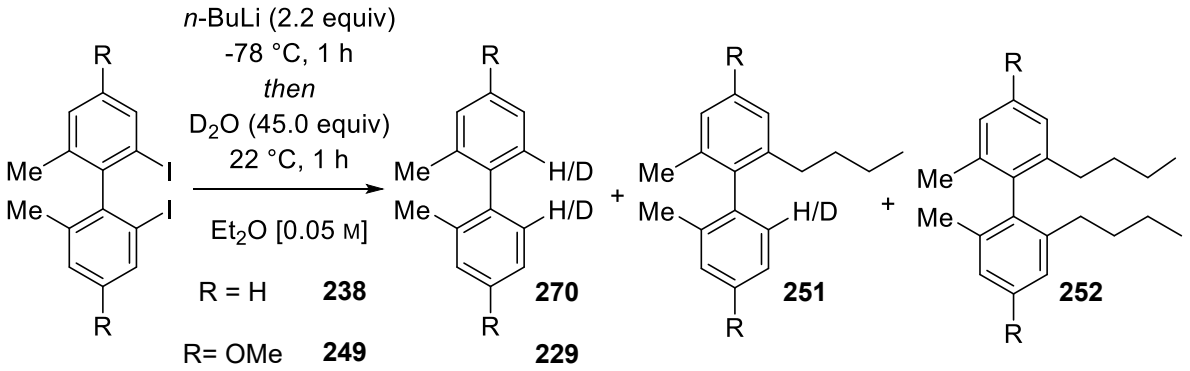

#	Variations	Products[a]				
	R = H	$(ArH/D)_2$ [%]	Deuteration [%]	ArH/D-ArBu [%]	Deuteration [%]	$(ArBu)_2$ [%]
1	None	95	94	0	–	–
2	THF	5	–	90	96	–
3[b]	THF, stir at 22 °C for 1 h before D_2O addition	4	–	59	<10	41
4	THF, *n*-BuLi (4.4 equiv), stir at 22 °C for 1 h before D_2O addition	45	<10	9	-	0
	R = OMe					
5	*n*-BuLi (4.4 equiv)	88	89	–	–	–

Reactions were performed on a 0.10 mmol scale. [a] Conversion to product according to ^{1}H-NMR using 1,3,5-trimethoxybenzene as an internal standard. [b] suspected 41% conversion to $(ArBu)_2$ product, sum of products >100%.

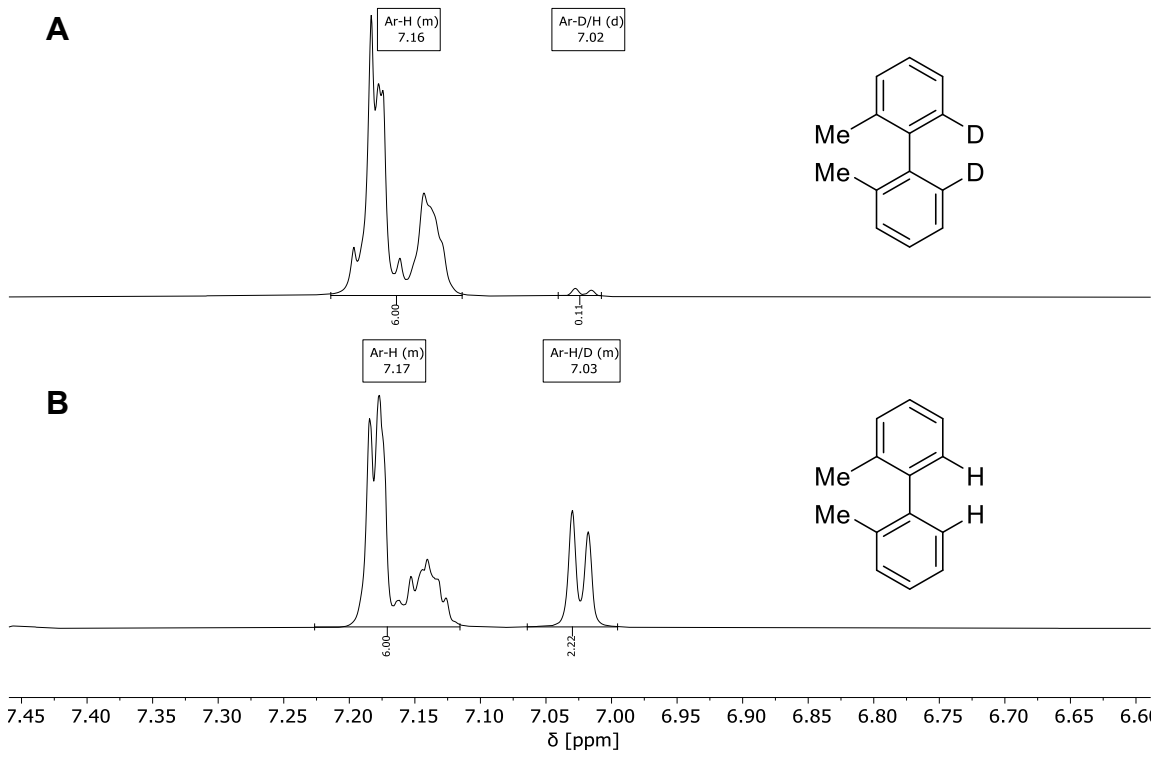

Figure 14: Halogen-metal exchange and subsequent quenching of 2,2′-diiodobiaryl **238** to form proto-halogenation product **270**. (A) Metal-Halogen exchange terminated with D_2O. (B) Metal-Halogen exchange terminated with H_2O.

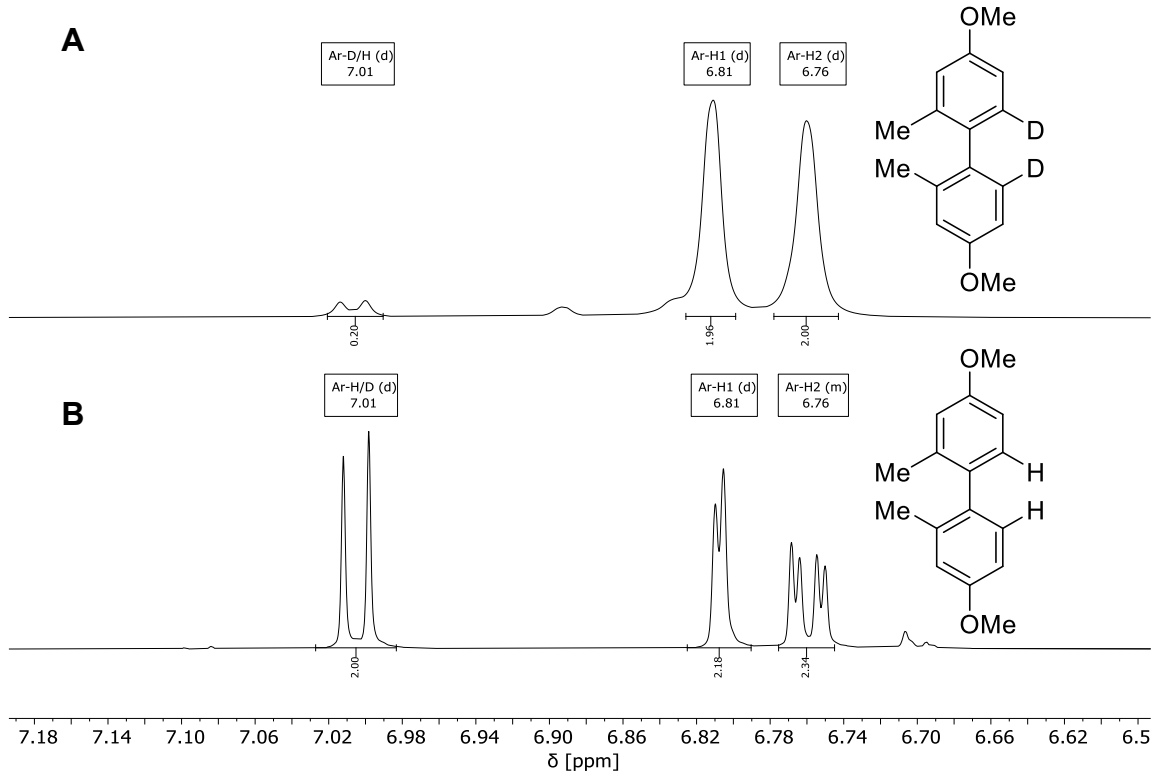

Figure 15: Halogen-metal exchange and subsequent quenching of 2,2′-diiodobiaryl **249** to form proto-halogenation product **229**. (A) Metal-Halogen exchange terminated with D_2O. (B) Metal-Halogen exchange terminated with H_2O.

With the metal halogen exchange step confirmed to proceed with high efficacy the next step of this reaction was probed. Different 'electrophilic' oxygen sources were investigated (Table 13, entries 1 – 10). Overall, molecular oxygen dried by various methods generally gave unselective conversions with large quantities of protonation side products. Either drying of the oxygen was insufficient, or another means of protonation was present as indicated by the deuteration experiments before. This protonation source could not be identified. Thus, nitrobenzene was further investigated as the oxygenating agent. In addition to the desired product **27**, the investigations were initiated with the synthesis of **253**. The use of *t*-BuLi instead of *n*-BuLi as a stronger base to better avoid protonation *via* the forming alkyl iodide did not result in a more selective product formation (Table 13, entry 11 vs 12). In addition to these metal halogen exchange reactions, transition metal catalysis using Cu[252] and Pd[253] by established protocols was investigated but resulted in no conversion to product (*ee* of the reisolated starting material **249** was retained) (Table 13, entries 13 and 14). In the end, biphenol **27** could be obtained in yields of 55 – 62% on up to 3.5 mmol scale following a protocol by *Ke et al.*[81a]. Recrystallization enriched the enantiomeric excess (>99%*ee*) with overall yields of 47% (S_a) and 47% (R_a) for the whole transformation.

Overall, a new method could be established that uses cyclic diaryliodonium salts to obtain both enantiomers of BIPOL (**27**) with >99%*ee*. A yield of 30% over five steps starting from cyclic iodonium salt **237** and 17% over eight steps, starting from commercially available starting materials was achieved. The reaction could be scaled up to 3.5 mmol scale. Valuable intermediate **239** was obtained that can serve as the starting point for various transformations (Chapter 6.2).

Table 13: Optimization of the dehalo-oxygenation *via* metal halogen exchange.

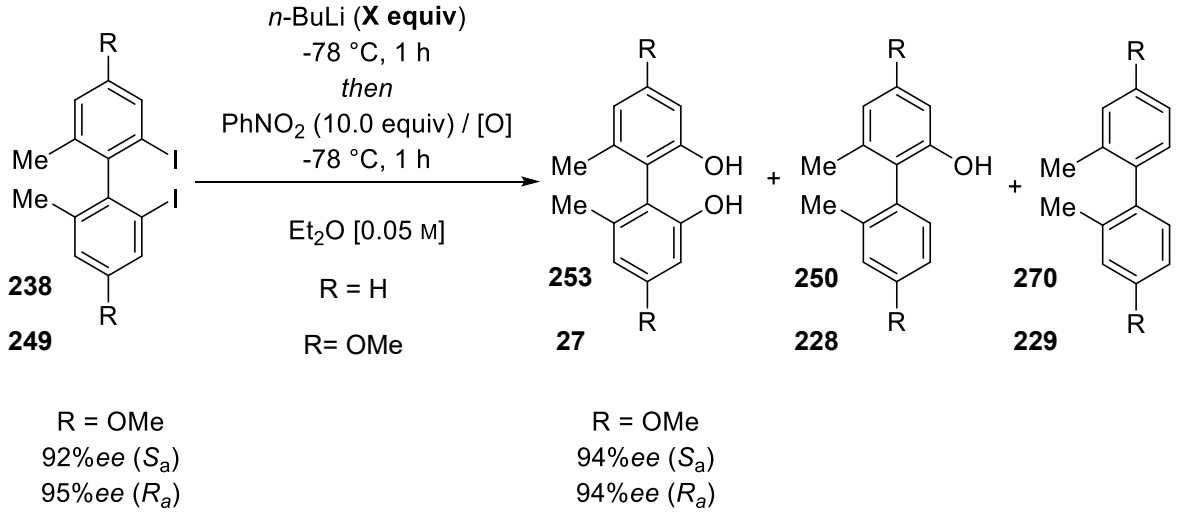

#	Variations	Products[a]			
R = H	***n*-BuLi (2.2 equiv)**	$(ArOH)_2$ [%]	$(ArH)_2$ [%]	ArH-ArOH [%]	$(ArI)_2$ [%]
1	None	44	29	24	0
2	[O] = Oxygen flask dried over acetone/dry ice trap	11	27	24	7
3	[O] = Oxygen balloon dried over Sicapent®	20	33	27	0
4	[O] = Oxygen balloon dried over Sicapent® Equip balloon, stir for 16 h at −78 °C	17	23	31	0
5	[O] = Oxygen balloon dried over Sicapent® Equip balloon, stir for 1 h at 22 °C	17	22	30	0
6	[O] = Oxygen balloon dried over Sicapent® Equip balloon, stir for 16 h at 22 °C	15	23	30	0
7	[O] = Oxygen balloon dried over $CaCl_2$	22	15	33	0
8	[O] = Oxygen balloon dried over Sicapent® Quench with D_2O after 1 h O_2 at 22 °C	16	30[c]	28	0
9	*n*-BuLi (4.4 equiv), [O] = Oxygen balloon dried over Sicapent®	28	15	35	0
10	*t*-BuLi (4.4 equiv), [O] = Oxygen balloon dried over Sicapent®	16	14	23	17
11	*n*-BuLi (4.4 equiv)	54 (**44**)[b]	27	11	0
12	*t*-BuLi (4.4 equiv)	26	45	0	0
13	Conditions: CuI (20 mol%), dibenzoylmethane (1.0 equiv), KOH (6.0 equiv), DMSO:H_2O (1:1) [0.25 M][252]	2	0	0	95
R = OMe	***n*-BuLi (4.4 equiv)**				
14	Conditions: $Pd(dba)_2$ (5 mol%), *t*-BuBrettPhos (20 mol%), KOH (6.0 equiv), H_2O (40 equiv), dioxane [0.25 M][253][d]	0	0	6	81
15	*n*-BuLi (2.2 equiv)	21	16	26	27
16	None	56±1 (**54**)[b]	16±1	16±1	0
17	$PhNO_2$ solution in Et_2O at -78 °C	52	14	23	0
18	$PhNO_2$ solution in Et_2O at 22 °C	22	16	26	0
19	–95 °C[e]	59	8	18	0
20	0.40 mmol scale	52	7	15	0
21	1.97 mmol scale	(**55**)[b]	–	–	–
22	3.49 mmol scale	(**62**)[b]	–	–	–

Reactions were performed on 0.10 mmol scale. Entries with standard deviation performed as duplicates. [a] Conversion to product according to ^{1}H-NMR using 1,3,5-trimethoxybenzene as an internal standard. [b] isolated yield. [c] 25% deuterated according to ^{1}H-NMR. [d] positive control using 4-iodo anisol gave conversion to product [e] methanol:liquid N_2 bath, temperature according to thermometer

5.2.3 Synthesis of enantioenriched biflavones and bichalcones

The results of the following chapter were published in Klischan et al. Org. Lett. ***2024***[228] *as well as in Mazzone et al. Front. Chem.* ***2024***.[224]

With a scalable and reliable synthesis of biphenol **27** established, the application of this method was to be shown by the synthesis of enantiopure biflavones and bichalcones. As discussed before, racemic bichalcone **166** (Chapter 5.1.3) and racemic biflavone **181** (Chapter 5.1.4) were of particular interest for further investigations due to high bioactivities against microbes and/or malignant human cell lines with low cytotoxicity towards healthy human cell lines. Following a literature known protocol by *Greb et al.,*[102] the Friedel-Crafts acetylation was conducted. Both enantiomers of acetophenone dimer **134** were isolated in yields of 75 – 78% (Scheme 60).

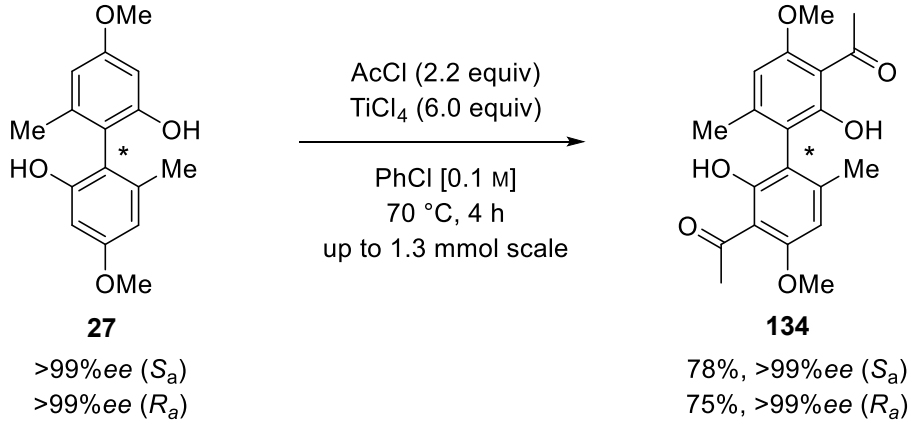

27
>99%*ee* (S_a)
>99%*ee* (R_a)

134
78%, >99%*ee* (S_a)
75%, >99%*ee* (R_a)

Scheme 60: Synthesis of both enantiomers and racemic mixture of 8,8′′-biphenol **183** starting from enantiopure biphenol **27** and racemic acetophenone **134**.

5.2.3.1 Synthesis of enantiopure bichalcones

First, enantiopure bichalcone **166** was synthesized. The *Claisen-Schmidt* condensation proceeded smoothly albeit with lower yields compared to the racemic mixture (88%, Chapter 5.1.3). to provide both enantiomers of bichalcones **166** in yields of 54 – 61%. The increased solubility of enantiopure bichalcone **166** in comparison to the racemic mixture was crucial in successful column chromatographic isolation yet may have also contributed to the formation of more flavanone side products. Assessment of the bioactivity performed by *Flaminia Mazzone* revealed that the (R_a)-enantiomer exhibited higher activity against *T. gondii* than then (S_a)-enantiomer while overall only being slightly more active than the racemic mixture (Scheme 61). The overall activity and selectivity indices of **166** exceeded those of pyrimethamine (lit.: $IC_{50\ T.\ gondii}$ 0.4 µM, SI > 202)[225] as the benchmark treatment for toxoplasmosis.[226]

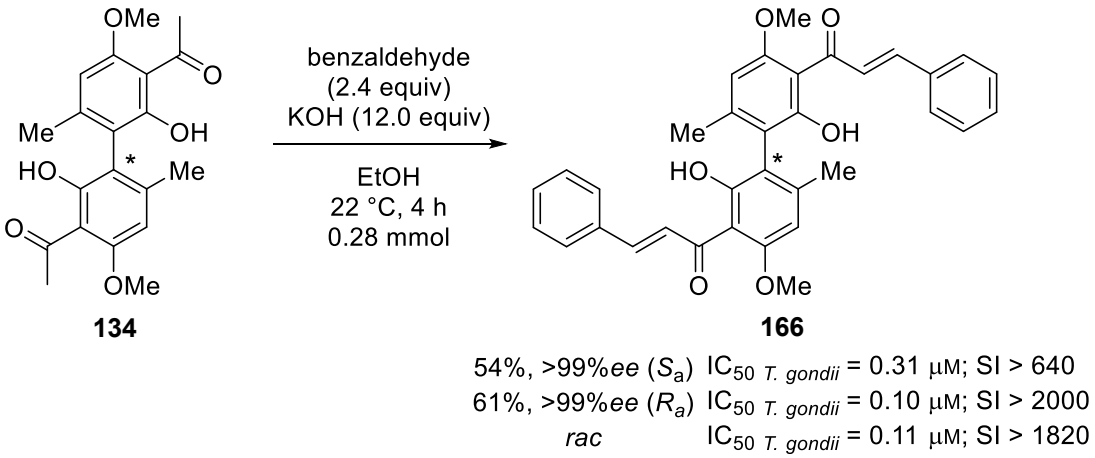

Scheme 61: *Claisen-Schmidt* condensation of enantiopure biacetophenone **134** to synthesize both enantiomers of bichalcone **166**.

Stability experiments revealed that while stable in DMSO at -20 °C for several months, particularly at elevated temperatures in MeOH with KOH emulating reaction conditions, a deterioration could be observed (Table 14). This is in line with lower yields observed for the enantiopure compounds.

Table 14: Stability experiments using bichalcone **166** under various conditions.

#	Variations	Time	Purity [%]
1	22 °C, DMSO	24 h	76
2	40 °C, DMSO	24 h	77
3	−20 °C, DMSO	6 months	96
3	40 °C, MeOH, KOH	24 h	36
4	40 °C, MeOH	24 h	90

To identify these side products, a reaction at 70 °C was performed on the same scale. Indeed, a complex mixture was observed by ^{1}H-NMR (Scheme 62A). This mixture was subjected to HRMS analysis using Bruker® timsTOF Pro (PASEF®) to identify the number of isomers present. In total, six isomeric peaks could be extracted (Scheme 62C), which is in line with the expected total number of isomers for bichalcone **166** (1x), flavanone-chalcones **254** (2x) and biflavanones **255** (3x) (Scheme 62B).

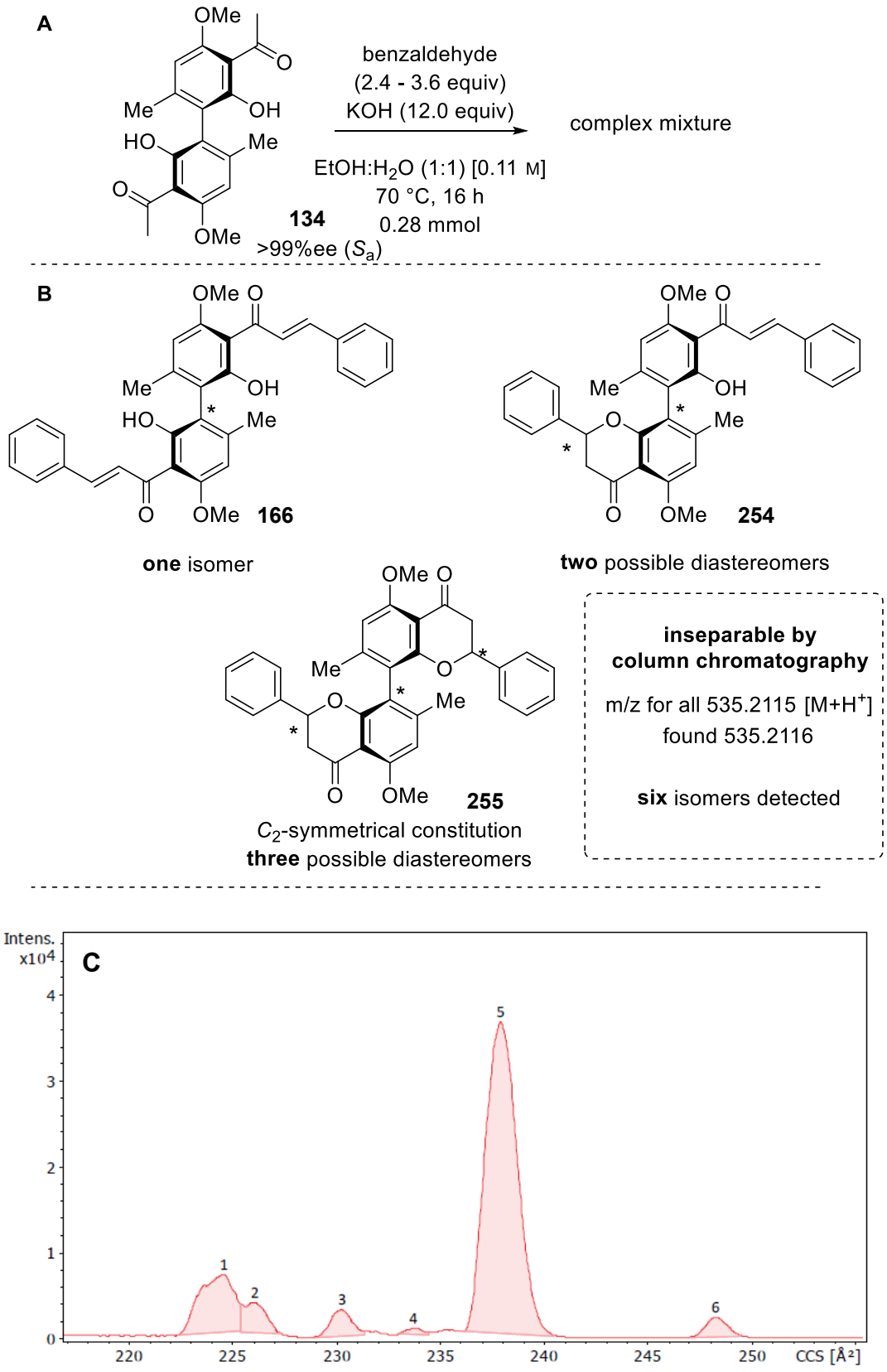

Scheme 62: (A) Bichalcone synthesis at 70 °C for 18 h, complex mixture according to ^{1}H-NMR. (B) Possible flavanone-chalcone and flavanone-flavanone diastereomers (C) Extracted mobilogram for [M+H^{+}] of 535.2115 theoretical m/z 535.2115 of the crude product separated by trapped ion mobility using collisional cross section (CCS) analysis.

5.2.3.2 Synthesis of Enantiopure Biflavones

With both enantiomers of biphenol **27** in hand, brominated biflavone **183** was synthesized (Scheme 63A). *Claisen-Schmidt* condensation gave both enantiomers in somewhat lower yields compared to the racemic compound (37% (S_a), 50% (R_a), 97% *rac* see Chapter 5.1.3). This is attributed to column chromatographic isolation to obtain the bichalcones in adequate purity (m.p., optical rotation, HPLC). The main impurities removed during the column chromatographic isolation were flavanone type side product (Chapter 5.2.3.1). Thus, yields should be able to be improved for this synthesis. An x-ray structure (measured by Dr. *Wolfgang Frey*) of bichalcone (R_a)-**169** was obtained, supporting the assignment of the absolute configuration (Figure 16).

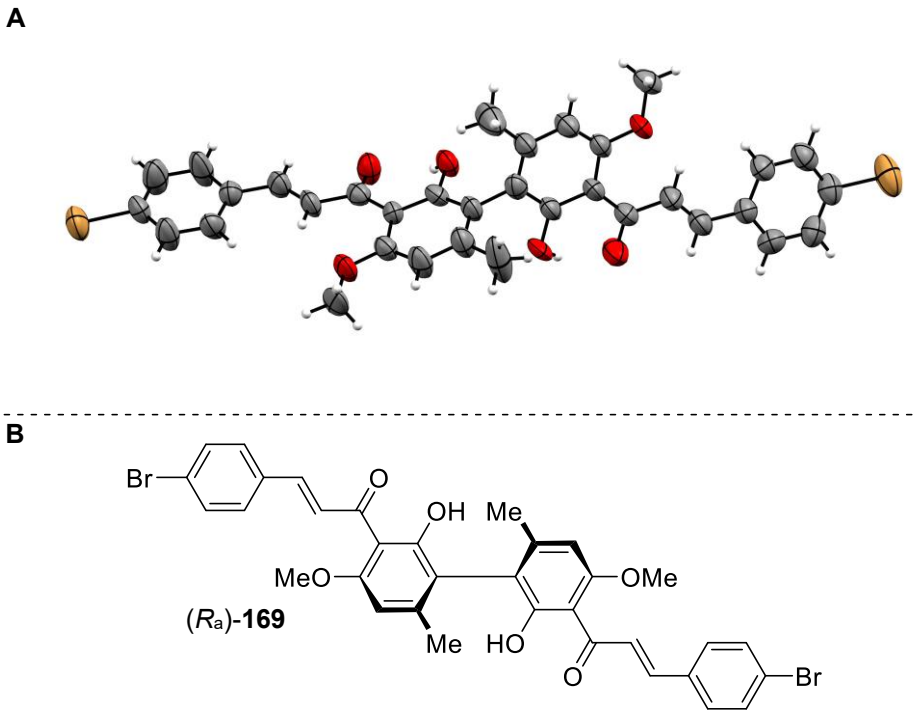

Figure 16: (A) X-ray structure, ORTEP at 50% probability. (B) Lewis structure interpretation.

Oxidative cyclization gave both enantiomers of brominated biflavone **183** in yields of 77 – 92%. The high enantiomeric excess >99%*ee* was retained over this sequence. Finally, the synthesis of amino biflavone **181**—identified as the most active biflavone (Chapter 5.1.4)—was conducted *via* palladium catalysis (Scheme 63B). Both enantiomers were obtained in yields of 79% (S_a) and 90% (R_a). The bioactivity was assessed by *Céline David*.[228] The IC_{50} value of the enantiopure biflavones was somewhat lower than of the racemic mixture (5.7 µM (S_a), 4.2 µM (S_a), 3.7 µM (*rac*)). Thus, the bioactivity could not be improved compared to the previous best hit regarding the activity against HeLa cells. The vastly different solubility of the racemic mixture compared to the enantiopure biflavones may influence the pharmacokinetics.

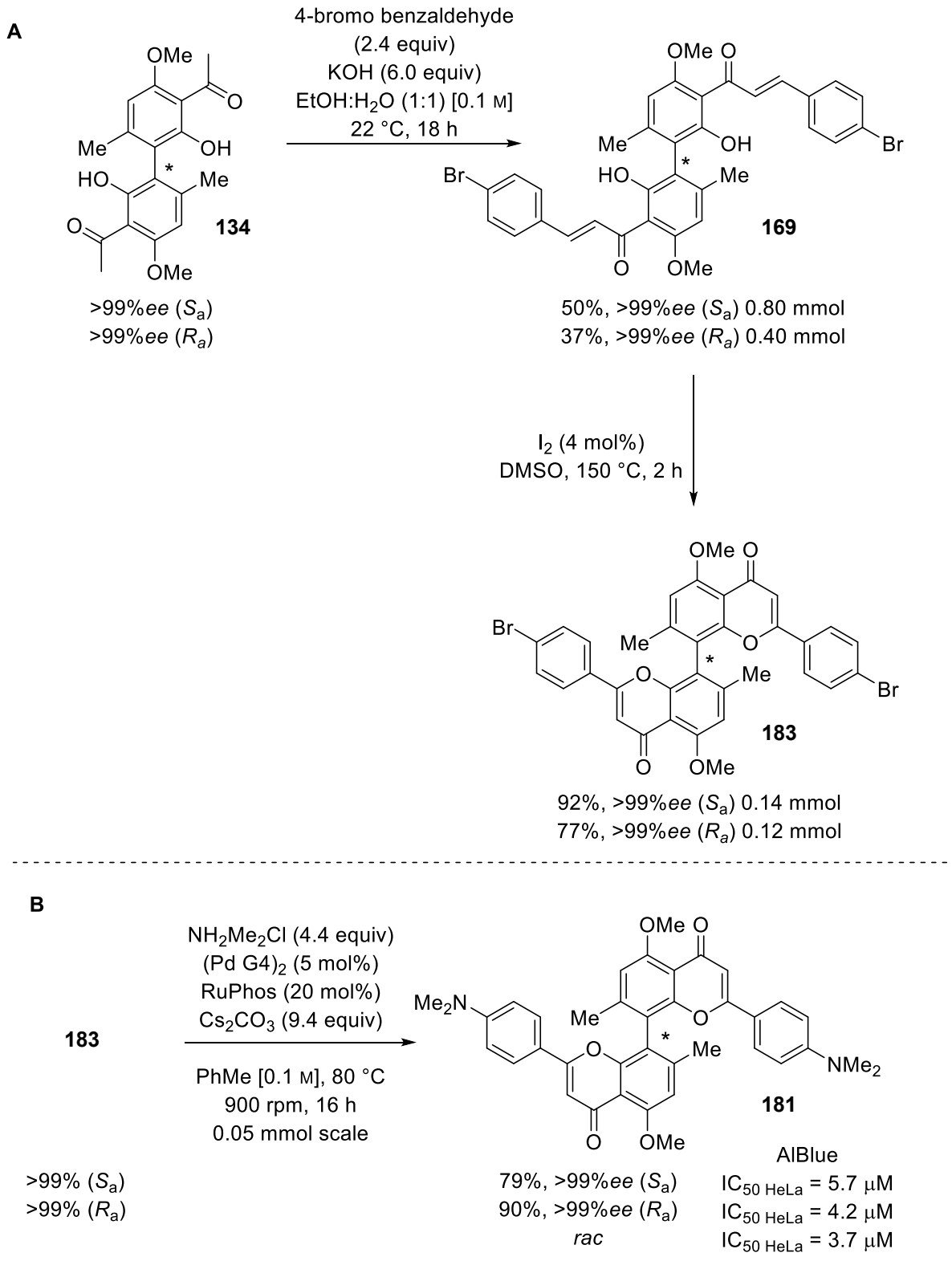

Scheme 63: Synthesis of both enantiomers and racemic mixture of 8,8″-biphenol **183** starting from enantiopure biphenol **27** and racemic acetophenone **134**. (B) Synthesis and bioactivity of biflavones (S_a)-**181** and (R_a)-**181**.

5.3 *Catellani* Reaction

The following chapter contains results obtained by Max Schlamkow as part of a bachelor's thesis.[254]

2-Aminobiaryls can be accessed by several methods (Chapter 5.2). A one-pot approach could shorten synthetic routes and enable access to novel tri-*ortho* substituted 2-aminobiaryls limited by the availability of commercial starting material (compare **240**, 5.2.2.1) (Figure 17). In particular, methoxylated 2-aminobiaryls, a substitution pattern common in polyketide- and terpenoid-based natural products,[27, 90, 102, 255] (Chapter 4.3) are not easily accessible *via* established methods. The following protocols were based on combining investigations towards di-*ortho* 2-morpholino biaryls[195] with an ammonia surrogate[194]. These 2-aminobiaryls serve a purpose in being starting materials for the synthesis of cyclic diaryliodonium salts (Chapter 5.2), as intermediates towards transition metal catalyzed transformations[201] and common structural motif in ligand and natural product synthesis.

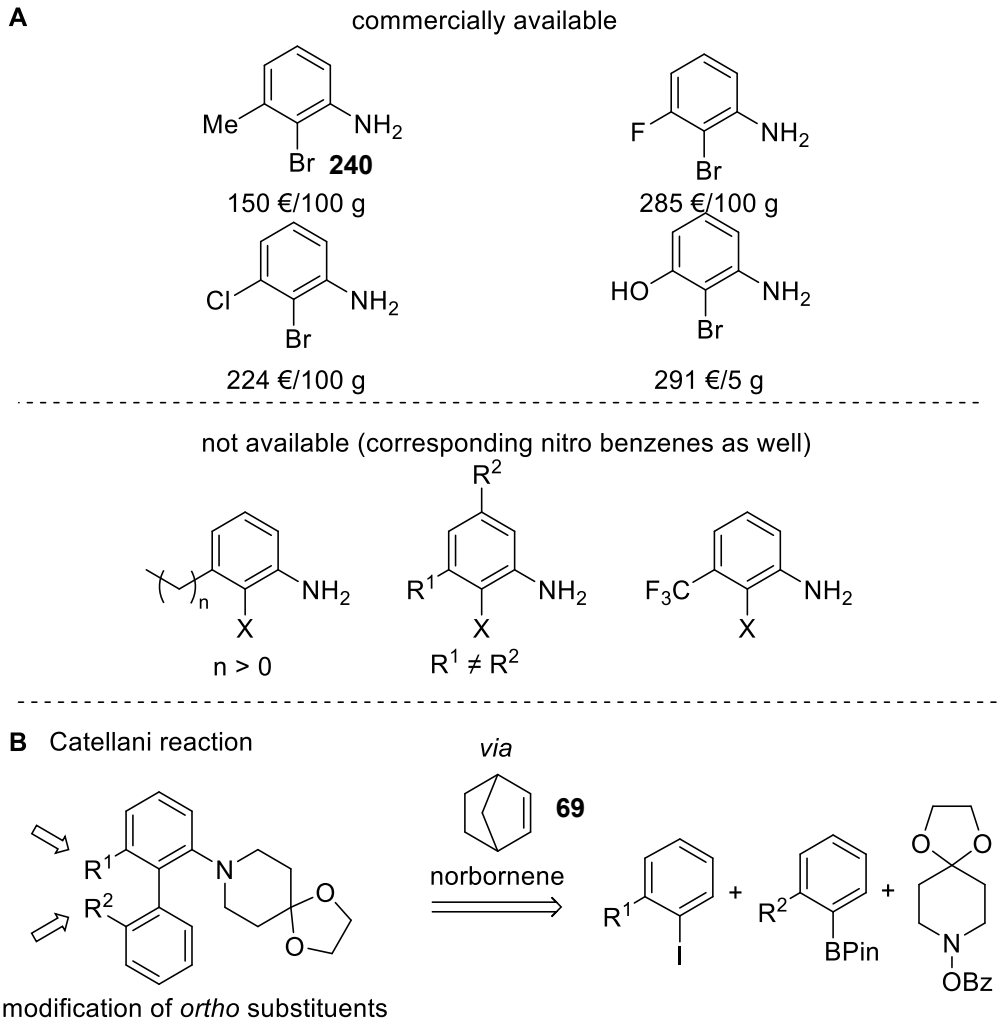

Figure 17: (A) Commercially available and selection of unavailable anilines. The corresponding nitro benzenes were unavailable as well.[243] (B) Strategy to access 2-aminobiaryls using norbornene.

5.3.1 Boronic acid esters

For the transformation described herein as well as a subsequent chapter (5.4), a range of boronic acid esters were required. These were synthesized following the previously established *Masuda* borylation (Chapter 5.2.1.1). Iodides as well as bromides were accepted and readily transformed into the corresponding aryl boronic acid esters (Scheme 64). The *Masuda* borylation gave good to acceptable yields for most aryl halides. For the sterically demanding and electron-deficient CF_3-substituted product **257**, significant proto-dehalogenation was observed resulting in lower yields. Overall, a diverse variety of aryl boronic acid esters was obtained on up to 50 mmol scale. Boronic acid ester **260** was synthesized by *Max Schlamkow* as part of a bachelor's thesis.[254]

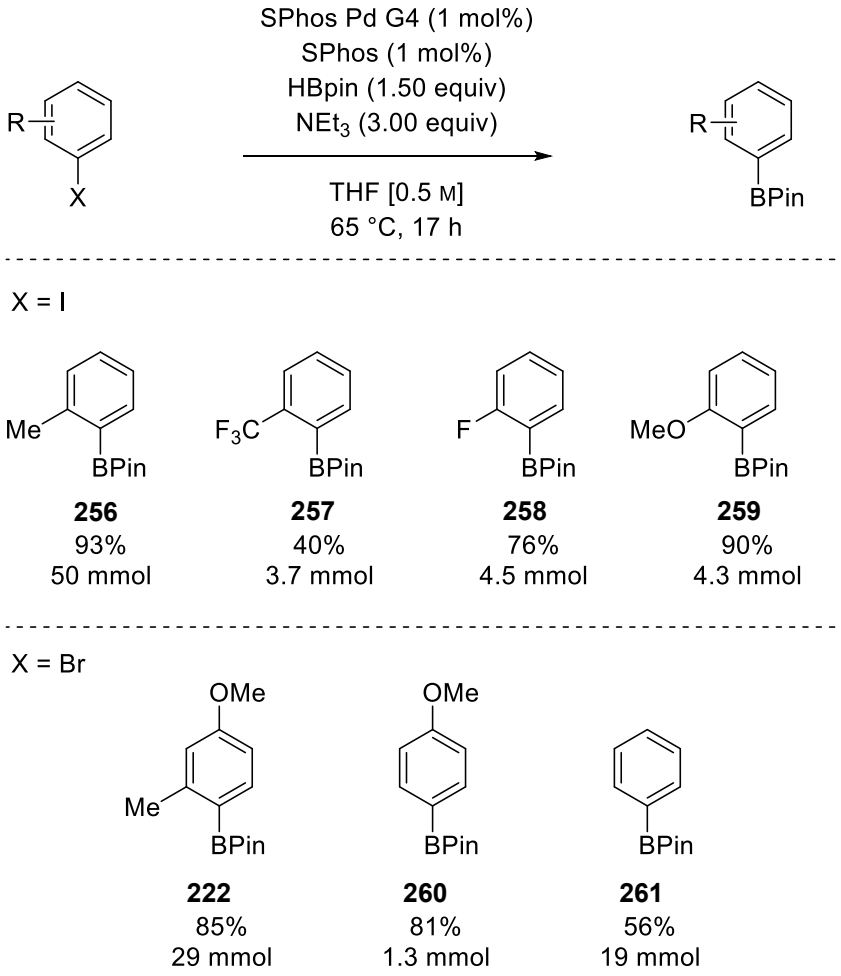

Scheme 64: Scope of the palladium-catalyzed *Masuda* borylation including previously discussed examples.

5.3.2 Initial protocol

In the bachelor's thesis of *Max Schlamkow,* the *Catellani* reaction (Chapter 4.5.4) to obtain tri-*ortho* substituted 2-aminobiaryls was investigated (Scheme 65).[254] In this initial protocol, microwave vials capped with a natural rubber septum were used. After a comprehensive ligand screening (2-furyl)$_3$P was identified as the most suitable ligand though conversions were incomplete unless high catalyst loadings were employed (10 mol% (Pd G4)$_2$ (**205**)). The optimal conditions in this approach effectively used 20 mol% Pd and thus a multifold of the reported catalyst loading.[195] A small scope of 2-amino biaryls was synthesized (**263** – **265**) using *O*-benzoyl hydroxylamine **262** with yields of 23 – 48%.

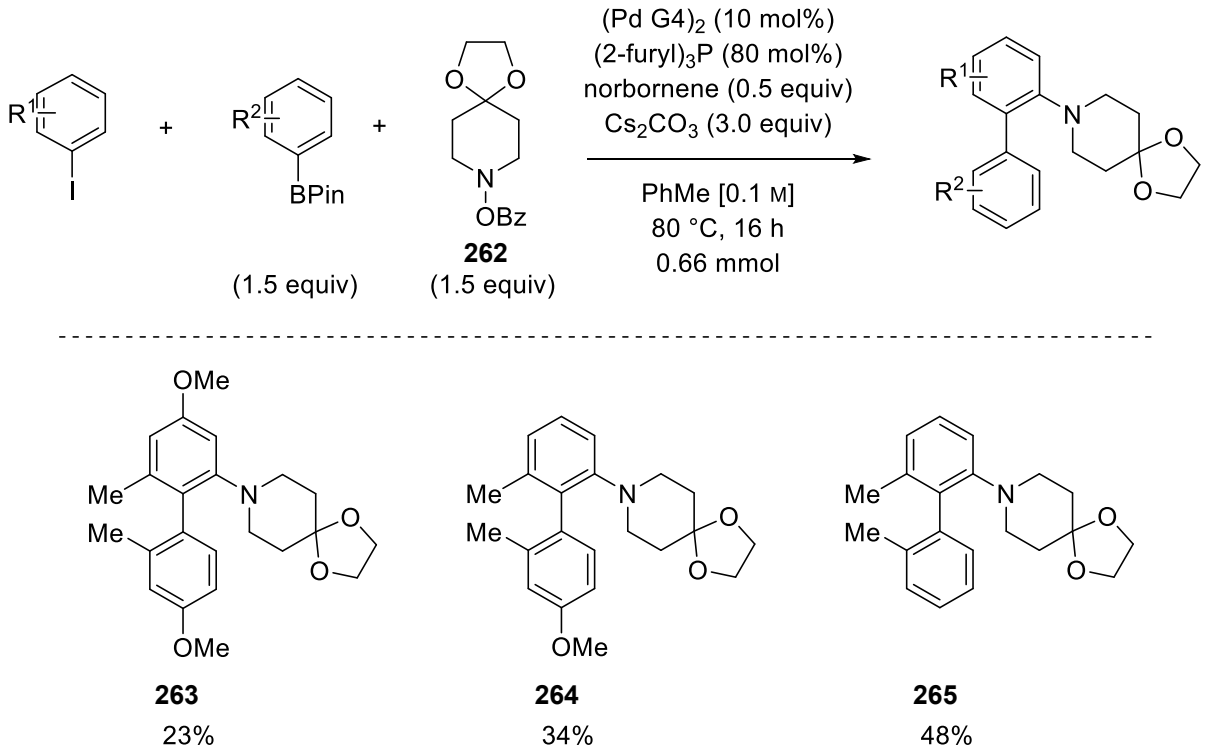

Scheme 65: Conditions and scope towards tri-*ortho* substituted 2-aminobiaryls for the initial palladium-catalyzed *Catellani* reaction.[254]

Additionally, the use of more bulky substrates such as very bulky aryl iodide **110** and aryl boronic acid ester **257** gave no conversion to product **266** (Scheme 66). Instead, a norbornene addition product **267** could be isolated as a single diastereomer. Thus, the limitations of this initial protocol were apparent with bulky and electron-rich substrates resulting in little conversion to product.

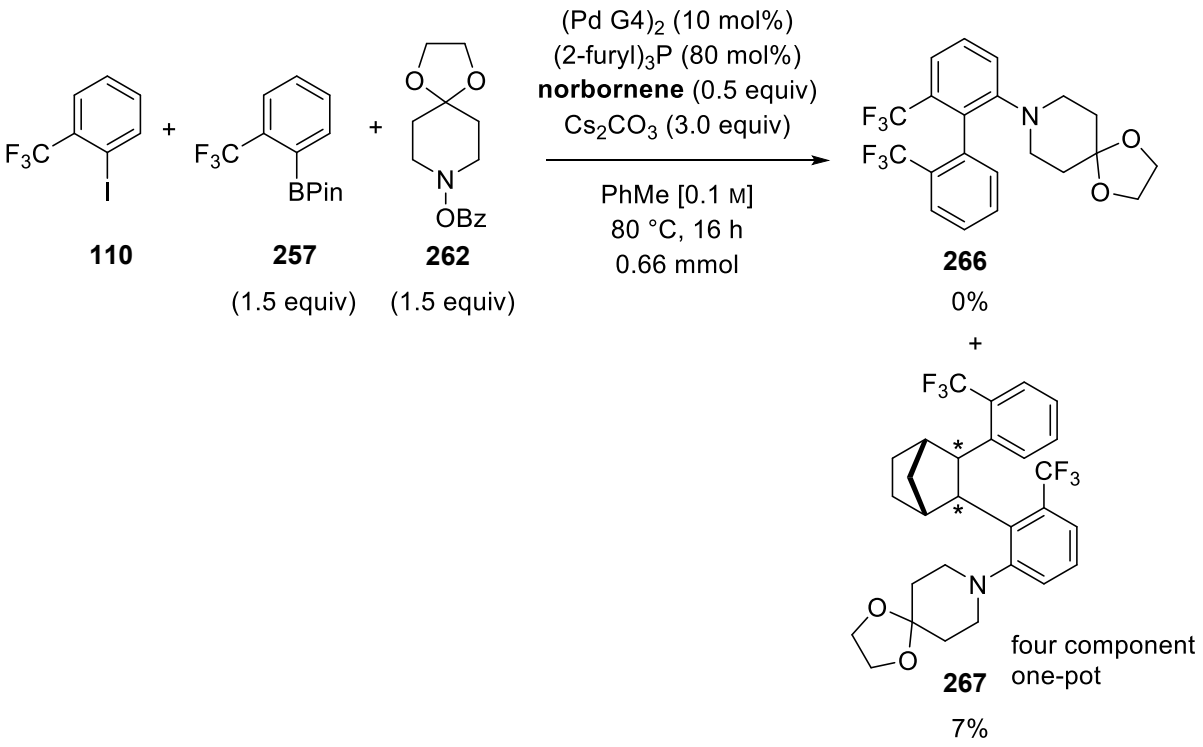

Scheme 66: Multi component palladium-catalyzed *Catellani* reaction and synthesis of **267**.

In the following optimization the coupling of aryl iodide **68**, aryl boronic acid ester **256**, and *O*-hydroxyl benzoyl amine **262** was investigated. The synthesis of *O*-benzoyl hydroxylamine **262** proceeded smoothly starting from amine **271** and provided the desired product in a yield of 72%.

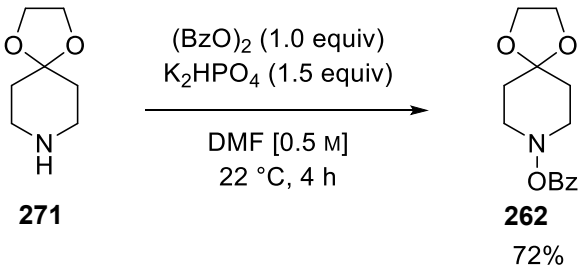

Scheme 67: Oxidation of 4,4-ethylenedioxy-piperidine using dibenzoyl peroxide.

The choice of the base is in many cases crucial for the selectivity of reactions and can vary dramatically even between different metal cations.[256] This influence was probed on a small scale (Table 15). Based on the 'cesium effect'[172] (Chapter 4.5.2) observed in transition metal catalyzed C–H activations, only Cs_2CO_3 gave any conversion of starting material while K_2CO_3 or KOAc did not. This highlights the importance of Cs_2CO_3 commonly observed in palladium-catalyzed transformations.[173] Crushing the Cs_2CO_3 to increase surface area and thus the solid-liquid interface gave an unsignificant change of product distribution (Table 15 entries 1 and 4). Large quantities of water were suspected to be introduced by this crushing process.

Over the course of these reactions in addition to the desired product **265**, several side products could be observed under these conditions that will be discussed in the following optimization tables. The main observed side products in this reaction are ortho functionalization with subsequent proto dehalogenation (**268**) (*m*-ArNR$_2$) the result of benzoyl hydroxylamine elimination,[257] electronically inverse *Buchwald-Hartwig* coupling (**269**) (*o*-ArNR$_2$)[258] and *Suzuki*-cross coupling (**270**) ((ArH)$_2$).

Table 15: Base screening for the synthesis of 2-aminobiaryl **265**. Common side products observed in the reaction mixture.

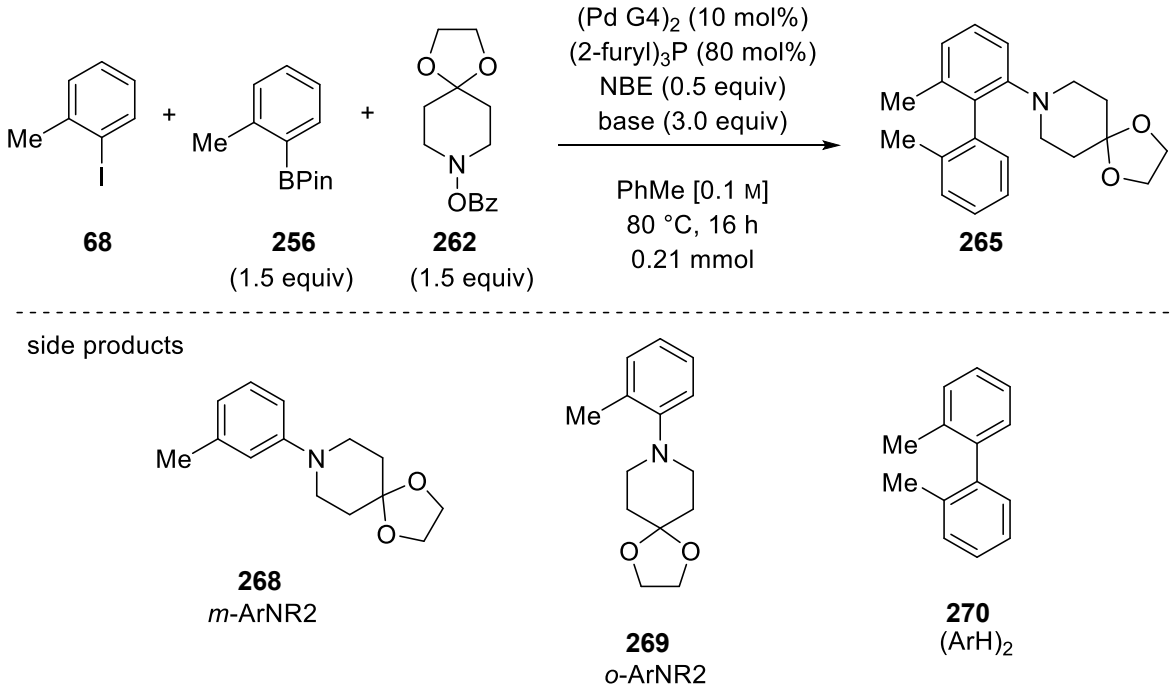

#	Base	Conversion[a] [%]	Product 265 [%]	*m*-ArNR$_2$ 268 [%]	*o*-ArNR$_2$ 269 [%]
1	Cs_2CO_3	72	30	36	31
2	K_2CO_3	0	0	0	0
3	KOAc	0	0	0	0
4	Cs_2CO_3[b]	69	26	36	32

Relative conversions to products according to ^{1}H-NMR. [a] Conversion of aryl iodide **68**. [b] Crushed using mortar and pestle (significant amounts of water suspected).

5.3.3 Improved protocol

As stated before, the initial protocol suffered from high catalyst loading and a narrow substrate scope. Additionally, reproducibility issues were encountered attributed to insufficient stirring caused by the reaction vessel. Before investigating a substrate scope, these issues had to be resolved. To mitigate this and potentially increase yields, the reaction setup was changed to a system common in transition metal catalyzed transformations.[160d, 259] By using a 2 dram (2 dr.) vial setup (8 mL volume cylindrical shape, short stir bar) sealed with PTFE tape, capped with a rubber lined PTFE cap under an argon atmosphere and by stirring the reaction in an oil bath, reliable results were obtained (see Chapter 7.1, Figure 29). Additionally, a 2 dr. vial also allowed for a higher stirring speed of 900 rpm.

The volatility of norbornene required careful handling of the reagents as excessive purging with inert gas could result in quick evaporation. With this new set-up, it was investigated if the palladium loading could be decreased. Moreover, the palladium source was reevaluated. Pd-catalyst $(Pd\ G4)_2$ (**205**) gave the highest conversion to product and a higher relative ratio of desired product to side products (Table 16, entries 1 and 3) compared to $Pd(OAc)_2$. The Pd-loading could be lowered from 10 mol% to 2.5 mol% without substantially lowering conversion to the desired product (32% vs 31%). $Pd(dba)_2$ (freshly purchased, efficacy benchmarked)[145] gave lower overall conversions. Interestingly using this Pd^0-source as the catalyst generated only traces of the *Suzuki*-side product **270**, indicating that activation of the Pd^{II}-sources may partially be caused by reduction of the boronic acid ester. A temperature screening revealed 90 °C as the optimum of this reaction (Table 16, entries 3 and 5 – 7). Overall, side product **269** (*o*-$ArNR_2$) was not observed under any of these conditions in contrast to the previous protocol.

Table 16: Temperature and Pd-source screening conditions of the *Catellani* reaction for the synthesis of tri-*ortho*-substituted 2-aminobiaryls.

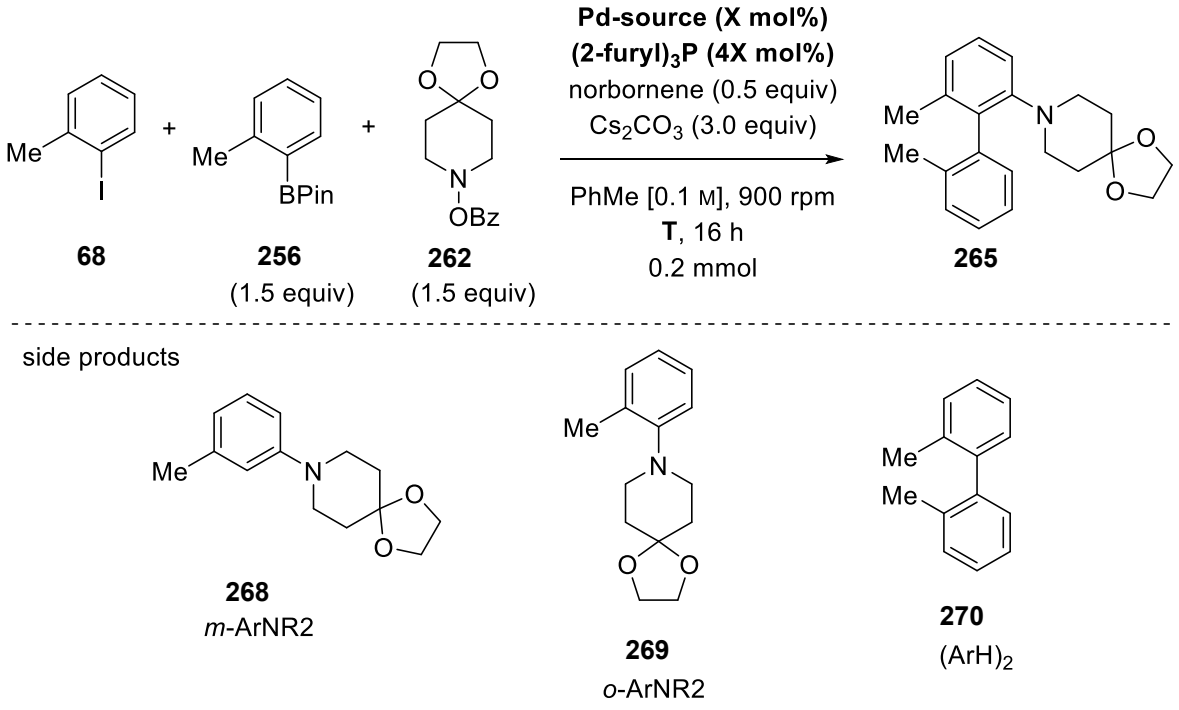

#	T [°C]	Pd-source[a]	[Pd] [mol%]	Conversion[b] [%]	Product **265** [%]	*m*-ArNR$_2$ **268** [%]	*o*-ArNR$_2$ **269** [%]	(ArH)$_2$ **270** [%]
1	80	$Pd(OAc)_2$	5	61	24	16	0	3
2	80	$(Pd\ G4)_2$	10	100	32	19	0	5
3	80	$(Pd\ G4)_2$	2.5	86	31	13	0	3
4	90	$Pd(dba)_2$	5	49	27	9	0	0
5	**90**	$(Pd\ G4)_2$	2.5	68	**42**	14	0	2
6	100	$(Pd\ G4)_2$	2.5	67	20	13	0	2
7	110	$(Pd\ G4)_2$	2.5	100	4	5	0	61

Reactions carried out on a 0.2 mmol scale. [a] Ligand to Pd ratio 4:1 based on absolute amount of Pd provided (2.5 mol% $(Pd\ G4)_2$ (**205**) would provide 5 mol% Pd. [b] Conversion of starting material **68** and to products according to ^{1}H-NMR with 1,3,5-trimethoxybenzene as internal standard.

To investigate if Pd G4 activation was taking place, the formation of carbazole **208** was quantified (Table 17). Additionally, it was investigated if the benzoate liberated during the catalytic cycle inhibits catalyst activity. Over the course of the reaction up to 1.5 equivalents of benzoic acid would be released. Addition of benzoic acid (1.0 equivalent), with additional Cs_2CO_3 to account for the deprotonation, suffered from low reproducibility (Table 17, entry 1). The addition of benzoic acid (1.0 equivalent) without base compensation gave no conversion to product yet comparable activation of the Pd G4 source (Table 17, entry 2). Similar experiments have been conducted by *Shi et al.* to rationalize *ipso*-hydrogenation.[194] These

results implied that a higher ratio of benzoic acid to base does indeed inhibit reaction rates. An increase in base equivalents however did not increase conversions to product (Table 17, entry 3). The carbazole formed rarely exceeded 50 %. This may indicate that G4 activation is incomplete. Other means of palladium activation such as reduction by boronic acid esters may still constitute the remaining Pd^{II} reduction.

Table 17: Investigation of base promoted formation of carbazole **208** in the presence of benzoic acid.

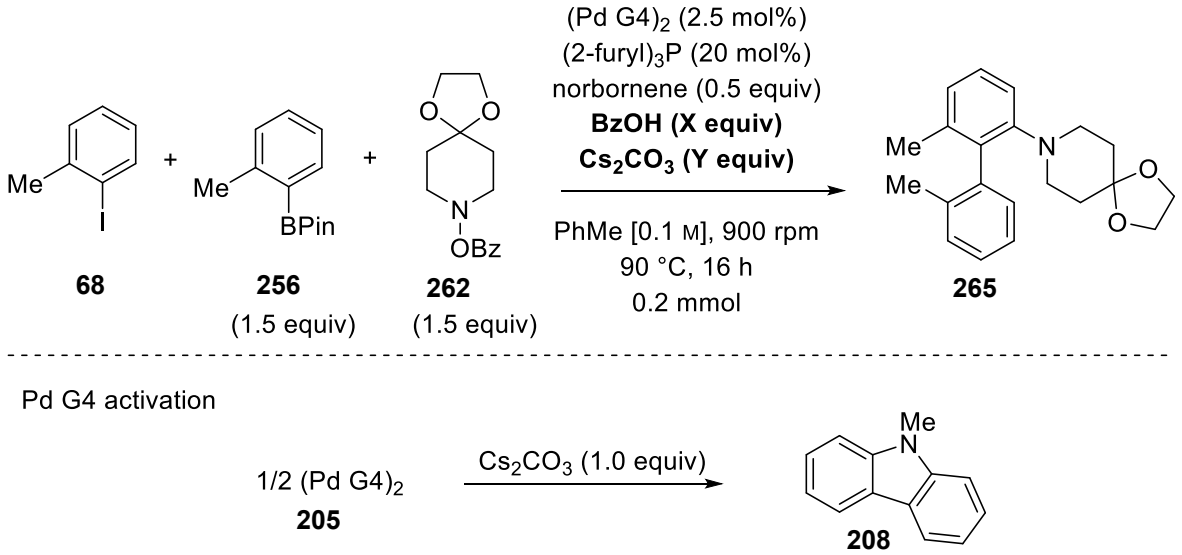

#	BzOH [equiv]	Cs_2CO_3 [equiv]	Conversion[a] [%]	Product **265** [%]	*m*-$ArNR_2$ **268** [%]	Carbazole **208** [%]
1[b]	1.0	4.0	78±32	17±18	11±1	23±24
2	2.0	4.0	50	0	4	41
3	-	4.0	77	36	16	44

Reactions carried out on a 0.2 mmol scale. [a] Conversion of starting material **68** according to ^{1}H-NMR with 1,3,5-trimethoxy benzene as internal standard. [b] Reaction performed as duplicates.

With these assessments in place, the influence of the ligand was investigated (Table 18). Generally, phosphines containing sp^3-C–P bonds are more electron rich than those with sp^2-hybridized substituents.[260] The employed ligand tris(2-trifuryl) phosphine is classified as an electron-deficient phosphine ligand and poor σ–donor due to the high s-character of the lone pair and electron withdrawing heteroaryl substituents.[260] This is in line with the previous observation of electron-rich substrates giving lower conversions to product (Scheme 65). Thus, electron-deficient ligands should facilitate the reductive elimination step which in turn should decrease the amount of side product **268**. Several ligands were screened including the tetrafluoroborate salt of electron-rich tricyclohexyl phosphine which gave *Suzuki*-coupling product **270** as the main product supporting the hypothesis (Table 18, entry 1). Electron-

deficient polyfluorinated triaryl phosphines gave varying results. While tris(pentafluorophenyl)phosphine gave side product **269** as the main product—otherwise not observed under these conditions—bulky $(3,5\text{-}(CF_3)_2C_6H_3)_3P$ and $(4\text{-}CF_3C_6H_3)_3P$ gave unselective conversions (Table 18, entries 2 – 4). Lowering the mol% of ligand relative to Pd gave overall less conversion of starting material and to product (Table 18, entry 5). As such, other ligands than tris(2-trifuryl) phosphine appeared too unwieldy for this transformation.

Table 18: Ligand screening conditions of the *Catellani* reaction for the synthesis of tri-*ortho*-substituted 2-aminobiaryls.

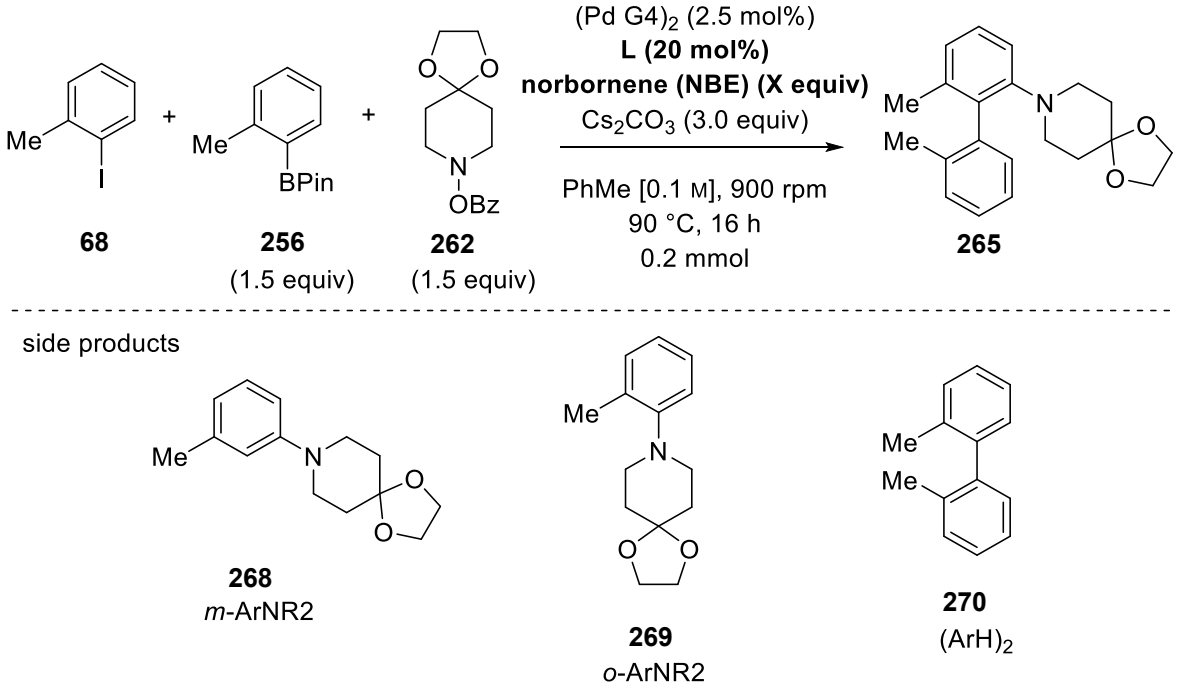

#	Ligand L	NBE [equiv]	Conversion[a] [%]	Product 265 [%]	*m*-ArNR$_2$ 268 [%]	*o*-ArNR$_2$ 269 [%]	(ArH)$_2$ 270 [%]
1[b]	$Cy_3P\cdot HBF_4$	0.5	89	15	19	0	36
2	$(4\text{-}CF_3C_6H_4)_3P$	0.5	68	17	13	0	8
3	$(Ph_F)_3P$	0.5	38	0	4	16	2
4	$(3,5\text{-}(CF_3)_2C_6H_3)_3P$	0.5	62	5	8	0	4
5	$(2\text{-furyl})_3P$ (10 mol%)	1.0	51	14	12	0	0

[a] Conversion of starting material **68** and to products according to ^{1}H-NMR with 1,3,5-trimethoxybenzene as internal standard. [b] 3.2 equiv Cs_2CO_3.

Next, the influence of norbornene and water were investigated (Table 19). Increasing the equivalents of norbornene—which in theory would suffice in catalytic amounts—gave greater

conversion of starting material and to product **265** (1.0 equiv). On the other hand, 2.0 equivalents of norbornene gave lower conversion to product. Excess of norbornene could push the equilibrium of the reaction towards incorporating norbornene into the final product as was observed before (Scheme 66). The addition of molecular sieve as a drying agent is literature known for similar reactions,[261] yet resulted in less product formation under these conditions (Table 19, entry 3). The addition of water drastically increased the formation of side product **268** (*m*-ArNR$_2$), resulting from the proto-depalladation (Table 19, entry 3).

Table 19: Norbornene and additive screening conditions of the *Catellani* reaction for the synthesis of tri-*ortho*-substituted 2′-aminobiaryls.

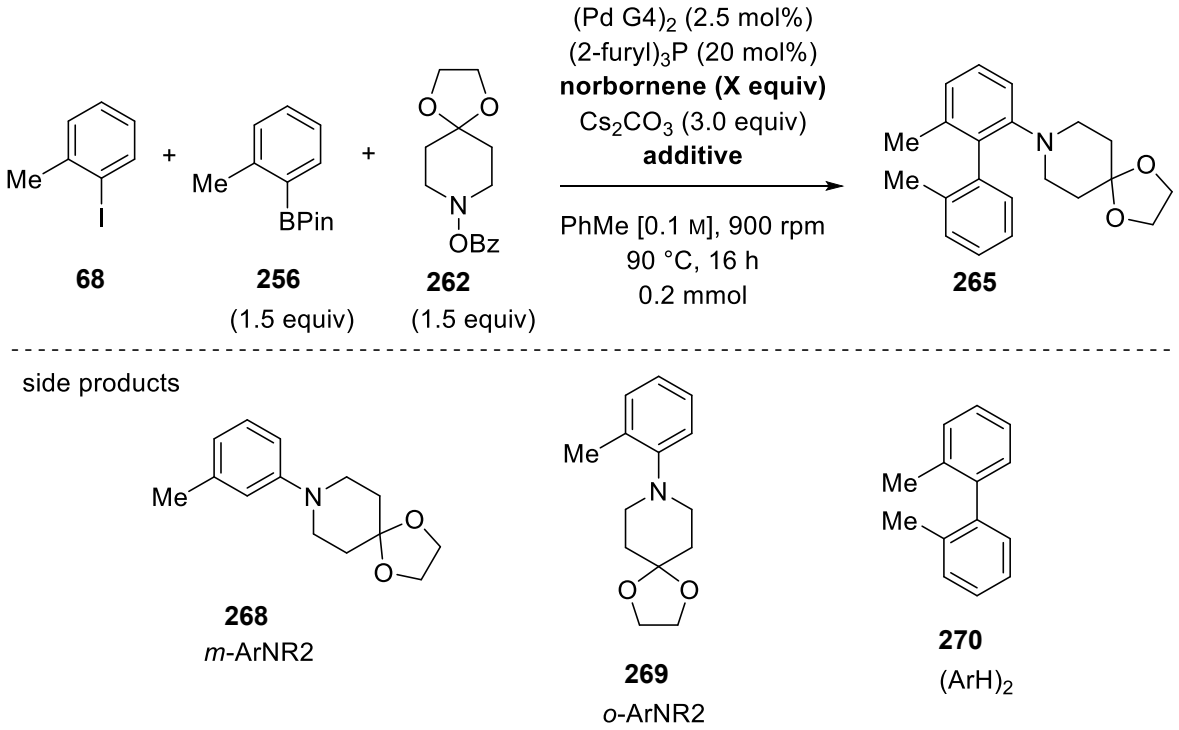

#	norbornene [equiv]	additive	Conversion[a] [%]	Product 265 [%]	*m*-ArNR$_2$ 268 [%]	*o*-ArNR$_2$ 269 [%]	(ArH)$_2$ 270 [%]
1	**1.0**	None	79	**47**	12	0	2
2	2.0	None	81	40	10	0	2
3	1.0	4 Å MS (2 weight equiv)	63	30	10	0	1
4[b]	0.5	50 µL H_2O	64	26	31	0	1

Reactions carried out on a 0.2 mmol scale. [a] Conversion of starting material **68** according to ^{1}H-NMR with 1,3,5-trimethoxy benzene as internal standard. [b] The reaction mixture was a solution rather than a suspension as was the case when using flame dried Cs_2CO_3.

Overall, the previously established protocol[254] could be improved by lowering the Pd-loading from effectively 20 mol% Pd to 5 mol% Pd and increasing selectivity towards product formation. Efforts towards understanding the incomplete conversion of aryl iodide starting material were undertaken. Benzoic acid was identified as a potential inhibitor.

5.4 Palladacycles as stereodynamic intermediates

In this chapter, the use of 2-iodobiaryls as precursors for palladacycles is discussed. The stereodynamics of these palladium complex intermediates would be investigated. After determining if the system is indeed stereodynamic, efforts towards asymmetric catalysis using chiral ligands would be undertaken.

Cyclic diaryliodonium salts are useful stereodynamic intermediates in the synthesis of enantioenriched biaryls (Chapter 5.2). These useful key-intermediates suffer from poor functional group tolerance as especially electron-rich substrates are not well accepted (Chapter 5.2.1). These electron-rich substrates are particularly important for the construction of dimeric polyketides. Stereodynamic palladium complexes have seen use in literature for the construction of axially chiral products (Chapter 4.5.3) but are generally tailor-made solutions and not applicable for structural motifs in polyketide-based natural product synthesis.[174] Various experimental methods exist to determine the rate of racemization for atropisomers compiled in a recent review.[262] Additionally, computational chemistry and DFT calculations in particular are powerful tools to calculate theoretical rotational barriers.[102, 263] Such methods are benchmarked for biaryls.[264] With methods towards 2-iodobiaryls established (Chapter 5.2.1), these readily available starting materials could be employed to experimentally verify the stereodynamic nature of the system. In combination with chiral ligands, enantioselective synthesis could be conducted. Additionally, efforts towards isolating the catalytically relevant palladacycles would be undertaken to determine the rotational barrier of the system. *Lu et al.* published the synthesis of 2,2′-disilylbiphenyls **272** starting from 2-iodobiaryls **273** *via* the formation of a palladacycle intermediate.[179] The mechanism proceeds *via* a Pd^{IV} intermediate (**IV**) (Scheme 68). The reductive elimination **d)** to form the first Si-C bond (**V**) in the final product would be the stereodetermining step. Thus, a chiral ligand coordinating the Pd^{II} species (**III**) and Pd^{IV} species (**IV**) would result in stereoselectivity *via* diastereomeric transition states.

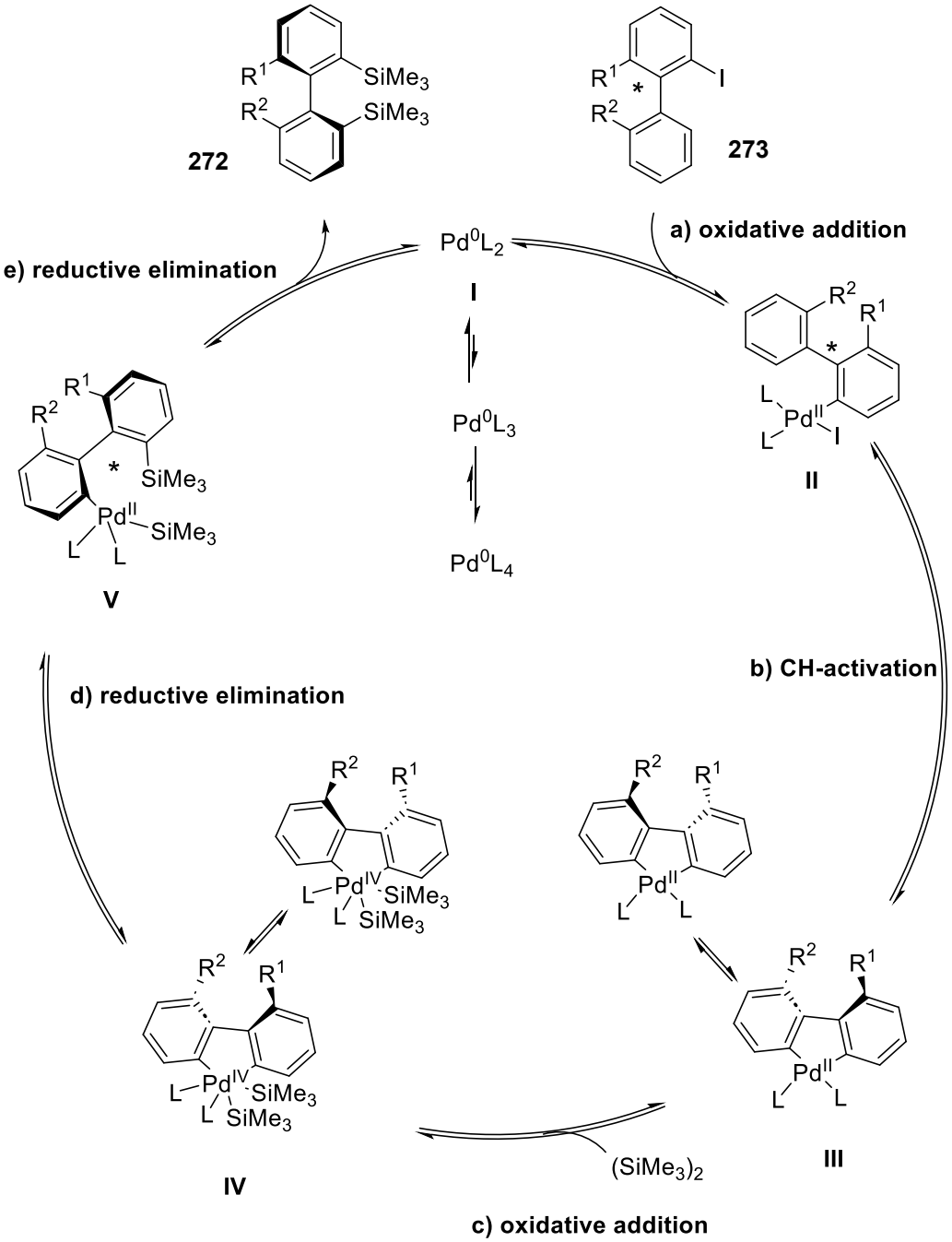

Scheme 68: Proposed catalytic cycle of the stereoselective silylation of 2-iodobiaryls.

Adding on to this, the use of di-*ortho* substituted biaryls would give enantioenriched 2,2′-disilylbiaryls **274** *via* desymmetrization of the achiral starting material **275** (Scheme 69A). Using tri-*ortho* substituted biaryls **273** the mechanism would instead proceed *via* dynamic kinetic asymmetric transformation (DYKAT) towards tetra-*ortho*-substituted products **272** (Scheme 69B).

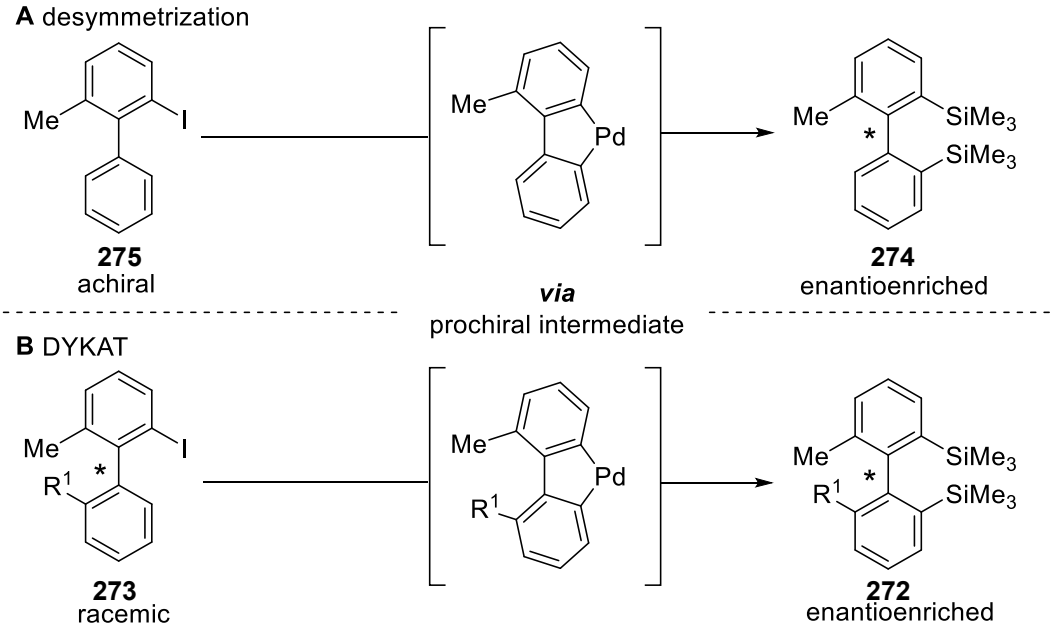

Scheme 69: Enantioselective synthesis of 2,2'-disilylbiaryls starting from (A) achiral di-*ortho* substituted biaryls *via* desymmetrization or (B) racemic tri-*ortho* substituted biaryls *via* DYKAT.

5.4.1 Starting material synthesis

To access a variety of 2-iodobiaryls the previously obtained *Masuda* borylation products were used to synthesize a small library of boronic acid esters (Chapter 5.2.1.1). The palladium-catalyzed *Suzuki* cross coupling following the previously established conditions was conducted (Chapter 5.2.1.2). Commercially available **240** was crucial in the investigation of this synthesis route (compare Chapters 5.2.3.2 and 5.3). Generally, 1 mol% palladium catalyst sufficed for scaled up reactions (Scheme 70). Key was the use of anhydrous K_3PO_4 by thorough drying and degassing of both THF and H_2O. The drying of K_3PO_4 served a dual purpose of degassing and defining the exact amount of H_2O present in the reaction. As such, a small library of 2-aminobiaryls was synthesized.

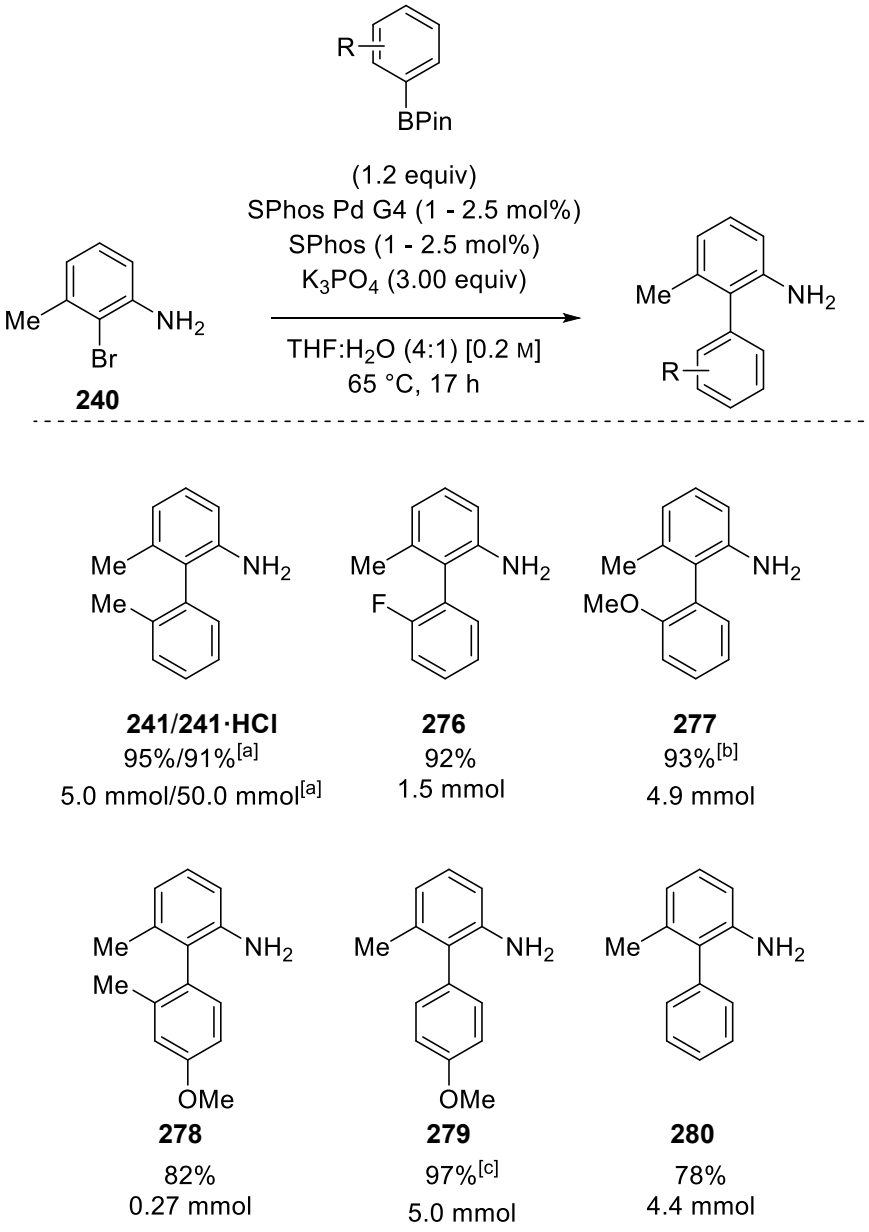

Scheme 70: Scope of 2-aminobiaryls. [a] Isolated as hydrochloride salt. [b] Relative to boronic acid ester **259**, using 1.5 equiv aryl iodide. [c] Boronic acid instead of boronic acid ester as starting material.

The *Sandmeyer* reaction following the previously established conditions again proceeded smoothly in providing 2-iodobiaryls for further investigations in yields of 77 – 94% (Scheme 71).

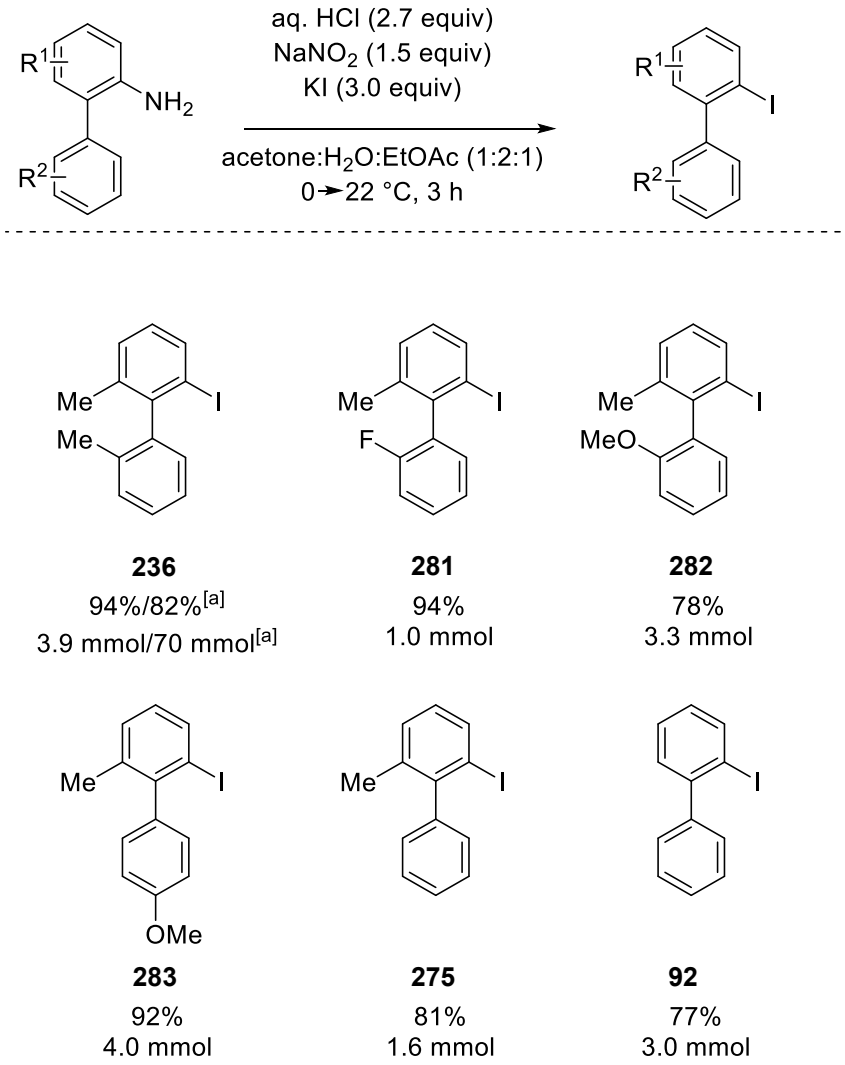

Scheme 71: Scope of *Sandmeyer* reaction towards 2-iodobiaryls. [a] Starting from **241·HCl** with aq. HCl (1.7 equiv).

5.4.2 Palladacycle synthesis attempts

The synthesis of palladacycles was attempted to investigate if the rotational barrier of the biaryl-axis could be determined experimentally and if such systems are stereodynamic in the first place. Additionally, the formation of the 5-membered palladacycle bearing two substituents *ortho* to the biaryl C–C axis was probed as the steric bulk may influence reactivities. In accordance with a protocol by *Yang et al.* the synthesis of palladacycle **284** using 2-iodobiaryl **283** was conducted (Scheme 72).[184] No palladacycle product could be observed. Instead, the ^{1}H-NMR data suggested the presence of the oxidative addition complex **285**. The palladacycle complex could be distinguished from the oxidative addition complex by ^{1}H-NMR through the signals of the C_2-symmetrical 4-methoxy-benzene moiety of complex **285**.

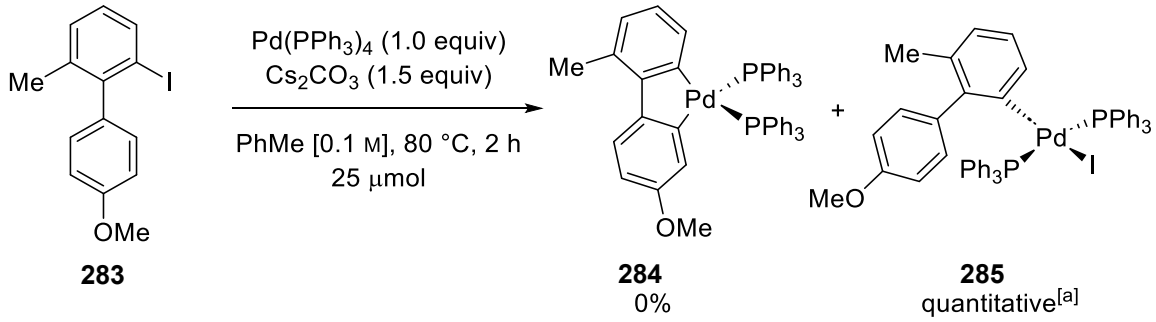

283 **284** 0% **285** quantitative[a]

Scheme 72: Oxidative addition of 2-iodobiaryl **283** to form palladium(II) complex **285**. [a] Major CH_2Cl_2 impurity.

Further substrates were investigated to probe steric or electronic effects but again instead of **286** and **287** only gave the oxidative addition complexes **288** and **289**(Scheme 73A). The presence of Cs_2CO_3 did not influence the selectivity of the transformation. On a sidenote, a multiplet with a coupling constant of 416 Hz for palladium complex **285** in ^{31}P-NMR could be observed for ox. add. complex **289** (Scheme 73B). This can be rationalized as a *trans*-$^{2}J_{P\text{-}P}$ coupling[265] with diastereotopic phosphorous atoms resulting from the axial chirality of the biaryl. Thus, both the retention of chirality of the aryl-aryl bond in this oxidative addition complex is supported as well as the *trans*-configuration.

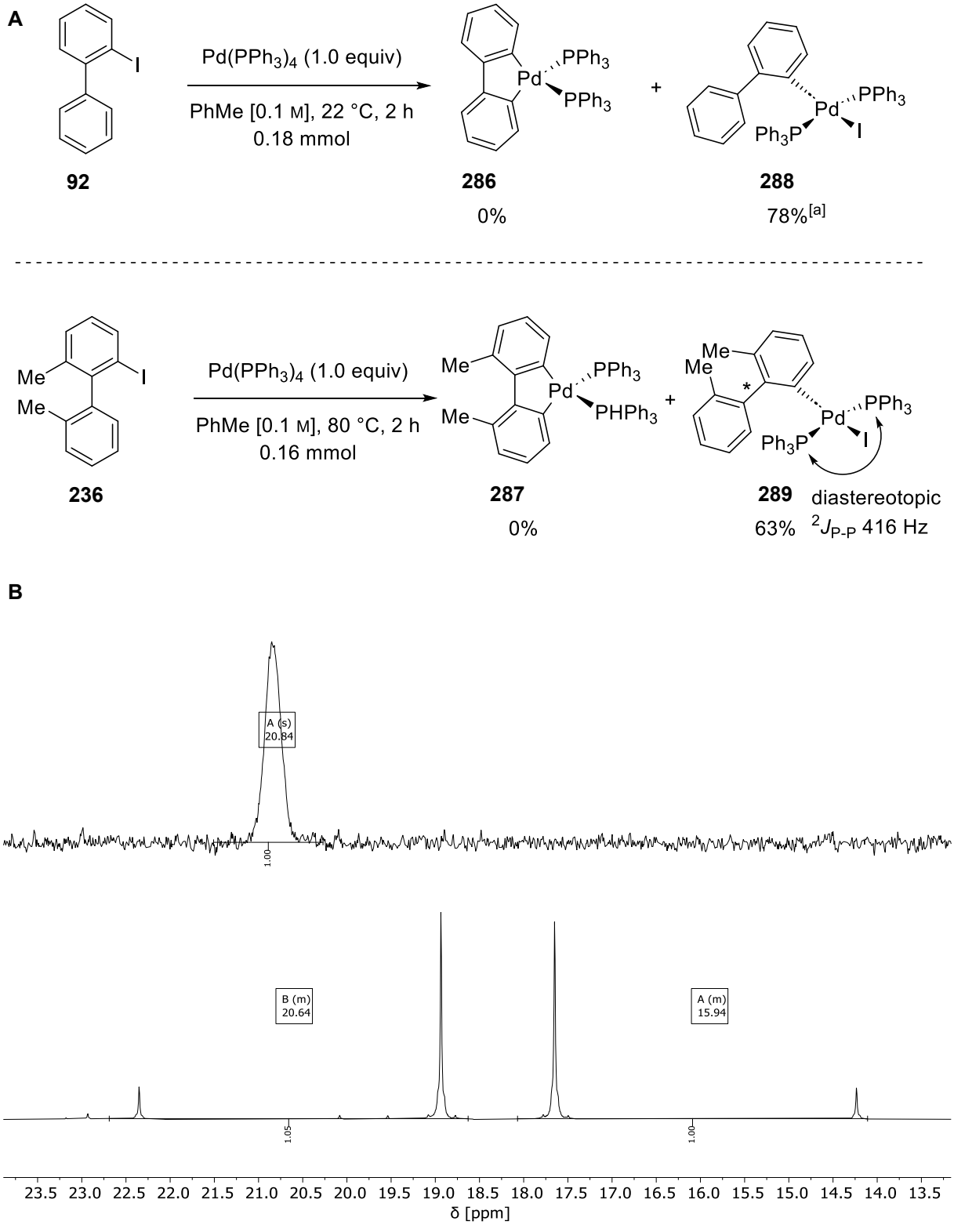

Scheme 73: (A) Oxidative addition of 2-iodobiaryls to form Pd^{II} complexes [a] minor CH_2Cl_2 impurity. (B) Top: ^{31}P NMR spectrum of **288**. Bottom: ^{31}P NMR spectrum of **289** exerting ^{31}P-^{31}P coupling.

Efforts were next directed at investigating if an increase in temperature would result in cyclization. Still, no conversion to product and only formation of triphenyl phosphine oxide ($OPPh_3$) could be observed at 110 °C (Scheme 74). Over the course of the reaction, free PPh_3 was also observed implying an equilibrium of coordination and decoordination. The addition

of 2.0 equivalents of PPh_3 to account for this again resulted in full oxidation of the ligands and thus deterioration of the complex.

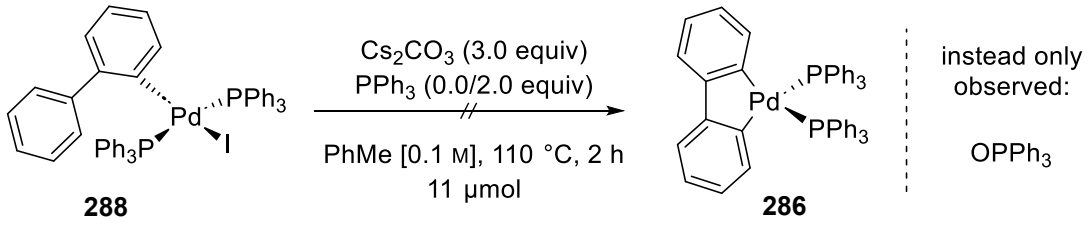

Scheme 74: Base mediated cyclization of palladium complex **288**.

5.4.3 DFT calculations

Because no palladacycle could be isolated, efforts were instead directed towards theoretical calculations of the rotational barrier. All calculations were performed at 298.15 K. First, the transition state of the palladacycle was investigated to probe if stereodynamics along the aryl-aryl bond could be observed. The geometries of relevant ground states were calculated using various DFT[100]-methods (density functional theory) benchmarked for transition metal complexes (Table 20)[266] using the Orca (5.0.1)[267] quantum chemistry software packages. The functionals used included TPSS[268] with the D4 dispersion correction[269] and def2-SVP[270] basis set, M06L[271] with def2-SVP and the B97-3c composite method[272]. Thus, obtained ground states were confirmed by the absence of imaginary frequences after an analytical frequency calculation (AnFreq). Electronic energies were then calculated based on these geometries using ωB97M-V[273] with the def2-TZVPP basis set benchmarked for palladium complexes[266]. Transition states were identified by relaxed surface scan (RSS) starting from the ground states and confirmed to be first order saddle points by the presence of exactly one imaginary frequency. The temperature dependency of $\Delta G^{\ddagger}_{e}$ is recognized though DFT as well as rotational barrier calculations were conducted for 298.15 K.[262] The derivation of the following equation is discussed in a publication by *Rickhaus et al.*[274] The equation, required to quantify the half-time of racemization, is derived from the equation for a 1st order kinetic process (1). The Eyring-Polanyi equation provides the enantiomerization rate constant (2). Combining these equations, equation (3) can be formed.

$$t_{1/2}^{rac} = \frac{ln(2)}{2k_e} \quad (1)$$

$$k_e = \left(\frac{k_B T}{h}\right) e^{\frac{-\Delta G_e^{\ddagger}}{RT}} \quad (2)$$

$$t_{1/2}^{rac} = \frac{\ln(2)}{2\left(\frac{k_B T}{h}\right)} e^{\frac{\Delta G_e^{\ddagger}}{RT}} \quad (3)$$

R: gas constant (8.314 J K^{-1}), T: temperature [K], k_B: Boltzmann constant (1.381 × 10^{-23} J K^{-1}), *h*: Planck constant (6.626 × 10^{-34} J s).

Though $\Delta G^{\ddagger}_{e}$ varied depending on the method employed, overall energies implied racemization occurring on time scales of milliseconds to nanoseconds (10^{-3} to 10^{-9} s) at 25 °C (Table 20). These initial results support the hypothesis that 5-membered dibenzo palladacycles should be stereodynamic. More thorough calculations to determine a more accurate rotational barrier would be postponed until confirmation by experimental data was in place.

Table 20: $\Delta G^{\ddagger}_{e}$ calculated by different methods [a] free energies were calculated at the ωB97M-V/def2-TZVPP//M06L/def2-SVP, ωB97M-V/def2-TZVPP//TPSS-D4/def2-SVP and ωB97M-V/def2-TZVPP//B97-3c levels of theory.

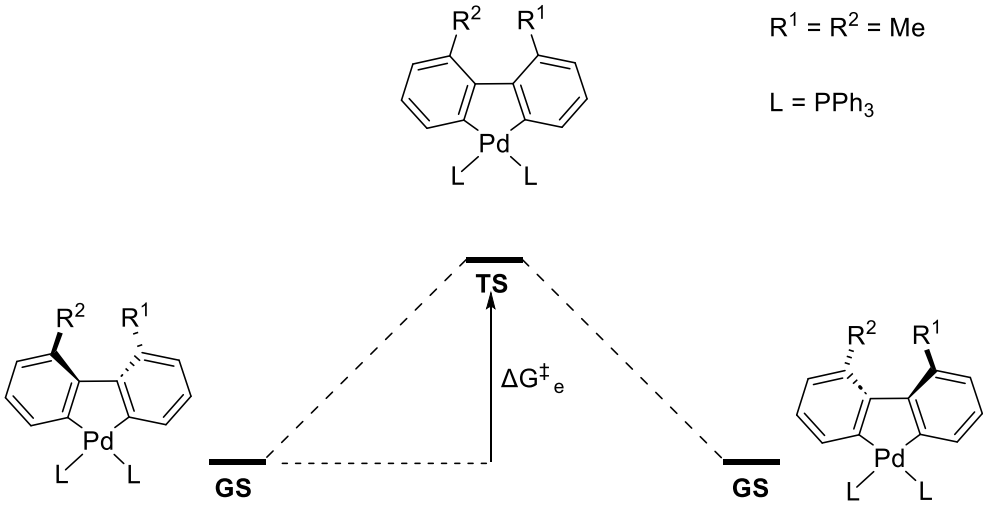

DFT Method	$\Delta G^{\ddagger}_{e}$ [kcal mol^{-1}]	$t_{1/2}$ [s]
B97-3c	6.060	$1.5 \cdot 10^{-9}$
M06L	13.03	$1.9 \cdot 10^{-4}$
TPSS D4	5.625	$7.4 \cdot 10^{-10}$

5.4.4 Silylation

With DFT calculations supporting the stereodynamic property of the palladacycle, the enantioselective transformation of such complexes was attempted. A silylation protocol involving a Pd^{IV}-palladacycle was chosen for these investigations. Initial reproduction attempts of the original protocol were inconsistent with literature.[179] Conversions of starting material varied drastically (Scheme 75A). Additionally, a side product could be observed when using 2-iodobiaryl **236** (Scheme 75B). This sp^3-C–H activation side product **291** was detected by ^{1}H-NMR and APCI-MS but could not be isolated. The presence of this side product and absence of the desired product hinted towards an insufficient oxidative addition of $(SiMe_3)_2$ to the Pd^{II}-complex.

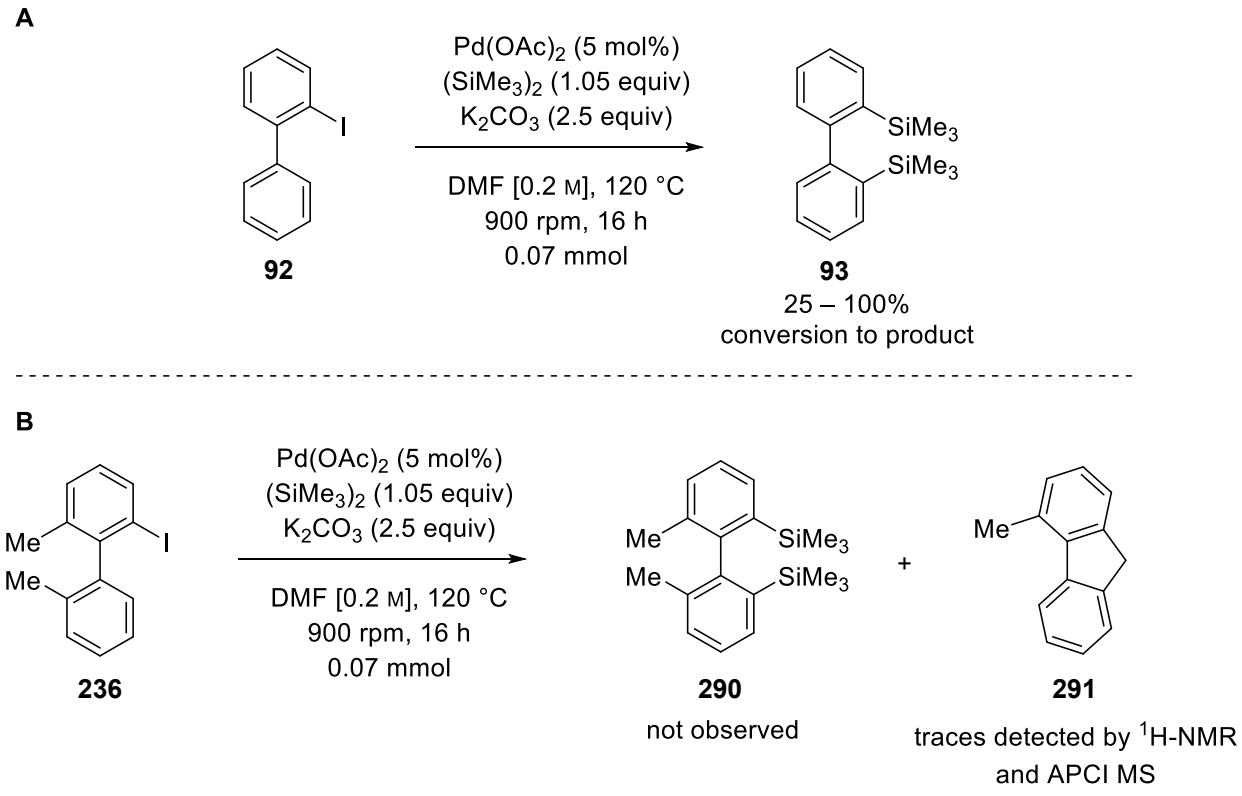

Scheme 75: Initial experiment towards 2,2′-silyl biaryls (A) Strong variation in conversion to product **93**. (B) observed cyclized side product **291**

It was observed that the addition of silane reagent to the reaction vessel as the last step was crucial in the reproducibility of the reaction due to high volatility of said silane. In their original publication *Lu et al.*[179] reported a degassing step freezing the reaction mixture with subsequent evacuation and refilling with N_2, possibly to avoid palladium mediated oxidation of silanes.[275] This observation in combination with the previously observed side product hinted towards insufficient amounts of silane present in solution. To accurately determine if the freeze-degassing step is crucial for full conversion, reactions were performed in duplicates (Table 21).

Including a freezing step as described in the original protocol actually decreased conversion of starting material and conversion to product. Thus, this freezing step was omitted for any subsequent investigations.

Table 21: Investigation on the necessity of degassing the reaction mixture *via* freeze-pump-thaw of the palladium catalyzed silylation.

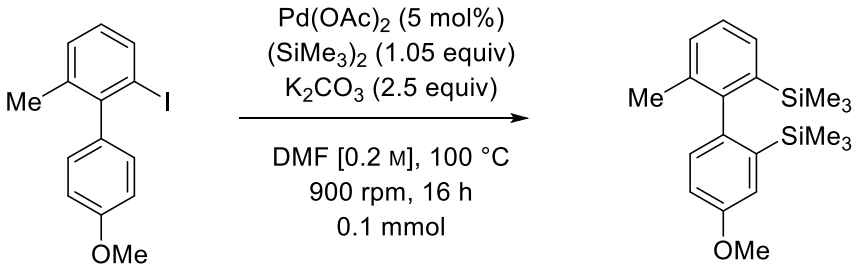

283 **292**

#	Freezing step	Conversion[a] [%]	Product [%]
1	no	98±0	69±2
2	yes	59±8	34±3

Reactions performed on a 0.1 mmol scale as duplicates. Conversions by ^{1}H NMR using 1,3,5-trimethoxybenzene as internal standard. [a] Conversion of starting material **283**.

With the reproducibility issues resolved, next the use of chiral ligands was investigated. Typical chiral ligands in palladium chemistry include axially chiral bidentate phosphine ligands (BINAP (**57**)), amino acid-based ligands (L-Leucine (**59**))[96, 155d, 276] or *P*-chiral monodentate ligands (BIDIME (**61**)) (Figure 18). It was originally believed that phosphine ligands cannot stabilized Pd^{IV}-complexes but this has shown to be false *via* the isolation of various such complexes.[147]

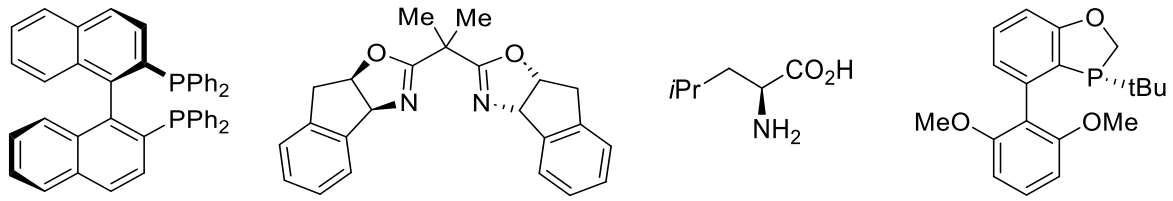

(*S*$_a$)-BINAP (**57**) **L1** L-Leucine (**59**) (*R*)-BIDIME (**61**)

Figure 18: Chiral ligands.

BINAP (**57**) and L-Leucine (**59**) as ligands gave low conversion of starting material **283** (Table 22, entries 1 – 2). This implies strong binding of the ligand to the palladium complex, inhibiting turnover. On the other hand, **L1** and BIDIME (**61**) gave conversions to product but no stereoselectivity implying weak coordination of the ligand or decoordination prior to the relevant transition state (Table 22, entries 3 – 4).

Table 22: Enantioselective silylations using various ligands.

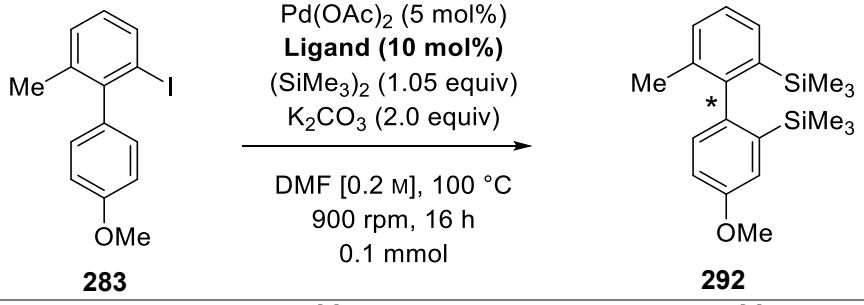

283 **292**

#	Ligand	Conversion[a] [%]	Conversion to product[a] [%]	ee [%]
1	(*S*a)-BINAP	12	0	–
2	L-Leucine	3	0	–
3	**L1**	57	48	0
4	(*R*)-BIDIME	100	81	0

Reactions performed on a 0.1 mmol scale. [a] According to ^{1}H-NMR with 1,3,5-trimethoxybenzene as internal standard.

Solvents are known to coordinate to palladium complexes.[277] To probe if DMF coordinates the palladium and thus competes with the chiral ligand in these reactions inhibiting product formation, solvent mixtures with PhMe were investigated. A 1:1 solvent mixture toluene:DMF gave incomplete conversion to product while any less DMF even in the presence of ligands gave no conversion to product (Table 23). Such solvent mixtures have successfully been applied in literature.[167]

Table 23: Solvent screening of the palladium-catalyzed silylation.

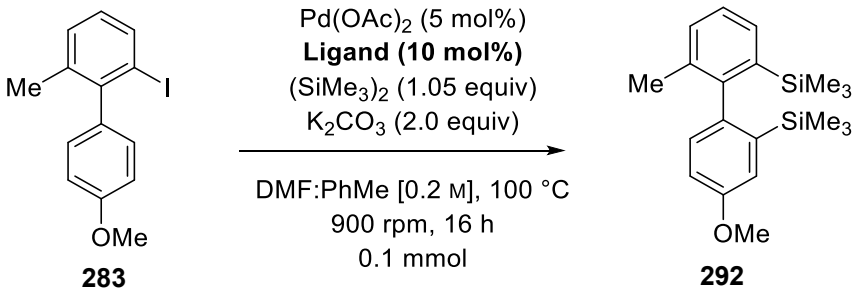

283 **292**

#	Ligand	Solvent (DMF:PhMe)	Conversion[a] [%]	Product[a] [%]
1	-	5:5	63	36
2	-	1:9	0	0
3	PPh_3	PhMe	6	0
4	L-Leucine	PhMe	0	0
5	Boc-L-Valine	PhMe	1	0

Reactions performed on a 0.1 mmol scale. [a] according to ^{1}H-NMR with 1,3,5-trimethoxybenzene as internal standard.

In summary, the importance of silane volatility could be shown. Moreover, preliminary calculations implied the palladacyclic intermediate to be stereodynamic. Next steps should further investigate if chiral ligands can be used in reactions involving palladacycles to leverage these stereodynamic intermediates.

5.5 Chiral Acetylene

A manuscript containing the following chapter and results is currently in preparation.[278]

The use of oxabicycles as acetylene analogues[279] and as a chiral transient auxiliary[259a] has been shown in recent literature. The following chapter focusses on investigating the mechanisms taking place in the stereoselective synthesis of indenes (Scheme 76). Indenes are pharmaceutically relevant scaffolds present in a variety of medicinally relevant drugs.[280] Therefore new methods should be explored to widen the accessible range of substitution patterns as well as to enantioenrich the desired products. Results obtained from the initial study by *Abel-Snape et al.* using a chiral enantioenriched oxabicycle with a chiral amide sidechain needed to be verified first.[259a] Furthermore, studies using racemic oxabicycles were conducted to investigate key-intermediates to probe the surprising implications on diastereo-, regio- and stereoselectivities (Chapters 5.5.4). Efforts were directed towards identifying the absolute configuration of the pre-retro-*Diels-Alder* intermediates (prDA) and final products. Finally, DFT calculations were conducted to rationalize observed ratios.

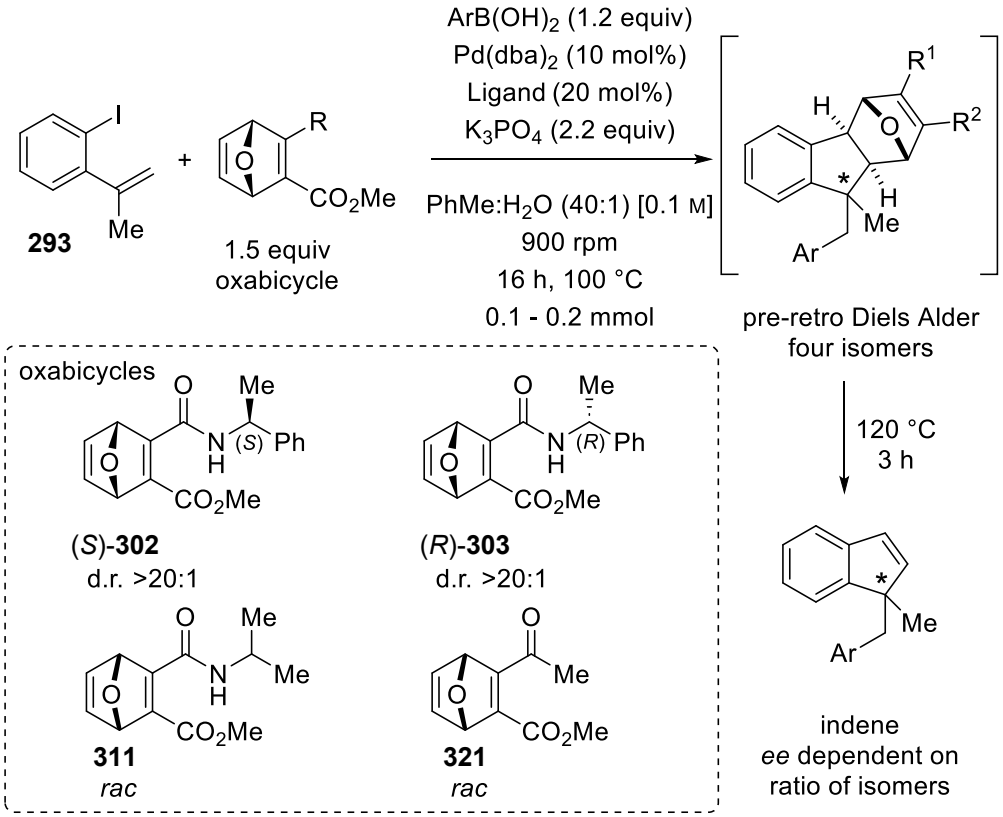

Scheme 76: Stereoselective synthesis of indenes *via* pre-retro-*Diels-Alder* intermediates.

5.5.1 Reaction Mechanism

Abel-Snape et al. proposed a catalytic cycle for the synthesis of indenes (Scheme 77).[259a] As of the writing of this thesis, *Han et al.* in a recent publication discusses the viability of the proposed mechanism.[281] Their findings support the 'alkene-first'-mechanism described hereafter. The catalytic cycle is comprised of several key steps that may influence the stereoselectivity. Starting from palladium complex **I**, oxidative addition **a)** of aryl iodide **293** generates palladium complex **II**. Next coordination **b)** of the oxabicycle forms palladium complex **III** followed by migratory insertion **c)** to form palladium complex **IV**. This migratory insertion step is thought to selectively proceed *exo*. Then a 5-exo-trig cyclization[282] **d)** generates palladium complex **V**. Ligand coordination (**VI**) followed by transmetalation **e)** generates the final palladium complex **VII**. Reductive elimination regenerates **I** by extruding a pre-retro-*Diels-Alder* (prDA) intermediate. The relative stereochemistry of these prDA intermediates is determined by the various steps in the catalytic cycle. It is important to note that certain simplifications have been made for this catalytic cycle. Moreover, the transmetalation step **e)** may occur earlier in the catalytic cycle and then influence subsequent steps. The formation of the indene final product proceeds *via* an off-cycle, thermically induced retro-*Diels-Alder* reaction of the prDA intermediate.

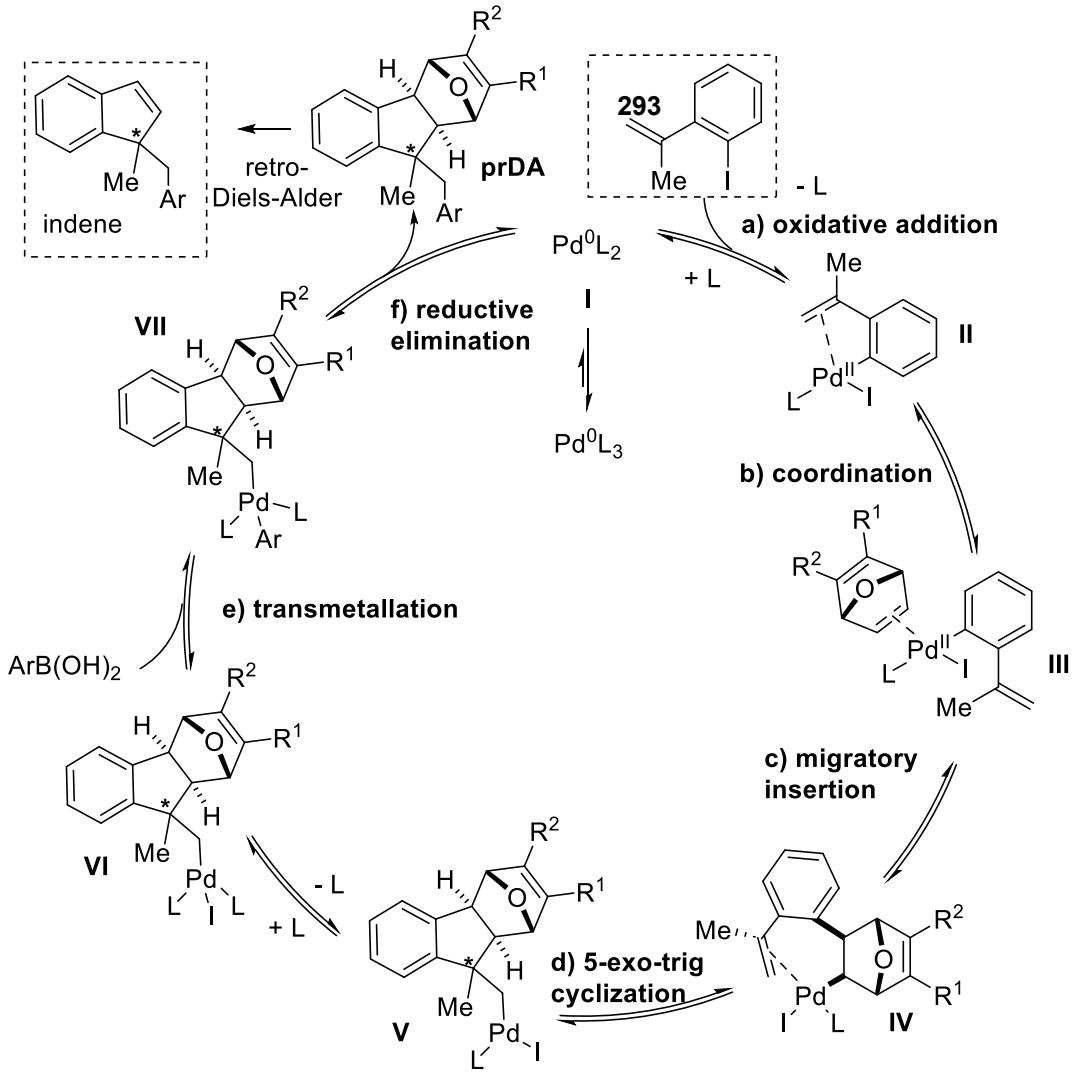

Scheme 77: Proposed catalytic cycle of the synthesis of indenes using oxabicycles. In accordance with *Abel-Snape et al.*[259a]

Expanding on this mechanism, a rational for the observed stereoselectivity of the reaction reported by *Abel-Snape et al.* can be formulated. The stereoselective implications of these steps become apparent by looking at the migratory insertion **c)** as well as the cyclization **d)**. In case of the oxabicycle being C_s-symmetrical ($R^1 = R^2$) (e.g. **296**) (Scheme 78), **IVa** and **IVb** are enantiomers of one another. The ratio should be 1:1 unless chiral ligands are used. The subsequent ratio of **Vaa** and **Vab** corresponds to a diastereomeric ratio (d.r.). The ratio of the enantiocomplementary **Vba** and **Vbb** should mirror this ratio. Under *Curtin-Hammet* control this diastereomeric ratio will depend on the ΔG of the relevant transition state. The resulting indene should be generated based on these ratios. In case of a C_s-symmetrical oxabicycle the enantiomeric ratio will be 1:1 after the retro-*Diels-Alder*.

In case of the use of a chiral oxabicycle ($R^1 \neq R^2$), the insertion does not result in two enantiomers but in two constitutional isomers **IVa** and **IVb** (Scheme 78). This constitutes a

regioisomeric ratio (r.r.). The cyclization of **IVa** again results in different diastereomers **Vaa** and **Vab**. The diastereomeric ratio of these does not necessarily mirror the diastereomic ratio of **Vba** and **Vbb**. Unless the d.r. of this step is 1:1 for both pairs, or the r.r. is 1:1, the resulting indenes will be enantioenriched. The enantiomeric excess will correspond to the ratios (both regioisomeric- and diastereomeric-) of the prDA intermediates observed (r.r. **IVa** vs **IVb**; d.r. **Vaa** vs **Vab** and d.r. **Vba** and **Vbb**). These ratios will be the same even if the chiral oxabicycle is employed as a racemic mixture.

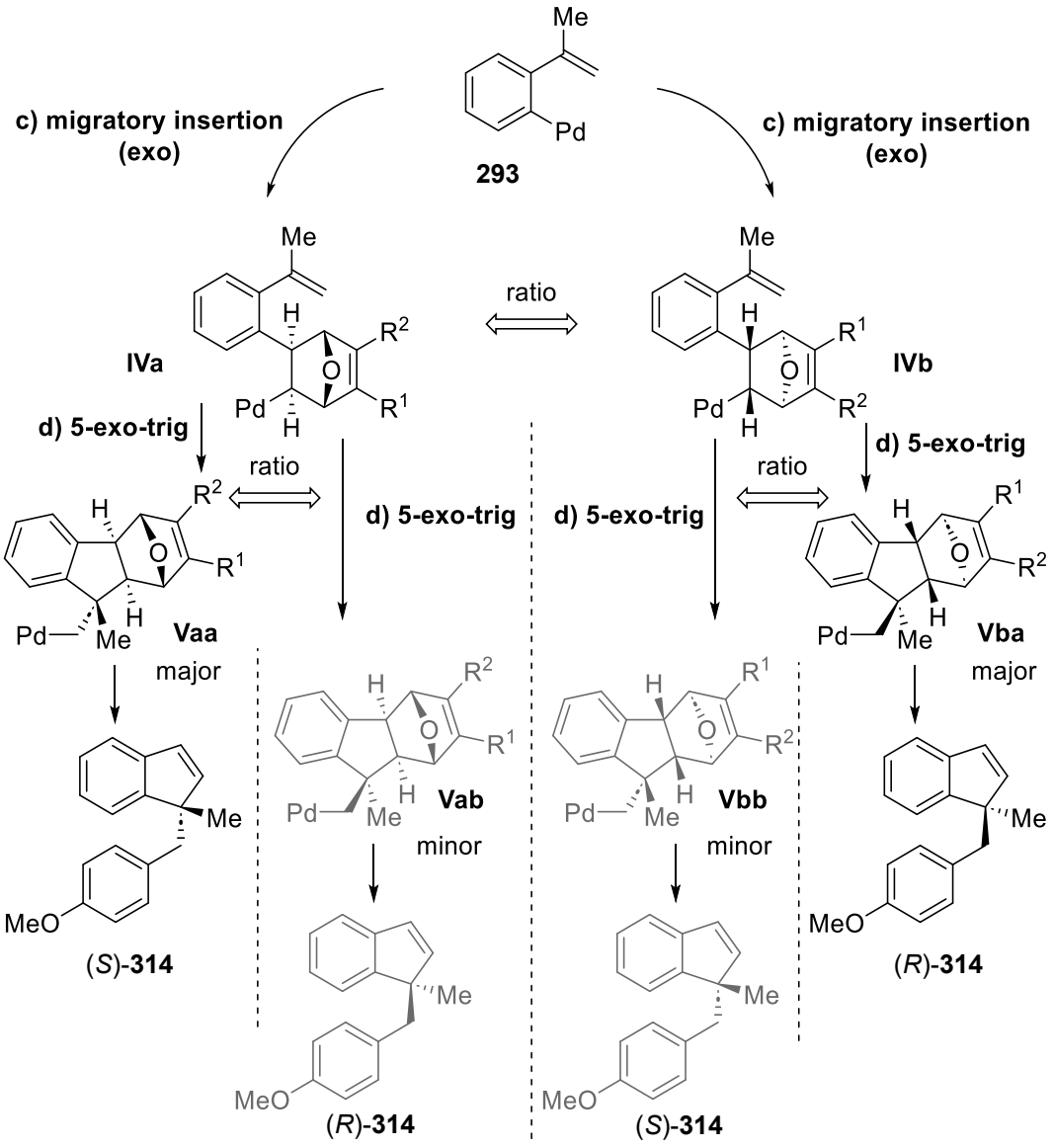

Scheme 78: Visualization of the exo-insertion of an oxabicycles and subsequent 5-exo-trig cyclization forming the relevant isomers. Ratios observed are indicative for enantiomeric ratio.

The prDA intermediate ratios will be discussed following optimization efforts using enantiopure oxabicycles to synthesize enantioenriched indenes. The observed prDA intermediate isomer ratios will be compared with the enantiomeric excess of the enantioselective reaction to probe the validity of this hypothesis.

5.5.2 Substrate syntheses

To investigate the synthesis of enantiopure indenes, starting materials needed to be synthesized first. The substrate **293** for the catalytic reaction was synthesized *via* a literature known procedure over two steps.[259a] Starting from commercially available acetophenone **294,** the *Sandmeyer* reaction to form **295** and subsequent *Wittig*-olefination proceeded smoothly to provide the substrate in a yield of 70% over two separate steps on a 10 mmol scale (1.1 g product **293**) (Scheme 79A), or in a yield of 78% over two steps on a 20 mmol scale (3.8 g product **293**) (Scheme 79B). Using KO*t*-Bu as an anhydrous solution in THF ensured proper and quantitative activation of the ylide in the second step.

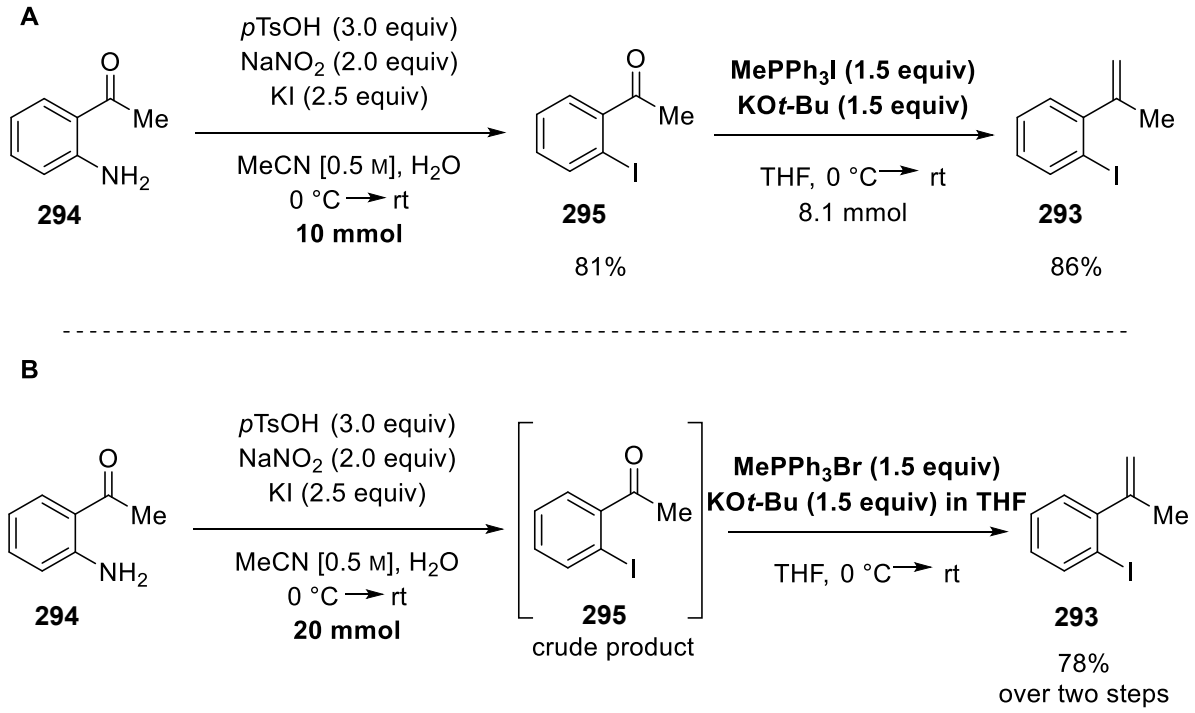

Scheme 79: *Sandmeyer* reaction for the synthesis of substrate **293** for catalytic reactions.

Next, oxabicycle **296** was synthesized by a literature known *Diels-Alder* [4+2]-cycloaddition of alkyne **297** with furan (**298**) (Scheme 80A).[279a] The product could be isolated in a yield of 70%. Overall, the product decomposed over time, gradually turning from a pale yellow to a dark orange and eventually a dark brown color, even when stored under argon at −20 °C. Additionally, dimethyl oxabicycle **299** was synthesized using furan **300** to be used in further investigations (Scheme 80B). No decomposition of **299** synthesized under the given conditions was observed over time. The lack of allylic hydrogens may play a role in the stability of this compound class.

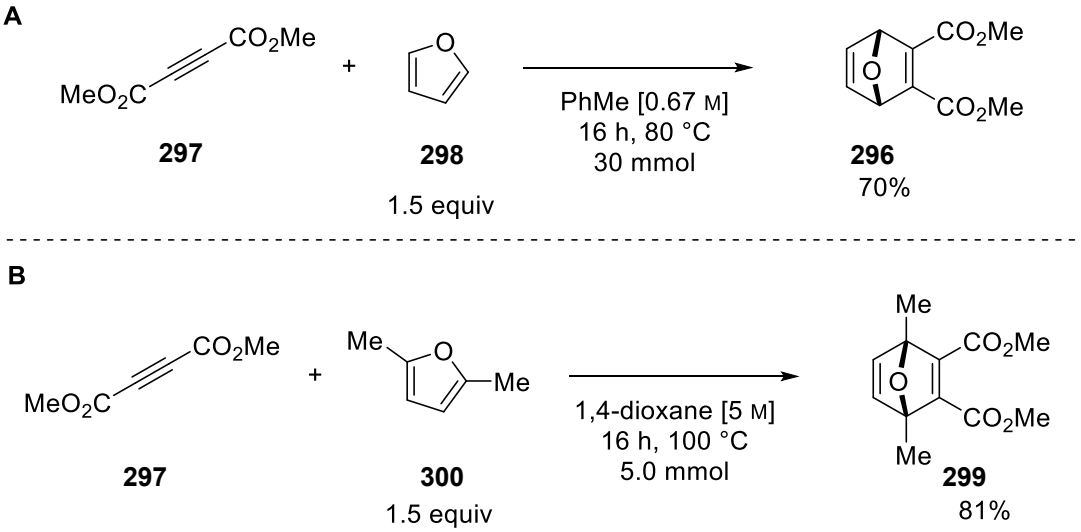

Scheme 80: Synthesis of oxabicycles *via Diels-Alder* [4+2]-cycloaddition.

Next, the synthesis of chiral oxabicycles was conducted. As outlined in the abstract, the aim of the initial investigations was to determine if the chirality of the amine in the oxabicycle amide played a role in the stereoselectivity determining step. In order to do this, starting material **301** for the amide coupling had to be synthesized first. Desymmetrization of C_s-symmetrical oxabicycle **296** was conducted by hydrolysis *via* a literature known protocol[259a] to provide the racemic chiral oxabicycle **301** in a yield of 61%. After implementing an improved workup protocol making use of a base wash, the yield could be increased to 78% (Scheme 81).

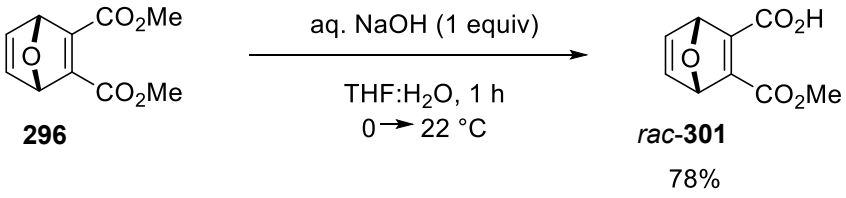

Scheme 81: Hydrolysis of C_s-symmetrical oxabicycle **301**.

Moving forward, the synthesis of oxabicycle amides **302** and **303** was performed according to a literature known procedure.[259a] Amide couplings using oxabicycle **301** have been reported in literature yet suffer from low yields.[283] To avoid wasting precious enantiopure oxabicycle **301** provided by *Greg Hughes*, reactions were performed using the racemic material first. Indeed, conversion to the desired products using coupling reagent DMTMM (**304**) and *α*-methylbenzylamine (**305**) was undesirably low (57%) (Table 24).

Table 24: DMTMM coupling towards oxabicycles **302** and **303**.

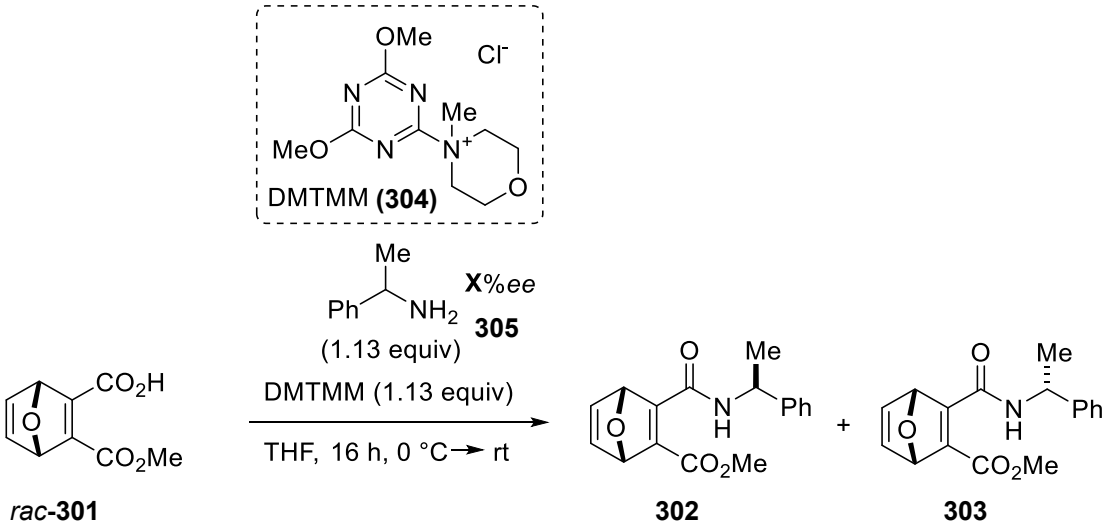

Entry	Amine [%*ee*]	yield [%]	d.r. (302:303)	*ee* [%][c]
1	98 (*S*)	57	1.16:1[a]	98/98
2	0 (*rac*)	53	1.29:1[b]	0/0

HPLC conditions: 0.5 mL/min, hexanes:*i*PrOH/9:1, IA-CHIRALPAK®, 22 °C. Isolated yields. [a] according to HPLC after column purification, [b] according to ^{1}H NMR after column purification. [c] enantiomeric excess by HPLC for **302**/**303**

To investigate if coupling agents other than DMTMM (**304**) would also provide the desired oxabicycle amides, a small range of typical, literature known amide coupling reagents were used (Scheme 82). In all cases a combination of a racemic mixture of mono acid oxabicycle **301** and (*S*)-*α*-methylbenzylamine ((*S*)-**305**) was employed. No product formation was observed using these alternative coupling strategies.

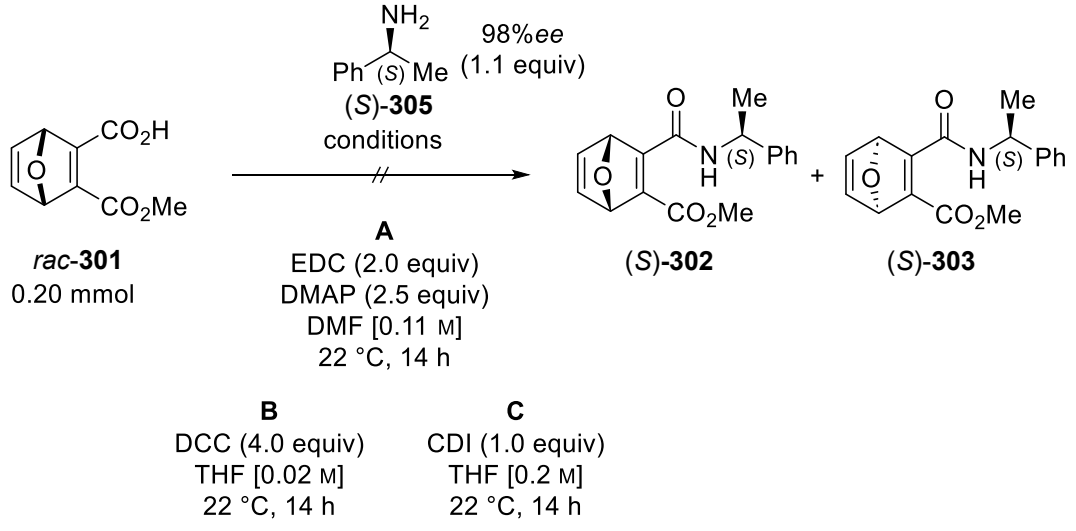

Scheme 82: Various amide coupling strategies.

After column chromatographic isolation of multiple batches of oxabicycle amide **302**, ^{1}H-NMR analysis not only showed the expected signals (Figure 19A), but also in multiple cases a further set of shifted peaks (Figure 19B). A mass analysis of this mixture revealed virtually identical mass chromatograms with the same m/z (300.3 $[M+H]^{+}$ and 353.3) as for a sample without impurities according to ^{1}H-NMR. Thus, the observed 'impurity' might have the same m/z. An isomerization experiment stirring the mixture of **302** and unknown impurity in toluene at 80 °C resulted in these impurity peaks (6.62 and 6.28 ppm) disappearing. At the same time new peak sets appeared (Figure 19B to C). The ratio of product:impurity pre stirring in PhMe at 80 °C was 7:3 while after stirring the ratio of product:new impurities was 8:2.

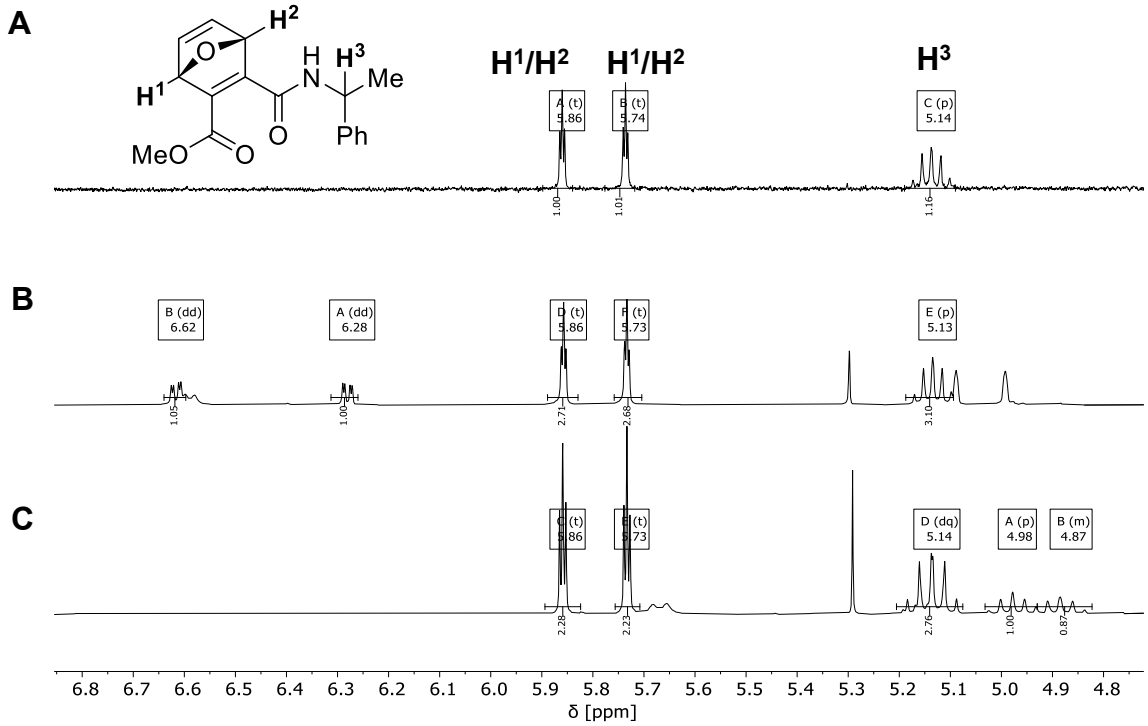

Figure 19: (A) Isolated **302** without additional peak set. (B) product **302** after a column chromatographic isolation attempt showing additional peaks. (C) Same product as **B** after stirring in toluene for 1.5 h at 80 °C, peak sets observed for **A** are no longer present, additional peaks are now visible.

5.5.2.1 Optimization of racemic amide coupling

To improve yields and address the seemingly inconsistent formation of side products, reaction conditions were screened using benzhydrylamine (**306**) to avoid formation of diastereomeric mixtures (Table 25). Experiments were set up in triplicates. Lower temperature (0 °C) was found to be crucial in increasing conversion to the desired product *rac*-**307**. Furthermore, using DMF as the solvent increased yields, yet poor removal of trace amounts of DMF made the use of THF more facile. Pre-stirring the DMTMM and acid was done to assure sequential formation of the activated carboxylate with subsequent substitution by the amine. Additional equivalents of amine were added to investigate if activation of the DMTMM was dependent on the presence of excess amine. No major side product formation (compare Figure 19) was observed using these conditions.

Table 25: Optimization of the amide coupling using DMTMM.

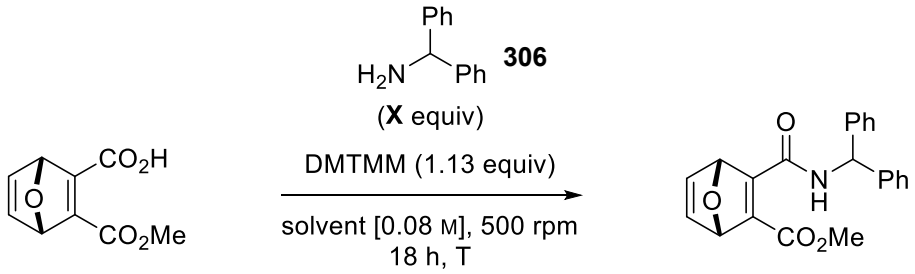

rac-**301** *rac*-**307**

#	Pre-stir with DMTMM[a]	Solvent	Amine [equiv]	T [°C]	Product [%]
1	No	THF	1.13	22	31±1
2	No	THF	1.13	22	32±2
3	No	THF	1.13	0	46±3
4	No	THF	2.00	0	38±0
5	Yes	THF	2.00	0	43±6
6	No	THF [0.25 M]	1.13	0	43
7	No	DMF	1.13	0	53
8	Yes	DMF	2.00	0	16

All reactions were performed on a 0.1 mmol scale. Conversion of starting material **68** and to products according to ^{1}H-NMR with 1,3,5-trimethoxybenzene as internal standard. Reactions with standard deviation performed as triplicates. [a] Pre-stirring refers to the addition of DMTMM and oxabicycle mono acid **301** and stirring at 0 °C for 10 min before the addition of amine **306**.

As outlined in the introduction, the influence of amine side chain was to be probed in the catalytical transformation. Therefore, a racemic dedicated library was synthesized. The use of benzylamine as the primary (1°) amine only gave the desired product **308** in trace amounts. The low steric bulk of the 1° amine may result in side product formation not observed for 2° amines.

The crude ^{1}H NMR revealed the presence of additional peaks akin to the ones previously observed for **303** and **302**. The use of isopropylamine (**309**), adamantylamine (**310**), or benzylhydrylamine (**306**) gave the corresponding products **311**, **312**, and **307** in acceptable yields (47 – 60%). The sterically bulky adamantyl group gave the highest yield, in line with the proposed importance of sterically bulky amines. The crude ^{1}H NMR contained little side products.

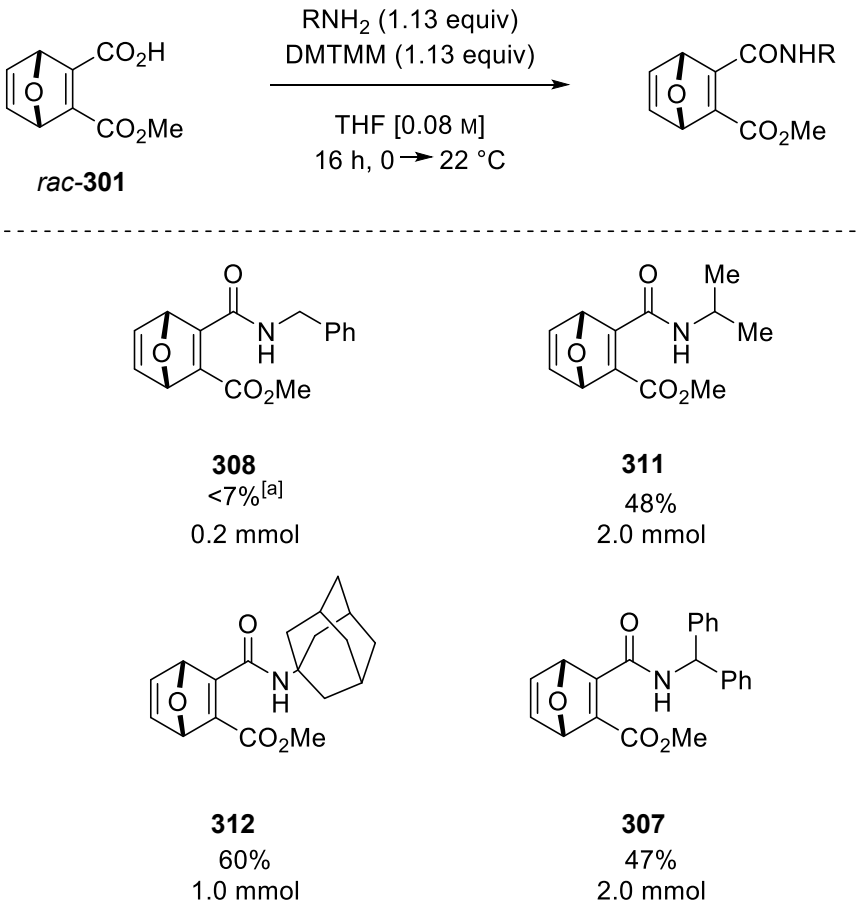

Scheme 83: Scope of oxabicycle amides synthesized. [a] major impurity persists after column chromatographic isolation.

5.5.3 Indene synthesis

5.5.3.1 Investigations on the Pd-source

Before commencing with the enantioselective synthesis of indenes, first, the influence of scale regarding yield was assessed as the original protocol was conducted on 0.2 mmol scale using oxabicycle **296**. Due to limited quantities of enantiopure oxabicycle mono acid **301** being readily available, a 0.1 mmol scale would conserve starting material. Additionally, the use of $(Pd\ G4)_2$ (**205**) in addition to the originally employed $Pd(dba)_2$ as the Pd-source was investigated. The reaction using boronic acid ester **313** gave *rac*-**314** in lower yields on 0.1 mmol scale (71%) compared to 0.2 mmol scale (80%) (lit.: 85%)[259a] (Table 26, entries 1 – 2). Using $(Pd\ G4)_2$ (**205**) as the Pd-source gave comparable yields of 80–83% (Table 26, entries 3 – 4) to the reported yield using $Pd(dba)_2$ (lit.: 85%).[259a] An additional 0.1 equivalents of K_3PO_4 were added when using $(PdG4)_2$ (**205**) to account for Pd G4-precatalyst deprotonation in addition to 0.2 equivalents accounting for the liberation of phosphine HBF_4 adduct. Degassing the PhMe by sparging did not significantly affect the yields.

Table 26: Synthesis of indene **314** using oxabicycle **296**.

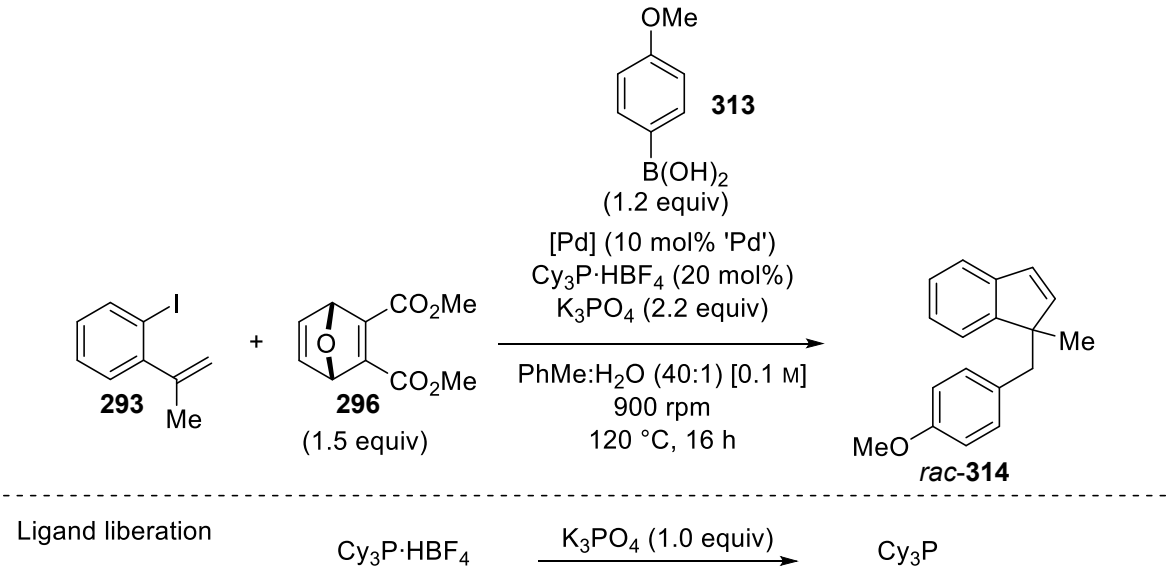

#	Pd source	K_3PO_4 [equiv]	scale [mmol]	Product [%]
1	$Pd(dba)_2$	2.2	0.2	80
2	$Pd(dba)_2$	2.2	0.1	71
3	$(PdG4)_2$	2.3	0.2	83
4[a]	$(PdG4)_2$	2.3	0.2	80

[a] degassed PhMe by sparging for 30 min.

In addition to the *Suzuki* termination, alternative terminating agents were considered as these could have an influence on the enantioselectivity via the early transmetalation mechanism (Chapter 5.5.1). The decarboxylative *Sonogashira* termination using phenyl propiolic acid (**315**) towards indene *rac*-**316** was first tested in a racemic fashion to see if the yield of this reaction could be increased using $(Pd\ G4)_2$ (**205**) (Table 27). The resulting yield (72%) was lower than the reported yield using $(Pd\ G4)_2$ (**205**) (lit.: 79%).[259a] Degassing the toluene by sparging again did not affect the yield (72%).

Table 27: Synthesis of indene **316** *via* decarboxylative *Sonogashira* termination.

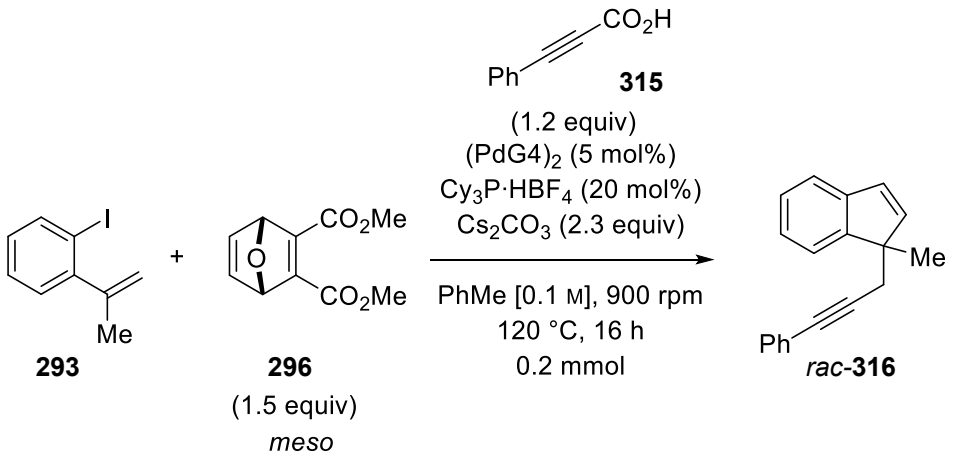

#	Variations	Product [%]
1	None	72
2	Degassed PhMe[a]	72

Reactions performed on a 0.2 mmol scale. [a] degassed PhMe by sparging for 30 min. As a dinuclear palladium-complex $(Pd\ G4)_2$ contributes twice as much palladium as $Pd(dba)_2$. Therefore, 5 mol% $(Pd\ G4)_2$ correspond to 10 mol% palladium nuclei.

5.5.3.2 Enantioselective synthesis of indenes with chiral oxabicycles

With assessments towards racemic oxabicycles and indenes in place, the synthesis of enantioenriched oxabicycles was investigated next. Using enantiopure oxabicycle mono acid **296** (99%*ee*) in combination with enantiomerically enriched *α*-methyl-benzylamine (**305**) (99%ee (*R*) or (*S*)) the enantio- and diastereoenriched amide oxabicycles (*S*)-**302** and (*R*)-**303** were synthesized (Scheme 84).

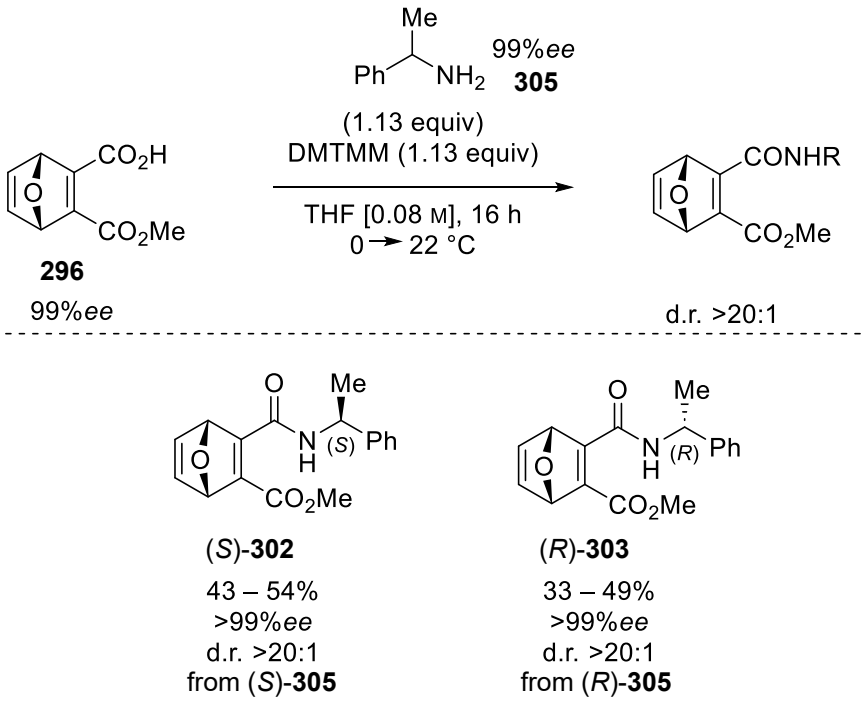

Scheme 84: Synthesis of enantio- and diastereoenriched oxabicycle amides (*S*)-**302** and (*R*)-**303**. Diastereomeric ratio determined by ^{1}H-NMR, enantiomeric excess determined by chiral HPLC.

Additionally, chiral phosphoramidite ligand (*S,S*)-**L3** was synthesized according to literature known protocols (Scheme 85) as it was found to function as a chiral ligand with mediocre induction of stereoselectivity (lit.: 37%*ee* of product) in the indene synthesis.[259a] This was done to investigate if the use of chiral oxabicycles in combination with this chiral ligand would have a synergistic effect. The synthesis proceeded smoothly starting from tartaric acid ester **317** via acetal protected **318** to TADDOL **319** in a yield of 46% over two steps. The ligand (*S,S*)-**L3** was then obtained in a yield of 53% by precipitation.

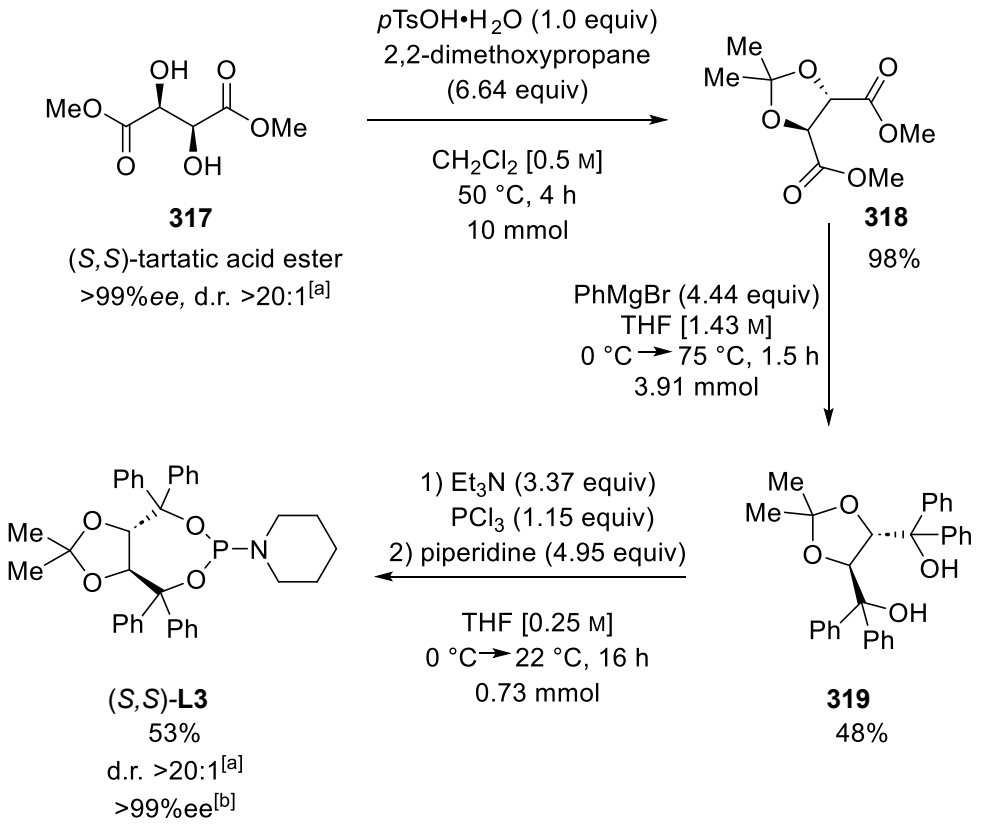

Scheme 85: Synthesis of ligand **L3**. [a] Relative to *meso*-**317** or (*S,R*)-**L3** respectively according to ^{1}H-NMR. [b] Inferred from starting material.

With starting materials and ligand in hand, the enantioselective synthesis of indenes was investigated. It was first explored if the reported 31%*ee,* when using chiral oxabicycle amide (*S*)**-302** (4.3:1 d.r.) in combination with an achiral ligand ($Cy_3P{\cdot}HBF_4$), could be improved (Table 28, entry 1).[259a] Indeed, a marked increase to 52%*ee* could be observed when using (*S*)**-302** (>20:1 d.r.) (Table 28, entry 2). The use of oxabicycle amide (*S*)**-302** with the aforementioned additional irremovable impurity according to ^{1}H-NMR-analysis was also investigated. While yields were lower (36% vs 46%, Table 28, entries 2 and 3), the enantiomeric excess was not significantly affected. Next, the combination of chiral ligand with chiral oxabicycle was probed. While (*S,S*)-**L3** in combination with oxabicycle **296** resulted in an enantiomeric excess of 42%*ee* (lit.: 37%*ee*[259a]), a combination of ligand (*S,S*)-**L3** with chiral oxabicycle (*R*)-**303** (>20:1 d.r.) only gave 27%*ee*. This showed a clear mismatch between ligand and chiral oxabicycle.[10][284] The cause for this may be the different electronic properties of phosphoramidite ligand **L3** (electron-deficient, π-acceptor) compared to a trialkyl ligand like Cy_3P (electron-rich, σ-donor).[285] To probe if the ligand has a large influence on the selectivity of the reaction, achiral PPh_3 was employed as a less electron-rich σ-donor. Indeed, using this

[10] The combination of (*R,R*)-**L3** with (*S*)-**302** (4.3:1 d.r.) was conducted by Xavier Abel-Snape and also gave lower enantioselectivity than either effect alone.

oxabicycle-ligand combination 30 – 45%*ee* of the **opposite enantiomer** was obtained (Table 28, entry 9).

Table 28: Enantioselective synthesis of indene **314**

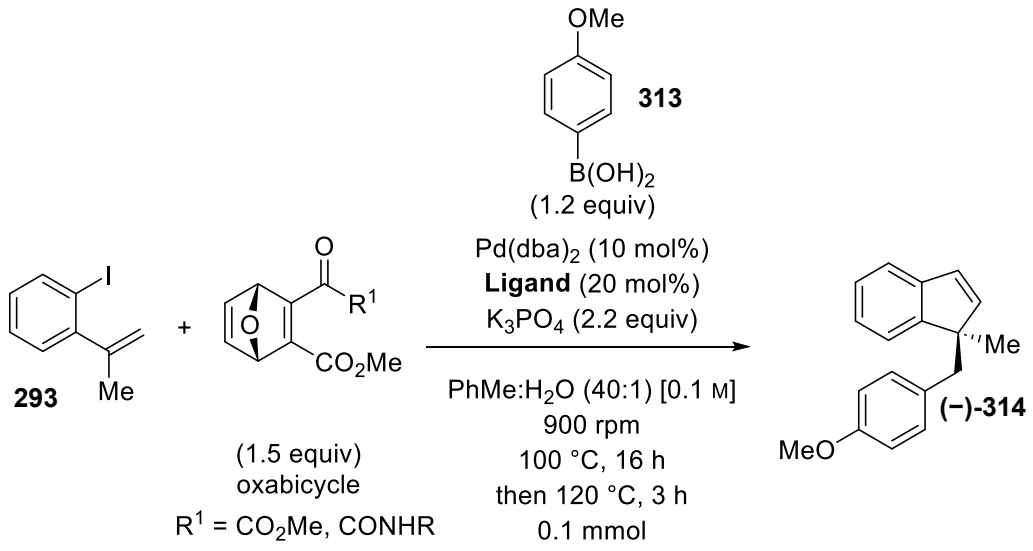

#	Oxabicycle	d.r. oxabicycle 302:303	Ligand	Product[d] [%]	*ee* [%]
1	(*S*)-**302**	4.3:1	$Cy_3P{\cdot}HBF_4$	– (50)	32[259a]
2	(*S*)-**302**	>20:1	$Cy_3P{\cdot}HBF_4$	50 (46)	**52**
3[a]	(*S*)-**302**	>20:1	$Cy_3P{\cdot}HBF_4$	32 (36)	50
4[a]	(*R*)-**303**	1:>20	$Cy_3P{\cdot}HBF_4$	41 (42)	48
5	**296**	–	(*R,R*)-**L3**	– (41)	−37[259a]
6	**296**	–	(*S,S*)-**L3**	28 (27)	42
7[a]	(*R*)-**303**	1:>20	(*S,S*)-**L3**	26 (25)	27
8[b]	(*S*)-**302**	>20:1	$Cy_3P{\cdot}HBF_4$	23 (26)	52
9[c][e]	(*S*)-**302**	>20:1	PPh_3	– (18)	**−(30 – 45)**[e]

Absolute configuration known by x-ray crystal structures. d.r. determined by ^{1}H-NMR. Enantiomeric excess of chiral oxabicycles >99%*ee* according to chiral HPLC [a] oxabicycle contained major impurities according to ^{1}H-NMR (iminoic acid); [b] at 90 °C instead of 100 °C; [c] 2.0 equiv K_3PO_4; [d] Conversion of starting material **293** and to product **314** according to ^{1}H-NMR with 1,3,5-trimethoxybenzene as internal standard isolated yield in brackets. [e] Impurity present, *ee* approximated.

Under the assumption that the two diastereomers, of the 4.3:1 d.r mixture reported in literature, would give the opposite enantiomer with the same selectivity, the *ee* should correspond to the theoretical ratio obtained when using a 4.3:1 mixture of diastereopure (>20:1 d.r) oxabicycles (*S*)-**302**:(*S*)-**303**. If the *ee* of the resulting product does not correspond to the theoretically calculated *ee*, then non-linear effects such as oxabicycle Pd-coordination should play a role in the catalytic cycle.

In the following section calculation and comparison of the theoretical enantiomeric excess according to observed enantioselectivites with batches of oxabicycle with various d.r. will be conducted.

The relative amount of major enantiomer formed $e1_{4.3:1}$ (enantioselectivity using a 4.3:1 d.r. mixture of oxabicycle, equation 5) is formed with a selectivity $e1_{>20:1}$ (enantioselectivity using a >20:1 d.r. mixture of oxabicycle) proportional to the major diastereomer (*S*)-**302** (d_1; in this case 0.81[11]) in addition to the same but opposite selectivity (1 – $e1_{>20:1}$) of the minor diastereomer (*S*)-**303** (1 − d_1; in this case 0.19) (equation 5).

$$ee = \frac{e1 - e2}{e1 + e2} \tag{4}$$

$$e1_{4.3:1} = d_1 * e1_{>20:1} + (1 - d_1) * (1 - e1_{>20:1}) \tag{5}$$

$$e1_{>20:1} = \frac{e1_{4.3:1} - 1 + d_1}{(2 * d_1 - 1)} \tag{6}$$

$$e1_{>20:1} = \frac{0.655 - 1 + 0.81}{(2 * 0.81 - 1)} = 0.75\ (50\%ee) \tag{7}$$

$e1_{4.3:1}$ = 0.655 is the observed relative peak area according to HPLC of the major enantiomer using d.r. 4.3:1 (0.81:0.19) ((*S*)-**302**:(*S*)-**303**). d_1 is the relative amount of the major diastereomer (*S*)-**302** (0.81). $e1_{>20:1}$ is the relative peak area of the major enantiomer using >20:1 d.r. ((*S*)-**302**:(*S*)-**303**).

By reforming the equation solving for the selectivity of enantiomer formation $e1_{>20:1}$ (6) and inserting the values (7) for the given literature known data (4.3:1, 31%*ee*),[259a] the obtained selectivity is $e1_{>20:1}$ = 0.75 (7). The expected enantiomeric excess is therefore 50%*ee*. This is in good agreement with the experimentally observed value using (*S*)-**302** (Table 28, entry 2, 52%*ee*). A reaction using (*R*)-**303** should therefore exhibit an enantioselectivity of 50%*ee,* which correlated well with the observed selectivity of 48%*ee* (Table 28, entry 2). Thus, the hypothesis of the stereogenic information of the amine not significantly influencing the enantioselectivity could be supported by the experimental data. Additionally, this implied that the oxabicycle does not serve as a ligand during the transformation which would result in non-linear effects.

[11] 4.3/5.3 = 0.81

To see if the terminating agent had an influence on the enantioselectivity of the reaction, the decarboxylative *Sonogashira* reaction was investigated in combination with chiral ligand (*S,S*)-**L3** (Scheme 86). Unfortunately, separation of the enantiomers was not possible by HPLC.

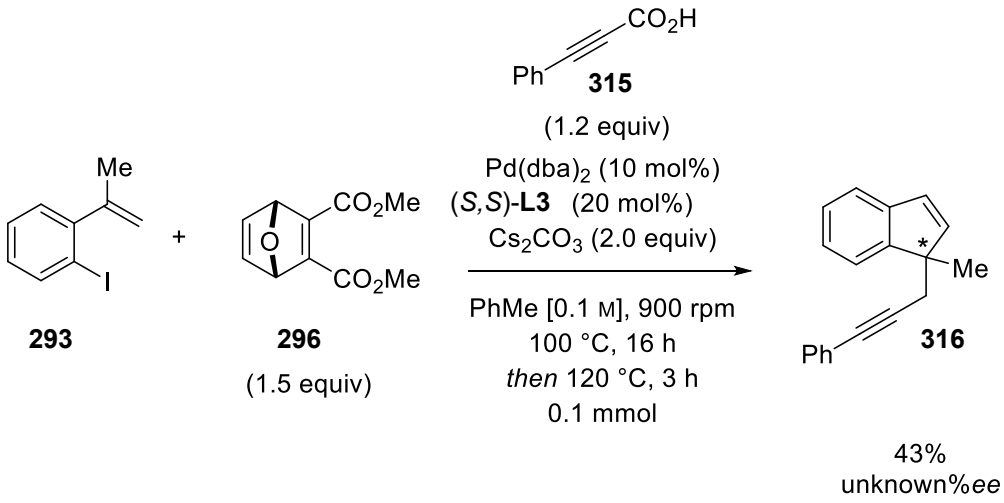

Scheme 86: Decarboxylative *Sonogashira* termination with chiral ligand (*S,S*)-**L3**.

In summary, it could be shown that the choice of ligand in this reaction had a significant effect on the stereoselectivity. A switch from trialkyl phosphine to triaryl phosphine ligand inverted the stereoselectivity of the reaction. Additionally, the use of phosphoramidite ligand (*S,S*)-**L3** showed a mismatch when using chiral oxabicycle (*S*)-**302**. The stereogenic center on the amide side chain did not significantly affect the *ee* of the reaction. This highlighted, that only the stereogenic information of the bicycle itself played a role in the stereoselectivity of the reaction. Non-linear effects could also be ruled out.

5.5.3.3 Oxabicycle Scope

With these promising results in place, alternative non-C_2 symmetrical oxabicycles in addition to the amide/ester oxabicycle system were investigated. These oxabicycles would serve as new potential chiral oxabicycles in the palladium-catalyzed indene synthesis. Modification of the electron withdrawing groups should result in a more selective insertion of the oxabicycle into the palladium complex. The reasoning for this was, that the enantioselectivity depends on the electronic effects of the carbonyls. A more pronounced electronic discrimination of these groups could result in a greater stereoselectivity. First, the racemic ester acid **301** was employed. In deprotonated form this carboxylate would serve as a readily available and relatively electron-rich oxabicycle. No conversion to product was observed for both the *Suzuki* termination (Scheme 87A) and for the decarboxylative *Sonogashira* termination (Scheme 87B) even in the presence of additional base to account for the carboxylic acid proton abstraction. Strong coordination of the carboxylate to the palladium complex was thought to be responsible for the lack of conversion to product.

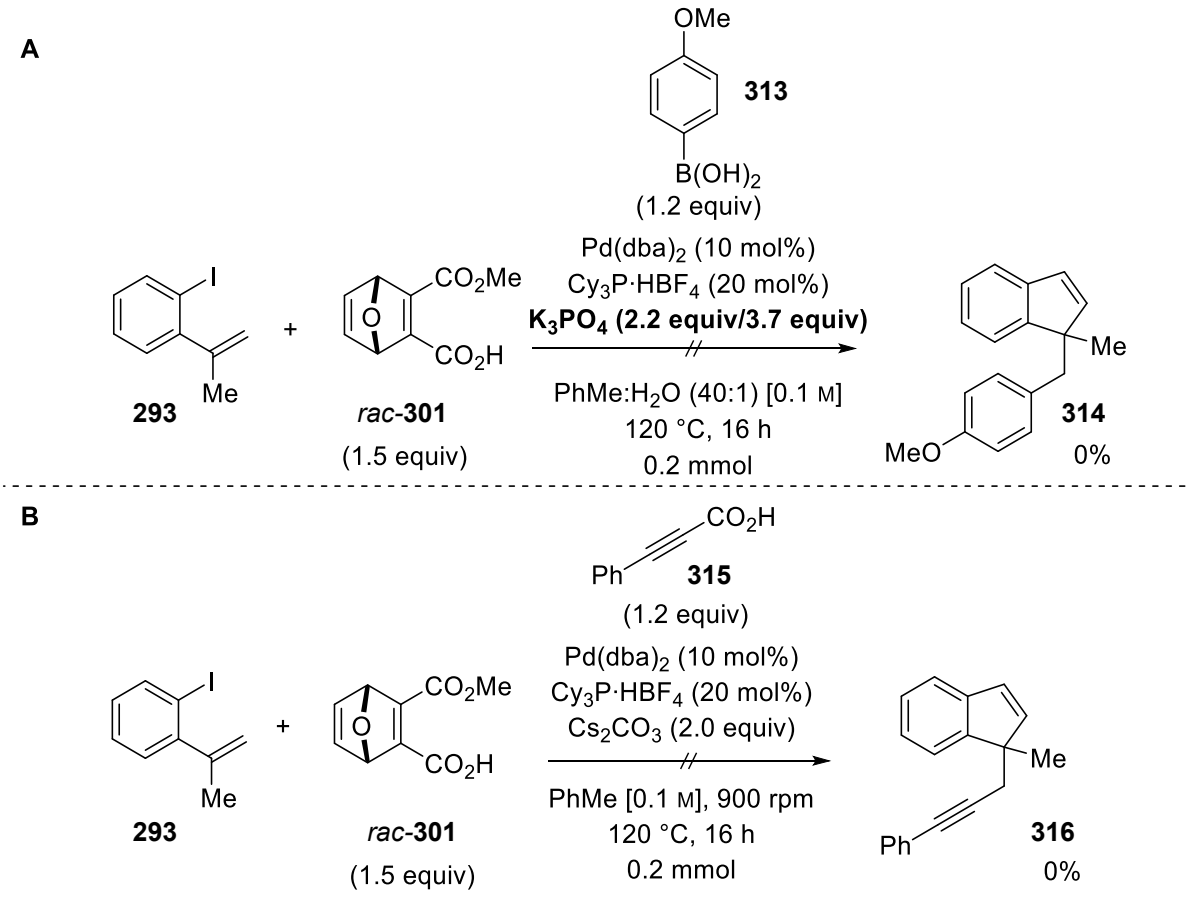

Scheme 87: (A) Indene synthesis with *Suzuki* termination using oxabicycle mono acid **296**. (B) Indene synthesis with decarboxylative *Sonogashira* termination using oxabicycle mono acid **296**.

Instead, efforts were directed at synthesizing other oxabicycles. The two strategies to obtain modified oxabicycles were to either modify existing oxabicycle mono acid **301** (Scheme 88A),

or to synthesize the oxabicycle *via* de-novo strategy akin to the synthesis of **296** (Scheme 88B). The former would bear the advantage of leveraging the already established separation of the enantiomers while the latter would make use of readily accessible propiolates **320**.

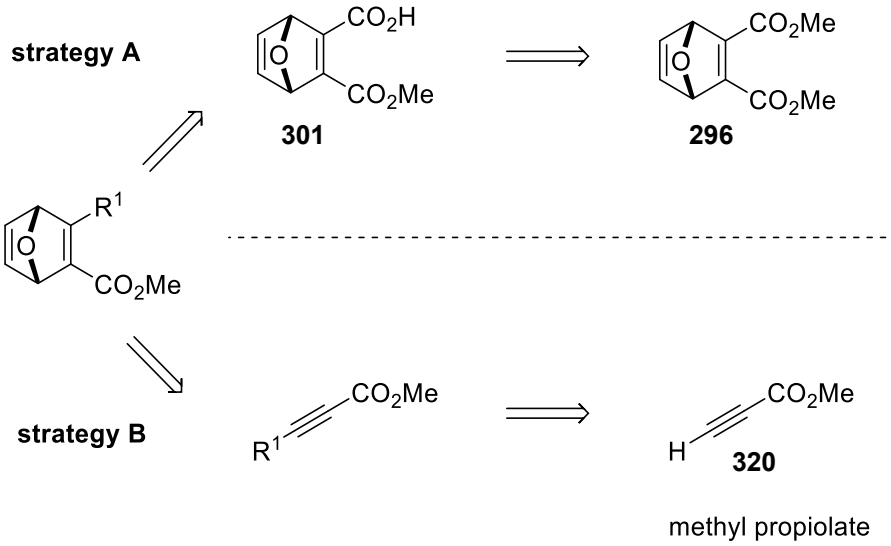

Scheme 88: Synthesis strategies for chiral oxabicycles. (A) modification of oxabicycle **301**. (B) synthesis of oxabicycle *via* modified alkynes via *Diels-Alder* [4+2]-cycloaddition.

Next, transformation of oxabicycle mono acid **301** into keto ester **321** *via* an acyl chloride intermediate **322** was investigated (Scheme 89). Only a complex mixture was obtained in this procedure according to ^{1}H NMR yet full conversion of **301** was observed. A reaction control to investigate the formation of **322** also showed a complex mixture. The m/z of the desired product could not be observed in the crude product after the addition of MeMgBr. Alternatively, the use of dimethyl malonate as the methylating agent followed by decarboxylation was investigated (Scheme 89). Again, reaction control of the acyl chloride revealed a complex ^{1}H NMR indicating the formation of the acyl chloride to be difficult under the employed conditions. Neither the desired product **321**, nor intermediate **323**, nor keto acid **324** could be detected by APCI-MS.

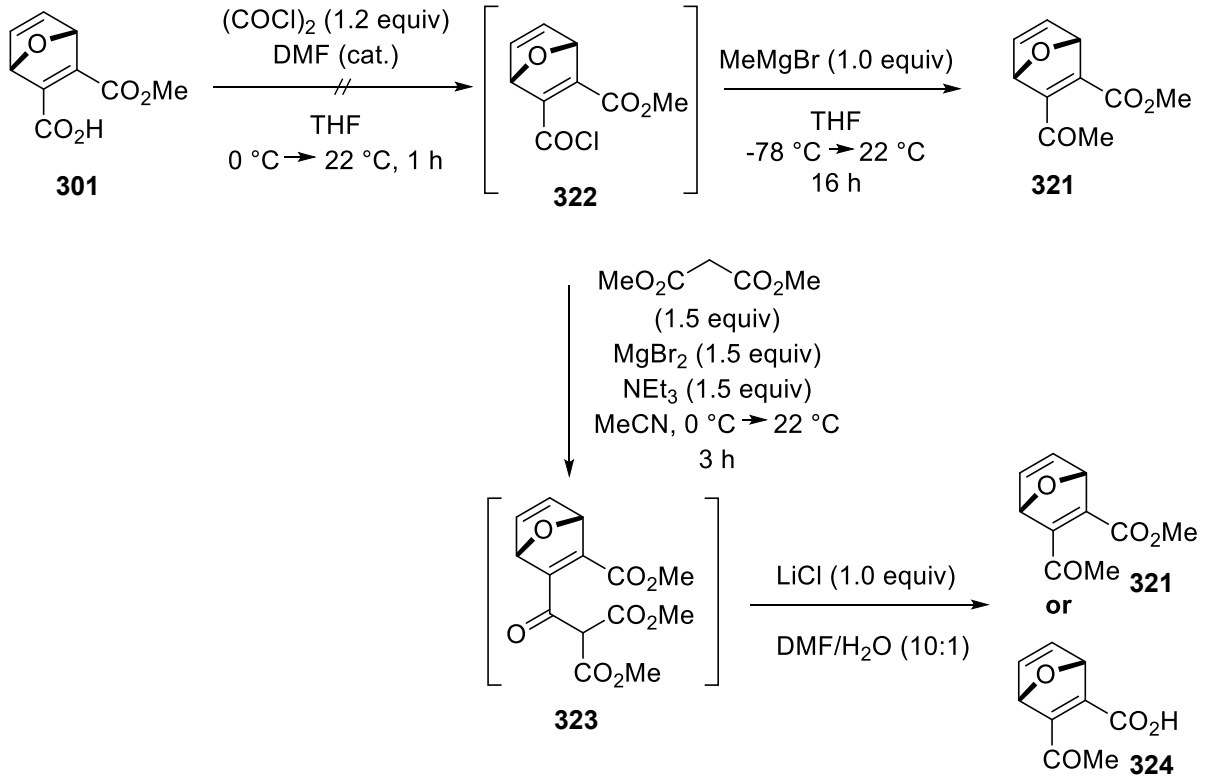

Scheme 89: Attempted synthesis of chiral oxabicycle **321** *via* formation of acid chloride **322** starting from oxabicycle **301** and subsequent methylation.

As modification of the mono acid **301** appeared difficult, de-novo synthesis of oxabicycles was investigated next. Acetylation of methyl propiolate (**320**) and subsequent *Diels-Alder* [4+2]-cycloaddition would provide the aforementioned desired product **321**. The reaction, based on literature known conditions,[286] gave an inseparable mixture of desired product **325** and acetylation side product **326** in a ratio of 2:1 according to ^{1}H NMR (Scheme 90A). A repeat experiment drying the CH_2Cl_2, *i*-Pr_2EtN and methyl propiolate (**320**) using 3 Å molecular sieve and adding AcCl at 22 °C gave a 1:1 mixture (**325**:**326**) in a lower total yield (7%). A *Diels-Alder* [4+2]-cycloaddition of the 2:1 mixture gave product **321** in a yield of 23% (Scheme 90B). A one pot approach using the crude mixture gave the desired product **321** in a yield of 13% over two steps (Scheme 90C).

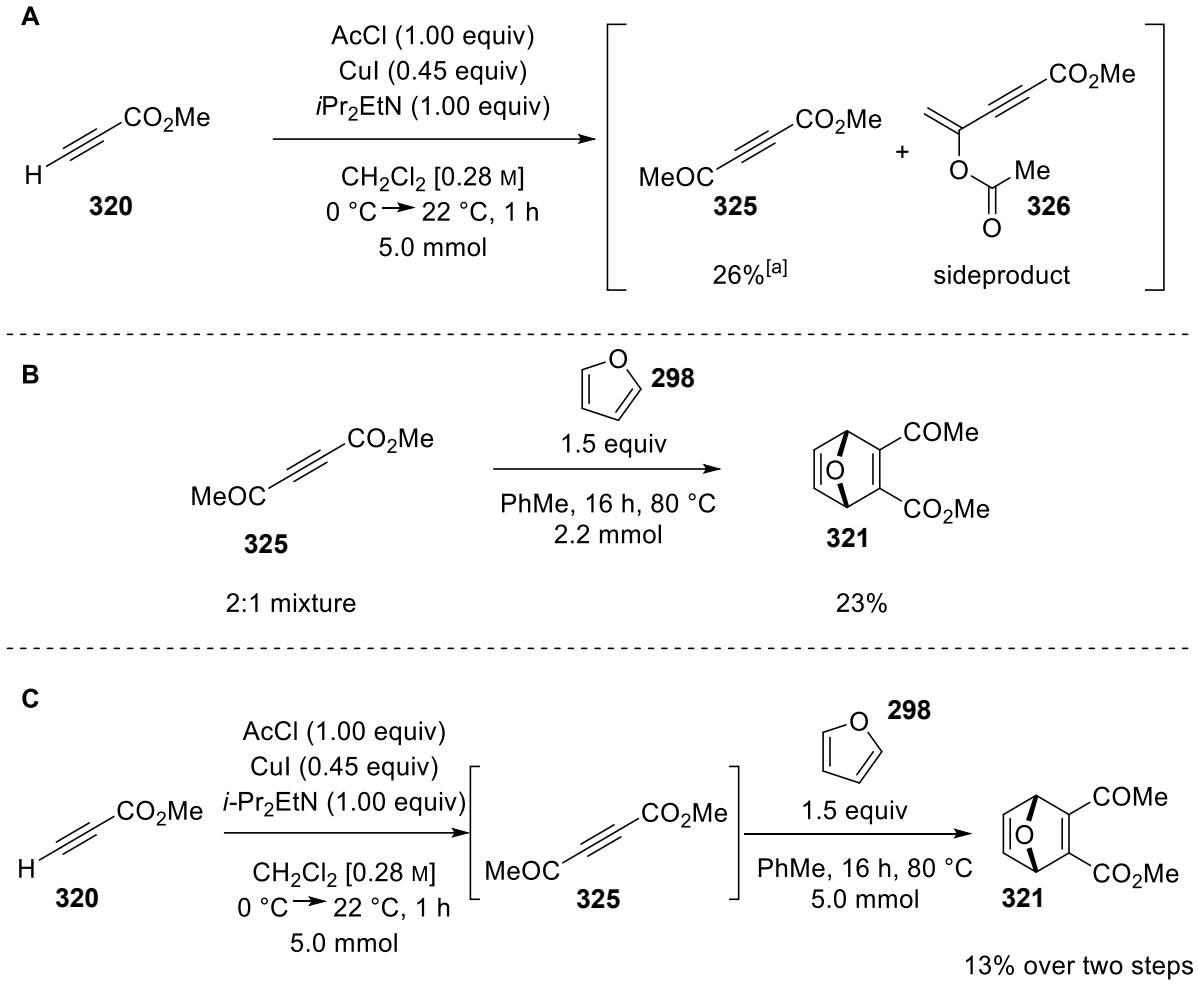

Scheme 90: (A) Synthesis of **325** *via* acetylation of methyl propiolate (**320**). (B) [4+2] cyclization to form a racemic mixture of chiral oxabicycle **321**. [a] Not isolated 2:1 mixture of **325**:**326**, theoretical amount of **325** calculated by ratio in ^{1}H-NMR. (C) One pot approach.

The driving force of the retro-*Diels-Alder* reaction in the end is proposed to be the extrusion of an electronically deficient furan.[279a] To probe if this retro-*Diels-Alder* reaction still occurs with less electronically withdrawing substituents, the synthesis of oxabicycle **327** *via* bromination of methyl propiolate,, subsequent *Diels-Alder* cyclization, and finally *Suzuki-Miyaura* cross-coupling was attempted. Brominated alkyne **328** was highly volatile, thus, direct transformation over two steps was conducted (Scheme 91A). The resulting product **329** could not be isolated and was only obtained as a mixture with alkyne **328**. The palladium-catalyzed transformation using this mixture was conducted nevertheless to see if any product formation could be observed (Scheme 91B). Unfortunately, the desired product could not be detected but instead several main side products could be observed. The analytical data implied the formation of furan **330** as a side product and implied the presence of a pre-retro-*Diels-Alder* intermediate. A mass corresponding to a compound akin to **331** (m/z $[M+H]^+$ 383.2) and also the presence of the aforementioned furan **330** (m/z $[M+H]^+$ 203.1) and trace amounts of stilbene (m/z $[M+H]^+$ 180.1) could be detected by APCI-MS. The ^{1}H-NMR data of furan **330** was also in accordance

with literature.[287] Even though no product could be obtained, these results implied that the retro-*Diels-Alder* of these oxabicycles with less electron withdrawing substituents proceeds at temperatures of 80 °C and thus, broadens the scope of oxabicycles of potential interest. The literature known extrusion of furan *via* retro-*Diels-Alder* is known to proceed at 100 – 120 °C.[259a]

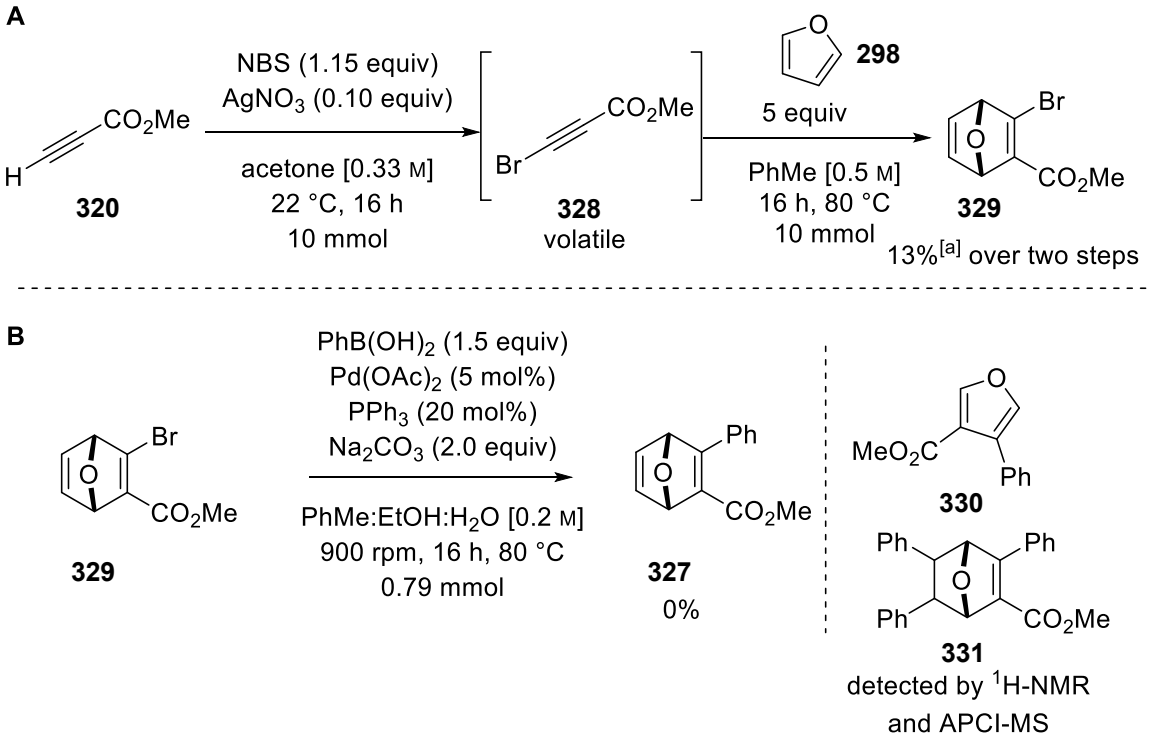

Scheme 91: (A) Bromination of methyl propiolate (**320**) and subsequent *Diels-Alder* cyclization of brominated product **328** and furan to synthesize oxabicycle **329**. (B) *Suzuki* coupling of oxabicycle **329** for the synthesis of aryl oxabicycles with detected sideproducts. [a] obtained as a 1:1 mixture of **328**:**329**.

In summary, a new oxabicycle **321** could be synthesized. Oxabicycle acid **301** could not be employed as a viable chiral auxiliary for the palladium-catalyzed transformation. Moreover, modification of oxabicycle acid **301** appeared difficult as did the late-stage modification of brominated oxabicycle **329**.

5.5.4 Mechanistic investigations

With experimental data on the stereoselectivity of the reaction at hand, the proposed mechanism of the enantioenrichment was probed. The two relevant steps, namely the regioselective insertion and diastereoselective cyclization were to be investigated separately. As stated in the introduction of this chapter (Chapter 5.5.1), the use of racemic oxabicycles should give a probe into the enantioselectivity of the reaction by isolating the pre-retro-*Diels-Alder* (prDA) products.

5.5.4.1 Diastereoselectivity

First, the diastereoselectivity using oxabicycle **296** was investigated (Scheme 92A). This way, the influence of ligands, time, and temperature on the 5-*exo*-trig migratory insertion to generate the quaternary carbon could be probed. If no diastereoselectivity is observed, then no enantioenrichment of the final product should be observed either. From data obtained by *Xavier Abel-Snape* in the previous study,[259a] the ratio of diastereomers as a function of time (Scheme 92B) and temperature (Scheme 92C) could be extracted. A strong relationship was found in both cases with the ratio of major to minor diastereomer increasing over time and decreasing at higher temperatures. The change in ratio implies that either interconversion of the minor diastereomer to the major one occurs over time, or that the retro-*Diels-Alder* reaction to form the indene may proceed at a faster rate than the minor diastereomer.

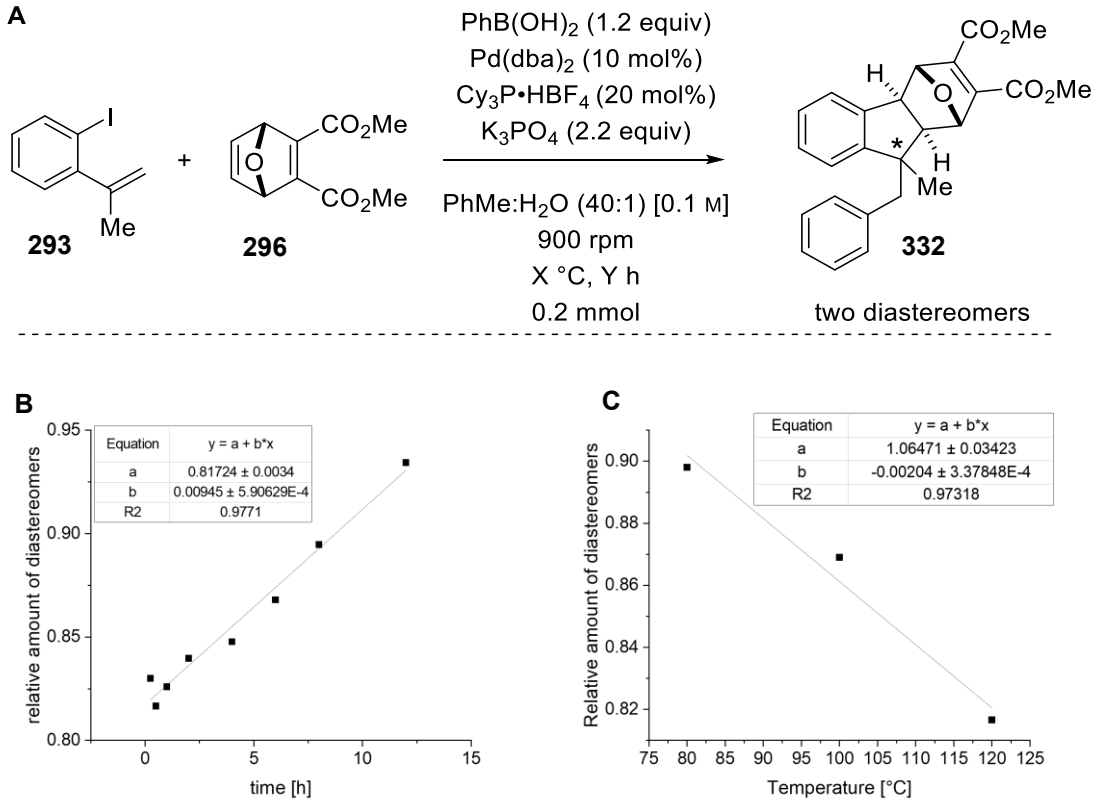

Scheme 92: Results obtained from unpublished data provided by *Xavier Abel-Snape*.[284] (A) Synthesis of pre-retro-*Diels-Alder* intermediate **332** using oxabicycle **296**. (B) Relative amount of the major diastereomer over time at 120 °C according to ^{1}H-NMR data over time. (C) Relative amount of diastereomers at different temperatures after 30 min according to ^{1}H-NMR data.

Going back to the results reported in Table 28, using PPh_3 as the ligand inverted the enantioselectivity of the reaction. Additionally, the use of ligand **L3** in combination with chiral oxabicycle (*R*)-**303** gave enantioselectivities lower (27%ee) than either case on its own (48%*ee* and 42%*ee* respectively). The hypothesis was, that the stereoelectronic effects of the ligand influence regioselectivities, diastereoselectivities, or both. To probe the extend of this influence, the diastereomeric ratio of the oxabicycle **296** derived pre-retro-*Diels-Alder* product **332** was investigated (Table 29). It was observed, that while the use of $Cy_3P\ HBF_4$ and *i*-$Pr_3P{\cdot}HBF_4$ gave similar results (Table 29, entries 1 and 2), $Me_3P{\cdot}HBF_4$ and *t*-$Bu_3P{\cdot}HBF_4$ as ligands gave inversion of diastereoselectivity in addition to low conversion to product according to ^{1}H NMR (Table 29, entries 3 and 4). PPh_3 gave inversion of the diastereoselectivity and a d.r. of 1.0:4.0 yet incomplete conversion. A reaction using trialkyl phosphines therefore predominantly formed one diastereomer while triaryl phosphines resulted in an excess of the complementary diastereomer. Various substituted aryl phosphines were investigated (Table 29, entries 6 – 10). The use of $(4\text{-}CF_3C_6H_4)_3P$ gave a ratio of 1.0:4.9 with full conversion of aryl iodide and 50% conversion to products. The use of sterically bulkier or more electron-rich aryl phosphines gave low conversions to product. Finally, TADDOL based ligand (*S,S*)-**L3** gave a d.r. of 1.7:1.0

(Table 29, entry 11) while (2-furyl)$_3$P implied a high diastereoselectivity of 1.0:10 but very low conversion to product (Table 29, entry 12). It is important to note that, in addition to the diastereoselectivity, the enantioselectivity of prDA intermediate formation using (*S,S*)-**L3** ultimately determines the *ee* of the product (compare mechanism discussed in chapter 5.5.1). These results highlight that an inversion of diastereoselectivity can take place when using a different class of ligands (PAr$_3$ vs PAlkyl$_3$). Only small amounts of indene formation were observed under these conditions (<5% relative to the prDA intermediates).

Table 29: Diastereoselectivity of the 5-*exo* trig cyclization generating pre-retro-*Diels-Alder* intermediate **332**.

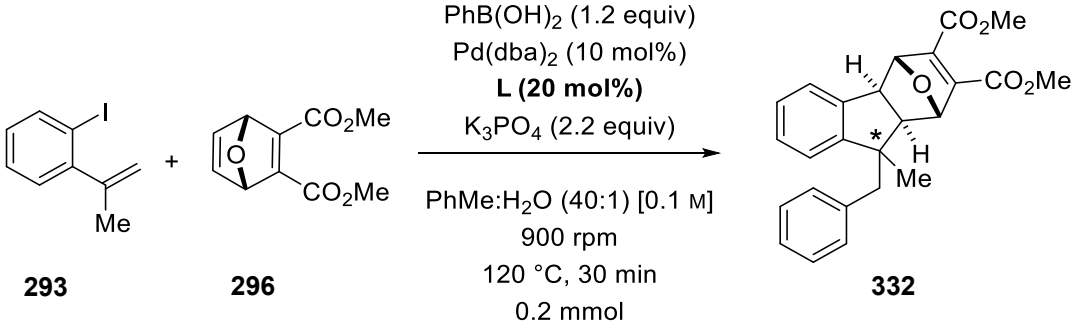

293 **296** **332**

#	L	Conversion [%]	Products[b] [%]	d.r.
1	$Cy_3P \cdot HBF_4$	100	96	**4.5:1.0**
2	*i*-$Pr_3P \cdot HBF_4$	100	78	3.5:1.0
3[a]	*t*-$Bu_3P \cdot HBF_4$	100	14	1.0:3.3
4	$Me_3P \cdot HBF_4$	100	37	1.0:1.2
5	PPh_3	25	18	**1.0:4.0**
6	(4-$OMeC_6H_4)_3P$	27	>5	–
7	(4-$CF_3C_6H_4)_3P$	100	42	**1.0:4.5**
8	(2-$CF_3C_6H_4)_3P$	29	12	1.0:2.5
9	(4-$MeC_6H_4)_3P$	16	>5	–
10	(3,5-$(CF_3)_2C_6H_4)_3P$	75	6	1.0:6.1
11	**L3**	100	63	1.7:1.0
12	(2-furyl)$_3$P	93	12	1.0:10

^{1}H NMR conversions of starting material **293** and to products according to ^{1}H-NMR with 1,3,5-trimethoxybenzene as internal standard. [a] major side product formation. [b] Sum of both diastereomers and indene.

Next, it was investigated if the choice of terminating agent had an influence on the diastereoselectivity by using various boronic acids (Table 30). This would probe if the competing catalytic cycle as proposed by *Han et al.* played a role in the catalytic cycle of this mechanism.[281] Varying the electronic and steric properties of the arene should influence the relevant transition states. No strong relationship between the diastereoselectivity and aryl boronic acid could be observed for the d.r. of the prDA intermediates **333** – **336**, therefore indicating transmetalation either not taking place or not influencing the diastereoselectivity of the 5-*exo*-trig cyclization. Separation of the diastereomers was only possible for the major diastereomer of **334**. Again, only low formation of indene was observed (<5% relative to the prDA intermediates). Low isolated yields can be attributed to cumbersome isolation efforts.

Table 30: Diastereoselectivity of the 5-*exo* trig cyclization generating pre-retro-*Diels-Alder* intermediates depending on the terminating aryl boronic acid.

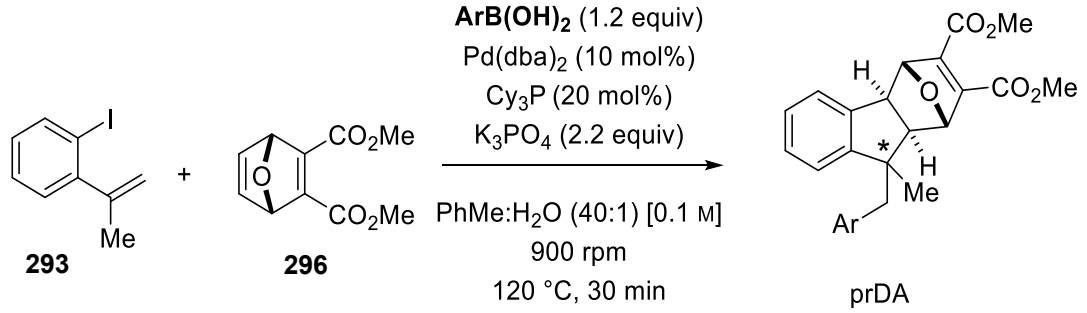

Entry	Ar	prDA products	Conversion [%]	Products[b] [%]	d.r.
1	(4-OMeC$_6$H$_4$)-	**333**	100	54 (11)	4.3:1.0
2	(4-CF$_3$C$_6$H$_4$)-	**334**	48	48 (22)	4.8:1.0
3	(2-OMeC$_6$H$_4$)-	**335**	78	52	4.8:1.0
4	(2-MeC$_6$H$_4$)-	**336**	88	65 (67)	4.7:1.0

^{1}H NMR Conversions of starting material **293** and to products according to ^{1}H-NMR with 1,3,5-trimethoxybenzene as internal standard. [a] major side product formation. [b] Sum of both diastereomers and indene (isolated yield of mixture of diastereomers in brackets).

Thus, the influence of ligand and boronic acid on the diastereoselectivity of the 5-*exo*-trig cyclization step were successfully shown. An inversion of diastereoselectivity was observed when employing triaryl phosphines compared to 2° trialkyl phosphines implying that this step might be of relevance for the previously observed switch in enantioselectivity when using the same ligands.

5.5.4.2 Regioselectivity

With data for the diastereoselectivity in hand the regioselectivity was investigated next. As discussed in the introduction (Chapter 5.5.4), in comparison to the use of oxabicycle **296**, a chiral oxabicycle should result in a prDA product with four isomers, comprised of two regioisomeric sets of diastereomers (Scheme 93).

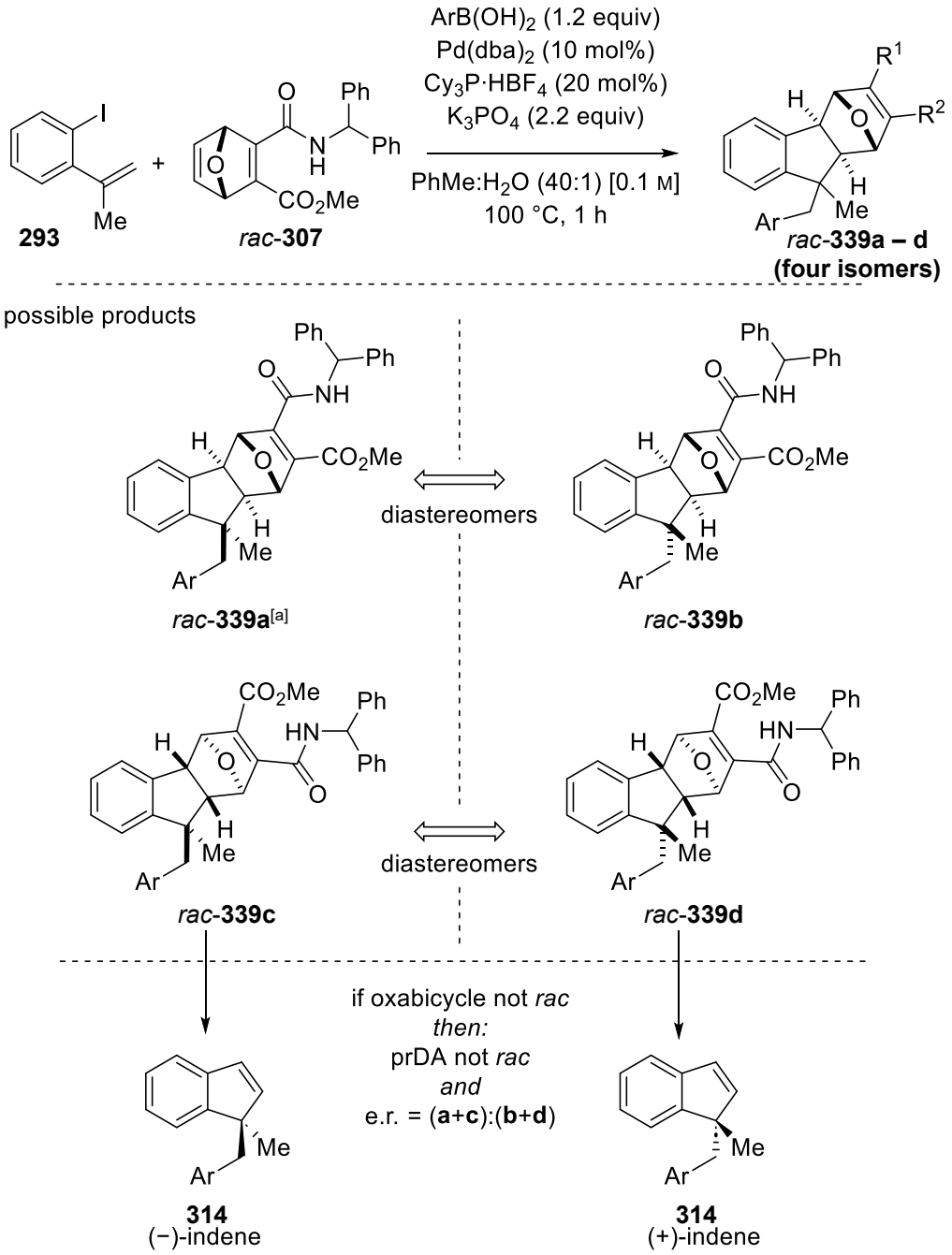

Scheme 93: Synthesis of pre-retro-*Diels-Alder* intermediates using racemic oxabicycles. The ratio of the four isomers (**339a – d**) formed should correspond to the observed ratio of enantiomers when using enantiopure oxabicycle (Chapter 5.5.3.2). Isomers **339a** and **339c** should correspond to one enantiomer while **339b** and **339d** should correspond to the other enantiomer. [a] x-ray structure obtained.

The validity of this hypothesis was tested with various oxabicycles to identify if a switch in regioselectivity takes place. As proposed, four isomeric peak sets could be identified by ^{1}H-NMR (Figure 20). The absolute and relative configuration of these isomers could be assigned using NMR and x-ray structures (Chapter 5.5.4.3). Isomers **a** and **c** were identified as comprising the same absolute configuration on the quaternary carbon center when using enantiopure oxabicycles. The same holds true for isomers **b** and **d**. Even when using racemic oxabicycles in combination with achiral ligands, the ratio of these isomers should correspond to the e.r. observed for the enantioselective reaction.

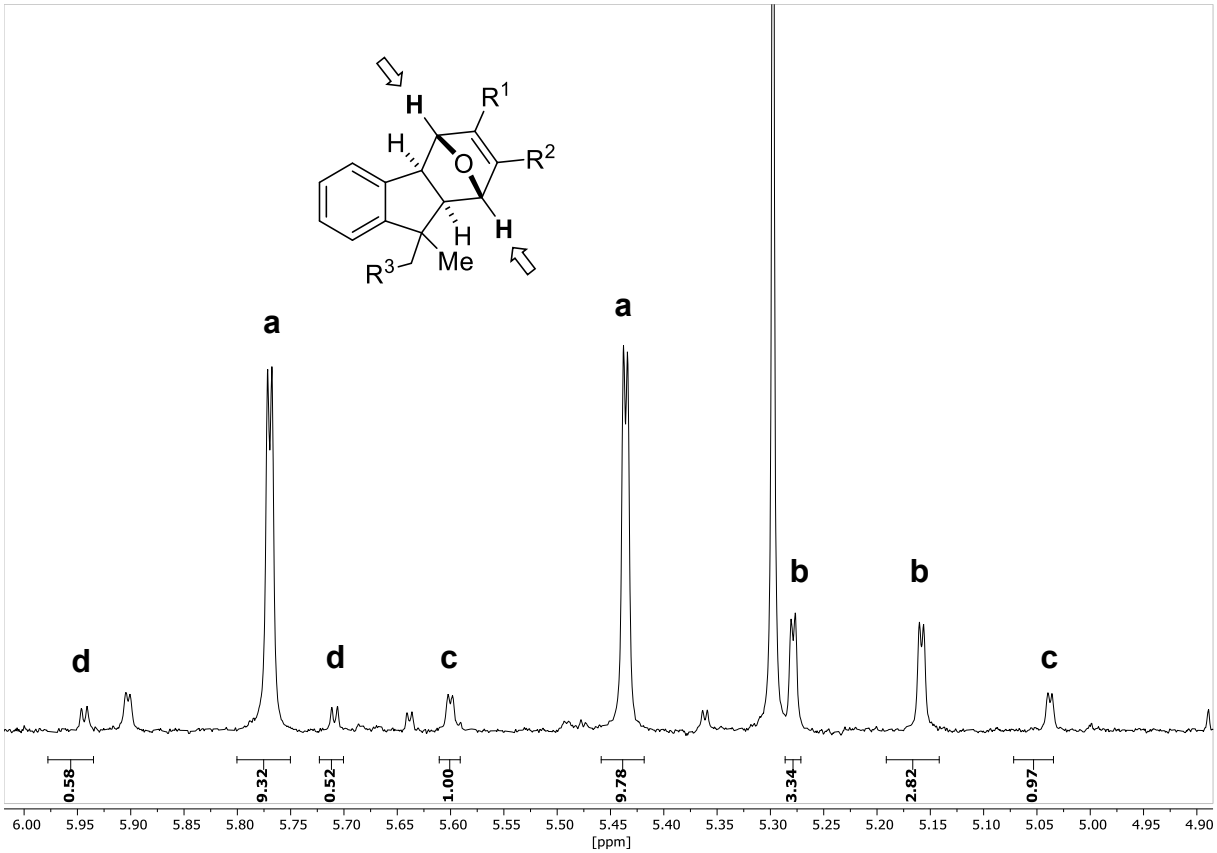

Figure 20: ^{1}H-NMR spectrum of pre-retro-*Diels-Alder* product **339** after one column chromatographic purification showing all relevant isomeric signals.

Overall, fewer overlapping peaks were observed in the ^{1}H-NMR when using boronic acid **337** compared to boronic acid **313** making determination of ratios more reliable. First, amide oxabicycles **311** and **307** were investigated. An isomeric ratio of 75:25 of the prDA intermediates (**a**+**c**:**b**+**d**) (compare Scheme 93) was observed in both cases (**338** and **339**) (Table 31, entries 1 – 2). This ratio corresponds immaculately to the experimentally observed 48 – 52%*ee* (e.r. 75:25) when using oxabicycle amides (*S*)-**302** and (*R*)-**303** (Table 28, entries 2 – 4). This result supports the assignment of the isomer pairs as well as the proposed mechanism of the regio- and diastereoselectivity determining the enantiomeric excess. Next, the use of PPh_3 was investigated. Indeed, a prDA isomeric ratio of 38:62 (Table 31, entry 3) (**a**+**c**:b+**d**) implied

the formation of the opposite enantiomer, though lower than the experimentally observed −(35 – 45)%*ee* (33:67 – 28:72) (Table 28, entry 9). This could be attributed to the low conversion of starting material **293** and thus inaccurate integers according to ^{1}H-NMR. The r.r. (**a**+**b**:**c**+**d**) of Ar_3P versus $Alkyl_3P$ revealed, that the same regioisomer should be preferred by both ligand classes. Only the d.r. **a**:**b** was inverted under these conditions, the same as observed in the previous section. Interestingly, when using ligand (*S,S*)-**L3**, an expected e.r. of 52:48 was obtained not in line with the experimentally observed 27%*ee* (Table 28, entry 7). The enantioselectivity of the reaction using ligand **L3** cannot solely be explained by the ratio of isomers (Table 31, entries 4) as additional peaks not part of the original four isomers (**a** – **d**) were observed in ^{1}H-NMR, indicative of additional isomer formation. This could be the result of *endo*-selective oxabicycle insertion. Additionally, using racemic oxabicycle does not reveal if one enantiomer of those racemic prDA products is preferentially formed. Thus, in this case, the ratio of prDA intermediates using racemic oxabicycles does not necessarily reflect the ratio of enantiopure oxabicycles. The previously synthesized keto-ester oxabicycle **321** gave an isomeric ratio of 1.8:1.0 though not all peaks could clearly be identified. Isolation was not possible, and no identification of the relative configuration of prDA products **340** could be made. Nevertheless, a ratio of major peaks was observed indicating either diastereoselectivity or regioselectivity.

Table 31: Synthesis of pre-retro-*Diels-Alder* intermediates to determine ratio of regioisomers.

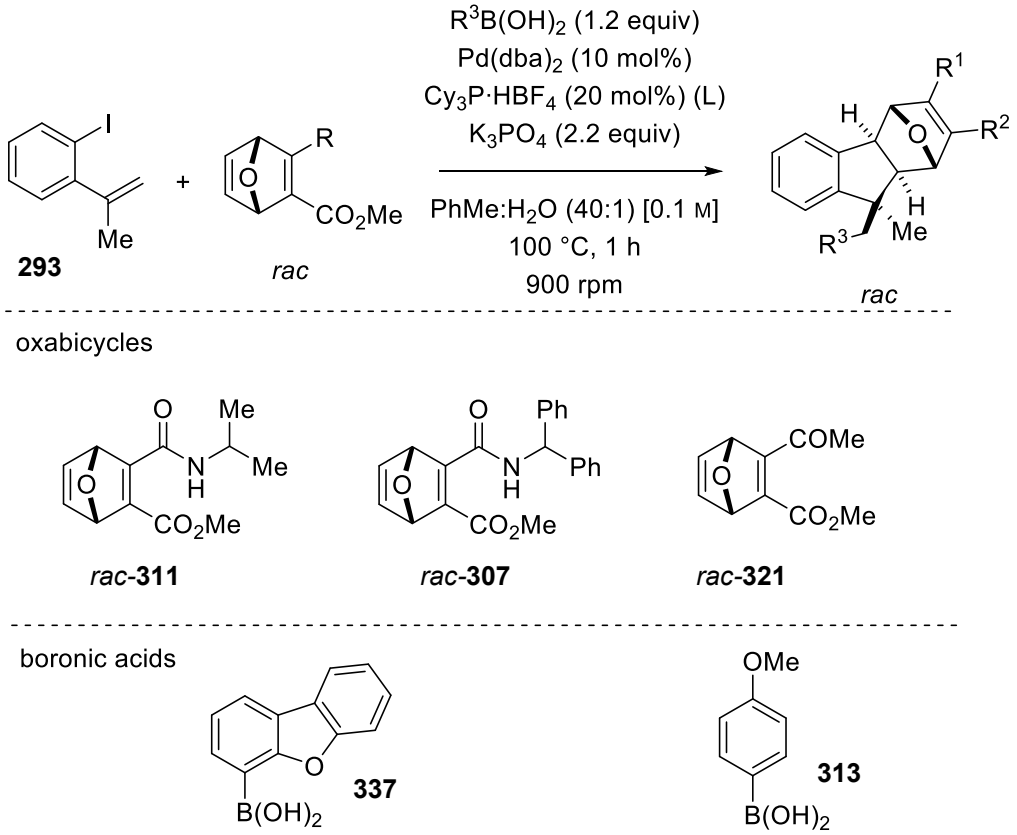

#	Variations	Oxabicycle:prDA	Ratio isomers (a:b:c:d)[a]				e.r.[b]	Products [%]
	R^3 = 337		**a**	**b**	**c**	**d**		
1	None	**311**:**338**	10.04	2.50	1.00	1.25	75:25	51[d]
2	None	**307**:**339**	20.30	6.54	1.94	1	75:25	58
3	PPh_3 as L	**307**:**339**	1.00	3.97	2.49	1.77	38:62	11
4[c]	(*S,S*)-**L3** as L	**307**:**339**	3.54	4.18	2.03	1.00	52:48	32
5[c]	R^3 = **313**	**321**:**340**	1.79	1.00	–	–	–	33

^{1}H NMR Conversions of starting material **293** and to products (isomers **a** – **d**) according to ^{1}H-NMR with 1,3,5-trimethoxybenzene as internal standard. [a] relative ratio according to ^{1}H NMR integers. [b] theoretical e.r. derived from the ratio of isomers. [c] major additional peaks in ^{1}H NMR. [d] isolated yield, mixture of isomers.

Overall, the use of racemic oxabicycles as a probe into the enantioselectivity of the reaction was successfully shown. As outlined in the introductory statement (Chapter 5.5.1), the correlation of prDA intermediate isomeric ratio to the observed enantiomeric ratios could be shown. Therefore, racemic starting materials can indeed be used to predict enantiomeric excess. As such, racemic oxabicycles like **321**, obtained by de-novo synthesis strategy, (Chapter 5.5.3.3) can easily be investigated without the need for lengthy method establishment to separate the

isomers, without knowing the cost-benefit ratio first. Additionally, it could be observed that the regioselectivity of the trialkyl phosphine ligand can be attributed to the high r.r. (Table 31, entries 1 and 2, **a**+**b**:**c**+**d** is 9:1) while the use of a triaryl phosphine ligand heavily depended on a favorable d.r. to achieve high enenatiomeric excess.

5.5.4.3 Determination of relative and absolute configuration

The constitution of the major isomer **338a** was resolved using an x-ray structure measured by Dr. *Alan Lough* (Figure 21).

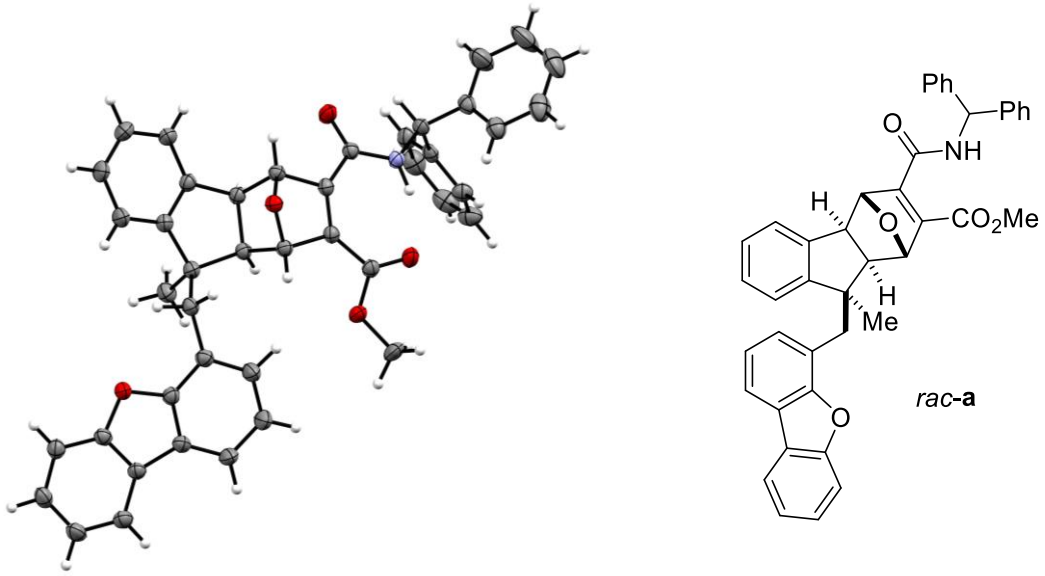

Figure 21: (A) X-ray structure of pre-retro-*Diels-Alder* product *rac* **339**a. ORTEP with a probability of 50%. (B) Lewis structure interpretation. The ^{1}H-NMR of the single crystal was in accordance with the major isomer **339a**.

To assure the assigned relative configuration corresponded to the major observed isomer, 2D-NMR studies were conducted. In particular, the ^{1}H-NMR spectra of the isomeric peak pattern (**a** – **d**) of **338** and **339** strongly resembled one another. Thus, it was deduced that the relative configurations should be in agreements with one another. Weak NOESY coupling suggested that the methyl ester moiety is closer to the 1-H hydrogen (Figure 23A and B). This would be in accordance with either **338a** or **b** Figure 22A. Coupling between 1-Me and 3-H was observed (Figure 23C) while coupling between the methyl moiety of the quaternary carbon and 1-H was completely absent (Figure 23C) corresponding to the constitution and relative configuration of the major isomer **338a** (Figure 22B). The relative configuration of the remaining isomer **b** – **d** could subsequently be assigned by NOESY and by HMBC following the same reasoning by *Xavier Abel-Snape*.[284]

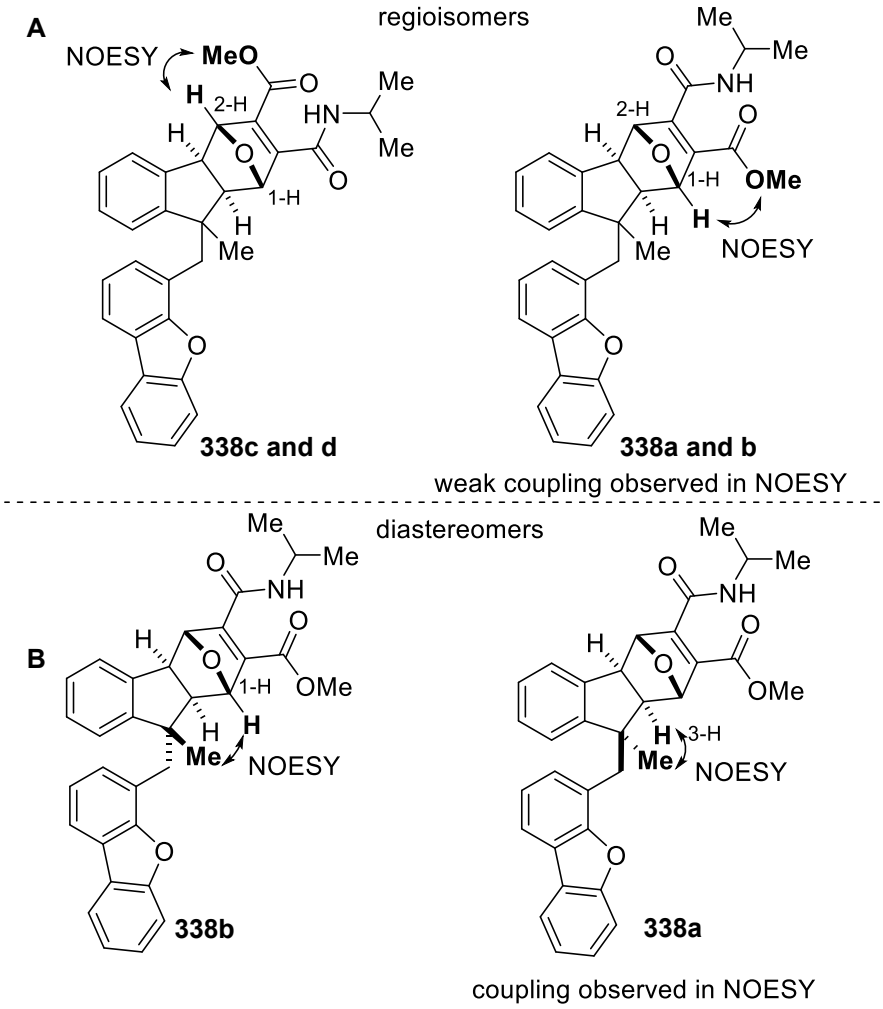

Figure 22: Determination of the structural isomer and relative configuration of the major pre-retro-*Diels-Alder* product **338** by (A) NOESY coupling of the bridgehead proton 1-H to the methoxy ester and (B) NOESY coupling of the methyl group with 3-H.

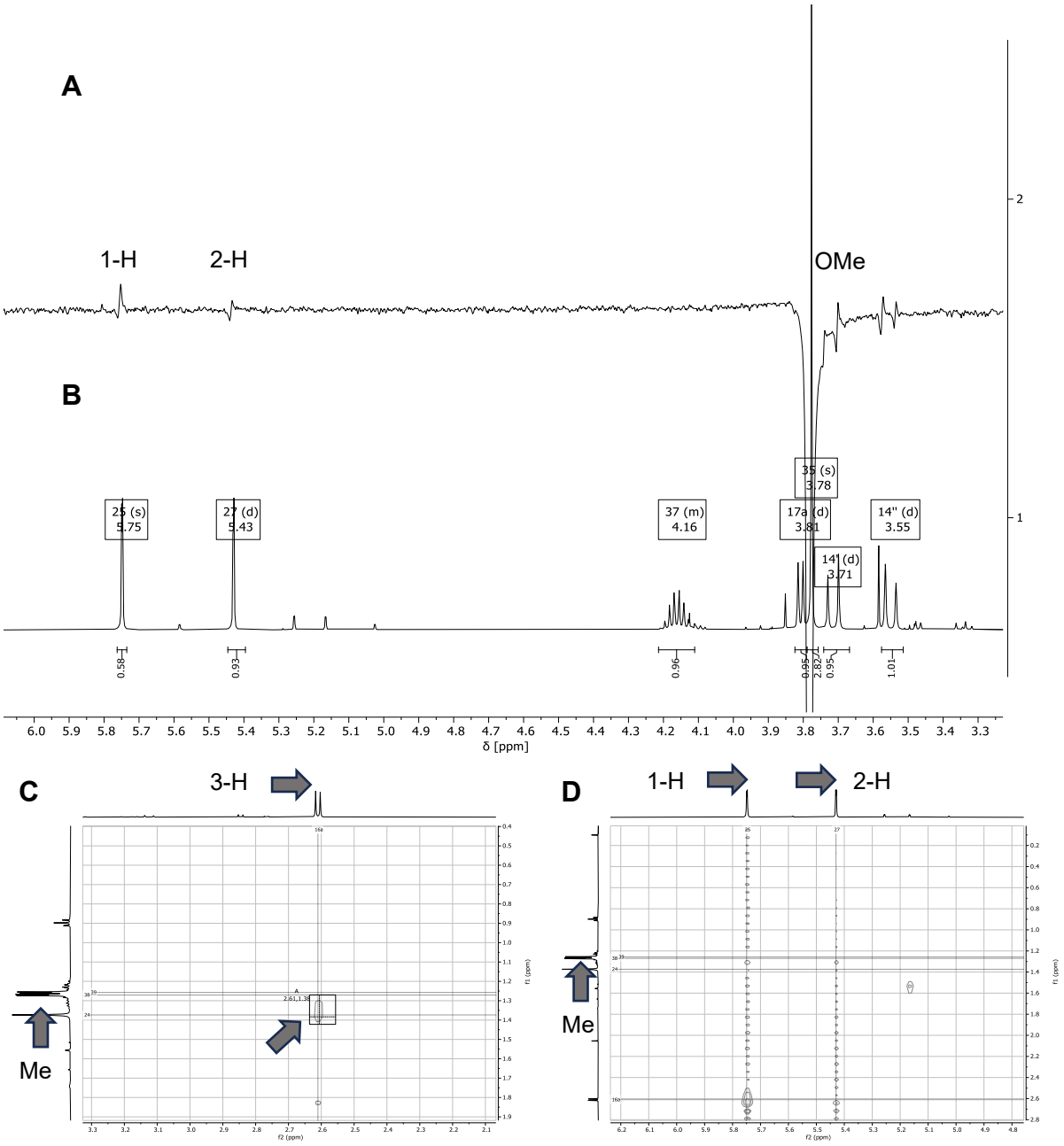

Figure 23: (A) 1D-NOESY of the weak excitation of the methoxy ester of the oxabicycle scaffold of pre-retro-*Diels-Alder* intermediate **338a**. (B) Excerpt of ^{1}H NMR of pre-retro-*Diels-Alder* intermediate **338**a. Weak coupling between the methoxy group and 1-H observed. (C) 2D-NOESY spectrum of pre-retro-*Diels-Alder* product **338**a showing coupling between Me and 3-H. (D) Absence of NOESY coupling between either 2-H or 1-H and the quaternary methyl group.

Before obtaining a crystal structure, the strength of the NOESY coupling was to be improved to unambiguously assign the isomers **a** – **d**. Oxabicycle **299** was chosen due to the potential closeness of the methyl groups to the methoxy group. In literature oxabicycle **299** was unfit for the palladium-catalyzed cyclization.[279a] A reaction under standard conditions (Chapter 5.5.3.1) was set up to investigate if this was either due to unreported insufficient retro-*Diels-Alder* reaction or due to actual low formation of the pre-retro-*Diels-Alder* product **341**. Full conversion of aryl iodide **293** was observed yet only 3% conversion to indene **314** according to

^{1}H-NMR was detected (Scheme 94). No significant amounts of pre-retro-*Diels-Alder* product could be detected either. Thus, it was concluded that synthesis and isolation of the corresponding pre-retro-*Diels-Alder* intermediate **341** would be very difficult at such low conversions to products.

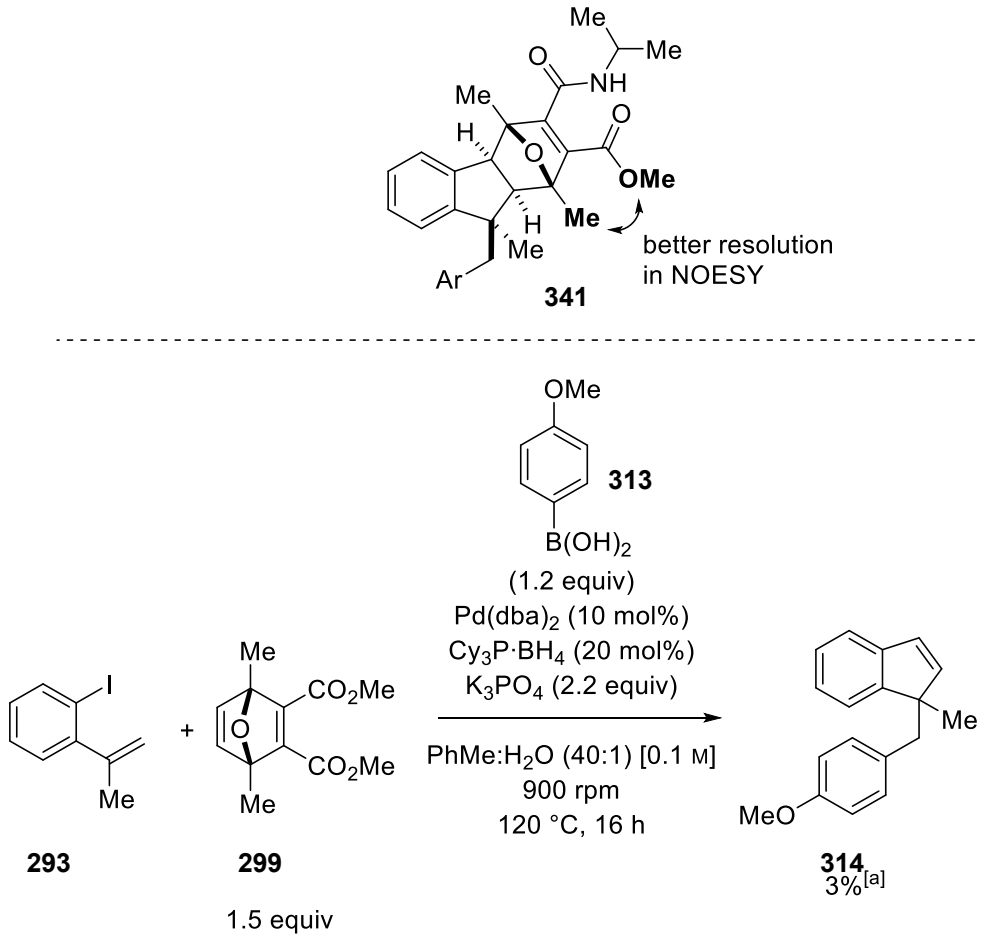

Scheme 94: Synthesis of indene **293** using oxabicycle **299**. [a] Conversions to product according to ^{1}H NMR with 1,3,5-trimethoxybenzene as internal standard.

Courtesy of the obtained x-ray structure of **338a** in addition to an x-ray structure of **307** obtained by *Xavier Abel-Snape*,[284] the absolute configuration of (−)-indene could be assigned as (*R*) (Scheme 95). As indenes generally were isolated as oils, crystallization of these compounds and thus direct determination of the configuration was not possible.

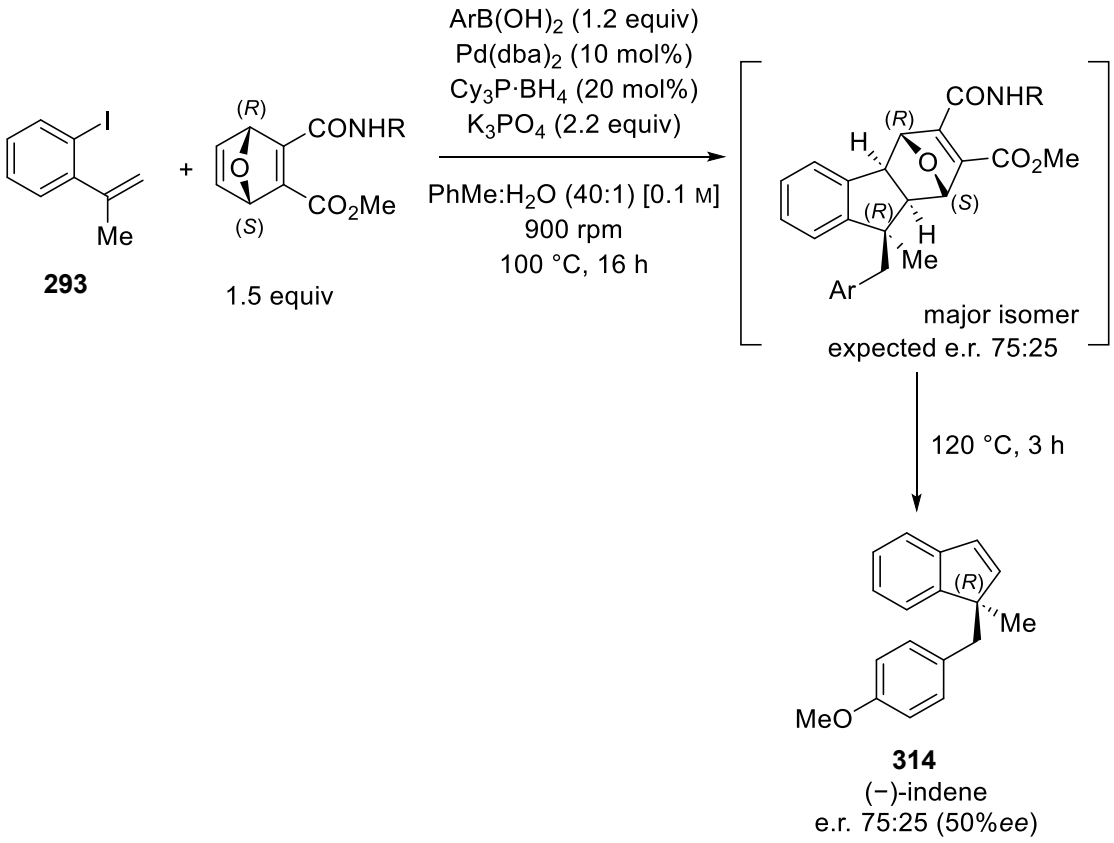

Scheme 95: Determination of absolute configuration of indene **314** *via* pre-retro-*Diels-Alder* products.

5.5.5 DFT Calculations

To rationalize the observed regioselectivities, DFT calculations were conducted. To accurately investigate the mechanism both *trans*- and *cis*-complexes were calculated (Figure 24A). Both regioisomers of the oxabicycle coordination and migratory insertion (Chapter 5.5.4) were computed to then determine the ΔG between the relevant transition states (Figure 24B). The α-complex refers to the regioisomers **c** and **d** while the β-complex refers to **a** and **b**. Independently in a very recent publication by *Han et al.* the underlying mechanism using oxabicycle (OBC) **296** was probed by investigating the relevant transition states of the involved complexes.[281] In addition to the alkene-insertion-first mechanism, they investigated the boronic acid transmetalation-first mechanism, where the iodide is substituted with a phenyl moiety. Both the PPh_3-complex as well as the *i*-Pr_3P complex were calculated to probe both a triarylphosphine ligand as well as a trialkylphosphine ligand. *i*-Pr_3P was chosen over Cy_3P to limit the amount of possible ligand conformers.

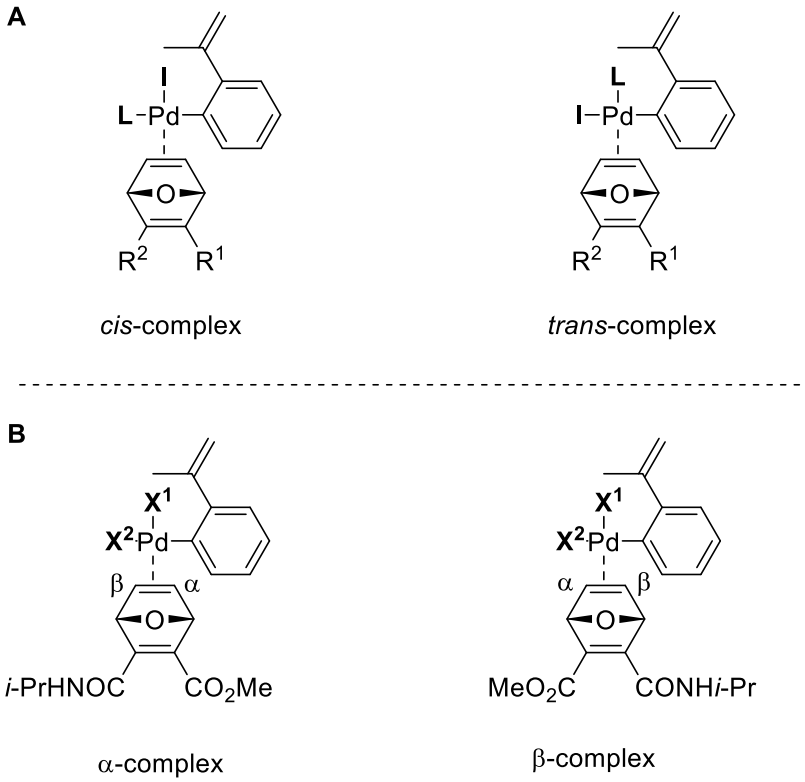

Figure 24: (A) Constitution of ligand and iodide for palladium complexes relevant for DFT calculations. The descriptors *trans* and *cis* refer to the relative position of the iodide and aryl substituents. (B) Regioisomeric complexes formed during the coordination of oxabicycle **311**.

DFT[100]-calculations were carried out using the Orca (5.0.4)[267] quantum chemistry software packages. All calculations were performed at 298.15 K. Energies were calculated by first pre-optimizing the crudely generated structure, using the GFN2-xTB[288] method and obtaining a conformer ensemble, using the conformer rotamer ensemble sampling tool (CREST)[289] and

subsequently condensed, using the censo[290] extension to a smaller subset of conformers. Such measures are taken to reduce the ambiguity of the system but are still subject to error. The energetically most favored ground state may not correspond to the energetically lowest transition state, as has been shown in literature.[291] *Cis*- and *trans*-conformers were extracted from the CREST ensembles. Next, geometries were calculated for the lowest energy conformer using the TPSS[268] functional with the D4 dispersion correction[269] with def2-SVP[270] basis set. Thus obtained ground states were confirmed by the absence of imaginary frequences after an analytical frequency calculation (AnFreq). Electronic energies were calculated using ωB97M-V,[273] using the def2-TZVPP basis set benchmarked for palladium complexes[266]. Transition states were identified by relaxed surface scan (RSS) of the same lowest energy conformers and confirmed to be first order saddle points by the presence of exactly one imaginary frequency. Hirshfeld charges[292] and condensed Fukui functions[293] (CFF) were considered for amide oxabicycle (*S*)-**302** to cheaply quantify regioselectivities and calculated using Multiwfn (3.8)[294] but gave inconclusive results. The following relevant palladium complexes were calculated: The oxabicycle-uncoordinated complex **Pd-1**, the resulting coordinated π-complex **Pd-2** of loose oxabicycle coordination, the σ-complex **Pd-3** after migratory insertion and C–C bond formation and the transition state **TS1** between σ- and π-complex (Scheme 96). The free energy of oxabicycle (OBC) **311** was also calculated *via* the same method.

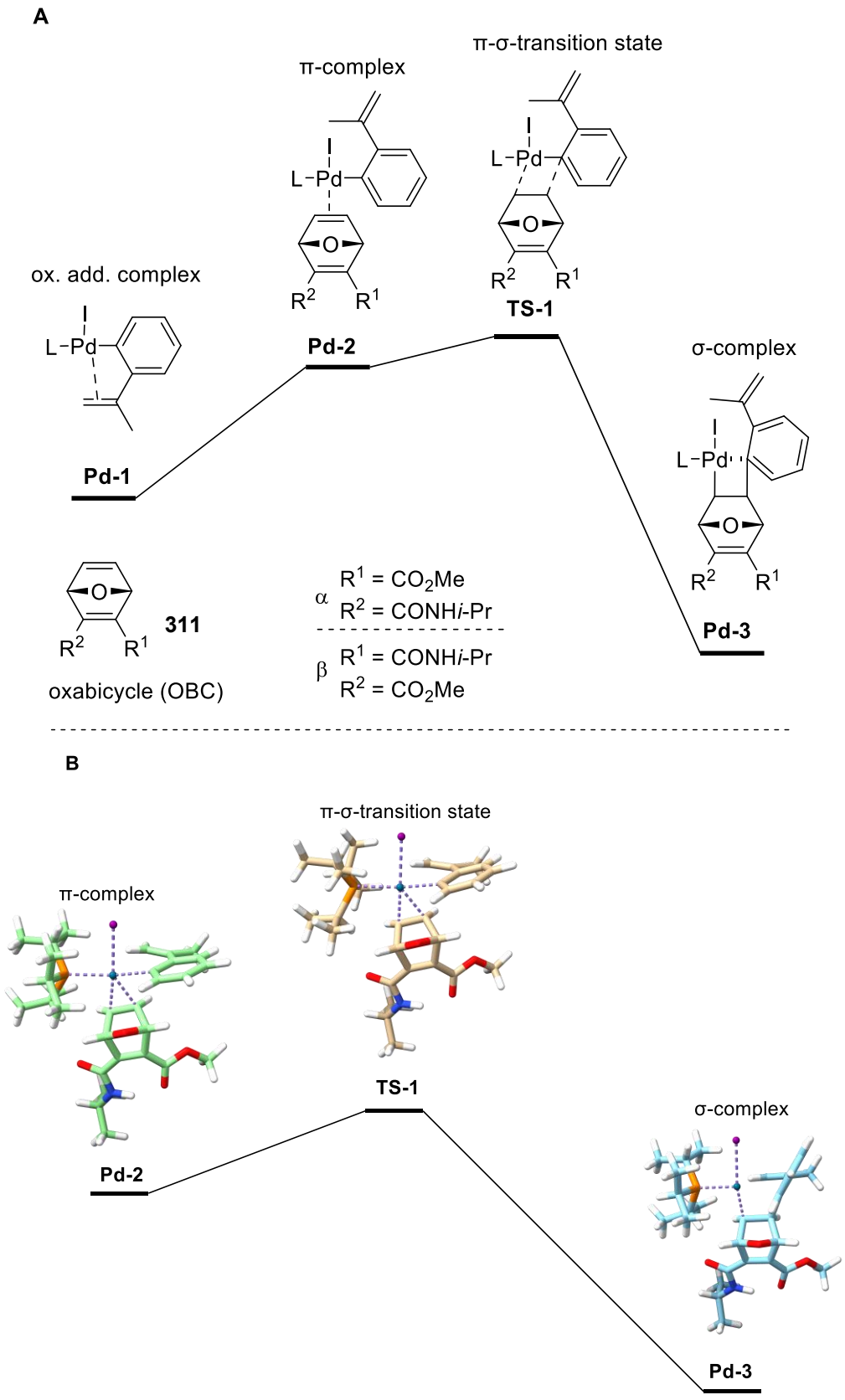

Scheme 96: (A) Schematic energy profile for the migratory insertion of oxabicycle **311** to the *cis*-oxidative addition complex **Pd-1** to form the *π*-complex (**Pd-2**) and then the *σ*-complex (**Pd-3**) *via* transition state (**TS1**). Same energy profile is applicable to the *trans*-complexes. (B) Exemplary structures of the energy profile using 3D-depictions of the optimized calculated structures.

The energies calculated followed comparable energetic pathways to the literature reported values (Table 32).[281] The formation of the π-complex starting from the mono-phosphine ligated complex **Pd-1** is energetically disfavored. The subsequent *σ*-complex (**Pd-3**) is energetically favored, though much more so for the *cis*-complex compared to the *trans*-complex ($\Delta G_{trans\text{-}cis}$ 3.9 kcal·mol^{-1} up to 13.5 kcal·mol^{-1}). If the reaction proceeds under kinetic control, the relative energies of transition state **TS-1** should be proportional to the regioisomeric ratios observed. The calculated relevant free energies as well as geometries of the aforementioned palladium-complex transition state **TS-1** closely resembled the energies and geometries of **Pd-2**. A comparison of the free energies revealed that the *α*-complex of **TS-1** is energetically more favored compared to the *β*-regioisomer. Therefore, a selectivity for the *α*-complex would be expected in all cases. This is in contradiction with the experimentally observed selectivity of the insertion. This discrepancy could be explained by various means. For one, the identified transition state **TS-1** is not the selectivity determining step. Additionally, the energetically lowest ground state conformer, the transition state geometries were based on, may not represent the energetically lowest conformer in the transition state. In addition, the alkene-first mechanism investigated by these calculations may not be the rate-determining pathway, instead coordination of an arene *via* transmetalation, as was shown to be plausible by *Han et al.* may yield energetically lower and thus the actually relevant transition states.[281]

Table 32: Lowest energy conformers of *σ*- and *π*-complexes were first identified by CREST and subsequent CENSO optimization. Free energies were calculated at the *ω*B97M-V/def2-TZVPP//TPSS-D4/def2-SVP levels of theory. Both *cis* and *trans* complexes were calculated. All energies relative to *trans*-Pd-complexes **Pd-1** + OBC **311**.

Pd-complex	**L = *i*-Pr$_3$P**			**L = PPh$_3$**		
	α	*β*	$\Delta G_{\alpha\text{-}\beta}$	*α*	*β*	$\Delta G_{\alpha\text{-}\beta}$
cis	kcal·mol^{-1}			kcal·mol^{-1}		
Pd-1 + OBC	6.9		–	4.8		–
Pd-2 (*π*)	11.9	13.7	−1.80	8.9	10.0	−1.14
TS-1 (*π*-*σ*)	**12.8**	**14.3**	**−1.52**	**12.4**	**13.6**	**−1.24**
Pd-3 (*σ*)	-24.6	-22.4	−2.24	-21.8	-20.7	−1.04
trans						
Pd-1 + OBC	0.0		–	0.0		–
Pd-2 (*π*)	7.0	6.6	0.410	3.8	7.5	−3.69
TS-1 (*π*-*σ*)	**12.1**	**12.5**	**−0.390**	**11.9**	**12.7**	**−0.878**
Pd-3 (*σ*)	-11.1	-12.6	1.57	-13.1	-16.8	3.67

Interestingly even though π- and *σ*-complexes varied strongly between *cis*- and *trans*-complexes, the free energy of the transition state **TS-1** of all calculated complexes using the same ligand were comparable. Under *Curtin-Hammet* conditions, the ratio of regioisomers formed would thus depend on the regioisomeric ratios of both the *cis*- and the *trans*-complex **TS-1**.

To account for lower energy conformers in the transition states,[291] the geometries of the obtained transition states **TS-1** (Table 32) were subjected to constrained conformer ensemble calculations (using CREST[289]). This was done by constraining the movement of all atoms except for those of the ligand (L) and the alkene sidechain of the aryl moiety (Table 33, blue). The resulting conformer ensemble geometries were energetically ranked by calculating single point energies at the TPSS-D4/def2-SVP level of theory. The lowest energy conformer of this ensemble was then subjected to a constrained geometry optimization by fixing the C–C bond (Table 33, red). This constrained geometry was used as the basis for a subsequent transition state geometry optimization. The transition state was again confirmed by the presence of a single imaginary frequency. The thus obtained energies (Table 33) were overall lower than the previously obtained energies starting from the lowest energy conformer ground states (Table 32). The hypothesis of the energetically lowest ground state conformer not necessarily corresponding to the energetically lowest transition state could therefore be supported. Only the *cis*-*α*-*i*-Pr_3P-complex was higher in energy than the previously obtained corresponding transition state complex (13.3 kcal mol^{-1} vs. 12.8 kcal mol^{-1}). The relative free energies obtained *via* this method implied, that the opposite—meaning *β instead of α*—regioisomer should be favored. This is in drastic contrast to the previously calculated relative free energies which implied the experimentally minor regioisomers (Table 31, Scheme 91 **c**+**d**, corresponding to *α*) would be favored. This clearly highlights the importance of obtaining accurate conformer profiles to determine exact ratios.

Table 33: Lowest energy conformers of *σ*-*π*-transition state. Based on geometries obtained from previous calculations (Table 32Table 33) using CREST.[289] Moieties subjected to conformer sampling (blue). Fixed C–C bond during constrained optimization (red). Free energies were calculated at the *ω*B97M-V/def2-TZVPP//TPSS-D4/def2-SVP levels of theory. Both *trans*- and *cis*-complexes were calculated. All energies relative to *trans*-Pd-complexes **Pd-1** + OBC **311** (Table 32).

π-σ-transition state

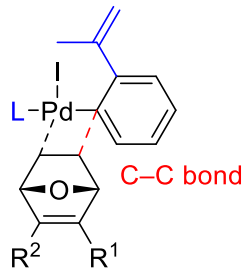

TS-1

Pd-complex	**L = *i*-Pr$_3$P**			**L = PPh$_3$**		
	α	*β*	$\Delta G_{\alpha-\beta}$	*α*	*β*	$\Delta G_{\alpha-\beta}$
cis	kcal·mol^{-1}			kcal·mol^{-1}		
TS-1 (π-σ)	**13.3**	**14.0**	**−0.690**	**12.4**	**12.1**	**0.275**
trans						
TS-1 (π-σ)	**11.8**	**9.9**	**1.95**	**11.5**	**11.5**	**0.0445**

With these optimized transition state energies calculated, the expected ratios of *α* and *β* conformers were determined *via* the Boltzmann distribution (8) of these energetically lowest transition states. For both ligand systems, a distribution was calculated at 298.15 K and 373.15 K. This was done because energy calculations were conducted at the former temperature while reactions were performed at the latter. The implications of the obtained energies (and thus Boltzmann distributions) were, that the *trans*-pathway is energetically favored. Still, the *cis*-pathway contributes significantly to the observed ratios, in particular when considering the Ph$_3$P ligated complexes.

$$N_x = \frac{e^{-\left(\frac{G_{rel}(x)}{k_B * T}\right)}}{\sum_i^n e^{-\left(\frac{G_{rel}(i)}{k_B * T}\right)}} \qquad (8)$$

N_x: relative Boltzmann population of transition state x, $G_{rel}(x)$: relative energy of transition state x, sum over all transition states, *trans* and *cis* of the *α* and *β* isomers.

Table 34: Relative Boltzmann population distribution (N_x) of the transition states **TS-1** (π-σ) at different temperatures.

Pd-complex	**L = *i*-Pr$_3$P**		**L = PPh$_3$**	
	α	*β*	*α*	*β*
298.15 K				
cis				
TS-1 (π-σ)	0.7%	0%	8.7%	14%
trans				
TS-1 (π-σ)	3.6%	96%	37%	40%
Σ	**4.3%**	**96%**	**46%**	**54%**
373.15 K				
cis				
TS-1 (π-σ)	1.8%	0%	11%	16%
trans				
TS-1 (π-σ)	6.6%	91%	35%	38%
Σ	**8.4%**	**92%**	**46%**	**54%**

The experimentally obtained ratios of regioisomers (**a**+**b**:**c**+**d**) (Table 31, entries 1 and 2) were then compared to the obtained theoretical ratios (Table 34). These ratios match very closely for both ligand systems with the alkyl phosphine ligand preferring the *β*-regioisomer (9:1) and the triaryl phosphine ligand giving an almost 1:1 mixture (Table 35). The validity of the calculations and implication of kinetic control taking place could thus be supported.

Table 35: Comparison of experimentally observed regioisomeric ratios at 373.15 K (Table 31, entries 1 and 2) and computationally calculated regioisomeric ratios at 373.15 K (Table 34, last entry). [a] Cy_3P for experimental data, *i*-Pr_3P for computational calculations. [b] Using oxabicycle **307** instead of **311**.

Ligand	**Experimental (a+b:c+d)**	**Computational (*β*:*α*)**
Alkyl$_3$P[a]	85:15 (90:10)[b]	92:8
PPh$_3$	54:46[b]	54:46

In conclusion, the ratios of the calculations could be shown to be in accordance with the experimental data. Moreover, it could be shown that while the *trans*-pathway dominates the mechanism, the *cis*-pathway still significantly contributes to the observed ratios. Additionally, the necessity of investigating energetically higher lying conformers as the catalytically active species[291] could be shown.

5.5.6 Scope expansion

A brief investigation into additional uses of oxabicycles beyond indene synthesis was conducted. Spiroindenes can be synthesized using norbornadiene in a Catellani-type reaction with *O*-benzoyl hydroxylamine **342**.[201] The reaction proceeds *via* intramolecular termination and formation of a quinoid moiety. The applicability of oxabicycle **296** as a substitute was tested (Table 36). ^{1}H-NMR-revealed little conversion to the expected product following the conditions by *Fan et al.* (Figure 25).[201] MS data supported the presence of spiroindene **343** in the crude reaction mixture (m/z 294 APCI) and the presence of furan **344** (m/z. GC-MS EI 184.1) with incomplete conversion of 2-iodobiaryl **345**. Under conditions more akin to the synthesis of indenes (Table 36) no product formation was observed. Formation of furan **344** was again observed (16%). No ^{1}H-NMR signals corresponding to pre-retro-*Diels-Alder* product **346** were observed in either case with corresponding masses not being detectable by APCI-MS or EI-MS analyses.

Table 36: Palladium-catalyzed Domino reaction for the synthesis of spiroindenes using oxabicycle **296**.

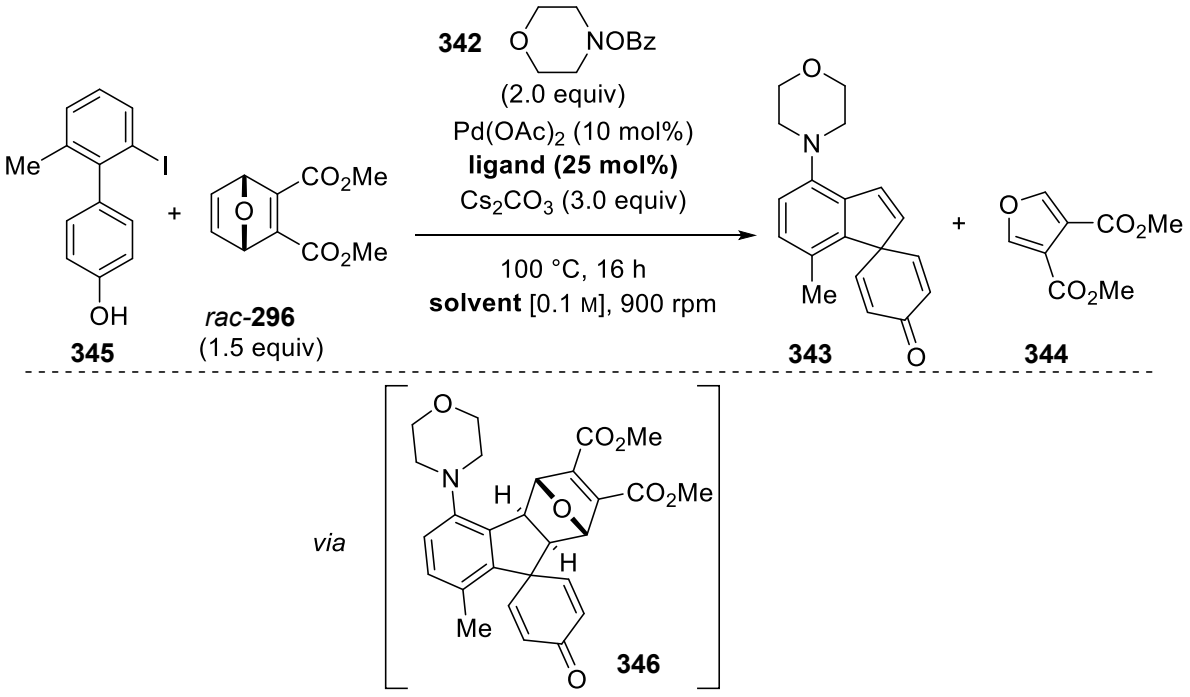

#	Ligand	solvent	ArI [%]	Product [%]	Furan [%]	$BzONR_2$ [%]
1	$(4\text{-OMe-}C_6H_4)_3P$	DME	26	2[a]	8	0
2	$Cy_3P{\cdot}HBF_4$[b]	PhMe	3	0	16	29

Conversions to products according to ^{1}H NMR with 1,3,5-trimethoxybenzene as internal standard. [a] suspected product. [b] Cs_2CO_3 (3.2 equiv)

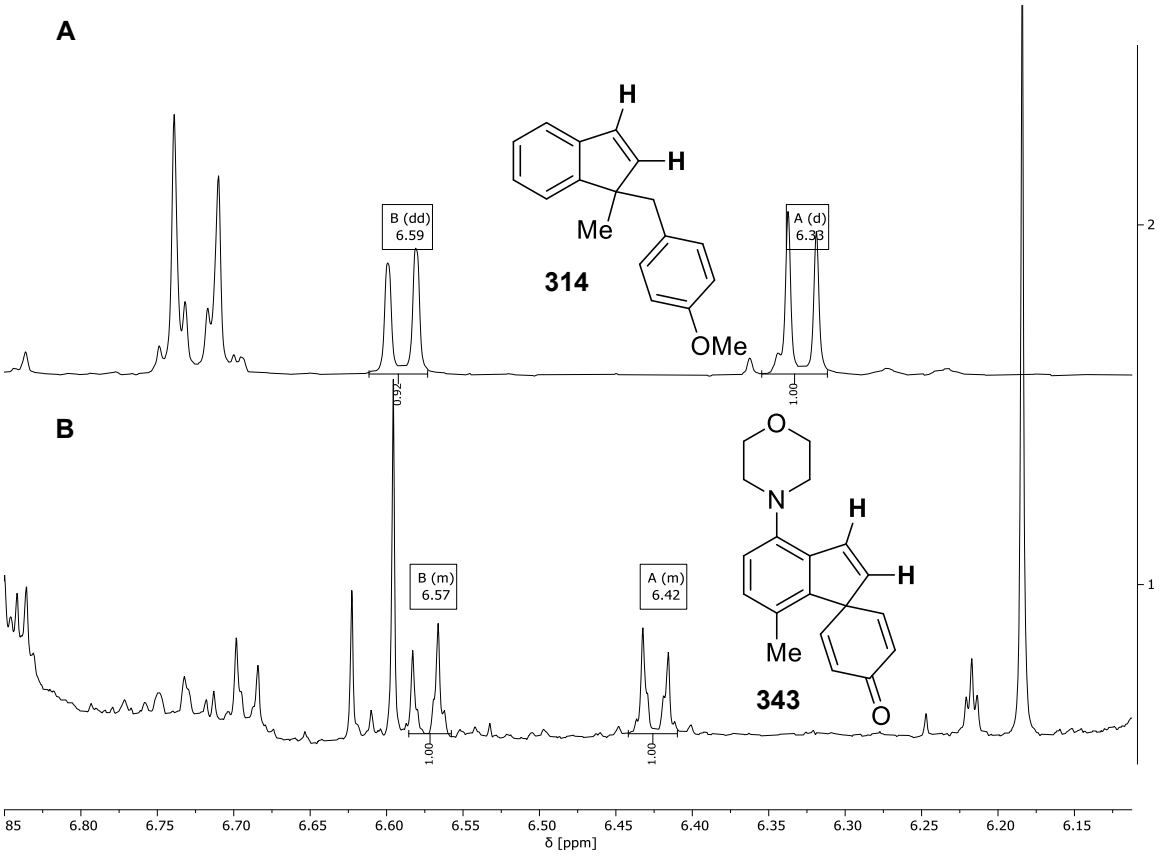

Figure 25: (A) Indene signals of **344**. (B) Suspected indene signals of **343** According to ^{1}H-NMR.

6 Outlook

6.1 Flavonoids

Over the course of the biological evaluation of biflavones, the first non-C_2-symmetrical 8,8″-biflavone **219** (B,B′-unsymmetrical) was synthesized. This compound exerts higher bioactivity than the corresponding C_2-symmetrical biflavone **217** (6.3 μM vs. 15.9 μM) (Figure 26A). Investigations on a scope of B,B′-C_2-unsymmetrical biflavones would therefore give insight into the structure activity relationship (Figure 26B). Additionally, the mode of action should further be probed. By identifying the biological target of the employed amino biflavones, more rational drug design could be employed. Furthermore, utilizing the *meta*-selective borylation, other A,A′-C_2-unsymmetrical biflavones **367** could be accessible and thus libraries expanded with existing methodology. Furthermore, the best hits obtained thus far should be screened against further human cell lines such as *cis*-platinum resistant human cancer cell lines to evaluate the usefulness of these drug candidates against therapy resistant pathogens.

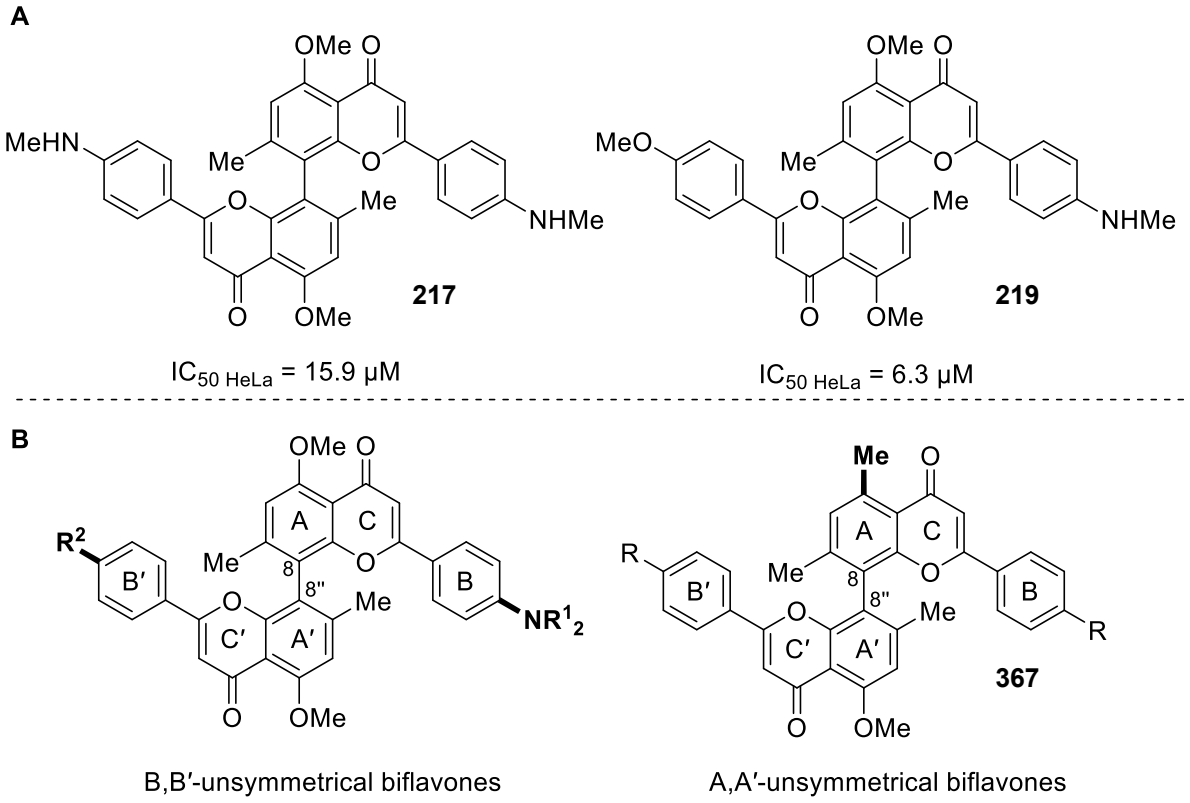

Figure 26: (A) Bioactive synthesized 8,8″-biflavones. (B) Non C_2-symmetrical biflavones as a scope of novel natural product inspired lead structures.

In addition to these investigations, the newly identified bichalcone **166** could be used as a lead structure for further investigations. Isomerization *in vivo* to a mixture of various flavanone type side products could play a role in the activity of this compound. Stereoselective synthesis of flavanones has been investigated thoroughly in literature.[295] Thus, starting from chalcones (**136**) *via* organocatalysts could provide the flavanones (**368**) in an enantioselective manner (Scheme 97A).[296] These conditions could then be transferred to the bichalcones (Scheme 97B) to provide the corresponding chalcone-flavanone (**254**) and biflavanones (**255**). The diastereoselectivity of this reaction should be investigated even in the absence of chiral organocatalyst. First experiments at identifying these side products have been conducted (Chapter 5.2.3.1) but diastereo- and chemoselectivities have barely been investigated.

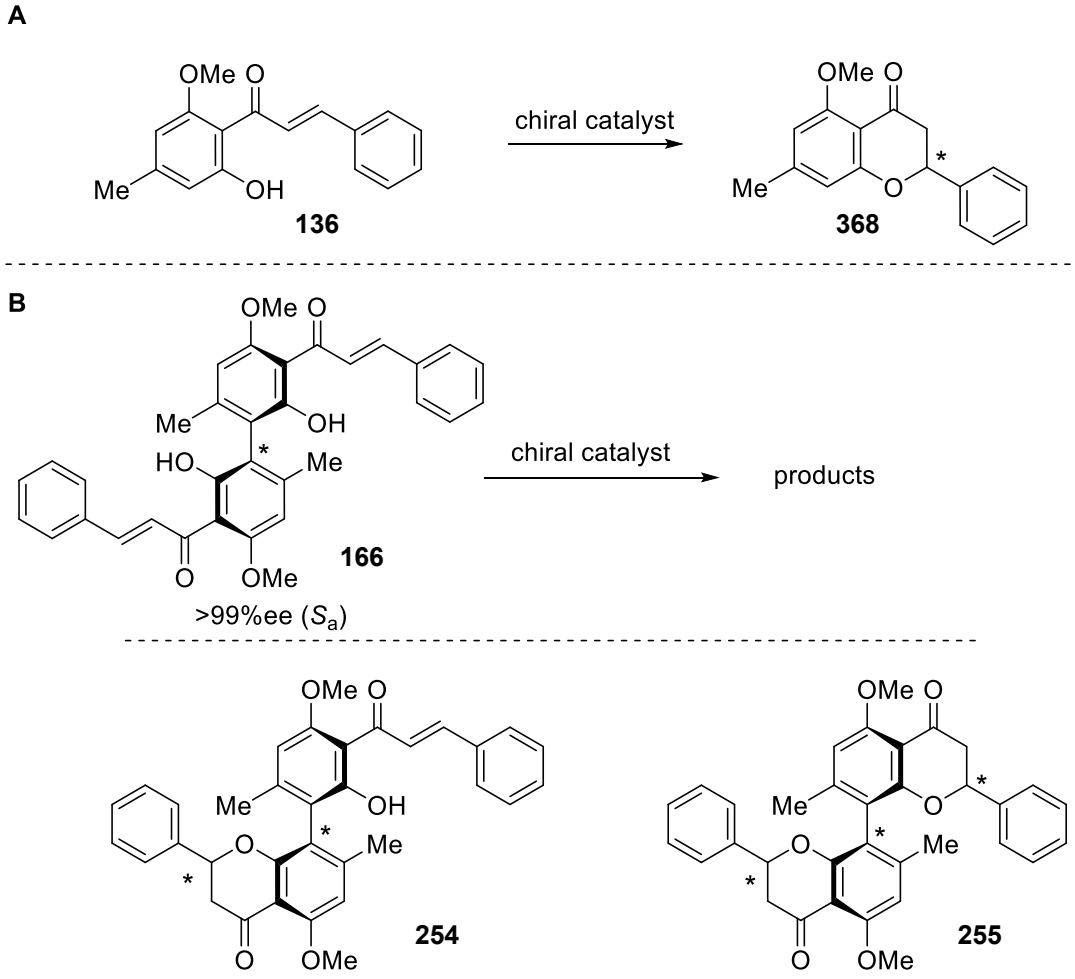

Scheme 97: (A) Cyclization of chalcones to flavanones using chiral catalysts. (B) Cyclization of bichalcones to flavanone type products.

6.2 Scope of biaryls

Overall, the synthesis sequence of the biphenol **27** synthesis was able to provide both enantiomers of the desired product in a yield of 17% over 8 steps. The yield of several steps in this sequence should be able to be improved. Multiple bottlenecks were identified. First the formation of the iodonium salt resulted in less than quantitative isolation of the desired product. It was suspected that the remainder of the product remained in solution due to the excess of benzoic acid. Column chromatographic isolation did not result in product isolation but isolation of small amounts of the benzoate salt **369** (Scheme 98). A base wash with subsequent NaOTf could be attempted to increase the yield of this step.

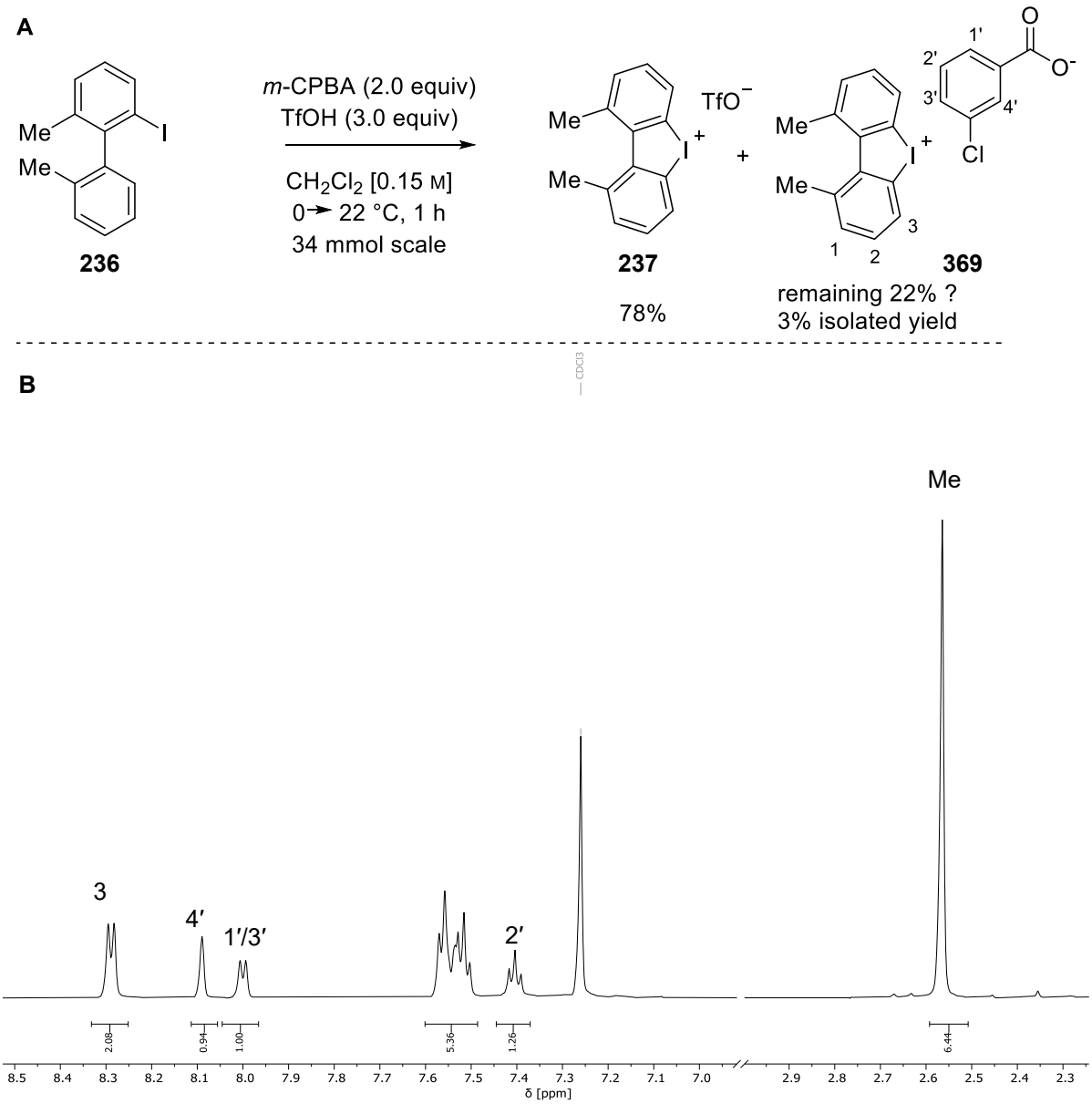

Scheme 98: (A) Synthesis of iodonium salt with isolated side product **369**. (B) 1H-NMR spectrum of benzoate salt **369**.

Next the Oxone® mediated oxidation could be tweaked to improve the obtained yields (Scheme 99). Milder conditions could be attempted to avoid overoxidation of the aryl iodide. Additionally, isolation of the desired product by base-wash could be attempted to remove the need for column chromatographic isolation.

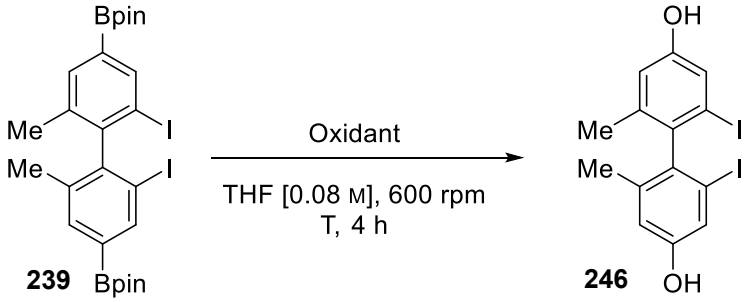

Scheme 99: Boronic acid ester oxidation.

Lastly, the halogen-oxygen exchange to generate the desired biphenol **27** only proceeded with acceptable yields of 45% after recrystallization (Chapter 5.2.2.5). To mitigate this, a change in strategy could be attempted. Literature known ring opening using benzoates to obtain non-C_2-symmetrical **370** (Scheme 100A) should be considered.[79] Subsequent halogen-oxygen exchange of biaryl **371** would elongate the synthesis route but improve yields (Scheme 100B).[79] Conveniently, the same chiral ligands are used in this transformation as the ones used for the halide ring opening (Chapter 5.2.2.2).[81]

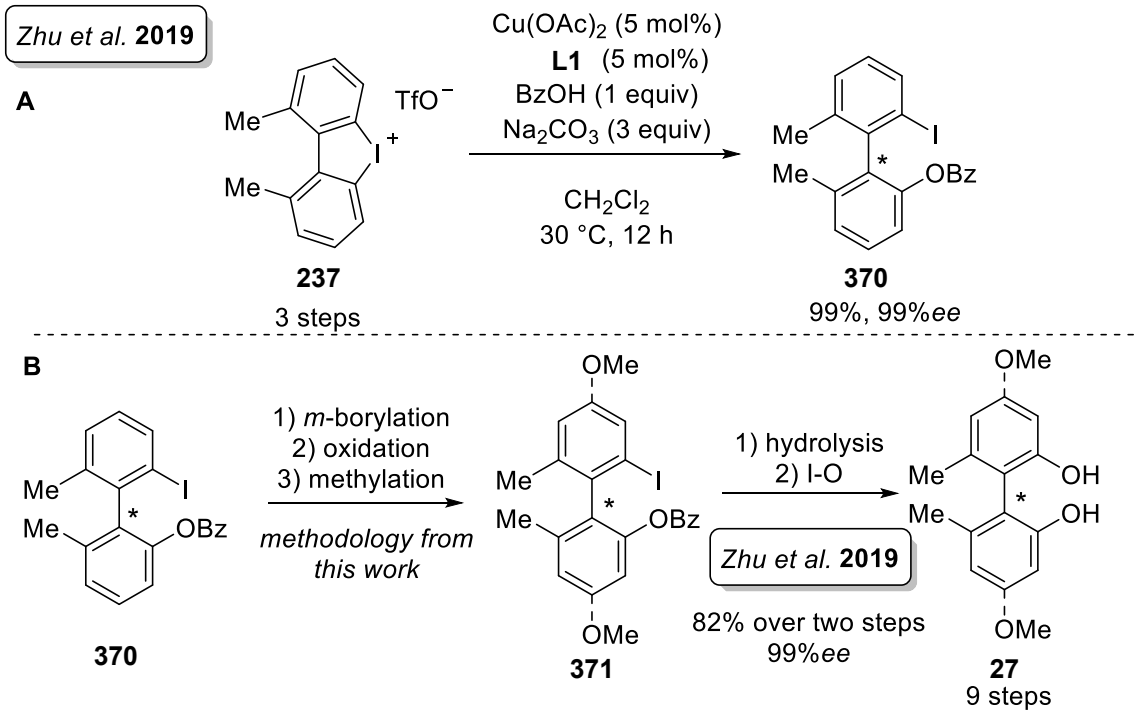

Scheme 100: Alternative route using a benzoate for the stereoselective ring opening.

With a high yielding protocol for the synthesis of borylated biaryls established (Chapter 5.2.2), several additional applications can be imagined. Hydrolysis of the esters to obtain the analogous boronic acids **372**[297] could make these structures intriguing candidates for novel axially chiral copolymers[298] or covalent organic frameworks (COF) **373** (Scheme 101).[299] In particular linear axially chiral conjugated polymers **374** have recently been investigated and would benefit greatly from the established methodology[300] and be accessible by simple literature known bromine substitution (**375**) of the boronic acid esters.[194]

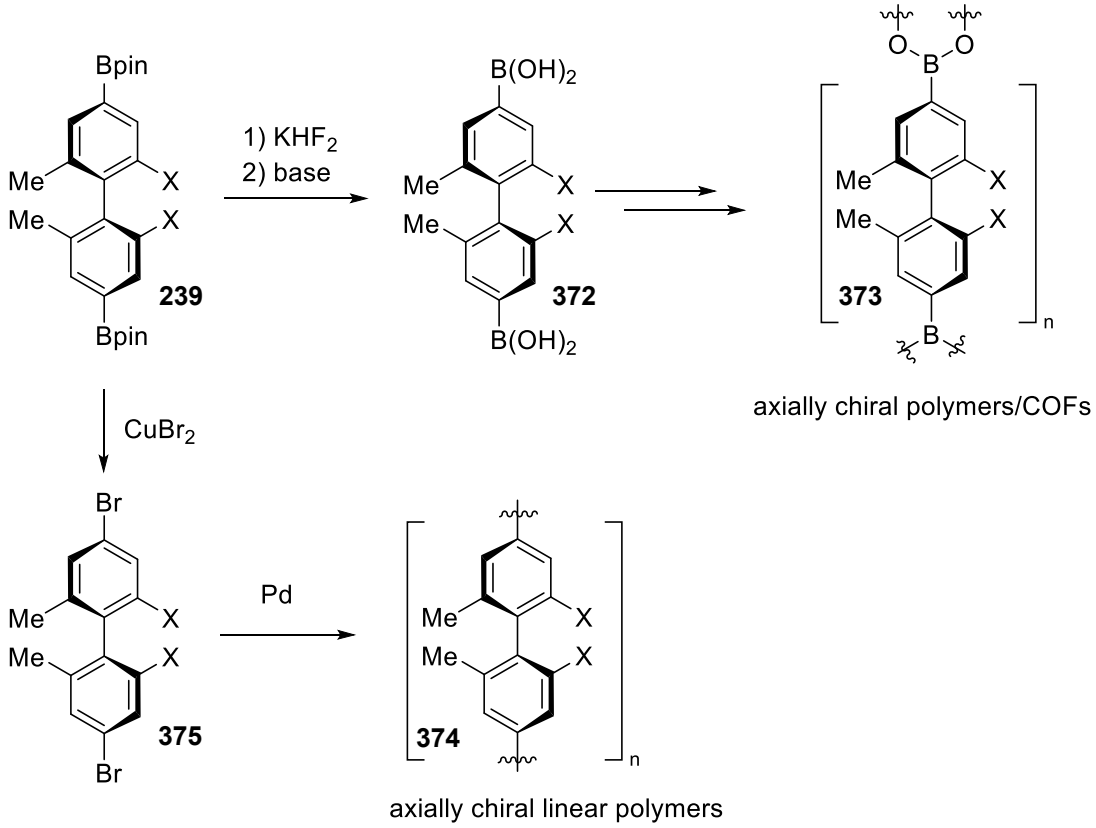

Scheme 101: Application of diborylated biaryls in the construction of axially chiral polymers.

In addition to the investigated C_2-symmetrical building blocks, non-C_2-symmetrical cyclic diaryliodonium salts **376** should be considered in combination with the borylation methodology to obtain a scope of electronically modified non-C_2-symmetrical dihalobiaryls **377**. These analogues could find applications in the synthesis of *P*-chiral dibenzophospholes **378**, a class of fairly unflexible arylphoshpine ligands in transition metal-catalyzed reactions (Scheme 102).[155b] The axial-to-point chirality transfer and the stereoelectronic implications of the arene substitution are currently under investigation by M.Sc. *Dominic Baderman* (Institute of Bioorganic Chemistry, Heinrich-Heine University).

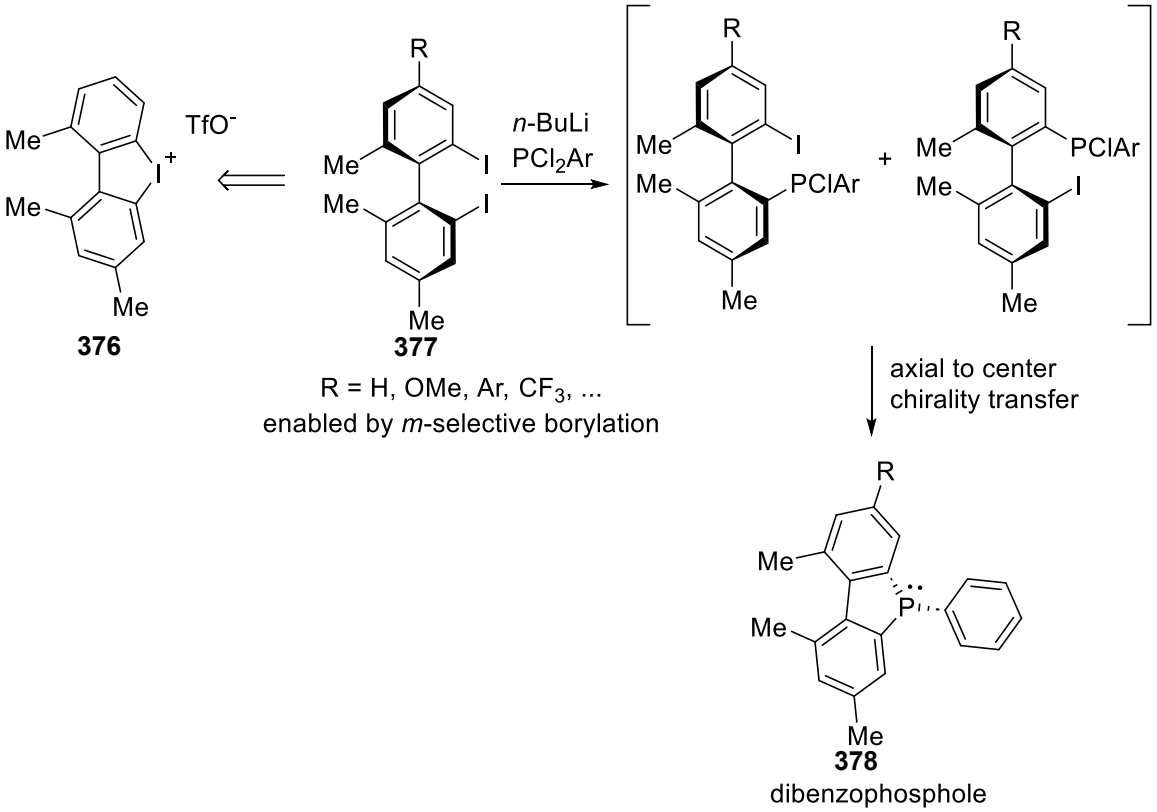

Scheme 102: Application of the *meta*-selective borylation for non-C_2-symmetrical substrates and their use in the construction of *P*-chiral dibenzophospholes.

6.3 Catellani

Low conversions of starting material and small amounts of *ipso* hydrogenation side product formation were observed over the course of the reaction using the improved protocol (Chapter 5.3.3). Inactivation of the palladium catalyst was thought to be responsible for the low conversion of starting material. Benzoyl hydroxylamine derivates such as 4-methoxyphenyl- (**379**), perfluorophenyl- (**380**), and 4-trifluoromethylphenylcarboxylates (**381**) have been reported in literature and could thus be used as alternative reagents (Figure 27A).[261, 301] The substituent were shown to have a clear effect on the reactivity in transition metal catalyzed reactions.[302] Thus electronically modifying the hydroxyl amino benzoate may result in less palladium inhibition and therefore higher conversions to product. To investigate the *ipso*-hydrogenation, the mode of action of this side product formation would need to be identified. Deuterium labeling studies suggest the incorporation of the *ortho*-hydrogen.[160a] Kinetic studies could be conducted to see if side product formation is linear or increases over time. Additionally, the influence of water should further be investigated. A relevant influence could be observed indicating a setup in a glovebox-type environment may be required for higher conversions to product. Finally, a scope should be synthesized to further probe the applicability of this protocol especially for sterically more congested systems (Figure 27B).

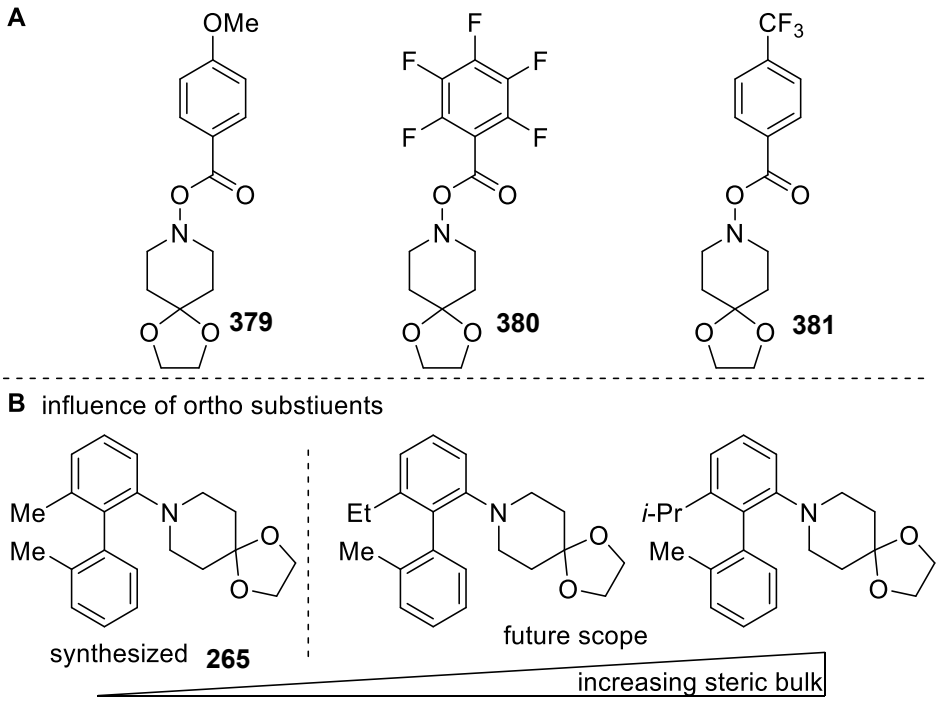

Figure 27: (A) Variously substituted benzoyl hydroxylamines to investigate product formation. (B) Scope of 2-aminobiaryls by increasing steric bulk of the ortho substituents.

6.4 Silylation

In the context of these investigations, the stereodynamics of the system at room temperature was supported by computational studies. Further DFT calculations are required to verify these results. A preliminary ligand screening revealed tight binding of bidentate L-L and L-X type ligands. Modifications of the reaction conditions beyond solvent screening should be conducted to attest the viability of this approach. Various amide ligands employed in literature contain protected carboxylates to mitigate tight binding which should also be explored.[276, 303] Additionally, a deracemization strategy could be investigated based on reversible C–I bond cleavage developed by the *Lautens* group (Scheme 103).[304]

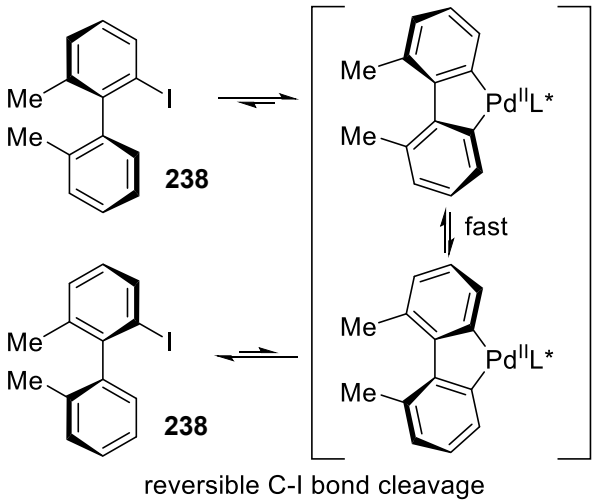

Scheme 103: Pd-catalyzed deracemization by reversible C-I bond cleavage using a chiral ligand.

6.5 Chiral Acetylene

In investigating the enantioselective synthesis of indenes, racemic mixtures of chiral oxabicycles as acetylene analogues could be used to probe the stereoselectivity of the reaction (Chapter 5.5). Therefore, without the need for enantioenriched oxabicycles, de-novo synthesis of such electronically modified analogues should be viable (Figure 28A). The synthesis of ketone/ester oxabicycle **321** should be improved to evaluate other electron-deficient systems such as keto-amide **382**. Additional oxabicycles obtained from substituted alkynes like methyl phenylpropiolate **383** or methyl propiolate **384** could be of interest. These assessments are currently undergoing further investigations.[278] Moreover, to exclude other species from being catalytically relevant and further validate the results, variously substituted Pd-complexes should be investigated. Further candidates for investigation include various substitutions of the palladium besides iodide (Figure 28B). The transition state between uncoordinated complex and both regioisomeric π-complexes **TS-2** could also be relevant in determining the regioselectivity under the *Curtin-Hammett* paradigm (Figure 28C).[305] As such, the mechanism

is still under scrutiny and must be probed further. In the end, the optimized oxabicycle system should be tested using the same methods to verify the applicability of the model.

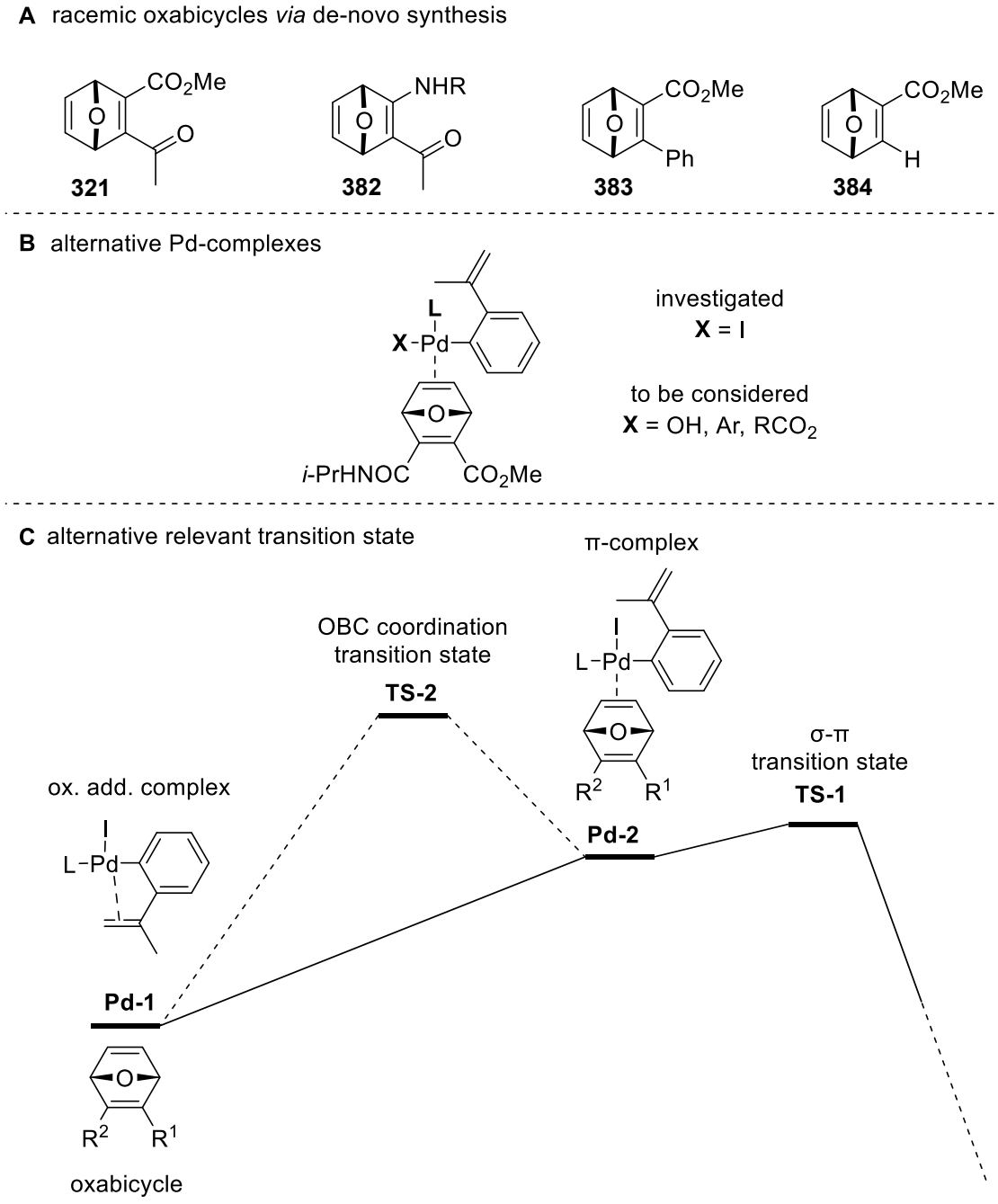

Figure 28: (A) Scope of oxabicycles to consider for the synthesis of prDA intermediates to assess the regio- and diastereoselectivities. (B) Alternative substituents X-type ligands on the relevant palladium complexes to assert the catalytically relevant transition states. (C) Alternative transition state to consider for the observed regioselectivity.

7 Experimental

7.1 General information

All chemicals not synthesized or present in the group were purchased from *Sigma-Aldrich Co.*, *Alfa Aesar GmbH & Co. KG*, *Merck KGaA* or *Fluorochem Ltd.* All reactants were used without any further purification unless stated otherwise. Methanol was dried using activated molecular sieve (3 Å). DMSO was degassed *via* freeze-pump-thaw. Anhyd. diethylether and dichloromethane were taken from the solvent purifier *MB SPS-800* by *MBraun*. Silica gel 60 (0.040 – 0.063 mm, 230 – 400 mesh) by *Machery Nagel* used for synthesis was dried in an oven at 110 °C over night. Anhyd. solid reagents were stored in a desiccator under an atmosphere of N_2.

Working under inert conditions

All glassware and stirring bars used for reactions under anhyd. or inert conditions were put in an oven at 110 °C for at least 12 h. When removing glassware from the oven it was sealed airtight using septa and stopcocks. It was then attached to a Schlenk-line and left to cool under nitrogen-gas, which was itself dried over *SICAPENT*®, for several minutes. Glassware was then dried using Schlenk-technique by heating the glassware under vacuum for several minutes and then letting it cool to room temperature under N_2-flow. This process was repeated three times. Septa were only opened briefly during the addition of reactants under N_2-countercurrent. Liquid reactants, solvents and solutions of reactants were transferred using syringes flushed three times with N_2.

Laboratory devices

Solvents were removed using rotary evaporators at a bath temperature of 40 °C under reduced pressure. Analytic balance AE 163 by Mettler Toledo was used to determine and weigh yields and reactants. Sonication of reactions was conducted using ultrasonic cleaning bath T310 by Elma Schmidbauer GmbH. Distillations of liquid aldehydes were conducted using Kugelrohrofen *Glass Oven B-580* and *Glass Oven B-585* by *Büchi* under reduced pressure.

Chromatography

For thin layer chromatography (TLC) silica gel plates (*Polygram® SIL G/UV 254*) by *Machery-Nagel* with fluorescent indicator. Spots were made visible under UV light, using aqueous potassium permanganate solution, cerium ammonium molybdate stain (CAM), anisaldehyde. Column chromatographic purification was conducted using the appropriate solvent mixture and

silica gel 60 (0.040 – 0.063 mm, 230 – 400 mesh) by *Machery Nagel* in cylindric glass columns by applying pressure with compressed air.

Analytical devices

^{1}H-, ^{13}C-, DEPT-135-, COSY-, HSQC-, HMBC-NMR spectra were measured on the spectrometer *Bruker Avance/DRX 600* at a frequency of 600 MHz (^{1}H) and 151 MHz (^{13}C). ^{19}F-, ^{11}B- and select ^{1}H- and ^{13}C-NMR spectra were measured on the spectrometer *Bruker Avance/DRX 300* at a frequency of 282 MHz (^{19}F), 96 MHz (^{11}B), 300 MHz (^{1}H) and 75 MHz (^{13}C). Additional select ^{1}H-, ^{13}C and ^{31}P- spectra (most spectra related to chapter 5.5) were measured on Bruker Avance III NMR Spectrometer (400 MHz ^{1}H), Varian MercuryPlus NMR Spectrometer (400 MHz ^{1}H) and Agilent DD2 NMR Spectrometer (500 MHz ^{1}H). Deuterated chloroform with or without 0.03 vol% TMS ($CDCl_3$) or deuterated d^{6}-DMSO were used as solvent. The ^{1}H- and ^{13}C-spectra were referenced to the solvent peak ($CDCl_3$ δ = 7.26 ppm (^{1}H), δ = 77.16 ppm (^{13}C)). Data was evaluated using the software *MNova* (*MestReNova*) version 14.1.2 by *Mestrelab Research*. Coupling constants *J* were given in Hz and chemical shifts δ in ppm (parts per million). Multiplicities are abbreviated as the following: singlet (s), broad singlet (brs), doublet (d), triplet (t), quartet (q), multiplet (m).

High resolution mass spectrometry (HRMS) was measured at the Heinrich Heine University Düsseldorf (Applied Biosystems/ MDS SCIEXQ Model Trap 4000) with electron spray ionization (ESI). Low resolution mass spectrometry was conducted using the express**ion** CMS system by Advion, Inc. in combination with an atmospheric pressure chemical ionization (APCI) or electron spray ionization (ESI). Gas chromatographic mass spectrometry (GC-MS) was conducted using the Thermo Scientific TRACE 1310 gas chromatograph (ISQ QD Single Quadrupole Mass Spectrometer, Helium). Elemental analyses were measured at the Heinrich Heine University Düsseldorf (Elementar, Vario Micro Cube). Furthermore, melting points (Stuart Scientific, Melting Point Apparatus SMP3), HPLC chromatograms (Thermo Scientific, Dionex UltiMate 3000 Column Comportment) and optical rotation (A.Krüss, P8000-TF) were measured with the appropriate devices. IR spectra were recorded using a *SpectrumTwo FT-IR* by *PerkinElmer* with attenuated total reflection (ATR). The absorption bands were given in units of wave numbers (cm^{-1}).

X-ray

X-ray crystallographic data for compounds **166**, **169** and **239** were measured by Wolfgang Frey at the Department for Single Crystal Diffractometry of the Institute of Organic Chemistry at the University of Stuttgart. Data was collected using a Bruker Kappa APEXII Duo diffractometer.

X-ray crystallographic data for compound **339** was measured by Alan Lough at the X-ray Crystallography Lab of the Dept. of Chemistry, University of Toronto, Canada. Data was collected using a Bruker Kappa APEX-DUO CMOS PHOTON II diffractometer.

The indicated deposition numbers (CCDC #) contain the supplementary crystallographic data for this paper. These data are provided free of charge by the joint Cambridge Crystallographic Data Centre and Fachinformationszentrum Karlsruhe Access Structures service.

Structures were visualized using the CCDC software Mercury (2023.2.0).

Chemicals

n-BuLi in hexanes was titrated using diphenyl acetic acid as the indicator in triplicates. Commercial nitrobenzene was washed with aq. NaOH solution (2 M), dist. water, HCl (1 M), dist. water and sat. aq. NaCl solution and dried over $MgSO_4$. Then vacuum distillation was performed at 90 °C, $8 \cdot 10^{-1}$mbar (head temperature 67 °C). After a stable head temperature was reached the liquid was collected into a round bottom flask charged with CaH_2. The nitrobenzene distilled this way was stored under argon and sealed airtight. DMSO was degassed by freeze pump thaw method (3x freezing under N_2, thawing under vacuum, typically $2 \cdot 10^{-1}$ – $2 \cdot 10^{-2}$ mbar. Morpholine was distilled prior to use at 50 °C and $1.9 \cdot 10^{-1}$ mbar. Benzylamine was distilled prior to use at 170 °C and $2.3 \cdot 10^{-1}$ mbar. $TMSCF_3$ was distilled using a Kugelrohrofen® prior to use (22 °C, $1.3 \cdot 10^{-1}$ mbar). Benzophenone imine was distilled using a Kugelrohrofen® prior to use (160 °C, $7 \cdot 10^{-2}$ mbar).

Working with transition metal catalyst

Stir bars used in transition metal catalyzed reactions were cleaned of trace metal impurities by stirring in a bath of conc. aqua regia (HNO_3:HCl, 1:3). Reactions were performed in 2 dram (2 dr.) vial (ThermoScientific National B7999-3) equipped with a PTFE lined cap (ThermoScientific National B7995-15) and a stir bar (Fisher cat no. 14-513-57, 12 x 4.5 mm). Hot vials equipped with stir bars (110 °C for 24 h) were taken out of the oven and immediately capped with a rubber stopper (Saint-Gobain Natural Rubber Folding Skirt Stoppers cat. no. 407010-50) and equipped with Argon filled balloons with an additional needle as an outlet. An

oil bath equipped with a stir bar was used as the heating source for such reactions. Solid reagents were weighed without gloves to avoid electrostatic discharging while using the analytical balances. After adding all non-volatile reagents, the outlet needle was removed. After adding all remaining reagents, the screw thread of the vial was lined with PTFE tape (in the same direction as the threading). The reactions were then sealed by removing the septum still equipped with the balloon swiftly and screwing on the PTFE lined cap, screwing on the lid tightly. The vial was the sealed with PTFE tape.

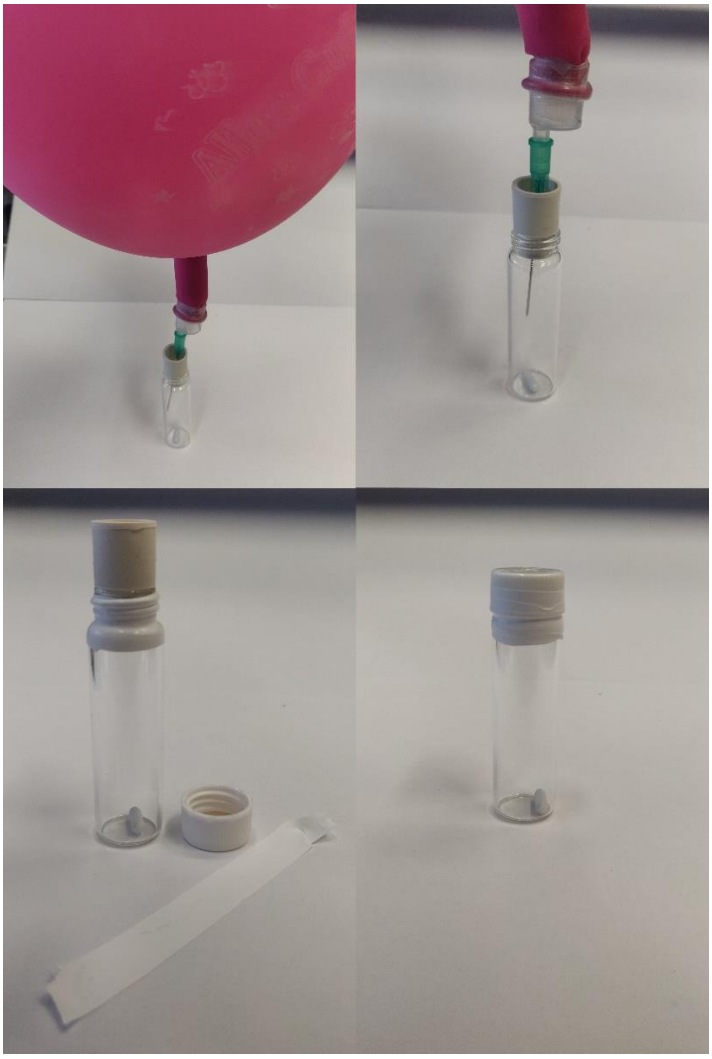

Figure 29: Setup using 2 dram vials. Top left: vial capped with argon balloon. Top right: Zoom in to show stirring bar. Bottom left: threading lined with PTFE-tape (clockwise). Bottom right: septum removed and replaced with PTFE-lined rubber cap, sealed with PTFE-tape (clockwise).

Working with internal standard

If conversions to product(s) according to ^{1}H-NMR are reported, the following general procedure was conducted. Reaction mixtures were worked up (extraction or filtration where applicable). Then a defined amount of internal standard (1,3,5-trimethoxy benzene) (around 6

– 20 mg) was weighed into a glass vial avoiding electrostatic discharge on the analytical balance. Then the internal standard was transferred to the crude product by dissolving in EtOAc und transferring by Pasteur pipette, making sure to rinse all glass ware thoroughly. Then solvents of the crude product were removed in vacuo, making sure not to heat the heating bath above 45 °C and not to set the vacuum below 100 mbar.

^{1}H-NMR experiments for the quantification of conversions to product were conducted at a d1-delay of 10 seconds. Variation of this delay of a complex mixture and integration over a fixed interval relative to 1,3,5-trimethoxy benzene as an internal standard are displayed in Table 37. The relative integers are in good agreement with one another except for a d1-time of 1 second. Therefore, quantifications using 1,3,5-trimethoxybenzene should be accurate.

Table 37: d1-time-dependant relative integer using 1,3,5-trimethoxy benzene as internal standard.

Entry	d1-time [s]	Integer (6.5 – 8.2 ppm)
1	1	9.01
2	5	8.82
3	10	8.85
4	20	8.76
5	90	8.83

DMF extraction

The extraction efficiency of the aq. workup was investigated. A solution of 1,3-dimethoxybenzene (0.10±0.02 mmol) in DMF (0.5 mL), was extracted with EtOAc (3 mL) and an aq. wash (1x H_2O, 3x sat. aq. NaCl solution) in a vial using a pipette performed and the organic phase dried over $MgSO_4$. Most DMF could be removed. The procedure gave an extraction efficiency of 99±7% in triplicates (1,3,5-trimethoxybenzene (0.10±0.03 mmol) according to ^{1}H-NMR). Any compound less polar than 1,3,5-trimethoxybenzene should be extracted similarly well under these conditions.

Computational software and details

DFT[100]-calculations were carried out using the Orca (5.0.4 or 5.0.1)[267] quantum chemistry software packages. The conformer rotamer ensemble sampling tool (CREST)[289] based on the xTB[288] package was used to identify conformers. The censo[290] extension was used to identify the lowest lying conformers. Obtained ground states were confirmed by the absence of imaginary frequences after an analytical frequency calculation (AnFreq). Transition states were

identified by relaxed surface scan (RSS) of the same lowest energy conformers and confirmed to be first order saddle points by the presence of exactly one imaginary frequency. Hirshfeld charges[292] and condensed Fukui functions[293] (CFF) were calculated using Multiwfn (3.8).[294] Methods and base sets used for energy calculations and geometry optimizations are mentioned where applicable. Structures were visualized using the software Avogadro (1.2.0) or UCSF ChimeraX (1.2.5). All energies were calculated at 298.15 K and in gas phase unless specified otherwise.

7.2 Experimental Procedures

7.2.1 Lipshutz Synthesis

7.2.1.1 1,3-Dimethoxy-5-methylbenzene (123)

A 500 mL round bottom flask equipped with stir bar was charged with 5-methylbenzene-1,3-diol (10.0 g, 1.00 equiv, 80.6 mmol), acetone (180 mL, 0.44 M), K_2CO_3 (31.8 g, 2.86 equiv, 230 mmol). The reaction mixture was cooled to 0 °C under stirring and Me_2SO_4 (16.8 mL, 2.20 equiv, 177 mmol) added. The reaction mixture was then stirred at 65 °C for 4.5 h. Aq. sat. Na_2SO_3-solution (100 mL) was added, and the mixture stirred vigorously at 40 °C for 30 min. The aq. phase extracted with EtOAc (3x). The combined organic phases were washed with sat. aq. NaCl solution, dried over $MgSO_4$ and solvents removed in vacuo. The crude product was then dissolved in CH_2Cl_2, washed with aq. NaOH solution (2x, 1 M) and the combined aq. phases dried over $MgSO_4$. The product was isolated as an amber oil in a yield of 11.4 g (74.9 mmol, 93%). The analytical data were in accordance with literature.[102]

^{1}H NMR (600 MHz, $CDCl_3$): δ 2.32 (s, 3H, Me), 3.79 (s, 6H, OMe), 6.31 (d, $^4J_{2\text{-}4}$ = 2.3 Hz, 1H, 2-H), 6.36 (d, $^4J_{2\text{-}4}$ = 2.4 Hz, 2H, 4+6-H). **^{13}C NMR** (151 MHz, $CDCl_3$): δ 21.91 (Me), 55.31 (OMe), 97.64 (C-2), 107.20 (C-4+6), 140.31 (C-5), 160.84 (C-1+3). **IR (ATR film) [cm^{-1}]:** 2940, 2836, 1597, 1461, 1318, 1203, 1147, 1056, 1067, 917, 825, 682. **TLC** (petroleum ether:EtOAc 7:3 v/v): R_f = 0.67 **APCI-MS:** m/z: ([M + H$^+$]): found: 153.0

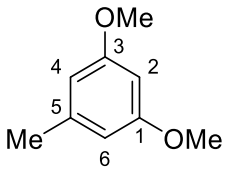

123

7.2.1.2 3-Methoxy-5-methylphenol (124)

A 500 mL Schlenk round bottom flask equipped with stir bar was charged with 1,3-dimethoxy-5-methylbenzene (**123**) (11.3 g, 1.0 equiv, 74.3 mmol), DMF (120 mL, 0.53 M) and NaH suspension in petroleum oil (60 weight%) (6.53 g, 2.2 equiv, 163 mmol) The reaction mixture was cooled to 0 °C and a solution of *n*-propanethiol (13.5 mL, 2.0 equiv, 149 mmol) in DMF (20.0 mL, 7.4 M) was slowly. A reflux condenser was equipped, a gas wash bottle filled with dilute bleach (4 weight% NaOCl) solution equipped to the top of the condenser *via* tubing and the reaction mixture stirred at 170 °C for 3 h. After letting the reaction cool to ambient temperature, H_2O (100 mL) was added, and the mixture extracted with petroleum ether (3x).

Then aq. HCl solution (4 M) was added until pH 1. The aq. phase was then extracted with Et_2O (3x), the combined organic phases washed with sat. aq. NaCl-solution and dried over $MgSO_4$ and solvents removed in vacuo. The product was isolated by Kugelrohr® distillation and subsequent washing with cold H_2O (3x) in EtOAc as a yellow oil in a yield of 9.27 g (67.1 mmol, 90%). The analytical data were in accordance with literature.[102]

^{1}H NMR (600 MHz, $CDCl_3$): δ 2.27 (s, 3H, Me), 3.76 (s, 3H, OMe), 6.30 (d, $^4J_{2\text{-}4,2\text{-}6}$ = 2.3 Hz, 1H, 2-H), 6.33 (d, $^4J_{4\text{-}6,2\text{-}6}$ = 2.2 Hz, 1H, 6-H), 6.36 (d, $^4J_{2\text{-}4,4\text{-}6}$ = 2.4 Hz, 1H, 4-H). **^{13}C NMR** (151 MHz, $CDCl_3$): δ 21.55 (Me), 55.28 (OMe), 98.77 (C-2), 107.42 (C-4), 109.03 (C-6), 140.72 (C-5), 156.61 (C-1), 160.61 (C-3). **IR (ATR film) [cm^{-1}]:** 3353, 1591, 1507, 1472, 1336, 1154, 1064, 926, 829, 684, 613, 499. **TLC** (petroleum ether:EtOAc 7:3 v/v): R_f = 0.42 **APCI-MS:** m/z: ([M + H$^+$]): found: 139.1 **Melting point**: 61 – 63 °C **Boiling point**: 91 – 93 °C ($2\cdot10^{-2}$ mbar)

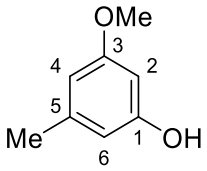

124

7.2.1.3 3-Methoxy-5-methylphenyl acetate (125)

A dry 250 mL round bottom flask equipped with stir bar was charged with NaH (suspension in mineral oil 60 weight%) (1.73 g, 1.00 equiv, 43.4 mmol) and anhydr. CH_2Cl_2 (80 mL, 0.54 M) was added at 0 °C. Then phenol **124** (6.00 g, 1.00 equiv, 43.4 mmol) was added at 0 °C and the reaction mixture stirred at 22 °C for 30 min. The solution was cooled to 0 °C and AcCl (3.25 mL, 1.05 equiv, 45.6 mmol) slowly added. The reaction mixture was stirred at 22 °C for 1 h. H_2O (100 mL) was added, the aq. phase extracted with EtOAc (3x), the combined organic phases washed with sat. aq. NaCl solution, dried over $MgSO_4$ and the solvents removed in vacuo. The product was isolated as a yellow oil in a yield of 7.85 g (43.6 mmol, 100%). The analytical data were in accordance with literature.[102]

^{1}H NMR (600 MHz, $CDCl_3$): δ 2.28 (s, 3H, OCO*Me*), 2.32 (s, 3H, Me), 3.77 (s, 3H, OMe), 6.45 (d, $^4J_{2\text{-}4,2\text{-}6}$ = 2.3 Hz, 1H, 2-H), 6.51 (t, $^4J_{4\text{-}6,2\text{-}6}$ = 1.8 Hz, 1H, 6-H), 6.60 (dd, $^4J_{4\text{-}6,2\text{-}4}$ = 2.6, 1.4 Hz, 1H, 4-H). **^{13}C NMR** (151 MHz, $CDCl_3$): δ 21.26 (OCO*Me*), 21.68 (Me), 55.47 (OMe), 104.73 (C-2), 112.67 (C-4), 114.71 (C-6), 140.44 (C-1), 151.54 (C-5), 160.40 (C-3), 169.68

(O*CO*Me). **IR (ATR film) [cm^{-1}]:** 2924, 1767, 1606, 1468, 1369, 1204, 1127, 1063, 1025, 826, 677, 583. **APCI-MS:** m/z: ([M + H$^+$]): found: 181.0; 139.0 (M - OAc$^-$ +H_2O)

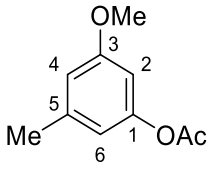

125

7.2.1.4 2-Bromo-5-methoxy-3-methylphenyl acetate (126)

A 1000 mL round bottom flask equipped with stir bar was charged with arene **125** (7.00 g, 1.00 equiv, 38.9 mmol) and acetonitrile (53 mL, 0.73 M). The reaction mixture was cooled to -40 °C and NBS (7.12 g, 1.03 equiv, 40.0 mmol) added. The reaction mixture left to warm up to ambient temperature over night. After 18 h, sat. aq. Na_2SO_3 solution was added, and the aq. phase extracted with CH_2Cl_2 (3x). The combined organic phases were washed with sat. aq. NaCl solution, dried over $MgSO_4$ and solvents removed in vacuo. The product was obtained as a mixture of regioisomers (86:14) as an orange oil in a yield of 10.1 g (38.9 mmol) and used in the next step without further purification. NMR data reported for the major regioisomer. The analytical data were in accordance with literature.[102]

^{1}H NMR (600 MHz, $CDCl_3$): δ 2.89 (s, 3H, Me), 2.95 (s, 3H, OAc), 4.30 (s, 3H, OMe), 7.09 (d, $^4J_{4\text{-}6}$ = 3.0 Hz, 1H, 4/6-H), 7.26 (d, $^4J_{4\text{-}6}$ = 3.0 Hz, 1H, 4/6-H). **^{13}C NMR** (151 MHz, $CDCl_3$) δ 20.86, 23.40, 55.55, 106.90, 109.36, 114.29, 140.20, 148.93, 158.92, 168.66. **APCI-MS:** m/z: ([M + H$^+$]): found: 258.

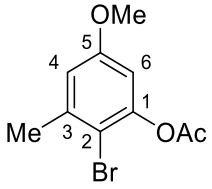

126

7.2.1.5 2-Bromo-5-methoxy-3-methylphenol (128)

A 500 mL round bottom flask equipped with stir bar was charged with arene **126** (mixture of regioisomers 86:14) (10.1 g, 1.0 equiv, 39.0 mmol), Na_2CO_3 (4.96 g, 1.2 equiv, 46.8 mmol) and MeOH (120 mL, 0.33 M). The reaction mixture was stirred at 85 °C for 40 mins and then at 22 °C for 21.5 h. Aq. HCl-solution (1 M, 100 mL) was added and the aq. phase extracted with

Et_2O (3x). The combined organic phases were washed with sat. aq. NaCl solution, dried over $MgSO_4$ and solvent removed in vacuo. The product was isolated by Kugelrohr® distillation (at no more than 110 °C) as white solids in a yield of 6.14 g (28.3 mmol, 73%) over two steps. The analytical data were in accordance with literature.[102] **^{1}H NMR** (600 MHz, $CDCl_3$): δ 2.36 (s, 3H, Me), 3.76 (d, ^5J = 1.3 Hz, 3H, OMe), 5.63 (s, 1H, OH), 6.42 (d, $^4J_{4\text{-}6}$ = 2.9 Hz, 1H, H-4), 6.46 (d, $^4J_{6\text{-}4}$ = 2.9 Hz, 1H, H-6). **^{13}C NMR** (151 MHz, $CDCl_3$): δ 23.33 (Me), 55.56 (OMe), 98.95 (C-6), 104.11 (C-2), 109.30 (C-4), 139.01 (C-3), 153.14 (C-1), 159.74(C-5). **IR (ATR film) [cm^{-1}]:** 3339, 2959, 1582, 1481, 1341, 1305, 1254, 1194, 1162, 1018, 836, 809, 624, 550. **TLC** (petroleum ether:EtOAc 7:3 v/v): R_f = 0.56 **APCI-MS:** m/z: ([M + H$^+$]): found: 216.9 **Melting Point**: 73 – 75 °C **Boiling point**: 100°C ($2.5 \cdot 10^{-2}$ mbar)

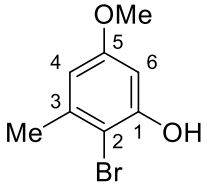

128

As a side product of the distillation the regioisomer **129** was obtained as a 94:6 mixture (**129**:**128**) in a yield of 1.67 g (7.70 mmol, 20%). The analytical data were in accordance with literature.[102]

^{1}H NMR (600 MHz, $CDCl_3$): δ 2.35 (s, 3H, Me), 3.85 (d, J = 3.6 Hz, 3H, OMe), 4.88 (s, 1H, OH), 6.31 (d, $^4J_{4\text{-}6}$ = 2.7 Hz, 1H, 6-H), 6.36 (d, $^4J_{4\text{-}6}$ = 2.7 Hz, 1H, 2-H). **^{13}C NMR** (151 MHz, $CDCl_3$): δ 23.30 (Me), 56.31 (OMe), 97.77 (C-6), 104.93 (C-4), 109.60 (C-2), 140.14 (C-3), 155.24 (C-1), 156.84 (C-5). **TLC** (petroleum ether:EtOAc 7:3 v/v): R_f = 0.42 **APCI-MS:** m/z: ([M + H$^+$]): found: 216.9 **Melting Point**: 122 – 124 °C

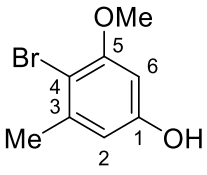

129

7.2.1.6 2-Bromo-5-methoxy-1-(methoxymethoxy)-3-methylbenzene (29)

A dry 250 mL round bottom flask equipped with stir bar was charged with phenol **128** (7.00 g, 1.0 equiv, 32.3 mmol) and DMF (100 mL, 0.33 M). The solution was cooled to 0 °C and NaH (suspension in mineral oil 60 weight%) (1.68 g, 1.3 equiv, 41.9 mmol) was slowly added under

stirring and the mixture stirred at 22 °C for 1.15 h. Then chlormethyl-methylether (2.94 mL, 1.2 equiv, 38.7 mmol) was added at 0 °C and the reaction stirred at 22 °C for 50 min. H_2O (100 mL) was added, the aq. phase extracted with Et_2O (3x), the combined organic phases washed with sat. aq. NaCl-solution, dried over $MgSO_4$ and solvents removed in vacuo. The product was isolated by Kugelrohr® distillation as a colorless oil in a yield of 8.43 g (32.3 mmol, 99%). The analytical data were in accordance with literature.[102]

^{1}H NMR (600 MHz, $CDCl_3$): δ 2.38 (s, 3H, Me), 3.51 (s, 3H, $CH_2O\underline{Me}$), 3.75 (s, 3H, OMe), 5.21 (s, 2H, $\underline{CH_2}OMe$), 6.48 (d, $^4J_{4\text{-}6}$ = 2.8 Hz, 1H, H-4), 6.59 (d, $^4J_{4\text{-}6}$ = 2.8 Hz, 1H, H-6). **^{13}C NMR** (151 MHz, $CDCl_3$): δ 23.57 (Me), 55.38 (OMe), 56.28 ($CH_2O\underline{Me}$), 95.18 ($\underline{CH_2}OMe$), 100.50 (C-6), 106.23 (C-2), 109.28 (C-4), 139.77 (C-3), 154.46 (C-1), 159.14 (C-5). **IR (ATR film) [cm^{-1}]:** 2947, 1581, 1468, 1322, 1156, 1048, 1025, 996, 929, 826, 604. **TLC** (petroleum ether:EtOAc 7:3 v/v): R_f = 0.56 **APCI-MS:** m/z: ([M + H$^+$]): found: 261.0 **Boiling point:** 120°C ($8 \cdot 10^{-2}$ mbar)

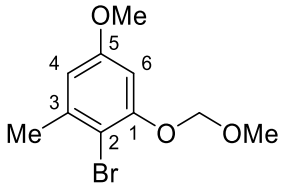

29

7.2.1.7 4,4'-Dimethoxy-2,2'-bis(methoxymethoxy)-6,6'-dimethyl-1,1'-biphenyl (28)

A dry 250 mL Schlenk round bottom flask equipped with stir bar was charged brominated arene **29** (2.00 mL, 1.00 equiv, 10.8 mmol) and the vessel evacuated and backfilled with N_2 (3x). Degassed (sparging) anhydrous THF (40 mL, 0.27 M) was added, and the mixture cooled to -78 °C. A solution of *t*-BuLi in pentanes (1.7 M, 11.1 mL, 1.75 equiv, 18.9 mmol) was added dropwise under stirring continuing to stir at that temperature for 15 mins. Then a solution of CuCN·2 LiCl (1.0 M, 5.40 mL, 5.40 mmol) was added dropwise and the reaction stirred for a further 15 mins at -78 °C. A separate dry 100 mL round bottom flask was charged with bichinone **30** (4.85 g, 1.1 equiv, 11.9 mmol) and the vessel evacuated and backfilled with N_2 (3x) and degassed anhydrous THF (80 mL, 0.15 M) was added and the resulting solution transferred *via* a cannulation to the reaction vessel at -78 °C. The resulting mixture was stirred for 30 mins at -78 °C, then at 22 °C for 30 mins. MeOH (5 mL) was added, solvents removed in vacuo and the resulting solids filtered over a pad of Celite® washing with MeOH. The solid residues were left to stand over night and then collected and submitted to recycling by

recrystallization from *i*-PrOH to provide bichinone **30**. To the filtrate was added aq. KPi-buffer (1 M, pH 7) and the aq. phase extracted with CH_2Cl_2 (3x), the combined org. phases washed with aq. NaCl solution and dried over $MgSO_4$. The product was isolated by column chromatography (petroleum ether:EtOAc 8:2 v/v) as a colorless oil in a yield of 1.68 g (4.64 mmol, 86%). The analytical data were in accordance with literature.[102]

^{1}H NMR (600 MHz, $CDCl_3$): δ 1.95 (s, 3H, Me), 3.30 (d, $^4J_{OMe\text{-}CH2}$ = 1.3 Hz, 3H, $CH_2O\underline{Me}$), 3.82 (d, $^4J_{OMe\text{-}CH2}$ = 1.3 Hz, 3H, OMe), 4.97 (d, $^2J_{CH2\text{-}CH2}$ = 6.8 Hz, 1H, $\underline{CH_2}$OMe-H_a), 5.02 (d, $^2J_{CH2\text{-}CH2}$ = 6.7 Hz, 1H, $\underline{CH_2}$OMe-H_b), 6.52 (d, $^4J_{3\text{-}5}$ = 2.4 Hz, 1H, 5-H), 6.64 (d, $^4J_{3\text{-}5}$ = 2.4 Hz, 1H, 3-H). **^{13}C NMR** (151 MHz, $CDCl_3$): δ 20.26 (Me), 55.32 (OMe), 55.85 ($CH_2O\underline{Me}$), 94.95 ($\underline{CH_2}$OMe), 99.66 (C-3), 108.54 (C-5), 119.87 (C-1), 139.51 (C-6), 155.98 (C-2), 159.48 (C-4). **IR (ATR film) [cm^{-1}]:** 2949, 1600, 1460, 1306, 1215, 1151, 1035, 987, 927, 827, 627, 522. **TLC** (petroleum ether:EtOAc 8:2 v/v): R_f = 0.29 **APCI-MS:** m/z: ([M + Na^+]): found: 385.2 **Boiling point:** >115°C ($8\cdot10^{-2}$ mbar)

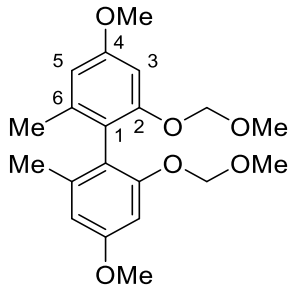

28

7.2.1.8 3,3',5,5'-Tetra-tert-butyl-[1,1'-bi(cyclohexylidene)]-2,2',5,5'-tetraene-4,4'-dione (30)

A 500 mL round bottom flask equipped with stir bar was charged with 2,6-di-*tert*-butylphenol (18.3 g, 1.0 equiv, 88.6 mmol), *i*-PrOH (180 mL, 0.49 M), and aq. KOH solution (30 mL, 11.9 M, 4.0 equiv, 356 mmol). A rubber stopper with an outlet was equipped and a stream of O_2 using a balloon was bubbled through solution at 22 °C under stirring for 24 h. H_2O (100 mL) and CH_2Cl_2 (100 mL) were added and the organic phase separated and solvents removed in vacuo. The resulting solids were recrystallized from *i*-PrOH (110 mL). Solids were collected and the pure product isolated in a yield of 7.09 g (17.6 mmol, 39%). The analytical data were in accordance with literature.[102]

^{1}H NMR (600 MHz, $CDCl_3$): δ 1.36 (s, 36H), 7.70 (s, 4H, C($\underline{CH_3)_3}$). **^{13}C NMR** (151 MHz, $CDCl_3$): δ 29.74 C($\underline{CH_3)_3}$), 36.17 ($\underline{C}(CH_3)_3$), 126.16 (C-2), 136.28 (C-1),

150.59 (C-3), 186.62 (C-4). **IR (ATR film) [cm^{-1}]:** 2953, 1603, 1566, 1451, 1355, 1258, 1097, 1035, 897, 885, 836, 817, 742, 518. **APCI-MS:** m/z: ([M + H^{+}]): found: 409.3 **Melting point:** 245 – 246 °C

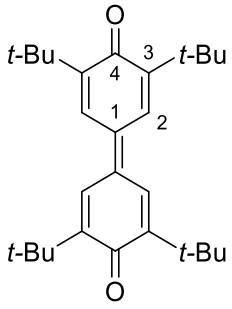

30

7.2.2 Chalcones and Flavones

The following chapter is a revised version of results published in Klischan et al. ACS Omega ***2023****,*[108b]

7.2.2.1.1 2-Phenyl-4H-chromen-4-one (194)

A round bottom flask equipped with stir bar was charged with I_2 (93.2 mg, 5 mol%, 0.367 mmol), DMSO (75 mL, 0.1 M), 2'-hydroxyacetophenone (**193**) (1.00 g, 1.00 equiv, 7.34 mmol) and pyrrolidine (0.303 mL, 0.5 equiv, 3.67 mmol). The reaction mixture was stirred at 150 °C for 23 h. H_2O and a solution of aq. $Na_2S_2O_3$ (10 % w/w) were added, the aq. phase extracted with EtOAc (3x) and solvents removed in vacuo. The product was obtained by column chromatography (petroleum ether:EtOAc 80:20 v/v) as orange needles (256 mg) with trace impurities. Recrystallization (petroleum ether:EtOAc) gave the final product as pink needles in a yield of 140 mg (0.630 mmol, 9%). The analytical data were in accordance with literature.[306]

^{1}H NMR (600 MHz, $CDCl_3$): δ 6.85 (s, 1H, 3-H), 7.39 – 7.46 (m, 1H, 6-H), 7.51 – 7.56 (m, 3H, 4'+3'-H), 7.58 (d, $^3J_{7\text{-}8}$ = 8.4 Hz, 1H, 8-H), 7.71 (ddd, $^3J_{7\text{-}8}$ = 8.6 Hz, $^3J_{7\text{-}6}$ = 7.1 Hz, $^4J_{7\text{-}5}$ = 1.7 Hz, 1H, 7-H), 7.94 (dd, $^3J_{2'\text{-}3'}$ = 7.7 Hz, $^4J_{3'\text{-}4'}$ = 2.0 Hz, 2H, 2'-H), 8.24 (dd, J = 8.0, 1.7 Hz, 1H, 5-H). **^{13}C NMR** (151 MHz, $CDCl_3$): δ 107.71 (C-3), 118.25 (C-8), 124.05 (C-4a), 125.43 (C-6), 125.88 (C-5), 126.49 (C-2'), 129.22 (C-3'), 131.81 (C-4'), 131.92 (C-1'), 133.99 (C-7), 156.44 (C-8a), 163.68 (C-2), 178.64 (C-4). **IR (ATR film) [cm^{-1}]:** 3517, 3065, 1646, 1569, 1462, 1378, 1217, 1125, 902, 764, 680. **TLC** (petroleum ether:EtOAc, 8:2 v/v): R_f = 0.16 **ESI-MS**: m/z [M + H$^+$]: found: 223.1.

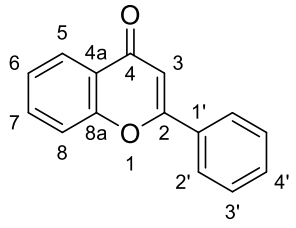

194

7.2.2.2 Synthesis of Starting Materials

7.2.2.2.1 1-(2,6-Dihydroxy-4-methylphenyl)ethan-1-one (131)

A 500 mL round bottom flask fitted with a Schlenk-stopcock equipped with stir bar was charged with 5-methylbenzen-1,3-diol (**122**) (20.0 g, 161 mmol, 1.0 equiv), $AlCl_3$ (64.5 g, 3.0 equiv, 483 mmol) and anhydr. chlorobenzene. A gas washing bottle was equipped and filled with aq. KOH-solution (300 mL, 1 M). Acetyl chloride (16.1 mL, 1.4 equiv, 226 mmol) was carefully added at 0 °C. After complete addition the reaction mixture was heated at 70 °C for 17 h. After

full conversion a gas washing bottle was equipped and filled with aq. KOH-solution (300 mL, 1 M) to quench excess HCl-gas. The reaction mixture was cooled to 0 °C Water (300 mL) was carefully added to the reaction mixture. The aq. phase was extracted with CH_2Cl_2 (4x 140 mL) and the combined organic phase washed with sat. NaCl-solution and dried over $MgSO_4$. Solids were filtered off and the solvent removed *in vacuo*. The product was isolated by recrystallization from PhMe (40 mL) as amorphous yellow solids in a yield (23.5 g, 141 mmol, 88 %). The analytical data were in accordance with literature.[215a]

^{1}H NMR (600 MHz, $CDCl_3$): δ 2.23 (s, 3H, Me), 2.74 (s, 3H, COMe), 6.24 (s, 2H, 3-H), 9.88-10.40 (brs, 2H, OH). **^{13}C NMR** (151 MHz, $CDCl_3$): δ 21.98 (Me), 33.25 (CO*Me*), 108.36 (C-1), 109.24 (C-3), 148.18 (C-4), 161.39 (C-2), 204.79 (*CO*Me).**IR (ATR film) [cm^{-1}]:** 3324, 3155, 2260, 1739, 1633, 1577, 1514, 1422, 1373, 1207, 1084, 1077, 957, 922, 816, 721, 527. **TLC** (petroleum ether:EtOAc, 95:5 v/v): R_f = 0.42 **ESI-MS**: m/z [M + H^+]: found: 167.1. **Melting point:** 143 – 148 °C (144 – 146 °C)[215a]

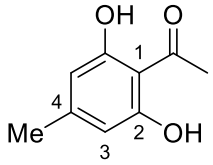

131

7.2.2.2.2 1-(2,4,6-Trihydroxyphenyl)ethan-1-one (132)

A 500 mL round bottom flask equipped with stir bar was charged with 1,3,5-trihydroxybenzene (**130**) (30.0 g, 1.0 equiv, 238 mmol) and EtOAc (240 mL, 1 M). Then Ac_2O (27.0 mL, 1.2 equiv, 285 mmol) was added. $BF_3 \cdot Et_2O$ (33.2 mL, 1.1 equiv, 262 mmol) was carefully added at 22 °C. A reflux condenser was equipped, and the resulting mixture was stirred for 5 h at 65 °C. After full conversion an aq. solution of NaOH (1 M) was added until pH 3. H_2O (100 mL) was added, and the aq. phase was extracted with EtOAc (4x 140 mL) and the combined organic phase washed with sat. NaCl-solution and dried over $MgSO_4$ and solvents removed in vacuo. The product was obtained by recrystallization from H_2O (130 mL) amorphous orange solids in a yield of 37.5 g (222 mmol, 94 %). The analytical data were in accordance with literature.[215b] **^{1}H NMR** (600 MHz, DMSO-d_6): δ 3.36 (s, 3H, COMe), 5.79 (s, 2H, 3-H), 10.37 (s, 1H, 4-OH), 12.23 (s, 2H, 2-OH).**^{13}C NMR** (151 MHz, DMSO-d_6): δ 32.27 (CO*Me*), 94.48 (C-3), 103.99 (C-1), 164.22 (C-2/4), 164.70 (C-2/4), 202.37 (*CO*Me). **IR (ATR film) [cm^{-1}]:** 3535, 3459, 3105, 3042, 2901, 2781, 2605, 1622, 1529, 1453, 1409, 1361, 1278, 1242, 1205, 1165, 1087,

1064, 1021, 962, 811, 757, 657, 612, 571, 524. **TLC** (petroleum ether:EtOAc, 95:5 v/v): R_f = 0.42 **ESI-MS:** m/z [M + H^+]: found: 169.1. **Melting point:** 215 – 217 °C (216 – 217 °C)[307]

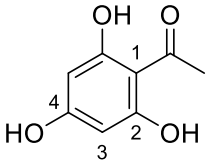

132

7.2.2.2.3 1-(2-Hydroxy-6-methoxy-4-methylphenyl)ethan-1-one (133)

A 500 mL round bottom flask equipped with stir bar was charged with acetophenone **131** (19.0 g, 1.0 equiv, 115 mmol) and K_2CO_3 (17.4 g, 1.1 equiv, 126 mmol) and acetone (800 mL, 0.14 M). Me_2SO_4 (11.9 mL, 1.1 equiv, 126 mmol) was slowly added at 22 °C. After full addition a reflux condenser was equipped, and the reaction mixture stirred at 60 °C for 2 h. After full conversion, a solution of aq. Na_2SO_3 (100 mL, 10 %) was added and the reaction mixture left to stir for an additional 2 h at 40 °C. After letting the mixture cool to 22 °C, a solution of aq. HCl (100 mL, 1 M) was carefully added until no more gas evolution was observed. The aq. Phase was then extracted using EtOAc (3x 150 mL). The combined organic phases were washed with sat. aq. NaCl-solution (100 mL) and dried over $MgSO_4$. Solids were filtered off and the solvents removed in vacuo. The product was obtained as off-white solids in a yield of 17.4 g (96.6 mmol, 84 %). The analytical data were in accordance with literature.[215c]

^{1}H NMR (600 MHz, $CDCl_3$): δ 2.29 (s, 3H, Me), 2.63 (s, 3H, CO*Me*), 3.86 (s, 3H, OMe), 6.17-6.19 (m, 1H, 3/5-H), 6.37 (dd, $^4J_{3\text{-}5}$ = 1.6 Hz, 1H, 3/5-H), 13.36 (s, 1H, OH). **^{13}C NMR** (151 MHz, $CDCl_3$): δ 22.46 (Me), 33.45 (CO*Me*), 55.61 (OMe), 102.51, 109.32, 111.10, 147.83 (C-4), 161.50 (C-2), 164.85 (C-6), 204.50 (*CO*Me). **IR (ATR film) [cm^{-1}]:** 3014, 2972, 2944, 2852, 2612, 2394, 1618, 1595, 1466, 1452, 1419, 1370, 1311, 1288, 1261, 1220, 1188, 1112, 1028, 1014, 968, 939, 854, 826, 749, 657, 606, 592, 547, 529. **TLC** (petroleum ether:EtOAc, 95:5 v/v): R_f = 0.42 **ESI-MS:** m/z [M + H^+]: found: 181.1. **Melting point:** 78 – 82 °C (79 °C)[215c]

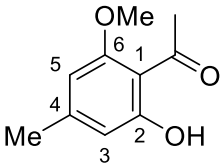

7.2.2.2.4 1-(2-Hydroxy-4,6-dimethoxyphenyl)ethan-1-one (47)

A 500 mL round bottom flask equipped with stir bar was charged with acetophenone **132** (37.5 g, 1.0 equiv, 223 mmol) and K_2CO_3 (64.7 g, 2.1 equiv, 468 mmol) and (500 mL). Me_2SO_4 (44.4 mL, 2.1 equiv, 468 mmol) was slowly added at 22 °C. After full addition a reflux condenser was equipped, and the reaction mixture stirred at 65 °C for 4 h. After full conversion, a solution of aq. Na_2SO_3 (150 mL, 10 %) was added and the reaction mixture left to stir for an additional 2 h at 40 °C. After letting the mixture cool to 22 °C, a solution of aq. HCl (150 mL, 1 M) was carefully added until no more gas evolution was observed. The aq. Phase was then extracted using EtOAc (3x 200 mL). The combined organic phases were washed with sat. aq. NaCl-solution (100 mL) and dried over $MgSO_4$. Solids were filtered off and the solvent removed *in vacuo*. The crude product was recrystallized from MeOH (55 mL). The product was obtained as amorphous off-white solids in a yield of (32.2 g, 164 mmol, 74 %). The analytical data is in accordance with literature.[215d]

^{1}H NMR (600 MHz, $CDCl_3$): δ 2.59 (s, 3H, CO*Me*), 3.80 (s, 3H, OMe), 3.84 (s, 3H, OMe), 5.90 (d, $^3J_{3\text{-}5}$ = 2.4 Hz, 1H, 3/5-H), 6.04 (d, $^3J_{3\text{-}5}$ = 2.4 Hz, 1H, 3/5-H), 14.03 (s, 1H, OH) **^{13}C NMR** (151 MHz, $CDCl_3$): δ 32.96 (CO*Me*), 55.63 (OMe), 90.85, 93.67, 106.16, 163.05 (C-2), 166.23 (C-4/6), 167.71 (C-4/6), 203.22 (*CO*Me). **IR (ATR film) [cm^{-1}]:** 3098, 3007, 2936, 2845, 2598, 1582, 1457, 1439, 1422, 1439, 1365, 1324, 1264, 1206, 1156, 1114, 1082, 1044, 1029, 961, 940, 893, 833, 812, 744, 713, 690, 658, 597, 557, 533. **TLC** (petroleum ether:EtOAc, 6:4 v/v): R_f = 0.59 **ESI-MS**: m/z [M + H$^+$]: found: 197.1. **Melting point:** 78 – 80 °C (78 – 80 °C)[308]

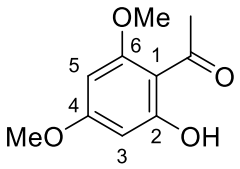

47

7.2.2.2.5 *rac*-1-(2-Hydroxy-6-methoxy-4-methylphenyl)ethan-1-one (134)

Preparation of $FeCl_3$ on SiO_2 ($FeCl_3/SiO_2$) 50% w/w: A 1000 mL round bottom flask was charged with anhyd. $FeCl_3$ (17.3 g, 4.8 equiv), 107 mmol) anhyd. MeOH (45 mL), anhyd. Et_2O

(500 mL) and anhyd. SiO_2 (17.26 g). The resulting brown suspension was sonicated for 15 min. The solvent was removed *in vacuo* at 40 °C until a brown slurry remained. The remaining solvent was slowly removed *in vacuo* at 60 °C over 3 h. The resulting fine, orange powder was stored under N_2 and used for synthesis the following day. *Oxidative coupling:* A 1000 mL round bottom flask was charged with acetophenone **133** (8.00 g, 1.0 equiv, 44.4 mmol) and anhyd. CH_2Cl_2 (900 mL, 0.05 M). $FeCl_3/SiO_2$ (50% w/w, 69.1 g, 4.8 equiv) was added at once and the resulting black suspension sonicated for 15 min. Solvent was then removed at 43 °C *in vacuo* on a rotary evaporator. Reaction controls were performed by TLC and ^{1}H-NMR by taking an aliquot and conducting a mini workup as described below. After 3.45 h to the black powder were added aq. HCl-solution (1 M, 50 mL) and CH_2Cl_2 (50 mL). The mixture was filtered over a pad of Celite® and the filter cake washed with CH_2Cl_2 (700 mL). The filter cake was kept for further washing once most of the water was evaporated. The aq. layer was separated and washed with CH_2Cl_2 (4 x 100 mL). The combined organic layers were washed with aq. Na_2EDTA-sol. (50 mM, 200 mL) and sat. NaCl-solution (100 mL) and dried over $MgSO_4$. Solids were filtered off and solvent removed in vacuo. The crude product was isolated by washing with acetone (15 mL) and subsequent removal of the acetone. The solids were collected. The acetone washing-solution was removed in vacuo and the process repeated with the then obtained residual crude product twice over. The product was isolated as pale yellow solids in a yield of 4.58 g (12.8 mmol 58%). The analytical data is in accordance with literature.[102]

In a further experiment following a literature known procedure[102] a 50 mL Schlenk-vial equipped with stir bar was charged with biaryl **27** (343 mg, 1.0 equiv, 1.25 mmol, >99%*ee* S_a) and anhydr. chlorobenzene (12.5 mL, 0.1 M). The solution was stirred at 0 °C (600 rpm), acetyl chloride (200 µL, 2.2 equiv, 2.75 mmol) added dropwise and then the mixture stirred at room temperature for 30 minutes. Then $TiCl_4$ (820 µL, 6.0 equiv, 7.50 mmol) was added dropwise and the reaction mixture stirred at 70 °C for 4 h. Then the dark brown mixture was slowly transferred into a 250 mL Erlenmeyer beaker equipped with stir bar with K_2HPO_4/KH_2PO_4-buffer (KPi-buffer, 1 M, 100 mL, pH 7) at 0 °C. The pH was then adjusted to pH 4 by the addition of 1 M HCl-solution. The resulting white suspension was then stirred for 15 min, sonicated for 15 min, and then stirred for 30 min. The mixture was filtered over a pad of celite using a wide Buchner-type funnel. The filter cake was washed with CH_2Cl_2 (100 mL), H_2O (100 mL), then again with CH_2Cl_2 (800 mL). The filter cake was then transferred into an Erlenmeyer flask and stirred with CH_2Cl_2 (250 mL) overnight. The suspension was then again filtered over celite. The filtrates were combined, and the aqueous phase extracted with CH_2Cl_2 (4x 250 mL). The combined aqueous phases were washed with sat. aq. NaCl solution, dried

over $MgSO_4$ and solvents removed in vacuo. The product was isolated by washing the crude product with acetone (10 mL). The remaining product in the wash fraction was isolated by column chromatography (CH_2Cl_2:PhMe 9:1 v/v to CH_2Cl_2:MeOH 99:1 v/v). The thus combined isolated product was obtained as yellow solids (332 mg [washed] + 20 mg [column], 0.98 mmol, 78%, >99%*ee* S_a).

A further experiment using biaryl **27** (233 mg, 1.0 equiv, 0.85 mmol, >99%*ee* R_a) gave the product as yellow solids (181 mg [washed] + 48 mg [column], 0.64 mmol, 75%, >99%*ee* R_a).

^{1}H NMR (600 MHz, $CDCl_3$): δ 2.06 (s, 3H, Me), 2.67 (s, 3H, CO*Me*), 3.93 (s, 3H, OMe), 6.38 (s, 1H, 5-H), 13.68 (s, 1H, OH). **^{13}C NMR** (151 MHz, $CDCl_3$): δ 20.97 (Me), 33.66 (CO*Me*), 55.58 (OMe), 102.97 (C-5), 109.41 (C-3), 117.38 (C-1), 147.54 (C-6), 160.79 (C-4), 162.40 (C-2), 204.77 (*C*OMe). **IR (ATR film) [cm^{-1}]:** 1599, 1360, 1283, 1202, 1119, 9693, 865, 834, 655, 573, 534. **TLC** (petroleum ether:EtOAc, 7:3 v/v): R_f = 0.32 **TLC** (CH_2Cl_2:PhMe, 9:1 v/v): R_f = 0.25 **HR-MS (ESI):** m/z calculated for $[C_{20}H_{23}O_6]^+$ ([M + H$^+$]): 359.1489, found: 359.1492.

Melting point: 233 – 235 °C (*rac*) (233 – 236 °C)[102]

231 – 235 °C (S_a, >99%*ee* HPLC) (209 – 210)[102]

231 – 234 °C (R_a, >99%*ee* HPLC)

HPLC: Lux® Amylose-1 (Phenomenex) 250 ° 4.6 mm, 25 °C, 0.5 mL min^{-1}, 274 nm, *n*-heptane:*i*-PrOH 50:50 (v/v) $t_R(S_a)$ = 7.5 min, $t_R(R_a)$ = 10.4 min

Optical rotation: $[\alpha]^{25}_D$ = +49.0 (±0.4, triplicate) (c = 0.96, $CHCl_3$, S_a, >99%*ee* by chiral HPLC) +43.1[102]

X-ray: 27 mg of **134** were dissolved in 1.5 mL CH_2Cl_2, filtered over a syringe filter into a vial with a loose cap and the solvent left to evaporate over time. CCDC 2269309

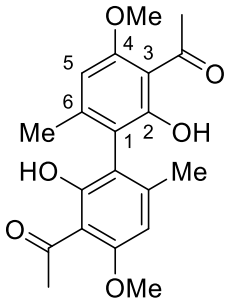

134

7.2.2.2.6 *rac*-1-(2-Hydroxy-4,6-dimethoxyphenyl)ethan-1-one (49)

Preparation of $FeCl_3 \cdot 6H_2O$ on SiO_2 ($FeCl_3/SiO_2$) 50% w/w: A 2000 mL round bottom flask was charged with $FeCl_3 \cdot 6H_2O$ (50.0 g, 186 mmol, 4.6 equiv), Et_2O (1000 mL) and anhyd. SiO_2 (50.0 g). The resulting brown suspension was sonicated for 15 min. The solvent was removed *in vacuo* at 40 °C until a fine bright yellow powder remained. The product was stored under N_2 and used for synthesis the following day. *Oxidative coupling:* A 2000 mL round bottom flask was charged with acetophenone **47** (8.00 g, 40.8 mmol, 1.0 equiv) and CH_2Cl_2 (750 mL). $FeCl_3/SiO_2$ (50% w/w, 100.0 g, 4.6 equiv) was added at once and the resulting black suspension sonicated for 15 min. Solvent was then removed at 42 °C *in vacuo* on a rotary evaporator. Reaction controls were performed by TLC and ^{1}H-NMR by taking an aliquot and conducting a mini workup as described below. After 6.5 h to the black powder were added H_2O (50 mL) and EtOAc (50 mL) at 0 °C. The resulting mixture was sonicated at 0 °C for 15 min. The mixture was filtered over a pad of Celite® and the filter cake washed with EtOAc (800 mL). The filter cake was kept for further washing once most of the water was evaporated. The aq. layer was separated and washed with EtOAc (5 x 300 mL). The combined organic layers were washed with Na_2EDTA-sol. (50 mM, 300 mL) and sat. NaCl-solution (200 mL) and dried over $MgSO_4$. Solids were filtered off and solvent removed *in vacuo*. The product was isolated by recrystallization from acetone (40 mL) as tan solids in a yield of 4.10 g (10.5 mmol, 52%). The analytical data is in accordance with literature.[69]

^{1}H NMR (600 MHz, $CDCl_3$): δ 2.63 (s, 3H, CO*Me*), 3.82 (s, 3H, OMe), 3.95 (s, 3H, OMe), 6.08 (s, 1H, 5-H), 13.98 (s, 1H, OH). **^{13}C NMR** (151 MHz, $CDCl_3$): δ 33.31 (CO*Me*), 55.57 (OMe), 56.03 (OMe), 86.53 (C-1), 102.68 (C-5), 106.33 (C-3), 163.43 (C-2), 164.08 (C-4/6), 164.17 (C-4/6), 203.47 (CO*Me*). **IR (ATR film) [cm^{-1}]:** 3003, 2946, 2889, 2846, 1613, 1590, 1468, 1404, 1374, 1276, 1214, 1125, 956, 800, 591, 529. **TLC** (petroleum ether:EtOAc, 6:4 v/v): R_f = 0.24 **APCI-MS:** found: [M+H$^+$] 391.3 **Melting point:** 239 °C (brown discoloration) 252.8 – 254.0 °C (211 – 212 °C)[69]

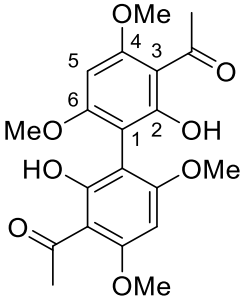

49

7.2.2.3 General Procedure 1 (GP1): Chalcone Monomer

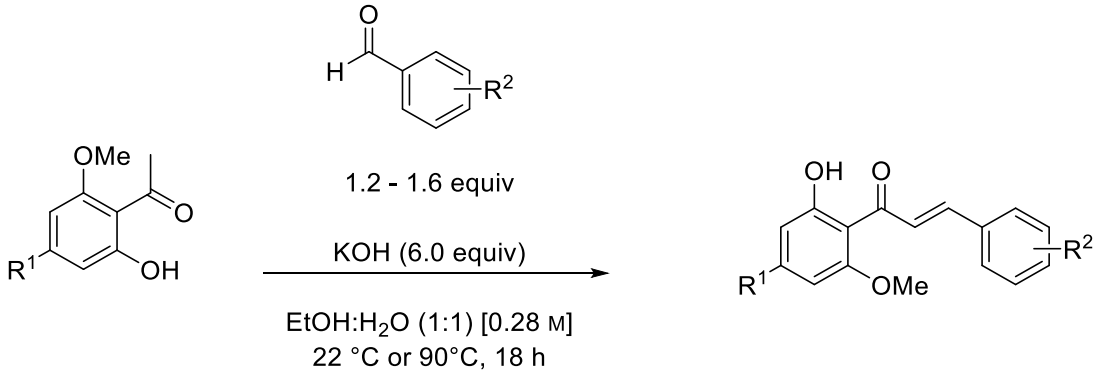

A vial equipped with stir bar was charged with acetophenone (250 mg, 1.0 equiv), ethanol (0.56 M) and aq. KOH solution (3 M, 6.0 equiv). The mixture was stirred for 5 min until all solids were dissolved. Aldehyde (1.2 equiv) was added at once. The reaction was stirred at room temperature unless stated otherwise. If stated, after 6 h another portion of aldehyde was added (0.6 equiv). The reaction mixture was left to stir over night unless stated otherwise. Reaction control was performed by TLC and ^{1}H-NMR. After the completion of the reaction aq. HCl (1 M, 10 mL) was added unless stated otherwise. Solids precipitate, which were collected by filtration over a pad of Celite® washing the solids with methanol (1 mL). The solids were then dissolved in CH_2Cl_2, MeOH (10% v/v) was added, and the solvent removed *in vacuo*. The product was isolated by washing with MeOH (4 mL) at 70 °C and discarding the wash solution.

7.2.2.3.1 (*E*)-1-(2-Hydroxy-6-methoxy-4-methylphenyl)-3-(4-methoxyphenyl)prop-2-en-1-one (135)

The title compound was synthesized in accordance with **GP1** with acetophenone **133** (200 mg, 1.0 equiv, 1.11 mmol) and 4-methoxybenzaldehyde (0.242 mL, 1.2 equiv+ 0.6 equiv, 2.00 mmol). The product was isolated as orange solids in a yield of 228 mg (0.762 mmol, 69%).

^{1}H NMR (600 MHz, $CDCl_3$): δ 2.33 (s, 3H, Me), 3.86 (s, 3H, OMe), 3.94 (s, 3H, OMe), 6.24 (d, $^{4}J_{3\text{-}5}$ = 1.5 Hz, 1H, 5-H), 6.44 (dd, $^{4}J_{3\text{-}5}$ = 1.5, 0.8 Hz, 1H, 3-H), 6.94 (d, $^{3}J_{2'\text{-}3'}$ = 8.8 Hz, 2H, 3'-H), 7.58 (d, $^{3}J_{2'\text{-}3'}$ = 8.8 Hz, 2H, 2'-H), 7.80 (s, 2H, 5'+6'-H), 13.49 (s, 1H, OH). **^{13}C NMR** (151 MHz, $CDCl_3$): δ 22.53 (Me), 55.56 (4'-OMe), 56.01 (6-OMe), 103.00 (C-5), 110.01 (C-1), 111.52 (C-3), 114.56 (C-3'), 125.51 (C-6'), 128.43 (C-1'), 130.34 (C-2'), 142.87 (C-5'), 147.51 (C-4), 161.02 (C-6), 161.64 (C-4'), 165.33 (C-2), 193.94 (CO). **IR (ATR film) [cm^{-1}]:** 3003, 2838, 1627, 1605, 1561, 1511, 1483, 1457, 1422, 1410, 1305, 1289, 1255, 1223, 1207, 1172, 1113, 1035, 982, 828, 814, 768, 742, 722, 662, 557, 539. **HR-MS (ESI):** m/z

calculated for $[C_{18}H_{19}O_4]^+$ ([M + H^+]): 299.1278, found: 299.1284. **Melting point:** 113 – 114 °C

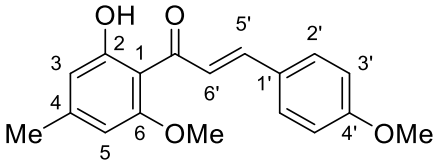

135

7.2.2.3.2 (*E*)-1-(2-Hydroxy-6-methoxy-4-methylphenyl)-3-phenylprop-2-en-1-one (136)

The title compound was synthesized in accordance with **GP**1 with acetophenone **133** (270 mg, 1.0 equiv, 1.50 mmol) and benzaldehyde (0.184 mL, 1.2 equiv, 1.80 mmol). The product was isolated as orange solids in a yield of 261 mg (0.974 mmol, 65%).

^{1}H NMR (600 MHz, $CDCl_3$): δ 2.33 (s, 3H, Me), 3.94 (s, 3H, OMe), 6.24 (s, 1H, 5-H), 6.45 (s, 1H, 3-H), 7.36 – 7.46 (m, 3H, 3'+4'-H), 7.56 – 7.66 (m, 2H, 2'-H), 7.80 (d, $^3J_{5'\text{-}6'}$ = 15.6 Hz, 1H, 5'-H), 7.89 (d, $^3J_{5'\text{-}6'}$ = 15.6 Hz, 1H, 6'-H), 13.37 (s, 1H, OH) **^{13}C NMR** (151 MHz, $CDCl_3$): δ 22.59 (Me), 56.01 (OMe), 102.97 (C-5), 109.89 (C-1), 111.46 (C-3), 127.83 (C-6'), 128.56 (C-2'), 129.04 (C-3'), 130.31 (C-4'), 135.61 (C-1'), 142.72 (C-5'), 147.89 (C-4), 161.04 (C-6), 165.31 (C-2), 194.02 (CO). **IR (ATR film) [cm^{-1}]:** 3091, 3036, 2980, 2951, 1641, 1576, 1495, 1459, 1418, 1378, 1344, 1284, 1232, 1216, 1168, 1124, 1082, 985, 954, 878, 853, 824. **HR-MS (ESI):** m/z calculated for $[C_{17}H_{17}O_3]^+$ ([M + H^+]): 269.1172, found: 269.1173. **Melting point:** 169 – 171 °C

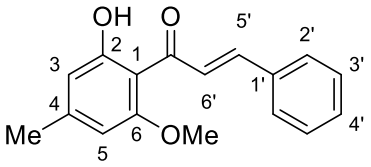

136

7.2.2.3.3 (*E*)-3-(4-(Dimethylamino)phenyl)-1-(2-hydroxy-6-methoxy-4-methylphenyl)prop-2-en-1-one (137)

The title compound was synthesized in accordance with **GP**1 with acetophenone **133** (250 mg, 1.0 equiv, 1.39 mmol) and 4-(dimethylamino)benzaldehyde (373 mg, 1.2 equiv + 0.6 equiv,

2.50 mmol) at 90 °C. The product was isolated as red solids in a yield of 264 mg (0.848 mmol, 61%).

^{1}H NMR (600 MHz, $CDCl_3$): δ 2.31 (s, 3H, Me), 3.04 (s, 6H, NMe_2), 3.93 (s, 3H, OMe), 6.22 (d, $^4J_{3\text{-}5}$ = 1.6 Hz, 1H, 5-H), 6.43 (d, $^4J_{3\text{-}5}$ = 1.6 Hz, 1H, 3-H), 6.70 (d, $^3J_{2'\text{-}3'}$ = 8.6 Hz, 2H, 3'-H), 7.50 – 7.55 (m, 2H, 2'-H), 7.74 (d, $^3J_{5'\text{-}6'}$ = 15.4 Hz, 1H, 5'-H), 7.84 (d, $^3J_{5'\text{-}6'}$ = 15.4 Hz, 1H, 6'-H), 13.72 (s, 1H, OH). **^{13}C NMR** (151 MHz, $CDCl_3$): δ 22.47 (Me), 40.28 (NMe_2), 55.93 (OMe), 102.90 (C-5), 110.06 (C-1), 111.40 (C-3), 112.00 (C-3'), 122.40 (C-6'), 123.41 (C-1'), 130.59 (C-2'), 144.39 (C-5'), 146.89 (C-4), 152.02 (C-4'), 160.88 (C-6), 165.24 (C-2), 193.67 (CO). **IR (ATR film) [cm^{-1}]:** 3121, 3009, 2968, 2808, 2645, 2169, 2052, 1628, 1593, 1525, 1476, 1462, 1435, 1413, 1375, 1336, 1296, 1257, 1223, 1198, 1168, 1113, 1069, 1031, 984, 948, 883, 838, 819, 807, 768, 732, 711, 680, 665, 638, 600, 546, 529, 514, 501, 470 **HR-MS (ESI):** m/z calculated for $[C_{19}H_{22}O_3N]^+$ ([M + H^+]): 312.1594, found: 312.1596. **Melting point:** 182 – 183 °C

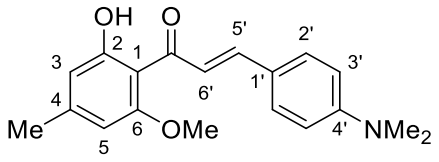

137

7.2.2.3.4 (*E*)-1-(2-Hydroxy-6-methoxy-4-methylphenyl)-3-(4-(trifluoromethyl)phenyl)prop-2-en-1-one (138)

The title compound was synthesized in accordance with **GP1** with acetophenone **133** (250 mg, 1.0 equiv, 1.39 mmol) and 4-(trifluoromethyl)benzaldehyde (0.34 mL, 1.2 equiv + 0.6 equiv, 2.50 mmol). The product was isolated as orange solids in a yield of 299 mg (0.890 mmol, 64%).

^{1}H NMR (600 MHz, $CDCl_3$): δ 2.36 (s, 3H, Me), 3.97 (s, 3H, OMe), 6.27 (s, 1H, 5-H), 6.48 (s, 1H, 3-H), 7.69 (d, $^3J_{2'\text{-}3'}$ = 8.1 Hz, 2H, 3'-H), 7.72 (d, $^3J_{2'\text{-}3'}$ = 8.1 Hz, 2H, 2'-H), 7.78 (d, $^3J_{5'\text{-}6'}$ = 15.7 Hz, 1H, 5'-H), 7.94 (d, $^3J_{5'\text{-}6'}$ = 15.7 Hz, 1H, 6'-H), 13.26 (d, *J* = 2.3 Hz, 1H, OH). **^{13}C NMR** (151 MHz, $CDCl_3$): δ 22.63 (Me), 56.05 (OMe), 103.00 (C-5), 109.77 (C-1), 111.53 (C-3), 124.05 (q, $^1J_{F\text{-}C}$ = 272.1 Hz, CF_3), 125.98 (q, $^3J_{F\text{-}C}$ = 3.8 Hz, C-3'), 128.53 (C-2'), 130.21 (C-6'), 131.62 (q, $^2J_{F\text{-}C}$ = 32.6 Hz, C-4'), 139.06 (C-1'), 140.37 (C-5'), 148.42 (C-4), 161.03 (C-6), 165.40 (C-2), 193.63 (CO). **^{19}F NMR** (282 MHz, $CDCl_3$): δ -62.77. **IR (ATR film) [cm^{-1}]:** 3746, 3123, 3051, 2974, 1635, 1614, 1565, 1487, 1456, 1410, 1368, 1317, 1287, 1266, 1223, 1169, 1066, 1031, 1015, 983, 909, 843, 813, 768, 747, 732, 683, 666, 626, 593, 558, 530, 506,

492 **HR-MS (ESI):** m/z calculated for $[C_{18}H_{16}O_3F_3]^+$ ([M + H^+]): 337.1046, found: 337.1050. **Melting point:** 124 – 126 °C

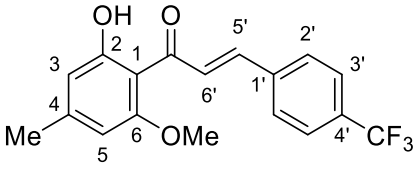

138

7.2.2.3.5 (*E*)-3-(4-Bromophenyl)-1-(2-hydroxy-6-methoxy-4-methylphenyl)prop-2-en-1-one (139)

The title compound was synthesized in accordance with **GP1** with acetophenone **133** (250 mg, 1.0 equiv, 1.39 mmol) and 4-bromobenzaldehyde (309 mg, 1.2 equiv, 1.66 mmol). The product was isolated as yellow solids in a yield of 261 mg (0.754 mmol, 54%).

^{1}H NMR (600 MHz, $CDCl_3$): δ 2.33 (s, 3H, Me), 3.93 (s, 3H, OMe), 6.23 (d, ^4J = 1.6 Hz, 1H, 5-H), 6.45 (s, 1H, 3-H), 7.46 (d, $^3J_{2',3'}$ = 8.4 Hz, 2H, 2'-H), 7.54 (d, $^3J_{2',3'}$ = 8.4 Hz, 2H, 3'-H), 7.70 (d, $^3J_{5',6'}$ = 15.6 Hz, 1H, 5'-H), 7.85 (d, $^3J_{5',6'}$ = 15.6 Hz, 1H, 6'-H), 13.30 (s, 1H, OH). **^{13}C NMR** (151 MHz, $CDCl_3$): δ 22.60 (Me), 56.04 (OMe), 102.98 (C-5), 109.82 (C-1), 111.51 (C-3), 124.48 (C-4'), 128.43 (C-6'), 129.88 (C-2'), 132.28 (C-3'), 134.56 (C-1'), 141.20 (C-5'), 148.13 (C-4), 161.00 (C-6), 165.36 (C-2), 193.74 (CO). **IR (ATR film) [cm^{-1}]:** 2970, 2850, 1632, 1571, 1486, 1454, 1402, 1369, 1331, 1270, 1222, 1206, 1159, 1114, 1072, 1031, 1009, 979, 945, 874, 820, 790, 764, 712, 595, 572, 557, 529 **HR-MS (ESI):** m/z calculated for $[C_{17}H_{16}O_3Br]^+$ ([M + H^+]): 347.0277, found: 347.0279. **Melting point:** 122 – 124 °C

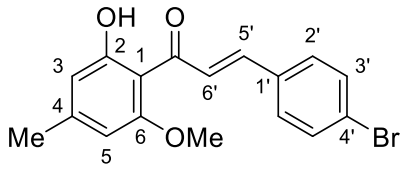

139

7.2.2.3.6 (*E*)-3-(3-Bromophenyl)-1-(2-hydroxy-6-methoxy-4-methylphenyl)prop-2-en-1-one (140)

The title compound was synthesized in accordance with **GP**1 with acetophenone **133** (250 mg, 1.0 equiv, 1.39 mmol) and 3-bromobenzaldehyde (0.200 mL, 1.2 equiv, 1.66 mmol). The product was isolated as yellow solids in a yield of 279 mg (0.806 mmol, 58%).

^{1}H NMR (600 MHz, $CDCl_3$): δ 2.33 (s, 3H, Me), 3.94 (s, 3H, OMe), 6.24 (d, $^4J_{3\text{-}5}$ = 1.5 Hz, 1H, 5-H), 6.43 – 6.46 (m, 1H, 3-H), 7.28 (t, $^3J_{4'\text{-}5',5'\text{-}6'}$ = 7.8 Hz, 1H, 5'-H), 7.51 (dd, $^3J_{4'\text{-}5'}$ = 7.9 Hz, $^4J_{3'\text{-}4'}$ = 1.8 Hz, 2H, 6'+4'-H), 7.67 (d, $^3J_{7'\text{-}8'}$ = 15.6 Hz, 1H, 7'-H), 7.74 (t, $^4J_{2'\text{-}4',2'\text{-}6'}$ = 1.8 Hz, 1H, 2'-H), 7.84 (d, $^3J_{7'\text{-}8'}$ = 15.6 Hz, 1H, 8'-H), 13.27 (s, 1H, OH). **^{13}C NMR** (151 MHz, $CDCl_3$): δ 22.61 (Me), 56.09 (OMe), 102.99 (C-5), 109.79 (C-1), 111.49 (C-3), 123.15 (C-3'), 127.21 (C-8'), 129.18 (C-6'), 130.53 (C-5'), 131.03 (C-2'), 132.97 (C-4'), 137.80 (C-1'), 140.70 (C-7'), 148.23 (C-4), 161.03 (C-6), 165.35 (C-2), 193.65 (CO). **IR (ATR film) [cm^{-1}]:** 2918, 2850, 1633, 1571, 1454, 1410, 1368, 1329, 1307, 1276, 1222, 1204, 1159, 1114, 1072, 1031, 978, 945, 898, 863, 815, 787, 760, 699, 667, 626, 606, 583, 557, 529, 485. **HR-MS (ESI):** m/z calculated for $[C_{17}H_{16}O_3Br]^+$ ([M + H$^+$]): 347.0277, found: 347.0278. **Melting point:** 123 – 124 °C

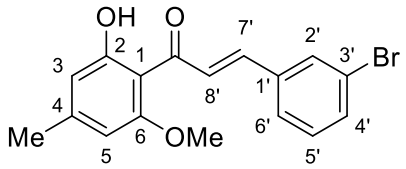

140

7.2.2.3.7 (*E*)-3-(2-Bromophenyl)-1-(2-hydroxy-6-methoxy-4-methylphenyl)prop-2-en-1-one (141)

The title compound was synthesized in accordance with **GP**1 with acetophenone **133** (250 mg, 1.0 equiv, 1.39 mmol) and 2-bromobenzaldehyde (0.191 mL, 1.2 equiv, 1.66 mmol). The product was isolated as yellow solids in a yield of 347 mg (1.00 mmol, 72%).

^{1}H NMR (600 MHz, $CDCl_3$): δ 2.33 (s, 3H, Me), 3.92 (s, 3H, OMe), 6.23 (s, 1H, 5-H), 6.45 (s, 1H, 3-H), 7.23 (td, $^3J_{3'\text{-}4',4'\text{-}5'}$ = 7.6 Hz, $^4J_{4'\text{-}6'}$ = 1.6 Hz, 1H, 4'-H), 7.35 (t, $^3J_{4'\text{-}5',5'\text{-}6'}$ = 7.5 Hz, 1H, 5'-H), 7.63 (dd, $^3J_{3'\text{-}4'}$ = 8.0 Hz, $^4J_{3'\text{-}5'}$ = 1.2 Hz, 1H, 3'-H), 7.69 (dd, $^3J_{5'\text{-}6'}$ = 7.9 Hz, $^4J_{4'\text{-}6'}$ = 1.6 Hz, 1H, 6'-H), 7.80 (d, $^3J_{7'\text{-}8'}$ = 15.4 Hz, 1H, 7'-H), 8.11 (d, $^3J_{7'\text{-}8'}$ = 15.5 Hz, 1H, 8'-H), 13.29 (s, 1H, OH). **^{13}C NMR** (151 MHz, $CDCl_3$): δ 22.61 (Me), 56.03 (OMe), 102.95 (C-5), 109.80 (C-1), 111.50 (C-3), 126.07 (C-2'), 127.77 (C-5'), 128.03 (C-6'), 130.45 (C-8'), 131.10

(C-4'), 133.69 (C-3'), 135.66 (C-1'), 140.78 (C-7'), 148.17 (C-4), 161.02 (C-6), 165.38 (C-2), 193.65 (CO). **IR (ATR film) [cm^{-1}]:** 3065, 1629, 1577, 1487, 1466, 1451, 1438, 1367, 1334, 1278, 1225, 1208, 1191, 1159, 1113, 1049, 1025, 996, 966, 944, 893, 858, 839, 813, 768, 745, 713, 656, 625, 606, 561, 530, 511, 489. **HR-MS (ESI):** m/z calculated for $[C_{17}H_{16}O_3Br]^+$ ([M + H$^+$]): 347.0277, found: 347.0281. **Melting point:** 162 – 164 °C

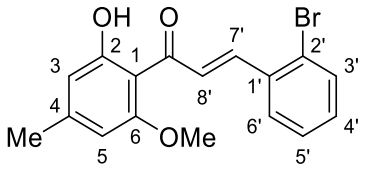

141

7.2.2.3.8 (*E*)-1-(2-Hydroxy-4,6-dimethoxyphenyl)-3-(4-methoxyphenyl)prop-2-en-1-one or Flavokavain A (142)

The title compound was synthesized in accordance with **GP1** with acetophenone **47** (250 mg, 1.0 equiv, 1.27 mmol) and 4-methoxybenzaldehyde (0.280 mL, 1.2 equiv + 0.6 equiv, 2.29 mmol) The product was isolated as yellow solids in a yield of 292 mg (0.927 mmol, 73%). The analytical data were in accordance with literature.[309]

^{1}H NMR (600 MHz, $CDCl_3$): δ 3.84 (s, 3H, OMe), 3.86 (s, 3H, OMe), 3.92 (s, 3H, OMe), 5.97 (dd, $^4J_{3\text{-}5}$ = 5.1, 2.4 Hz, 1H, 5-H), 6.11 (d, $^4J_{3\text{-}5}$ = 2.3 Hz, 1H, 3-H), 6.93 (d, $^3J_{2'\text{-}3'}$ = 8.8 Hz, 2H, 3'-H), 7.57 (d, $^3J_{2'\text{-}3'}$ = 8.7 Hz, 2H, 2'-H), 7.80 (m, 2H, 5'+6'-H), 14.43 (s, 1H, OH). **^{13}C NMR** (151 MHz, $CDCl_3$): δ 55.39 (OMe), 55.56 (OMe), 55.84 (OMe), 91.26 (C-5), 93.86 (C-3), 106.41 (C-1), 114.38 (C-3'), 125.19 (C-6'), 128.37 (C-1'), 130.10 (C-2'), 142.45 (C-5'), 161.38 (C-4/6/4'), 162.48 (C-4/6/4'), 166.03 (C-4/6/4'), 168.38 (C-2), 192.61 (CO). **IR (ATR film) [cm^{-1}]:** 3005, 2838, 1622, 1580, 1559, 1511, 1488, 1455, 1440, 1421, 1391, 1344, 1304, 1289, 1255, 1216, 1172, 1158, 1112, 984, 939, 870, 828, 766, 721, 697, 674, 615, 559, 539, 520 **HR-MS (ESI):** m/z calculated for $[C_{18}H_{19}O_5]^+$ ([M + H$^+$]): 315.1227, found: 315.1230. **Melting point:** 113 – 114 °C (110 °C)[310]

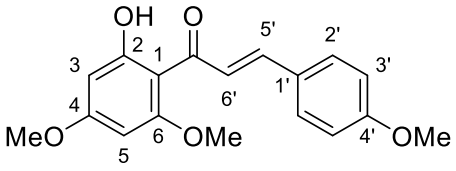

142

7.2.2.3.9 (*E*)-1-(2-Hydroxy-4,6-dimethoxyphenyl)-3-phenylprop-2-en-1-one (143)

The title compound was synthesized in accordance with **GP**1 with acetophenone **47** (250 mg, 1.0 equiv, 1.27 mmol) and benzaldehyde (0.233 mL, 1.2 equiv + 0.6 equiv, 2.29 mmol) at 50 °C. The product was isolated as yellow solids in a yield of 130 mg (0.458 mmol, 36%). The analytical data were in accordance with literature.[309]

^{1}H NMR (600 MHz, $CDCl_3$): δ 3.84 (s, 3H, OMe), 3.92 (s, 3H, OMe), 5.97 (d, $^4J_{3\text{-}5}$ = 2.4 Hz, 1H, 5-H), 6.11 (d, $^4J_{3\text{-}5}$ = 2.4 Hz, 1H, 3-H), 7.36 – 7.44 (m, 3H, 3'+4'-H), 7.58 – 7.63 (m, 2H, 2'-H), 7.79 (d, $^3J_{5',6'}$ = 15.6 Hz, 1H, 5'-H), 7.91 (d, $^3J_{5',6'}$ = 15.6 Hz, 1H, 6'-H), 14.31 (s, 1H, OH). **^{13}C NMR** (151 MHz, $CDCl_3$): δ 55.59 (OMe), 55.87 (OMe), 91.31 (C-5), 93.86 (C-3), 106.41 (C-1), 127.60 (C-6'), 128.36 (C-2'), 128.88 (C-3'), 130.04 (C-4'), 135.64 (C-1'), 142.32 (C-5'), 162.55 (C-4/6), 166.27 (C-4/6), 168.43 (C-2), 192.67 (CO). **IR (ATR film) [cm^{-1}]:** 3082, 3059, 3025, 3004, 2969, 2940, 2849, 1615, 1558, 1494, 1415, 1340, 1284, 1211, 1155, 1112, 1072, 1055, 1033, 984, 939, 888, 869, 818, 788, 742, 691, 673, 647, 623, 577, 562, 534, 495, 459 **HR-MS (ESI):** m/z calculated for $[C_{17}H_{17}O_4]^+$ ([M + H$^+$]): 285.1121, found: 285.1122. **Melting point:** 83 – 84 °C (85 – 86 °C)[309]

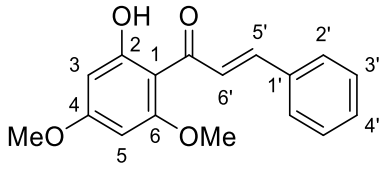

143

7.2.2.3.10 (*E*)-3-(4-(Dimethylamino)phenyl)-1-(2-hydroxy-4,6-dimethoxyphenyl)prop-2-en-1-one (144)

The title compound was synthesized in accordance with **GP1** with acetophenone **47** (250 mg, 1.0 equiv, 1.27 mmol) and 4-(dimethylamino)benzaldehyde (228 mg, 1.2 equiv, 1.53 mmol) at 90 °C. The product was isolated as red solids in a yield of 296 mg (0.906 mmol, 71%). The analytical data were in accordance with literature.[311]

^{1}H NMR (600 MHz, $CDCl_3$): δ 3.03 (s, 6H, NMe_2), 3.82 (s, 3H, OMe), 3.91 (s, 3H, OMe), 5.95 (d, $^4J_{3\text{-}5}$ = 2.4 Hz, 1H, 5-H), 6.10 (d, $^4J_{3\text{-}5}$ = 2.4 Hz, 1H, 3-H), 6.69 (d, $^3J_{2',3'}$ = 8.5 Hz, 2H, 3'-H), 7.52 (d, $^3J_{2',3'}$ = 8.7 Hz, 2H, 2'-H), 7.75 (d, $^3J_{5',6'}$ = 15.3 Hz, 1H, 5'-H), 7.83 (d, $^3J_{5',6'}$ = 15.4 Hz, 1H, 6'-H), 14.66 (s, 1H, OH). **^{13}C NMR** (151 MHz, $CDCl_3$): δ 40.16 (NMe_2), 55.52

(OMe), 55.78 (OMe), 91.12 (C-5), 93.83 (C-3), 106.45 (C-1), 111.90 (C-3'), 122.09 (C-6'), 123.40 (C-1'), 130.37 (C-2'), 143.99 (C-5'), 151.84 (C-4'), 162.39 (C-4/6), 165.63 (C-4/6), 168.31 (C-2), 192.47 (CO). **IR (ATR film) [cm^{-1}]:** 3004, 2962, 2850, 1621, 1587, 1528, 1481, 1436, 1415, 1379, 1346, 1296, 1209, 1172, 1154, 1111, 1031, 1001, 986, 941, 920, 864, 810, 765, 711, 677, 638, 616, 547, 516, 503, 461. **HR-MS (ESI):** m/z calculated for $[C_{19}H_{22}O_4]^+$ ($[M + H^+]$): 328.1543, found: 328.1546. **Melting point:** 203 – 204 °C (153 °C)[310]

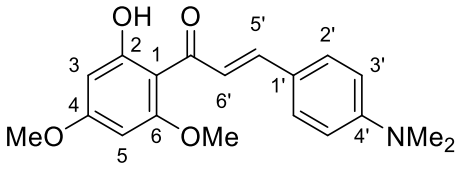

144

7.2.2.3.11 (*E*)-1-(2-Hydroxy-4,6-dimethoxyphenyl)-3-(4-(trifluoromethyl)phenyl)prop-2-en-1-one (145)

The title compound was synthesized in accordance with **GP1** with acetophenone **47** (250 mg, 1.0 equiv, 1.27 mmol) and 4-(trifluoromethyl)benzaldehyde (0.309 mL, 1.2 equiv + 0.6 equiv, 2.29 mmol). The product was isolated as yellow solids in a yield of 293 mg (0.831 mmol, 65%). **^{1}H NMR** (600 MHz, $CDCl_3$): δ 3.84 (s, 3H, OMe), 3.92 (s, 3H, OMe), 5.97 (d, $^4J_{3\text{-}5}$ = 2.4 Hz, 1H, 5-H), 6.11 (d, $^4J_{3\text{-}5}$ = 2.4 Hz, 1H, 3-H), 7.65 (d, $^3J_{2'\text{-}3'}$ = 8.3 Hz, 2H, 3'-H), 7.68 (d, $^3J_{2'\text{-}3'}$ = 8.3 Hz, 2H, 2'-H), 7.74 (d, $^3J_{5'\text{-}6'}$ = 15.6 Hz, 1H, H-5'), 7.93 (d, $^3J_{5'\text{-}6'}$ = 15.6 Hz, 1H, 6'-H), 14.14 (s, 1H, OH). **^{13}C NMR** (151 MHz, $CDCl_3$): δ 55.78 (OMe), 56.05 (OMe), 91.53 (C-5), 94.00 (C-3), 106.43 (C-1), 124.07 (q, $^1J_{F\text{-}C}$ = 272.1 Hz, CF_3), 125.96 (q, $^3J_{F\text{-}C}$ = 3.8 Hz, C-3'), 128.47 (C-2'), 130.12 (C-6'), 131.51 (q, $^2J_{F\text{-}C}$ = 32.6 Hz, C-4'), 139.19 (C-1'), 140.13 (C-5'), 162.65 (C-4/6), 166.72 (C-4/6), 168.66 (C-2), 192.32 (CO). **^{19}F NMR** (282 MHz, $CDCl_3$): δ -62.76. **IR (ATR film) [cm^{-1}]:** 3022, 2980, 2948, 1633, 1613, 1579, 1488, 1456, 1438, 1414, 1342, 1324, 1287, 1216, 1101, 1067, 1030, 1016, 955, 936, 906, 872, 838, 827, 815, 768, 750, 732, 693, 676, 605, 590, 535, 504, 461 **HR-MS (ESI):** m/z calculated for $[C_{18}H_{16}O_4F_3]^+$ ($[M + H^+]$): 353.0995, found: 353.0997. **Melting point:** 148 – 149 °C

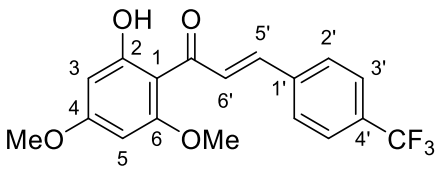

145

7.2.2.3.12 (*E*)-3-(4-Bromophenyl)-1-(2-hydroxy-4,6-dimethoxyphenyl)prop-2-en-1-one (146)

The title compound was synthesized in accordance with **GP1** with acetophenone **47** (250 mg, 1.0 equiv, 1.27 mmol) and 4-bromobenzaldehyde (423 mg, 1.2 equiv + 0.6 equiv, 2.29 mmol) The product was isolated as a yellow solid in a yield of 356 mg (0.983 mmol, 77%). The analytical data were in accordance with literature.[309]

^{1}H NMR (600 MHz, $CDCl_3$): δ 3.82 (s, 3H, OMe), 3.90 (s, 3H, OMe), 5.94 (d, $^4J_{3\text{-}5}$ = 2.4 Hz, 1H, 5-H), 6.09 (d, $^4J_{3\text{-}5}$ = 2.4 Hz, 1H, 3-H), 7.44 (d, $^3J_{2'\text{-}3'}$ = 8.2 Hz, 2H, 3'-H), 7.52 (d, $^3J_{2'\text{-}3'}$ = 8.2 Hz, 2H, 2'-H), 7.67 (d, $^3J_{5'\text{-}6'}$ = 15.6 Hz, 1H, 5'-H), 7.85 (d, $^3J_{5'\text{-}6'}$ = 15.6 Hz, 1H, 6'-H), 14.23 (s, 1H, OH). **^{13}C NMR** (151 MHz, $CDCl_3$): δ 55.72 (OMe), 55.99 (OMe), 91.42 (C-5), 93.95 (C-3), 106.39 (C-1), 124.30 (C-4'), 128.26 (C-6'), 129.78 (C-2'), 132.20 (C-3'), 134.63 (C-1'), 140.88 (C-5'), 162.58 (C-4/6), 166.49 (C-4/6), 168.57 (C-2), 192.40 (CO). **IR (ATR film) [cm^{-1}]:** 3016, 2996, 2978, 1627, 1586, 1564, 1484, 1440, 1420, 1336, 1303, 1289, 1272, 1215, 1158, 1114, 1069, 1029, 1007, 986, 973, 936, 891, 818, 792, 758, 709, 666, 604, 564, 534, 505, 483, 460. **HR-MS (ESI):** m/z calculated for $[C_{17}H_{16}O_4Br]^+$ ($[M + H^+]$): 363.0226, found: 363.0231. **Melting point:** 169 – 170 °C (166 °C)[312] (150-151 °C)[309]

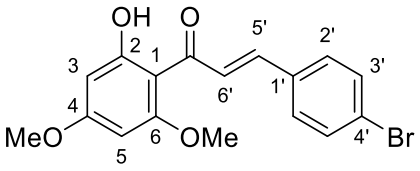

146

7.2.2.3.13 (*E*)-3-(3-Bromophenyl)-1-(2-hydroxy-4,6-dimethoxyphenyl)prop-2-en-1-one (147)

The title compound was synthesized in accordance with **GP1** with acetophenone **47** (250 mg, 1.0 equiv, 1.27 mmol) and 3-bromobenzaldehyde (0.269 mL, 1.2 equiv + 0.6 equiv, 2.29 mmol). The product was isolated as a yellow solid in a yield of 310 mg (0.856 mmol, 67%). The analytical data were in accordance with literature.[313]

^{1}H NMR (600 MHz, $CDCl_3$): δ 3.83 (s, 3H, OMe), 3.92 (s, 3H, OMe), 5.96 (d, $^4J_{3\text{-}5}$ = 2.4 Hz, 1H, 5-H), 6.10 (d, $^4J_{3\text{-}5}$ = 2.4 Hz, 1H, 3-H), 7.27 (t, $^3J_{4'\text{-}5',5'\text{-}6'}$ = 7.9 Hz, 1H, 5'-H), 7.49 (dd, ^3J

= 7.9 Hz, ^{4}J = 1.8 Hz, 2H, 4'+6'-H), 7.66 (d, $^{3}J_{7'-8'}$ = 15.6 Hz, 1H, 7'-H), 7.72 (t, $^{4}J_{2'-4',2'-6'}$ = 1.8 Hz, 1H, 2'-H), 7.85 (d, $^{3}J_{7'-8'}$ = 15.6 Hz, 1H, 8'-H), 14.18 (s, 1H, OH). **^{13}C NMR** (151 MHz, $CDCl_3$): δ 55.75 (OMe), 56.07 (OMe), 91.47 (C-5), 93.96 (C-3), 106.42 (C-1), 123.12 (C-3'), 127.12 (C-8'), 129.05 (C-6'), 130.49 (C-5'), 130.99 (C-2'), 132.84 (C-4'), 137.90 (C-1'), 140.43 (C-7'), 162.63 (C-4/6), 166.59 (C-4/6), 168.59 (C-2), 192.35 (CO). **IR (ATR film) [cm^{-1}]:** 2942, 2852, 1619, 1578, 1469, 1454, 1440, 1416, 1392, 1340, 1319, 1303, 1262, 1216, 1158, 1114, 1072, 1055, 1030, 983, 939, 911, 863, 819, 787, 758, 688, 670, 647, 624, 582, 564, 533, 492 **HR-MS (ESI):** m/z calculated for $[C_{17}H_{16}O_4Br]^+$ ([M + H$^+$]): 363.0226, found: 363.0230. **Melting point:** 115 – 116 °C

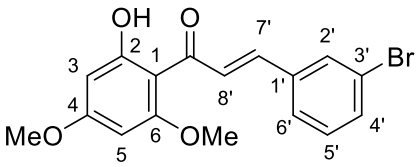

147

7.2.2.3.14 (*E*)-3-(2-Bromophenyl)-1-(2-hydroxy-4,6-dimethoxyphenyl)prop-2-en-1-one (148)

The title compound was synthesized in accordance with **GP1** with acetophenone **47** (250 mg, 1.0 equiv, 1.27 mmol) and 2-bromobenzaldehyde (0.181 mL, 1.2 equiv, 1.53 mmol). The product was isolated as yellow solids in a yield of 385 mg (1.06 mmol, 83%). The analytical data were in accordance with literature.[314]

^{1}H NMR (600 MHz, $CDCl_3$): δ 3.83 (s, 3H, OMe), 3.89 (s, 3H, OMe), 5.95 (d, $^{4}J_{3-5}$ = 2.4 Hz, 1H, 5-H), 6.10 (d, $^{4}J_{3-5}$ = 2.4 Hz, 1H, 3-H), 7.21 (td, $^{3}J_{3'-4',4'-5'}$ = 7.6 Hz, $^{4}J_{4'-6'}$ = 1.6 Hz, 1H, 4'-H), 7.34 (td, $^{3}J_{4'-5',5'-6'}$ = 7.6 Hz, $^{4}J_{3'-5'}$ = 1.3 Hz, 1H, 5'-H), 7.62 (dd, $^{3}J_{3'-4'}$ = 8.1 Hz, $^{4}J_{3'-5'}$ = 1.2 Hz, 1H, 3'-H), 7.67 (dd, $^{3}J_{5'-6'}$ = 7.8 Hz, $^{4}J_{4'-6'}$ = 1.7 Hz, 1H, 6'-H), 7.81 (d, $^{3}J_{7'-8'}$ = 15.5 Hz, 1H, 7'-H), 8.09 (d, $^{3}J_{7'-8'}$ = 15.5 Hz, 1H, 8'-H), 14.21 (s, 1H, OH). **^{13}C NMR** (151 MHz, $CDCl_3$): δ 55.73 (OMe), 56.01 (OMe), 91.41 (C-5), 93.96 (C-3), 106.41 (C-1), 125.96 (C-2'), 127.75 (C-5'), 127.99 (C-6'), 130.32 (C-8'), 130.98 (C-4'), 133.62 (C-3'), 135.73 (C-1'), 140.51 (C-7'), 162.62 (C-4/6), 166.55 (C-4/6), 168.60 (C-2), 192.34 (CO). **IR (ATR film) [cm^{-1}]:** 3005, 2976, 1627, 1579, 1565, 1490, 1464, 1437, 1416, 1343, 1321, 1307, 1269, 1216, 1160, 1113, 1048, 1027, 971, 939, 874, 814, 797, 770, 744, 695, 663, 646, 622, 586, 535, 507. **HR-MS (ESI):** m/z calculated for $[C_{17}H_{16}O_4Br]^+$ ([M + H$^+$]): 363.0226, found: 363.0233. **Melting point:** 147 – 148 °C (146 -147 °C)[314]

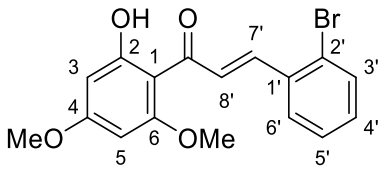

148

7.2.2.3.15 (*E*)-1-(2-Hydroxy-6-methoxy-4-methylphenyl)-3-(pyridin-2-yl)prop-2-en-1-one (149)

A 25 mL round bottom flask was charged with acetophenone **47** (270 mg, 1.0 equiv, 1.50 mmol), MeOH (5 mL, 0.3 M), pyridine-2-carbaldehyde (0.143 mL, 1.0 equiv, 1.50 mmol) and an aq. solution of NaOMe (6.25 M, 1.00 mL, 4.2 equiv, 6.25 mmol). The reaction mixture was stirred for 24 h. Aq. KPi buffer (1 M, K_2HPO_4/KH_2PO_4 pH 7) was added, the aq. Phase extracted with CH_2Cl_2 (3x), the combined org phases washed with sat. aq. NaCl solution, dried over $MgSO_4$, solids filtered off and solvents removed in vacuo. The product was isolated by column chromatography (petroleum ether:EtOAc 65:35 v/v) as orange solids in a yield of 147 mg (0.540 mmol, 36%).

^{1}H NMR (600 MHz, $CDCl_3$): δ 2.33 (s, 3H, Me), 3.94 (s, 3H, OMe), 6.23 (s, 1H, H-3), 6.44 (s, 1H, H-5), 7.27 – 7.30 (m, 1H, H-5’’), 7.48 (d, $^3J_{3'',4''}$ = 7.8 Hz, 1H, H-3’’), 7.72 (m, 1H, H-4’’), 7.73 (d, J = 15.4 Hz, 1H, H-2’), 8.31 (d, J = 15.3 Hz, 1H, H-3’), 8.68 (d, $^3J_{5'',6''}$ = 4.4 Hz, 1H, H-6’’), 13.29 (s, 1H, OH). **^{13}C NMR** (151 MHz, $CDCl_3$): δ 22.63 (Me), 56.10 (OMe), 102.96 (C-3), 109.97 (C-1), 111.31 (C-5), 124.11 (C-5’’), 124.93 (C-3’’), 131.82 (C-3’), 136.87 (C-2’), 140.81 (C-4’’), 148.29 (C-4), 150.29 (C-6’’), 154.05 (C-2’’), 161.29 (C-2), 165.31 (C-6), 194.32 (C-1’). **IR (ATR film) [cm^{-1}]:** 2953, 1633, 1573, 1466, 1429, 1322, 1216, 1188, 981, 814, 753. **TLC** (petroleum ether:EtOAc, 5:5 v/v): R_f = 0.45

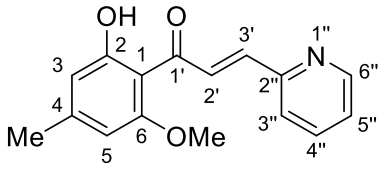

149

7.2.2.3.15.1 5-Methoxy-7-methyl-2-(pyridin-2-yl)chroman-4-one (197)

As a side product **197** was obtained in analytical quantities.

^{1}H NMR (600 MHz, $CDCl_3$): δ 2.37 (s, 3H, Me), 3.07 (dd, $^2J_{3a\text{-}3b}$ = 15.2 Hz, $^3J_{2\text{-}3}$ = 9.7 Hz, 1H, H-3_a), 3.54 (dd, $^2J_{3a\text{-}3b}$ = 15.1 Hz, $^3J_{2\text{-}3}$ = 3.4 Hz, 1H, H-3_b), 3.94 (s, 3H, OMe), 5.11 (dd, *J* = 9.7, 3.4 Hz, 1H, H-2), 6.27 (s, 1H), 6.44 – 6.47 (m, 1H), 7.16 (dd, *J* = 7.5, 4.9 Hz, 1H), 7.25 (d, *J* = 8.0 Hz, 2H), 7.62 (td, *J* = 7.6, 1.8 Hz, 1H), 8.57 (d, *J* = 5.0 Hz, 1H). **TLC** (CH_2Cl_2:MeOH, 98:2 v/v): R_f = 0.16

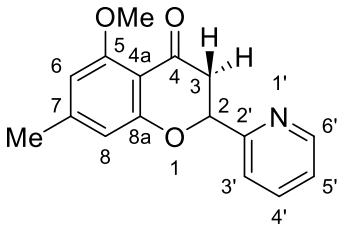

197

7.2.2.4 General Procedure 2 (GP2): Flavone Monomer

A 10 mL microwave vial equipped with stir bar was charged with chalcone (100 mg, 1.00 equiv) and capped with a septum. Degassed DMSO (1.70 mL) and a solution of I_2 in degassed DMSO (78.8 mM, 4 mol%) were added. The reaction solution was then heated to 150 °C and stirred for 3 h. After complete conversion sat. aq. Na_2SO_3 solution (4 mL) was added. The aq. phase was extracted with ethyl acetate (3x 20 mL). The combined org. layers were washed with cold water (3x 20 mL) and sat. NaCl solution (2x 20 mL) and the solvent removed *in vacuo*. The product was isolated by filtration over a plug of silica (CH_2Cl_2:MeOH, 9:1 v/v).

7.2.2.4.1 5-Methoxy-2-(4-methoxyphenyl)-7-methyl-4*H*-chromen-4-one (150)

The title compound was synthesized in accordance with **GP2** with chalcone **135** (100 mg, 1.0 equiv, 0.335 mmol) and I_2 (78.8 mM, 173 µL, 4 mol%, 0.0134 mmol). The product was isolated as white solids in a yield of 81.0 mg (0.274 mmol, 81%).

^{1}H NMR (600 MHz, $CDCl_3$): δ 2.46 (s, 3H, Me), 3.88 (s, 3H, OMe), 3.98 (s, 3H, OMe), 6.62 (s, 1H, 6-H), 6.63 (s, 1H, 3-H), 6.94 (dd, $^4J_{6\text{-}8}$ = 1.6, 0.8 Hz, 1H, 8-H), 7.00 (d, $^3J_{2'\text{-}3'}$ = 8.9 Hz, 2H, 3'-H), 7.83 (d, $^3J_{2'\text{-}3'}$ = 8.9 Hz, 2H, 2'-H). **^{13}C NMR** (151 MHz, $CDCl_3$): δ 22.42 (Me), 55.63 (OMe), 56.59 (OMe), 107.88 (C-3+6), 110.39 (C-8), 112.60 (C-4a), 114.54 (C-3'), 124.13 (C-1'), 127.86 (C-2'), 145.01 (C-7), 158.44 (C-8a), 159.67 (C-5), 161.04 (C-2), 162.28 (C-5), 178.34 (CO). **IR (ATR film) [cm^{-1}]:** 2840, 1639, 1606, 1575, 1512, 1483, 1423, 1377, 1340, 1300, 1220, 1180, 1115, 1050, 955, 903, 833, 611, 586. **HR-MS (ESI):** m/z calculated for $[C_{18}H_{17}O_4]^+$ ($[M + H^+]$): 297.1121, found: 297.1126. **Melting point:** 173 – 174 °C

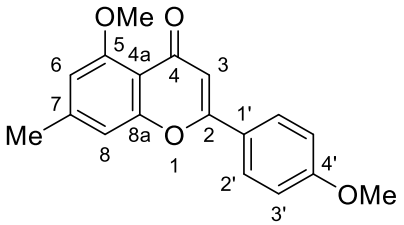

150

7.2.2.4.2 5-Methoxy-7-methyl-2-phenyl-4*H*-chromen-4-one (151)

The title compound was synthesized in accordance with **GP1** with chalcone **136** (100 mg, 1.0 equiv, 0.373 mmol) and I_2 (78.8 mM, 192 µL, 4 mol%, 0.0149 mmol). The product was isolated as white solids in a yield of 90.3 mg (0.339 mmol, 90%).

^{1}H NMR (600 MHz, $CDCl_3$): δ 2.45 (s, 3H, Me), 3.98 (s, 3H, OMe), 6.62 (s, 1H, 6-H), 6.70 (s, 1H, 3-H), 6.95 (s, 1H, 8-H), 7.49 (m, 3H, 3'+4'-H), 7.87 (dd, J = 7.5, 2.3 Hz, 2H, 2'-H). **^{13}C NMR** (151 MHz, $CDCl_3$): δ 22.40 (Me), 56.55 (OMe), 107.93 (C-3), 109.17 (C-6), 110.39 (C-8), 112.62 (C-4a), 126.14 (C-2'/3'), 129.05 (C-2'/3'), 131.34 (C-4'), 131.77 (C-1'), 145.26 (C-7), 158.45 (C-8a), 159.65 (C-5), 160.97 (C-2), 178.28 (CO). **IR (ATR film) [cm^{-1}]:** 3068, 2914, 2851, 2236, 1637, 1610, 1577, 1566, 1482, 1463, 1449, 1410, 1375, 1337, 1298, 1263, 1219, 1188, 1163, 1118, 1079, 1049, 1014, 1001, 973, 956, 919, 901, 848, 825, 769, 729, 691, 676, 610, 566, 545, 528, 488. **HR-MS (ESI):** m/z calculated for $[C_{17}H_{15}O_3]^+$ ([M + H$^+$]): 267.1016, found: 267.1020. **Melting point:** 162 – 163 °C

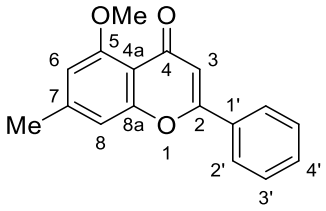

151

7.2.2.4.3 2-(4-(Dimethylamino)phenyl)-5-methoxy-7-methyl-4*H*-chromen-4-one (152)

The title compound was synthesized in accordance with **GP2** with chalcone **137** (100 mg, 1.0 equiv, 0.321 mmol) and I_2 (78.8 mM, 162 µL, 4 mol%, 0.0128 mmol). The product was isolated as orange solids in a yield of 50.0 mg (0.162 mmol, 50%).

^{1}H NMR (600 MHz, $CDCl_3$): δ 2.44 (s, 3H, Me), 3.05 (s, 6H, NMe_2), 3.97 (s, 3H, OMe), 6.57 (s, 1H, 3-H), 6.60 (s, 1H, 6-H), 6.73 (d, $^3J_{2',3'}$ = 8.9 Hz, 2H, 3'-H), 6.92 (s, 1H, 8-H), 7.76 (d, ^3J = 8.9 Hz, 2H, 2'-H). **^{13}C NMR** (151 MHz, $CDCl_3$): δ 22.38 (Me), 40.24 (NMe_2), 56.54 (OMe), 106.13 (C-3), 107.60 (C-6), 110.36 (C-8), 111.76 (C-3'), 112.55 (C-4a), 118.36 (C-1'), 127.49 (C-2'), 144.54 (C-7), 152.37 (C-4'), 158.38 (C-8a), 159.53 (C-5), 161.89 (C-2), 178.42 (CO). **IR (ATR film) [cm^{-1}]:** 2924, 2853, 2235, 1629, 1597, 1523, 1481, 1463, 1445, 1412, 1366, 1339, 1300, 1253, 1223, 1197, 1170, 1118, 1092, 1049, 1015, 972, 947, 914, 776, 758,

728, 677, 643, 611, 577, 541, 528, 510, 480 **HR-MS (ESI):** m/z calculated for $[C_{19}H_{20}NO_3]^+$ ($[M + H^+]$): 310.1438, found: 310.1441. **Melting point:** 198 °C (decomposition)

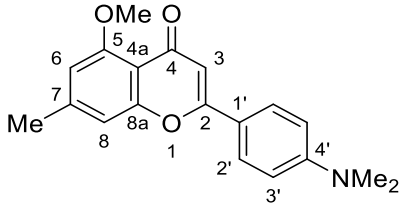

152

7.2.2.4.4 5-Methoxy-7-methyl-2-(4-(trifluoromethyl)phenyl)-4*H*-chromen-4-one (153)

The title compound was synthesized in accordance with **GP2** with chalcone **138** (100 mg, 1.0 equiv, 0.297 mmol) and I_2 (78.8 mM, 152 µL, 4 mol%, 0.0119 mmol). The product was isolated as white solids in a yield of 65.7 mg (0.196 mmol, 66%).

^{1}H NMR (600 MHz, $CDCl_3$): δ 2.46 (s, 3H, Me), 3.98 (s, 3H, OMe), 6.64 (s, 1H, 6-H), 6.74 (s, 1H, 3-H), 6.96 (s, 1H, 8-H), 7.75 (d, $^3J_{2',3'}$ = 8.2 Hz, 2H, 3'-H), 7.98 (d, $^3J_{2',3'}$ = 8.1 Hz, 2H, 2'-H). **^{13}C NMR** (151 MHz, $CDCl_3$): δ 22.44 (Me), 56.59 (OMe), 108.19 (C-6), 110.34 (C-3+8), 112.63 (C-4a), 122.91 (q, $^1J_{F-C}$ = 271.2 Hz, CF_3), 126.07 (q, $^3J_{F-C}$ = 3.8 Hz, C-3'), 126.48 (C-2'), 132.97 (q, $^2J_{F-C}$ = 32.8 Hz, C-4'), 135.23 (C-1'), 145.73 (C-7), 158.35 (C-8a), 159.23 (C-2), 159.73 (C-5), 177.89 (CO). **^{19}F NMR** (282 MHz, $CDCl_3$): δ -62.95. **IR (ATR film) [cm^{-1}]:** 3074, 2920, 1645, 1612, 1567, 1518, 1486, 1466, 1417, 1379, 1319, 1295, 1257, 1219, 1202, 1159, 1114, 1071, 1049, 1016, 958, 902, 889, 849, 823, 776, 731, 702, 677, 649, 635, 612, 585, 566, 551, 530, 497. **HR-MS (ESI):** m/z calculated for $[C_{18}H_{14}O_3F_3]^+$ ($[M + H^+]$): 335.0890, found: 335.0895. **Melting point:** 226 – 228 °C

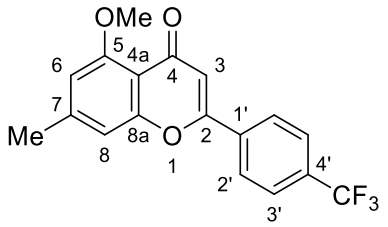

153

7.2.2.4.5 2-(4-Bromophenyl)-5-methoxy-7-methyl-4*H*-chromen-4-one (154)

The title compound was synthesized in accordance with **GP2** with chalcone **139** (100 mg, 1.0 equiv, 0.288 mmol) and I_2 (78.8 mM, 147 µL, 4 mol%, 0.0115 mmol). The product was isolated as white solids in a yield of 90.5 mg (0.262 mmol, 91%).

^{1}H NMR (600 MHz, $CDCl_3$): δ 2.46 (s, 3H, Me), 3.98 (s, 3H, OMe), 6.64 (s, 1H, 6-H), 6.69 (s, 1H, 3-H), 6.94 (s, 1H, 8-H), 7.63 (d, $^3J_{2'\text{-}3'}$ = 8.6 Hz, 2H, 3'-H), 7.74 (d, $^3J_{2'\text{-}3'}$ = 8.6 Hz, 2H, 2'-H). **^{13}C NMR** (151 MHz, $CDCl_3$): δ 22.48 (Me), 56.60 (OMe), 108.05 (C-3), 109.29 (C-6), 110.35 (C-8), 112.54 (C-4a), 126.02 (C-4'), 127.61 (C-2'), 130.71 (C-1'), 132.39 (C-3'), 145.53 (C-7), 158.34 (C-8a), 159.67 (C-2), 159.95 (C-5), 178.13 (CO). **IR (ATR film) [cm^{-1}]:** 3072, 2236, 1612, 1588, 1567, 1483, 1463, 1404, 1375, 1334, 1300, 1265, 1218, 1188, 1164, 1120, 1074, 1048, 1008, 956, 828, 776, 731, 677, 644, 566, 550, 529, 495, 475. **HR-MS (ESI):** m/z calculated for $[C_{17}H_{14}O_3Br]^+$ ([M + H^+]): 345.0121, found: 345.0121. **Melting point:** 203 – 206 °C

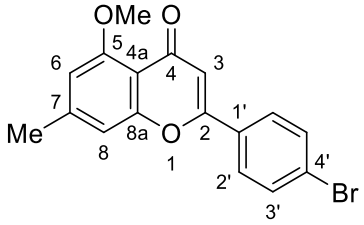

154

7.2.2.4.6 2-(3-Bromophenyl)-5-methoxy-7-methyl-4*H*-chromen-4-one (155)

The title compound was synthesized in accordance with **GP2** with chalcone **140** (100 mg, 1.0 equiv, 0.288 mmol) and I_2 (78.8 mM, 147 µL, 4 mol%, 0.0115 mmol). The product was isolated as white solids in a yield of 92.1 mg (0.266 mmol, 92%).

^{1}H NMR (600 MHz, $CDCl_3$): δ 2.39 (s, 3H, Me), 3.91 (s, 3H, OMe), 6.56 (s, 1H, 6-H), 6.57 (s, 1H, 3-H), 6.86 (t, $^4J_{6\text{-}8}$ = 1.1 Hz, 1H, 8-H), 7.29 (t, $^3J_{4'\text{-}5',5'\text{-}6}$ = 7.9 Hz, 1H, 5'-H), 7.54 (ddd, ^3J = 8.0 Hz, ^4J = 2.0 Hz, J = 1.0 Hz, 1H, 4'-H), 7.68 (dt, ^3J = 7.9 Hz, ^4J = 1.4 Hz, 1H, 6'-H), 7.92 (t, $^4J_{2'\text{-}4',2'\text{-}6'}$ = 1.9 Hz, 1H, 2'-H). **^{13}C NMR** (151 MHz, $CDCl_3$): δ 22.28 (Me), 56.37 (OMe), 107.88 (C-3), 109.44 (C-6), 110.17 (C-8), 112.29 (C-4a), 123.08 (C-2'), 124.44 (C-6'), 128.84 (C-3'), 130.40 (C-5'), 133.49 (C-1'), 133.99 (C-4'), 145.44 (C-7), 158.03 (C-8a), 158.97 (C-2), 159.40 (C-5), 177.71 (CO). **IR (ATR film) [cm^{-1}]:** 2921, 1644, 1613, 1560, 1483, 1465, 1417, 1375, 1301, 1266, 1217, 1165, 1121, 1098, 1077, 1050, 998, 977, 956, 846, 825, 791, 744, 721,

693, 612, 566, 529, 487. **HR-MS (ESI):** m/z calculated for $[C_{17}H_{14}O_3Br]^+$ ($[M + H^+]$): 345.0121, found: 345.0125. **Melting point:** 165 – 166 °C

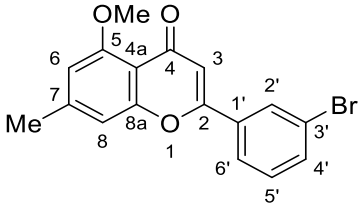

155

7.2.2.4.7 2-(2-Bromophenyl)-5-methoxy-7-methyl-4*H*-chromen-4-one (156)

The title compound was synthesized in accordance with **GP2** with chalcone **141** (100 mg, 1.0 equiv, 0.288 mmol) and I_2 (78.8 mM, 147 µL, 4 mol%, 0.0115 mmol). The product was isolated as white solids in a yield of 76.4 mg (0.221 mmol, 76%).

^{1}H NMR (600 MHz, $CDCl_3$): δ 2.45 (s, 3H, Me), 3.99 (s, 3H, OMe), 6.45 (s, 1H, 3-H), 6.64 (s, 1H, 6-H), 6.88 (s, 1H, 8-H), 7.35 (td, $^3J_{3'\text{-}4',4'\text{-}5'}$ = 7.7 Hz, $^4J_{4'\text{-}6'}$ = 1.7 Hz, 1H, 4'-H), 7.43 (td, $^3J_{4'\text{-}5',5'\text{-}6'}$ = 7.5 Hz, $^4J_{3'\text{-}5'}$ = 1.2 Hz, 1H, 5'-H), 7.55 (dd, $^3J_{5'\text{-}6'}$ = 7.7 Hz, $^4J_{4'\text{-}6'}$ = 1.7 Hz, 1H, 6'-H), 7.70 (dd, $^3J_{3'\text{-}4'}$ = 8.0 Hz, $^4J_{3'\text{-}5'}$ = 1.1 Hz, 1H, 3'-H). **^{13}C NMR** (151 MHz, $CDCl_3$): δ 22.43 (Me), 56.58 (OMe), 108.06 (C-3), 110.45 (C-6), 112.62 (C-8), 114.33 (C-4a), 122.05 (C-2'), 127.70 (C-5'), 130.98 (C-6'), 131.81 (C-4'), 134.02 (C-1'), 134.05 (C-3'), 145.50 (C-7), 158.71 (C-8a), 159.75 (C-2), 161.65 (C-5), 177.90 (CO). **IR (ATR film) [cm^{-1}]:** 2931, 1650, 1616, 1483, 1466, 1436, 1411, 1332, 1298, 1267, 1217, 1164, 1117, 1061, 1040, 1026, 854, 764, 727, 683, 567, 545, 500. **HR-MS (ESI):** m/z calculated for $[C_{17}H_{14}O_3Br]^+$ ($[M + H^+]$): 345.0121, found 345.0125. **Melting point:** 146 – 148 °C

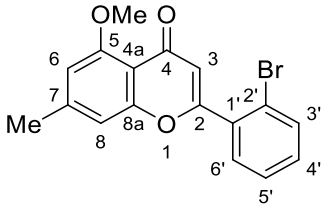

156

7.2.2.4.8 5,7-Dimethoxy-2-(4-methoxyphenyl)-4*H*-chromen-4-one or apigenin trimethyl ether (157)

The title compound was synthesized in accordance with **GP2** with chalcone **142** (100 mg, 1.0 equiv, 0.318 mmol) and I_2 (78.8 mM, 162 µL, 4 mol%, 0.0127 mmol). The product was isolated as white solids in a yield of 35.7 mg (0.114 mmol, 36%). The analytical data were in accordance with literature.[315]

^{1}H NMR (600 MHz, $CDCl_3$): δ 3.88 (s, 3H, OMe), 3.91 (s, 3H, OMe), 3.96 (s, 3H, OMe), 6.37 (d, $^4J_{6\text{-}8}$ = 2.3 Hz, 1H, 6-H), 6.56 (d, $^4J_{6\text{-}8}$ = 2.3 Hz, 1H, 8-H), 6.60 (s, 1H, 3-H), 7.00 (d, $^3J_{2'\text{-}3'}$ = 8.9 Hz, 2H, 3'-H), 7.82 (d, $^3J_{2'\text{-}3'}$ = 8.9 Hz, 2H, 2'-H). **^{13}C NMR** (151 MHz, $CDCl_3$): δ 55.62 (OMe), 55.87 (OMe), 56.59 (OMe), 93.02 (C-8), 96.25 (C-6), 107.92 (C-3), 109.46 (C-4a), 114.53 (C-3'), 124.09 (C-1'), 127.76 (C-2'), 160.03 (C-8a), 160.83 (C-5), 161.12 (C-2), 162.22 (C-4'), 164.07 (C-7), 177.75 (CO). **IR (ATR film) [cm^{-1}]:** 2941, 1640, 1605, 1513, 1491, 1460, 1422, 1347, 1301, 1259, 1218, 1202, 1180, 1161, 1114, 1057, 1032, 908, 833, 773, 620, 599, 559. **HR-MS (ESI):** m/z calculated for $[C_{18}H_{17}O_5]^+$ ([M + H$^+$]): 313.1071, found: 313.1075. **Melting point:** 155 – 157°C (155 – 157 °C)[315]

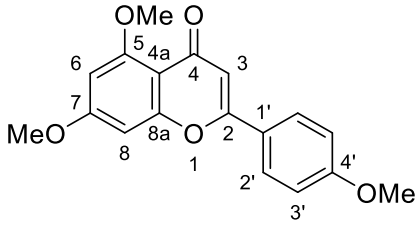

157

7.2.2.4.9 5,7-Dimethoxy-2-phenyl-4*H*-chromen-4-one or Dimethyl-chrysin (158)

The title compound was synthesized in accordance with **GP2** with chalcone **143** (100 mg, 1.0 equiv, 0.352 mmol) and I_2 (78.8 mM, 178 µL, 4 mol%, 0.0141 mmol). The product was isolated as white solids in a yield of 80.1 mg (0.284 mmol, 80%). The analytical data were in accordance with literature.[316]

^{1}H NMR (600 MHz, $CDCl_3$): δ 3.91 (s, 3H, OMe), 3.95 (s, 3H, OMe), 6.37 (d, $^4J_{6\text{-}8}$ = 2.3 Hz, 1H, 6-H), 6.57 (d, $^4J_{6\text{-}8}$ = 2.3 Hz, 1H, 8-H), 6.68 (s, 1H, 3-H), 7.47 – 7.52 (m, 3H, 3'+4'-H), 7.84 – 7.90 (m, 2H, 2'-H). **^{13}C NMR** (151 MHz, $CDCl_3$): δ 55.89 (OMe), 56.57 (OMe), 93.02 (C-8), 96.35 (C-6), 109.26 (C-4a), 109.52 (C-3), 126.09 (C2'/3'), 129.06 (C-2'/3'), 131.29 (C-4'), 131.75 (C-1'), 160.08 (C-8a), 160.78 (C-5), 161.12 (C-2), 164.22 (C-7), 177.69 (CO). **IR (ATR film) [cm^{-1}]:** 3017, 2948, 2922, 2844, 2326, 2226, 2015, 1646, 1605, 1491, 1465, 1451,

1422, 1392, 1348, 1302, 1268, 1215, 1204, 1189, 1161, 1120, 1104, 1079, 1058, 1035, 1022, 1000, 962, 949, 915, 851, 819, 803, 766, 723, 689, 642, 614, 556, 530, 483. **HR-MS (ESI):** m/z calculated for $[C_{17}H_{15}O_4]^+$ ([M + H^+]): 283.0965, found: 283.0969. **Melting point:** 80 °C (brown discoloration), 141 – 142.1 °C (145 – 146 °C)[316]

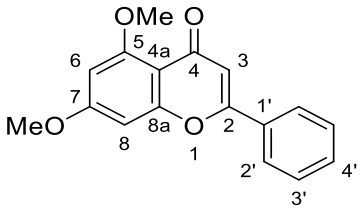

158

7.2.2.4.10 2-(4-(dimethylamino)phenyl)-5,7-dimethoxy-4*H*-chromen-4-one (159)

The title compound was synthesized in accordance with **GP2** with chalcone **144** (100 mg, 1.0 equiv, 0.306 mmol) and I_2 (78.8 mM, 157 µL, 4 mol%, 0.0122 mmol). The product was isolated as orange solids in a yield of 37.1 mg (0.114 mmol, 37%).

^{1}H NMR (600 MHz, $CDCl_3$): δ 3.06 (s, 6H, NMe_2), 3.91 (s, 3H, OMe), 3.95 (s, 3H, OMe), 6.36 (d, $^4J_{6\text{-}8}$ = 2.3 Hz, 1H, 6-H), 6.55 (s, 2H, 3+8-H), 6.74 (d, $^3J_{2',3'}$ = 9.0 Hz, 2H, 3'-H), 7.75 (d, $^3J_{2',3'}$ = 9.0 Hz, 2H, 2'-H). **^{13}C NMR** (151 MHz, $CDCl_3$): δ 40.25 (NMe_2), 55.83 (OMe), 56.57 (OMe), 93.03 (C-8), 96.03 (C-6), 106.23 (C-3), 111.83 (C-3'), 112.16 (C-4a), 118.48 (C-1'), 127.44 (C-2'), 152.39 (C-4'), 160.00 (C-8a), 161.04 (C-5), 161.72 (C-2), 163.79 (C-7), 177.87 (CO). **IR (ATR film) [cm^{-1}]:** 2943, 1635, 1601, 1525, 1489, 1458, 1369, 1347, 1303, 1253, 1217, 1200, 1161, 1117, 1057, 1029, 1002, 908, 819, 729, 674, 642, 618, 592, 511, 467. **HR-MS (ESI):** m/z calculated for $[C_{19}H_{20}NO_4]^+$ ([M + H^+]): 326.1387, found: 326.1388. **Melting point:** 211 – 214 °C

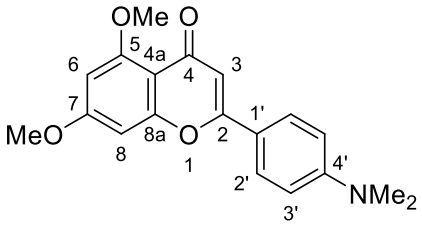

159

7.2.2.4.11 5,7-Dimethoxy-2-(4-(trifluoromethyl)phenyl)-4*H*-chromen-4-one (160)

The title compound was synthesized in accordance with **GP2** with chalcone **145** (100 mg, 1.0 equiv, 0.284 mmol) and I_2 (78.8 mM, 147 µL, 4 mol%, 0.0114 mmol). The product was isolated as white solids in a yield of 26.8 mg (0.0765 mmol, 27%). The analytical data were in accordance with literature.[317]

^{1}H NMR (600 MHz, $CDCl_3$): δ 3.91 (s, 3H, OMe), 3.95 (s, 3H, OMe), 6.38 (d, $^4J_{6\text{-}8}$ = 2.3 Hz, 1H, 6-H), 6.57 (d, $^4J_{6\text{-}8}$ = 2.3 Hz, 1H, 8-H), 6.70 (s, 1H, 3-H), 7.74 (d, $^3J_{2',3'}$ = 8.1 Hz, 2H, 3'-H), 7.97 (d, $^3J_{2',3'}$ = 8.1 Hz, 2H, 2'-H). **^{13}C NMR** (151 MHz, $CDCl_3$): δ 55.80 (OMe), 56.45 (OMe), 92.88 (C-8), 96.41 (C-6), 109.36 (C-4a), 110.30 (C-3), 123.68 (q, J = 272.2 Hz, CF_3), 125.91 (q, J = 3.8 Hz, C-3'), 126.26 (C-2'), 132.77 (q, J = 32.8 Hz, C-4'), 135.02 (C-1'), 158.87 (C-8a), 159.84 (C-5), 161.04 (C-2), 164.34 (C-7), 177.11 (CO). **^{19}F NMR** (282 MHz, $CDCl_3$): δ -62.93. **IR (ATR film) [cm^{-1}]:** 2945, 2240, 1645, 1574, 1491, 1459, 1416, 1386, 1322, 1295, 1264, 1218, 1203, 1161, 1070, 1057, 1027, 1016, 908, 841, 807, 731, 675, 635, 616, 586, 564, 528, 514, 493, 468. **HR-MS (ESI):** m/z calculated for $[C_{18}H_{14}F_3O_4]^+$ ([M + H$^+$]): 351.0839, found: 351.0843. **Melting point:** 185 – 186 °C

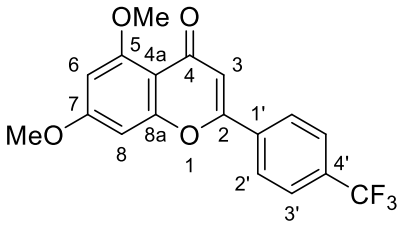

160

7.2.2.4.12 2-(4-Bromophenyl)-5,7-dimethoxy-4*H*-chromen-4-one (161)

The title compound was synthesized in accordance with **GP2** with chalcone **146** (100 mg, 1.0 equiv, 0.275 mmol) and I_2 (78.8 mM, 142 µL, 4 mol%, 0.0110 mmol). The product was isolated as white solids in a yield of 92.6 mg (0.257 mmol, 93%). The analytical data were in accordance with literature.[318]

^{1}H NMR (600 MHz, $CDCl_3$): δ 3.90 (s, 3H, OMe), 3.94 (s, 3H, OMe), 6.36 (d, $^4J_{6\text{-}8}$ = 2.3 Hz, 1H, 6-H), 6.54 (d, $^4J_{6\text{-}8}$ = 2.3 Hz, 1H, 8-H), 6.63 (s, 1H, 3-H), 7.61 (d, $^3J_{2',3'}$ = 8.6 Hz, 2H, 3'-H), 7.71 (d, $^3J_{2',3'}$ = 8.6 Hz, 2H, 2'-H). **^{13}C NMR** (151 MHz, $CDCl_3$): δ 55.91 (OMe), 56.57 (OMe), 92.93 (C-8), 96.40 (C-6), 109.33 (C-3), 109.38 (C-4a), 125.88 (C-4'), 127.47 (C-2'), 130.60 (C-1'), 132.33 (C-3'), 159.64 (C-8a), 159.91 (C-5), 161.06 (C-2), 164.28 (C-7), 177.44

(CO). **IR (ATR film) [cm^{-1}]:** 2842, 1644, 1607, 1572, 1488, 1459, 1422, 1404, 1380, 1341, 1277, 1217, 1202, 1161, 1118, 1105, 1073, 1057, 1008, 905, 827, 773, 738, 718, 674, 635, 616, 529, 491, 475. **HR-MS (ESI):** m/z calculated for $[C_{17}H_{14}O_4Br]^+$ ($[M + H^+]$): 361.0070, found: 361.0073. **Melting point:** 194 – 195 °C (197 – 198 °C)[318]

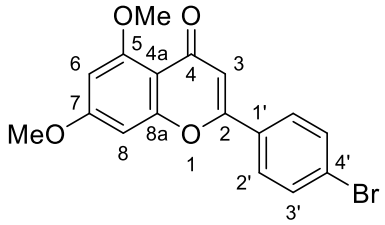

161

7.2.2.4.13 2-(3-Bromophenyl)-5,7-dimethoxy-4*H*-chromen-4-one (162)

The title compound was synthesized in accordance with **GP2** with chalcone **147** (100 mg, 1.0 equiv, 0.275 mmol) and I_2 (78.8 mM, 142 µL, 4 mol%, 0.0110 mmol). The product was isolated as white solids in a yield of 84.9 mg (0.235 mmol, 85%). The analytical data were in accordance with literature.[319]

^{1}H NMR (600 MHz, $CDCl_3$): δ 3.92 (s, 3H, OMe), 3.96 (s, 3H, OMe), 6.39 (d, $^4J_{6\text{-}8}$ = 2.3 Hz, 1H, 6-H), 6.58 (d, $^4J_{6\text{-}8}$ = 2.3 Hz, 1H, 8-H), 6.65 (s, 1H, 3-H), 7.37 (t, $^3J_{4'\text{-}5',5'\text{-}6'}$ = 7.9 Hz, 1H, 5'-H), 7.63 (dd, $^3J_{4',5'}$ = 8.0 Hz, $^4J_{2'\text{-}4'}$ = 1.5 Hz, 1H, 4'-H), 7.77 (dt, $^3J_{6'\text{-}5'}$ = 7.9 Hz, $^4J_{2'\text{-}6'}$ = 1.4 Hz, 1H, 6'-H), 8.03 (d, $^4J_{2'\text{-}4',2'\text{-}6'}$ = 1.9 Hz, 1H, 2'-H). **^{13}C NMR** (151 MHz, $CDCl_3$): δ 55.82 (OMe), 56.46 (OMe), 92.85 (C-8), 96.41 (C-6), 109.35 (C-4a), 109.75 (C-3), 123.16 (C-2'), 124.50 (C-6'), 128.93 (C-2'), 130.45 (C-5'), 133.66 (C-1'), 134.00 (C-4'), 158.95 (C-8a), 159.84 (C-5), 161.00 (C-2), 164.26 (C-7), 177.21 (CO). **IR (ATR film) [cm^{-1}]:** 2949, 1649, 1609, 1571, 1489, 1421, 1384, 1268, 1201, 1160, 1115, 1099, 1063, 1024, 910, 854, 825, 764, 728, 636, 611, 566, 554, 531, 504, 480. **HR-MS (ESI):** m/z calculated for $[C_{17}H_{14}O_4Br]^+$ ($[M + H^+]$): 361.0070, found: 361.0077. **Melting point:** 134 – 136 °C (278 – 280 °C)[320] The melting point diverged strongly from the literature reported value.

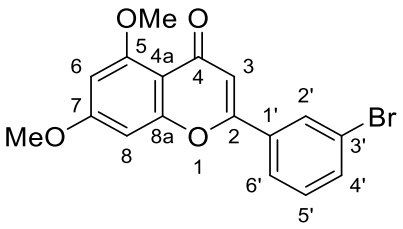

162

7.2.2.4.14 2-(2-Bromophenyl)-5,7-dimethoxy-4*H*-chromen-4-one (163)

The title compound was synthesized in accordance with **GP2** with chalcone **148** (100 mg, 1.0 equiv, 0.275 mmol) and I_2 (78.8 mM, 142 µL, 4 mol%, 0.0110 mmol). The product was isolated as white solids in a yield of 292.3 mg (0.255 mmol, 92%).

^{1}H NMR (600 MHz, $CDCl_3$): δ 3.88 (s, 3H, OMe), 3.96 (s, 3H, OMe), 6.39 (d, $^4J_{6\text{-}8}$ = 2.3 Hz, 1H, 6-H), 6.43 (s, 1H, 3-H), 6.50 (d, $^4J_{6\text{-}8}$ = 2.3 Hz, 1H, 8-H), 7.35 (td, $^3J_{3'\text{-}4',4'\text{-}5'}$ = 7.7 Hz, $^4J_{4'\text{-}6'}$ = 1.7 Hz, 1H, 4'-H), 7.43 (td, $^3J_{4'\text{-}5',5'\text{-}6'}$ = 7.5 Hz, $^4J_{3'\text{-}5'}$ = 1.2 Hz, 1H, 5'-H), 7.54 (dd, $^3J_{5'\text{-}6'}$ = 7.6 Hz, $^4J_{4'\text{-}6'}$ = 1.7 Hz, 1H, 6'-H), 7.70 (dd, $^3J_{3'\text{-}4'}$ = 8.1 Hz, $^4J_{3'\text{-}5'}$ = 1.2 Hz, 1H, 3'-H). **^{13}C NMR** (151 MHz, $CDCl_3$): δ 55.89 (OMe), 56.59 (OMe), 92.99 (C-8), 96.51 (C-6), 109.48 (C-3), 114.41 (C-4a), 122.05 (C-2'), 127.71 (C-5'), 130.98 (C-6'), 131.80 (C-4'), 133.97 (C-1'), 134.02 (C-3'), 160.35 (C-7), 161.20 (C-8a), 161.34 (C-2), 164.35 (C-5), 177.28 (CO). **IR (ATR film) [cm^{-1}]:** 2843, 1644, 1607, 1489, 1459, 1421, 1383, 1334, 1306, 1269, 1217, 1202, 1161, 1119, 1101, 1079, 1057, 1028, 997, 965, 953, 916, 876, 846, 824, 790, 772, 754, 726, 692, 674, 643, 616, 566, 529, 483 **HR-MS (ESI):** m/z calculated for $[C_{17}H_{14}O_4Br]^+$ ($[M + H^+]$): 361.0070, found: 361.0074. **Melting point:** 162 – 163 °C

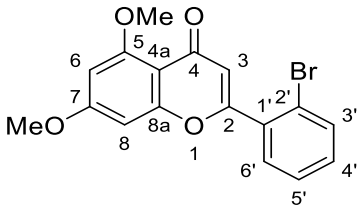

163

7.2.2.5 General Procedure 3 (GP3): Bichalcones

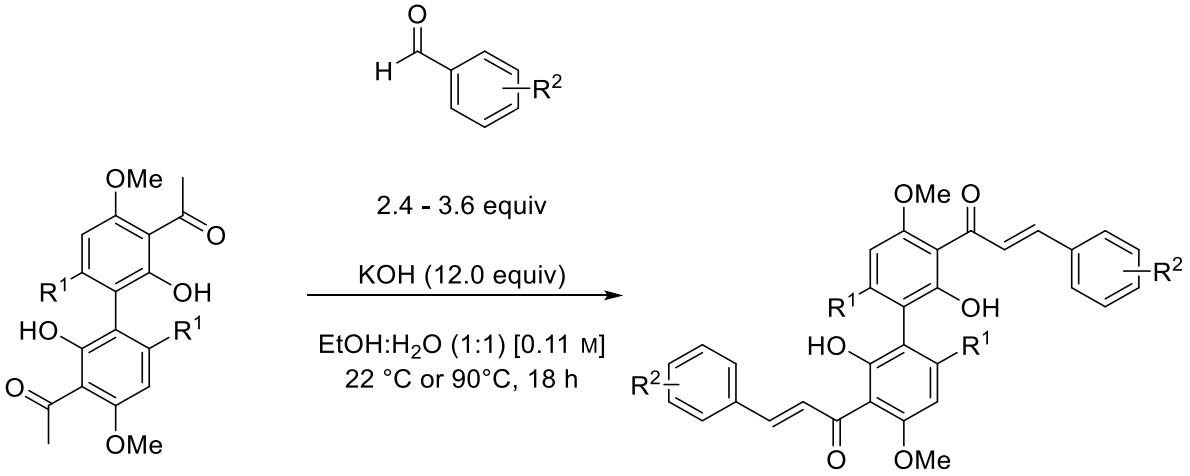

A vial equipped with stir bar was charged with acetophenone dimer (200 mg, 1.0 equiv), ethanol (0.22 M) and aq. KOH solution (3 M, 12.0 equiv). The mixture was stirred for 5 min until all solids were dissolved. Aldehyde (2.4 equiv) was added at once. The reaction was stirred at room temperature unless stated otherwise. If stated, after 6 h another portion of aldehyde was added (1.2 equiv). The reaction mixture was left to stir over night unless stated otherwise. Reaction control was performed by TLC and ^{1}H-NMR. After the completion of the reaction aq. HCl (1 M, 10 mL) was added unless stated otherwise. Solids precipitate, which were collected by filtration over a pad of Celite® washing the solids with methanol (1 mL). The solids were then dissolved in CH_2Cl_2, MeOH (10% v/v) was added, and the solvent removed *in vacuo*. The product was isolated by washing with MeOH (10 mL) at 22 °C and discarding the wash solution.

7.2.2.5.1 *rac*-(2*E*,2'*E*)-1,1'-(2,2'-Dihydroxy-4,4'-dimethoxy-6,6'-dimethyl-[1,1'-biphenyl]-3,3'-diyl)bis(3-(4-methoxyphenyl)prop-2-en-1-one) (165)

The title compound was synthesized in accordance with **GP3** with acetophenone **134** (200 mg, 1.0 equiv, 0.558 mmol) and 4-methoxybenzaldehyde (0.244 mL, 2.4 equiv + 1.2 equiv, 2.01 mmol). The product was isolated as orange solids in a yield of 278 mg (0.467 mmol, 83%).

^{1}H NMR (600 MHz, $CDCl_3$): δ 2.11 (s, 6H, Me), 3.86 (s, 6H, OMe), 3.99 (s, 6H, OMe), 6.43 (s, 2H, 5-H), 6.94 (d, $^3J_{2'\text{-}3'}$ = 8.7 Hz, 4H, 3'-H), 7.58 (d, $^3J_{2'\text{-}3'}$ = 8.7 Hz, 4H, 2'-H), 7.79 (d, $^3J_{5'\text{-}6'}$ = 15.6 Hz, 2H, 5'-H), 7.84 (d, $^3J_{5'\text{-}6'}$ = 15.6 Hz, 2H, 6'-H), 13.80 (s, 2H, OH). **^{13}C NMR** (151 MHz, $CDCl_3$): δ 20.87 (Me), 55.40 (OMe), 55.77 (OMe), 103.30 (C-5), 109.96 (C-1), 114.38 (C-3'), 117.73 (C-3), 125.66 (C-6'), 128.37 (C-1'), 130.16 (C-2'), 142.50 (C-5'), 147.05 (C-6), 160.12 (C-4), 161.41 (C-4'/2), 162.70 (C-2/4'), 194.03 (CO). **IR (ATR film) [cm^{-1}]:** 2970, 2839, 1623, 1603, 1558, 1510, 1464, 1422, 1363, 1327, 1304, 1291, 1256, 1216, 1170, 1114, 1037, 908, 871, 828, 770, 647, 619, 559, 536, 521, 487. **HR-MS (ESI):** m/z

calculated for $[C_{36}H_{35}O_8]^+$ ([M + H^+]): 595.2327, found: 595.2335. **Melting point:** 212 – 214 °C

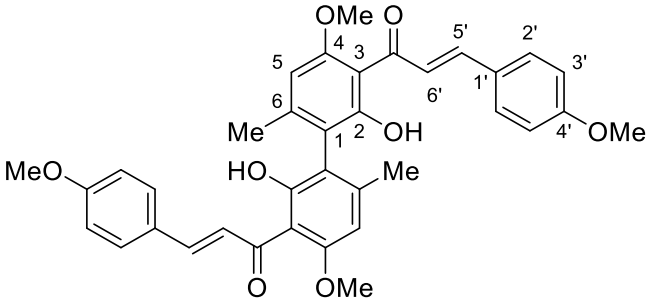

165

7.2.2.5.2 *rac*-(2*E*,2'*E*)-1,1'-(2,2'-Dihydroxy-4,4'-dimethoxy-6,6'-dimethyl-[1,1'-biphenyl]-3,3'-diyl)bis(3-phenylprop-2-en-1-one) (166)

The title compound was synthesized in accordance with **GP3** with biacetophenone **134** (200 mg, 1.0 equiv, 0.558 mmol) and benzaldehyde (0.205 mL, 2.4 equiv + 1.2 equiv, 2.01 mmol). The product was isolated as orange solids in a yield of 263 mg (0.492 mmol, 88%).

A vial equipped with a stir bar was charged with biacetophenone **134** (100 mg, 0.279 mmol, 1.0 equiv, >99%*ee* S_a) and ethanol (1.0 mL, 0.28 M) and an aqueous solution of KOH (1.12 mL, 3.35 mmol, 12.0 equiv). Once fully dissolved, benzaldehyde (67.7 µL, 0.670 mmol, 2.4 equiv) were added at once. The mixture was stirred for 4 h at 22 °C after which aq. HCl-solution (1 M, 4 mL) was added. The forming solids were filtered off and washed with MeOH:H_2O (8:2, 10 mL). The solids were then dissolved into a round bottom flask using CH_2Cl_2 and solvents removed in vacuo. The product was isolated by column chromatography (100% CH_2Cl_2). The isolated product was suspended in *n*-pentane (2 × 5 mL) and sonicated to remove traces of CH_2Cl_2. The solvent was then removed in vacuo. The product was isolated as orange amorphous solids in a yield of 81.0 mg (0.152 mmol, 54%, >99%*ee* S_a).

In a repeat experiment starting from (100 mg, 0.279 mmol, 1.0 equiv, >99%*ee* R_a) the product was isolated as orange amorphous solids in a yield of 91.1 mg (0.170 mmol, 61%, >99%*ee* R_a).

^{1}H NMR (600 MHz, $CDCl_3$): δ 2.12 (s, 6H, Me), 4.00 (s, 6H, OMe), 6.44 (s, 2H, 5-H), 7.37 – 7.45 (m, 6H, 3'+4'-H), 7.59 – 7.65 (m, 4H, 2'-H), 7.80 (d, $^3J_{5',6'}$ = 15.6 Hz, 2H, 5'-H), 7.94 (d, $^3J_{5',6'}$ = 15.6 Hz, 2H, 6'-H), 13.71 (s, 2H, OH). **^{13}C NMR** (151 MHz, $CDCl_3$): δ 21.06 (Me),

55.96 (OMe), 103.50 (C-5), 110.07 (C-3), 117.82 (C-1), 128.16 (C-6'), 128.56 (C-2'), 129.04 (C-3'), 130.24 (C-4'), 135.76 (C-1'), 142.55 (C-5'), 147.57 (C-6), 160.38 (C-4), 162.89 (C-2), 194.30 (CO). **IR (ATR film) [cm^{-1}]:** 3104, 3026, 2970, 2942, 2250, 1628, 1609, 1564, 1448, 1388, 1361, 1329, 1272, 1214, 1179, 1115, 1073, 1038, 976, 948, 907, 869, 817, 789, 758, 725, 688, 647, 565, 534, 494. **TLC** (100% CH_2Cl_2): R_f = 0.36 (yellow spot) **HR-MS (ESI):** m/z calculated for $[C_{34}H_{31}O_6]^+$ ([M + H$^+$]): 535.2115, found: 535.2122.

Melting point: 213 – 215 °C (*rac*)

190 – 192 °C (S_a)

191 – 192 °C (R_a)

Elemental analysis (calcd., found for $C_{34}H_{30}O_6$): C (76.39, 76.31), H (5.66, 5.59). (*rac*)

Elemental analysis (calcd., found for $C_{34}H_{30}O_6$): C (76.39, 76.13), H (5.66, 5.62). (S_a)

Elemental analysis (calcd., found for $C_{34}H_{30}O_6$): C (76.39, 75.91), H (5.66, 5.72). (R_a)

Chiral HPLC: >99% ee (S_a)

>99% ee (R_a)

Purity: >99% (normal phase HPLC), >99% (reversed phase HPLC) (S_a)

>99% (normal phase HPLC), >99% (reversed phase HPLC) (R_a)

96% (reversed phase HPLC), (elemental Analysis) (*rac*)

Optical rotation: $[\alpha]^{20}_D$ = +128.7 (±0.1, duplicate) (*c* = 0.964, $CHCl_3$, S_a, >99%*ee*)

HPLC: Lux® Amylose-1 (*Phenomenex*) 250 ° 4.6 mm, 25 °C, 0.5 mL min^{-1}, 331 nm, *n*-heptane:*i*-propanol 50:50 (v/v): $t_R(S_a)$ = 14.7 min, $t_R(R_a)$ = 24.2 min.

X-ray: 166 was dissolved in a glass vial in EtOH, layered with *n*-pentane and solvent left to mix at 22 °C over time sealed with a plastic cap. CCDC 2342256

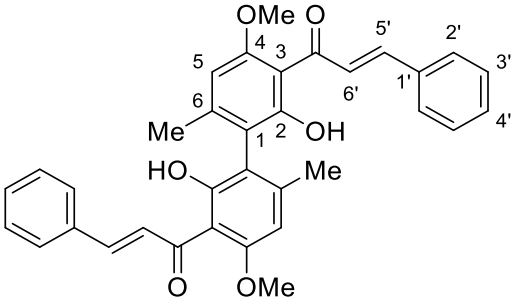

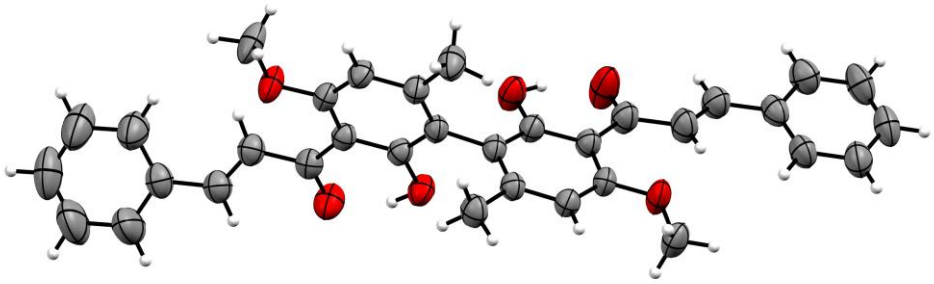

166

CCDC 2342256

Figure 30: *rac*-bichalcone **166**. Top: Lewis structure interpretation Bottom: Crystal structure shown as Oak Ridge Thermal Ellipsoid Plot (ORTEP) of the racemic mixture, ellipsoids are shown at 50% probability. Detailed information can be found in cif-format under the given CCDC deposition number.

7.2.2.5.3 *rac*-(2*E*,2'*E*)-1,1'-(2,2'-Dihydroxy-4,4'-dimethoxy-6,6'-dimethyl-[1,1'-biphenyl]-3,3'-diyl)bis(3-(4-(dimethylamino)phenyl)prop-2-en-1-one) (167)

The title compound was synthesized in accordance with **GP3** with acetophenone **134** (200 mg, 1.0 equiv, 0.558 mmol) and 4-(dimethylamino)benzaldehyde (200 mg, 1.34 mmol, 2.4 equiv) at 90 °C. The product was isolated as red solids in a yield of 175 mg (0.282 mmol, 50%).

Scale up: A 50 mL round bottom flask was charged with acetophenone **134** (1.00 g, 1.0 equiv, 2.79 mmol), 4-(dimethylamino)benzaldehyde (1.00 g, 2.4 equiv, 6.69 mmol) and EtOH (10 mL). Aq. KOH-solution was added (3 M, 11.0 mL, 12.0 equiv, 33.5 mmol). The reaction mixture was stirred at 90 °C. After 24 h, 4-(dimethylamino)benzaldehyde (500 mg, 1.2 equiv, 3.35 mmol) was added. After an additional 24 h heating was stopped, KPi-buffer (1 M, pH 7, 20 mL) was added. The organic phases were extracted using CH_2Cl_2 (3x 100 mL). The combined organic phases were washed with sat. aq. NaCl-solution (50 mL) and dried over $MgSO_4$. The solvent was removed *in vacuo*. The mixture was then resuspended in MeOH (10 mL). Aq. KOH-solution was added (3 M, 11.0 mL, 12.0 equiv, 33.5 mmol). Then 4-(dimethylamino)benzaldehyde (500 mg, 1.2 equiv, 3.35 mmol) was added and the mixture stirred at 90 °C for 16 h. the reaction was stopped, KPi-buffer (1 M, pH 7, 20 mL) was added. The organic phases were extracted using CH_2Cl_2 (3x 100 mL). The combined organic phases

were washed with sat. aq. NaCl-solution (50 mL) and dried over $MgSO_4$. MeOH (15 mL) was added to the solution and the solvent was carefully removed *in vacuo*. The resulting mixture was macerated with MeOH (15 mL). The solids were filtered off and washed with copious amounts of MeOH. The product was obtained as red solids in a yield of 607 mg (0.978 mmol, 35%).

^{1}H NMR (600 MHz, $CDCl_3$): δ 2.10 (s, 6H, Me), 3.04 (s, 12H, NMe_2), 3.98 (s, 6H, OMe), 6.41 (s, 2H, 5-H), 6.70 (d, $^3J_{2'\text{-}3'}$ = 8.6 Hz, 4H, 3'-H), 7.53 (d, $^3J_{2'\text{-}3'}$ = 8.5 Hz, 4H, 2'-H), 7.78 (d, $^3J_{5'\text{-}6'}$ = 15.4 Hz, 2H, 5'-H), 7.84 (d, $^3J_{5'\text{-}6'}$ = 15.5 Hz, 2H, 6'-H), 13.96 (s, 2H, OH). **^{13}C NMR** (151 MHz, $CDCl_3$): δ 20.98 (Me), 40.30 (NMe_2), 55.87 (OMe), 103.40 (C-5), 110.29 (C-3), 112.07 (C-3'), 118.01 (C-1), 122.95 (C-6'), 123.69 (C-1'), 130.54 (C-2'), 144.05 (C-5'), 146.58 (C-4), 152.03 (C-4'), 160.15 (C-6), 162.83 (C-2), 193.97 (CO). **IR (ATR film) [cm^{-1}]:** 1602, 1543, 1525, 1472, 1445, 1414, 1364, 1316, 1298, 1228, 1211, 1167, 1113, 1067, 979, 947, 866, 815, 732, 703, 651, 613, 569, 541, 469. **HR-MS (ESI):** m/z calculated for $[C_{38}H_{41}N_2O_6]^+$ ([M + H$^+$]): 621.2959, found: 621.2962. **Melting point:** 265 °C (decomposition)

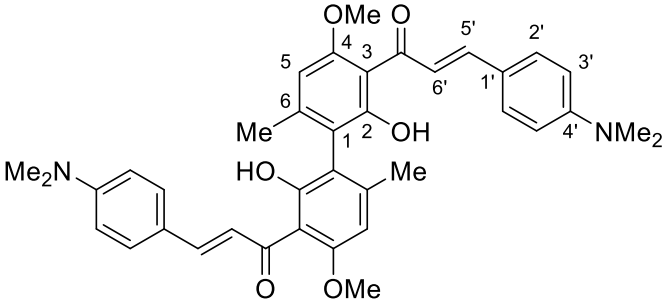

167

7.2.2.5.4 *rac*-(2*E*,2'*E*)-1,1'-(2,2'-Dihydroxy-4,4'-dimethoxy-6,6'-dimethyl-[1,1'-biphenyl]-3,3'-diyl)bis(3-(4-(trifluoromethyl)phenyl)prop-2-en-1-one) (168)

The title compound was synthesized in accordance with **GP3** with acetophenone **134** (200 mg, 1.0 equiv, 0.558 mmol) and 4-(trifluoromethyl)benzaldehyde (0.274 mL, 2.4 equiv + 1.2 equiv, 2.01 mmol). The product was isolated as orange solids in a yield of 232 mg (0.346 mmol, 62%).

^{1}H NMR (600 MHz, $CDCl_3$): δ 2.12 (s, 6H, Me), 4.00 (s, 6H, OMe), 6.45 (s, 2H, 5-H), 7.67 (d, $^3J_{2'\text{-}3'}$ = 8.2 Hz, 4H, 3'-H), 7.71 (d, $^3J_{2'\text{-}3'}$ = 8.1 Hz, 4H, 3'-H), 7.76 (d, $^3J_{5'\text{-}6'}$ = 15.6 Hz, 2H, 5'-H), 7.97 (d, $^3J_{5'\text{-}6'}$ = 15.7 Hz, 2H, 6'-H), 13.59 (s, 2H, OH). **^{13}C NMR** (151 MHz, $CDCl_3$): δ 21.10 (Me), 56.03 (OMe), 103.55 (C-5), 109.97 (C-3), 117.77 (C-1), 124.09 (q, $^1J_{F\text{-}C}$ = 271.5,

CF_3), 126.00 (q, $^3J_{F\text{-}C}$ = 3.8 Hz, C-3'), 128.54 (C-2'), 130.49 (C-6'), 131.65 (q, $^2J_{F\text{-}C}$ = 33.4 Hz, C-2'), 139.17 (C-1'), 140.30 (C-5'), 148.08 (C-4), 160.41 (C-6), 162.94 (C-2), 193.93 (CO). **^{19}F NMR** (282 MHz, $CDCl_3$): δ -62.76. **IR (ATR film) [cm^{-1}]:** 2946, 2852, 1609, 1570, 1481, 1452, 1414, 1389, 1362, 1321, 1288, 1273, 1216, 1180, 1116, 1068, 1034, 1017, 979, 954, 834, 734, 716, 673, 652, 593, 571, 535. **HR-MS (ESI):** m/z calculated for $[C_{36}H_{29}F_6O_6]^+$ ($[M + H^+]$): 671.1863, found: 671.1866. **Melting point:** 208 – 209 °C

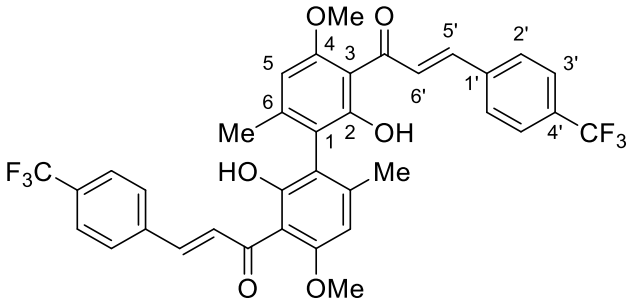

168

7.2.2.5.5 *rac*-(2*E*,2'*E*)-1,1'-(2,2'-Dihydroxy-4,4'-dimethoxy-6,6'-dimethyl-[1,1'-biphenyl]-3,3'-diyl)bis(3-(4-bromophenyl)prop-2-en-1-one) (169)

The title compound was synthesized in accordance with **GP3** with acetophenone **134** (200 mg, 1.0 equiv, 0.558 mmol) and 4-bromobenzaldehyde (248 mg, 2.4 equiv, 1.34 mmol). The product was isolated as orange solids in a yield of 364 mg (0.527 mmol, 94%).

A further experiment using biaryl **134** (1.43 g, 1.0 equiv, 4.00 mmol, *rac*) gave the product as orange crystalline solids (2.67 g, 3.88 mmol, 97%, *rac*). After the addition of HCl-solution, the solids were filtered off, washed with water and then MeOH (10 mL). The solids were then dissolved using CH_2Cl_2, washed with sat. aq. NaCl solution and dried over $MgSO_4$. MeOH was added (10 mL) and the solvents carefully removed in vacuo. The analytical data were in accordance with literature.[108b]

^{1}H NMR (600 MHz, $CDCl_3$): δ 2.11 (s, 6H, Me), 3.99 (s, 6H, OMe), 6.43 (s, 2H, 5-H), 7.47 (d, $^3J_{2',3'}$ = 8.5 Hz, 4H, 2'-H), 7.54 (d, $^3J_{2',3'}$ = 8.4 Hz, 3H, 3'-H), 7.71 (d, $^3J_{5',6'}$ = 15.6 Hz, 2H, 5'-H), 7.90 (d, $^3J_{5',6'}$ = 15.6 Hz, 2H, 6'-H), 13.65 (s, 2H, OH). **^{13}C NMR** (151 MHz, $CDCl_3$): δ 21.06 (Me), 56.00 (OMe), 103.51 (C-5), 110.00 (C-3), 117.80 (C-1), 124.43 (C-4'), 128.73 (C-6'), 129.88 (C-2'), 132.29 (C-3'), 134.68 (C-1'), 141.07 (C-5'), 147.79 (C-6), 160.35 (C-4), 162.90 (C-2), 194.02 (CO). **IR (ATR film) [cm^{-1}]:** 2970, 2941, 2848, 2251, 1627, 1605, 1559, 1485, 1389, 1359, 1323, 1213, 1178, 1141, 1114, 1072, 1035, 1009, 979, 946, 908, 875, 819,

801, 786, 731, 648, 632, 604, 571, 535, 507, 491. **HR-MS (ESI):** m/z calculated for $[C_{34}H_{29}O_6Br_2]^+$ ($[M + H^+]$): 691.0325, found: 691.0324.

Melting point: 230 – 236 °C (*rac*)

233 – 237 °C (decomposition) (S_a, >99%*ee* HPLC)

227 – 230 °C (decomposition) (R_a, >99%*ee* HPLC)

HPLC: CHIRALPAK® IA (Daciel) 250 ° 4.6 mm, 25 °C, 0.5 mL min^{-1}, 335 nm, *n*-heptane:*i*-PrOH 50:50 (v/v) $t_R(S_a)$ = 25.5 min, $t_R(R_a)$ = 40.9 min

Optical rotation: $[\alpha]^{25}_D$ = +69.4 (±0.6, duplicate) (c = 1.01, $CHCl_3$, S_a, >99%*ee* by chiral HPLC)

X-ray: (*R*)-**169** was dissolved in $CDCl_3$, filtered over a syringe filter into a vial and the solvent left to evaporate over time. CCDC 2342250

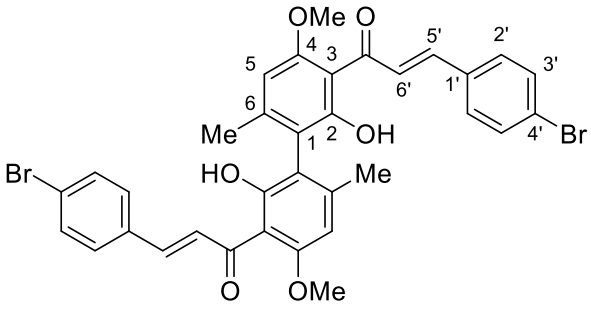

169

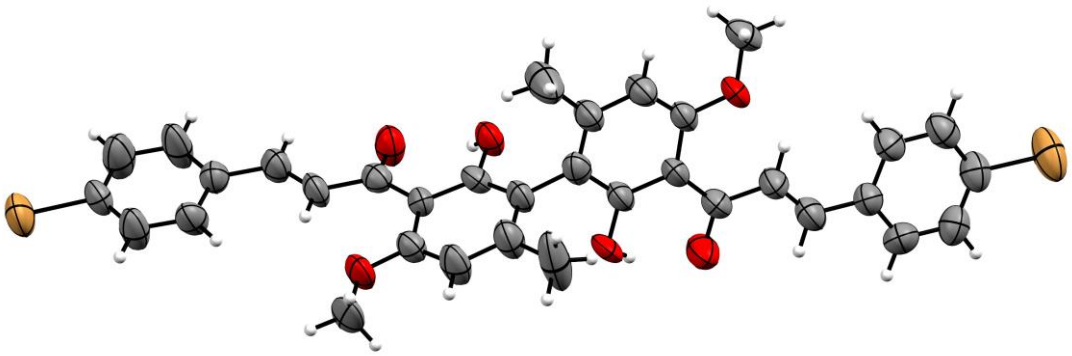

(*R*)-**169 isomer 1**

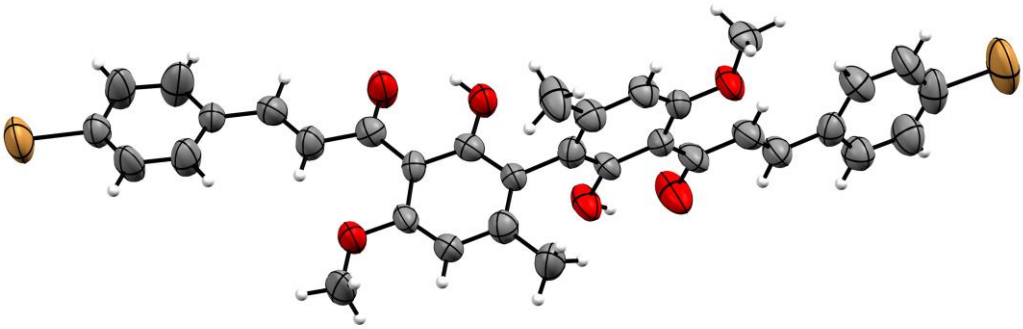

(*R*)-**169 isomer 2**

CCDC 2342250

Figure S1: Bichalcone **239**. Top Lewis structure interpretation Middle and bottom: Crystal structure (two conformers) shown as Oak Ridge Thermal Ellipsoid Plot (ORTEP) of the (*R*)-enantiomer, ellipsoids are shown at 50% probability. Detailed information can be found in cif-format under the given CCDC deposition number.

7.2.2.5.6 *rac*-(2*E*,2'*E*)-1,1'-(2,2'-Dihydroxy-4,4'-dimethoxy-6,6'-dimethyl-[1,1'-biphenyl]-3,3'-diyl)bis(3-(3-bromophenyl)prop-2-en-1-one) (170)

The title compound was synthesized in accordance with **GP3** with acetophenone **134** (200 mg, 1.0 equiv, 0.558 mmol) and 3-bromobenzaldehyde (0.156 mL, 2.4 equiv, 1.34 mmol). The product was isolated as orange solids in a yield of 335 mg (0.484 mmol, 86%).

^{1}H NMR (600 MHz, $CDCl_3$): δ 2.11 (s, 6H, Me), 4.00 (s, 6H, OMe), 6.44 (s, 2H, 5-H), 7.29 (t, $^{3}J_{4'\text{-}5',5'\text{-}6'}$ = 7.8 Hz, 2H, 5'-H), 7.51 (dt, J = 8.1, 1.5 Hz, 4H, 4'+6'-H), 7.68 (d, $^{3}J_{7'\text{-}8'}$ = 15.6 Hz, 2H, 7'-H), 7.74 (t, $^{4}J_{2'\text{-}4',2'\text{-}6'}$ = 1.8 Hz, 2H, 2'-H), 7.89 (d, $^{3}J_{7'\text{-}8'}$ = 15.6 Hz, 2H, 8'-H), 13.63 (s, 2H, OH). **^{13}C NMR** (151 MHz, $CDCl_3$): δ 21.09 (Me), 56.04 (OMe), 103.51 (C-5), 109.92 (C-3), 117.71 (C-1), 123.15 (C-3'), 127.20 (C-8'), 129.43 (C-6'), 130.53 (C-5'), 131.06 (C-2'), 132.94 (C-4'), 137.88 (C-1'), 140.62 (C-7'), 147.92 (C-6), 160.37 (C-4), 162.90 (C-2), 193.93 (CO). **IR (ATR film) [cm^{-1}]:** 2922, 1630, 1469, 1389, 1323, 1274, 1180, 1116, 1035, 907, 864, 795, 778, 730, 648. **HR-MS (ESI):** m/z calculated for $[C_{34}H_{29}O_6Br_2]^+$ ([M + H$^+$]): 691.0325, found: 691.0324. **Melting point:** 110 °C (decomposition)

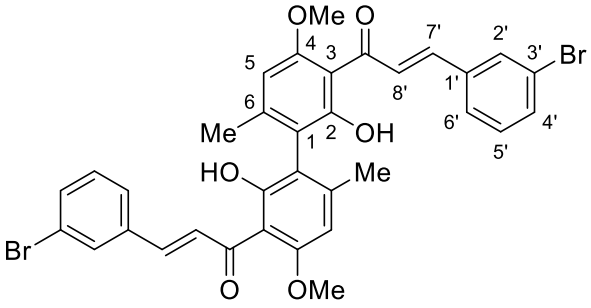

170

7.2.2.5.7 *rac*-(2*E*,2*'E*)-1,1'-(2,2'-Dihydroxy-4,4'-dimethoxy-6,6'-dimethyl-[1,1'-biphenyl]-3,3'-diyl)bis(3-(2-bromophenyl)prop-2-en-1-one) (171)

The title compound was synthesized in accordance with **GP3** with acetophenone **134** (200 mg, 1.0 equiv, 0.558 mmol) and 2-bromobenzaldehyde (0.156 mL, 2.4 equiv, 1.34 mmol). The product was isolated as orange solids in a yield of 253 mg (0.365 mmol, 65%).

^{1}H NMR (600 MHz, $CDCl_3$): δ 2.11 (s, 6H, Me), 3.98 (s, 6H, OMe), 6.43 (s, 2H, 5-H), 7.24 (td, $^3J_{3'\text{-}4',4'\text{-}5'}$ = 7.7 Hz, $^4J_{4'\text{-}6'}$ = 1.6 Hz, 2H, 4'-H), 7.36 (td, $^3J_{4'\text{-}5',5'\text{-}6'}$ = 7.4 Hz, $^4J_{3'\text{-}5'}$ = 1.0 Hz, 2H, 5'-H), 7.64 (dd, $^3J_{3'\text{-}4'}$ = 8.0 Hz, $^4J_{3'\text{-}5'}$ = 1.3 Hz, 2H, 3'-H), 7.70 (dd, $^3J_{5'\text{-}6'}$ = 7.8 Hz, $^4J_{4'\text{-}6'}$ = 1.6 Hz, 2H, 6'-H), 7.85 (d, $^3J_{7'\text{-}8'}$ = 15.5 Hz, 2H, 7'-H), 8.11 (d, $^3J_{7'\text{-}8'}$ = 15.6 Hz, 2H, 8'-H), 13.61 (s, 2H, OH). **^{13}C NMR** (151 MHz, $CDCl_3$): δ 20.93 (Me), 55.83 (OMe), 103.33 (C-5), 109.85 (C-3), 117.63 (C-1), 125.88 (C-2'), 127.62 (C-5'), 127.96 (C-6'), 130.69 (C-8'), 130.86 (C-4'), 133.54 (C-3'), 135.70 (C-1'), 140.43 (C-7'), 147.70 (C-6), 160.21 (C-4), 162.79 (C-2), 193.76 (CO). **IR (ATR film) [cm^{-1}]:** 2851, 1610, 1573, 1465, 1361, 1214, 1180, 1117, 1027, 907, 730, 535. **HR-MS (ESI):** m/z calculated for $[C_{34}H_{29}O_6Br_2]^+$ ($[M + H^+]$): 691.0325, found: 691.0323. **TLC** (petroleum ether:EtOAc, 6:4 v/v): R_f = 0.44 **Melting point:** 220 – 221 °C

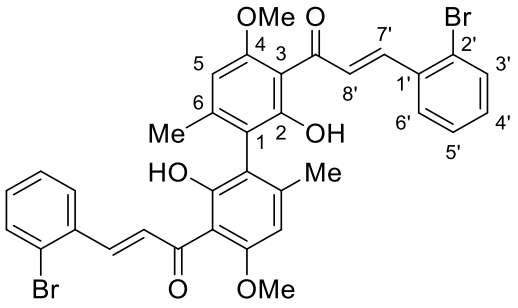

171

7.2.2.5.8 *rac*-(2*E*,2'*E*)-1,1'-(2,2'-Dihydroxy-4,4',6,6'-tetramethoxy-[1,1'-biphenyl]-3,3'-diyl)bis(3-(4-methoxyphenyl)prop-2-en-1-one) (172)

The title compound was synthesized in accordance with **GP3** with acetophenone **49** (200 mg, 1.0 equiv, 0.512 mmol) and 4-methoxybenzaldehyde (0.149 mL, 2.4 equiv, 1.23 mmol). The product was isolated as yellow solids in a yield of 145 mg (0.231 mmol, 45%). The analytical data is in accordance with literature.[113b]

^{1}H NMR (600 MHz, $CDCl_3$): δ 3.86 (s, 12H, OMe), 4.01 (s, 6H, OMe), 6.14 (s, 2H, 5-H), 6.93 (d, $^3J_{2',3'}$ = 8.6 Hz, 4H, 3'-H), 7.56 (d, $^3J_{2',3'}$ = 8.5 Hz, 4H, 2'-H), 7.76 (d, $^3J_{5',6'}$ = 15.5 Hz, 2H, 5'-H), 7.82 (d, $^3J_{5',6'}$ = 15.6 Hz, 2H, 6'-H), 14.20 (s, 2H, OH). **^{13}C NMR** (151 MHz, $CDCl_3$): δ 55.55 (OMe), 55.98 (OMe), 56.08 (OMe), 87.20 (C-5), 103.27 (C-1), 106.93 (C-3), 114.50 (C-3'), 125.90 (C-6'), 128.69 (C-1'), 130.18 (C-2'), 142.07 (C-5'), 161.40 (C-4/6/4'), 162.93 (C-4/6/4'), 164.02 (C-4/6/4'), 164.78 (C-2), 193.18 (CO). **IR (ATR film) [cm^{-1}]:** 1739, 1622, 1604, 1510, 1466, 1407, 1371, 1290, 1255, 1215, 1171, 1122, 829, 801, 776, 603, 559, 539, 520. **HR-MS (ESI):** m/z calculated for $[C_{36}H_{35}O_{10}]^+$ ($[M + H^+]$): 627.2225, found: 627.2227. **Melting point:** 284 – 285 °C (282 – 285 °C)[113b]

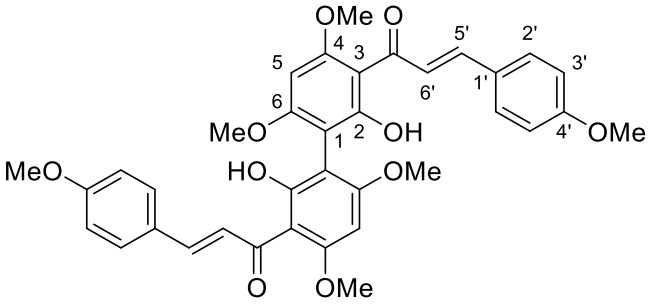

172

7.2.2.5.9 *rac*-(2*E*,2'*E*)-1,1'-(2,2'-Dihydroxy-4,4',6,6'-tetramethoxy-[1,1'-biphenyl]-3,3'-diyl)bis(3-phenylprop-2-en-1-one) (173)

The title compound was synthesized in accordance with **GP3** with acetophenone **49** (200 mg, 1.0 equiv, 0.512 mmol) and benzaldehyde (0.188 mL, 2.4 equiv + 1.2 equiv, 1.84 mmol). The product was isolated as yellow solids in a yield of 65.8 mg (0.116 mmol, 23%).

^{1}H NMR (600 MHz, $CDCl_3$): δ 3.86 (s, 6H, OMe), 4.02 (s, 6H, NMe_2), 6.15 (s, 2H, 5-H), 7.37 – 7.44 (m, 6H, 3'+4'-H), 7.61 (d, $^3J_{2',3'}$ = 7.1 Hz, 4H, 2'-H), 7.77 (d, $^3J_{5',6'}$ = 15.6 Hz, 2H, 5'-H), 7.91 (d, $^3J_{5',6'}$ = 15.6 Hz, 2H, 6'-H), 14.11 (s, 2H, OH). **^{13}C NMR** (151 MHz, $CDCl_3$): δ 56.00 (OMe), 56.10 (OMe), 87.20 (C-5), 103.20 (C-1), 106.90 (C-3), 128.25 (C-6'), 128.47 (C-

2'), 129.00 (C-3'), 130.04 (C-4'), 135.94 (C-1'), 141.97 (C-5'), 163.06 (C-4/6), 164.25 (C-4/6), 164.80 (C-2), 193.25 (CO). **IR (ATR film) [cm^{-1}]:** 2918, 2850, 1737, 1617, 1560, 1470, 1450, 1435, 1373, 1331, 1287, 1217, 1179, 1155, 1122, 1037, 870, 804, 762, 726, 703, 685, 662, 633, 576, 532, 477. **HR-MS (ESI):** m/z calculated for $[C_{34}H_{31}O_8]^+$ ([M + H$^+$]): 567.2013, found: 567.2020. **Melting point:** 272 °C (decomposition)

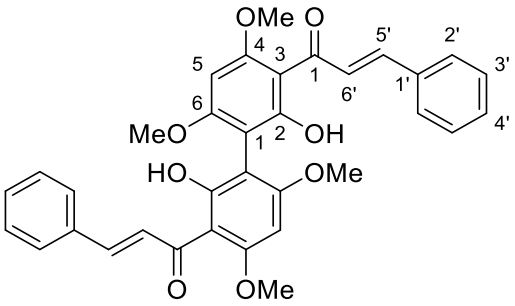

173

7.2.2.5.10 *rac*-(2*E*,2'*E*)-1,1'-(2,2'-Dihydroxy-4,4',6,6'-tetramethoxy-[1,1'-biphenyl]-3,3'-diyl)bis(3-(4-(dimethylamino)phenyl)prop-2-en-1-one) (174)

The title compound was synthesized in accordance with **GP3** with acetophenone **49** (200 mg, 1.0 equiv, 0.512 mmol) and 4-(dimethylamino)benzaldehyde (183 mg, 2.4 equiv, 1.23 mmol) at 90 °C. The product was isolated as red solids in a yield of 80.2 mg (0.123 mmol, 24%). (Due to poor solubility in $CDCl_3$, and d_6-DMSO only a ^{1}H NMR spectrum could be obtained.)

^{1}H NMR (600 MHz, $CDCl_3$): δ 3.04 (s, 12H, OMe), 3.84 (s, 6H, OMe), 4.00 (s, 6H), 6.13 (s, 2H), 6.70 (d, ^3J = 8.6 Hz, 4H), 7.52 (d, ^3J = 8.5 Hz, 4H), 7.76 (d, $^3J_{\text{E-alkene}}$ = 15.4 Hz, 2H), 7.81 (d, $^3J_{\text{E-alkene}}$ = 15.4 Hz, 2H), 14.37 (s, 2H, OH). **IR (ATR film) [cm^{-1}]:** 2850, 1598, 1542, 1527, 1467, 1434, 1411, 1370, 1334, 1295, 1214, 1168, 1114, 1038, 996, 982, 970, 863, 818, 776, 722, 702, 662, 605, 543. **HR-MS (ESI):** m/z calculated for $[C_{38}H_{41}N_2O_8]^+$ ([M + H$^+$]): 653.2857, found: 653.2851. **Melting point:** 303 °C (decomposition)

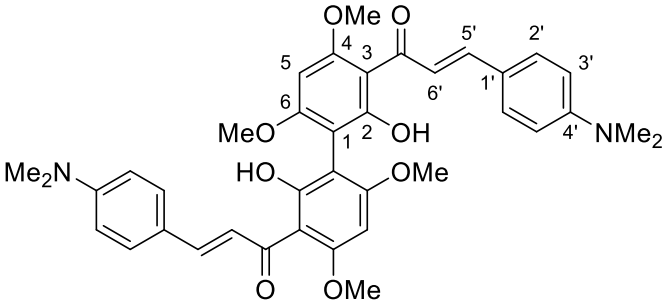

174

7.2.2.5.11 *rac*-(2*E*,2′*E*)-1,1'-(2,2'-Dihydroxy-4,4',6,6'-tetramethoxy-[1,1'-biphenyl]-3,3'-diyl)bis(3-(4-(trifluoromethyl)phenyl)prop-2-en-1-one) (175)

The title compound was synthesized in accordance with **GP3** with acetophenone **49** (200 mg, 1.0 equiv, 0.512 mmol) and 4-(trifluoromethyl)benzaldehyde (0.168 mL, 2.4 equiv, 1.23 mmol). The product was isolated as yellow solids in a yield of 95.0 mg (0.135 mmol, 27%).

^{1}H NMR (600 MHz, $CDCl_3$): δ 3.87 (s, 6H, OMe), 4.02 (s, 6H, OMe), 6.15 (s, 2H, 5-H), 7.66 (d, $^{3}J_{2'-3'}$ = 8.2 Hz, 4H, 3'-H), 7.69 (d, $^{3}J_{2'-3'}$ = 8.2 Hz, 4H, 2'-H), 7.73 (d, $^{3}J_{5'-6'}$ = 15.7 Hz, 2H, 5'-H), 7.94 (d, $^{3}J_{5'-6'}$ = 15.7 Hz, 2H, 6'-H), 13.99 (s, 2H, OH). **^{13}C NMR** (151 MHz, $CDCl_3$): δ 56.05 (OMe), 56.12 (OMe), 87.21 (C-5), 103.14 (C-1), 106.80 (C-3), 124.12 (q, $^{1}J_{F-C}$ = 271.3 Hz, CF_3), 125.96 (q, $^{3}J_{F-C}$ = 3.8 Hz, C-3'), 128.45 (C-2'), 130.61 (C-6'), 131.46 (q, $^{2}J_{F-C}$ = 32.7 Hz, C-4'), 139.36 (C-1'), 139.75 (C-5'), 163.13 (C-4/6), 164.57 (C-4/6), 164.83 (C-2), 192.79 (CO). **^{19}F NMR** (282 MHz, $CDCl_3$): δ -62.74. **IR (ATR film) [cm^{-1}]:** 2921, 2852, 1731, 1611, 1566, 1467, 1405, 1321, 1286, 1215, 1122, 1067, 1032, 1016, 954, 907, 834, 775, 732, 649, 597, 531. **HR-MS (ESI):** m/z calculated for $[C_{36}H_{29}F_6O_8]^+$ ([M + H$^+$]): 703.1761, found: 703.1767. **Melting point:** 251 °C (decomposition)

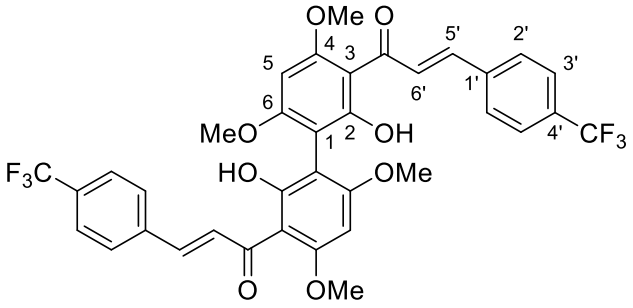

175

7.2.2.5.12 *rac*-(2*E*,2′*E*)-1,1'-(2,2'-Dihydroxy-4,4',6,6'-tetramethoxy-[1,1'-biphenyl]-3,3'-diyl)bis(3-(4-bromophenyl)prop-2-en-1-one) (176)

The title compound was synthesized in accordance with **GP3** with acetophenone **49** (200 mg, 1.0 equiv, 0.512 mmol) and 4-bromobenzaldehyde (227 mg, 2.4 equiv, 1.23 mmol). The product was isolated as yellow solids in a yield of 203 mg (0.280 mmol, 55%).

^{1}H NMR (600 MHz, $CDCl_3$): δ 3.86 (s, 6H, OMe), 4.01 (s, 6H, OMe), 6.14 (s, 2H, 5-H), 7.45 (d, $^3J_{2',3'}$ = 8.4 Hz, 4H, 3'-H), 7.53 (d, $^3J_{2',3'}$ = 8.3 Hz, 4H, 2'-H), 7.67 (d, $^3J_{5',6'}$ = 15.6 Hz, 2H, 5'-H), 7.88 (d, $^3J_{5',6'}$ = 15.6 Hz, 2H, 6'-H), 14.05 (s, 2H, OH). **^{13}C NMR** (151 MHz, $CDCl_3$): δ 56.03 (OMe), 56.10 (OMe), 87.20 (C-5), 103.17 (C-1), 106.83 (C-3), 124.19 (C-4'), 128.83 (C-6'), 129.79 (C-2'), 132.24 (C-3'), 134.86 (C-1'), 140.51 (C-5'), 163.05 (C-4/6), 164.38 (C-4/6), 164.80 (C-2), 192.92 (CO). **IR (ATR film) [cm^{-1}]:** 2918, 2850, 1738, 1628, 1556, 1486, 1471, 1436, 1399, 1372, 1328, 1291, 1214, 1180, 1154, 1090, 1073, 1033, 1009, 974, 820, 648, 631. **HR-MS (ESI):** m/z calculated for $[C_{34}H_{29}Br_2O_8]^+$ ($[M + H^+]$): 723.0220, found: 723.0224. **Melting point:** 274 °C (decomposition)

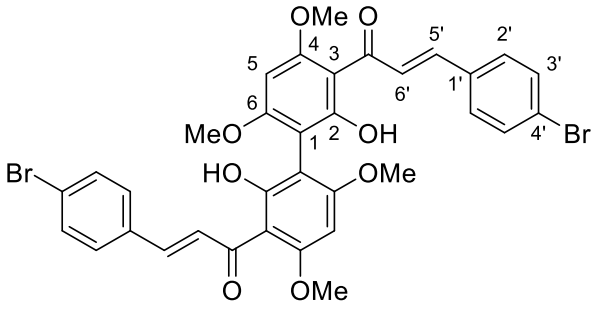

176

7.2.2.5.13 *rac*-(2*E*,2′*E*)-1,1'-(2,2'-Dihydroxy-4,4',6,6'-tetramethoxy-[1,1'-biphenyl]-3,3'-diyl)bis(3-(3-bromophenyl)prop-2-en-1-one) (177)

The title compound was synthesized in accordance with **GP3** with acetophenone **49** (200 mg, 1.0 equiv, 0.512 mmol) and 3-bromobenzaldehyde (0.143 mL, 2.4 equiv, 1.23 mmol). The product was obtained as yellow solids (124 mg). 3:1 Mix of Chalcone:Flavanone with mono-addition product present (according to ^{1}H-NMR).

^{1}H NMR (600 MHz, $CDCl_3$): δ 3.86 (s, 6H, OMe), 4.03 (s, 6H, OMe), 6.15 (s, 2H), 7.29 (t, *J* = 7.9 Hz, 2H), 7.50 (d, *J* = 7.8 Hz, 4H), 7.65 (d, $^3J_{\text{E-alkene}}$ = 15.5 Hz, 2H), 7.73 (s, 2H), 7.87 (d, $^3J_{\text{E-alkene}}$ = 15.6 Hz, 2H), 14.03 (s, 2H, OH). **HR-MS (ESI):** m/z calculated for $[C_{34}H_{29}Br_2O_8]^+$ ($[M + H^+]$): 723.0221, found: 723.0224.

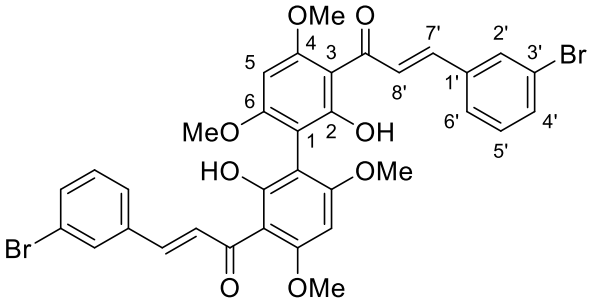

177

7.2.2.5.14 *rac*-(2*E*,2′*E*)-1,1'-(2,2'-Dihydroxy-4,4',6,6'-tetramethoxy-[1,1'-biphenyl]-3,3'-diyl)bis(3-(2-bromophenyl)prop-2-en-1-one) (178)

The title compound was synthesized in accordance with **GP3** with acetophenone **49** (200 mg, 1.0 equiv, 0.512 mmol) and 2-bromobenzaldehyde (0.143 mL, 2.4 equiv, 1.23 mmol), 1.5 h reaction time. The product was obtained as yellow solids (84.7 mg). 5:1 Mix of Chalcone:Flavanone with mono-addition product present (according to ^{1}H-NMR).

^{1}H NMR (600 MHz, $CDCl_3$): δ 3.86 (s, 6H, OMe), 4.00 (s, 6H, OMe), 6.13 (s, 2H), 7.22 (t, *J* = 7.7 Hz, 2H), 7.35 (t, *J* = 7.8 Hz, 2H), 7.63 (d, *J* = 8.0 Hz, 2H), 7.69 (d, *J* = 7.6 Hz, 3H), 7.82 (d, $^{3}J_{\text{E-alkene}}$ = 15.6 Hz, 2H), 8.07 (d, $^{3}J_{\text{E-alkene}}$ = 15.6 Hz, 2H), 13.96 (s, 2H, OH). **HR-MS (ESI):** m/z calculated for $[C_{34}H_{29}Br_2O_8]^+$ ($[M + H^+]$): 723.0216, found: 723.0224.

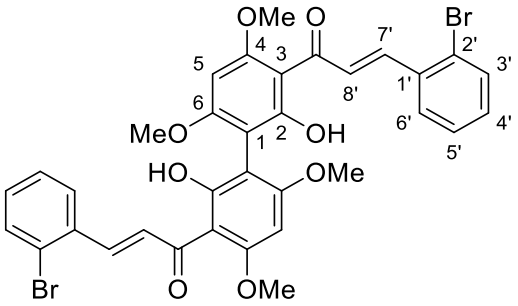

178

7.2.2.6 General Procedure 4 (GP4): Biflavones

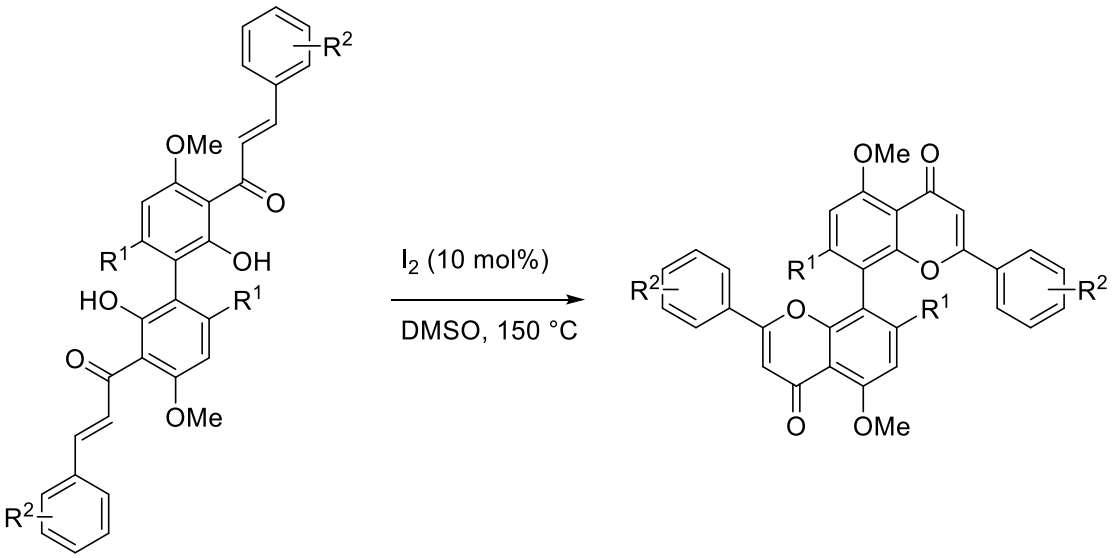

A 10 mL microwave vial with stir bar was charged with bichalcone (30 mg, 1.00 equiv) and capped with a septum. Degassed DMSO (0.24 mL) and a solution of I_2 in degassed DMSO (78.8 mM, 10 mol%) were added. The reaction solution was then heated to 150 °C and stirred for 3 h unless stated otherwise. After complete conversion sat. aq. Na_2SO_3 solution (4 mL) was added. The aq. phase was extracted with ethyl acetate (3x 20 mL). The combined org. layers were washed with cold water (3x 20 mL) and sat. NaCl solution (2x 20 mL) and the solvent removed in vacuo. The product was isolated by column chromatography unless otherwise stated.

7.2.2.6.1 *rac*-5,5'-Dimethoxy-2,2'-bis(4-methoxyphenyl)-7,7'-dimethyl-4*H*,4'*H*-[8,8'-bichromene]-4,4'-dione (179)

The title compound was synthesized in accordance with **GP4** with bichalcone **165** (30.0 mg, 1.00 equiv, 50.7 µmol) and I_2 (78.8 mM, 64.3 µL, 10 mol%, 5.07 µmol) in 1 h. The product was isolated by column chromatography (EtOAc:MeOH, 95:5 v/v) as white solids in a yield of 15.8 mg (26.8 µmol, 53%). The analytical data were in accordance with literature.[108a]

^{1}H NMR (600 MHz, $CDCl_3$): δ 2.18 (s, 6H, Me), 3.79 (s, 6H, OMe), 4.11 (s, 6H, OMe), 6.64 (s, 2H, 3-H), 6.78 (d, $^3J_{2',3'}$ = 8.9 Hz, 4H, 3'-H), 6.88 (s, 2H, 6-H), 7.23 (d, $^3J_{2',3'}$ = 8.9 Hz, 4H, 2'-H). **^{13}C NMR** (151 MHz, $CDCl_3$): δ 20.76 (Me), 55.63 (OMe), 56.72 (OMe), 107.23 (C-3), 108.34 (C-6), 112.96 (C-4a), 114.66 (C-3'), 116.56 (C-8), 123.48 (C-1'), 127.32 (C-2'), 144.67 (C-7), 155.77 (C-8a), 159.28 (C-5), 160.94 (C-2), 162.32 (C-5), 178.62 (CO). **IR (ATR film) [cm^{-1}]:** 2844, 2238, 1605, 1576, 1512, 1496, 1478, 1464, 1442, 1423, 1371, 1335, 1301, 1207, 1116, 1062, 1031, 976, 956, 909, 730, 644, 590. **TLC** (EtOAc:MeOH, 95:5 v/v): R_f = 0.26 **HR-MS (ESI):** m/z calculated for $[C_{36}H_{31}O_8]^+$ ([M + H$^+$]): 591.2013, found: 591.2020. **Melting point:** 295 – 296 °C

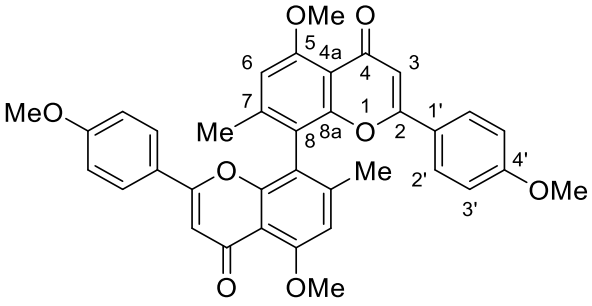

179

7.2.2.6.2 *rac*-5,5'-Dimethoxy-7,7'-dimethyl-2,2'-diphenyl-4*H*,4'*H*-[8,8'-bichromene]-4,4'-dione (180)

The title compound was synthesized in accordance with **GP**4 with bichalcone **166** (30.0 mg, 1.00 equiv, 56.5 µmol) and I_2 (78.8 mM, 71.7 µL, 10 mol%, 5.65 µmol). The product was isolated by column chromatography (EtOAc:MeOH, 98:2 v/v) as white solids in a yield of 6.2 mg (12 µmol, 21%).

^{1}H NMR (600 MHz, $CDCl_3$): δ 2.19 (s, 6H, Me), 4.11 (s, 6H, OMe), 6.73 (s, 2H, 3-H), 6.89 (s, 2H, 6-H), 7.26 – 7.33 (m, 8H, 2'+3'-H), 7.34 – 7.40 (m, 2H, 4'-H). **^{13}C NMR** (151 MHz, $CDCl_3$): δ 20.65 (Me), 56.57 (OMe), 108.28 (C-3), 108.50 (C-6), 112.92 (C-4a), 116.35 (C-8), 125.44 (C-2'/3'), 129.01 (C-2'/3'), 131.09 (C-4'), 131.29 (C-1'), 144.81 (C-7), 155.66 (C-8a), 159.20 (C-5), 160.64 (C-2), 178.44 (CO). **IR (ATR film) [cm^{-1}]:** 3005, 2848, 1640, 1597, 1578, 1495, 1479, 1464, 1450, 1370, 1333, 1307, 1281, 1258, 1207, 1189, 1122, 1062, 976, 955, 908, 850, 771, 730, 689, 665, 645, 612, 551, 531. **TLC** (EtOAc:MeOH, 98:2 v/v): R_f = 0.28 **HR-MS (ESI):** m/z calculated for $[C_{34}H_{27}O_6]^+$ ($[M + H^+]$): 531.1802, found: 531.1805. **Melting point:** 296 °C

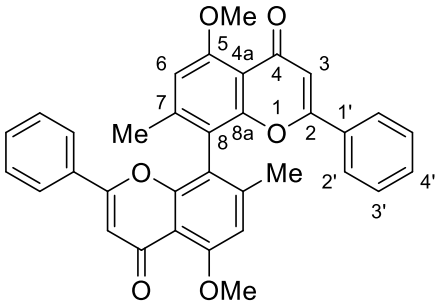

180

7.2.2.6.3 *rac*-2,2'-Bis(4-(dimethylamino)phenyl)-5,5'-dimethoxy-7,7'-dimethyl-4*H*,4*'H*-[8,8'-bichromene]-4,4'-dione (181)

The title compound was synthesized in accordance with **GP4** with bichalcone **167** (30.0 mg, 1.00 equiv, 48.6 µmol) and I_2 (78.8 mM, 61.7 µL, 10 mol%, 4.86 µmol). The product was isolated by column chromatography (EtOAc:CH_2Cl_2:MeOH, 7:2.5:0.5 v/v) as orange solids in a yield of 6.3 mg (10 µmol, 21%).

In a further experiment the reaction was scaled up with bichalcone **167** (575 mg, 1.00 equiv, 0.927 mmol) and I_2 (78.8 mM, 1.18 mL, 10 mol%, 92.7 µmol). The product was isolated as orange solids in a yield of 123 mg (0.199 mmol, 21 %).

^{1}H NMR (600 MHz, $CDCl_3$): δ 2.17 (s, 6H, Me), 2.97 (s, 12H, NMe_2), 4.10 (s, 6H, OMe), 6.51 (d, $^3J_{2',3'}$ = 9.1 Hz, 4H, 3'-H), 6.58 (s, 2H, 3-H), 6.86 (s, 2H, 6-H), 7.16 (d, $^3J_{2',3'}$ = 9.0 Hz, 4H, 2'-H). **^{13}C NMR** (151 MHz, $CDCl_3$): δ 20.71 (Me), 40.17 (NMe_2), 56.64 (OMe), 105.38 (C-3), 108.02 (C-6), 111.79 (C-3'), 112.83 (C-4a), 116.66 (C-8), 117.70 (C-1'), 127.05 (C-2'), 144.20 (C-7), 152.28 (C-4'), 155.70 (C-8a), 159.00 (C-5), 161.92 (C-2), 178.80 (C-4). **IR (ATR film) [cm^{-1}]:** 2923, 2237, 1731, 1604, 1591, 1524, 1495, 1364, 1335, 1302, 1284, 1251, 1197, 1171, 1120, 1063, 908, 819, 761, 728, 662, 642, 582, 570, 544, 531, 512. **TLC** (EtOAc:CH_2Cl_2:MeOH, 7:2.5:0.5 v/v): R_f = 0.16 **HR-MS (ESI):** m/z calculated for $[C_{38}H_{37}N_2O_6]^+$ ([M + H$^+$]): 617.2646, found: 617.2653. **Melting point:** 196 – 197 °C

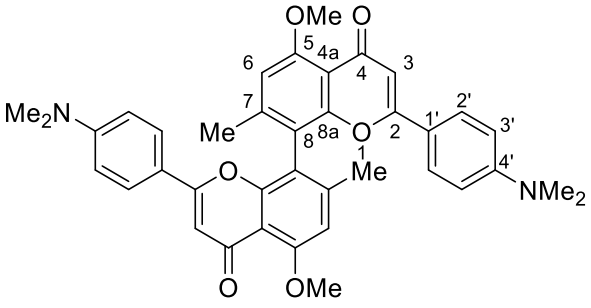

181

7.2.2.6.4 *rac*-5,5'-Dimethoxy-7,7'-dimethyl-2,2'-bis(4-(trifluoromethyl)phenyl)-4*H*,4*'H*-[8,8'-bichromene]-4,4'-dione (182)

The title compound was synthesized in accordance with **GP4** with bichalcone **168** (30.0 mg, 1.00 equiv, 45.0 µmol) and I_2 (78.8 mM, 57.1 µL, 10 mol%, 4.50 µmol) for 2 h. The product was isolated by column chromatography (petroleum ether:EtOAc:isopropanol, 6:3:1 v/v) as a white viscous semi-solid in a yield of 8.5 mg (13 µmol, 28%).

^{1}H NMR (600 MHz, $CDCl_3$): δ 2.21 (s, 6H, Me), 4.12 (s, 6H, OMe), 6.78 (s, 2H, 3-H), 6.93 (s, 2H, 6-H), 7.40 (d, $^{3}J_{2',3'}$ = 8.2 Hz, 4H, 3'-H), 7.56 (d, $^{3}J_{2',3'}$ = 8.3 Hz, 4H, 2'-H). **^{13}C NMR** (151 MHz, $CDCl_3$): δ 20.83 (Me), 56.78 (OMe), 108.68 (C-6), 109.89 (C-3), 113.06 (C-4a), 116.21 (C-8), 123.61 (q, $^{1}J_{F-C}$ = 272.1 Hz, CF_3), 125.84 (C-2'), 126.22 (q, $^{3}J_{F-C}$ = 3.7 Hz, C-3'), 133.12 (q, $^{2}J_{F-C}$ = 33.1 Hz, C-4'), 134.59 (C-1'), 145.37 (C-7), 155.68 (C-8a), 159.03 (C-2), 159.52 (C-5), 178.08 (CO). **^{19}F NMR** (282 MHz, $CDCl_3$): δ -63.13. **IR (ATR film) [cm^{-1}]:** 2854, 1817, 1646, 1600, 1579, 1497, 1480, 1466, 1445, 1417, 1323, 1295, 1207, 1125, 1063, 1015, 977, 957, 909, 844, 777, 731, 625, 557, 532, 518. **TLC** (petroleum ether:EtOAc:isopropanol, 6:3:1 v/v): R_f = 0.21 **HR-MS (ESI):** m/z calculated for $[C_{36}H_{25}F_6O_6]^+$ ([M + H$^+$]): 667.1555, found: 667.1550. **Melting point:** 263 – 265 °C

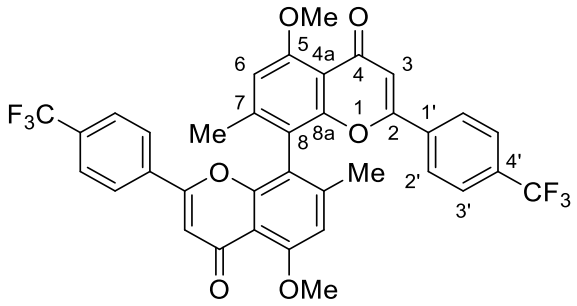

182

7.2.2.6.5 *rac*-2,2'-Bis(4-bromophenyl)-5,5'-dimethoxy-7,7'-dimethyl-4*H*,4'*H*-[8,8'-bichromene]-4,4'-dione (183)

The title compound was synthesized in accordance with **GP4** with bichalcone **169** (30.0 mg, 1.00 equiv, 43.6 µmol) and I_2 (78.8 mM, 55.3 µL, 10 mol%, 4.36 µmol). The product was obtained as white solids in a yield of 27.7mg (40.1 µmol, 92%).

A further experiment following **GP4** using bichalcone **169** (1.29 g, 1.0 equiv, 1.86 mmol, *rac*) gave the product as off-white solids (1.22 g, 1.77 mmol, 95%, *rac*).

In a further experiment, a 2-dr. vial equipped with stir bar was charged with bichalcone **169** (96.9 mg, 1.0 equiv, 140 µmol, >99% *ee* S_a) and a solution of iodine in degassed DMSO (0.08 M, 175 µL, 0.1 equiv, 14.0 µmol). The reaction was stirred at 150 °C for 2 h. Sat. aq. Na_2SO_3 (1 mL) solution was added and the aq. phase extracted with CH_2Cl_2 (3x 15 mL). The combined org. phases were washed with sat. aq. NaCl solution, water (3x) sat. aq. NaCl solution again, dried over $MgSO_4$ and solvents removed in vacuo. The product was obtained as off-white solids in a yield of 89.0 mg (129 µmol, 92%, >99%*ee* S_a).

A further experiment using bichalcone **169** (83.1 mg, 1.0 equiv, 120 µmol, >99% *ee* R_a) gave the product as off-white solids in a yield of 63.2 mg (91.8 µmol, 77%, >99%*ee* R_a).

A further experiment using bichalcone **169** (1.29 g, 1.0 equiv, 1.86 mmol, *rac*) gave the product as off-white solids in a yield of 1.22 g (1.77 mmol, 95%, *rac*). The analytical data were in accordance with literature.[108b]

^{1}H NMR (600 MHz, $CDCl_3$): δ 2.18 (s, 6H, Me), 4.10 (s, 6H, OMe), 6.69 (s, 2H, 3-H), 6.89 (s, 2H, 6-H), 7.14 (d, $^3J_{2'\text{-}3'}$ = 8.7 Hz, 4H, 2′-H), 7.42 (d, $^3J_{2'\text{-}3'}$ = 8.7 Hz, 4H, 3′-H). **^{13}C NMR** (151 MHz, $CDCl_3$): δ 20.82 (Me), 56.74 (OMe), 108.49 (C-6), 108.77 (C-3), 112.94 (C-4a), 116.23 (C-8), 126.19 (C-4′), 126.93 (C-3′), 130.08 (C-1′), 132.49 (C-2′), 145.14 (C-7), 155.62 (C-8a), 159.37 (C-5), 159.72 (C-2), 178.26 (C=O). **IR (ATR film) [cm^{-1}]:** 3005, 2931, 2851, 2240, 1773, 1638, 1597, 1562, 1479, 1464, 1403, 1368, 1329, 1303, 1275, 1260, 1207, 1187, 1167, 1122, 1061, 1030, 1008, 977, 955, 907, 830, 794, 681, 645, 626, 573, 557, 532, 499, 478. **TLC** (CH_2Cl_2:MeOH, 98:2 v/v): R_f = 0.15 **HR-MS (ESI):** m/z calculated for $[C_{34}H_{25}O_4Br_2]^+$ ([M + H$^+$]): 687.0012, found: 687.0017.

Melting point: 245 °C (decomposition) (*rac*)

270 °C (decomposition) (S_a, >99%*ee* HPLC)

270 °C (decomposition) (R_a, >99%*ee* HPLC)

HPLC: Lux® Amylose-1 (Phenomenex) 250 ° 4.6 mm, 25 °C, 0.5 mL min^{-1}, 331 nm, *n*-heptane:*i*-PrOH 50:50 (v/v) $t_R(S_a)$ = 18.0 min, $t_R(R_a)$ = 24.3 min

Optical rotation: $[\alpha]^{25}_D$ = +25.7 (±0.1, duplicate) (c = 1.08, $CHCl_3$, S_a, >99%*ee* by chiral HPLC)

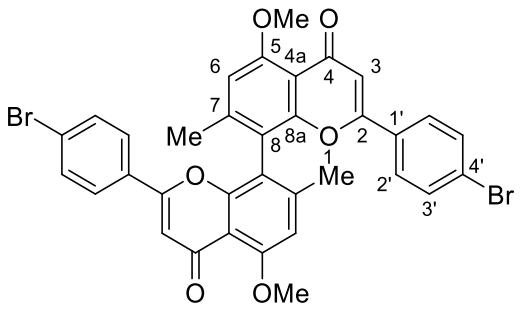

183

7.2.2.6.6 *rac*-2,2'-Bis(3-bromophenyl)-5,5'-dimethoxy-7,7'-dimethyl-4*H*,4'*H*-[8,8'-bichromene]-4,4'-dione (184)

The title compound was synthesized in accordance with **GP4** with bichalcone **170** (30.0 mg, 1.00 equiv, 43.6 µmol) and I_2 (78.8 mM, 55.3 µL, 10 mol%, 4.36 µmol) for 1 h. The product was isolated by column chromatography (EtOAc 100%) as white solids 25.4 mg (36.9 µmol, 86%).

^{1}H NMR (600 MHz, $CDCl_3$): δ 2.24 (s, 6H, Me), 4.11 (s, 6H, OMe), 6.70 (s, 2H, 3-H), 6.94 (s, 2H, 6-H), 7.18 (t, $^3J_{4'\text{-}5',5'\text{-}6'}$ = 7.9 Hz, 2H, 5'-H), 7.31 (dt, $^3J_{5'\text{-}6'}$ = 8.0 Hz, $^4J_{2'\text{-}6',4'\text{-}6'}$ = 1.4 Hz, 2H, 6'-H), 7.34 (t, $^4J_{2'\text{-}4',2'\text{-}6'}$ = 1.9 Hz, 2H, 2'-H), 7.49 (ddd, $^3J_{4'\text{-}5'}$ = 8.0 Hz, $^4J_{2'\text{-}4',4'\text{-}6'}$ = 2.0, 1.0 Hz, 2H, 4'-H). **^{13}C NMR** (151 MHz, $CDCl_3$): δ 20.84 (Me), 56.73 (OMe), 108.62 (C-6), 109.16 (C-3), 113.03 (C-4a), 116.16 (C-8), 123.38 (C-2'), 123.91 (C-6'), 128.77 (C-3'), 130.58 (C-5'), 133.21 (C-1'), 134.18 (C-4'), 145.20 (C-7), 155.49 (C-8a), 158.77 (C-2), 159.50 (C-5), 178.11 (CO). **IR (ATR film) [cm^{-1}]:** 2851, 2241, 1642, 1598, 1561, 1496, 1478, 1442, 1417, 1367, 1299, 1266, 1206, 1124, 1062, 998, 956, 917, 847, 790, 730, 692, 646, 619, 571, 551, 532. **TLC** (EtOAc 100%): R_f = 0.26 **HR-MS (ESI):** m/z calculated for $[C_{34}H_{25}O_4Br_2]^+$ ([M + H$^+$]): 687.0012, found: 687.0005. **Melting point:** 276 – 278 °C

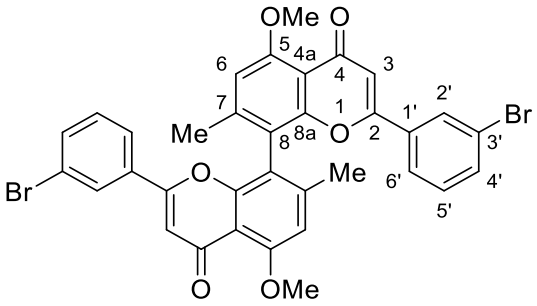

184

7.2.2.6.7 *rac*-2,2'-Bis(2-bromophenyl)-5,5'-dimethoxy-7,7'-dimethyl-4*H*,4'*H*-[8,8'-bichromene]-4,4'-dione (185)

The title compound was synthesized in accordance with **GP4** with bichalcone **171** (30.0 mg, 1.00 equiv, 43.6 µmol) and I_2 (78.8 mM, 55.3 µL, 10 mol%, 4.36 µmol) for 2 h. The product was obtained as white solids in a yield of 16.5 mg (24.0 µmol, 55%).

^{1}H NMR (600 MHz, $CDCl_3$): δ 2.12 (s, 6H, Me), 4.02 (s, 6H, OMe), 6.46 (s, 2H, 3-H), 6.78 (s, 2H, 6-H), 7.20 (td, $^3J_{3'\text{-}4',4'\text{-}5'}$ = 7.4, 6.9 Hz, $^4J_{4'\text{-}6'}$ = 2.0 Hz, 2H, 4'-H), 7.21 – 7.29 (m, 4H, 5'+6'-H), 7.51 (dd, $^3J_{3'\text{-}4'}$ = 7.8 Hz, $^4J_{3'\text{-}5'}$ = 1.5 Hz, 2H, 3'-H). **^{13}C NMR** (151 MHz, $CDCl_3$): δ 20.93

(Me), 56.54 (OMe), 108.54 (C-3), 113.00 (C-8), 114.33 (C-4a), 116.56 (C-1), 121.57 (C-2'), 127.67 (C-5'), 130.73 (C-6'), 131.78 (C-4'), 133.49 (C-1'), 134.22 (C-3'), 144.91 (C-7), 156.39 (C-8a), 159.23 (C-2), 161.62 (C-5), 178.19 (CO). **IR (ATR film) [cm^{-1}]:** 3300, 2924, 2869, 2852, 1733, 1653, 1600, 1562, 1496, 1464, 1437, 1370, 1327, 1279, 1263, 1206, 1115, 1065, 976, 954, 912, 855, 763, 733, 703, 680, 645, 612. **HR-MS (ESI):** m/z calculated for $[C_{34}H_{25}O_4Br_2]^+$ ([M + H$^+$]): 687.0012, found: 687.0011. **Melting point:** 250 °C (decomposition)

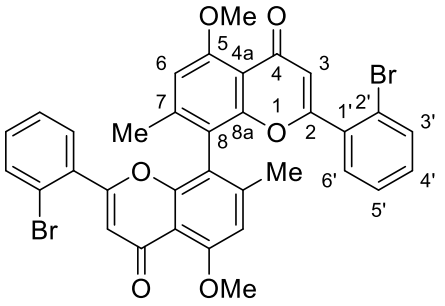

185

7.2.2.6.8 *rac*-5,5',7,7'-Tetramethoxy-2,2'-bis(4-methoxyphenyl)-4*H*,4'*H*-[8,8'-bichromene]-4,4'-dione or Hexa-O-methylcupressuflavone (186)

The title compound was synthesized in accordance with **GP4** with bichalcone **172** (30.0 mg, 1.00 equiv, 48.2 µmol) and I_2 (78.8 mM, 61.2 µL, 10 mol%, 4.82 µmol). The product was isolated by column chromatography (EtOAc:MeOH, 9:1 v/v) as white solids in a yield of 23.1 mg (37.1 µmol, 77%). The analytical data were in accordance with literature.[113b]

^{1}H NMR (600 MHz, $CDCl_3$): δ 3.77 (s, 6H, OMe), 3.86 (s, 6H, OMe), 4.12 (s, 6H, OMe), 6.58 (s, 2H, 6-H), 6.59 (s, 2H, 3-H), 6.77 (d, $^3J_{2',3'}$ = 8.9 Hz, 4H, 3'-H), 7.29 (d, $^3J_{2',3'}$ = 8.9 Hz, 4H, 2'-H). **^{13}C NMR** (151 MHz, $CDCl_3$): δ 55.47 (OMe), 56.13 (OMe), 56.60 (OMe), 91.78 (C-6), 102.13 (C-8), 106.80 (C-3), 109.05 (C-4a), 114.39 (C-3'), 123.54 (C-1'), 127.15 (C-2'), 156.57 (C-8a), 160.66 (C-2/5/7/4'), 161.29 (C-2/5/7/4'), 161.74 (C-2/5/7/4'), 162.03 (C-2/5/7/4'), 178.14 (CO). **IR (ATR film) [cm^{-1}]:** 1637, 1593, 1465, 1424, 1388, 1338, 1304, 1180, 1111, 1033, 919, 834, 588, 567. **TLC** (EtOAc:MeOH, 9:1 v/v): R_f = 0.22 **HR-MS (ESI):** m/z calculated for $[C_{36}H_{31}O_{10}]^+$ ([M + H$^+$]): 623.1912, found: 623.1912. **Melting point:** 240 °C (brown discoloration) 285 – 286 °C. (294 – 295 °C)[113b]

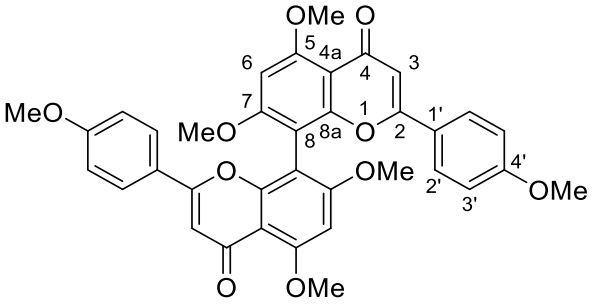

186

7.2.2.6.9 *rac*-5,5',7,7'-Tetramethoxy-2,2'-diphenyl-4*H*,4'*H*-[8,8'-bichromene]-4,4'-dione (187)

Synt The title compound was synthesized in accordance with **GP4** with bichalcone **173** (30.0 mg, 1.00 equiv, 53.3 µmol) and I_2 (78.8 mM, 67.6 µL, 10 mol%, 5.33 µmol) for 2 h. The product was isolated by column chromatography (EtOAc:MeOH, 98:2 v/v) as white solids in a yield of 17.6 mg (31.3 µmol, 59%). The analytical data were in a accordance with literature.[56b]

^{1}H NMR (600 MHz, $CDCl_3$): δ 3.85 (s, 6H, OMe), 4.12 (s, 6H, OMe), 6.59 (s, 2H, 6-H), 6.68 (s, 2H, 3-H), 7.28 (d, $^3J_{2'\text{-}3'}$ = 7.4 Hz, 4H, 3'-H), 7.33 – 7.40 (m, 6H, 2'+4'-H). **^{13}C NMR** (151 MHz, $CDCl_3$): δ 56.25 (OMe), 56.72 (OMe), 91.92 (C-6), 102.19 (C-8), 108.36 (C-4a), 109.29 (C-3), 125.56 (C-2'/3'), 129.01 (C-2'/3'), 131.23 (C-4'), 131.42 (C-1'), 156.77 (C-8a), 160.62 (C-5), 161.51 (C-2), 161.99 (C -7), 178.19 (CO). **IR (ATR film) [cm^{-1}]:** 3067, 2844, 2238, 1635, 1590, 1508, 1491, 1465, 1450, 1435, 1388, 1333, 1299, 1265, 1214, 1190, 1172, 1125, 1109, 1087, 1036, 1022, 957, 917, 849, 812, 771, 728, 689, 672, 644, 618, 570, 546, 514. **TLC** (EtOAc:MeOH, 98:2 v/v): R_f = 0.12 **HR-MS (ESI):** m/z calculated for $[C_{34}H_{27}O_8]^+$ ([M + H$^+$]): 563.1700, found: 563.1707. **Melting point:** 312 – 313 °C (318 – 319 °C)[56b]

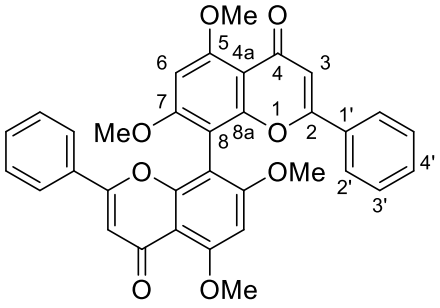

187

7.2.2.6.10 *rac*-2,2'-Bis(4-(dimethylamino)phenyl)-5,5',7,7'-tetramethoxy-4*H*,4'*H*-[8,8'-bichromene]-4,4'-dione (188)

The title compound was synthesized in accordance with **GP4** with bichalcone **174** (30.0 mg, 1.00 equiv, 46.3 µmol) and I_2 (78.8 mM, 58.8 µL, 10 mol%, 4.63 µmol). The product was isolated by column chromatography (CH_2Cl_2:EtOAc:MeOH, 5:4.5:0.5 v/v) as orange solids in a yield of 7.7 mg (12 µmol, 26%).

^{1}H NMR (600 MHz, $CDCl_3$): δ 2.95 (s, 12H, Me), 3.86 (s, 6H, OMe), 4.11 (s, 6H, OMe), 6.50 (d, $^3J_{2'\text{-}3'}$ = 8.9 Hz, 4H, 3'-H), 6.53 (s, 2H, 6-H), 6.56 (s, 2H, 3-H), 7.21 (d, $^3J_{2'\text{-}3'}$ = 9.0 Hz, 4H, 2'-H). **^{13}C NMR** (151 MHz, $CDCl_3$): δ 40.19 (NMe_2), 56.24 (OMe), 56.71 (OMe), 91.82 (C-6), 102.44 (C-8), 105.21 (C-3), 109.21 (C-3'), 111.78 (C-4a), 118.11 (C-1'), 127.09 (C-2'), 152.25 (C-4'), 156.70 (C-8a), 161.21 (C-5), 161.61 (C-2), 161.82 (C-7), 178.44 (CO). **IR (ATR film) [cm^{-1}]:** 2942, 2234, 1630, 1601, 1586, 1524, 1487, 1465, 1434, 1387, 1366, 1336, 1305, 1253, 1214, 1198, 1171, 1124, 1064, 1030, 1001, 947, 917, 840, 819, 783, 766, 729, 664, 643, 582, 563, 513, 486. **TLC** (CH_2Cl_2:EtOAc:MeOH, 5:4.5:0.5 v/v): R_f = 0.14 **HR-MS (ESI):** m/z calculated for $[C_{38}H_{37}N_2O_8]^+$ ($[M + H^+]$): 649.2544, found: 649.2546.

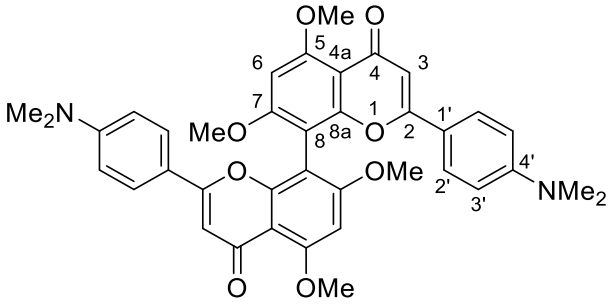

188

7.2.2.6.11 *rac*-5,5',7,7'-Tetramethoxy-2,2'-bis(4-(trifluoromethyl)phenyl)-4*H*,4'*H*-[8,8'-bichromene]-4,4'-dione (189)

The title compound was synthesized in accordance with **GP4** with bichalcone **175** (30.0 mg, 1.00 equiv, 42.9 µmol) and I_2 (78.8 mM, 54.4 µL, 10 mol%, 4.29 µmol) for 2 h. The product was isolated by column chromatography (petroleum ether:EtOAc:*i*PrOH, 2:7:1 v/v) as white solids in a yield of 17.7 mg (25.3 µmol, 59%).

^{1}H NMR (600 MHz, $CDCl_3$): δ 3.89 (s, 6H, OMe), 4.15 (s, 6H, OMe), 6.62 (s, 2H, 6-H), 6.73 (s, 2H, 3-H), 7.46 (d, $^3J_{2'\text{-}3'}$ = 8.2 Hz, 4H, 3'-H), 7.56 (d, $^3J_{2'\text{-}3'}$ = 8.3 Hz, 4H, 2'-H). **^{13}C NMR** (151 MHz, $CDCl_3$): δ 56.32 (OMe), 56.77 (OMe), 92.04 (C-6), 101.94 (C-8), 109.24

(C-4a), 109.63 (C-3), 123.64 (q, $^{1}J_{F\text{-}C}$ = 271.8 Hz, CF_3), 125.80 (C-2'), 126.09 (q, $^{3}J_{F\text{-}C}$ = 3.6 Hz, C-3'), 132.92 (q, $^{2}J_{F\text{-}C}$ = 32.9 Hz, C-4'), 134.79 (C-1'), 156.67 (C-8a), 158.84 (C-5), 161.72 (C-2), 162.24 (C-7), 177.67 (CO). **^{19}F NMR** (282 MHz, $CDCl_3$): δ -63.08. **IR (ATR film) [cm^{-1}]:** 1622, 1594, 1416, 1388, 1324, 1216, 1170, 1128, 1070, 1027, 958, 919, 843, 812. **TLC** (petroleum ether:EtOAc:*i*PrOH, 2:7:1 v/v): R_f = 0.35 **HR-MS (ESI):** m/z calculated for $[C_{36}H_{25}N_2O_8]^+$ ([M + H$^+$]): 699.1448, found: 699.1450. **Melting point:** 261 – 262 °C

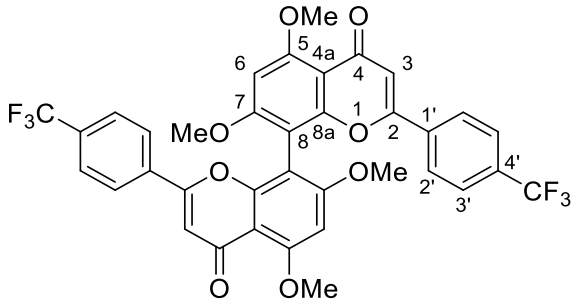

189

7.2.2.6.12 *rac*-2,2'-Bis(4-bromophenyl)-5,5',7,7'-tetramethoxy-4*H*,4'*H*-[8,8'-bichromene]-4,4'-dione (190)

The title compound was synthesized in accordance with **GP4** with bichalcone **176** (30.0 mg, 1.00 equiv, 41.6 µmol) and I_2 (78.8 mM, 52.8 µL, 10 mol%, 4.16 µmol) for 2 h. The product was isolated by column chromatography (petroleum ether:EtOAc:*i*PrOH, 2:7:1 v/v) as white solids in a yield of 20.9 mg (29.0 µmol, 70%).

^{1}H NMR (600 MHz, $CDCl_3$): δ 3.86 (s, 6H, OMe), 4.12 (s, 6H, OMe), 6.58 (s, 2H, 6-H), 6.64 (s, 2H, 3-H), 7.20 (d, $^{3}J_{2',3'}$ = 8.4 Hz, 4H, 3'-H), 7.42 (d, $^{3}J_{2',3'}$ = 8.5 Hz, 4H, 2'-H). **^{13}C NMR** (151 MHz, $CDCl_3$): δ 56.28 (OMe), 56.74 (OMe), 91.93 (C-6), 101.96 (C-8), 108.51 (C-3), 109.17 (C-4a), 125.95 (C-4'), 126.92 (C-2'), 130.30 (C-1'), 132.35 (C-3'), 156.60 (C-5), 159.53 (C-2), 161.60 (C-2), 162.07 (C-7), 177.85 (CO). **IR (ATR film) [cm^{-1}]:** 2885, 2239, 1638, 1590, 1508, 1487, 1465, 1435, 1403, 1388, 1331, 1302, 1274, 1215, 1190, 1171, 1127, 1107, 1073, 1027, 1009, 958, 828, 782, 730, 687, 644, 626, 572, 545, 517, 477. **TLC** (petroleum ether:EtOAc:*i*PrOH, 2:7:1 v/v): R_f = 0.21 **HR-MS (ESI):** m/z calculated for $[C_{34}H_{25}O_8Br_2]^+$ ([M + H$^+$]): 718.9911, found: 718.9915. **Melting point:** 251 – 255 °C

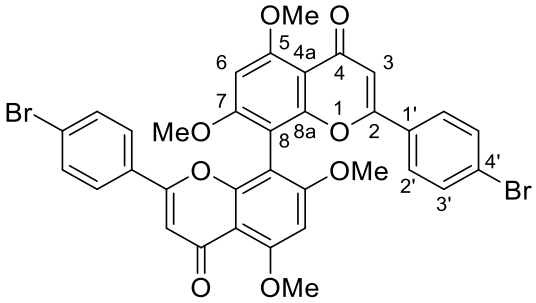

190

7.2.2.6.13 *rac*-2,2'-Bis(2-bromophenyl)-5,5',7,7'-tetramethoxy-4H,4'H-[8,8'-bichromene]-4,4'-dione (192)

The title compound was synthesized in accordance with **GP4** with bichalcone **178** (30.0 mg, 1.00 equiv, 41.6 µmol) and I_2 (78.8 mM, 52.8 µL, 10 mol%, 4.16 µmol) for 1 h. The product was isolated by column chromatography (EtOAc:MeOH, 9:1 v/v) as white solids in a yield of 16.7 mg (23.2 µmol, 56%).

^{1}H NMR (600 MHz, $CDCl_3$): δ 3.84 (s, 6H, OMe), 4.06 (s, 6H, OMe), 6.47 (s, 2H, 6-H), 6.50 (s, 2H, 3-H), 7.23 (ddd, *J* = 7.8, 4.0, 2.4 Hz, 4H), 7.27 – 7.29 (m, 2H), 7.53 – 7.57 (m, 2H). **^{13}C NMR** (151 MHz, $CDCl_3$): δ 56.20 (OMe), 56.58 (OMe), 91.98 (C-6), 102.18 (C-8), 109.12 (C-3), 114.04 (C-4a), 121.57 (C-2'), 127.62, 130.63, 131.65, 133.50 (C-1'), 134.24, 157.33 (C-7), 161.14 (C-8a), 161.41 (C-2), 162.13 (C-5), 177.82 (CO). **IR (ATR film) [cm^{-1}]:** 2923, 1649, 1588, 1520, 1482, 1360, 1246, 1201, 1163, 1110, 1034, 814. **TLC** (EtOAc:MeOH, 9:1 v/v): R_f = 0.32 **HR-MS (ESI):** m/z calculated for $[C_{34}H_{25}O_8Br_2]^+$ ([M + H$^+$]): 718.9911, found: 718.9916. **Melting point:** 260 °C (decomposition)

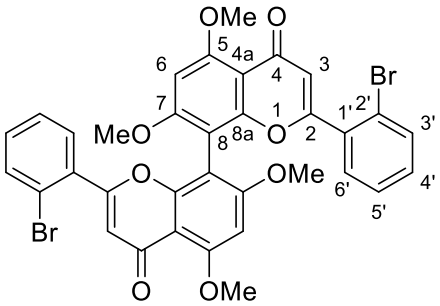

192

7.2.2.7 Miscellaneous Syntheses

7.2.2.7.1 1-(3-Chloro-2-hydroxy-6-methoxy-4-methylphenyl)ethan-1-one (199) and 1-(3-chloro-6-hydroxy-2-methoxy-4-methylphenyl)ethan-1-one (198)

A microwave vial with fitted stir bar was charged with acetophenone **133** (200 mg, 1.00 equiv, 1.11 mmol), CH_2Cl_2 (8 mL, 0.14 M), N-chlorosuccinimide (156 mg, 1.05 equiv, 1.17 mmol) and $FeCl_3$ (18.0 mg, 0.10 equiv, 0.111 mmol). The reaction was stirred at 22 °C for 20 h. After full conversion a solution of Na_2SO_3 (10 mL, 10%, aq.) was added. The resulting mixture was extracted with CH_2Cl_2 (2x 20 mL). The combined organic phase was washed with sat. aq. NaCl-solution and dried over $MgSO_4$. Solids were filtered off and the solvent was removed *in vacuo*. The product was isolated by column chromatography (petroleum ether:EtOAc, 8:2 v/v) as yellow-green crystals in a yield of 107 mg (49.9 µmol, 45 %).

^{1}H NMR (600 MHz, $CDCl_3$): δ 2.41 (s, 3H, Me), 2.67 (d, *J* = 0.8 Hz, 3H, CO*Me*), 3.90 (s, 3H, OMe), 6.31 (s, 1H, 5-H), 14.10 (s, 1H, OH). **^{13}C NMR** (151 MHz, $CDCl_3$): δ 21.54 (Me), 33.55 (CO*Me*), 55.82 (OMe), 103.35 (C-5), 109.97 (C-1), 114.64 (C-3), 145.23 (C-4), 159.44 (C-6), 160.18 (C-2), 204.61 (*CO*Me). **IR (ATR film) [cm^{-1}]:** 3014, 2990, 2955, 2929, 2854, 2685, 1624, 1595, 1561, 1404, 1372, 1286, 1264, 1215, 1124, 877, 825, 634. **TLC** (petroleum ether:EtOAc, 95:5 v/v): R_f = 0.19 **HR-MS (ESI):** m/z calculated for $[C_{10}H_{12}ClO_3]^+$ ($[M + H^+]$): 215.0469 found: 215.0473 **Melting point:** 118 – 120 °C

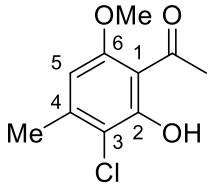

199

Additionally, product **198** was isolated as a yellow oil that solidified after a while in a yield of 112 mg (52.2 µmol, 47 %).

^{1}H NMR (600 MHz, $CDCl_3$): δ 2.37 (s, 3H, Me), 2.73 (s, 3H, CO*Me*), 3.90 (s, 3H, OMe), 6.69 (s, 1H, 5-H), 12.70 (s, 1H, OH). **^{13}C NMR** (151 MHz, $CDCl_3$): δ 21.31 (Me), 31.95 (CO*Me*), 61.62 (OMe), 114.23 (C-1), 116.15 (C-5), 119.01 (C-3), 146.25 (C-4), 157.75 (C-2), 161.74 (C-6)), 204.33 (*CO*Me). **IR (ATR film) [cm^{-1}]:** 2987, 2945, 2858, 1634, 1609, 1557, 1456, 1392, 1366, 1287, 1232, 1195, 1098, 1076, 1011, 961, 827, 783, 669, 611, 544. **TLC** (petroleum ether:EtOAc, 95:5 v/v): R_f = 0.42 **HR-MS (ESI):** m/z calculated for $[C_{10}H_{12}ClO_3]^+$ ($[M + H^+]$): 215.0469 found: 215.0469 **Melting point:** 44 – 45 °C

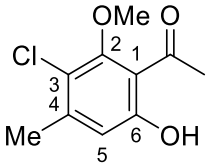

198

7.2.2.7.2 1-(3-Chloro-2-hydroxy-4,6-dimethoxyphenyl)ethan-1-one (200) and 1-(3-chloro-6-hydroxy-2,4-dimethoxyphenyl)ethan-1-one (48)

A microwave vial equipped with stir bar was charged with acetophenone **47** (50.0 mg, 1.00 equiv, 0.250 mmol), CH_2Cl_2 (2 mL, 0.125 M), N-chlorosuccinimide (35.6 mg, 1.05 equiv, 0.263 mmol) and $FeCl_3$ (4.1 mg, 0.10 equiv, 25 µmol). The reaction was stirred at 22 °C for 20 h. After full conversion a solution of Na_2SO_3 (10 mL, 10%, aq.) was added. The resulting mixture was extracted with CH_2Cl_2 (2x 20 mL). The combined organic phase was washed with sat. aq. NaCl-solution and dried over $MgSO_4$. Solids were filtered off and the solvent was removed *in vacuo*. The product was isolated by column chromatography (petroleum ether:EtOAc, 7:3 v/v) as a yellow solid in a yield of 20.8 mg (9.02 µmol, 36 %). The analytical data were in accordance with literature.[217]

^{1}H NMR (600 MHz, $CDCl_3$): δ 2.65 (s, 3H, CO*Me*), 3.95 (s, 3H, 4-OMe), 3.99 (s, 3H, 6-OMe), 6.03 (s, 1H, 5-H), 14.46 (s, 1H, OH). **^{13}C NMR** (151 MHz, $CDCl_3$): δ 33.14 (CO*Me*), 55.73 (C-4-OMe), 56.23 (C-6-OMe), 86.53 (C-5), 102.03 (C-3), 106.34 (C-1), 160.97 (C-4), 161.65 (C-2), 161.78 (C-6), 203.44 (*CO*Me). **IR (ATR film) [cm^{-1}]:** 2989, 2950, 1742, 1629, 1585, 1563, 1466, 1422, 1362, 1287, 1265, 1217, 1135, 1105, 902, 786. **TLC** (petroleum ether:EtOAc, 7:3 v/v): R_f = 0.24 **APCI-MS:** found: [M+H$^+$] 231.1 **Melting point:** 190 – 192 °C

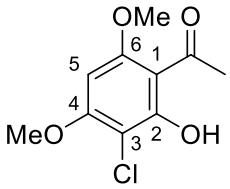

200

Additionally, product **48** was obtained as a yellow solid in a yield of 10.7 mg (4.64 µmol, 19 %). The analytical data were in accordance with literature.[217]

^{1}H NMR (600 MHz, $CDCl_3$): δ 2.70 (s, 3H, CO*Me*), 3.92 (s, 3H, OMe), 3.92 (s, 3H, OMe), 6.32 (s, 1H, 5-H), 13.49 (s, 1H, OH). **^{13}C NMR** (151 MHz, $CDCl_3$): δ 31.54 (CO*Me*), 56.70 (OMe), 61.55 (OMe), 97.25 (C-5), 108.14 (C-3), 109.88 (C-1), 159.32 (C-2), 161.58 (C-4), 164.68 (C-6), 203.27 (*CO*Me). **IR (ATR film) [cm^{-1}]:** 3006, 2978, 2947, 2851, 1618, 1589, 1438, 1397, 1363, 1251, 1210, 1106, 1076, 820. **TLC** (petroleum ether:EtOAc, 9:1 v/v): R_f = 0.42 **APCI-MS:** found: [M+H$^+$] 231.1 **Melting point:** 85 – 86 °C

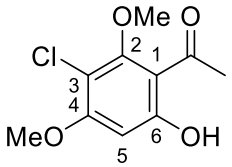

48

7.2.2.7.3 1-(3,5-Dichloro-2-hydroxy-6-methoxy-4-methylphenyl)ethan-1-one (201)

To a microwave vial with fitted stirrer were added acetophenone **133** (90.1 mg, 1.0 equiv, 0.500 mmol), N-chlorosuccinimide (333.8 mg, 5.0 equiv, 2.50 mmol) and $FeCl_3$ (8.1 mg, 0.1 equiv, 50 µmol) and dissolved in CH_2Cl_2 (4 mL). The reaction was stirred at 22 °C for 48 h. After full conversion a solution of Na_2SO_3 (10 mL, 10%, aq.) was added. The resulting mixture was extracted with CH_2Cl_2 (2x 20 mL). The combined organic phase was washed with sat. aq. NaCl-solution and dried over $MgSO_4$. Solids were filtered off and the solvent was removed *in vacuo*. The product was isolated by column chromatography (petroleum ether:EtOAc 85:15, v/v) as yellow solids in a yield of 43.3 mg (0.174 mmol 35 %).

^{1}H NMR (600 MHz, $CDCl_3$): δ 2.45 (s, 3H, Me), 2.54 (s, 3H, CO*Me*), 3.96 (s, 3H, OMe). **^{13}C NMR** (151 MHz, $CDCl_3$): δ 18.03 (Me), 33.05 (CO*Me*), 62.45 (OMe), 80.41 (C-3/5), 116.96 (C-1), 129.59 (C-3/5), 146.07 (C-4), 163.85 (C-6), 176.17 (C-2), 199.30 (*CO*Me). **IR (ATR film) [cm^{-1}]:** 3007, 2953, 2854, 1707, 1655, 1604, 1445, 1326, 1280, 1248, 1176, 1032, 925, 801, 767, 740, 663, 568. **TLC** (petroleum ether:EtOAc, 8:2 v/v): R_f = 0.28 **HR-MS (ESI):** m/z calculated for $[C_{10}H_{11}Cl_2O_3]^+$ ([M + H$^+$]): 249.0080 found: 249.0082 **Melting point:** 108 – 111 °C

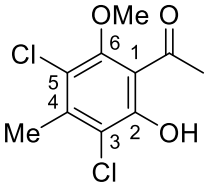

7.2.2.7.4 5-Hydroxy-7-methyl-2-phenylchroman-4-one (196)

A 50 mL round bottom flask equipped with stir bar was charged with MeOH (5 mL) and sodium (201 mg, 2.92 equiv, 4.38 mmol). After full dissolution of the sodium, acetophenone **131** (249 mg, 1.00 equiv, 1.50 mmol) was added followed by benzaldehyde (152 µL, 1.00 equiv, 1.50 mmol). The mixture was stirred for 62 h at 22 °C. Then aq. HCl-solution (1 M) was added and the precipitating solids filtered off. The product was isolated by column chromatography (petroleum ether:EtOAc 7:3 v/v to 100% EtOAc to 100% CH_2Cl_2) as an orange viscous oil in a yield of 170 mg (0.669 mmol, 45%).

^{1}H NMR (600 MHz, $CDCl_3$): 2.32 (s, 3H, Me), 2.86 (dd, $^2J_{3a\text{-}3b}$ = 17.2 Hz, $^3J_{2\text{-}3}$ = 3.1 Hz, 1H, H-3a), 3.10 (dd, $^2J_{3a\text{-}3b}$ = 17.1 Hz, $^3J_{2\text{-}3}$ = 13.1 Hz, 1H, H-3b), 5.42 (dd, $^3J_{2\text{-}3}$ = 13.2, 3.0 Hz, 1H, H-2), 6.37 (d, *J* = 1.6 Hz, 1H, H-6/8), 6.41 (d, *J* = 1.6 Hz, 1H, H-8/6), 11.75 (s, 1H, OH). **TLC** (petroleum ether:EtOAc, 7:3 v/v): R_f = 0.78

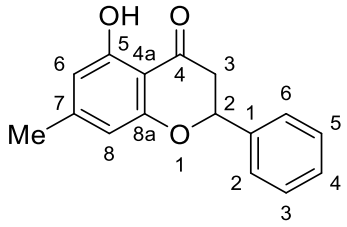

196

7.2.2.7.5 *rac*-2,2'-Bis(4-(dimethylamino)phenyl)-5,5'-dihydroxy-7,7'-dimethyl-4H,4'H-[8,8'-bichromene]-4,4'-dione (204)

A flame dried 25 mL Schlenk round bottom flask equipped with stir bar was charged with biflavone **181** (40.0 mg, 1.0 equiv, 64.9 µmmol) and anhydr. CH_2Cl_2 (2.5 mL, 0.026 M). The solution was cooled to -78 °C and a solution of BCl_3 in CH_2Cl_2 (1 M, 0.143 mL, 2.2 equiv, 0.143 mmol) added dropwise. The reaction mixture in the cooling bath was left to warm to 22 °C while stirring for 16 h. KPi-buffer (K_2HPO_4/KH_2PO_4, 1 M, pH 7, 10 mL) was added, the aqueous phase extracted with CH_2Cl_2 (3x 10 mL), the combined organic phases washed with sat. aq. NaCl-solution (20 mL), dried over $MgSO_4$ and solvents removed in vacuo. The crude product was isolated by column chromatography (EtOAc:MeOH, 9:1 v/v) as orange crystals in a yield of 16.9 mg (28.7 µmol 44 %).

^{1}H NMR (600 MHz, $CDCl_3$): δ 2.15 (s, 6H, Me), 3.01 (s, 12H, NMe_2), 6.56 (s, 2H), 6.58 (d, ^{3}J = 9.0 Hz, 4H), 6.87 (s, 2H), 7.28 (d, ^{3}J = 9.0 Hz, 4H), 12.99 (s, 2H). **^{13}C NMR** (151 MHz, $CDCl_3$): δ 20.78, 40.17, 102.04, 109.12, 111.85, 112.58, 113.33, 117.29, 127.63, 146.42, 152.81, 153.79, 160.16, 165.32, 183.41. **IR (ATR film) [cm^{-1}]:** 2923, 1649, 1588, 1520, 1482, 1360, 1246, 1201, 1163, 1110, 1034, 814. **TLC** (petroleum ether:EtOAc, 55:45 v/v): R_f = 0.3 **HR-MS (ESI):** m/z calculated for $[C_{36}H_{33}N_2O_6]^+$ ([M + H^+]): 589.2333, found: 589.2340 **Melting point:** 280 – 283 °C

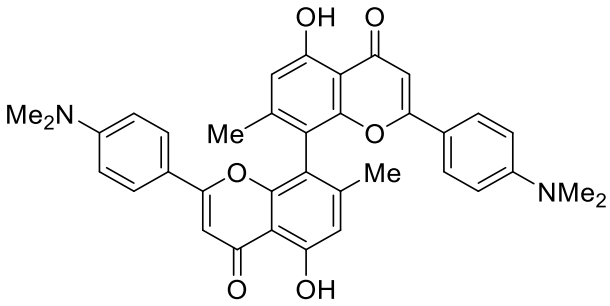

204

7.2.2.8 General Procedure 5 (GP5): *Buchwald* Hartwig Amination

The following chapter contains results obtained by Daniel Grudzinski as part of a bachelor's thesis.[206] Parts of the following chapter will be published in a peer-reviewed journal, a manuscript is currently in preparation.[228]

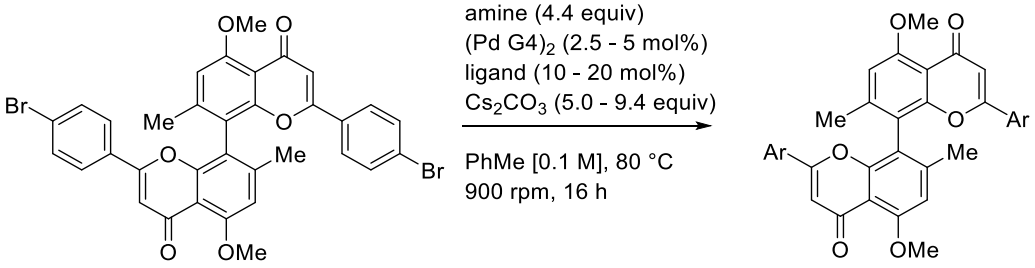

Hydrochloride amine (**GP5a**)

A 2-dr. vial equipped with stir bar which were dried at 110 °C over night was left to cool under Argon-atmosphere. The vial was then charged with Cs_2CO_3 (306 mg, 9.40 equiv, 0.940 mmol), biflavone **183** (68.8 mg, 1.00 equiv, 0.100 mmol), ligand (10 – 20mol%), $(Pd\ G4)_2$ (**205**) (3.8 mg, 5 mol%, 10.0 µmol) and hydrochloride amine (4.4 equiv) in that order. Then PhMe (1 mL, 0.1 M) was added, the reaction vessel capped and sealed using PTFE tape and then stirred at 80 °C for 16 h (900 rpm). After letting the reaction cool, the reaction was filtered over a pad of silica into a vial containing a defined amount of 1,3,5-trimethoxybenzene (0.4 – 0.8 equiv), washing with CH_2Cl_2:MeOH (9:1 v/v). The solvent was removed and conversion to product determined by ^{1}H-NMR. The product was isolated by column chromatography (CH_2Cl_2:EtOAc 1:9 v/v to CH_2Cl_2:MeOH 96:4 v/v).

Amine (**GP5b**)

A 2-dr. vial equipped with stir bar which were dried at 110 °C over night was left to cool under Argon-atmosphere. The vial was then charged with Cs_2CO_3 (306 mg, 9.40 equiv, 0.940 mmol), biflavone **183** (68.8 mg, 1.00 equiv, 0.100 mmol), ligand (10 – 20mol%), $(Pd\ G4)_2$ (**205**) (3.8 mg, 5 mol%, 10.0 µmol). Then a solution of amine in PhMe (1 mL, 4.4 equiv, 0.440 mmol) prepared in a separate dry vial was added (making sure not to purge the vial with an argon balloon so volatile amines wouldn't evaporate), the reaction vessel capped and sealed using PTFE tape and then stirred at 80 °C for 16 h. After letting the reaction cool, the reaction was filtered over a pad of silica into a vial containing a defined amount of 1,3,5-trimethoxybenzene (0.4 – 0.8 equiv), washing with CH_2Cl_2:MeOH (9:1 v/v). The solvent was removed and conversion to product determined by ^{1}H-NMR. The product was isolated by column chromatography (CH_2Cl_2:EtOAc 1:9 v/v to CH_2Cl_2:MeOH 96:4 v/v).

7.2.2.8.1 2,2'-Bis(4-(dimethylamino)phenyl)-5,5'-dimethoxy-7,7'-dimethyl-4*H*,4*'H*-[8,8'-bichromene]-4,4'-dione (181)

The title compound was synthesized according to **GP5a** using biflavone **183** (68.8 mg, 1.0 equiv, 100 µmol, *rac*), RuPhos (9.3 mg, 20 mol%, 20 µmol), $(Pd\ G4)_2$ (**205**) (1.9 mg, 2.5 mol%,2.5 µmol) and dimethylamine hydrochloride (35.9 mg, 4.40 equiv, 0.440 mmol). The product was isolated as yellow solids in a yield of 51.3 mg (83.5 µmol, 83%, *rac*).

Enantiopure

A further experiment following **GP5a** using biflavone **183** (34.4 mg, 1.0 equiv, 50.0 µmol, >99%*ee* S_a), RuPhos (4.7 mg, 20 mol%, 10 µmol), $(Pd\ G4)_2$ (**205**) (1.9 mg, 5 mol%,2.5 µmol) and dimethylamine hydrochloride (17.9 mg, 2.20 equiv, 0.220 mmol) gave the product as pale-yellow solids in a yield of 24.2 mg (39.4 µmol, 79%, >99%*ee* S_a). (81% conversion to product according to ^{1}H-NMR) (isolation by column chromatography CH_2Cl_2:EtOAc 9:1 v/v to CH_2Cl_2:MeOH 97:3)

A further experiment following **GP5a** using biflavone **183** (34.4 mg, 1.0 equiv, 50.0 µmol, >99%*ee* R_a), RuPhos (4.7 mg, 20 mol%, 10 µmol), $(Pd\ G4)_2$ (**205**) (1.9 mg, 5 mol%,2.5 µmol) and dimethylamine hydrochloride (17.9 mg, 2.20 equiv, 0.220 mmol) gave the product as pale-yellow solids in a yield of 27.8 mg (45.2 µmol, 90%, >99%*ee* R_a). (89% conversion to product according to ^{1}H-NMR) (isolation by column chromatography CH_2Cl_2:EtOAc 9:1 v/v to CH_2Cl_2:MeOH 97:3) The analytical data were in accordance with literature (7.2.2.6.3).[108b]

TLC (EtOAc:CH_2Cl_2:MeOH, 7:2.5:0.5 v/v): R_f = 0.16

TLC (EtOAc:CH_2Cl_2:MeOH, 96:4 v/v): R_f = 0.29

Melting point: 196 - 199 °C (*rac*)

HPLC: Lux® Amylose-1 (Phenomenex) 250 ° 4.6 mm, 25 °C, 0.5 mL min^{-1}, 331 nm, *n*-heptane:*i*-PrOH 50:50 (v/v) $t_R(S_a)$ = 9.53 min, $t_R(R_a)$ = 12.8 min.

Optical rotation: $[\alpha]^{25}_D$ = +44.0 (±1.1, duplicate) (c = 0.250, CH_2Cl_2, S_a, >99%ee by chiral HPLC)

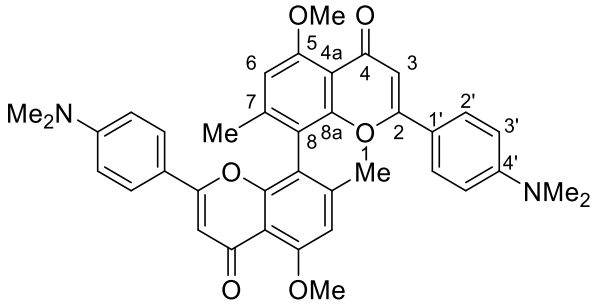

181

7.2.2.8.2 *rac*-2,2'-Bis(4-(diethylamino)phenyl)-5,5'-dimethoxy-7,7'-dimethyl-4H,4'H-[8,8'-bichromene]-4,4'-dione (212)

The title compound was synthesized according to **GP5b** using RuPhos (9.3 mg, 20 mol%, 20 µmol), (Pd G4)$_2$ (**205**) (3.8 mg, 5 mol%, 5.0 µmol) and diethylamine (32.2 mg, 4.40 equiv, 0.440 mmol). The product was isolated as yellow solids in a yield of 50.0 mg (74.5 µmol, 75%).

^{1}H NMR (600 MHz, $CDCl_3$): δ 1.07 – 1.16 (m, 12H, $CH_2\underline{CH_3}$), 2.13 (d, J = 1.7 Hz, 6H, Me), 3.31 (q, $^3J_{CH2\text{-}CH3}$ = 7.2 Hz, 8H, $\underline{CH_2}CH_3$), 4.08 (s, 6H, OMe), 6.46 (d, $^3J_{2'\text{-}3'}$ = 8.6 Hz, 4H, 3'-H), 6.55 (d, J = 2.0 Hz, 2H, 3-H), 6.83 (s, 2H, 6-H), 7.10 – 7.15 (m, 4H, 2'-H). **^{13}C NMR** (151 MHz, $CDCl_3$): δ 12.56 ($CH_2\underline{CH_3}$), 20.63 (Me), 44.44 ($\underline{CH_2}CH_3$), 56.55 (OMe), 104.91 (C-3), 108.00 (C-6), 111.19 (C-3'), 112.76 (C-4a), 116.60 (C-8), 116.67 (C-1'), 127.32 (C-2'), 144.11 (C-7), 149.89 (C-4'), 155.62 (C-8a), 158.91 (C-5), 162.02 (C-2), 178.80 (C-4). **IR (ATR film) [cm^{-1}]**: 3474, 2969, 2924, 2851, 1635, 1602, 1590, 1374, 1333, 1200, 1119, 1061, 817 **TLC** (CH_2Cl_2:MeOH, 95:5 v/v): R_f = 0.57 **HR-MS (ESI):** m/z calculated for $[C_{42}H_{45}N_2O_6]^+$ ([M + H$^+$]): 673.3272, found: 673.3274 (-0.3 ppm). **Melting point:** 173 – 176 °C

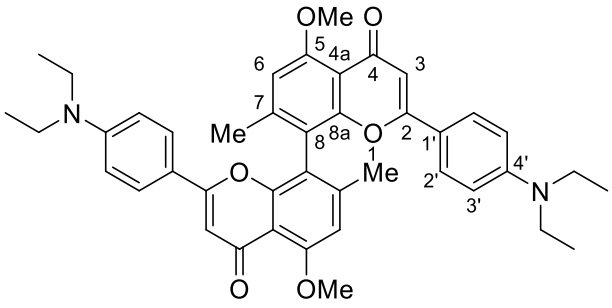

212

7.2.2.8.3 *rac*-5,5'-Dimethoxy-7,7'-dimethyl-2,2'-bis(4-(pyrrolidin-1-yl)phenyl)-4H,4'H-[8,8'-bichromene]-4,4'-dione (213)

The title compound was synthesized according to **GP5b** using RuPhos (9.3 mg, 20 mol%, 20 µmol), (Pd G4)$_2$ (**205**) (1.9 mg, 2.5 mol%,2.5 µmol) and pyrrolidine (31.3 mg, 4.40 equiv, 0.440 mmol). The product was isolated as yellow solids in a yield of 56.2 mg (84.3 µmol, 84%).

^{1}H NMR (600 MHz, $CDCl_3$): δ 1.95 – 2.01 (m, 8H, 2''-H), 2.16 (s, 6H, Me), 3.27 (d, $^3J_{1'',2''}$ = 6.5 Hz, 8H, 1''-H), 4.09 (s, 6H, OMe), 6.36 (d, $^3J_{2',3'}$ = 8.6 Hz, 4H, 3'-H), 6.56 (s, 2H, 3-H), 6.84 (s, 2H, 6-H), 7.15 (d, $^3J_{2',3'}$ = 8.5 Hz, 4H, 2'-H). **^{13}C NMR** (151 MHz, $CDCl_3$): δ 20.71 (Me), 25.55 (C-2''), 47.64 (C-1''), 56.65 (OMe), 105.04 (C-3), 108.01 (C-6), 111.75 (C-3'), 112.85 (C-4a), 116.71 (C-8), 117.02 (C-1'), 127.20 (C-3'), 144.14 (C-7), 149.88 (C-4'), 155.72 (C-8a), 159.00 (C-5), 162.19 (C-2), 178.82 (C-4). **IR (ATR film) [cm^{-1}]**: 3507, 2968, 2847, 1632, 1603, 1589, 15221, 1371, 1336, 1194, 1118, 1062, 815. **TLC** (CH_2Cl_2:MeOH, 95:5 v/v): R_f = 0.65 **HR-MS (ESI):** m/z calculated for $[C_{42}H_{41}N_2O_8]^+$ ([M + H$^+$]): 669.2959, found: 669.2956 (0.5 ppm). **Melting point:** 281 – 285 °C (brown discoloration)

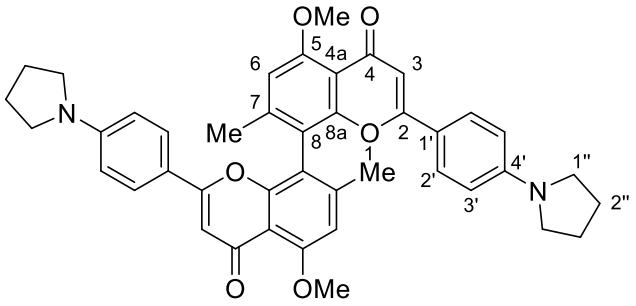

213

7.2.2.8.4 *rac*-5,5'-Dimethoxy-7,7'-dimethyl-2,2'-bis(4-morpholinophenyl)-4H,4'H-[8,8'-bichromene]-4,4'-dione (214)

The title compound was synthesized according to **GP5b** using RuPhos (9.3 mg, 20 mol%, 20 µmol), (Pd G4)$_2$ (**205**) (1.9 mg, 2.5 mol%, 2.5 µmol) and morpholine (39.3 mg, 4.40 equiv, 0.440 mmol). The product was isolated as yellow solids in a yield of 65.6 mg (93.9 µmol, 94%)

^{1}H NMR (600 MHz, $CDCl_3$): δ 2.17 (s, 6H, Me), 3.19 (t, $^3J_{1'',2''}$ = 4.8 Hz, 8H, 1''-H), 3.81 (t, $J_{1'',2''}$ = 4.9 Hz, 8H, 2''-H), 4.09 (s, 6H, OMe), 6.60 (s, 2H, 3-H), 6.66 – 6.74 (m, 4H, 3'-H), 6.85 (s, 2H, 6-H), 7.17 (d, $^3J_{2',3'}$ = 8.7 Hz, 4H, 2'-H). **^{13}C NMR** (151 MHz, $CDCl_3$): δ 20.72 (Me), 47.84 (C-1'), 56.64 (OMe), 66.65 (C-2''), 106.35 (C-3), 108.19 (C-6), 112.83 (C-4a), 114.49 (C-3'), 116.56 (C-8), 121.03 (C-1'), 127.00 (C-2'), 144.50 (C-7), 153.10 (C-4'), 155.72

(C-8a), 159.09 (C-5), 161.27 (C-2), 178.74 (C-4). **IR (ATR film) [cm^{-1}]**: 3492, 2957, 2924, 2852, 1633, 1602, 1517, 1378, 1332, 1232, 1202, 1119, 1064, 928, 825 **TLC** (CH_2Cl_2:MeOH, 95:5 v/v): R_f = 0.62 **HR-MS (ESI):** m/z calculated for $[C_{42}H_{41}N_2O_8]^+$ ([M + H$^+$]): 701.2857, found: 701.2869 (-1.6 ppm). **Melting point:** 233 – 258 °C (brown discoloration)

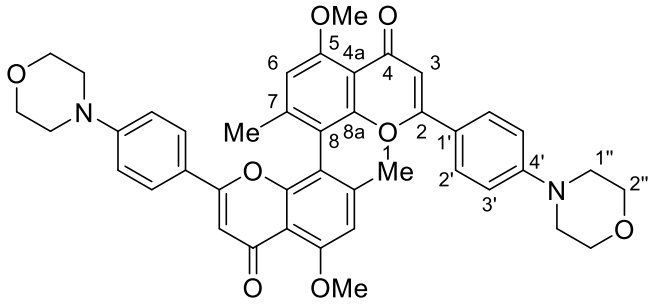

214

7.2.2.8.5 *rac*-5,5'-Dimethoxy-7,7'-dimethyl-2,2'-bis(4-(piperidin-1-yl)phenyl)-4H,4'H-[8,8'-bichromene]-4,4'-dione (215)

The title compound was synthesized according to **GP5b** using BrettPhos (9.3 mg, 20 mol%, 20 µmol), (Pd G4)$_2$ (**205**) (3.8 mg, 5 mol%, 5.0 µmol) and piperidine (37.5 mg, 4.40 equiv, 0.440 mmol). The product was isolated as yellow solids in a yield of 56.5 mg (81.3 µmol, 81%).

^{1}H NMR (600 MHz, $CDCl_3$): δ 1.61 (m, 12H, 2''+3''-H), 2.17 (s, 6H, Me), 3.25 (t, $^3J_{1'',-2''}$ = 5.0 Hz, 8H, 1''-H), 4.09 (s, 6H, OMe), 6.58 (s, 2H, 3-H), 6.70 (d, $^3J_{2',-3'}$ = 8.7 Hz, 4H, 3'-H), 6.84 (s, 2H, 6-H), 7.14 (d, $^3J_{2',-3'}$ = 8.6 Hz, 4H, 2'-H). **^{13}C NMR** (151 MHz, $CDCl_3$): δ 20.72 (Me), 24.42 (C-3''), 25.37 (C-2''), 48.94 (C-1''), 56.64 (OMe), 105.87 (C-3), 108.11 (C-6), 112.85 (C-4a), 114.57 (C-3'), 116.63 (C-8), 119.29 (C-1'), 127.07 (C-2'), 144.33 (C-7), 153.24 (C-4'), 155.72 (C-8a), 159.05 (C-5), 161.56 (C-2), 178.77 (C-4). **IR (ATR film) [cm^{-1}]**: 3477, 2930, 2847, 1633, 1603, 1516, 1383, 1336, 1234, 1199, 1061, 1024, 828. **TLC** (CH_2Cl_2:MeOH, 95:5 v/v): R_f = 0.61 **HR-MS (ESI):** m/z calculated for $[C_{44}H_{45}N_2O_6]^+$ ([M + H$^+$]): 697.3272, found: 697.3281 (-1.3 ppm). **Melting point:** 195 – 208 °C (brown discoloration)

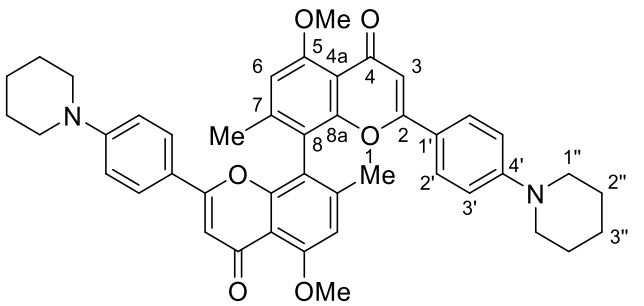

215

7.2.2.8.6 *rac*-2,2'-Bis(4-(azetidin-1-yl)phenyl)-5,5'-dimethoxy-7,7'-dimethyl-4H,4'H-[8,8'-bichromene]-4,4'-dione (216)

The title compound was synthesized according to **GP5b** using RuPhos (9.3 mg, 20 mol%, 20 µmol), (Pd G4)$_2$ (**205**) (3.8 mg, 5 mol%, 10.0 µmol) and azetidine (25.1 mg, 4.40 equiv, 0.440 mmol). The product was isolated as yellow solids in a yield of 50.0 mg (78.2 µmol, 78%).

^{1}H NMR (600 MHz, $CDCl_3$): δ 2.16 (s, 6H, Me), 2.36 (p, $^3J_{1'',2''}$ = 7.3 Hz, 4H, 2''-H), 3.87 – 3.93 (m, 8H, 1''-H), 4.09 (s, 6H, OMe), 6.18 – 6.25 (m, 4H, 3'-H), 6.56 (s, 2H, 3-H), 6.84 (s, 2H, 6-H), 7.06 – 7.15 (m, 4H, 2'-H). **^{13}C NMR** (151 MHz, $CDCl_3$): δ 16.71 (C-2''), 20.72 (Me), 51.86 (C-1''), 56.64 (OMe), 105.46 (C-3), 108.04 (C-6), 110.80 (C-3'), 112.77 (C-4a), 116.62 (C-8), 118.52 (C-1'), 126.93 (C-2'), 144.27 (C-7), 153.46 (C-4'), 155.68 (C-8a), 159.00 (C-5), 161.94 (C-2), 178.81 (C-4). **IR (ATR film) [cm^{-1}]**: 3469, 2930, 2855, 2233, 1634, 1604, 1518, 1477, 1365, 1335, 1298, 1246, 1183, 1119, 1060, 907, 825, 724, 646. **TLC** (CH_2Cl_2:MeOH, 96:4 v/v): R_f = 0.38 **HR-MS (ESI):** m/z calculated for $[C_{40}H_{37}N_2O_6]^+$ ([M + H$^+$]): 641.2646, found: 641.2652 (-1.0 ppm). **Melting point:** 275 °C (decomposition) (*rac*)

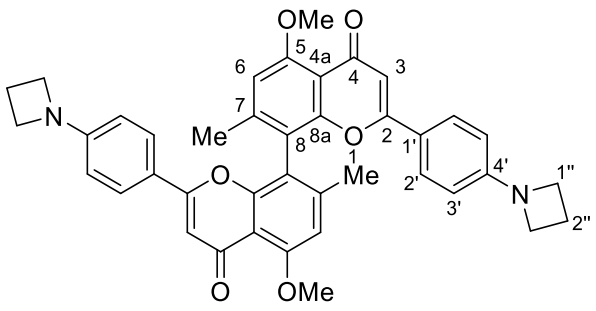

216

7.2.2.8.7 *rac*-2,2'-Bis(4-(benzylamino)phenyl)-5,5'-dimethoxy-7,7'-dimethyl-4H,4'H-[8,8'-bichromene]-4,4'-dione (218)

The title compound was synthesized according to **GP5b** using RuPhos (9.3 mg, 20 mol%, 20 µmol), (Pd G4)$_2$ (**205**) (3.8 mg, 5 mol%, 5.0 µmol) and morpholine (47.1 mg, 4.40 equiv, 0.440 mmol). The product was isolated as yellow solids in a yield of 24.9 mg (33.7 µmol, 34%).

^{1}H NMR (600 MHz, $CDCl_3$): δ 2.15 (s, 6H, Me), 4.07 (s, 6H, OMe), 4.33 (s, 4H, CH_2), 6.47 (d, $^3J_{2',3'}$ = 8.5 Hz, 4H, 3'-H), 6.56 (s, 2H, 3-H), 6.83 (s, 2H, 6-H), 7.11 (d, $^3J_{2',3'}$ = 8.6 Hz, 4H.

2'-H), 7.27 – 7.37 (m, 10H, Ph). **^{13}C NMR** (151 MHz, $CDCl_3$): δ 20.74 (Me), 47.77 (CH_2), 56.66 (OMe), 105.66 (C-3), 108.13 (C-6), 112.73 (C-3'), 112.84 (C-4a), 116.60 (C-8), 119.51 (C-1'), 127.40 (C-2'), 127.51, 127.67 (C-4''), 128.93, 138.39, 144.37 (C-7), 150.65 (C-4'), 155.69 (C-8a), 159.09 (C-5), 161.74 (C-2), 178.75 (C-4). **IR (ATR film) [cm^{-1}]**: 3321, 2929, 2847, 1632, 1603, 1591, 1525, 1370, 1332, 1251, 1183, 1120, 1060, 826, 733, 699. **TLC** (CH_2Cl_2:MeOH, 95:5 v/v): R_f = 0.64 **HR-MS (ESI):** m/z calculated for $[C_{48}H_{41}N_2O_6]^+$ ([M + H^+]): 741.2959, found: 741.2965 (-0.8 ppm). **Melting point:** 286 – 290 °C (brown discoloration)

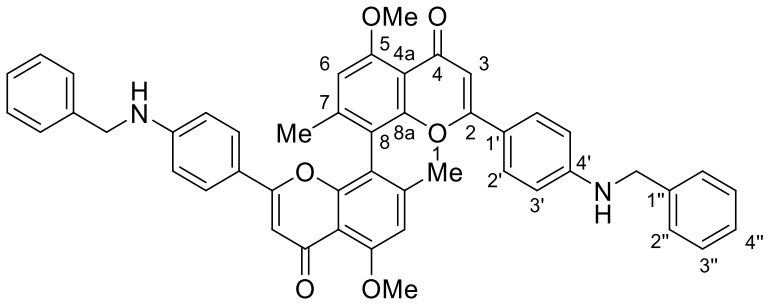

218

7.2.2.8.8 *rac*-5,5'-Dimethoxy-7,7'-dimethyl-2,2'-bis(4-(methylamino)phenyl)-4H,4'H-[8,8'-bichromene]-4,4'-dione (217)

The title compound was synthesized according to **GP5a** using BrettPhos (10.7 mg, 20 mol%, 20.0 µmol), $(Pd\ G4)_2$ (**205**) (3.8 mg, 5 mol%, 5.0 µmol) and methylamine hydrochloride (25.1 mg, 4.40 equiv, 0.440 mmol). The product was isolated as yellow solids in a yield of 4.6 mg (7.81 µmol, 8%).

^{1}H NMR (600 MHz, $CDCl_3$): δ 2.17 (s, 6H, Me), 2.82 (s, 6H, NH*Me*), 4.09 (s, 6H, OMe), 6.38 – 6.48 (m, 4H, 3'-H), 6.56 (s, 2H, 3-H), 6.84 (s, 2H, 6-H), 7.05 – 7.18 (m, 4H, 2'-H). **^{13}C NMR** (151 MHz, $CDCl_3$): δ 20.73 (Me), 30.31 (NH*Me*), 56.63 (OMe), 105.47 (C-3), 108.05 (C-6), 112.16 (C-3'), 112.80 (C-4a), 116.61 (C-8), 118.92 (C-1'), 127.30 (C-2'), 144.32 (C-7), 151.81 (C-4'), 155.68 (C-8a), 159.03 (C-5), 161.86 (C-2), 178.84 (C-4). **IR (ATR film) [cm^{-1}]:** 3340, 2930, 2233, 1633, 1588, 1535, 1330, 1246, 1193, 1125, 1064, 829, 731. **TLC** (CH_2Cl_2:MeOH, 96:4 v/v): R_f = 0.19 **HR-MS (ESI):** m/z calculated for $[C_{36}H_{33}N_2O_6]^+$ ([M + H^+]): 589.2333, found: 589.2339 (-1.0 ppm).

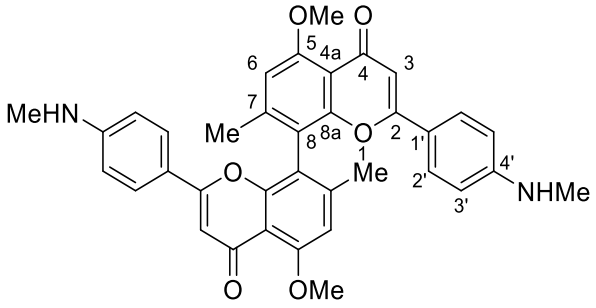

217

7.2.2.8.8.1 *rac*-2-(4-Bromophenyl)-5,5'-dimethoxy-7,7'-dimethyl-2'-(4-(methylamino)phenyl)-4H,4'H-[8,8'-bichromene]-4,4'-dione (219)

The title compound was isolated as a sideproduct during the synthesis of **217** as orange solids in a yield of 4.4 mg (7.46 µmol, 7%)

^{1}H NMR (600 MHz, $CDCl_3$): δ 2.17 (s, 3H, Me/Me'), 2.18 (s, 3H, Me/Me'), 2.83 (s, 3H, NH*Me*), 3.78 (s, 3H, OMe''), 4.09 (s, 3H, OMe/OMe'), 4.10 (s, 3H, OMe/OMe'), 6.46 (d, $^{3}J_{2'''-3'''}$ = 8.5 Hz, 2H, 3'''-H), 6.58 (s, 1H, 3'-H), 6.63 (s, 1H, 3-H), 6.78 (d, $^{3}J_{2''-3''}$ = 8.9 Hz, 2H, 3''-H), 6.86 (s, 1H, 6'-H), 6.87 (s, 1H, 6-H), 7.13 (d, $^{3}J_{2'''-3'''}$ = 8.8 Hz, 2H, 2'''-H), 7.23 (d, $^{3}J_{2''-3''}$ = 8.9 Hz, 1H, 2''-H). **^{13}C NMR** (151 MHz, $CDCl_3$): δ 20.74, 20.79, 30.44 (NHMe), 55.62 (OMe''), 56.67, 56.68, 105.54, 107.10, 108.09, 108.26, 112.36, 112.81, 114.61, 116.41, 116.66, 123.41, 127.30, 127.33, 144.32, 144.79, 151.62, 151.65, 155.73, 159.11, 159.13, 161.00, 161.81, 162.25, 178.75 (C-4), 178.79. **IR (ATR film) [cm^{-1}]:** 3340, 2938, 2249, 1740, 1633, 1595, 1368, 1330, 1254, 1186, 1118, 1057, 829, 731. **TLC** (CH_2Cl_2:MeOH, 96:4 v/v): R_f = 0.25 **HR-MS (ESI):** m/z calculated for $[C_{36}H_{32}NO_7]^+$ ([M + H$^+$]): 590.2173, found: 590.2169 (0.7 ppm).

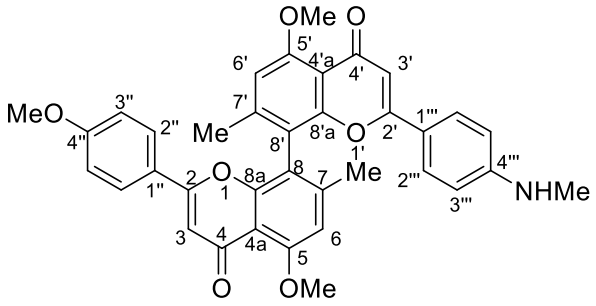

219

7.2.2.8.9 5-Methoxy-7-methyl-2-(4-morpholinophenyl)-4H-chromen-4-one (210)

A 2 d.r. vial was charged with readily available flavone[108b] **154** (34.5 mg, 1.00 equiv, 0.100 mmol), RuPhos (18.6 mg, 40 mol%, 40.0 µmol), (Pd G4)$_2$ (**205**) (1.9 mg, 2.5 mol%, 2.5 µmol). A separate dry vial was charged with morpholine (38.4 mg, 4.40 equiv, 0.440 mmol) (making sure not to purge the vial with an argon balloon so the volatile amine wouldn't evaporate) and PhMe (2 mL). Then that solution of amine in PhMe (1 mL, 2.20 equiv, 0.220 mmol) was added, the reaction vessel capped and sealed using PTFE tape and then stirred at 80 °C for 16 h. After letting the reaction cool, the reaction was filtered over a pad of silica into a vial containing a defined amount of 1,3,5-trimethoxybenzene (0.4 – 0.8 equiv), washing with CH_2Cl_2:MeOH (7:3 v/v). The solvent was removed and conversion to product determined by ^{1}H-NMR. The product was isolated by column chromatography (CH_2Cl_2:MeOH 97:3 v/v to CH_2Cl_2:EtOAc 7:3 v/v) as brown solids in a yield of 31.4 mg (89.4 µmol, 89%)

^{1}H NMR (600 MHz, $CDCl_3$): δ 2.44 (s, 3H, Me), 3.28 (t, $^3J_{1'',2''}$ = 4.8 Hz, 4H, 1''-H), 3.87 (t, $^3J_{1'',2''}$ = 4.8 Hz, 4H, 2''-H), 3.97 (s, 3H, OMe), 6.60 (s, 2H, 3-H + 6-H), 6.93 (s, 1H, 8-H), 6.95 (d, $^3J_{2',3'}$ = 8.4 Hz, 2H, 3'-H), 7.78 (d, $^3J_{2',3'}$ = 8.4 Hz, 2H, 2'-H). **^{13}C NMR** (151 MHz, $CDCl_3$): δ 22.39 (Me), 48.05 (C-1''), 56.53 (OMe), 66.74 (C-2''), 107.08 (C-3), 107.74 (C-6), 110.35 (C-8), 112.52 (C-4a), 114.59 (C-3'), 121.84 (C-1'), 127.48 (C-2'), 144.87 (C-7), 153.20 (C-4'), 158.37 (C-8a), 159.56 (C-5), 161.27 (C-2), 178.40 (C-4). **IR (ATR film) [cm^{-1}]**: 3466, 2920, 2847, 1633, 1603, 1517, 1481, 1377, 1335, 1233 1203, 1118, 1049, 926, 826 **TLC** (CH_2Cl_2:MeOH, 95:5 v/v): R_f = 0.46 **HR-MS (ESI):** m/z calculated for $[C_{21}H_{22}NO_4]^+$ ([M + H^+]): 352.1543, found: 352.1549 (-1.5 ppm). **Melting point:** 218 – 221 °C (brown discoloration)

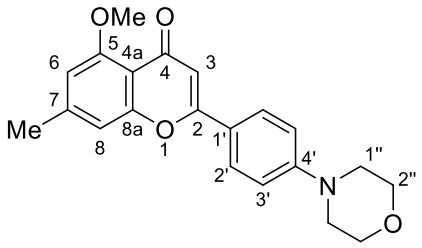

214

7.2.2.8.10 2-(4-(Benzylamino)phenyl)-5-methoxy-7-methyl-4H-chromen-4-one (211)

A 2 d.r. vial was charged with readily available flavone[108b] **154** (34.5 mg, 1.00 equiv, 0.100 mmol), RuPhos (4.7 mg, 10 mol%, 10 µmol), (Pd G4)$_2$ (**205**) (1.9 mg, 2.5 mol%,

2.5 µmol). A separate dry vial was charged with benzylamine (47.1 mg, 4.40 equiv, 0.440 mmol) (making sure not to purge the vial with an argon balloon so the volatile amine wouldn't evaporate) and PhMe (2 mL). Then that solution of amine in PhMe (1 mL, 2.20 equiv, 0.220 mmol) was added, the reaction vessel capped and sealed using PTFE tape and then stirred at 80 °C for 16 h. After letting the reaction cool, the reaction was filtered over a pad of silica into a vial containing a defined amount of 1,3,5-trimethoxybenzene (0.4 – 0.8 equiv), washing with CH_2Cl_2:MeOH (7:3 v/v). The solvent was removed and conversion to product determined by ^{1}H-NMR. The product was isolated by column chromatography (CH_2Cl_2:MeOH 97:3 v/v to CH_2Cl_2:EtOAc 7:3 v/v) as orange solids in analytical quantities. (54% conversion to product according to ^{1}H-NMR).

^{1}H NMR (600 MHz, $CDCl_3$): δ 2.44 (s, 3H, Me), 3.97 (s, 3H, OMe), 4.41 (s, 2H, CH_2), 6.57 (s, 1H, 3-H), 6.60 (s, 1H, 6-H), 6.64 – 6.72 (m, 2H, 3'-H), 6.91 (s, 1H, 8-H), 7.30 (m, 1H, 4''-H), 7.36 (m, 4H, 2''-H +3''-H), 7.66 – 7.75 (m, 2H, 2'-H). **^{13}C NMR** (151 MHz, $CDCl_3$): δ 22.39 (Me), 47.92 (CH_2), 56.55 (OMe), 106.36 (C-3), 107.68 (C-6), 110.34 (C-8), 112.52 (C-4a), 112.71 (C-3'), 120.09 (C-1'), 127.54 (C-2''/3''), 127.71 (C-4''), 127.81 (C-2'), 128.96 (C-2''/3''), 138.53 (C-1''), 144.68 (C-7), 150.69 (C-4'), 158.37 (C-8a), 159.56 (C-5), 161.74 (C-2), 178.43 (C-4). **IR (ATR film) [cm^{-1}]**: 3307, 2921, 2848, 1638, 1599, 1526, 1479, 1348, 1253, 1192, 1122, 1050, 837, 817, 698 **TLC** (CH_2Cl_2:MeOH, 96:4 v/v): R_f = 0.35 **HR-MS (ESI):** m/z calculated for $[C_{21}H_{22}NO_4]^+$ ([M + H$^+$]): 372.1595, found: 352.1594 (-0.2 ppm). **Melting point:** 250 – 251 °C

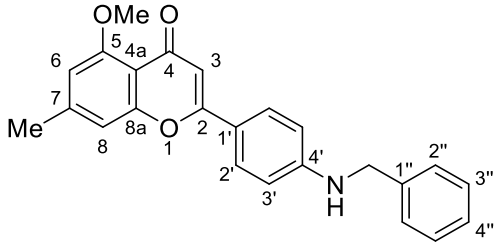

211

7.2.3 General Procedure 6 (GP6): *Masuda* Borylation

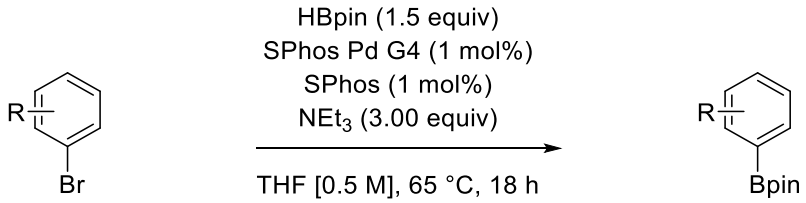

An appropriately sized Schlenk round bottom flask equipped with a stir bar was charged with aryl halide (1.000 equiv), SPhos Pd G4 (1 mol%) and SPhos (1 mol%) (or $(Pd\ G4)_2$ (**205**) (0.5 mol%) and SPhos (2.0 mol%) respectively) and capped with a rubber septum. The mixture was evacuated and backfilled with N_2 (3x). Anhydr. degassed (by sparging for 20 min) THF was added. The reaction was heated to 65 °C. After 5 mins HBpin (1.500 equiv) and NEt_3 (3.000 equiv) were added. The yellow-orange reaction mixture turns black and turbid after a short while and was stirred overnight. After full conversion (grey suspension) the reaction mixture was cooled to room temperature. Methanol was added and the crude mixture filtered over a pad of Celite® washing with EtOAc and solvents removed in vacuo. The product was isolated as stated either by distillation, an additional aq. washing step or column chromatography.

7.2.3.1 2-(4-Methoxy-2-methylphenyl)-4,4,5,5-tetramethyl-1,3,2-dioxaborolane (222)

The title compound was synthesized in accordance with **GP6** with 1-bromo-4-methoxy-2-methylbenzene (4.00 mL, 28.91 mmol, 1.000 equiv), $(Pd\ G4)_2$ (**205**) (110.9 mg, 0.14 mmol, 0.5 mol%), SPhos (237 mg, 0.58 mmol, 2.0 mol%), HBpin (6.29 mL, 43.36 mmol, 1.500 equiv), NEt_3 (12.09 mL, 86.72 mmol, 3.000 equiv) in THF (70 mL). The product was isolated by Kugelrohr distillation ($2 \cdot 10^{-1}$ mbar, 110 °C). The white solids in the collection bulb were removed and the remaining liquid subjected to the same procedure twice over until no more white solid crystallizes in the collection bulb. Then the product was isolated from the remaining mixture by Kugelrohr® distillation ($2 \cdot 10^{-1}$ mbar, 160 °C) as a colorless liquid in a yield of 6.13 g (24.7 mmol, 85%). The analytical data were in accordance with literature.[321]

^{1}H NMR (600 MHz, $CDCl_3$): δ 1.34 (s, 12H, $B(OC\underline{Me}_2)_2$), 2.55 (s, 3H, Me), 3.81 (s, 3H, OMe), 6.70 – 6.74 (m, 2H, 3-H + 5-H), 7.74 (d, $^3J_{6\text{-}5} = 9.0$ Hz, 1H, 6-H). **^{13}C NMR** (151 MHz, $CDCl_3$): δ 22.54 (Me), 25.00 ($B(OC\underline{Me}_2)_2$), 55.09 (OMe), 83.23 ($B(O\underline{C}Me_2)_2$), 110.24 (C-5), 115.63 (C-3), 120.33 (C-1), 137.97 (C-6), 147.35 (C-2), 161.82 (C-4). **^{11}B NMR** (96 MHz, $CDCl_3$): δ 30.52. **IR (ATR film) [cm^{-1}]:** 2980, 2932, 2828, 1602, 1347, 1314, 1290, 1273, 1233, 1146,

1128, 1041, 860, 660. **TLC** (petroleum ether:EtOAc 98:2 v/v): R_f = 0.3 **APCI-MS:** m/z: ([M + H^+]): found: 249.3 **Boiling point:** 160 °C ($2 \cdot 10^{-1}$ mbar) **Density**: 1.13 g/cm^3

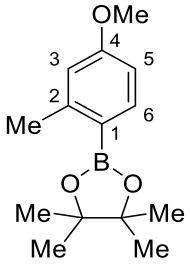

222

7.2.3.2 4,4,5,5-Tetramethyl-2-phenyl-1,3,2-dioxaborolane (261)

The title compound was synthesized in accordance with **GP6** with bromobenzene (3.00 g, 19.11 mmol, 1.000 equiv), $(Pd\ G4)_2$ (**205**) (73.3 mg, 0.096 mmol, 0.5 mol%), SPhos (78.4 mg, 0.191 mmol, 2.0 mol%), HBpin (4.16 mL, 28.66 mmol, 1.500 equiv), NEt_3 (8.00 mL, 4.01 mmol, 3.000 equiv) in THF (40 mL). The product was isolated by column chromatography (petroleum ether: EtOAc, 97.5:2.5 v/v) as a colorless liquid in a yield of 2.20 g (10.8 mmol, 56%). The analytical data were in accordance with literature.[322]

^{1}H NMR (600 MHz, $CDCl_3$): δ 1.36 (s, 12H, $B(OC\underline{Me}_2)_2$), 7.38 (t, $^3J_{3\text{-}4;3\text{-}2}$ = 7.6 Hz, 2H, 3-H), 7.47 (t, $^3J_{4\text{-}3}$ = 7.4 Hz, 1H, 4-H), 7.82 (d, $^3J_{2\text{-}3}$ = 7.9 Hz, 2H, 2-H). **^{13}C NMR** (151 MHz, $CDCl_3$): δ 25.01 ($B(OC\underline{Me}_2)_2$), 83.90 ($B(O\underline{C}Me_2)_2$), 127.84 (C-3), 131.38 (C-4), 134.88 (C-2). **^{11}B NMR** (96 MHz, $CDCl_3$): δ 31.00. **IR (ATR film) [cm^{-1}]:** 3054, 3022, 2952, 2922, 1552, 1456, 1441, 1174, 1127, 1010, 826, 764, 736, 700, 637, 524. **APCI-MS:** m/z: ([M + H^+]): found: 205.2

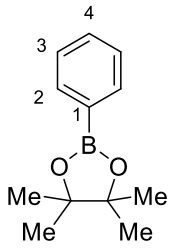

261

7.2.3.3 4,4,5,5-Tetramethyl-2-(o-tolyl)-1,3,2-dioxaborolane (256)

The title compound was synthesized in accordance with **GP6** with 1-bromo-2-methylbenzene (10.00 g, 45.86 mmol, 1.00 equiv), SPhos Pd G4 (364.3 mg, 0.46 mmol,

1 mol%), SPhos (188.3 mg, 0.46 mmol, 1 mol%), HBpin (9.98 mL, 68.80 mmol, 1.50 equiv), NEt_3 (19.18 mL, 137.59 mmol, 3.00 equiv) in THF (120 mL). The product was isolated *via* Kugelrohr distillation ($9.5 \cdot 10^{-2}$ mbar, 62 °C). The white solids in the collection bulb were removed and the remaining liquid subjected to the same procedure twice over until no more white solid crystallizes in the collection bulb. Then the product was isolated from the remaining mixture by Kugelrohr® distillation ($8 \cdot 10^{-2}$ mbar, 85 °C) as a colorless liquid in a yield of 9.29 g (42.6 mmol, 93%).

In a different batch the title compound was synthesized in accordance with **GP1** with 1-bromo-2-methylbenzene (6.4 mL, 50.0 mmol, 1.00 equiv), Sphos Pd G4 (397.1 mg, 0.5 mmol, 1 mol%), SPhos (205.3 mg, 0.5 mmol, 1 mol%), HBpin (10.9 mL, 75.0 mmol, 1.50 equiv), NEt_3 (20.9 mL, 50.0 mmol, 3.00 equiv) in THF (100 mL, 0.5 M). The crude product was suspended in *n*-pentane and filtered over a plug of silica to remove pinacol. The product was isolated as a colorless liquid in a yield of 9.96 g (45.5 mmol, 91%). The analytical data were in accordance with literature.[323]

^{1}H NMR (600 MHz, $CDCl_3$): δ 1.35 (s, 12H, B(OC*Me*$_2$)$_2$), 2.54 (s, 3H, Me), 7.13 – 7.19 (m, 2H, H-2, 4-H), 7.32 (td, $^3J_{3\text{-}4}$ = 7.5, $^4J_{3\text{-}5}$ = 1.6 Hz, 1H, 3-H), 7.76 (dd, $^3J_{5\text{-}4}$ = 7.7, $^4J_{5\text{-}3}$ = 1.6 Hz, 1H, 5-H). **^{13}C NMR** (151 MHz, $CDCl_3$): δ 22.36 (Me), 25.04 (B(OC*Me*$_2$)$_2$), 83.54 (B(O*C*Me$_2$)$_2$), 124.84 (C-4), 129.91 (C-2), 130.92 (C-3), 135.99 (C-5), 144.97 (C-1). **^{11}B NMR** (96 MHz, $CDCl_3$): δ 31.11. **IR (ATR film) [cm^{-1}]:** 2978, 2929, 1601, 1439, 1380, 1344, 1311, 1265, 1144, 1072, 1043, 963, 861, 729, 659. **TLC** (petroleum ether:EtOAc 98:2 v/v): R_f = 0.47 **APCI-MS:** m/z: ([M + H$^+$]): found: 219.1 **Boiling point:** 85 °C ($8 \cdot 10^{-2}$ mbar)

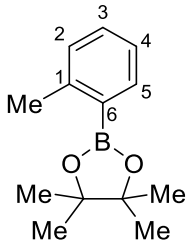

256

7.2.3.4 2-(2-Methoxyphenyl)-4,4,5,5-tetramethyl-1,3,2-dioxaborolane (259)

The title compound was synthesized in accordance with **GP6** with 2-bromoanisole (1.00 g, 4.27 mmol, 1.000 equiv), (Pd G4)$_2$ (**205**) (16.4 mg, 0.02 mmol, 0.5 mol%), SPhos (17.5 mg, 0.02 mmol, 2.0 mol%), HBpin (930 µL, 6.41 mmol, 1.500 equiv), NEt_3 (1.79 mL, 12.82 mmol, 3.000 equiv) in THF (10 mL). The product was isolated *via* Kugelrohr distillation ($5.5 \cdot 10^{-}$

^{2} mbar, 102 °C). The product was collected from the collection bulbs and redissolved in pentane and washed with sat. aq. Na_2CO_3-solution (2x 50 mL). The solvent was removed *in vacuo*. The product was isolated as white solids in a yield of 902 mg (3.84 mmol, 90%). The analytical data were in accordance with literature.[324]

^{1}H NMR (600 MHz, $CDCl_3$): δ 1.35 (d, J = 1.2 Hz, 12H, B(OCMe_2)$_2$), 3.83 (d, J = 1.1 Hz, 3H, OMe), 6.86 (d, $^{3}J_{3\text{-}4}$ = 8.3 Hz, 1H, 3-H), 6.94 (t, $^{3}J_{5\text{-}4;5\text{-}6}$ = 7.3 Hz, 1H, 5-H), 7.35 – 7.43 (m, 1H, 4-H), 7.67 (d, $^{3}J_{5\text{-}6}$ = 7.6 Hz, 1H, 6-H). **^{13}C NMR** (151 MHz, $CDCl_3$): δ 24.97 (B(OCMe_2)$_2$), 55.96 (Me), 83.58 (B(O*C*Me$_2$)$_2$), 110.60 (C-3), 120.33 (C-5), 132.58 (C-4), 136.84 (C-6), 164.31 (C-2). **^{11}B NMR** (96 MHz, $CDCl_3$): δ 30.71. **IR (ATR film) [cm^{-1}]:** 2978, 2931, 2834, 1601, 1577, 1489, 1433, 1354, 1249, 1145, 1074, 861, 762, 659. **HR-MS (ESI):** m/z calculated for $[C_{13}H_{20}BO_3]^+$ ([M + H$^+$]): 235.1500, found: 235.1508.

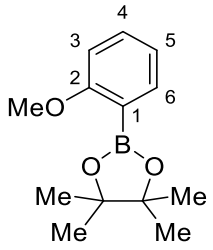

259

7.2.3.5 2-(4-Methoxyphenyl)-4,4,5,5-tetramethyl-1,3,2-dioxaborolane (260)

The title compound was synthesized in accordance with **GP6** with 4-bromoanisole (167 µL, 1.30 mmol, 1.00 equiv), SPhos Pd G4 (11 mg, 0.013 mmol, 1.0 mol%), SPhos (5.5 mg, 0.013 mmol, 1.0 mol%), HBpin (291 µL, 2.00 mmol, 1.50 equiv), NEt_3 (559 µL, 4.01 mmol, 3.00 equiv) in THF (2.50 mL). The product was isolated by column chromatography (petroleum ether: EtOAc, 95:5 v/v) as a colorless liquid in a yield of 255 mg (1.09 mmol, 84%). The analytical data were in accordance with literature.[321]

^{1}H NMR (600 MHz, $CDCl_3$): δ 1.33 (s, 12H, B(OCMe_2)$_2$), 3.83 (s, 3H, OMe), 6.90 (d, $^{3}J_{2\text{-}3}$ = 8.6 Hz, 2H, 3-H), 7.75 (d, $^{3}J_{2\text{-}3}$ = 8.5 Hz, 2H, 2-H). **^{13}C NMR** (151 MHz, $CDCl_3$): δ 24.88 (B(OC$\underline{Me}_2$)$_2$), 55.09 (OMe), 83.55 (B(O$\underline{C}$Me$_2$)$_2$), 113.32 (C-3),120.63 (C-1), 136.53 (C-2), 162.17 (C-4). **^{11}B NMR** (96 MHz, $CDCl_3$): δ 30.38. **IR** (ATR film) **[cm^{-1}]**: 2978, 2936, 2839, 1605, 1397, 1361, 1318, 1278, 1248, 1144, 1092, 1031, 656. **APCI-MS:** m/z: ([M + H$^+$]): found: 235.2

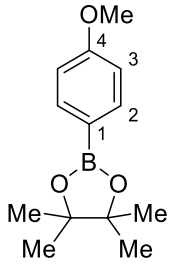

260

7.2.3.6 2-(2-Fluorophenyl)-4,4,5,5-tetramethyl-1,3,2-dioxaborolane (258)

The title compound was synthesized in accordance with **GP6** with 1-bromo-2-fluorobenzene (1.00 g, 4.50 mmol, 1.00 equiv), SPhos Pd G4 (35.8 mg, 0.05 mmol, 1 mol%), SPhos (18.5 mg, 0.05 mmol, 1 mol%), HBpin (980 µL, 6.76 mmol, 1.50 equiv), NEt_3 (1.88 mL, 13.51 mmol, 3.00 equiv) in THF (9 mL). The product was isolated by column chromatography (petroleum ether: CH_2Cl_2, 8:2 v/v) as a colorless liquid (m.p. lit 53°C [325]) in a yield of 757 mg (3.41 mmol, 76%). The analytical data were in accordance with literature.[326]

^{1}H NMR (600 MHz, $CDCl_3$): δ 1.36 (s, 12H, B(OC*Me*$_2$)$_2$), 7.02 (t, $^3J_{H\text{-}3,F\text{-}2;H\text{-}3,H\text{-}4}$ = 8.9 Hz, 1H, 3-H), 7.13 (t, $^3J_{H\text{-}5,H\text{-}4;H\text{-}5,H\text{-}6}$ = 7.3 Hz, 1H, 5-H), 7.43 (tdd, *J* = 7.7, 5.5, 1.9 Hz, 1H, 4-H), 7.74 (ddd, *J* = 7.8, 6.0, 1.9 Hz, 1H, 6-H). **^{13}C NMR** (151 MHz, $CDCl_3$): δ 24.96 (B(OC*Me*$_2$)$_2$), 84.03 (B(O*C*Me$_2$)$_2$), 115.38 (d, $^2J_{C\text{-}F}$ = 23.9 Hz, C-3), 123.72 (d, $^4J_{5\text{-}F}$ = 3.2 Hz, C-5), 133.40 (d, $^3J_{4\text{-}F}$ = 8.7 Hz, C-4), 136.95 (d, $^3J_{6\text{-}F}$ = 8.0 Hz, C-6), 167.33 (d, $^1J_{2\text{-}F}$ = 250.7 Hz, C-2). **^{11}B NMR** (96 MHz, $CDCl_3$): δ 30.14 (brs). **^{19}F NMR** (282 MHz, $CDCl_3$): δ -102.64 (dt, $^3J_{C\text{-}2,C\text{-}3}$ = 9.3 Hz, $^4J_{C\text{-}2,C\text{-}4}$ = 5.9 Hz). **IR (ATR film) [cm^{-1}]:** 2981, 2934, 1616, 1489, 1447, 1356, 1214, 1145, 1112, 767, 657. **TLC** (petroleum ether:CH_2Cl_2 8:2 v/v): R_f = 0.1 **APCI-MS:** m/z: ([M + H^+]): found: 223.2

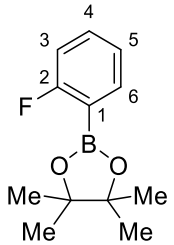

258

7.2.3.7 2-(2-(Trifluoromethyl)phenyl)-4,4,5,5-tetramethyl-1,3,2-dioxaborolane (257)

The title compound was synthesized in accordance with **GP6** with 1-bromo-2-(trifluoromethyl)benzene (1.00 g, 3.68 mmol, 1.00 equiv), $(Pd\ G4)_2$ (**205**) (28.4 mg, 0.04 mmol, 1 mol%), SPhos (30.2 mg, 0.07 mmol, 4 mol%), HBpin (800 µL, 6.41 mmol, 1.50 equiv), NEt_3 (1.54 mL, 12.82 mmol, 3.00 equiv) in THF (9 mL). The product was isolated *via* Kugelrohr distillation ($5.5 \cdot 10^{-2}$ mbar, 102 °C). The product was isolated by column chromatography (petroleum ether: EtOAc, 97:3 v/v) as a colorless liquid in a yield of 396 mg (1.46 mmol, 40%). The analytical data were in accordance with literature.[327]

^{1}H NMR (600 MHz, $CDCl_3$): δ 1.40 (d, J = 1.7 Hz, 12H, $B(OC\mathit{Me}_2)_2$), 7.53 (m, 2H, 4-H + 5-H), 7.69 (d, $^3J_{3\text{-}4}$ = 6.3 Hz, 1H, 3-H), 7.75 (d, $^3J_{6\text{-}5}$ = 6.1 Hz, 1H, 6-H). **^{13}C NMR** (151 MHz, $CDCl_3$): δ 24.61 ($B(OC\mathit{Me}_2)_2$), 84.49 ($B(OC\mathrm{Me}_2)_2$), 124.42 (q, $^1J_{C\text{-}F}$ = 273.4 Hz, CF_3), 125.25 (q, $^3J_{3\text{-}F}$ = 5.0 Hz, C-3), 129.96 (C-5), 130.71 (C-4), 133.82 (q, $^2J_{2\text{-}F}$ = 31.4 Hz, C-2), 134.71 (C-6). **^{11}B NMR** (96 MHz, $CDCl_3$): δ 31.20 **^{19}F NMR** (282 MHz, $CDCl_3$): δ -59.67 **IR (ATR film) [cm^{-1}]:** 2982, 2932, 1499, 1352, 1315, 1138, 1098, 1046, 962, 857, 774, 663. **TLC** (petroleum ether:Et_2O 96:4 v/v): R_f = 0.38 **APCI-MS:** m/z: ([M + H$^+$]): found: 273.2

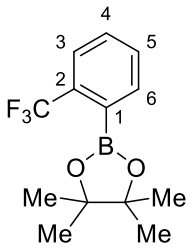

257

7.2.4 General Procedure 7 (GP7): *Suzuki-Miyaura* cross coupling

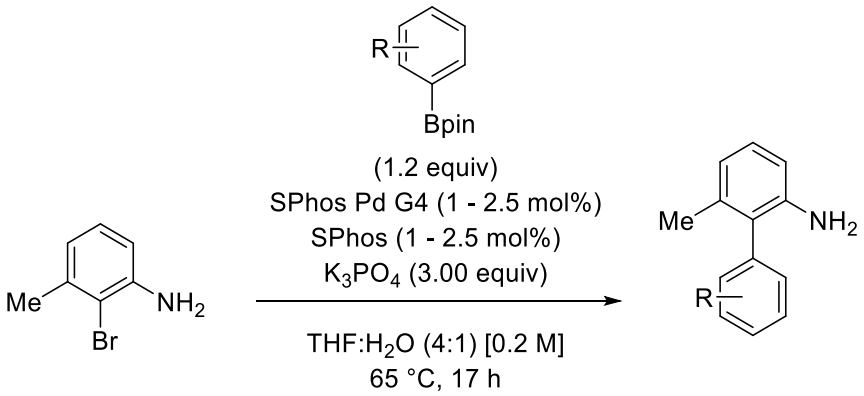

An appropriately sized dry Schlenk round-bottom flask equipped with stir bar was charged with aryl halide (1.00 equiv) aryl boronic acid ester (1.20 equiv), SPhos Pd G4 (1 mol% or 2.5 mol%) and SPhos (1 mol% or 2.5 mol%) and capped with a rubber septum. Anhydr. THF (0.21 M, degassed by sparging for 20 min) was added. In a separate vial K_3PO_4 (3.00 equiv) was dried at 80 °C overnight in vacuo and then dissolved in degassed water (2.5 M, degassed by sparging for 20 min) and then added at once. The reaction was then heated to 65 °C and stirred over night. After completion, the reaction mixture was filtered over a pad of Celite® and the solvent removed in vacuo. The product was isolated *via* column chromatography unless stated otherwise.

7.2.4.1 4'-Methoxy-2',6-dimethyl-[1,1'-biphenyl]-2-amine (278)

The title compound was synthesized according to **GP7** starting from 2-bromo-3-methylaniline (33.6 µL, 1.00 equiv, 270 µmol) and boronic acid ester **222** (97.8 µL, 1.50 equiv, 400 µmol) and SPhos Pd G4 (5.3 mg, 6.8 µmol, 2.5 mol%). The product was isolated by column chromatography (petroleum ether:EtOAc 95:5 v/v) as an amber oil in a yield of 50.1 mg (220 µmol, 82%).

^{1}H NMR (600 MHz, $CDCl_3$): δ 1.92 (s, 3H, Me), 2.04 (s, 3H, Me′), 3.36 (s, 2H, NH_2), 3.84 (s, 3H, OMe′), 6.62 (d, $^3J_{3\text{-}4}$ = 7.8 Hz, 1H, 3-H), 6.69 (d, ^3J = 7.2 Hz, 1H, 5-H), 6.83 (dd, $^3J_{5',6'}$ = 8.3 Hz, $^4J_{5',3'}$ = 2.7 Hz, 1H, 5′-H), 6.88 (d, $^4J_{3',5'}$ = 2.7 Hz, 1H, 3′-H), 7.02 (d, $^3J_{5',6'}$ = 8.3 Hz, 1H, 6′-H), 7.05 (t, $^3J_{4\text{-}5;4\text{-}3}$ = 7.8 Hz, 1H, 4-H). **^{13}C NMR** (151 MHz, $CDCl_3$): δ 19.72 (Me′), 20.38 (Me), 55.34 (OMe′), 112.00 (C-5′), 112.57 (C-3), 116.04 (C-3′), 119.91 (C-5), 126.86 (C-1), 127.91 (C-4), 129.81 (C-1′), 130.99 (C-6′), 137.55 (C-6), 138.68 (C-2′), 144.38 (C-2), 159.12 (C-4′). **IR (ATR film) [cm^{-1}]:** 3469, 3376, 3022, 2952, 2918, 2835, 1608, 1507, 1465, 1291, 1236, 1159, 1051, 1003, 778, 748. **TLC** (petroleum ether:EtOAc 95:5 v/v): R_f = 0.23 **HR-MS (ESI):** m/z calculated for $[C_{15}H_{18}NO]^+$ ([M + H$^+$]): 228.1383, found: 228.1387.

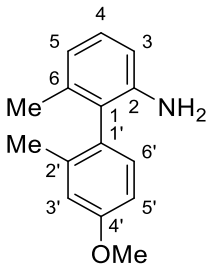

278

7.2.4.2 2',6-Dimethyl-[1,1'-biphenyl]-2-amine (241)

The title compound was synthesized according to **GP7** starting from 2-bromo-3-methylaniline (625 µL, 1.00 equiv, 5.00 mmol) and boronic acid ester **256** (1.80 g, 1.20 equiv, 7.50 mmol) and SPhos Pd G4 (99.3 mg, 125 µmol, 2.5 mol%). The product was isolated by column chromatography (petroleum ether:EtOAc 95:5 v/v) as an amber oil in a yield of 933 mg (4.73 mmol, 95%). The analytical data were in accordance with literature. [75]

^{1}H NMR (600 MHz, $CDCl_3$): δ 1.92 (s, 3H, Me), 2.08 (s, 3H, Me′), 3.34 (s, 2H, NH_2), 6.63 (d, $^3J_{3\text{-}4}$ = 7.9 Hz, 1H, 3-H), 6.70 (d, $^3J_{5\text{-}4}$ = 7.5 Hz, 1H, 5-H), 7.07 (dd, $^3J_{4\text{-}3,4\text{-}5}$ = 7.7 Hz, 1H, 4-H), 7.10 – 7.15 (m, 1H, 6′-H), 7.25 – 7.31 (m, 2H, 4′-H + 5′-H), 7.30 – 7.35 (m, 1H, 3′-H). **^{13}C NMR** (151 MHz, $CDCl_3$): δ 19.40 (Me′), 20.32 (Me), 112.67 (C-3), 119.97 (C-5), 126.73 (C-5′), 127.21 (C-1), 127.80 (C-4′), 127.99 (C-4), 130.01 (C-6′), 130.58 (C-3′), 136.97 (C-6), 137.23 (C-2′), 137.61 (C-1′), 143.87 (C-2). **IR (ATR film) [cm^{-1}]:** 3468, 3378, 3060, 2921, 1668, 1610, 1464, 1303, 1004, 765. **TLC** (petroleum ether:EtOAc 95:5 v/v): R_f = 0.23 (penH:EtOAc 8:2 R_f = 0.37) **HR-MS (ESI):** m/z calculated for $[C_{14}H_{16}N]^+$ ([M + H^+]): 198.1277, found: 198.1280.

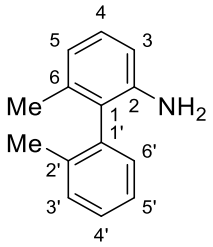

241

7.2.4.3 2',6-Dimethyl-[1,1'-biphenyl]-2-amine hydrochloride (241·HCl)

The title compound was synthesized according to **GP7** starting from 2-bromo-3-methylaniline (2.46 mL, 1.00 equiv, 20.0 mmol) and boronic acid ester **256** (1.08 g, 1.20 equiv, 5.28 mmol) and SPhos Pd G4 (159 mg, 0.20 mmol, 1 mol%). The crude product was dissolved in pentane.

Aq. HCl-solution (1 M), was added and the two phase mixture stirred vigorously forming off-white solids immediately. The solids were filtered off, washed with copious *n*-pentane, and dried in a desiccator over night. The product was isolated as an off-white solid in a yield of 4.43 g (19.0 mmol, 95%).

In an additional reaction the title compound was synthesized according to **GP2** starting from 2-bromo-3-methylaniline (6.16 mL, 1.00 equiv, 50.0 mmol) and o-tolylboronic acid (8.16 g, 1.20 equiv, 60.0 mmol) and SPhos Pd G4 (397 mg, 0.500 mmol, 1 mol%). The product was isolated as off-white solids in a yield of 10.2 g (43.8 mmol, 91%).

^{1}H NMR (600 MHz, $CDCl_3$): δ 1.99 (s, 3H, CH_3), 2.02 (s, 3H, CH_3), 7.08 – 7.15 (m, 3H, Ar-H), 7.26 (dd, *J* = 7.6, 1.9 Hz, 1H, Ar-H), 7.30 (d, *J* = 1.6 Hz, 1H, Ar-H), 7.43 (dd, *J* = 5.5, 3.7 Hz, 1H, Ar-H), 9.60 (s, 3H, NH_3^+). **^{13}C NMR** (151 MHz, $CDCl_3$): δ 19.94 (CH_3), 20.00 (CH_3), 121.96, 126.58, 128.28, 128.77, 128.79, 130.05, 130.34, 130.91, 133.88, 136.06, 137.09, 138.41. **IR (ATR film) [cm^{-1}]:** 2850, 2596, 1584, 1528, 1463, 778, 763, 743, 730. **HR-MS (ESI):** m/z calculated for $[C_{14}H_{16}N]^+$ ([M - Cl^-]): 198.1277, found: 198.1280. **Melting point:** 173 – 180 °C

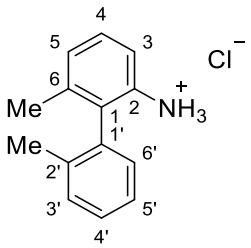

241·HCl

7.2.4.4 6-Methyl-[1,1'-biphenyl]-2-amine (280)

The title compound was synthesized according to **GP7** starting from 2-bromo-3-methylaniline (542 µL, 1.00 equiv, 4.40 mmol) and boronic acid ester **261** (1.08 g, 1.20 equiv, 5.28 mmol) and SPhos Pd G4 (34.9 mg, 44.0 µmol, 1 mol%). The product was isolated by column chromatography (petroleum ether:EtOAc 95:5 v/v) as an amber oil in a yield of 628 mg (3.43 mmol, 78%). The analytical data were in accordance with literature.[328]

^{1}H NMR (600 MHz, $CDCl_3$): δ 2.00 (s, 3H, Me), 3.44 (s, 2H, NH_2), 6.64 (d, ^3J = 8.0 Hz, 1H, 3-H), 6.70 (d, $^3J_{4\text{-}5}$ = 7.5 Hz, 1H, 5-H), 7.06 (dd, $^3J_{4\text{-}5}$ = 7.7 Hz, 1H, 4-H), 7.24 – 7.27 (m, 2H, 2′-H), 7.36 (td, $^3J_{3'\text{-}4',4'\text{-}5'}$ = 7.4 Hz, $^4J_{4'\text{-}2',4'\text{-}6'}$ = 1.4 Hz, 1H, 4′-H), 7.47 (td, $^3J_{2'\text{-}3',3'\text{-}4'}$ = 7.6 Hz, $^4J_{3'\text{-}5'}$ = 1.4 Hz, 2H, 3′-H). **^{13}C NMR** (151 MHz, $CDCl_3$): δ 20.74 (Me), 112.92 (C-3), 120.16 (C-5), 127.40 (C-4′), 127.97 (C-1), 128.12 (C-4), 129.25 (C-3′), 130.03 (C-2′), 137.10 (C-6),

138.43 (C-1′), 144.18 (C-2). **IR (ATR film) [cm^{-1}]:** 3469, 3376, 3059, 3022, 2921, 1609, 1583, 1465, 1301, 776, 739, 704, 565. **TLC** (petroleum ether:EtOAc 98:2 v/v): R_f = 0.3 **HR-MS (ESI):** m/z calculated for $[C_{13}H_{14}N]^+$ ([M + H$^+$]): 184.1121, found: 184.1125.

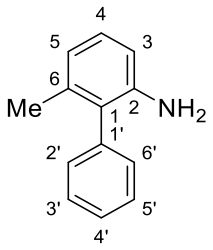

280

7.2.4.5 2'-Methoxy-6-methyl-[1,1'-biphenyl]-2-amine (277)

The title compound was synthesized according to **GP7** starting from 2-bromo-3-methylaniline (560 µL, 1.25 equiv, 4.54 mmol) and boronic acid ester **259** (843 mg, 1.00 equiv, 3.60 mmol) and SPhos Pd G4 (23.8 mg, 0.30 mmol, 0.8 mol%). The product was isolated by column chromatography (petroleum ether:EtOAc 9:1 to 8:2 v/v) as an amber oil in a yield of 715 mg (3.35 mmol, 93% relative to boronic acid ester **259**).

^{1}H NMR (600 MHz, $CDCl_3$): δ 1.99 (s, 3H, Me), 3.43 (s, 2H, NH_2), 3.77 (s, 3H, OMe), 6.64 (d, $^3J_{3\text{-}4}$ = 8.0 Hz, 1H, 3-H), 6.72 (d, $^3J_{4\text{-}5}$ = 7.5 Hz, 1H, 5-H), 7.03 (d, $^3J_{3'\text{-}4'}$ = 8.3 Hz, 1H, 3′-H), 7.03 – 7.07 (m, 2H, 5′-H), 7.08 (d, $^3J_{4\text{-}3,4\text{-}5}$ = 8.0 Hz, 1H, 4-H), 7.16 (dd, $^3J_{6'\text{-}5'}$ = 7.3 Hz, $^4J_{6'\text{-}4'}$ = 1.8 Hz, 1H, 6′-H), 7.37 (td, $^3J_{4'\text{-}3',4'\text{-}5'}$ = 7.9 Hz, $^4J_{4'\text{-}6'}$ = 1.8 Hz, 1H, 4′-H). **^{13}C NMR** (151 MHz, $CDCl_3$): δ 20.40 (Me), 55.76 (OMe), 111.57 (C-3′), 112.91 (C-1), 119.98 (C-5), 121.36 (C-5′), 124.38 (C-1), 126.63 (C-3′), 128.13 (C-4), 129.18 (C-4′), 131.65 (C-6′), 137.81 (C-6), 144.32 (C-2), 157.28 (C-2′). **IR (ATR film) [cm^{-1}]:** 3468, 3373, 3063, 3022, 2951, 2834, 1610, 1498, 1464, 1433, 1294, 1257, 1232, 1120, 1051, 1025, 1002, 776, 765, 545. **TLC** (petroleum ether:EtOAc 9:1 v/v): R_f = 0.18 **HR-MS (ESI):** m/z calculated for $[C_{14}H_{16}NO]^+$ ([M + H$^+$]): 214.1226, found: 214.1233.

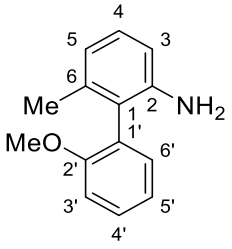

277

7.2.4.6 2'-Fluoro-6-methyl-[1,1'-biphenyl]-2-amine (276)

The title compound was synthesized according to **GP7** starting from 2-bromo-3-methylaniline (185 µL, 1.00 equiv, 1.50 mmol), boronic acid ester **258** (401 mg, 1.20 equiv, 1.81 mmol), SPhos Pd G4 (29.9 mg, 37.5 µmol, 2.5 mol%) and SPhos (15.4 mg, 37.5 mmol, 2.5 mol%). The product was isolated by column chromatography (petroleum ether:EtOAc 95:5 v/v) as an amber oil in a yield of 279 mg (1.39 mmol, 92%).

^{1}H NMR (600 MHz, $CDCl_3$): δ 2.02 (s, 3H, Me), 3.44 (s, 2H, NH_2), 6.64 (d, $^3J_{3\text{-}4}$ = 8.0 Hz, 1H, 3-H), 6.72 (d, $^3J_{4\text{-}5}$ = 7.5 Hz, 1H, 5-H), 7.09 (t, $^3J_{4\text{-}3,4\text{-}5}$ = 7.8 Hz, 1H, 4-H), 7.19 (t, $^3J_{3'\text{-}4',3'\text{-}2'F}$ = 8.8 Hz, 1H, 3′-H), 7.22 – 7.29 (m, 2H, 5′-H +6′-H), 7.35 – 7.40 (m, 1H, 4′-H). **^{13}C NMR** (151 MHz, $CDCl_3$): δ 20.27 (Me), 112.91 (C-3), 116.25 (d, $^2J_{3'\text{-}F}$ = 22.2 Hz, C-3′), 120.00 (C-5), 121.08 (C-1), 124.75 (d, J = 3.8 Hz, C-5′), 125.18 (d, $^2J_{1'\text{-}F}$ = 17.5 Hz, C-1′), 128.73 (C-4′), 129.62 (d, $^3J_{4'\text{-}F}$ = 8.1 Hz, C-4′), 132.12 (d, $^3J_{6'\text{-}F}$ = 3.8 Hz, C-6′), 137.75 (C-6), 144.30 (C-2), 160.07 (d, $^1J_{2'\text{-}F}$ = 246.0 Hz, C-2′). **^{19}F NMR** (282 MHz, $CDCl_3$): δ -102.65 **IR (ATR film) [cm^{-1}]:** 3470, 3378, 3065, 2924, 1614, 1582, 1467, 1446, 1305, 1210, 1107, 824, 760. **TLC** (petroleum ether:EtOAc 8:2 v/v): R_f = 0.44 **HR-MS (ESI):** m/z calculated for $[C_{13}H_{12}FN]^+$ ([M + H$^+$]): 202.1027, found: 202.1030.

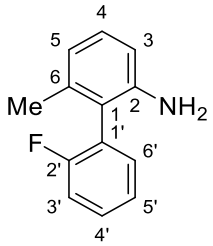

276

7.2.4.7 4'-Methoxy-6-methyl-[1,1'-biphenyl]-2-amine (279)

The title compound was synthesized according to **GP7** starting from 2-bromo-3-methylaniline (625 µL, 1.00 equiv, 5.00 mmol) (4-methoxyphenyl)boronic acid (912 mg, 1.20 equiv, 6.00 mmol), SPhos Pd G4 (87.3 mg, 125 µmol, 2.5 mol%) and SPhos (51.3 mg, 125 mmol, 2.5 mol%). The product was isolated by column chromatography (*n*-pentane:EtOAc 95:5 to 8:2 v/v) as an amber oil in a yield of 1.03 g (4.84 mmol, 97%). The analytical data were in accordance with literature.[201]

^{1}H NMR (600 MHz, $CDCl_3$): δ 2.02 (s, 3H, Me), 3.52 (s, 2H, NH_2), 3.86 (s, 3H, OMe), 6.64 (d, $^3J_{3\text{-}4}$ = 7.9 Hz, 1H, 3-H), 6.70 (dt, $^3J_{4\text{-}5}$ = 7.5 Hz, $^4J_{3\text{-}5}$ = 1.0 Hz, 1H, 5-H), 7.01 (d, $^3J_{2'\text{-}3'}$ = 8.6 Hz, 2H, 2′-H), 7.05 (t, $^3J_{4\text{-}3,4\text{-}5}$ = 7.7 Hz, 1H, 4-H), 7.18 (d, $^3J_{2'\text{-}3'}$ = 8.7 Hz, 2H, 3′-H).

^{13}C NMR (151 MHz, $CDCl_3$): δ 20.81 (Me), 55.40 (OMe), 112.87 (C-3), 114.66 (C-2′), 120.17 (C-5), 127.64 (C-1), 127.97 (C-4), 130.34 (C-1′), 131.08 (C-3′), 137.54 (C-6), 144.41 (C-2), 158.87 (C-4′).**IR (ATR film) [cm^{-1}]:** 3461, 3370, 2953, 1611, 1520, 1486, 1239, 1171, 1084, 829. **TLC** (pentanes:EtOAc 8:2 v/v): R_f = 0.19 **HR-MS (ESI):** m/z calculated for $[C_{14}H_{16}NO]^+$ ($[M + H^+]$): 214.1226, found: 214.1227. **Melting point:** 76 – 78 °C

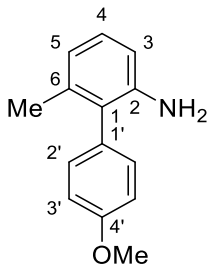

279

7.2.5 General Procedure 8 (GP8): *Sandmeyer* reaction

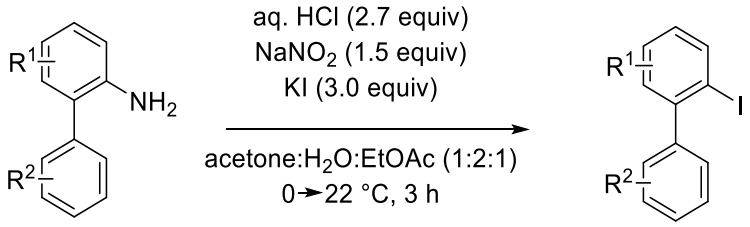

An appropriately sized vessel equipped with stir bar was charged with 2-aminobiaryl (1.0 equiv) and dissolved in acetone (1.00 M). A solution of aq. HCl (1.70 M, 2.7 equiv) was added and the reaction mixture stirred at 0 °C for 5 min. Aq. $NaNO_2$ (0.86 M, 1.5 equiv) solution was added. The reaction was stirred at 0 °C for 30 min. EtOAc (1.00 M regarding the amine) was added and a solution of aq. KI (3.00 M, 3.0 equiv) was added dropwise *via* syringe pump over 1 h at 0 °C. The reaction was stirred at 22 °C for an additional 1 h. Then aq. sat. Na_2SO_3 was added and the mixture extracted with EtOAc (3x), washed with aq. sat. NaCl-solution and dried over $MgSO_4$. Solvents were removed in vacuo and the crude product then suspended in pentane and filtered over a plug of silica washing with pentane (check with TLC for any remaining product stuck to silica). Solvents were removed in vacuo and the product isolated without further purification.

7.2.5.1 2-Iodo-1,1'-biphenyl (92)

The title compound was synthesized according to **GP8** starting from 2-amino-1,1'-biphenyl (500 mg, 1.0 equiv, 2.95 mmol). The product was isolated as a colorless oil in a yield of 635 mg (2.27 mmol, 77%). The analytical data were in accordance with literature.[329]

^{1}H NMR (600 MHz, $CDCl_3$): δ 7.07 (td, $^3J_{4\text{-}3,4\text{-}5}$ = 7.6 Hz, $^4J_{4\text{-}6}$ = 1.7 Hz, 1H, 4-H), 7.35 (dd, *J* = 7.6, 1.8 Hz, 1H), 7.37 – 7.41 (m, 2H), 7.40 – 7.46 (m, 1H, 5-H), 7.44 – 7.49 (m, 3H), 8.00 (dd, $^3J_{3\text{-}4}$ = 7.9 Hz, $^4J_{3\text{-}4}$ = 1.3 Hz, 1H, 3-H). **^{13}C NMR** (151 MHz, $CDCl_3$): δ 98.75 (C-2), 127.77, 128.08, 128.24 (C-5), 128.90 (C-4), 129.40, 130.21, 139.62 (C-3), 144.34, 146.77. **IR (ATR film) [cm^{-1}]:** 3052, 1960, 1459, 1413, 1017, 1005, 743, 698, 649, 614, 550. **TLC** (petroleum ether:EtOAc 9:1 v/v): R_f = 0.75 **APCI-MS:** m/z: ([M - I$^-$]): found: 153.1 **GC-MS(EI-MS):** m/z: ([M$^+$]): 280.1 (100).

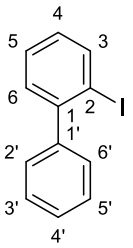

7.2.5.2 2-Iodo-2',6-dimethyl-1,1'-biphenyl (236)

The title compound was synthesized according to **GP8** starting from 2-aminobiaryl **241** (762 mg, 1.0 equiv, 3.86 mmol). The product was isolated as a red oil in a yield of 1.12 g (3.65 mmol, 94%).

The title compound was also synthesized according to **GP8** starting from 2-aminobiaryl **241·HCl** (16.36 g, 1.0 equiv, 70.00 mmol) with aq. HCl (1.7 M, 70.0 mL, 1.7 equiv, 119 mmol). The product was isolated as a colorless oil in a yield of 17.71 g (57.47 mmol, 82%).

^{1}H NMR (600 MHz, $CDCl_3$): δ 2.01 (s, 3H, Me′), 2.03 (s, 3H, Me), 6.96 (t, ^3J = 7.8 Hz, 1H, 4-H), 6.99 (dd, $^3J_{5',6'}$ = 7.4, 1.4 Hz, 1H, 6′-H), 7.25 (d, $^3J_{4-5}$ = 7.6 Hz, 1H, 5-H), 7.26 – 7.34 (m, 3H, 3′-H, 4′-H, 5′-H), 7.79 (d, $^3J_{3-4}$ = 8.0 Hz, 1H, 3-H). **^{13}C NMR** (151 MHz, $CDCl_3$): δ 19.63 (Me′), 21.91 (Me), 101.18 (C-2), 126.23 (C-5′), 127.96 (C-4), 128.89 (C-4′), 129.00 (C-6′), 129.84 (C-5), 130.22 (C-3′), 135.52 (C-2′), 136.57 (C-3), 137.81 (C-6), 144.06 (C-1′), 145.91 (C-1). **IR (ATR film) [cm^{-1}]:** 3050, 3016, 2971, 2947, 2919, 2858, 1555, 1454, 1439, 1173, 1115, 1008, 828, 758, 741, 727, 638, 461. **TLC** (petroleum ether:EtOAc 95:5 v/v): R_f = 0.63 **APCI-MS:** m/z: ([M^+]): found: 308.1. ([M - I^-]): found: 181.2

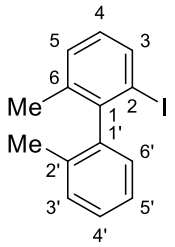

236

Via 2',6-dimethyl-[1,1'-biphenyl]-2-diazonium salt.

^{1}H NMR (600 MHz, $CDCl_3$): δ 2.10 (s, 3H), 2.20 (s, 3H), 7.24 (d, J = 7.6 Hz, 1H), 7.26 (s, 2H), 7.41 (dd, J = 17.2, 8.0 Hz, 2H), 7.49 (t, J = 7.6 Hz, 1H), 7.80 (t, J = 8.1 Hz, 1H), 8.02 (d, J = 7.8 Hz, 1H), 9.13 (d, J = 8.3 Hz, 1H).

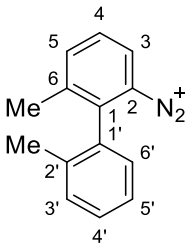

236-N_2^+

7.2.5.3 2-Iodo-4,4'-dimethoxy-2',6-dimethyl-1,1'-biphenyl (231)

The title compound was synthesized according to **GP8** starting from 2-aminobiaryl **221** (207 mg, 1.0 equiv, 0.80 mmol). The product was isolated as a colorless oil that slowly solidified over time in a yield of 215 mg (0.58 mmol, 73%).

^{1}H NMR (600 MHz, $CDCl_3$): δ 1.97 (s, 3H, Me′), 1.99 (s, 3H, Me), 3.81 (s, 3H, OMe), 3.84 (s, 3H, OMe′), 6.78 – 6.82 (m, 2H, 5-H + 5′-H), 6.82 (d, $^4J_{3'\text{-}5'}$ = 2.7 Hz, 1H, 3′-H), 6.88 (d, $^3J_{5'\text{-}6'}$ = 8.3 Hz, 1H, 6′-H), 7.31 (d, $^4J_{3\text{-}5}$ = 2.6 Hz, 1H, 3-H). **^{13}C NMR** (151 MHz, $CDCl_3$): δ 20.03 (Me′), 22.39 (Me), 55.26 (OMe′), 55.55 (OMe), 102.18 (C-2), 111.31 (C-5′), 115.45 (C-3′), 116.13 (C-5), 121.30 (C-3), 130.55 (C-6′), 136.45 (C-1′), 137.58 (C-2′), 138.25 (C-1), 138.75 (C-6), 158.87 (C-4), 159.11 (C-4′). **IR (ATR film) [cm^{-1}]:** 2997, 2953, 2834, 1594, 1548, 1465, 1436, 1291, 1258, 1237, 1213, 1161, 1131, 1059, 847, 790. **TLC** (petroleum ether:EtOAc 8:2 v/v): R_f = 0.71 **TLC** (petroleum ether:PhMe 7:3 v/v): R_f = 0.51 **HR-MS (ESI):** m/z calculated for $[C_{16}H_{18}IO_2]^+$ ([M + H$^+$]): 369.0346, found: 369.0340. **Melting point:** 81 – 83 °C

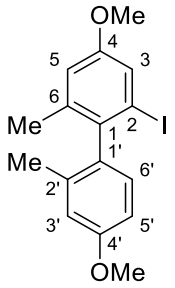

231

4,4'-Dimethoxy-2,2'-dimethyl-1,1'-biphenyl (**229**)

As a side product **229** could be isolated in analytical quantities. The analytical data were in accordance with literature.[330]

^{1}H NMR (600 MHz, $CDCl_3$): δ 2.03 (s, 6H, Me), 3.83 (s, 6H, OMe), 6.76 (dd, $^3J_{5\text{-}6}$ = 8.4 Hz, $^4J_{5\text{-}3}$ = 2.6 Hz, 2H, 5-H), 6.81 (d, $^4J_{3\text{-}5}$ = 2.7 Hz, 2H, 3-H), 7.00 (d, $^3J_{5\text{-}6}$ = 8.3 Hz, 2H, 6-H). **^{13}C NMR** (151 MHz, $CDCl_3$): δ 20.33 (Me), 55.34 (OMe), 110.88 (C-5), 115.30 (C-3), 130.86

(C-6), 133.95 (C-1), 137.82 (C-2), 158.67 (C-4). **IR (ATR film) [cm^{-1}]:** 2997, 2937, 2834, 1605, 1572, 1488, 1465, 1290, 1239, 1161, 1127, 1056, 810, 570. **TLC** (petroleum ether:PhMe 7:3 v/v): R_f = 0.48 **APCI-MS:** m/z: ([M + H$^+$]): found: 243.2 **Melting point:** 76 – 81 °C

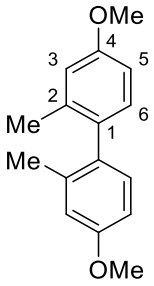

229

7.2.5.4 2-Iodo-6-methyl-1,1'-biphenyl (275)

The title compound was synthesized according to **GP8** starting from 2-aminobiaryl **275** (300 mg, 1.0 equiv, 1.64 mmol). The product was isolated as a colorless oil in a yield of 392 mg (1.33 mmol, 81%).

^{1}H NMR (600 MHz, $CDCl_3$): δ 2.10 (s, 3H, Me), 6.95 (td, *J* = 7.8, 1.5 Hz, 1H), 7.13 (d, *J* = 8.1 Hz, 2H), 7.24 (d, *J* = 7.6 Hz, 1H), 7.37 – 7.42 (m, 1H), 7.42 – 7.51 (m, 2H), 7.79 (d, *J* = 7.9 Hz, 1H). **^{13}C NMR** (151 MHz, $CDCl_3$): δ 22.35, 101.01, 127.59, 128.53, 129.10, 129.86, 136.62, 137.78, 144.57, 146.41. **IR (ATR film) [cm^{-1}]:** 3054, 3022, 2922, 1552, 1441, 1174, 1127, 1010, 826, 764, 700, 637. **APCI-MS:** m/z: ([M$^+$]): found: 294.1. ([M - I$^-$]): found: 167.1

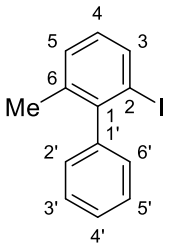

275

7.2.5.5 2-Iodo-2'-methoxy-6-methyl-1,1'-biphenyl (282)

The title compound was synthesized according to **GP8** starting from 2-aminobiaryl **277** (700 mg, 1.0 equiv, 3.28 mmol). The product was isolated as a colorless oil in a yield of 825 mg (2.54 mmol, 78%).

^{1}H NMR (600 MHz, $CDCl_3$): δ 2.08 (s, 3H, Me), 3.77 (s, 3H, OMe), 6.95 (t, $^3J_{4\text{-}3,4\text{-}5}$ = 7.8 Hz, 1H, 4-H), 7.00 (t, ^3J = 7.9 Hz, 2H, 3′-H +6′-H), 7.03 – 7.07 (m, 1H, 5′-H), 7.23 (d, $^3J_{5\text{-}4}$ = 7.6

Hz, 1H, 5-H), 7.37 – 7.42 (m, 1H, 4′-H), 7.77 (d, $^{3}J_{3\text{-}4}$ = 7.9 Hz, 1H, 3-H). **^{13}C NMR** (151 MHz, $CDCl_3$): δ 21.91 (Me), 55.81 (OMe), 101.81 (C-2), 111.33 (C-6′), 120.83 (C-5′), 129.02 (C-4), 129.37 (C-4′), 129.61 (C-5), 130.71 (C-3′), 133.29 (C-1′), 136.43 (C-3), 138.50 (C-6), 143.41 (C-1), 156.32 (C-2′). **IR (ATR film) [cm^{-1}]:** 3050, 3002, 2955, 2833, 1599, 1582, 1497, 1460, 1434, 1295, 1263, 1242, 1229, 1178, 1116, 1026, 829, 798, 753, 634, 565. **HR-MS (ESI):** m/z calculated for $[C_{14}H_{14}IO_2]^+$ ([M + H$^+$]): 342.0349, found: 342.0351.

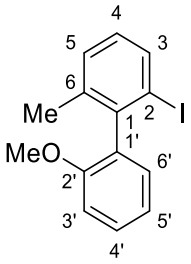

282

7.2.5.6 2'-Fluoro-2-iodo-6-methyl-1,1'-biphenyl (281)

The title compound was synthesized according to **GP8** starting from 2-aminobiaryl **276** (200 mg, 1.0 equiv, 0.99 mmol). The product was isolated as a colorless oil in a yield of 291 mg (0.93 mmol, 94%).

^{1}H NMR (600 MHz, $CDCl_3$): δ 2.12 (s, 3H, Me), 6.99 (t, $^{3}J_{4\text{-}3,4\text{-}5}$ = 7.8 Hz, 1H, 4-H), 7.13 (td, $^{3}J_{6'\text{-}5'}$ = 7.4 Hz, 1.8 Hz, 1H, 6′-H), 7.17 (ddd, $^{3}J_{2'\text{F-}3'}$ = 9.4 Hz, $^{3}J_{3'\text{-}4'}$ 8.2 Hz, $^{4}J_{3'\text{-}5'}$ = 1.1 Hz, 1H, 3′-H), 7.23 (dd, $^{3}J_{5'\text{-}4',5'\text{-}6'}$ = 7.5 Hz, $^{4}J_{5'\text{-}3'}$ = 1.2 Hz, 1H, 5′-H), 7.25 – 7.27 (m, 2H, 5-H), 7.41 (dddd, $^{3}J_{4'\text{-}3'}$ = 8.6 Hz, $^{3}J_{4'\text{-}5'}$ = 7.2 Hz, $^{4}J_{4'\text{-}2'\text{F}}$ = 5.2 Hz, 1.8 Hz, 1H, 4′-H), 7.77 – 7.81 (m, 1H, 3-H). **^{13}C NMR** (151 MHz, $CDCl_3$): δ 21.88 (Me), 101.01 (C-2), 115.96 (d, $^{2}J_{3'\text{-}2'\text{F}}$ = 21.7 Hz, C-3′), 124.34 (d, $^{4}J_{5'\text{-}2'\text{F}}$ = 3.7 Hz, C-5′), 129.75 (C-4), 129.81 (C-5), 129.97 (d, $^{3}J_{4'\text{-}2'\text{F}}$ = 8.2 Hz, C-4′), 131.46 (d, $^{3}J_{6'\text{-}2'\text{F}}$ = 3.5 Hz, C-6′), 131.70 (d, $^{2}J_{1'\text{-}2'\text{F}}$ = 17.0 Hz, C-1′), 136.69 (C-3), 138.61 (C-6), 140.62 (C-1), 159.22 (d, $^{1}J_{2'\text{-}2'\text{F}}$ = 245.7 Hz, C-2′). **IR (ATR film) [cm^{-1}]:** 3055, 2924, 1554, 1497, 1451, 1441, 1255, 1209, 1107, 819, 756. **APCI-MS:** m/z: ([M + H$^+$]): found: 311.9.

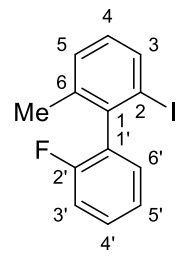

281

7.2.5.7 4'-Methoxy-2-iodo-6-methyl-1,1'-biphenyl (283)

The title compound was synthesized according to **GP8** starting from 2-aminobiaryl **276** (853 mg, 1.0 equiv, 4.00 mmol). The product was isolated as orange solids in a yield of 1.195 g (3.69 mmol, 92%). The analytical data were in accordance with literature.[201]

^{1}H NMR (600 MHz, $CDCl_3$): δ 2.10 (s, 3H, Me), 3.87 (s, 3H, OMe), 6.93 (t, $^3J_{4\text{-}3,4\text{-}5}$ = 7.7 Hz, 1H, 4-H), 6.96 – 7.01 (m, 2H, 3′-H), 7.02 – 7.08 (m, 2H, 2′-H), 7.22 (dt, $^3J_{5\text{-}4}$ = 7.6 Hz, $^4J_{5\text{-}3}$ = 1.0 Hz, 1H, 5-H), 7.74 – 7.81 (m, 1H, 3-H). **^{13}C NMR** (151 MHz, $CDCl_3$): δ 22.46 (Me), 55.35 (OMe), 102.03 (C-2), 113.85 (C-2′), 128.99 (C-6), 129.84 (C-5), 130.24 (C-3′), 136.59 (C-3), 137.09 (C-1′), 138.23 (C-6), 146.12 (C-1), 158.96 (C-4′). **IR (ATR film) [cm^{-1}]:** 2953, 2832, 1611, 1512, 1444, 1292, 1246, 1171, 1034, 822, 769. **TLC** (pentanes:EtOAc 95:5 v/v): R_f = 0.62 **HR-MS (ESI):** m/z calculated for $[C_{14}H_{13}NaO]^+$ ($[M + Na^+]$): 346.9903, found: 346.9897. **Melting point:** 66 – 68 °C

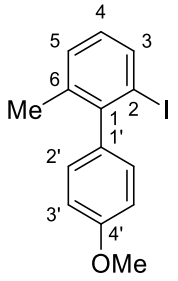

283

7.2.6 Electron-rich Cyclic Diaryl Iodonium Salt Synthesis

7.2.6.1 4,4'-Dimethoxy-2-(methoxymethoxy)-2',6-dimethyl-1,1'-biphenyl (225)

A dry microwave vial equipped with stir bar was charged with K_3PO_4 (489 mg, 3.00 equiv, 2.28 mmol), SPhos Pd G4 (3.0 mg, 0.5 mol%, 3.8 µmol) and SPhos (1.6 mg, 0.5 mol%, 3.8 µmol). The vial was sealed, evacuated, and backfilled with N_2 (3x). A separate dry flask was charged with aryl bromide **29** (141 µL, 1.00 mmol, 0.76 mmol) and aryl boronic acid ester **222** (277 µL, 1.50 equiv, 1.14 mmol). The flask was briefly evacuated and backfilled with N_2 (3x). The contents of the second vessel were transferred into the microwave vial by dissolving in degassed THF (3.2 mL, 0.24 M). Then H_2O (0.8 mL, 4:1 v/v regarding THF:H_2O) was added to the microwave vial and the reaction stirred at 65 °C for 17 h. The reaction was filtered through a plug of silica washing with EtOAc and solvents removed in vacuo. The product was isolated by column chromatography (petroleum ether:EtOAc 95:5 v/v) as a colorless oil in a yield of 216 mg (0.73 mmol, 94%).

^{1}H NMR (600 MHz, $CDCl_3$): δ 1.95 (s, 3H, Me), 2.02 (s, 3H, Me′), 3.30 (s, 3H, $OCH_2O\underline{Me}$), 3.82 (s, 3H, OMe), 3.83 (s, 3H, OMe′), 5.00 (s, 2H, $O\underline{CH_2}OMe$), 6.51 (d, $^4J_{5\text{-}3}$ = 2.4 Hz, 1H, 5-H), 6.63 (d, $^4J_{3\text{-}5}$ = 2.5 Hz, 1H, 3-H), 6.77 (dd, $^3J_{5'\text{-}6'}$ = 8.3 Hz, $^4J_{5'\text{-}3'}$ = 2.7 Hz, 1H, 5′-H), 6.82 (d, $^4J_{3'\text{-}5'}$ = 2.7 Hz, 1H, 3′-H), 6.96 (d, $^3J_{6'\text{-}5'}$ = 8.3 Hz, 1H, 6′-H). **^{13}C NMR** (151 MHz, $CDCl_3$): δ 20.10 (Me′), 20.64 (Me), 55.22 (OMe′), 55.41 (OMe), 55.96 ($OCH_2O\underline{Me}$), 94.82 ($O\underline{CH_2}OMe$), 99.50 (C-3), 108.49 (C-5), 110.96 (C-5′), 115.23 (C-3′), 123.81 (C-1), 129.84 (C-1′), 131.27 (C-6′), 138.57 (C-2′), 139.04 (C-6), 155.76 (C-2), 158.63 (C-4′), 159.41 (C-4). **IR (ATR film) [cm^{-1}]:** 2996, 2952, 2834, 1604, 1576, 1465, 1303, 1236, 1146, 1042, 997, 924, 841, 600. **TLC** (petroleum ether:EtOAc 9:1 v/v): R_f = 0.27 **HR-MS (ESI):** m/z calculated for $[C_{18}H_{23}O_4]^+$ ([M + H^+]): 303.1591, found: 303.1599. **Boiling point:** 90 °C ($5\cdot10^{-2}$ mbar)

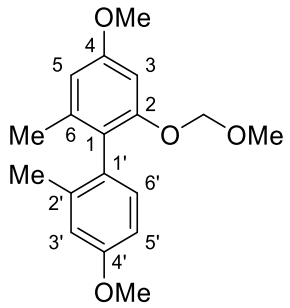

225

7.2.6.2 4,4'-Dimethoxy-2',6-dimethyl-[1,1'-biphenyl]-2-ol (228)

A dry Schlenk vial equipped with stir bar was charged with K_3PO_4 (1.44 mg, 3.00 equiv, 11.5 mmol), SPhos Pd G4 (30.4 mg, 1 mol%, 38.2 µmol) and SPhos (15.7 mg, 1 mol%, 38.2 µmol). The vial was sealed, evacuated, and backfilled with N_2 (3x). A separate dry flask was charged with aryl bromide **228** (830 mg, 1.00 mmol, 3.82 mmol) and aryl boronic acid ester **222** (1.21 mL, 1.30 equiv, 4.97 mmol). The flask was briefly evacuated and backfilled with N_2 (3x). The contents of the second vessel were transferred into the microwave vial by dissolving in degassed THF (16 mL, 0.24 M). Then H_2O (4 mL, 4:1 v/v regarding THF:H_2O) was added to the microwave vial and the reaction stirred at 65 °C for 17 h. The reaction was filtered through a plug of silica washing with EtOAc and solvents removed in vacuo. The product was isolated by column chromatography (petroleum ether:EtOAc 9:1 v/v) as white solids in a yield of 800 mg (3.10 mmol, 81%).

The title compound was alternatively synthesized by charging a 50 mL round-bottom flask equipped with stir bar with biaryl **225** (523 mg, 1.0 equiv, 1.73 mmol), MeOH (10 mL, 0.17 M) and aq. HCl-solution (519 µL, 1.0 M, 0.3 equiv, 0.52 mmol). The reaction mixture was stirred for 3 h at 70 °C. The aq. phase was then extracted using CH_2Cl_2 (3x), the combined organic phases were washed with sat. aq. NaCl-solution, dried over $MgSO_4$ and solvents removed in vacuo. The product was isolated as a colorless oil in a yield of 448 mg (1.73 mmol, 99%).

^{1}H NMR (600 MHz, $CDCl_3$): δ 1.95 (s, 3H, Me), 2.05 (s, 3H, Me′), 3.81 (s, 3H, OMe), 3.84 (s, 3H, OMe′), 4.66 (s, 1H, OH), 6.43 (d, $^4J_{3\text{-}5}$ = 2.5 Hz, 1H, 3-H), 6.44 (d, $^4J_{5\text{-}3}$ = 2.5 Hz, 1H, 5-H), 6.84 (dd, $^3J_{5'\text{-}6'}$ = 8.3 Hz, ^4J = 2.7 Hz, 1H, 5′-H), 6.90 (d, $^4J_{3'\text{-}5'}$ = 2.7 Hz, 1H, 3′-H), 7.07 (d, $^3J_{6'\text{-}5'}$ = 8.3 Hz, 1H, 6′-H). **^{13}C NMR** (151 MHz, $CDCl_3$): δ 19.86 (Me′), 20.33 (Me), 55.31 (OMe), 55.33 (OMe′), 97.92 (H-3), 108.02 (H-5), 112.21 (H-5′), 116.32 (H-3′), 119.65 (H-1), 126.17 (H-1′), 132.34 (H-6′), 138.62 (H-6), 140.07 (H-2′), 154.06 (H-2), 159.78 (H-4′), 159.88 (H-4). **IR (ATR film) [cm^{-1}]:** 3528 (broad signal), 2999, 2955, 2836, 1607, 1581, 1487, 1236, 1147, 1067, 838. **TLC** (petroleum ether:EtOAc 8:2 v/v): R_f = 0.23 **HR-MS (ESI):** m/z calculated for $[C_{16}H_{19}O_3]^+$ ([M + H$^+$]): 259.1329, found: 259.1333. **Melting point:** 76 –81 °C **Boiling point:** 150 °C ($2\cdot10^{-1}$ mbar)

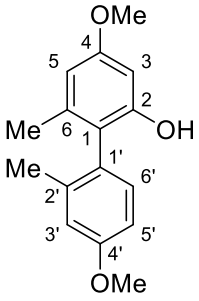

228

7.2.6.3 3-Methoxy-5-methylphenyl trifluoromethanesulfonate (232)

A 250 mL round bottom flask equipped with stir bar was charged with phenol **124** (1.07 g, 1.0 equiv, 7.75 mmol), toluene (12 mL, 0.65 M) and an aq. solution of K_3PO_4 (12 mL, 1.93 M, 3.0 equiv, 23.2 mmol). The mixture was cooled to 0 °C and Tf_2O (1.56 mL, 1.2 equiv, 9.30 mmol) added dropwise under vigorous stirring. The cooling bath was removed, and the reaction stirred at 22 °C for 1 h. The reaction mixture was diluted with H_2O (20 mL), and the aq. phase extracted with EtOAc (3x), the combined org. phases washed with H_2O (3x), sat. aq. NaCl-solution, dried over $MgSO_4$ and solvents removed in vacuo. The product was isolated by Kugelrohr® distillation as a colorless liquid in a yield of 1.92 g (7.11 mmol, 92%). The analytical data were in accordance with literature.[331]

^{1}H NMR (600 MHz, $CDCl_3$): δ 2.36 (s, 3H, Me), 3.80 (s, 3H, OMe), 6.61 (t, $^4J_{2\text{-}4,2\text{-}6}$ = 2.4 Hz, 1H, 2-H), 6.68 (d, $^4J_{2\text{-}4,2\text{-}6}$ = 2.2 Hz, 1H, 6-H), 6.71 – 6.74 (m, 1H, 4-H). **^{13}C NMR** (151 MHz, $CDCl_3$): δ 21.73 (Me), 55.77 (OMe), 104.62 (C-2), 114.11 (C-6), 114.99 (C-4), 118.87 (q, $^1J_{F\text{-}C}$ = 320.4 Hz, CF_3), 141.54 (C-5), 150.19 (C-1), 160.72 (C-3). **^{19}F NMR** (282 MHz, $CDCl_3$): δ -27.96. **IR (ATR film) [cm^{-1}]:** 2946, 2842, 1618, 1421, 1245, 1208, 1141, 1106, 1062, 963, 932, 849, 822, 612. **TLC** (petroleum ether:EtOAc 7:3 v/v): R_f = 0.72 **APCI-MS:** m/z: ([M + H$^+$]): 271.1 **HR-MS (ESI):** m/z calculated for $[C_8H_{11}O_2]^+$ ([M – OTf$^-$ + H_2O^+]): 139.0754, found: 139.0733. **elemental analysis** (calcd., found for $C_9H_9F_3O_4S$): C (40.00, 39.32), H (3.36, 3.34), S (11.86, 11.64).**Boiling point:** 68°C ($2.5\cdot10^{-2}$ mbar).

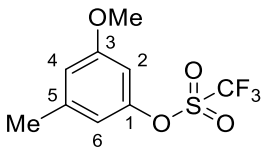

232

7.2.6.4 N-(3-Methoxy-5-methylphenyl)-1,1-diphenylmethanimine (233)

A dry microwave vial was charged with triflate **232** (35.4 µL, 1.00 equiv, 0.200 mmol) and benzophenone imine (36.9 µL, 1.10 equiv, 0.220 mmol) and briefly evacuated and backfilled with N_2 (3x). Anhydrous, degassed toluene (0.4 mL, 0.5 M) was added. A separate dry microwave vial equipped with stir bar was charged with *rac*-BINAP (6.2 mg, 5 mol%, 10.0 µmol), BINAP Pd G4 **205** (10.1 mg, 5 mol%, 10.0 µmol) and Cs_2CO_3 (163 mg, 2.50 equiv, 0.500 mmol). The reaction vial was evacuated and backfilled with N_2. Toluene (0.6 mL) was added and the mixture stirred for 15 min at 80 °C. Then the mixture from the first vial was added and reaction vial stirred at 110 C for 40 min. Solvents were removed in vacuo. The product was isolated by column chromatography (petroleum ether:CH_2Cl_2 3:7 v/v) in a yield of 53.0 mg (0.176 mmol, 88%).

^{1}H NMR (600 MHz, $CDCl_3$): δ 2.16 (s, 3H, Me), 3.62 (d, *J* = 1.2 Hz, 3H, OMe), 6.10 (s, 1H), 6.17 (s, 1H), 6.31 (s, 1H), 7.11 – 7.20 (m, 2H), 7.26 – 7.30 (m, 2H), 7.40 (t, *J* = 7.5 Hz, 2H), 7.70 – 7.77 (m, 2H). **TLC** (petroleum ether:CH_2Cl_2 3:7 v/v): R_f = 0.23 **APCI-MS:** m/z: ([M + H^+]): 302.1 **HR-MS (ESI):** m/z calculated for $[C_{21}H_{20}NO]^+$ ([M + H^+]): 302.1539, found: 302.1542.

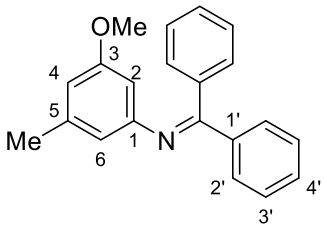

233

7.2.6.5 4,4'-Dimethoxy-2',6-dimethyl-[1,1'-biphenyl]-2-yl trifluoromethanesulfonate (230)

A dry 250 mL round bottom flask equipped with stir bar was charged with phenol **228** (2.01 g, 1.0 equiv, 7.79 mmol), CH_2Cl_2 (45 mL, 0.17 M) and NEt_3 (1.30 mL, 1.2 equiv, 9.34 mmol). The reaction mixture was cooled to 0 °C and Tf_2O (1.57 mL, 1.2 equiv, 9.34 mmol) was added dropwise under vigorous stirring. The cooling bath was removed, and the reaction mixture stirred at 22 °C for 2.5 h. The mixture was cooled to 0 °C, aq. KPi-solution (1 M, pH 7, 30 mL) added. The aq. phase was extracted with EtOAc (3x), the combined org. phases washed with sat. aq. NaCl-solution, dried over MgSO4 and solvents removed in vacuo. The product was isolated by column chromatography (petroleum ether:EtOAc 95:5 v/v) as a colorless oil in a yield of 2.63 g (6.74 mmol, 87%).

^{1}H NMR (600 MHz, $CDCl_3$): δ 2.01 (s, 3H, Me′), 2.05 (s, 3H, Me), 3.83 (s, 3H, OMe′), 3.84 (s, 3H, OMe), 6.73 (d, $^4J_{3\text{-}5}$ = 2.5 Hz, 1H, 3-H), 6.80 (dd, $^3J_{5',6'}$ = 8.3 Hz, ^2J = 2.7 Hz, 1H, 5′-H), 6.84 (d, $^4J_{3',5'}$ = 2.7 Hz, 1H, 3′-H), 6.86 (d, $^4J_{5\text{-}3}$ = 2.5 Hz, 1H, 5-H), 7.01 (d, $^3J_{6',5'}$ = 8.4 Hz, 1H, 6′-H). **^{13}C NMR** (151 MHz, $CDCl_3$): δ 19.90 (Me′), 20.65 (Me), 55.28 (OMe′), 55.73 (OMe), 104.70 (C-3), 111.27 (C-5′), 115.51 (Ar-C), 115.55 (Ar-C), 118.46 (q, $^1J_{C\text{-}F}$ = 320.2 Hz, CF_3), 126.08 (C-1′), 127.01 (C-1), 131.73 (C-6′), 138.57 (C-2′), 140.98 (C-6), 148.08 (C-2), 159.27 (C-4), 159.60 (C-4′). **^{19}F NMR** (282 MHz, $CDCl_3$): δ -74.51. **IR (ATR film) [cm^{-1}]:** 3006, 2942, 2839, 1738, 1611, 1568, 1483, 1420, 1242, 1208, 1141, 1062, 968, 823, 602. **TLC** (petroleum ether:EtOAc 8:2 v/v): R_f = 0.74 **HR-MS (ESI):** m/z calculated for $[C_{17}H_{17}F_3O_5S]^+$ ($[M + H^+]$): 391.0822, found: 391.0824. **Boiling point:** 180 °C ($1.2 \cdot 10^{-1}$ mbar)

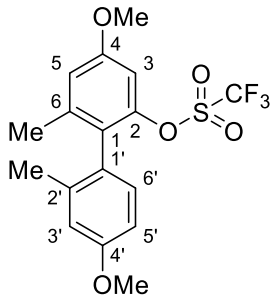

230

7.2.6.6 N-Benzyl-4,4'-dimethoxy-2',6-dimethyl-[1,1'-biphenyl]-2-amine (235)

A dry 25 mL round bottom flask was charged with triflate **230** (1.40 g, 1.00 equiv, 3.59 mmol) and benzylamine (431 µL, 1.10 equiv, 3.94 mmol) and briefly evacuated and backfilled with N_2 (3x). Anhydrous, degassed toluene (9 mL, 0.4 M) was added. A separate dry Schlenk round bottom flask equipped with stir bar was charged with *rac*-BINAP (44.7 mg, 2 mol%, 71.7 µmol), BINAP Pd G4 **205** (72.2 mg, 2 mol%, 71.7 µmol) and Cs_2CO_3 (2.92 g, 2.50 equiv, 8.97 mmol). The reaction vial was evacuated and backfilled with N_2. Toluene (31 mL) was added and the mixture stirred for 15 min at 80 °C. Then the mixture from the first vial was added and reaction vial stirred at 110 C for 19 h. Solvents were removed in vacuo. The product was isolated by column chromatography (petroleum ether:CH_2Cl_2 95:5 v/v) in a yield of 1.18 g (3.41 mmol, 95%).

^{1}H NMR (600 MHz, $CDCl_3$): δ 1.90 (s, 3H, Me), 2.06 (s, 3H, Me′), 3.75 (s, 3H, OMe), 3.84 (s, 3H, OMe′), 3.86 (s, 1H, NH), 4.27 (s, 2H, $\underline{CH_2}$Ph), 6.10 (d, $^4J_{3\text{-}5}$ = 2.5 Hz, 1H, 3-H), 6.22 (d, $^4J_{5\text{-}3}$ = 2.4 Hz, 1H, 5-H), 6.82 (dd, $^3J_{5',6'}$ = 8.3 Hz, $^4J_{5',3'}$ = 2.7 Hz, 1H, 5′-H), 6.88 (d, $^4J_{3',5'}$ = 2.7 Hz, 1H, 3′-H), 7.03 (d, $^3J_{6',5'}$ = 8.3 Hz, 1H, 6′-H), 7.19 – 7.24 (m, 3H, Ph), 7.28 (t, J = 7.5

Hz, 2H, Ph). **^{13}C NMR** (151 MHz, $CDCl_3$): δ 19.85 (Me′), 20.71 (Me), 48.20 (<u>*CH*$_2$</u>Ph), 55.08 (OMe), 55.29 (OMe′), 95.12 (C-3), 103.29 (C-5), 112.07 (C-5′), 116.07 (C-3′), 119.62 (C-1), 127.07, 127.10, 128.65, 129.27 (C-1′), 131.96 (C-6′), 137.96 (C-6), 139.56 (C-2′), 139.70, 146.72, 159.12 (C-4′), 159.77 (C-4). **IR (ATR film) [cm^{-1}]:** 3423, 2925, 2852, 1739, 1602, 1583, 1494, 1451, 1362, 1362, 1237, 1292, 1167, 1069, 822, 734, 699. **TLC** (petroleum ether:EtOAc 95:5 v/v): R_f = 0.17 **HR-MS (ESI):** m/z calculated for $[C_{23}H_{26}NO_2]^+$ ([M + H$^+$]): 348.1958, found: 348.1972.

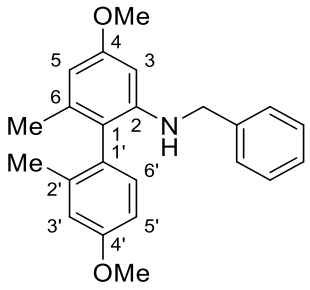

235

7.2.6.7 4'-Methoxy-6-methyl-[1,1'-biphenyl]-2-amine (221)

A 250 mL Schlenk tube equipped with stir bar was charged with 2-aminobiaryl **235** (1.18 g, 1.00 equiv, 3.41 mmol) and degassed (sparging) EtOAc (100 mL, 0.03 M) and $Pd(OH)_2$/C (15 weight%) (160 mg, 5 mol%, 0.171 mmol). An atmosphere exchange was performed by equipping a H_2-balloon with a closed stopcock fitting. The flask was evacuated until the EtOAc started boiling. Then the vacuum valve was closed and the H_2 valve opened. The H_2-balloon stopcock was closed again, and the process repeated twice over. Then the reaction mixture was stirred for 2.20 h at 22 °C. The reaction mixture was then filtered over a pad of Celite® washing with EtOAc (300 mL) and solvents removed in vacuo. The product was isolated as an amber oil in a yield of 821 mg (3.19 mmol, 93%).

^{1}H NMR (600 MHz, $CDCl_3$): δ 1.91 (s, 3H, Me), 2.05 (s, 3H, Me′), 3.79 (s, 3H, OMe), 3.82 (s, 3H, OMe′), 6.24 (d, $^4J_{3\text{-}5}$ = 2.5 Hz, 1H, 3-H), 6.31 (d, $^4J_{5\text{-}3}$ = 2.5 Hz, 1H, 5-H), 6.80 (dd, $^3J_{5',6'}$ = 8.3 Hz, $^4J_{5',3'}$ = 2.7 Hz, 1H, 5′-H), 6.86 (d, $^4J_{3',5'}$ = 2.7 Hz, 1H, 3′-H), 7.02 (d, $^3J_{6',5'}$ = 8.3 Hz, 1H, 6′-H). **^{13}C NMR** (151 MHz, $CDCl_3$): δ 19.81 (Me′), 20.63 (Me), 55.18 (OMe), 55.29 (OMe′), 98.53 (C-3), 106.02 (C-5), 111.86 (C-5′), 115.98 (C-3′), 120.23 (C-1), 129.41 (C-1′), 131.64 (C-6′), 138.68 (C-6), 139.24 (C-2′), 144.66 (C-2), 159.10 (C-4′), 159.46 (C-4). **IR (ATR film) [cm^{-1}]:** 3468, 3375, 2998, 2952, 2917, 2837, 1738, 1604, 1581, 1486, 1446, 1339, 1292, 1235, 1198, 1160, 1066, 825. **TLC** (petroleum ether:EtOAc 8:2 v/v): R_f = 0.38 **HR-MS (ESI):**

m/z calculated for $[C_{16}H_{20}NO_2]^+$ ($[M + H^+]$): 258.1489, found: 258.1494 **Melting point:** 81 – 82 °C

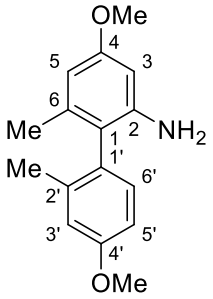

221

7.2.7 Non-Electron-rich Cyclic Diaryl Iodonium Salt Synthesis

The following chapter contains results obtained by Daniel Grudzinski as part of a bachelor's thesis.[206] Parts of the following chapter will be published in a peer-reviewed journal, two manuscript containing these results are in preparation.[228]

7.2.7.1 Synthesis of Box-ligand

7.2.7.1.1 (3aS,3a'S,8aR,8a'R)-2,2'-(Propane-2,2-diyl)bis(3a,8a-dihydro-8H-indeno[1,2-d]oxazole) ((*S*,*S*)-L1)

A 250 mL two-necked round bottom flask was charged with $Zn(OTf)_2$ (579 mg, 1.0 equiv, 1.59 mmol) and dried under vacuum at 125 °C for 2 h. Dimethylmalonitrile (150 mg, 1.0 equiv, 1.59 mmol) and anhydr. toluene (10 mL) and (1S,2R)-2-aminoindanol (476 mg, 2.0 equiv, 3.19 mmol) were added in that order. The sides of the reaction flask were flushed with additional anhydr. toluene (10 mL, 0.16 M). A reflux condenser was equipped, and the mixture stirred at 120 °C for 24 h. EtOAc (100 mL) was added, and the organic mixture extracted with sat. aq. NaCl-solution (3x) and sat. aq. $NaHCO_3$-solution (3x) and dried over $MgSO_4$. Solvent was removed in vacuo. The product was isolated by column chromatography (petroleum ether:EtOAc 7:3 v/v to 100% MeOH) and subsequent tituration from acetone by the addition of petroleum ether. The product could be obtained as white solids in a yield of 130 mg (0.227 mmol, 23 %). The analytical data were in accordance with literature.[242a, 332]

^{1}H NMR (600 MHz, $CDCl_3$): δ 1.42 (s, 6H, Me), 2.95 (d, $^2J_{8\text{-}8}$ = 17.8 Hz, 2H, H_a-8), 3.30 (dd, $^2J_{8\text{-}8}$ = 17.9 Hz, $^3J_{8\text{-}8a}$ = 7.1 Hz, 2H, 8-H_b), 5.19 – 5.34 (m, 2H, 8a-H), 5.52 (d, $^3J_{3a\text{-}8a}$ = 7.9 Hz, 2H, 3a-H), 7.23 (d, *J* = 7.4 Hz, 3H, H-Ar), 7.47 – 7.53 (m, 2H, 7-H). **^{13}C NMR** (151 MHz, $CDCl_3$): δ 24.04 (C*Me*$_2$), 38.61 (*C*Me$_2$), 39.80 (C-8), 76.63 (C-3a), 83.35 (C-8a), 125.22, 125.81 (C-7), 127.49, 128.48 (C-5), 139.89 (C-3b), 141.99 (C-7a), 169.27 (C-2). **IR (ATR film) [cm^{-1}]:** 2983, 2938, 2922, 1741, 1646, 1483, 1456, 1350, 1236, 1148, 1117, 998, 857, 751, 734, 606. **TLC** (CH_2Cl_2:MeOH 98:2 v/v): R_f = 0.23 **APCI-MS:** m/z: ([M + H$^+$]): found: 359.2. **Melting point:** 77 – 79 °C

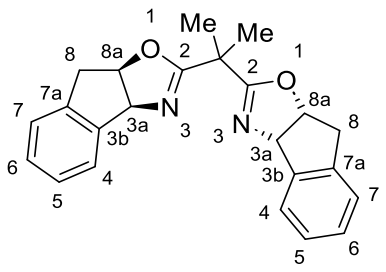

L1

7.2.7.1.1.1 2-((3aS,8aR)-3a,8a-Dihydro-8H-indeno[1,2-d]oxazol-2-yl)-2-methylpropanenitrile (244)

The mono-addition product was obtained as off-white solids in a yield of 96.3 mg (0.268 mmol, 27 %).

^{1}H NMR (600 MHz, $CDCl_3$): δ 1.60 (s, 3H, Me), 1.64 (s, 3H, Me), 3.29 (d, $^2J_{8\text{-}8}$ = 18.1 Hz, 1H, 8'-H), 3.48 (dd, $^2J_{8\text{-}8}$ = 18.1, 7.0 Hz, 1H, 8-H_a), 5.43 – 5.54 (m, 1H, 8-H_b), 5.62 (d, $J_{3a\text{-}8a}$ = 7.9 Hz, 1H, 3a-H), 7.30 (dq, *J* = 8.4, 5.1 Hz, 3H, 5-H + 6-H + 7-H), 7.47 – 7.56 (m, 1H, 4-H). **^{13}C NMR** (151 MHz, $CDCl_3$): δ 25.38 (Me), 25.42 (Me), 33.42 (*C*Me_2), 39.71 (C-8), 76.86 (C-3a), 84.62 (C-8a), 121.28 (CN), 125.46, 125.76 (C-4), 127.68, 128.89 (C-6), 139.56 (C-7a), 141.10 (C-3b), 165.63 (C-2). **IR (ATR film) [cm^{-1}]:** 2992, 2941, 2925, 2244, 1659, 1460, 1345, 1291, 1240, 1130, 997, 856, 749, 620. **TLC** (CH_2Cl_2:MeOH 98:2 v/v): R_f = 0.64 (petroleum ether:EtOAc 7:3 v/v): R_f = 0.25 **APCI-MS:** m/z: ([M + H^+]): found: 227.1

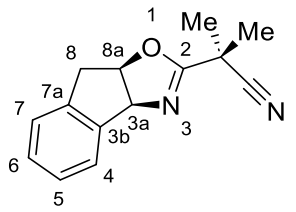

244

7.2.7.2 Biphenol Synthesis

7.2.7.2.1 1,9-Dimethyldibenzo[b,d]iodol-5-ium (237)

A 1000 mL round bottom flask was charged with biaryl **236** (10.5 g, 1.0 equiv, 33.9 mmol), CH_2Cl_2 (226 mL, 0.15 M). To the stirred solution was added *m*-CPBA (15.6 g, 2.0 equiv, 67.8 mmol). After full dissolution of the *m*-CPBA, the solution was cooled to 0 °C and TfOH (9.00 mL, 3.0 equiv, 102 mmol) added dropwise *via* a dropping funnel. The resulting suspension was stirred at room temperature for 1 h. The solvent was removed in vacuo and the resulting crude product suspended in Et_2O. The resulting mixture was stirred for 20 min and the solids collected by filtration and washed with additional Et_2O. The product was obtained as off-white solids in a yield of 12.0 g (26.4 mmol, 78%). The analytical data were in accordance with literature.[81a]

^{1}H NMR (600 MHz, $CDCl_3$): δ 2.57 (s, 6H, Me), 7.53 (t, $^3J_{3\text{-}2,3\text{-}4}$ = 7.8 Hz, 2H, 3-H), 7.58 (d, $^3J_{2\text{-}3}$ = 7.6 Hz, 2H, 2-H), 8.25 (d, $^3J_{4\text{-}3}$ = 8.0 Hz, 2H, 4-H). **^{13}C NMR** (151 MHz, $CDCl_3$): δ 24.11 (Me), 120.11 (C-5), 128.92 (C-4), 130.34 (C-3), 133.97 (C-2), 140.52 (C-1), 141.92 (C-6). **^{19}F NMR** (282 MHz, $CDCl_3$): δ -78.02. **IR (ATR film) [cm^{-1}]:** 3485 (broad), 3103, 3081,

1442, 1287, 1239, 1224, 1163, 1025, 777, 696, 636, 574, 516. **TLC** (petroleum ether:EtOAc 2:8 v/v): R_f = 0.21 **HR-MS (ESI):** m/z calculated for $[C_{14}H_{12}I]^+$ ([M - OTf^-]): 306.9979, found: 306.9978. **Melting point:** 170 – 171 °C

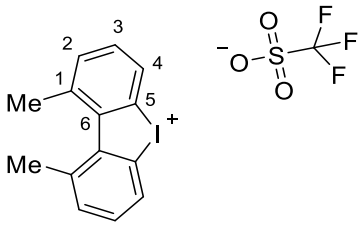

237

7.2.7.2.1.1 1,9-Dimethyldibenzo[b,d]iodol-5-ium 3-chlorobenzoate (369)

The benzoate salt was obtained column chromatographic isolation (petroleum ether:EtOAc 2:8 v/v) of the Et_2O wash fraction in a yield of 547 mg (1.18 mmol, 3%)

^{1}H NMR (600 MHz, $CDCl_3$): δ 2.56 (s, 6H, Me), 7.40 (t, *J* = 7.9 Hz, 1H, 2'-H), 7.47 – 7.60 (m, 6H, 1-H + 2-H + 1'/3'-H), 8.00 (d, *J* = 7.7 Hz, 1H, 1'/3'-H), 8.05 – 8.15 (m, 1H, 4'-H), 8.29 (d, *J* = 7.9 Hz, 2H, 3-H).

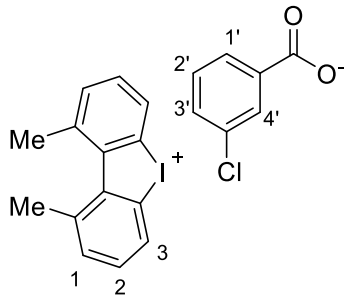

369

7.2.7.2.2 2,2'-Diiodo-6,6'-dimethyl-1,1'-biphenyl (238)

A dry 500 mL round bottom flask was charged with CuI (171 mg, 5 mol%, 0.900 mmol) and bisoxazoline ligand (*S,S*)-**L2** (452 mg, 7.5 mol%, 1.35 mmol). Anhydr. CH_2Cl_2 (180 mL, 0.1 M) was added and the mixture stirred for 10 min. Iodonium salt **237** (8.21 g, 1.0 equiv, 18.0 mmol) was added and once fully dissolved flame dried NaI (3.24 g, 1.2 equiv, 21.6 mmol) was added at once. A septum and Argon balloon were equipped, and the reaction stirred for 24 h at room temperature. The reaction mixture was washed with saturated aqueous Na_2SO_3 solution, washed with sat. aq. NaCl solution and dried over $MgSO_4$. Solvent was removed in vacuo and the crude product suspended in *n*-pentane. The crude product was then filtered over a plug of silica

washing with copious amounts of *n*-pentane until no more product elution could be detected by TLC. The product was obtained as white crystalline solids in a yield of 6.70 g (15.4 mmol, 86%, 91%*ee* S_a).

A further experiment on the same scale with ligand (*R,R*)-**L2** gave the enantiocomplementary product as white crystalline solids in a yield of 6.30 g (14.8 mmol, 82%, 94%*ee* R_a).

A further experiment with CuI (14.3 mg, 5 mol%, 7.50 µmol), anhydr. CH_2Cl_2 (15 mL, 0.1 M), iodonium salt **237** (684 mg, 1.0 equiv, 1.50 mmol) and TBAI (554 mg, 1.0 equiv, 1.50 mmol) without ligand gave the racemic product as white solids in a yield of 608 mg (1.40 mmol, 93%, *rac*). The analytical data were in accordance with literature.[81a]

^{1}H NMR (600 MHz, $CDCl_3$): δ 2.01 (s, 3H, Me), 7.00 (t, $^3J_{4\text{-}3,4\text{-}5}$ = 7.8 Hz, 1H, 4-H), 7.28 (d, $^3J_{5\text{-}4}$ = 7.6 Hz, 1H, 5-H), 7.81 (d, $^3J_{3\text{-}4}$ = 7.9 Hz, 1H, 3-H). **^{13}C NMR** (151 MHz, $CDCl_3$): δ 21.55 (Me), 100.80 (C-2), 129.55 (C-4), 130.20 (C-5), 136.93 (C-3), 137.72 (C-6), 147.61 (C-1). **IR (ATR film) [cm^{-1}]:** 2978, 2934, 2835, 1600, 1575, 1490, 1457, 1432, 1387, 1353, 1315, 1272, 1247, 1145, 1125, 1073, 1046, 1026, 963, 862, 829, 760, 659. **TLC** (petroleum ether:EtOAc 9:1 v/v): R_f = 0.68 **APCI-MS:** m/z: ([M + H$^+$]): found: 433.8.

Melting point: 94 – 96 °C (*rac*)

92 – 93 °C (S_a, 92%*ee* HPLC) (93 – 95 °C)[333]

HPLC: Chiralpak® IC (Daciel) 250 ° 4.6 mm, 25 °C, 0.5 mL min^{-1}, 225 nm, *n*-heptane:*i*-PrOH 99.9:0.1 (v/v) $t_R(S_a)$ = 10.0 min, $t_R(R_a)$ = 11.1 min

Optical rotation: $[\alpha]^{25}_D$ = +35.0 (±0.1, duplicate) (c = 0.970, $CHCl_3$, S_a, 92%ee by chiral HPLC)

$[\alpha]^{27.5}_D$ = +26.8 (c = 0.970, $CHCl_3$, S_a, 92%ee by chiral HPLC) −21.0 (R_a)[81a]

$[\alpha]^{20}_D$ = +28.2 (c = 0.970, $CHCl_3$, S_a, 92%ee by chiral HPLC)

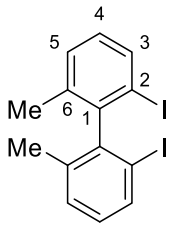

238

7.2.7.2.3 2,2'-(2,2'-Diiodo-6,6'-dimethyl-[1,1'-biphenyl]-4,4'-diyl)bis(4,4,5,5-tetramethyl-1,3,2-dioxaborolane) (239)

A dry 250 mL Schlenk-vial equipped with a stir bar was charged with biaryl **238** (4.34 g, 1.00 equiv, 10.0 mmol, 91%*ee* S_a) and B_2pin_2 (5.33 g, 2.10 equiv, 21.0 mmol). A separate dry Schlenk-flask equipped with a stir bar was charged with $(Ir(COD)OMe)_2$ (199 mg, 3 mol%, 0.30 mmol), dtbpy (161 mg, 6 mol%, 0.60 mmol), and THF (50 mL). The catalyst mixture was stirred for 5 min and then added to the reaction mixture. The flask was sealed with PTFE band and the reaction mixture stirred at 700 rpm at 75 °C for 16 h. MeOH (20 mL) was added to quench HBpin. The crude mixture was filtered over a plug of silica washing with petroleum ether:EtOAc (9:1, 5000 mL) until no more product was detectable by TLC (product elutes poorly on silica). Solvent was removed *in vacuo* until 500 mL remained. The organic phase was then washed with sat. aq. $NaHCO_3$ (3x 100 mL) to remove pinacol, the org. phase dried over $MgSO_4$ and solvent removed in vacuo. The isolated product was obtained as white solids in a yield of 6.74 g (9.83 mmol, 98%, 95%*ee* S_a).

A further experiment using biaryl **238** (4.34 g, 1.00 equiv, 10.0 mmol, 94%*ee* R_a) gave the enantiocomplementary product as white solids in a yield of 6.75 g (9.84 mmol, 98%, 95%*ee* R_a).

^{1}H NMR (600 MHz, $CDCl_3$): δ 1.36 (s, 12H, $B(OC\mathit{Me}_2)_2$), 1.98 (s, 3H, Me), 7.68 (s, 1H, 5-H), 8.23 (s, 1H, 3-H). **^{13}C NMR** (151 MHz, $CDCl_3$): δ 21.20 (Me), 25.05 ($B(OC\mathit{Me}_2)_2$), 25.07 ($B(OC\mathit{Me}_2)_2$), 84.29 ($B(O\mathit{C}Me_2)_2$), 100.39 (C-2), 130.87 (brs, C-4), 136.31 (C-5), 136.90 (C-6), 142.98 (C-3), 150.21 (C-1). **^{11}B NMR** (96 MHz, $CDCl_3$): δ 31.52. **IR (ATR film) [cm^{-1}]:** 2978, 2928, 1595, 1527, 1423, 1371, 1339, 1314, 1270, 1237, 1213, 1141, 1124, 1006, 966, 909, 888, 852, 801, 732, 697, 684, 648, 579. **TLC** (petroleum ether:EtOAc 95:5 v/v): $R_f = 0.35$ **HR-MS (ESI):** m/z calculated for $[C_{26}H_{38}B_2NI_2O_4]^+$ ($[M + NH_4^+]$): 704.1071, found: 704.1078.

Melting point: 262 – 268 °C (*rac*)

267 – 270 °C (S_a, 98%*ee* HPLC)

HPLC: Lux® Amylose-1 (Phenomenex) 250 ° 4.6 mm, 10 °C, 0.5 mL min^{-1}, 222 nm, *n*-heptane:*i*-PrOH 99:1 (v/v) $t_R(S_a) = 6.5$ min, $t_R(R_a) = 6.8$ min

Optical rotation: $[\alpha]^{25}_D = +20.3$ (±0.4, duplicate) (c = 1.00, $CHCl_3$, S_a, 98%*ee* by chiral HPLC)

X-ray: 239 was dissolved in a glass vial in little Et_2O, layered with *n*-pentane and solvent left to mix at 22 °C over time sealed with a plastic cap. CCDC 2342278

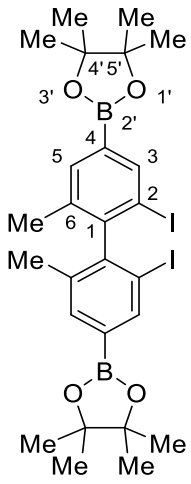

239

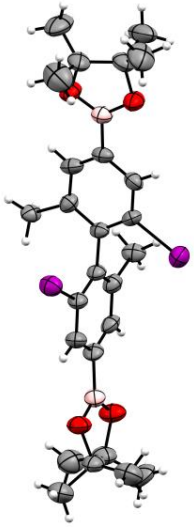

(*S*)-**239**

CCDC 2342278

Figure S2: 2,2′-diiodobiaryl **239**. Left: Lewis structure interpretation Right: Crystal structure shown as Oak Ridge Thermal Ellipsoid Plot (ORTEP) of the (*S*)-enantiomer, ellipsoids are shown at 50% probability. Detailed information can be found in cif-format under the given CCDC deposition number.

7.2.7.2.4 2,2'-Diiodo-6,6'-dimethyl-[1,1'-biphenyl]-4,4'-diol (246)

A 250 mL round bottom flask equipped with stir bar was charged with biaryl **239** (2.74 g, 1.0 equiv, 4.00 mmol, 95%*ee* S_a) and THF (50 mL, 0.08 M). A solution of Oxone® (2.45 g, 4.0 equiv, 8.00 mmol) in water (48.0 mL) was added and the suspension stirred at 600 rpm at room temperature for 24 h. Aqueous 10% Na_2SO_3 solution (100 mL) was added, and the suspension stirred for 5 min. The aq. phase was extracted using CH_2Cl_2 (3x 150 mL) and the combined organic phases washed with sat. aq. NaCl solution and dried over $MgSO_4$. The solvent was removed in vacuo. The product was isolated by column chromatography (petroleum ether:EtOAc 7:3 v/v). and obtained as white solids in a yield of 1.58 g (3.39 mmol, 85%, 92%*ee* S_a).

A further experiment using biaryl **239** (2.74 g, 1.00 equiv, 4.00 mmol, 95%*ee* R_a) gave the enantiocomplementary product as white solids in a yield of 1.52 g (3.26 mmol, 82%, 94%*ee* R_a).

^{1}H NMR (600 MHz, $CDCl_3$): δ 1.96 (s, 6H, Me), 4.80 (s, 2H, OH), 6.78 (d, $^4J_{5\text{-}3}$ = 2.5 Hz, 2H, 5-H), 7.30 (d, $^4J_{3\text{-}5}$ = 2.5 Hz, 2H, 3-H).

^{13}C NMR (151 MHz, $CDCl_3$): δ 21.85 (Me), 101.87 (C-1), 117.36 (C-5), 123.52 (C-3), 139.13 (C-6), 140.14 (C-1), 155.31 (C-4).

IR (ATR film) [cm^{-1}]: 3342 (broad), 1595, 1566, 1441, 1415, 1328, 1270, 1198, 1131, 1112, 1007, 972, 909, 854, 795, 733, 614.

TLC (petroleum ether:EtOAc 6:4 v/v): $R_f = 0.52$

APCI-MS: m/z: ([M + H^+]): found: 467.0

Elemental analysis (calcd., found for $C_{14}H_{12}I_2O_2$): C (36.08, 36.37), H (2.60, 2.87)

Melting point: 171 – 173 °C (*rac*)

162 – 167 °C (S_a, 97%*ee* HPLC)

HPLC: Lux® Amylose-1 (Phenomenex) 250 ° 4.6 mm, 25 °C, 0.5 mL min^{-1}, 205 nm, *n*-heptane:*i*-PrOH 80:20 (v/v) $t_R(S_a) = 12.4$ min, $t_R(R_a) = 11.3$ min

Optical rotation: $[\alpha]^{25}_D = +26.2$ (±0.2, duplicate) (c = 0.30, $CHCl_3$, S_a, 97%*ee* by chiral HPLC)

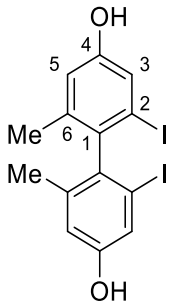

246

2,2'-Diiodo-6,6'-dimethyl-[1,1'-biphenyl]-4-ol (**248**) was obtained as a sideproduct in analytical quantities.

^{1}H NMR (600 MHz, $CDCl_3$): δ 1.95 (s, 3H, Me), 2.02 (s, 3H, Me′), 5.00 (s, 1H, OH), 6.79 (d, $^4J_{5\text{-}3} = 2.5$ Hz, 1H, 5-H), 6.98 (t, $^3J_{4'\text{-}3',4'\text{-}5'} = 7.7$ Hz, 1H, 4′-H), 7.26 (d, $^3J_{5'\text{-}4'} = 7.5$ Hz, 1H, 5′-H), 7.32 (d, $^4J_{3\text{-}5} = 2.5$ Hz, 1H, 3-H), 7.79 (d, $^3J_{3'\text{-}4'} = 7.9$ Hz, 1H, 3′-H). **^{13}C NMR** (151 MHz, $CDCl_3$): δ 21.65 (Me), 21.74 (Me), 100.63 (C-2), 102.07 (C-2′), 117.45 (C-5), 123.61 (C-3), 129.52 (C-4′), 130.12 (C-5′), 136.83 (C-3′), 138.35, 138.54, 140.63 (C-1), 147.19 (C-1′), 155.34 (C-4). **IR (ATR film) [cm^{-1}]:** 3389 (broad), 3038, 2924, 2847, 1603, 1565, 1448, 1442, 1420, 1275, 1206, 1122, 1000, 847, 804, 763, 732. **TLC** (petroleum ether:EtOAc 6:4 v/v): $R_f = 0.69$ **APCI-MS:** m/z: ([M + H^+]): found: 451.0 **Elemental analysis** (calcd., found for $C_{14}H_{12}I_2O$): C (37.36, 37.13), H (2.69, 2.85)

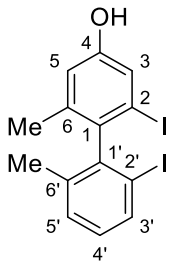

248

7.2.7.2.5 2,2'-Diiodo-4,4'-dimethoxy-6,6'-dimethyl-1,1'-biphenyl (249)

A 100 mL round bottom flask equipped with stir bar was charged with biaryl **246** (1.86 g, 1.0 equiv, 4.00 mmol, 92%*ee* S_a) and acetone (20 mL, 0.2 M). K_2CO_3 (1.66 g, 3.0 equiv, 12.0 mmol) was added and stirred at 700 rpm. The reaction was cooled to 0 °C and Me_2SO_4 (0.84 mL, 2.2 equiv, 8.80 mmol) was added dropwise. A reflux condenser was equipped, and the reaction mixture stirred at 65 °C for 2 h. Saturated aqueous Na_2SO_3 (10 mL) solution was added and the reaction stirred at 40 °C for 20 min to quench excess Me_2SO_4. The aq. phase was then extracted using EtOAc (3x 50 mL), the combined organic phases were washed with sat. aq. NaCl solution, dried over $MgSO_4$ and solvents removed in vacuo. The product was obtained as a white solids in a yield of 1.76 g (3.56 mmol, 89%, 92%*ee* S_a).

A further experiment using biaryl **246** (1.32 g, 1.00 equiv, 2.83 mmol, 94%*ee* R_a) gave the product as a white solid in a yield of 1.32 g (2.68 mmol, 95%, 95%*ee* R_a).

^{1}H NMR (600 MHz, $CDCl_3$): δ 1.98 (s, 6H, Me), 3.82 (s, 6H, OMe), 6.83 (d, $^4J_{5\text{-}3}$ = 2.6 Hz, 2H, 5-H), 7.33 (d, $^4J_{3\text{-}5}$ = 2.5 Hz, 2H, 3-H). **^{13}C NMR** (151 MHz, $CDCl_3$): δ 22.04 (Me), 55.51 (OMe), 102.03 (C-2), 116.36 (C-5), 121.56 (C-3), 138.77 (C-1), 140.16 (C-6), 159.23 (C-4). **IR (ATR film) [cm^{-1}]:** 2925, 2834, 1593, 1540, 1464, 1426, 1283, 1252, 1214, 1131, 1056, 987, 851, 775, 730, 586, 495. **TLC** (petroleum ether:EtOAc 7:3 v/v): R_f = 0.65 **HR-MS (ESI):** m/z calculated for $[C_{16}H_{17}I_2O_2]^+$ ([M + H$^+$]): 494.9313, found: 494.9310.

Melting point: 96 – 98 °C (*rac*)

109 – 113 °C (S_a, 98%*ee* HPLC)

HPLC: Chiralpak® IC (Daciel) 250 ° 4.6 mm, 25 °C, 0.5 mL min^{-1}, 208 nm, *n*-heptane:*i*-PrOH 99.9:0.1 (v/v) $t_R(S_a)$ = 8.9 min, $t_R(R_a)$ = 8.5 min

Optical rotation: $[\alpha]^{25}_D$ = +31.9 (±0.1, duplicate) (c = 0.99, $CHCl_3$, S_a, 98%*ee* by chiral HPLC)

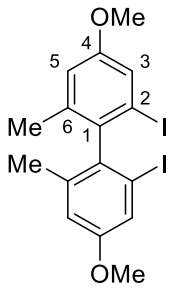

249

7.2.7.2.6 4,4'-Dimethoxy-6,6'-dimethyl-[1,1'-biphenyl]-2,2'-diol (27)

A dry 250 mL Schlenk-vial equipped with stir bar was charged with biaryl **249** (1.72 g, 1.0 equiv, 3.49 mmol, 94%*ee* S_a) and anhydrous Et_2O (70 mL, 0.05 M). To the stirred (700 rpm) solution at -78 °C was added a solution of *n*-BuLi in hexanes (2.5 M, 6.15 mL, 4.4 equiv, 15.6 mmol). The mixture was stirred at -78 °C for 1 h. Then freshly distilled nitrobenzene (3.58 mL, 10.0 equiv, 34.9 mmol) was added at once at -78 °C. The mixture was then stirred at -78 °C for 1 h. The reaction was left to warm to room temperature and stirred for 30 min. Then MeOH (20 mL) was added and the reaction was stirred for 10 min. K_2HPO_4/KH_2PO_4-buffer (KPi-buffer, 1 M, pH 7, 40 mL) was added and the aq. phase extracted with EtOAc (3x 100 mL). The combined organic phases were washed with sat. aq. NaCl solution, dried over $MgSO_4$ and solvents removed in vacuo. The product was isolated by column chromatography (petroleum ether:EtOAc 75:25 v/v) and obtained as off-white solids in a yield of 645 mg (2.35 mmol, 67%, 94%*ee* S_a). The product was recrystallized (petroleum ether:EtOAc 4:6 v/v, 5.2 mL) to provide the product as off-white solids in a yield of 463 mg (1.69 mmol, 48%, >99%*ee* S_a).

A further experiment using biaryl **249** (974 mg, 1.0 equiv, 1.97 mmol, 94%*ee* R_a) gave the product as white solids in a yield of 311 mg (1.14 mmol, 58%, 94%*ee* R_a). After recrystallization the product was obtained as off-white solids in a yield of 254 mg (0.93 mmol, 47%, >99%*ee* R_a). The analytical data were in accordance with literature.[102]

^{1}H NMR (600 MHz, $CDCl_3$): δ 1.97 (s, 6H, Me), 3.81 (s, 6H, OMe), 4.84 (s, 2H, OH), 6.47 (d, $^4J_{3\text{-}5}$ = 2.5 Hz, 2H, 3-H), 6.49 (d, $^4J_{5\text{-}3}$ = 2.5 Hz, 2H, 5-H). **^{13}C NMR** (151 MHz, $CDCl_3$): δ 19.78 (Me), 55.28 (OMe), 98.44 (C-3), 108.95 (C-5), 111.27 (C-1), 140.46 (C-6), 155.44 (C-2), 161.13 (C-4). **IR (ATR film) [cm^{-1}]:** 3446 (broad), 2946, 2839, 1615, 1576, 1480, 1441, 1330, 1300, 1195, 1148, 1070, 1040, 836. **TLC** (petroleum ether:EtOAc, 7:3 v/v): R_f = 0.26 **APCI-MS:** m/z: ([M + H$^+$]): found: 275.

Melting point: 148 – 150 °C (*rac*) (148 – 150 °C)[102]

170 – 172 °C (S_a, >99%*ee* HPLC) (172 – 174°C)[102]

169 – 171 °C (R_a, >99%*ee* HPLC)

HPLC: Lux® Amylose-1 (Phenomenex) 250 ° 4.6 mm, 25 °C, 0.5 mL min^{-1}, 205 nm, *n*-heptane:*i*-PrOH 50:50 (v/v) $t_R(S_a)$ = 14.5 min, $t_R(R_a)$ = 53.1 min

Optical rotation: $[\alpha]^{25}_D = -31.1$ (±0.7, duplicate) (c = 0.98, $CHCl_3$, S_a, >99%*ee* by chiral HPLC) −31.9[102]

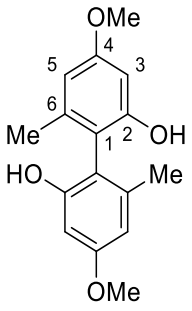

27

7.2.7.3 Miscellaneous Syntheses

7.2.7.3.1 6,6'-Dimethyl-[1,1'-biphenyl]-2,2'-diol (253)

A microwave vial equipped with stir bar was charged with 2,2′-diiodo biaryl **238** (43.3 mg, 1.0 equiv, 0.100 mmol) and anhydr. Et_2O (2.0 mL, 0.05 M). To the stirred (700 rpm) solution at -78 °C was added a solution of *n*-BuLi in pentanes (2.5 M, 88.0 µL, 2.2 equiv, 0.220 mmol). The mixture was stirred at -78 °C for 1 h. Then, freshly distilled nitrobenzene (103 µL, 10.0 equiv, 1.00 mmol) was added at once at -78 °C. The mixture was then stirred at -78 °C for 1 h. The reaction was left to warm to room temperature and stirred for 30 min. Then MeOH (2.0 mL) was added, and the reaction was stirred for 10 min H_2O (10 mL) was added, the aq. phase extracted with CH_2Cl_2 (3x) and the combined org. phases discarded. Then HCl-solution (1 M, 2.0 mL) was added and the aq. phase extracted with CH_2Cl_2 (3x 20 mL). The combined organic phases were washed with sat. aq. NaCl solution, dried over $MgSO_4$ and solvents removed in vacuo. The product was obtained as off-white solids in a yield of 11.2 mg (52.3 µmol, 52%). The analytical data were in accordance with literature.[81a, 334]

^{1}H NMR (600 MHz, $CDCl_3$): δ 2.01 (s, 6H, Me), 4.72 (s, 2H, OH), 6.90 (d, $^3J_{3\text{-}4}$ = 8.2 Hz, 2H, 3-H), 6.93 (d, $^3J_{5\text{-}4}$ = 7.5 Hz, 2H, 5-H), 7.17 – 7.35 (m, 2H, 4-H). **^{13}C NMR** (151 MHz, $CDCl_3$): δ 19.60 (Me), 113.30 (C-3), 119.68 (C-1), 122.73 (C-5), 130.25 (C-4), 139.07 (C-6), 153.96

(C-2). **IR (ATR film) [cm^{-1}]:** 3484 (broad signal), 2930, 1580, 1466, 1338, 1277, 1262, 1178, 776, 746. **Melting point**: °C (163 – 164 °C) (*rac*) (159 – 160 °C)[335] **APCI-MS:** m/z: ([M + H$^+$]): found: 215.2

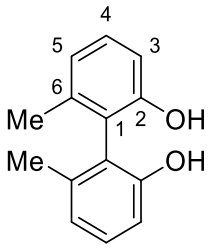

253

7.2.7.3.2 2-Butyl-2',6-dimethyl-1,1'-biphenyl-6'-*d* (251)

A microwave vial equipped with stir bar was charged with 2,2′-diiodo biaryl **238** (43.4 mg, 1.0 equiv, 0.100 mmol) and anhydr. Et_2O (2.0 mL, 0.05 M). To the stirred (700 rpm) solution at -78 °C was added a solution of *n*-BuLi in hexanes (2.5 M, 88.0 µL, 4.4 equiv, 0.220 mmol). The mixture was stirred at -78 °C for 1 h. Then D_2O (100 µL, 45.0 equiv, 4.50 mmol) was added at once at -78 °C. The mixture was left to warm to room temperature and stirred for 30 min. Then MeOH (2.0 mL) was added and the reaction was stirred for 10 min. K_2HPO_4/KH_2PO_4-buffer (KPi-buffer, 1 M, pH 7, 5.0 mL) was added and the aq. phase extracted with EtOAc (3x 20 mL). The combined organic phases were washed with sat. aq. NaCl solution, dried over $MgSO_4$ and solvents removed in vacuo. 1,3,5-trimethoxybenzene (12.5 mg) was added to determine the conversion to product according to ^{1}H NMR (90%). The product was isolated by filtration over silica washing with *n*-pentane and solvents removed in vacuo. The title compound was isolated as a colorless oil in analytical quantaties.

^{1}H NMR (600 MHz, $CDCl_3$): δ 0.75 (t, $^3J_{4'',3''}$ = 7.4 Hz, 3H, 4''-H), 1.16 (qd, $^3J_{3'',4'',3'',2''}$ = 7.2 Hz, $^4J_{3'',1''}$ = 3.4 Hz, 2H, 3''-H), 1.38 (dqd, $^3J_{2'',1''}$ = 8.8 Hz, $^3J_{2'',3''}$ = 7.4 Hz, $^4J_{2'',4''}$ = 1.7 Hz, 2H, 2''-H), 1.93 (s, 3H, Me), 1.96 (s, 3H, Me'), 2.17 (ddd, $^2J_{1a,1b}$ = 13.7 Hz, $^3J_{1'',2''}$ = 8.8 Hz, *J* = 7.0 Hz, 1H, 1_a''-H), 2.24 – 2.32 (m, 1H, 1_b''-H), 7.03 (d, $^3J_{6',5'}$ = 7.3 Hz, 0H, 6'-D), 7.10 (d, $^3J_{3',4'}$ = 7.5 Hz, 1H, 3'-H), 7.13 (d, $^3J_{5',4',5',6'}$ = 7.6 Hz, 1H, 5'-H), 7.20 (t, *J* = 7.6 Hz, 1H, ArH), 7.22 (dd, *J* = 7.1, 2.3 Hz, 1H, ArH), 7.24 – 7.31 (m, 3H, ArH). **^{13}C NMR** (151 MHz, $CDCl_3$): δ 13.95 (C-4''), 19.74 (Me'), 20.60 (Me), 22.68 (C-3''), 33.11 (C-2''), 33.19 (C-1''), 125.73, 126.47 (C-3), 127.08, 127.10, 127.27 (C-3'), 129.96, 136.00, 136.12, 136.94, 140.23, 140.73, 140.76. **IR (ATR film) [cm^{-1}]:** 2953, 2923, 2862, 1740, 1459, 1383, 1011, 799, 761, 655. **TLC** (100% petroleum ether): R_f = 0.56 **GC-MS(EI-MS):** m/z: ([M$^+$]): found: 239.3

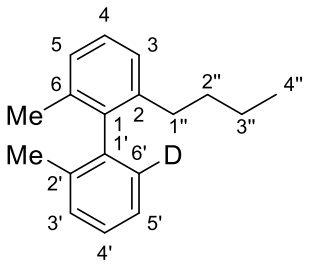

251

7.2.8 *Catellani* Reaction

7.2.8.1 1,4-Dioxa-8-azaspiro[4.5]decan-8-yl benzoate (262)

A 50 mL round bottom flask equipped with stir bar was charged with dibenzoyl peroxide (75 weight%, 1.13 g, 1.0 equiv, 3.50 mmol), K_2HPO_4 (914 mg, 1.5 equiv, 5.25 mmol), and DMF (7 mL, 0.5 M). The suspension was stirred at 0 °C and 4,4-ethylenedioxy-piperidine (449 mg, 1.0 equiv, 3.50 mmol) added. The reaction mixture was stirred at 22 °C for 4 h. H_2O (20 mL) was added and the aq. phase extracted using EtOAc (3x). The combined organic phases were washed with sat. Aq. NaCl solution, dried over $MgSO_4$ and solvents removed in vacuo. The product was isolated by column chromatography (petroleum ether:EtOAc 6:4 v/v) as a colorless oil in a yield of 665 mg (2.53 mmol, 72%). The analytical data is in accordance with literature.[336] (Though the product is reported as a solid instead of an oil)

^{1}H NMR (600 MHz, $CDCl_3$): δ 1.97 (t, 4H, 2′-H), 3.26 (s, 2H, 1′a-H), 3.45 (s, 2H, 1′b-H), 3.99 (d, 4H, 3′-H), 7.44 (t, 2H, 3-H), 7.56 (t, 1H, 4-H), 8.01 (d, 2H, 2-H). **^{13}C NMR** (151 MHz, $CDCl_3$): δ 32.60 (C-2′), 51.00 (C-1′), 64.38 (C-3′/ CR_2O_2), 64.54 (C-3′/CR_2O_2), 106.05 (C-1), 128.43 (C-3), 129.45 (C-2), 133.08 (C-4), 164.77 (CO_2). **IR (ATR film) [cm^{-1}]:** 2964, 2880, 1736, 1451, 1246, 1153, 1118, 1084, 1064, 1037, 1025, 969, 947, 919, 709, 679. **TLC** (*n*-pentane:EtOAc 4:6 v/v): R_f = 0.41 **APCI-MS:** m/z: ([M + H$^+$]): found: 264.1

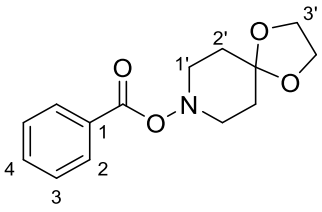

262

7.2.8.2 Morpholino benzoate (342)

A 50 mL round bottom flask equipped with stir bar was charged with dibenzoyl peroxide (75 weight%, 5.00 g, 1.0 equiv, 20.64 mmol), K_2HPO_4 (5.40 g, 1.5 equiv, 31.0 mmol), and DMF (50 mL, 0.5 M). The suspension was stirred at 0 °C and morpholine (2.2 mL, 1.0 equiv, 24.7 mmol) added. The reaction mixture was stirred at 22 °C for 4 h. H_2O (20 mL) was added and the aq. phase extracted using EtOAc (3x). The combined organic phases were washed with sat. Aq. NaCl solution, dried over $MgSO_4$ and solvents removed in vacuo. The product was

isolated by column chromatography (petroleum ether:EtOAc 6:4 v/v) as white solids in a yield of 716 mg (3.5 mmol, 17%). The analytical data is in accordance with literature.[337]

^{1}H NMR (600 MHz, $CDCl_3$): δ 3.05 (m, 2H, 1'-H), 3.46 (m, 2H, 1'-H), 3.87 (m, 2H, 2'-H), 3.99 (m, 2H, 2'-H), 7.45 (m, 2H, 3-H), 7.58 (m, 1H, 4-H), 8.02 (m, 2H, 2-H). **^{13}C NMR** (151 MHz, $CDCl_3$): δ 52.00 (C-1'), 65.86 (C-2'), 128.46 (C-3), 129.16 (C-1), 129.46 (C-2), 133.21 (C-4), 164.60 (CO_2). **IR (ATR film) [cm^{-1}]:** 1738, 1452, 1248, 1102, 1085, 1066, 1049, 1035, 1009, 858, 709 **TLC** (petroleum ether:EtOAc 6:4 v/v): R_f = 0.38 **APCI-MS:** m/z: ([M-$C_4H_8NO_2$]): found: 105.0 [M-$C_7H_5O_2$]$^+$ found: 86.0 **Melting point**: 83 °C

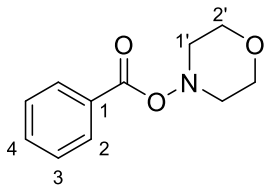

342

7.2.8.3 (±)-8-(2',6-Dimethyl-[1,1'-biphenyl]-2-yl)-1,4-dioxa-8-azaspiro[4.5]decan (265)

A dry microwave vial equipped with stir bar and N_2 balloon was charged with 1-iodo-2-methylbenzene (26.0 µL, 1.0 equiv, 0.208 mmol), Cs_2CO_3 (202 mg, 3.0 equiv, 0.624 mmol), $(2\text{-furyl})_3P$ (38.0 mg, 80.0 mol%, 0.168 mmol) and $(Pd\ G4)_2$ (**205**) (16 mg, 10 mol%, 20.8 µmol). The vial was evacuated and backfilled with N_2 (3x). Solutions of boronic acid ester **222** (0.500 mL, 75.0 µL, 1.5 equiv, 0.312 mmol), amine benzoate **262** (0.500 mL, 80.0 µL, 1.5 equiv, 0.312 mmol) and norbornene (0.500 mL, 9.70 mg, 0.5 equiv, 0.105 mmol) taken from stock solutions each prepared in separate dry microwave vials in anhydrous degassed toluene beforehand (4x amount each) were added to the reaction vessel. Then anhydrous degassed toluene (0.250 mL) was added to the reaction vessel. The balloon was removed, the vial sealed with Parafilm® and the reaction mixture stirred at 500 rpm at 80 °C in a sand bath for 24 h. The resulting mixture was then filtered over a pad of Celite® and solvents removed in vacuo. The product was isolated by column chromatography (petroleum ether:EtOAc 95:5 v/v) as a colorless oil in a yield of 31.9 mg (0.100 mmol, 48%).

^{1}H NMR (600 MHz, $CDCl_3$): δ 1.36 (m, 2H, 8_a-H), 1.44 (m, 2H, 8_b-H), 1.98 (s, 3H, Me), 2.02 (s, 3H, Me′), 2.76 (m, 2H, 7_a-H), 2.96 (m, 2H, 7_b-H), 3.89 (s, 4H, 10-H), 6.91 (d, $^3J_{3\text{-}4}$ = 7.9 Hz,

1H, 3-H), 6.98 (d, $^{3}J_{4\text{-}5}$ = 7.6 Hz, 1H, 5-H), 7.08 (m, 1H, 5′-H), 7.19 (m, 3H, 4/4′/6′-H), 7.24 (m, 1H, 3′-H). **^{13}C NMR** (151 MHz, $CDCl_3$): δ 19.63 (Me′), 20.70 (Me), 35.32 (C-8), 50.06 (C-7), 64.10 (C-10), 107.16 (C-9), 117.10 (C-3), 124.78 (C-5), 125.30 (C-4), 126.65 (C-6′), 127.64 (C-4′), 129.92 (C-3′), 130.48 (C-5′), 136.38 (C-1), 136.71 (C-1′), 137.15 (C-6), 139.20 (C-2′), 151.43 (C-2). **IR (ATR film) [cm^{-1}]:** 2954, 1459, 1362, 1340, 1232, 1141, 1115, 1059, 1038, 910, 763, 748. **TLC** (petroleum ether:EtOAc 95:5 v/v): R_f = 0.29 **HR-MS (ESI):** m/z calculated for $[C_{21}H_{26}NO_2]^+$ ([M + H$^+$]): 324.1958, found: 324.1965 **APCI-MS:** m/z: ([M + H$^+$]): found: 324.1

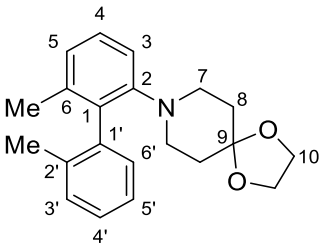

265

7.2.8.3.1 8-(*m*-Tolyl)-1,4-dioxa-8-azaspiro[4.5]decane (268)

Side product **268** was isolated in analytical quantities.

^{1}H NMR (600 MHz, $CDCl_3$): δ 1.85 (dd, $^{3}J_{8\text{-}7}$ = 6.7, 4.4 Hz, 4H, 8-H), 2.32 (d, J = 2.3 Hz, 3H, Me), 3.32 (dd, $^{3}J_{7\text{-}8}$ = 6.9, 4.2 Hz, 4H, 7-H), 4.00 (d, $^{3}J_{10a\text{-}10b}$ = 1.9 Hz, 4H, 10-H), 6.67 (d, $^{3}J_{4\text{-}3/5}$ = 7.5 Hz, 1H, 5/3-H), 6.77 (d, $^{3}J_{4\text{-}3/5}$ = 7.5 Hz, 1H, 3/5-H), 6.79 (s, 1H, 1-H), 7.15 (td, $^{3}J_{4\text{-}3,4\text{-}5}$ = 7.7, J = 2.0 Hz, 1H, 4-H). **IR (ATR film) [cm^{-1}]:** 2955, 2926, 2879, 2829, 1601, 1581, 1494, 1465, 1364, 1340, 1240, 1411, 1101, 1036, 945, 911, 771, 695. **TLC** (petroleum ether:EtOAc 95:5 v/v): R_f = 0.12 **HR-MS (ESI):** m/z calculated for $[C_{14}H_{20}NO_2]^+$ ([M + H$^+$]): 234.1489, found: 234.1491

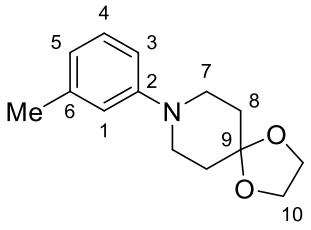

268

7.2.8.4 (±)-8-(4,4'-Dimethoxy-2',6-dimethyl-[1,1'-biphenyl]-2-yl)-1,4-dioxa-8-azaspiro[4.5]decan (263)

A dry microwave vial equipped with stir bar and N_2 balloon was charged with aryl iodide **354** (180 mg, 1.0 equiv, 0.726 mmol), Cs_2CO_3 (709 mg, 3.0 equiv, 2.18 mmol), $(2\text{-furyl})_3P$ (135 mg, 80.0 mol%, 0.581 mmol) and $(Pd\ G4)_2$ (**205**) (56.0 mg, 10 mol%, 72.5 µmol). The vial was evacuated and backfilled with N_2 (3x). Solutions of boronic acid ester **222** (2.00 mL, 264 µL, 1.5 equiv, 1.09 mmol), amine benzoate **262** (2.00 mL, 282 µL, 1.5 equiv, 0.312 mmol) and norbornene (2.00 mL, 34.0 mg, 0.5 equiv, 0.363 mmol) taken from stock solutions each prepared in separate dry microwave vials in anhydrous degassed toluene beforehand (4x amount each) were added to the reaction vessel. Then anhydrous degassed toluene (1.00 mL) was added to the reaction vessel. The balloon was removed, the vial sealed with Parafilm® and the reaction mixture stirred at 500 rpm at 80 °C in a sand bath for 24 h. The resulting mixture was then filtered over a pad of Celite® and solvents removed in vacuo. The product was isolated by column chromatography (petroleum ether:EtOAc 9:1 v/v) as brown solids in a yield of 64.9 mg (0.169 mmol, 23%).

^{1}H NMR (600 MHz, $CDCl_3$): δ 1.40 (m, 2H, 8a-H), 1.46 (m, 2H, 8b-H), 1.96 (s, 3H, Me), 2.00 (s, 3H, Me'), 2.77 (m, 2H, 7a-H), 2.95 (m, 2H, 7b-H), 3.81 (s, 3H, OMe/OMe'), 3.82 (s, 3H, OMe/OMe'), 3.89 (s, 4H, 10-H), 6.50 (d, $^4J_{3\text{-}5}$ = 2.5 Hz, 1H, 3-H), 6.52 (d, $^4J_{3\text{-}5}$ = 2.5 Hz, 1H, 5-H), 6.75 (dd, $^3J_{5'\text{-}6'}$ = 8.4 Hz, $^4J_{5'\text{-}3'}$ = 2.7 Hz, 1H, 5'-H), 6.79 (d, $^4J_{3'\text{-}5'}$ = 2.7 Hz, 1H, 3'-H), 6.98 (d, $^3J_{6'\text{-}5'}$ = 8.4 Hz, 1H, 6'-H). **^{13}C NMR** (151 MHz, $CDCl_3$): δ 20.00 (Me'), 21.10 (Me), 35.33 (C-8), 49.86 (C-7), 55.10 (OMe+OMe'), 64.12 (C-10), 103.60 (C-3), 107.18 (C-9), 108.93 (C-5), 110.84 (C-5'), 115.13 (C-3'), 128.74 (C-1), 131.38 (C-1'), 131.92 (C-6'), 138.26 (C-2'), 138.49 (C-6), 153.00 (C-2), 158.13 (C-4'), 158.88 (C-4). **IR (ATR film) [cm^{-1}]:** 2954, 1598, 1578, 1465, 1440, 1292, 1237, 1165, 1141, 1117, 1076 **TLC** (petroleum ether:EtOAc 9:1 v/v): R_f = 0.23 **HR-MS (ESI):** m/z calculated for $[C_{23}H_{30}NO_4]^+$ ($[M + H^+]$): 384.2175, found: 384.2176 **Melting point:** 127 °C – 128 °C.

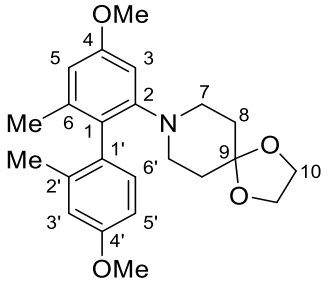

263

7.2.8.4.1 8-(3-Methoxy-5-methylphenyl)-1,4-dioxa-8-azaspiro[4.5]decane (347)

Side product **347** was isolated in analytical quantities.

^{1}H NMR (600 MHz, $CDCl_3$): δ 1.82 (m, 4H, 8-H), 2.28 (s, 3H, Me), 3.31 (m, 4H, 7-H), 3.77 (s, 3H, OMe), 3.98 (s, 4H, 10-H), 6.23 (s, 1H, 5-H), 6.30 (s, 1H, 3-H), 6.39 (s, 1H, 1-H). **^{13}C NMR** (151 MHz, $CDCl_3$): 22.03 (Me), 31.55 (C-8), 47.71 (C-7), 55.13 (OMe), 64.33 (C-10), 100.13 (C-3), 105.36 (C-5), 107.26 (C-9), 110.31 (C-1), 139.76 (C-6), 152.16 (C-2), 160.53 (C-4). **IR (ATR film) [cm^{-1}]:** 2955, 2931, 1590, 1466, 1363, 1198, 1162, 1104, 1072, 1038, 946, 827 **TLC** (petroleum ether:EtOAc 9:1 v/v): R_f = 0.17 **HR-MS (ESI):** m/z calculated for $[C_{14}H_{20}NO_2]^+$ ([M + H$^+$]): 264.1594, found: 264.1598

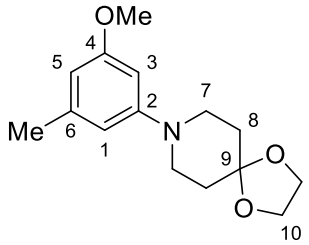

347

7.2.8.4.2 8-(4-Methoxy-2-methylphenyl)-1,4-dioxa-8-azaspiro[4.5]decane (348)

Side product **348** was isolated in analytical quantities.

^{1}H NMR (600 MHz, $CDCl_3$): δ 1.86 (m, 4H, 2'-H), 2.30 (s, 3H, Me), 2.91 (m, 4H, 1'-H), 3.76 (s, 3H, OMe), 4.00 (s, 4H, 4'-H), 6.69 (dd, $^3J_{3\text{-}2}$ = 8.6 Hz, $^4J_{3\text{-}5}$ = 3.0 Hz, 1H, 3-H), 6.75 (d, $^4J_{3\text{-}5}$ = 3.0 Hz, 1H, 5-H), 7.00 (d, $^3J_{2\text{-}3}$ = 8.6 Hz, 1H, 2-H). **^{13}C NMR** (151 MHz, $CDCl_3$): 17.77 (Me), 35.73 (C-2'), 50.71 (C-1'), 55.37 (OMe), 61.28 (C-4'), 107.22 (C-3'), 111.03 (C-3), 116.49 (C-5), 120.32 (C-2), 134.49 (C-6), 145.34 (C-1), 155.52 (C-4). **IR (ATR film) [cm^{-1}]:** 2954, 2926, 1501, 1467, 1209, 1140, 1102, 1047, 916, 804. **TLC** (petroleum ether:EtOAc 9:1 v/v): R_f = 0.27 **HR-MS (ESI):** m/z calculated for $[C_{14}H_{20}NO_2]^+$ ([M + H$^+$]): 264.1594, found: 264.1598

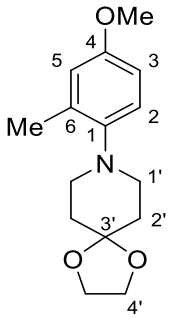

7.2.8.5 (±)-8-(4'-Methoxy-2',6-dimethyl-[1,1'-biphenyl]-2-yl)-1,4-dioxa-8-azaspiro[4.5]decan (264)

A dry microwave vial equipped with stir bar and N_2 balloon was charged with 1-iodo-2-methylbenzene (26.0 µL, 1.0 equiv, 0.208 mmol), Cs_2CO_3 (202 mg, 3.0 equiv, 0.624 mmol), $(2\text{-furyl})_3P$ (38.0 mg, 80.0 mol%, 0.168 mmol) and $(Pd\ G4)_2$ (**205**) (16 mg, 10 mol%, 20.8 µmol). The vial was evacuated and backfilled with N_2 (3x). Solutions of boronic acid ester **222** (0.500 mL, 80.0 µL, 1.5 equiv, 0.312 mmol), amine benzoate **262** (0.500 mL, 80.0 µL, 1.5 equiv, 0.312 mmol) and norbornene (0.500 mL, 9.70 mg, 0.5 equiv, 0.105 mmol) taken from stock solutions each prepared in separate dry microwave vials in anhydrous degassed toluene beforehand (4x amount each) were added to the reaction vessel. Then anhydrous degassed toluene (0.250 mL) was added to the reaction vessel. The balloon was removed, the vial sealed with Parafilm® and the reaction mixture stirred at 500 rpm at 80 °C in a sand bath for 24 h. The resulting mixture was then filtered over a pad of Celite® and solvents removed in vacuo. The product was isolated by column chromatography (petroleum ether:EtOAc 95:5 v/v) as a colorless oil in a yield of 24.6 mg (69.6 µmol, 34%).

^{1}H NMR (600 MHz, $CDCl_3$): δ 1.41 (m, 2H, 8a-H), 1.47 (m, 2H, 8b-H), 1.98 (s, 3H, Me), 2.00 (s, 3H, Me'), 2.77 (m, 2H, 7a-H), 2.96 (m, 2H, 7b-H), 3.83 (s, 3H, OMe'), 3.90 (s, 4H, 10-H), 6.76 (dd, $^3J_{5',6'}$ = 8.3 Hz, $^4J_{5',3'}$ = 2.7 Hz, 1H, 5'-H), 6.80 (d, $^4J_{3',5'}$ = 2.7 Hz, 1H, 3'-H), 6.93 (d, $^3J_{3,4}$ = 8.0 Hz, 1H, 3-H), 6.97 (d, $^3J_{5,4}$ = 7.5 Hz, 1H, 5-H), 6.99 (d, $^3J_{6',5'}$ = 8.3 Hz, 1H, 6'-H), 7.19 (dd, $^3J_{4,3}$ = 8.0 Hz, $^3J_{4,5}$ = 7.5 Hz, 1H, 4-H). **^{13}C NMR** (151 MHz, $CDCl_3$): δ 19.95 (Me'), 20.76 (Me), 35.39 (C-8), 49.99 (C-7), 55.10 (OMe'), 64.12 (C-10), 107.20 (C-9), 110.85 (C-5'), 115.16 (C-3'), 116.96 (C-3), 124.68 (C-5), 127.51 (C-4), 131.37 (C-6'), 131.55 (C-1'), 136.30 (C-1), 137.67 (C-6), 137.77 (C-2'), 151.78 (C-2), 158.21 (C-4'). **IR (ATR film) [cm^{-1}]:** 2953, 1607, 1505, 1459, 1234, 1140, 1114, 1058, 911, 756 **TLC** (petroleum ether:EtOAc 9:1 v/v): R_f = 0.32 **HR-MS (ESI):** m/z calculated for $[C_{22}H_{28}NO_3]^+$ ([M + H$^+$]): 354.2064, found: 354.2072

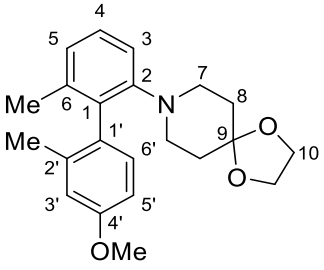

7.2.8.6 (±)-8-(3-(Trifluoromethyl)-2-(3-(2-(trifluoromethyl)phenyl)bicyclo[2.2.1]heptan-2-yl)phenyl)-1,4-dioxa-8-azaspiro[4.5]decane (267)

A dry microwave vial equipped with stir bar and N_2 balloon was charged with 1-iodo-2-(trifluoro)methylbenzene (180 mg, 1.0 equiv, 0.662 mmol), Cs_2CO_3 (647 mg, 3.0 equiv, 1.99 mmol), (2-furyl)$_3$P (123 mg, 80.0 mol%, 0.529 mmol) and (Pd G4)$_2$ (**205**) (50.8 mg, 10 mol%, 66.2 µmol). The vial was evacuated and backfilled with N_2 (3x). Solutions of boronic acid ester **257** (2.00 mL, 270 mg, 1.5 equiv, 0.993 mmol), amine benzoate **262** (2.00 mL, 261 mg, 1.5 equiv, 0.993 mmol) and norbornene (2.00 mL, 31.2 mg, 0.5 equiv, 0.331 mmol) taken from stock solutions each prepared in separate dry microwave vials in anhydrous degassed toluene beforehand (4x amount each) were added to the reaction vessel. Then anhydrous degassed toluene (0.400 mL) was added to the reaction vessel. The balloon was removed, the vial sealed with Parafilm® and the reaction mixture stirred at 500 rpm at 80 °C in a sand bath for 24 h. The resulting mixture was then filtered over a pad of Celite® and solvents removed in vacuo. The product was isolated by column chromatography (petroleum ether:EtOAc 9:1 v/v) as a colorless oil as a single diastereomer in a yield of 24.5 mg (46.6 µmol, 7%).

^{1}H NMR (600 MHz, $CDCl_3$): δ 1.43 (dd, *J* = 10.7, 4.9 Hz, 2H, 6a-H + 7a-H), 1.62 (q, *J* = 11.5, 9.2 Hz, 2H, 5a-H), 1.74 (d, *J* = 9.3 Hz, 3H, 5b-H + 6b-H + 2a'''-H), 1.85 (dd, *J* = 13.0, 2.9 Hz, 1H, 2b'''-H), 2.11 (td, *J* = 12.9, 4.5 Hz, 2H, 2c'''-H + 2d'''-H), 2.15 – 2.19 (m, 1H, 4-H), 2.68 (d, *J* = 10.1 Hz, 1H, 7b-H), 2.79 (td, *J* = 12.7, 2.5 Hz, 1H, 1a'''-H), 2.94 – 3.01 (m, 1H, 1b'''-H), 3.03 – 3.05 (m, 1H, 1-H), 3.05 – 3.10 (m, 1H, 1c''''-H), 3.31 – 3.40 (m, 1H, 1d''''-H), 3.82 (s, 2H, 2-H + 3-H), 3.98 – 4.09 (m, *J* = 4.5 Hz, 4H, 4'''-H), 6.98 (p, *J* = 7.8, 7.3 Hz, 2H, 5'-H + 6'-H), 7.04 (t, *J* = 7.5 Hz, 1H, 4'-H), 7.16 (t, *J* = 7.9 Hz, 1H, 5''-H), 7.31 (d, *J* = 7.8 Hz, 1H, 4''-H), 7.49 (d, *J* = 7.8 Hz, 1H, 3'-H), 7.54 (d, *J* = 8.0 Hz, 1H, 6''-H). **^{13}C NMR** (151 MHz, $CDCl_3$): δ 30.77 (C-5), 32.71 (C-21), 34.78 (C-2a'''), 35.74 (C-2b'''), 38.49 (C-7), 41.65 (C-1), 46.23 (C-4), 51.04 (C-1a'''), 51.38 (C-3), 53.91 (C-2), 56.94 (C-1b'''), 64.51 (C-4'''), 106.98 (C-3'''), 123.62 (q, $^1J_{C\text{-}F}$ ~ 270 Hz, CF_3'), 124.77 (q, *J* = 7.1 Hz, C-4''), 125.11 (C-4'), 125.44 (d, $^1J_{C\text{-}F}$ ~ 270 Hz, CF_3''), 126.23 (q, *J* = 6.3 Hz, C-6'), 127.17 (C-5''), 127.95 (C-6''), 128.49 (d, *J* = 26.8 Hz), 128.91 (q, *J* = 29.1, 28.6 Hz, C-2'), 129.28 (C-5'/C-6'), 129.72 (C-5'/C-6'), 131.65 (q, *J* = 27.7 Hz, C-3''), 138.54 (C-2''), 142.49 (C-1'), 155.16 (C-1''). **^{19}F NMR** (282 MHz, $CDCl_3$): δ -58.52 (q, *J* = 8.1 Hz), -57.71 (q, *J* = 8.1 Hz).

IR (ATR film) [cm^{-1}]: 2958, 2931, 2876, 1457, 1434, 1364, 1307, 1228, 1158, 1114, 1104, 1036, 944, 909, 817, 770, 756, 736, 676, 654, 547. **TLC** (petroleum ether:EtOAc 9:1 v/v): R_f = 0.18 **HR-MS (ESI):** m/z calculated for $[C_{28}H_{30}F_6NO_2]^+$ ([M + H$^+$]): 526.2175, found: 526.2173

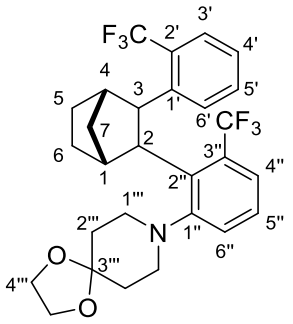

267

7.2.9 Palladium complexes

7.2.9.1 N-Methyl-[1,1'-biphenyl]-2-amine (207)

A dry 250 mL Schlenk round bottom flask equipped with stir bar was charged with 2-amino biphenyl (2.00 g, 1.00 equiv, 11.8 mmol) and anhydrous THF (40 mL, 0.30 M). The mixture was cooled to 0 °C, *n*-BuLi in hexanes(2.3 M, 5.40 mL, 1.05 equiv, 12.4 mmol) was added dropwise and the reaction mixture stirred at 0 °C for 1 h. Iodomethane (740 µL, 1.01 equiv, 11.9 mmol) was added dropwise and the reaction stirred for a further 30 mins at 22 °C. Sat. aq. $NaHCO_3$ solution (25 mL) and H_2O (25 mL)were added and the aq. phase extracted with Et_2O (3x), the combined org. phases dried over $MgSO_4$ and solvents removed in vacuo. The product was obtained as a 95:5 mixture of mono and dimethylated products according to ^{1}H NMR and used in the next step without further isolation in a yield of 2.15 g. The ^{1}H-NMR data was in accordance with literature.[153]

^{1}H NMR (600 MHz, $CDCl_3$): δ 2.76 – 2.83 (m, 3H, NH*Me*), 3.96 (s, 1H, N*H*Me), 6.68 – 6.72 (m, 1H), 6.78 (td, *J* = 7.4, 1.1 Hz, 1H), 7.09 (dd, *J* = 7.4, 1.7 Hz, 1H), 7.28 (dd, *J* = 7.8, 1.7 Hz, 1H), 7.35 (tt, *J* = 6.6, 1.8 Hz, 1H), 7.40 – 7.48 (m, 4H).

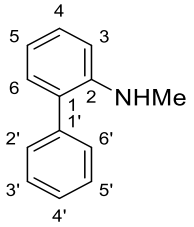

207

7.2.9.2 Bis-((2'-(methylamino)-[1,1'-biphenyl]-2-yl)((methylsulfonyl)oxy)palladium(II)) (Pd G4)$_2$ (205)

A 100 mL round bottom flask equipped with stir bar was charged with 2-aminobiaryl **207** (2.15 g, 1.0 equiv, 11.7 mmol) and THF (30 mL). Methanesulfonic acid (720 µL, 0.95 equiv, 11.1 mmol) was added dropwise and the reaction mixture stirred at 22 °C for 15 mins. $Pd(OAc)_2$ (2.48 g, 0.95 equiv, 11.1 mmol) was added in one portion, the walls of the vessel rinsed off using THF (15 mL). The flask was capped with a rubber septum and the mixture stirred at 50 °C for 1 h. Solvents were removed in vacuo, Et_2O (40 mL) was added and the mixture sonicated for 1 h. The precipitating tan solids were filtered off washing with additional Et2O and dried in vacuo. The product was obtained without any additional isolation step as tan solids in a yield of 4.23 g (5.52 mmol, 94%). The analytical data were in accordance with literature.[153]

^{1}H NMR (600 MHz, $CDCl_3$): δ 2.61 (s, 6H), 2.80 (s, 7H), 6.98 (t, *J* = 7.5 Hz, 2H), 7.08 (t, *J* = 7.3 Hz, 2H), 7.11 – 7.18 (m, 3H), 7.22 (t, *J* = 7.5 Hz, 3H), 7.34 (d, *J* = 7.6 Hz, 2H), 7.53 (d, *J* = 7.7 Hz, 2H). **^{13}C NMR** (151 MHz, $CDCl_3$): δ 39.50, 44.57, 120.69, 124.83, 125.91, 126.59, 127.44, 128.00, 128.82, 134.36 (d, *J* = 74.1 Hz), 139.03 (d, *J* = 53.6 Hz), 140.84. **ESI-MS:** m/z: ([M - $MeSO_3^-$ + 2 MeCN]): found: 370.1 (100), 372.1 (84), 369.1 (78) (MeCN:H_2O 8:2 v/v + 0.1% HCO_2H)

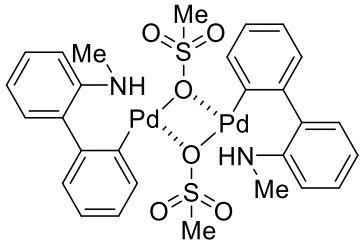

205

7.2.9.3 *trans*-Bis(triphenylphosphine)-([1,1'-biphenyl]-2-yl)palladium(II) iodide (286)

A microwave vial equipped with stir bar was charged with $Pd(PPh_3)_4$ (202 mg, 1.0 equiv, 0.178 mmol) and 2'-iodo biphenyl (**92**) (50.0 mg, 1.0 equiv, 0.178 mmol) and dissolved in anhydr. degassed toluene (1.75 mL, 0.1 M). The vessel was sealed and stirred at 22 °C for 14 h. The solvent was removed in vacuo and a mixture *n*-pentane:Et_2O (5:1) was added. The mixture was sonicated for 5 min and the resulting precipitate filtered off and washed with the *n*-

pentane:Et_2O mixture. The product was obtained as tan solids with irremovable CH_2Cl_2 impurity in a yield of 131 mg.

^{1}H NMR (300 MHz, $CDCl_3$): δ 6.31 (t, *J* = 7.2 Hz, 1H), 6.58 (dt, *J* = 14.6, 7.5 Hz, 2H), 6.96 – 7.06 (m, 1H), 7.13 – 7.35 (m, 41H), 7.35 – 7.43 (m, 3H). **^{31}P NMR** (122 MHz, $CDCl_3$) δ 20.84 (s). **ESI-MS:** m/z: ([M - I^-]): found: 783.1, 784.1, 785.1 (low temperature, low fragmentation, MeCN:H_2O 8:2 v/v + 0.1% HCO_2H)

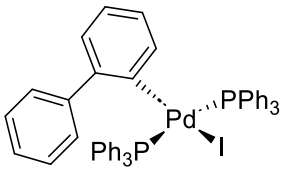

286

7.2.9.4 *trans*-Bis(triphenylphosphine)-(4'-methoxy-6-methyl-[1,1'-biphenyl]-2-yl)palladium(II) iodide (284)

A 2-dr. vial equipped with stir bar was charged with Cs_2CO_3 (12.2 mg, 1.5 equiv, 37.5 μmol) and flame dried. $Pd(PPh_3)_4$ (28.9 mg, 1.0 equiv, 25.0 μmol) and 2'-iodo biaryl **236** (8.10 mg, 1.0 equiv, 25.0 μmol) and dissolved in anhydr. degassed toluene (0.2 mL, 0.125 M). The vessel was sealed and stirred at 80 °C for 9 h. The solvent was removed in vacuo and a mixture pentanes:Et_2O (5:1) was added. The mixture was sonicated for 5 min and the resulting precipitate filtered off and washed with the pentanes:Et_2O mixture. The solids were then dissolved in CH_2Cl_2, flushed into a round bottom flask and solvents removed in vacuo. The title complex was obtained with a major impurity of CH_2Cl_2, washing with pentanes did not result in a dry product (26.1 mg).

^{1}H NMR (400 MHz, $CDCl_3$): δ 1.71 (s, 3H, Me), 3.93 (s, 3H, Me), 6.25 (t, *J* = 7.5 Hz, 1H), 6.49 (d, *J* = 7.4 Hz, 1H), 6.58 (d, *J* = 8.6 Hz, 2H), 6.74 (d, *J* = 8.6 Hz, 2H), 6.80 (d, *J* = 7.7 Hz, 1H), 7.21 (t, *J* = 7.5 Hz, 15H), 7.33 (t, *J* = 7.2 Hz, 8H). **^{31}P NMR** (162 MHz, $CDCl_3$) δ 20.20 (s).

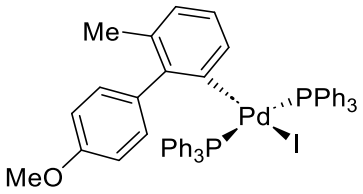

284

7.2.9.5 *trans*-Bis(triphenylphosphine)-(2'-6-dimethyl-[1,1'-biphenyl]-2-yl)palladium(II) iodide (287)

A microwave vial equipped with stir bar was charged with $Pd(PPh_3)_4$ (183 mg, 1.0 equiv, 0.162 mmol) and 2'-iodo biaryl **236** (50.0 mg, 1.0 equiv, 0.162 mmol) and dissolved in anhydr. degassed toluene (1.75 mL, 0.09 M). The vessel was sealed and stirred at 80 °C for 4 h. The solvent was removed in vacuo and a mixture *n*-pentane:Et_2O (5:1) was added. The mixture was sonicated for 5 min and the resulting precipitate filtered off and washed with the *n*-pentane:Et_2O mixture. The product was isolated as tan solids in a yield of 94.9 mg (0.101 mmol, 63%).

^{1}H NMR (300 MHz, $CDCl_3$) δ 1.07 (s, 3H, Me), 1.75 (s, 3H, Me), 6.21 (t, J = 7.5 Hz, 1H), 6.46 (d, J = 7.3 Hz, 1H), 6.83 (d, J = 7.6 Hz, 1H), 7.09 (dt, J = 23.5, 8.1 Hz, 13H), 7.30 (dq, J = 19.6, 6.3 Hz, 18H), 7.54 (t, J = 8.2 Hz, 6H), 7.69 (d, J = 7.1 Hz, 1H), 7.89 (d, J = 7.4 Hz, 1H). **^{13}C NMR** (76 MHz, $CDCl_3$): δ 18.18 (Me), 20.42 (Me), 124.61, 125.14, 126.34, 126.79, 127.72 (dd, J = 8.6, 1.7 Hz), 127.96 (dd, J = 8.2, 1.6 Hz), 129.79 (dd, J = 12.7, 2.0 Hz), 130.64, 132.48 (d, J = 8.5 Hz), 132.96 (dd, J = 8.7, 3.7 Hz), 133.48 (d, J = 8.9 Hz), 134.84 – 135.61 (m), 136.38, 137.08, 142.80, 142.97, 155.79. **^{31}P NMR** (122 MHz, $CDCl_3$) δ 15.96 (d, $^2J_{P\text{-}P}$ = 414.1 Hz), 20.65 (d, $^2J_{P\text{-}P}$ = 416.1 Hz). **ESI-MS:** m/z: ([M - I^- -2 PPh_3 + MeCN]): found: 590.2 (100), 592.2 (85), 589.2 (80) and ([M - I^- -2 PPh_3]): found: 549.2 (100), 551.2 (85), 548.2 (80) (MeCN:H_2O 8:2 v/v + 0.1% HCO_2H)

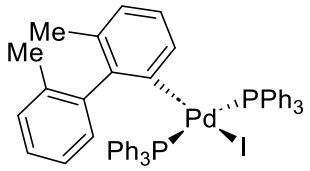

287

7.2.10 Silylation

7.2.10.1 2,2'-Bis(trimethylsilyl)-1,1'-biphenyl (93)

A microwave vial equipped with stir bar was charged with $Pd(OAc)_2$ (1.60 mg, 5 mol%, 7.14 µmol), 2-iodo biphenyl (**92**) (25.0 µL, 1.00 equiv, 143 µmol), K_2CO_3 (50.0 mg, 2.50 equiv, 360 µmol), PivOH (7.29 mg, 0.50 equiv, 70.0 µmol) $(TMS)_2$ (30.9 µL, 1.05 equiv, 151 µmol) and anhydr. degassed DMF (0.6 mL, 0.24 M). The mixture was frozen in liquid N_2, evacuated, and backfilled with N_2 (10x). The reaction mixture was stirred at 120 °C for 1 h. After cooling to 22 °C the reaction was filtered over a pad of Celite® EtOAc (4 mL) added and organic phase washed with H_2O (3x). The combined organic phases were dried over $MgSO_4$, and solvents removed in vacuo. The product was obtained in analytical quantities. The analytical data were

in accordance with literature.[338] MS-data could not be obtained by EI, ESI or APCI ionization methods.

^{1}H NMR (600 MHz, $CDCl_3$): δ -0.07 (s, 18H, $SiMe_3$), 7.13 – 7.18 (m, 2H, Ar-H), 7.30 – 7.36 (m, 4H, Ar-H), 7.56 – 7.61 (m, 2H, Ar-H). **^{13}C NMR** (151 MHz, $CDCl_3$): δ 0.49 ($SiMe_3$), 126.55, 127.86, 130.05, 134.46, 139.01 (C-2), 150.07 (C-1). **IR (ATR film) [cm^{-1}]:** 3051, 2953, 1421, 1247, 1122, 835, 772, 756, 728, 690, 621.

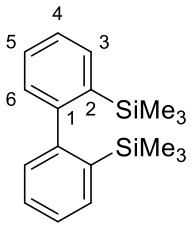

93

7.2.10.2 (6-Methyl-[1,1'-biphenyl]-2,2'-diyl)bis(trimethylsilane) (274)

A microwave vial equipped with stir bar was charged with $Pd(OAc)_2$ (1.60 mg, 5 mol%, 7.14 µmol), 2-iodo biphenyl (**92**) (25.0 µL, 1.00 equiv, 143 µmol), K_2CO_3 (50.0 mg, 2.50 equiv, 360 µmol), L-Leucine (1.70 mg, 0.10 equiv, 7.00 µmol) $(TMS)_2$ (30.9 µL, 1.05 equiv, 151 µmol) and anhydr. degassed DMF (0.6 mL, 0.24 M). The mixture was frozen in liquid N_2, evacuated, and backfilled with N_2 (10x). The reaction mixture was stirred at 120 °C for 1 h. After cooling to 22 °C the reaction was filtered over a pad of Celite® EtOAc (4 mL) added and organic phase washed with H_2O (3x). The combined organic phases were dried over $MgSO_4$, and solvents removed in vacuo. The product was isolated by column chromatography (100% *n*-pentane) as a colorless oil in a yield of 16.3 mg (52.1 µmol, 37%). The analytical data were in accordance with literature.[179] MS-data could not be obtained by EI, ESI or APCI ionisation methods.

^{1}H NMR (600 MHz, $CDCl_3$): δ -0.11 (s, 9H, $SiMe_3'$), -0.10 (s, 9H, $SiMe_3$), 1.95 (s, 3H, Me), 7.07 (dd, $^3J_{6'\text{-}5'}$ = 6.6 Hz, $^4J_{6'\text{-}4'}$ = 1.8 Hz, 1H, 6′-H), 7.21 (d, $^3J_{5\text{-}4}$ = 7.5 Hz, 1H, 5-H), 7.26 (t, $^3J_{4\text{-}3,4\text{-}5}$ = 7.5 Hz, 1H, 4-H), 7.33 (dd, $^3J_{4'\text{-}3'}$ = 7.2 Hz, $^3J_{4'\text{-}5'}$ = 5.6 Hz, 1H, 4′-H), 7.36 (dd, $^3J_{5'\text{-}6'}$ = 7.1, $^3J_{5'\text{-}4'}$ = 5.6 Hz, 1H, 5′-H), 7.43 (d, $^3J_{3\text{-}4}$ = 7.3 Hz, 1H, 3-H), 7.59 (dd, $^3J_{4'\text{-}3'}$ = 7.3 Hz, $^4J_{3'\text{-}5'}$ = 1.7 Hz, 1H, 3′-H). **^{13}C NMR** (151 MHz, $CDCl_3$): δ 0.32 ($SiMe_3'$), 0.63 ($SiMe_3$), 21.22 (Me), 126.41 (C-4′), 126.84 (C-4), 128.41 (C-5′), 129.81 (C-6′), 130.37 (C-5), 131.83 (C-3), 134.85 (C-3′), 135.89 (C-6), 139.29 (C-2), 139.44 (C-2′), 148.44 (C-1′), 149.17 (C-1). **IR (ATR film) [cm^{-1}]:** 3050, 2954, 2895, 1405, 1248, 1121, 836, 759, 731, 690. **TLC** (100% petroleum ether):

R_f = 0.52. **HPLC**: CHIRALCEL® OD-H 250 ° 4.6 mm, 10 °C, 0.5 mL min^{-1}, 254 nm, *n*-heptane:*i*-PrOH 95:5 (v/v) $t_R(1)$ = 21 min, $t_R(2)$ = 23 min

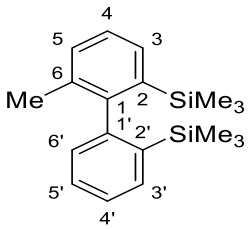

274

7.2.10.3 (4-Methoxy-6'-methyl-[1,1'-biphenyl]-2,2'-diyl)bis(trimethylsilane) (292)

A microwave vial equipped with stir bar was charged with $Pd(OAc)_2$ (1.12 mg, 5 mol%, 5.00 µmol), 2-iodo biphenyl (**92**) (32.4 mg, 1.00 equiv, 100 µmol), K_2CO_3 (27.6 mg, 2.50 equiv, 200 µmol), *(R)*-BIDIME (3.30 mg, 10 mol%, 10.0 µmol) and a solution of $(TMS)_2$ in anhydr. degassed DMF (500 µL, 0.21 M, 1.05 equiv, 105 µmol). The vial was sealed with Parafilm® reaction mixture was stirred at 120 °C (900 rpm) for 16 h. After cooling to 22 °C the reaction was filtered over a pad of silica with EtOAc, the organic phase washed with H_2O (1x) and sat. aq. NaCl solution (3x), dried over $MgSO_4$ and solvents removed in vacuo. The product was isolated by column chromatography (*n*-pentane:EtOAc 95:5 v/v) as a colorless oil in a yield of 23.2 mg (67.7 µmol, 68%).

^{1}H NMR (600 MHz, $CDCl_3$): δ -0.10 (s, 9H, $SiMe_3$), -0.09 (s, 9H, $SiMe_3$), 1.95 (s, 3H, Me), 3.87 (s, 3H, OMe), 6.89 (dd, $^3J_{5\text{-}6}$ = 8.3 Hz, $^4J_{5\text{-}3}$ = 2.8 Hz, 1H, 5-H), 6.99 (d, $^3J_{6\text{-}5}$ = 8.3 Hz, 1H, 6-H), 7.13 (d, $^4J_{3\text{-}5}$ = 2.8 Hz, 1H, 3-H), 7.20 (ddd, $^3J_{5'\text{-}4'}$ = 7.5 Hz, $^4J_{5'\text{-}3'}$ = 1.5 Hz, *J* = 0.8 Hz, 1H, 5′-H), 7.24 (t, $^3J_{4'\text{-}3',4'\text{-}5'}$ = 7.4 Hz, 1H, 4′-H), 7.37 – 7.45 (m, 1H, 3′-H). **^{13}C NMR** (151 MHz, $CDCl_3$): δ 0.25 ($SiMe_3$), 0.73 ($SiMe_3$), 21.25 (Me), 55.27 (OMe), 112.86 (C-5), 120.75 (C-3), 126.78 (C-4′), 130.34 (C-5′), 130.92 (C-6), 131.82 (C-3′), 136.49 (C-6′), 139.83 (C-2′), 140.88 (C-1), 141.06 (C-2), 148.90 (C-1′), 157.92 (C-4). **IR (ATR film) [cm^{-1}]:** 2953, 1603, 1459, 1254, 1140, 1049, 875, 822, 761, 693. **TLC** (petroleum ether:EtOAc 95:5 v/v): R_f = 0.6 **APCI-MS:** m/z: ([M + H^+]): found: 343.2.

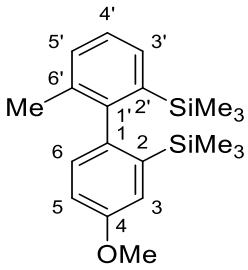

292

7.2.11 Chiral Acetylene

Parts of the following chapter will be published in a peer-reviewed journal, a manuscript is currently in preparation.[278]

7.2.12 Substrate Synthesis

7.2.12.1.1 1-(2-Iodophenyl)ethan-1-one (295)

A 250 mL round-bottom flask equipped with stir bar was charged with 2′-aminoacetophenone (1.35 g, 1.0 equiv, 10.0 mmol), $TsOH \cdot H_2O$ (5.71 g, 3.0 equiv, 30.0 mmol) and MeCN (20 mL, 0.5 M) and cooled to 0 °C. A solution of $NaNO_2$ (1.38 g, 2.0 equiv, 20.0 mmol) in H_2O (3 mL, 6.67 M) was added dropwise followed by the dropwise addition of a solution of KI (4.15 g, 2.5 equiv, 50.0 mmol) in H_2O (9 mL, 5.56 M). The reaction mixture was stirred at 0 °C for 10 min, then left to warm up to rt for an additional 30 min. Water (30 mL) was added and sat. aq. $NaHCO_3$ solution was added until pH ~9-10. Sat. aq. $Na_2S_2O_3$ solution (10 mL) was added and the mixture extracted with EtOAc (3x 60 mL). The combined organic phases were dried over $MgSO_4$ and solvent was removed in vacuo. The title compound was isolated *via* column chromatography (9:1 petroleum ether:EtOAc) as an amber oil in a yield of 2.00 g (8.13 mmol, 81%). The analytical data were in accordance with literature.[339]

^{1}H NMR (600 MHz, $CDCl_3$): δ 2.61 (s, 3H, Me), 7.12 (ddd, $^3J_{4\text{-}3}$ = 7.9 Hz, $^3J_{4\text{-}5}$ = 7.3 Hz, $^4J_{4\text{-}6}$ = 1.7 Hz, 1H, 4-H), 7.41 (td, $^3J_{5\text{-}4,5\text{-}6}$ = 7.5 Hz, $^4J_{5\text{-}3}$ = 1.1 Hz, 1H, 5-H), 7.46 (dd, $^3J_{6\text{-}5}$ = 7.7 Hz, $^4J_{6\text{-}4}$ = 1.7 Hz, 1H, 6-H), 7.93 (dd, $^3J_{3\text{-}4}$ = 8.0 Hz, $^4J_{3\text{-}5}$ = 1.1 Hz, 1H, 3-H). **^{13}C NMR** (151 MHz, $CDCl_3$): δ 29.63 (Me), 91.08 (C-2), 128.20 (C-5), 128.45 (C-6), 131.94 (C-4), 141.01 (C-3), 144.17 (C-1), 201.92 (*C*OMe). **IR (ATR film) [cm^{-1}]:** 3378, 3067, 2999, 1686, 1673, 1421, 1353, 1239, 1087, 1019, 753, 594. **TLC** (*n*-pentane:EtOAc, 95:5 v/v): R_f = 0.24 **APCI-MS:** m/z: ([M + H$^+$]): found: 246.9.

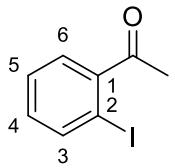

295

7.2.12.1.2 1-Iodo-2-(prop-1-en-2-yl)benzene (293)

A 250 mL round-bottom flask equipped with stir bar was charged with 2′-aminoacetophenone (2.70 g, 1.0 equiv, 20 mmol), $TsOH \cdot H_2O$ (11.41 g, 3.0 equiv, 60 mmol) and MeCN (80 mL. 0.25 M) and cooled to 0 °C. A solution of $NaNO_2$ (2.76 g, 2.0 equiv, 40 mmol) in H_2O (6 mL, 6.67 M) was added dropwise followed by the dropwise addition of a solution of KI (8.30 g, 2.5 equiv, 50 mmol) in H_2O (9 mL, 5.56 M). The reaction mixture was stirred at 0 °C for 10 min,

then left to warm up to rt for an additional 30 min. Water (30 mL) was added and sat. aq. $NaHCO_3$ solution was added until pH ~9-10. Sat. aq. $Na_2S_2O_3$ solution (10 mL) was added, and the mixture extracted with EtOAc (3x 60 mL). The combined organic phases were dried over $MgSO_4$ and solvent was removed in vacuo. The crude product was filtered through a silica plug and used without further isolation in the next step. (**A**)

A dry 250 mL round-bottom flask equipped with stir bar was charged with $MePPh_3I$ (12.12 g, 1.5 equiv, 30 mmol) was dissolved in anhydr. THF (100 mL) and cooled to 0 °C. KO*t*-Bu (3.37 g, 1.5 equiv, 30 mmol) was slowly added (reaction turns bright yellow). The reaction was left to warm to 22 °C and then stirred for 30 min. The reaction mixture was again cooled to 0 °C and a solution of crude 2′-iodoacetophenone **295** (**A**) (4.921 g, 1.0 equiv, 20 mmol) in THF (20 mL) was added dropwise. The reaction was left to stir at 22 °C for 12 h. The reaction mixture was diluted with pentanes (100 mL) and filtered through a silica pad washing with a 80:20/pentanes:EtOAc solvent mixture (300 mL). The solvent was removed and the product isolated *via* column chromatography (100% pentanes). The product was obtained as a colorless oil in a yield of 3.80 g (15.6 mmol, 78%) over two steps.

In a repeat experiment the title compound was synthesized starting from isolated **295.**

A dry 250 mL round-bottom flask equipped with stir bar was charged with $MePPh_3Br$ (2.92 g, 1.5 equiv, 8.17 mmol) and THF (100 mL) and cooled to 0 °C. A solution of KO*t*Bu in THF (8.18 mL, 1 M, 1.5 equiv, 8.17 mmol) was slowly added (reaction turns bright yellow). The reaction was stirred at 0 °C for 30 min. A solution of 2'-Iodoacetophenone (1.34 g, 1.0 equiv, 5.45 mmol) in THF (22 mL, 0.25 M) was added dropwise. The reaction was left to stir at 22 °C for 12 h. The reaction mixture was diluted with pentanes (50 mL) and filtered through a silica pad washing with a 80:20/pentanes:EtOAc solvent mixture (250 mL). The solvent was removed and the product isolated *via* column chromatography (100% pentanes). The product was obtained as a colorless oil in a yield of 1.14 g (7.03 mmol, 86%). The analytical data were in accordance with literature.[340]

^{1}H NMR (600 MHz, $CDCl_3$): δ 2.07 (t, $^4J_{Me,CH2}$ = 1.3 Hz, 3H, Me), 4.90 (dd, $^2J_{CH2-CH2}$ = 1.9, $^4J_{Me,CH2}$ = 1.0 Hz, 1H, H_a-C=$\underline{CH_2}$), 5.23 (p, $^4J_{Me,CH2}$ = 1.6 Hz, 1H, H_b-C=$\underline{CH_2}$), 6.94 (td, $^3J_{5\text{-}4,5\text{-}6}$ = 7.6, $^4J_{5\text{-}3}$ = 1.7 Hz, 1H, 5-H), 7.18 (dd, $^3J_{3\text{-}4}$ = 7.6 Hz, $^4J_{3\text{-}5}$ = 1.7 Hz, 1H, 3-H), 7.30 (td, $^3J_{4\text{-}3,4\text{-}5}$ = 7.5 Hz, $^4J_{4\text{-}6}$ = 1.2 Hz, 1H, 4-H), 7.84 (dd, $^3J_{6\text{-}5}$ = 7.9 Hz, $^4J_{6\text{-}4}$ 1.2 Hz, 1H, 6-H). **^{13}C NMR** (151 MHz, $CDCl_3$): δ 24.02 (Me), 97.05 (C-1), 116.17 (C=$\underline{C}H_2$), 128.17 (C-4), 128.51 (C-5), 128.64 (C-3), 139.33 (C-6), 148.54 ($\underline{C}$=CH_2), 148.98 (C-2). **IR (ATR film) [cm$^-$**

[1]: 3075, 2968, 2908, 1640, 1468, 1428, 1374, 1010, 905, 758, 726, 646, 548. **TLC** (*n*-pentane:EtOAc, 95:5 v/v): R_f = 0.70 **APCI-MS:** m/z: ([M – I^-]): found: 117.1.

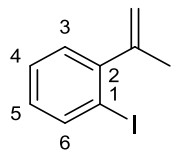

293

7.2.12.1.3 Dimethyl 7-oxabicyclo[2.2.1]hepta-2,5-diene-2,3-dicarboxylate (296)

A 250 mL round-bottom flask equipped with stir bar was charged with dimethyl acetylene dicarboxylate (3.69 mL, 1.0 equiv, 30.0 mmol), furan (3.27 mL, 1.5 equiv, 45.0 mmol) and toluene (45 mL, 0.67 M). A relux condenser was equipped and the reaction left to stir at 80 °C for 16 h. The solvent was removed and the product isolated by column chromatography (pentanes:EtOAc 90:10 to 80:20 v/v) as a pale-yellow oil in a yield of 4.40 g (20.9 mmol, 70%). The analytical data were in accordance with literature.[279a] [341]

^{1}H NMR (600 MHz, $CDCl_3$): δ 3.84 (s, 6H, $CO_2\underline{\textit{Me}}$), 5.70 (t, $^3J_{2\text{-}3}$ = 1.0 Hz, 2H, 2-H), 7.24 (t, $^3J_{3\text{-}2}$ = 1.1 Hz, 2H, 3-H). **^{13}C NMR** (151 MHz, $CDCl_3$): δ 52.51 ($CO_2\underline{\textit{Me}}$), 85.22 (C-2), 143.40 (C-3), 153.16 (C-1), 163.39 ($\underline{C}O_2$Me). **IR (ATR film) [cm^{-1}]:** 3461, 2961, 1724, 1633, 1436, 1269, 1216, 1118, 1034, 882, 708. **TLC** (pentanes:EtOAc, 70:30 v/v): R_f = 0.69. **APCI-MS:** m/z: ([M – CO_2Me^-]): found: 151.

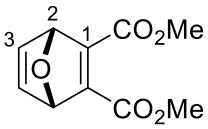

296

7.2.12.1.4 *cis*-3-(Methoxycarbonyl)-7-oxabicyclo[2.2.1]hepta-2,5-diene-2-carboxylic acid (301)

A 100 mL round-bottom flask equipped with stir bar was charged with oxabicycle **296** (424 mg, 1.0 equiv, 2.00 mmol) and THF (13 mL, 0.15 M) and cooled to 0 °C. A solution of aq. NaOH (0.25 M, 8 mL, 1.0 equiv, 2.00 mmol) was added dropwise. The reaction was stirred at 22 °C for 30 min. A solution of aq. HCl (1 M, 1.0 equiv, 2.00 mmol) was added and the reaction mixture extracted with EtOAc (3x 50 mL) and dried over $MgSO_4$. The product was isolated *via* column chromatography (pentanes:EtOAc 90:10 to 80:20 v/v to CH_2Cl_2:EtOAc:AcOH 85:10:5 v/v). The product was isolated as tan solids in a yield of 238 mg (1.21 mmol, 61%).

In a different batch a 100 mL round-bottom flask equipped with stir bar was charged with oxabicycle **296** (1.00 g, 1.0 equiv, 4.72 mmol) and THF (55 mL, 0.15 M) and cooled to 0 °C. A solution of aq. NaOH (0.25 M, 18.9 mL, 1.0 equiv, 4.72 mmol) was added dropwise. After stirring the reaction mixture at 22 °C for 30 min, the reaction mixture was extracted with pentanes (3x), then EtOAc (2x) and the combined organic phases discarded. The aq. phase was then acidified with aq. HCl-solution (1 M, 4.72 mL, 1.0 equiv, 4.72 mmol). The aq. phase was extracted with EtOAc (3x), the combined organic phases were washed with sat. aq. NaCl-solution dried over $MgSO_4$ and the solvent removed in vacuo. The crude product was resuspended in CH_2Cl_2 filtered over a plug of silica washing with a mixture of pentanes:EtOAc (6:4). The product was obtained as tan solids in a yield of 624 mg (3.18 mmol, 67%).

^{1}H NMR (400 MHz, $CDCl_3$): δ 3.99 (s, 3H), 5.79 (t, *J* = 1.8 Hz, 1H), 5.84 (t, *J* = 1.8 Hz, 1H), 7.19 (dd, *J* = 5.3, 1.9 Hz, 1H), 7.28 (dd, *J* = 5.3, 2.0 Hz, 1H). **IR (ATR film) [cm^{-1}]:** 3446 (broad signal), 2984, 2635, 1717, 1611, 1444, 1269, 1231, 877, 847, 760, 698. **TLC** (CH_2Cl_2:EtOAc:AcOH, 85:10:5 v/v): R_f = 0.30 **APCI-MS:** m/z: ([M – MeO^- + H_2O]): 183.1 **Melting point:** 137 °C – 140 °C (*rac*).

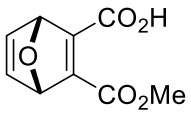

301

7.2.12.1.5 Dimethyl-1,4-dimethyl-7-oxabicyclo[2.2.1]hepta-2,5-diene-2,3-dicarboxylate (299)

A 250 mL round-bottom flask equipped with stir bar was charged with DMAD (0.615 mL, 1.0 equiv, 5.00 mmol), furan (0.810 mL, 1.5 equiv, 7.50 mmol) and 1,4-dioxane (1 mL, 5 M). A relux condenser was equipped and the reaction left to stir at 100 °C for 15 h. The solvent was removed and the product isolated by column chromatography (90:10 to 80:20/pentanes:EtOAc). The title compound was isolated as a pale-yellow oil in a yield of 968 mg (4.06 mmol, 81%). The analytical data were in accordance with literature.[341]

^{1}H NMR (300 MHz, $CDCl_3$): δ 1.79 (s, 6H, Me), 3.80 (s, 6H, CO_2Me), 6.95 (s, 2H, H-3). **TLC** (pentanes:EtOAc, 70:30 v/v): R_f = 0.52

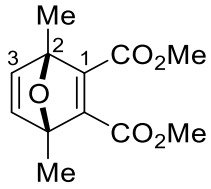

299

7.2.12.1.6 Methyl 4-oxopent-2-ynoate (325)

A flame dried 50 mL round bottom flaks equipped with stir bar was charged with CuI (429 mg, 0.45 equiv, 2.25 mmol), methyl propiolate (445 µL, 1.00 equiv, 5.00 mmol) and CH_2Cl_2 (15 mL, 0.33 M). The deep yellow slurry was stirred at 0 °C. A solution of AcCl (357 µL, 1.00 equiv, 5.00 mmol) in CH_2Cl_2 (3 mL, 1.67 M) was added dropwise and the reaction mixture stirred for 1 h. The mixture was filtered over a pad of silica washing with copious EtOAc. The solvent was removed and isolation by column chromatograph (pentanes:EtOAc 8:2 v/v) was attempted. The product was obtained as a 2:1 mixture with side product **326** in a yield of 278 mg (calculating the theoretical amount of substance gives 1.32 mmol, 26%), sideproduct **326** (0.66 mmol).

^{1}H NMR (300 MHz, $CDCl_3$): 2.42 (d, J = 0.4 Hz, 3H), 3.85 (d, J = 0.4 Hz, 3H). **APCI-MS:** m/z: ([M + H^+]): 126.9 **TLC** (pentanes:EtOAc, 80:20 v/v): R_f = 0.31

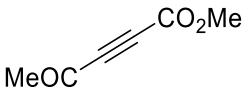

325

Methyl 4-acetoxypent-4-en-2-ynoate (**326**)

The title compound was isolated by column chromatography (pentanes:EtOAc 8:2 v/v) in analytical quantities.

^{1}H NMR (400 MHz, $CDCl_3$) δ 2.15 (s, 3H, CO*Me*), 3.77 (s, 3H, CO_2*Me*), 5.47 (d, $^2J_{CH2\text{-}CH2}$ = 2.0 Hz, 1H, H-4 CH_2-H_a), 5.56 (d, $^2J_{CH2\text{-}CH2}$ = 2.0 Hz, 1H, H-4 CH_2-H_b). **^{13}C NMR** (126 MHz, $CDCl_3$) δ 20.65 (COMe), 53.03 (CO_2Me), 79.26 (C-1/2), 80.13 (C-1/2), 117.50 (C-4), 134.29 (C-3), 153.47 (*C*OMe), 167.95 (*C*O_2Me). **APCI-MS:** m/z: ([M + H^+]): 168.8 **TLC** (pentanes:EtOAc, 80:20 v/v): R_f = 0.31

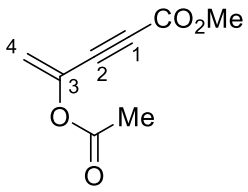

326

7.2.12.1.7 *rac*-Methyl (1S,4R)-3-acetyl-7-oxabicyclo[2.2.1]hepta-2,5-diene-2-carboxylate (321)

A flame dried 50 mL round bottom flaks equipped with stir bar was charged with CuI (428.5 mg, 0.45 equiv, 2.25 mmol). CH_2Cl_2 (15 mL) then methyl propiolate (445 µL, 1.00 equiv, 5.00 mmol) were added. The deep yellow slurry was stirred at 0 °C. A solution of AcCl (357 µL, 1.00 equiv, 5.00 mmol) in CH_2Cl_2 (3 mL) was added dropwise and the reaction mixture stirred for 1 h. The mixture was filtered over a pad of silica washing with copious EtOAc. The solvent was removed and the crude product (**325**) used in the next step without further isolation.

A 50 mL round bottom flask equipped with stir bar was charged with alkyne **325**, furan (546 µL, 1.5 equiv, 5.00 mmol) and dissolved in toluene (7.5 mL, 0.67 M). A reflux condenser was equipped, and the mixture stirred at 80 °C for 16 h. The solvent was removed *in vacuo* and the crude product isolated by flash chromatography (95:5 to 85:15/pentanes:EtOAc). The title compound was isolated as a colorless oil in a yield of 122 mg (0.628 mmol, 13%) over two steps.

^{1}H NMR (500 MHz, $CDCl_3$): δ 2.55 (s, 3H, CO*Me*), 3.83 (s, 3H, CO_2*Me*), 5.59 – 5.63 (m, 1H, 1-H/4-H), 5.73 (t, $^3J_{4\text{-}5/1\text{-}6}$ = 1.8 Hz, 1H, 1-H/4-H), 7.15 (dd, $^3J_{5\text{-}6}$ = 5.3 Hz, $^3J_{4\text{-}5/1\text{-}6}$ = 1.9 Hz, 1H, 5-H/6-H), 7.20 (dd, $^3J_{5\text{-}6}$ = 5.3 Hz, $^3J_{4\text{-}5/1\text{-}6}$ = 2.0 Hz, 1H, 5-H/6-H). **^{13}C NMR** (151 MHz, $CDCl_3$): δ 30.56 (CO*Me*), 52.49 (CO_2*Me*), 85.50 (C-1/C-4), 85.65 (C-1/C-4), 142.66 (C-5/C-6), 143.26 (C-5/C-6), 149.85, 161.04, 163.18 (*C*O_2Me), 196.99 (*C*OMe). **APCI-MS:** m/z: ([M + H^+]): 195.0 **TLC** (pentanes:EtOAc, 80:20 v/v): R_f = 0.20

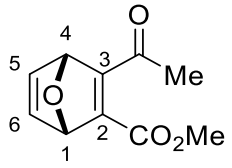

321

7.2.12.1.8 Methyl (1S,4R)-3-bromo-7-oxabicyclo[2.2.1]hepta-2,5-diene-2-carboxylate (329)

A 100 mL round bottom flask was charged with methyl propiolate (**320**) (0.841 g, 1.00 equiv, 10.0 mmol), acetone (30 mL, 0.33 M), N-bromosuccinimide (2.05 g, 1.15 equiv, 11.5 mmol) and silver nitrate (0.170 g, 0.1 equiv, 1.00 mmol) in this order. The solution was stirred at 22 °C for 16 h. The solvent was removed in vacuo, the grey solids resuspended in *n*-pentane, filtered over a pad of Celite®, and the solvent carefully removed in vacuo (product is volatile). The obtained product (**328**) was used in the next step without further isolation.

A 50 mL round bottom flask was charged with 3-bromopropiolate (**328**) (1.63 g, 1.0 equiv, 10.0 mmol), furan (3.40 g, 5.0 equiv, 50.0 mmol) and toluene (20 mL, 0.5 M) and stirred at 80 °C for 16 h. Solvents were removed *in vacuo* and the crude product isolated *via* column chromatography (*n*-pentane:EtOAc 80:20 v/v). The product was obtained as a mixture (**328**:**329** 1:1 according to ^{1}H-NMR) as a yellow oil in a yield of 499 mg over two steps.

^{1}H NMR (600 MHz, $CDCl_3$): δ 3.79 (s, 3H, $CO_2\underline{Me}$), 5.32 (t, *J* = 1.7 Hz, 1H), 5.70 (t, *J* = 1.7 Hz, 1H), 7.19 (dd, *J* = 5.3, 1.9 Hz, 1H), 7.23 (dd, *J* = 5.3, 1.8 Hz, 1H). **TLC** (*n*-penH:EtOAc, 7:3 v/v): R_f = 0.5

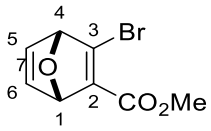

329

Intermediate product **328** could only be identified by ^{1}H-NMR due to being unstable.

^{1}H NMR (600 MHz, $CDCl_3$): δ 3.79 (s, 3H). **TLC** (penH:EtOAc, 9:1 v/v): R_f = 0.4

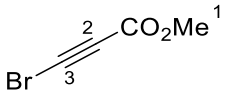

328

7.2.12.2 General procedure 9 (GP9): Synthesis of oxabicycle-amides

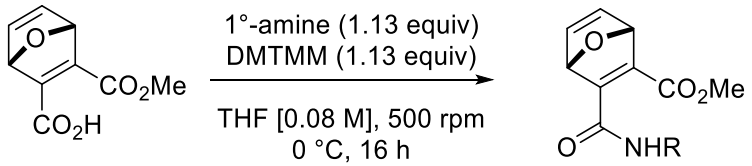

An appropriately sized reaction vessel equipped with stir bar was charged with oxabicycle **301** (1.00 equiv) and THF (0.08 M). The solution was cooled to 0 °C, 1° amine (1.13 equiv) added, and the mixture stirred for 5 min. DMTMM (1.13 equiv) was added at once. The mixture was left to stir for 16 h at 0 °C at 500 rpm. The crude reaction mixture was filtered through a plug of silica. The product was isolated by column chromatography (pentanes:EtOAc 90:10 to 80:20 v/v).

7.2.12.2.1 Methyl (1R,4S)-3-(((S)-1-phenylethyl)carbamoyl)-7-oxabicyclo[2.2.1]hepta-2,5-diene-2-carboxylate (302)

The title compound was synthesized according to **GP9**. Starting from oxabicycle **301** (98.1 mg, 1.00 equiv, 0.500 mmol, 98%*ee*) and (*S*)-(−)-*α*-Methylbenzylamine (73.0 µL, 1.13 equiv, 0.565 mmol, 98%*ee*). The product was obtained as a mixture of isomers (d.r. >20:1 **302**:**303** according to ^{1}H-NMR) with a minor unidentified impurity as a pale-yellow oil in a yield of 72.7 mg (0.243 mmol, 49%). In a repeat experiment, the product was isolated as white solids in a yield of 49.9 mg (0.167 mmol, 33%). In a repeat experiment, the product was obtained as beige solids in a yield of 67.0 mg (0.224 mmol, 45%). The analytical data were in accordance with literature.[259a]

^{1}H NMR (400 MHz, $CDCl_3$) δ 1.55 (d, $^{3}J_{CH\text{-}CH3}$ = 6.9 Hz, 3H, Me), 3.84 (s, 3H, CO_2Me), 5.13 (p, $^{3}J_{CH\text{-}CH3}$ = 7.0 Hz, 1H, *CH*R_3), 5.73 (t, $^{3}J_{4\text{-}5/1\text{-}6}$ = 1.8 Hz, 1H, 1/4-H), 5.86 (t, $^{3}J_{4\text{-}5/1\text{-}6}$ = 1.9 Hz, 1H, 1/4-H), 7.13 (dd, $^{3}J_{5\text{-}6}$ = 5.3 Hz, $^{3}J_{4\text{-}5/1\text{-}6}$ = 1.9 Hz, 1H, 5/6-H), 7.20 (dd, $^{3}J_{5\text{-}6}$ = 5.2 Hz, $^{3}J_{4\text{-}5/1\text{-}6}$ = 2.0 Hz, 1H, 5/6-H), 7.29 – 7.35 (m, 5H, ArH), 9.28 (s, 1H, NHR_2). **HR-MS (DART):** m/z calculated for $[C_{17}H_{18}NO_4]^+$ ([M + H^+]): 300.1230, found: 300.1221. **TLC** (pentanes:EtOAc, 7:3 v/v): R_f = 0.59

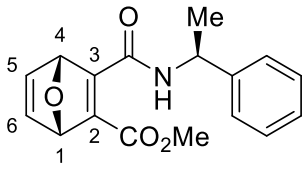

(*S*)-**302**

7.2.12.2.2 Methyl (1R,4S)-3-(((R)-1-phenylethyl)carbamoyl)-7-oxabicyclo[2.2.1]hepta-2,5-diene-2-carboxylate (303)

The title compound was synthesized according to **GP9**. Starting from oxabicycle **301** (98.1 mg, 1.00 equiv, 0.500 mmol, 98% ee) and (*R*)-(−)-*α*-Methylbenzylamine (73.0 µL, 1.13 equiv, 0.565 mmol, 98% ee). The product was obtained as a mixture of isomers (d.r. 11:1 **303**:**302**

according to NMR) with a minor unidentified impurity presumed to be some type of tautomer as a pale-yellow oil in a yield of 63.6 mg (0.212 mmol, 43%). In a repeat experiment the product (d.r. >20:1 **303**:**302** according to ^{1}H-NMR) was obtained with a major unidentified impurity presumed to be the same tautomer as a pale-yellow oil in a yield of 80.7 mg (0.270 mmol, 54%).

^{1}H NMR (400 MHz, $CDCl_3$) δ 1.51 (d, $^{3}J_{CH\text{-}CH3}$ = 6.9 Hz, 3H, Me), 3.88 (s, 3H, CO_2Me), 5.12 (p, $^{3}J_{CH\text{-}CH3}$ = 7.0 Hz, 1H, <u>*CH*</u>R_3), 5.74 (t, $^{3}J_{4\text{-}5/1\text{-}6}$ = 1.8 Hz, 1H, 1/4-H), 5.82 (t, $^{3}J_{4\text{-}5/1\text{-}6}$ = 1.8 Hz, 1H, 1/4-H), 7.17 (dd, $^{3}J_{5\text{-}6}$ = 5.3 Hz, $^{3}J_{4\text{-}5/1\text{-}6}$ = 1.9 Hz, 1H, 5/6-H), 7.23 – 7.30 (m, 1H, 5/6-H), 7.34 – 7.39 (m, 5H, ArH), 9.27 (d, $^{3}J_{NH\text{-}CH}$ = 7.5 Hz, 1H, NHR_2). **TLC** (pentanes:EtOAc, 7:3 v/v): R_f = 0.58

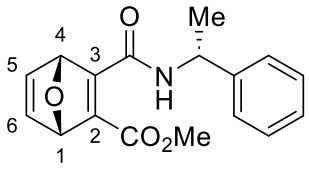

(*R*)-**303**

7.2.12.2.3 Mixtures of 302 and 303

In another reaction according to **GP**9. Starting from oxabicycle **301** (45.0 mg, 1.00 equiv, 0.229 mmol, unknown *ee*) and (*S*)-(−)-*α*-methylbenzylamine (33.5 µL, 1.13 equiv, 0.259 mmol, 98% ee). The product was obtained as a mixture of diastereomers (d.r. 1.2:1 **303**:**302**) as a pale-yellow oil in a yield of 37.7 mg (0.126 mmol, 59%).

In a repeat experiment using oxabicycle **301** (98.1 mg, 1.00 equiv, 0.500 mmol, *rac*) and (*S*)-(−)-*α*-methylbenzylamine (73.0 µL, 1.13 equiv, 0.565 mmol, 98% ee) the product was obtained as a mixture of diastereomers (d.r. 1.2:1 (*S*)-**303**:(*S*)-**302** according to ^{1}H-NMR) as a pale-yellow oil in a yield of 85.6 mg (0.286 mmol, 57%).

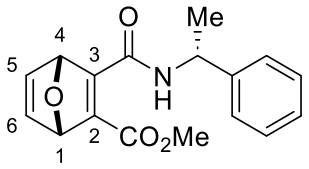

In another reaction according to **GP**9. Starting from oxabicycle **301** (39.2 mg, 1.00 equiv, 0.200 mmol, *rac*) and (±)-*α*-methylbenzylamine (29.1 µL, 1.13 equiv, 0.226 mmol, *rac*). The product was obtained as a mixture of racemic diastereomers (d.r. 1:1.3 *rac*-**303**:*rac*-**302** according to ^{1}H-NMR) as a pale-yellow oil in a yield of 32.3 mg (0.108 mmol, 54 %).

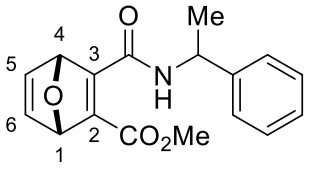

7.2.12.2.4 Methyl (1R,4S)-3-(benzylcarbamoyl)-7-oxabicyclo[2.2.1]hepta-2,5-diene-2-carboxylate (308)

The title compound was synthesized according to **GP**9. Starting from oxabicycle **301** (39.2 mg, 1.00 equiv, 0.200 mmol, *rac*) and benzylamine (25.8 µL, 1.13 equiv, 0.226 mmol). The product was obtained as a pale-yellow oil in a yield of 3.9 mg with a major inseparable impurity according to ^{1}H-NMR. ^{1}H-NMR spectrum reported for suspected product.

^{1}H NMR (400 MHz, $CDCl_3$) δ 3.82 (s, 3H, CO_2Me), 4.49 (dd, *J* = 15.0, 5.7 Hz, 1H, CH_2-a), 4.57 (dd, *J* = 15.0, 5.9 Hz, 1H, CH_2-b), 5.74 (t, *J* = 1.8 Hz, 1H, 1/4-H), 5.89 (t, *J* = 1.8 Hz, 1H, 1/4-H), 7.17 (dd, *J* = 5.3, 1.9 Hz, 1H, 5/6-H), 7.24 – 7.38 (m, 9H, ArH), 9.23 (s, 1H, NHR_2).

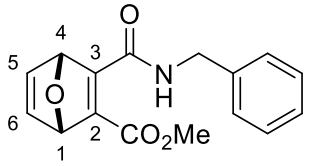

308

7.2.12.2.5 Methyl (1R,4S)-3-(isopropylcarbamoyl)-7-oxabicyclo[2.2.1]hepta-2,5-diene-2-carboxylate (311)

The title compound was synthesized according to **GP9**. Starting from oxabicycle **301** (392 mg, 1.00 equiv, 2.00 mmol, *rac*) and isopropylamine (194 µL, 1.13 equiv, 2.26 mmol). The product was obtained as a pale-yellow solid in a yield of 227 mg (0.956 mmol, 48%).

^{1}H NMR (400 MHz, $CDCl_3$) δ 1.15 (d, $^{3}J_{CH3\text{-}CH}$ = 6.6 Hz, 3H, CH$\underline{CH_3}$-a), 1.18 (d, $^{3}J_{CH3\text{-}CH}$ = 6.5 Hz, 3H, CH$\underline{CH_3}$-b), 3.81 (d, *J* = 0.5 Hz, 3H, CO_2Me), 4.00 – 4.10 (m, 1H, $\underline{CH}CH_3$), 5.66 – 5.70 (m, 1H, 1/4-H), 5.77 – 5.82 (m, 1H, 1/4-H), 7.12 (ddd, $^{3}J_{5\text{-}6}$ = 5.3 Hz, $^{4}J_{5\text{-}4/6\text{-}1}$ = 1.9, 0.5 Hz, 1H, 5/6-H), 7.21 (ddd, $^{3}J_{5\text{-}6}$ = 5.3 Hz, $^{4}J_{5\text{-}4/6\text{-}1}$ = 2.1, 0.6 Hz, 1H, 5/6-H), 8.68 (s, 1H, NHR_2).
^{13}C NMR (126 MHz, $CDCl_3$) δ 22.44 (CH$\underline{CH_3}$-a), 22.50 (CH$\underline{CH_3}$-b), 41.71 ($\underline{CH}CH_3$), 52.72 ($CO_2\underline{Me}$), 84.91 (C-1/4), 85.75 (C-1/4), 142.85 (C-5/6), 143.44 (C-5/6), 145.98 (C-2/3), 160.55

(C-2/3), 162.75 (*C*ONHR), 164.92 (*C*O_2Me). **HR-MS (DART):** m/z calculated for $[C_{12}H_{16}NO_4]^+$ ([M + H^+]): 238.1074, found: 238.1074. **IR (ATR film) [cm^{-1}]:** 3300, 2982, 2959, 2932, 1703, 1544, 1258, 1216, 886, 696. **Melting point:** 62 – 67 °C

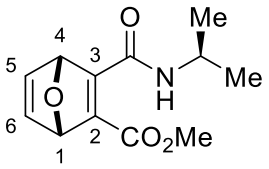

311

7.2.12.2.6 Methyl (1R,4S)-3-(benzhydrylcarbamoyl)-7-oxabicyclo[2.2.1]hepta-2,5-diene-2-carboxylate (307)

The title compound was synthesized according to **GP9**. Starting from oxabicycle **301** (392 mg, 1.00 equiv, 2.00 mmol, *rac*) and benzhydrylamine (390 µL, 1.13 equiv, 2.26 mmol). The product was obtained as a white solid in a yield of 338 mg (0.934 mmol, 47%).

^{1}H NMR (500 MHz, $CDCl_3$) δ 3.84 (s, 3H, CO_2Me), 5.75 (t, $^3J_{4\text{-}5/1\text{-}6}$ = 1.8 Hz, 1H, 1/4-H), 5.88 (t, $^3J_{4\text{-}5/1\text{-}6}$ = 1.8 Hz, 1H, 1/4-H), 6.30 (d, $^3J_{NH\text{-}CH}$ = 8.4 Hz, 1H, *CH*Ph_2), 7.16 (dd, $^3J_{5\text{-}6}$ = 5.3 Hz, $^3J_{4\text{-}5/1\text{-}6}$ = 1.9 Hz, 1H, 5/6-H), 7.24 (dd, $^3J_{5\text{-}6}$ = 5.3, $^3J_{4\text{-}5/1\text{-}6}$ = 2.1 Hz, 1H, 5/6-H), 7.23 – 7.37 (m, 10H, CH*Ph*$_2$), 9.79 (d, $^3J_{NH\text{-}CH}$ = 8.4 Hz, 1H, NHR_2). **^{13}C NMR** (126 MHz, $CDCl_3$) δ 53.04 (CO_2*Me*), 57.51 (*CH*Ph_2), 85.13 (C-1/4), 85.96 (C-1/4), 127.37, 127.49, 127.54, 128.80, 128.83, 141.64, 141.68, 142.94 (C-5/6), 143.65 (C-5/6), 146.99 (C-2/3), 160.67 (C-2/3), 162.37 (*C*ONHR), 165.04 (*C*O_2Me). **IR (ATR film) [cm^{-1}]:** 3273, 2951, 1691, 1652, 1616, 1538, 1269, 1222, 881, 698. **TLC** (petroleum ether:EtOAc 7:3 v/v): R_f = 0.38 **HR-MS (DART):** m/z calculated for $[C_{12}H_{16}NO_4]^+$ ([M + H^+]): 362.1387, found: 362.1392. **Melting point:** 135 – 138 °C

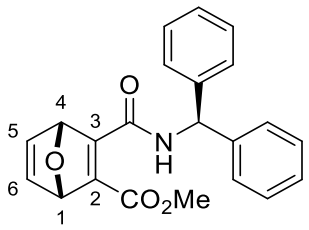

307

7.2.12.2.7 Methyl (1R,4S)-3-(((adamantan-1-yl)carbamoyl)-7-oxabicyclo[2.2.1]hepta-2,5-diene-2-carboxylate (312)

The title compound was synthesized according to **GP9**. Starting from oxabicycle **301** (196 mg, 1.00 equiv, 1.00 mmol, *rac*) and 1-adamantylamine (170 mg, 1.13 equiv, 1.13 mmol). The product was isolated as a pale-yellow solid in a yield of 197 mg (0.598 mmol, 60%).

^{1}H NMR (500 MHz, $CDCl_3$) δ 1.69 (d, $^3J_{2'\text{-}3'}$ = 3.1 Hz, 6H, 2′-H), 2.06 (d, $^3J_{4'\text{-}3'}$ = 2.6 Hz, 6H, 4′-H), 2.08 (d, $^3J_{3'\text{-}2',3'\text{-}4'}$ = 3.3 Hz, 3H, 3′-H), 3.84 (d, J = 0.6 Hz, 3H, CO_2Me), 5.71 (t, $^3J_{1\text{-}6/4\text{-}5}$ = 1.8 Hz, 1H, 1/4-H), 5.79 (t, $^3J_{1\text{-}6/4\text{-}5}$ = 2.2 Hz, 1H, 1/4-H), 7.14 (dd, $^3J_{5\text{-}6}$ = 5.3 Hz, $^3J_{1\text{-}6/4\text{-}5}$ = 1.9 Hz, 1H, 5/6-H), 7.24 (ddd, $^3J_{5\text{-}6}$ = 5.3 Hz, $^3J_{1\text{-}6/4\text{-}5}$ = 2.1 Hz, J = 0.7 Hz, 1H, 5/6-H), 8.56 (s, 1H, NHR_2). **^{13}C NMR** (126 MHz, $CDCl_3$) δ 29.50 (C-3′), 36.49 (C-2′), 41.37 (C-4′), 52.49 ($CO_2\underline{Me}$), 52.77 (C-1′), 85.05 (C-1/4), 85.94 (C-1/4), 142.86 (C-5/6), 143.50 (C-5/6), 145.20 (C-2/3), 160.56 (C-2/3), 163.88 (<u>C</u>ONHR), 165.11 (<u>C</u>O_2Me). **TLC** (pentanes:EtOAc, 7:3 v/v): R_f = 0.52

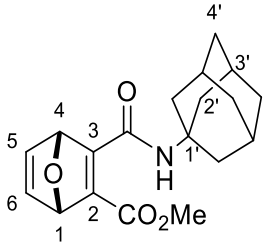

312

7.2.12.3 Indene Syntheses

7.2.12.3.1 General procedure 10 (GP10): Synthesis of pre-retro-*Diels-Alder* products starting from *C*$_s$-symmetrical oxabicycle

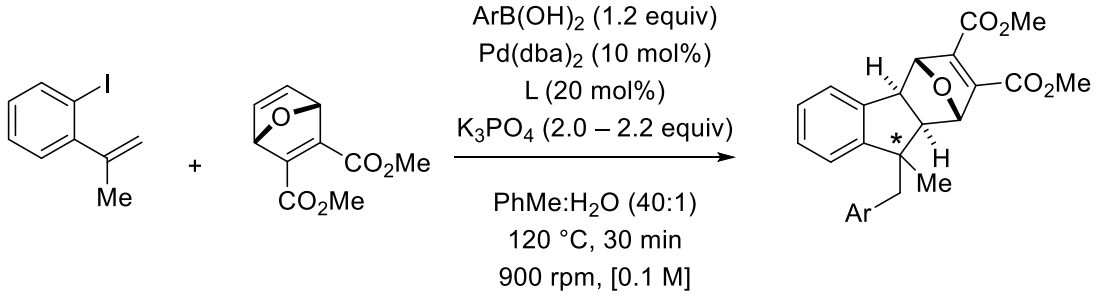

A 2-dr. vial equipped with stir bar which were dried at 110 °C over night was left to cool under Argon-atmosphere. The vial was then charged with aryl iodide (48.8 mg, 1.0 equiv, 0.200 mmol), flame dried K_3PO_4 (93.4 mg, 2.2 equiv 0.440 mmol), aryl boronic acid (1.2 equiv, 0.240 mmol), ligand (20 mol%, 0.040 mmol) and $Pd(dba)_2$ (11.5 mg, 10 mol%, 0.020 mmol)

in that order. A separate flame dried vial was charged with oxabicycle **296** (1.5 equiv, 0.300 mmol) and anhydr. PhMe (2 mL, 0.15 M). This solution was transferred into the reaction vessel, H_2O (50 µL, 0.00375 M) was added, the reaction vessel capped and sealed using PTFE tape and then stirred at 120 °C for 30 min (900 rpm). After letting the reaction cool, the reaction was filtered over a pad of silica into a vial containing a defined amount of 1,3,5-trimethoxybenzene (0.4 – 0.8 equiv), washing with EtOAc. The solvent was removed and conversion to product determined by ^{1}H-NMR. The product was isolated by column chromatography.

7.2.12.3.1.1 Dimethyl (1S,4R,4aS,9R,9aR)-9-methyl-9-(4-(trifluoromethyl)benzyl)-4,4a,9,9a-tetrahydro-1H-1,4-epoxyfluorene-2,3-dicarboxylate (334)

The title compound was synthesized according to **GP10** using 4-(trifluoromethyl)phenylboronic acid (45.6 mg, 1.2 equiv, 0.240 mmol) and $Cy_3P{\cdot}HBF_4$ (14.8 mg, 20 mol%, 0.040 mmol) and isolated by column chromatography (*n*-pentane:EtOAc, 9:1 v/v) as a colorless oil in a yield of 21.0 mg (0.044 mmol, 22%).

^{1}H NMR (600 MHz, $CDCl_3$): δ 1.29 (s, 3H, Me), 2.64 (d, $^3J_{9a\text{-}4a}$ = 7.2 Hz, 1H, 9a-H), 3.22 (d, $^2J_{CH2\text{-}CH2}$ = 14.4 Hz, 1H, CH_2-H_a), 3.28 (d, $^2J_{CH2\text{-}CH2}$ = 14.5 Hz, 1H, CH_2-H_b), 3.76 (d, $^3J_{4a\text{-}9a}$ = 7.2 Hz, 1H, 4a-H), 3.87 (s, 3H, $CO_2\underline{Me}_a$), 3.90 (s, 3H, $CO_2\underline{Me}_b$), 5.19 (d, $^4J_{4\text{-}1}$ = 1.1 Hz, 1H, 4-H), 5.50 (d, $^4J_{1\text{-}4}$ = 1.1 Hz, 1H, 1-H), 6.69 (d, $^3J_{8\text{-}7}$ = 7.7 Hz, 1H, 8-H), 7.15 (t, $^3J_{7\text{-}6,7\text{-}8}$ = 7.5 Hz, 1H, 7-H), 7.24 (td, $^3J_{6\text{-}5,6\text{-}7}$ = 7.4 Hz, $^4J_{6\text{-}8}$ = 1.1 Hz, 1H, 6-H), 7.36 (d, $^3J_{5\text{-}6}$ = 7.1 Hz, 1H, 5-H), 7.46 (d, $^3J_{2'\text{-}3'}$ = 8.0 Hz, 2H, 2'-H), 7.61 (d, $^3J_{3'\text{-}2'}$ = 8.0 Hz, 2H, 3'-H). **^{13}C NMR** (151 MHz, $CDCl_3$): δ 31.69 (Me), 42.65 (CH_2), 47.17 (C-9), 51.76 (H-4a), 52.57 ($CO_2\underline{Me}_a$), 52.63 ($CO_2\underline{Me}_b$), 55.43 (C-9a), 83.25 (C-1), 85.78 (C-4), 124.08 (C-8), 124.30 (C-5), 124.49 (q, $^1J_{C\text{-}F}$ = 271.8 Hz, CF_3), 125.03 (q, $^3J_{3'\text{-}CF3}$ = 3.8 Hz, C-3'), 127.51 (C-6), 127.65 (C-7), 128.80 (q, $^2J_{4'\text{-}CF3}$ = 32.5 Hz, C-4'), 131.27 (C-2'), 139.64 (C-4b), 142.89 (C-1'), 144.50 (C-2), 145.30 (C-3), 152.72 (C-8a), 162.97 ($\underline{CO}_2Me_{a/b}$), 163.14 ($\underline{CO}_2Me_{a/b}$). **^{19}F NMR** (282 MHz, $CDCl_3$) δ -62.25. **IR (ATR film) [cm^{-1}]:** 2954, 1725, 1633, 1485, 1320, 1267, 1213, 1114, 1061, 931. **TLC** (*n*-pentane:EtOAc, 8:2 v/v): R_f = 0.5 **HR-MS (ESI):** m/z calculated for $[C_{26}H_{24}F_3O_5]^+$ ($[M + H^+]$): 473.1570, found: 473.1573.

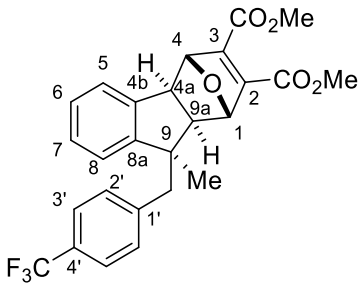

334

7.2.12.3.1.2 Dimethyl (1S,4R,4aS,9R,9aR)-9-(4-methoxybenzyl)-9-methyl-4,4a,9,9a-tetrahydro-1H-1,4-epoxyfluorene-2,3-dicarboxylate (333)

The title compound was synthesized according to **GP10** using 4-methoxyphenylboronic acid (36.5 mg, 1.2 equiv, 0.240 mmol) and $Cy_3P{\cdot}HBF_4$ (14.8 mg, 20 mol%, 0.040 mmol) and isolated by column chromatography (*n*-pentane:CH_2Cl_2:EtOAc, 5:4.5:0.5 v/v) as a mixture of isomers as an amber oil in a yield of 9.9 mg (11%, 5:1 d.r.). (NMR spectra reported for the major isomer)

^{1}H NMR (600 MHz, $CDCl_3$): δ 1.28 (s, 3H, Me), 2.59 (dd, $^3J_{9a\text{-}4a}$ = 7.1, 1.5 Hz, 1H, 9a-H), 3.10 (d, $^2J_{CH2\text{-}CH2}$ = 14.4 Hz, 1H, CH_2-H_a), 3.16 (d, $^2J_{CH2\text{-}CH2}$ = 14.4 Hz, 1H, CH_2-H_b), 3.73 (d, $^3J_{4a\text{-}8a}$ = 7.1 Hz, 1H, 4a-H), 3.84 (s, 3H, OMe), 3.87 (s, 3H, CO_2Me_a), 3.89 (s, 3H, CO_2Me_b), 5.18 (d, $^4J_{4\text{-}1}$ = 1.0 Hz, 1H, 4-H), 5.55 (d, $^4J_{1\text{-}4}$ = 1.1 Hz, 1H, 1-H), 6.73 (d, $^3J_{8\text{-}7}$ = 7.7 Hz, 1H, 8-H), 6.87 – 6.91 (m, 2H, 3'-H), 7.10 – 7.15 (m, 1H, 7-H), 7.20 – 7.23 (m, 1H, 6-H), 7.23 – 7.26 (m, 2H, 2'-H), 7.34 (d, $^3J_{5\text{-}6}$ = 7.3 Hz, 1H, 5-H). **^{13}C NMR** (151 MHz, $CDCl_3$): δ 31.88 (Me), 41.86 (CH_2), 47.30 (C-9), 51.59 (C-4a), 52.52 ($CO_2\underline{Me}_b$), 52.58 ($CO_2\underline{Me}_a$), 55.41 (OMe), 55.43 (C-9a), 83.25 (C-1), 85.70 (C-4), 113.52 (C-3'), 124.11 (C-8), 124.40 (C-5), 127.23 (C-6), 127.50 (C-7), 130.54 (C-1'), 131.97 (C-2'), 139.70 (C-4b), 144.92 (C-2), 145.14 (C-3), 153.31 (C-8a), 158.27 (C-4'), 163.04 ($\underline{CO}_2Me_{a/b}$), 163.20 ($\underline{CO}_2Me_{a/b}$). **TLC** (*n*-pentane:CH_2Cl_2:EtOAc, 5:4.5:0.5 v/v): R_f = 0.25 **HR-MS (ESI):** m/z calculated for $[C_{26}H_{26}O_6]^+$ ($[M + H^+]$): 435.1802, found: 435.1809.

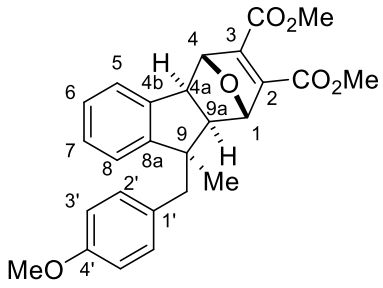

333

7.2.12.3.1.3 Dimethyl (1S,4R,4aS,9R,9aR)-9-methyl-9-(2-methylbenzyl)-4,4a,9,9a-tetrahydro-1H-1,4-epoxyfluorene-2,3-dicarboxylate (336)

The title compound was synthesized according to **GP10** using *o*-tolylboronic acid (32.6 mg, 1.2 equiv, 0.240 mmol) and $Cy_3P{\cdot}HBF_4$ (14.8 mg, 20 mol%, 0.040 mmol) and isolated by column chromatography (*n*-pentane:EtOAc, 9:1 v/v) as a mixture of isomers as a yellow oil in a yield of 55.8 mg (67%, 5:1 d.r.). (NMR spectra reported for the major isomer)

^{1}H NMR (600 MHz, $CDCl_3$): δ 1.32 (s, 3H, Me), 1.98 (s, 3H, Me'), 2.67 (d, $^3J_{9a\text{-}4a}$ = 7.2 Hz, 1H, 9a-H), 2.88 (d, $^2J_{CH2\text{-}CH2}$ = 15.3 Hz, 1H, CH_2-H_a), 3.25 (d, $^2J_{CH2\text{-}CH2}$ = 15.3 Hz, 1H, CH_2-H_b), 3.67 (d, $^3J_{4a\text{-}9a}$ = 7.2 Hz, 1H, 4a-H), 3.78 (s, 3H, $CO_2\underline{Me}$), 3.80 (s, 3H, $CO_2\underline{Me}$), 5.10 (d, $^4J_{4\text{-}1}$ = 1.1 Hz, 1H, 4-H), 5.33 (d, $^4J_{1\text{-}4}$ = 1.1 Hz, 1H, 1-H), 6.57 (d, $^3J_{8\text{-}7}$ = 7.7 Hz, 1H, 8-H), 7.02 (td, $^3J_{7\text{-}6,7\text{-}8}$ = 7.4 Hz, $^4J_{7\text{-}5}$ = 0.9 Hz, 1H, 7-H), 7.09 (dd, *J* = 8.8, 1.8 Hz, 2H, ArH (3'-H)), 7.11 – 7.16 (m, 3H, ArH (6-H)), 7.25 (d, $^3J_{5\text{-}6}$ = 7.5 Hz, 1H, 5-H), 7.36 (d, $^3J_{6'\text{-}5'}$ = 7.5 Hz, 1H, 6'-H). **^{13}C NMR** (151 MHz, $CDCl_3$): δ 20.35 (Me'), 31.33 (Me), 39.05 (CH_2), 47.10 (C-9), 52.01 (C-4a), 52.40 ($CO_2\underline{Me}$), 52.49 ($CO_2\underline{Me}$), 55.14 (C-9a), 83.49 (C-1), 85.60 (C-4), 123.89 (C-8), 124.01 (C-5), 125.45, 126.24, 127.21 (C-6), 127.54 (C-7), 130.13, 130.44 (C-3'), 136.89, 138.30 (C-1'), 139.38 (C-4b), 144.93 (C-2), 145.14 (C-3), 148.89 (C-2'), 153.54 (C-8a), 163.00 ($\underline{CO_2}$Me), 163.06 ($\underline{CO_2}$Me). **TLC** (*n*-pentane:EtOAc, 8:2 v/v): R_f = 0.41 **HR-MS (ESI):** m/z calculated for $[C_{26}H_{27}O_5]^+$ ($[M + H^+]$): 419.1853, found: 419.1854.

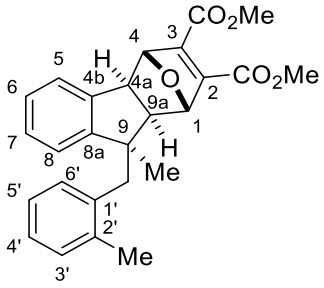

336

7.2.12.3.2 General procedure 11 (GP11): Synthesis of pre-retro-*Diels-Alder* products starting from chiral oxabicycles

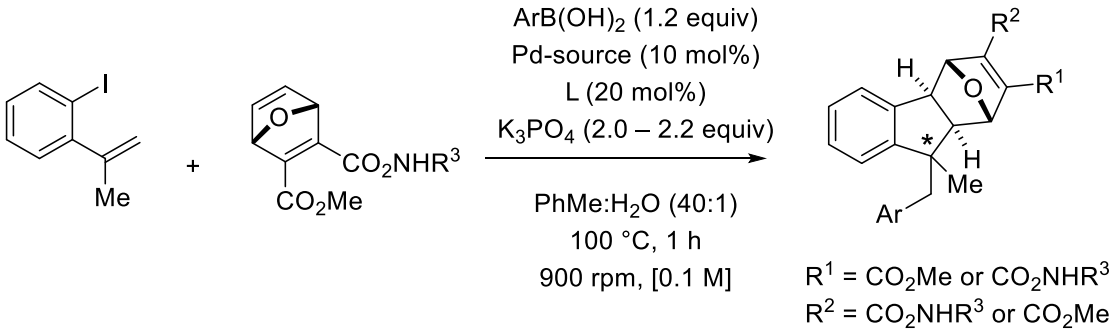

A 2-dr. vial which was dried at 110 °C over night was equipped with stir bar and left to cool under Argon-atmosphere. A 2-dr. vial equipped with stir bar which were dried at 110 °C over night was left to cool under Argon-atmosphere. The vial was then charged with aryl iodide **293** (1.0 equiv), flame dried K_3PO_4 (2.2 equiv), aryl boronic acid (1.2 equiv), ligand (20 mol%) and $Pd(dba)_2$ (10 mol%) in that order. A separate flame dried vial was charged with oxabicycle (1.5 equiv) and toluene (0.15 M). This solution was transferred into the reaction vessel, H_2O (0.00375 M) was added, the reaction vessel capped and sealed using PTFE tape and then stirred at 100 °C for 1 h (900 rpm). After letting the reaction cool, the reaction was filtered over a pad of silica into a vial containing a defined amount of 1,3,5-trimethoxybenzene (0.4 – 0.8 equiv), washing with EtOAc. The solvent was removed and conversion to product determined by ^{1}H-NMR. The product was isolated by column chromatography.

7.2.12.3.2.1 Methyl (1S,4R,4aS,9R,9aR)-9-(dibenzo[b,d]furan-4-ylmethyl)-3-(isopropylcarbamoyl)-9-methyl-4,4a,9,9a-tetrahydro-1H-1,4-epoxyfluorene-2-carboxylate (338)

The title compound was synthesized according to **GP11** using aryl iodide **293** (73.2 mg, 1.00 equiv, 0.300 mmol), K_3PO_4 (140 mg, 2.2 equiv, 0.660 mmol), 4-(dibenzofuranyl)boronic acid (**337**) (76.3 mg, 1.2 equiv, 0.360 mmol), $Cy_3P{\cdot}HBF_4$ (22.1 mg, 20 mol%, 0.060 mmol) and $Pd(dba)_2$ (17.3 mg, 10 mol%, 0.030 mmol), oxabicycle **311** (107 mg, 1.5 equiv, 0.450 mmol), toluene (3 mL, 0.15 M) and H_2O (75.0 µL, 0.00375 M). The title compound was isolated by column chromatography (*first*: pentanes:EtOAc 9:1 to 8:2 v/v *then* pentanes:CH_2Cl_2:EtOAc 50:45:5 v/v) as a mixture of isomers as white solids in a yield of 26.4 mg (0.051 mmol, 51%).

^{1}H NMR (500 MHz, $CDCl_3$) δ 1.26 (d, $^3J_{CH3\text{-}CH}$ = 2.5 Hz, 3H, CHMe*Me*), 1.27 (d, $^3J_{CH3\text{-}CH}$ = 2.4 Hz, 3H, CH*Me*Me), 1.37 (s, 3H, Me), 2.61 (d, $^3J_{9a\text{-}4a}$ = 7.1 Hz, 1H, 9a-H), 3.55 (d, $^2J_{CH2\text{-}CH2}$ = 15.2 Hz, 1H, CH_2-H_a), 3.71 (d, $^2J_{CH2\text{-}CH2}$ = 15.3 Hz, 1H, CH_2-H_b), 3.78 (s, 3H, CO_2Me), 3.81 (d, $^3J_{4a\text{-}9a}$ = 7.0 Hz, 1H, 4a-H), 4.11 – 4.21 (m, 1H, *CH*MeMe), 5.43 (d, $^4J_{4\text{-}1}$ = 1.2 Hz, 1H, H-

4), 5.75 (s, 1H, 1-H), 7.07 (dt, $^{3}J_{8\text{-}7}$ = 7.7 Hz, $^{4}J_{8\text{-}6}$ = 0.8 Hz, 1H, 8-H), 7.19 – 7.23 (m, 1H, 7-H), 7.28 (td, $^{3}J_{6\text{-}5,6\text{-}7}$ = 7.4 Hz, $^{4}J_{6\text{-}8}$ = 1.2 Hz, 1H, 6-H), 7.35 (t, $^{3}J_{2'\text{-}1',2'\text{-}3'}$ = 7.6 Hz, 1H, 2'-H), 7.37 (td, *J* = 7.4, 1.0 Hz, 1H, ArH), 7.45 – 7.50 (m, 1H, 5-H), 7.55 (dd, $^{3}J_{3'\text{-}2'}$ = 7.5 Hz, $^{4}J_{3'\text{-}1'}$ = 1.2 Hz, 1H, 3'-H), 7.61 (dt, *J* = 8.2, 0.8 Hz, 1H, ArH), 7.91 (dd, $^{3}J_{1'\text{-}2'}$ = 7.7 Hz, $^{4}J_{1'\text{-}3'}$ = 1.2 Hz, 1H, 1'-H), 7.99 (ddd, *J* = 7.7, 1.3, 0.6 Hz, 1H, ArH), 8.82 (d, $^{3}J_{\text{NH-CH}}$ = 7.5 Hz, 1H, <u>*NH*</u>R_2). **^{13}C NMR** (126 MHz, $CDCl_3$) δ 22.54 (CHMe<u>*Me*</u>), 22.64 (CH<u>*Me*</u>Me), 32.09 (Me), 35.24 (CH_2), 41.76 (<u>*CH*</u>MeMe), 47.94 (C-9), 51.33 (C-4a), 52.76 (CO_2<u>*Me*</u>), 55.27 (C-9a), 83.69 (C-1), 86.81 (C-4), 111.87, 118.77, 120.77, 122.31, 122.84 (C-2'), 123.32 (C-8), 123.46, 124.08, 124.48, 124.67 (possibly C-5), 127.24 (possibly C-5), 127.47 (C-6), 127.66 (C-7), 129.28 (C-3'), 138.43, 140.03 (C-4b), 153.56 (C-8a), 154.24, 155.75 (C-4a'), 156.01, 160.48 (<u>*C*</u>ONR_2), 165.01 (<u>*C*</u>O_2Me). **TLC** (pentanes:EtOAc, 7:3 v/v): R_f = 0.58 **TLC** (pentanes:EtOAc, pentanes:CH_2Cl_2:EtOAc 5:4.5:0.5 v/v): R_f = 0.29

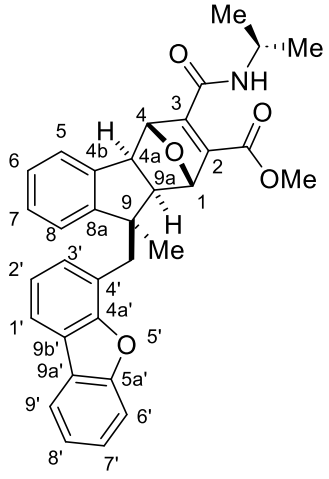

338

7.2.12.3.2.2 Methyl (1S,4R,4aS,9R,9aR)-3-(benzhydrylcarbamoyl)-9-(dibenzo[b,d]furan-4-ylmethyl)-9-methyl-4,4a,9,9a-tetrahydro-1H-1,4-epoxyfluorene-2-carboxylate (339)

The title compound was synthesized according to **GP11** using aryl iodide **293** (48.8 mg, 1.00 equiv, 0.200 mmol), K_3PO_4 (93.4 mg, 2.2 equiv, 0.440 mmol), 4-(dibenzofuranyl)boronic acid (**337**) (50.9 mg, 1.2 equiv, 0.240 mmol), $Cy_3P{\cdot}HBF_4$ (14.7 mg, 20 mol%, 0.040 mmol) and $Pd(dba)_2$ (11.5 mg, 10 mol%, 0.020 mmol), oxabicycle **311** (108 mg, 1.5 equiv, 0.300 mmol), toluene (2 mL, 0.15 M) and H_2O (50.0 µL, 0.00375 M). The title compound was obtained as a mixture (3.7:1) of isomers by column chromatography (*first*: pentanes:EtOAc 9:1 to 8:2 v/v *then* pentanes:CH_2Cl_2:EtOAc 50:49:1 to 50:47.5:2.5 v/v) as white solids in a yield of 69.3 mg (0.107 mmol, 54%). (NMR spectra reported for the major isomer)

^{1}H NMR (300 MHz, $CDCl_3$) δ 1.35 (s, 3H, Me), 2.58 (d, *J* = 7.1 Hz, 1H, 9a-H), 3.54 (d, *J* = 15.1 Hz, 1H, CH_2-H_a), 3.70 (d, *J* = 15.3 Hz, 1H, CH_2-H_b), 3.74 (s, 3H, OMe), 5.43 (d, *J* = 1.2 Hz, 1H, 1/4-H), 5.77 (d, *J* = 1.3 Hz, 1H, 1/4-H), 6.33 (d, *J* = 8.2 Hz, 1H, 4a-H), 7.05 (d, *J* = 7.3 Hz, 1H, ArH), 7.13 – 7.50 (m, 25H, ArH), 7.54 (d, *J* = 7.6 Hz, 1H, ArH), 7.55 – 7.64 (m, 1H, ArH), 7.90 (dd, *J* = 7.6, 1.2 Hz, 1H, ArH), 7.94 – 8.03 (m, 1H, ArH), 9.86 (d, *J* = 8.3 Hz, 1H, CO*NH*Ph_2). **TLC** (pentanes:EtOAc, 7:3 v/v): R_f = 0.42 **HR-MS (ESI):** m/z calculated for $[C_{43}H_{36}O_5N]^+$ ([M + H^+]) (ppm -2.5): 646.2572, found: 646.2588.

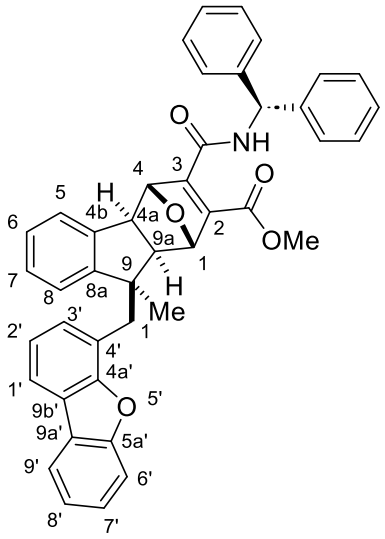

339

7.2.12.3.3 General procedure 12 (GP12): Catalytic reactions Suzuki termination

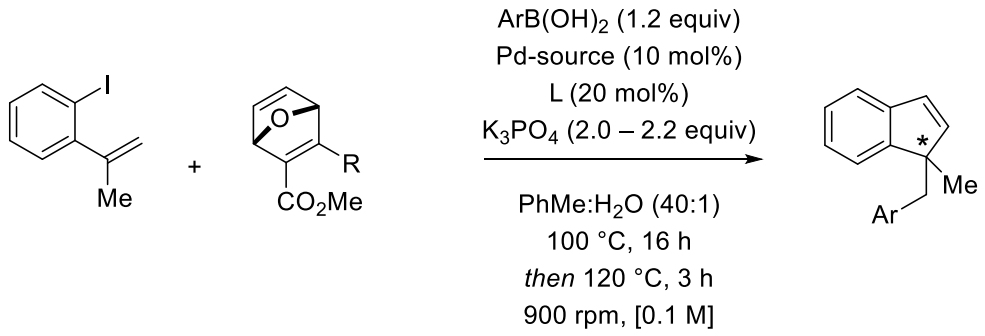

A 2-dr. vial equipped with stir bar which were dried at 110 °C over night was left to cool under Argon-atmosphere. The vial was then charged with aryl iodide **293** (24.4 mg, 1.0 equiv, 0.100 mmol), flame dried K_3PO_4 (46.7 mg, 2.2 equiv 0.220 mmol), aryl boronic acid (1.2 equiv, 0.120 mmol), ligand (20 mol%, 0.020 mmol) and palladium source (10 mol%, 0.010 mmol) in that order. A separate flame dried vial was charged with oxabicycle (1.5 equiv, 0.150 mmol) and anhydr. PhMe (1 mL, 0.15 M). This solution was transferred into the reaction vessel, H_2O

(25.0 µL, 0.00375 M) was added, the reaction vessel capped and sealed using PTFE tape and then stirred at 100 °C for 16 h. The vessel was then stirred at 120 °C for 3 h (900 rpm). After letting the reaction cool, the reaction was filtered over a pad of silica into a vial containing a defined amount of 1,3,5-trimethoxybenzene (0.4 – 0.8 equiv), flushing with additional EtOAc. The solvent was removed and conversion to product determined by ^{1}H-NMR. The product was isolated by column chromatography (pentanes:EtOAc 95:5 to 75:25 v/v).

7.2.12.3.3.1 1-(4-Methoxybenzyl)-1-methyl-1H-indene (314)

The title compound was synthesized in accordance with **GP12** using 4-methoxy boronic acid (18.4 mg, 1.2 equiv, 0.120 mmol), $Pd(dba)_2$ (5.8 mg, 10 mol%, 0.010 mmol), $Cy_3P{\cdot}HBF_4$ (7.4 mg, 20 mol%, 0.020 mmol) and oxabicycle **302** (44.9 mg, 1.5 equiv, 0.150 mmol, 99%*ee*, *d.r.* >20:1). The product was isolated as a colorless oil in a yield of 11.8 mg (0.047 mmol, 47%, 50%*ee*). The analytical data were in accordance with literature.[259a]

^{1}H NMR (300 MHz, CDCl3) δ 1.29 (s, 3H, Me), 2.80 (d, *J* = 13.2 Hz, 1H, CH_2-H_a), 2.94 (d, *J* = 13.2 Hz, 1H, CH_2-H_b), 3.76 (s, 3H, OMe), 6.33 (d, *J* = 5.5 Hz, 1H, 2/3-H), 6.59 (dd, *J* = 5.5, 0.6 Hz, 1H, 2/3-H), 6.68 – 6.85 (m, 2H, 2'/3'-H), 6.88 – 6.99 (m, 2H, 2'/3'-H), 7.15 – 7.25 (m, 3H), 7.26 – 7.31 (m, 1H). **HPLC:** Chiralpak® AS-H 250 ° 4.6 mm, 25 °C, 0.5 mL min^{-1}, 254 nm, hexanes 100% t_R(*R*) = 16 min, t_R(*S*) = 25 min **TLC** (pentanes:EtOAc, 8:2 v/v): R_f = 0.29

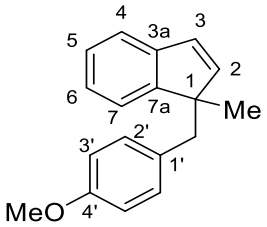

314

7.2.12.3.4 General procedure 13 (GP13): Catalytic reactions decarboxylative Sonogashira termination

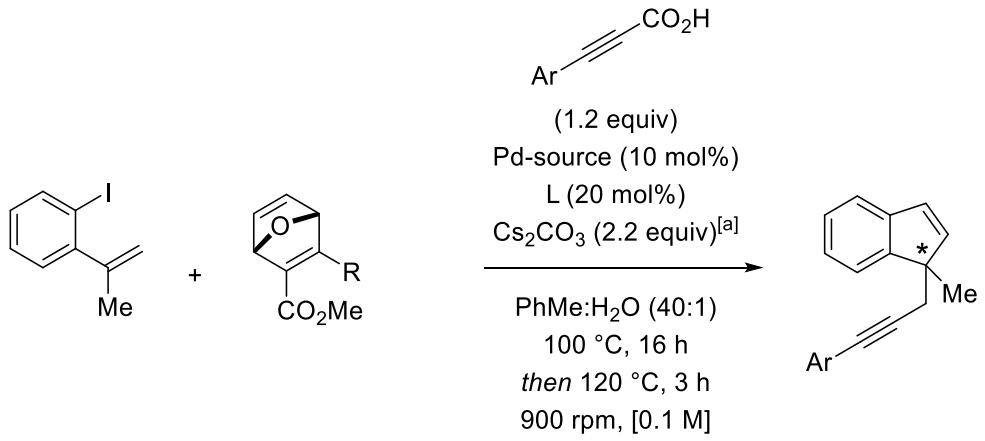

A 2-dr. vial equipped with stir bar which were dried at 110 °C over night was left to cool under Argon-atmosphere. The vial was then charged with aryl iodide **293** (48.8 mg, 1.0 equiv, 0.200 mmol), Cs_2CO_3 (143 mg, 2.2 equiv, 0.440 mmol), aryl propiolic acid (1.2 equiv, 0.240 mmol), ligand (20 mol%, 0.020 mmol) and Pd-source (10 mol%, 0.020 mmol) in that order. A separate flame dried vial was charged with oxabicycle (1.5 equiv, 0.30 mmol) and anhydr. PhMe (2 mL, 0.15 M). This solution was transferred into the reaction vessel, the reaction vessel capped and sealed using PTFE tape and then stirred at 120 °C for 16 h (900 rpm). After letting the reaction cool, the reaction was filtered over a pad of silica into a vial containing a defined amount of 1,3,5-trimethoxybenzene (0.4 – 0.8 equiv), washing with EtOAc. The solvent was removed and conversion to product determined by ^{1}H-NMR. The product was isolated by column chromatography (pentanes:CH_2Cl_2 95:5 v/v).

7.2.12.3.4.1 1-(3-Phenylprop-2-yn-1-yl)-1-methyl-1H-indene (316)

The title compound was synthesized according to **GP13** using phenylpropiolic acid (35.1 mg, 1.2 equiv, 0.240 mmol), $Pd(dba)_2$ (11.5 mg, 10 mol%, 0.020 mmol) and ligand (*S*),(*S*)-**L3** (23.2 mg, 20 mol%, 0.040 mmol). The product was isolated as a colorless oil in a yield of 20.8 mg (0.085 mmol, 43%). Separation of the enantiomers by HPLC was impossible. The analytical data were in accordance with literature.[259a]

^{1}H NMR (300 MHz, $CDCl_3$): δ 1.50 (s, 3H, Me), 2.57 (d, *J* = 16.6 Hz, 1H, CH_2-H_a), 2.72 (d, *J* = 16.6 Hz, 1H, CH_2-H_a), 6.53 (d, *J* = 5.5 Hz, 1H, 2/3-H), 6.73 (d, *J* = 5.5 Hz, 1H, 2/3-H), 7.17 – 7.24 (m, 1H), 7.28 – 7.32 (m, 4H), 7.38 – 7.43 (m, 2H), 7.44 – 7.53 (m, 2H). **TLC** (pentanes:EtOAc, 95:5 v/v): R_f = 0.37

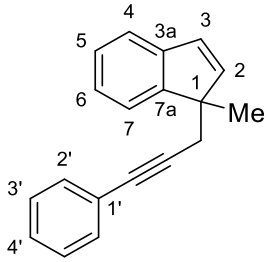

316

7.2.12.4 Miscellaneous Syntheses

7.2.12.4.1 (1S,4R)-3-(Benzhydrylcarbamoyl)-7-oxabicyclo[2.2.1]hepta-2,5-diene-2-carboxylic acid (351)

A scintillation vial equipped with stir bar was charged with oxabicycle **307** (72.3 mg, 1.0 equiv, 0.200 mmol) was dissolved in THF (20 mL, 0.15 M) and cooled to 0 °C. A solution of aq. NaOH (0.25 M, 0.800 mL, 1.0 equiv, 0.200 mmol) was added dropwise. After stirring the reaction mixture at 22 °C for 30 min, the reaction mixture was extracted with EtOAc (3x) and the collected organic phases discarded. The aq. phase was then neutralized adding KPi-buffer (1 M, 0.200 mL, 1.0 equiv, 0.200 mmol) and then acidified with aq. HCl-solution (1 M, 0.600 mL, 1.0 equiv, 0.600 mmol). The aq. phase was extracted with EtOAc (3x), the combined organic phases were washed with sat. aq. NaCl-solution, dried over $MgSO_4$ and the solvent removed in vacuo. The product was obtained as white solids in a yield of 48.3 mg (0.139 mmol, 70%).

^{1}H NMR (500 MHz, $CDCl_3$) δ 5.75 (t, $^3J_{1\text{-}6/4\text{-}5}$ = 1.8 Hz, 1H, 1/4-H), 5.81 (t, $^3J_{1\text{-}6/4\text{-}5}$ = 1.8 Hz, 1H, 1/4-H), 6.30 (d, $^3J_{CH\text{-}NH}$ = 8.0 Hz, 1H; *CH*Ph_2), 7.18 (dd, $^3J_{5\text{-}6}$ = 5.3 Hz, $^3J_{5\text{-}6/6\text{-}1}$ = 1.9 Hz, 1H, 5/6-H), 7.22 (dd, $^3J_{5\text{-}6}$ = 5.3 Hz, $^3J_{5\text{-}4/6\text{-}1}$ = 1.9 Hz, 1H, 5/6-H), 7.22 – 7.35 (m, 10H, CH*Ph*$_2$), 8.53 (s, 1H, NHR_2). **^{13}C NMR** (126 MHz, $CDCl_3$) δ 57.89 (*CH*Ph_2), 84.81 (C-1/4), 85.31 (C-1/4), 127.30, 127.40, 127.90, 128.87, 140.18, 140.23, 142.55 (C-5/6), 143.69 (C-5/6), 161.79 (CONHR), 164.82 (CO_2H).

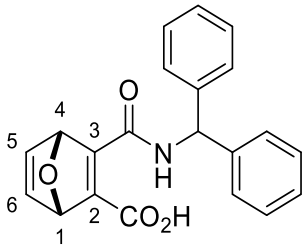

351

7.2.12.4.2 (1S,4R,4aS,9R,9aR)-9-(Dibenzo[b,d]furan-4-ylmethyl)-3-(isopropylcarbamoyl)-9-methyl-4,4a,9,9a-tetrahydro-1H-1,4-epoxyfluorene-2-carboxylic acid (353)

A scintillation vial equipped with stir bar was charged with pre-retro-*Diels-Alder* product **338** (mixture of regioisomers 4:1) (72.3 mg, 1.0 equiv, 0.200 mmol) was dissolved in THF (0.15 M, 1.33 mL) and cooled to 0 °C. A solution of aq. NaOH (0.25 M, 0.800 mL, 1.0 equiv, 0.200 mmol) was added dropwise. After stirring the reaction mixture at 22 °C for 30 min, the reaction mixture was extracted with EtOAc (3x). The organic phases were dried over $MgSO_4$ and the solvent removed in vacuo. The aq. phase was then neutralized adding KPi-buffer (1 M, 0.200 mL, 1.0 equiv, 0.200 mmol) and then acidified with aq. HCl-solution (1 M, 0.200 mL, 1.0 equiv, 0.200 mmol). The aq. phase was extracted with EtOAc (3x), the combined organic phases were washed with sat. aq. NaCl-solution, dried over $MgSO_4$ and the solvent removed in vacuo. The two organic extracts were combined and subjected to column chromatography (9:1/CH_2Cl_2:EtOAc to 8.8:1:0.2/CH_2Cl_2:EtOAc:AcOH) to obtain the desired product as a mixture of regioisomers (5:1) as off-white solids in a yield of 58.1 mg (0.114 mmol, 57%, 59% based on recovered starting material).

^{1}H NMR (500 MHz, $CDCl_3$) δ 1.32 (d, $^3J_{CH\text{-}CH3}$ = 2.0 Hz, 3H, CHMe*Me*), 1.33 (d, $^3J_{CH\text{-}CH3}$ = 2.0 Hz, 3H, CHMe*Me*), 2.12 (s, 3H, Me), 2.70 (d, $^3J_{9a\text{-}4a}$ = 7.2 Hz, 1H, 4a/9a-H), 3.52 (d, $^2J_{CH2\text{-}CH2}$ = 14.6 Hz, 1H, CH_2-H_a), 3.67 (d, $^2J_{CH2\text{-}CH2}$ = 14.6 Hz, 1H, CH_2-H_b), 3.74 (d, $^3J_{4a\text{-}9a}$ = 7.1 Hz, 1H, 4a/9a-H), 4.26 (dp, $^3J_{CH\text{-}CH3}$ = 7.7, 6.5 Hz, 1H, *CH*MeMe), 5.24 (d, $^4J_{1\text{-}4}$ = 1.0 Hz, 1H, 1/4-H), 5.83 (d, $^4J_{1\text{-}4}$ = 1.1 Hz, 1H, 1/4-H), 6.92 – 6.96 (m, 1H, ArH), 7.15 (tdd, *J* = 7.3, 1.3, 0.7 Hz, 1H, ArH), 7.24 (td, *J* = 7.4, 1.1 Hz, 1H, ArH), 7.33 – 7.39 (m, 3H, ArH), 7.45 (ddd, *J* = 8.4, 7.3, 1.4 Hz, 1H, ArH), 7.56 (dd, *J* = 7.5, 1.2 Hz, 1H, ArH), 7.56 – 7.60 (m, 1H, ArH), 7.88 (dd, *J* = 7.6, 1.2 Hz, 1H, ArH), 7.97 (ddd, *J* = 7.6, 1.3, 0.6 Hz, 1H, ArH). **^{13}C NMR** (126 MHz, $CDCl_3$) δ 22.48, 22.49, 31.76, 35.72, 43.05, 47.91, 49.09, 51.96, 55.20, 84.15, 85.26, 111.88, 118.96, 120.81, 122.71, 122.74, 122.82, 123.94, 124.00, 124.47, 124.81, 127.11, 127.35, 127.88, 129.87, 139.08, 139.44, 153.77, 155.87, 156.08.

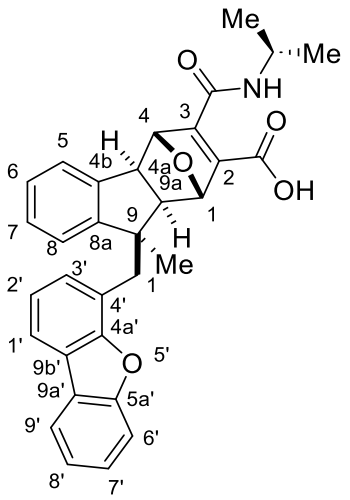

353

7.2.12.5 Ligand Syntheses

7.2.12.5.1 Tris(3,5-bis(trifluoromethyl)phenyl)phosphane (352)

Under inert atmosphere a 250 mL Schlenk round-bottom flask equipped with stir bar was charged with Mg turnings (705 mg, 3.0 equiv, 29.0 mmol) and an I_2 crystal. The round-bottom flask was heated with a heat gun until a violet gas started to form. Then the round-bottom flask was cooled to 0 °C. Bromobenzene (5.00 mL, 3.0 equiv, 29.0 mmol) in Et_2O (14.5 mL, 2 M) was added dropwise. After complete addition a reflux condenser was equipped and the mixture was stirred at 60 °C for 1 h until all Mg was consumed. Then the reaction mixture was cooled to 0 °C and a solution of PCl_3 (845 µL, 1.0 equiv, 9.65 mmol) in Et_2O (14.5 mL) was added dropwise at a rate that kept the solution reluxing. Then the reaction mixture was stirred at 22 °C for 1 h. H_2O (20 mL) was added, the aq. phase was extracted with Et_2O (3x), the combined organic phases washed with sat. aq. NaCl solution, dried over $MgSO_4$ and solvents removed in vacuo. The product was isolated by recrystallization from MeOH as off-white solids in a yield of 1.34 g (2.51 mmol, 9%).

^{1}H NMR (600 MHz, $CDCl_3$): δ 7.75 (dd, $^3J_{2\text{-}P}$ = 6.9 Hz, $^4J_{2\text{-}4}$ = 1.6 Hz, 2H, 2-H), 7.99 (s, 1H, 4-H). **^{13}C NMR** (151 MHz, $CDCl_3$): δ 122.85 (q, $^1J_{C\text{-}F}$ = 273.3 Hz, CF_3), 124.57 (p, $^3J_{4\text{-}CF3}$ = 3.7 Hz, C-4), 133.11 (dd, $^2J_{3\text{-}CF3}$ = 33.8, 6.9 Hz, C-3), 133.27 – 133.56 (m, C-2), 137.52 (d, $^1J_{C\text{-}P}$ = 17.6 Hz, C-1). **^{19}F NMR** (282 MHz, $CDCl_3$): δ -63.14. **^{31}P NMR** (122 MHz, $CDCl_3$) δ -4.21 (p, $^1J_{1\text{-}P}$ = 7.1 Hz). **IR (ATR film) [cm^{-1}]:** 1353, 1284, 1133, 746, 685. **APCI-MS:** m/z: ([M + H$^+$]): found: 670.9. **Melting point:** 100 – 101 °C

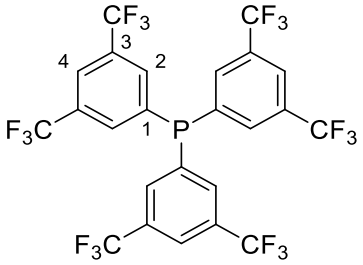

352

7.2.12.5.2 Dimethyl (4S,5S)-2,2-dimethyl-1,3-dioxolane-4,5-dicarboxylate (318)

A round-bottom flask was charged with (−)-Dimethyl D-tartrate (1.78 g, 10.0 mmol, 1.0 equiv), CH_2Cl_2 (20 mL, 0.5 M) *p*TsOH·H_2O (0.951 g, 5 mmol, 0.5 equiv) and 2,2-Dimethoxypropane (8.14 mL, 66.4 mmol, 6.64 equiv). The mixture was stirred at 60 °C for 4 h. The solvent was removed in vacuo, H2O was added and the suspension extracted with EtOAc (3x), washed with sat. aq. NaCl-solution, dried over $MgSO_4$ and the solvent removed in vacuo. The product was obtained as a brown oil in a yield of 2.15 g (9.84 mmol, 98%). The analytical data were in accordance with literature.[342]

^{1}H NMR (400 MHz, $CDCl_3$) δ 1.48 (d, *J* = 1.6 Hz, 6H, CMe_2), 3.81 (d, *J* = 1.5 Hz, 6H, CO_2Me), 4.80 (s, 2H, CHR_2).

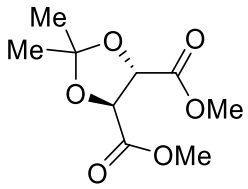

318

7.2.12.5.3 ((4S,5S)-2,2-Dimethyl-1,3-dioxolane-4,5-diyl)bis(diphenylmethanol) (319)

Under inert atmosphere a round-bottom flask equipped with stir bar was charged with Mg turnings (445 mg, 18.3 mmol, 4.67 equiv) and an I_2 crystal. The round-bottom flask was heated with a heat gun until a violet gas started to form. Then the round-bottom flask was cooled to 0 °C. Bromobenzene (1.82 mL, 17.4 mmol, 4.44 equiv) in THF (12.2 mL, 1.43 M) was added dropwise. After complete addition the mixture was stirred at 60 °C for 1 h until all Mg was consumed. Then the reaction mixture was cooled to 0 °C and diester **318** (0.855 mL, 3.91 mmol, 1.0 equiv) in THF (8.7 mL, 0.45 M) was added dropwise. The reaction was then stirred at 80 °C for 1.5 h. The reaction mixture was then cooled to 0 °C and sat. aq. NH_4Cl-

solution was slowly added. The suspension was extracted with EtOAc (3x), washed with sat. aq. NaCl-solution, dried over MgSO4 and the solvent removed in vacuo. The crude product was dissolved in EtOAc (3 mL), pentanes (200 mL) were added and then *i*-PrOH (1 mL) was added and the mixture cooled to -20 °C. The solvent was then removed, pentanes (80 mL) were added, the solids sonicated and the solvent removed *via* pipette. Pentanes were added again (10 mL) and the solvent removed *via* pipette. The remaining solids were collected as the product as pale yellow solids in a yield of 885 mg (1.90 mmol, 49%). The analytical data were in accordance with literature.[342]

^{1}H NMR (400 MHz, $CDCl_3$) δ 1.04 (s, 6H, CMe_2), 3.86 (s, 2H, OH), 4.61 (s, 2H, CHR_2), 7.20 – 7.37 (m, 16H, ArH), 7.50 – 7.55 (m, 4H, ArH).

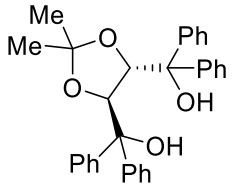

319

7.2.12.5.4 1-((3aS,8aS)-2,2-Dimethyl-4,4,8,8-tetraphenyltetrahydro-[1,3]dioxolo[4,5-e][1,3,2]dioxaphosphepin-6-yl)piperidine (L3)

A scintillation vial equipped with stir bar was charged with diole **319** (339 mg, 0.725 mmol, 1.00 equiv) was dissolved in anhydr. THF (2.9 mL, 0.25 M) and cooled to 0 °C. Et_3N (341 µL, 2.45 mmol, 3.37 equiv) was added then PCl_3 (73.0 µL, 0.835 mmol, 1.15 equiv) was added and the reaction stirred at 22 °C for 30 min. The yellow suspension is then cooled to 0 °C, piperidine (355 µL, 3.59 mmol, 4.95 equiv) was added and the reaction mixture stirred for 16 h at 22 °C. The reaction mixture is diluted with Et_2O (10 mL), filtered over a pad of Celite® washing with Et_2O. The solvent is removed and the product isolated *via* column chromatography (pentanes:Et_2O:Et_3N 99:0:1 to 96:3:1 v/v). The product was obtained as white solids in a yield of 221 mg (0.381 mmol, 53%). The analytical data were in accordance with literature.[259a]

^{1}H NMR (300 MHz, $CDCl_3$) δ 0.27 (s, 3H, Me_a), 0.86 (d, J = 15.2 Hz, 2H, CH_2), 1.30 (s, 3H, Me_b), 1.56 – 1.65 (m, 4H, CH_2), 3.08 – 3.34 (m, 4H, CH_2), 4.75 (d, J = 8.5 Hz, 1H, CHR_2-H_a), 5.15 (dd, $^3J_{CHR2a-CHR2b}$ = 8.5 Hz, $J_{P-CHR2b}$ = 3.4 Hz, 1H, CHR_2-H_b), 7.17 – 7.25 (m, 5H, ArH), 7.27 – 7.35 (m, 7H, ArH), 7.39 – 7.43 (m, 2H, ArH), 7.44 – 7.51 (m, 2H, ArH), 7.62 (dd, J = 7.2, 1.5 Hz, 2H, ArH), 7.72 – 7.78 (m, 2H, ArH).

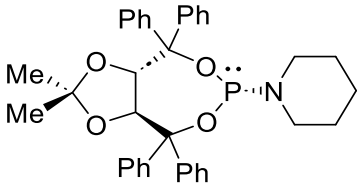

L3

7.2.13 Miscellaneous Syntheses

7.2.13.1 2'-Iodo-6'-methyl-[1,1'-biphenyl]-4-ol (345)

In accordance with a literature procedure[201] a Schlenk-flask was charged with 2-iodobiaryl **283** (162 mg, 1.0 equiv, 500 µmol) and CH_2Cl_2 (0.125 M, 4 mL) and stirred at 0 °C. A solution of BBr_3 in hexanes (1 M, 1.00 mL, 2.0 equiv, 1.00 mmol) was added dropwise. The reaction mixture was stirred at 22 °C for 3 h. Water (10 mL) was added at 0 °C and the aq. phase extracted with CH_2Cl_2 (3x), washed with sat. NaCl-solution and dried over $MgSO_4$. Most of the solvent was removed in vacuo and the crude product filtered over a plug of silica flushing with additional CH_2Cl_2. The product was obtained as off-white solids in a yield of 149 mg (480 µmol, 96%). The analytical data were in accordance with literature.[201]

^{1}H NMR (600 MHz, $CDCl_3$): δ 2.10 (s, 3H, Me), 4.94 (s, 1H, OH), 6.92 (d, $^3J_{3\text{-}2}$ = 8.5 Hz, 2H, 3-H), 6.93 (t, $^3J_{4'\text{-}3',4'\text{-}5'}$ = 7.5 Hz, 1H, 4′-H), 7.00 (d, $^3J_{2\text{-}3}$ = 8.5 Hz, 2H, 2-H), 7.22 (d, $^3J_{5'\text{-}4'}$ = 7.6 Hz, 1H, 5′-H), 7.78 (d, $^3J_{3'\text{-}4'}$ = 7.9 Hz, 1H, 3′-H). **^{13}C NMR** (151 MHz, $CDCl_3$): δ 22.43 (Me), 101.96 (C-2′), 115.43 (C-3), 129.03 (C-4′), 129.86 (C-6′), 130.48 (C-2), 136.60 (C-3′), 137.33 (C-1), 138.19 (C-1′), 145.99 (C-6′), 154.91 (C-4). **IR (ATR film) [cm^{-1}]:** 3336 (broad), 1610, 1511, 1435, 1229, 1168, 1129, 809, 771, 565. **TLC** (petroleum ether:EtOAc 7:3 v/v): R_f = 0.5 **APCI-MS:** m/z: ([M^+]): found: 310.1. ([M - I^-]): found: 183.2 **Melting point:** 106 °C – 111 °C.

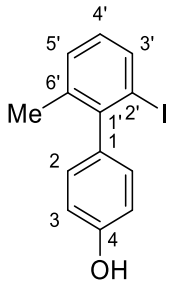

345

7.2.13.2 1-Iodo-4-methoxy-2-methylbenzene (354)

A round bottom flask equipped with stir bar was charged with $FeCl_3$ (33 mg, 5 mol%, 0.20 mmol) and NIS (1.01 g, 1.10 equiv, 4.50 mmol) CH_2Cl_2 (2 mL, 2 M). The mixture was cooled to -78°C and 1-methoxy-3-methylbenzene (515 µL, 1.00 equiv, 4.09 mmol) was added. The mixture was stirred for 2 h. Then n-pentane (5 mL) and H_2O (5 mL) were added. The aq. phase was extracted with petroleum ether (3x) and the combined organic phases dried over $MgSO_4$. The product was obtained by recrystallization from *n*-pentane (0.2 mL g^{-1}) as white

solids in a yield of 894 mg (3.60 mmol, 88%). The analytical data were in accordance with literature.[343]

^{1}H NMR (600 MHz, $CDCl_3$): δ 2.40 (s, 3H, Me), 3.77 (s, 3H, OMe), 6.48 (dd, $^3J_{5\text{-}6}$ = 8.7 Hz, $^4J_{5\text{-}3}$ = 3.0 Hz, 1H, 5-H), 6.82 (d, $^4J_{3\text{-}5}$ = 3.0 Hz, 1H, 3-H), 7.66 (d, $^3J_{6\text{-}5}$ = 8.6 Hz, 1H, 6-H). **^{13}C NMR** (151 MHz, $CDCl_3$): δ 28.37 (Me), 55.45 (OMe), 89.79 (C-1), 113.51 (C-5), 116.01 (C-3), 139.47 (C-6), 142.51 (C-2), 160.04 (C-4). **IR (ATR film) [cm^{-1}]:** 2999, 2954, 1589, 1568, 1471, 1290, 1238, 1163, 1056, 1012, 844, 798, 590. **TLC** (petroleum ether:EtOAc 8:2 v/v): R_f = 0.63 **APCI-MS:** m/z: ([M + H$^+$]): found: 248.0 **Melting point:** 43 – 45 °C. (43 – 45 °C)[344] **Boiling point:** 105 °C (2·10^{-1} mbar) (129 – 130 °C (16 mbar))[345]

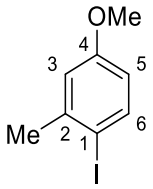

354

7.2.13.3 5,5'-Dibromo-4,4'-dimethoxy-6,6'-dimethyl-[1,1'-biphenyl]-2,2'-diol (355)

A vial equipped with stir bar was charged with biphenol **27** (50.0 mg, 1.00 equiv, 0.182 mmol), CH_2Cl_2 (600 µL, 0.33 M) and dissolved by sonication. Then NBS (66.2 mg, 2.04 equiv, 0.365 mmol) was added at 0 °C and the reaction stirred at 22 °C for 8 h. Sat. aq. Na_2SO_3 solution was added. The aq. phase was extracted with CH_2Cl_2 (3x), and the combined organic phases washed with sat. aq. NaCl solution, dried over $MgSO_4$ and solvents removed in vacuo. The product was isolated as white solids in a yield of 35.4 mg (81.9 µmol, 46%).

^{1}H NMR (600 MHz, $CDCl_3$): δ 2.10 (s, 6H, Me), 3.92 (s, 6H, OMe), 4.79 (s, 2H, OH), 6.56 (s, 2H, 3-H). **^{13}C NMR** (151 MHz, $CDCl_3$): δ 20.61 (Me), 31.08, 56.51 (OMe), 97.87 (C-3), 106.35 (C-5), 112.49 (C-1), 140.10 (C-6), 154.45 (C-2), 157.74 (C-4). **IR (ATR film) [cm^{-1}]:** 3475, 3012, 2941, 2842, 1602, 1565, 1444, 1414, 1339, 1220, 1157, 1099, 1035, 937, 827, 724, 624, 523. **TLC** (petroleum ether:EtOAc 7:3 v/v): R_f = 0.31 **HR-MS (ESI):** m/z calculated for $[C_{16}H_{17}Br_2O_4]^+$ ([M + H$^+$]): 430.9488, found: 430.9488. **Melting point:** 205 °C (decomposition, starts turning grey).

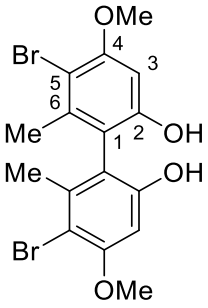

355

Unsuccessful syntheses

7.2.13.4 Synthesis of methyl 3-(((S)-1-phenylethyl)carbamoyl)-7-oxabicyclo[2.2.1]hepta-2,5-diene-2-carboxylate (302)

A vial equipped with stir bar was charged with oxabicycle **301** (39.2 mg, 1.0 equiv, 0.200 mmol, *rac*), (*S*)-(−)-*α*-methylbenzylamine (28.4 µL, 1.1 equiv, 0.220 mmol, 99%*ee*) and anhydr. DMF (1.82 mL, 0.11 M). DMAP (61.1 mg, 2.5 equiv, 0.500 mmol) and N-(3-Dimethylaminopropyl)-N′-ethylcarbodiimide (EDC) (76.6 mg, 2.0 equiv, 0.400 mmol) were added in this order and the reaction stirred at 22 °C for 14 h. Reaction control was performed by TLC (70:30/pentanes:EtOAc). Water (5 mL) and CH_2Cl_2 (15 mL) were added. The organic phase was separated, washed with cold water (2x 10 mL), sat. aq. NaCl-solution and dried over $MgSO_4$. No product formation could be observed by ^{1}H NMR and TLC.

A vial equipped with stir bar was charged with CDI (32.4 mg, 1.0 equiv, 0.200 mmol) and anhydr. THF (0.25 mL, 0.8 M). Oxabicycle **301** (39.2 mg, 1.0 equiv, 0.200 mmol, *rac*) was added and the reaction mixture stirred for 90 min. Then a solution of (*S*)-(−)-*α*-methylbenzylamine (28.4 µL, 1.1 equiv, 0.220 mmol, 99%*ee*) in anhydr. THF (0.83 mL, 0.27 M) was added dropwise. The reaction was stirred at 22 °C for 14 h. Reaction control was performed by TLC (70:30/pentanes:EtOAc). H_2O (5 mL) and CH_2Cl_2 (15 mL) were added. The organic phase was separated, washed with sat. aq. NaCl-solution and dried over $MgSO_4$. No product formation could be observed by ^{1}H NMR and TLC.

A vial equipped with stir bar was charged with oxabicycle **301** (39.2 mg, 1.0 equiv, 0.200 mmol, *rac*), (*S*)-(−)-*α*-methylbenzylamine (28.4 µL, 1.1 equiv, 0.220 mmol, 99%*ee*) and anhydr. THF (8.7 mL, 0.023 M). The mixture was cooled to 0 °C, DCC (41.3 mg, 4.0 equiv, 0.800 mmol) was added and the reaction stirred at 22 °C for 14 h. Reaction control was performed by TLC (70:30/pentanes:EtOAc). Water (5 mL) and CH_2Cl_2 (15 mL) were added. The organic phase was separated, washed with cold water (2x 10 mL), sat. aq. NaCl-solution and dried over $MgSO_4$. No product formation could be observed by ^{1}H NMR and TLC.

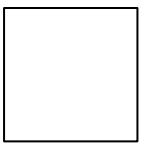

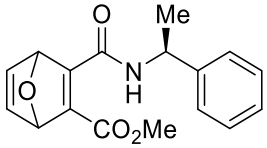

302

7.2.13.5 Synthesis of methyl 4-hydroxy-4-phenylbut-2-ynoate (364)

A flame dried 50 mL round bottom flask was charged with LiHMDS in THF (1 M, 5.50 mL, 1.1 equiv, 5.50 mmol) and cooled to -78 °C. Methyl propiolate (444 µL, 1.0 equiv, 5.00 mmol) was added dropwise and the reaction stirred for 1 h. Benzaldehyde (561 µL, 5.5 equiv, 5.50 mmol) was added dropwise and the reaction stirred for 2 h. The solvent was removed in vacuo. No product formation could be observed by ^{1}H NMR and TLC.

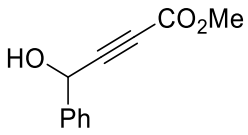

364

7.2.13.6 Synthesis of (1*R*,4*S*)-N^2-benzhydryl-N^3,N^3-dimethyl-7-oxabicyclo[2.2.1]hepta-2,5-diene-2,3-dicarboxamide (356)

A solution of dimethylamine in THF was prepared by dissolving dimethylamine hydrochloride (23.2 mg, 2.26 equiv, 0.284 mmol) in THF (2.84 mL, 0.1 M). K_2CO_3 (23.2 mg, 4.52 equiv, 0.568 mmol) was added and the resulting mixture stirred for 5 min. Solids were filtered off over a cotton plug.

A 2-dr. vial was charged with oxabicycle **351** (43.7 mg, 1.0 equiv, 0.126 mmol) and THF (0.08 M, 1.5 mL). The solution was cooled to 0 °C, dimethyl amine in THF (1.42 mL, 0.1 M, 1.13 equiv, 0.142 mmol) added and the mixture stirred for 5 min. DMTMM (23.1 mg, 1.13 equiv, 0.142 mmol) was added at once. The mixture was left to stir for 16 h at 0 °C and left to warm to 22 °C. Full consumption of starting material was observed yet no product formation could be observed by ^{1}H NMR and APCI MS.

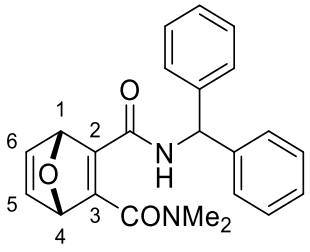

356

7.2.13.7 Synthesis of methyl (1S,4R)-3-phenyl-7-oxabicyclo[2.2.1]hepta-2,5-diene-2-carboxylate (327)

A 2 d.r. vial was charged with an aq. solution of sodium carbonate (2 M, 788 µL, 2.00 equiv, 1.58 mmol), phenyl boronic acid (144 mg, 1.50 equiv, 1.18 mmol), triphenylphosphine (41.3 mg, 20 mol%, 0.158 mmol) and $Pd(OAc)_2$ (8.9 mg, 5 mol%, 39.4 µmol). A separate vial was charged with oxabicycle **329** (182 mg, 1.00 equiv, 0.788 mmol) and toluene (3.94 mL, 0.20 M) and that solution added to vial 1. Ethanol (56 µL, 1.54 equiv, 1.21 mmol) was added, the vial sealed, and the reaction mixture stirred at 80 °C for 16 h (900 rpm). No product formation could be observed by ^{1}H NMR, APCI MS and TLC. A major side product was observed.

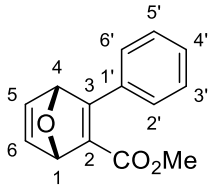

327

7.2.13.8 Synthesis of methyl (1S,4R)-3-(trifluoromethyl)-7-oxabicyclo[2.2.1]hepta-2,5-diene-2-carboxylate (357)

A dry 2 dr. vial equipped with stir bar was charged with oxabicycle **301** (19.6 mg, 1.0 equiv, 0.100 mmol), PPh_3 (36.7 mg, 1.4 equiv, 0.140 mmol) and anhydrous THF (0.5 mL, 0.2 M). The reaction mixture was cooled to 0 °C and NBS (26.7 mg, 1.5 equiv, 0.150 mmol) was added in one portion. The reaction mixture was stirred at 22 °C for 15 mins. A separate dry vial equipped with stir bar was charged with CuI (38.1 mg, 2.0 equiv, 0.200 mmol), flame dried CsF (22.8 mg, 1.5 equiv, 0.150 mmol) and THF (0.5 mL). Freshly distilled $TMSCF_3$ (37.0 µL, 2.5 equiv, 0.250 mmol) was added and the mixture stirred at 22 °C for 10 mins (500 rpm). The contents of vial 1 were transferred to vial 2. The reaction mixture was stirred at 22 °C for 1 h. The mixture was diluted with *n*-pentane (2 mL). The crude mixture was filtered over a pad of Celite® flushing with EtOAc. The solvent was removed in vacuo. No product formation could be observed by ^{1}H NMR, ^{19}F NMR, APCI MS and TLC.

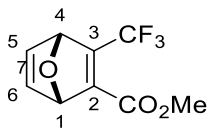

357

7.2.13.9 Resolution attempt of 3-(methoxycarbonyl)-7-oxabicyclo[2.2.1]hepta-2,5-diene-2-carboxylic acid (301)

A scintillation vial was charged with oxabicycle **301** (130 mg, 1.0 equiv, 0.660 mmol) and THF (10 mL). Then (*S*)-(-)-α-methylbenzylamine (85.0 µL, 1.0 equiv, 0.660 mmol) was added and stirred for 1 min. The forming solids were filtered off and washed with THF (20 mL). The solids were then dissolved in CH_2Cl_2 (20 mL). Dilute aq. HCl was added and the mixture stirred until all solids were dissolved. The org. phase was washed with dilute aq. HCl (2 x 10 mL), sat. aq. NaCl-solution and the organic phase dried over $MgSO_4$. Solvents were removed in vacuo and the product obtained as an off-white solid in a yield of 50.6 mg. (No RP column available, all normal phase columns available incompatible with carboxylic acids, thus only indirect determination of *ee* possible).

To determine the *ee*, the product was subjected to amide coupling according to **GP**9 with *(S)*-(-)-a-methylbenzylamine to provide a mixture of diastereomers. The product was obtained as a mixture of tautomers as a pale-yellow oil in a yield of 37.7 mg (63%) with a d.r. of 1:1. Thus little to no resolution was achieved (compare ratio to 7.2.12.2.3 Mixtures of **302** and **303**).

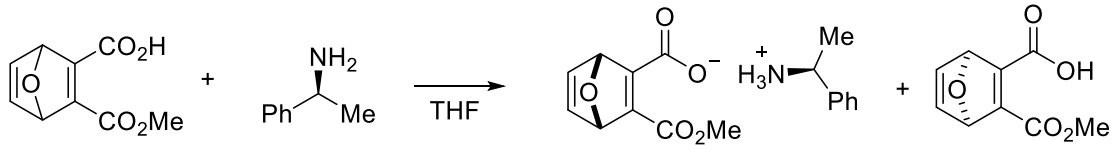

7.2.13.9.1.1 Synthesis of 7'-methyl-4'-morpholinospiro[cyclohexane-1,1'-indene]-2,5-dien-4-one

Following the reagent order outlined in **GP12** a reaction was set up with Cs_2CO_3 (104 mg, 3.2 equiv, 0.320 mmol), aryl iodide **345** (31.0 mg, 1.00 equiv, 0.100 mmol), *O*-benzoyl hydroxylamine **342** (41.4 mg, 2.0 equiv, 0.200 mmol), oxabicycle **296** (31.5 mg, 1.5 equiv, 0.150 mmol), $Pd(OAc)_2$ (2.3 mg, 10 mol%, 0.010 mmol), $Cy_3P{\cdot}HBF_4$ (7.4 mg, 20 mol%, 0.020 mmol) and PhMe (1.00 mL, 0.10 M). No product was obtained.

Following the reagent order outlined in **GP12** a reaction was set up with Cs_2CO_3 (97.7 mg, 3.0 equiv, 0.300 mmol), aryl iodide **345** (31.0 mg, 1.00 equiv, 0.100 mmol), *O*-benzoyl hydroxylamine **342** (41.4 mg, 2.0 equiv, 0.200 mmol), oxabicycle **296** (31.5 mg, 1.5 equiv, 0.150 mmol), $Pd(OAc)_2$ (2.3 mg, 10 mol%, 0.010 mmol), $(4\text{-}OMeC_6H_4)_3P{\cdot}HBF_4$ (8.8 mg, 25 mol%, 0.025 mmol) and 1,2-dimethoxyethane (glyme) (1.00 mL, 0.10 M). No product was obtained.

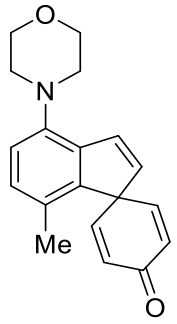

343

7.2.13.9.1.2 Synthesis of methyl 4-hydroxy-4-phenylbut-2-ynoate

A dry 25 mL round bottom flask was charged with methyl propiolate (**320**) (444 µL, 1.0 equiv, 5.54 mmol). The round bottom flask was cooled to -78 °C and a solution of LiHMDS in THF (1 M, 5.5 mL, 1.0 equiv, 5.5 mmol) was added dropwise. The mixture was stirred for 1 h. Then benzaldehyde (561 µL, 1.1 equiv, 6.05 mmol) was added and the reaction mixture stirred for 2 h at -78 °C. The reaction mixture was then left to warm to room temperature. Aq. dilute HCl-solution was added, and the aq. phase extracted with EtOAc. No product could be obtained.

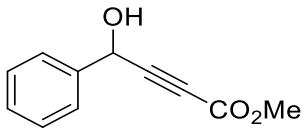

343

7.3 HPLC Chromatograms

7.3.1 Silylation

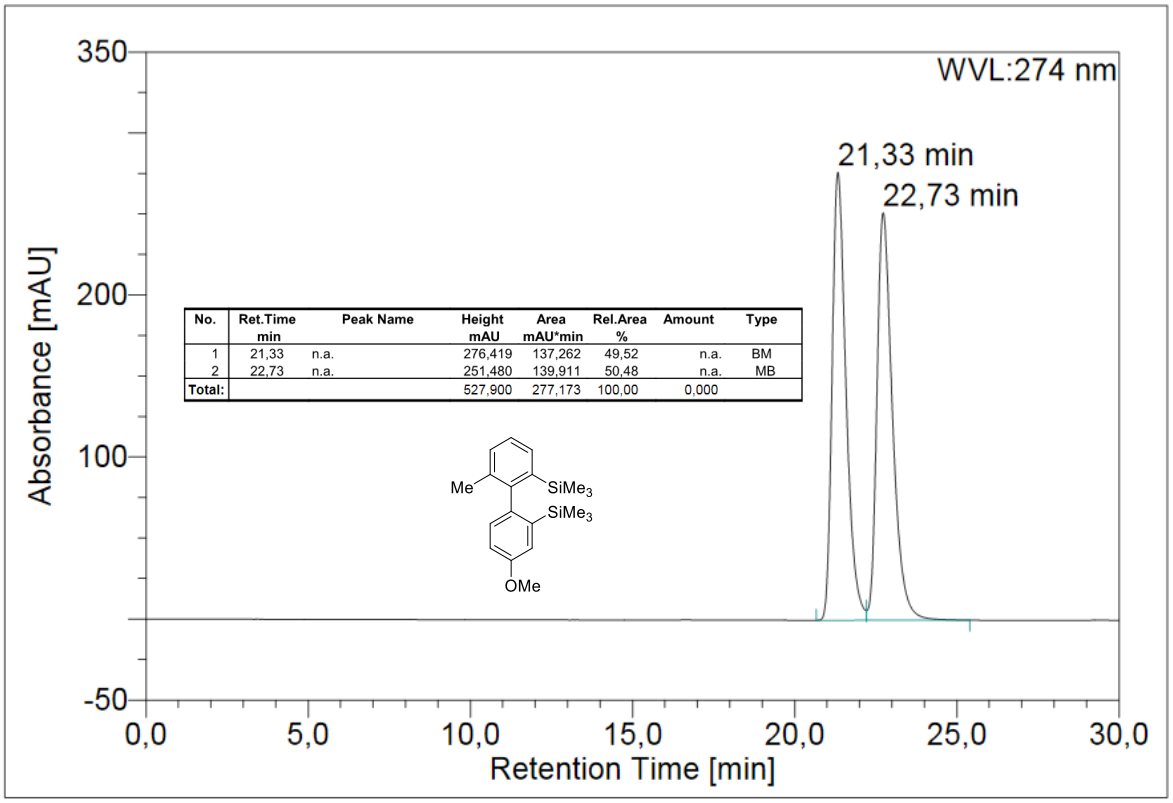

No.	Ret.Time min	Peak Name	Height mAU	Area mAU*min	Rel.Area %	Amount	Type
1	21,33	n.a.	276,419	137,262	49,52	n.a.	BM
2	22,73	n.a.	251,480	139,911	50,48	n.a.	MB
Total:			527,900	277,173	100,00	0,000	

Figure 31: HPLC Chromatogram of biaryl **292** (*rac*) CHIRALCEL® OD-H 250 ° 4.6 mm, 10 °C, 0.5 mL min^{-1}, 254 nm, *n*-heptane:*i*-PrOH 95:5 (v/v).

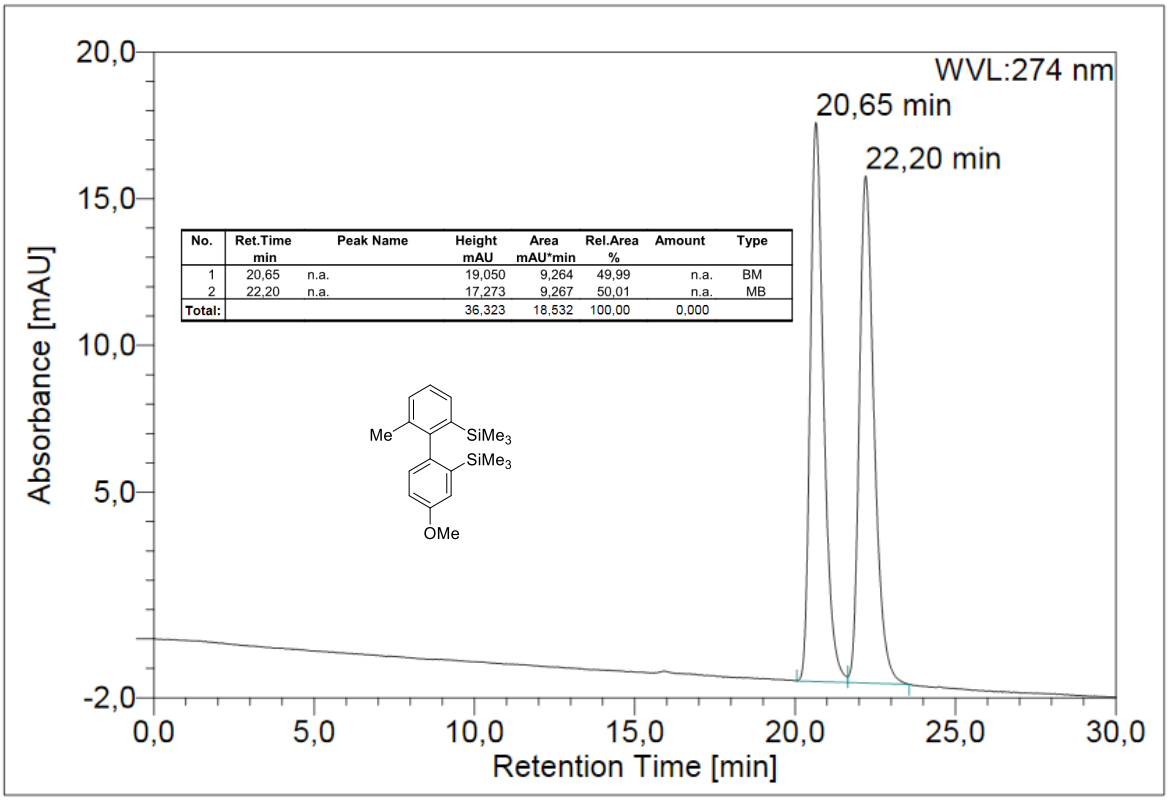

No.	Ret.Time min	Peak Name	Height mAU	Area mAU*min	Rel.Area %	Amount	Type
1	20,65	n.a.	19,050	9,264	49,99	n.a.	BM
2	22,20	n.a.	17,273	9,267	50,01	n.a.	MB
Total:			36,323	18,532	100,00	0,000	

Figure 32: HPLC Chromatogram of synthesis of biaryl **292** using (*S*)-BIDIME. CHIRALCEL® OD-H 250 ° 4.6 mm, 10 °C, 0.5 mL min^{-1}, 254 nm, *n*-heptane:*i*-PrOH 95:5 (v/v).

7.3.2 Chiral flavonoids via cyclic diaryl iodonium salt

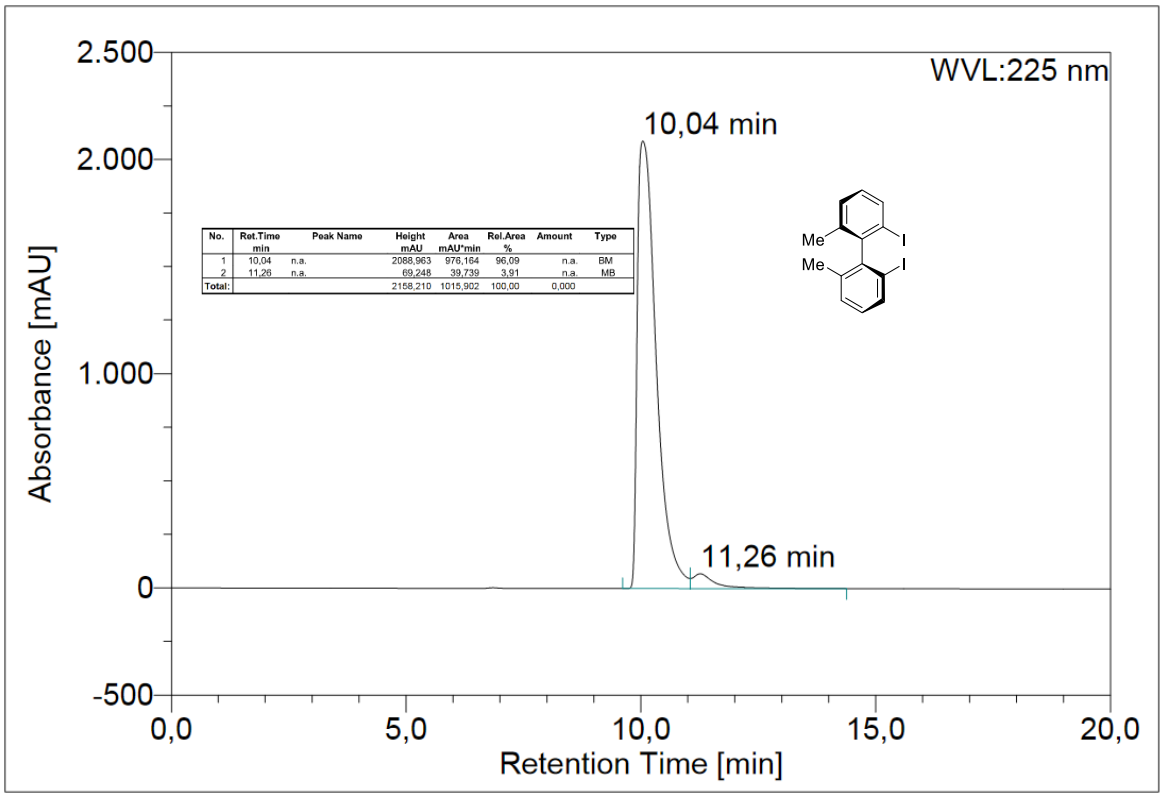

No.	Ret.Time min	Peak Name	Height mAU	Area mAU*min	Rel.Area %	Amount	Type
1	10,04	n.a.	2088,963	976,164	96,09	n.a.	BM
2	11,26	n.a.	69,248	39,739	3,91	n.a.	MB
Total:			2158,210	1015,902	100,00	0,000	

Figure 33: HPLC Chromatogram of biaryl **246** 92%*ee* (S_a). Chiralpak® IC (Daciel) 250 ° 4.6 mm, 25 °C, 0.5 mL min-1, 225 nm, n-heptane:i-PrOH 99.9:0.1 (v/v) tR(Sa) = 10.0 min, tR(Ra) = 11.1 min.

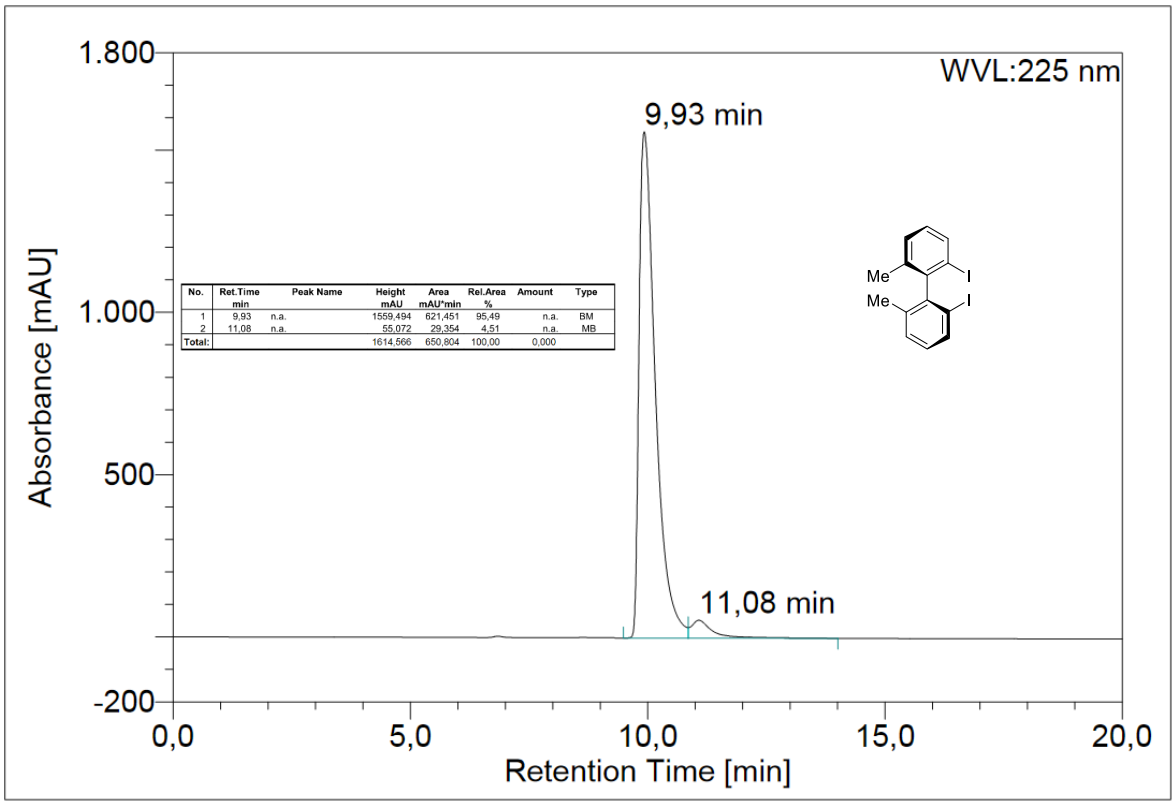

No.	Ret.Time min	Peak Name	Height mAU	Area mAU*min	Rel.Area %	Amount	Type
1	9,93	n.a.	1559,494	621,451	95,49	n.a.	BM
2	11,08	n.a.	55,072	29,354	4,51	n.a.	MB
Total:			1614,566	650,804	100,00	0,000	

Figure 34: HPLC Chromatogram of biaryl **246** 91%*ee* (S_a) Chiralpak® IC (Daciel) 250 ° 4.6 mm, 25 °C, 0.5 mL min-1, 225 nm, n-heptane:i-PrOH 99.9:0.1 (v/v) tR(Sa) = 10.0 min, tR(Ra) = 11.1 min.

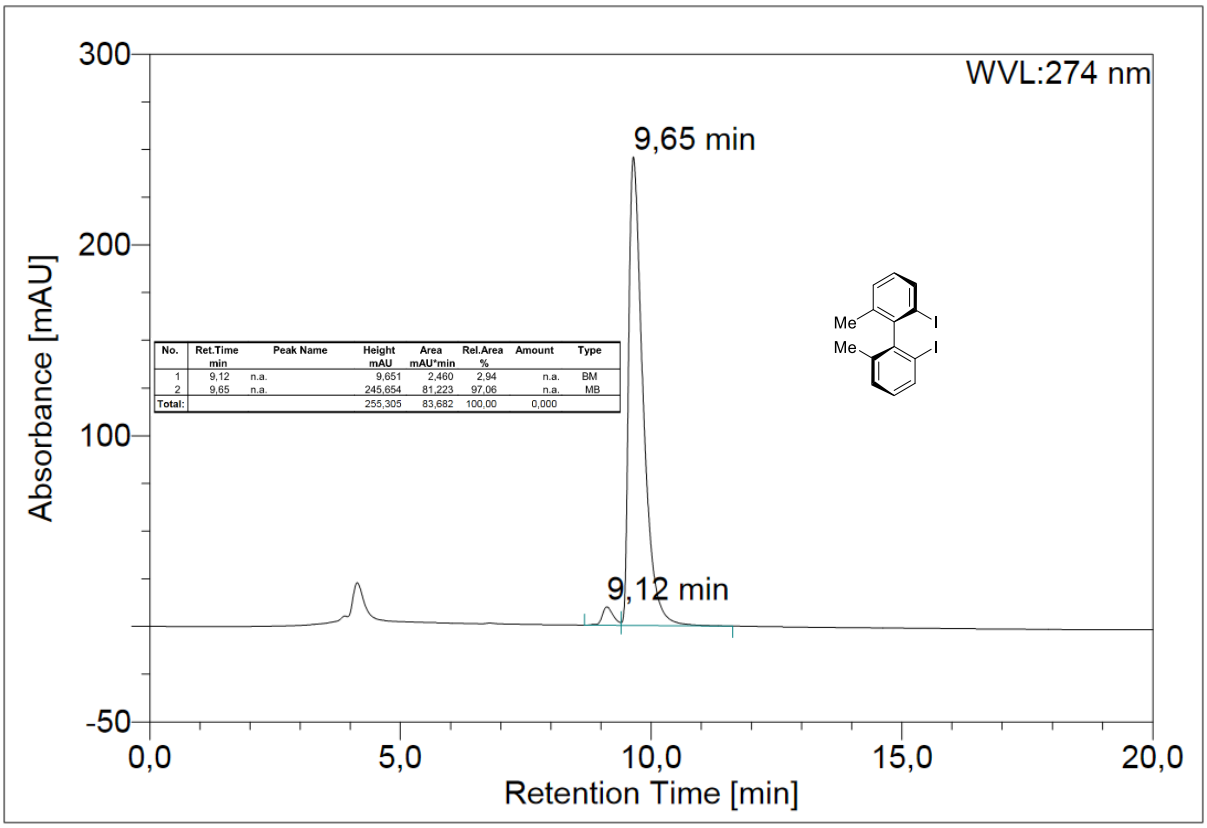

Figure 35: HPLC Chromatogram of biaryl **246** 94%*ee* (R_a). Chiralpak® IC (Daciel) 250 ° 4.6 mm, 25 °C, 0.5 mL min-1, 225 nm, n-heptane:i-PrOH 99.9:0.1 (v/v) tR(Sa) = 10.0 min, tR(Ra) = 11.1 min.

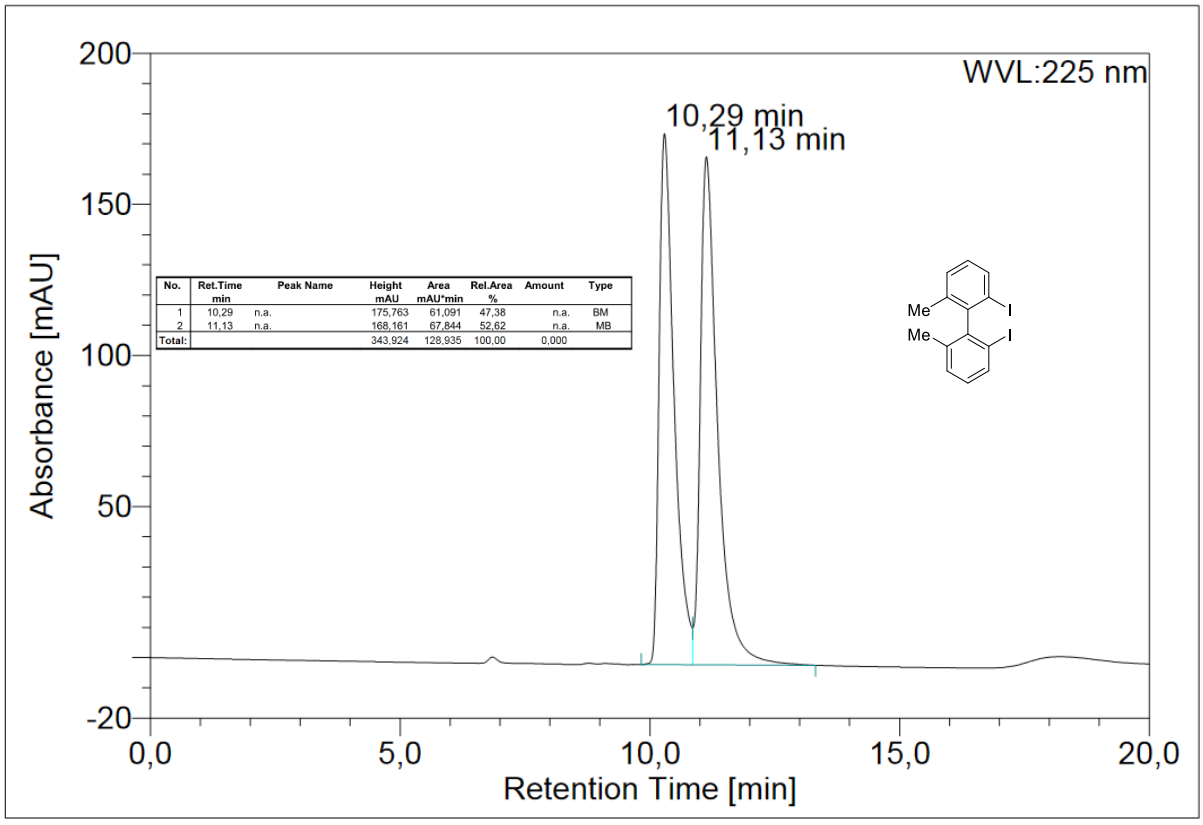

Figure 36: HPLC Chromatogram of biaryl *rac*-**238**. Chiralpak® IC (Daciel) 250 ° 4.6 mm, 25 °C, 0.5 mL min-1, 225 nm, n-heptane:i-PrOH 99.9:0.1 (v/v) tR(Sa) = 10.0 min, tR(Ra) = 11.1 min.

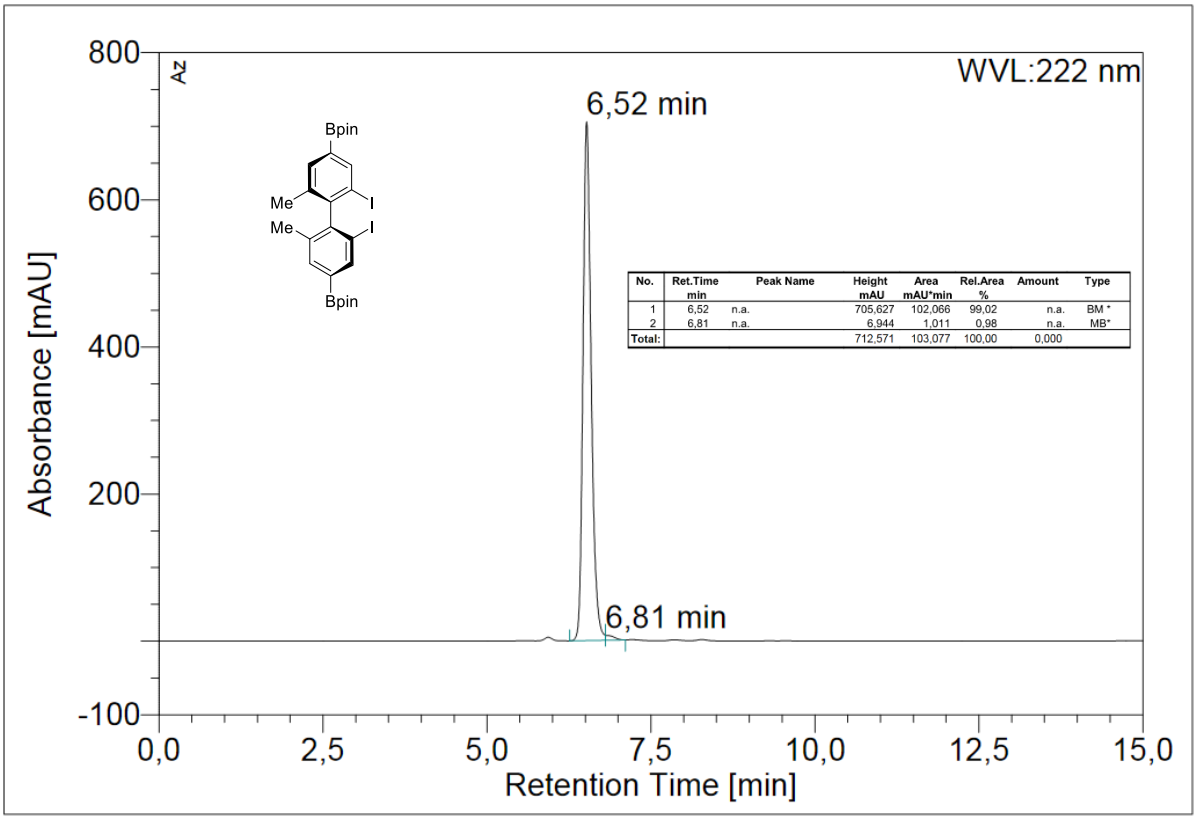

Figure 37: HPLC Chromatogram of biaryl **239** 98%*ee* (S_a). Lux® Amylose-1 (Phenomenex) 250 ° 4.6 mm, 10 °C, 0.5 mL min^{-1}, 222 nm, *n*-heptane:*i*-PrOH 99:1 (v/v) $t_R(S_a)$ = 6.5 min, $t_R(R_a)$ = 6.8 min.

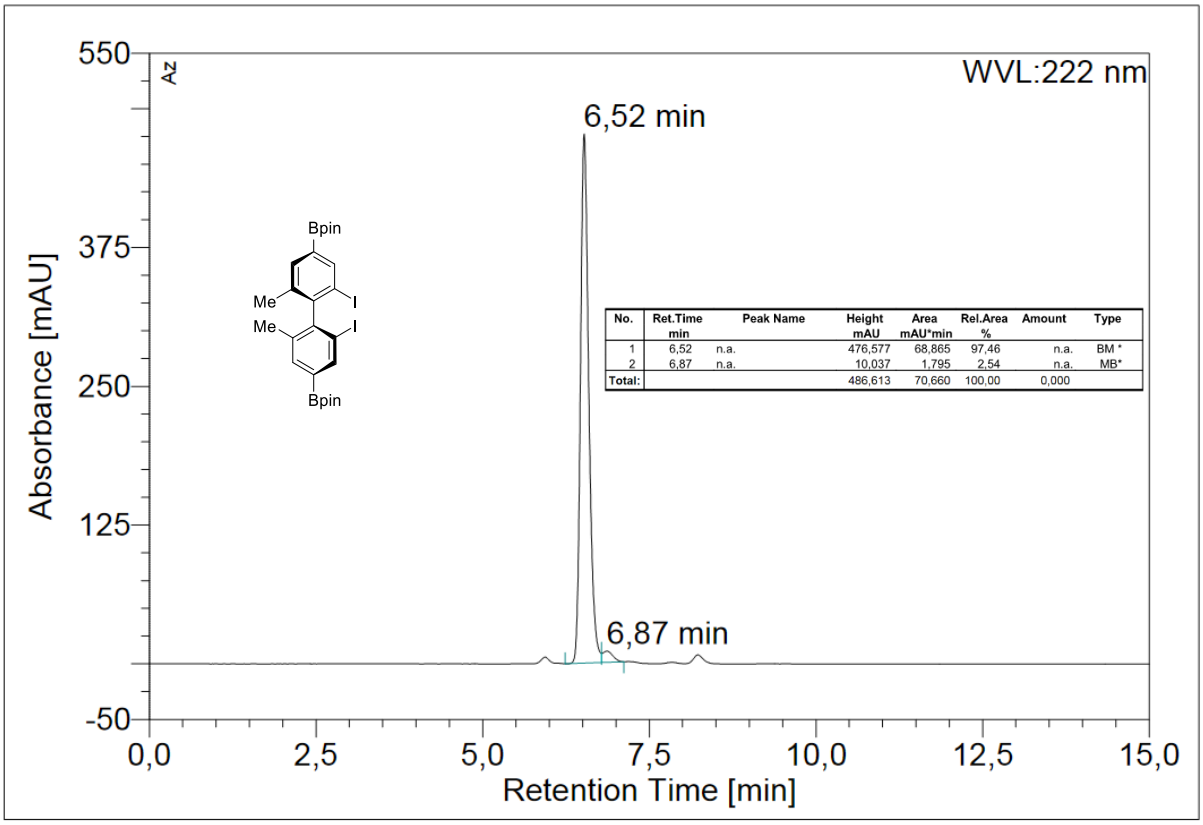

Figure 38: HPLC Chromatogram of biaryl **239** 95%*ee* (S_a). Lux® Amylose-1 (Phenomenex) 250 ° 4.6 mm, 10 °C, 0.5 mL min^{-1}, 222 nm, *n*-heptane:*i*-PrOH 99:1 (v/v) $t_R(S_a)$ = 6.5 min, $t_R(R_a)$ = 6.8 min.

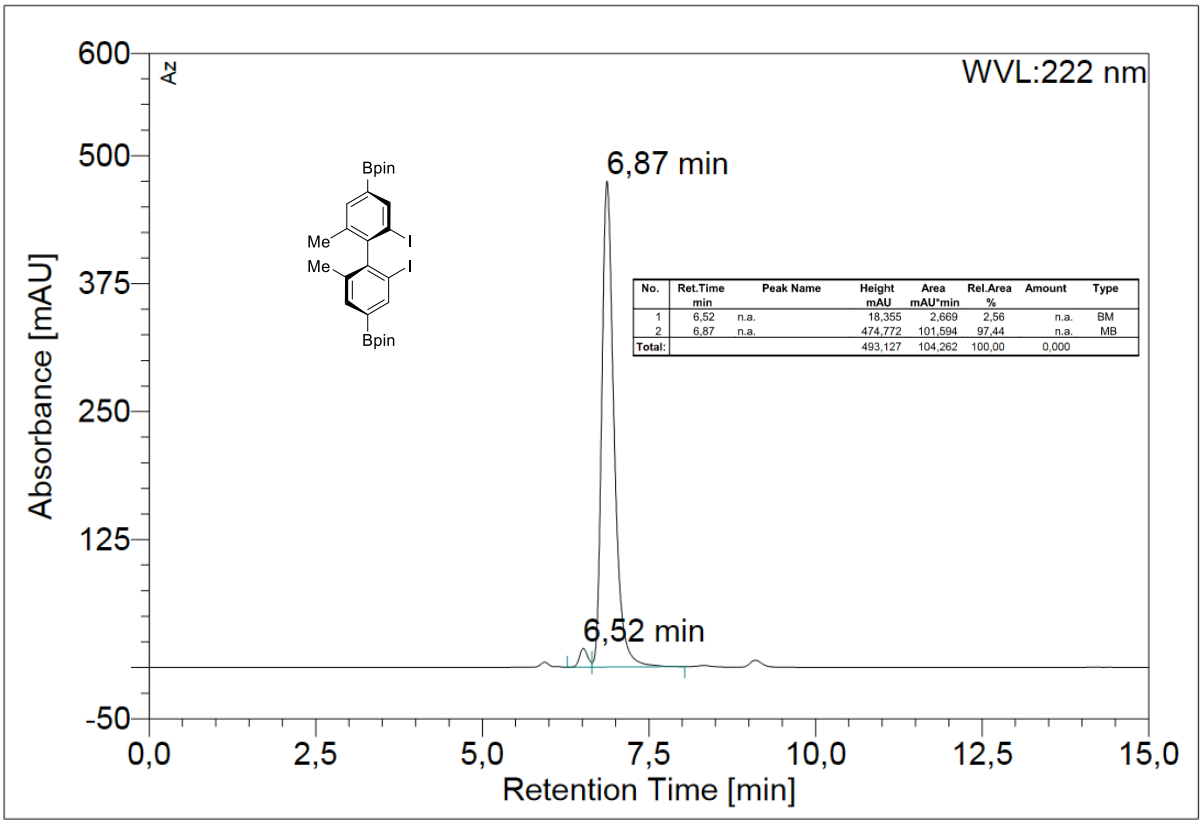

Figure 39: HPLC Chromatogram of biaryl **239** 95%*ee* (R_a). Lux® Amylose-1 (Phenomenex) 250 ° 4.6 mm, 10 °C, 0.5 mL min^{-1}, 222 nm, *n*-heptane:*i*-PrOH 99:1 (v/v) $t_R(S_a)$ = 6.5 min, $t_R(R_a)$ = 6.8 min.

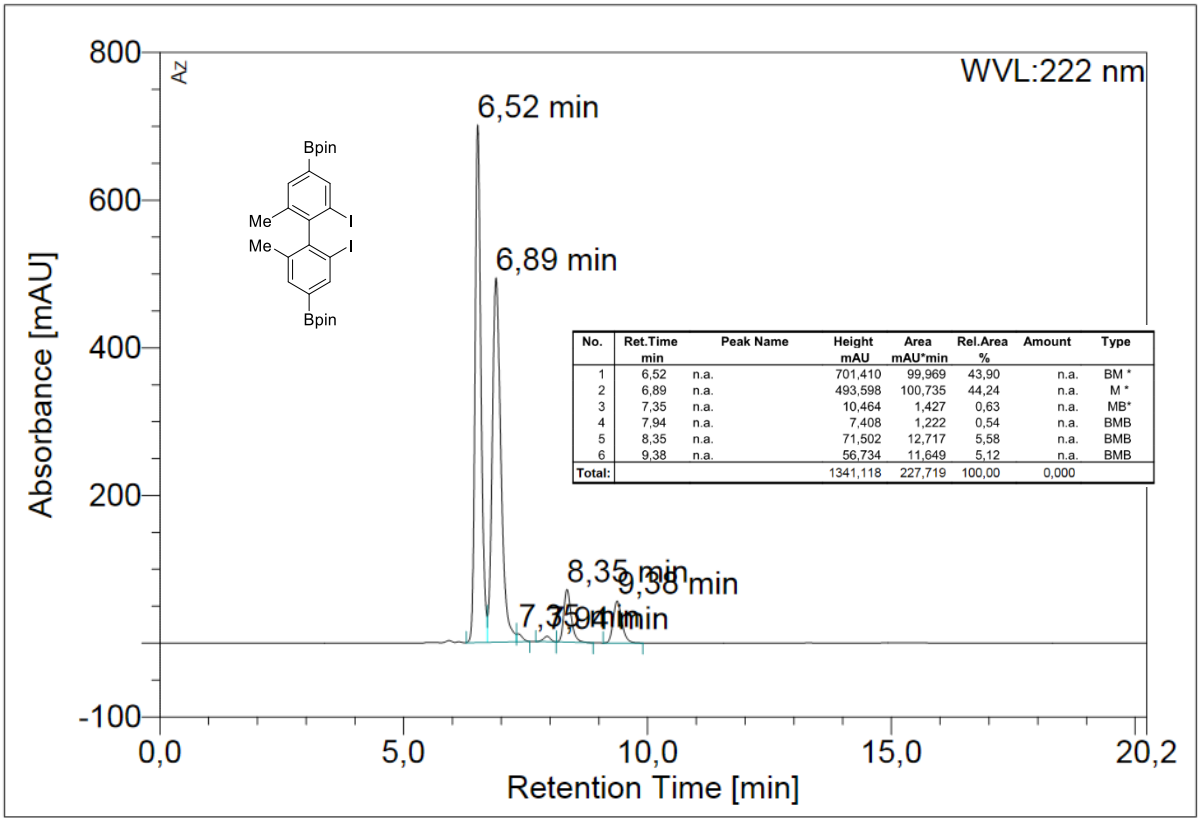

Figure 40: HPLC Chromatogram of biaryl *rac*-**239**. Lux® Amylose-1 (Phenomenex) 250 ° 4.6 mm, 10 °C, 0.5 mL min^{-1}, 222 nm, *n*-heptane:*i*-PrOH 99:1 (v/v) $t_R(S_a)$ = 6.5 min, $t_R(R_a)$ = 6.8 min.

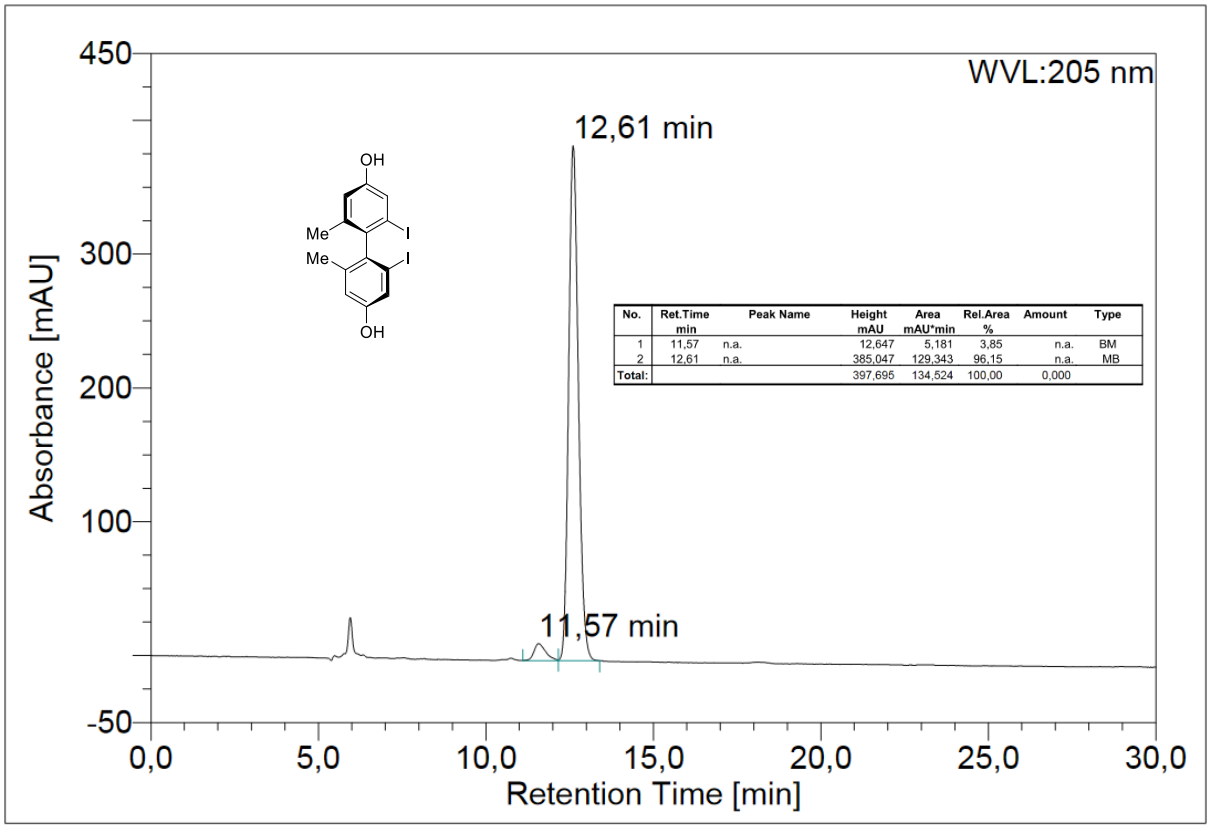

Figure 41: HPLC Chromatogram of biaryl **246** 92%*ee* (S_a). Lux® Amylose-1 (Phenomenex) 250 ° 4.6 mm, 25 °C, 0.5 mL min^{-1}, 205 nm, *n*-heptane:*i*-PrOH 80:20 (v/v) $t_R(S_a)$ = 12.4 min, $t_R(R_a)$ = 11.3 min.

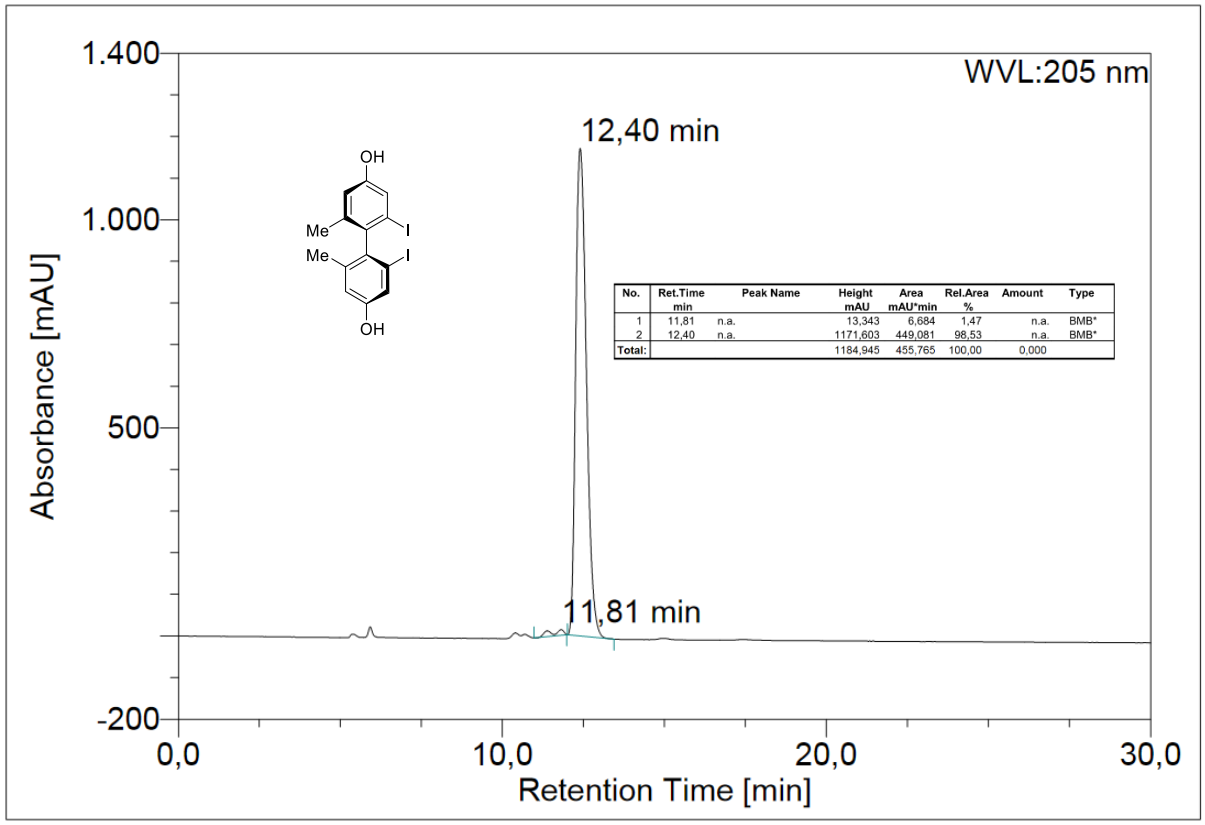

Figure 42: HPLC Chromatogram of biaryl **246** 97%*ee* (S_a). Lux® Amylose-1 (Phenomenex) 250 ° 4.6 mm, 25 °C, 0.5 mL min^{-1}, 205 nm, *n*-heptane:*i*-PrOH 80:20 (v/v) $t_R(S_a)$ = 12.4 min, $t_R(R_a)$ = 11.3 min.

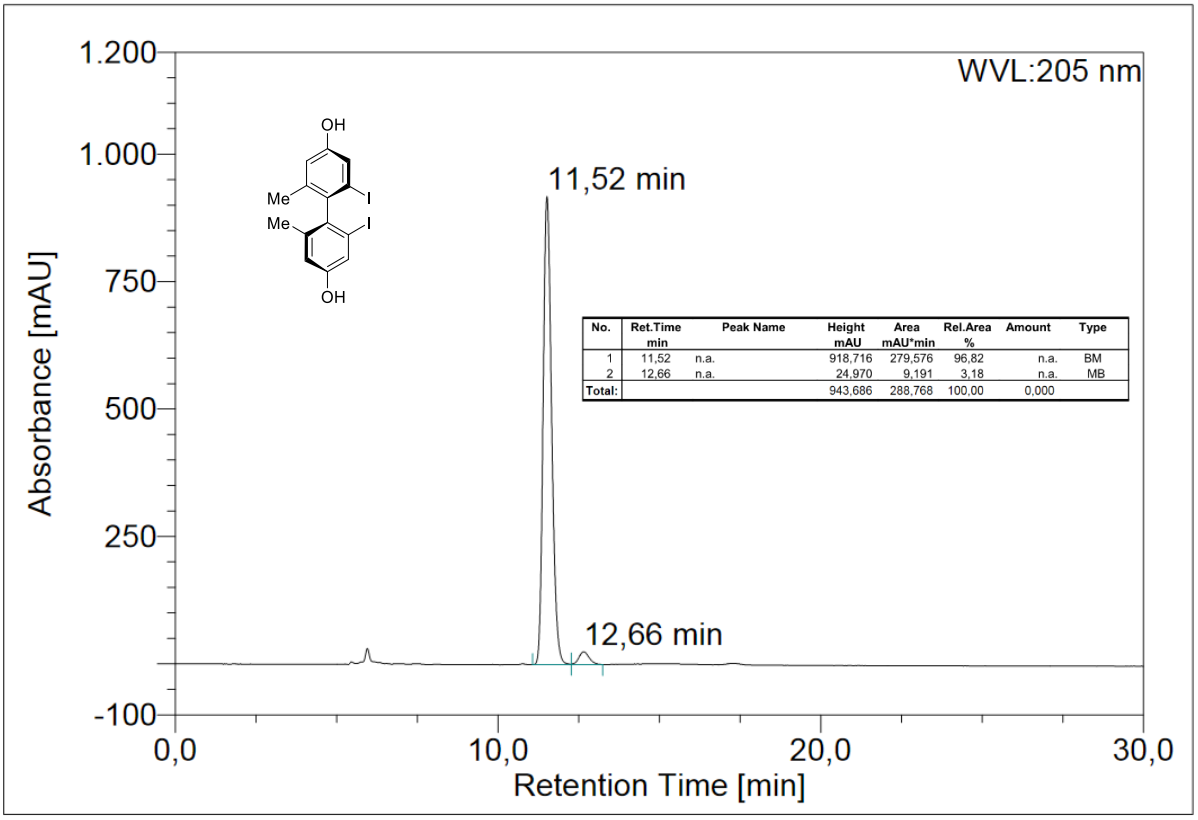

No.	Ret.Time min	Peak Name	Height mAU	Area mAU*min	Rel.Area %	Amount	Type
1	11,52	n.a.	918,716	279,576	96,82	n.a.	BM
2	12,66	n.a.	24,970	9,191	3,18	n.a.	MB
Total:			943,686	288,768	100,00	0,000	

Figure 43: HPLC Chromatogram of biaryl **246** 94%*ee* (R_a). Lux® Amylose-1 (Phenomenex) 250 ° 4.6 mm, 25 °C, 0.5 mL min^{-1}, 205 nm, *n*-heptane:*i*-PrOH 80:20 (v/v) $t_R(S_a)$ = 12.4 min, $t_R(R_a)$ = 11.3 min.

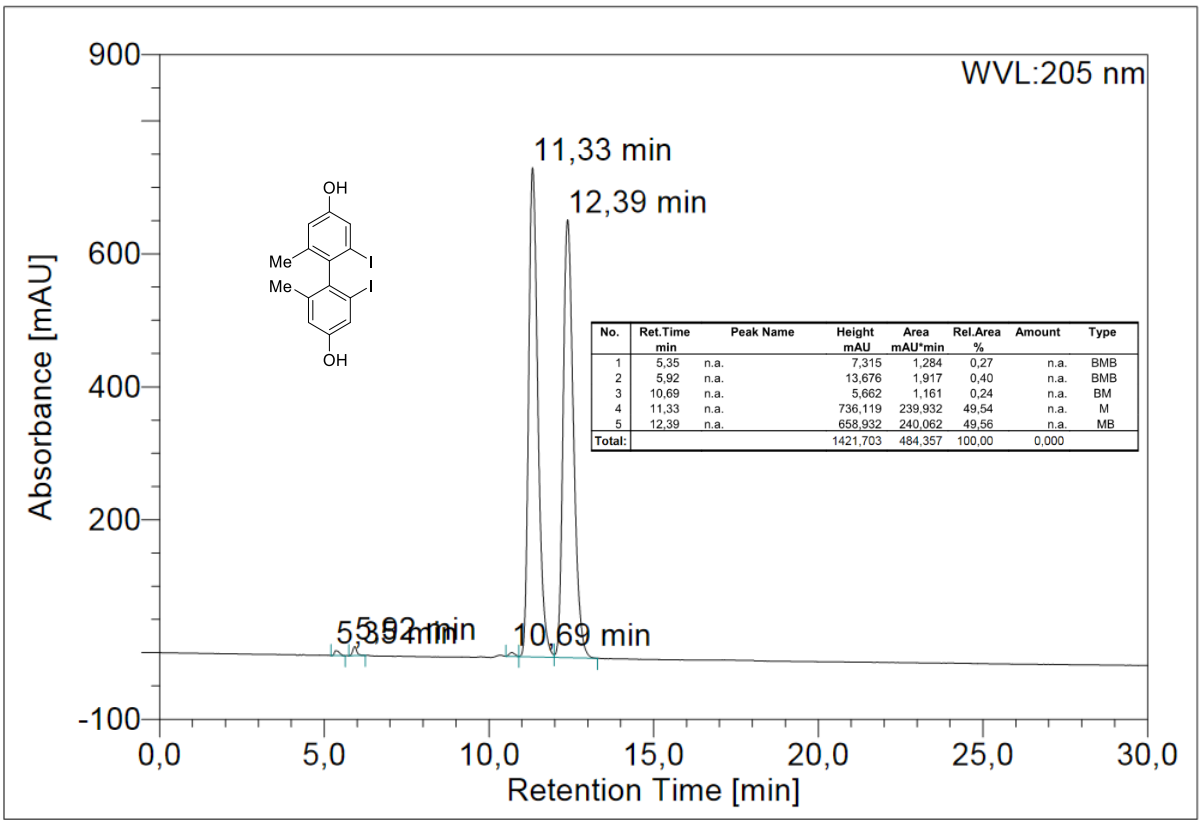

No.	Ret.Time min	Peak Name	Height mAU	Area mAU*min	Rel.Area %	Amount	Type
1	5,35	n.a.	7,315	1,284	0,27	n.a.	BMB
2	5,92	n.a.	13,676	1,917	0,40	n.a.	BMB
3	10,69	n.a.	5,662	1,161	0,24	n.a.	BM
4	11,33	n.a.	736,119	239,932	49,54	n.a.	M
5	12,39	n.a.	658,932	240,062	49,56	n.a.	MB
Total:			1421,703	484,357	100,00	0,000	

Figure 44: HPLC Chromatogram of biaryl *rac*-**246**. Lux® Amylose-1 (Phenomenex) 250 ° 4.6 mm, 25 °C, 0.5 mL min^{-1}, 205 nm, *n*-heptane:*i*-PrOH 80:20 (v/v) $t_R(S_a)$ = 12.4 min, $t_R(R_a)$ = 11.3 min.

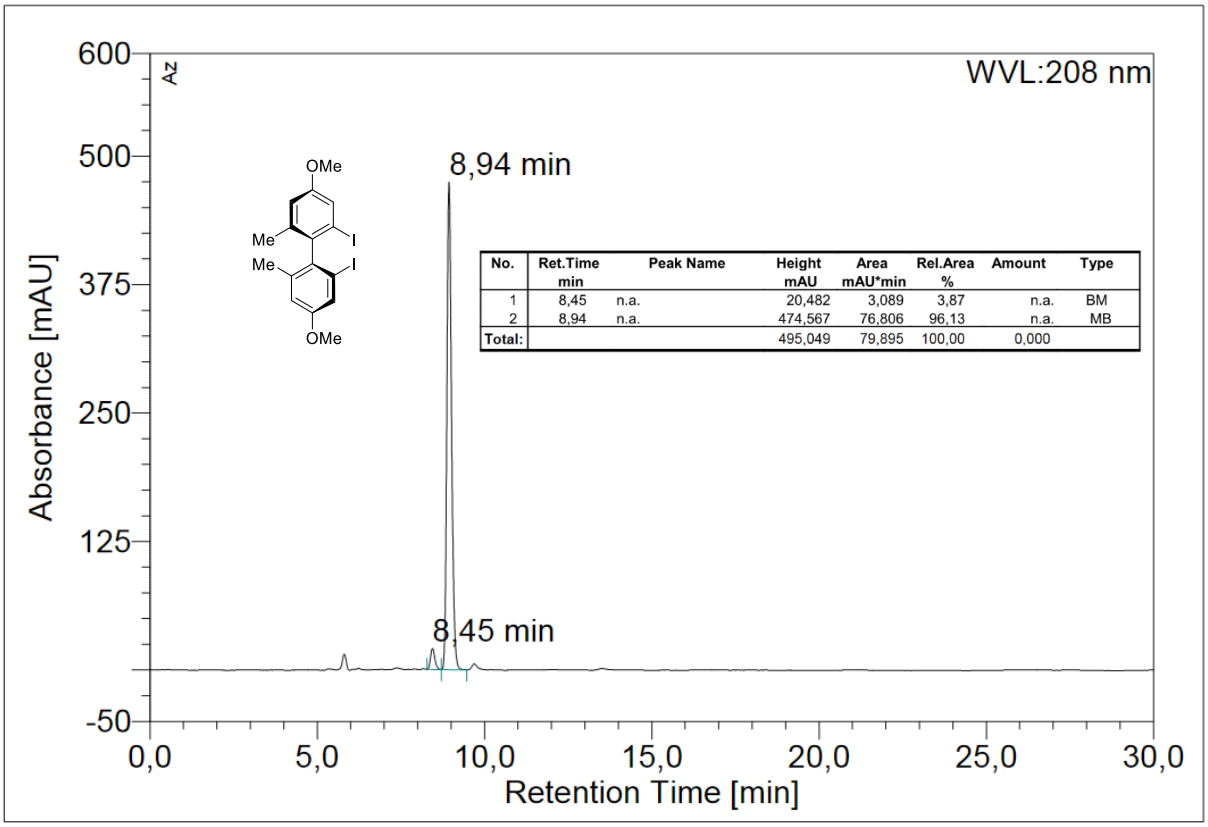

No.	Ret.Time min	Peak Name	Height mAU	Area mAU*min	Rel.Area %	Amount	Type
1	8,45	n.a.	20,482	3,089	3,87	n.a.	BM
2	8,94	n.a.	474,567	76,806	96,13	n.a.	MB
Total:			495,049	79,895	100,00	0,000	

Figure 45: HPLC Chromatogram of biaryl **249** 92%*ee* (S_a). Chiralpak® IC (Daciel) 250 ° 4.6 mm, 25 °C, 0.5 mL min^{-1}, 208 nm, *n*-heptane:*i*-PrOH 99.9:0.1 (v/v) $t_R(S_a)$ = 8.9 min, $t_R(R_a)$ = 8.5 min.

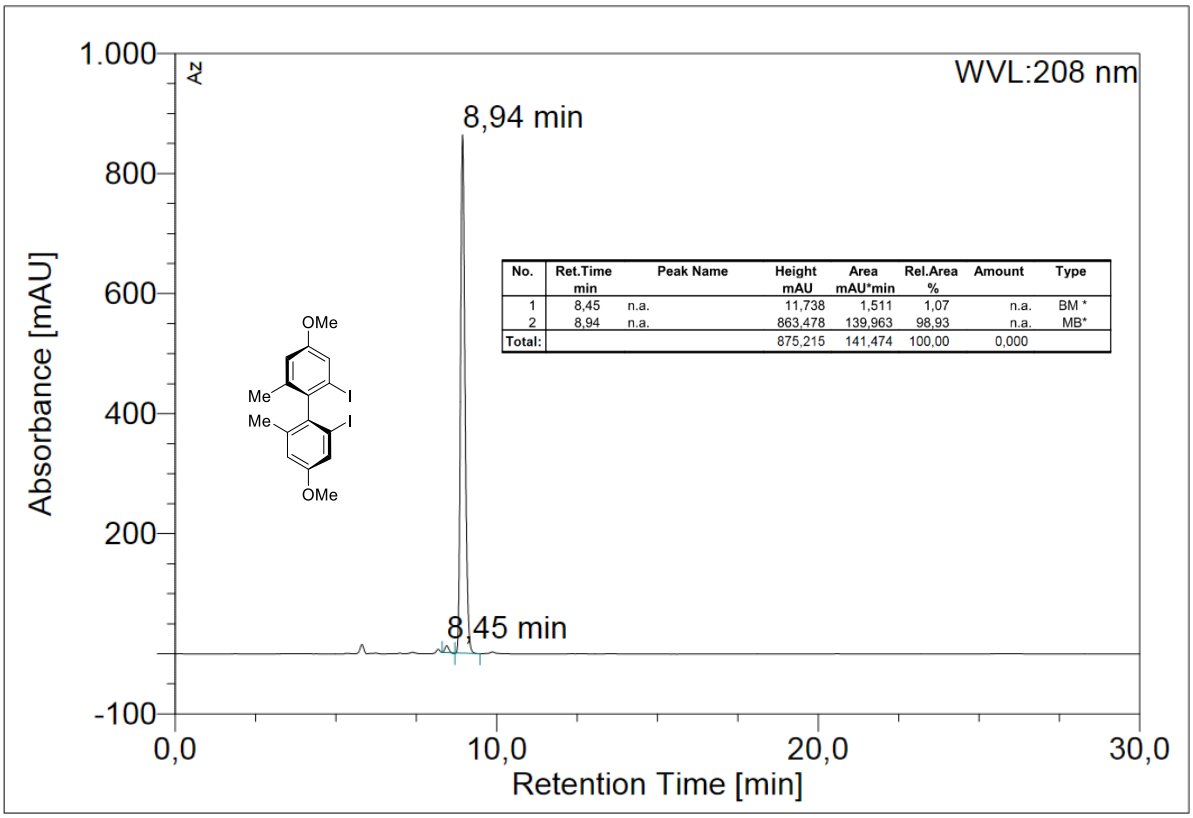

No.	Ret.Time min	Peak Name	Height mAU	Area mAU*min	Rel.Area %	Amount	Type
1	8,45	n.a.	11,738	1,511	1,07	n.a.	BM *
2	8,94	n.a.	863,478	139,963	98,93	n.a.	MB*
Total:			875,215	141,474	100,00	0,000	

Figure 46: HPLC Chromatogram of biaryl **249** 98%*ee* (S_a). Chiralpak® IC (Daciel) 250 ° 4.6 mm, 25 °C, 0.5 mL min^{-1}, 208 nm, *n*-heptane:*i*-PrOH 99.9:0.1 (v/v) $t_R(S_a)$ = 8.9 min, $t_R(R_a)$ = 8.5 min.

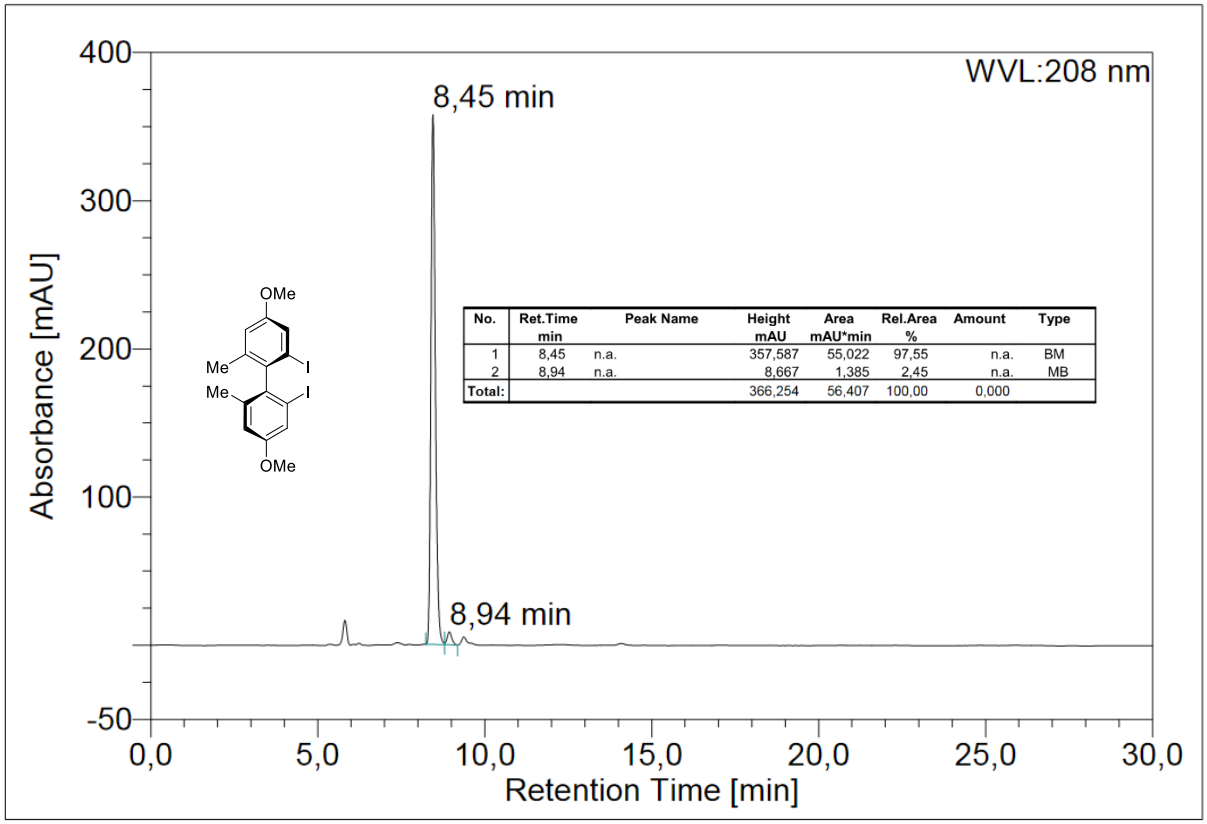

No.	Ret.Time min	Peak Name	Height mAU	Area mAU*min	Rel.Area %	Amount	Type
1	8,45	n.a.	357,587	55,022	97,55	n.a.	BM
2	8,94	n.a.	8,667	1,385	2,45	n.a.	MB
Total:			366,254	56,407	100,00	0,000	

Figure 47: HPLC Chromatogram of biaryl **249** 95%*ee* (R_a). Chiralpak® IC (Daciel) 250 ° 4.6 mm, 25 °C, 0.5 mL min^{-1}, 208 nm, *n*-heptane:*i*-PrOH 99.9:0.1 (v/v) $t_R(S_a)$ = 8.9 min, $t_R(R_a)$ = 8.5 min.

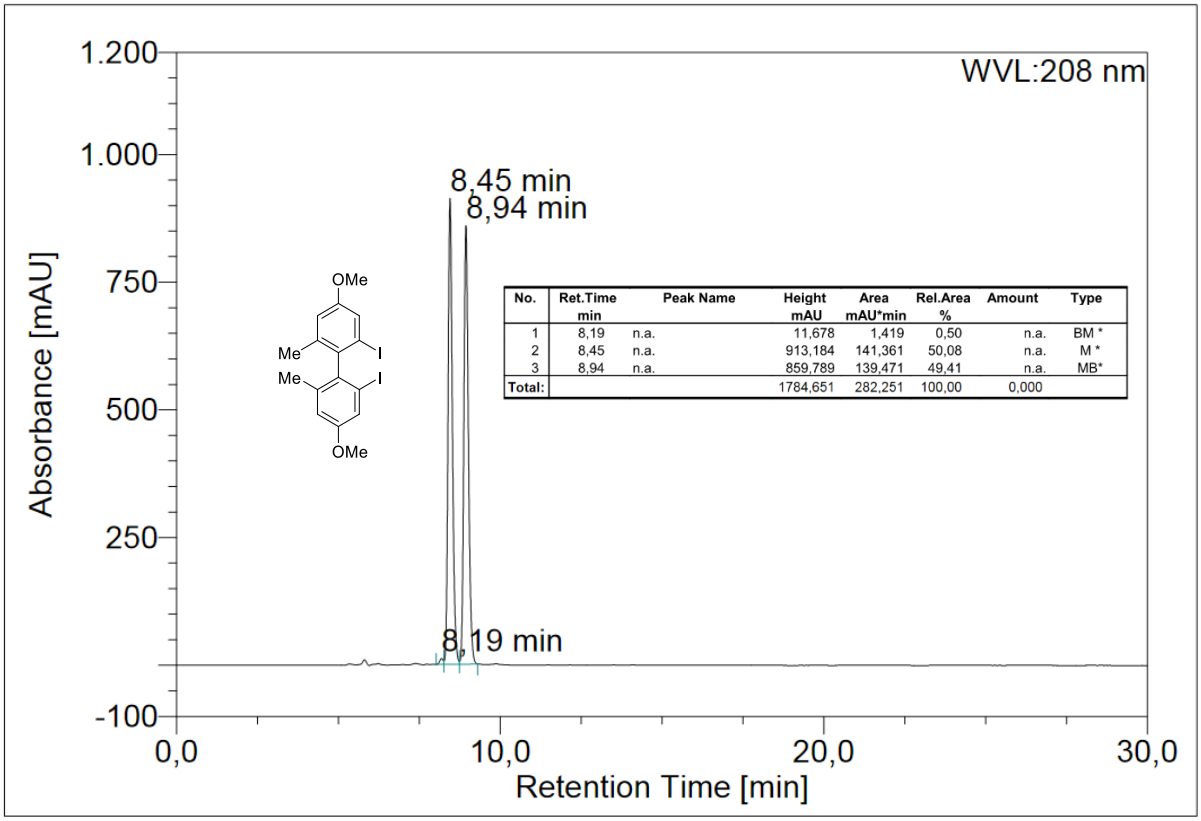

No.	Ret.Time min	Peak Name	Height mAU	Area mAU*min	Rel.Area %	Amount	Type
1	8,19	n.a.	11,678	1,419	0,50	n.a.	BM *
2	8,45	n.a.	913,184	141,361	50,08	n.a.	M *
3	8,94	n.a.	859,789	139,471	49,41	n.a.	MB*
Total:			1784,651	282,251	100,00	0,000	

Figure 48: HPLC Chromatogram of biaryl *rac*-**249**. Chiralpak® IC (Daciel) 250 ° 4.6 mm, 25 °C, 0.5 mL min^{-1}, 208 nm, *n*-heptane:*i*-PrOH 99.9:0.1 (v/v) $t_R(S_a)$ = 8.9 min, $t_R(R_a)$ = 8.5 min.

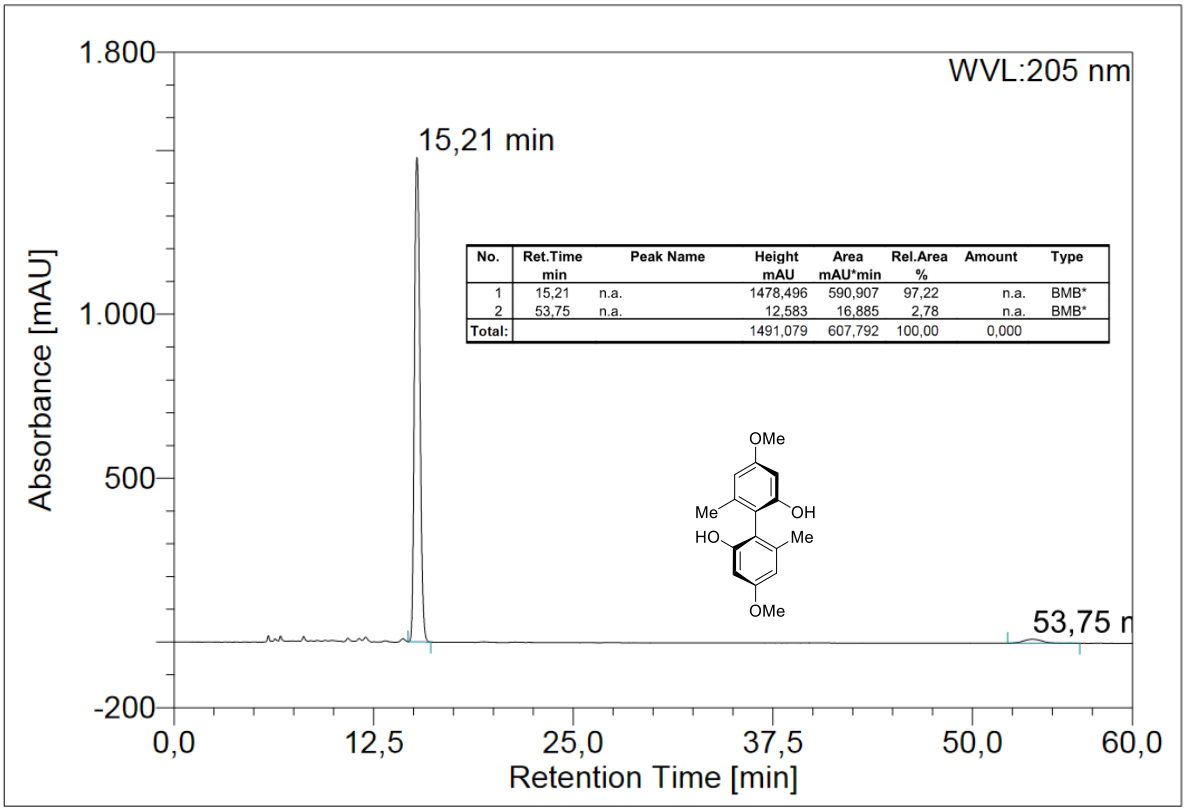

No.	Ret.Time min	Peak Name	Height mAU	Area mAU*min	Rel.Area %	Amount	Type
1	15,21	n.a.	1478,496	590,907	97,22	n.a.	BMB*
2	53,75	n.a.	12,583	16,885	2,78	n.a.	BMB*
Total:			1491,079	607,792	100,00	0,000	

Figure 49: HPLC Chromatogram of biaryl **27** 94%*ee* (S_a). Lux® Amylose-1 (Phenomenex) 250 ° 4.6 mm, 25 °C, 0.5 mL min-1, 205 nm, n heptane:i PrOH 50:50 (v/v) tR(Sa) = 14.5 min, tR(Ra) = 53.1 min.

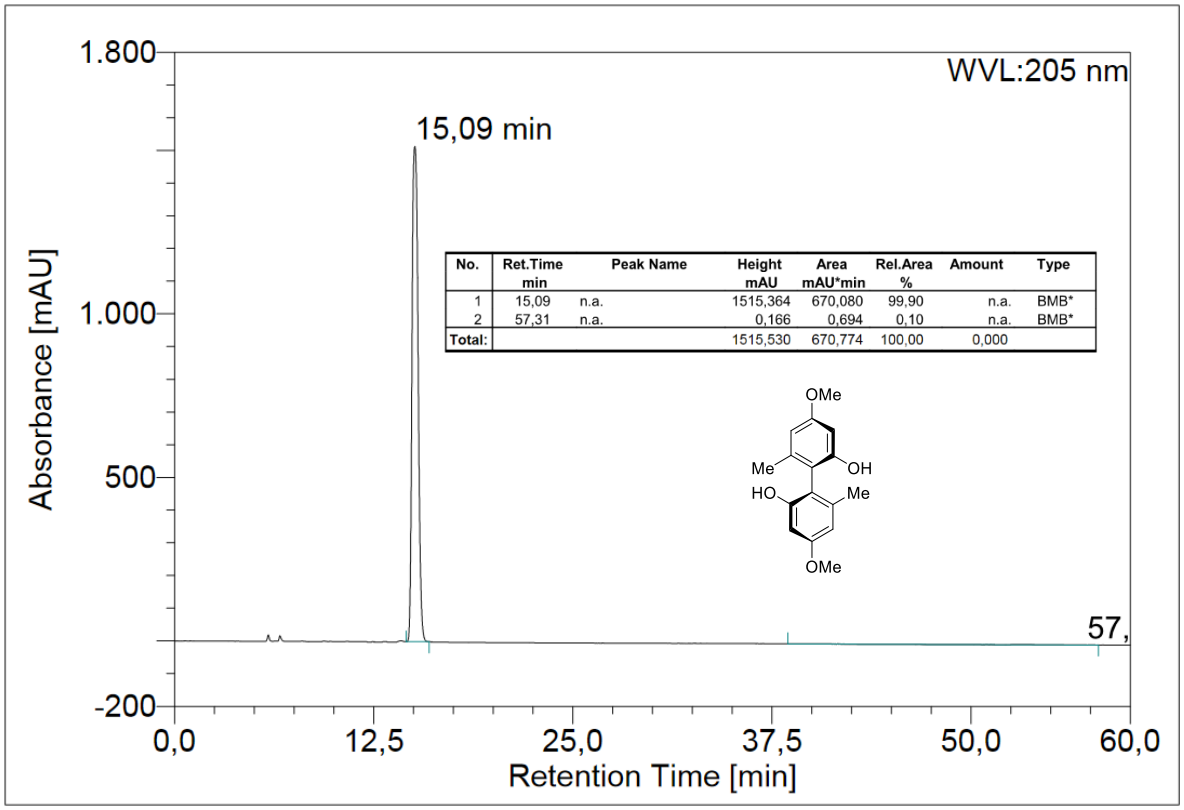

No.	Ret.Time min	Peak Name	Height mAU	Area mAU*min	Rel.Area %	Amount	Type
1	15,09	n.a.	1515,364	670,080	99,90	n.a.	BMB*
2	57,31	n.a.	0,166	0,694	0,10	n.a.	BMB*
Total:			1515,530	670,774	100,00	0,000	

Figure 50: HPLC Chromatogram of biaryl **27** >99%*ee* (S_a). Lux® Amylose-1 (Phenomenex) 250 ° 4.6 mm, 25 °C, 0.5 mL min-1, 205 nm, n heptane:i PrOH 50:50 (v/v) tR(Sa) = 14.5 min, tR(Ra) = 53.1 min

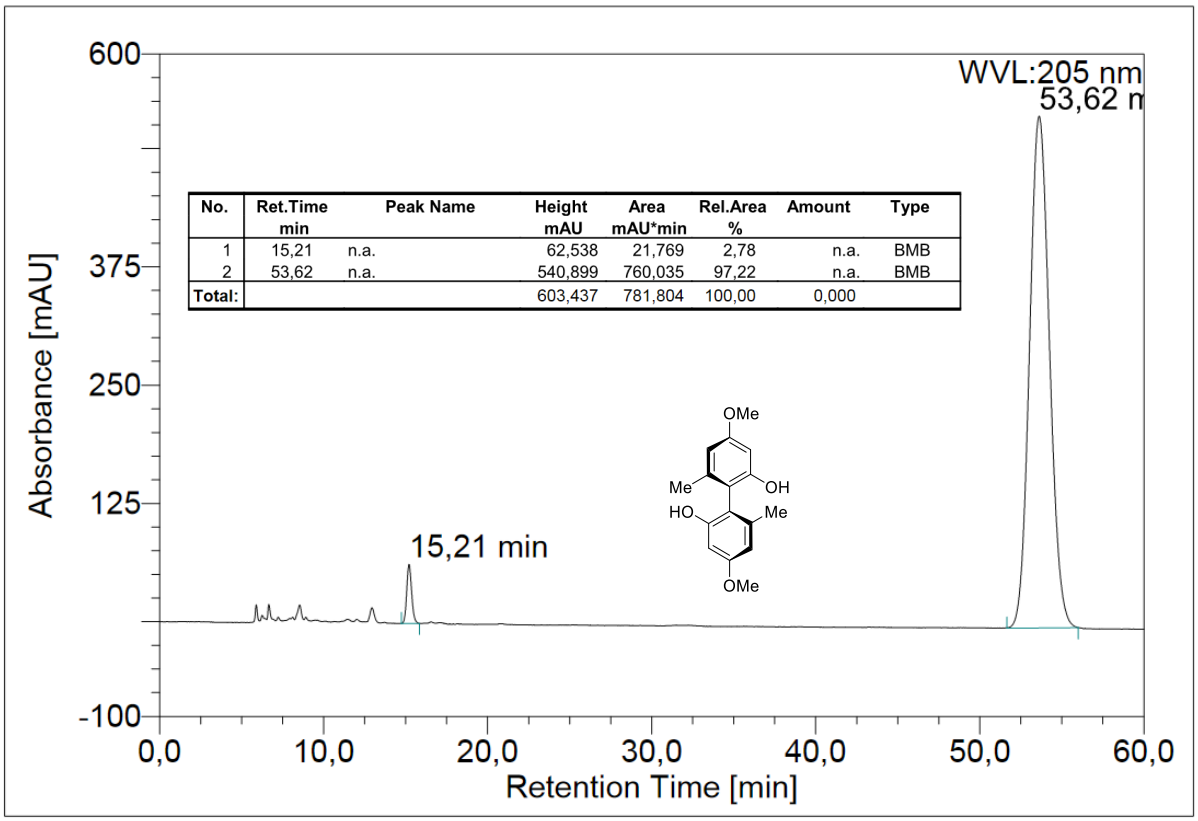

No.	Ret.Time min	Peak Name	Height mAU	Area mAU*min	Rel.Area %	Amount	Type
1	15,21	n.a.	62,538	21,769	2,78	n.a.	BMB
2	53,62	n.a.	540,899	760,035	97,22	n.a.	BMB
Total:			603,437	781,804	100,00	0,000	

Figure 51: HPLC Chromatogram of biaryl **27** 94%*ee* (R_a). Lux® Amylose-1 (Phenomenex) 250 ° 4.6 mm, 25 °C, 0.5 mL min-1, 205 nm, n heptane:i PrOH 50:50 (v/v) tR(Sa) = 14.5 min, tR(Ra) = 53.1 min.

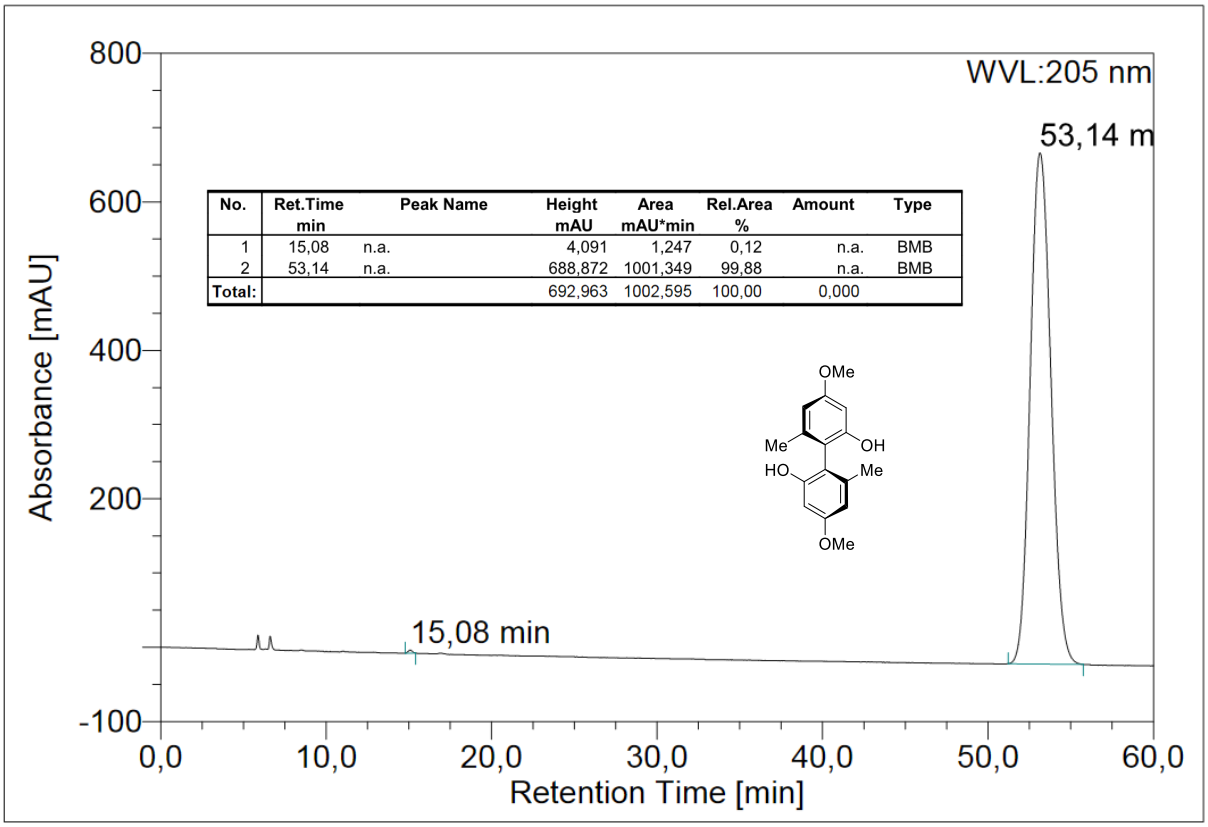

No.	Ret.Time min	Peak Name	Height mAU	Area mAU*min	Rel.Area %	Amount	Type
1	15,08	n.a.	4,091	1,247	0,12	n.a.	BMB
2	53,14	n.a.	688,872	1001,349	99,88	n.a.	BMB
Total:			692,963	1002,595	100,00	0,000	

Figure 52: HPLC Chromatogram of biaryl **27** >99%*ee* (R_a). Lux® Amylose-1 (Phenomenex) 250 ° 4.6 mm, 25 °C, 0.5 mL min-1, 205 nm, n heptane:i PrOH 50:50 (v/v) tR(Sa) = 14.5 min, tR(Ra) = 53.1 min.

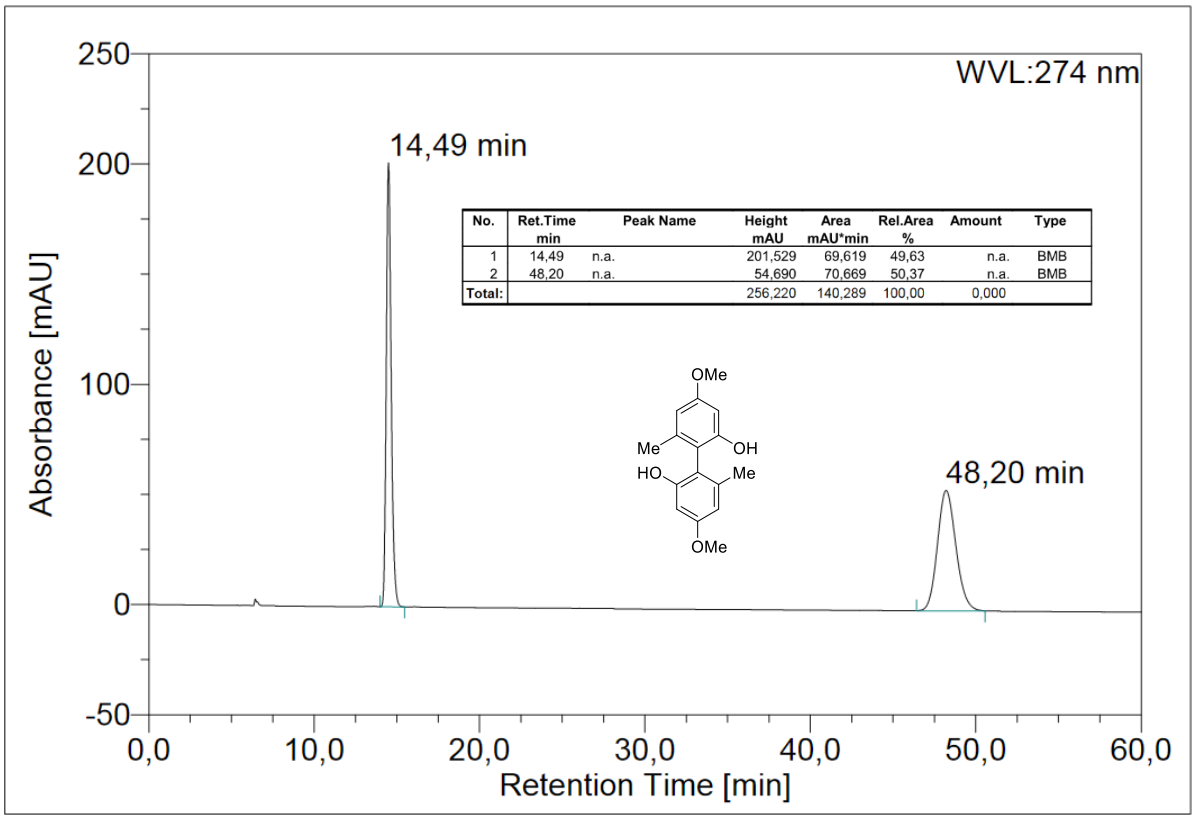

No.	Ret.Time min	Peak Name	Height mAU	Area mAU*min	Rel.Area %	Amount	Type
1	14,49	n.a.	201,529	69,619	49,63	n.a.	BMB
2	48,20	n.a.	54,690	70,669	50,37	n.a.	BMB
Total:			256,220	140,289	100,00	0,000	

Figure 53: HPLC Chromatogram of biaryl *rac*-**27**. Lux® Amylose-1 (Phenomenex) 250 ° 4.6 mm, 25 °C, 0.5 mL min-1, 205 nm, n heptane:i PrOH 50:50 (v/v) tR(Sa) = 14.5 min, tR(Ra) = 53.1 min.

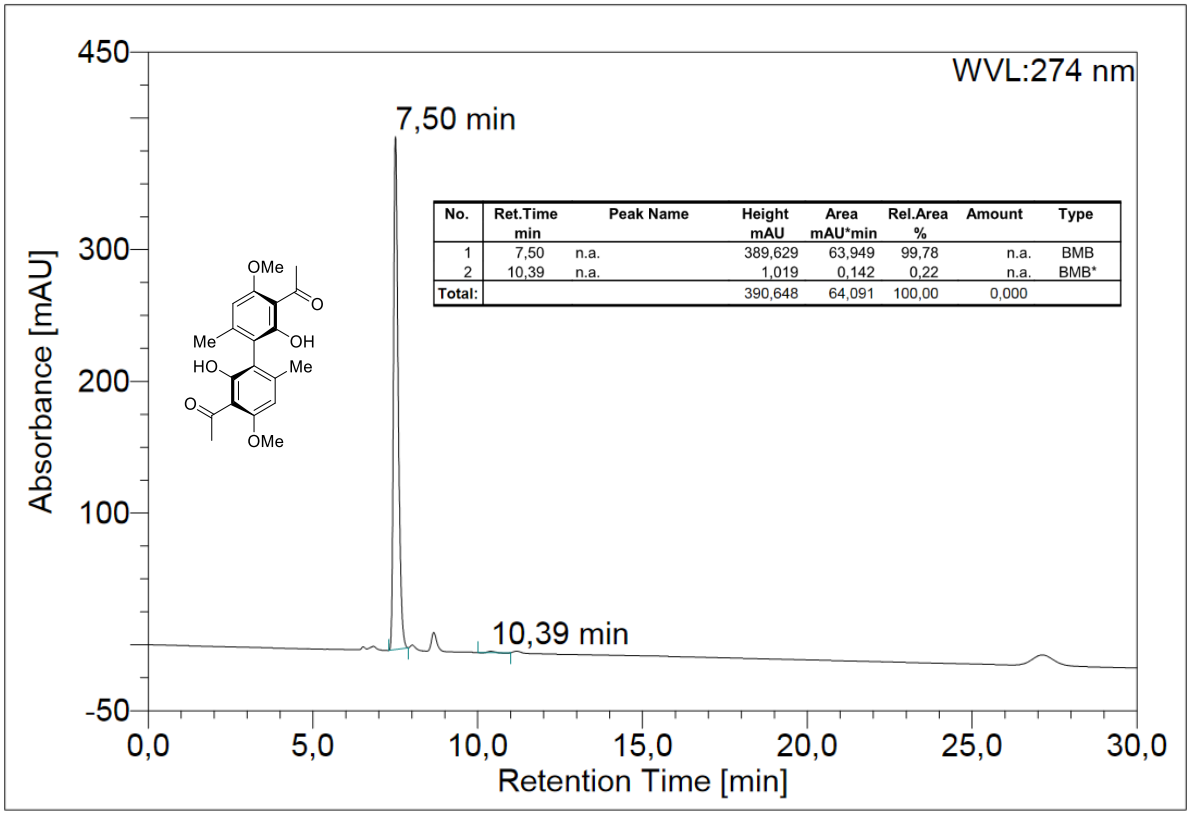

No.	Ret.Time min	Peak Name	Height mAU	Area mAU*min	Rel.Area %	Amount	Type
1	7,50	n.a.	389,629	63,949	99,78	n.a.	BMB
2	10,39	n.a.	1,019	0,142	0,22	n.a.	BMB*
Total:			390,648	64,091	100,00	0,000	

Figure 54: HPLC Chromatogram of biaryl **134** >99%*ee* (S_a). Lux® Amylose-1 (Phenomenex) 250 ° 4.6 mm, 25 °C, 0.5 mL min-1, 274 nm, n heptane:i PrOH 50:50 (v/v) tR(Sa) = 7.5 min, tR(Ra) = 10.4 min

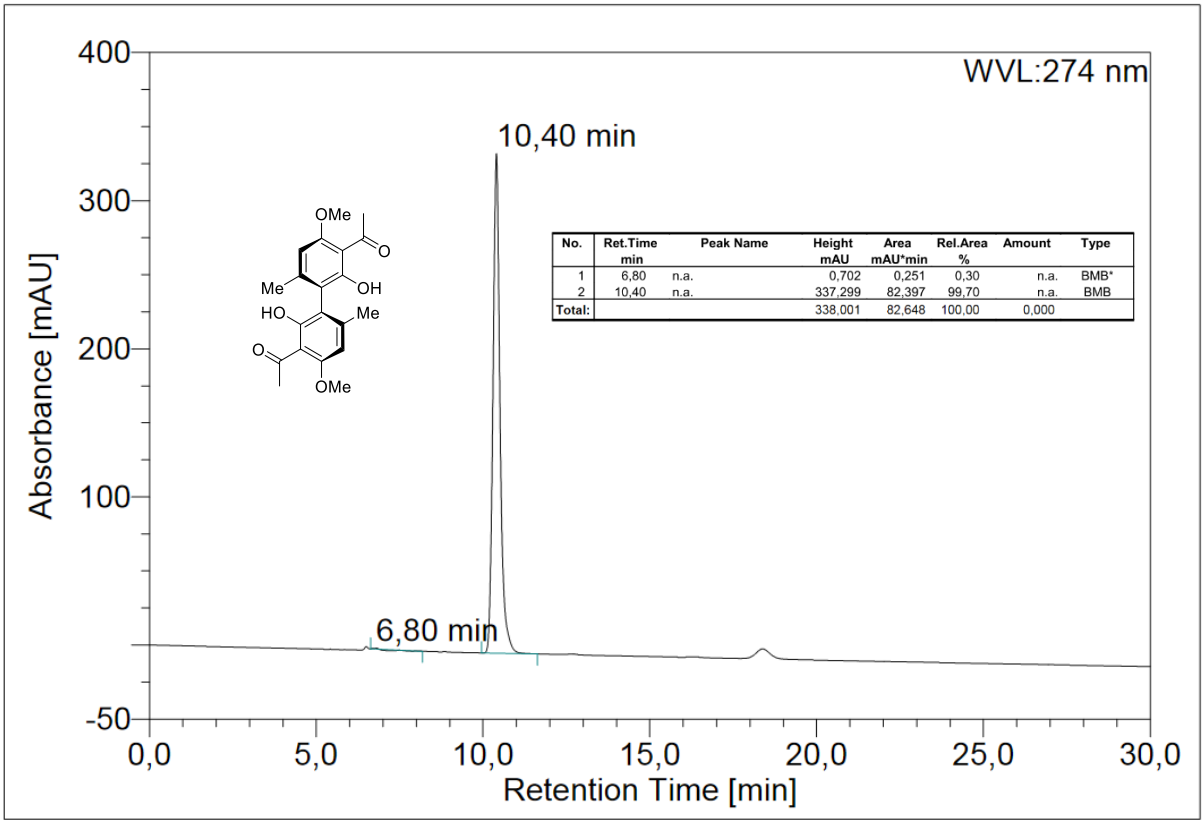

No.	Ret.Time min	Peak Name	Height mAU	Area mAU*min	Rel.Area %	Amount	Type
1	6,80	n.a.	0,702	0,251	0,30	n.a.	BMB*
2	10,40	n.a.	337,299	82,397	99,70	n.a.	BMB
Total:			338,001	82,648	100,00	0,000	

Figure 55: HPLC Chromatogram of biaryl **134** >99%*ee* (R_a). Lux® Amylose-1 (Phenomenex) 250 ° 4.6 mm, 25 °C, 0.5 mL min-1, 274 nm, n heptane:i PrOH 50:50 (v/v) tR(Sa) = 7.5 min, tR(Ra) = 10.4 min.

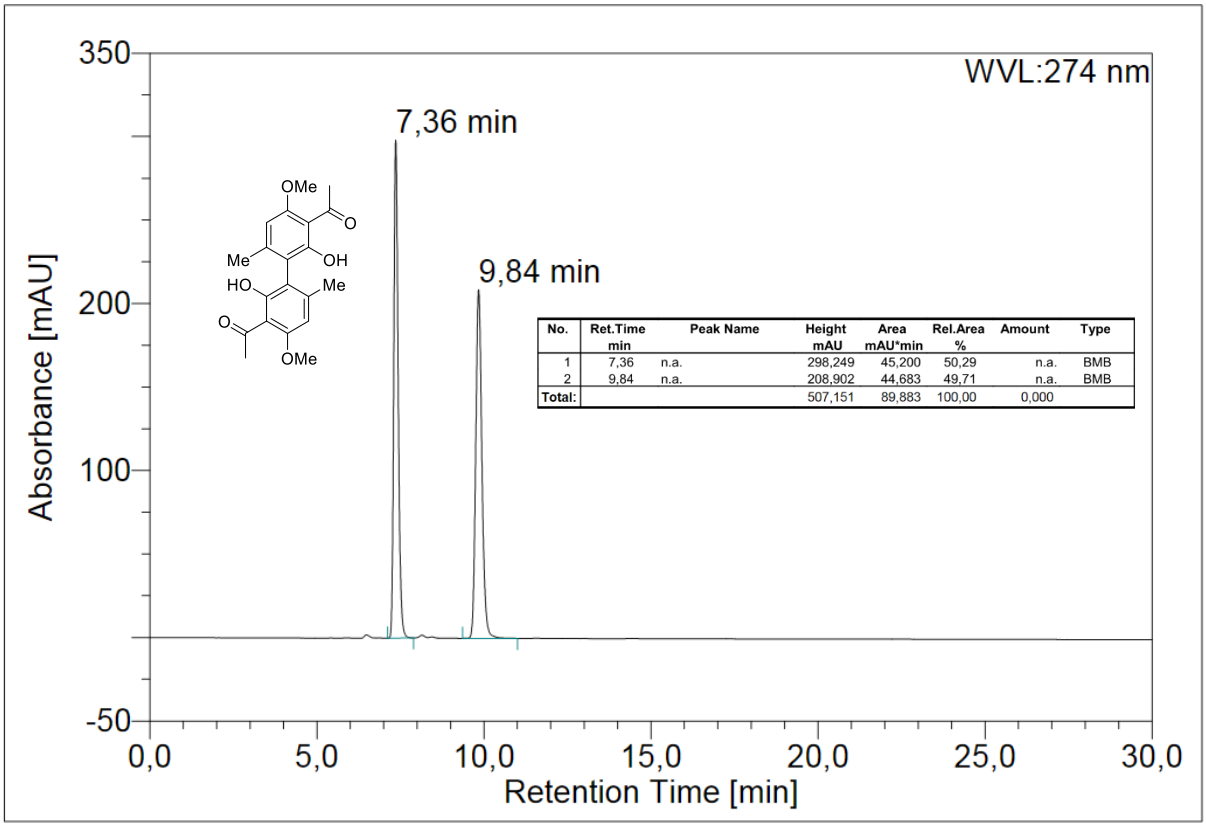

No.	Ret.Time min	Peak Name	Height mAU	Area mAU*min	Rel.Area %	Amount	Type
1	7,36	n.a.	298,249	45,200	50,29	n.a.	BMB
2	9,84	n.a.	208,902	44,683	49,71	n.a.	BMB
Total:			507,151	89,883	100,00	0,000	

Figure 56: HPLC Chromatogram of biaryl *rac*-**134**. Lux® Amylose-1 (Phenomenex) 250 ° 4.6 mm, 25 °C, 0.5 mL min-1, 274 nm, n heptane:i PrOH 50:50 (v/v) tR(Sa) = 7.5 min, tR(Ra) = 10.4 min.

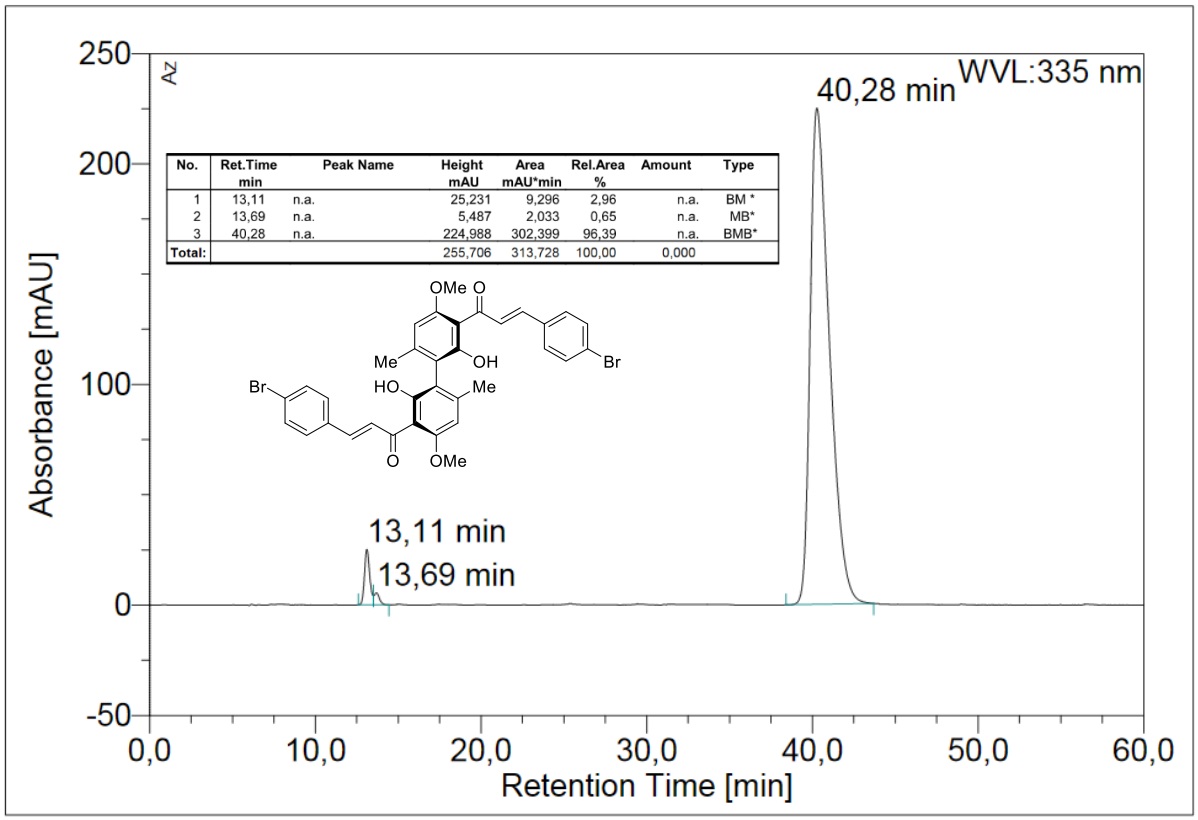

No.	Ret.Time min	Peak Name	Height mAU	Area mAU*min	Rel.Area %	Amount	Type
1	13,11	n.a.	25,231	9,296	2,96	n.a.	BM *
2	13,69	n.a.	5,487	2,033	0,65	n.a.	MB*
3	40,28	n.a.	224,988	302,399	96,39	n.a.	BMB*
Total:			255,706	313,728	100,00	0,000	

Figure 57: HPLC Chromatogram of biaryl **169** >99%*ee* (S_a). CHIRALPAK® IA (Daciel) 250 ° 4.6 mm, 25 °C, 0.5 mL min-1, 335 nm, n heptane:i PrOH 50:50 (v/v) tR(Sa) = 25.5 min, tR(Ra) = 40.9 min.

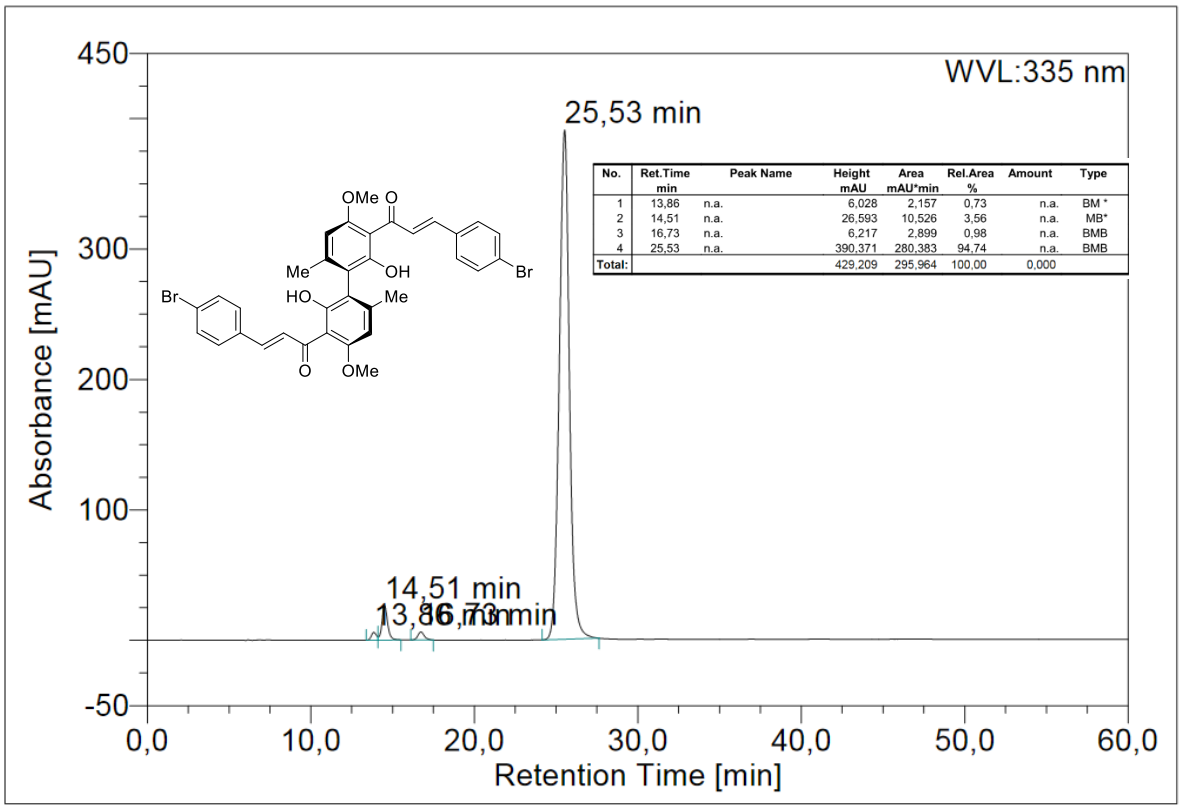

No.	Ret.Time min	Peak Name	Height mAU	Area mAU*min	Rel.Area %	Amount	Type
1	13,86	n.a.	6,028	2,157	0,73	n.a.	BM *
2	14,51	n.a.	26,593	10,526	3,56	n.a.	MB*
3	16,73	n.a.	6,217	2,899	0,98	n.a.	BMB
4	25,53	n.a.	390,371	280,383	94,74	n.a.	BMB
Total:			429,209	295,964	100,00	0,000	

Figure 58: HPLC Chromatogram of biaryl **169** >99%*ee* (R_a). CHIRALPAK® IA (Daciel) 250 ° 4.6 mm, 25 °C, 0.5 mL min-1, 335 nm, n heptane:i PrOH 50:50 (v/v) tR(Sa) = 25.5 min, tR(Ra) = 40.9 min.

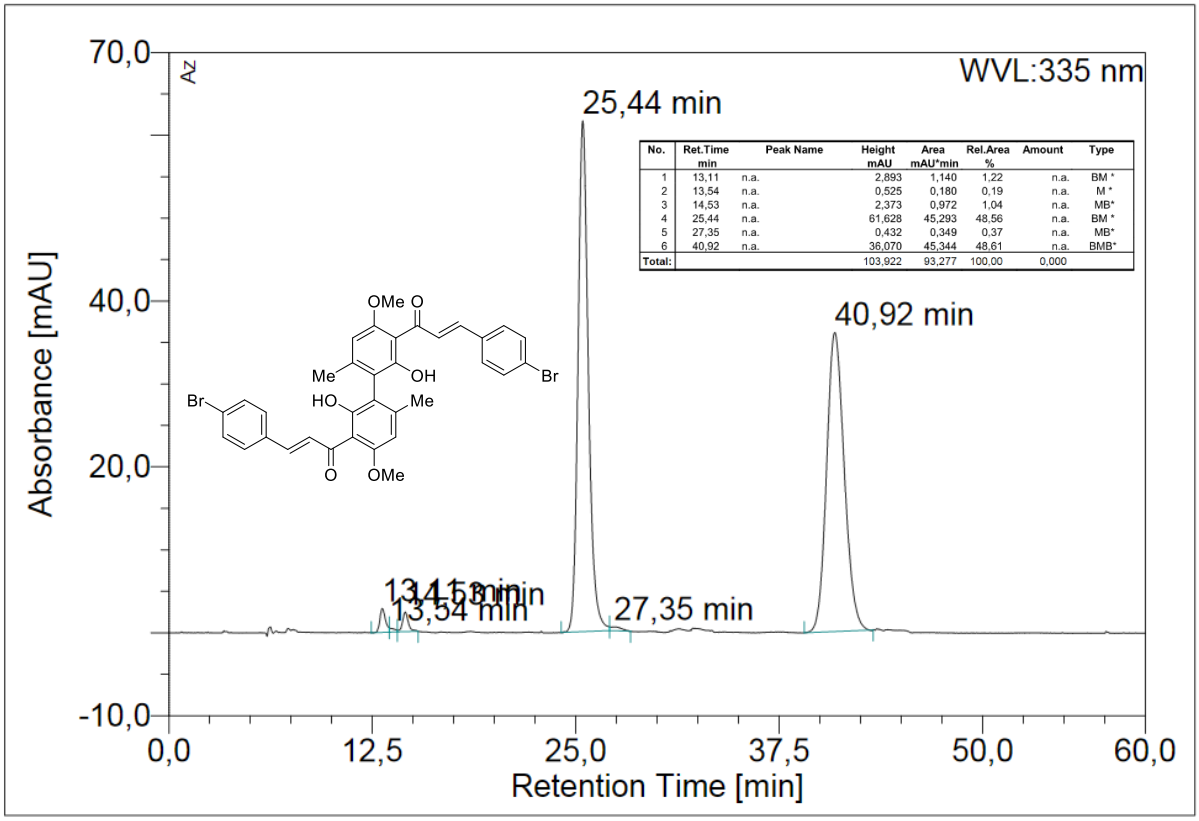

No.	Ret.Time min	Peak Name	Height mAU	Area mAU*min	Rel.Area %	Amount	Type
1	13,11	n.a.	2,893	1,140	1,22	n.a.	BM *
2	13,54	n.a.	0,525	0,180	0,19	n.a.	M *
3	14,53	n.a.	2,373	0,972	1,04	n.a.	MB*
4	25,44	n.a.	61,628	45,293	48,56	n.a.	BM *
5	27,35	n.a.	0,432	0,349	0,37	n.a.	MB*
6	40,92	n.a.	36,070	45,344	48,61	n.a.	BMB*
Total:			103,922	93,277	100,00	0,000	

Figure 59: HPLC Chromatogram of biaryl *rac*-**169**. HPLC Chromatogram of biaryl **169** >99%*ee* (R_a). CHIRALPAK® IA (Daciel) 250 ° 4.6 mm, 25 °C, 0.5 mL min-1, 335 nm, n heptane:i PrOH 50:50 (v/v) tR(Sa) = 25.5 min, tR(Ra) = 40.9 min.

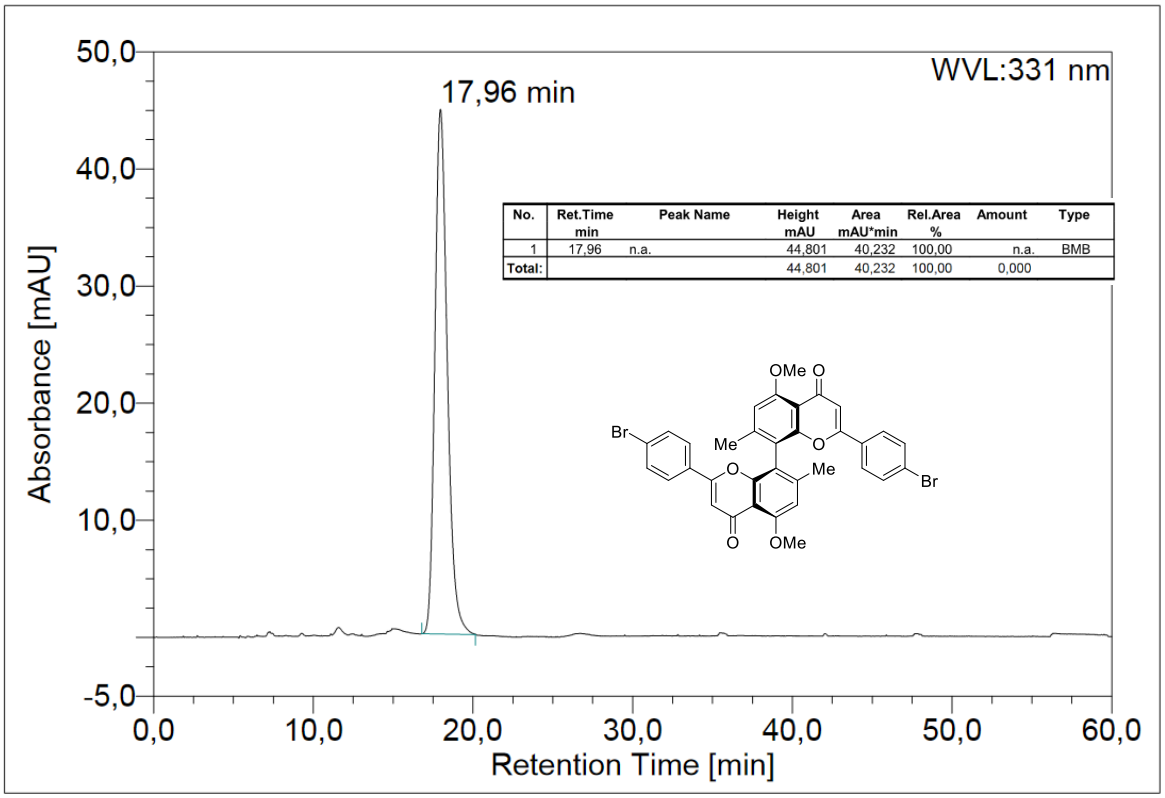

No.	Ret.Time min	Peak Name	Height mAU	Area mAU*min	Rel.Area %	Amount	Type
1	17,96	n.a.	44,801	40,232	100,00	n.a.	BMB
Total:			44,801	40,232	100,00	0,000	

Figure 60: HPLC Chromatogram of biaryl **183** >99%*ee* (S_a). Lux® Amylose-1 (Phenomenex) 250 ° 4.6 mm, 25 °C, 0.5 mL min^{-1}, 331 nm, *n*-heptane:*i*-PrOH 50:50 (v/v) $t_R(S_a)$ = 18.0 min, $t_R(R_a)$ = 24.3 min.

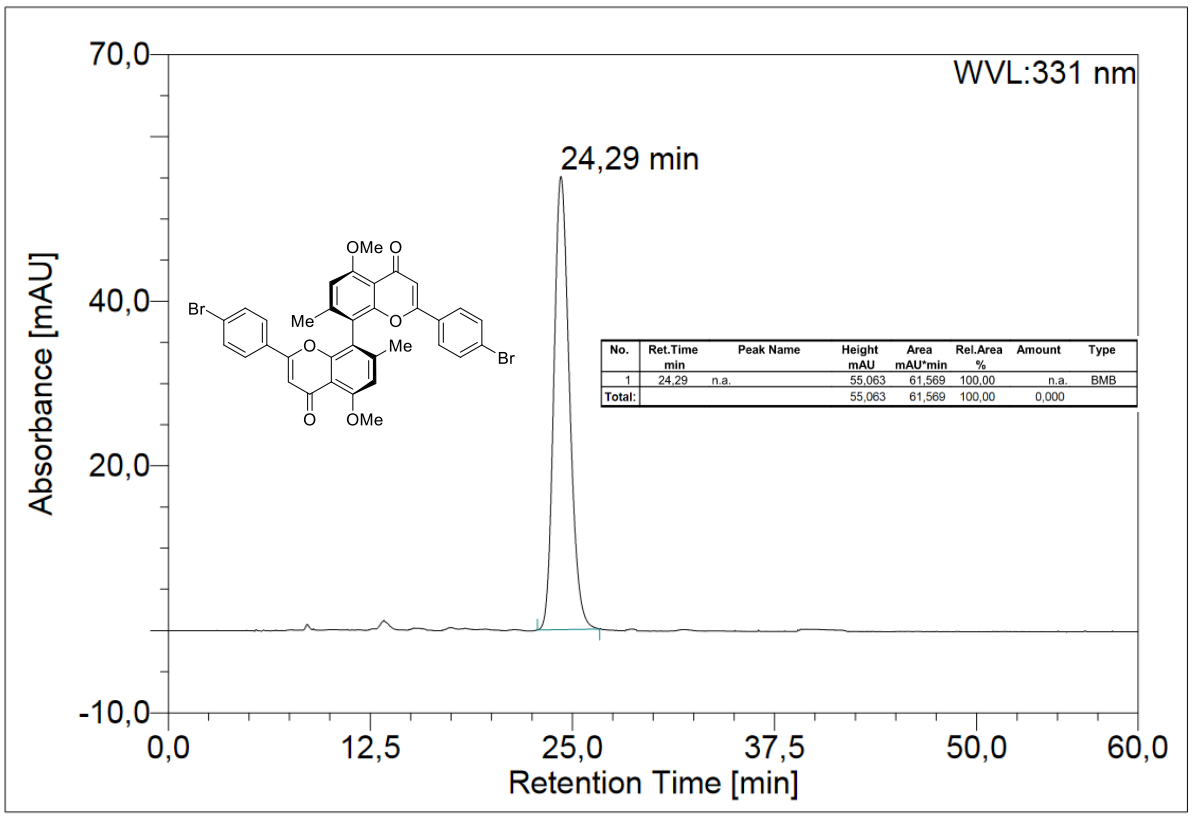

Figure 61: HPLC Chromatogram of biaryl **183** >99%*ee* (R_a). Lux® Amylose-1 (Phenomenex) 250 ° 4.6 mm, 25 °C, 0.5 mL min^{-1}, 331 nm, *n*-heptane:*i*-PrOH 50:50 (v/v) $t_R(S_a)$ = 18.0 min, $t_R(R_a)$ = 24.3 min.

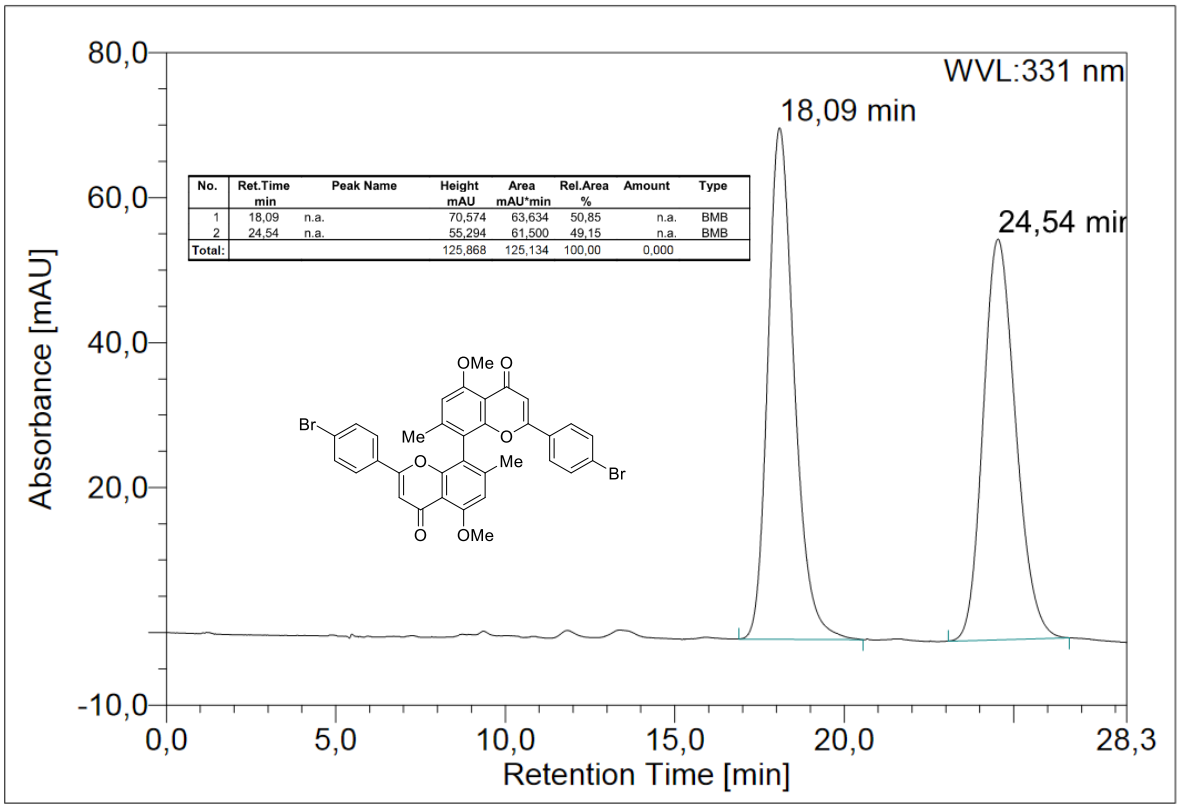

Figure 62: HPLC Chromatogram of biaryl *rac*-**183**. Lux® Amylose-1 (Phenomenex) 250 ° 4.6 mm, 25 °C, 0.5 mL min^{-1}, 331 nm, *n*-heptane:*i*-PrOH 50:50 (v/v) $t_R(S_a)$ = 18.0 min, $t_R(R_a)$ = 24.3 min.

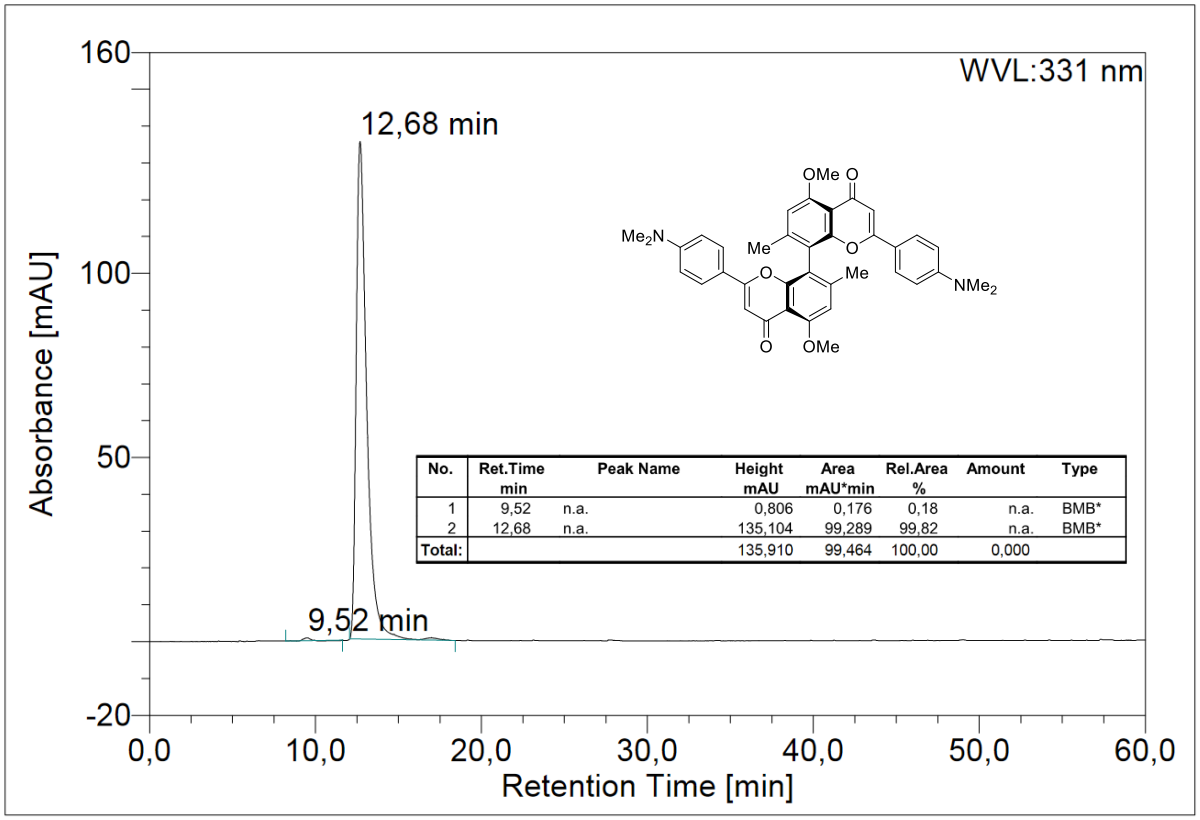

No.	Ret.Time min	Peak Name	Height mAU	Area mAU*min	Rel.Area %	Amount	Type
1	9,52	n.a.	0,806	0,176	0,18	n.a.	BMB*
2	12,68	n.a.	135,104	99,289	99,82	n.a.	BMB*
Total:			135,910	99,464	100,00	0,000	

Figure 63: HPLC Chromatogram of biaryl **181** >99%*ee* (S_a). Lux® Amylose-1 (Phenomenex) 250 ° 4.6 mm, 25 °C, 0.5 mL min^{-1}, 331 nm, *n*-heptane:*i*-PrOH 50:50 (v/v) $t_R(S_a)$ = 9.53 min, $t_R(R_a)$ = 12.8 min.

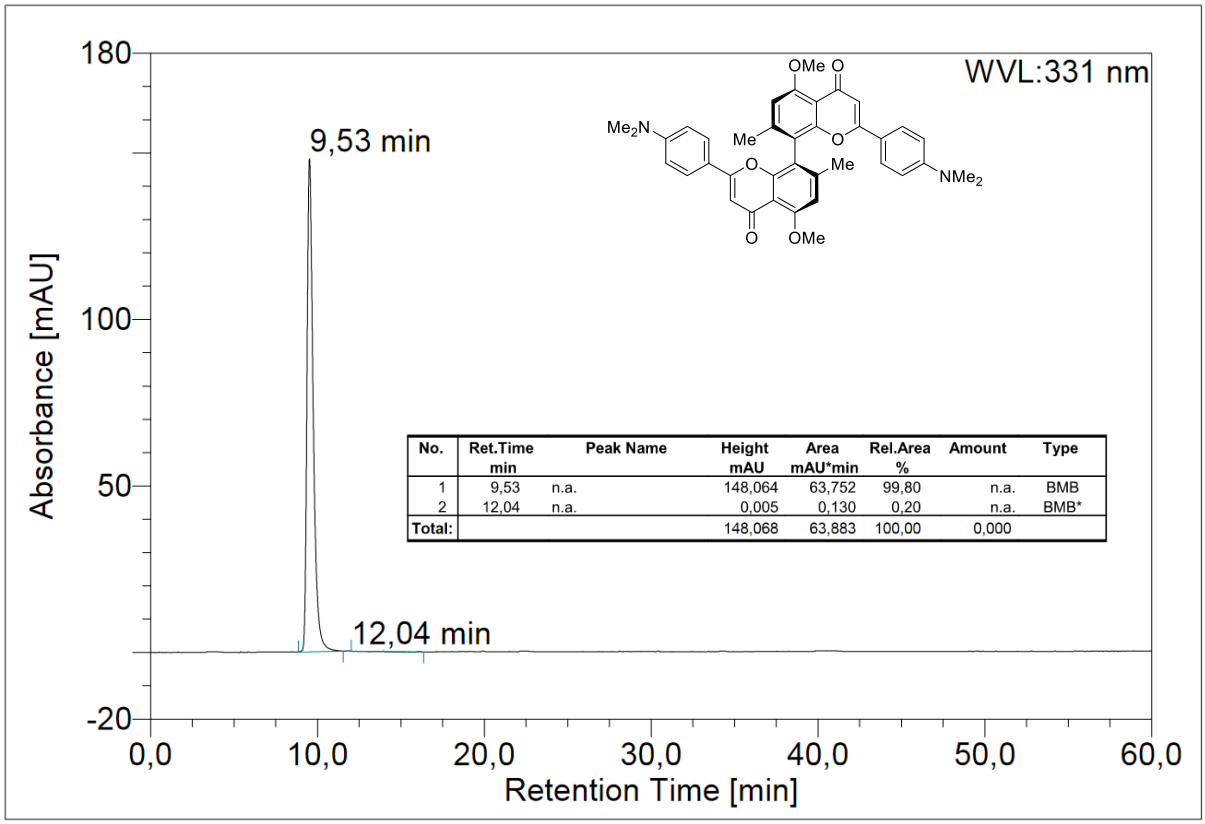

No.	Ret.Time min	Peak Name	Height mAU	Area mAU*min	Rel.Area %	Amount	Type
1	9,53	n.a.	148,064	63,752	99,80	n.a.	BMB
2	12,04	n.a.	0,005	0,130	0,20	n.a.	BMB*
Total:			148,068	63,883	100,00	0,000	

Figure 64: HPLC Chromatogram of biaryl **181** >99%*ee* (R_a). Lux® Amylose-1 (Phenomenex) 250 ° 4.6 mm, 25 °C, 0.5 mL min^{-1}, 331 nm, *n*-heptane:*i*-PrOH 50:50 (v/v) $t_R(S_a)$ = 9.53 min, $t_R(R_a)$ = 12.8 min.

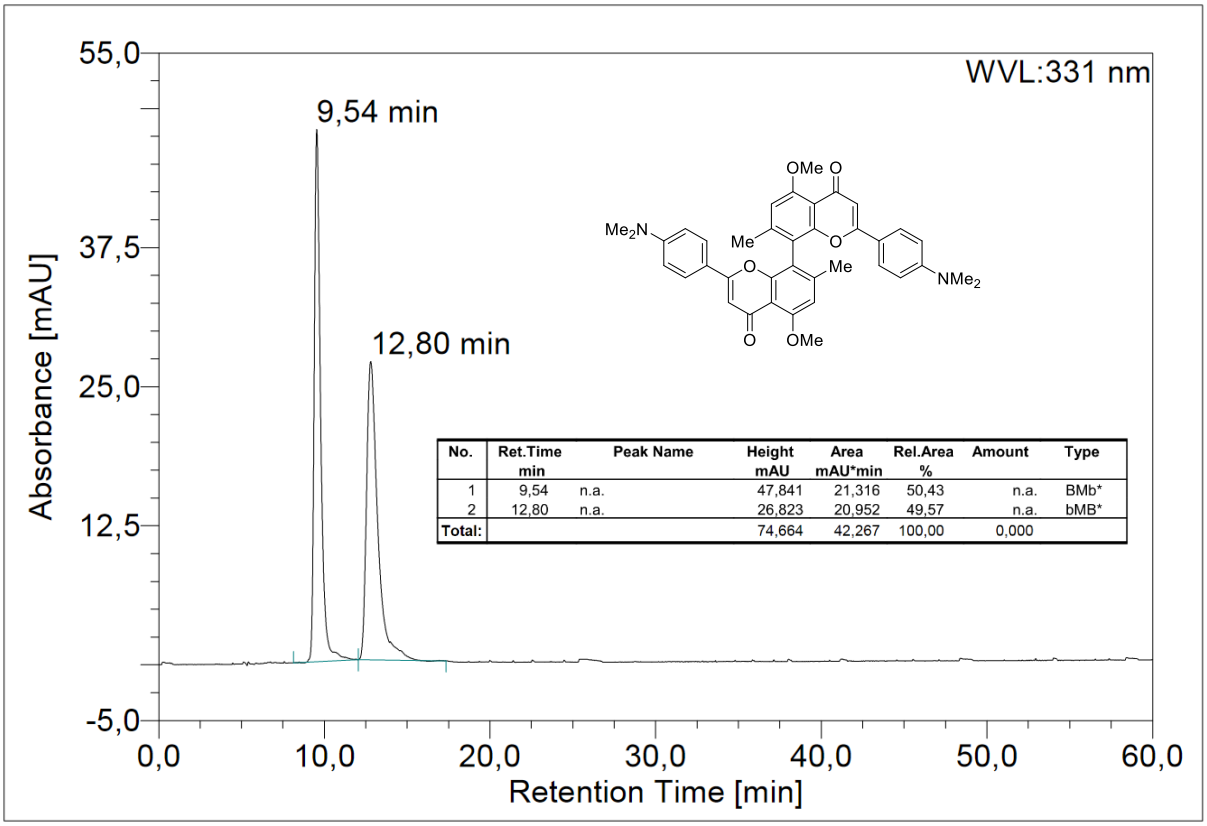

No.	Ret.Time min	Peak Name	Height mAU	Area mAU*min	Rel.Area %	Amount	Type
1	9,54	n.a.	47,841	21,316	50,43	n.a.	BMb*
2	12,80	n.a.	26,823	20,952	49,57	n.a.	bMB*
Total:			74,664	42,267	100,00	0,000	

Figure 65: HPLC Chromatogram of biaryl *rac*-**181**. Lux® Amylose-1 (Phenomenex) 250 ° 4.6 mm, 25 °C, 0.5 mL min^{-1}, 331 nm, *n*-heptane:*i*-PrOH 50:50 (v/v) $t_R(S_a)$ = 9.53 min, $t_R(R_a)$ = 12.8 min.

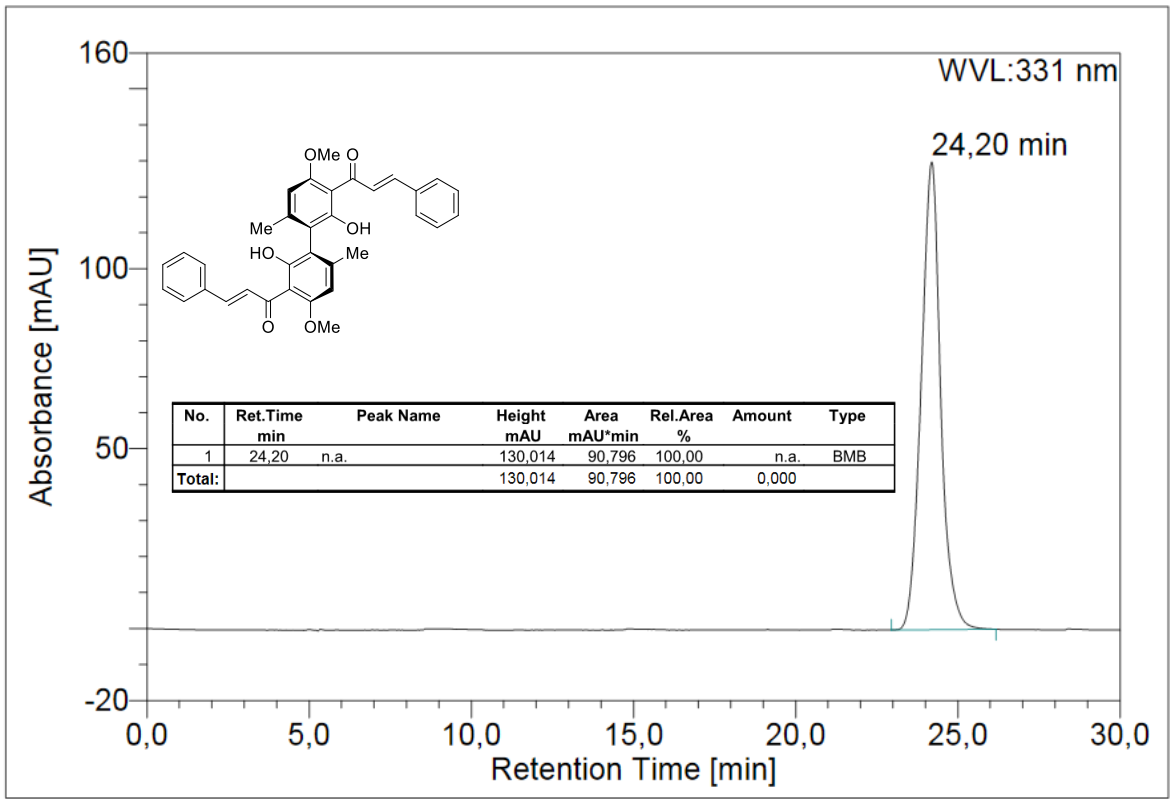

No.	Ret.Time min	Peak Name	Height mAU	Area mAU*min	Rel.Area %	Amount	Type
1	24,20	n.a.	130,014	90,796	100,00	n.a.	BMB
Total:			130,014	90,796	100,00	0,000	

Figure 66: HPLC Chromatogram of bichalcone **166** >99%*ee* (R_a). Lux® Amylose-1 (*Phenomenex*) 2504.6 mm, 25 °C, 0.5 mL min^{-1}, 331 nm, *n*-heptane:*i*-propanol 50:50 (v/v): $t_R(S_a)$ = 14.7 min, $t_R(R_a)$ = 24.2 min.

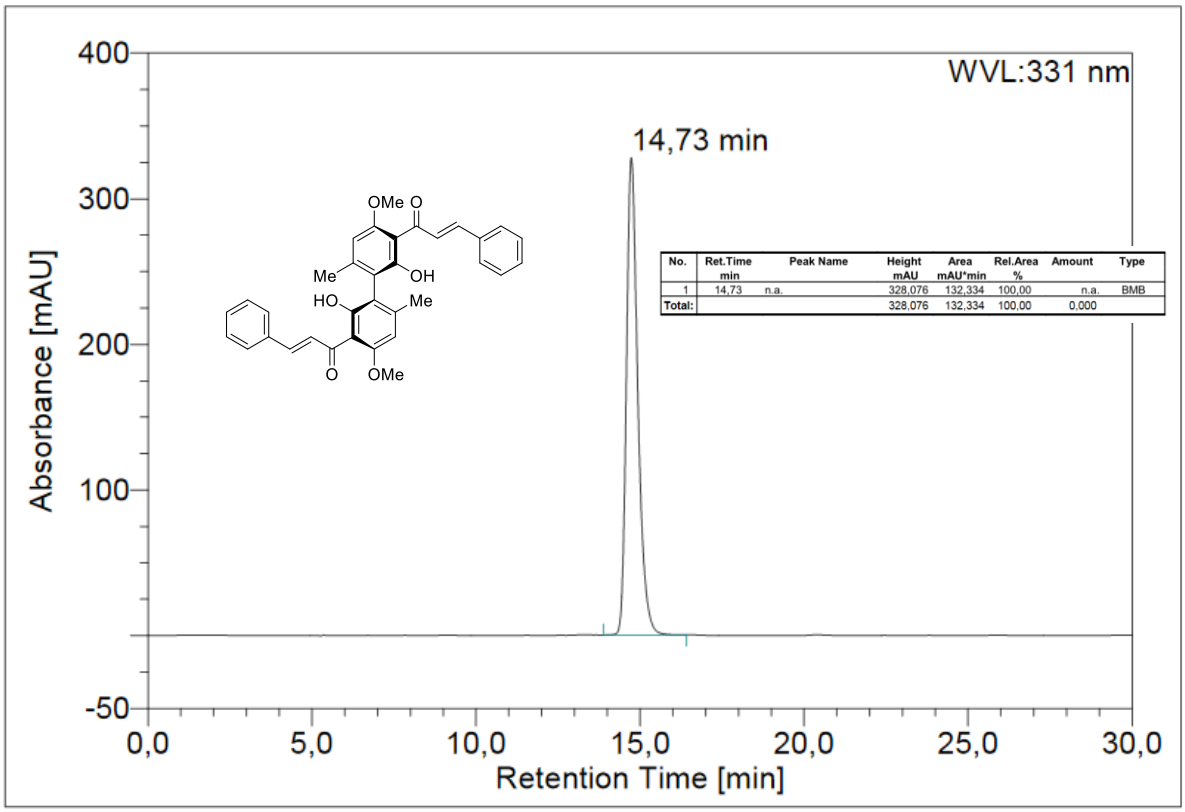

Figure 67: HPLC Chromatogram of bichalcone **166** >99%*ee* (S_a). Lux® Amylose-1 (*Phenomenex*) 2504.6 mm, 25 °C, 0.5 mL min^{-1}, 331 nm, *n*-heptane:*i*-propanol 50:50 (v/v): $t_R(S_a)$ = 14.7 min, $t_R(R_a)$ = 24.2 min.

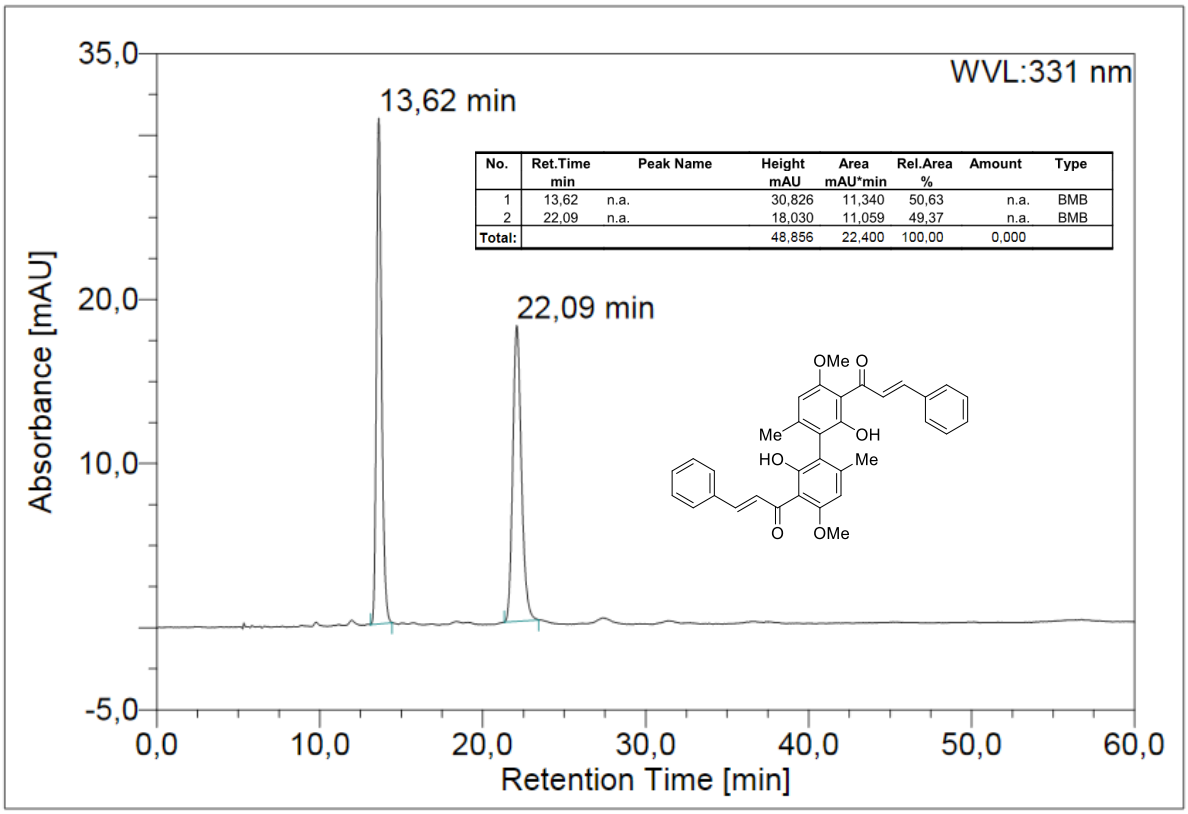

Figure 68: HPLC Chromatogram of bichalcone *rac*-**166**. Lux® Amylose-1 (*Phenomenex*) 2504.6 mm, 25 °C, 0.5 mL min^{-1}, 331 nm, *n*-heptane:*i*-propanol 50:50 (v/v): $t_R(S_a)$ = 14.7 min, $t_R(R_a)$ = 24.2 min.

7.3.3 Indenes

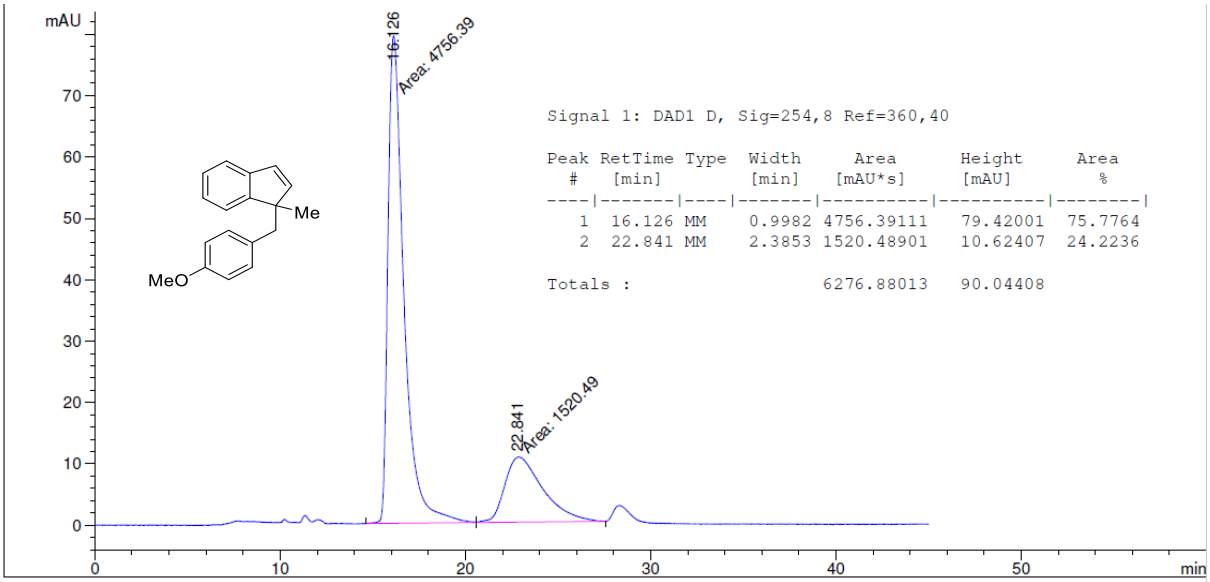

Figure 69: HPLC chromatogram of the enantiomeric excess of (−)-indene **314** using >20:1 d.r. chiral oxabicycle (*S*)-**302** (no additional peaks in ^{1}H NMR, oxabicycle is white crystalline solids). Chiralpak® AS-H 250 ° 4.6 mm, 25 °C, 0.5 mL min^{-1}, 254 nm, hexanes 100% t_R(*R*) = 16 min, t_R(*S*) = 25 min. Racemic standard in literature.[259a]

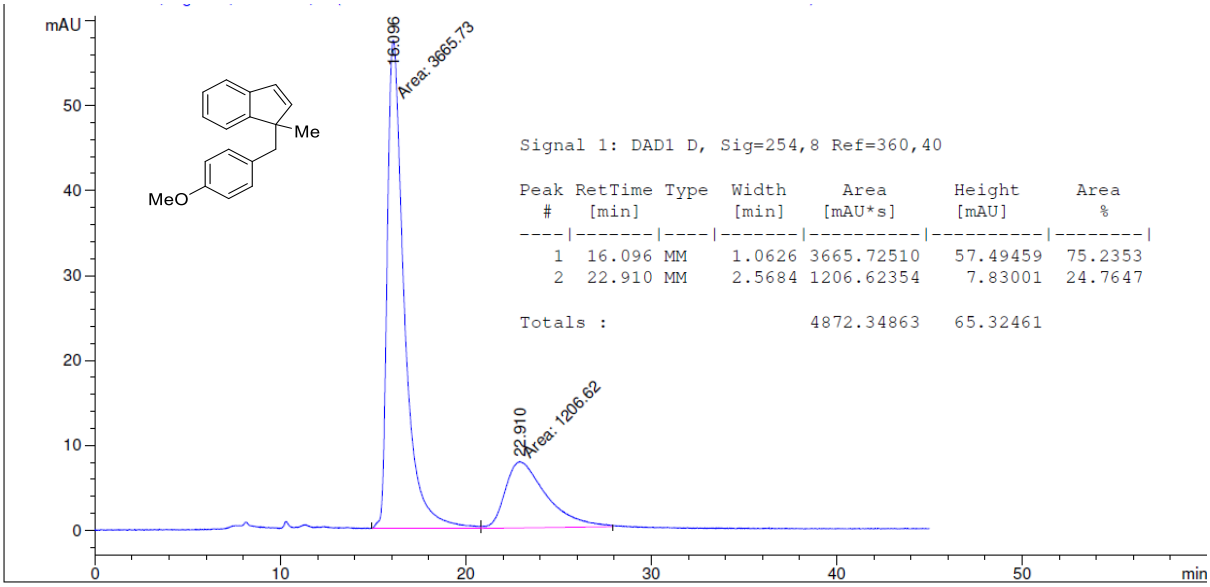

Figure 70: HPLC chromatogram of the enantiomeric excess of (−)-indene **314** using >20:1 d.r. chiral oxabicycle (*S*)-**302** (additional peaks in ^{1}H NMR, oxabicycle is slightly yellow oil). Chiralpak® AS-H 250 ° 4.6 mm, 25 °C, 0.5 mL min^{-1}, 254 nm, hexanes 100% t_R(*R*) = 16 min, t_R(*S*) = 25 min.

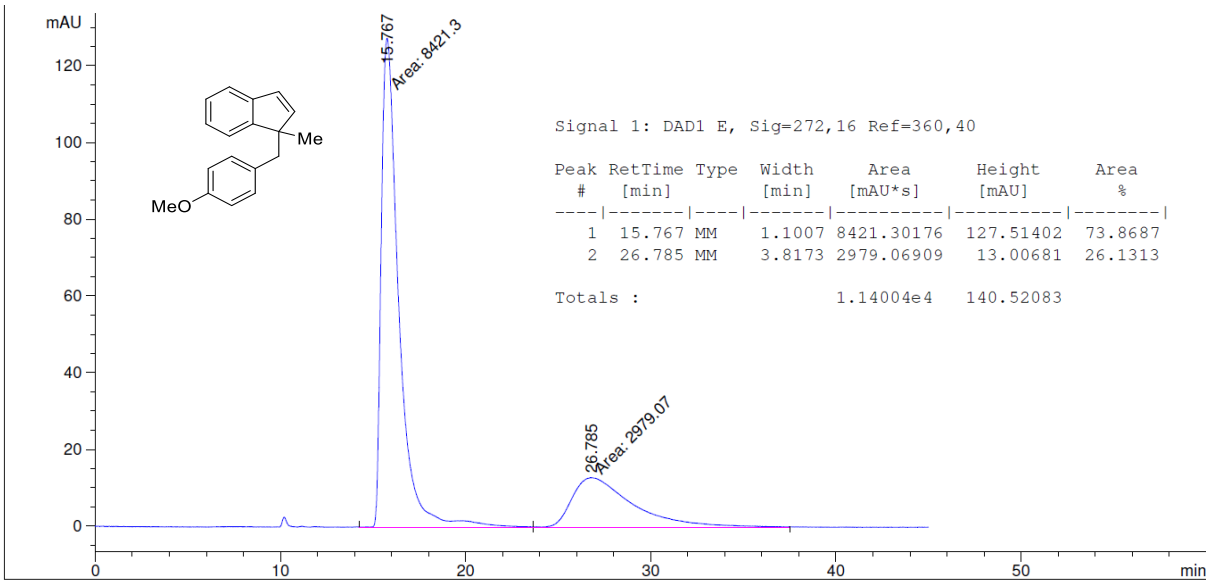

Figure 71: HPLC chromatogram of the enantiomeric excess of (−)-indene **314** using >20:1 d.r. chiral oxabicycle (*R*)-**303** (additional peaks in ^{1}H NMR, oxabicycle is slightly yellow oil). Chiralpak® AS-H 250 ° 4.6 mm, 25 °C, 0.5 mL min^{-1}, 254 nm, hexanes 100% t_R(*R*) = 16 min, t_R(*S*) = 25 min.

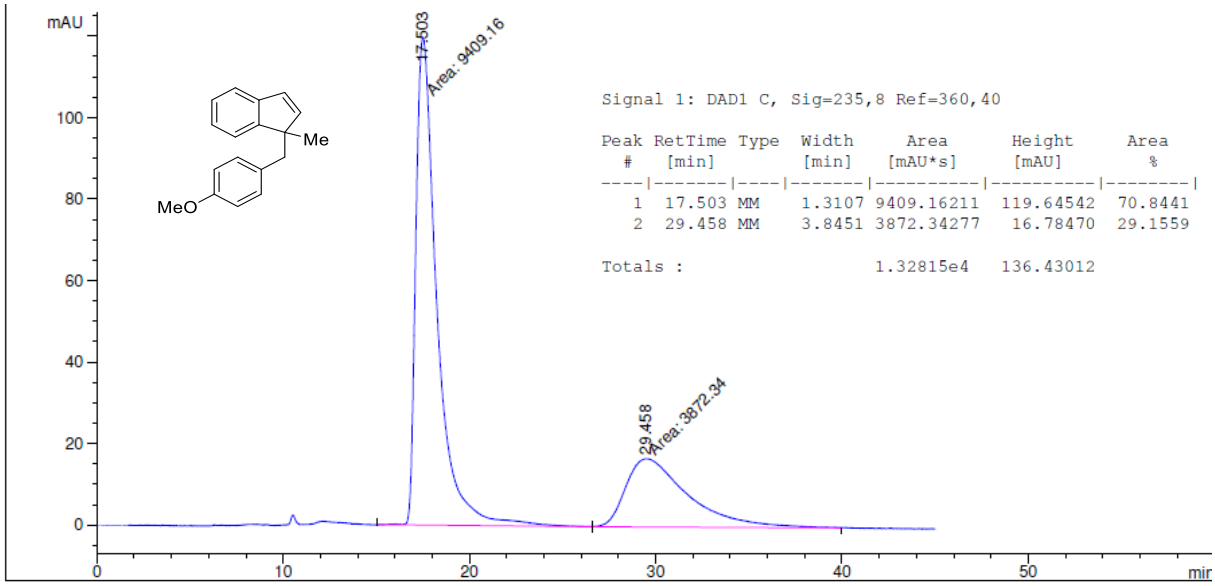

Figure 72: HPLC chromatogram of the enantiomeric excess of (−)-indene **314** using TADDOL Ligand **L3**. Chiralpak® AS-H 250 ° 4.6 mm, 25 °C, 0.5 mL min^{-1}, 254 nm, hexanes 100% t_R(*R*) = 16 min, t_R(*S*) = 25 min.

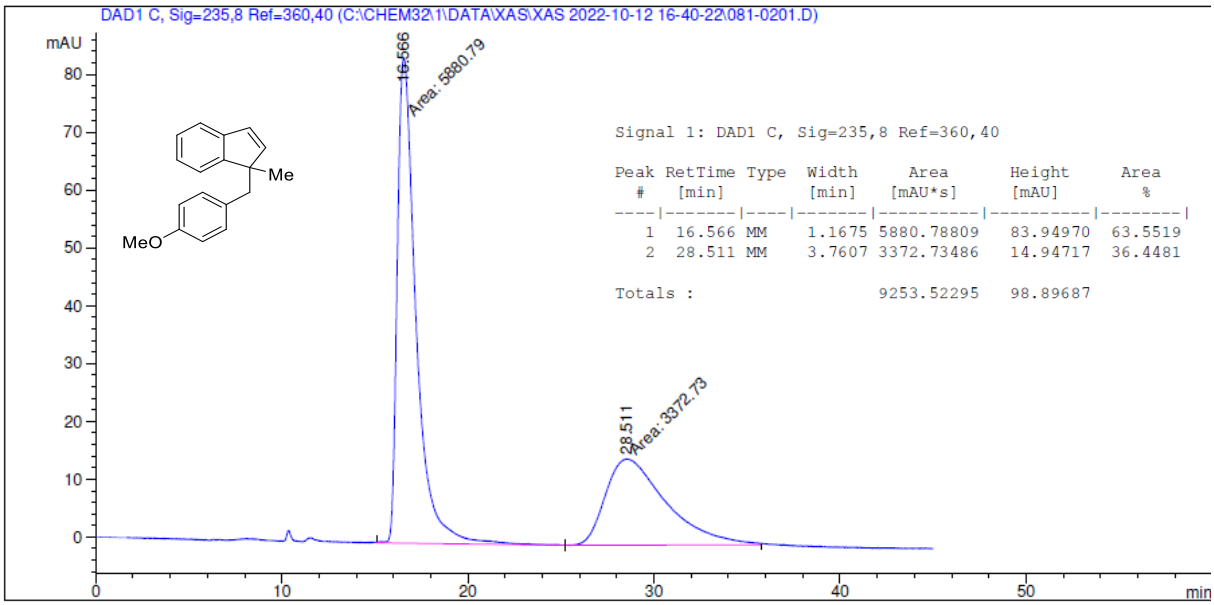

Figure 73: HPLC chromatogram of the enantiomeric excess of (−)-indene **314** using TADDOL **L3** and chiral oxabicycle (*S*)-**302**. Chiralpak® AS-H 250 ° 4.6 mm, 25 °C, 0.5 mL min^{-1}, 254 nm, hexanes 100% t_R(*R*) = 16 min, t_R(*S*) = 25 min.

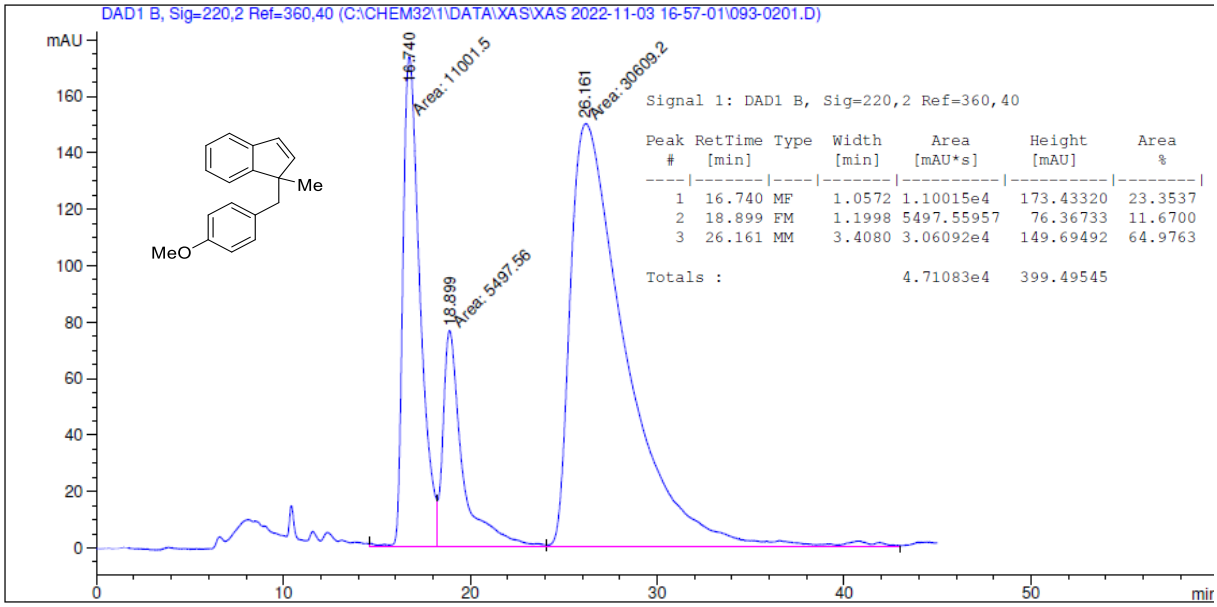

Figure 74: HPLC chromatogram of the enantiomeric excess of (+)-indene **314** using oxabicycle (*S*)-**302** and PPh_3 (impurity at 18.9 min retention time). Chiralpak® AS-H 250 ° 4.6 mm, 25 °C, 0.5 mL min^{-1}, 254 nm, hexanes 100% t_R(*R*) = 16 min, t_R(*S*) = 25 min.

7.3.4 Oxabicycles

Enantioenriched oxabicycle mono acid (*S*,*R*) (**a**,**b**) could be obtained through a cooperation with Dr. *Greg Hughes*. To obtain a chiral standard for the HPLC to determine *ee* and d.r. of the resulting product, a combination of racemic mono acid and racemic *α*-methylbenzylamine was coupled. The reasoning was, that even if a diastereoselectivity for the coupling takes place, the integers of the d.r. should be 1:1. Thus the enantiomeric ratio of the acid can be determined. A partial separation using the AD-H column and IA column were observed.

Table 38: Retention times of chiral oxabicycles **302** and **303**. HPLC conditions: 0.5 mL/min, hexanes:iPrOH (9:1 v/v), IA-CHIRALPAK®, 22 °C.

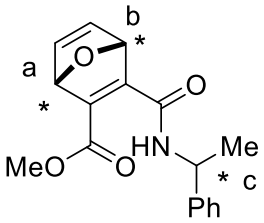

Entry	Oxabicycle	a, b, c	Retention time [min]
1	(*S*)-**302**	*(S) (R) (S)*	17.6
2	(*R*)-**303**	*(S) (R) (R)*	16.5
3	(*S*)-**303**	*(R) (S) (S)*	24.4
4	(*R*)-**302**	*(R) (S) (R)*	17.6

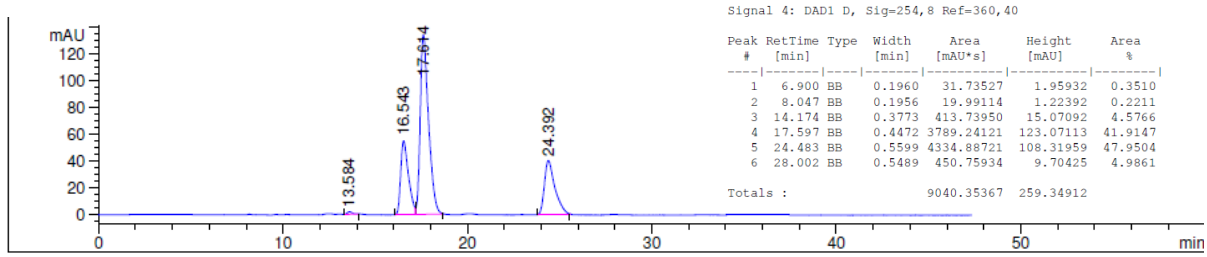

Figure 75: *rac*-**302**:*rac*-**303**, d.r. 1.3:1

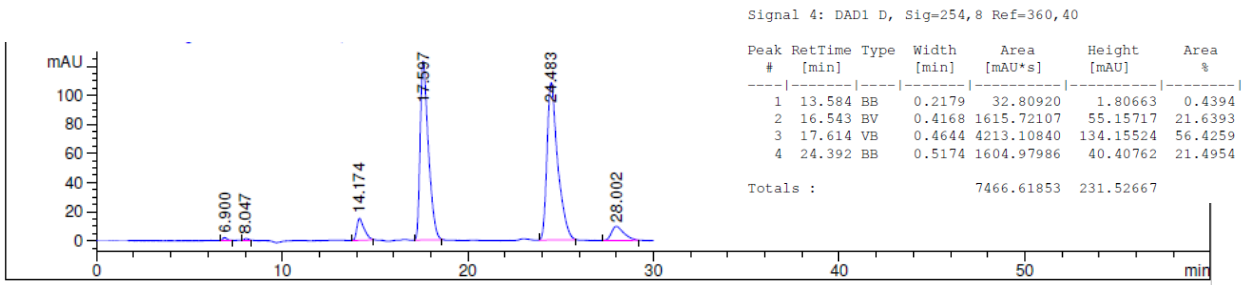

Figure 76: (*S*)-**302**:(*S*)-**303**, d.r. 1.14:1. Minor impurities.

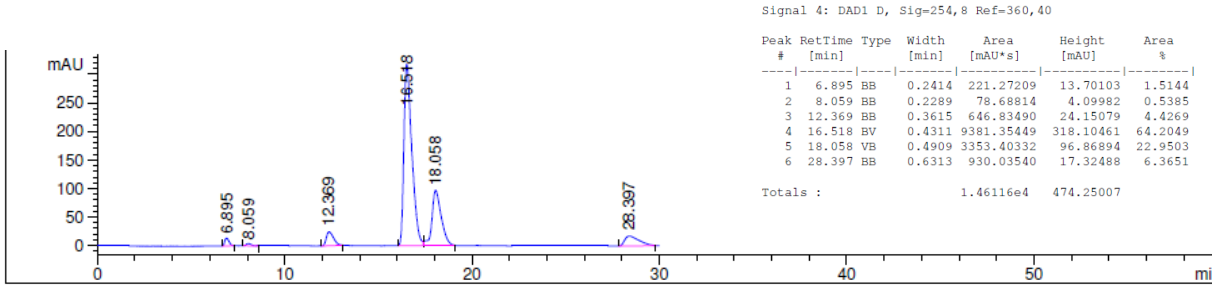

Signal 4: DAD1 D, Sig=254,8 Ref=360,40

Peak #	RetTime [min]	Type	Width [min]	Area [mAU*s]	Height [mAU]	Area %
1	6.895	BB	0.2414	221.27209	13.70103	1.5144
2	8.059	BB	0.2289	78.68814	4.09982	0.5385
3	12.369	BB	0.3615	646.83490	24.15079	4.4269
4	16.518	BV	0.4311	9381.35449	318.10461	64.2049
5	18.058	VB	0.4909	3353.40332	96.86894	22.9503
6	28.397	BB	0.6313	930.03540	17.32488	6.3651
Totals :				1.46116e4	474.25007	

Figure 77: (*S*)-**302**:(*S*)-**303** (d.r. 1:>20), major impurity at 18.1 min.

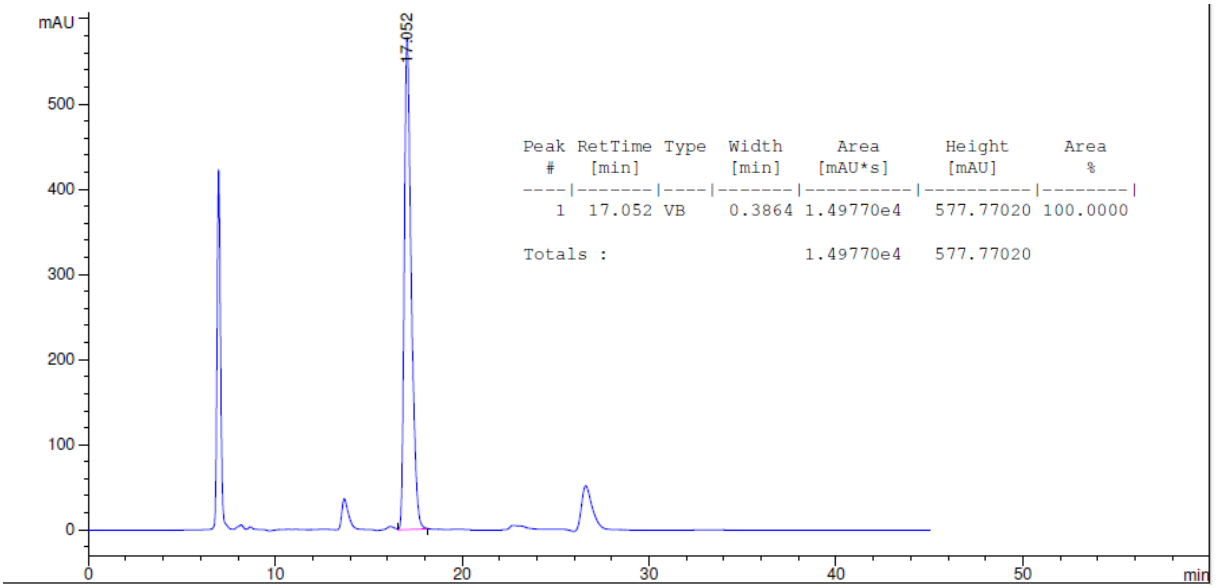

Peak #	RetTime [min]	Type	Width [min]	Area [mAU*s]	Height [mAU]	Area %
1	17.052	VB	0.3864	1.49770e4	577.77020	100.0000
Totals :				1.49770e4	577.77020	

Figure 78: (*S*)-**302**:(*S*)-**303** (d.r. >20:1). Major impurities.

8 References

[1] E. Brockway, T. H. de Brockway, L. Santos, *Diccionario náhuatl del norte del estado de Puebla*, 9683103022, Instituto Lingüístico de Verano, **2000**.

[2] D. L. Katz, K. Doughty, A. Ali, *Antioxid. Redox Signal.* **2011**, *15*, 2779-2811, doi.org/10.1089/ars.2010.3697, 'Cocoa and chocolate in human health and disease'.

[3] S. Zarrillo, N. Gaikwad, C. Lanaud, T. Powis, C. Viot, I. Lesur, O. Fouet, X. Argout, E. Guichoux, F. Salin, *Nat. Eco. Evo.* **2018**, *2*, 1879-1888, doi.org/10.1038/s41559-018-0697-x, 'The use and domestication of Theobroma cacao during the mid-Holocene in the upper Amazon'.

[4] a) L. M. Goh, P. J. Barlow, *Food Res. Int.* **2002**, *35*, 815-820, doi.org/10.1016/S0963-9969(02)00084-4, 'Antioxidant capacity in Ginkgo biloba'; b) D. Šamec, E. Karalija, S. Dahija, S. T. Hassan, *Plants* **2022**, *11*, 1381, doi.org/10.3390/plants11101381, 'Biflavonoids: Important contributions to the health benefits of Ginkgo (Ginkgo biloba L.)'.

[5] D. Tungmunnithum, A. Thongboonyou, A. Pholboon, A. Yangsabai, *Medicines* **2018**, *5*, 93, doi.org/10.3390/medicines5030093, 'Flavonoids and other phenolic compounds from medicinal plants for pharmaceutical and medical aspects: An overview'.

[6] A. N. Panche, A. D. Diwan, S. R. Chandra, *J. Nutr. Sci.* **2016**, *5*, e47, 'Flavonoids: an overview'.

[7] J. P. Spencer, *Brit. J. Nutr.* **2008**, *99*, ES60-ES77, doi.org/10.1017/S0007114508965776 'Flavonoids: modulators of brain function?'.

[8] R. J. Williams, J. P. Spencer, C. Rice-Evans, *Free Radic. Biol. Med.* **2004**, *36*, 838-849, doi.org/10.1016/j.freeradbiomed.2004.01.001, 'Flavonoids: antioxidants or signalling molecules?'.

[9] S. B. Lotito, B. Frei, *Free Radic. Biol. Med.* **2006**, *41*, 1727-1746, doi.org/10.1016/j.freeradbiomed.2006.04.033, 'Consumption of flavonoid-rich foods and increased plasma antioxidant capacity in humans: cause, consequence, or epiphenomenon?'.

[10] K. Yonekura-Sakakibara, Y. Higashi, R. Nakabayashi, *Front. Plant Sci.* **2019**, 943, doi.org/10.3389/fpls.2019.00943, 'The origin and evolution of plant flavonoid metabolism'.

[11] a) V. V. S. Murti, P. V. Raman, T. R. Seshadri, *Tetrahedron* **1967**, *23*, 397-404, doi.org/10.1016/S0040-4020(01)83325-1, 'Cupressuflavone, a new biflavonyl pigment'; b) R. J. Molyneux, A. C. Waiss Jr, W. F. Haddon, *Tetrahedron* **1970**, *26*, 1409-1416, doi.org/10.1016/S0040-4020(01)92970-9, 'Oxidative coupling of apigenin'; c) W. Rahman, S. P. Bhatnagar, *Tetrahedron Lett.* **1968**, *9*, 675-678, doi.org/10.1016/S0040-4039(00)75610-3, 'A new biflavonyl AC3 from Araucaria cunninghamii'; d) V. V. S. Murti, P. V. Raman, T. R. Seshadri, *Tetrahedron Lett.* **1964**, *5*, 2995-2997, doi.org/10.1016/0040-4039(64)83077-X, 'Cupressuflavone, a new member of the biflavonyl group'.

[12] a) S. Yu, H. Yan, L. Zhang, M. Shan, P. Chen, A. Ding, S. F. Y. Li, *Molecules* **2017**, *22*, 299, doi.org/10.3390/molecules22020299, 'A review on the phytochemistry, pharmacology, and pharmacokinetics of amentoflavone, a naturally-occurring biflavonoid'; b) H. P. Kim, H. Park, K. H. Son, H. W. Chang, S. S. Kang, *Arch. Pharmacal Res.* **2008**, *31*, 265-273, doi.org/10.1007/s12272-001-1151-3 'Biochemical pharmacology of biflavonoids: implications for anti-inflammatory action'; c) Y.-M. Lin, M. T. Flavin, R. Schure, F.-C. Chen, R. Sidwell, D. I. Barnard, J. H. Huffmann, E. R. Kern, *Planta Med.* **1999**, *65*, 120-125, doi.org/10.1016/j.biopha.2021.111596, 'Antiviral activities of biflavonoids'; d) M. Adnan, A. Rasul, G. Hussain, M. A. Shah, M. K. Zahoor, H. Anwar, I. Sarfraz, A. Riaz, M. Manzoor, Ş. Adem, *Food Chem. Toxicol.* **2020**, *145*, 111642, doi.org/10.1016/j.fct.2020.111642, 'Ginkgetin: A natural biflavone with versatile pharmacological activities'; e) L. F. Yamaguchi, M. J. Kato, P. Di Mascio, *Phytochem.* **2009**, *70*, 615-620, doi.org/10.1016/j.phytochem.2009.03.003, 'Biflavonoids from *Araucaria angustifolia* protect against DNA UV-induced damage'; f) V. S. Gontijo, M. H. Dos Santos, C. Viegas Jr, *Mini Rev. Med. Chem.* **2017**, *17*, 834-862, doi.org/10.2174/1389557517666161104130026, 'Biological and chemical aspects of natural biflavonoids from plants: a brief review'; g) D. Tasdemir, M. Kaiser, R. Brun, V. Yardley, T. J. Schmidt, F. Tosun, P. Rüedi, *Antimicrob. Agents Chemother.* **2006**, *50*, 1352-1364, doi.org/10.1128/aac.50.4.1352-1364.20, 'Antitrypanosomal and antileishmanial activities of

flavonoids and their analogues: in vitro, in vivo, structure-activity relationship, and quantitative structure-activity relationship studies'.

[13] W. H. Organization, *World health statistics 2023: monitoring health for the Sustainable Development Goals. CC BY-NC-SA 3.0 IGO.* , 978-92-4-007432-3, Geneva, **2023**.

[14] N. Vasan, J. Baselga, D. M. Hyman, *Nature* **2019**, *575*, 299-309, doi.org/10.1038/s41586-019-1730-1, 'A view on drug resistance in cancer'.

[15] A. Tagliabue, R. Rappuoli, *Front. Immunol.* **2018**, *9*, 1068, doi.org/10.3389/fimmu.2018.01068, 'Changing priorities in vaccinology: antibiotic resistance moving to the top'.

[16] M. Miethke, M. Pieroni, T. Weber, M. Brönstrup, P. Hammann, L. Halby, P. B. Arimondo, P. Glaser, B. Aigle, H. B. Bode, *Nat. Rev. Chem.* **2021**, *5*, 726-749, doi.org/10.1038/s41570-021-00313-1, 'Towards the sustainable discovery and development of new antibiotics'.

[17] D. J. Newman, G. M. Cragg, *J. Nat. Prod.* **2020**, *83*, 770-803, doi.org/10.1021/acs.jnatprod.9b01285, 'Natural Products as Sources of New Drugs over the Nearly Four Decades from 01/1981 to 09/2019'.

[18] G. Bringmann, C. Günther, M. Ochse, O. Schupp, S. Tasler, *Biaryls in nature: a multi-facetted class of stereochemically, biosynthetically, and pharmacologically intriguing secondary metabolites*, 3709172721, **2001**.

[19] S. T. Toenjes, J. L. Gustafson, *Future Med. Chem.* **2018**, *10*, 409-422, doi.org/10.4155/fmc-2017-0152, 'Atropisomerism in medicinal chemistry: challenges and opportunities'.

[20] J. Clayden, W. J. Moran, P. J. Edwards, S. R. LaPlante, *Angew. Chem. Int. Ed.* **2009**, *48*, 6398-6401, doi.org/10.1002/anie.200901719, 'The challenge of atropisomerism in drug discovery'.

[21] C.-Y. Sun, Q.-Y. Zhang, G.-J. Zheng, B. Feng, *Biomed. Pharmacother.* **2019**, *110*, 518-527, doi.org/10.1016/j.biopha.2018.12.010, 'Phytochemicals: Current strategy to sensitize cancer cells to cisplatin'.

[22] J.-S. Lou, L.-P. Zhao, Z.-H. Huang, X.-Y. Chen, J.-T. Xu, W. C.-S. Tai, K. W. Tsim, Y.-T. Chen, T. Xie, *Phytomedicine* **2021**, *80*, 153370, doi.org/10.1016/j.phymed.2020.153370, 'Ginkgetin derived from Ginkgo biloba leaves enhances the therapeutic effect of cisplatin via ferroptosis-mediated disruption of the Nrf2/HO-1 axis in EGFR wild-type non-small-cell lung cancer'.

[23] a) M. Frank, H. Niemann, P. Böhler, B. Stork, S. Wesselborg, W. Lin, P. Proksch, *Curr. Med. Chem.* **2015**, *22*, 3523-3532, doi.org/10.2174/0929867322666150716115300, 'Phomoxanthone A-from mangrove forests to anticancer therapy'; b) C. Wang, L. Engelke, D. Bickel, A. Hamacher, M. Frank, P. Proksch, H. Gohlke, M. U. Kassack, *Bioorg. Med. Chem.* **2019**, *27*, 115044, doi.org/10.1016/j.bmc.2019.115044, 'The tetrahydroxanthone-dimer phomoxanthone A is a strong inducer of apoptosis in cisplatin-resistant solid cancer cells'; c) B. Elsässer, K. Krohn, U. Flörke, N. Root, H. J. Aust, S. Draeger, B. Schulz, S. Antus, T. Kurtán, *Eur. J. Org. Chem.* **2005**, 4563-4570, doi.org/10.1002/ejoc.200500265, 'X - ray structure determination, absolute configuration and biological activity of phomoxanthone A'.

[24] H. Kikuchi, M. Isobe, M. Sekiya, Y. Abe, T. Hoshikawa, K. Ueda, S. Kurata, Y. Katou, Y. Oshima, *Org. Lett.* **2011**, *13*, 4624-4627, doi.org/10.1021/ol2018449, 'Structures of the dimeric and monomeric chromanones, gonytolides A–C, isolated from the fungus *Gonytrichum sp.* and their promoting activities of innate immune responses'.

[25] T. Qin, S. L. Skraba-Joiner, Z. G. Khalil, R. P. Johnson, R. J. Capon, J. A. Porco Jr, *Nat. Chem.* **2015**, *7*, 234-240, doi.org/10.1038/NCHEM.2173, 'Atropselective syntheses of (−) and (+) rugulotrosin A utilizing point-to-axial chirality transfer'.

[26] Y. S. Park, C. I. Grove, M. González-López, S. Urgaonkar, J. C. Fettinger, J. T. Shaw, *Angew. Chem. Int. Ed.* **2011**, *50*, 3730-3733, doi.org/10.1002/anie.201007298, 'Synthesis of (−)-Viriditoxin: A 6,6′-Binaphthopyran-2-one that Targets the Bacterial Cell Division Protein FtsZ'.

[27] G. Bringmann, A. J. Price Mortimer, P. A. Keller, M. J. Gresser, J. Garner, M. Breuning, *Angew. Chem.* **2005**, *117*, 5518-5563, doi.org/10.1002/ange.200462661, 'Atropselektive Synthese axial-chiraler Biaryle'.

[28] L. A. Nguyen, H. He, C. Pham-Huy, *Int. J. Biomed. Sci.* **2006**, *2*, 85-100, 'Chiral drugs: an overview'.

[29] H. Aldemir, R. Richarz, T. A. Gulder, *Angew. Chem. Int. Ed.* **2014**, *53*, 8286-8293, doi.org/10.1002/anie.201401075, 'The biocatalytic repertoire of natural biaryl formation'.

[30] J. Hassan, M. Sévignon, C. Gozzi, E. Schulz, M. Lemaire, *Chem. Rev.* **2002**, *102*, 1359-1470, doi.org/10.1021/cr000664r, 'Aryl− aryl bond formation one century after the discovery of the Ullmann reaction'.

[31] L. E. Zetzsche, J. A. Yazarians, S. Chakrabarty, M. E. Hinze, L. A. Murray, A. L. Lukowski, L. A. Joyce, A. R. Narayan, *Nature* **2022**, *603*, 79-85, doi.org/10.1038/s41586-021-04365-7, 'Biocatalytic oxidative cross-coupling reactions for biaryl bond formation'.

[32] L. E. Zetzsche, S. Chakrabarty, A. R. Narayan, *J. Am. Chem. Soc.* **2022**, *144*, 5214-5225, doi.org/10.1021/jacs.2c00224, 'The transformative power of biocatalysis in convergent synthesis'.

[33] a) E. Täuber, *Ber. Dtsch. Chem. Ges.* **1891**, *24*, 197-201, doi.org/10.1002/cber.18910240138, '*o*‐Dinitro‐und *o*‐Diamidodiphenyl und Synthese des Carbazols aus dem letzteren'; b) F. Ullmann, J. Bielecki, *Ber. Dtsch. Chem. Ges.* **1901**, *34*, 2174-2185, doi.org/10.1002/cber.190103402141, 'Ueber synthesen in der biphenylreihe'.

[34] G. H. Christie, J. Kenner, *J. Chem. Soc. T.* **1922**, *121*, 614-620, doi.org/10.1039/CT9222100614, 'LXXI. — The molecular configurations of polynuclear aromatic compounds. Part I. The resolution of γ-6: 6′-dinitro-and 4: 6: 4′: 6′-tetranitro-diphenic acids into optically active components'.

[35] M. Oki, *Topics in stereochemistry, Vol. 14*, ISBN: 978-0471237488, **1983**.

[36] G. Moss, P. Smith, D. Tavernier, *Pure Appl. Chem.* **1995**, *67*, 1307-1375, doi.org/10.1351/pac199567081307, 'Glossary of class names of organic compounds and reactivity intermediates based on structure (IUPAC Recommendations 1995)'.

[37] B. K. Lombe, D. Feineis, G. Bringmann, *Nat. Prod. Rep.* **2019**, *36*, 1513-1545, doi.org/10.1039/C9NP00024K, 'Dimeric naphthylisoquinoline alkaloids: polyketide-derived axially chiral bioactive quateraryls'.

[38] J. Mutanyatta, M. Bezabih, B. M. Abegaz, M. Dreyer, R. Brun, N. Kocher, G. Bringmann, *Tetrahedron* **2005**, *61*, 8475-8484, doi.org/10.1016/j.tet.2005.06.055, 'The first 6′-*O*-sulfated phenylanthraquinones: isolation from Bulbine frutescens, structural elucidation, enantiomeric purity, and partial synthesis'.

[39] C. Paniagua, A. Bilkova, P. Jackson, S. Dabravolski, W. Riber, V. Didi, J. Houser, N. Gigli-Bisceglia, M. Wimmerova, E. Budínská, *J. Exp. Botany* **2017**, *68*, 3287-3301, doi.org/10.1093/jxb/erx141, 'Dirigent proteins in plants: modulating cell wall metabolism during abiotic and biotic stress exposure'.

[40] O. F. Watts, J. Berreur, B. S. Collins, J. Clayden, *Acc. Chem. Res.* **2022**, *55*, 3362-3375, doi.org/10.1021/acs.accounts.2c00572, 'Biocatalytic Enantioselective Synthesis of Atropisomers'.

[41] A. Zask, J. Murphy, G. A. Ellestad, *Chirality* **2013**, *25*, 265-274, 'Biological stereoselectivity of atropisomeric natural products and drugs'.

[42] a) J. Wencel-Delord, A. Panossian, F. Leroux, F. Colobert, *Chem. Soc. Rev.* **2015**, *44*, 3418-3430, doi.org/10.1039/C5CS00012B, 'Recent advances and new concepts for the synthesis of axially stereoenriched biaryls'; b) P. Loxq, E. Manoury, R. Poli, E. Deydier, A. Labande, *Coordin. Chem. Rev.* **2016**, *308*, 131-190, doi.org/10.1016/j.ccr.2015.07.006, 'Synthesis of axially chiral biaryl compounds by asymmetric catalytic reactions with transition metals'; c) J. K. Cheng, S.-H. Xiang, S. Li, L. Ye, B. Tan, *Chem. Rev.* **2021**, *121*, 4805-4902, 'Recent advances in catalytic asymmetric construction of atropisomers'.

[43] P. Rodríguez-Salamanca, R. Fernández, V. Hornillos, J. M. Lassaletta, *Chem. Eur. J.* **2022**, *28*, e202104442, doi.org/10.1002/chem.202104442, 'Asymmetric Synthesis of Axially Chiral C−N Atropisomers'.

[44] G. Bringmann, A. J. Price Mortimer, P. A. Keller, M. J. Gresser, J. Garner, M. Breuning, *Angew. Chem. Int. Ed.* **2005**, *44*, 5384-5427, doi.org/10.1002/anie.200462661, 'Atroposelective synthesis of axially chiral biaryl compounds'.

[45] G. Keseru, M. Nogradi, *Stud. Nat. Prod. Chem.* **1997**, *20*, 263-322, doi.org/10.1016/S1572-5995(97)80033-6, 'Natural products by oxidative phenolic coupling phytochemistry, biosynthesis and synthesis'.

[46] G. Bringmann, S. Tasler, *Tetrahedron* **2001**, *57*, 331-343, doi.org/10.1016/S0040-4020(00)00940-6, 'Oxidative aryl coupling reactions: a biomimetic approach to configurationally unstable or axially chiral biaryl natural products and related bioactive compounds'.

[47] a) Y. E. Lee, T. Cao, C. Torruellas, M. C. Kozlowski, *J. Am. Chem. Soc.* **2014**, *136*, 6782-6785, doi.org/10.1021/ja500183z, 'Selective oxidative homo-and cross-coupling of phenols with aerobic catalysts'; b) Y. Nieves-Quinones, T. J. Paniak, Y. E. Lee, S. M. Kim, S. Tcyrulnikov, M. C. Kozlowski, *J. Am. Chem. Soc.* **2019**, *141*, 10016-10032, doi.org/10.1021/jacs.9b03890, 'Chromium-salen catalyzed cross-coupling of phenols: mechanism and origin of the selectivity'; c) H. Kang, Y. E. Lee, P. V. G. Reddy, S. Dey, S. E. Allen, K. A. Niederer, P. Sung, K. Hewitt, C. Torruellas, M. R. Herling, *Org. Lett.* **2017**, *19*, 5505-5508, doi.org/10.1021/acs.orglett.7b02552, 'Asymmetric oxidative coupling of phenols and hydroxycarbazoles'; d) J. Wu, M. C. Kozlowski, *ACS Catal.* **2022**, *12*, 6532-6549, doi.org/10.1021/acscatal.2c00318, 'Catalytic oxidative coupling of phenols and related compounds'.

[48] a) H. Shalit, A. Libman, D. Pappo, *J. Am. Chem. Soc.* **2017**, *139*, 13404-13413, doi.org/10.1021/jacs.7b05898, '*meso*-Tetraphenylporphyrin iron chloride catalyzed selective oxidative cross-coupling of phenols'; b) S. Narute, R. Parnes, F. D. Toste, D. Pappo, *J. Am. Chem. Soc.* **2016**, *138*, 16553-16560, doi.org/10.1021/jacs.6b11198, 'Enantioselective oxidative homocoupling and cross-coupling of 2-naphthols catalyzed by chiral iron phosphate complexes'; c) A. Libman, H. Shalit, Y. Vainer, S. Narute, S. Kozuch, D. Pappo, *J. Am. Chem. Soc.* **2015**, *137*, 11453-11460, doi.org/10.1021/jacs.5b06494, 'Synthetic and predictive approach to unsymmetrical biphenols by iron-catalyzed chelated radical–anion oxidative coupling'; d) E. Gaster, Y. Vainer, A. Regev, S. Narute, K. Sudheendran, A. Werbeloff, H. Shalit, D. Pappo, *Angew. Chem. Int. Ed.* **2015**, *54*, 4198-4202, doi.org/10.1002/anie.201409694, 'Significant Enhancement in the Efficiency and Selectivity of Iron-Catalyzed Oxidative Cross-Coupling of Phenols by Fluoroalcohols'.

[49] a) W. Hüttel, M. Nieger, M. Müller, *Synthesis* **2003**, 1803-1808, doi.org/10.1055/s-2003-41027, 'A Short and Efficient TotalSynthesis of the Naturally Occurring Coumarins Siderin, Kotanin, Isokotanin A and Desertorin C'; b) D. Drochner, W. Hüttel, M. Nieger, M. Müller, *Angew. Chem.* **2003**, *115*, 961-963, doi.org/10.1002/ange.200390216, 'Unselective Phenolic Coupling of Methyl 2-Hydroxy-4-methoxy-6-methylbenzoate—A Valuable Tool for the Total Synthesis of Natural Product Families'; c) H. Shalit, A. Dyadyuk, D. Pappo, *J. Org. Chem.* **2019**, *84*, 1677-1686, doi.org/10.1021/acs.joc.8b03084, 'Selective oxidative phenol coupling by iron catalysis'.

[50] M. Noji, M. Nakajima, K. Koga, *Tetrahedron Lett.* **1994**, *35*, 7983-7984, doi.org/10.1016/0040-4039(94)80028-6, 'A new catalytic system for aerobic oxidative coupling of 2-naphthol derivatives by the use of CuCl-amine complex: a practical synthesis of binaphthol derivatives'.

[51] a) D.-R. Hwang, C.-P. Chen, B.-J. Uang, *Chem. Commun.* **1999**, 1207-1208, doi.org/10.1039/A901934K, 'Aerobic catalytic oxidative coupling of 2-naphthols and phenols by $VO(acac)_2$'; b) Q.-X. Guo, Z.-J. Wu, Z.-B. Luo, Q.-Z. Liu, J.-L. Ye, S.-W. Luo, L.-F. Cun, L.-Z. Gong, *J. Am. Chem. Soc.* **2007**, *129*, 13927-13938, doi.org/10.1021/ja074322f, 'Highly enantioselective oxidative couplings of 2-naphthols catalyzed by chiral bimetallic oxovanadium complexes with either oxygen or air as oxidant'.

[52] M. Grzybowski, B. Sadowski, H. Butenschön, D. T. Gryko, *Angew. Chem. Int. Ed.* **2019**, *59*, 2998 –3027, doi.org/10.1002/anie.201904934, 'Synthetic Applications of Oxidative Aromatic Coupling—From Biphenols to Nanographenes'.

[53] A. Kumar, H. Sasai, S. Takizawa, *Acc. Chem. Res.* **2022**, *55*, 2949-2965, doi.org/10.1021/acs.accounts.2c00545, 'Atroposelective Synthesis of C–C Axially Chiral Compounds via Mono-and Dinuclear Vanadium Catalysis'.

[54] K. Tanaka, F. Toda, *Mol. Cryst. Liq.* **1990**, *187*, 49-52, doi.org/10.1080/00268949008036026, 'Oxidative coupling reactions of phenols with $FeCl_3$ in the solid state'.

[55] X. Yang, S. H. M. Lim, J. Lin, J. Wu, H. Tang, F. Zhao, F. Liu, C. Sun, X. Shi, Y. Kuang, *Nat. Commun.* **2022**, *13*, 6424, doi.org/10.1038/s41467-022-34123-w, 'Oxygen mediated oxidative couplings of flavones in alkaline water'.

[56] a) F.-J. Zhang, G.-Q. Lin, Q.-C. Huang, *J. Org. Chem.* **1995**, *60*, 6427-6430, doi.org/10.1021/jo00125a031, 'Synthesis, Resolution, and Absolute Configuration of Optically Pure 5,5''-Dihydroxy-4',4''', 7,7''-tetramethoxy-8,8''-biflavone and Its Derivatives'; b) F. J. Zhang, G. Q. Lin, *Chin. J. Chem.* **1997**, *15*, 464-471, doi.org/10.1002/cjoc.19970150513, 'Synthesis of the optically pure 5,5″‐dihydroxy‐7,7″‐dimethoxy‐8,8″‐biflavone and its derivatives'; c) C. Sambiagio, S. P. Marsden, A. J. Blacker, P. C. McGowan, *Chem. Soc. Rev.* **2014**, *43*, 3525-3550, doi.org/10.1039/C3CS60289C, 'Copper catalysed Ullmann type chemistry: from mechanistic aspects to modern development'.

[57] N. Miyaura, S. L. Buchwald, *Cross-coupling reactions: a practical guide, Vol. 219*, 978-3-540-42175-7, Springer, **2002**.

[58] a) N. Miyaura, T. Yanagi, A. Suzuki, *Synth. Commun.* **1981**, *11*, 513-519, doi.org/10.1080/00397918108063618, 'The palladium-catalyzed cross-coupling reaction of phenylboronic acid with haloarenes in the presence of bases'; b) N. Miyaura, A. Suzuki, *Chem. Rev.* **1995**, *95*, 2457-2483, doi.org/10.1021/cr00039a007, 'Palladium-catalyzed cross-coupling reactions of organoboron compounds'.

[59] K. Nicolaou, P. G. Bulger, D. Sarlah, *Angew. Chem. Int. Ed.* **2005**, *44*, 4442-4489, doi.org/10.1002/anie.200500368, 'Palladium‐catalyzed cross‐coupling reactions in total synthesis'.

[60] P. Ruiz-Castillo, S. L. Buchwald, *Chem. Rev.* **2016**, *116*, 12564-12649, doi.org/10.1021/acs.chemrev.6b00512, 'Applications of palladium-catalyzed C–N cross-coupling reactions'.

[61] a) R. Dorel, C. P. Grugel, A. M. Haydl, *Angew. Chem. Int. Ed.* **2019**, *58*, 17118-17129, doi.org/10.1002/anie.201904795, 'The Buchwald–Hartwig amination after 25 years'; b) D. G. Brown, J. Bostrom, *J. Med. Chem.* **2016**, *59*, 4443-4458, doi.org/10.1021/acs.jmedchem.5b01409, 'Analysis of past and present synthetic methodologies on medicinal chemistry: where have all the new reactions gone? Miniperspective'.

[62] F.-S. Han, *Chem. Soc. Rev.* **2013**, *42*, 5270-5298, doi.org/10.1039/C3CS35521G, 'Transition-metal-catalyzed Suzuki–Miyaura cross-coupling reactions: a remarkable advance from palladium to nickel catalysts'.

[63] a) The Nobel Foundation, Nobel Prize 2010 Akira Suzuki Facts, https://www.nobelprize.org/prizes/chemistry/2010/suzuki/facts/, Accessed: November 11, 2023; b) A. Suzuki, *Chem. Commun.* **2005**, 4759-4763, doi.org/10.1039/B507375H, 'Carbon–carbon bonding made easy'.

[64] a) K. Xu, W. Li, S. Zhu, T. Zhu, *Angew. Chem. Int. Ed.* **2019**, *58*, 17625-17630, doi.org/10.1002/anie.201910049, 'Atroposelective Arene Formation by Carbene-Catalyzed Formal [4+2] Cycloaddition'; b) G. Nishida, N. Suzuki, K. Noguchi, K. Tanaka, *Org. Lett.* **2006**, *8*, 3489-3492, doi.org/10.1021/ol0611550, 'Enantioselective synthesis of tetra-*ortho*-substituted axially chiral biaryls through rhodium-catalyzed double [2+2+2] cycloaddition'; c) T. Shibata, A. Sekine, A. Mitake, K. S. Kanyiva, *Angew. Chem. Int. Ed.* **2018**, *57*, 15862-15865, doi.org/10.1002/anie.201810174, 'Intramolecular Consecutive Dehydro‐Diels–Alder Reaction for the Catalytic and Enantioselective Construction of Axial Chirality'.

[65] a) X. Wu, T. Iwata, A. Scharf, T. Qin, K. D. Reichl, J. A. Porco Jr, *J. Am. Chem. Soc.* **2018**, *140*, 5969-5975, doi.org/10.1021/jacs.8b02535, 'Asymmetric synthesis of gonytolide A: strategic use of an aryl halide blocking group for oxidative coupling'; b) R. G. Giles, M. Sargent, *Aust. J. Chem.* **1986**, *39*, 2177-2181, doi.org/10.1071/CH9862177, 'Naturally-Occurring Dibenzofurans. X. A New Synthesis of Di-*O*-Methylstrepsilin'; c) D. Drochner, W. Hüttel, S. E. Bode, M. Müller,

U. Karl, M. Nieger, W. Steglich, *Eur. J. Org. Chem.* **2007**, 1749-1758, doi.org/10.1002/ejoc.200600899, 'Dimeric orsellinic acid derivatives: Valuable intermediates for natural product synthesis'; d) F. M. Hauser, P. J. F. Gauuan, *Org. Lett.* **1999**, *1*, 671-672, doi.org/10.1021/ol990758r, 'Total synthesis of (±)-Biphyscion'; e) M. Rahman, M. Riaz, U. R. Desai, *Chem. Biodivers.* **2007**, *4*, 2495-2527, doi.org/10.1002/cbdv.200790205, 'Synthesis of biologically relevant biflavanoids–a review'.

[66] T. T. Nguyen, *Eur. J. Org. Chem.* **2019**, 147-155, doi.org/10.1002/ejoc.201901557, 'The use of chiral *ortho*-auxiliaries/substituents and remote stereogenic centers in atropselective biaryl synthesis'.

[67] D. Zhang, Q. Wang, *Coordin. Chem. Rev.* **2015**, *286*, 1-16, doi.org/10.1016/j.ccr.2014.11.011, 'Palladium catalyzed asymmetric Suzuki–Miyaura coupling reactions to axially chiral biaryl compounds: Chiral ligands and recent advances'.

[68] J. A. Carmona, C. Rodríguez-Franco, R. Fernández, V. Hornillos, J. M. Lassaletta, *Chem. Soc. Rev.* **2021**, *50*, 2968-2983, doi.org/10.1039/D0CS00870B 'Atroposelective transformation of axially chiral (hetero) biaryls. From desymmetrization to modern resolution strategies'.

[69] H.-Y. Li, T. Nehira, M. Hagiwara, N. Harada, *J. Org. Chem.* **1997**, *62*, 7222-7227, doi.org/10.1021/jo970670w, 'Total Synthesis and Absolute Stereochemistry of the Natural Atropisomer of the Biflavone 4‘,4‘‘‘,7,7‘‘-Tetra-*O*-methylcupressuflavone'.

[70] H. Kagan, J. Fiaud, in *Topics in stereochemistry, Vol. 18*, John Wiley & Sons, Inc., United States of America, **1988**, pp. 249-330.

[71] R. S. Ward, *Tetrahedron: Asymmetry* **1995**, *6*, 1475-1490, doi.org/10.1016/0957-4166(95)00179-S, 'Dynamic kinetic resolution'.

[72] a) G. Bringmann, O. Schupp, *S. Afr. J. Chem.* **1994**, *47*, 83-102, 'Stereocontrolled'twisting'of biaryl systems–a new pathway to axial chirality'; b) G. Bringmann, M. Heubes, M. Breuning, L. Göbel, M. Ochse, B. Schöner, O. Schupp, *J. Org. Chem.* **2000**, *65*, 722-728, doi.org/10.1021/jo9913356, 'Atropisomerization barriers of configurationally unstable biaryl compounds, useful substrates for atroposelective conversions to axially chiral biaryls'; c) N. Chatterjee, A. Goswami, *Eur. J. Org. Chem.* **2017**, 3023-3032, doi.org/10.1002/ejoc.201601651, 'Synthesis and application of cyclic diaryliodonium salts: a platform for bifunctionalization in a single step'.

[73] J. Steinreiber, K. Faber, H. Griengl, *Chem. Eur. J.* **2008**, *14*, 8060-8072, doi.org/10.1002/chem.200701643, 'De-racemization of enantiomers versus de-epimerization of diastereomers—classification of dynamic kinetic asymmetric transformations (DYKAT)'.

[74] M. Huang, T. Pan, X. Jiang, S. Luo, *J. Am. Chem. Soc.* **2023**, *145*, 10917−10929, doi.org/10.1021/jacs.3c02622, 'Catalytic Deracemization Reactions'.

[75] K. Zhao, L. Duan, S. Xu, J. Jiang, Y. Fu, Z. Gu, *Chem* **2018**, *4*, 599-612, doi.org/10.1016/j.chempr.2018.01.017, 'Enhanced reactivity by torsional strain of cyclic diaryliodonium in Cu-catalyzed enantioselective ring-opening reaction'.

[76] F. Heinen, E. Engelage, A. Dreger, R. Weiss, S. M. Huber, *Angew. Chem. Int. Ed.* **2018**, *57*, 3830-3833, doi.org/10.1002/anie.201713012, 'Iodine(III) derivatives as halogen bonding organocatalysts'.

[77] M. Hou, R. Deng, Z. Gu, *Org. Lett.* **2018**, *20*, 5779-5783, doi.org/10.1021/acs.orglett.8b02477, 'Cu-Catalyzed Enantioselective Atropisomer Synthesis via Thiolative Ring Opening of Five-Membered Cyclic Diaryliodoniums'.

[78] Q. Li, M. Zhang, S. Zhan, Z. Gu, *Org. Lett.* **2019**, *21*, 6374-6377, doi.org/10.1021/acs.orglett.9b02267, 'Copper-Catalyzed Enantioselective Ring-Opening of Cyclic Diaryliodoniums and *O*-Alkylhydroxylamines'.

[79] K. Zhu, K. Xu, Q. Fang, Y. Wang, B. Tang, F. Zhang, *ACS Catal.* **2019**, *9*, 4951-4957, doi.org/10.1021/acscatal.9b00695, 'Enantioselective Synthesis of Axially Chiral Biaryls via Cu-Catalyzed Acyloxylation of Cyclic Diaryliodonium Salts'.

[80] Z. Chao, M. Ma, Z. Gu, *Org. Lett.* **2020**, *22*, 6441−6446, doi.org/10.1021/acs.orglett.0c02256, 'Cu-Catalyzed Site-Selective and Enantioselective Ring Opening of Cyclic Diaryliodoniums with 1,2,3-Triazoles'.

[81] a) J. Ke, B. Zu, Y. Guo, Y. Li, C. He, *Org. Lett.* **2020**, *23*, 329-333, doi.org/10.1021/acs.orglett.0c03833, 'Hexafluoroisopropanol-Enabled Copper-Catalyzed Asymmetric Halogenation of Cyclic Diaryliodoniums for the Synthesis of Axially Chiral 2,2′-Dihalobiaryls'; b) K. Zhu, Z. Song, Y. Wang, F. Zhang, *Org. Lett.* **2020**, *22*, 9356-9359, doi.org/10.1021/acs.orglett.0c03614, 'Synthesis of 2,2′-dihalobiaryls via Cu-catalyzed halogenation of cyclic diaryliodonium salts'.

[82] X. Zhang, K. Zhao, N. Li, J. Yu, L. Z. Gong, Z. Gu, *Angew. Chem. Int. Ed.* **2020**, *59*, 19899-19904, doi.org/10.1002/ange.202008431, 'Atroposelective Ring Opening of Cyclic Diaryliodonium Salts with Bulky Anilines Controlled by a Chiral Cobalt(III) Anion'.

[83] H. Cheng, J. Ma, P. Guo, *Adv. Synth. Catal.* **2023**, *365*, 1 - 29, doi.org/10.1002/adsc.202201326, 'Cyclic Diaryliodonium Salts: Eco‐Friendly and Versatile Building Blocks for Organic Synthesis'.

[84] M. Bielawski, 'Diaryliodonium Salts: Development of Synthetic Methodologies and *α*-Arylation of Enolates', Department of Organic Chemistry, Stockholm University **2011**.

[85] J. Malmgren, 'Iodonium Salts: Preparation, Chemoselectivity and Metal-Catalyzed Applications', Department of Organic Chemistry, Stockholm University **2014**.

[86] S. Mondal, B. Olofsson, *Trends Chem.* **2023**, *5*, 404-405, doi.org/10.1016/j.trechm.2023.02.004, 'Regioselective arylations via aryne intermediates'.

[87] M. Lanzi, Q. Dherbassy, J. Wencel‐Delord, *Angew. Chem. Int. Ed.* **2021**, 14852–14857, doi.org/10.1002/ange.202103625, 'Cyclic Diaryl λ^3-Bromanes as Original Aryne Precursors'.

[88] Y. Yoshida, S. Ishikawa, T. Mino, M. Sakamoto, *Chem. Commun.* **2021**, *57*, 2519-2522, doi.org/10.1039/D0CC07733J, 'Bromonium salts: diaryl-λ^3-bromanes as halogen-bonding organocatalysts'.

[89] M. Lanzi, T. Rogge, T. S. Truong, K. Houk, J. Wencel-Delord, *J. Am. Chem. Soc.* **2022**, *145*, 345-358, doi.org/10.1021/jacs.2c10090, 'Cyclic Diaryl λ^3-Chloranes: Reagents and Their C–C and C–O Couplings with Phenols via Aryne Intermediates'.

[90] G. Bringmann, T. Gulder, T. A. Gulder, M. Breuning, *Chem. Rev.* **2011**, *111*, 563-639, doi.org/10.1021/cr100155e, 'Atroposelective total synthesis of axially chiral biaryl natural products'.

[91] M. C. Kozlowski, B. J. Morgan, E. C. Linton, *Chem. Soc. Rev.* **2009**, *38*, 3193-3207, doi.org/10.1039/B821092F, 'Total synthesis of chiral biaryl natural products by asymmetric biaryl coupling'.

[92] a) G. Bringmann, J. Hinrichs, P. Henschel, J. Kraus, K. Peters, E. M. Peters, *Eur. J. Org. Chem.* **2002**, 1096-1106, doi.org/10.1002/1099-0690(200203)2002:6<1096::AID-EJOC1096>3.0.CO;2-Z, 'Atropo‐Enantioselective Synthesis of the Natural Bicoumarin (+)‐Isokotanin A via a Configurationally Stable Biaryl Lactone'; b) O. Baudoin, F. Guéritte, *Stud. Nat. Prod. Chem.* **2003**, *29*, 355-417, doi.org/10.1016/S1572-5995(03)80011-X, 'Natural bridged biaryls with axial chirality and antimitotic properties'; c) J. M. Lassaletta, R. Fernandez, *Atropisomerism and axial chirality*, 9781786346452, World Scientific, **2019**.

[93] H. Kang, M. R. Herling, K. A. Niederer, Y. E. Lee, P. Vasu Govardhana Reddy, S. Dey, S. E. Allen, P. Sung, K. Hewitt, C. Torruellas, *J. Org. Chem.* **2018**, *83*, 14362-14384, doi.org/10.1021/acs.joc.8b02083, 'Enantioselective vanadium-catalyzed oxidative coupling: development and mechanistic insights'.

[94] M. Isaka, S. Palasarn, K. Kocharin, J. Saenboonrueng, *J. Nat. Prod.* **2005**, *68*, 945-946, doi.org/10.1021/np058028h, 'A cytotoxic xanthone dimer from the entomopathogenic fungus *Aschersonia sp.* BCC 8401'.

[95] Z. Xiao, Y. Li, S. Gao, *Org. Lett.* **2017**, *19*, 1834-1837, doi.org/10.1021/acs.orglett.7b00592, 'Total synthesis and structural determination of the dimeric tetrahydroxanthone ascherxanthone A'.

[96] C. Qi, W. Wang, K. D. Reichl, J. McNeely, J. A. Porco Jr, *Angew. Chem.* **2018**, *130*, 2123-2126, doi.org/10.1002/ange.201711535, 'Total Synthesis of Aurofusarin: Studies on the Atropisomeric Stability of Bis-Naphthoquinones'.

[97] Y. Zhang, S.-M. Yeung, H. Wu, D. P. Heller, C. Wu, W. D. Wulff, *Org. Lett.* **2003**, *5*, 1813-1816, doi.org/10.1021/ol0275769, 'Highly enantioselective deracemization of linear and vaulted biaryl ligands'.

[98] M. Smrcina, M. Lorenc, V. Hanus, P. Sedmera, P. Kocovsky, *J. Org. Chem.* **1992**, *57*, 1917-1920, doi.org/10.1021/jo00032a055, 'Synthesis of enantiomerically pure 2,2'-dihydroxy-1,1'-binaphthyl, 2,2'-diamino-1,1'-binaphthyl, and 2-amino-2'-hydroxy-1,1'-binaphthyl. Comparison of processes operating as diastereoselective crystallization and as second order asymmetric transformation'.

[99] M. Smrcina, J. Polakova, S. Vyskocil, P. Kocovsky, *J. Org. Chem.* **1993**, *58*, 4534-4538, doi.org/10.1021/jo00069a010, 'Synthesis of enantiomerically pure binaphthyl derivatives. Mechanism of the enantioselective, oxidative coupling of naphthols and designing a catalytic cycle'.

[100] a) P. Hohenberg, W. Kohn, *Phys. Rev.* **1964**, *136*, B864-B871, doi.org/10.1103/PhysRev.136.B864, 'Inhomogeneous electron gas'; b) W. Kohn, L. J. Sham, *Phys. Rev.* **1965**, *140*, A1133-A1138, doi.org/10.1103/PhysRev.140.A1133, 'Self-consistent equations including exchange and correlation effects'.

[101] B. H. Lipshutz, F. Kayser, Z. P. Liu, *Angew. Chem., Int. Ed. Engl.* **1994**, *33*, 1842-1844, doi.org/10.1002/anie.199418421, 'Asymmetric synthesis of biaryls by intramolecular oxidative couplings of cyanocuprate intermediates'.

[102] J. Greb, T. Drennhaus, M. K. T. Klischan, Z. W. Schroeder, W. Frey, J. Pietruszka, *Chem. Eur. J.* **2023**, *29*, e202300941, doi.org/10.1002/chem.202300941, 'A Common C_2-Symmetric 2,2′-Biphenol Building Block and its Application in the Synthesis of (+)-di-*epi*-Gonytolide A'.

[103] R. Ganardi, J. Greb, B. Henssen, J. Pietruszka, *Adv. Synth. Catal.* **2023**, *365,*, 3512–3520, doi.org/10.1002/adsc.202300698, 'Atroposelective Total Synthesis of (+)-Isokotanin A via Combined Metal and Enzyme Catalysis'.

[104] Y. Inatomi, N. Iida, H. Murata, A. Inada, J. Murata, F. A. Lang, M. Iinuma, T. Tanaka, T. Nakanishi, *Tetrahedron Lett.* **2005**, *46*, 6533-6535, doi.org/10.1016/j.tetlet.2005.07.091, 'A pair of new atropisomeric cupressuflavone glucosides isolated from Juniperus communis var. depressa'.

[105] J.-F. Goossens, L. Goossens, C. Bailly, *Nat. Prod. Bioprospect.* **2021**, *11*, 365-377, doi.org/10.1007/s13659-021-00298-w, 'Hinokiflavone and related C–O–C-type biflavonoids as anti-cancer compounds: properties and mechanism of action'.

[106] N. Sirimangkalakitti, L. D. Juliawaty, E. H. Hakim, I. Waliana, N. Saito, K. Koyama, K. Kinoshita, *Bioorg. Med. Chem. Lett.* **2019**, *29*, 1994–1997, doi.org/10.1016/j.bmcl.2019.05.020, 'Naturally occurring biflavonoids with amyloid *β* aggregation inhibitory activity for development of anti-Alzheimer agents'.

[107] a) E. Al-Sayed, H. A. Gad, M. El-Shazly, M. M. Abdel-Daim, A. Nasser Singab, *Drug Dev. Res.* **2018**, *79*, 22-28, doi.org/10.1002/ddr.21417, 'Anti-inflammatory and analgesic activities of cupressuflavone from *Cupressus macrocarpa*: Impact on pro-inflammatory mediators'; b) A. Freitas, M. Almeida, C. Andrighetti-Fröhner, F. Cardozo, C. Barardi, M. Farias, C. Simões, *J. Ethnopharmacol.* **2009**, *126*, 512-517, doi.org/10.1016/j.jep.2009.09.005, 'Antiviral activity-guided fractionation from *Araucaria angustifolia* leaves extract'; c) J. A. Siddiqui, G. Swarnkar, K. Sharan, B. Chakravarti, G. Sharma, P. Rawat, M. Kumar, F. M. Khan, D. Pierroz, R. Maurya, *Mol. Cell. Endocrinol.* **2010**, *323*, 256-267, doi.org/10.1016/j.mce.2010.03.024, '8,8″-Biapigeninyl stimulates osteoblast functions and inhibits osteoclast and adipocyte functions: Osteoprotective action of 8,8″-biapigeninyl in ovariectomized mice'; d) E. Al-Sayed, M. M. Abdel-Daim, *Planta Med.* **2014**, *80*, 1665-1671, doi.org/10.1055/s-0034-1383211, 'Protective role of Cupressuflavone from *Cupressus macrocarpa* against carbon tetrachloride-induced hepato-and nephrotoxicity in mice'; e) H. Sasaki, Y. Kitoh, M. Tsukada, K. Miki, K. Koyama, L. D. Juliawaty, E. H. Hakim, K. Takahashi, K. Kinoshita, *Bioorg. Med. Chem. Lett.* **2015**, *25*, 2831-

2833, doi.org/10.1016/j.bmcl.2015.04.106, 'Inhibitory activities of biflavonoids against amyloid-*β* peptide 42 cytotoxicity in PC-12 cells'; f) J. C. DeForest, L. Du, P. M. Joyner, *J. Nat. Prod.* **2014**, *77*, 1093-1096, doi.org/10.1021/np4010739, '4′,4‴,7,7″-*Tetra-O*-methylcupressuflavone Inhibits Seed Germination of *Lactuca sativa*'.

[108] a) H. Kikuchi, T. Hoshikawa, S. Kurata, Y. Katou, Y. Oshima, *J. Nat. Prod.* **2016**, *79*, 1259-1266, doi.org/10.1021/acs.jnatprod.5b00829, 'Design and synthesis of Structure-Simplified derivatives of Gonytolide for the promotion of innate immune responses'; b) M. K. T. Klischan, F. Mazzone, L. Berning, J. Greb, M. Schlamkow, M. Haase, W. Frey, B. Stork, K. Pfeffer, J. Pietruszka, *ACS Omega* **2023**, *8*, 41816–41834, doi.org/10.1021/acsomega.3c06503, 'Modular Approach for the Synthesis and Bioactivity Profiling of 8,8′-Biflavones'.

[109] S. Natarajan, V. V. S. Murti, T. R. Seshadri, *Phytochem.* **1970**, *9*, 575-579, 'Biflavones of some Cupressaceae plants'.

[110] M. Ilyas, J. N. Usmani, S. P. Bhatnagar, M. Ilyas, W. Rahman, *Tetrahedron Lett.* **1968**, *9*, 5515-5517, doi.org/10.1016/S0040-4039(00)75549-3, 'WB1 and W11, the first optically active biflavones'.

[111] C. L. Covington, F. M. Junior, J. H. Silva, R. M. Kuster, M. B. de Amorim, P. L. Polavarapu, *J. Nat. Prod.* **2016**, *79*, 2530-2537, doi.org/10.1021/acs.jnatprod.6b00395, 'Atropoisomerism in biflavones: the absolute configuration of (−)-agathisflavone via chiroptical spectroscopy'.

[112] P. A. Wender, V. A. Verma, T. J. Paxton, T. H. Pillow, *Acc. Chem. Res.* **2008**, *41*, 40-49, doi.org/10.1021/ar700155p, 'Function-oriented synthesis, step economy, and drug design'.

[113] a) S. Ahmad, S. Razaq, *Tetrahedron Lett.* **1971**, *12*, 4633-4636, doi.org/10.1016/S0040-4039(01)97549-5, 'A new approach to the synthesis of symmetrical biflavones'; b) S. Ahmad, S. Razaq, *Tetrahedron* **1976**, *32*, 503-506, doi.org/10.1016/0040-4020(76)80071-3, 'New synthesis of biflavones of cupressuflavone series'; c) M. Parthasarathy, S. Gupta, *Indian J. Chem. B* **1984**, *23*, 227-230, 'Oxidative coupling of phloroacetophenone dimethyl ether, resacetophenone and resacetophenone monomethyl ether using silica-bound $FeCl_3$'; d) C. Y. Lee, C. H. Cheon, *Adv. Synth. Catal.* **2016**, *358*, 549-554, doi.org/10.1002/adsc.201500798, 'Diastereomeric Resolution of a Racemic Biarylboronic Acid and Its Application to Divergent Asymmetric Total Syntheses of Some Axially Chiral Natural Products'.

[114] N. Harada, H. Ono, H. Uda, M. Parveen, K. N. ud Din, B. Achari, P. K. Dutta, *J. Am. Chem. Soc.* **1992**, *114*, 7687-7692, doi.org/10.1021/ja00046a013 'Atropisomerism in natural products. Absolute stereochemistry of biflavone,(-)-4',4''', 7,7''-tetra-*O*-methylcupressuflavone, as determined by the theoretical calculation of CD spectra'.

[115] H. Sasaki, K. Miki, K. Kinoshita, K. Koyama, L. D. Juliawaty, S. A. Achmad, E. H. Hakim, M. Kaneda, K. Takahashi, *Bioorg. Med. Chem. Lett.* **2010**, *20*, 4558-4560, doi.org/10.1016/j.bmcl.2010.06.021, '*β*-Secretase (BACE-1) inhibitory effect of biflavonoids'.

[116] P. Coulerie, M. Nour, A. Maciuk, C. Eydoux, J.-C. Guillemot, N. Lebouvier, E. Hnawia, K. Leblanc, G. Lewin, B. Canard, *Planta Med.* **2013**, *79*, 1313-1318, doi.org/10.1055/s-0033-1350672, 'Structure-activity relationship study of biflavonoids on the Dengue virus polymerase DENV-NS5 RdRp'.

[117] B. Weniger, C. Vonthron-Sénécheau, M. Kaiser, R. Brun, R. Anton, *Phytomedicine* **2006**, *13*, 176-180, doi.org/10.1016/j.phymed.2004.10.008, 'Comparative antiplasmodial, leishmanicidal and antitrypanosomal activities of several biflavonoids'.

[118] T. D. Nelson, A. Meyers, *Tetrahedron Lett.* **1993**, *34*, 3061-3062, doi.org/10.1016/S0040-4039(00)93379-3, 'The synthesis of a useful chiral biaryl catalyst. An oxazoline-mediated Ullmann reaction'.

[119] A. P. R. Dianin, Z.; Khim, F., *Zh. Russ. Fiz.-Khim. O-va.* **1874**, *6*, 183-193, 'About Products from the Oxidation of Naphthols with Ferric Chloride'.

[120] T. C. Jempty, L. L. Miller, Y. Mazur, *J. Org. Chem.* **1980**, *45*, 749-751, doi.org/10.1021/jo01292a051 'Oxidative coupling reactions using silica-bound ferric chloride'.

[121] G.-Q. Lin, M. Zhong, *Tetrahedron Lett.* **1997**, *38*, 1087-1090, doi.org/10.1016/S0040-4039(96)02475-6, 'The first enantioselective synthesis of optically pure (*R*)-and (*S*)-5,5″-

dihydroxy-4′,4‴,7,7″-tetramethoxy-8,8″-biflavone and the reconfirmation of their absolute configuration'.

[122] R. Noyori, *Angew. Chem. Int. Ed.* **2002**, *41*, 2008-2022, doi.org/10.1002/1521-3773(20020617)41:12<2008::AID-ANIE2008>3.0.CO;2-4, 'Asymmetric catalysis: science and opportunities (Nobel lecture)'.

[123] S. Otsuka, A. Nakamura, T. Kano, K. Tani, *J. Am. Chem. Soc.* **1971**, *93*, 4301-4303, doi.org/10.1021/ja00746a041, 'Partial resolution of racemic tertiary phosphines with an asymmetric palladium complex'.

[124] A. Miyashita, A. Yasuda, H. Takaya, K. Toriumi, T. Ito, T. Souchi, R. Noyori, *J. Am. Chem. Soc.* **1980**, *102*, 7932-7934, doi.org/10.1021/ja00547a020, 'Synthesis of 2,2'-bis (diphenylphosphino)-1,1'-binaphthyl (BINAP), an atropisomeric chiral bis (triaryl) phosphine, and its use in the rhodium (I)-catalyzed asymmetric hydrogenation of. alpha.-(acylamino) acrylic acids'.

[125] The Nobel Foundation, Nobel Prize 2001 Ryoji Noyori Facts, https://www.nobelprize.org/prizes/chemistry/2001/noyori/facts/, Accessed: November 11, 2023.

[126] J. Yin, S. L. Buchwald, *J. Am. Chem. Soc.* **2000**, *122*, 12051-12052, doi.org/10.1021/ja005622z, 'A catalytic asymmetric Suzuki coupling for the synthesis of axially chiral biaryl compounds'.

[127] T. Hayashi, *Acc. Chem. Res.* **2000**, *33*, 354-362, doi.org/10.1021/ar990080f, 'Chiral monodentate phosphine ligand MOP for transition-metal-catalyzed asymmetric reactions'.

[128] R. Martin, S. L. Buchwald, *Acc. Chem. Res.* **2008**, *41*, 1461-1473, doi.org/10.1021/ar800036s, 'Palladium-catalyzed Suzuki−Miyaura cross-coupling reactions employing dialkylbiaryl phosphine ligands'.

[129] D. S. Surry, S. L. Buchwald, *Angew. Chem. Int. Ed.* **2008**, *47*, 6338-6361, doi.org/10.1002/anie.200800497, 'Biaryl phosphane ligands in palladium - catalyzed amination'.

[130] W. Tang, A. G. Capacci, X. Wei, W. Li, A. White, N. D. Patel, J. Savoie, J. J. Gao, S. Rodriguez, B. Qu, *Angew. Chem.* **2010**, *122*, 6015-6019, doi.org/10.1002/ange.201002404, 'A general and special catalyst for Suzuki–Miyaura coupling processes'.

[131] W. Tang, B. Qu, A. G. Capacci, S. Rodriguez, X. Wei, N. Haddad, B. Narayanan, S. Ma, N. Grinberg, N. K. Yee, *Org. Lett.* **2010**, *12*, 176-179, doi.org/10.1021/ol9025815, 'Novel, tunable, and efficient chiral bisdihydrobenzooxaphosphole ligands for asymmetric hydrogenation'.

[132] J. F. Teichert, B. L. Feringa, *Angew. Chem. Int. Ed.* **2010**, *49*, 2486-2528, doi.org/10.1002/anie.200904948, 'Phosphoramidites: privileged ligands in asymmetric catalysis'.

[133] A. H. de Vries, A. Meetsma, B. L. Feringa, *Angew. Chem., Int. Ed. Engl.* **1996**, *35*, 2374-2376, doi.org/10.1002/anie.199623741, 'Enantioselective conjugate addition of dialkylzinc reagents to cyclic and acyclic enones catalyzed by chiral copper complexes of new phosphorus amidites'.

[134] M. P. Carroll, P. J. Guiry, *Chem. Soc. Rev.* **2014**, *43*, 819-833, doi.org/10.1039/C3CS60302D, '*P*,*N* ligands in asymmetric catalysis'.

[135] V. Corti, G. Bertuzzi, *Synthesis* **2020**, *52*, 2450-2468, doi.org/10.1055/s-0040-1707814, 'Organocatalytic asymmetric methodologies towards the synthesis of atropisomeric *N*-heterocycles'.

[136] T. Akiyama, K. Mori, *Chem. Rev.* **2015**, *115*, 9277-9306, doi.org/10.1021/acs.chemrev.5b00041, 'Stronger Brønsted acids: recent progress'.

[137] a) A. S. Guram, S. L. Buchwald, *J. Am. Chem. Soc.* **1994**, *116*, 7901-7902, doi.org/10.1021/ja00096a059, 'Palladium-catalyzed aromatic aminations with in situ generated aminostannanes'; b) F. Paul, J. Patt, J. F. Hartwig, *J. Am. Chem. Soc.* **1994**, *116*, 5969-5970, doi.org/10.1021/ja00092a058 'Palladium-catalyzed formation of carbon-nitrogen bonds. Reaction intermediates and catalyst improvements in the hetero cross-coupling of aryl halides and tin amides'.

[138] L. Xu, F.-Y. Liu, Q. Zhang, W.-J. Chang, Z.-L. Liu, Y. Lv, H.-Z. Yu, J. Xu, J.-J. Dai, H.-J. Xu, *Nat. Catal.* **2021**, *4*, 71-78, doi.org/10.26434/chemrxiv.14237288.v1, 'The amine-catalysed Suzuki–Miyaura-type coupling of aryl halides and arylboronic acids'.

[139] a) Z. Novák, R. Adamik, J. T. Csenki, F. Béke, R. Gavaldik, B. Varga, B. Nagy, Z. May, J. Daru, Z. Gonda, *ChemRxiv* **2021**, doi.org/10.26434/chemrxiv.14071247.v1, 'Curse or Blessing? Influence of Impurities on Cross-Coupling—Guideline for Elucidating Catalysts'; b) M. Avanthay, R. B. Bedford, C. S. Begg, D. Boese, J. Clayden, S. A. Davis, J.-C. Eloi, G. P. Goryunov, I. V. Hartung, J. Heeley, *Nat. Catal.* **2021**, *4*, 994-998, doi.org/10.1038/s41929-021-00710-1, 'Identifying palladium culprits in amine catalysis'.

[140] a) H.-U. Blaser, A. Indolese, A. Schnyder, *Curr. Sci.* **2000**, *78*, 1336-1344, 'Applied homogeneous catalysis by organometallic complexes'; b) J. Wang, G. Dong, *Chem. Rev.* **2019**, *119*, 7478-7528, doi.org/10.1021/acs.chemrev.9b00079, 'Palladium/norbornene cooperative catalysis'.

[141] a) M. Catellani, F. Frignani, A. Rangoni, *Angew. Chem., Int. Ed. Engl.* **1997**, *36*, 119-122, doi.org/10.1002/chin.199716113, 'A Complex Catalytic Cycle Leading to a Regioselective Synthesis of *o*,*o*'-Disubstituted Vinylarenes'; b) N. Della Ca', M. Fontana, E. Motti, M. Catellani, *Acc. Chem. Res.* **2016**, *49*, 1389-1400, doi.org/10.1021/acs.accounts.6b00165, 'Pd/Norbornene: a winning combination for selective aromatic functionalization via C–H bond activation'.

[142] A. F. Littke, C. Dai, G. C. Fu, *J. Am. Chem. Soc.* **2000**, *122*, 4020-4028, doi.org/10.1021/ja0002058, 'Versatile catalysts for the Suzuki cross-coupling of arylboronic acids with aryl and vinyl halides and triflates under mild conditions'.

[143] M. R. Netherton, G. C. Fu, *Org. Lett.* **2001**, *3*, 4295-4298, doi.org/10.1021/ol016971g, 'Air-stable trialkylphosphonium salts: simple, practical, and versatile replacements for air-sensitive trialkylphosphines. Applications in stoichiometric and catalytic processes'.

[144] E. K. Reeves, O. R. Bauman, G. B. Mitchem, S. R. Neufeldt, *Isr. J. Chem.* **2020**, *60*, 406-409, doi.org/10.1002/ijch.201900082, 'Solvent Effects on the Selectivity of Palladium-Catalyzed Suzuki-Miyaura Couplings'.

[145] S. S. Zalesskiy, V. P. Ananikov, *Organometallics* **2012**, *31*, 2302-2309, doi.org/10.1021/om201217r, '$Pd_2(dba)_3$ as a precursor of soluble metal complexes and nanoparticles: Determination of palladium active species for catalysis and synthesis'.

[146] G. A. Morris, *Emagres* **2007**, 1-13, doi.org/10.1002/9780470034590.emrstm0119.pub2, 'Diffusion-ordered spectroscopy'.

[147] P. Sehnal, R. J. Taylor, I. J. Fairlamb, *Chem. Rev.* **2010**, *110*, 824-889, doi.org/10.1021/cr9003242, 'Emergence of palladium(IV) chemistry in synthesis and catalysis'.

[148] W. A. Carole, J. Bradley, M. Sarwar, T. J. Colacot, *Org. Lett.* **2015**, *17*, 5472-5475, doi.org/10.1021/acs.orglett.5b02835, 'Can palladium acetate lose its “saltiness”? Catalytic activities of the impurities in palladium acetate'.

[149] C. Amatore, A. Jutand, M. A. M'Barki, *Organometallics* **1992**, *11*, 3009-3013, doi.org/10.1021/om00045a012 'Evidence of the formation of zerovalent palladium from $Pd(OAc)_2$ and triphenylphosphine'.

[150] C. S. Wei, G. H. Davies, O. Soltani, J. Albrecht, Q. Gao, C. Pathirana, Y. Hsiao, S. Tummala, M. D. Eastgate, *Angew. Chem.* **2013**, *125*, 5934-5938, doi.com/10.1002/anie.201210252, 'The impact of palladium(II) reduction pathways on the structure and activity of palladium(0) catalysts'.

[151] P. R. Melvin, D. Balcells, N. Hazari, A. Nova, *ACS Catal.* **2015**, *5*, 5596-5606, doi.org/10.1021/acscatal.5b01291, 'Understanding precatalyst activation in cross-coupling reactions: alcohol facilitated reduction from Pd(II) to Pd(0) in precatalysts of the type (η^3-allyl) Pd(L)(Cl) and (η^3-indenyl) Pd(L)(Cl)'.

[152] M. R. Biscoe, B. P. Fors, S. L. Buchwald, *J. Am. Chem. Soc.* **2008**, *130*, 6686-6687, doi.org/10.1021/ja801137k, 'A new class of easily activated palladium precatalysts for facile C−N cross-coupling reactions and the low temperature oxidative addition of aryl chlorides'.

[153] N. C. Bruno, N. Niljianskul, S. L. Buchwald, *J. Org. Chem.* **2014**, *79*, 4161-4166, doi.org/10.1021/jo500355k, '*N*-Substituted 2-aminobiphenylpalladium methanesulfonate precatalysts and their use in C–C and C–N cross-couplings'.

[154] B. T. Ingoglia, C. C. Wagen, S. L. Buchwald, *Tetrahedron* **2019**, *75*, 4199-4211, doi.org/10.1016/j.tet.2019.05.003, 'Biaryl monophosphine ligands in palladium-catalyzed C–N coupling: An updated User's guide'.

[155] a) F. Schoenebeck, K. Houk, *J. Am. Chem. Soc.* **2010**, *132*, 2496-2497, doi.org/10.1021/ja9077528, 'Ligand-controlled regioselectivity in palladium-catalyzed cross coupling reactions'; b) K. Fourmy, D. H. Nguyen, O. Dechy-Cabaret, M. Gouygou, *Cat. Sci. Technol.* **2015**, *5*, 4289-4323, doi.org/10.1039/C4CY01701C, 'Phosphole-based ligands in catalysis'; c) A. J. Kendall, L. N. Zakharov, D. R. Tyler, *Inorg. Chem.* **2016**, *55*, 3079-3090, doi.org/10.1021/acs.inorgchem.5b02996, 'Steric and Electronic Influences of Buchwald-Type Alkyl-JohnPhos Ligands'; d) R. E. Plata, D. E. Hill, B. E. Haines, D. G. Musaev, L. Chu, D. P. Hickey, M. S. Sigman, J.-Q. Yu, D. G. Blackmond, *J. Am. Chem. Soc.* **2017**, *139*, 9238-9245, doi.org/10.1021/jacs.7b03716, 'A role for Pd(IV) in catalytic enantioselective C–H functionalization with monoprotected amino acid ligands under mild conditions'; e) K. Abe, M. Kitamura, H. Fujita, M. Kunishima, *Mol. Cat.* **2018**, *445*, 87-93, doi.org/10.1016/j.mcat.2017.11.008, 'Development of highly electron-deficient and less sterically-hindered phosphine ligands possessing 1,3,5-triazinyl groups'.

[156] K. Fagnou, M. Lautens, *Angew. Chem. Int. Ed.* **2002**, *41*, 26-47, doi.org/10.1002/1521-3773(20020104)41:1<26::AID-ANIE26>3.0.CO;2-9, 'Halide effects in transition metal catalysis'.

[157] L. M. Alcazar-Roman, J. F. Hartwig, *Organometallics* **2002**, *21*, 491-502, 'Mechanistic studies on oxidative addition of aryl halides and triflates to Pd (BINAP) 2 and structural characterization of the product from aryl triflate addition in the presence of amine'.

[158] J.-Q. Yu, Z. Shi, *C-H activation, Vol. 292*, 978-3-642-12355-9, Springer, **2010**.

[159] a) G. Bocelli, M. Catellani, S. Ghelli, *J. Organomet. Chem.* **1993**, *458*, C12-C15, doi.org/10.1016/0022-328X(93)80486-U, 'Regioselective ring opening of a palladium(IV) alkylaromatic metallacycle by benzyl group migration from palladium to the aromatic carbon and X-ray structure of the resulting palladium(II) complex'; b) E. Motti, A. Mignozzi, M. Catellani, *J. Mol. Catal.* **2003**, *204*, 115-124, doi.org/10.1016/S1381-1169(03)00290-5, 'A new type of palladium-catalysed aromatic cross-coupling combined with a Suzuki reaction: synthesis of selectively 2,3′-substituted 1,1′; 2′,1″-terphenyl derivatives'.

[160] a) A. Martins, M. Lautens, *Org. Lett.* **2008**, *10*, 5095-5097, doi.org/10.1021/ol802185x, 'Aromatic *ortho*-benzylation reveals an unexpected reductant'; b) A. Martins, D. A. Candito, M. Lautens, *Org. Lett.* **2010**, *12*, 5186-5188, doi.org/10.1021/ol1019037, 'Palladium-catalyzed reductive ortho-arylation: evidence for the decomposition of 1,2-dimethoxyethane and subsequent arylpalladium(II) reduction'; c) D. I. Chai, P. Thansandote, M. Lautens, *Chem. Eur. J.* **2011**, *17*, 8175-8188, doi.org/10.1002/chem.201100210, 'Mechanistic Studies of Pd‐Catalyzed Regioselective Aryl C-H Bond Functionalization with Strained Alkenes: Origin of Regioselectivity'; d) X. Abel-Snape, A. Whyte, M. Lautens, *Org. Lett.* **2020**, *22*, 7920-7925, doi.org/10.1021/acs.orglett.0c02850, 'Synthesis of aminated phenanthridinones via palladium/Norbornene catalysis'.

[161] J. Wencel-Delord, T. Dröge, F. Liu, F. Glorius, *Chem. Soc. Rev.* **2011**, *40*, 4740-4761, doi.org/10.1039/C1CS15083A, 'Towards mild metal-catalyzed C–H bond activation'.

[162] S. K. Sinha, S. Guin, S. Maiti, J. P. Biswas, S. Porey, D. Maiti, *Chem. Rev.* **2021**, *122*, 5682-5841, doi.org/10.1021/acs.chemrev.1c00220, 'Toolbox for distal C–H bond functionalizations in organic molecules'.

[163] a) H. Ge, B. Li, B. Lawrence, G. Li, *Angew. Chem. Int. Ed.* **2020**, *59*, 3078-3082, doi.org/10.1002/anie.201913126, 'Ligand‐Controlled Direct γ‐C‐H Arylation of Aldehydes'; b) P. Dolui, J. Das, H. B. Chandrashekar, S. Anjana, D. Maiti, *Angew. Chem. Int. Ed.* **2019**, *58*, 13773-13777, doi.org/10.1002/anie.201907262, 'Ligand‐Enabled Pd^{II}‐Catalyzed Iterative γ–C(sp^3)–H Arylation of Free Aliphatic Acid'; c) G. Xia, J. Weng, L. Liu, P. Verma, Z. Li, J.-Q. Yu, *Nat.*

Chem. **2019**, *11*, 571-577, doi.org/10.1038/s41557-019-0245-6, 'Reversing conventional site-selectivity in C(sp^3)–H bond activation'.

[164] S. Duan, Y. Xu, X. Zhang, X. Fan, *Chem. Commun.* **2016**, *52*, 10529-10532, doi.org/10.1039/C6CC04756D, 'Synthesis of 2,2′-biphenols through direct C (sp^2) – H hydroxylation of [1,1′-biphenyl]-2-ols'.

[165] D. Lapointe, K. Fagnou, *Chem. Lett.* **2010**, *39*, 1118-1126, doi.org/10.1246/cl.2010.1118, 'Overview of the mechanistic work on the concerted metallation–deprotonation pathway'.

[166] H.-Y. Sun, S. I. Gorelsky, D. R. Stuart, L.-C. Campeau, K. Fagnou, *J. Org. Chem.* **2010**, *75*, 8180-8189, doi.org/10.1021/jo101821r, 'Mechanistic analysis of azine *N*-oxide direct arylation: Evidence for a critical role of acetate in the $Pd(OAc)_2$ precatalyst'.

[167] M. Lafrance, K. Fagnou, *J. Am. Chem. Soc.* **2006**, *128*, 16496-16497, doi.org/10.1021/ja067144j, 'Palladium-catalyzed benzene arylation: incorporation of catalytic pivalic acid as a proton shuttle and a key element in catalyst design'.

[168] Y. Tan, J. F. Hartwig, *J. Am. Chem. Soc.* **2011**, *133*, 3308-3311, doi.org/10.1021/ja1113936, 'Assessment of the intermediacy of arylpalladium carboxylate complexes in the direct arylation of benzene: Evidence for C−H bond cleavage by “Ligandless” species'.

[169] S. I. Gorelsky, D. Lapointe, K. Fagnou, *J. Org. Chem.* **2012**, *77*, 658-668, doi.org/10.1021/jo202342q, 'Analysis of the palladium-catalyzed (aromatic) C–H bond metalation–deprotonation mechanism spanning the entire spectrum of arenes'.

[170] D. L. Davies, S. M. Donald, S. A. Macgregor, *J. Am. Chem. Soc.* **2005**, *127*, 13754-13755, doi.org/10.1021/ja052047w, 'Computational study of the mechanism of cyclometalation by palladium acetate'.

[171] D. L. Davies, S. A. Macgregor, C. L. McMullin, *Chem. Rev.* **2017**, *117*, 8649-8709, doi.org/10.1021/acs.chemrev.6b00839, 'Computational studies of carboxylate-assisted C–H activation and functionalization at group 8–10 transition metal centers'.

[172] G. Dijkstra, W. H. Kruizinga, R. M. Kellogg, *J. Org. Chem.* **1987**, *52*, 4230-4234, doi.org/10.1021/jo00228a015 'An assessment of the causes of the "cesium effect"'.

[173] a) T. J. Dent, 'Controlling and exploiting the caesium effect in palladium catalysed coupling reactions', University of Leeds **2019**; b) T. W. Lyons, K. L. Hull, M. S. Sanford, *J. Am. Chem. Soc.* **2011**, *133*, 4455-4464, doi.org/10.1021/ja1097918, 'Controlling site selectivity in Pd-catalyzed oxidative cross-coupling reactions'; c) M. Wang, X. Zhang, Y.-X. Zhuang, Y.-H. Xu, T.-P. Loh, *J. Am. Chem. Soc.* **2015**, *137*, 1341-1347, doi.org/10.1021/ja512212x, 'Pd-Catalyzed intramolecular C–N bond cleavage, 1, 4-migration, sp^3 c–h activation, and heck reaction: four controllable diverse pathways depending on the judicious choice of the base and ligand'.

[174] a) A. Ros, B. Estepa, P. Ramirez-Lopez, E. Alvarez, R. Fernandez, J. M. Lassaletta, *J. Am. Chem. Soc.* **2013**, *135*, 15730-15733, doi.org/10.1021/ja4087819, 'Dynamic kinetic cross-coupling strategy for the asymmetric synthesis of axially chiral heterobiaryls'; b) P. Ramirez-Lopez, A. Ros, B. Estepa, R. Fernandez, B. Fiser, E. Gomez-Bengoa, J. M. Lassaletta, *ACS Catal.* **2016**, *6*, 3955-3964, doi.org/10.1021/acscatal.6b00784, 'A dynamic kinetic C–P cross–coupling for the asymmetric synthesis of axially chiral *P*,*N* ligands'.

[175] Á. Mosquera, M. A. Pena, J. Perez Sestelo, L. A. Sarandeses, *Eur. J. Org. Chem.* **2013**, 2555-2562, doi.org/10.1002/ejoc.201300042, 'Synthesis of Axially Chiral 1,1′-Binaphthalenes by Palladium-Catalysed Cross-Coupling Reactions of Triorganoindium Reagents'.

[176] V. Bhat, S. Wang, B. M. Stoltz, S. C. Virgil, *J. Am. Chem. Soc.* **2013**, *135*, 16829-16832, doi.org/10.1021/ja409383f, 'Asymmetric synthesis of QUINAP via dynamic kinetic resolution'.

[177] M. Retbøll, A. J. Edwards, A. D. Rae, A. C. Willis, M. A. Bennett, E. Wenger, *J. Am. Chem. Soc.* **2002**, *124*, 8348-8360, doi.org/10.1021/ja0264091, 'Preparation of Benzyne Complexes of Group 10 Metals by Intramolecular Suzuki Coupling of *ortho*-Metalated Phenylboronic Esters: Molecular Structure of the First Benzyne-Palladium(0) Complex'.

[178] Y. Zhang, *Acc. Chem. Res.* **2022**, *55*, 3507-3518, doi.com/10.1021/acs.accounts.2c00627, 'Intermolecular Difunctionalization of C,C-Palladacycles Obtained by Pd(0)-Catalyzed C–H Activation'.

[179] A. Lu, X. Ji, B. Zhou, Z. Wu, Y. Zhang, *Angew. Chem. Int. Ed.* **2018**, *57*, 3233-3237, doi.org/10.1002/anie.201800330, 'Palladium‐Catalyzed C−H Silylation through Palladacycles Generated from Aryl Halides'.

[180] G. Shi, D. Chen, H. Jiang, Y. Zhang, Y. Zhang, *Org. Lett.* **2016**, *18*, 2958-2961, doi.org/10.1021/acs.orglett.6b01300, 'Synthesis of Fluorenes Starting from 2-Iodobiphenyls and CH_2Br_2 through Palladium-Catalyzed Dual C–C Bond Formation'.

[181] C. Cheng, X. Zuo, D. Tu, B. Wan, Y. Zhang, *Chem. Commun.* **2021**, *57*, 2939-2942, doi.org/10.1039/D1CC00398D 'Palladium-catalyzed diastereoselective cross-coupling of two aryl halides via C–H activation: synthesis of chiral eight-membered nitrogen heterocycles'.

[182] Y. Luo, S. Cheng, Y. Peng, X. Wang, J. Li, C. Gan, S. Luo, Q. Zhu, *CCS Chem.* **2022**, *4*, 2897-2905, doi.org/10.31635/ccschem.021.202101486, 'A new saddle-shaped aza analog of tetraphenylene: atroposelective synthesis and application as a chiral acylating reagent'.

[183] X.-C. Wang, H.-R. Wang, X. Xu, D. Zhao, *ChemRxiv* **2021**, doi.org/10.26434/chemrxiv.14510718.v1, 'Ring Expansion to 8-Membered Silacycles via Formal Cross-Dimerization of 5-Membered Palladacycles with Silacyclobutanes'.

[184] Y. Yang, B. Zhou, X. Zhu, G. Deng, Y. Liang, Y. Yang, *Org. Lett.* **2018**, *20*, 5402-5405, doi.org/10.1021/acs.orglett.8b02310, 'Palladium-Catalyzed Synthesis of Triphenylenes via Sequential C–H Activation and Decarboxylation'.

[185] C. C. Hsiao, Y. K. Lin, C. J. Liu, T. C. Wu, Y. T. Wu, *Adv. Synth. Catal.* **2010**, *352*, 3267-3274, doi.org/10.1002/adsc.201000651, 'Synthesis of Methylene‐Bridge Polyarenes through Palladium‐Catalyzed Activation of Benzylic Carbon‐Hydrogen Bond'.

[186] G. Karig, M.-T. Moon, N. Thasana, T. Gallagher, *Org. Lett.* **2002**, *4*, 3115-3118, doi.org/10.1021/ol026426v, 'C−H activation and palladium migration within biaryls under Heck reaction conditions'.

[187] A. Maleckis, J. W. Kampf, M. S. Sanford, *J. Am. Chem. Soc.* **2013**, *135*, 6618-6625, doi.org/10.1021/ja401557m, 'A Detailed Study of Acetate-Assisted C–H Activation at Palladium(IV) Centers'.

[188] L. F. Tietze, *Chem. Rev.* **1996**, *96*, 115-136, doi.org/10.1021/cr950027e, 'Domino reactions in organic synthesis'.

[189] E. Motti, N. Della Ca, S. Deledda, E. Fava, F. Panciroli, M. Catellani, *Chem. Commun.* **2010**, *46*, 4291-4293, doi.org/10.1039/C000526F, 'Palladium-catalyzed unsymmetrical aryl couplings in sequence leading to *o*-teraryls: dramatic olefin effect on selectivity'.

[190] M. Blanchot, D. A. Candito, F. Larnaud, M. Lautens, *Org. Lett.* **2011**, *13*, 1486-1489, doi.org/10.1021/ol200174g, 'Formal synthesis of nitidine and NK109 via palladium-catalyzed domino direct arylation/*N*-arylation of aryl triflates'.

[191] a) C. Amatore, M. Catellani, S. Deledda, A. Jutand, E. Motti, *Organometallics* **2008**, *27*, 4549-4554, doi.org/10.1021/om800015x, 'Rates of the oxidative addition of benzyl halides to a metallacyclic palladium(II) complex and of the reductive elimination from a benzyl-palladium(IV) complex'; b) D. J. Cárdenas, B. Martín-Matute, A. M. Echavarren, *J. Am. Chem. Soc.* **2006**, *128*, 5033-5040, doi.org/10.1021/ja056661j, 'Aryl transfer between Pd(II) centers or Pd(IV) intermediates in Pd-catalyzed domino reactions'.

[192] C.-T. Wang, M. Li, Y.-N. Ding, W.-X. Wei, Z. Zhang, X.-Y. Gou, R.-Q. Jiao, Y.-T. Wen, Y.-M. Liang, *Org. Lett.* **2021**, *23*, 786−791, doi.org/10.1021/acs.orglett.0c04018, 'Alkylation-Terminated Catellani Reactions by Cyclobutanol C–C Cleavage'.

[193] R. Li, F. Liu, G. Dong, *Org. Chem. Front.* **2018**, *5*, 3108-3112, doi.org/10.1039/C8QO00808F, 'Palladium-catalyzed asymmetric annulation between aryl iodides and racemic epoxides using a chiral norbornene cocatalyst'.

[194] H. Shi, D. J. Babinski, T. Ritter, *J. Am. Chem. Soc.* **2015**, *137*, 3775-3778, doi.org/10.1021/jacs.5b01082, 'Modular C–H functionalization cascade of aryl iodides'.

[195] C. Ye, H. Zhu, Z. Chen, *J. Org. Chem.* **2014**, *79*, 8900-8905, doi.org/10.1021/jo501544h, 'Synthesis of biaryl tertiary amines through Pd/norbornene joint catalysis in a remote C–H amination/Suzuki coupling reaction'.

[196] Z. Dong, G. Dong, *J. Am. Chem. Soc.* **2013**, *135*, 18350-18353, doi.org/10.1021/ja410823e, '*Ortho* vs *ipso*: site-selective Pd and norbornene-catalyzed arene C–H amination using aryl halides'.

[197] X. Dong, Q. Liu, Y. Dong, H. Liu, *Chem. Eur. J.* **2017**, *23*, 2481-2511, doi.org/10.1002/chem.201601607, 'Transition - Metal - Catalyzed Electrophilic Amination: Application of *O*-Benzoylhydroxylamines in the Construction of the C–N Bond'.

[198] P. Renaud, I. Bétrisey, *Synth. Commun.* **1995**, *25*, 3479-3491, doi.org/10.1080/00397919508013872, 'Radical Reductive Alkylation of Enamines: Conversion of the Products into Alkenes and Primary Amines'.

[199] P. Aschwanden, C. R. Stephenson, E. M. Carreira, *Org. Lett.* **2006**, *8*, 2437-2440, doi.org/10.1021/ol060876w, 'Highly enantioselective access to primary propargylamines: 4-piperidinone as a convenient protecting group'.

[200] L. Ding, X. Sui, Z. Gu, *ACS Catal.* **2018**, *8*, 5630-5635, doi.org/10.1021/acscatal.8b01037, 'Enantioselective synthesis of biaryl atropisomers via Pd/norbornene-catalyzed three-component cross-couplings'.

[201] L. Fan, J. Liu, L. Bai, Y. Wang, X. Luan, *Angew. Chem. Int. Ed.* **2017**, *56*, 14257-14261, doi.org/10.1002/anie.201708310, 'Rapid Assembly of Diversely Functionalized Spiroindenes by a Three-Component Palladium-Catalyzed C–H Amination/Phenol Dearomatization Domino Reaction'.

[202] R. Li, G. Dong, *J. Am. Chem. Soc.* **2020**, *142*, 17859-17875, doi.org/10.1021/jacs.0c09193, 'Structurally Modified Norbornenes: A Key Factor to Modulate Reaction Selectivity in the Palladium/Norbornene Cooperative Catalysis'.

[203] Z.-S. Liu, Y. Hua, Q. Gao, Y. Ma, H. Tang, Y. Shang, H.-G. Cheng, Q. Zhou, *Nat. Catal.* **2020**, *3*, 727-733, doi.org/10.1038/s41929-020-0494-1, 'Construction of axial chirality via palladium/chiral norbornene cooperative catalysis'.

[204] Q. Gao, C. Wu, S. Deng, L. Li, Z.-S. Liu, Y. Hua, J. Ye, C. Liu, H.-G. Cheng, H. Cong, *J. Am. Chem. Soc.* **2021**, *143*, 7253-7260, doi.org/10.1021/jacs.1c02405, 'Catalytic Synthesis of Atropisomeric *o*-Terphenyls with 1, 2-Diaxes via Axial-to-Axial Diastereoinduction'.

[205] Q. Feng, X. Ma, W. Bao, S.-J. Li, Y. Lan, Q. Song, *CCS Chem.* **2021**, 1-25, doi.org/10.31635/ccschem.021.202000725, 'Catalytic Atroposelective Catellani Reaction Enables to Construct Axially Chiral Biaryl Monophosphine Oxides'.

[206] D. Grudzinski, Bachelor's Thesis, 'Auf dem Weg zu neuartigen, enantiomerenreinen 8,8'-Biflavonen', Heinrich Heine University Düsseldorf **2023**.

[207] W. Zhang, K. Krohn, U. Flörke, G. Pescitelli, L. Di Bari, S. Antus, T. Kurtán, J. Rheinheimer, S. Draeger, B. Schulz, *Chem. Eur. J.* **2008**, *14*, 4913-4923, doi.org/10.1002/chem.200800035, 'New Mono-and Dimeric Members of the Secalonic Acid Family: Blennolides A–G Isolated from the Fungus *Blennoria sp*'.

[208] J. R. Cannon, T. M. Cresp, B. W. Metcalf, M. V. Sargent, G. Vinciguerra, J. A. Elix, *J. Chem. Soc. C* **1971**, 3495-3504, doi.org/10.1039/J39710003495, 'The bromination of some derivatives of resorcinol'.

[209] K.-H. Hellwich, in *Stereochemie—Grundbegriffe*, Springer, **2002**, pp. 40-41.

[210] S. S. Negus, *Biochem. Pharmacol.* **2006**, *71*, 1663-1670, doi.org/10.1016/j.bcp.2005.12.038, 'Some implications of receptor theory for in vivo assessment of agonists, antagonists and inverse agonists'.

[211] H. Adams, C. Werner, *Anaesthesist* **1997**, *46*, 1026-1042, doi.org/10.1007/s001010050503 'Vom Razemat zum Eutomer:(S)-Ketamin Renaissance einer Substanz? Renaissance einer Substanz?'.

[212] a) T. Eriksson, S. Björkman, B. Roth, P. Höglund, *J. Pharm, Pharmacol.* **2000**, *52*, 807-817, doi.org/10.1211/0022357001774660, 'Intravenous formulations of the enantiomers of thalidomide: pharmacokinetic and initial pharmacodynamic characterization in man'; b) W. M. Liu, S. J. Strauss, T. Chaplin, S. Shahin, D. J. Propper, B. D. Young, S. P. Joel, J. S. Malpas, *Haematologica* **2004**, *5*, 247-254, doi.org/10.1038/sj.thj.6200351, '(*S*)-Thalidomide has a

greater effect on apoptosis than angiogenesis in a multiple myeloma cell line'; c) H. R. Wiedemann, *Med. Welt* **1961**, *37*, 1863, 'Hinweis auf eine derzeitige Häufung hypo-und aplastischer Fehlbildung der Gliedmassen'.

[213] C. A. Kuttruff, M. D. Eastgate, P. S. Baran, *Nat. Prod. Rep.* **2014**, *31*, 419-432, doi.org/10.1039/C3NP70090A, 'Natural product synthesis in the age of scalability'.

[214] a) J. Wang, R.-G. Zhou, T. Wu, T. Yang, Q.-X. Qin, I. Li, B. Yang, J. Yang, *J. Chem. Res.* **2012**, *36*, 121-122, doi.org/10.3184/174751912X13285269293913, 'Total synthesis of apigenin'; b) P. Königs, B. Rinker, L. Maus, M. Nieger, J. Rheinheimer, S. Waldvogel, *J. Nat. Prod.* **2010**, *73*, 2064-2066, doi.org/10.1021/np1005604, 'Structural revision and synthesis of altechromone A'.

[215] a) F. Eiden, G. Patzelt, *Arch. Pharm.* **1985**, *318*, 328-340, doi.org/10.1002/ardp.19853180408, 'Darstellung und Reaktionen von 2-Acetyl-3-amino-5-hydroxy-2-cyclohexenonen; Benzol-Derivate aus Pyronen'; b) J.-Q. Hou, C. Guo, J.-J. Zhao, Q.-W. He, B.-B. Zhang, H. Wang, *J. Org. Chem.* **2017**, *82*, 1448-1457, doi.org/10.1021/acs.joc.6b02643, 'Frutescone A–G, tasmanone-based meroterpenoids from the aerial parts of *Baeckea frutescens*'; c) F. Eiden, E. G. Teupe, *Arch. Pharm.* **1981**, *314*, 223-227, doi.org/10.1002/ardp.19813140307, 'Über die Reaktion von 3,5-Diacetyl-2,6-dimethyl-4H-pyran-4-on mit Natriumalkanolaten'; d) T. D. Grayfer, P. Grellier, E. Mouray, R. H. Dodd, J. Dubois, K. Cariou, *Org. Lett.* **2016**, *18*, 708-711, doi.org/10.1021/acs.orglett.5b03676, 'Mallotojaponins B and C: total synthesis, antiparasitic evaluation, and preliminary SAR studies'.

[216] M. M. Naik, S. G. Tilve, V. P. Kamat, *Tetrahedron Lett.* **2014**, *55*, 3340-3343, 'Pyrrolidine and iodine catalyzed domino aldol-Michael-dehydrogenative synthesis of flavones'.

[217] M. Freitas, D. Ribeiro, S. M. Tome, A. M. Silva, E. Fernandes, *Eur. J. Med. Chem.* **2014**, *86*, 153-164, doi.org/10.1016/j.ejmech.2014.08.035, 'Synthesis of chlorinated flavonoids with anti-inflammatory and pro-apoptotic activities in human neutrophils'.

[218] W. Ge, Y. Wei, *Green Chem.* **2012**, *14*, 2066-2070, doi.org/10.1039/C2GC35337G, 'Iodine-catalyzed oxidative system for 3-sulfenylation of indoles with disulfides using DMSO as oxidant under ambient conditions in dimethyl carbonate'.

[219] H. Xue, L. Sigg, F. G. Kari, *Envir. Sci. Technol.* **1995**, *29*, 59-68, doi.org/10.1021/es00001a007 'Speciation of EDTA in natural waters: exchange kinetics of Fe-EDTA in river water'.

[220] F. Effenberger, *Angew. Chem. Int. Ed.* **2002**, *41*, 1699-1700, doi.org/10.1002/1521-3773(20020517)41:10<1699::AID-ANIE1699>3.0.CO;2-N, 'How attractive is bromine as a protecting group in aromatic chemistry?'.

[221] M. Dardé, D. Ajzenberg, J. Smith, *Population structure and epidemiology of Toxoplasma gondii*, Elsevier, **2007**.

[222] J. Flegr, J. Prandota, M. Sovičková, Z. H. Israili, *PLoS One* **2014**, *9*, e90203, doi.org/10.1371/journal.pone.0090203, 'Toxoplasmosis–a global threat. Correlation of latent toxoplasmosis with specific disease burden in a set of 88 countries'.

[223] E. a. ECDC, *EFSA Journal* **2019**, *17*, 5926, doi.org/10.2903/j.efsa.2019.5926, 'The European Union One Health 2018 Zoonoses Report'.

[224] F. Mazzone, M. K. T. Klischan, J. Greb, S. H. J. Smits, J. Pietruszka, K. Pfeffer, *Front. Chem.* **2024**, *12*, 1406307, doi.org/10.3389/fchem.2024.1406307, 'Synthesis and In Vitro Evaluation of Bichalcones as Novel Anti-Toxoplasma Agents'.

[225] B. Touquet, L. Pelissier, P. Cavailles, W. Yi, V. Bellini, C. Mercier, M.-F. Cesbron-Delauw, A. Boumendjel, D. Aldebert, *PLoS One* **2018**, *13*, e0201678, doi.org/10.1371/journal.pone.0201678, 'High-content imaging assay to evaluate *Toxoplasma gondii* infection and proliferation: a multiparametric assay to screen new compounds'.

[226] N. Konstantinovic, H. Guegan, T. Stäjner, S. Belaz, F. Robert-Gangneux, *Food Waterborne Parasitol.* **2019**, *15*, e00036, doi.org/10.1016/j.fawpar.2019.e00036, 'Treatment of toxoplasmosis: Current options and future perspectives'.

[227] R. Re, N. Pellegrini, A. Proteggente, A. Pannala, M. Yang, C. Rice-Evans, *Free Radic. Biol. Med.* **1999**, *26*, 1231-1237, 'Antioxidant activity applying an improved ABTS radical cation decolorization assay'.

[228] M. K. T. Klischan, C. David, D. Grudzinski, W. Frey, B. Stork, J. Pietruszka, *Org. Lett.* **2024**, *26*, 5258-5262, doi.org/10.1021/acs.orglett.4c01308, 'Application of Cyclic Diaryliodonium Salts in the Synthesis of Axially Chiral Natural Product Analogues'.

[229] a) D. Maiti, B. P. Fors, J. L. Henderson, Y. Nakamura, S. L. Buchwald, *Chem. Sci.* **2011**, *2*, 57-68, doi.org/10.1039/C0SC00330A, 'Palladium-catalyzed coupling of functionalized primary and secondary amines with aryl and heteroaryl halides: two ligands suffice in most cases'; b) B. P. Fors, N. R. Davis, S. L. Buchwald, *J. Am. Chem. Soc.* **2009**, *131*, 5766-5768, doi.org/10.1021/ja901414u, 'An efficient process for Pd-catalyzed C−N cross-coupling reactions of aryl iodides: insight into controlling factors'.

[230] J. Louie, F. Paul, J. F. Hartwig, *Organometallics* **1996**, *15*, 2794-2805, doi.org/10.1021/om960188o, 'Catalysis with Platinum-Group Alkylamido Complexes. The Active Palladium Amide in Catalytic Aryl Halide Aminations As Deduced from Kinetic Data and Independent Generation'.

[231] a) T. Z. Liu, S. D. Lee, R. S. Bhatnagar, *Toxoco. Lett.* **1979**, *4*, 469-473, doi.org/10.1016/0378-4274(79)90113-9, 'Toxicity of palladium'; b) J. Kielhorn, C. Melber, D. Keller, I. Mangelsdorf, *Int. J. Hyg. Environ. Health* **2002**, *205*, 417-432, doi.org/10.1078/1438-4639-00180, 'Palladium–a review of exposure and effects to human health'; c) M. Schmid, S. Zimmermann, H. F. Krug, B. Sures, *Environ. Int.* **2007**, *33*, 385-390, doi.org/10.1016/j.envint.2006.12.003, 'Influence of platinum, palladium and rhodium as compared with cadmium, nickel and chromium on cell viability and oxidative stress in human bronchial epithelial cells'.

[232] K. L. Billingsley, T. E. Barder, S. L. Buchwald, *Angew. Chem. Int. Ed.* **2007**, *46*, 5359-5363, doi.org/10.1002/anie.200701551, 'Palladium‐Catalyzed Borylation of Aryl Chlorides: Scope, Applications, and Computational Studies'.

[233] a) M. Murata, S. Watanabe, Y. Masuda, *J. Org. Chem.* **1997**, *62*, 6458-6459, doi.org/10.1021/jo970963p, 'Novel palladium(0)-catalyzed coupling reaction of dialkoxyborane with aryl halides: convenient synthetic route to arylboronates'; b) M. Murata, T. Oyama, S. Watanabe, Y. Masuda, *J. Org. Chem.* **2000**, *65*, 164-168, doi.org/10.1021/jo991337q, 'Palladium-catalyzed borylation of aryl halides or triflates with dialkoxyborane: A novel and facile synthetic route to arylboronates'.

[234] a) T. Ishiyama, M. Murata, N. Miyaura, *J. Org. Chem.* **1995**, *60*, 7508-7510, doi.org/10.1021/jo00128a024, 'Palladium(0)-catalyzed cross-coupling reaction of alkoxydiboron with haloarenes: a direct procedure for arylboronic esters'; b) T. Ishiyama, Y. Itoh, T. Kitano, N. Miyaura, *Tetrahedron Lett.* **1997**, *38*, 3447-3450, doi.org/10.1016/S0040-4039(97)00642-4, 'Synthesis of arylboronates via the palladium(0)-catalyzed cross-coupling reaction of tetra (alkoxo) diborons with aryl triflates'.

[235] a) X. Shen, A. M. Hyde, S. L. Buchwald, *J. Am. Chem. Soc.* **2010**, *132*, 14076-14078, doi.org/10.1021/ja107481a, 'Palladium-catalyzed conversion of aryl and vinyl triflates to bromides and chlorides'; b) A. Klapars, S. L. Buchwald, *J. Am. Chem. Soc.* **2002**, *124*, 14844-14845, doi.org/10.1021/ja028865v, 'Copper-catalyzed halogen exchange in aryl halides: An aromatic Finkelstein reaction'.

[236] D.-Y. Lee, J. F. Hartwig, *Org. Lett.* **2005**, *7*, 1169-1172, doi.org/10.1021/ol050141b, 'Zinc trimethylsilylamide as a mild ammonia equivalent and base for the amination of aryl halides and triflates'.

[237] R. A. Green, J. F. Hartwig, *Org. Lett.* **2014**, *16*, 4388-4391, doi.org/10.1021/ol501739g, 'Palladium-catalyzed amination of aryl chlorides and bromides with ammonium salts'.

[238] X. Jin, C. Uttamapinant, A. Y. Ting, *ChemBioChem* **2011**, *12*, 65-70, doi.org/10.1002/cbic.201000414, 'Synthesis of 7‐Aminocoumarin by Buchwald–Hartwig Cross Coupling for Specific Protein Labeling in Living Cells'.

[239] W. Liu, J. Li, P. Querard, C.-J. Li, *J. Am. Chem. Soc.* **2019**, *141*, 6755-6764, doi.org/10.1021/jacs.9b02684, 'Transition-metal-free C–C, C–O, and C–N cross-couplings enabled by light'.

[240] M. Bielawski, M. Zhu, B. Olofsson, *Adv. Synth. Catal.* **2007**, *349*, 2610-2618, doi.org/10.1002/adsc.200700373, 'Efficient and general one‐pot synthesis of diaryliodonium triflates: optimization, scope and limitations'.

[241] M. Bielawski, B. Olofsson, *Chem. Commun.* **2007**, 2521-2523, doi.org/10.1039/B701864A, 'High-yielding one-pot synthesis of diaryliodonium triflates from arenes and iodine or aryl iodides'.

[242] a) A. Cornejo, J. M. Fraile, J. I. García, M. J. Gil, V. Martínez-Merino, J. A. Mayoral, E. Pires, I. Villalba, *Synlett* **2005**, *2005*, 2321-2324, doi.org/10.1055/s-2005-872672, 'An efficient and general one-pot method for the synthesis of chiral bis(oxazoline) and pyridine bis(oxazoline) ligands'; b) S. Fu, H. Yang, G. Li, Y. Deng, H. Jiang, W. Zeng, *Org. Lett.* **2015**, *17*, 1018-1021, doi.org/10.1021/acs.orglett.5b00131, 'Copper(II)-catalyzed enantioselective intramolecular cyclization of *N*-alkenylureas'.

[243] BLDPharm, https://www.bldpharm.com/products/, Accessed: November 11, 2023.

[244] A. B. Lindstrom, M. J. Strynar, E. L. Libelo, *Envir. Sci. Technol.* **2011**, *45*, 7954-7961, doi.org/10.1021/es2011622, 'Polyfluorinated compounds: past, present, and future'.

[245] a) T. Ishiyama, Y. Nobuta, J. F. Hartwig, N. Miyaura, *Chem. Commun.* **2003**, 2924-2925, doi.org/10.1039/B311103B, 'Room temperature borylation of arenes and heteroarenes using stoichiometric amounts of pinacolborane catalyzed by iridium complexes in an inert solvent'; b) T. Ishiyama, J. Takagi, J. F. Hartwig, N. Miyaura, *Angew. Chem. Int. Ed.* **2002**, *41*, 3056-3058, doi.org/10.1002/1521-3773(20020816)41:16<3056::AID-ANIE3056>3.0.CO;2-%23, 'A Stoichiometric Aromatic C-H Borylation Catalyzed by Iridium(I)/2,2′‐Bipyridine Complexes at Room Temperature'; c) T. Ishiyama, J. Takagi, K. Ishida, N. Miyaura, N. R. Anastasi, J. F. Hartwig, *J. Am. Chem. Soc.* **2002**, *124*, 390-391, doi.org/10.1021/ja0173019, 'Mild iridium-catalyzed borylation of arenes. High turnover numbers, room temperature reactions, and isolation of a potential intermediate'.

[246] T. M. Boller, J. M. Murphy, M. Hapke, T. Ishiyama, N. Miyaura, J. F. Hartwig, *J. Am. Chem. Soc.* **2005**, *127*, 14263-14278, 'Mechanism of the mild functionalization of arenes by diboron reagents catalyzed by iridium complexes. Intermediacy and chemistry of bipyridine-ligated iridium trisboryl complexes'.

[247] a) J. F. Hartwig, *Chem. Soc. Rev.* **2011**, *40*, 1992-2002, doi.org/10.1039/C0CS00156B, 'Regioselectivity of the borylation of alkanes and arenes'; b) L. Xu, G. Wang, S. Zhang, H. Wang, L. Wang, L. Liu, J. Jiao, P. Li, *Tetrahedron* **2017**, *73*, 7123-7157, doi.org/10.1016/j.tet.2017.11.005, 'Recent advances in catalytic C−H borylation reactions'; c) I. A. Mkhalid, J. H. Barnard, T. B. Marder, J. M. Murphy, J. F. Hartwig, *Chem. Rev.* **2010**, *110*, 890-931, doi.org/10.1021/cr900206p, 'C−H activation for the construction of C−B bonds'.

[248] H. Deng, M. Bengsch, N. Tchorz, C. N. Neumann, *Chem. Eur. J.* **2022**, e202202074, doi.org/10.1002/chem.202202074, 'Sterically Controlled Late‐Stage Functionalization of Bulky Phosphines'.

[249] a) M. Anil Kumar, K. K. K. Reddy, M. V. Reddy, C. D. Reddy, C. S. Reddy, *Synth. Commun.* **2008**, *38*, 2089-2095, doi.org/10.1080/00397910802029349, 'Oxone as a mild, inexpensive, and environmentally benign oxidant for the *α*-thiocyanation of ketones'; b) K. S. Webb, D. Levy, *Tetrahedron Lett.* **1995**, *36*, 5117-5118, doi.org/10.1016/0040-4039(95)00963-D, 'A facile oxidation of boronic acids and boronic esters'.

[250] R. E. Maleczka, F. Shi, D. Holmes, M. R. Smith, *J. Am. Chem. Soc.* **2003**, *125*, 7792-7793, doi.org/10.1021/ja0349857, 'C−H activation/borylation/oxidation: A one-pot unified route to *meta*-substituted phenols bearing *ortho*-/*para*-directing groups'.

[251] N. Soldatova, P. Postnikov, A. A. Troyan, A. Yoshimura, M. S. Yusubov, V. V. Zhdankin, *Tetrahedron Lett.* **2016**, *57*, 4254-4256, doi.org/10.1016/j.tetlet.2016.08.038, 'Mild and efficient synthesis of iodylarenes using oxone as oxidant'.

[252] A. Tlili, N. Xia, F. Monnier, M. Taillefer, *Angewandte Chemie* **2009**, *121*, 8881-8884, doi.org/10.1002/ange.200903639, 'A very simple copper‐catalyzed synthesis of phenols employing hydroxide salts'.

[253] C. W. Cheung, S. L. Buchwald, *J. Org. Chem.* **2014**, *79*, 5351-5358, doi.org/10.1021/jo500662s, 'Palladium-catalyzed hydroxylation of aryl and heteroaryl halides enabled by the use of a palladacycle precatalyst'.

[254] M. Schlamkow, Bachelor's Thesis, 'Palladium-katalysierte Catellani-Reaktionen: Funktionalisierung von Aromaten für die Synthese Biaryl-basierter Naturstoffe', Fachhochschule Aachen **2021**.

[255] K. Dodou, *Exp. Opin. Inv. Drugs* **2005**, *14*, 1419-1434, doi.org/10.1517/13543784.14.11.1419, 'Investigations on gossypol: past and present developments'.

[256] T. Imamoto, T. Oshiki, T. Onozawa, M. Matsuo, T. Hikosaka, M. Yanagawa, *Heteroatom Chem.* **1992**, *3*, 563-575, doi.org/10.1002/hc.520030519, 'Synthesis and reactions of optically active phosphine‐boranes'.

[257] G. Li, S. Qian, C. Wang, J. You, *Angew. Chem.* **2013**, *125*, 7991-7994, doi.org/10.1002/ange.201303099, 'Palladium(II)‐Catalyzed Dehydrogenative Cross‐Coupling between Two C-H Bonds: Unexpected C-C Bond Formation'.

[258] C. He, C. Chen, J. Cheng, C. Liu, W. Liu, Q. Li, A. Lei, *Angew. Chem. Int. Ed.* **2008**, *47*, 6414-6417, doi.org/10.1002/ange.200801427, 'Aryl Halide Tolerated Electrophilic Amination of Arylboronic Acids with *N*‐Chloroamides Catalyzed by CuCl at Room Temperature'.

[259] a) X. Abel-Snape, G. Wycich, M. Lautens, *ACS Catal.* **2022**, *12*, 3291-3301, doi.org/10.1021/acscatal.1c06046, 'Synthesis of Indenes and Benzofulvenes via a Palladium-Catalyzed Three-Component Reaction'; b) A. D. Marchese, M. Wollenburg, B. Mirabi, X. Abel-Snape, A. Whyte, F. Glorius, M. Lautens, *ACS Catal.* **2020**, *10*, 4780-4785, doi.org/10.1021/acscatal.0c00841, 'Nickel-catalyzed enantioselective carbamoyl iodination: a surrogate for carbamoyl iodides'.

[260] a) N. G. Andersen, B. A. Keay, *Chem. Rev.* **2001**, *101*, 997-1030, doi.org/10.1021/cr000024o, '2-Furyl phosphines as ligands for transition-metal-mediated organic synthesis'; b) V. Farina, S. R. Baker, D. A. Benigni, C. Sapino Jr, *Tetrahedron Lett.* **1988**, *29*, 5739-5742, doi.org/10.1016/S0040-4039(00)82177-2, 'Palladium-catalyzed coupling between cephalosporin derivatives and unsaturated stannanes: A new ligand for palladium chemistry'.

[261] J. He, T. Shigenari, J. Q. Yu, *Angew. Chem. Int. Ed.* **2015**, *54*, 6545-6549, doi.org/10.1002/anie.201502075, 'Palladium(0)/PAr_3-Catalyzed Intermolecular Amination of C(sp^3)–H Bonds: Synthesis of β-Amino Acids'.

[262] J.-P. Heeb, J. Clayden, M. D. Smith, R. J. Armstrong, *Nat. Protoc.* **2023**, *18*, 1-27, doi.org/10.1038/s41596-023-00859-y, 'Interrogating the configurational stability of atropisomers'.

[263] M. Moussa, W. Ebrahim, M. Bonus, H. Gohlke, A. Mándi, T. Kurtán, R. Hartmann, R. Kalscheuer, W. Lin, Z. Liu, *RSC Adv.* **2019**, *9*, 1491-1500, doi.org/10.1039/C8RA09067J 'Co-culture of the fungus Fusarium tricinctum with Streptomyces lividans induces production of cryptic naphthoquinone dimers'.

[264] E. Masson, *Org. Biomol. Chem.* **2013**, *11*, 2859-2871, doi.org/10.1039/C3OB26704K, 'Torsional barriers of substituted biphenyls calculated using density functional theory: a benchmarking study'.

[265] F. B. Ogilvie, J. M. Jenkins, J. G. Verkade, *J. Am. Chem. Soc.* **1970**, *92*, 1916-1923, doi.org/10.1021/ja00710a022, '^{31}P-^{31}P spin-spin coupling in complexes containing two phosphorus ligands'.

[266] a) S. Dohm, A. Hansen, M. Steinmetz, S. Grimme, M. P. Checinski, *J. Chem. Theory Comput.* **2018**, *14*, 2596-2608, doi.org/10.1021/acs.jctc.7b01183, 'Comprehensive thermochemical benchmark set of realistic closed-shell metal organic reactions'; b) M. A. Iron, T. Janes, *J. Phys. Chem. A* **2019**, *123*, 3761-3781, doi.org/10.1021/acs.jpca.9b01546, 'Evaluating transition metal barrier heights with the latest density functional theory exchange–correlation functionals: the MOBH35 benchmark database'.

[267] F. Neese, F. Wennmohs, U. Becker, C. Riplinger, *J. Chem. Phys.* **2020**, *152*, 224108, doi.org/10.1063/5.0004608, 'The ORCA quantum chemistry program package'.

[268] J. Tao, J. P. Perdew, V. N. Staroverov, G. E. Scuseria, *Phys. Rev. Lett.* **2003**, *91*, 146401, doi.org/10.1103/PhysRevLett.91.146401, 'Climbing the density functional ladder: Nonempirical *meta*–generalized gradient approximation designed for molecules and solids'.

[269] E. Caldeweyher, S. Ehlert, A. Hansen, H. Neugebauer, S. Spicher, C. Bannwarth, S. Grimme, *J. Chem. Phys.* **2019**, *150*, doi.org/10.1063/1.5090222, 'A generally applicable atomic-charge dependent London dispersion correction'.

[270] F. Weigend, R. Ahlrichs, *Phys. Chem. Chem. Phys.* **2005**, *7*, 3297-3305, doi.org/10.1039/B508541A, 'Balanced basis sets of split valence, triple zeta valence and quadruple zeta valence quality for H to Rn: Design and assessment of accuracy'.

[271] Y. Zhao, D. G. Truhlar, *J. Chem. Phys.* **2006**, *125*, doi.org/10.1063/1.2370993, 'A new local density functional for main-group thermochemistry, transition metal bonding, thermochemical kinetics, and noncovalent interactions'.

[272] J. G. Brandenburg, C. Bannwarth, A. Hansen, S. Grimme, *J. Chem. Phys.* **2018**, *148*, 064104-(064101-064112), doi.org/10.1063/1.5012601, 'B97-3c: A revised low-cost variant of the B97-D density functional method'.

[273] N. Mardirossian, M. Head-Gordon, *J. Chem. Phys.* **2016**, *144*, doi.org/10.1063/1.4952647, '*ω*B97M-V: A combinatorially optimized, range-separated hybrid, *meta*-GGA density functional with VV10 nonlocal correlation'.

[274] M. Rickhaus, L. Jundt, M. Mayor, *Chimia* **2016**, *70*, 192-192, doi.org/10.2533/chimia.2016.192 'Determining Inversion Barriers in Atrop-isomers–A Tutorial for Organic Chemists'.

[275] T. Kamachi, K.-i. Shimizu, D. Yoshihiro, K. Igawa, K. Tomooka, K. Yoshizawa, *J. Phys. Chem. C* **2013**, *117*, 22967-22973, doi.org/10.1021/jp408269s, 'Oxidation of silanes to silanols on Pd nanoparticles: H_2 desorption accelerated by surface oxygen atom'.

[276] C. Zhu, Y. Zhang, J. Kan, H. Zhao, W. Su, *Org. Lett.* **2015**, *17*, 3418-3421, doi.org/10.1021/acs.orglett.5b01398, 'Ambient-temperature ortho C–H arylation of benzoic acids with aryl iodides with ligand-supported palladium catalyst'.

[277] E. K. Elias, S. M. Rehbein, S. R. Neufeldt, *Chem. Sci.* **2022**, *13*, 1618-1628, doi.org/10.1039/D1SC05862B, 'Solvent coordination to palladium can invert the selectivity of oxidative addition'.

[278] X. Abel-Snape, M. K. T. Klischan, C. Jans, J. Melder, B. Mirabi, A. Peloewetse, G. Hughes, J. Pietruszka, M. Lautens, **2022 - 2024**, 'A Chiral Acetylene Equivalent: An Enantioenriched Oxabicycle as a Chiral Auxiliary'.

[279] a) W. Lv, S. Wen, J. Yu, G. Cheng, *Org. Lett.* **2018**, *20*, 4984-4987, doi.org/10.1021/acs.orglett.8b02106, 'Palladium-catalyzed ortho-silylation of aryl iodides with concomitant arylsilylation of oxanorbornadiene: Accessing functionalized (Z)-β-substituted vinylsilanes and their analogues'; b) X. Abel-Snape, C. E. Johnson, B. Imbriaco, M. Lautens, *Chem. Sci.* **2023**, *14*, 5650-5655, doi.org/10.1039/D3SC01072D, 'Synthesis of spirooxindoles via formal acetylene insertion into a common palladacycle intermediate'; c) S. M. Parke, J. C. Lopez, S. Cui, A. M. LaPointe, G. W. Coates, *Angew. Chem. Int. Ed.* **2023**, *62*, e202301927, doi.org/10.1002/anie.202301927, 'Polyethylene Incorporating Diels–Alder Comonomers: A "Trojan Horse" Strategy for Chemically Recyclable Polyolefins'.

[280] A. Rinaldi, D. Scarpi, E. G. Occhiato, *Eur. J. Org. Chem.* **2019**, *2019*, 7401-7419, doi.org/10.1002/ejoc.201901425, 'Recent Advances in the Synthesis of Indenes'.

[281] C. Han, F. Zhao, Q. Lu, F. Liu, *J. Org. Chem.* **2023**, *88*, 15608−15614, doi.org/10.1021/acs.joc.3c01522, 'Computational Determination of the Mechanism of the Palladium-Catalyzed Domino Reaction of ortho-Iodostyrene, Oxanorbornadiene, and Phenylboronic Acid'.

[282] J. E. Baldwin, *J. Chem. Soc. Chem. Comm.* **1976**, 734-736, doi.org/10.1039/C39760000734, 'Rules for ring closure'.

[283] N. Sultan, R. Guillot, L. Blanco, S. Deloisy, *Synthesis* **2013**, 2018-2028, doi.org/10.1055/s-0033-1338802, 'Regioselective preparation of 7-oxanorborna-2,5-diene-2,3-dicarboxylic acid derivatives by the Diels–Alder reaction: A selective access to furans by retro-Diels–Alder reaction'.

[284] X. Abel-Snape, 'PhD Thesis', **2020 - 2024**.

[285] R. H. Crabtree, *The organometallic chemistry of the transition metals*, 9781118138076, John Wiley & Sons, **2009**.

[286] F. Feist, L. L. Rodrigues, S. L. Walden, T. W. Krappitz, T. R. Dargaville, T. Weil, A. S. Goldmann, J. P. Blinco, C. Barner-Kowollik, *J. Am. Chem. Soc.* **2020**, *142*, 7744-7748, doi.org/10.1021/jacs.0c02002, 'Light-induced ligation of *o*-quinodimethanes with gated fluorescence self-reporting'.

[287] F.-L. Haut, N. J. Feichtinger, I. Plangger, L. A. Wein, M. Müller, T.-N. Streit, K. Wurst, M. Podewitz, T. Magauer, *J. Am. Chem. Soc.* **2021**, *143*, 9002-9008, doi.org/10.1021/jacs.1c04835, 'Synthesis of Pyrroles via Consecutive 6π-Electrocyclization/Ring-Contraction of Sulfilimines'.

[288] C. Bannwarth, S. Ehlert, S. Grimme, *J. Chem. Theory Comput.* **2019**, *15*, 1652-1671, doi.org/10.1021/acs.jctc.8b01176, 'GFN2-xTB—An accurate and broadly parametrized self-consistent tight-binding quantum chemical method with multipole electrostatics and density-dependent dispersion contributions'.

[289] P. Pracht, F. Bohle, S. Grimme, *Phys. Chem. Chem. Phys.* **2020**, *22*, 7169-7192, doi.org/10.1039/C9CP06869D, 'Automated exploration of the low-energy chemical space with fast quantum chemical methods'.

[290] S. Grimme, F. Bohle, A. Hansen, P. Pracht, S. Spicher, M. Stahn, *J. Phys. Chem. A* **2021**, *125*, 4039-4054, doi.org/10.1021/acs.jpca.1c00971, 'Efficient Quantum Chemical Calculation of Structure Ensembles and Free Energies for Nonrigid Molecules'.

[291] A. K. Vitek, T. M. Jugovic, P. M. Zimmerman, *ACS Catal.* **2020**, *10*, 7136-7145, doi.org/10.1021/acscatal.0c00618, 'Revealing the strong relationships between ligand conformers and activation barriers: a case study of bisphosphine reductive elimination'.

[292] F. L. Hirshfeld, *Theor. Chim. Acta* **1977**, *44*, 129-138, doi.org/10.1007/BF00549096 'Bonded-atom fragments for describing molecular charge densities'.

[293] R. G. Parr, W. Yang, *J. Am. Chem. Soc.* **1984**, *106*, 4049-4050, doi.org/10.1021/ja00326a036 'Density functional approach to the frontier-electron theory of chemical reactivity'.

[294] T. Lu, F. Chen, *J. Comput. Chem.* **2012**, *33*, 580-592, doi.org/10.1002/jcc.22885, 'Multiwfn: a multifunctional wavefunction analyzer'.

[295] L. Meng, J. Wang, *Synlett* **2016**, *27*, 656-663, doi.org/10.1055/s-0035-1560987, 'Recent Progress on the Asymmetric Synthesis of Chiral Flavanones'.

[296] Y.-L. Zhang, Y.-Q. Wang, *Tetrahedron Lett.* **2014**, *55*, 3255-3258, doi.org/10.1016/j.tetlet.2014.04.032, 'Enantioselective biomimetic cyclization of 2′-hydroxychalcones to flavanones'.

[297] A. K. Yuen, C. A. Hutton, *Tetrahedron Lett.* **2005**, *46*, 7899-7903, doi.org/10.1016/j.tetlet.2005.09.101, 'Deprotection of pinacolyl boronate esters via hydrolysis of intermediate potassium trifluoroborates'.

[298] Y.-A. Kim, M. Kang, Y.-J. Jeon, K. Hwang, Y.-J. Kim, S.-Y. Jang, I.-B. Kim, G. Kwon, D.-Y. Kim, *J. Mat. Chem. C* **2017**, *5*, 10332-10342, doi.org/10.1039/C7TC02925J, 'Structure–property relationship of D–A type copolymers based on phenanthrene and naphthalene units for organic electronics'.

[299] L. Frey, J. J. Jarju, L. M. Salonen, D. D. Medina, *New J. Chem.* **2021**, *45*, 14879-14907, doi.org/10.1039/D1NJ01269J, 'Boronic-acid-derived covalent organic frameworks: from synthesis to applications'.

[300] D. W. Zhang, M. Li, C. F. Chen, *Angew. Chem. Int. Ed.* **2022**, *61*, e202213130, doi.org/10.1002/anie.202213130, 'Linear Axially Chiral Conjugated Polymers Exhibiting Ultralong Low-Temperature Phosphorescence and Intense Circularly Polarized Luminescence'.

[301] a) B. N. Hemric, A. W. Chen, Q. Wang, *ACS Catal.* **2019**, *9*, 10070-10076, doi.org/10.1021/acscatal.9b03076, 'Copper-Catalyzed 1,2-Amino Oxygenation of 1,3-Dienes: A Chemo-, Regio-, and Site-Selective Three-Component Reaction with *O*-Acylhydroxylamines and Carboxylic Acids'; b) J. Jeon, C. Lee, H. Seo, S. Hong, *J. Am. Chem. Soc.* **2020**, *142*, 20470-

20480, doi.org/10.1021/jacs.0c10333, 'NiH-catalyzed proximal-selective hydroamination of unactivated alkenes'.

[302] T. Kang, N. Kim, P. T. Cheng, H. Zhang, K. Foo, K. M. Engle, *J. Am. Chem. Soc.* **2021**, *143*, 13962-13970, doi.org/10.1021/jacs.1c07112, 'Nickel-catalyzed 1, 2-carboamination of alkenyl alcohols'.

[303] K. Khomthawee, N. Nilada, A. Homchuen, P. Saejueng, *Appl. Organomet. Chem.* **2023**, *37*, e6987, doi.org/10.1002/aoc.6987, 'Chitosan - Ethylenediaminetetraacetic acid - palladium composite for the Suzuki–Miyaura reaction'.

[304] A. D. Marchese, A. G. Durant, C. M. Reid, C. Jans, R. Arora, M. Lautens, *J. Am. Chem. Soc.* **2022**, *144*, 20554-20560, doi.org/10.1021/jacs.2c09716, 'Pd(0)/Blue Light Promoted Carboiodination Reaction–Evidence for Reversible C–I Bond Formation via a Radical Pathway'.

[305] P. Muller, *Pure Appl. Chem.* **1994**, *66*, 1077-1184, doi.org/10.1351/pac199466051077, 'Glossary of terms used in physical organic chemistry (IUPAC Recommendations 1994)'.

[306] K. Mal, A. Kaur, F. Haque, I. Das, *J. Org. Chem.* **2015**, *80*, 6400-6410, doi.org/10.1021/acs.joc.5b00846, 'PPh_3· HBr–DMSO: A reagent system for diverse chemoselective transformations'.

[307] V. K. Gujral, S. R. Gupts, K. S. Verma, *Indian J. Chem. B* **1979**, *17*, 40-41, 'Structure of undulatoside-B, a new chromone glycoside from Tecomella undulata'.

[308] R. Kant, D. Kumar, D. Agarwal, R. D. Gupta, R. Tilak, S. K. Awasthi, A. Agarwal, *Eur. J. Med. Chem.* **2016**, *113*, 34-49, doi.org/10.1016/j.ejmech.2016.02.041, 'Synthesis of newer 1,2,3-triazole linked chalcone and flavone hybrid compounds and evaluation of their antimicrobial and cytotoxic activities'.

[309] P. Boeck, C. A. B. Falcão, P. C. Leal, R. A. Yunes, V. Cechinel Filho, E. C. Torres-Santos, B. Rossi-Bergmann, *Bioorg. Med. Chem.* **2006**, *14*, 1538-1545, doi.org/10.1016/j.bmc.2005.10.005, 'Synthesis of chalcone analogues with increased antileishmanial activity'.

[310] C. Thieury, N. Lebouvier, R. Le Guével, Y. Barguil, G. Herbette, C. Antheaume, E. Hnawia, Y. Asakawa, M. Nour, T. Guillaudeux, *Bioorg. Med. Chem.* **2017**, *25*, 1817-1829, doi.org/10.1016/j.bmc.2017.01.049, 'Mechanisms of action and structure-activity relationships of cytotoxic flavokawain derivatives'.

[311] C. W. Mai, M. Yaeghoobi, N. Abd-Rahman, Y. B. Kang, M. R. Pichika, *Eur. J. Med. Chem.* **2014**, *77*, 378-387, doi.org/10.1016/j.ejmech.2014.03.002, 'Chalcones with electron-withdrawing and electron-donating substituents: anticancer activity against TRAIL resistant cancer cells, structure–activity relationship analysis and regulation of apoptotic proteins'.

[312] C. Sinyeue, M. Matsui, M. Oelgemöller, F. Bregier, V. Chaleix, V. Sol, N. Lebouvier, *Molecules* **2022**, *27*, 1781, doi.org/10.3390/molecules27061781, 'Synthesis and Investigation of Flavanone Derivatives as Potential New Anti-Inflammatory Agents'.

[313] İ. Akçok, A. Çağır, *Bioorg. Chem.* **2010**, *38*, 139-143, doi.org/10.1016/j.bioorg.2010.04.001, 'Synthesis of stilbene-fused 2′-hydroxychalcones and flavanones'.

[314] M. Cabrera, M. Simoens, G. Falchi, M. L. Lavaggi, O. E. Piro, E. E. Castellano, A. Vidal, A. Azqueta, A. Monge, A. L. de Cerain, *Bioorg. Med. Chem.* **2007**, *15*, 3356-3367, doi.org/10.1016/j.bmc.2007.03.031, 'Synthetic chalcones, flavanones, and flavones as antitumoral agents: Biological evaluation and structure–activity relationships'.

[315] M. Schwarz, R. F. Eno, S. Freitag-Pohl, C. R. Coxon, H. E. Straker, D. J. Wortley, D. J. Hughes, G. Mitchell, J. Moore, I. Cummins, *Org. Biomol. Chem.* **2021**, *19*, 9211-9222, doi.org/10.1039/D1OB01802G, 'Flavonoid-based inhibitors of the Phi-class glutathione transferase from black-grass to combat multiple herbicide resistance'.

[316] N. Basílio, J. C. Lima, L. Cruz, V. de Freitas, F. Pina, H. Ando, Y. Kimura, K. I. Oyama, K. Yoshida, *Eur. J. Org. Chem.* **2017**, 5617-5626, doi.org/10.1002/ejoc.201701009, 'Unveiling the 6,8-rearrangement in 8-phenyl-5,7-dihydroxyflavylium and 8-methyl-5,7-dihydroxyflavylium through host–guest complexation'.

[317] X. Zheng, J.-G. Cao, W.-D. Meng, F.-L. Qing, *Bioorg. Med. Chem. Lett.* **2003**, *13*, 3423-3427, doi.org/10.1016/S0960-894X(03)00752-2, 'Synthesis and anticancer effect of B-ring trifluoromethylated flavonoids'.

[318] T.-L. Shih, C.-E. Chou, W.-Y. Liao, C.-A. Hsiao, *Tetrahedron* **2014**, *70*, 3657-3664, doi.org/10.1016/j.tet.2014.04.022, 'Copper-mediated trimethylsilyl azide in amination of bromoflavonoids to synthesize unique aminoflavonoids'.

[319] C. Wu, D. Dunaway-Mariano, P. S. Mariano, *J. Org. Chem.* **2013**, *78*, 1910-1922, doi.org/10.1021/jo3018473, 'Design, synthesis, and evaluation of inhibitors of pyruvate phosphate dikinase'.

[320] J. Wang, T. Li, T. Zhao, T. Wu, C. Liu, H. Ding, Z. Li, J. Bian, *Eur. J. Med. Chem.* **2019**, *178*, 782-801, doi.org/10.1016/j.ejmech.2019.06.024, 'Design of wogonin-inspired selective cyclin-dependent kinase 9 (CDK9) inhibitors with potent in vitro and in vivo antitumor activity'.

[321] J. W. Clary, T. J. Rettenmaier, R. Snelling, W. Bryks, J. Banwell, W. T. Wipke, B. Singaram, *J. Org. Chem.* **2011**, *76*, 9602-9610, doi.org/10.1021/jo201093u, 'Hydride as a leaving group in the reaction of pinacolborane with halides under ambient grignard and barbier conditions. One-Pot synthesis of alkyl, aryl, heteroaryl, vinyl, and allyl pinacolboronic esters'.

[322] A. M. Mfuh, J. D. Doyle, B. Chhetri, H. D. Arman, O. V. Larionov, *J. Am. Chem. Soc.* **2016**, *138*, 2985-2988, doi.org/10.1021/jacs.6b01376, 'Scalable, metal-and additive-free, photoinduced borylation of haloarenes and quaternary arylammonium salts'.

[323] D. K. Scrafton, J. E. Taylor, M. F. Mahon, J. S. Fossey, T. D. James, *J. Org. Chem.* **2008**, *73*, 2871-2874, doi.org/10.1021/jo702584u, '"Click-fluors": modular fluorescent saccharide sensors based on a 1,2,3-triazole ring'.

[324] O. Baudoin, D. Guénard, F. Guéritte, *J. Org. Chem.* **2000**, *65*, 9268-9271, doi.org/10.1021/jo005663d, 'Palladium-Catalyzed Borylation of Ortho-Substituted Phenyl Halides and Application to the One-Pot Synthesis of 2,2'-Disubstituted Biphenyls'.

[325] R. Ding, Q. Liu, L. Zheng, *Chem. Eur. J.* **2023**, *29*, e202203792, doi.org/10.1002/chem.202203792, 'Piezoelectric Metal‐Organic Frameworks Mediated Mechanoredox Borylation and Arylation Reactions by Ball Milling'.

[326] S. Jin, H. T. Dang, G. C. Haug, R. He, V. D. Nguyen, V. T. Nguyen, H. D. Arman, K. S. Schanze, O. V. Larionov, *J. Am. Chem. Soc.* **2020**, *142*, 1603-1613, doi.org/10.1021/jacs.9b12519, 'Visible light-induced borylation of C–O, C–N, and C–X bonds'.

[327] E. Demory, V. Blandin, J. Einhorn, P. Y. Chavant, *Org. Process Res. Dev.* **2011**, *15*, 710–716, doi.org/10.1021/op2000089, 'Noncryogenic Preparation of Functionalized Arylboronic Esters through a Magnesium−Iodine Exchange with in Situ Quench'.

[328] Z. Zuo, J. Liu, J. Nan, L. Fan, W. Sun, Y. Wang, X. Luan, *Angew. Chem. Int. Ed.* **2015**, *54*, 15385-15389, doi.org/10.1002/anie.201508850, 'Highly Stereoselective Synthesis of Imine‐Containing Dibenzo [b,d] azepines by a Palladium(II)‐Catalyzed [5+2] Oxidative Annulation of *o*‐Arylanilines with Alkynes'.

[329] R. Wu, J. S. Schumm, D. L. Pearson, J. M. Tour, *J. Org. Chem.* **1996**, *61*, 6906-6921, doi.org/10.1021/jo960897b, 'Convergent synthetic routes to orthogonally fused conjugated oligomers directed toward molecular scale electronic device applications'.

[330] D. Vonlanthen, A. Rudnev, A. Mishchenko, A. Käslin, J. Rotzler, M. Neuburger, T. Wandlowski, M. Mayor, *Chem. Eur. J.* **2011**, *17*, 7236-7250, doi.org/10.1002/chem.201003763, 'Conformationally Controlled Electron Delocalization in n‐Type Rods: Synthesis, Structure, and Optical, Electrochemical, and Spectroelectrochemical Properties of Dicyanocyclophanes'.

[331] B. Jiang, M.-m. Li, P. Xing, Z.-g. Huang, *Org. Lett.* **2013**, *15*, 871-873, doi.org/10.1021/ol400030a, 'A concise formal synthesis of (−)-hamigeran B'.

[332] A. Bruneau, M. Roche, M. Alami, S. Messaoudi, *ACS Catal.* **2015**, *5*, 1386-1396, doi.org/10.1021/cs502011x, '2-aminobiphenyl palladacycles: the "most powerful" precatalysts in C–C and C–heteroatom cross-couplings'.

[333] K. Mislow, M. A. W. Glass, R. E. O'Brien, P. Rutkin, D. H. Steinberg, J. Weiss, C. Djerassi, *J. Am. Chem. Soc.* **1962**, *84*, 1455-1478, doi.org/10.1021/ja00867a023, 'Configuration, Conformation and Rotatory Dispersion of Optically Active Biaryls'.

[334] W. Kashikura, K. Mori, T. Akiyama, *Org. Lett.* **2011**, *13*, 1860-1863, doi.org/10.1021/ol200374m, 'Chiral phosphoric acid catalyzed enantioselective synthesis of *β*-amino-*α*,*α*-difluoro carbonyl compounds'.

[335] S. Kanoh, N. Tamura, M. Motoi, H. Suda, *B. Chem. Soc. Jpn.* **1987**, *60*, 2307-2309, doi.org/10.1246/bcsj.60.2307, 'Optical Resolution and Absolute Configuration of Axially Dissymmetric 2,2′-Dihydroxy-6,6′-dimethylbiphenyl'.

[336] S. Bouarfa, S. Graßl, M. Ivanova, T. Langlais, G. Bentabed‐Ababsa, F. Lassagne, W. Erb, T. Roisnel, V. Dorcet, P. Knochel, *Eur. J. Org. Chem.* **2019**, 3244-3258, doi.org/10.1002/ejoc.201900276, 'Copper‐and Cobalt‐Catalyzed Syntheses of Thiophene‐Based Tertiary Amines'.

[337] S. Bouarfa, S. Graßl, M. Ivanova, T. Langlais, G. Bentabed‐Ababsa, F. Lassagne, W. Erb, T. Roisnel, V. Dorcet, P. Knochel, *Eur. J. Org. Chem.* **2019**, 3244-3258, 'Copper‐and Cobalt‐Catalyzed Syntheses of Thiophene‐Based Tertiary Amines'.

[338] J.-W. F. Kaagman, M. Rep, M. Horáček, P. Sedmera, J. Čejka, V. Varga, K. Mach, *Collect. Czech. Chem. Commun.* **1996**, *61*, 1722-1728, doi.org/10.1135/cccc19961722 'Titanium-Catalyzed [4+2] and [6+2] Cycloadditions of 1,4-Bis (trimethylsilyl) buta-1,3-diyne'.

[339] A. Boelke, T. J. Kuczmera, L. D. Caspers, E. Lork, B. J. Nachtsheim, *Org. Lett.* **2020**, *22*, 7261-7266, doi.org/10.1021/acs.orglett.0c02593, 'Iodolopyrazolium salts: synthesis, derivatizations, and applications'.

[340] W. Ma, J. Fang, J. Ren, Z. Wang, *Org. Lett.* **2015**, *17*, 4180-4183, doi.org/10.1021/acs.orglett.5b01927, 'Lewis Acid Catalyzed Formal Intramolecular [3+3] Cross-Cycloaddition of Cyclopropane 1,1-Diesters for Construction of Benzobicyclo [2.2.2] octane Skeletons'.

[341] M. Murai, T. Ogita, K. Takai, *Chem. Commun.* **2019**, *55*, 2332-2335, doi.org/10.1039/C9CC00270G, 'Regioselective arene homologation through rhenium-catalyzed deoxygenative aromatization of 7-oxabicyclo [2.2.1] hepta-2,5-dienes'.

[342] D. Seebach, A. K. Beck, R. Imwinkelzied, S. Roggo, A. Wonnacott, *Helv. Chim. Acta* **1987**, *70*, 954-974, doi.org/10.1002/hlca.19870700406, 'Chirale alkoxytitan (IV) ‐ komplexe für enantioselektive nucleophile additionen an aldehyde und als Lewis‐Säuren in Diels‐Alder‐reaktionen'.

[343] G. J. Perry, J. M. Quibell, A. Panigrahi, I. Larrosa, *J. Am. Chem. Soc.* **2017**, *139*, 11527-11536, doi.org/10.1021/jacs.7b05155, 'Transition-metal-free decarboxylative iodination: new routes for decarboxylative oxidative cross-couplings'.

[344] T. Sato, M. Oki, *B. Chem. Soc. Jpn.* **1957**, *30*, 859-862, doi.org/10.1246/bcsj.30.859, 'Estrogenic Biphenyls. III. 2-Alkyl-4-methoxybiphenyl-4′-carboxylic Acids'.

[345] J. Cornforth, L. M. Huguenin, J. R. Wilson, *J. Chem. Soc., Perkin Trans. 1* **1987**, 871-875, doi.org/10.1039/P19870000871, 'Synthesis of substituted dibenzophospholes. Part 8. Synthesis and resolution of atropisomers of a 4,6-diaryldibenzophosphole'.

9 Appendix

9.1 NMR-Spectra

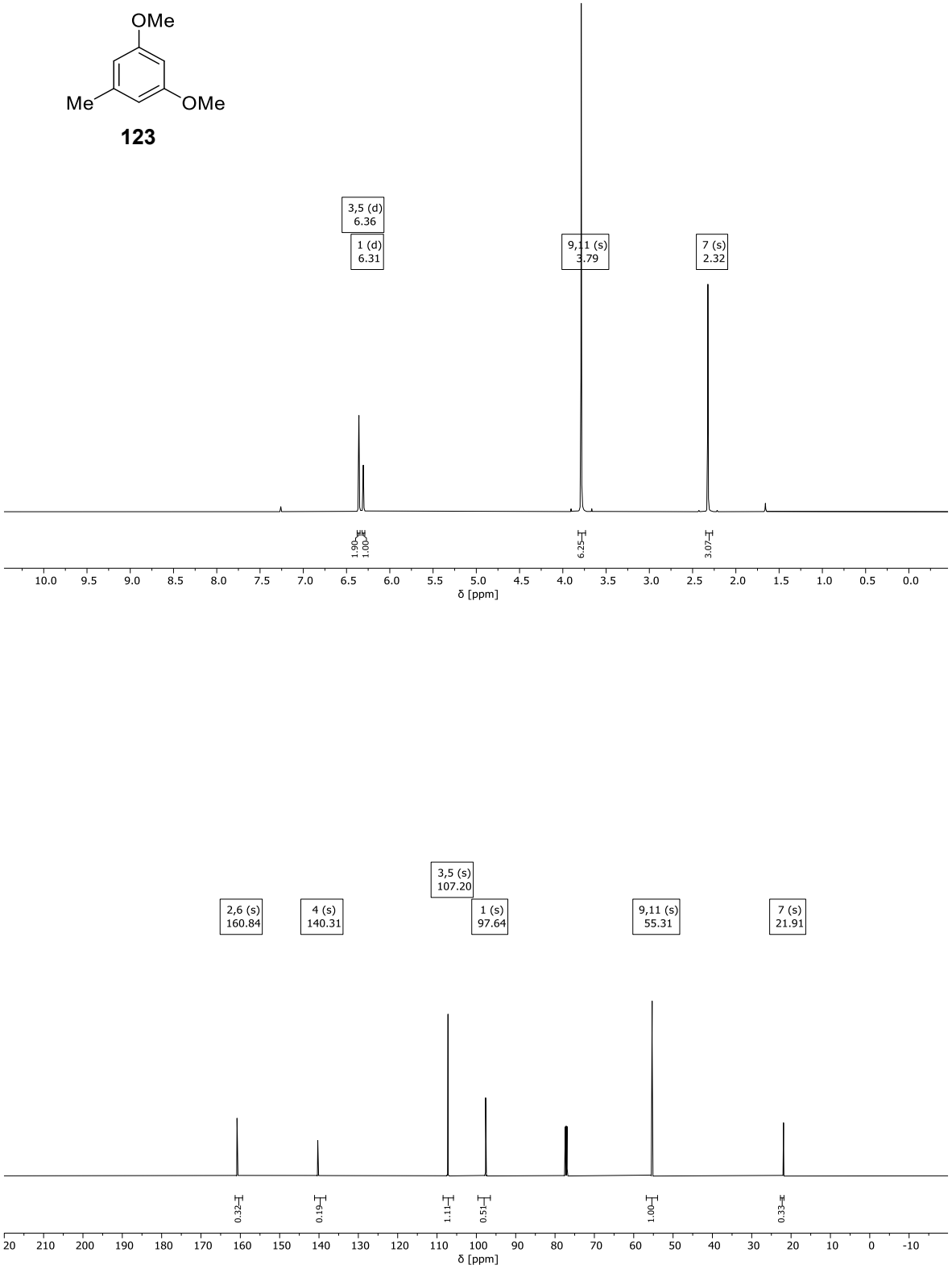

Figure 79: ^{1}H- and ^{13}C-NMR spectra (600 / 151 MHz, $CDCl_3$) of 1,3-dimethoxy-5-methylbenzene (**123**).

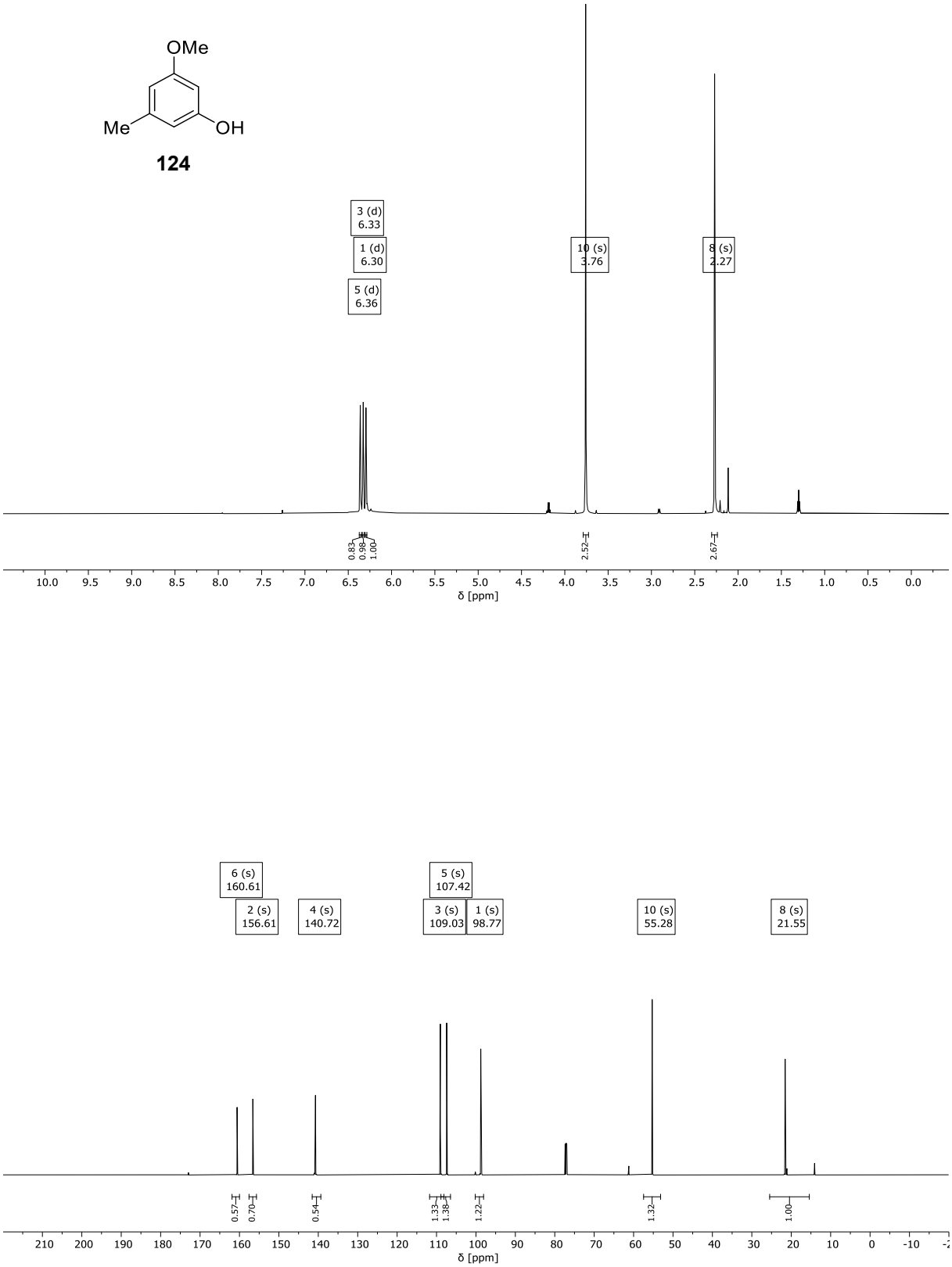

Figure 80: ^{1}H- and ^{13}C-NMR spectra (600 / 151 MHz, $CDCl_3$) of 3-methoxy-5-methylphenol (**124**).

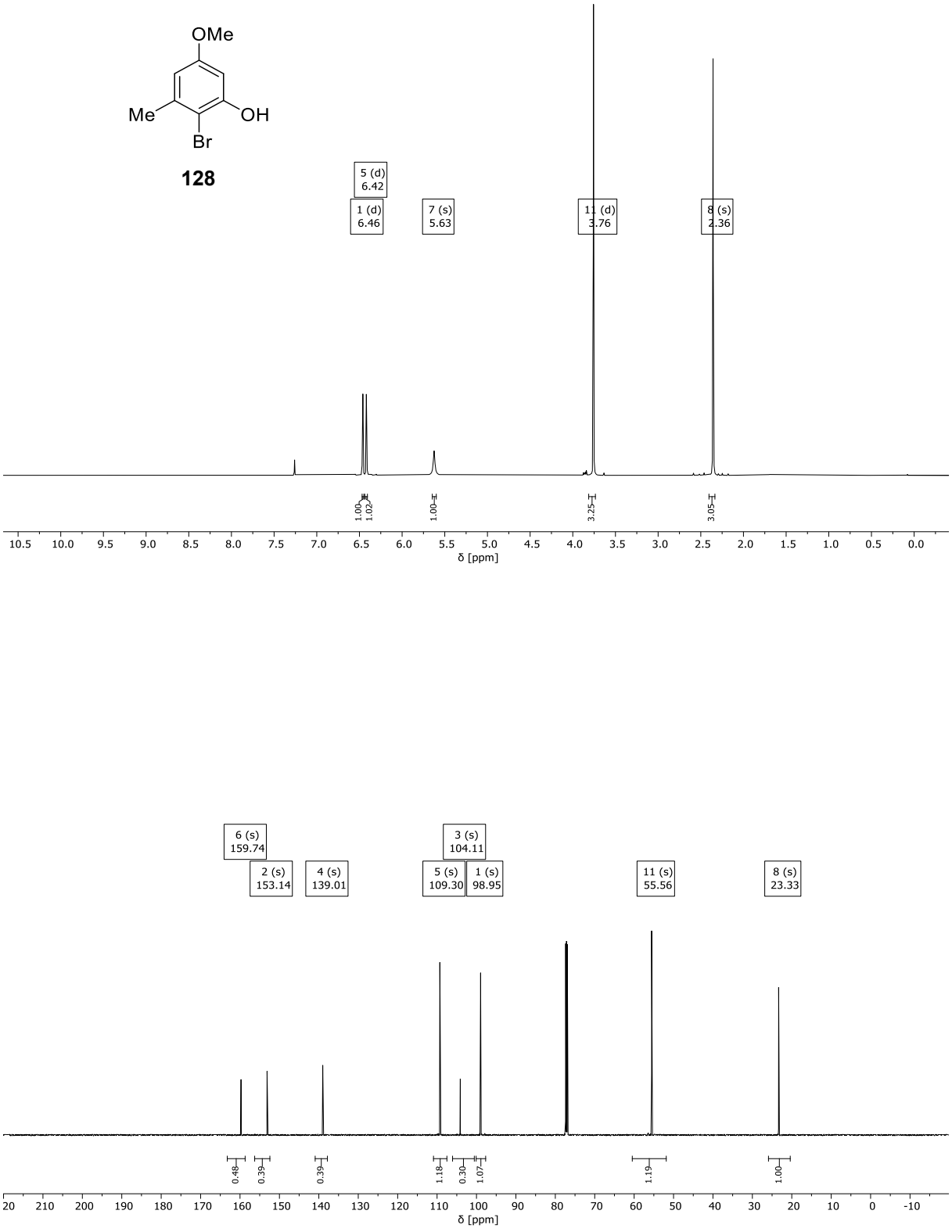

Figure 81: ^{1}H- and ^{13}C-NMR spectra (600 / 151 MHz, $CDCl_3$) of 2-bromo-5-methoxy-3-methylphenol (**128)**.

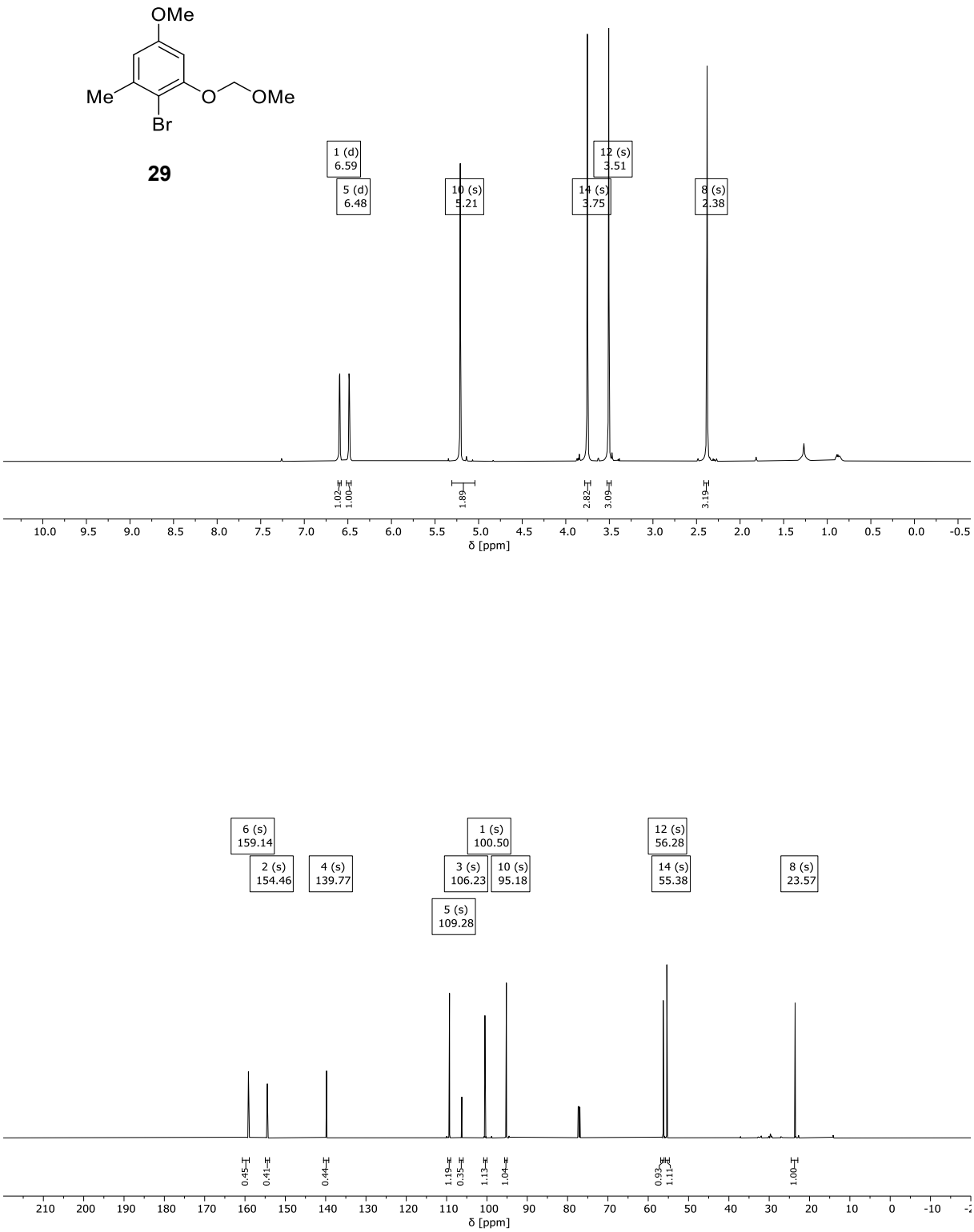

Figure 82: ^{1}H- and ^{13}C-NMR spectra (600 / 151 MHz, $CDCl_3$) of 2-bromo-5-methoxy-1-(methoxymethoxy)-3-methylbenzene (**29**).

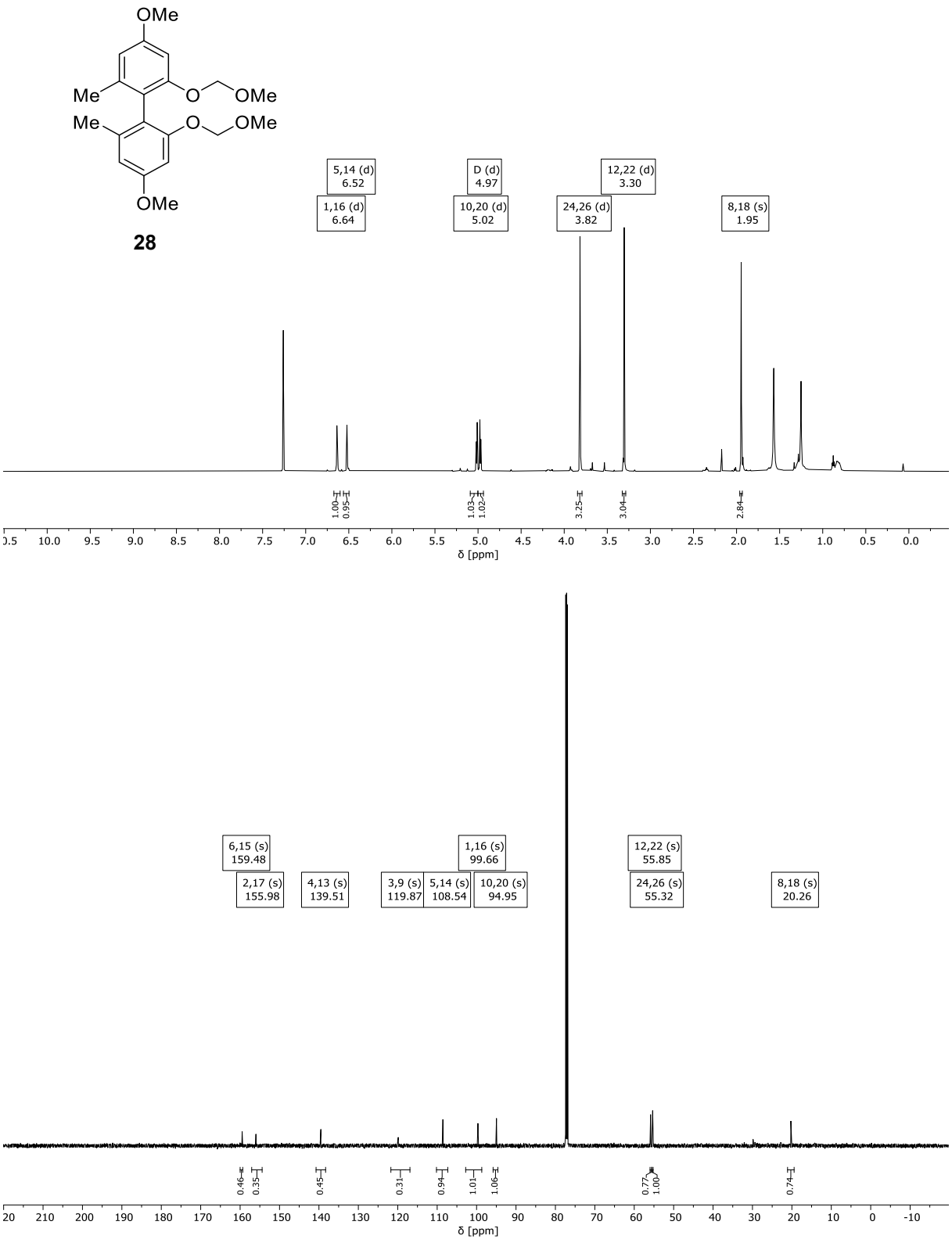

Figure 83 ^{1}H- and ^{13}C-NMR spectra (600 / 151 MHz, $CDCl_3$) of 4,4'-dimethoxy-2,2'-bis(methoxymethoxy)-6,6'-dimethyl-1,1'-biphenyl (**28**).

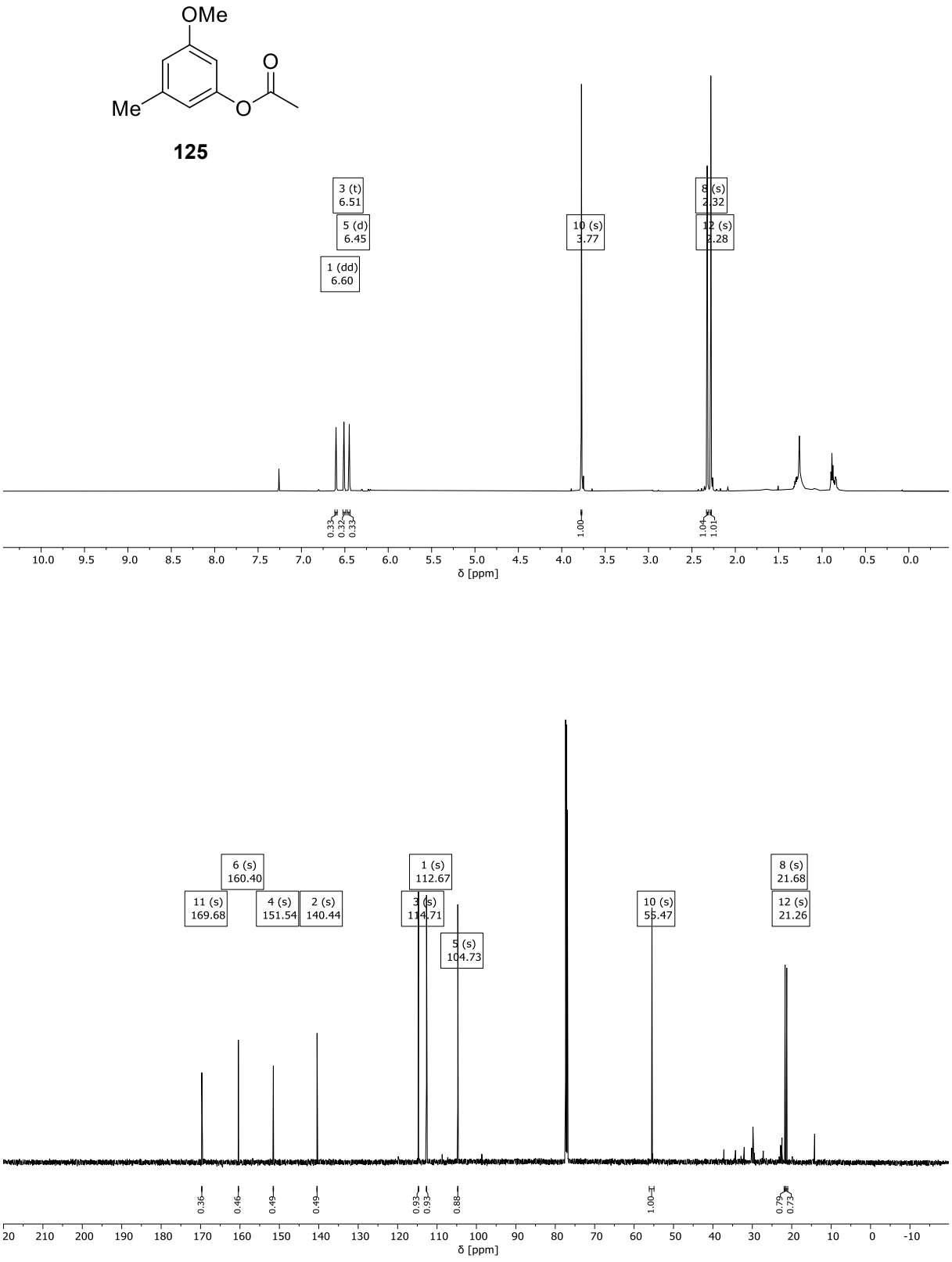

Figure 84: ^{1}H- and ^{13}C-NMR spectrum (600 / 151 MHz, $CDCl_3$) of 3-methoxy-5-methylphenyl acetate (**125**).

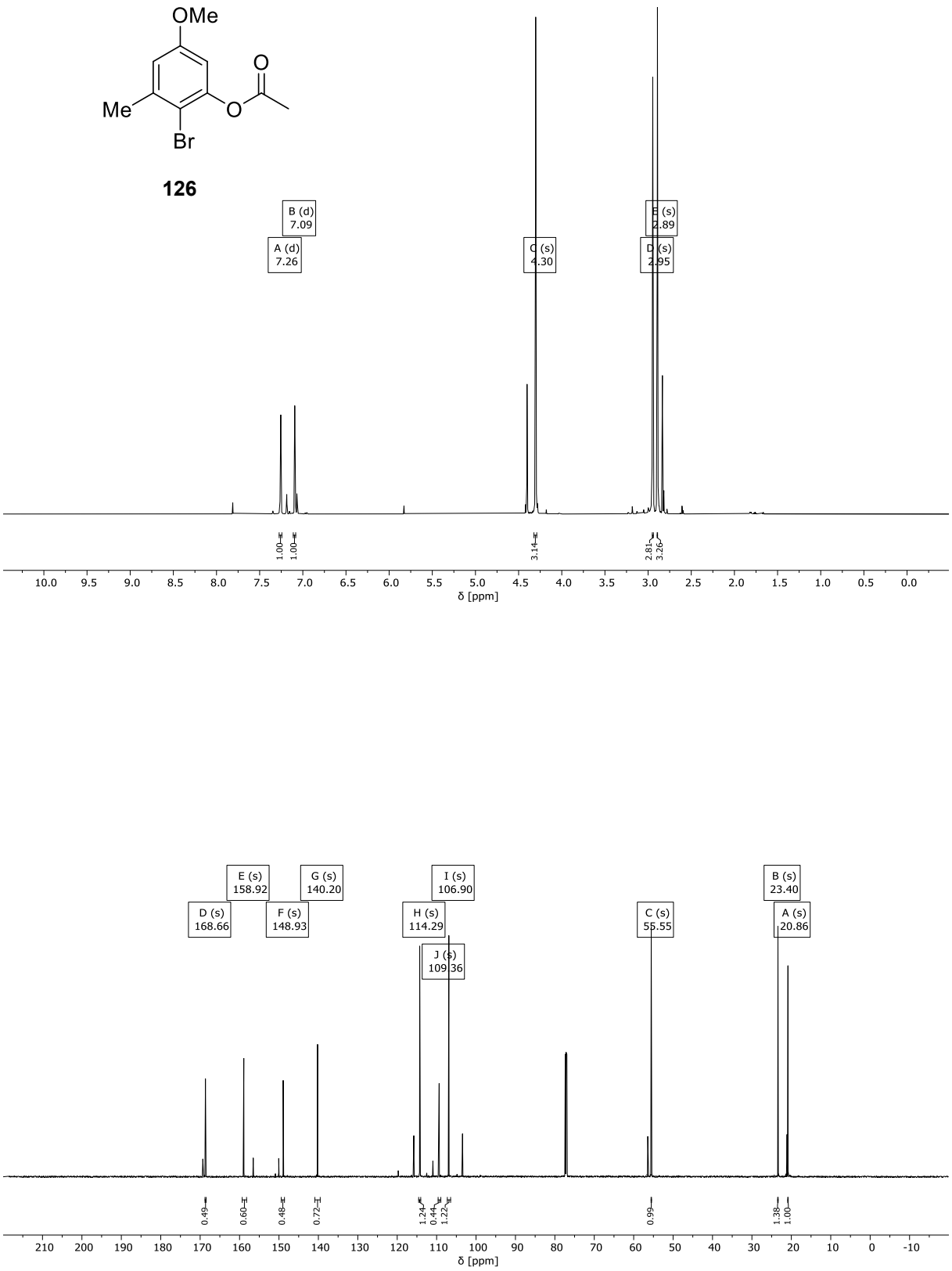

Figure 85: ^{1}H- and ^{13}C-NMR spectra (600 / 151 MHz, $CDCl_3$) of 2-bromo-5-methoxy-3-methylphenyl acetate (**126**).

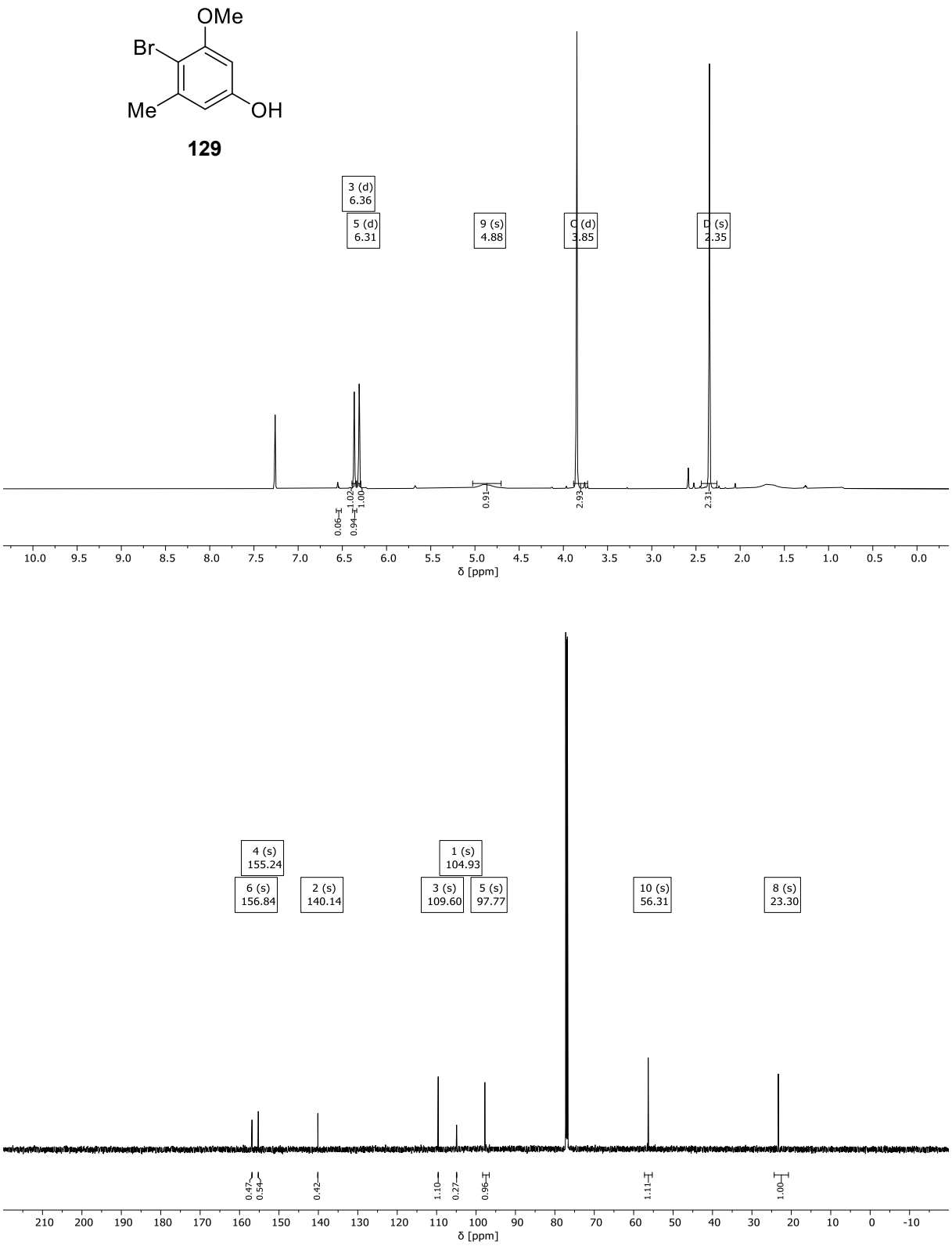

Figure 86: ^{1}H- and ^{13}C-NMR spectra (600 / 151 MHz, $CDCl_3$) of 4-bromo-3-methoxy-5-methylphenol (**129**).

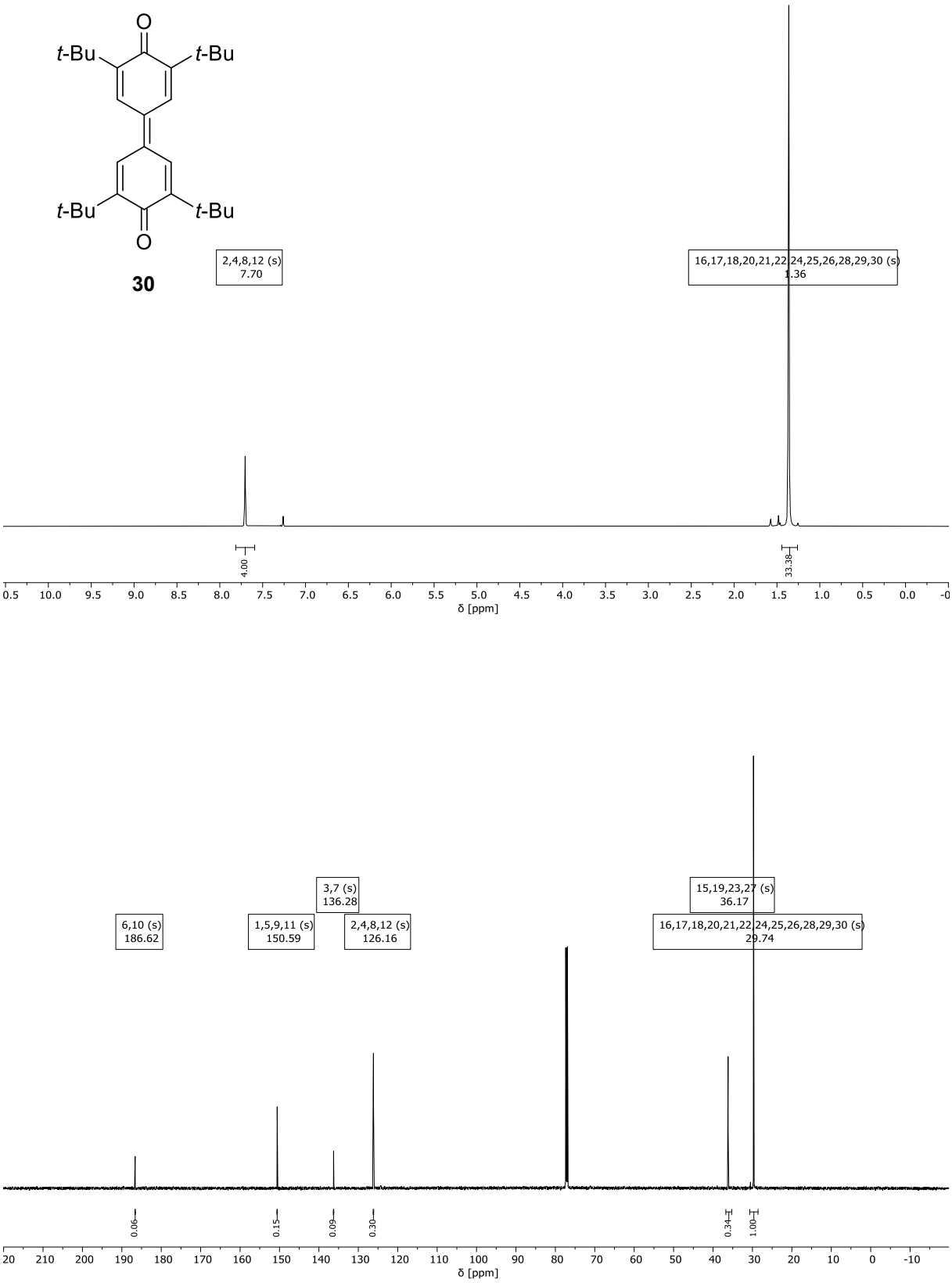

Figure 87: ^{1}H- and ^{13}C-NMR spectra (600 / 151 MHz, $CDCl_3$) of 3,3',5,5'-tetra-tert-butyl-[1,1'-bi(cyclohexylidene)]-2,2',5,5'-tetraene-4,4'-dione (**30**).

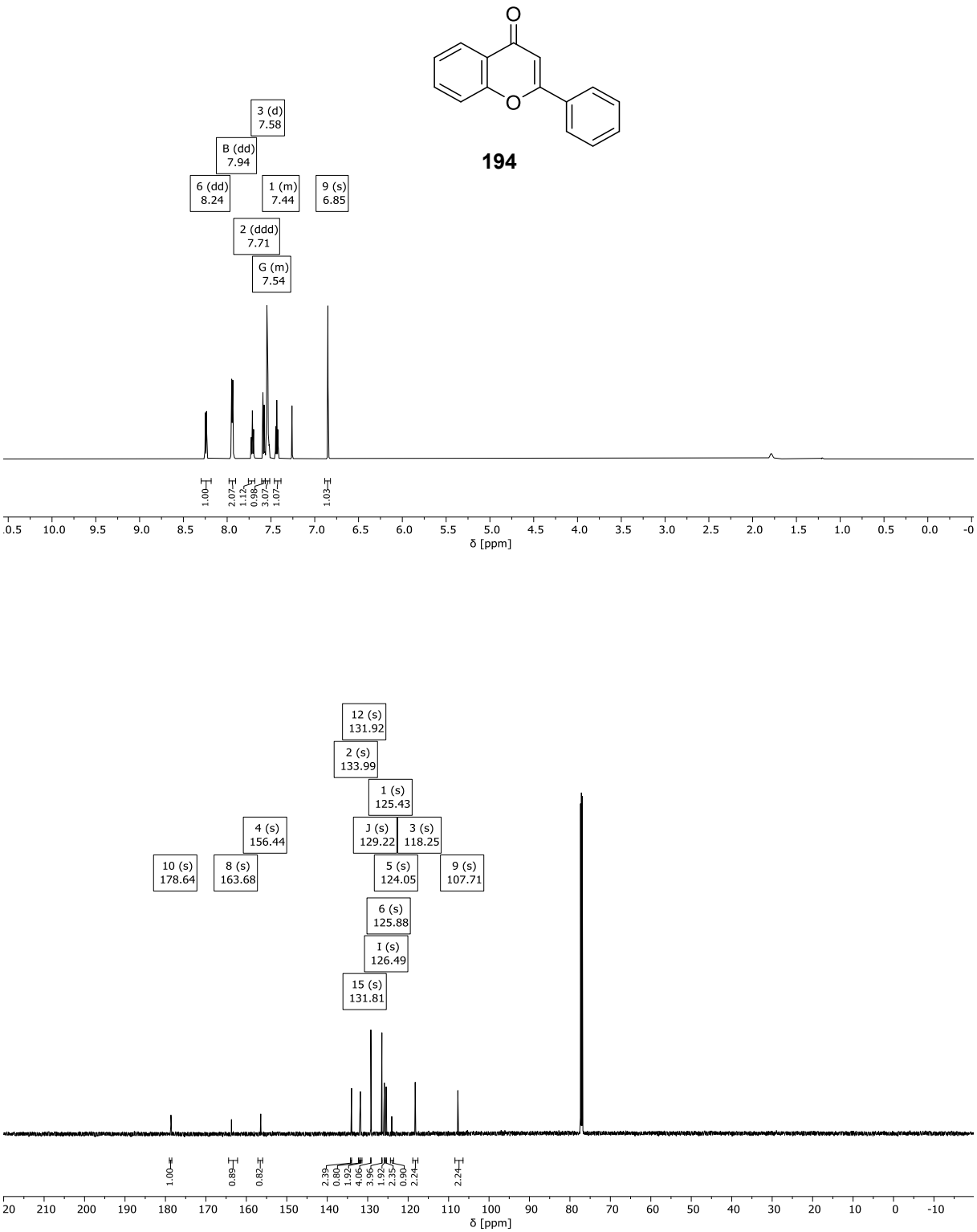

Figure 88: ^{1}H- and ^{13}C-NMR spectra (600 / 151 MHz, $CDCl_3$) of 2-phenyl-4H-chromen-4-one (**194**)

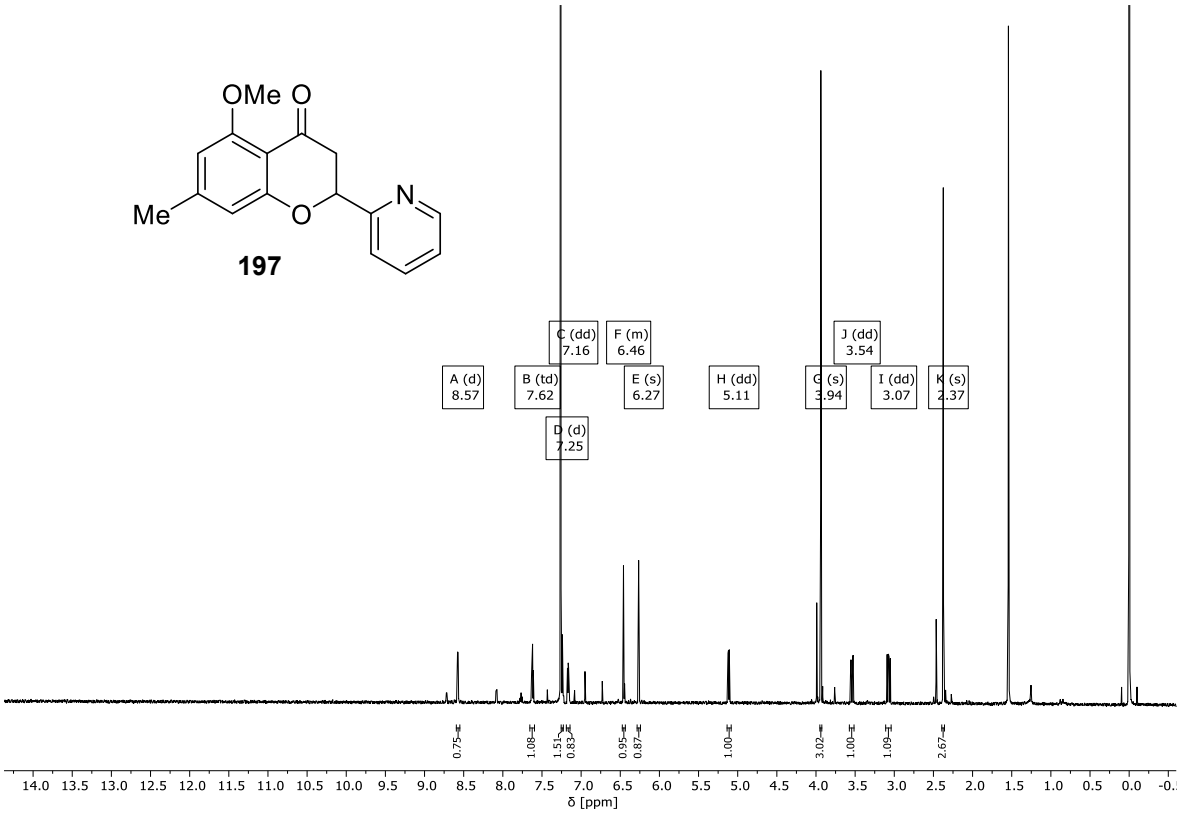

Figure 89: ^{1}H-NMR spectrum (600 MHz, $CDCl_3$) of 5-methoxy-7-methyl-2-(pyridin-2-yl)chroman-4-one (**197**).

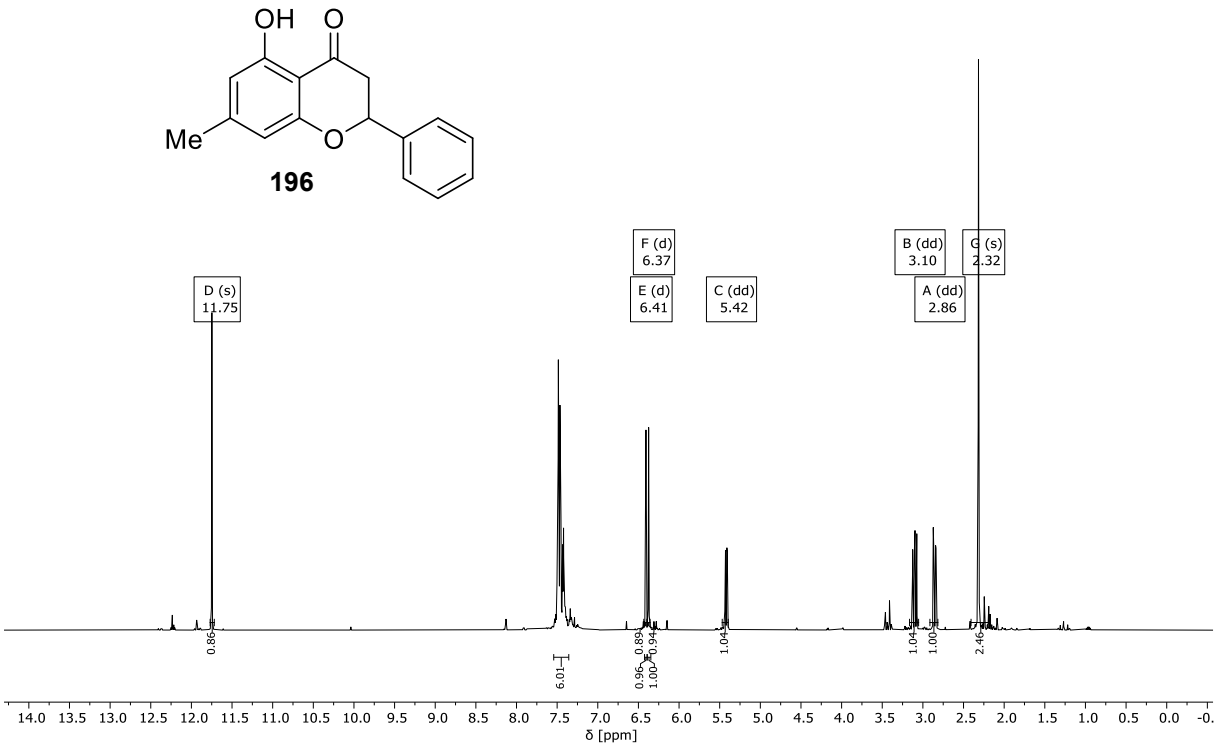

Figure 90: ^{1}H-NMR spectrum (600 MHz, $CDCl_3$) of 5-hydroxy-7-methyl-2-phenylchroman-4-one (**196**)

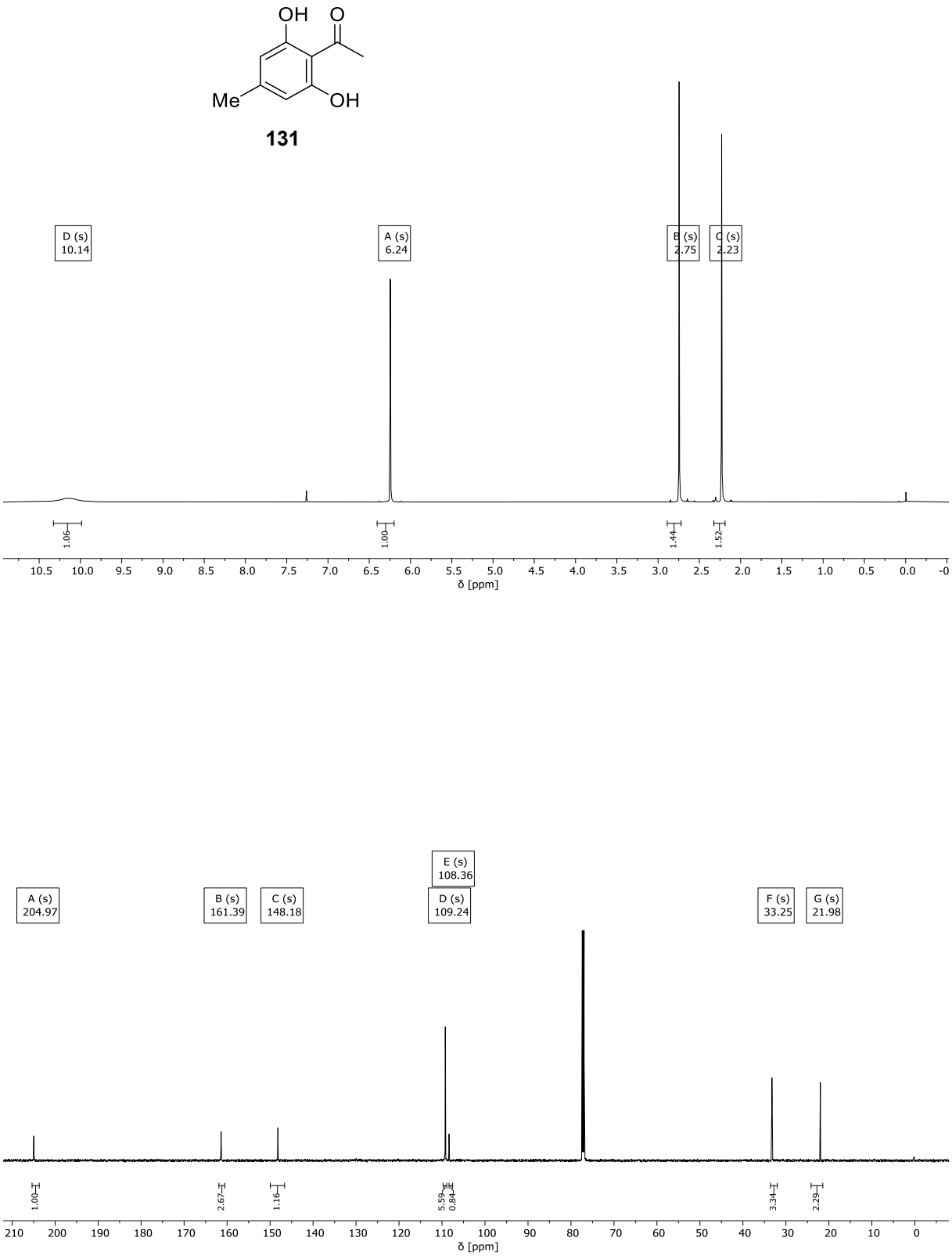

Figure 91: ^{1}H- and ^{13}C-NMR spectra (600 / 151 MHz, $CDCl_3$) of 1-(2,6-dihydroxy-4-methylphenyl)ethan-1-one (**131**)

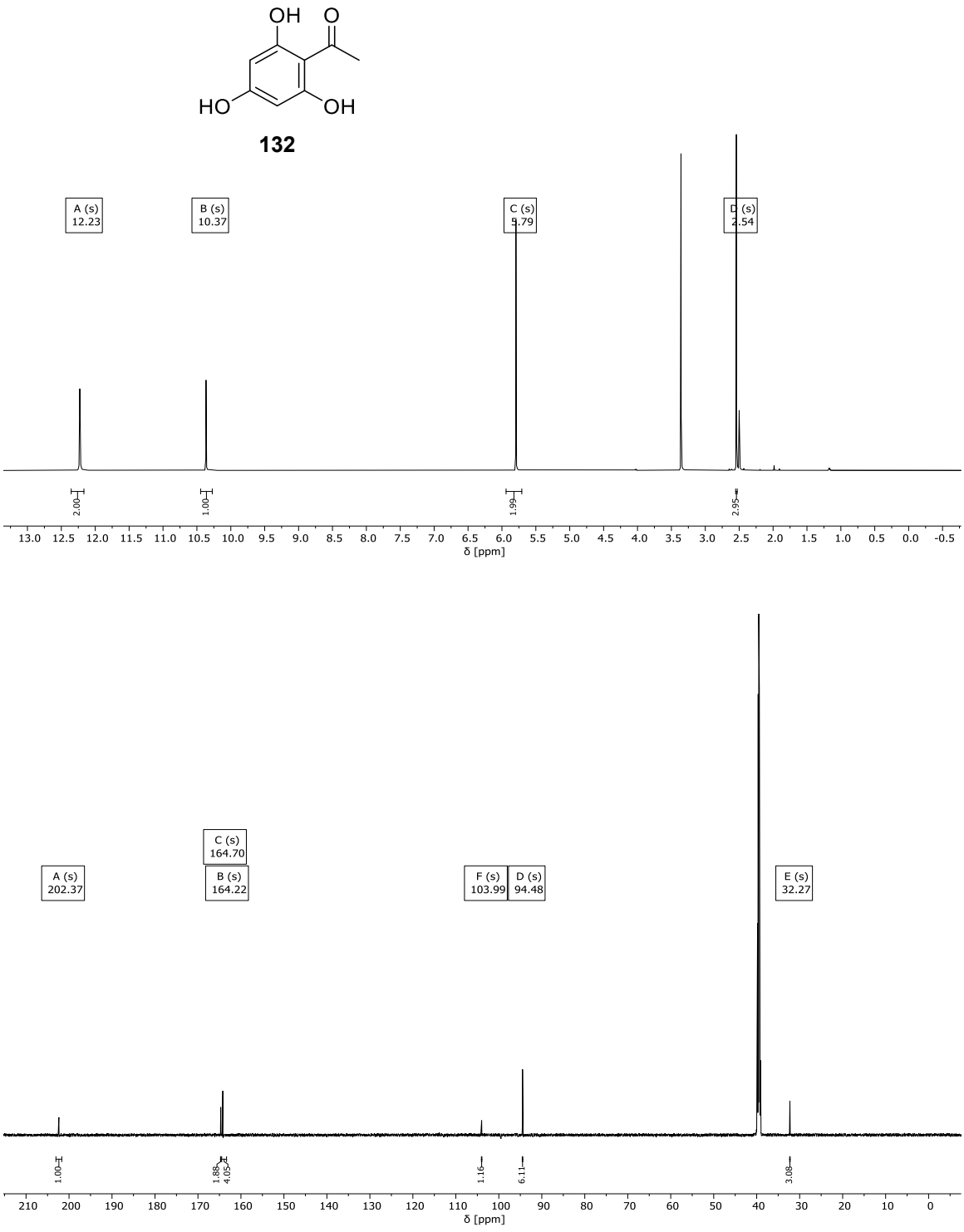

Figure 92: ^{1}H- and ^{13}C-NMR spectra (600 / 151 MHz, DMSO-d_6) of 1-(2,4,6-trihydroxyphenyl)ethan-1-one (**132**)

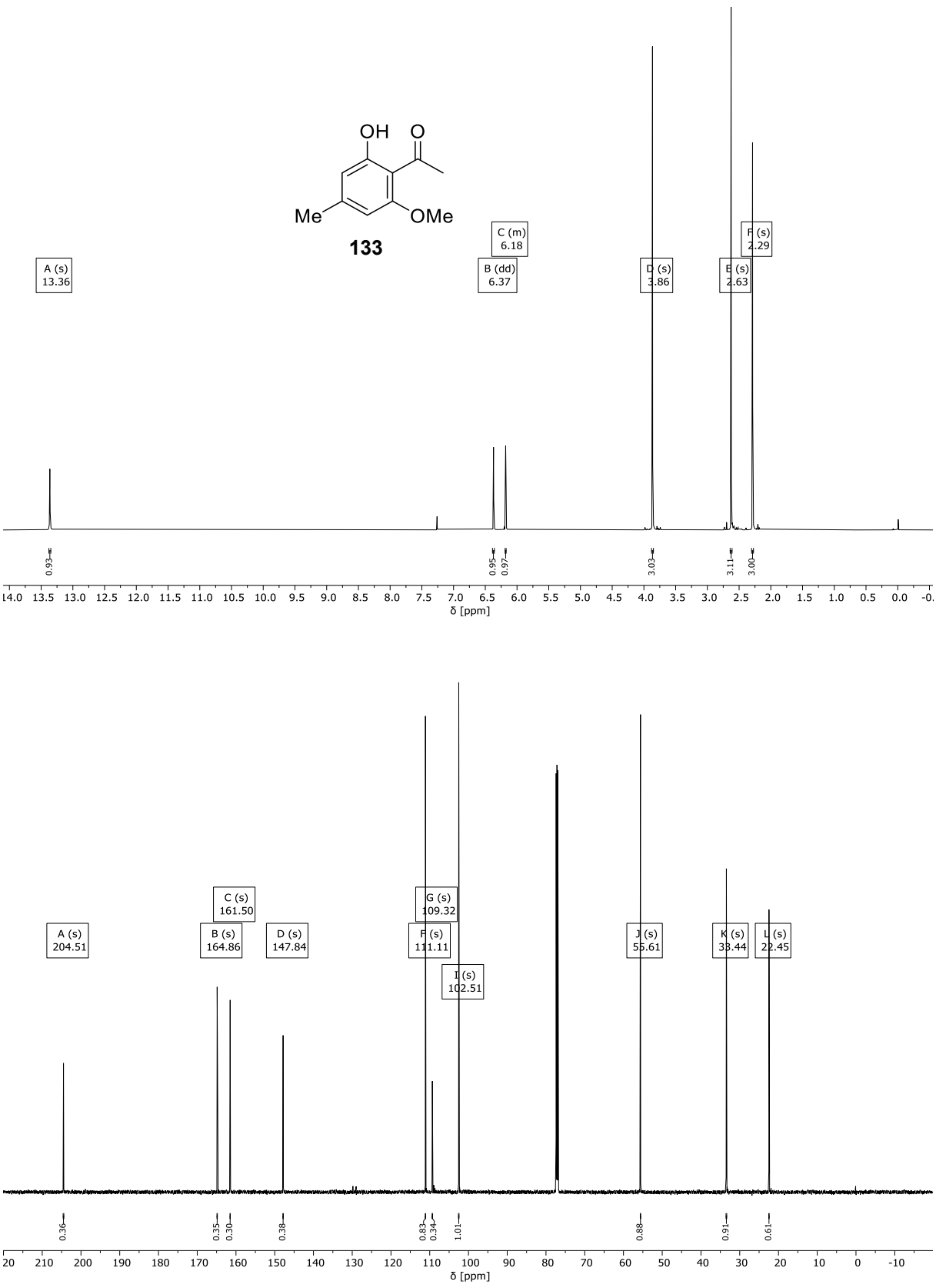

Figure 93: ^{1}H- and ^{13}C-NMR spectra (600 / 151 MHz, $CDCl_3$) of 1-(2-hydroxy-6-methoxy-4-methylphenyl)ethan-1-one (**133)**

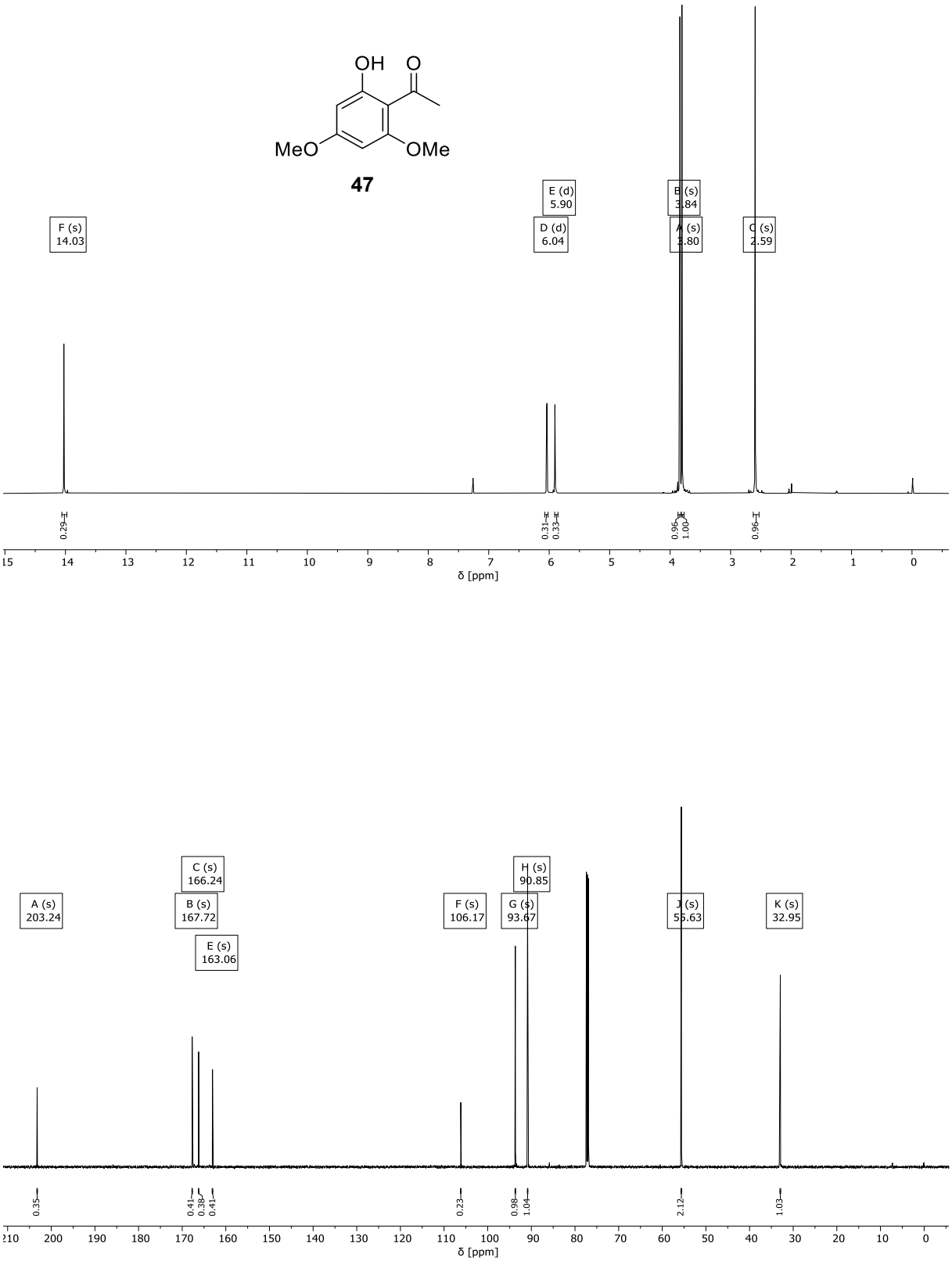

Figure 94: ^{1}H- and ^{13}C-NMR spectra (600 / 151 MHz, $CDCl_3$) of 1-(2-hydroxy-4,6-dimethoxyphenyl)ethan-1-one (**47**)

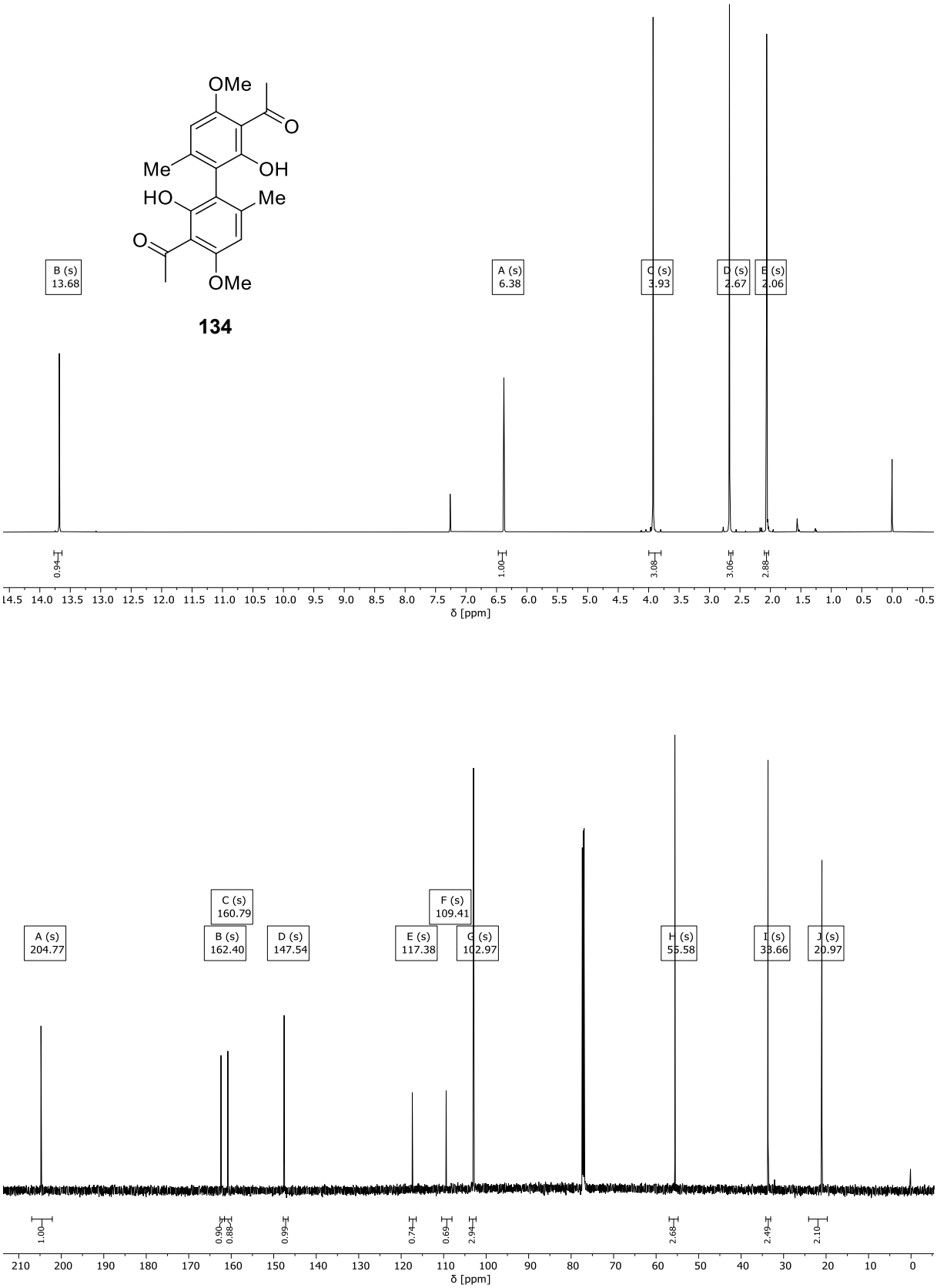

Figure 95: ^{1}H- and ^{13}C-NMR spectra (600 / 151 MHz, $CDCl_3$) of rac-1-(2-hydroxy-6-methoxy-4-methylphenyl)ethan-1-one (**134**)

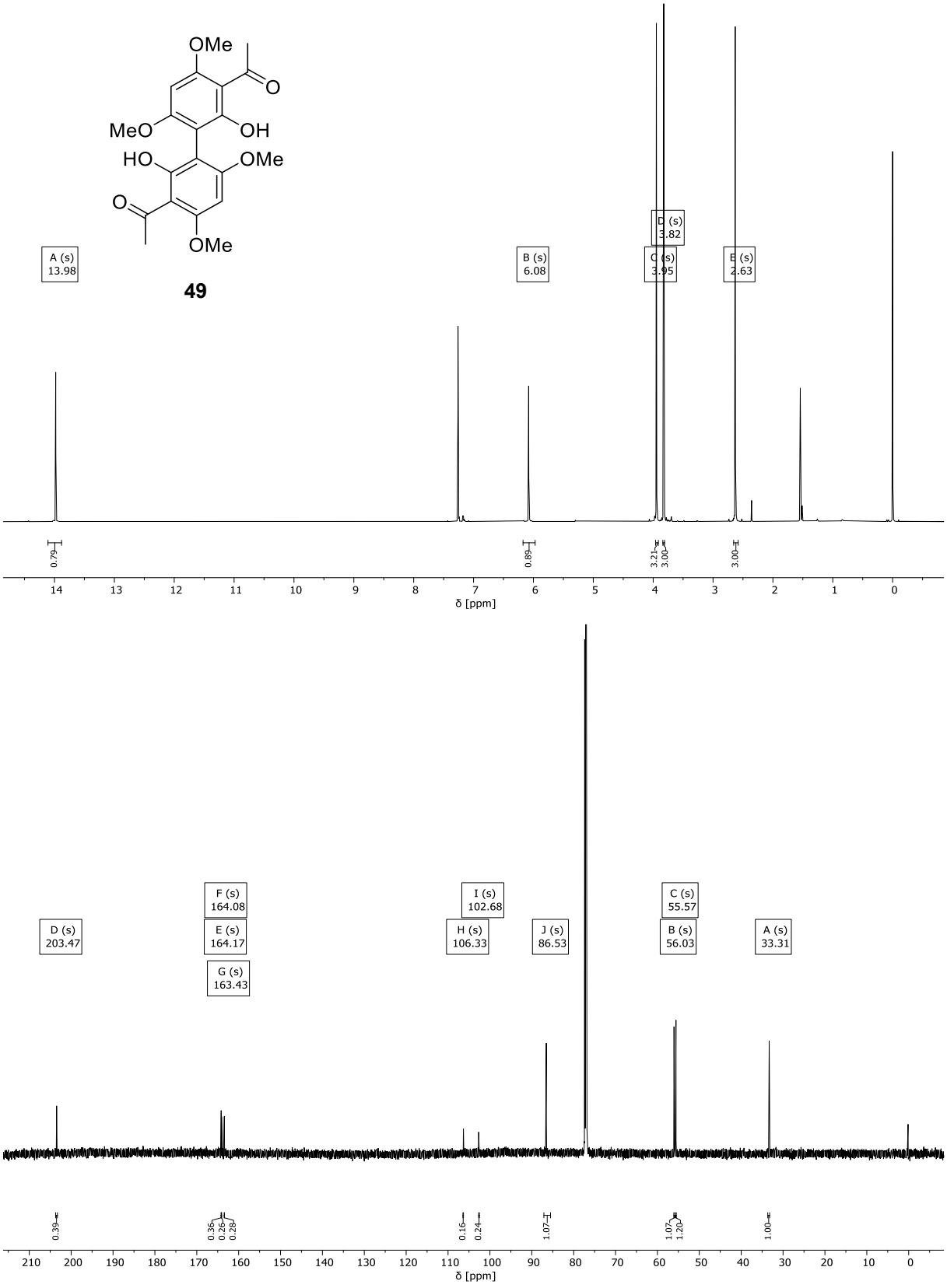

Figure 96: ^{1}H- and ^{13}C-NMR spectra (600 / 151 MHz, $CDCl_3$) of 1-(2-hydroxy-4,6-dimethoxyphenyl)ethan-1-one (**49**)

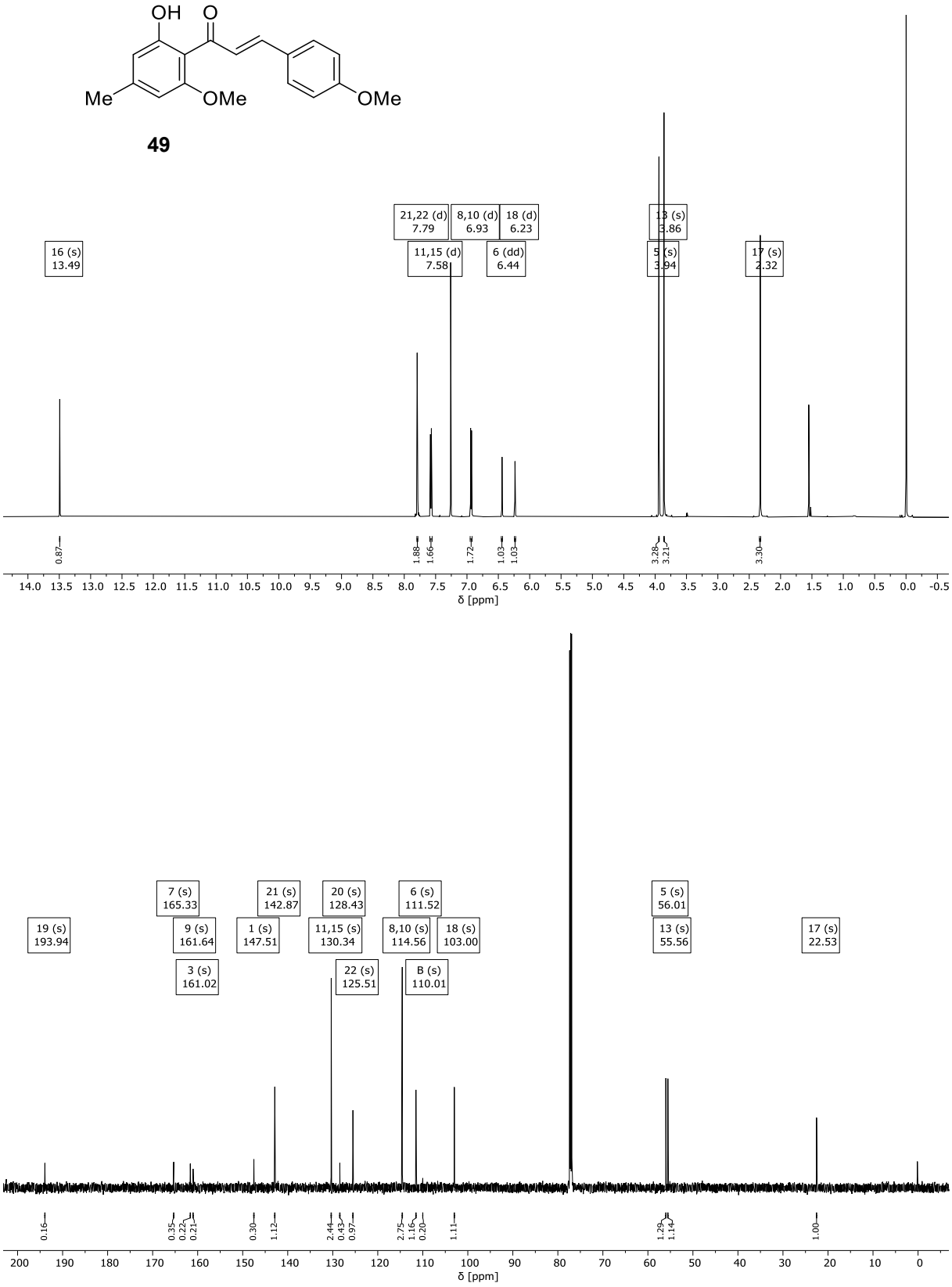

Figure 97: ^{1}H- and ^{13}C-NMR spectra (600 / 151 MHz, $CDCl_3$) of (*E*)-1-(2-hydroxy-6-methoxy-4-methylphenyl)-3-(4-methoxyphenyl)prop-2-en-1-one (**135)**

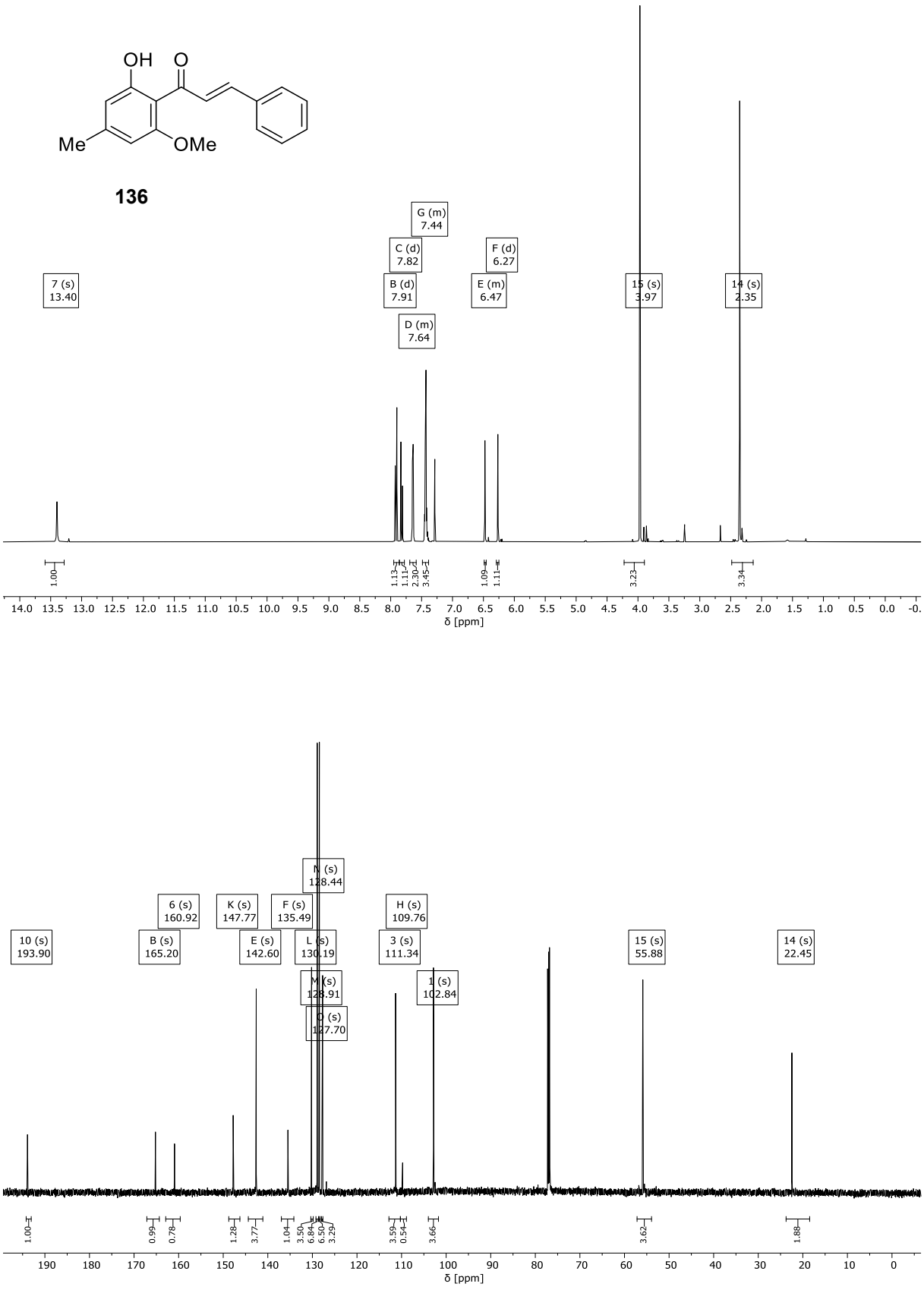

Figure 98: ^{1}H- and ^{13}C-NMR spectra (600 / 151 MHz, $CDCl_3$) of (*E*)-1-(2-hydroxy-6-methoxy-4-methylphenyl)-3-phenylprop-2-en-1-one (**136**)

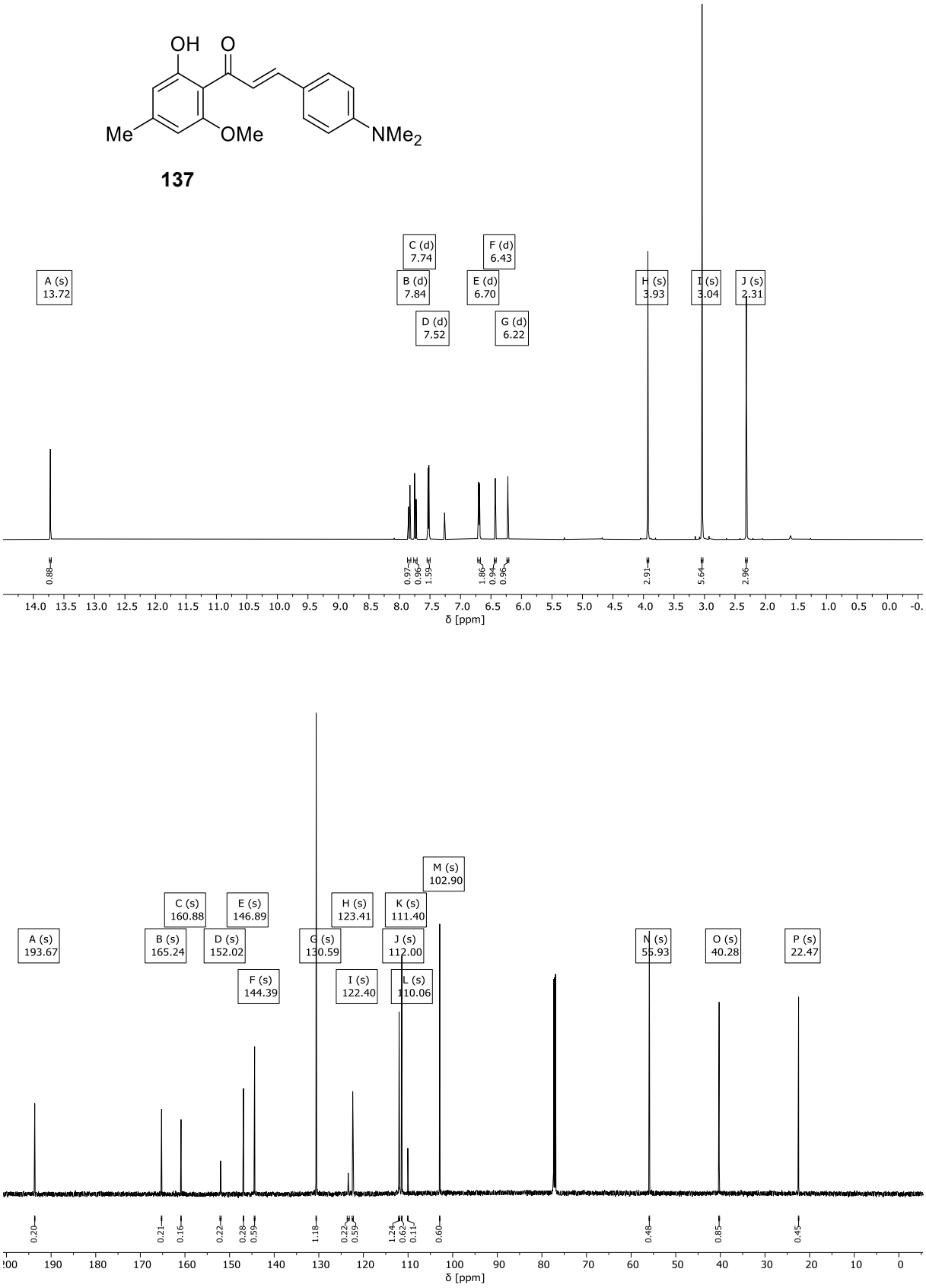

Figure 99: ^{1}H- and ^{13}C-NMR spectra (600 / 151 MHz, $CDCl_3$) of (*E*)-3-(4-(dimethylamino)phenyl)-1-(2-hydroxy-6-methoxy-4-methylphenyl)prop-2-en-1-one (**137)**

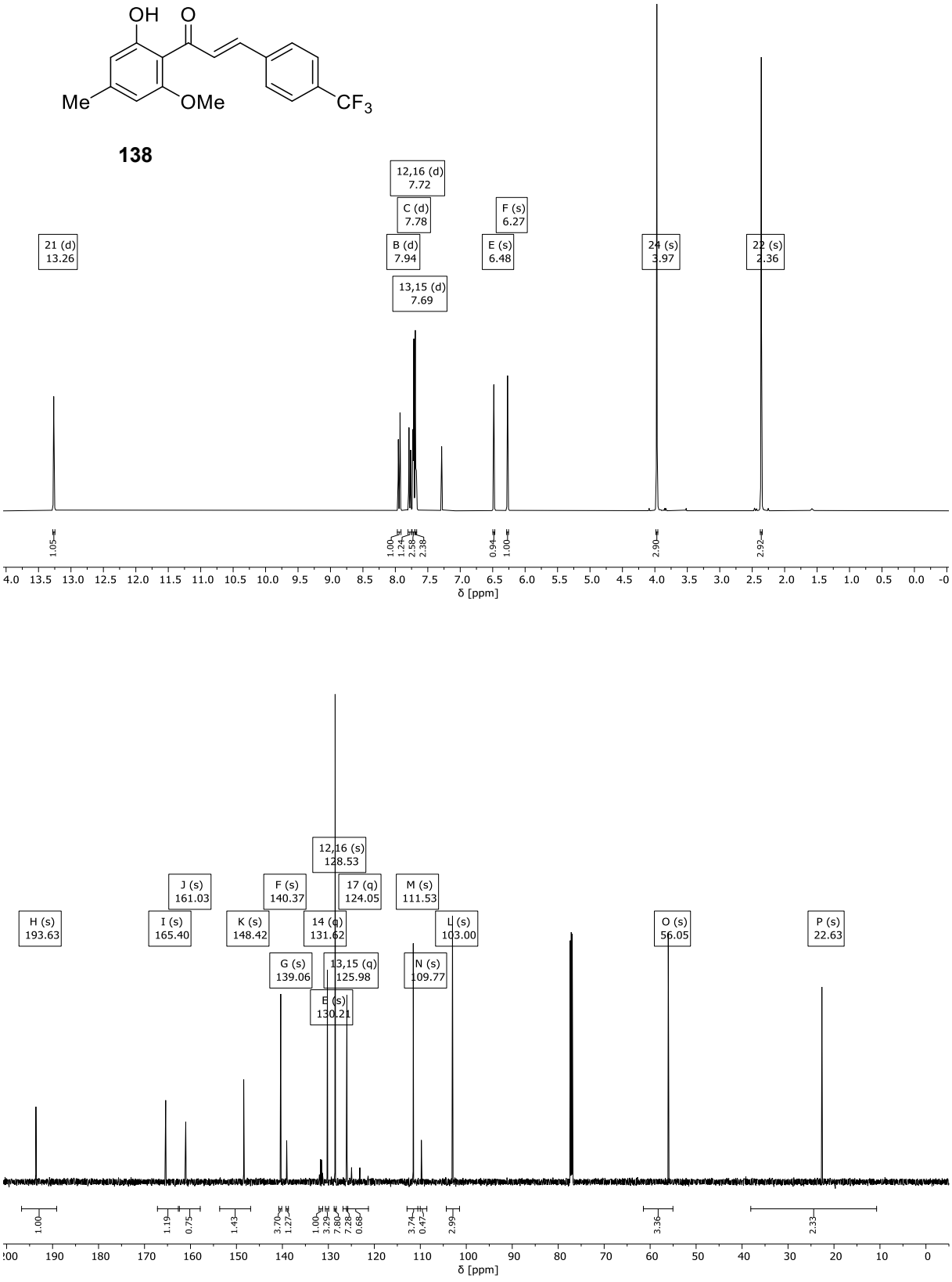

Figure 100: ^{1}H-, ^{13}C-NMR spectra (600 / 151 MHz, $CDCl_3$) of (*E*)-1-(2-hydroxy-6-methoxy-4-methylphenyl)-3-(4-(trifluoromethyl)phenyl)prop-2-en-1-one (**138**)

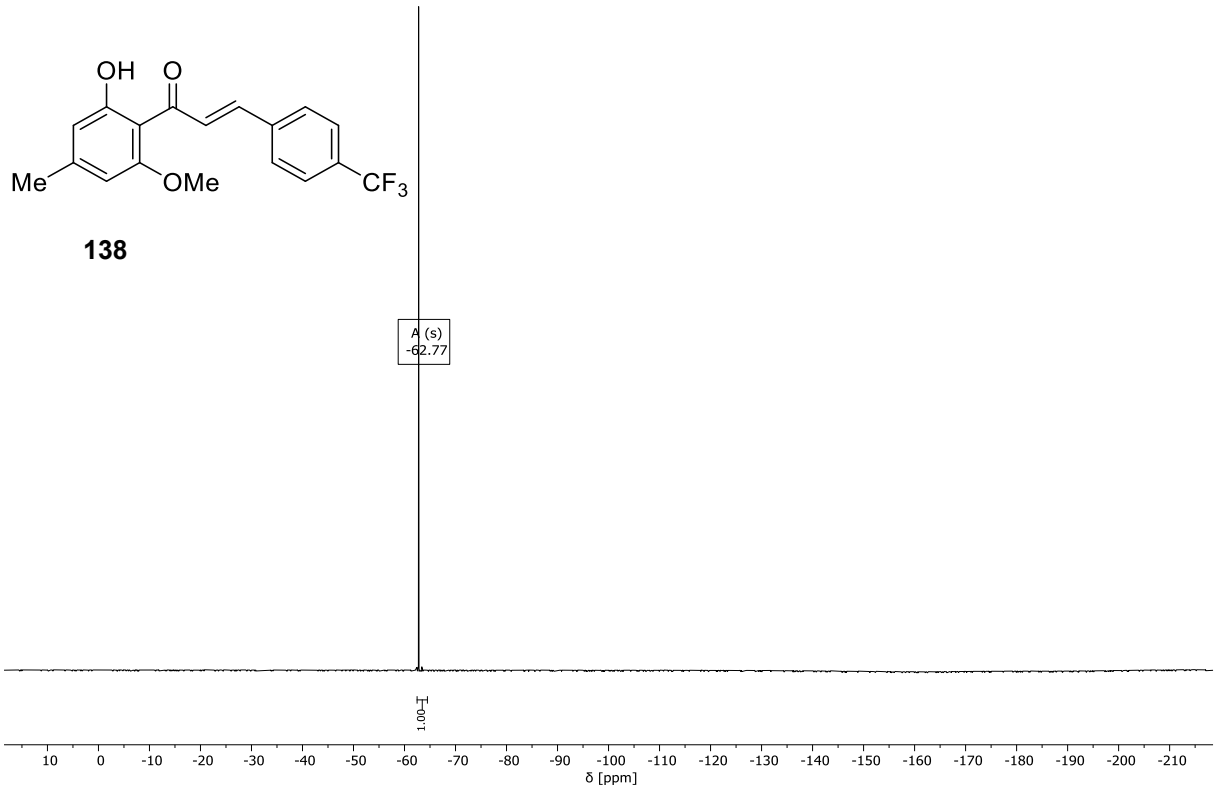

Figure 101: ^{19}F-NMR spectrum (282 MHz, $CDCl_3$) of (*E*)-1-(2-hydroxy-6-methoxy-4-methylphenyl)-3-(4-(trifluoromethyl)phenyl)prop-2-en-1-one (**138**)

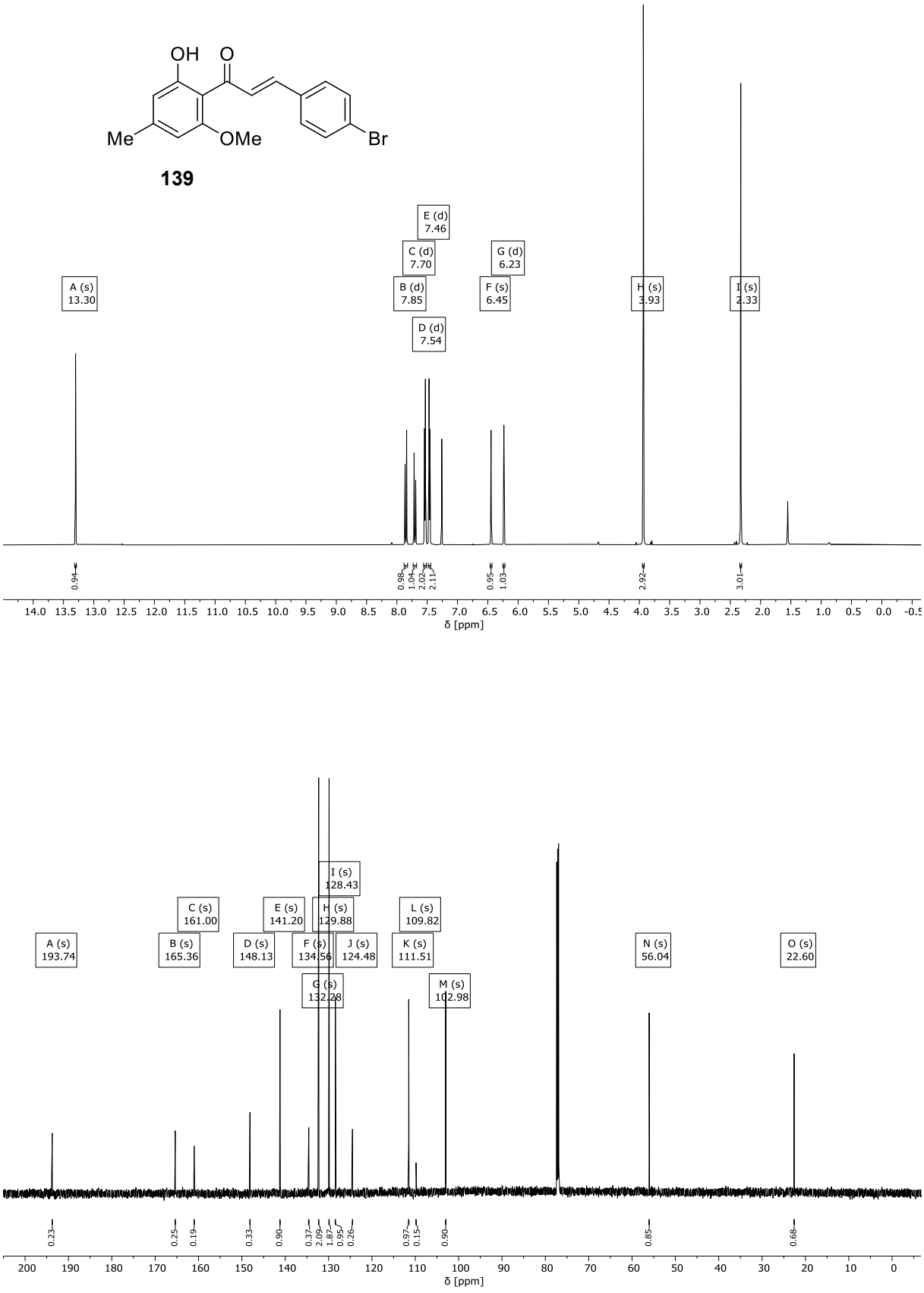

Figure 102: ^{1}H- and ^{13}C-NMR spectra (600 / 151 MHz, $CDCl_3$) of (*E*)-3-(4-bromophenyl)-1-(2-hydroxy-6-methoxy-4-methylphenyl)prop-2-en-1-one (**139**)

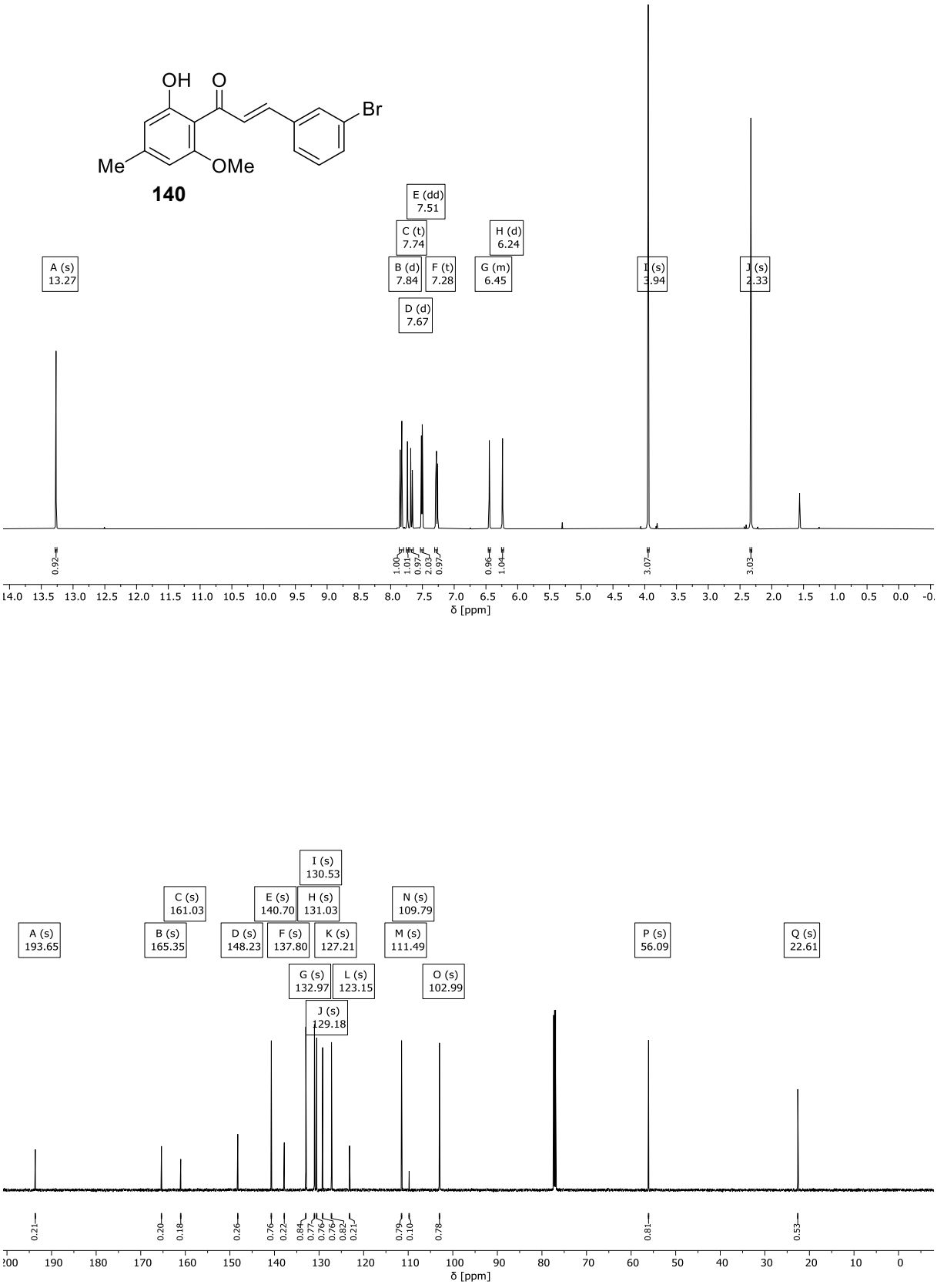

Figure 103: ^{1}H- and ^{13}C-NMR spectra (600 / 151 MHz, $CDCl_3$) of (*E*)-3-(3-bromophenyl)-1-(2-hydroxy-6-methoxy-4-methylphenyl)prop-2-en-1-one (**140**)

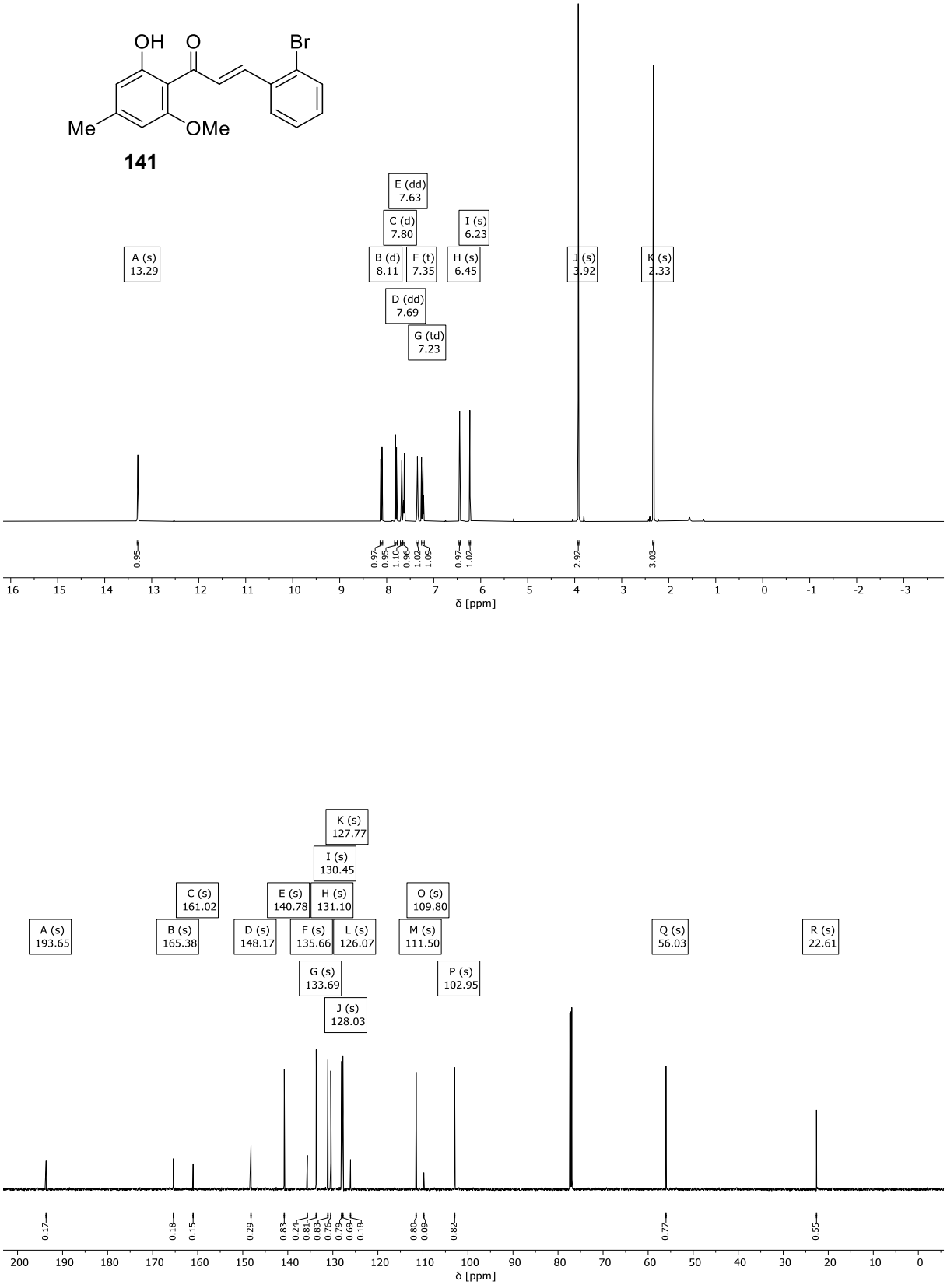

Figure 104: ^{1}H- and ^{13}C-NMR spectra (600 / 151 MHz, $CDCl_3$) of (*E*)-3-(2-bromophenyl)-1-(2-hydroxy-6-methoxy-4-methylphenyl)prop-2-en-1-one (**141**)

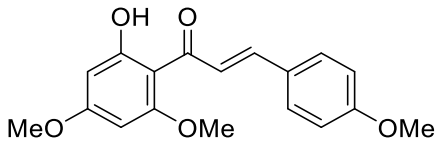

142

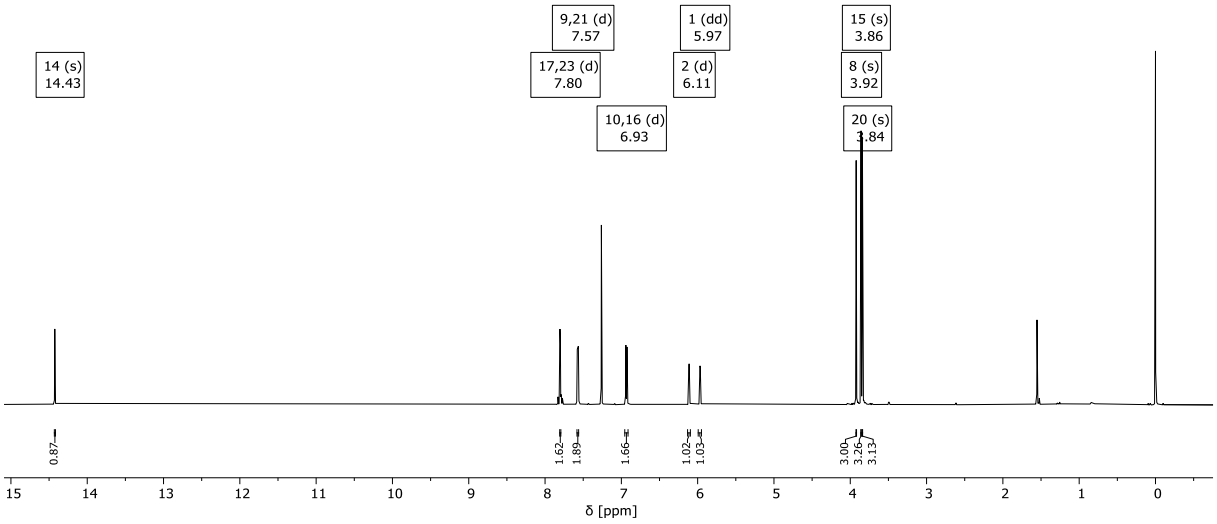

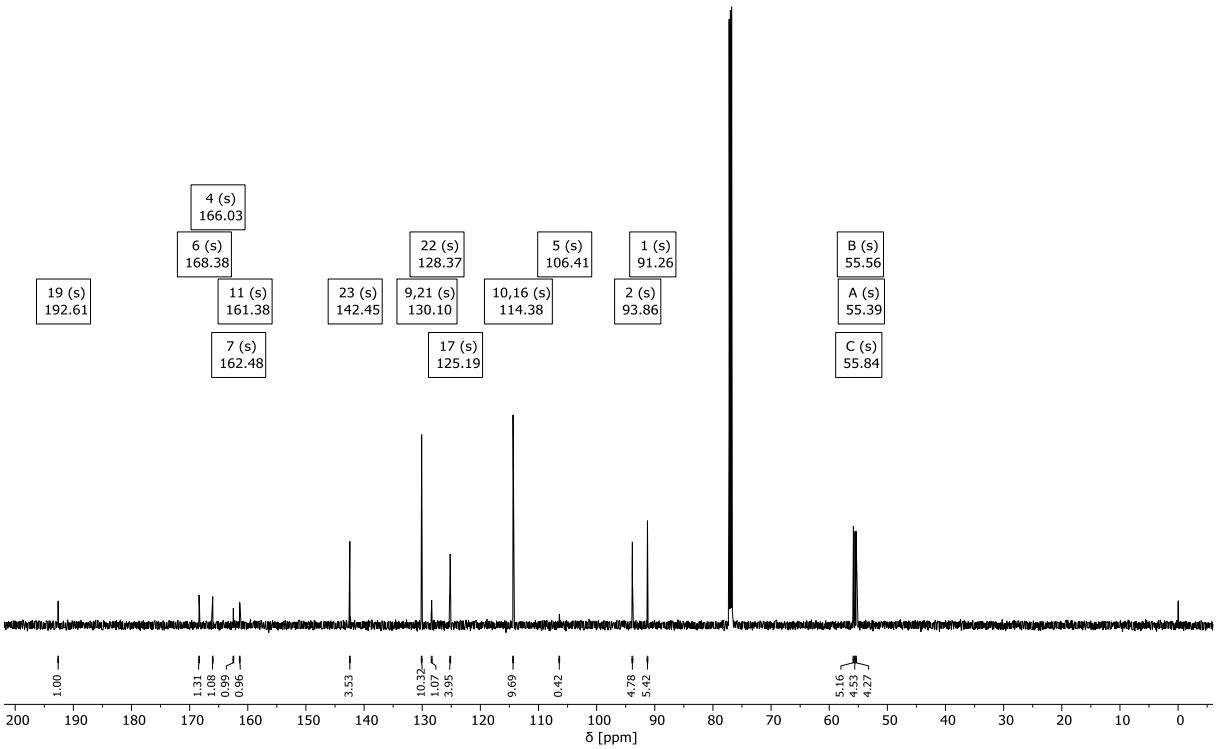

Figure 105: ^{1}H- and ^{13}C-NMR spectra (600 / 151 MHz, $CDCl_3$) of (E)-1-(2-hydroxy-4,6-dimethoxyphenyl)-3-(4-methoxyphenyl)prop-2-en-1-one (**142**)

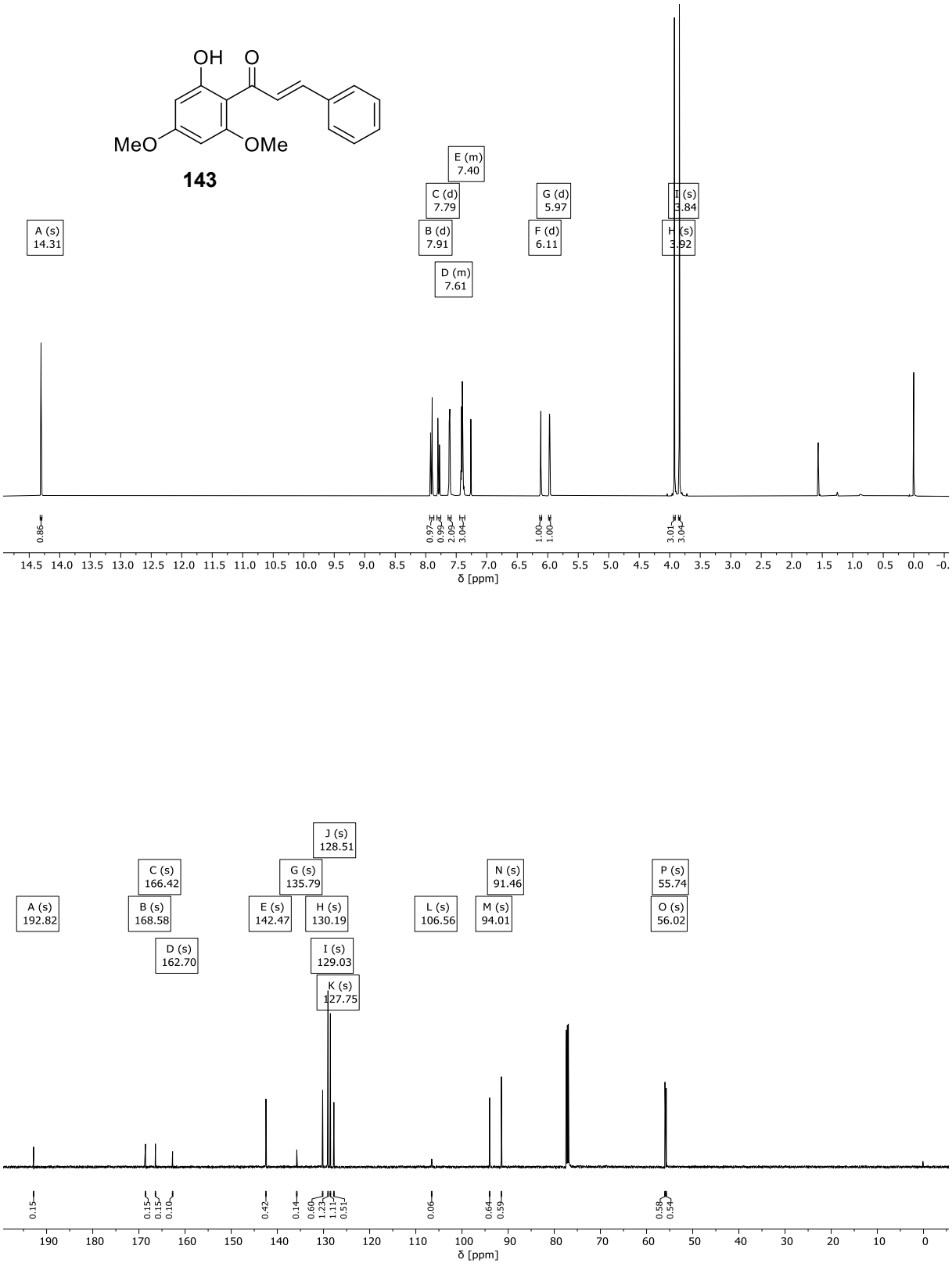

Figure 106: ^{1}H- and ^{13}C-NMR spectra (600 / 151 MHz, $CDCl_3$) of (E)-1-(2-hydroxy-4,6-dimethoxyphenyl)-3-phenylprop-2-en-1-one (**143)**

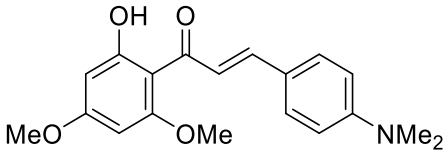

144

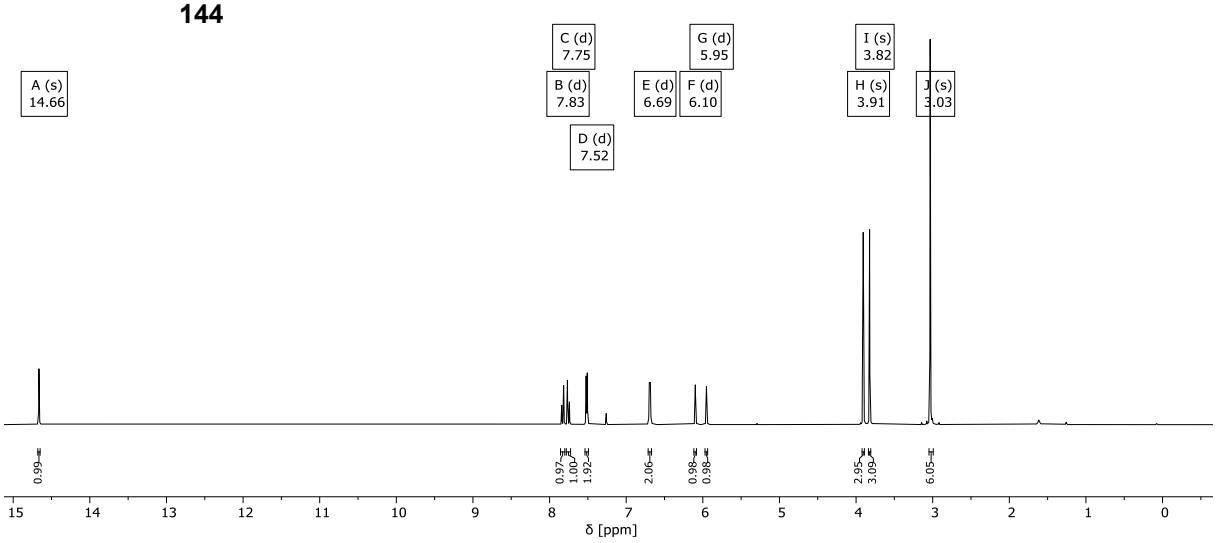

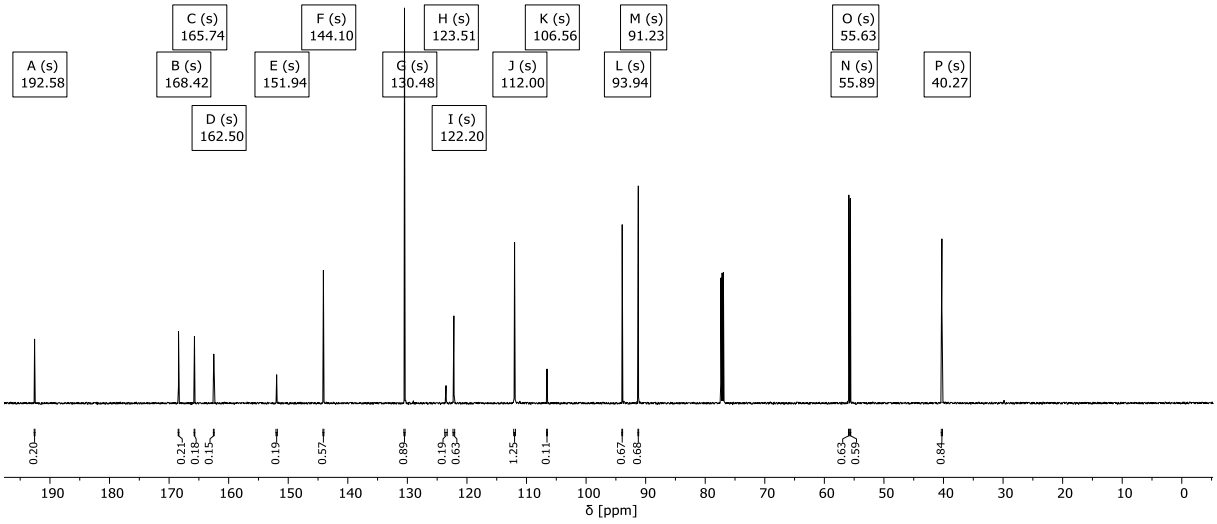

Figure 107: ^{1}H- and ^{13}C-NMR spectra (600 / 151 MHz, $CDCl_3$) of (*E*)-3-(4-(dimethylamino)phenyl)-1-(2-hydroxy-4,6-dimethoxyphenyl)prop-2-en-1-one (**144)**

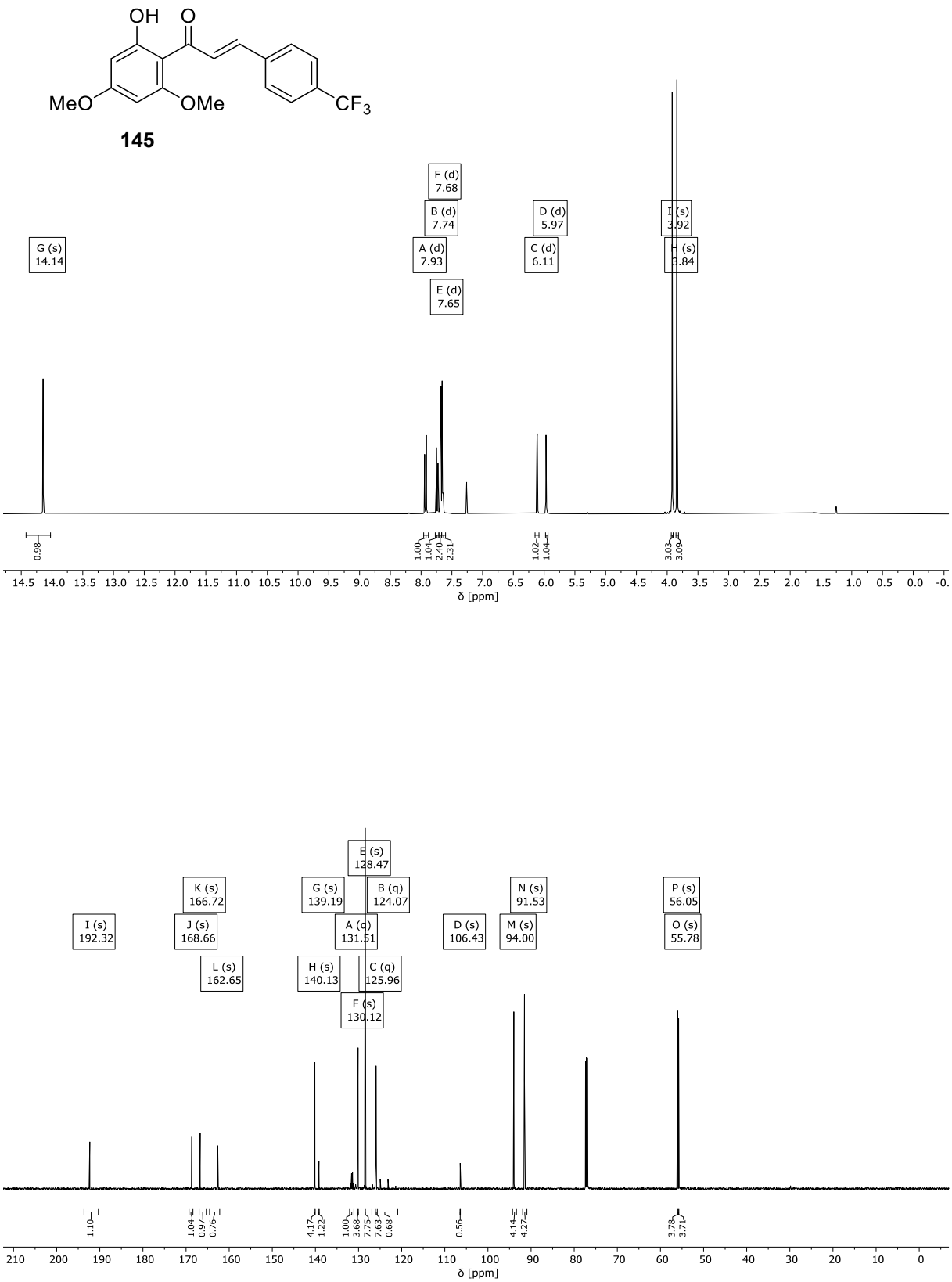

Figure 108: ^{1}H-, ^{13}C-NMR spectra (600 / 151 MHz, $CDCl_3$) of (*E*)-1-(2-hydroxy-4,6-dimethoxyphenyl)-3-(4-(trifluoromethyl)phenyl)prop-2-en-1-one (**145)**

Figure 109: ^{19}F-NMR spectrum (282 MHz, $CDCl_3$) of (*E*)-1-(2-hydroxy-4,6-dimethoxyphenyl)-3-(4-(trifluoromethyl)phenyl)prop-2-en-1-one (**145)**

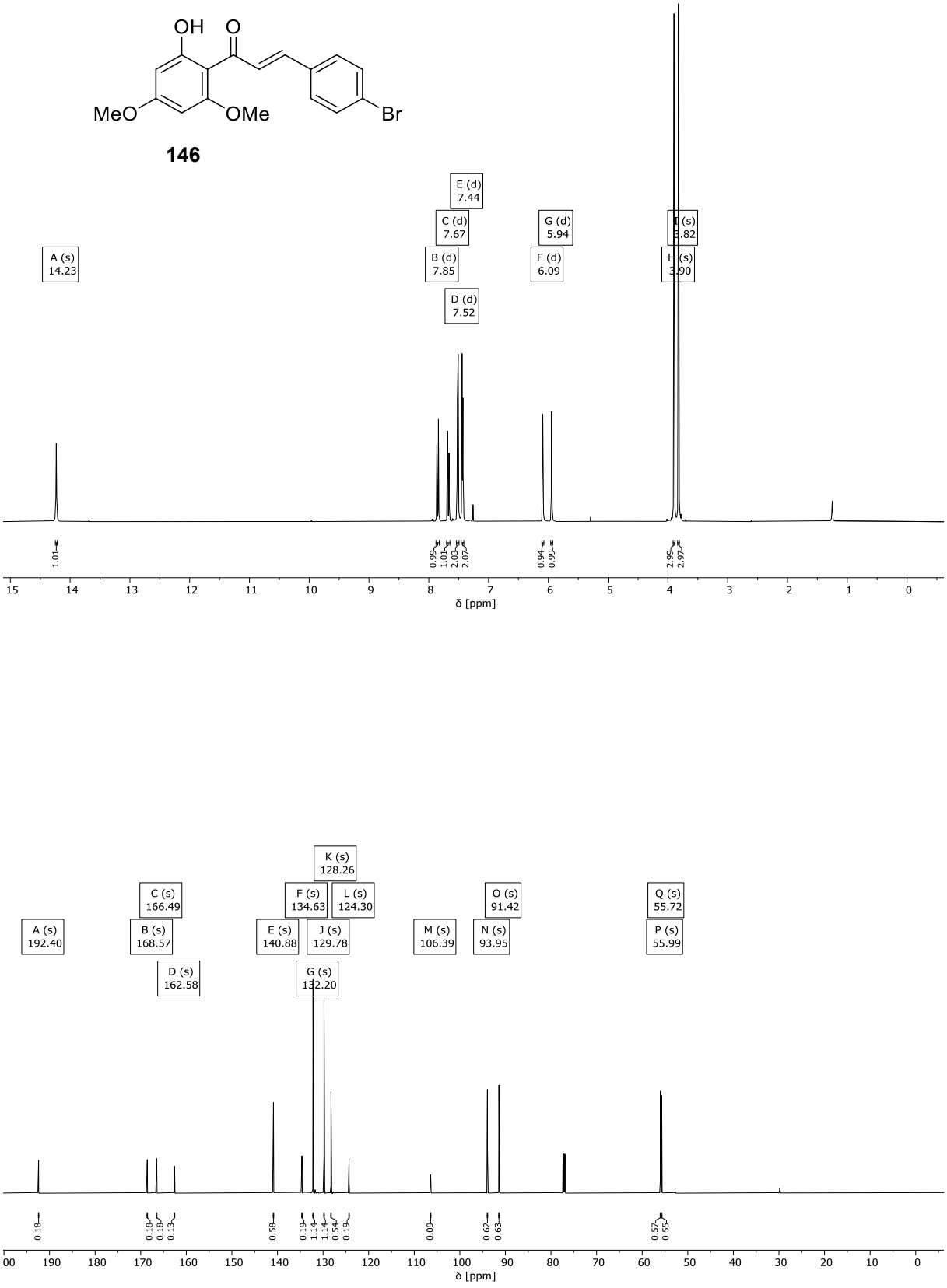

Figure 110: ^{1}H- and ^{13}C-NMR spectra (600 / 151 MHz, $CDCl_3$) of (*E*)-3-(4-bromophenyl)-1-(2-hydroxy-4,6-dimethoxyphenyl)prop-2-en-1-one (**146**)

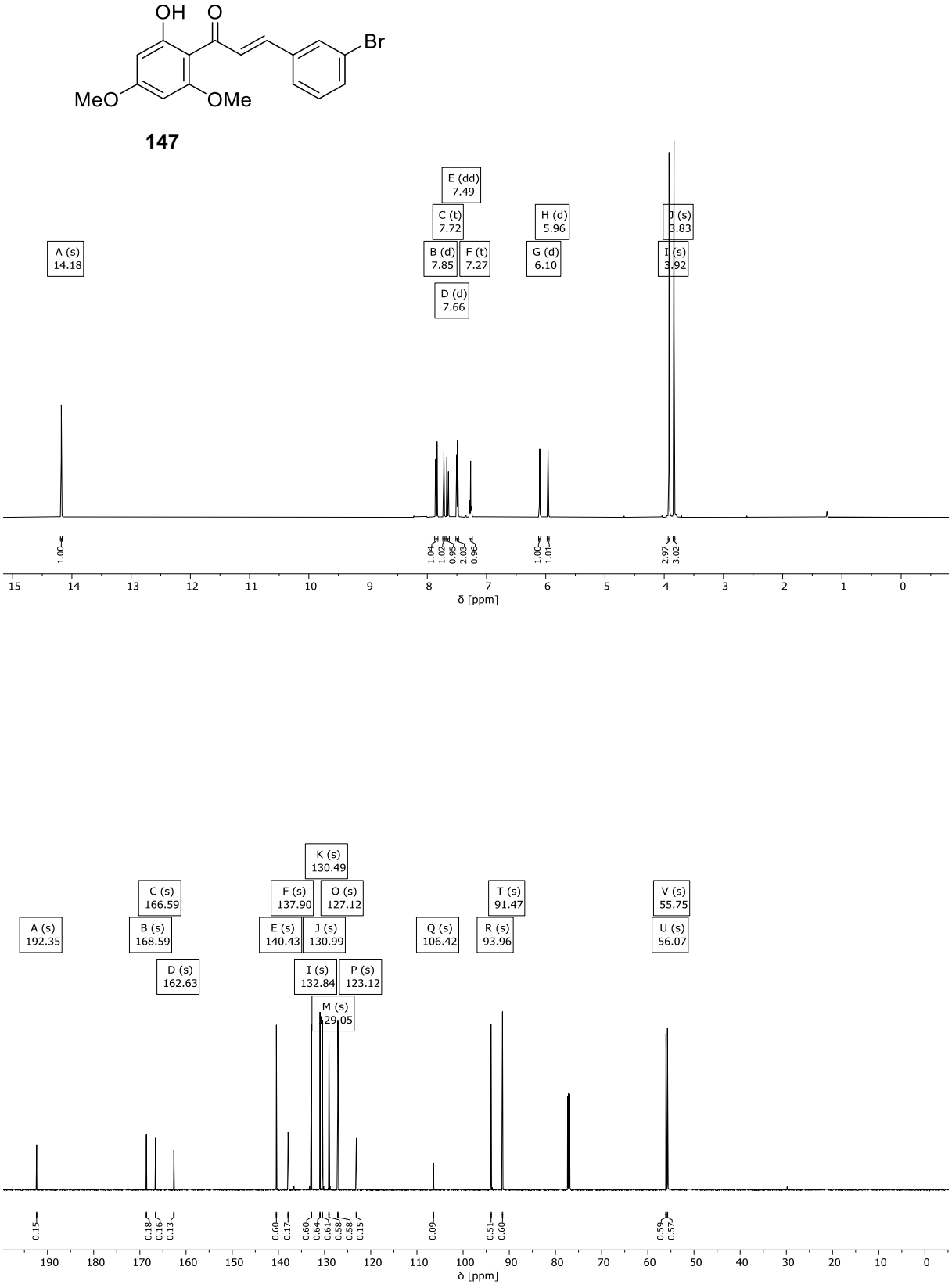

Figure 111: ^{1}H- and ^{13}C-NMR spectra (600 / 151 MHz, $CDCl_3$) of (*E*)-3-(3-bromophenyl)-1-(2-hydroxy-4,6-dimethoxyphenyl)prop-2-en-1-one (**147)**

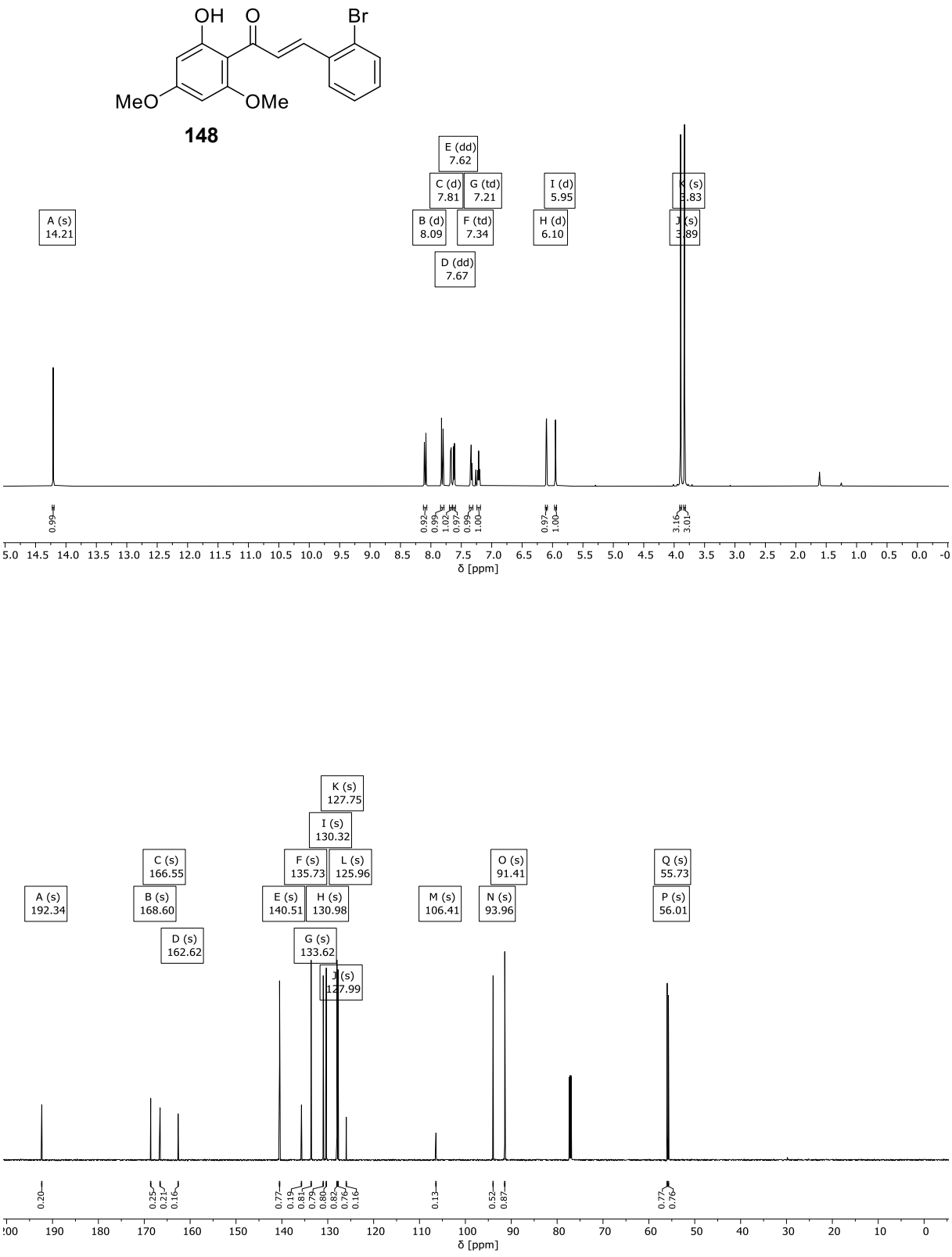

Figure 112: ^{1}H- and ^{13}C-NMR spectra (600 / 151 MHz, $CDCl_3$) of (*E*)-3-(2-bromophenyl)-1-(2-hydroxy-4,6-dimethoxyphenyl)prop-2-en-1-one (**148**)

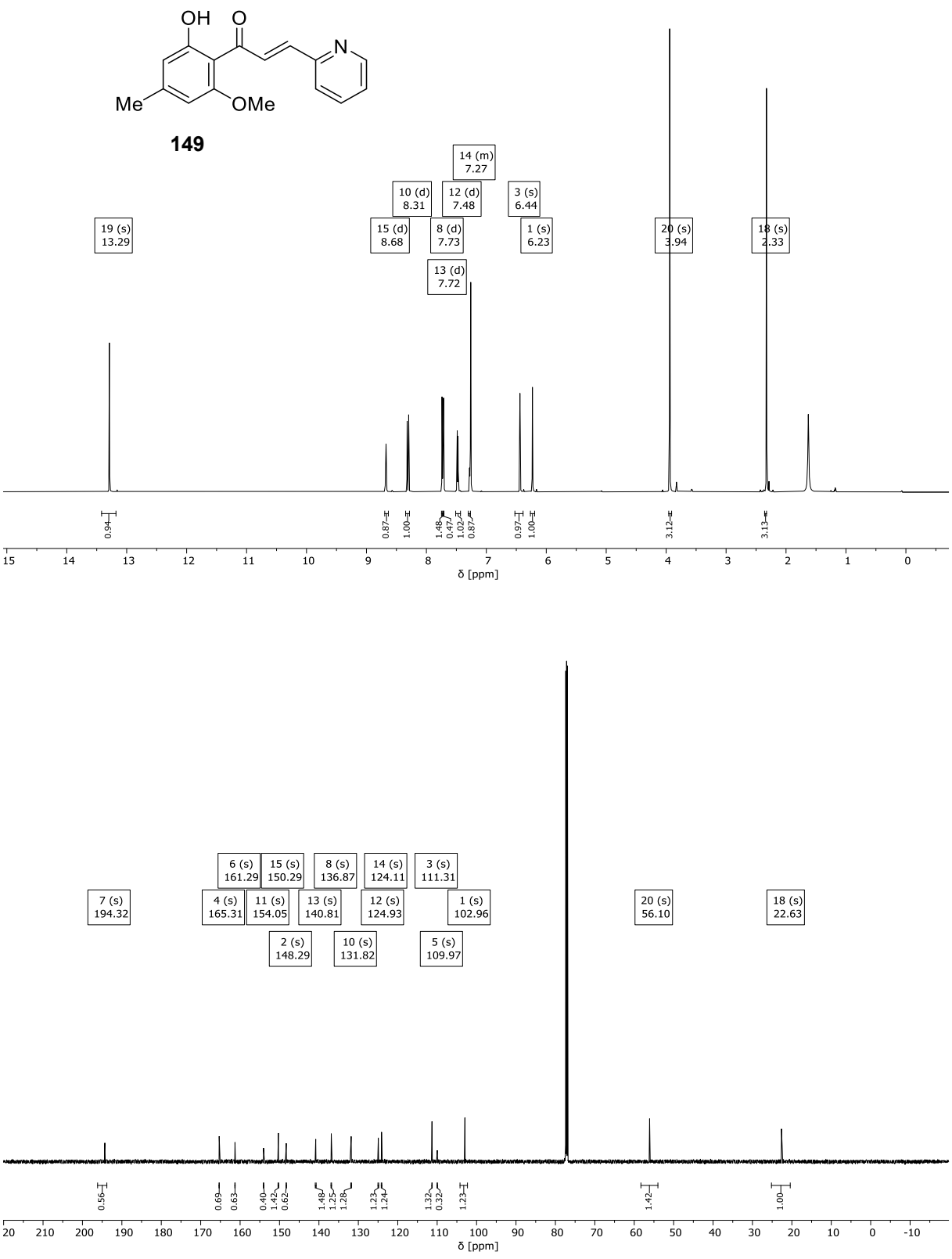

Figure 113: ^{1}H- and ^{13}C-NMR spectra (600 / 151 MHz, $CDCl_3$) of (*E*)-1-(2-hydroxy-6-methoxy-4-methylphenyl)-3-(pyridin-2-yl)prop-2-en-1-one (**149)**

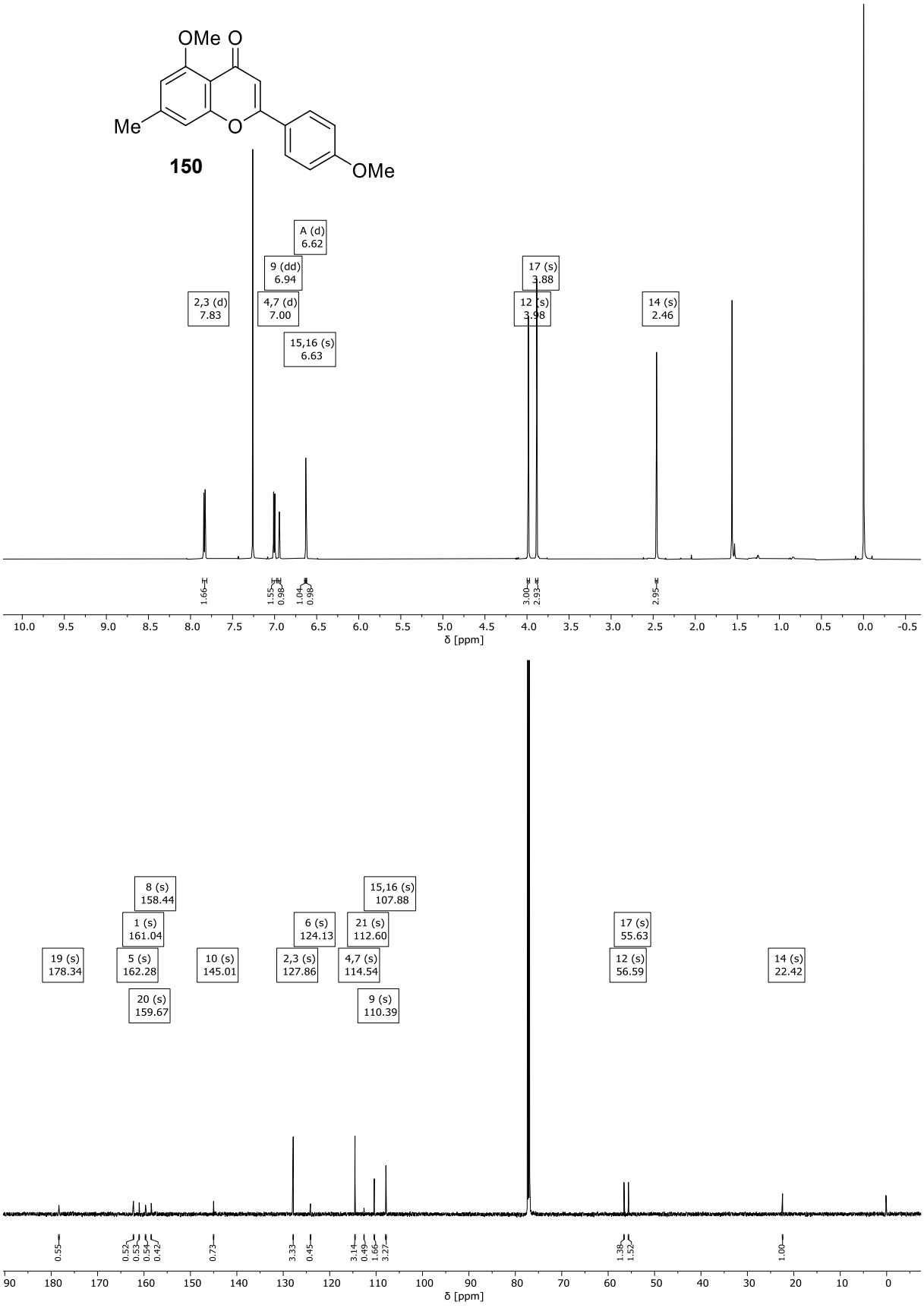

Figure 114: ^{1}H- and ^{13}C-NMR spectra (600 / 151 MHz, $CDCl_3$) of 5-methoxy-2-(4-methoxyphenyl)-7-methyl-4H-chromen-4-one (**150)**

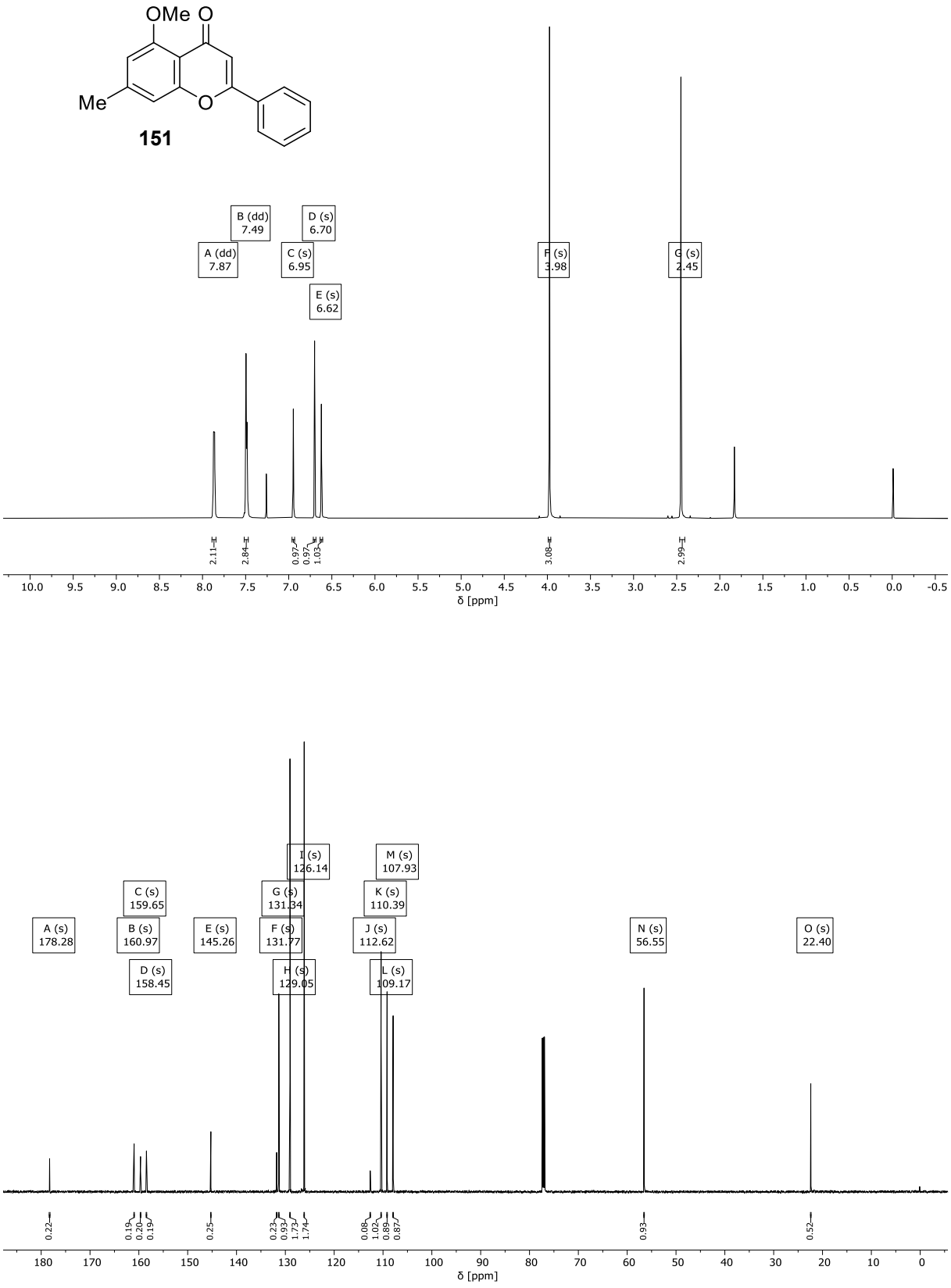

Figure 115: ^{1}H- and ^{13}C-NMR spectra (600 / 151 MHz, $CDCl_3$) of 5-methoxy-7-methyl-2-phenyl-4H-chromen-4-one (**151)**

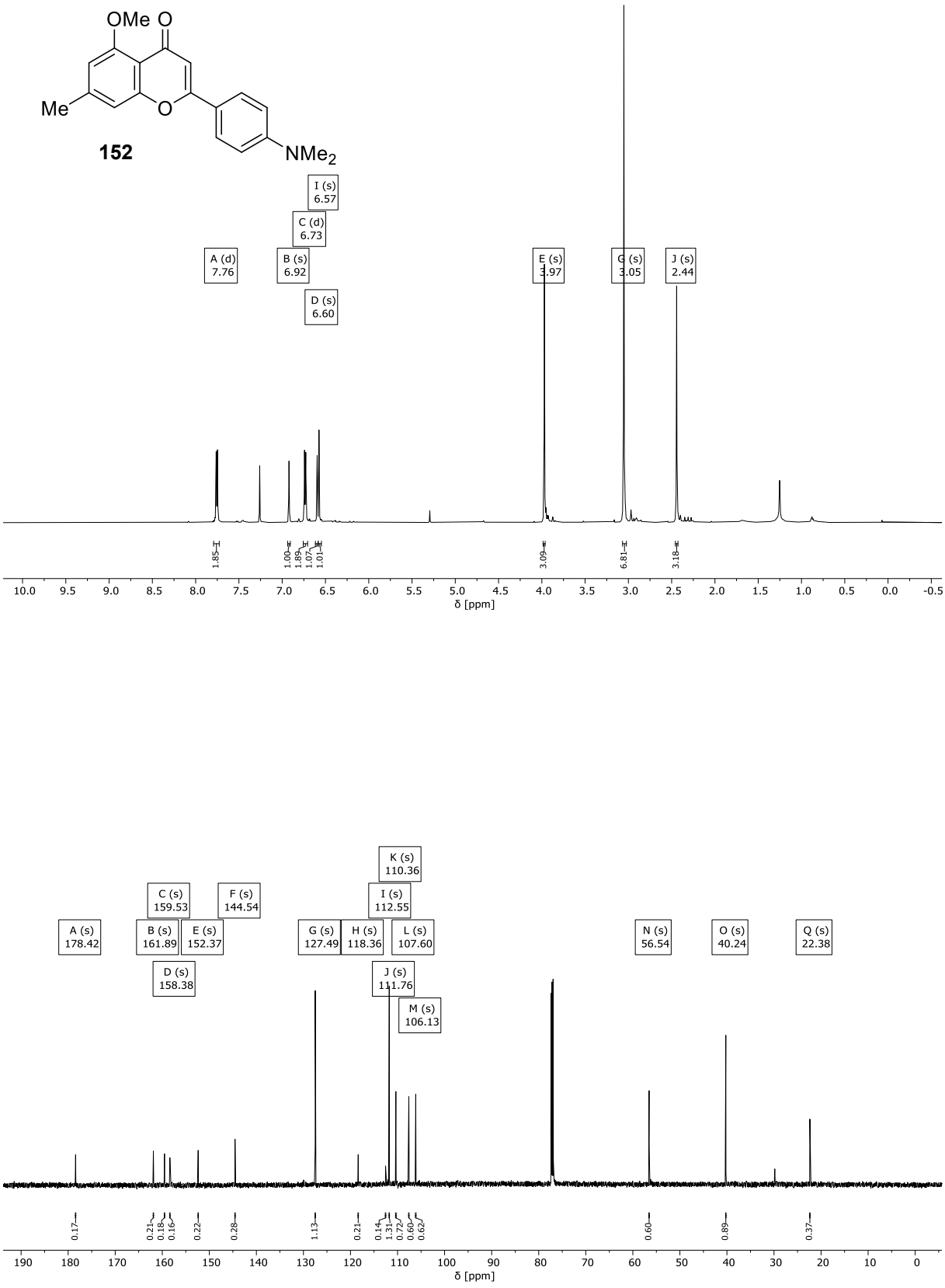

Figure 116: ^{1}H- and ^{13}C-NMR spectra (600 / 151 MHz, $CDCl_3$) of 2-(4-(dimethylamino)phenyl)-5-methoxy-7-methyl-4H-chromen-4-one (**152)**

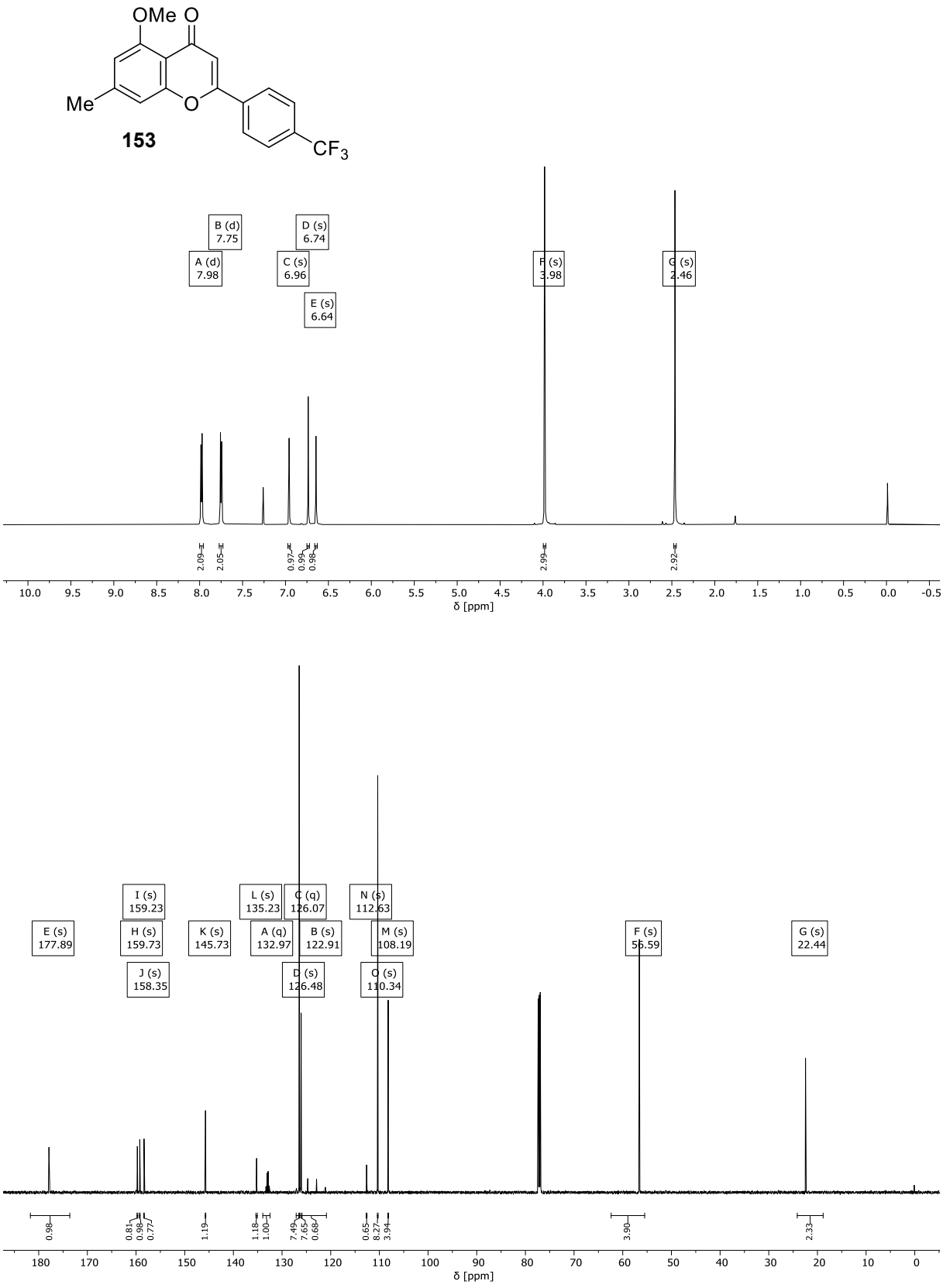

Figure 117: ^{1}H-, ^{13}C-spectra (600 / 151 MHz, $CDCl_3$) of 5-methoxy-7-methyl-2-(4-(trifluoromethyl)phenyl)-4H-chromen-4-one (**153)**

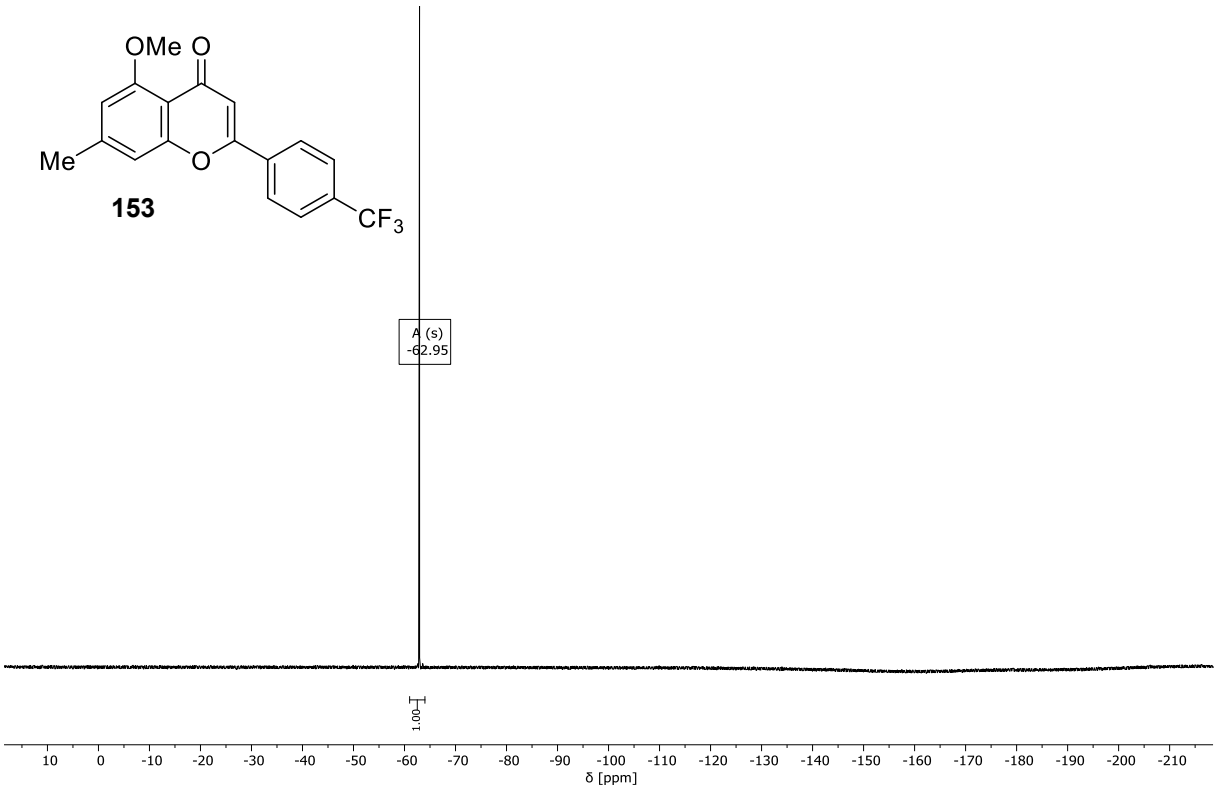

Figure 118: ^{19}F-NMR spectrum (282 MHz, $CDCl_3$) of 5-methoxy-7-methyl-2-(4-(trifluoromethyl)phenyl)-4H-chromen-4-one (**153)**

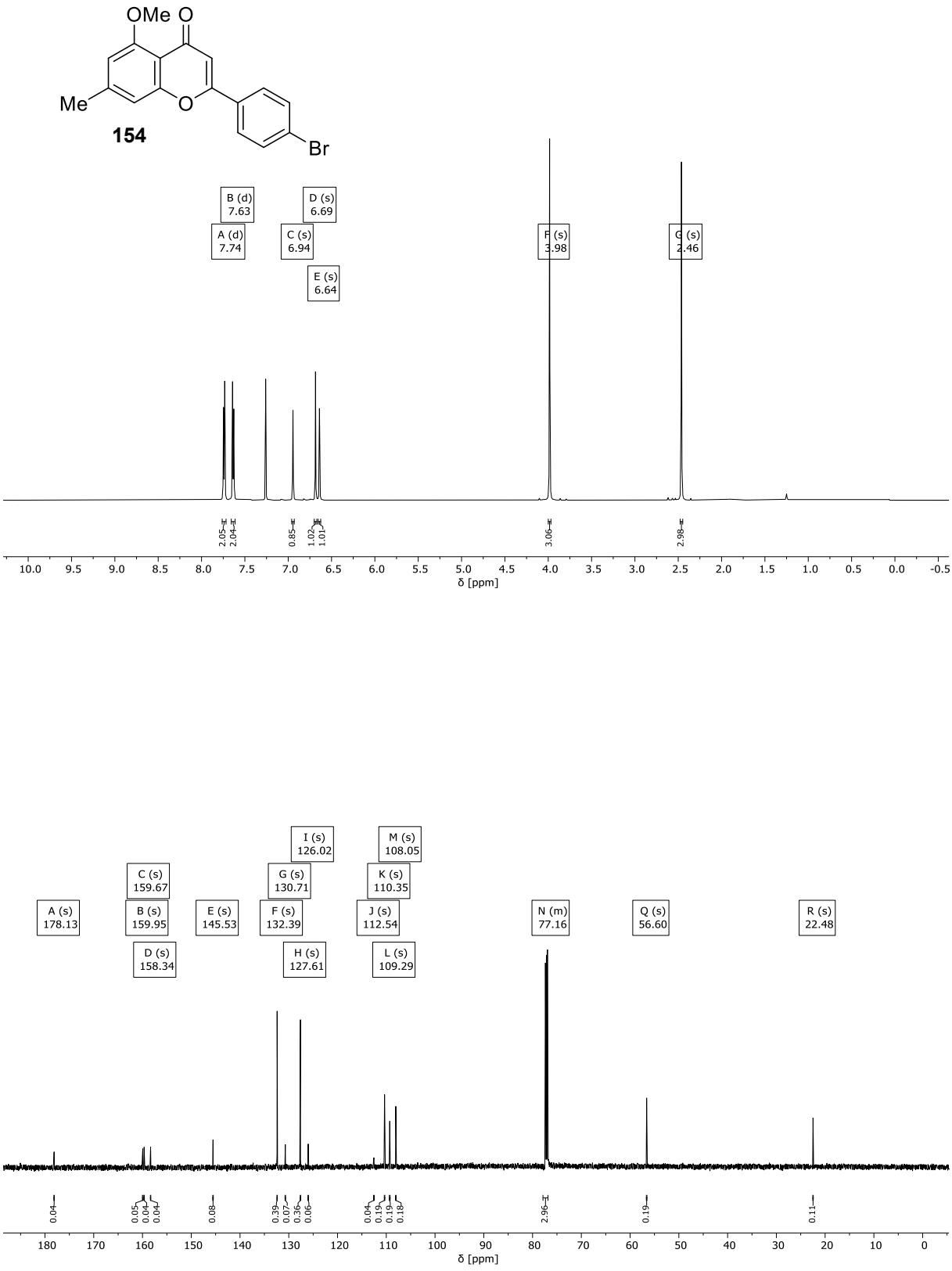

Figure 119: ^{1}H- and ^{13}C-NMR spectra (600 / 151 MHz, $CDCl_3$) of 2-(4-bromophenyl)-5-methoxy-7-methyl-4H-chromen-4-one (**154)**

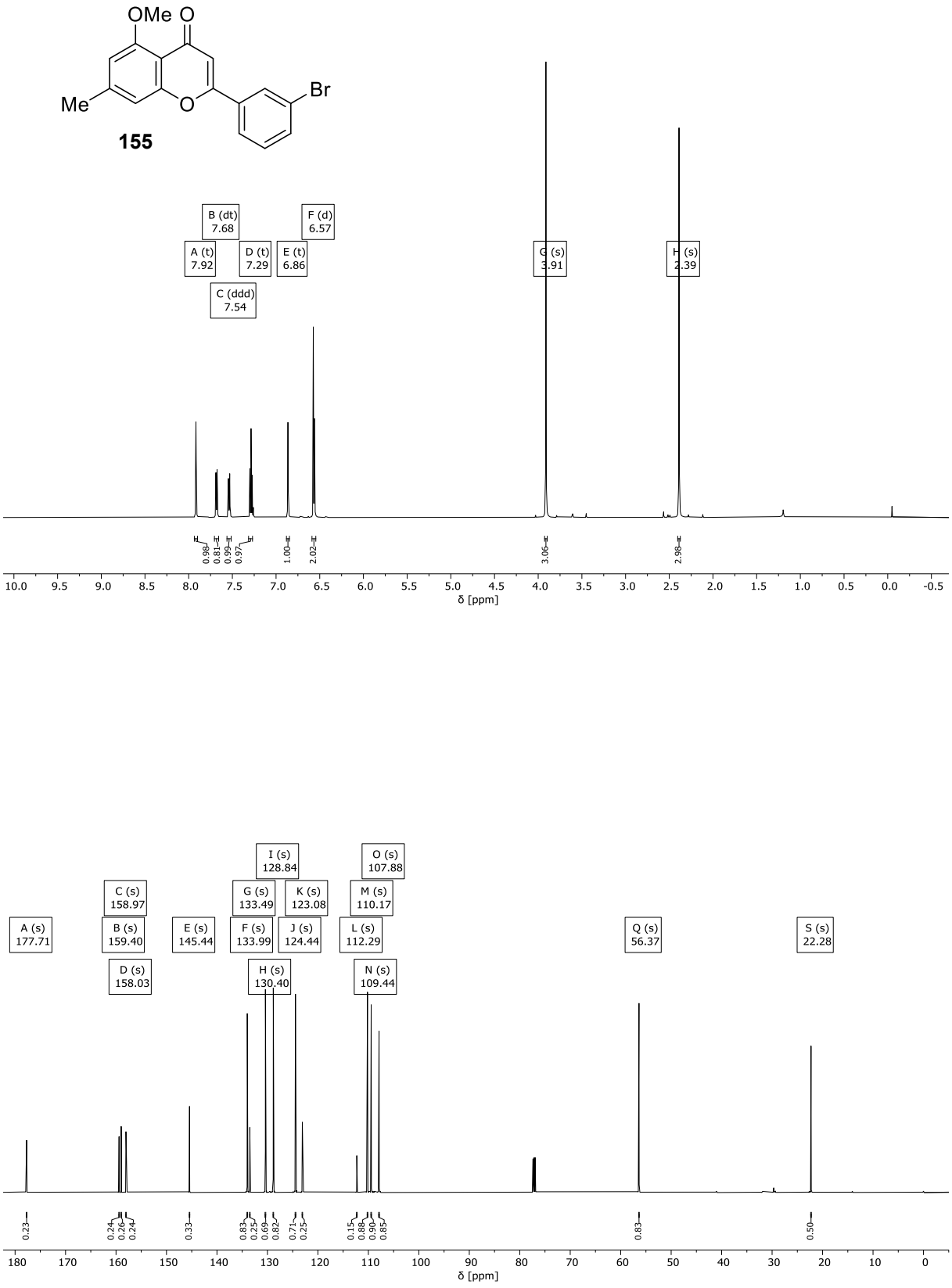

Figure 120: ^{1}H- and ^{13}C-NMR spectra (600 / 151 MHz, $CDCl_3$) of 2-(3-bromophenyl)-5-methoxy-7-methyl-4H-chromen-4-one (**155)**

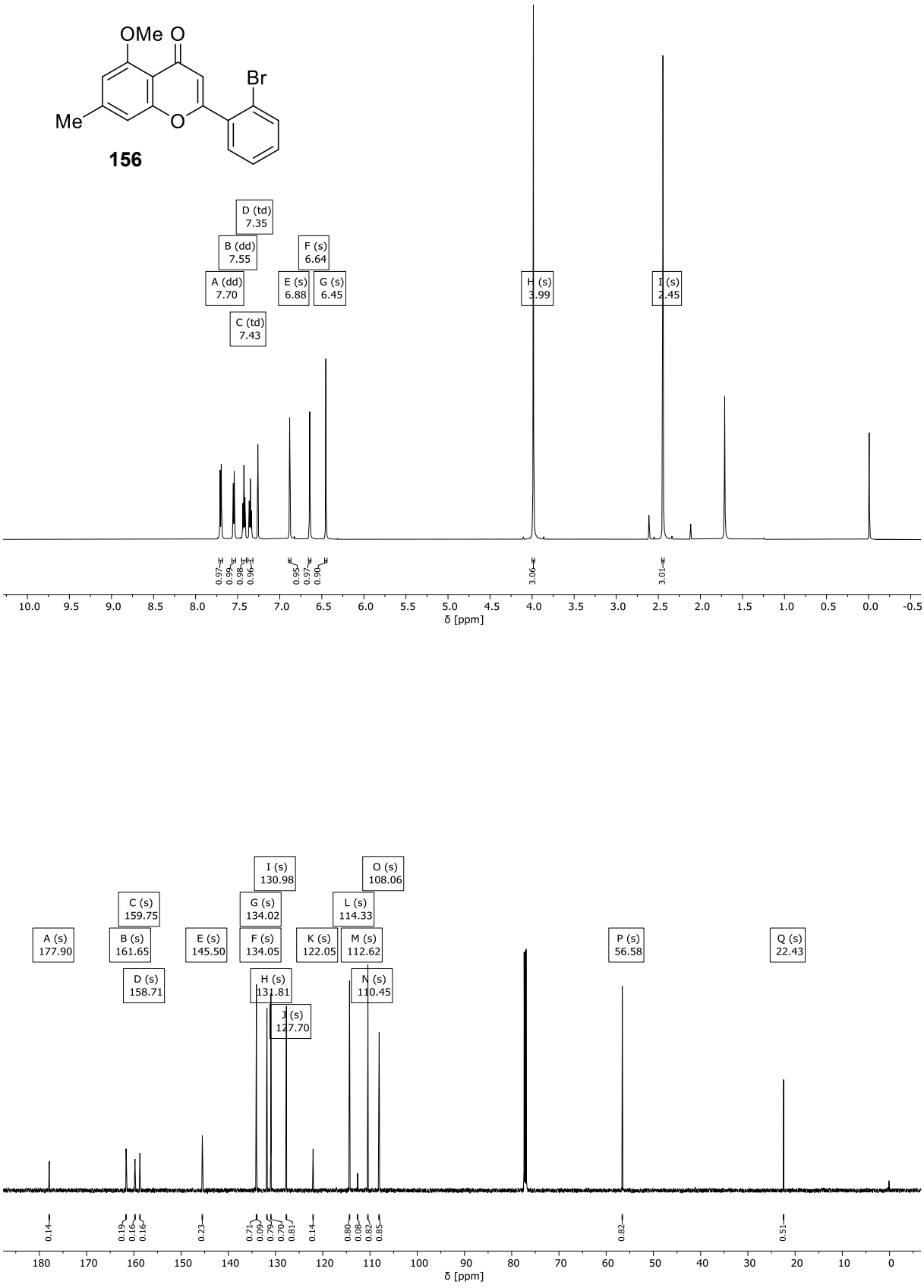

Figure 121: ^{1}H- and ^{13}C-NMR spectra (600 / 151 MHz, $CDCl_3$) of 2-(2-bromophenyl)-5-methoxy-7-methyl-4H-chromen-4-one (**156)**

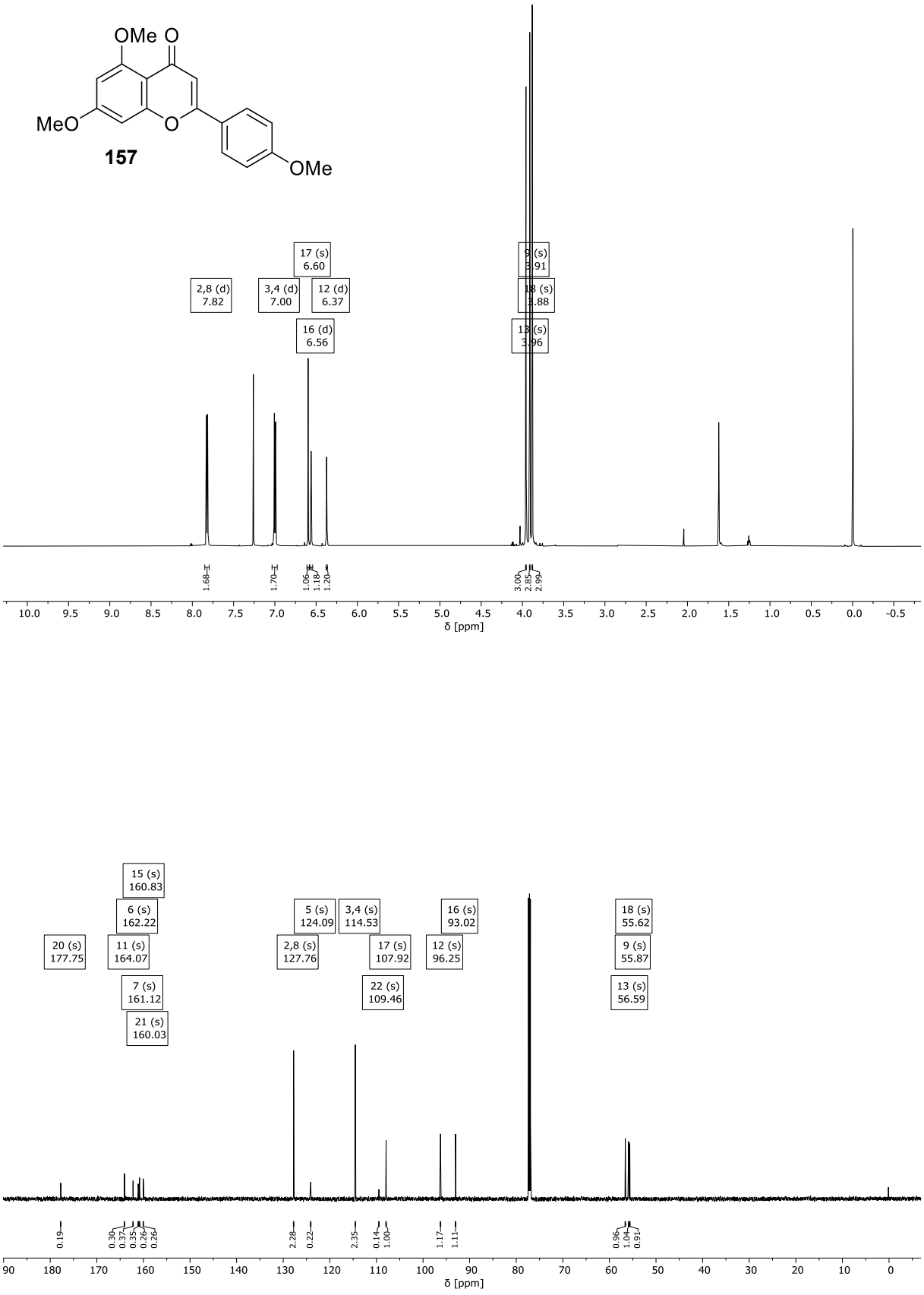

Figure 122: ^{1}H- and ^{13}C-NMR spectra (600 / 151 MHz, $CDCl_3$) of 5,7-dimethoxy-2-(4-methoxyphenyl)-4H-chromen-4-one (**157)**

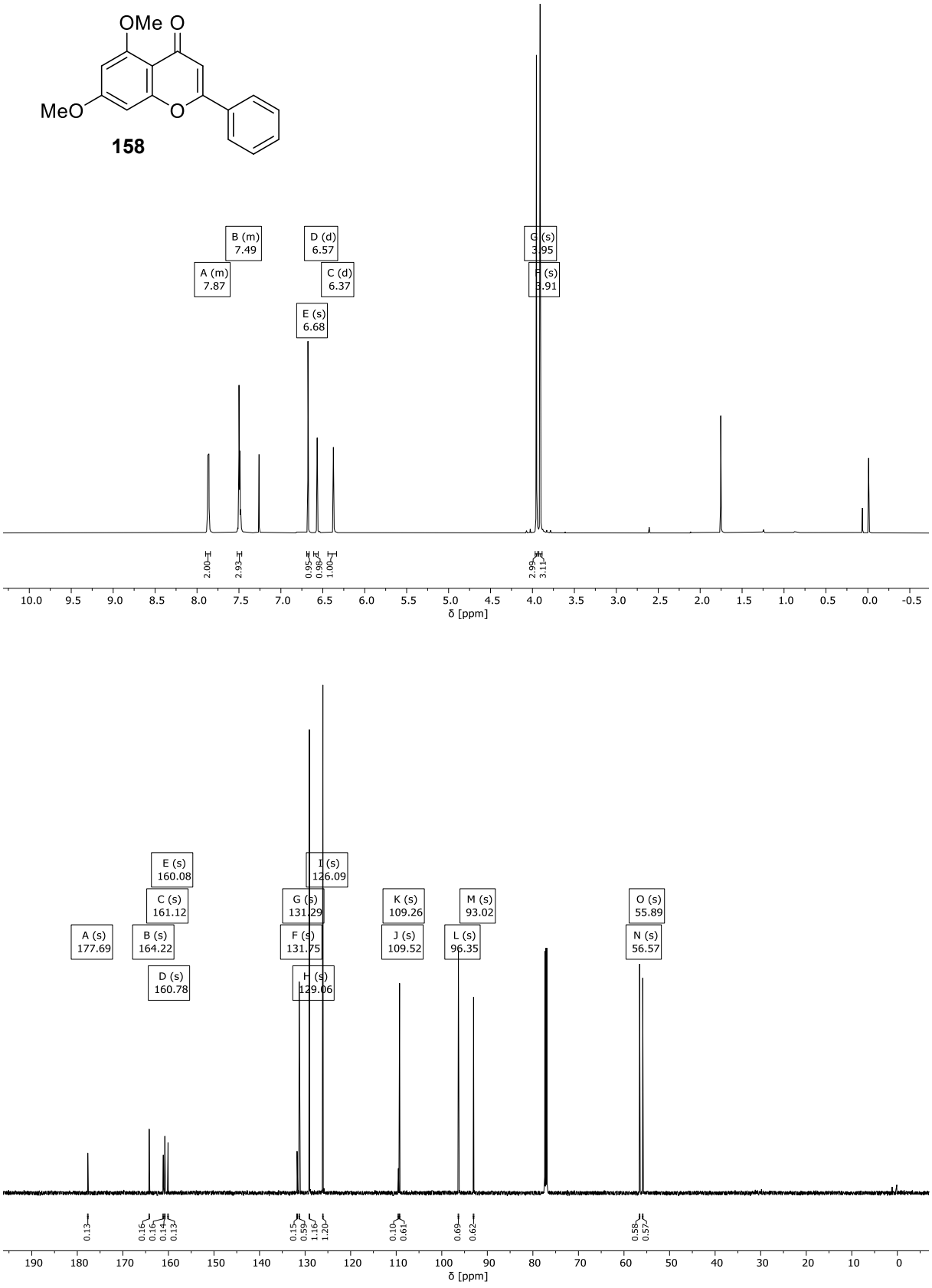

Figure 123: ^{1}H- and ^{13}C-NMR spectra (600 / 151 MHz, $CDCl_3$) of 5,7-dimethoxy-2-phenyl-4H-chromen-4-one (**158)**

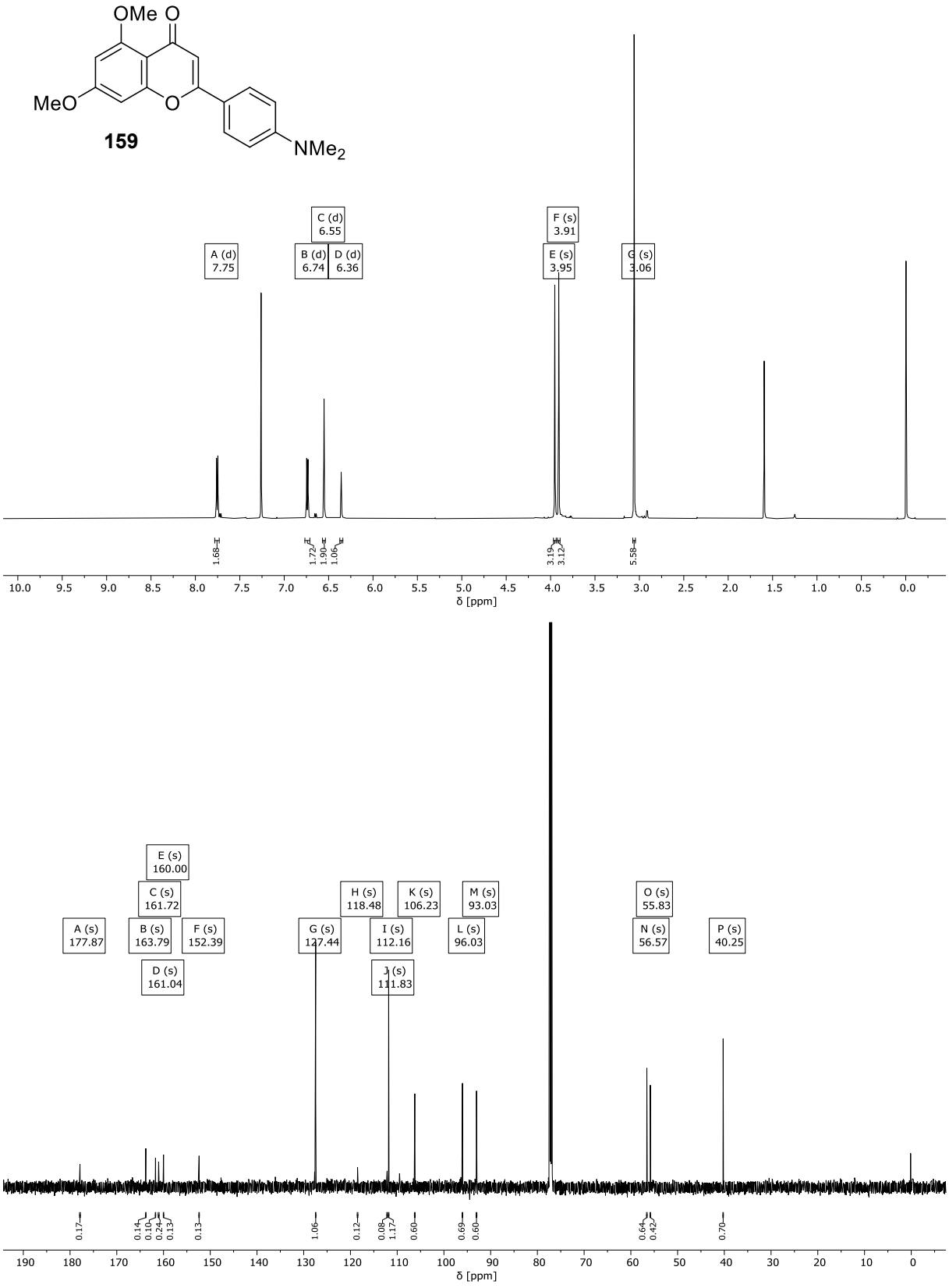

Figure 124: ^{1}H- and ^{13}C-NMR spectra (600 / 151 MHz, $CDCl_3$) of 2-(4-(dimethylamino)phenyl)-5,7-dimethoxy-4H-chromen-4-one (**159)**

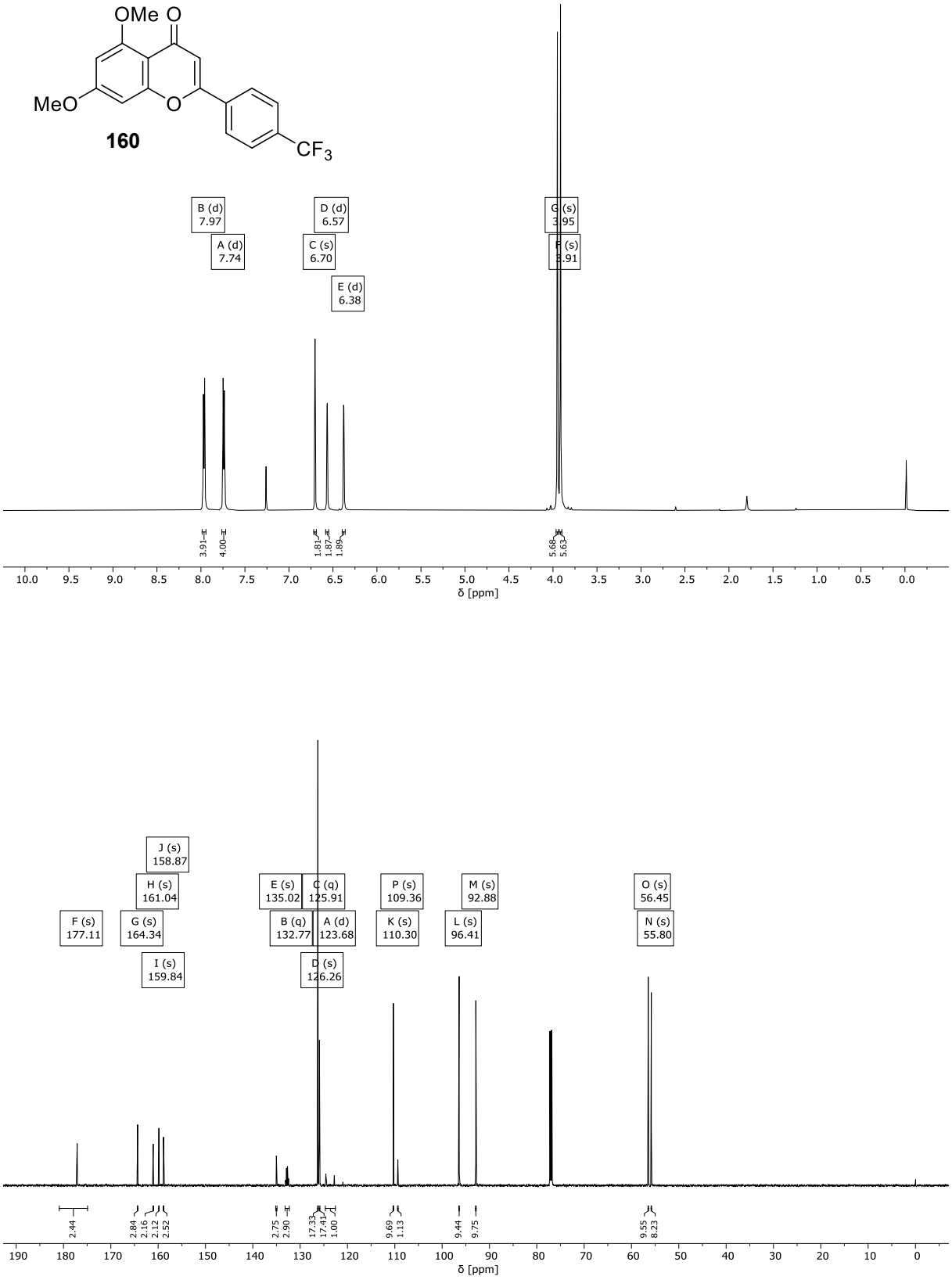

Figure 125: ^{1}H-, ^{13}C-NMR spectra (600 / 151 MHz, $CDCl_3$) of 5,7-dimethoxy-2-(4-(trifluoromethyl)phenyl)-4H-chromen-4-one (**160)**

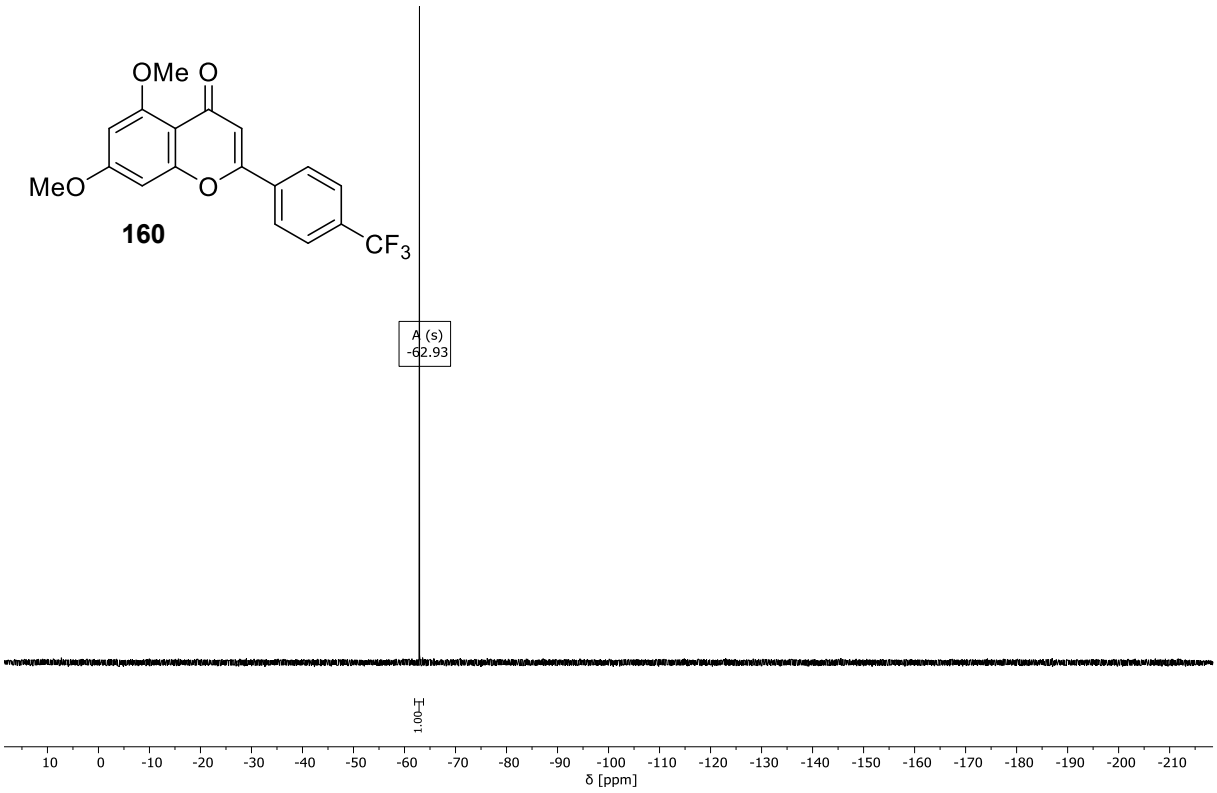

Figure 126: ^{19}F-NMR spectrum (282 MHz, $CDCl_3$) of 5,7-dimethoxy-2-(4-(trifluoromethyl)phenyl)-4H-chromen-4-one (**160)**

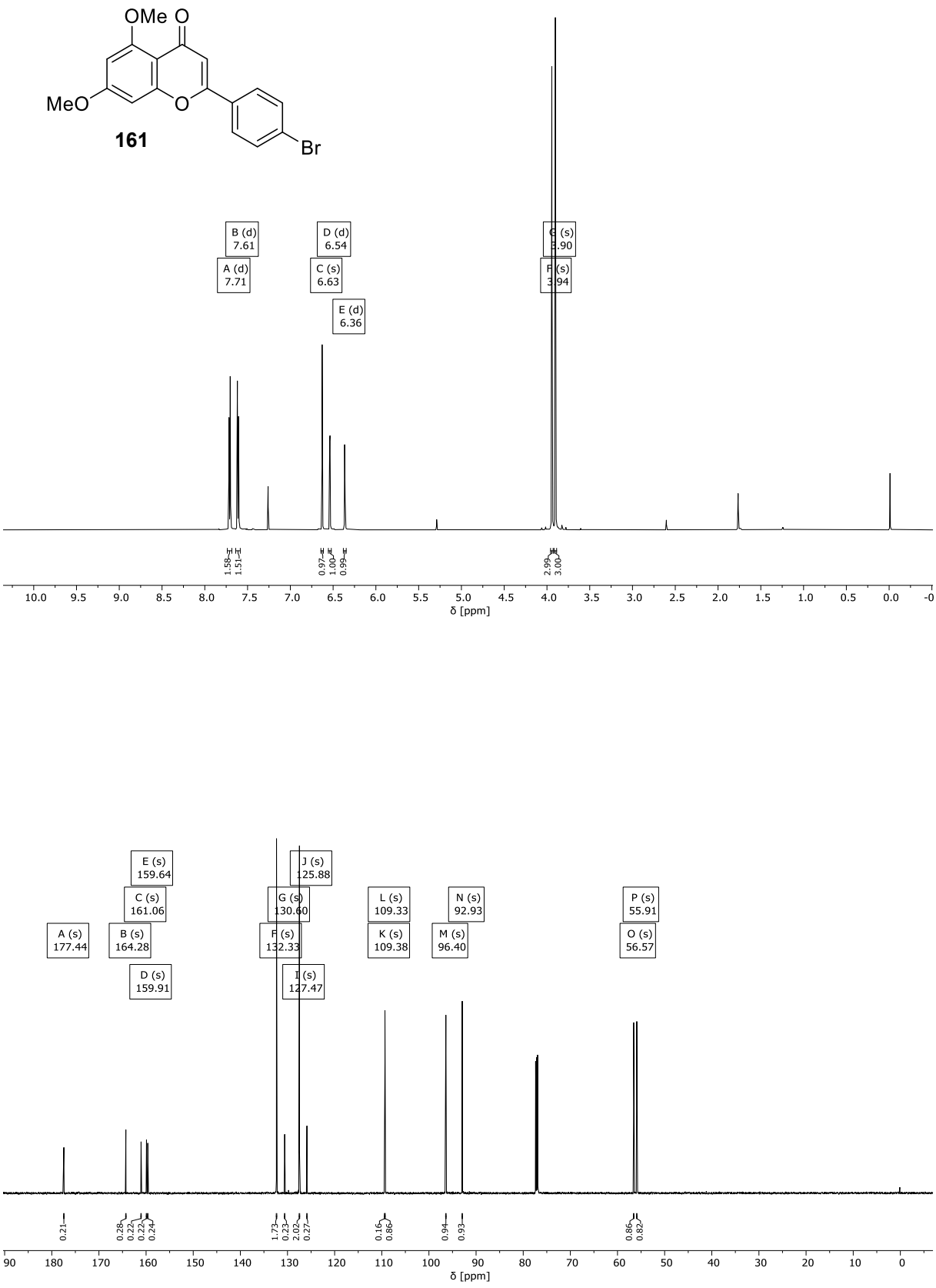

Figure 127: ^{1}H- and ^{13}C-NMR spectra (600 / 151 MHz, $CDCl_3$) of 2-(4-bromophenyl)-5,7-dimethoxy-4H-chromen-4-one (**161)**

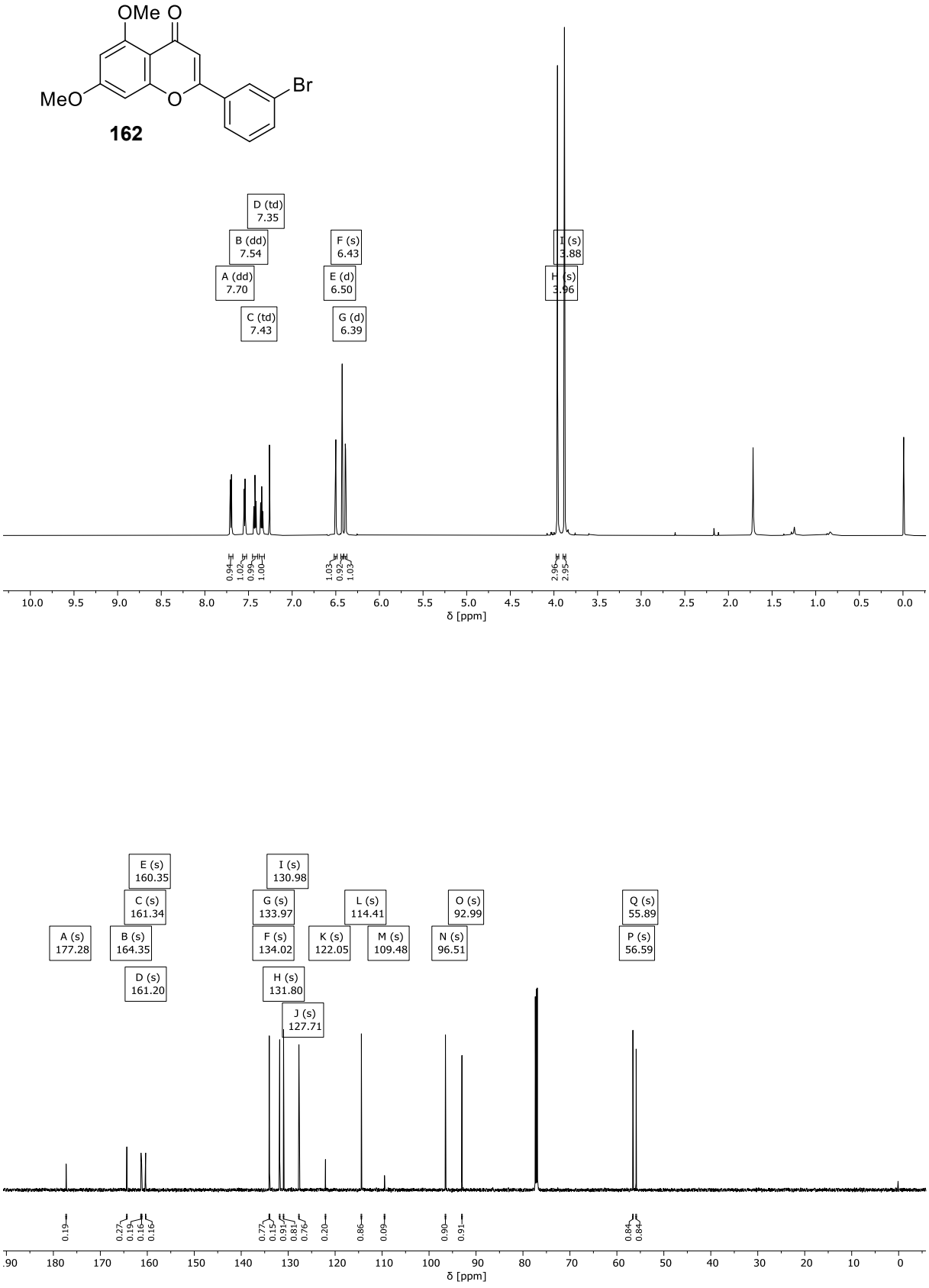

Figure 128: ^{1}H- and ^{13}C-NMR spectra (600 / 151 MHz, $CDCl_3$) of 2-(3-bromophenyl)-5,7-dimethoxy-4H-chromen-4-one (**162)**

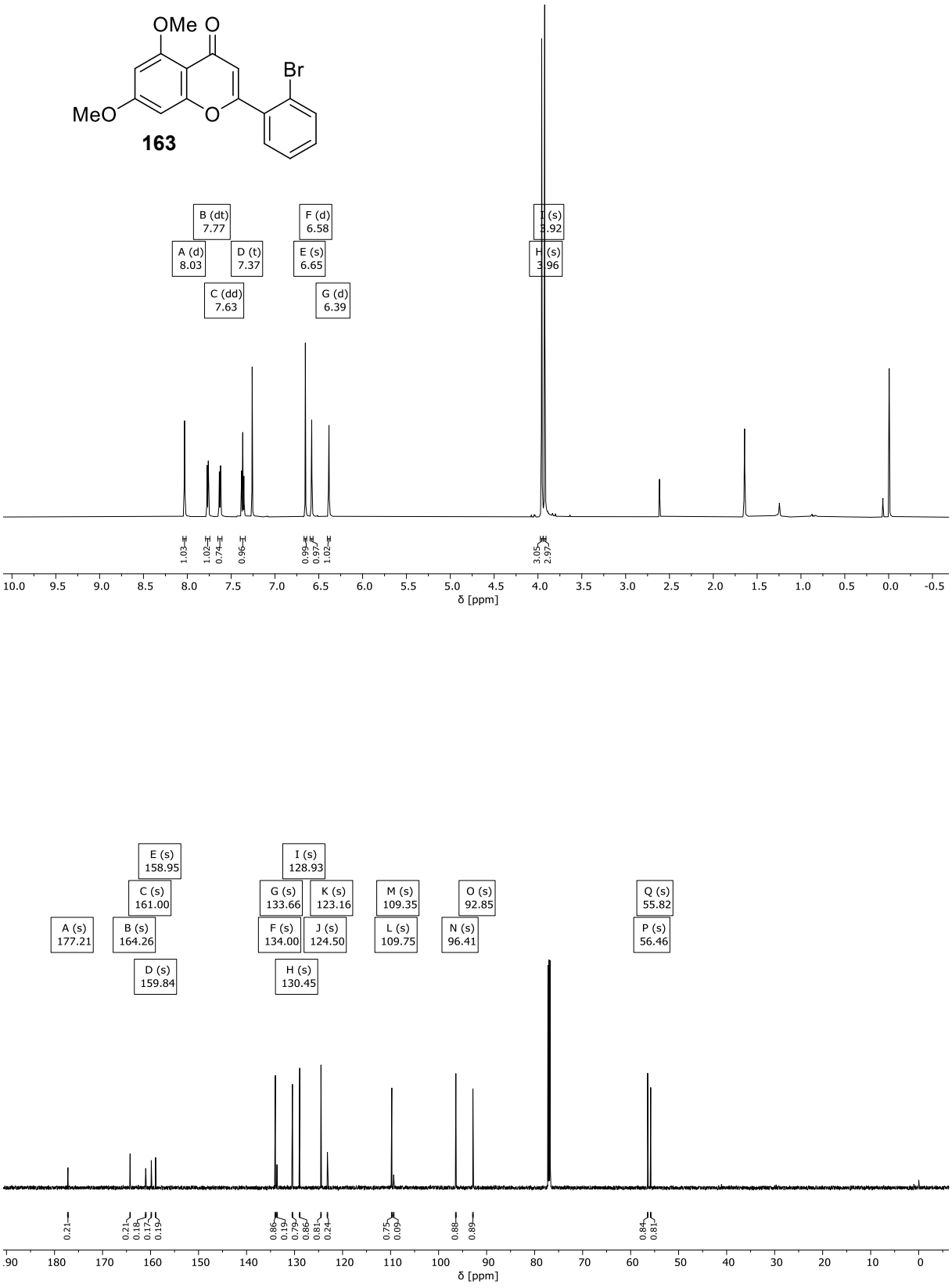

Figure 129: ^{1}H- and ^{13}C-NMR spectra (600 / 151 MHz, $CDCl_3$) of 2-(2-bromophenyl)-5,7-dimethoxy-4H-chromen-4-one (**163)**

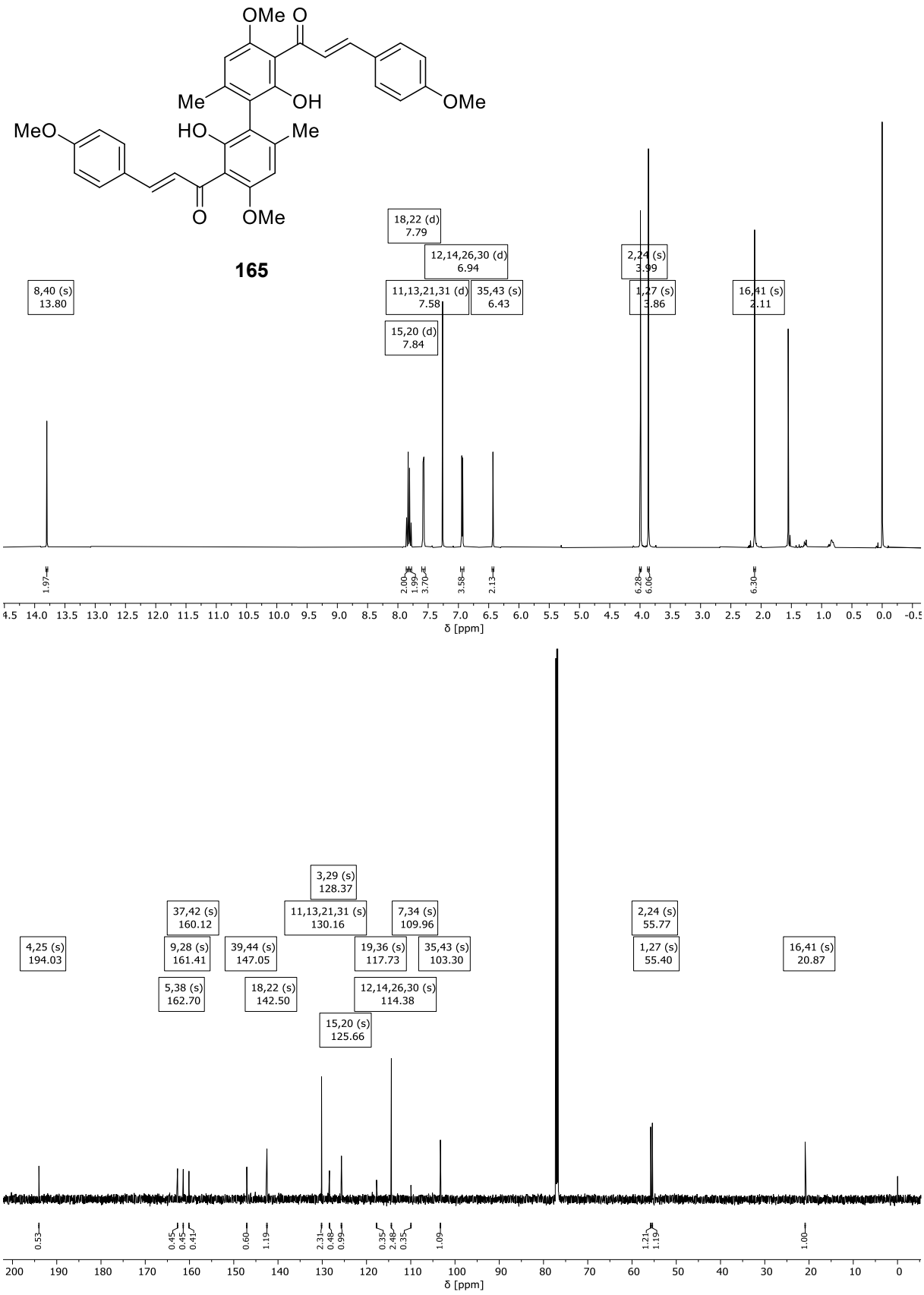

Figure 130: ^{1}H- and ^{13}C-NMR spectra (600 / 151 MHz, $CDCl_3$) of rac-(2*E*,2'*E*)-1,1'-(2,2'-dihydroxy-4,4'-dimethoxy-6,6'-dimethyl-[1,1'-biphenyl]-3,3'-diyl)bis(3-(4-methoxyphenyl)prop-2-en-1-one) (**165)**

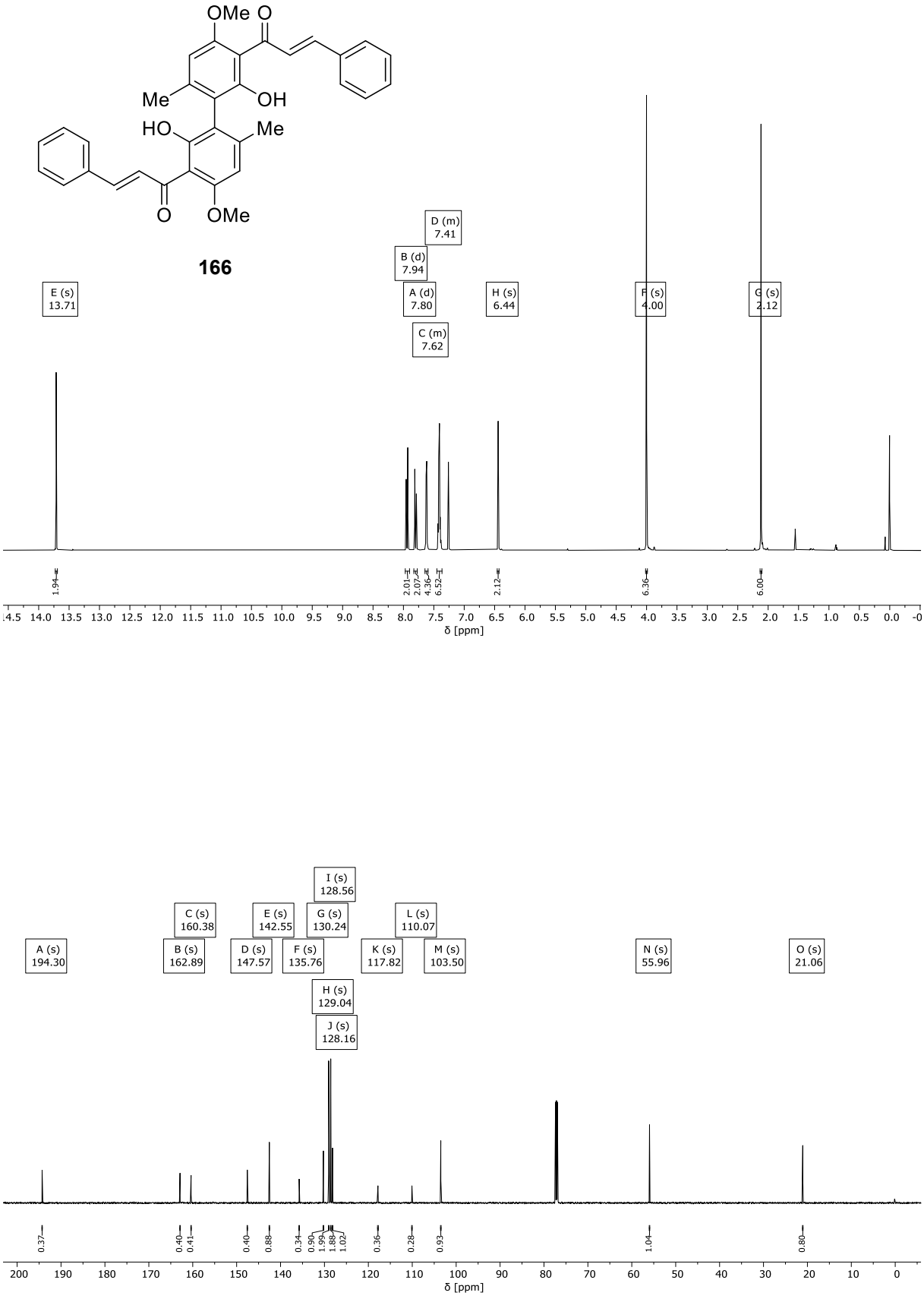

Figure 131: ^{1}H- and ^{13}C-NMR spectra (600 / 151 MHz, $CDCl_3$) of rac-(2E,2'E)-1,1'-(2,2'-dihydroxy-4,4'-dimethoxy-6,6'-dimethyl-[1,1'-biphenyl]-3,3'-diyl)bis(3-phenylprop-2-en-1-one) (**166)**

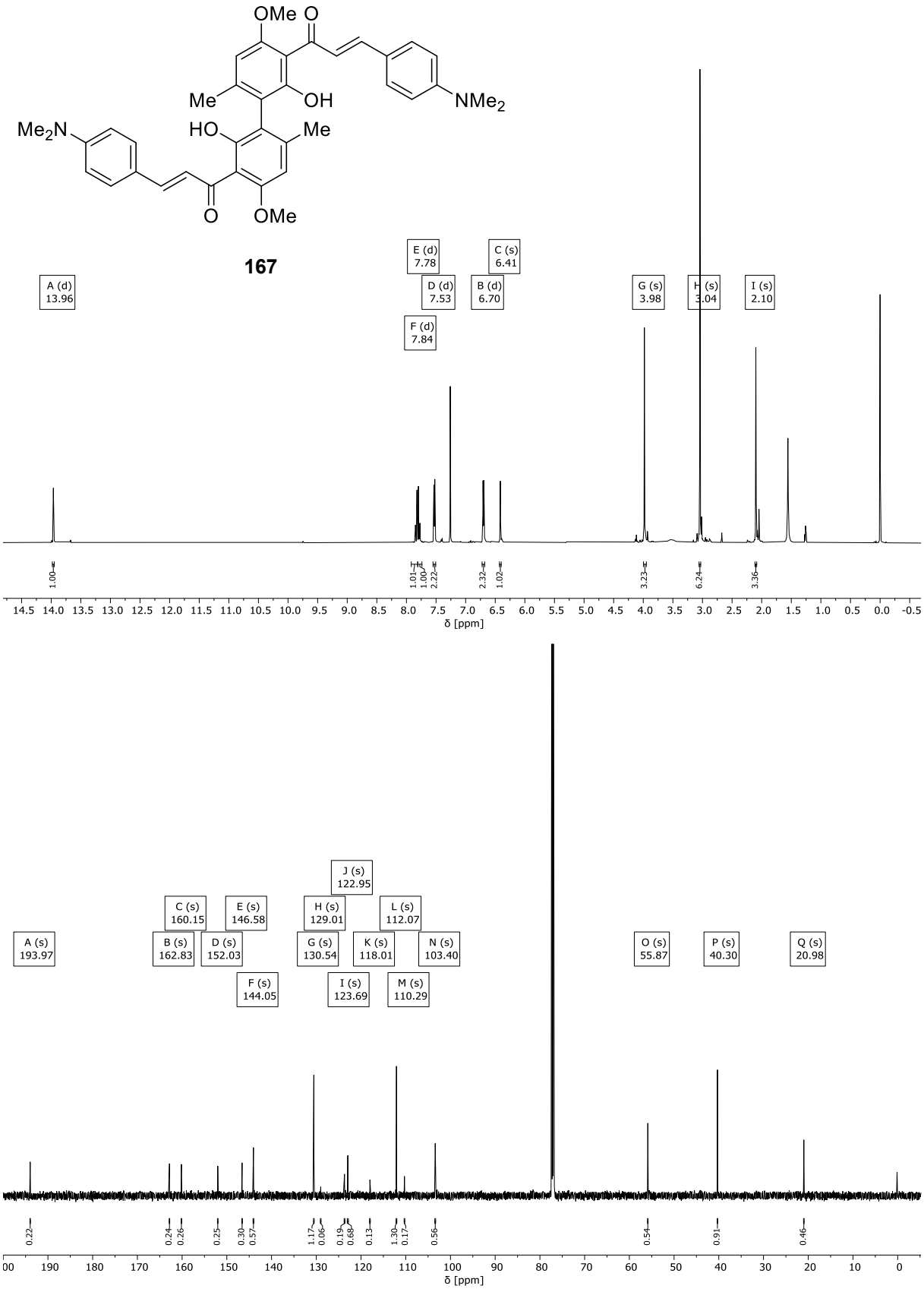

Figure 132: ^{1}H- and ^{13}C-NMR spectra (600 / 151 MHz, $CDCl_3$) of rac-(2E,2'E)-1,1'-(2,2'-dihydroxy-4,4'-dimethoxy-6,6'-dimethyl-[1,1'-biphenyl]-3,3'-diyl)bis(3-(4-(dimethylamino)phenyl)prop-2-en-1-one) (**167)**

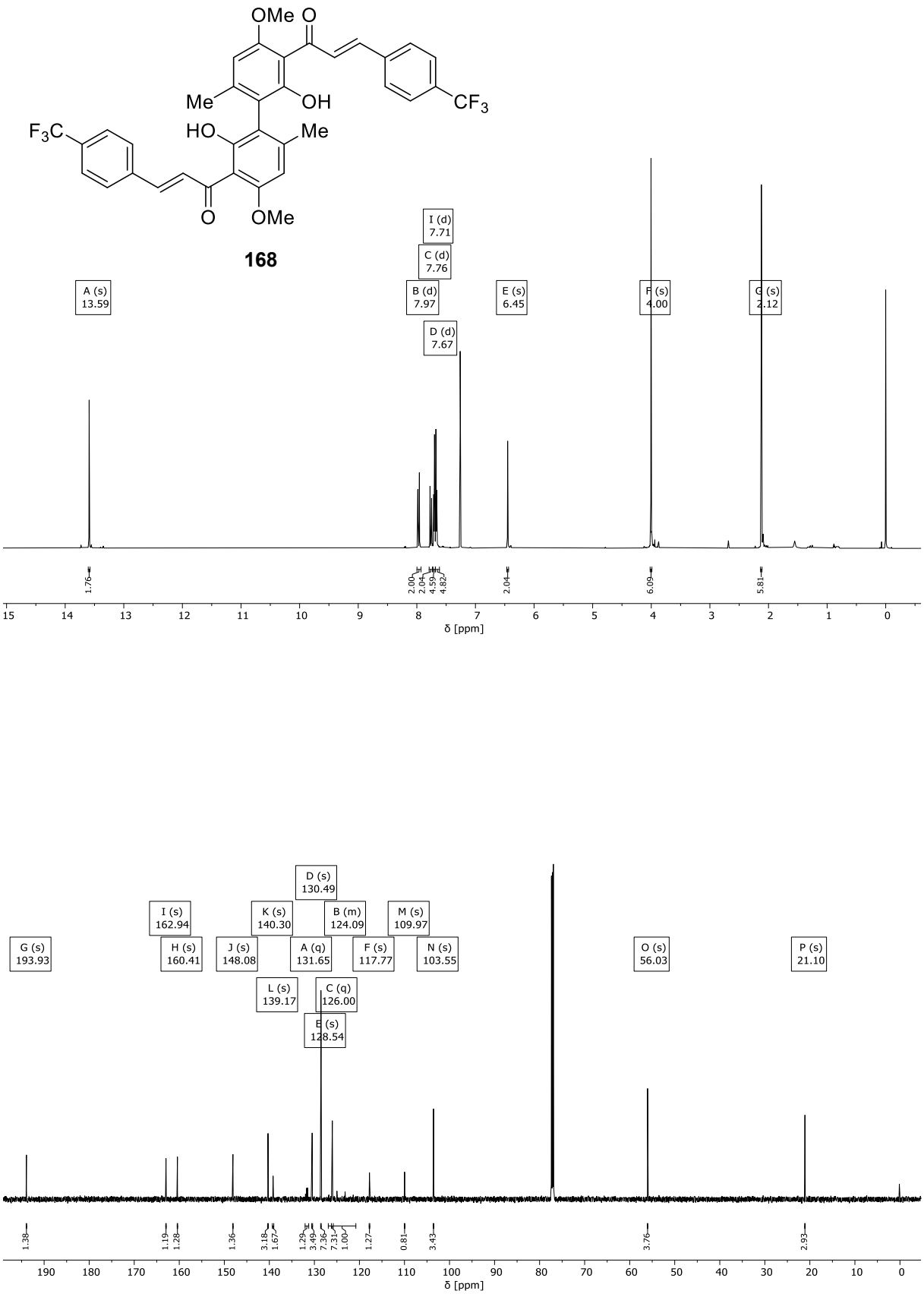

Figure 133: ^{1}H-, ^{13}C-spectra (600 / 151 MHz, $CDCl_3$) of rac-(2*E*,2'*E*)-1,1'-(2,2'-dihydroxy-4,4'-dimethoxy-6,6'-dimethyl-[1,1'-biphenyl]-3,3'-diyl)bis(3-(4-(trifluoromethyl)phenyl)prop-2-en-1-one) (**168)**

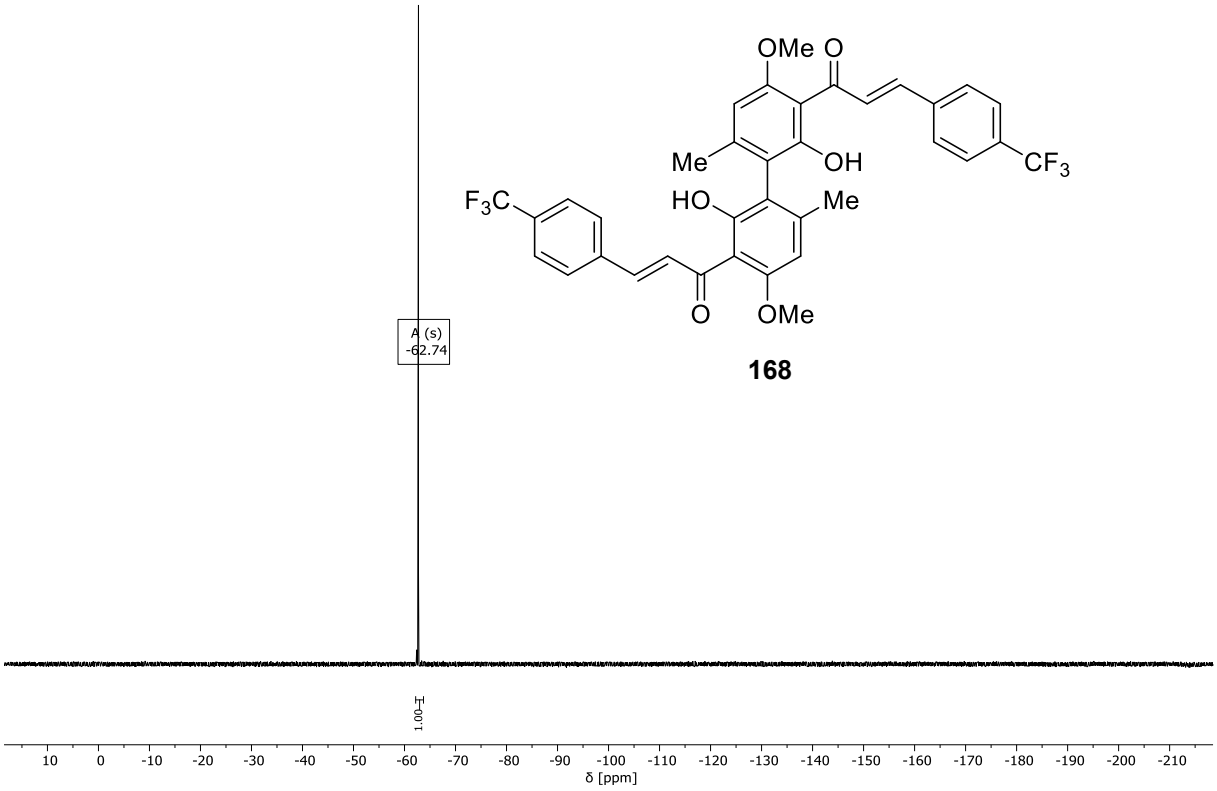

168

Figure 134: ^{19}F-NMR spectra (282 MHz, $CDCl_3$) of rac-(2*E*,2'*E*)-1,1'-(2,2'-dihydroxy-4,4'-dimethoxy-6,6'-dimethyl-[1,1'-biphenyl]-3,3'-diyl)bis(3-(4-(trifluoromethyl)phenyl)prop-2-en-1-one) (**168)**

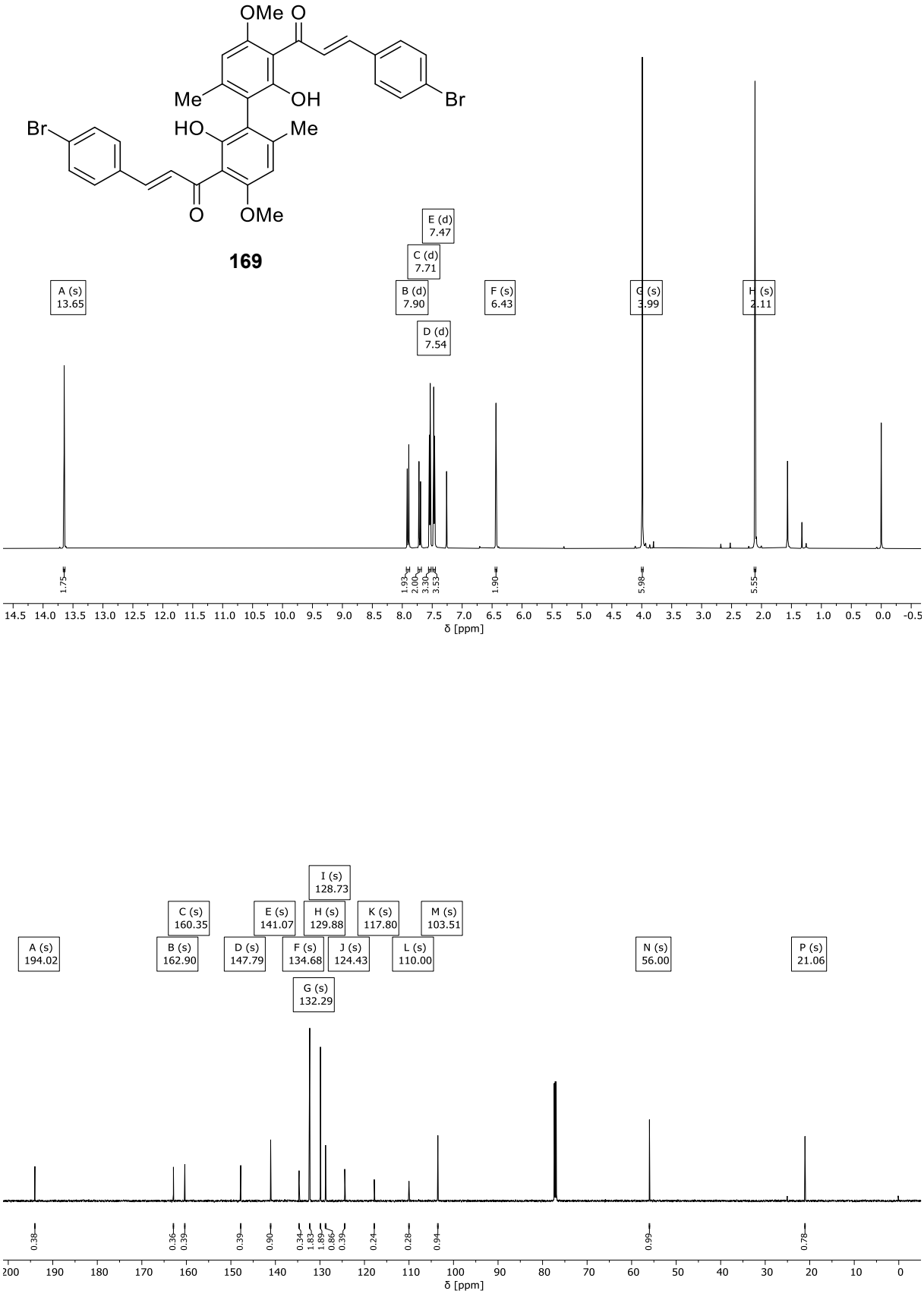

Figure 135: ^{1}H- and ^{13}C-NMR spectra (600 / 151 MHz, $CDCl_3$) of rac-(2*E*,2'*E*)-1,1'-(2,2'-dihydroxy-4,4'-dimethoxy-6,6'-dimethyl-[1,1'-biphenyl]-3,3'-diyl)bis(3-(4-bromophenyl)prop-2-en-1-one) (**169)**

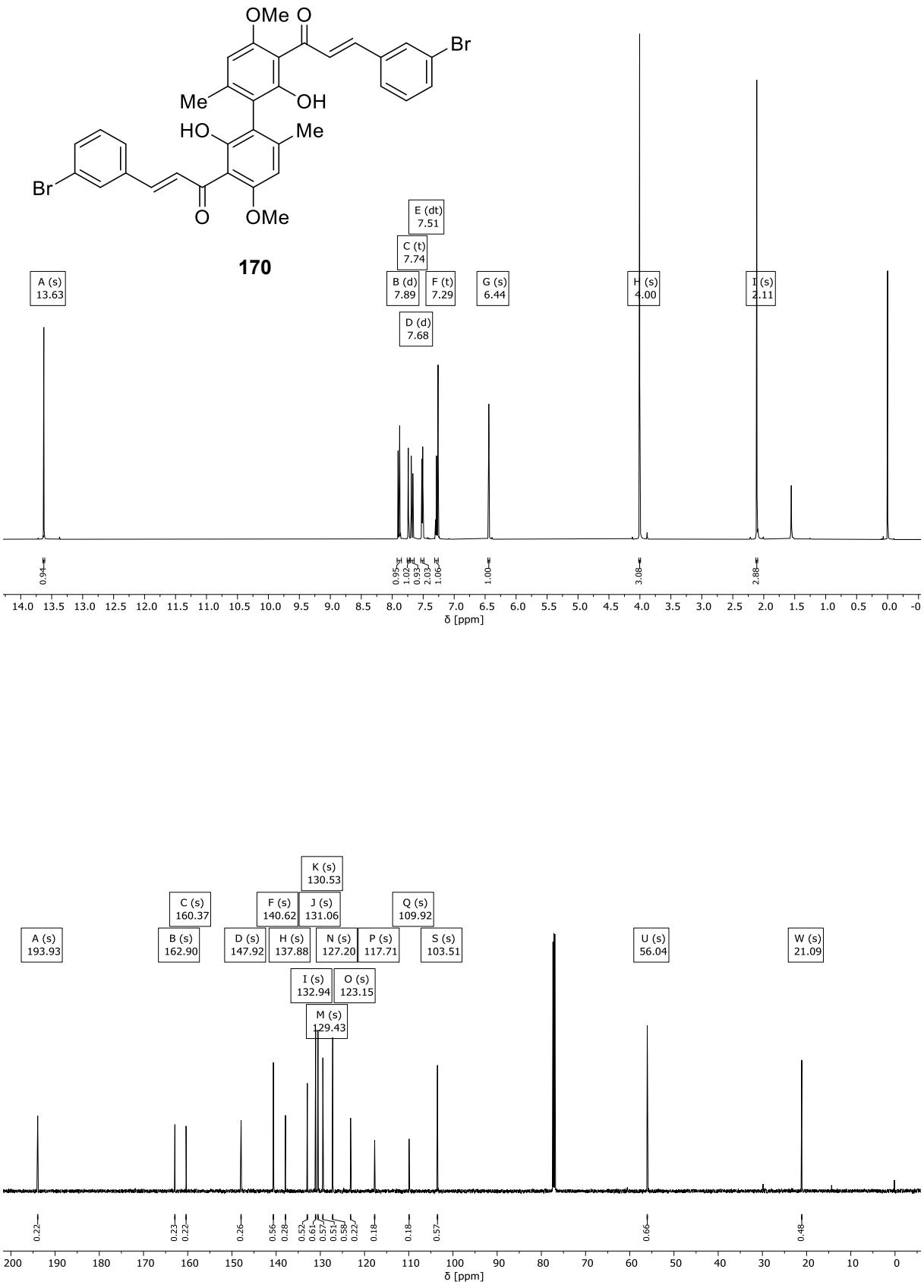

Figure 136: ^{1}H- and ^{13}C-NMR spectra (600 / 151 MHz, $CDCl_3$) of rac-(2*E*,2'*E*)-1,1'-(2,2'-dihydroxy-4,4'-dimethoxy-6,6'-dimethyl-[1,1'-biphenyl]-3,3'-diyl)bis(3-(3-bromophenyl)prop-2-en-1-one) (**170)**

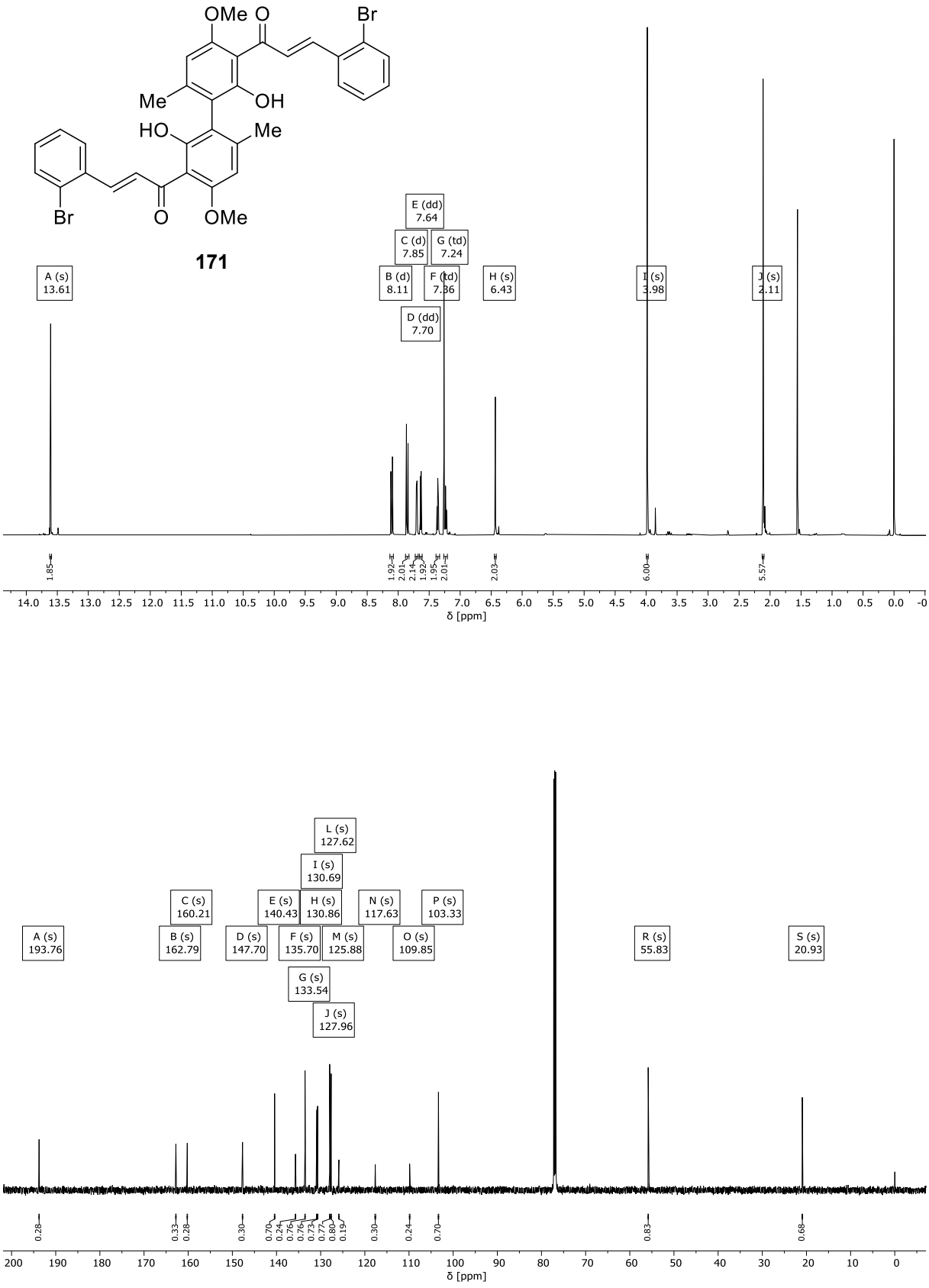

Figure 137: ^{1}H- and ^{13}C-NMR spectra (600 / 151 MHz, $CDCl_3$) of rac-(2*E*,2'*E*)-1,1'-(2,2'-dihydroxy-4,4'-dimethoxy-6,6'-dimethyl-[1,1'-biphenyl]-3,3'-diyl)bis(3-(2-bromophenyl)prop-2-en-1-one) (**171**)

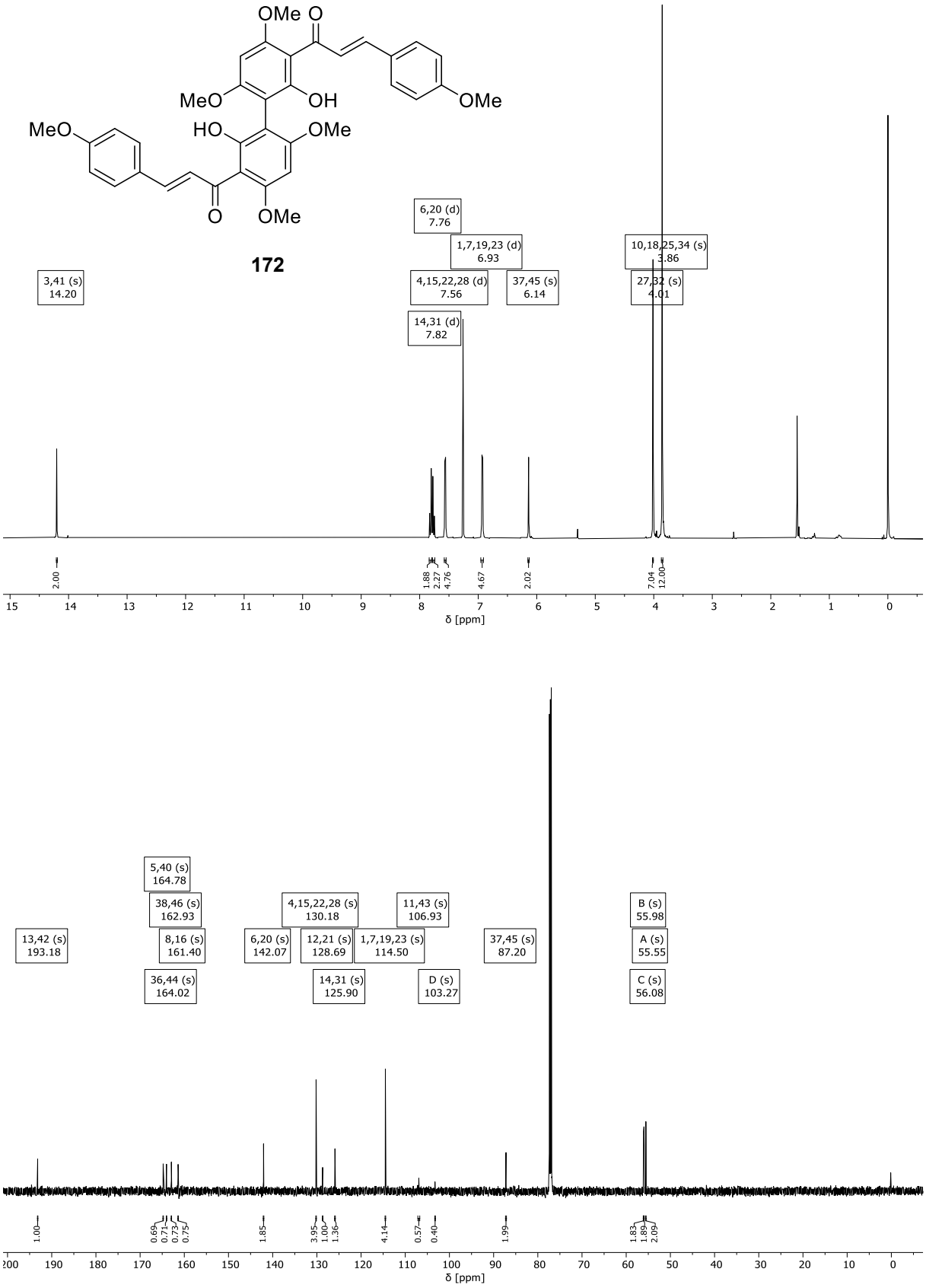

Figure 138: ^{1}H- and ^{13}C-NMR spectra (600 / 151 MHz, $CDCl_3$) of rac-(2*E*,2'*E*)-1,1'-(2,2'-dihydroxy-4,4',6,6'-tetramethoxy-[1,1'-biphenyl]-3,3'-diyl)bis(3-(4-methoxyphenyl)prop-2-en-1-one) (**172)**

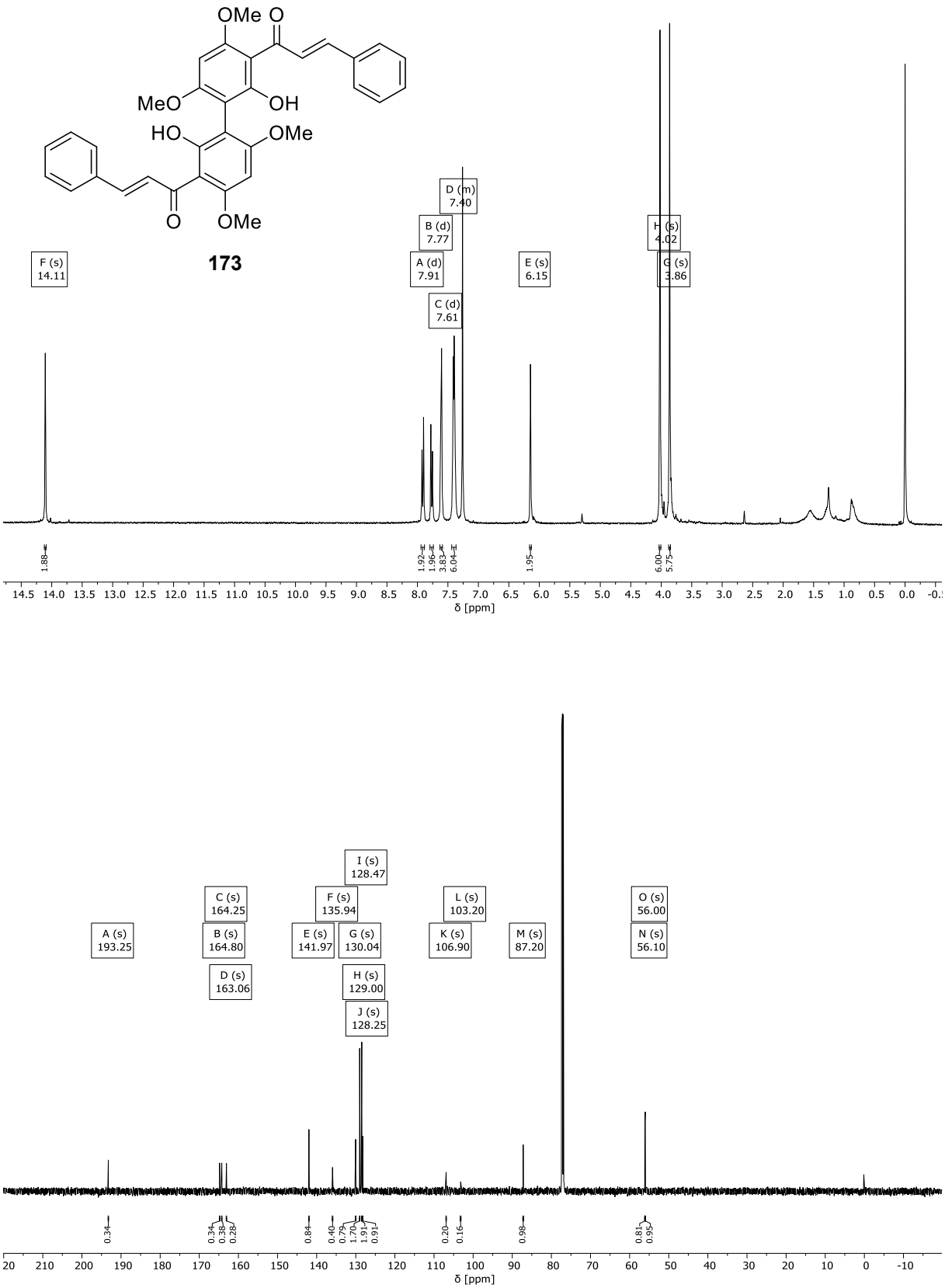

Figure 139: ^{1}H- and ^{13}C-NMR spectra (600 / 151 MHz, $CDCl_3$) of rac-(2*E*,2'*E*)-1,1'-(2,2'-dihydroxy-4,4',6,6'-tetramethoxy-[1,1'-biphenyl]-3,3'-diyl)bis(3-phenylprop-2-en-1-one) (**173)**

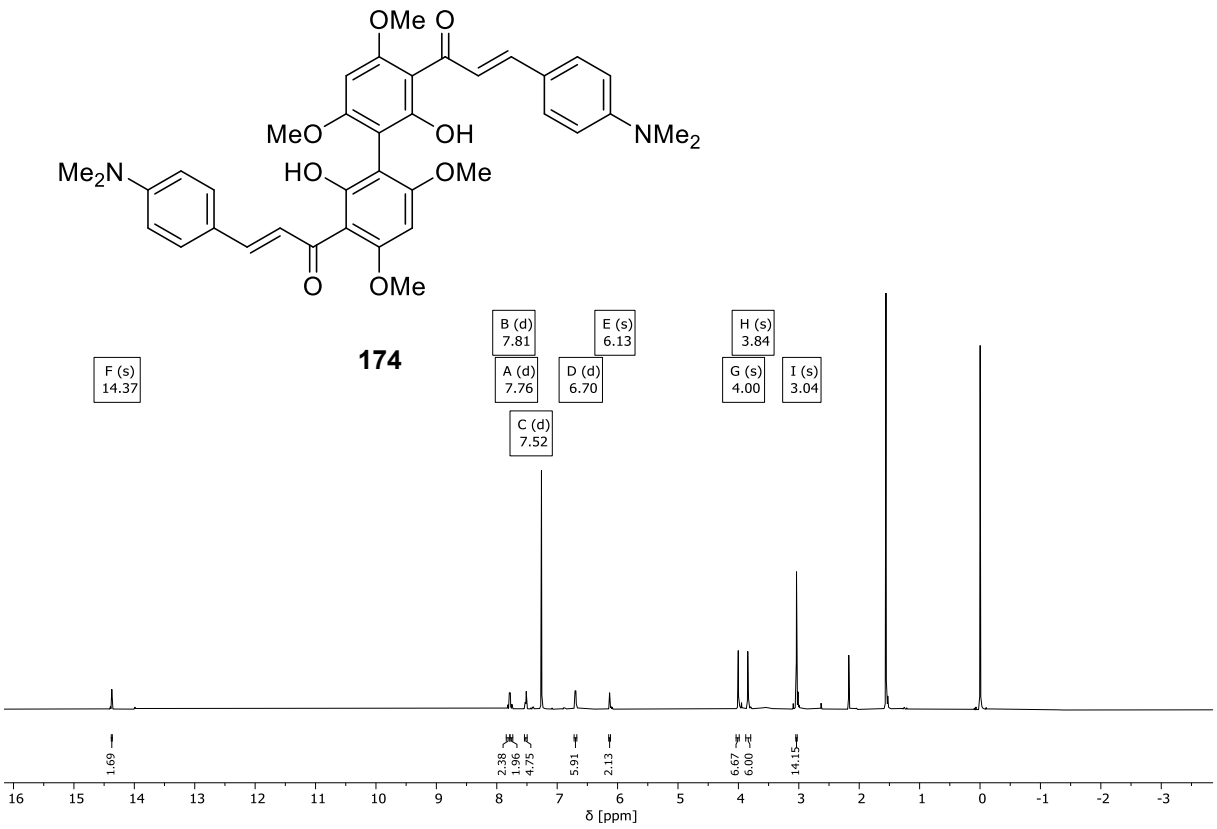

Figure 140: ^{1}H- spectrum (600 MHz, $CDCl_3$) of rac-(2*E*,2'*E*)-1,1'-(2,2'-dihydroxy-4,4',6,6'-tetramethoxy-[1,1'-biphenyl]-3,3'-diyl)bis(3-(4-(dimethylamino)phenyl)prop-2-en-1-one) (**174)**

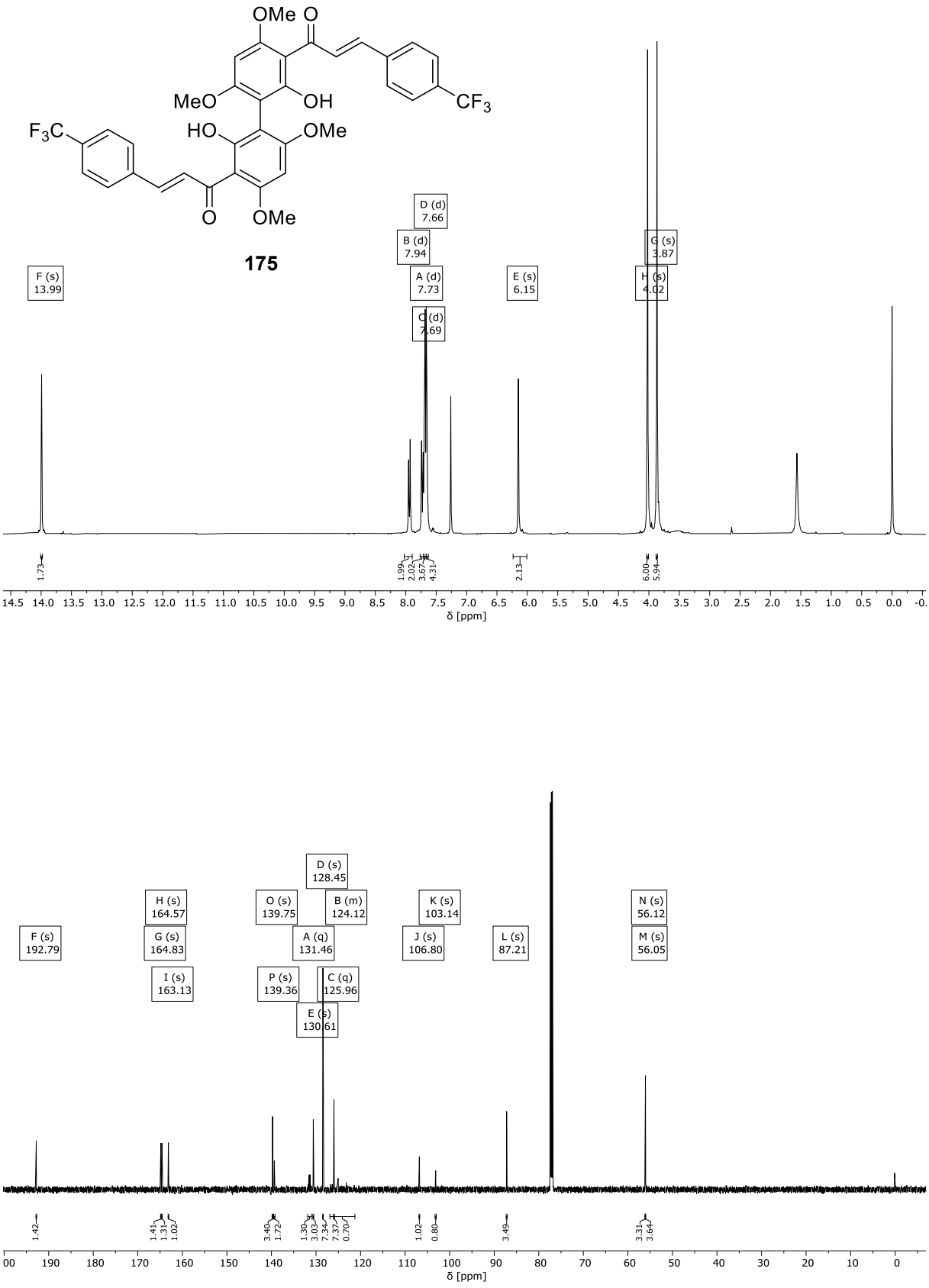

Figure 141: ^{1}H-, ^{13}C-NMR spectra (600 / 151 MHz, $CDCl_3$) of rac-(2*E*,2'*E*)-1,1'-(2,2'-dihydroxy-4,4',6,6'-tetramethoxy-[1,1'-biphenyl]-3,3'-diyl)bis(3-(4-(trifluoromethyl)phenyl)prop-2-en-1-one) (**175)**

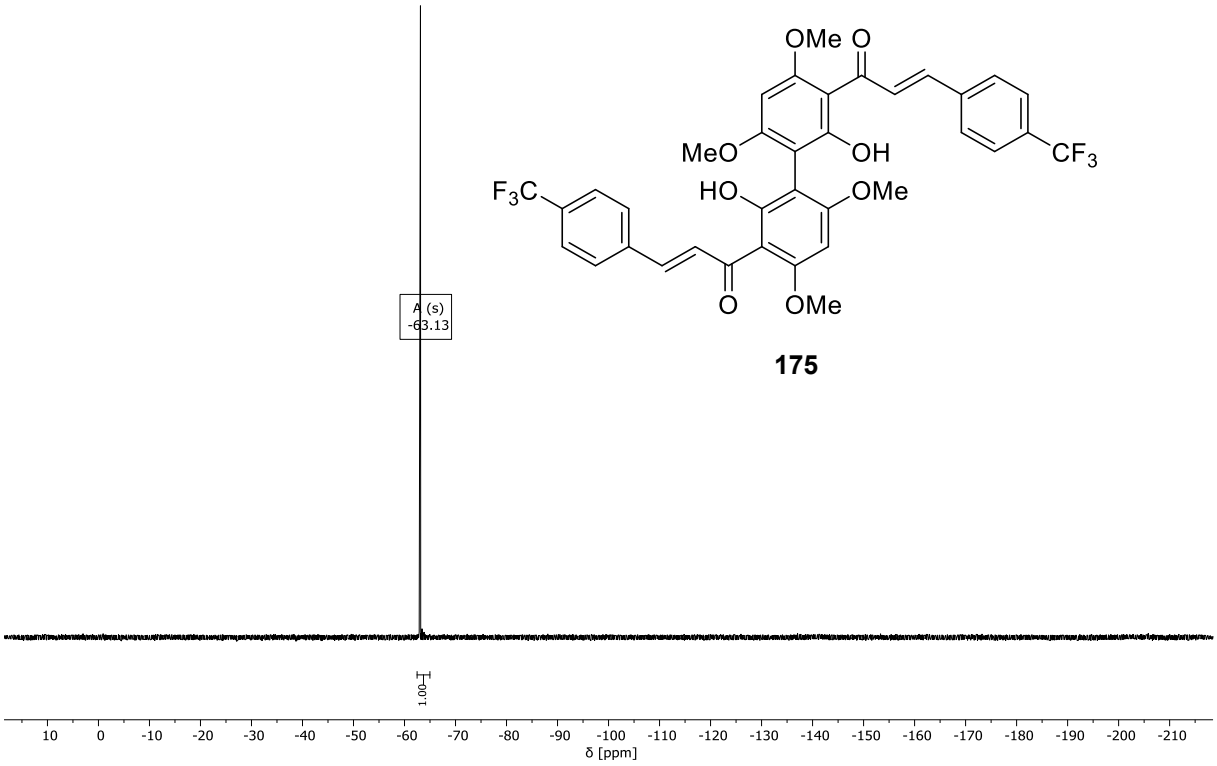

Figure 142: ^{19}F-NMR spectrum (282 MHz, $CDCl_3$) of rac-(2*E*,2'*E*)-1,1'-(2,2'-dihydroxy-4,4',6,6'-tetramethoxy-[1,1'-biphenyl]-3,3'-diyl)bis(3-(4-(trifluoromethyl)phenyl)prop-2-en-1-one) (**175)**

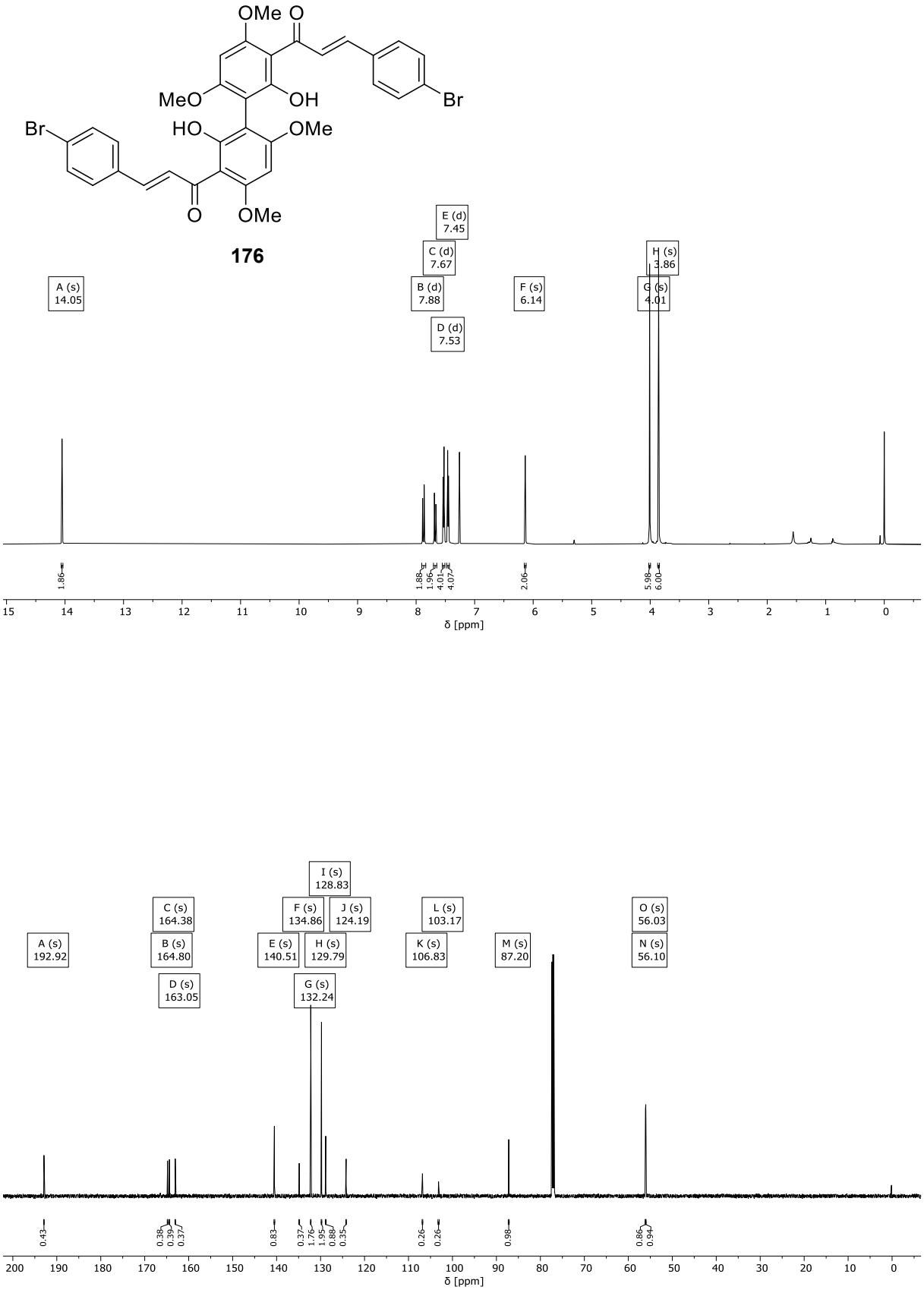

Figure 143: ^{1}H- and ^{13}C-NMR spectra (600 / 151 MHz, $CDCl_3$) of rac-(2*E*,2'*E*)-1,1'-(2,2'-dihydroxy-4,4',6,6'-tetramethoxy-[1,1'-biphenyl]-3,3'-diyl)bis(3-(4-bromophenyl)prop-2-en-1-one) (**176)**

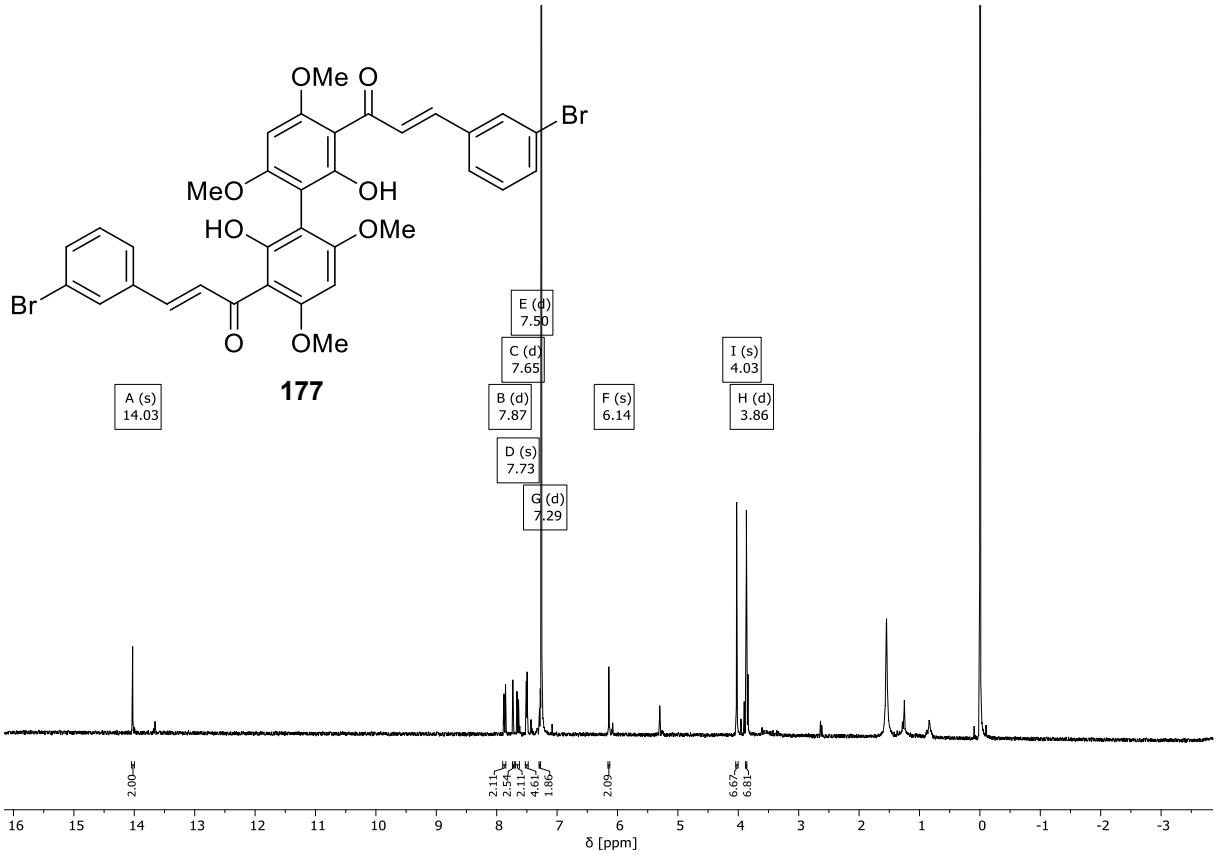

Figure 144: [1]H-NMR spectrum (600 MHz, CDCl3) of rac-(2*E*,2'*E*)-1,1'-(2,2'-dihydroxy-4,4',6,6'-tetramethoxy-[1,1'-biphenyl]-3,3'-diyl)bis(3-(3-bromophenyl)prop-2-en-1-one) (**177**)

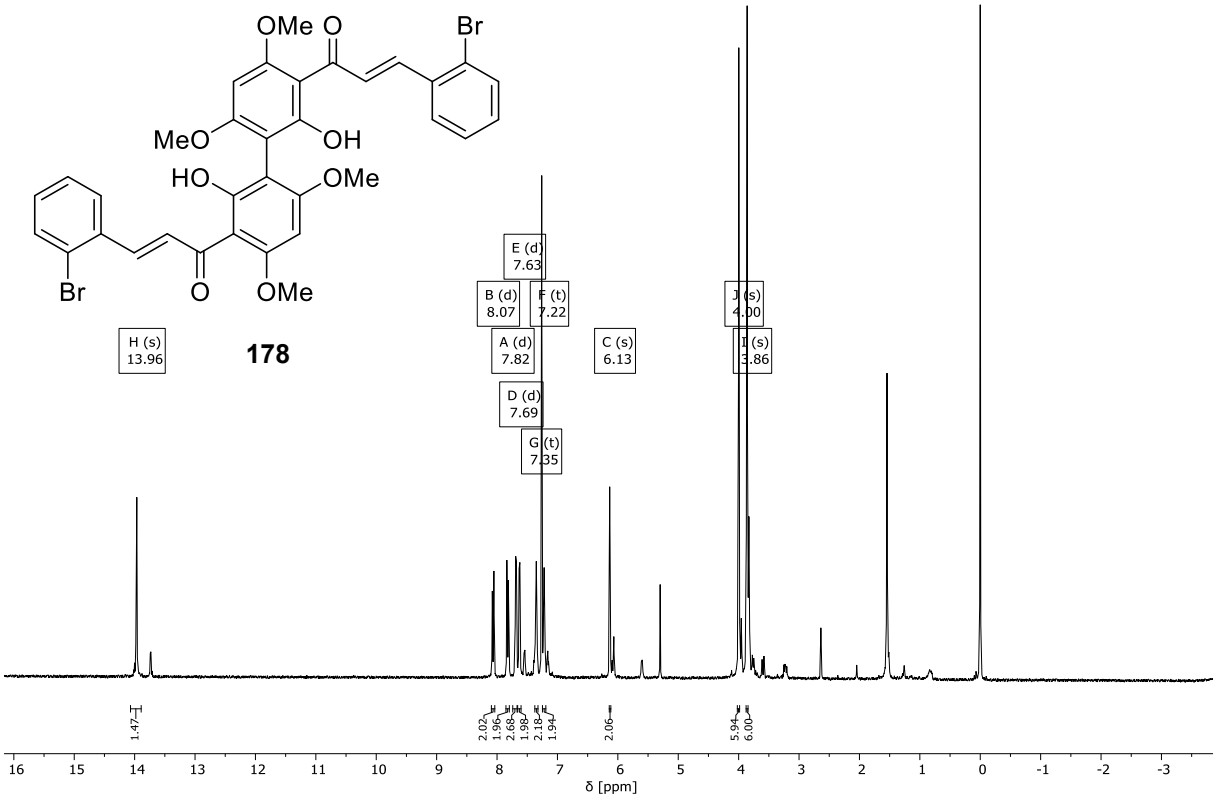

Figure 145: [1]H-spectrum (600 MHz, $CDCl_3$) of rac-(2*E*,2'*E*)-1,1'-(2,2'-dihydroxy-4,4',6,6'-tetramethoxy-[1,1'-biphenyl]-3,3'-diyl)bis(3-(2-bromophenyl)prop-2-en-1-one) (**178)**

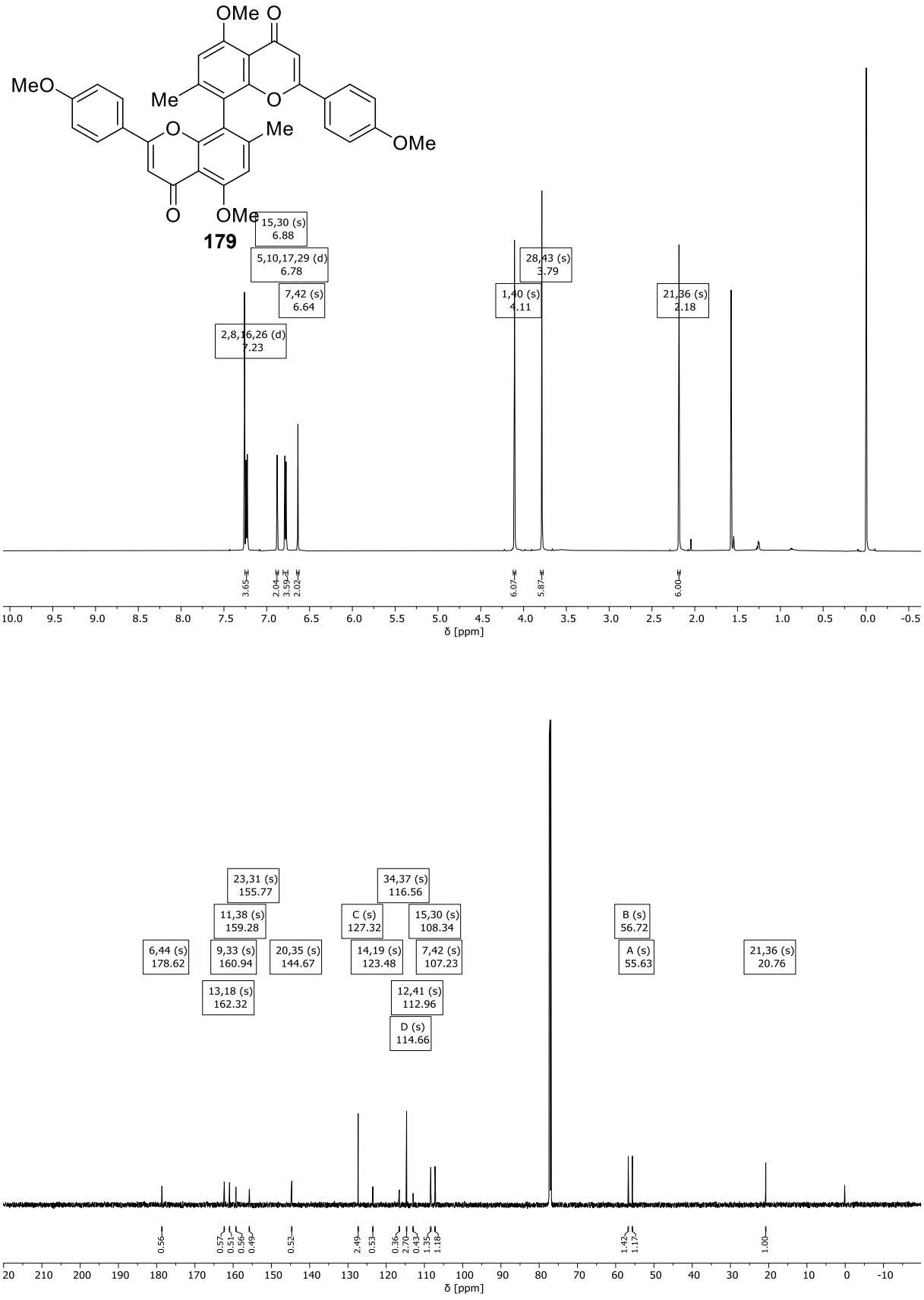

Figure 146: ^{1}H- and ^{13}C-NMR spectra (600 / 151 MHz, $CDCl_3$) of *rac*-5,5'-dimethoxy-2,2'-bis(4-methoxyphenyl)-7,7'-dimethyl-4H,4'H-[8,8'-bichromene]-4,4'-dione (**179**)

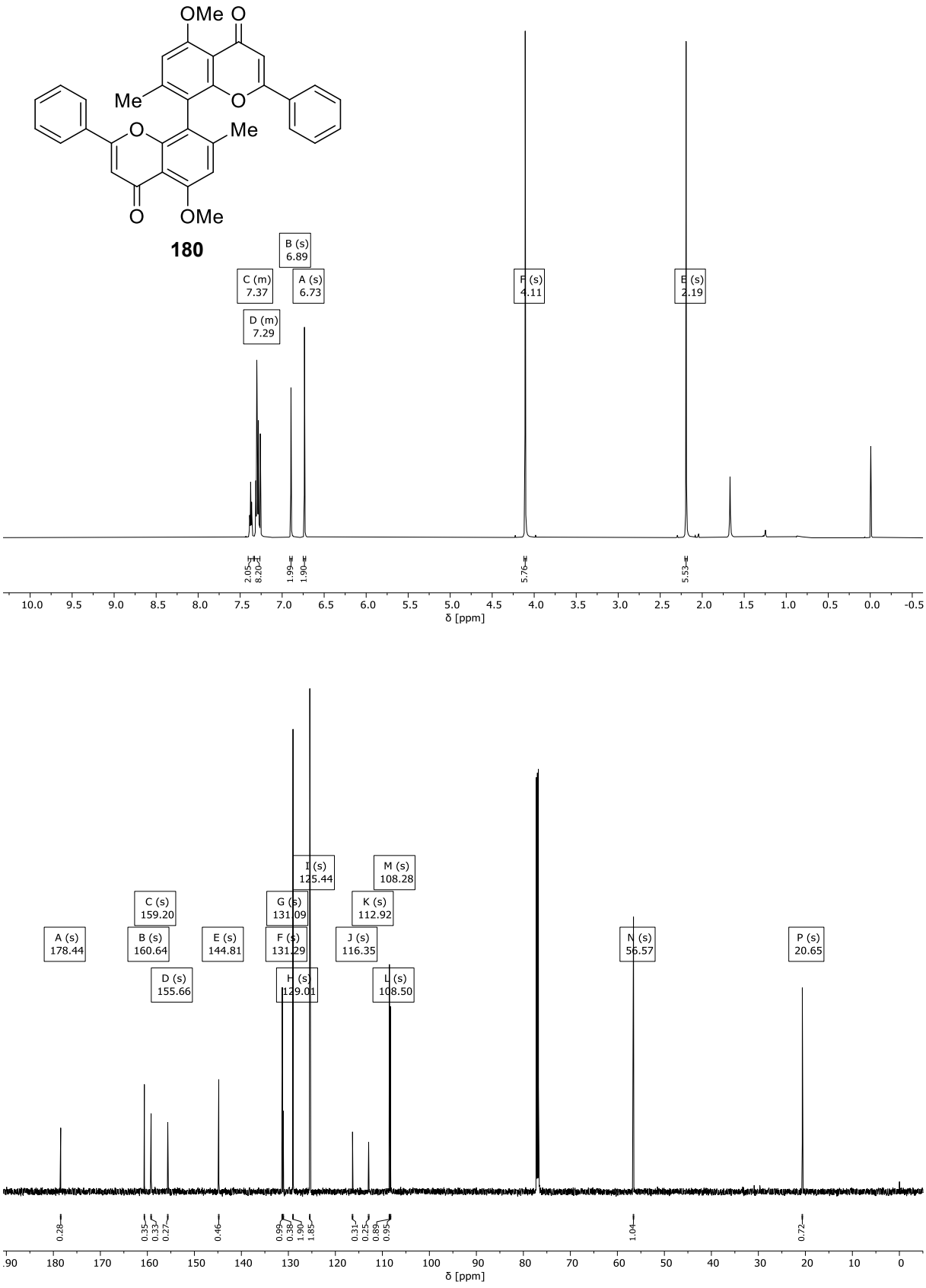

Figure 147: ^{1}H- and ^{13}C-NMR spectra (600 / 151 MHz, $CDCl_3$) of *rac*-5,5'-dimethoxy-7,7'-dimethyl-2,2'-diphenyl-4H,4'H-[8,8'-bichromene]-4,4'-dione (**180)**

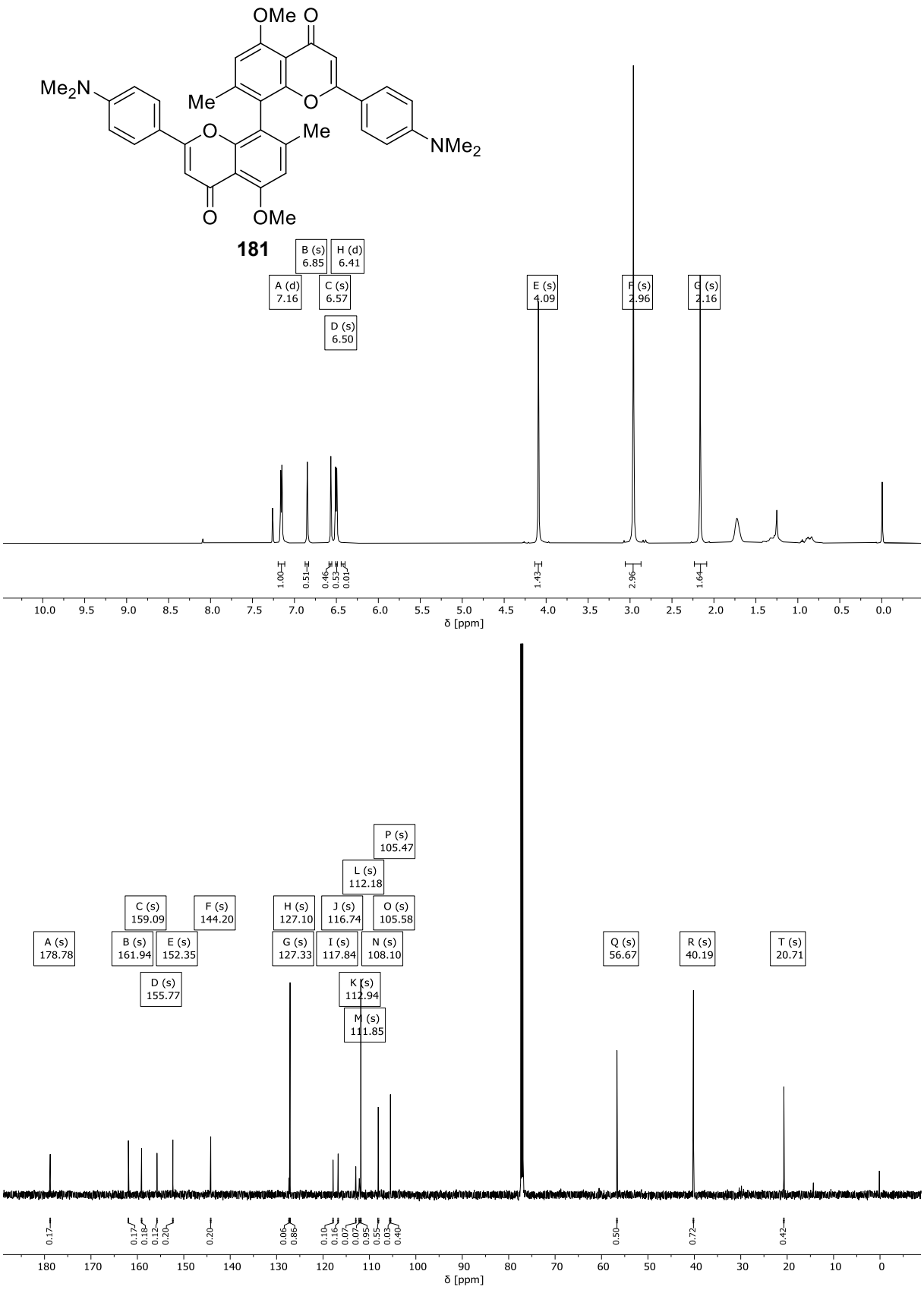

Figure 148: ^{1}H- and ^{13}C-NMR spectra (600 / 151 MHz, $CDCl_3$) of *rac*-2,2'-bis(4-(dimethylamino)phenyl)-5,5'-dimethoxy-7,7'-dimethyl-4H,4'H-[8,8'-bichromene]-4,4'-dione (**181)**

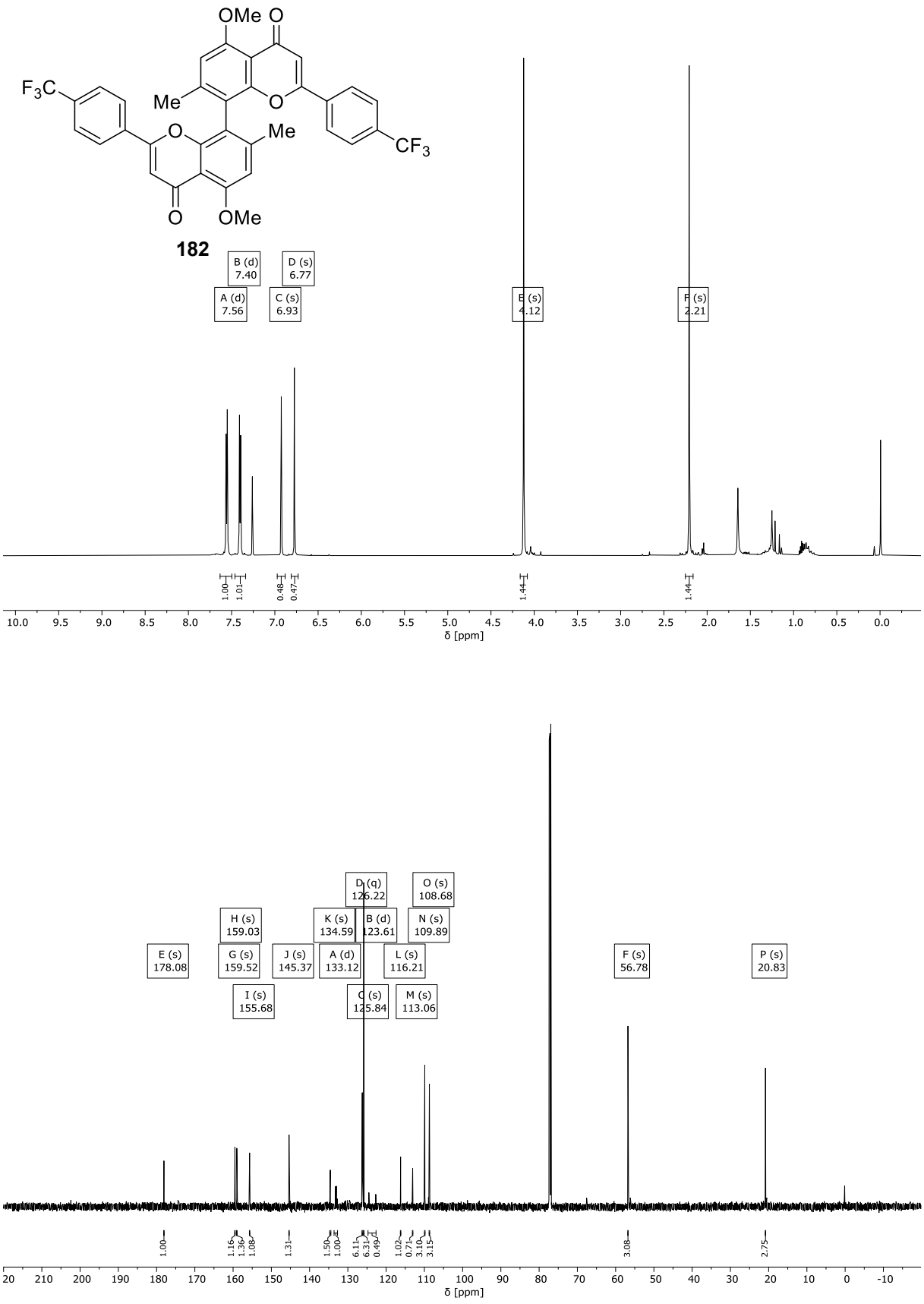

Figure 149: ^{1}H-, ^{13}C-NMR spectra (600 / 151 MHz, $CDCl_3$) of *rac*-5,5'-dimethoxy-7,7'-dimethyl-2,2'-bis(4-(trifluoromethyl)phenyl)-4H,4'H-[8,8'-bichromene]-4,4'-dione (**182)**

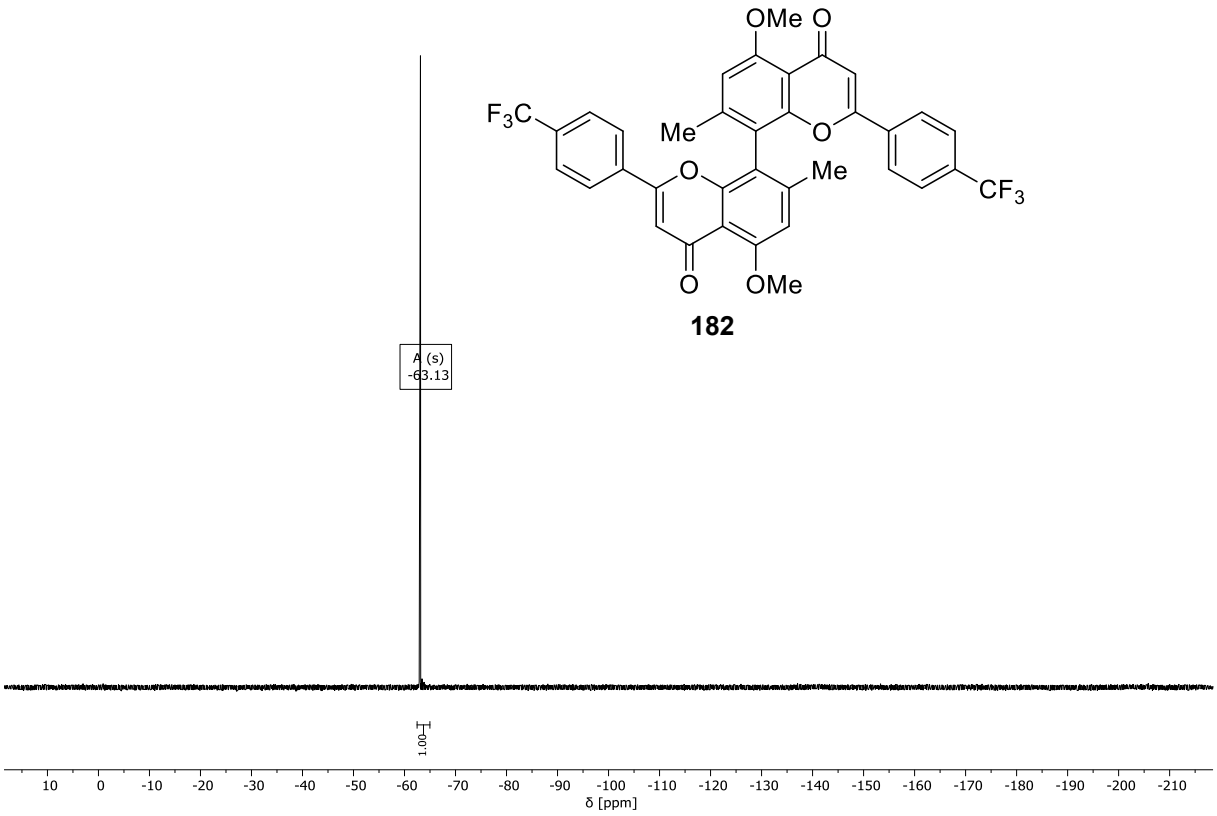

Figure 150: ^{19}F-NMR spectrum (282 MHz, $CDCl_3$) of *rac*-5,5'-dimethoxy-7,7'-dimethyl-2,2'-bis(4-(trifluoromethyl)phenyl)-4H,4'H-[8,8'-bichromene]-4,4'-dione (**182)**

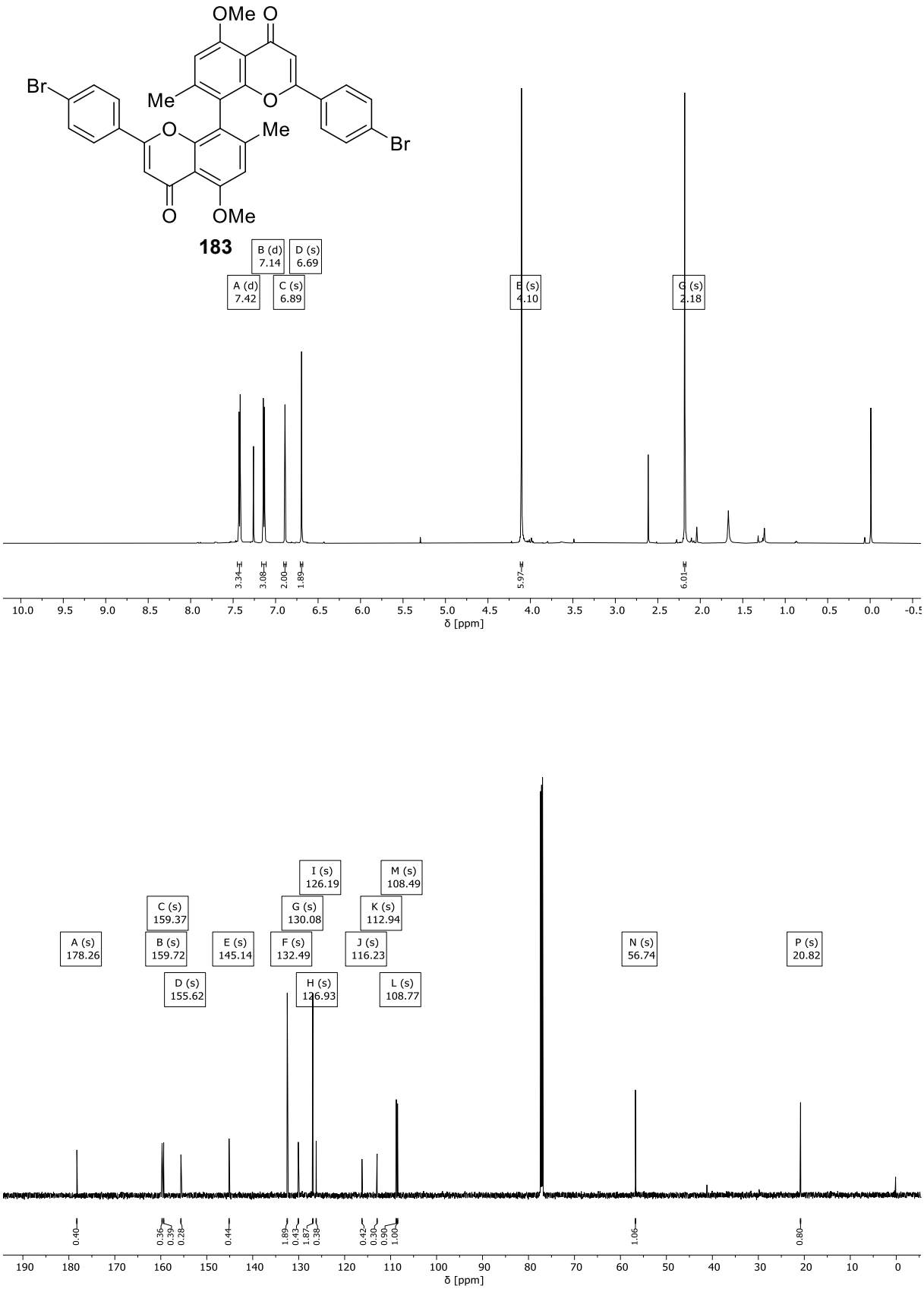

Figure 151: ^{1}H- and ^{13}C-NMR spectra (600 / 151 MHz, $CDCl_3$) of *rac*-2,2'-bis(4-bromophenyl)-5,5'-dimethoxy-7,7'-dimethyl-4H,4'H-[8,8'-bichromene]-4,4'-dione (**183)**

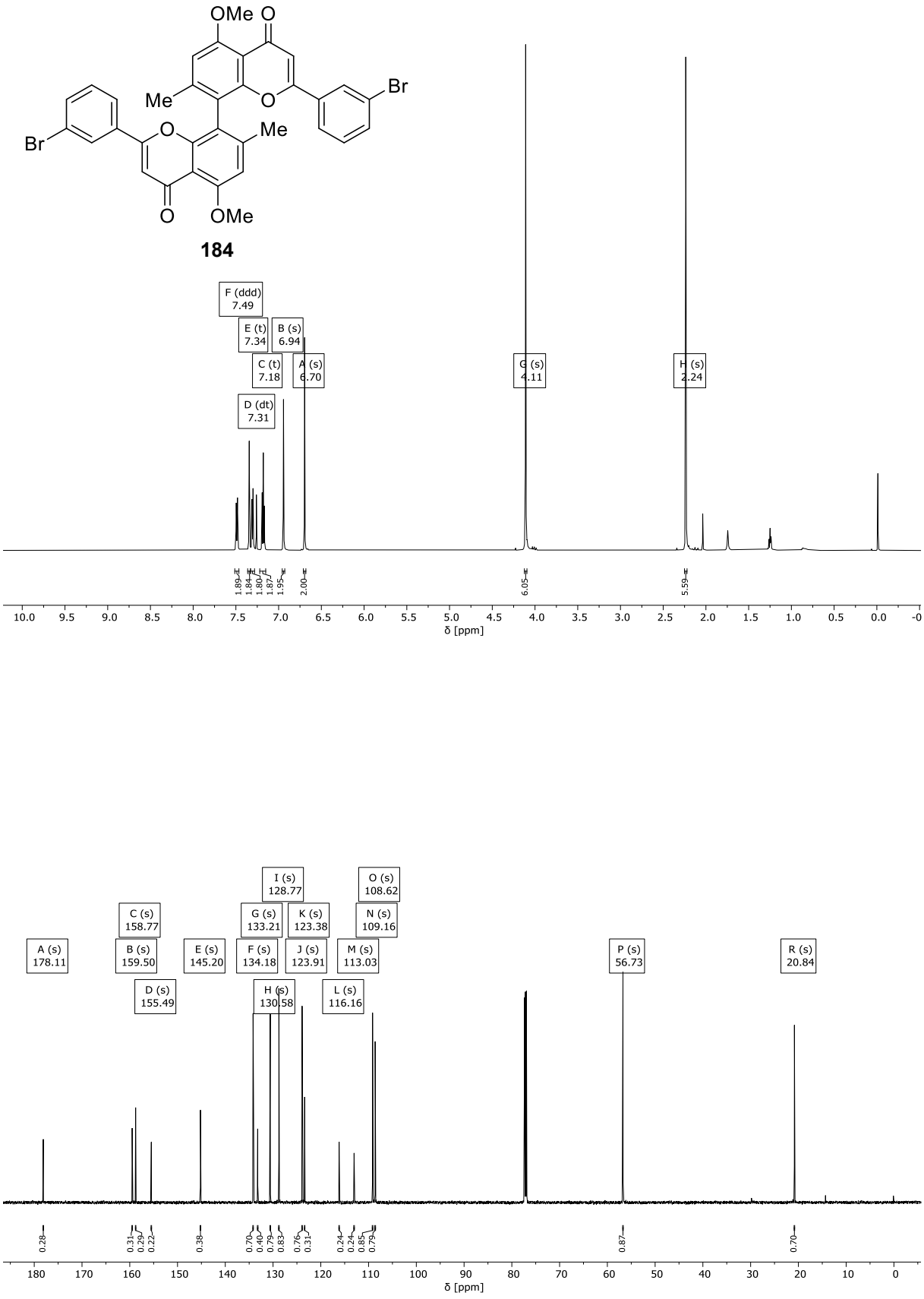

Figure 152: ^{1}H- and ^{13}C-NMR spectra (600 / 151 MHz, $CDCl_3$) of *rac*-2,2'-bis(3-bromophenyl)-5,5'-dimethoxy-7,7'-dimethyl-4H,4'H-[8,8'-bichromene]-4,4'-dione (**184)**

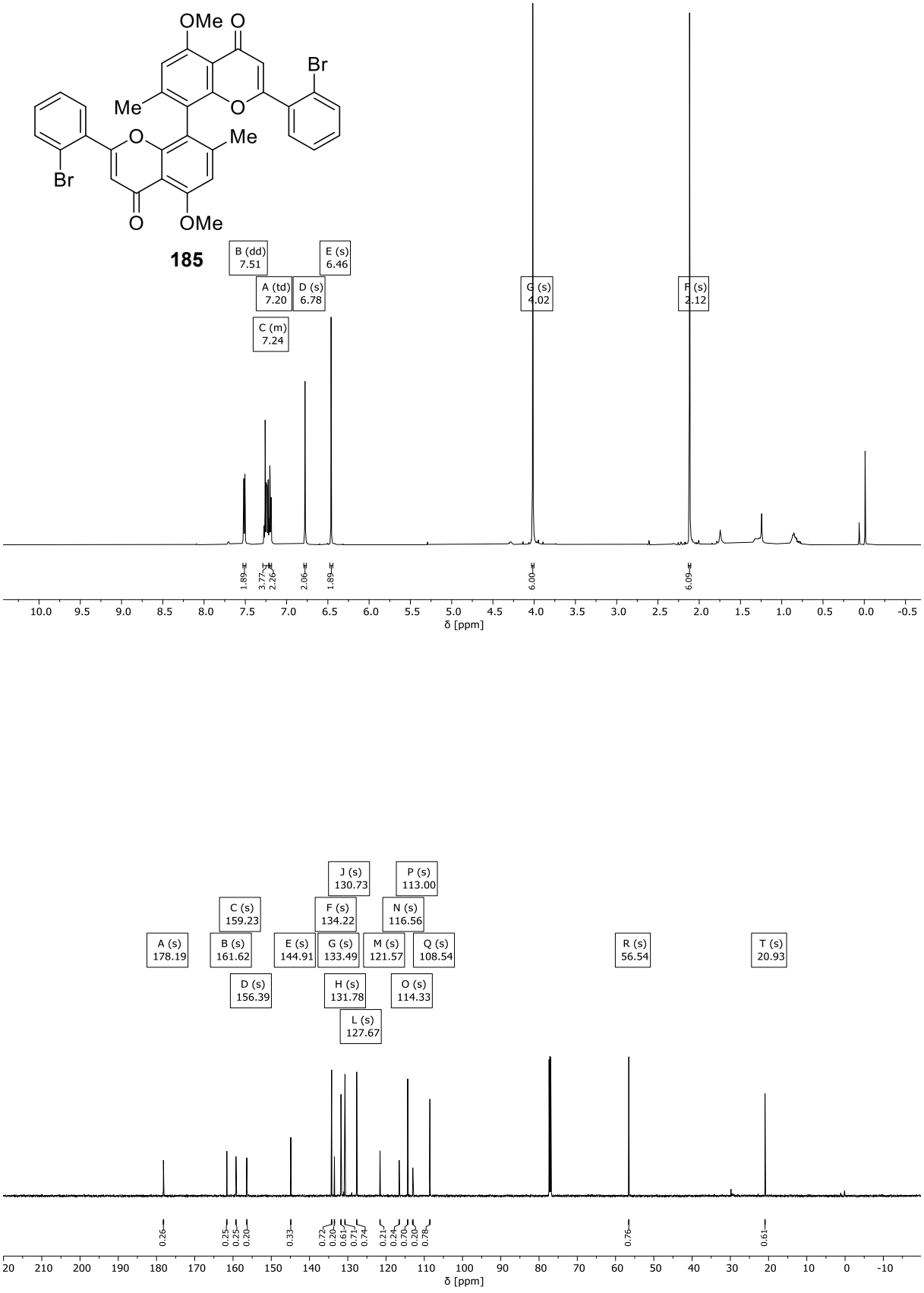

Figure 153: ^{1}H- and ^{13}C-NMR spectra (600 / 151 MHz, $CDCl_3$) of *rac*-2,2'-bis(2-bromophenyl)-5,5'-dimethoxy-7,7'-dimethyl-4H,4'H-[8,8'-bichromene]-4,4'-dione (**185)**

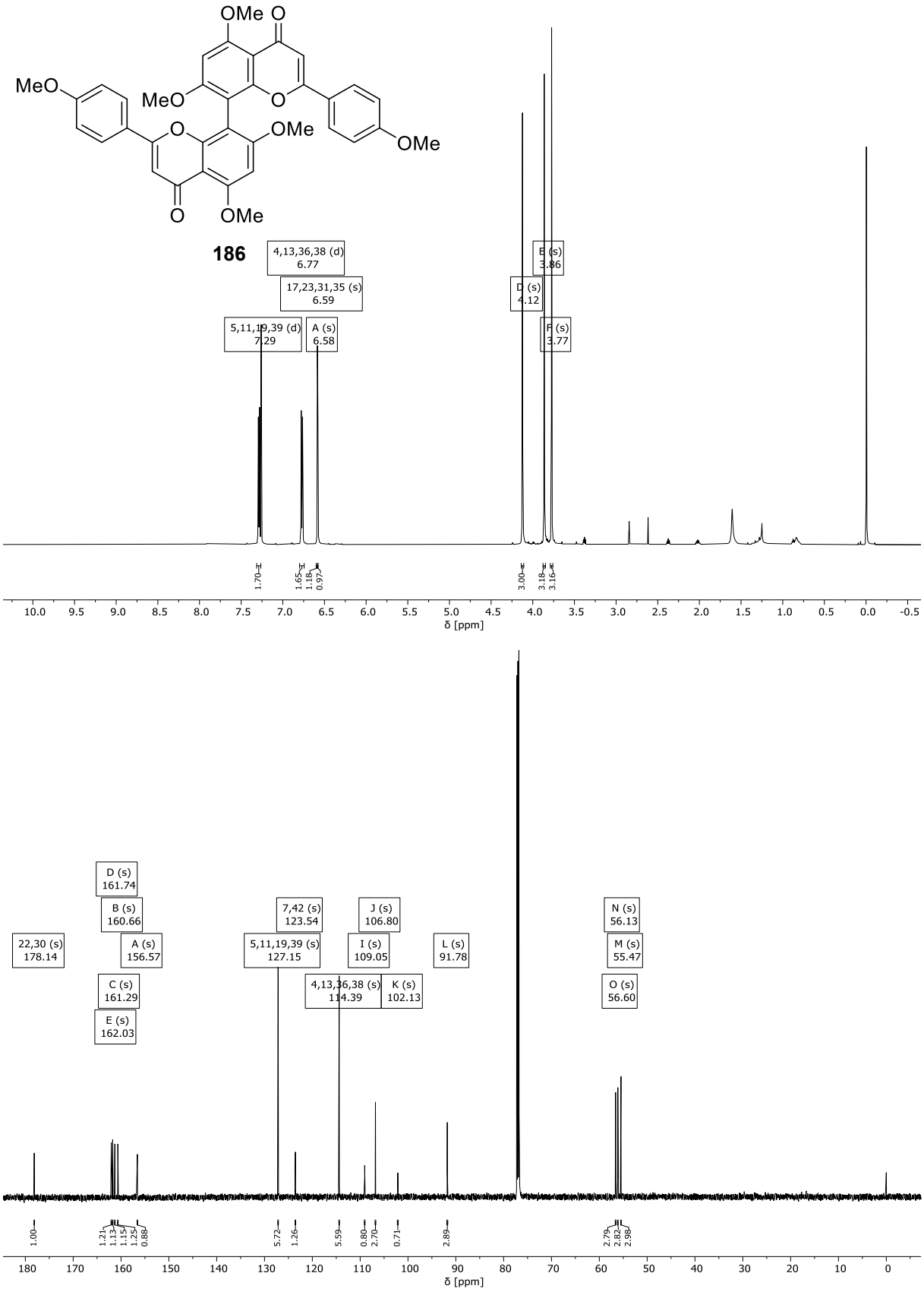

Figure 154: ^{1}H- and ^{13}C-NMR spectra (600 / 151 MHz, $CDCl_3$) of *rac*-5,5',7,7'-tetramethoxy-2,2'-bis(4-methoxyphenyl)-4H,4'H-[8,8'-bichromene]-4,4'-dione (**186)**

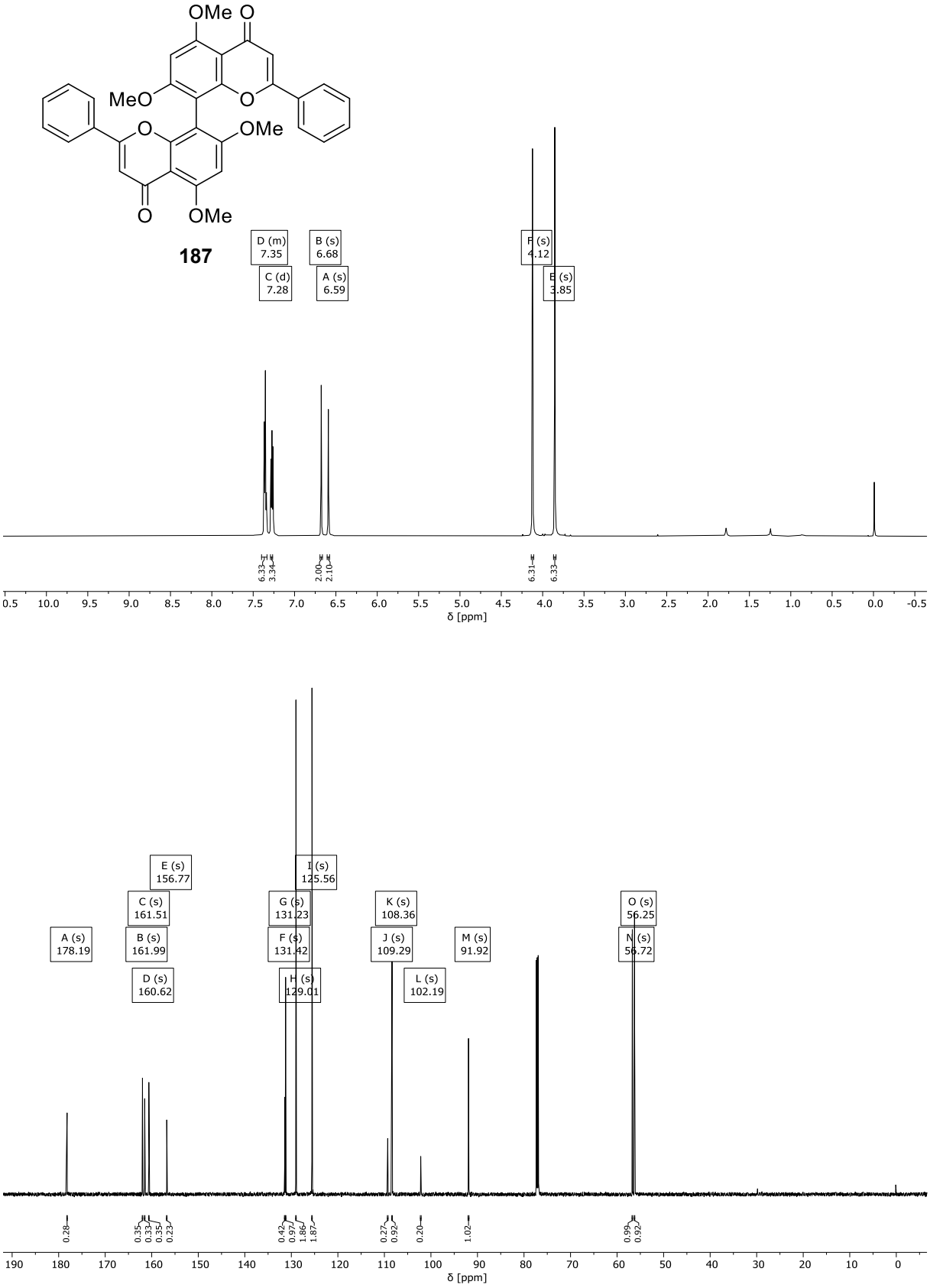

Figure 155: ^{1}H- and ^{13}C-NMR spectra (600 / 151 MHz, $CDCl_3$) of *rac*-5,5',7,7'-tetramethoxy-2,2'-diphenyl-4H,4'H-[8,8'-bichromene]-4,4'-dione (**187)**

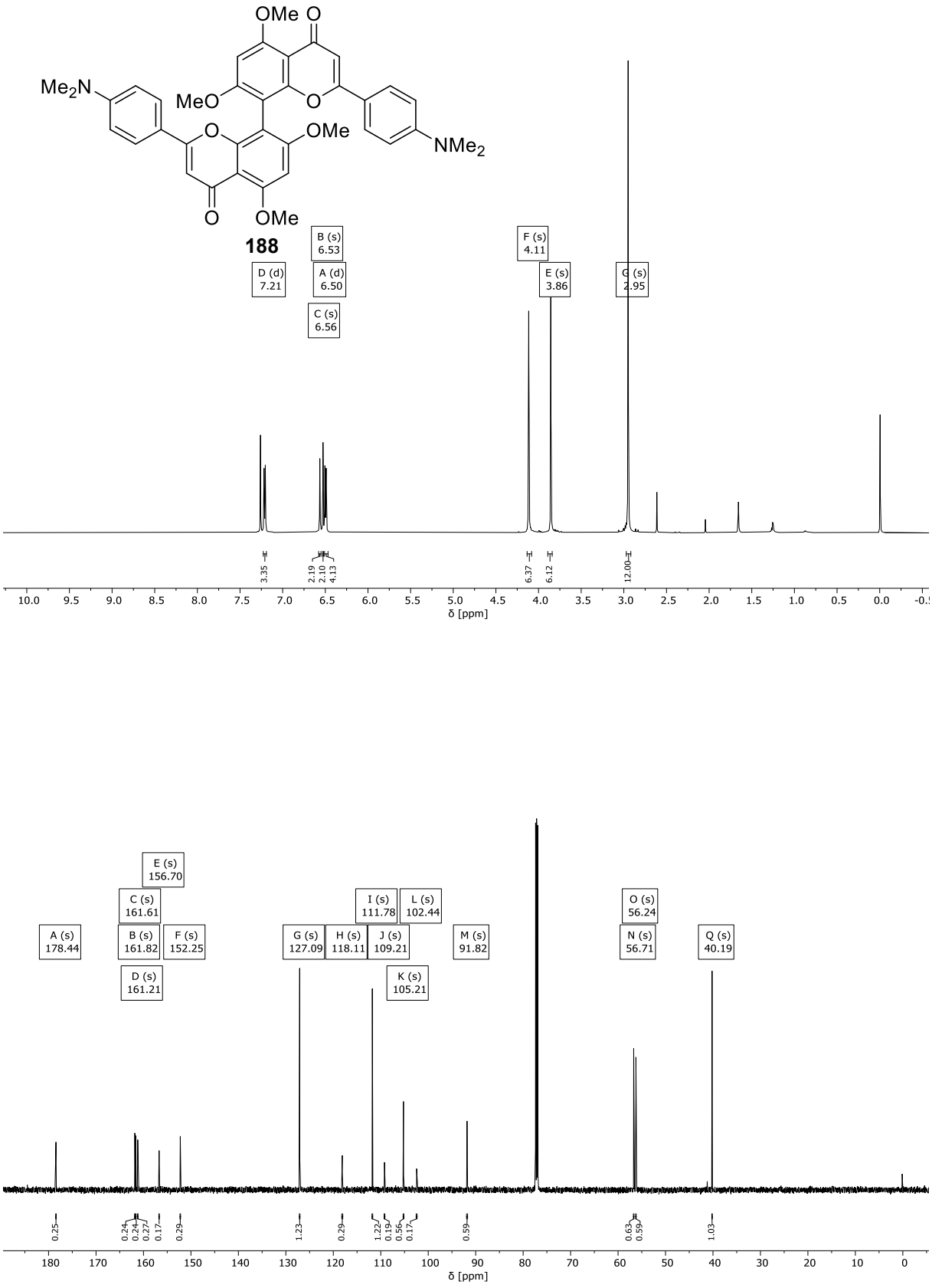

Figure 156: ^{1}H- and ^{13}C-NMR spectra (600 / 151 MHz, $CDCl_3$) of *rac*-2,2'-bis(4-(dimethylamino)phenyl)-5,5',7,7'-tetramethoxy-4H,4'H-[8,8'-bichromene]-4,4'-dione (**188)**

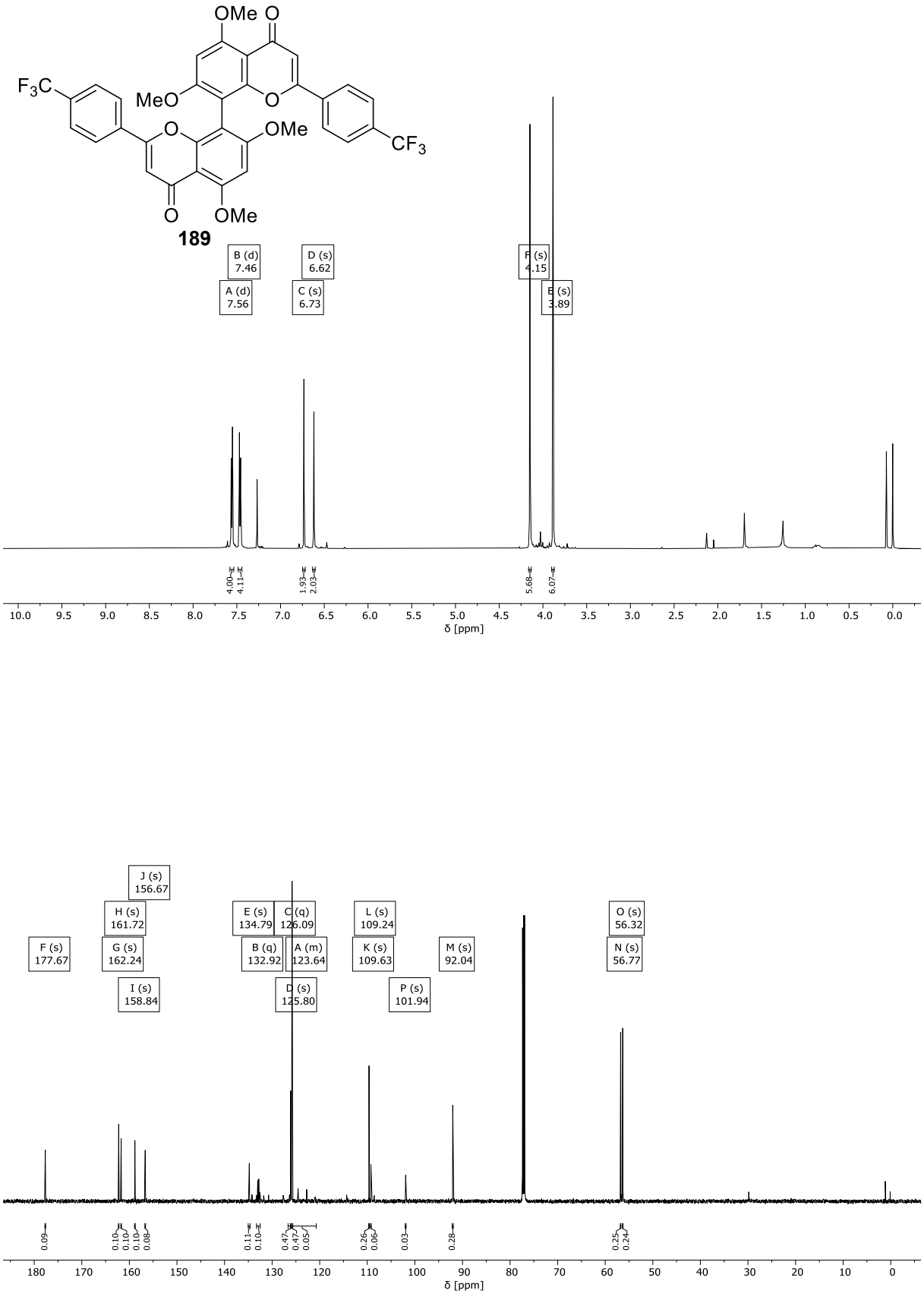

Figure 157: ^{1}H-, ^{13}C-NMR spectra (600 / 151 MHz, $CDCl_3$) of *rac*-5,5',7,7'-tetramethoxy-2,2'-bis(4-(trifluoromethyl)phenyl)-4H,4'H-[8,8'-bichromene]-4,4'-dione (**189**)

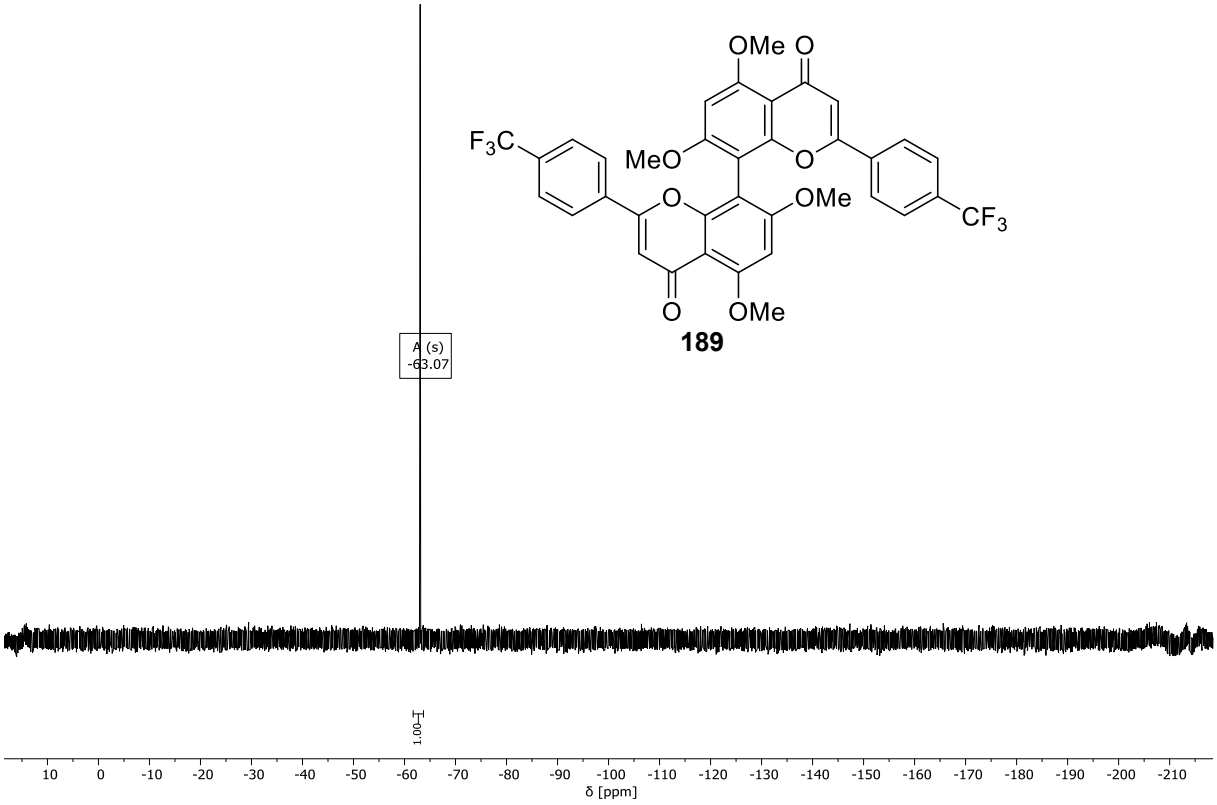

Figure 158: ^{19}F-NMR spectrum (282 MHz, $CDCl_3$) of *rac*-5,5',7,7'-tetramethoxy-2,2'-bis(4-(trifluoromethyl)phenyl)-4H,4'H-[8,8'-bichromene]-4,4'-dione (**189)**

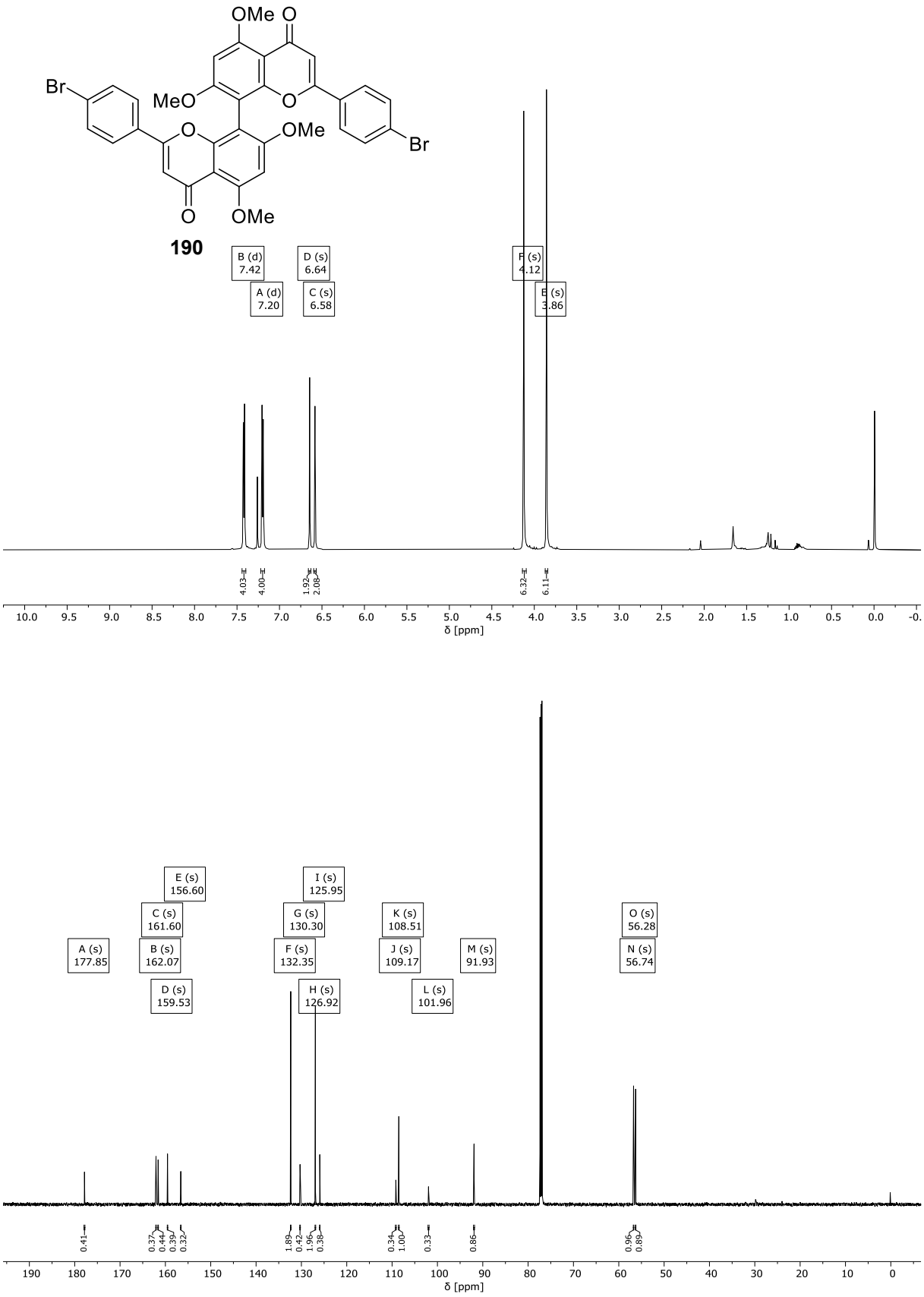

Figure 159: ^{1}H- and ^{13}C-NMR spectra (600 / 151 MHz, $CDCl_3$) of *rac*-2,2'-bis(4-bromophenyl)-5,5',7,7'-tetramethoxy-4H,4'H-[8,8'-bichromene]-4,4'-dione (**190)**

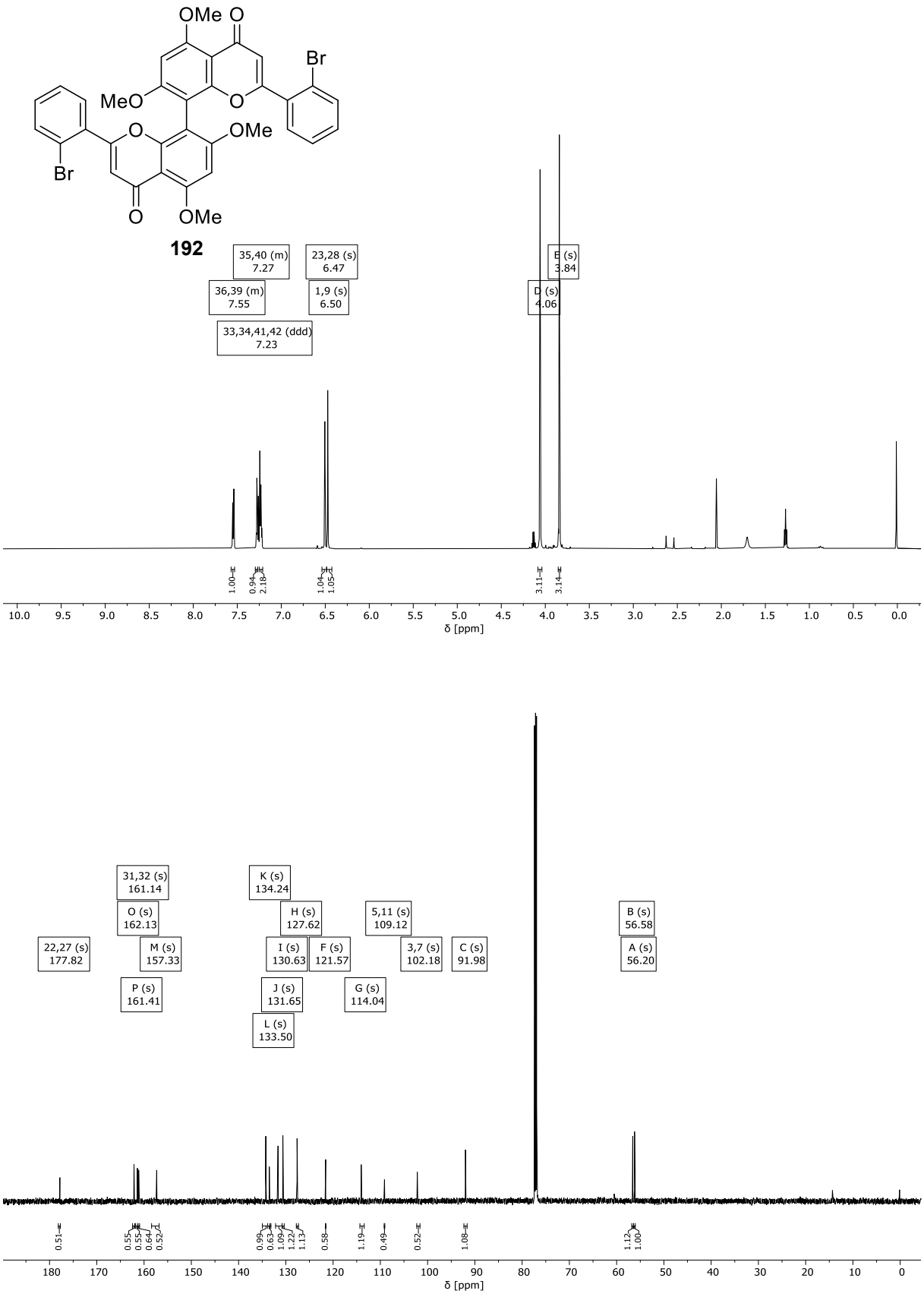

Figure 160: ^{1}H- and ^{13}C-NMR spectra (600 / 151 MHz, $CDCl_3$) of *rac*-2,2'-bis(2-bromophenyl)-5,5',7,7'-tetramethoxy-4H,4'H-[8,8'-bichromene]-4,4'-dione (**192)**

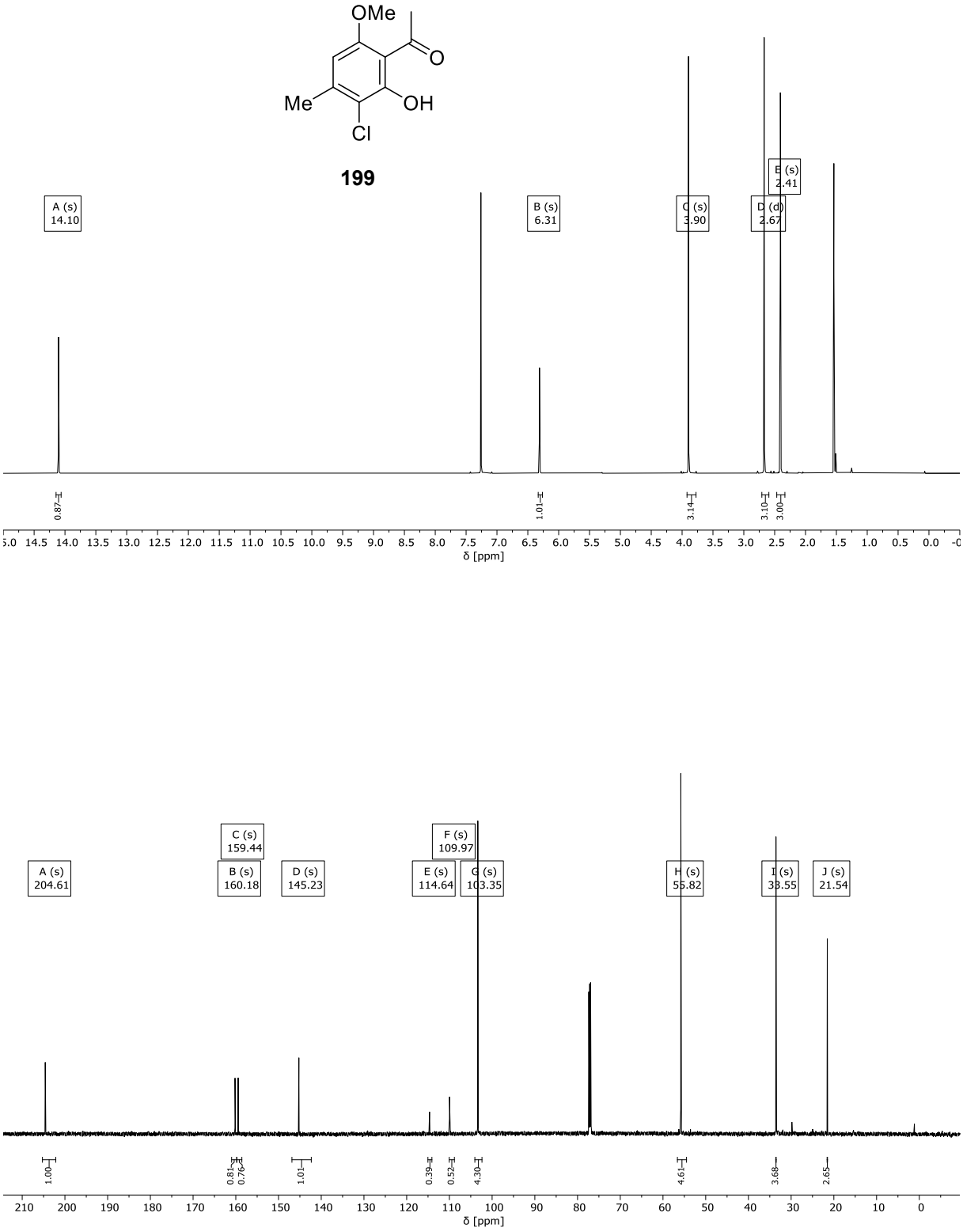

Figure 161: ^{1}H- and ^{13}C-NMR spectra (600 / 151 MHz, $CDCl_3$) of 1-(3-chloro-2-hydroxy-6-methoxy-4-methylphenyl)ethan-1-one (**199**)

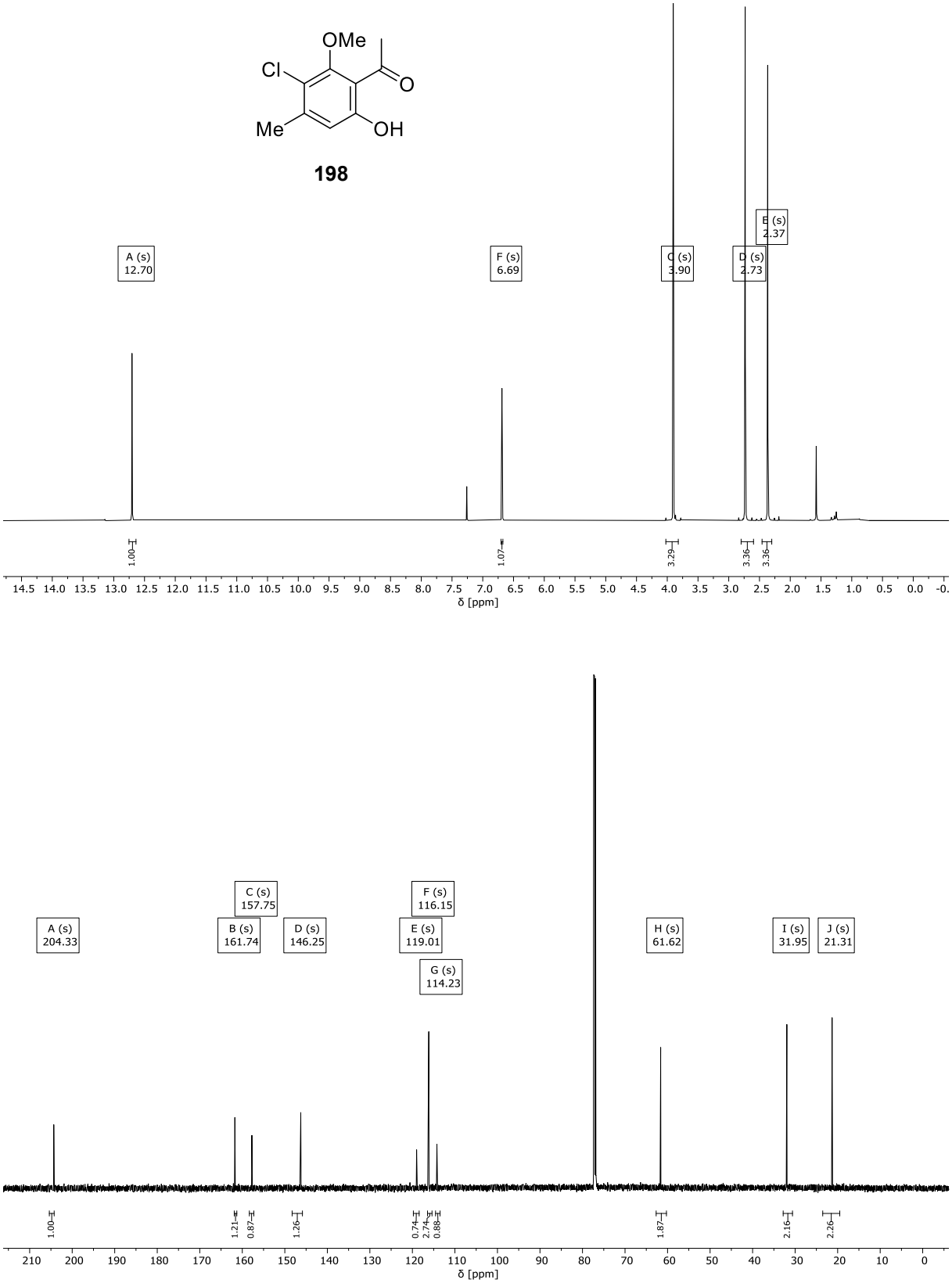

Figure 162: ^{1}H- and ^{13}C-NMR spectra (600 / 151 MHz, $CDCl_3$) of 1-(3-chloro-6-hydroxy-2-methoxy-4-methylphenyl)ethan-1-one (**198**)

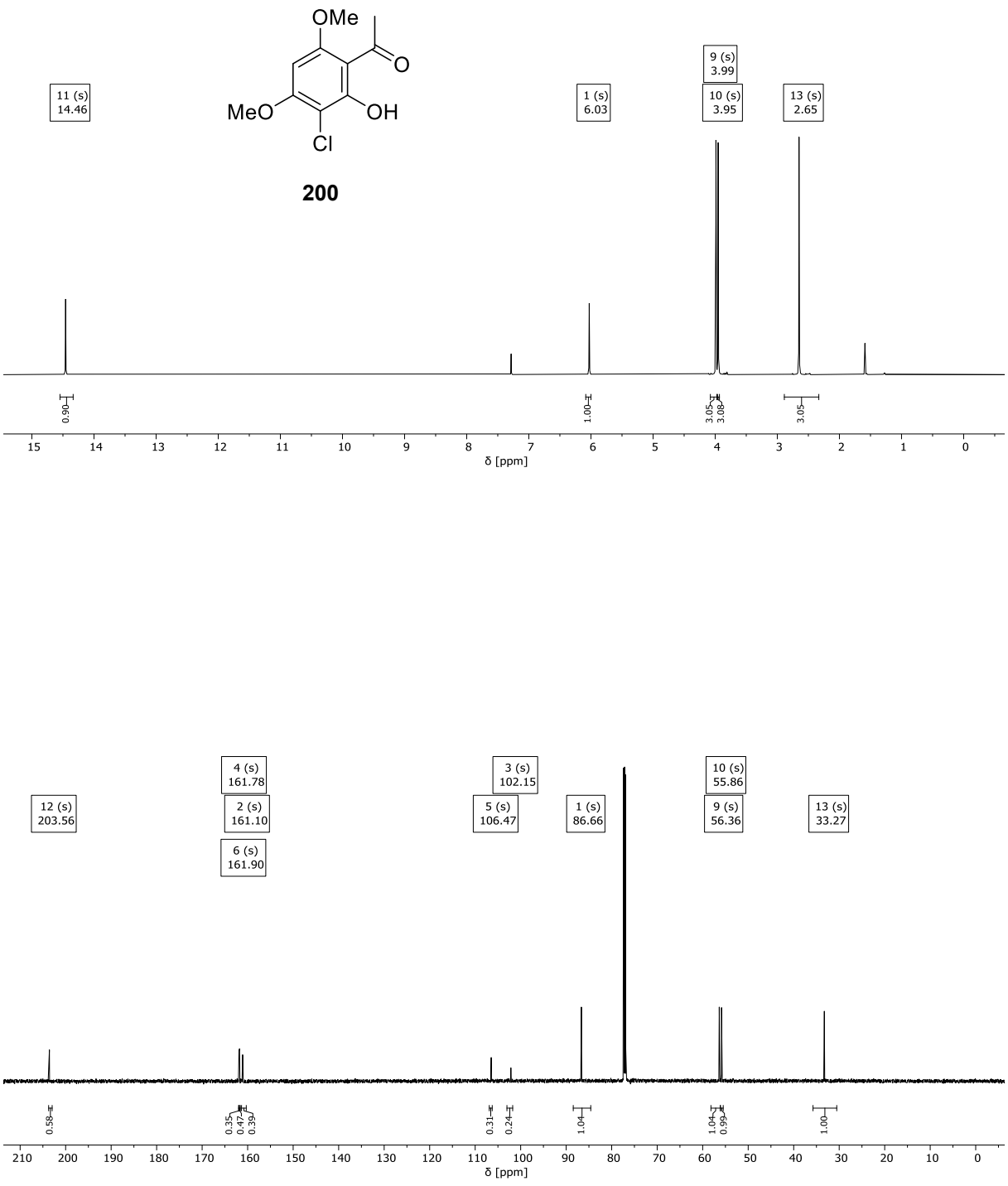

Figure 163: ^{1}H- and ^{13}C-NMR spectra (600 / 151 MHz, $CDCl_3$) of 1-(3-chloro-2-hydroxy-4,6-dimethoxyphenyl)ethan-1-one (**200**)

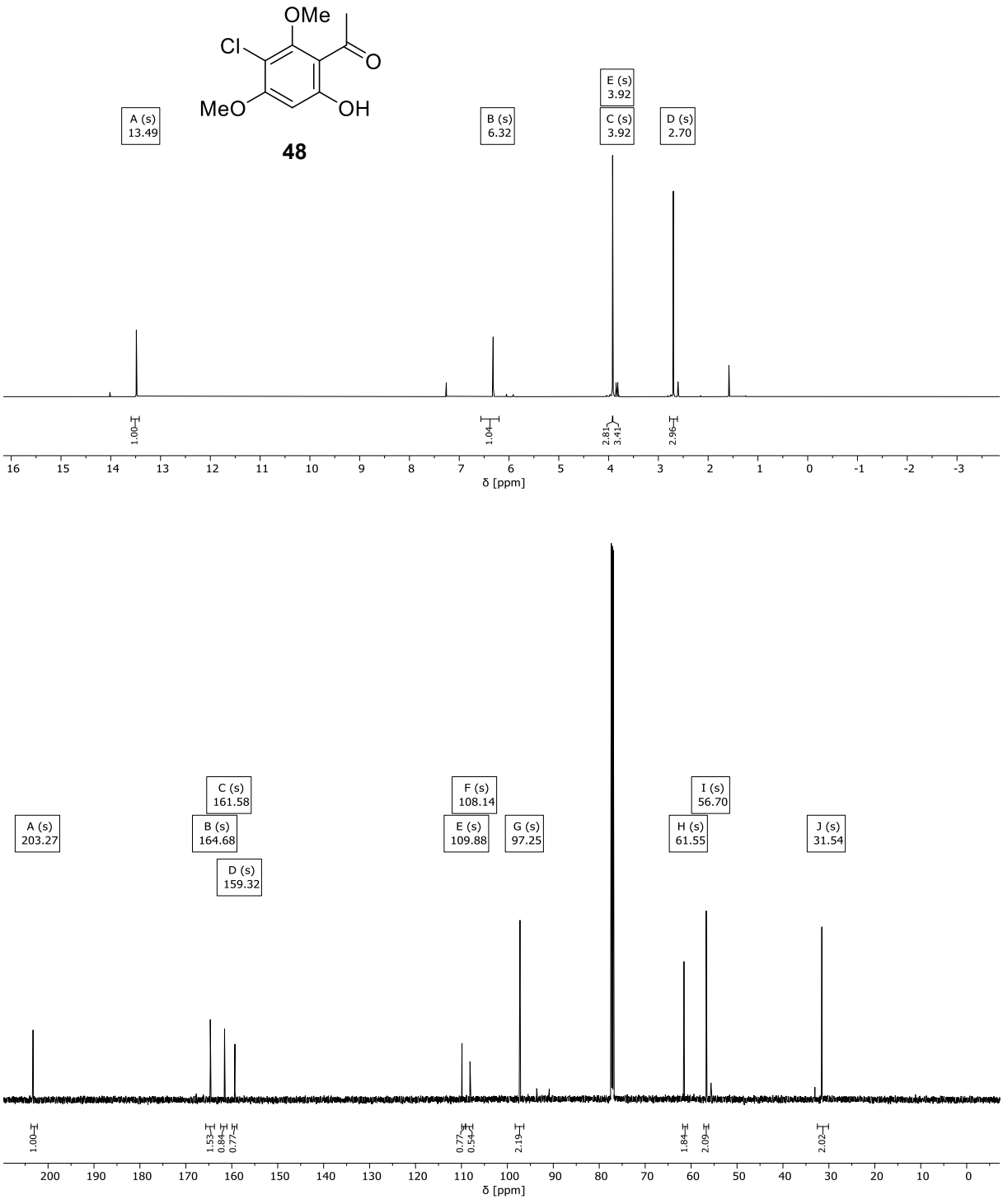

Figure 164: ^{1}H- and ^{13}C-NMR spectra (600 / 151 MHz, $CDCl_3$) of 1-(3-chloro-6-hydroxy-2,4-dimethoxyphenyl)ethan-1-one (**48**)

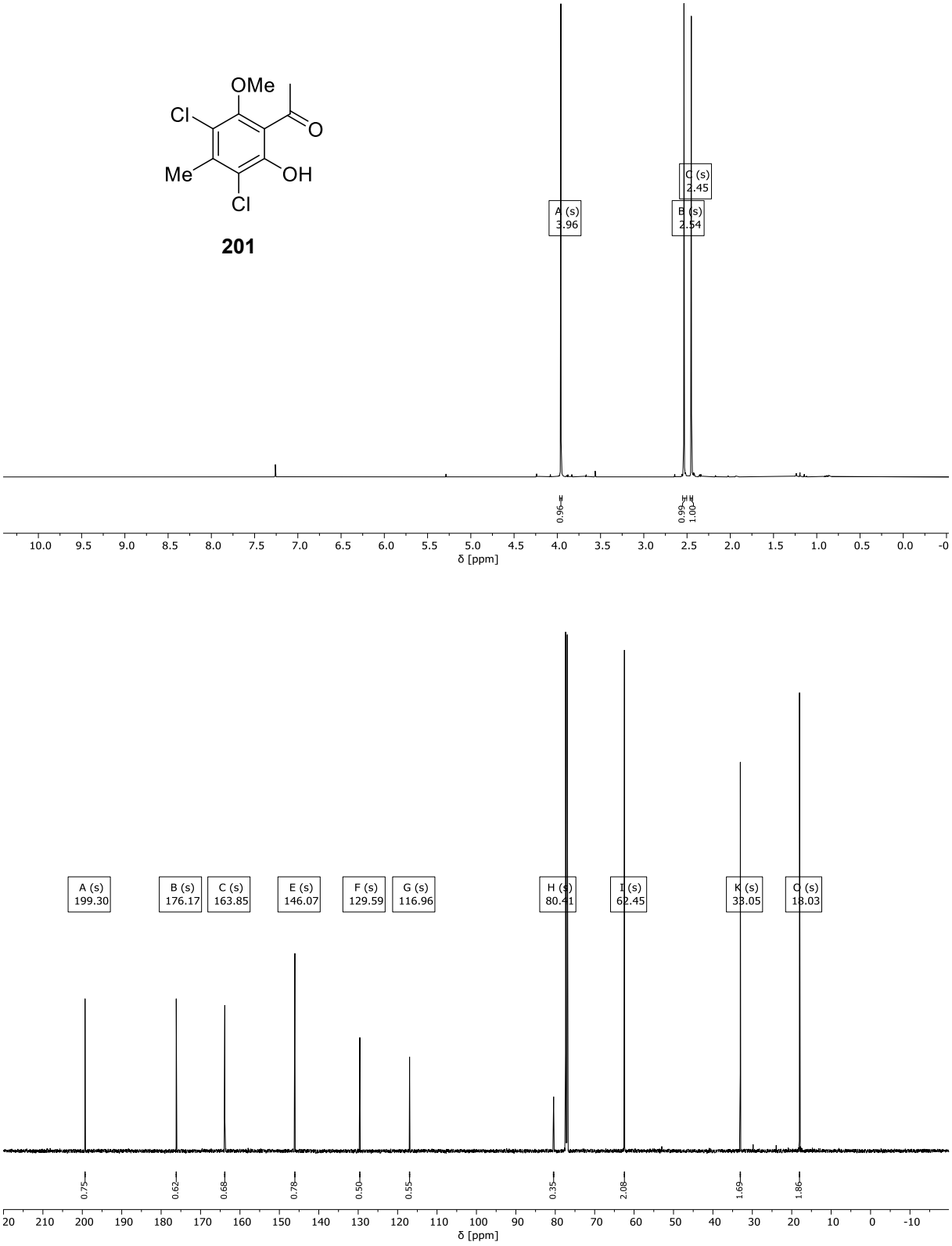

Figure 165: ^{1}H- and ^{13}C-NMR spectra (600 / 151 MHz, $CDCl_3$) of 1-(3,5-dichloro-2-hydroxy-6-methoxy-4-methylphenyl)ethan-1-one (**201**)

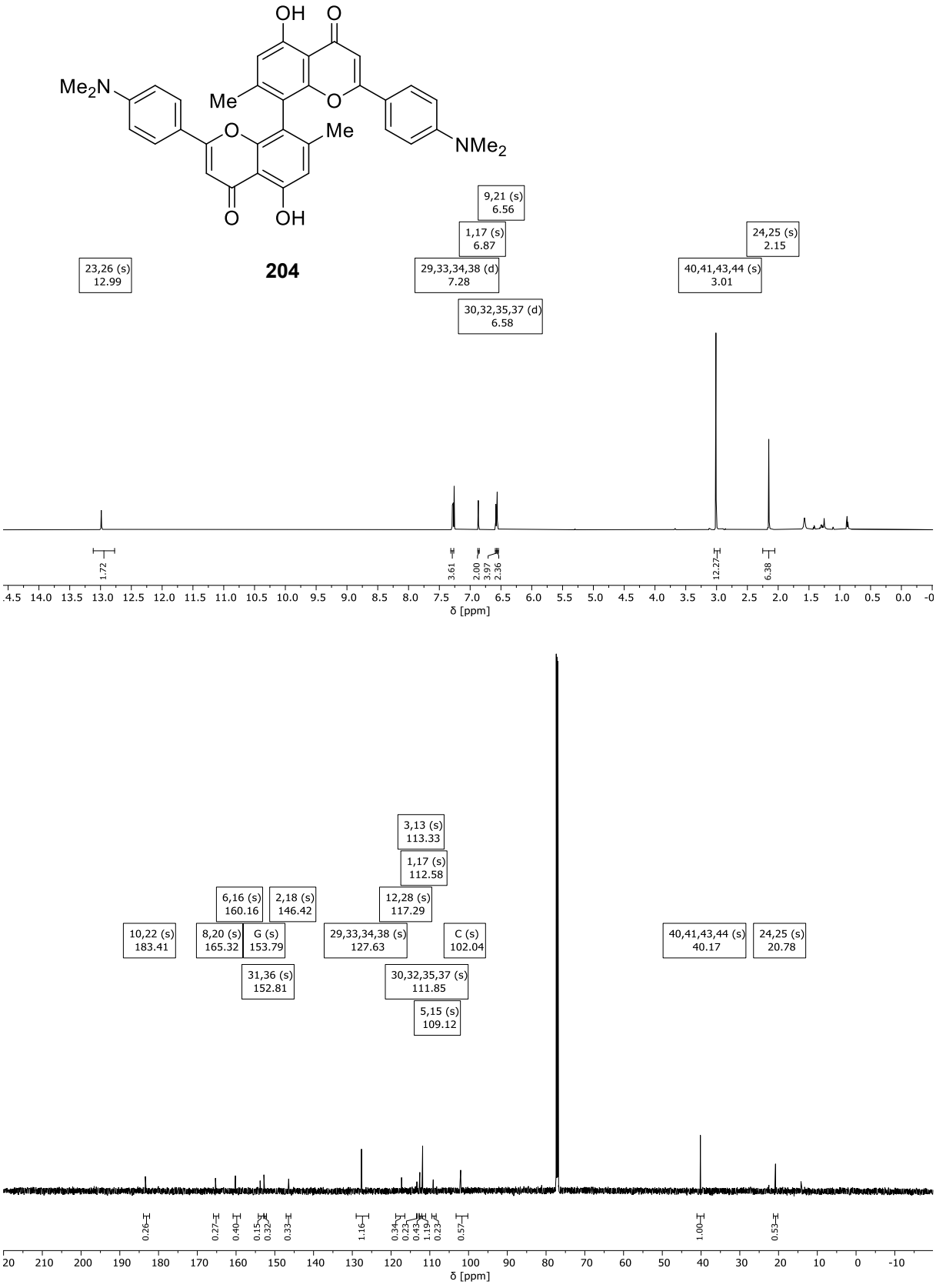

Figure 166: ^{1}H- and ^{13}C-NMR spectra (600 / 151 MHz, $CDCl_3$) of rac-2,2'-bis(4-(dimethylamino)phenyl)-5,5'-dihydroxy-7,7'-dimethyl-4H,4'H-[8,8'-bichromene]-4,4'-dione (**204**)

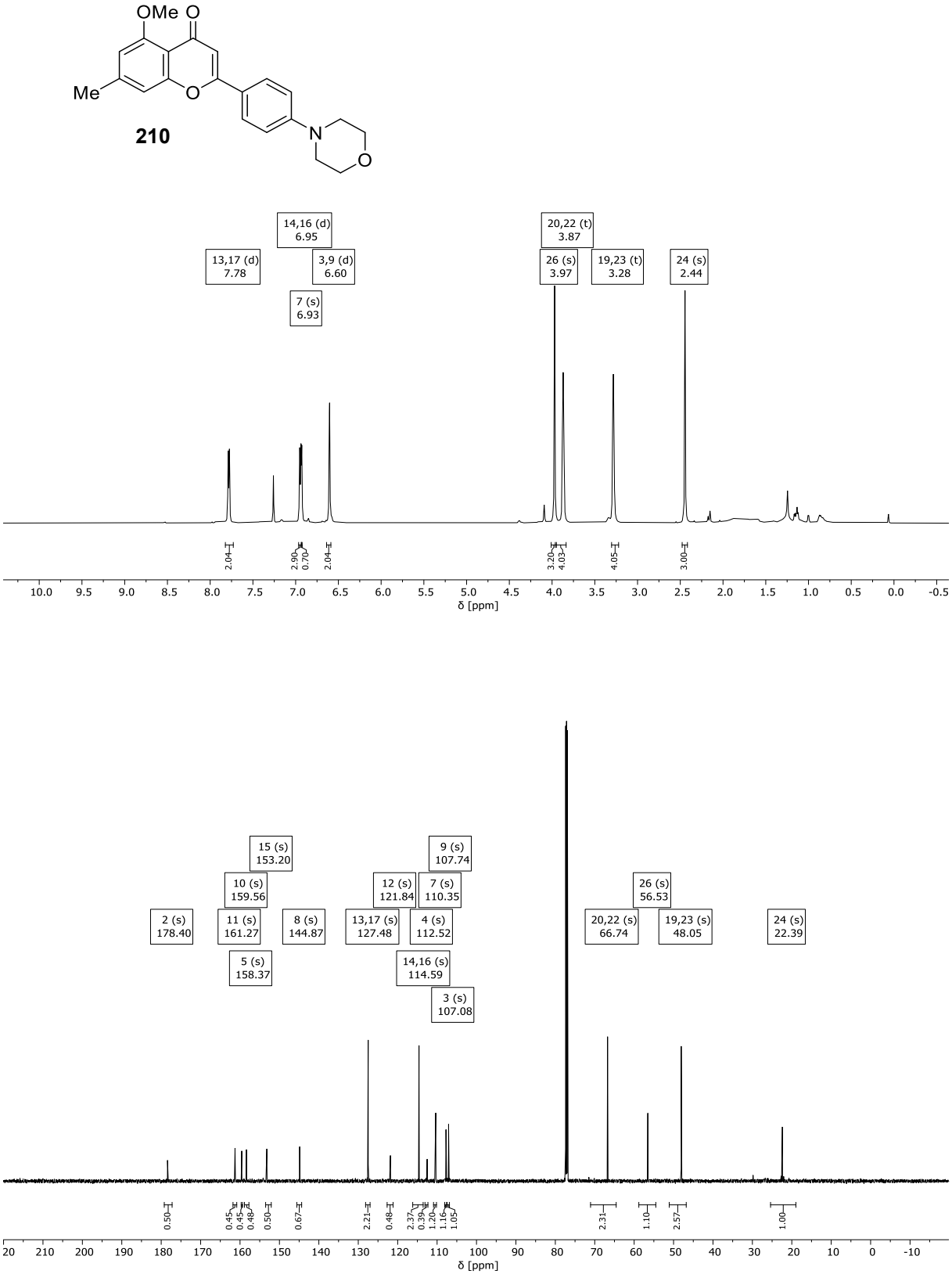

Figure 167: ^{1}H- and ^{13}C-NMR spectra (600 / 151 MHz, $CDCl_3$) of 5-methoxy-7-methyl-2-(4-morpholinophenyl)-4H-chromen-4-one (**210**).

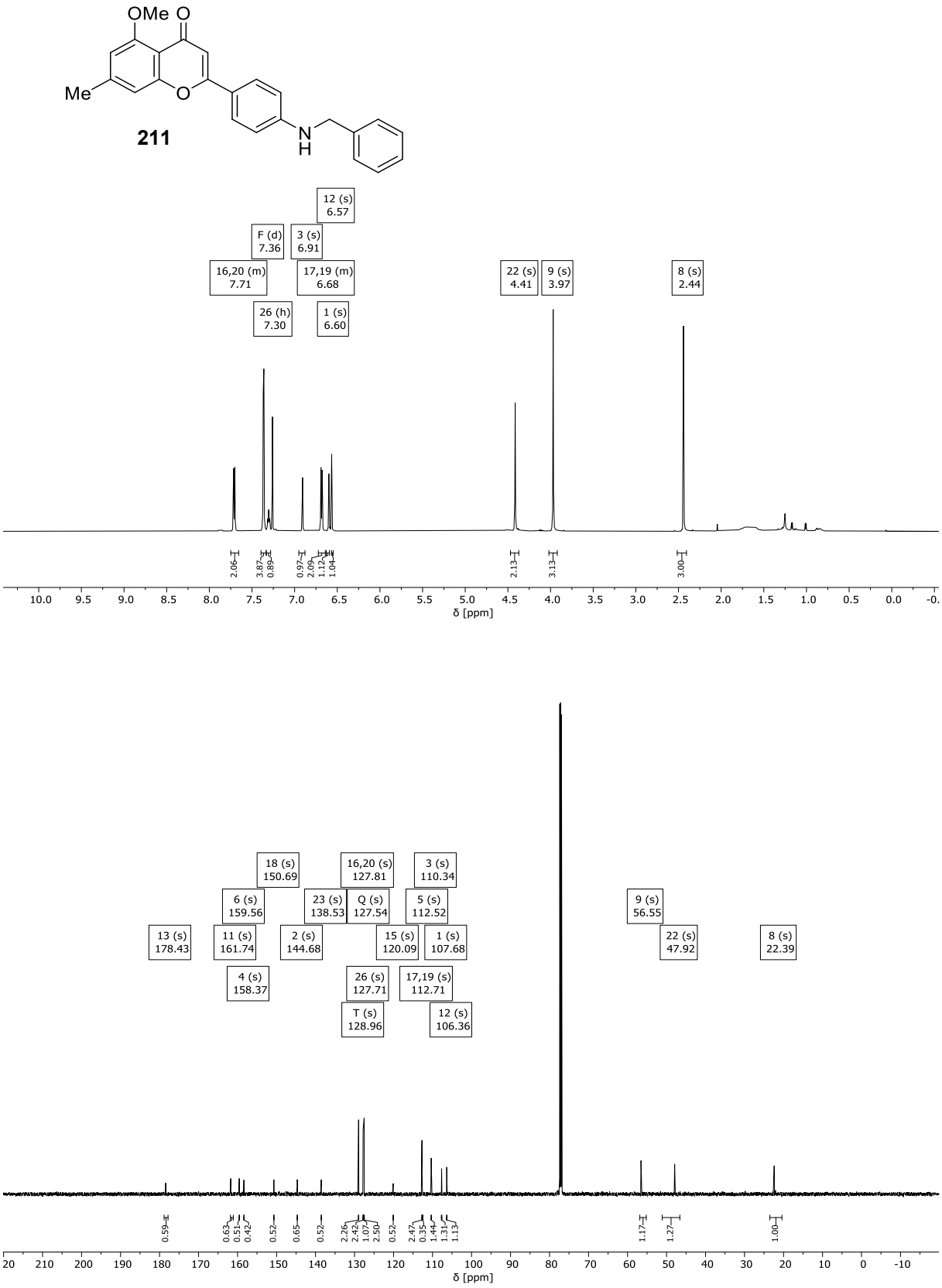

Figure 168: ^{1}H- and ^{13}C-NMR spectra (600 / 151 MHz, $CDCl_3$) of 2-(4-(benzylamino)phenyl)-5-methoxy-7-methyl-4H-chromen-4-one (**211**)

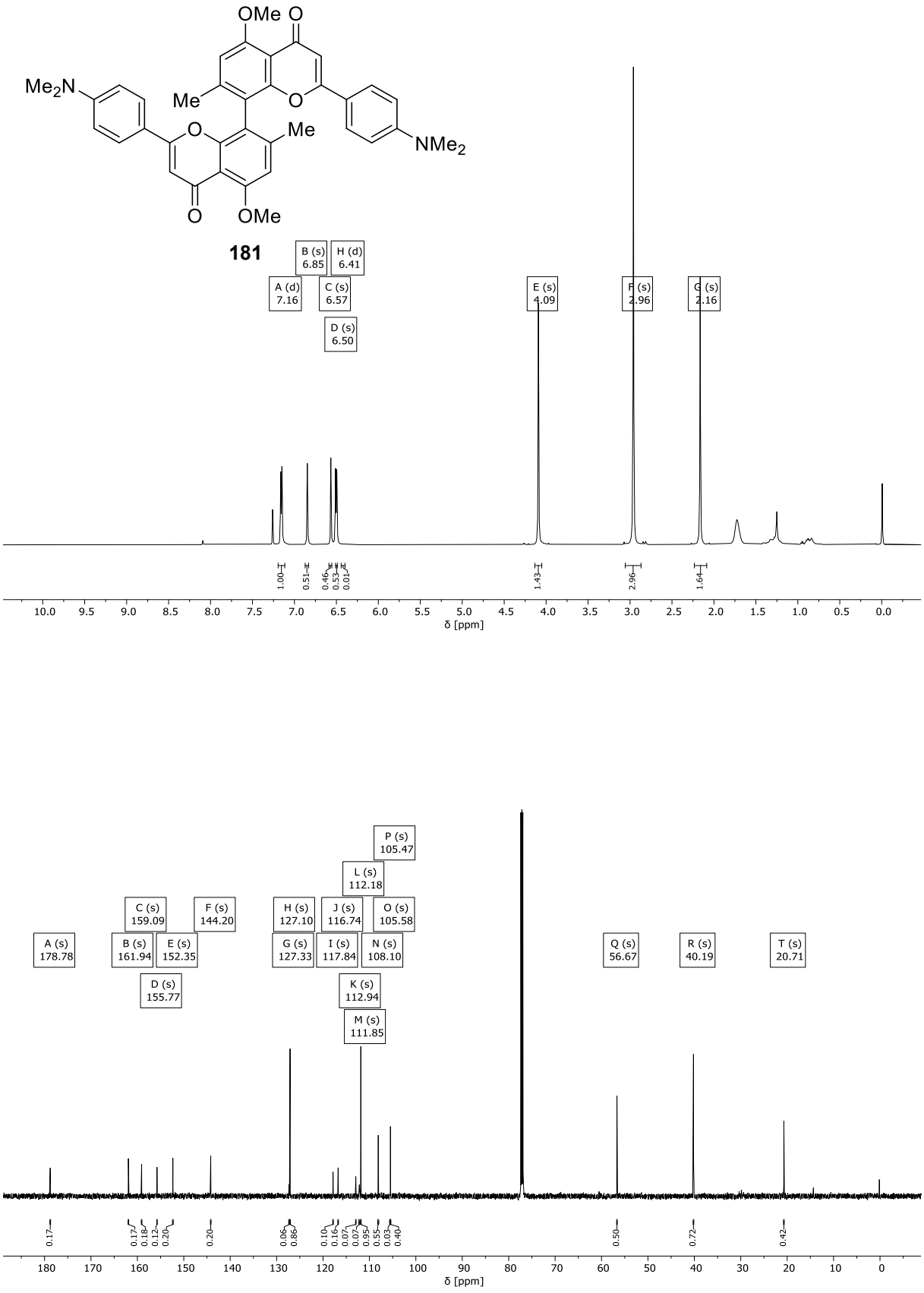

Figure 169: ^{1}H- and ^{13}C-NMR spectrum (600 / 151 MHz, $CDCl_3$) of *rac*-2,2'-bis(4-(dimethylamino)phenyl)-5,5'-dimethoxy-7,7'-dimethyl-4H,4'H-[8,8'-bichromene]-4,4'-dione (**181**)

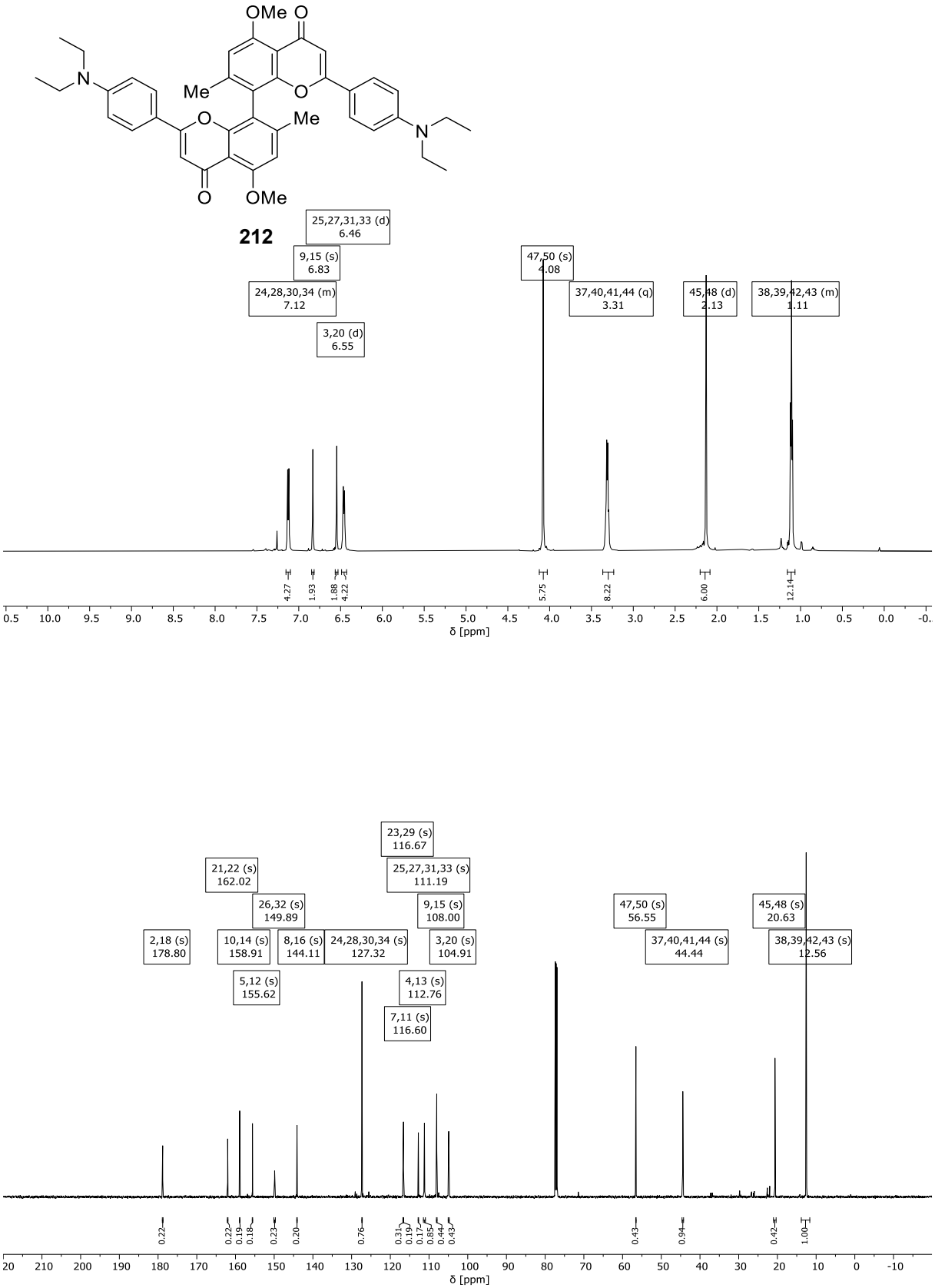

Figure 170: ^{1}H- and ^{13}C-NMR spectra (600 / 151 MHz, $CDCl_3$) of *rac*-2,2'-bis(4-(diethylamino)phenyl)-5,5'-dimethoxy-7,7'-dimethyl-4H,4'H-[8,8'-bichromene]-4,4'-dione (**212**).

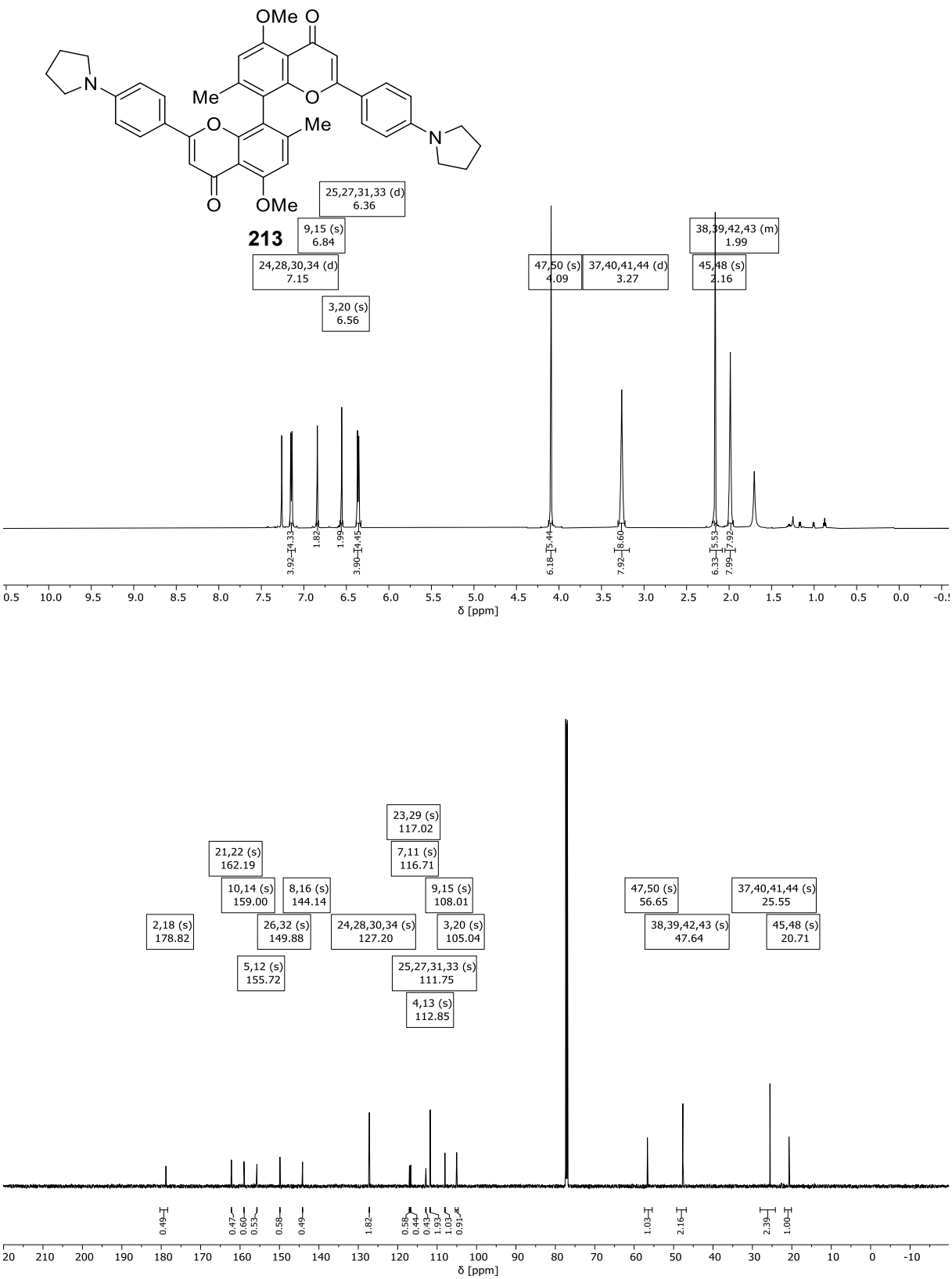

Figure 171: ^{1}H- and ^{13}C-NMR spectra (600 / 151 MHz, $CDCl_3$) of *rac*-5,5'-dimethoxy-7,7'-dimethyl-2,2'-bis(4-(pyrrolidin-1-yl)phenyl)-4H,4'H-[8,8'-bichromene]-4,4'-dione (**213**).

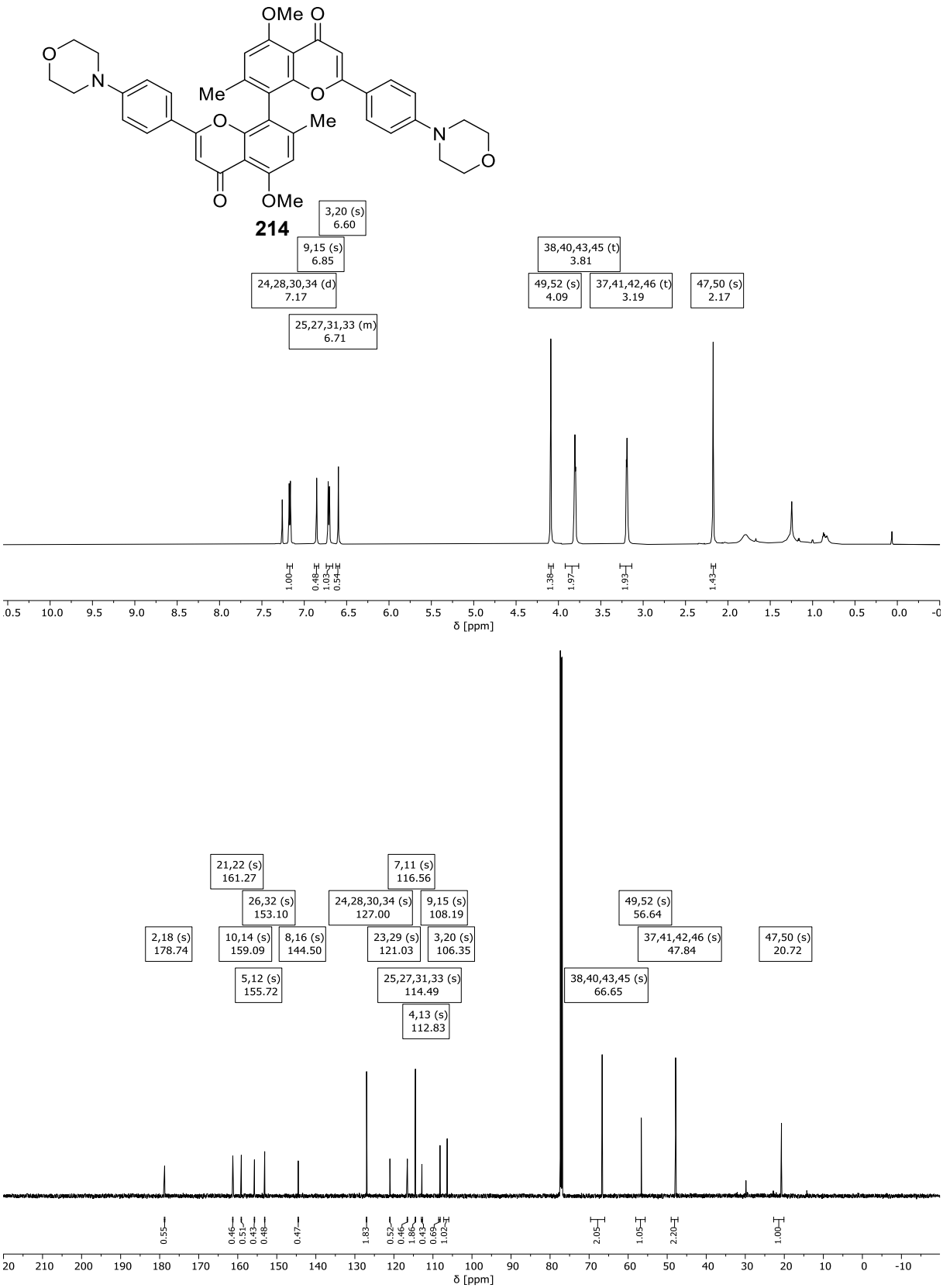

Figure 172: ^{1}H- and ^{13}C-NMR spectra (600 / 151 MHz, $CDCl_3$) of *rac*-5,5'-dimethoxy-7,7'-dimethyl-2,2'-bis(4-morpholinophenyl)-4H,4'H-[8,8'-bichromene]-4,4'-dione (**214**).

Figure 173: ^{1}H- and ^{13}C-NMR spectra (600 / 151 MHz, $CDCl_3$) of *rac*-5,5'-dimethoxy-7,7'-dimethyl-2,2'-bis(4-(piperidin-1-yl)phenyl)-4H,4'H-[8,8'-bichromene]-4,4'-dione (**215**).

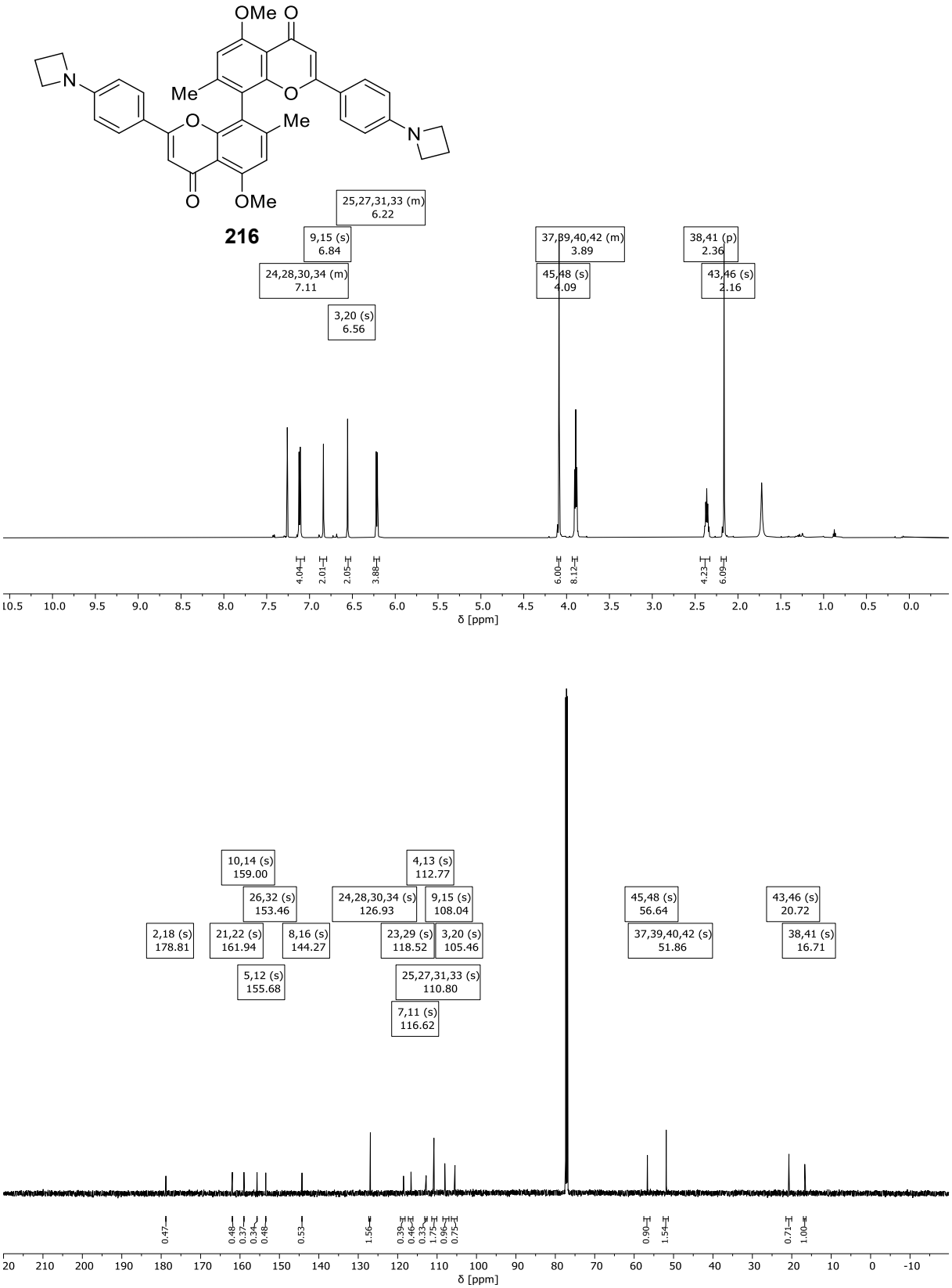

Figure 174: ^{1}H- and ^{13}C-NMR spectra (600 / 151 MHz, $CDCl_3$) of *rac*-2,2'-bis(4-(azetidin-1-yl)phenyl)-5,5'-dimethoxy-7,7'-dimethyl-4H,4'H-[8,8'-bichromene]-4,4'-dione (**216**).

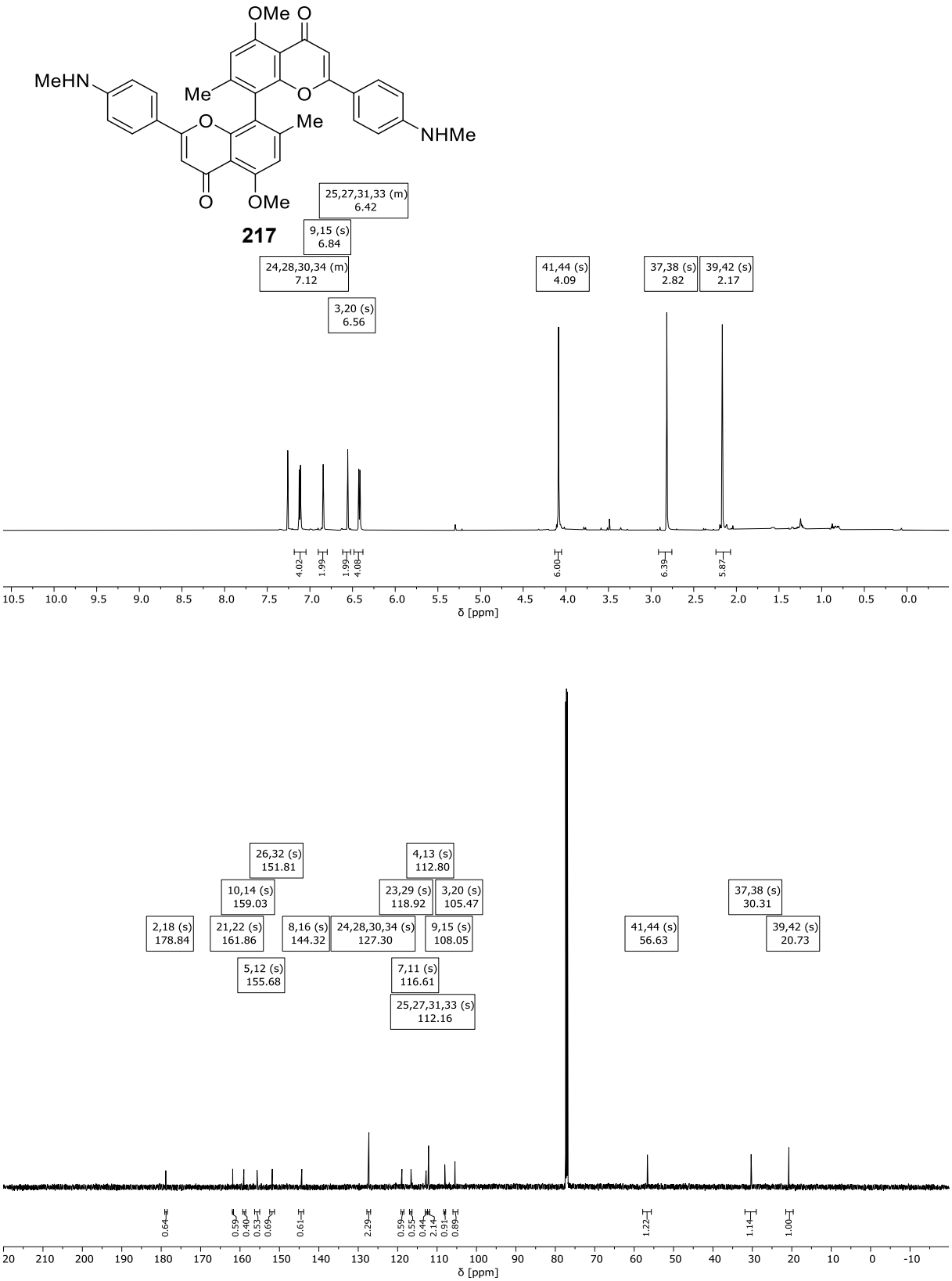

Figure 175: ^{1}H- and ^{13}C-NMR spectra (600 / 151 MHz, $CDCl_3$) of *rac*-5,5'-dimethoxy-7,7'-dimethyl-2,2'-bis(4-(methylamino)phenyl)-4H,4'H-[8,8'-bichromene]-4,4'-dione (**217**).

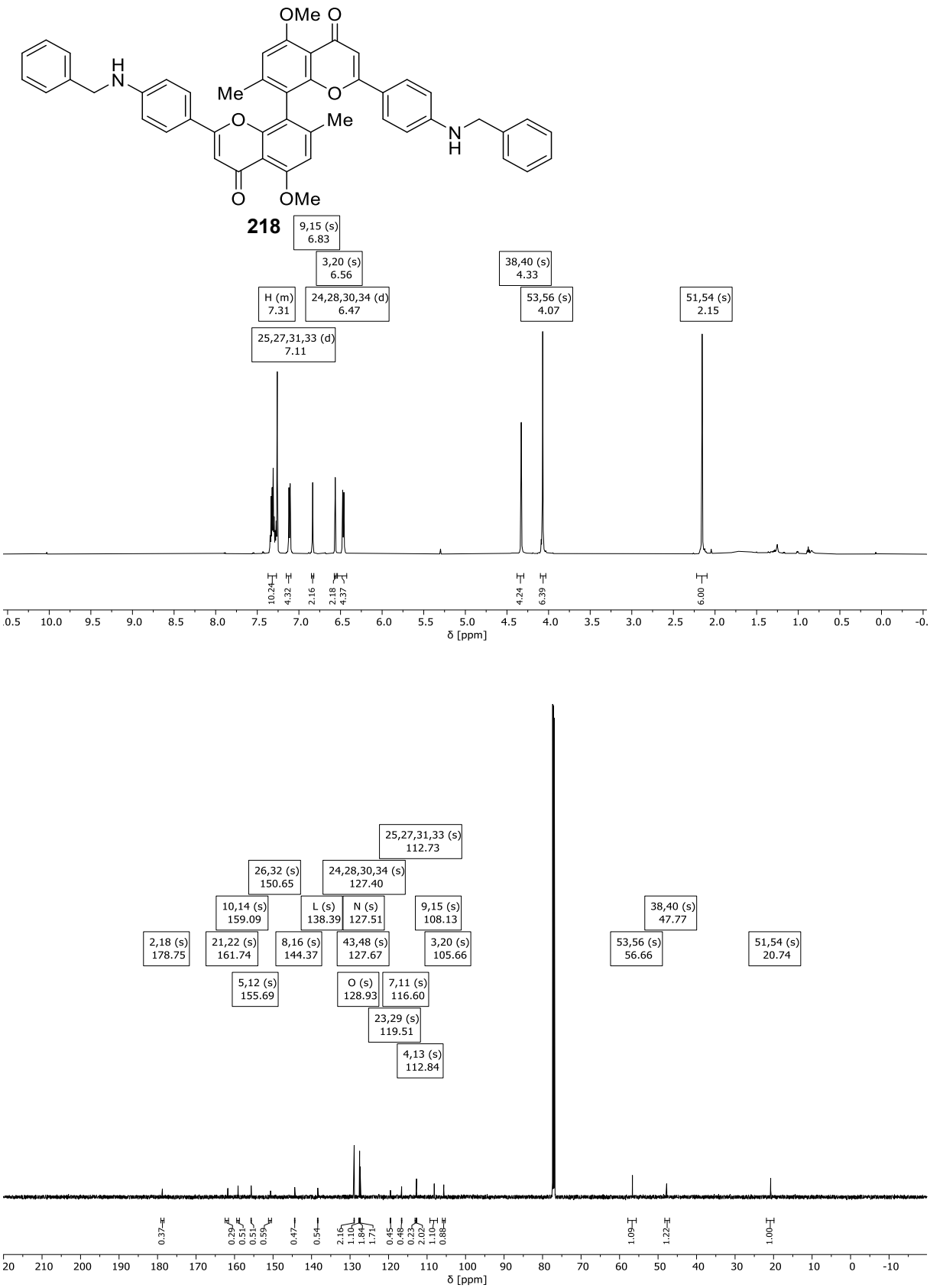

Figure 176: ^{1}H- and ^{13}C-NMR spectra (600 / 151 MHz, $CDCl_3$) of *rac*-2,2'-bis(4-(benzylamino)phenyl)-5,5'-dimethoxy-7,7'-dimethyl-4H,4'H-[8,8'-bichromene]-4,4'-dione (**218)**.

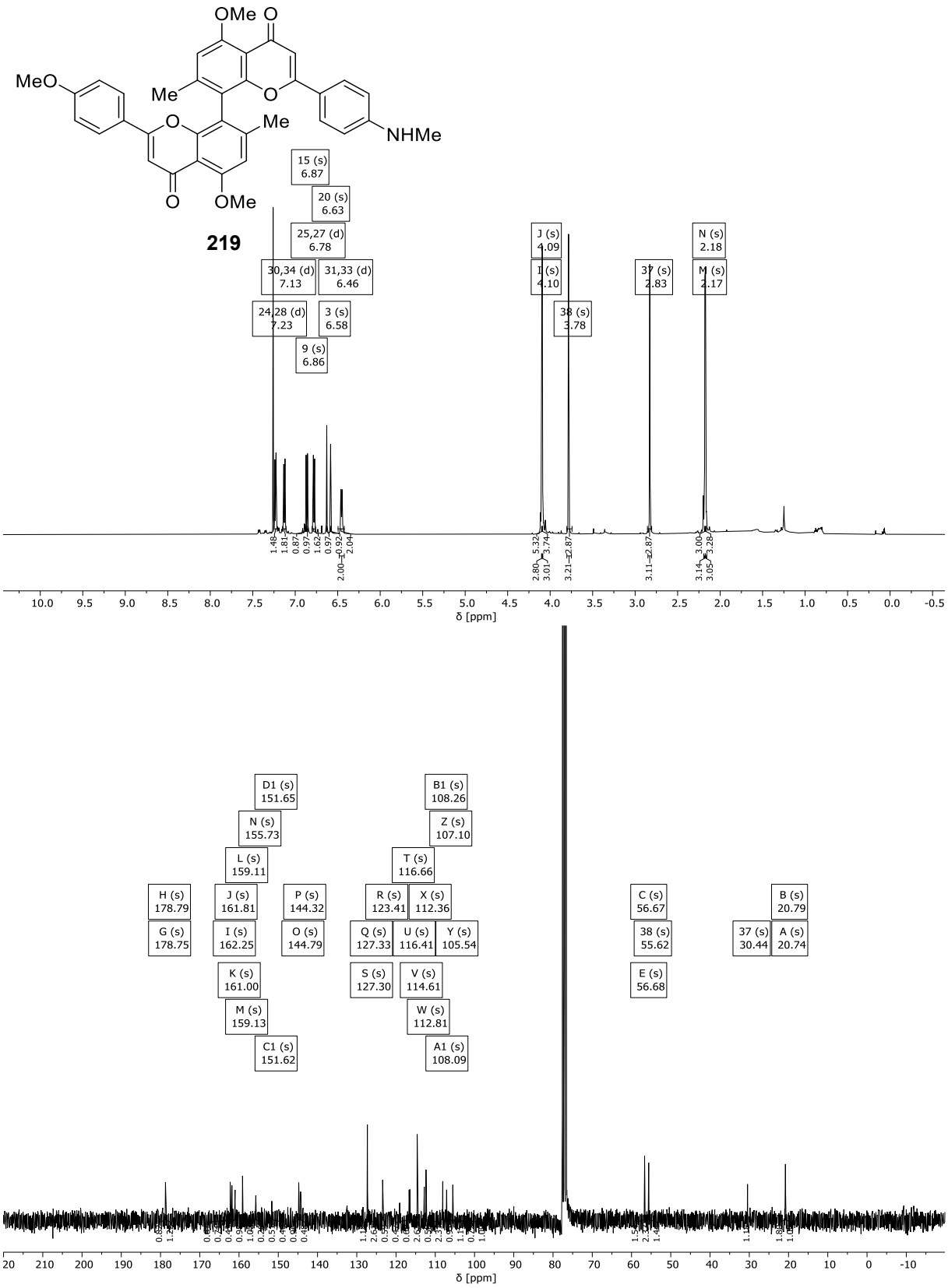

Figure 177: ^{1}H- and ^{13}C-NMR spectra (600 / 151 MHz, $CDCl_3$) of *rac*-5,5'-dimethoxy-2-(4-methoxyphenyl)-7,7'-dimethyl-2'-(4-(methylamino)phenyl)-4H,4'H-[8,8'-bichromene]-4,4'-dione (**219**).

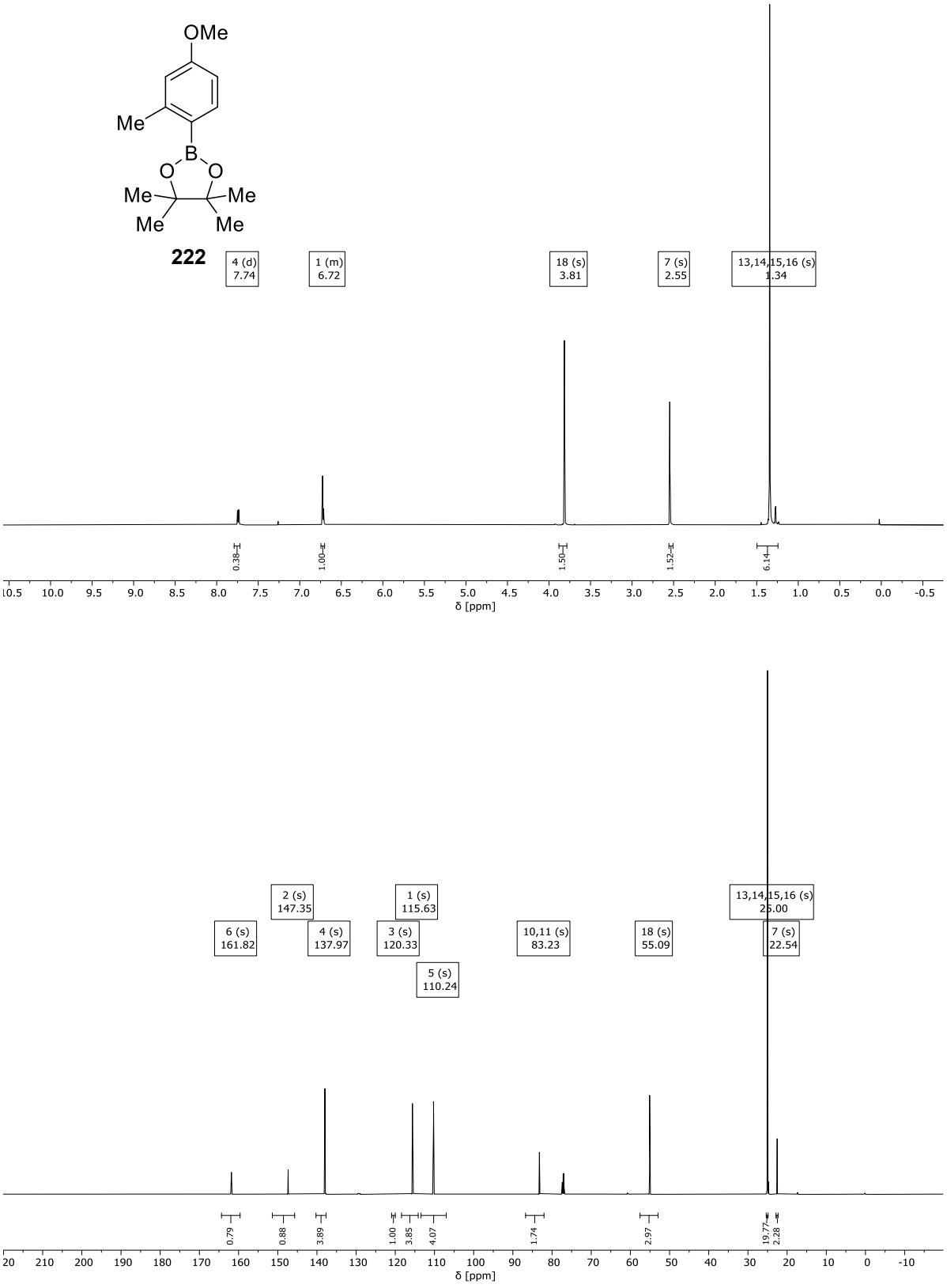

Figure 178: ^{1}H-, ^{13}C-NMR spectra (600 / 151 MHz, $CDCl_3$) of 2-(4-methoxy-2-methylphenyl)-4,4,5,5-tetramethyl-1,3,2-dioxaborolane (**222**).

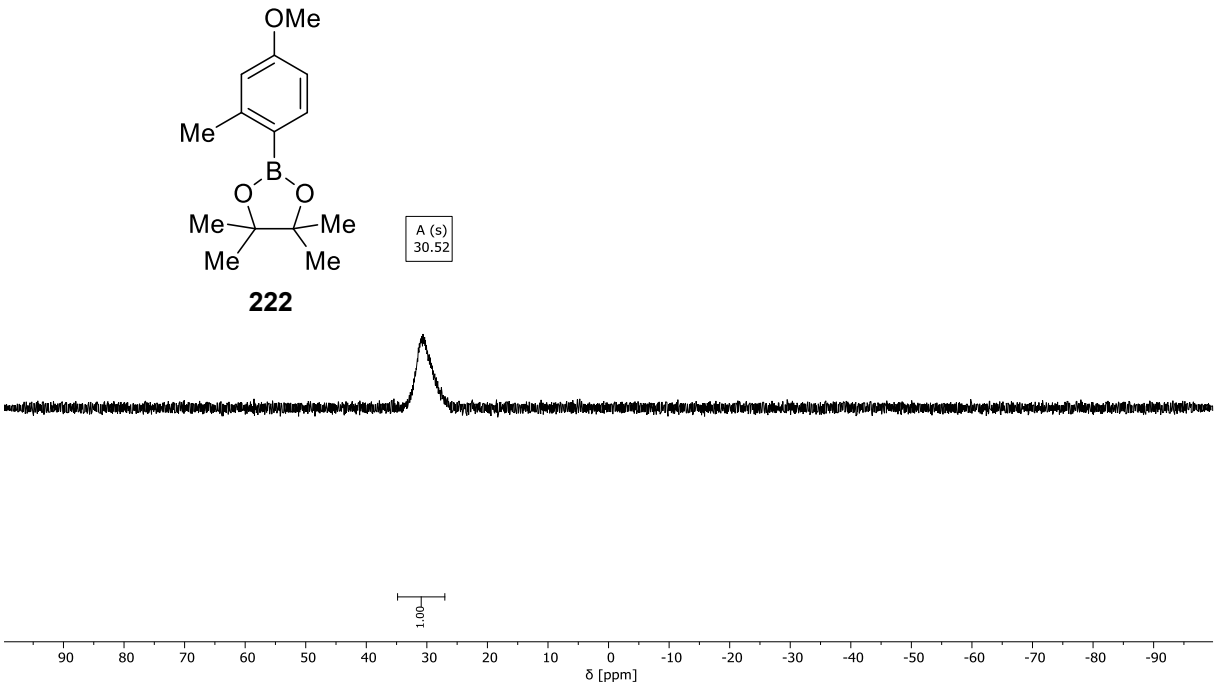

Figure 179: ^{11}B-NMR spectra (96 MHz, $CDCl_3$) of 2-(4-methoxy-2-methylphenyl)-4,4,5,5-tetramethyl-1,3,2-dioxaborolane (**222**).

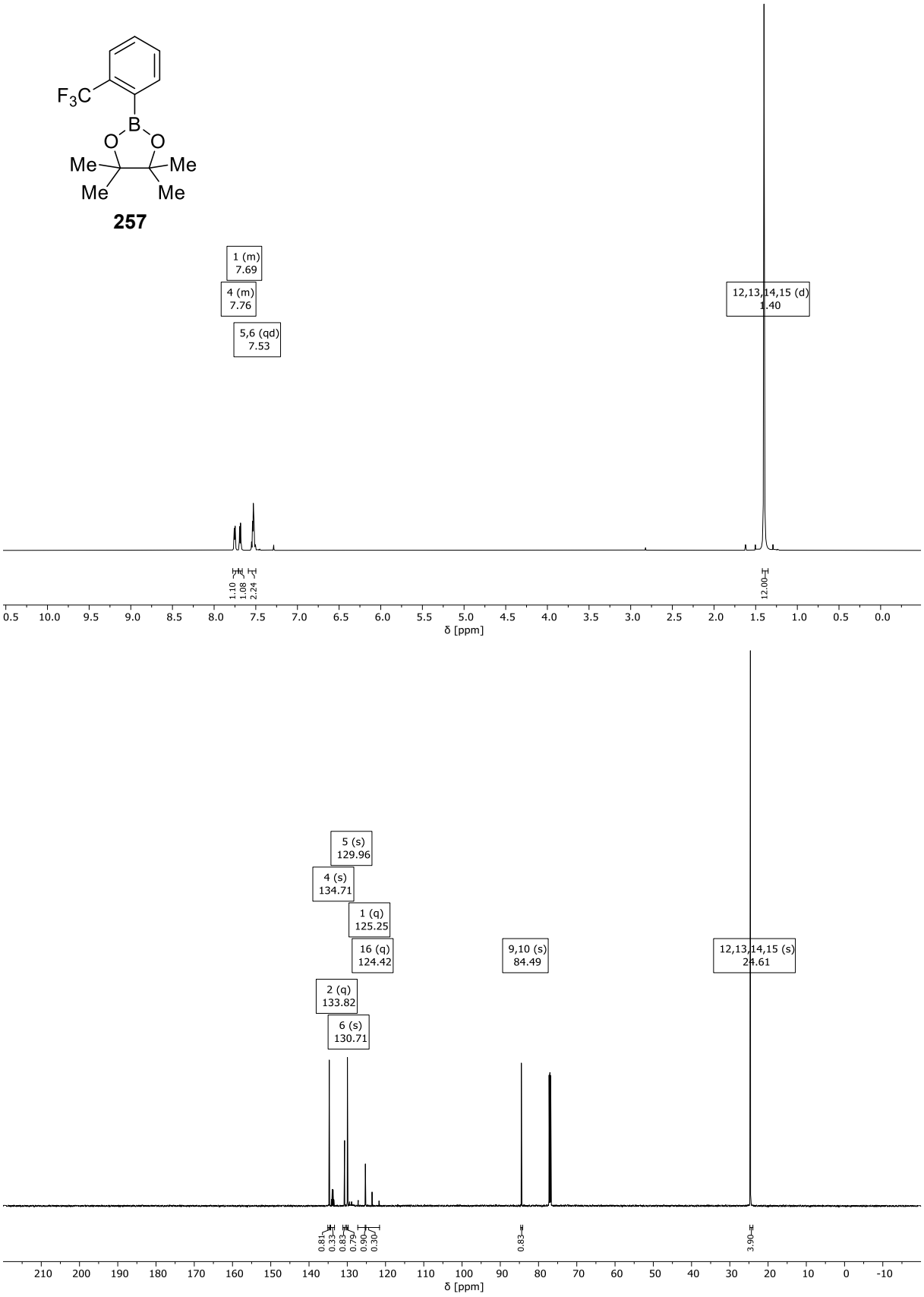

Figure 180: ^{1}H-, ^{13}C-NMR spectra (600 / 151 / 96 / 282 MHz, $CDCl_3$) of 4,4,5,5-tetramethyl-2-(2-(trifluoromethyl)phenyl)-1,3,2-dioxaborolane (**257**).

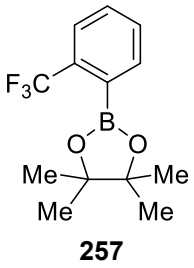

257

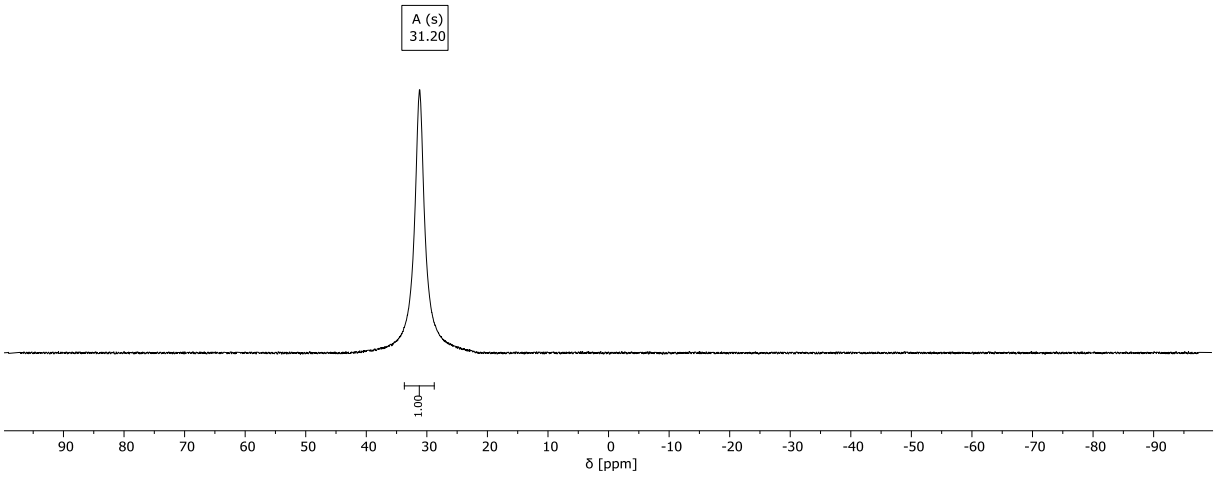

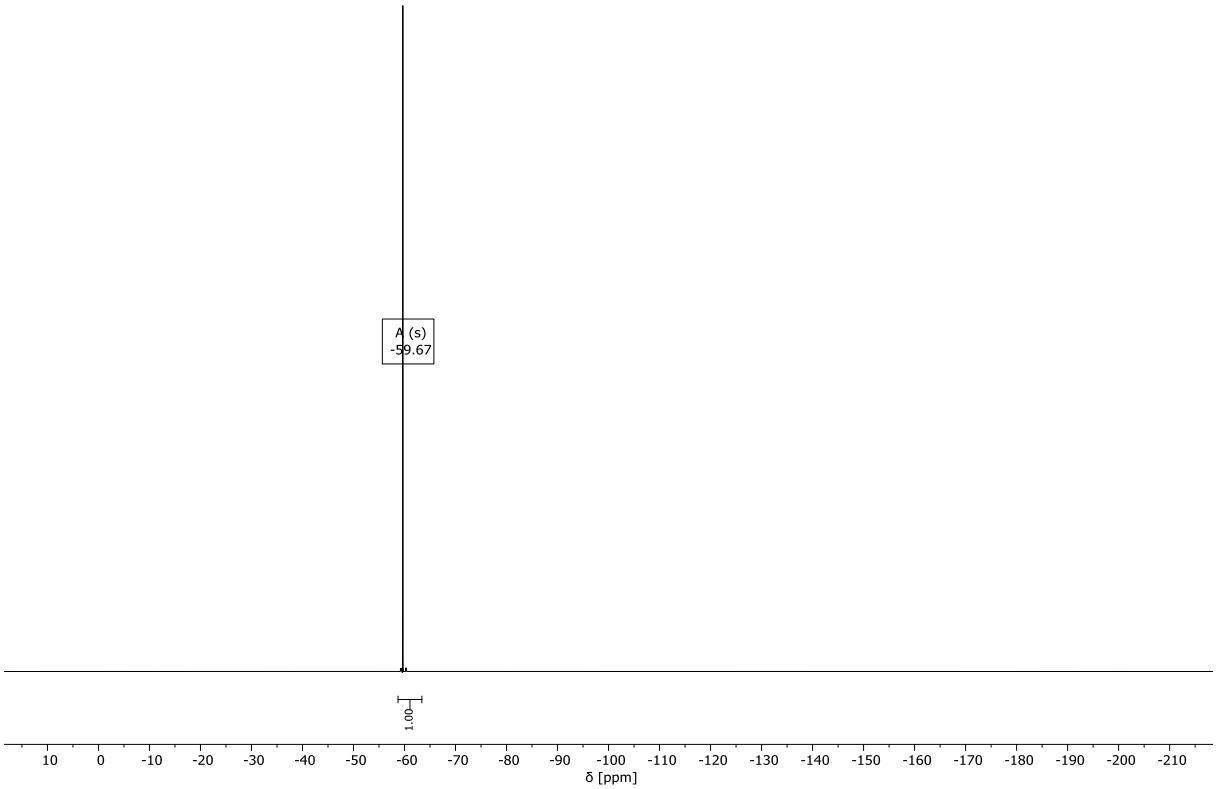

Figure 181: ^{11}B and ^{19}F-NMR spectra (96 / 282 MHz, $CDCl_3$) of 4,4,5,5-tetramethyl-2-(2-(trifluoromethyl)phenyl)-1,3,2-dioxaborolane (**257**).

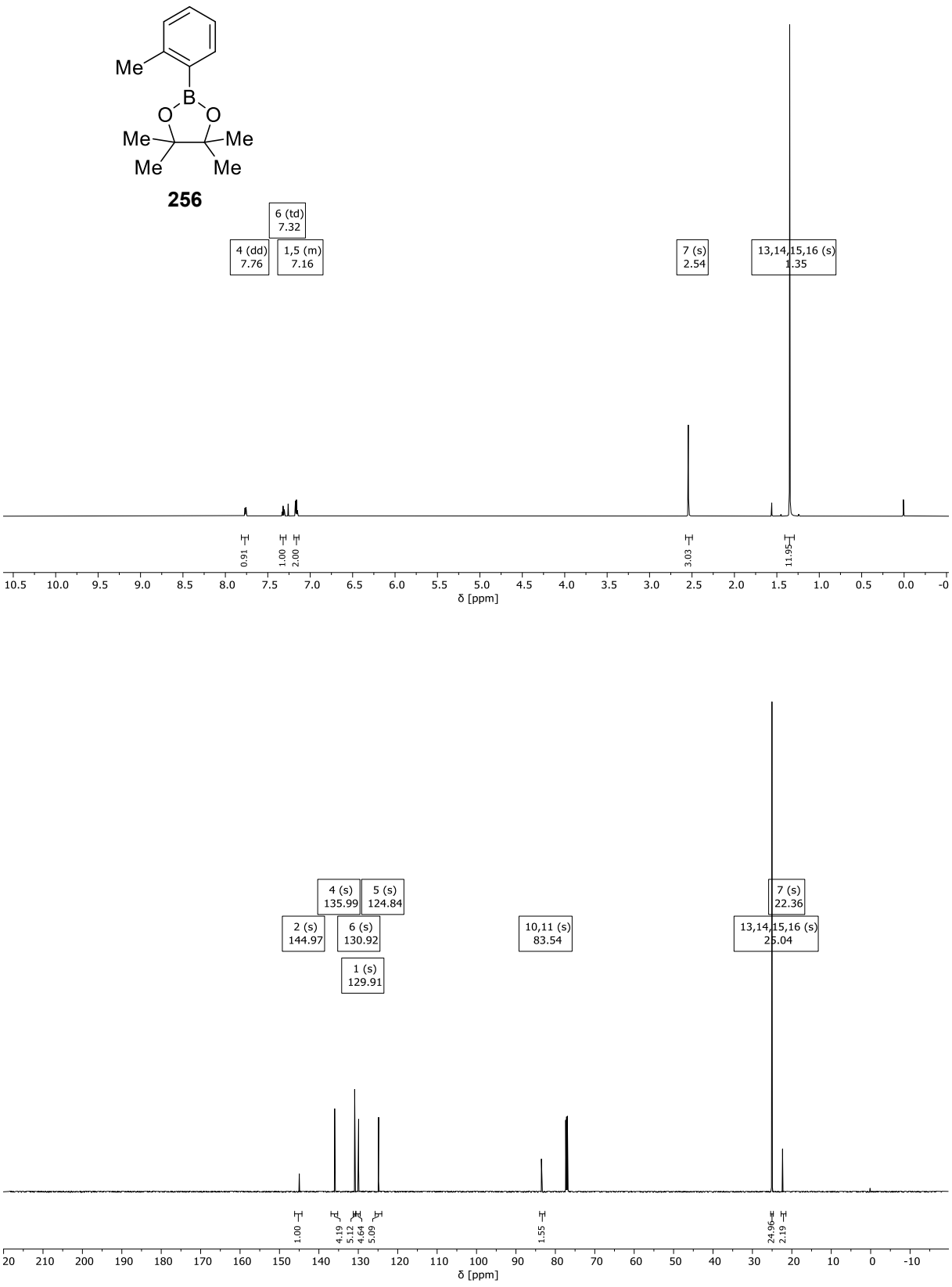

Figure 182: ^{1}H-, ^{13}C-NMR spectra (600 / 151 MHz, $CDCl_3$) of 4,4,5,5-tetramethyl-2-(o-tolyl)-1,3,2-dioxaborolane (**256**).

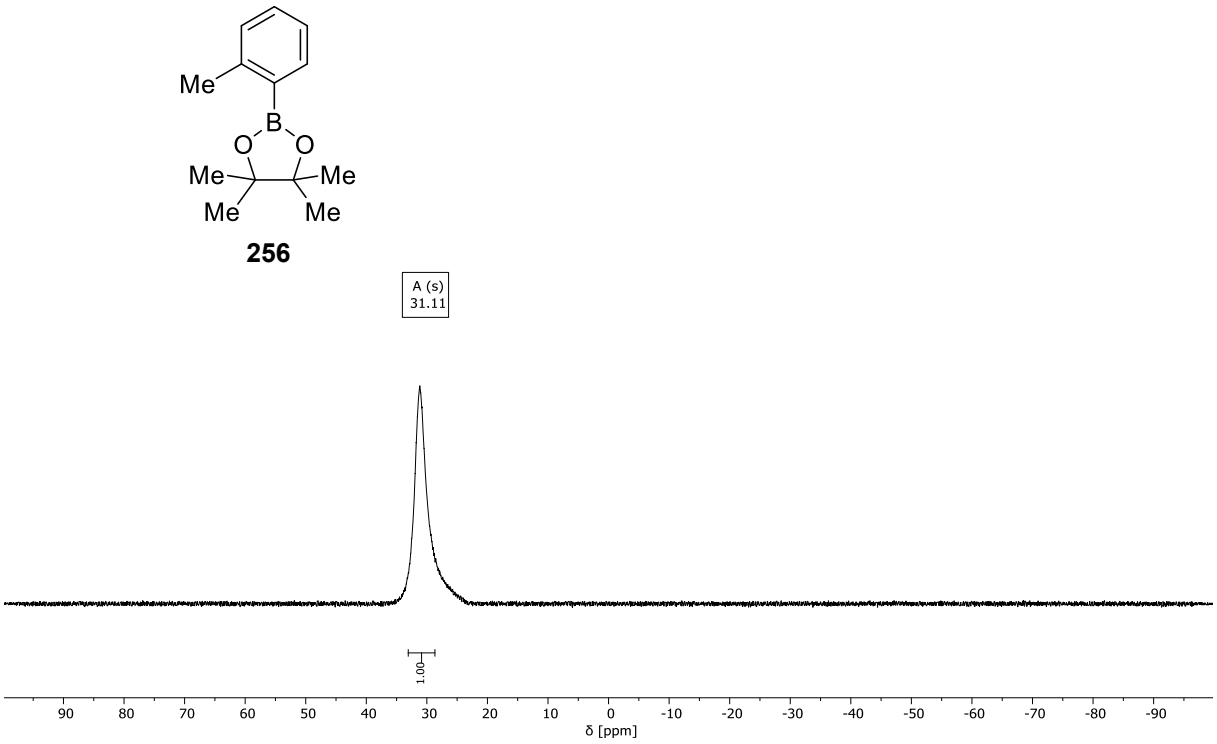

Figure 183: ^{11}B-NMR spectra (96 MHz, $CDCl_3$) of 4,4,5,5-tetramethyl-2-(o-tolyl)-1,3,2-dioxaborolane (**256**).

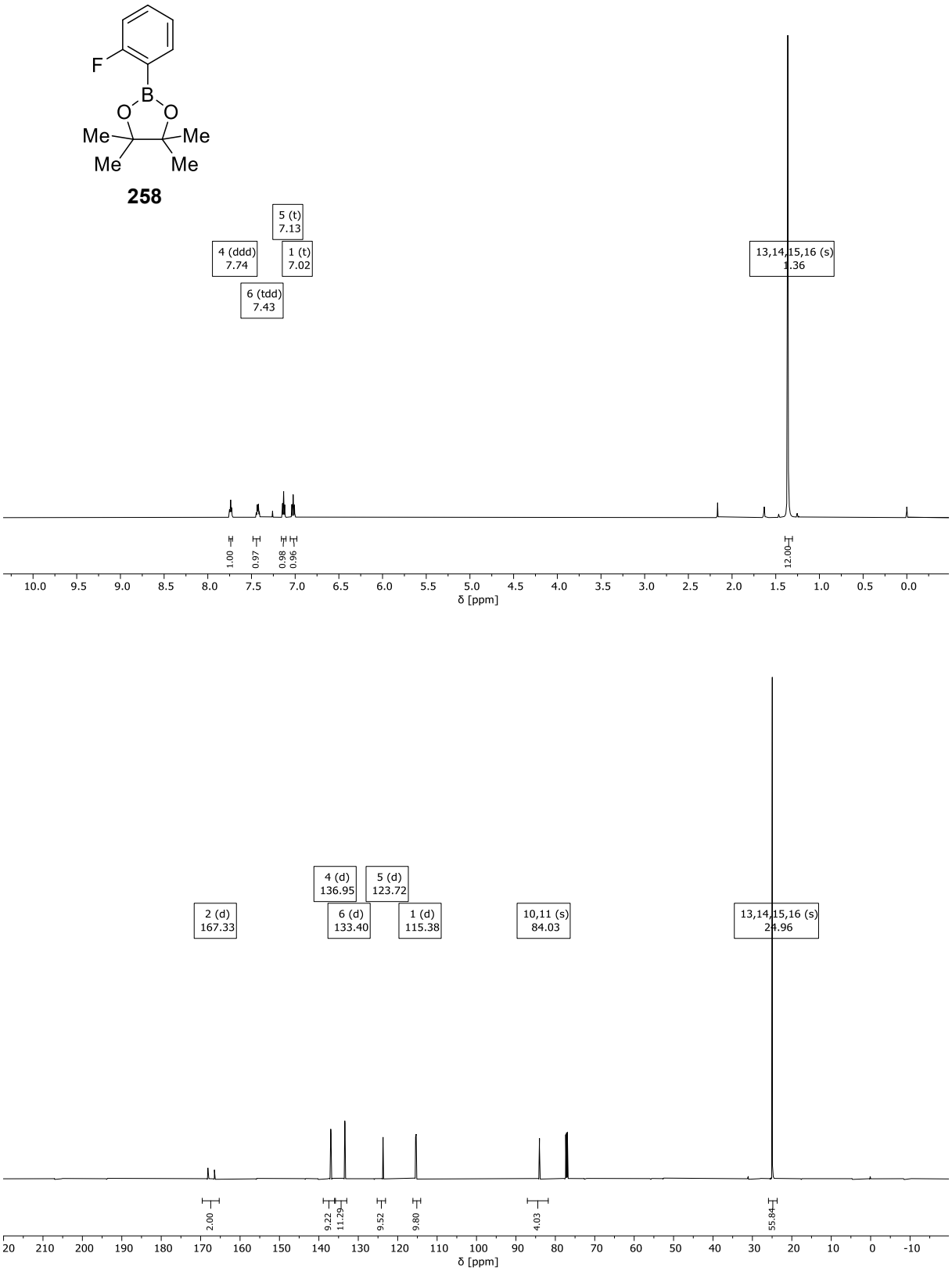

Figure 184: ^{1}H-, ^{13}C-NMR spectra (600 / 151 MHz, $CDCl_3$) of 2-(2-fluorophenyl)-4,4,5,5-tetramethyl-1,3,2-dioxaborolane (**258**).

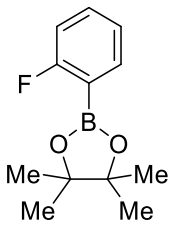

258

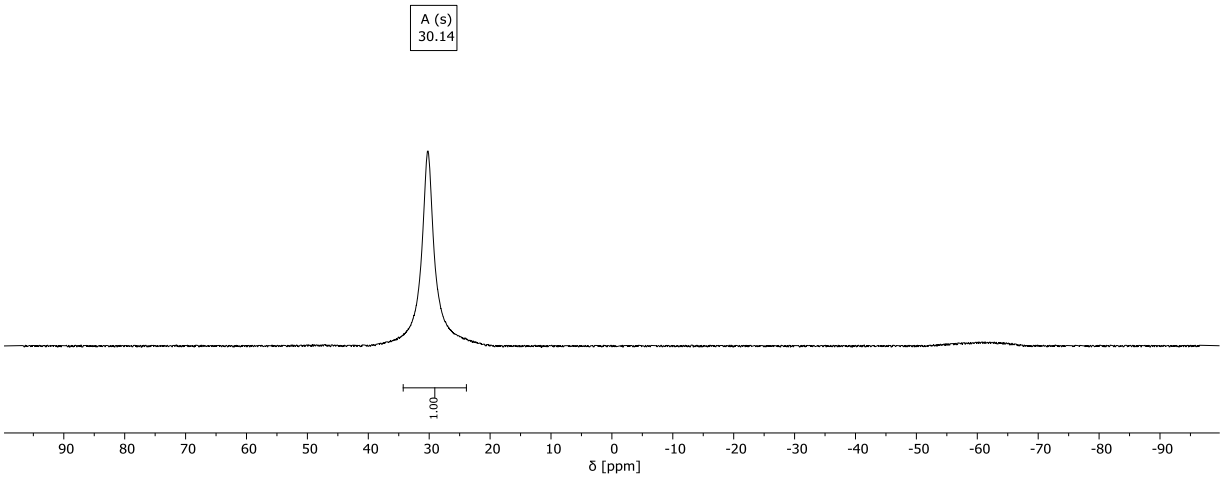

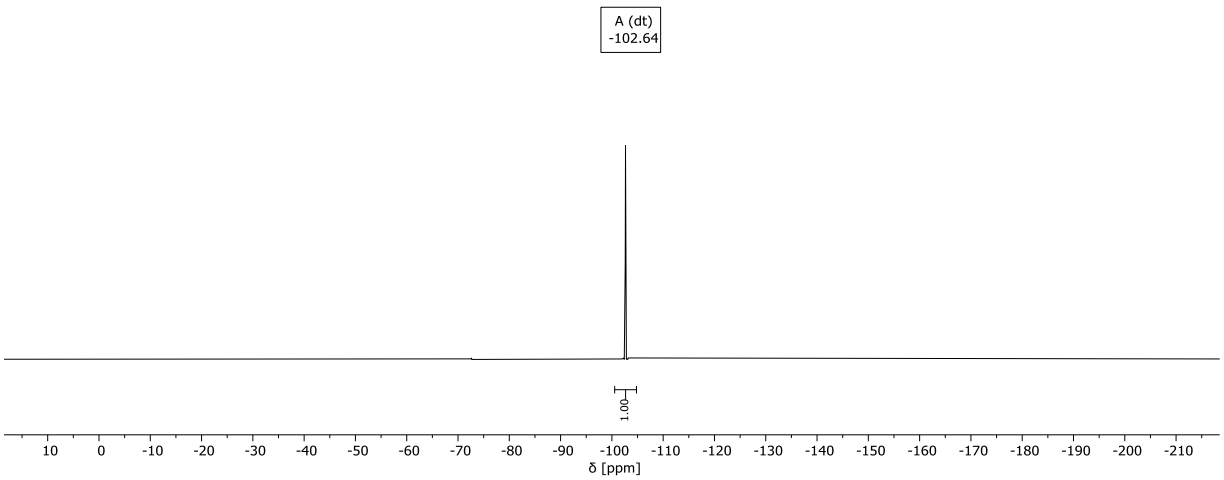

Figure 185: ^{11}B and ^{19}F-NMR spectra (96 / 282 MHz, $CDCl_3$) of 2-(2-fluorophenyl)-4,4,5,5-tetramethyl-1,3,2-dioxaborolane (**258**).

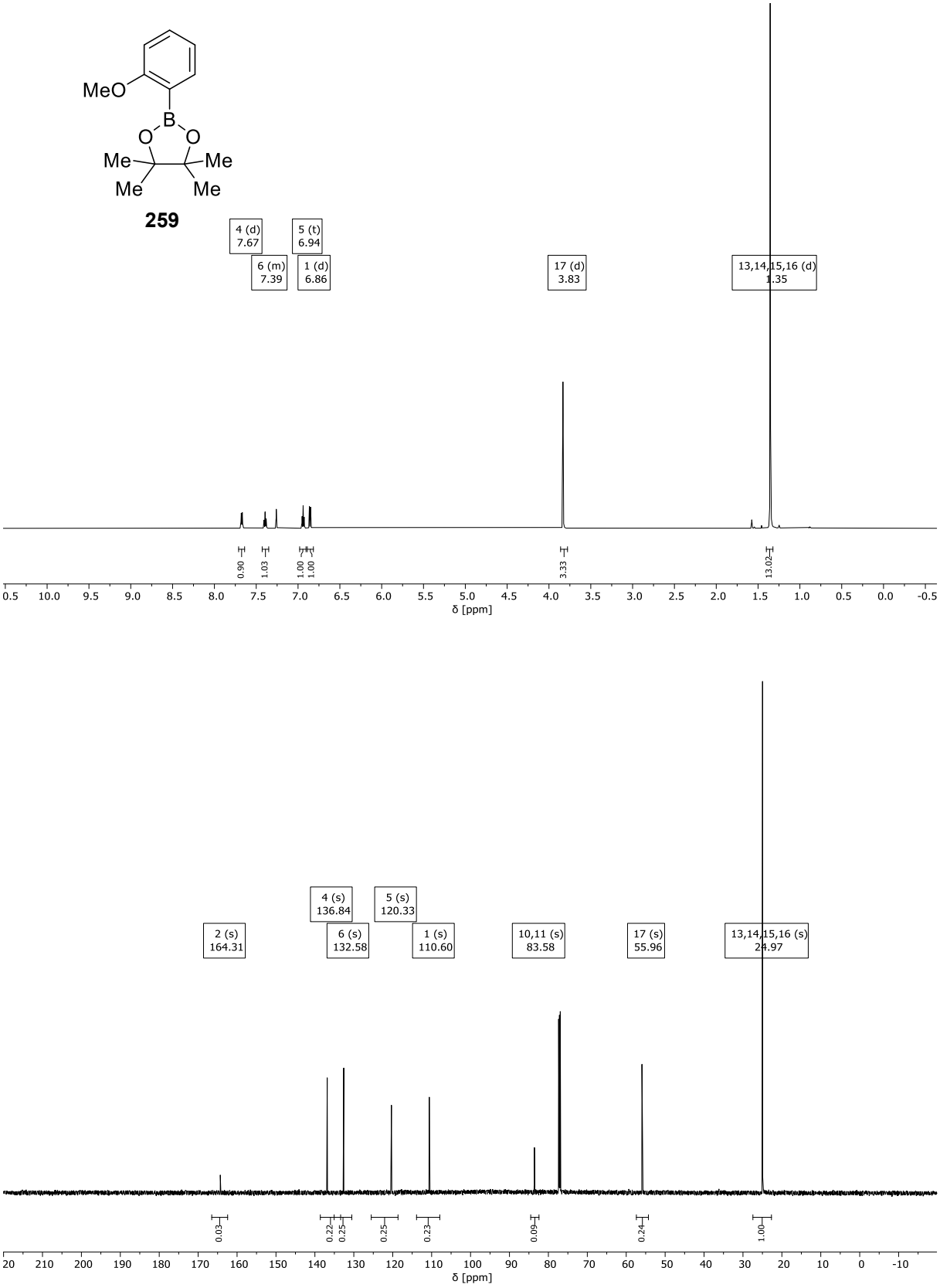

Figure 186: ^{1}H-, ^{13}C- and ^{11}B-NMR spectra (600 / 151 MHz, $CDCl_3$) of 2-(2-methoxyphenyl)-4,4,5,5-tetramethyl-1,3,2-dioxaborolane (**259**).

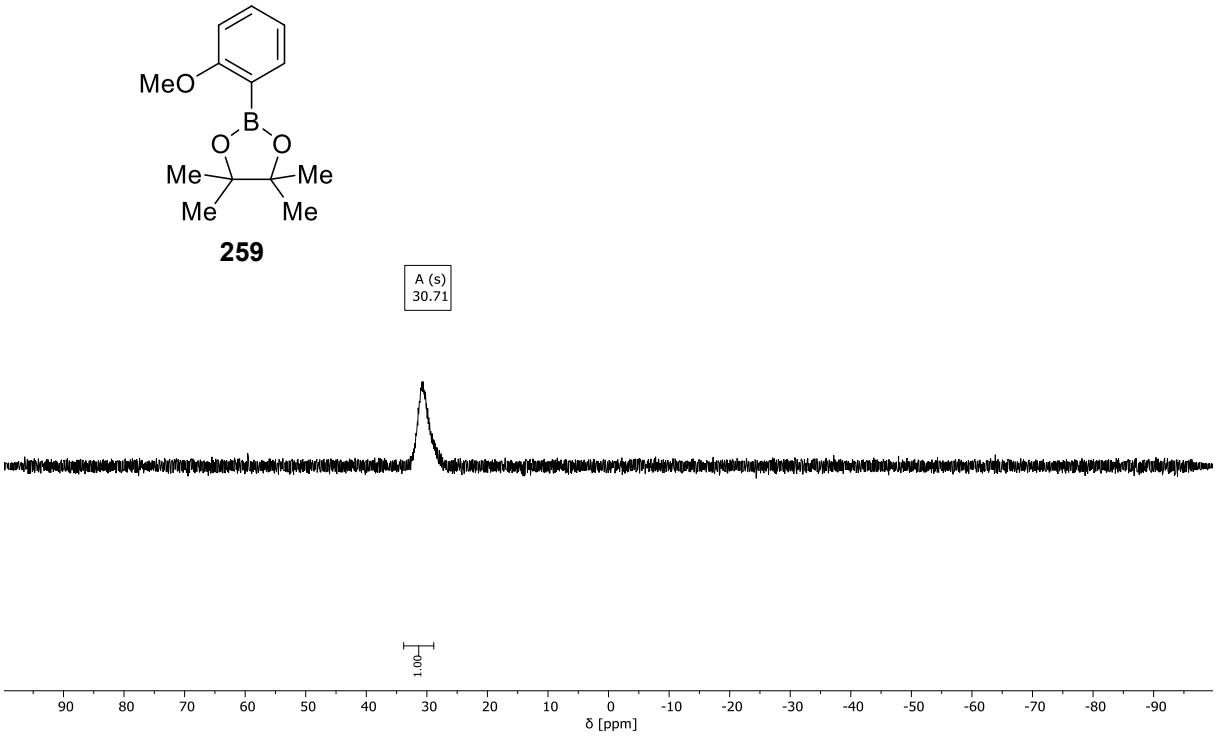

Figure 187: ^{11}B-NMR spectra (96 MHz, $CDCl_3$) of 2-(2-methoxyphenyl)-4,4,5,5-tetramethyl-1,3,2-dioxaborolane (**259**).

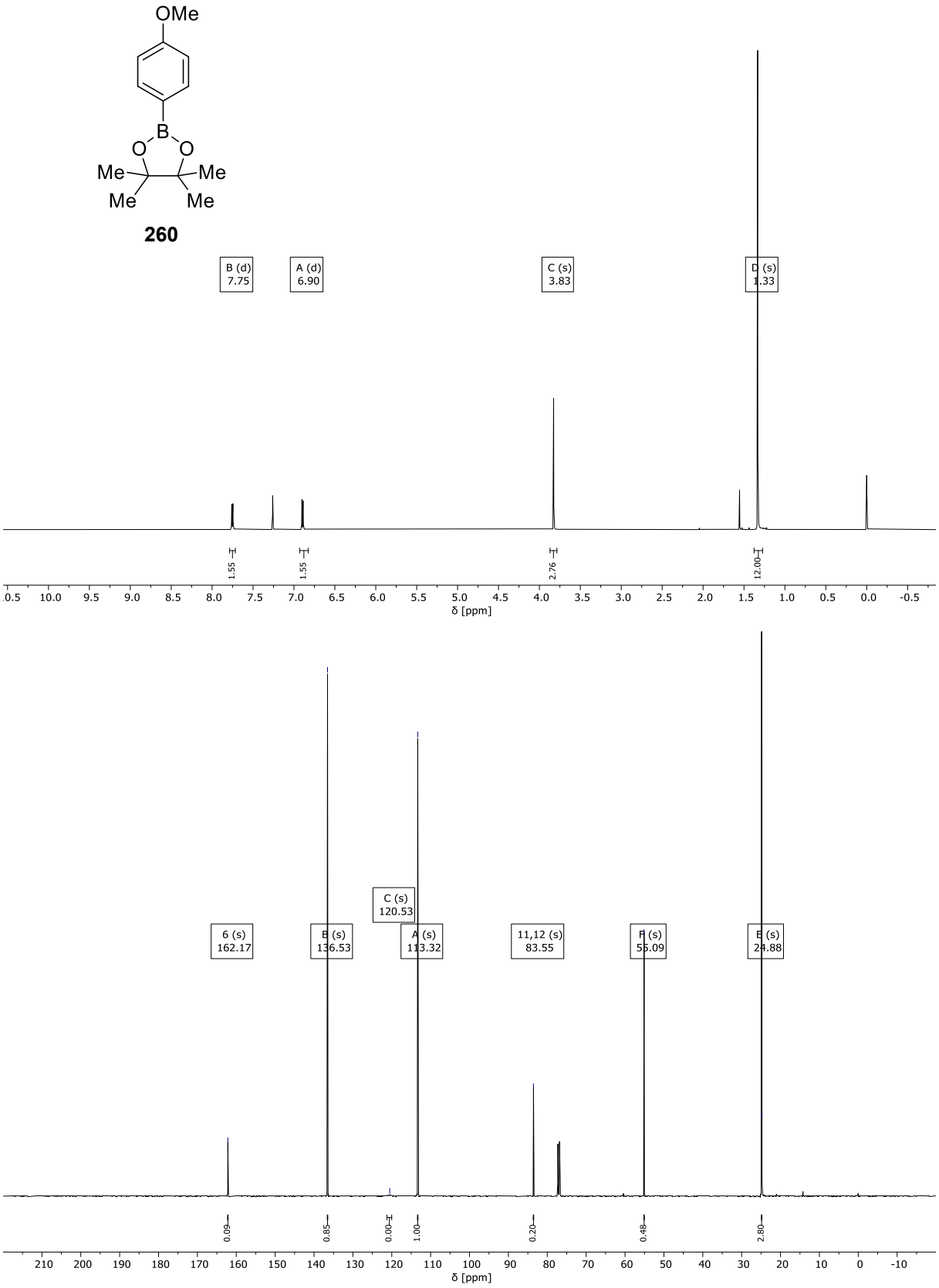

Figure 188: ^{1}H-, ^{13}C-NMR spectra (600 / 151 MHz, $CDCl_3$) of 2-(4-methoxyphenyl)-4,4,5,5-tetramethyl-1,3,2-dioxaborolane (**260**).

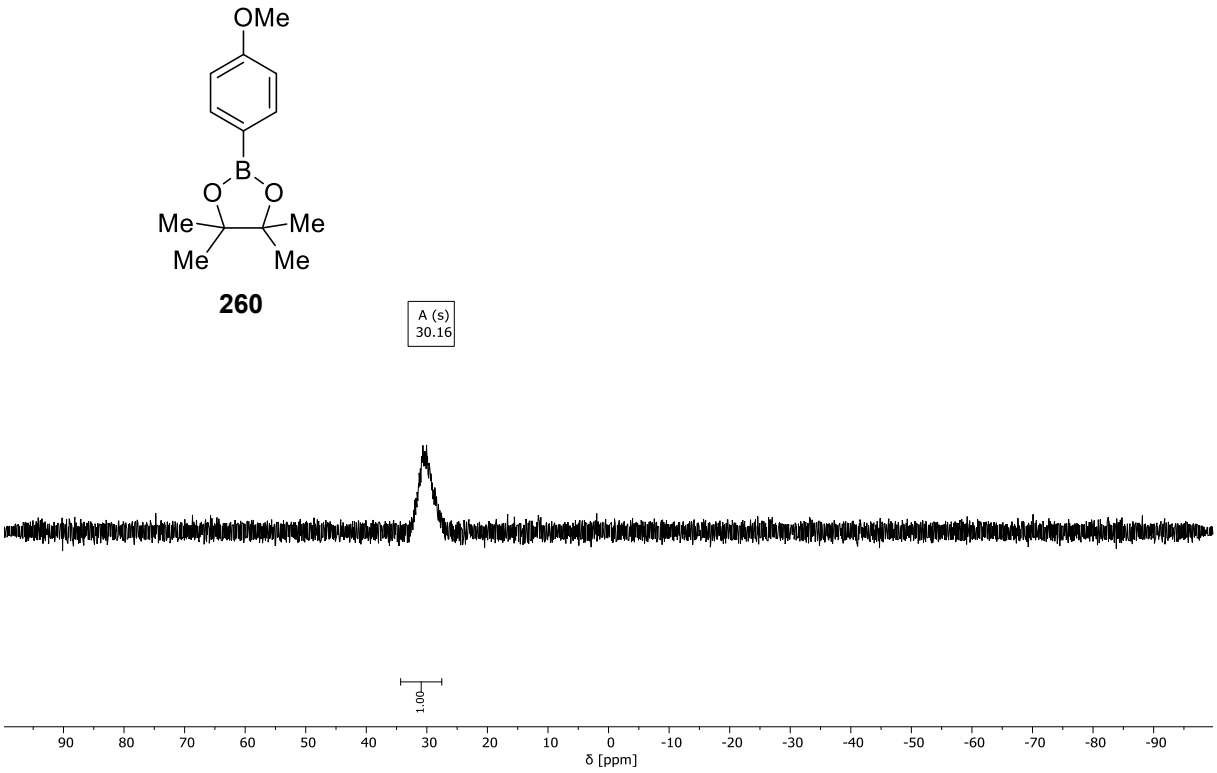

Figure 189: ^{11}B-NMR spectrum (96 MHz, $CDCl_3$) of 2-(4-methoxyphenyl)-4,4,5,5-tetramethyl-1,3,2-dioxaborolane (**260**).

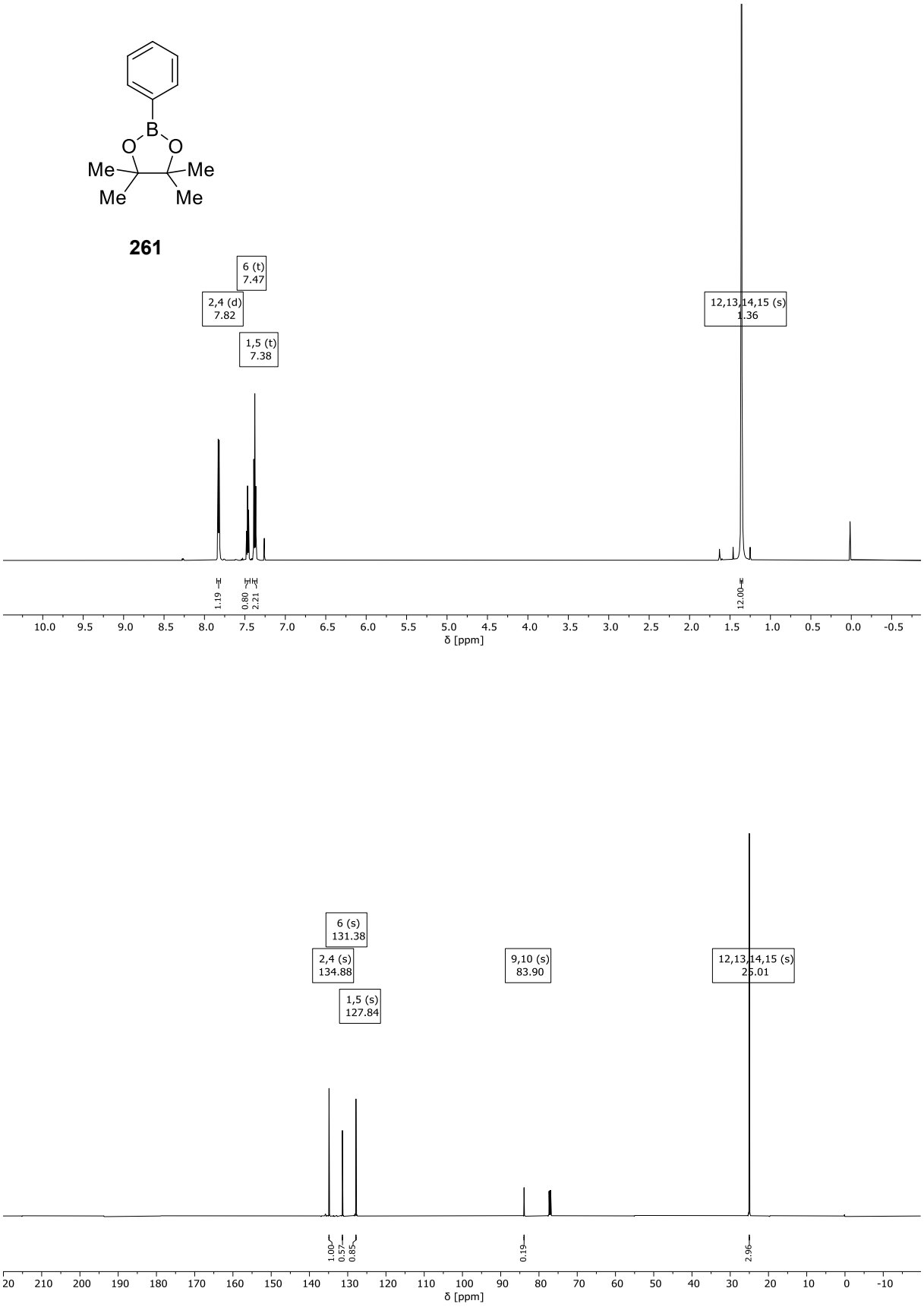

Figure 190: ^{1}H-, ^{13}C-NMR spectra (600 / 151 MHz, $CDCl_3$) of 4,4,5,5-tetramethyl-2-phenyl-1,3,2-dioxaborolane (**261**).

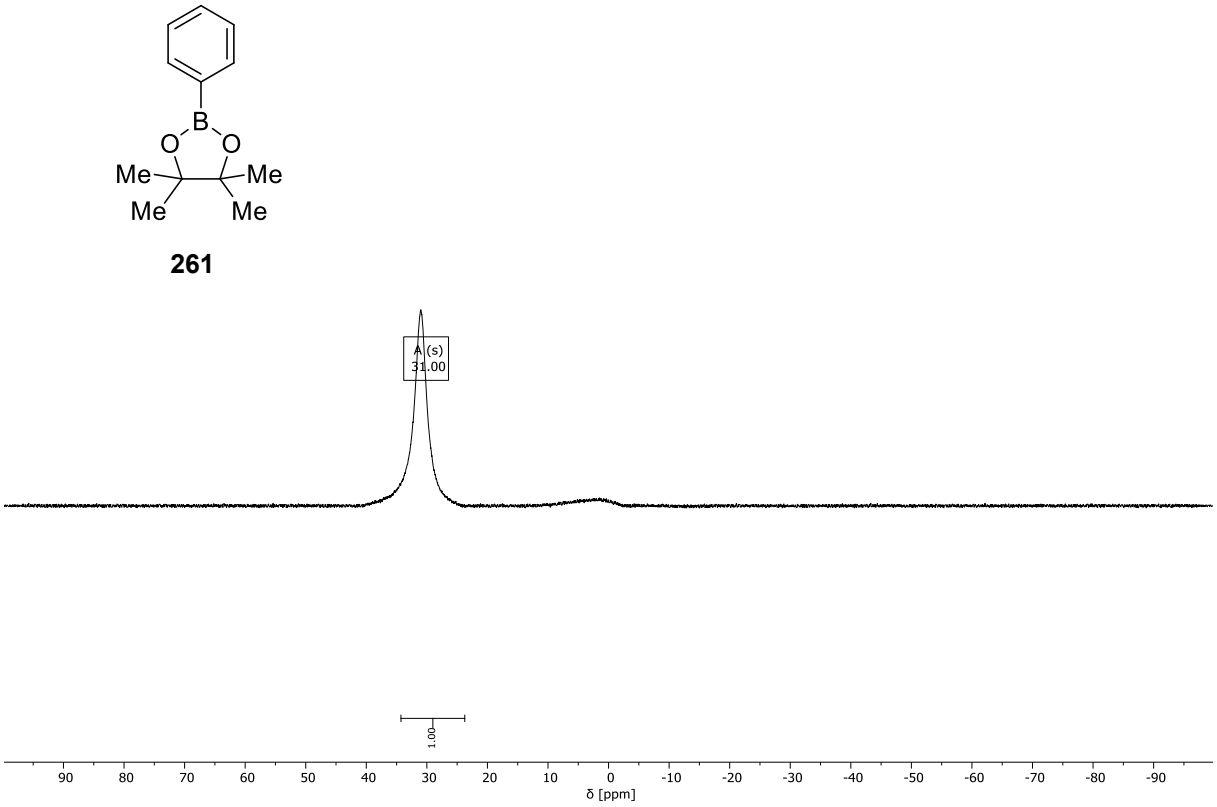

261

Figure 191: ^{11}B-NMR spectra (96 MHz, $CDCl_3$) of 4,4,5,5-tetramethyl-2-phenyl-1,3,2-dioxaborolane (**261**).

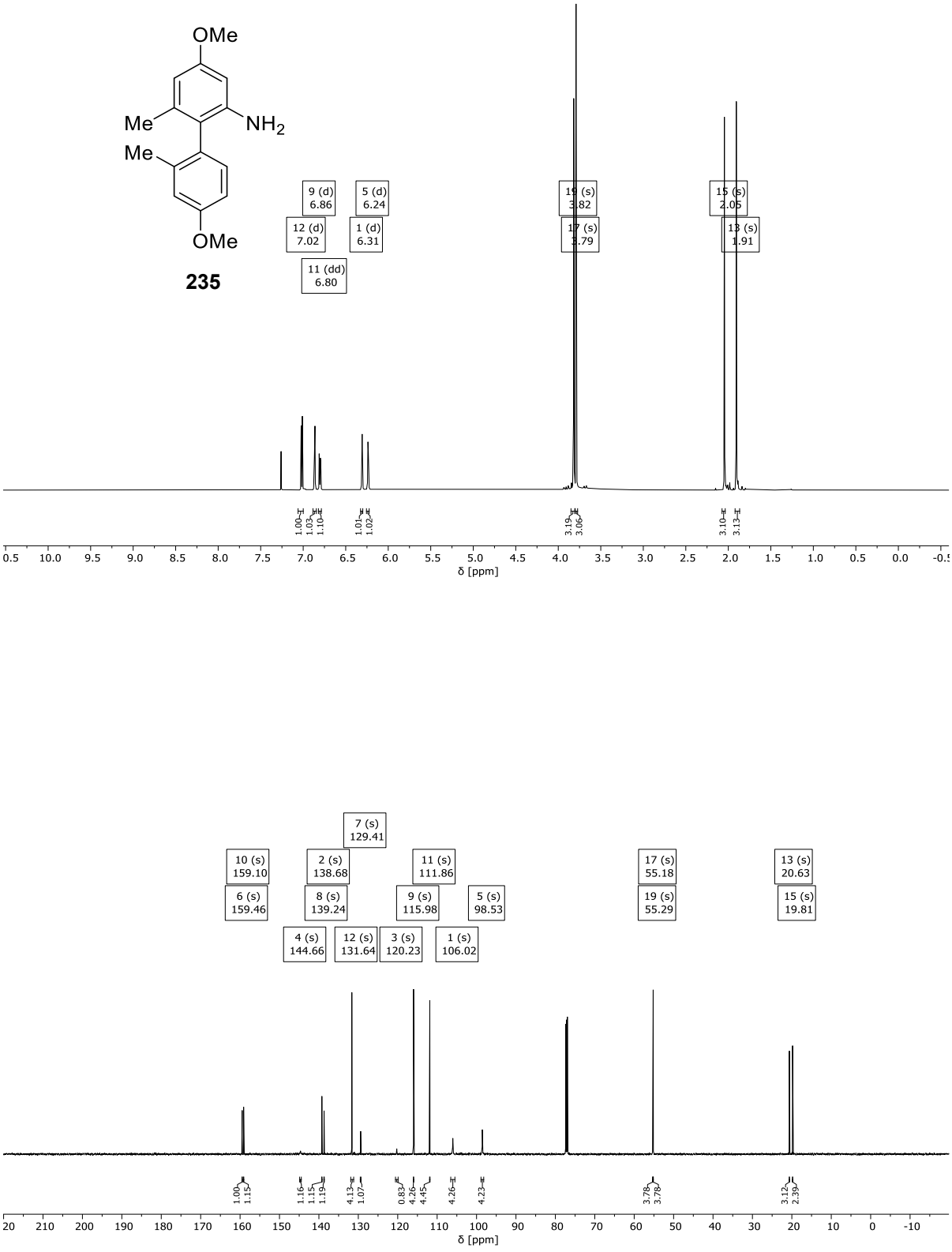

Figure 192: ^{1}H- and ^{13}C-NMR spectra (600 / 151 MHz, $CDCl_3$) of 4,4'-dimethoxy-2',6-dimethyl-[1,1'-biphenyl]-2-amine (**235**).

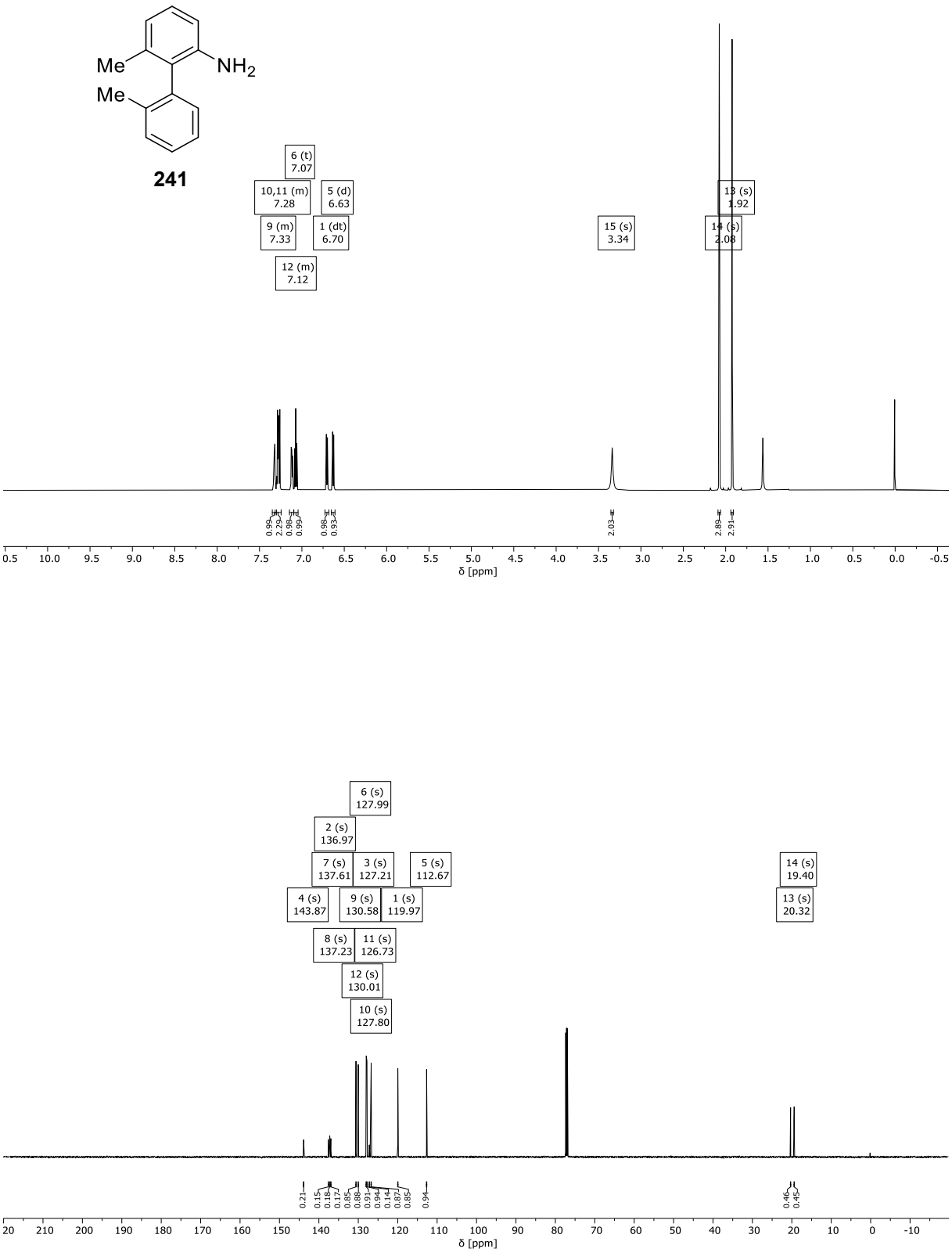

Figure 193: ^{1}H- and ^{13}C-NMR spectra (600 / 151 MHz, $CDCl_3$) of 2',6-dimethyl-[1,1'-biphenyl]-2-amine (**241**).

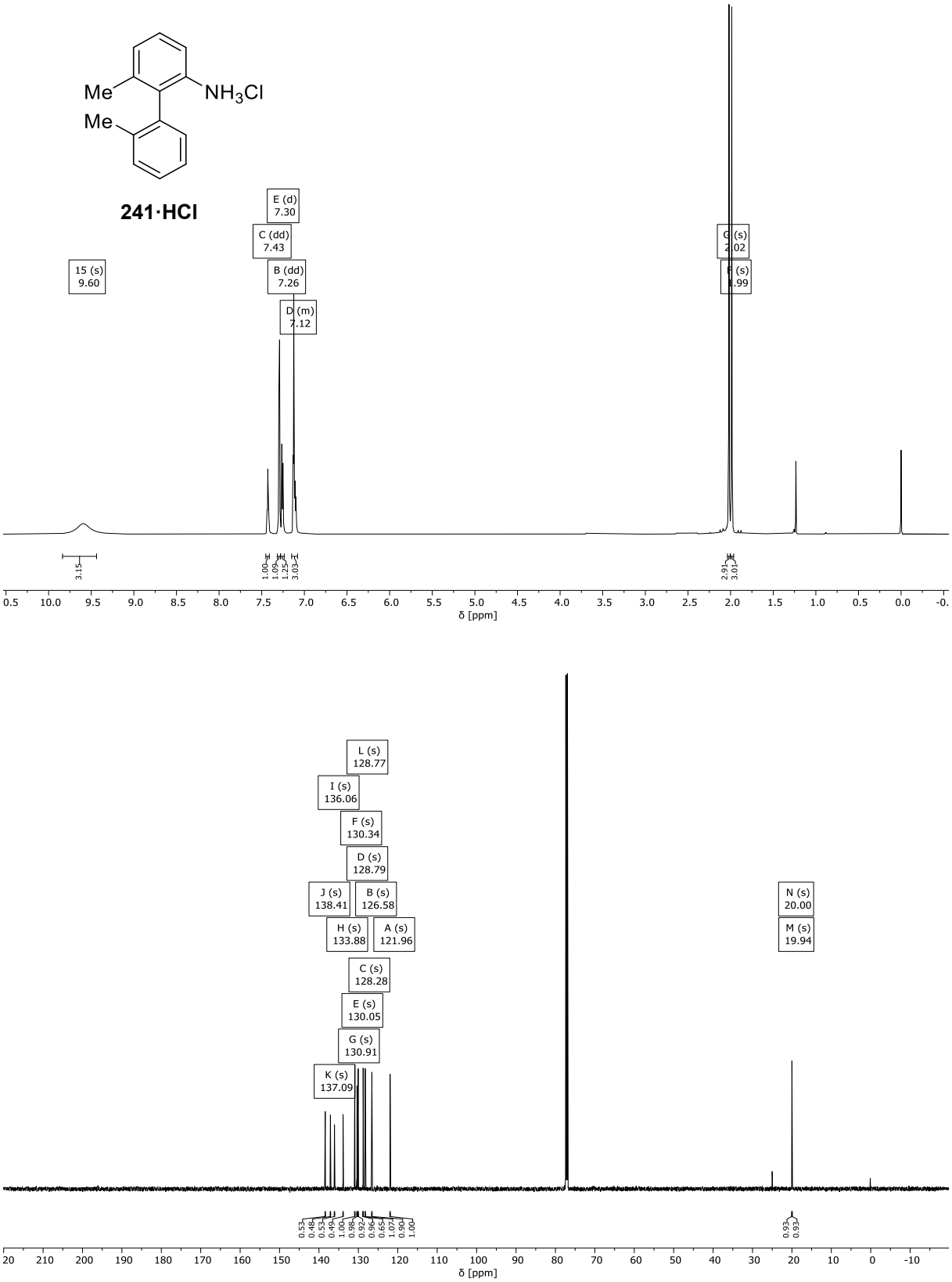

Figure 194: ^{1}H- and ^{13}C-NMR spectra (600 / 151 MHz, $CDCl_3$) of 2',6-dimethyl-[1,1'-biphenyl]-2-aminium chloride (**241·HCl**).

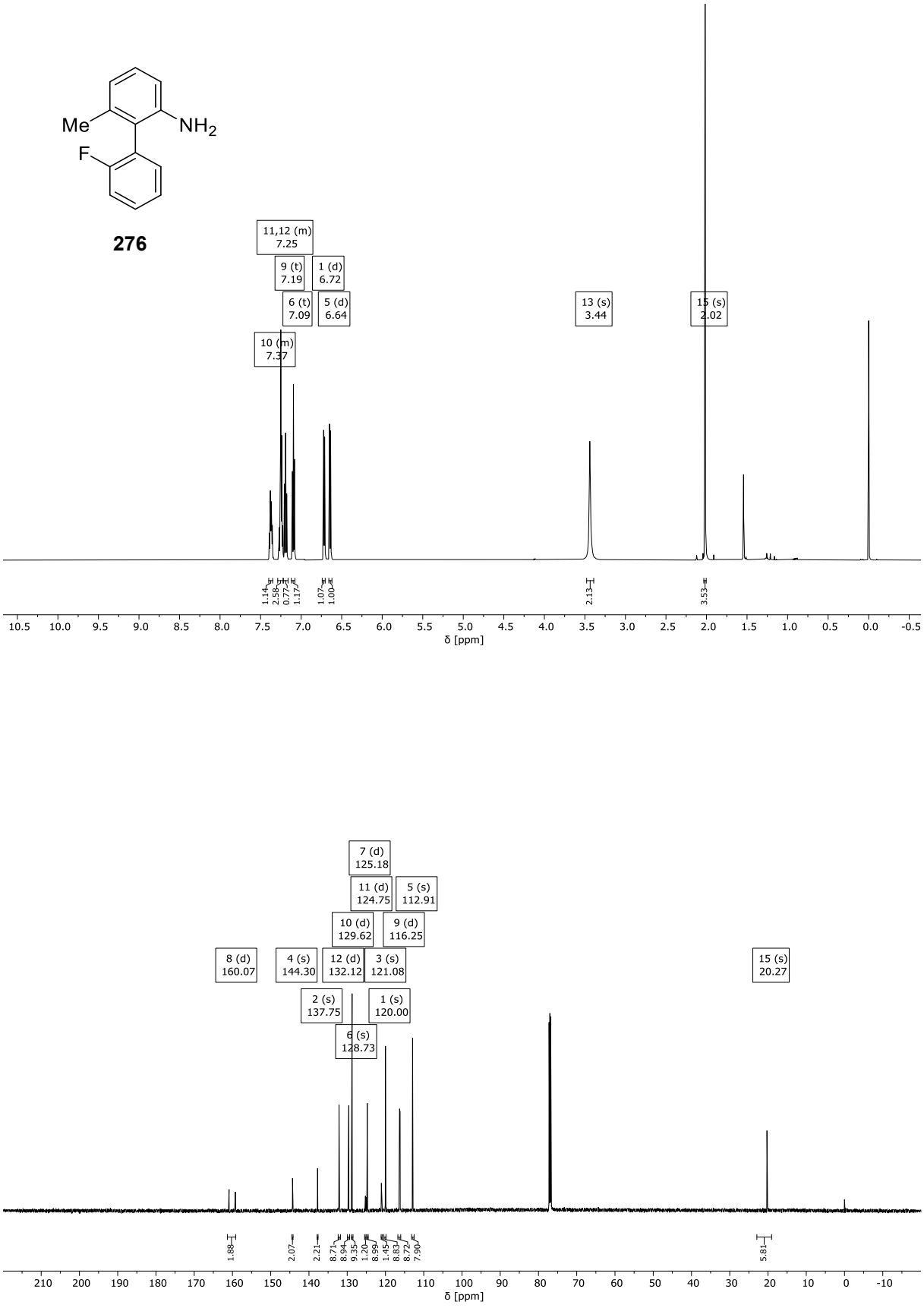

Figure 195: ^{1}H-, ^{13}C-NMR spectra (600 / 151 MHz, $CDCl_3$) of 2'-fluoro-6-methyl-[1,1'-biphenyl]-2-amine (**276**).

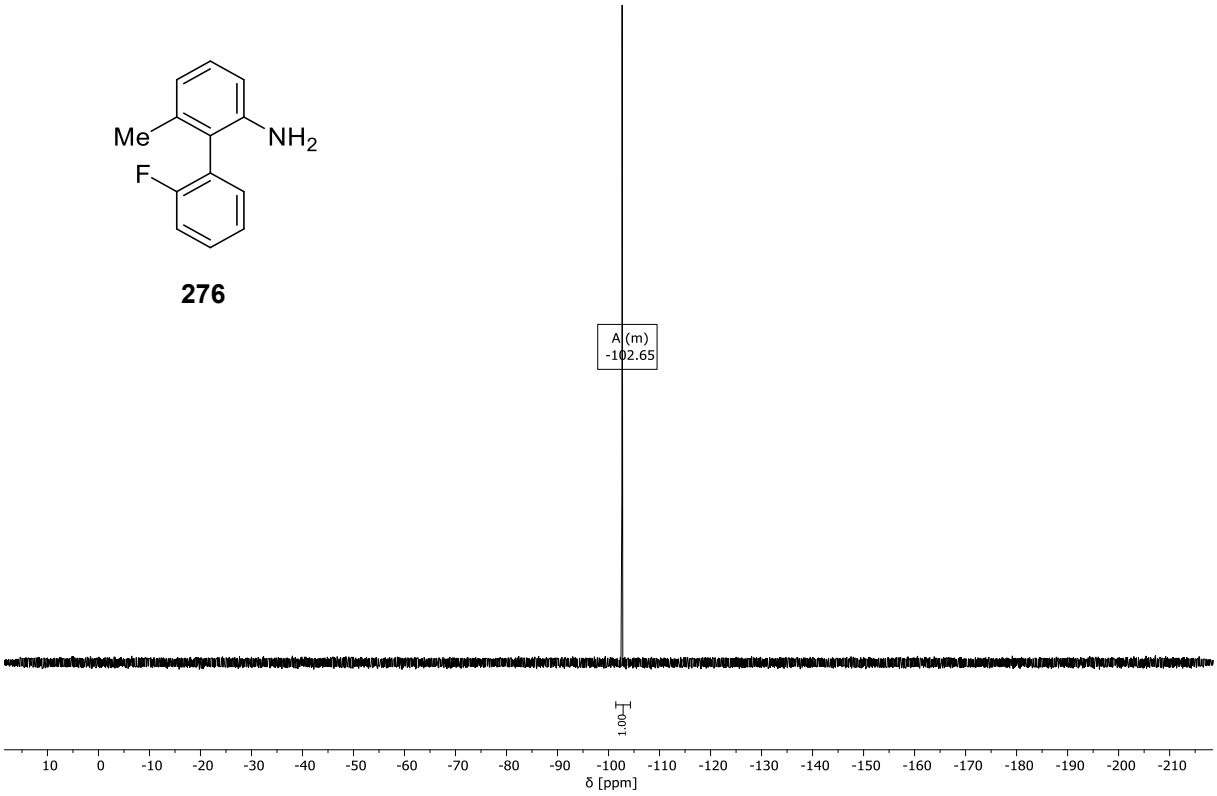

Figure 196: ^{19}F-NMR spectra (282 MHz, $CDCl_3$) of 2'-fluoro-6-methyl-[1,1'-biphenyl]-2-amine (**276**).

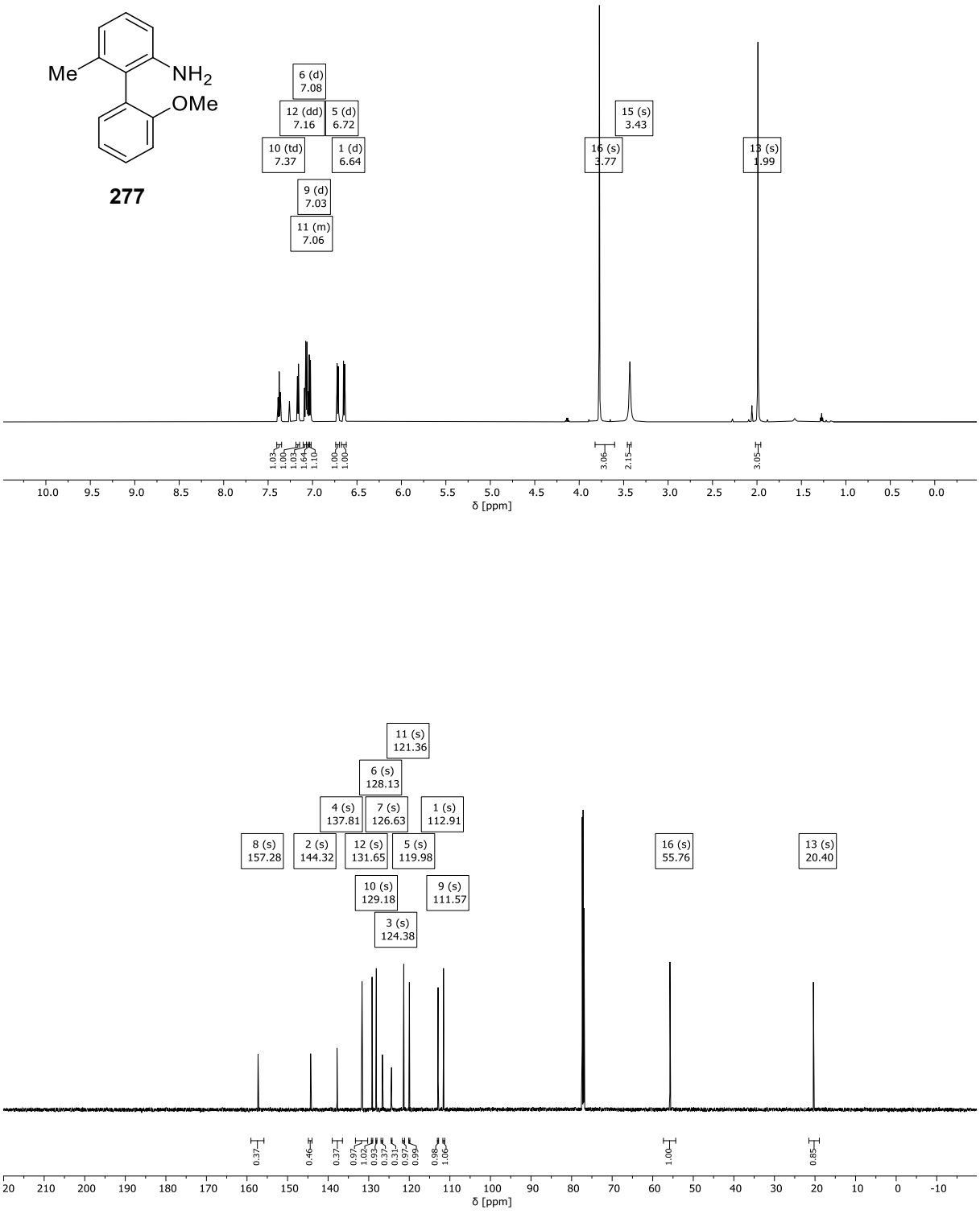

Figure 197: ^{1}H- and ^{13}C-NMR spectra (600 / 151 MHz, $CDCl_3$) of 2'-methoxy-6-methyl-[1,1'-biphenyl]-2-amine (**277**).

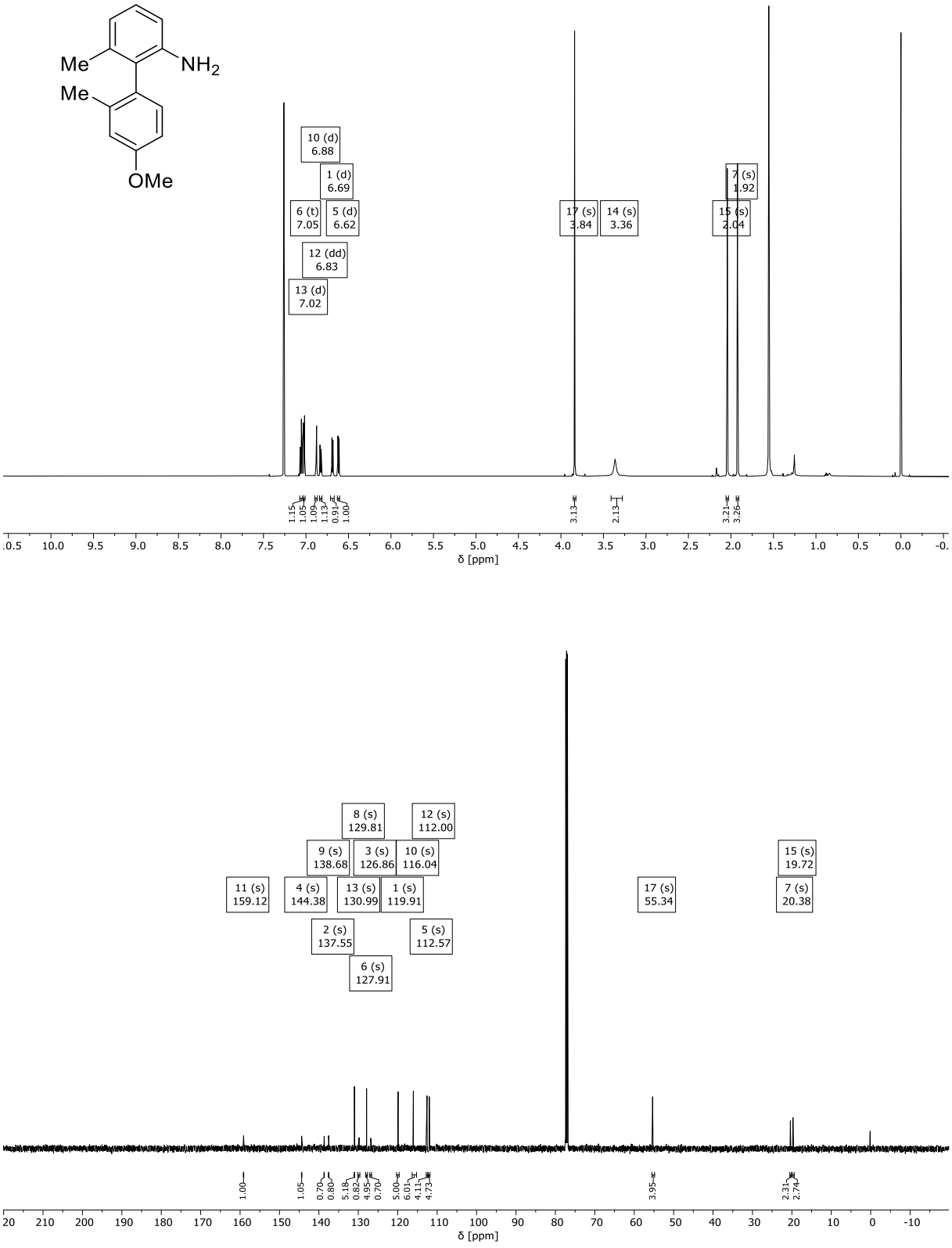

Figure 198: ^{1}H- and ^{13}C-NMR spectra (600 / 151 MHz, $CDCl_3$) of 4'-methoxy-2',6-dimethyl-[1,1'-biphenyl]-2-amine (**278**).

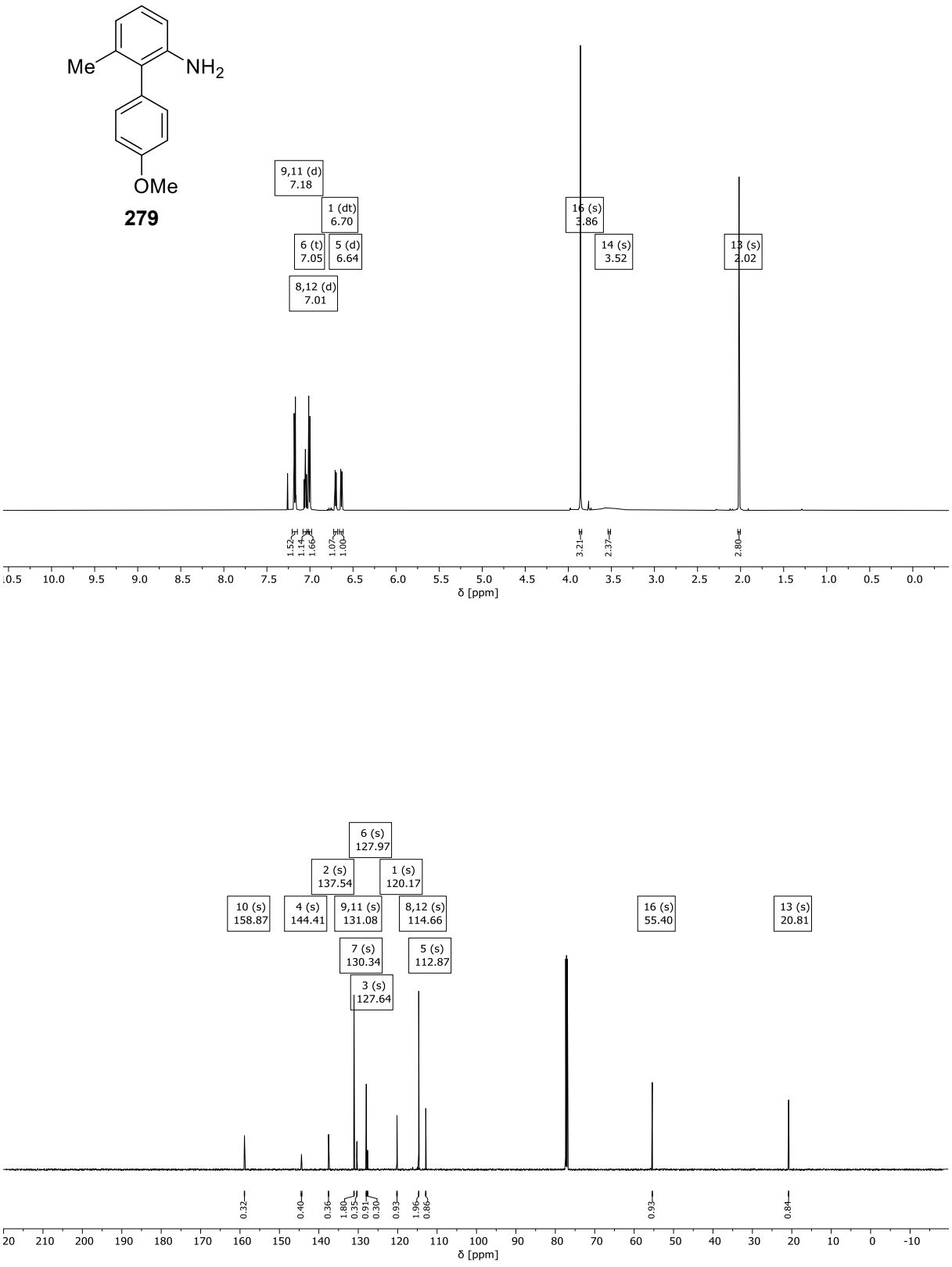

Figure 199: ^{1}H- and ^{13}C-NMR spectra (600 / 151 MHz, $CDCl_3$) of 4'-methoxy-6-methyl-[1,1'-biphenyl]-2-amine (**279**).

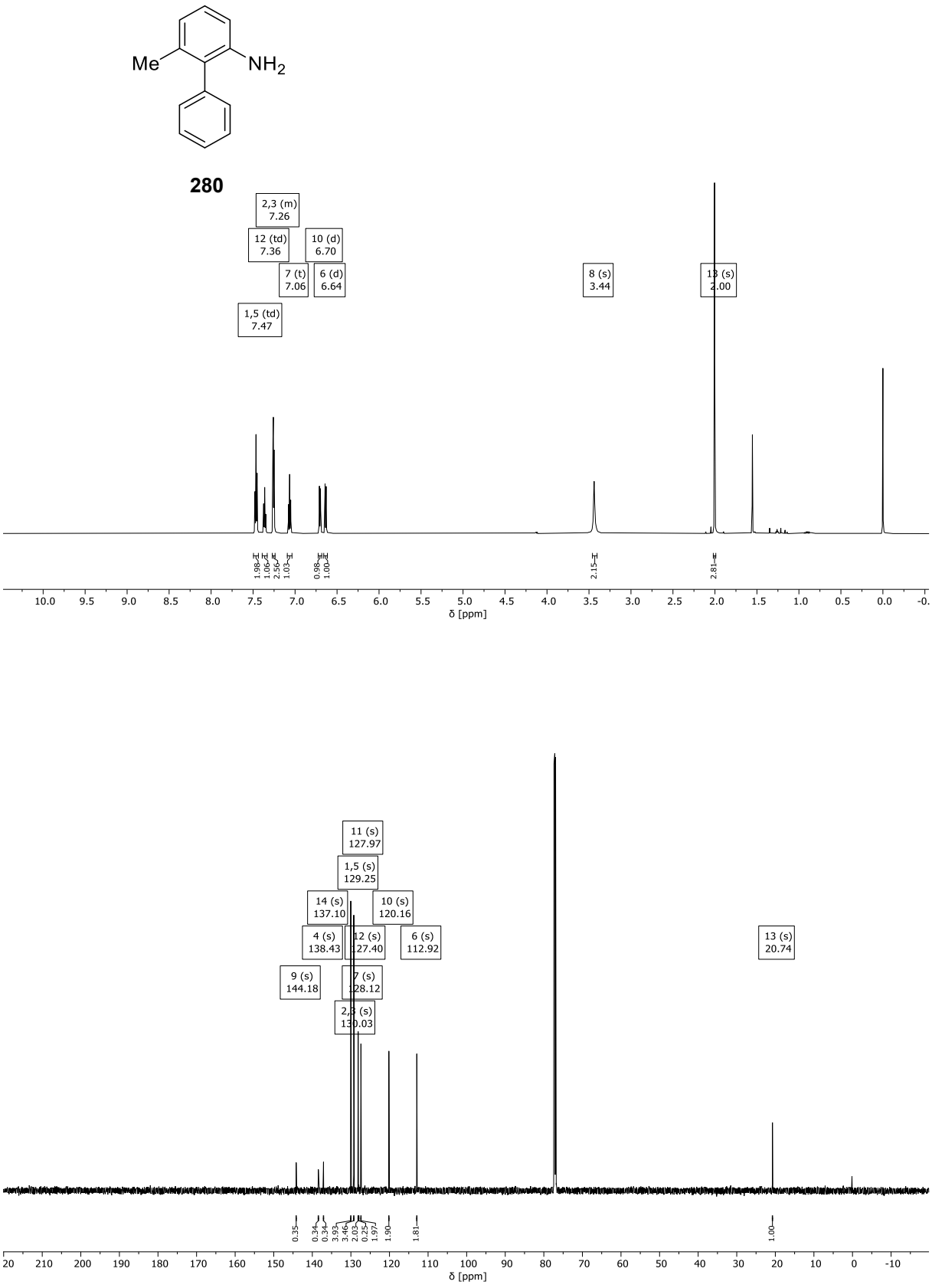

Figure 200: ^{1}H- and ^{13}C-NMR spectra (600 / 151 MHz, $CDCl_3$) of 6-methyl-[1,1'-biphenyl]-2-amine (**280**).

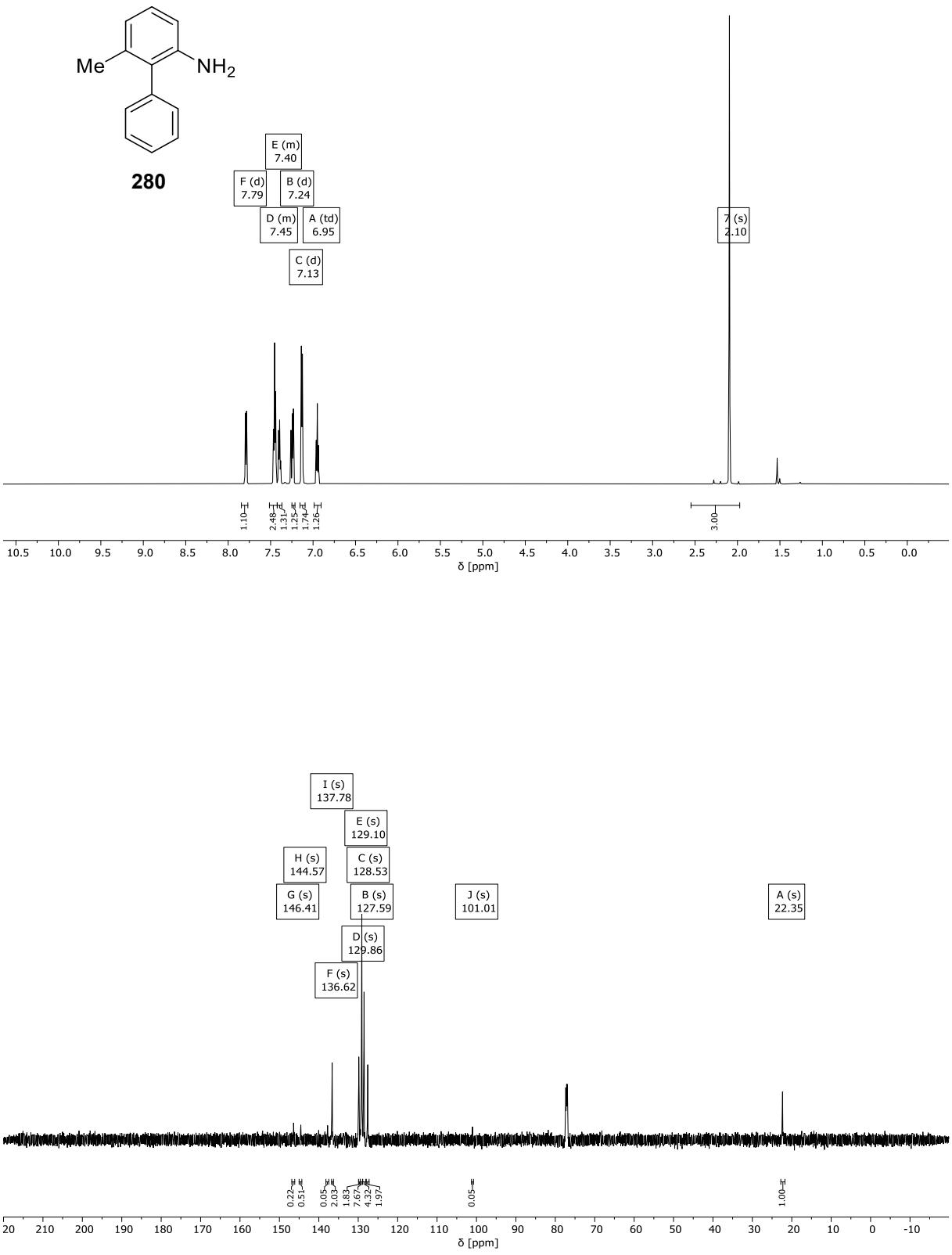

Figure 201: ^{1}H- and ^{13}C-NMR spectra (600 / 151 MHz, $CDCl_3$) of 6-methyl-[1,1'-biphenyl]-2-amine (**280**).

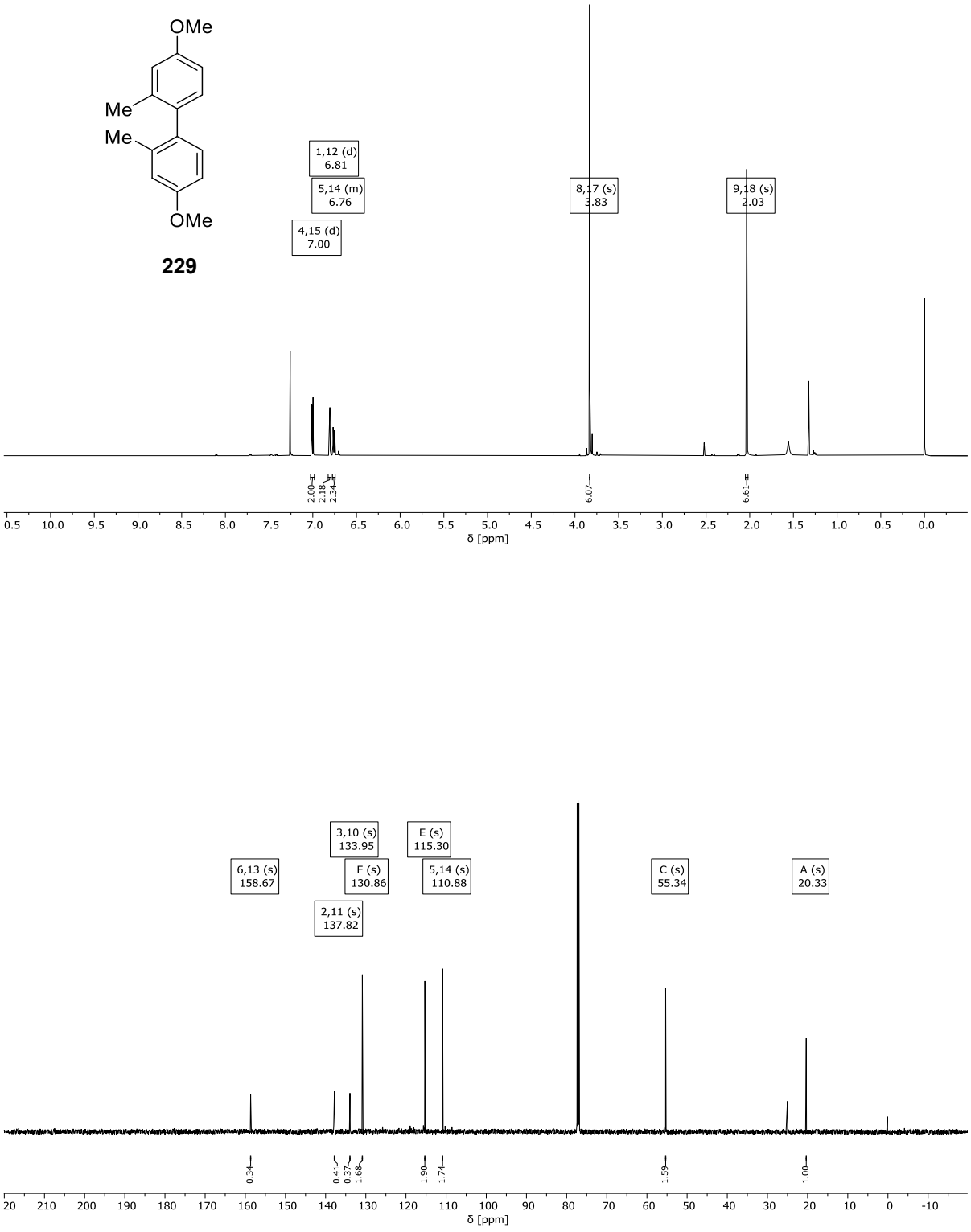

Figure 202: ^{1}H- and ^{13}C-NMR spectra (600 / 151 MHz, $CDCl_3$) of 4,4'-dimethoxy-2,2'-dimethyl-1,1'-biphenyl (**229**).

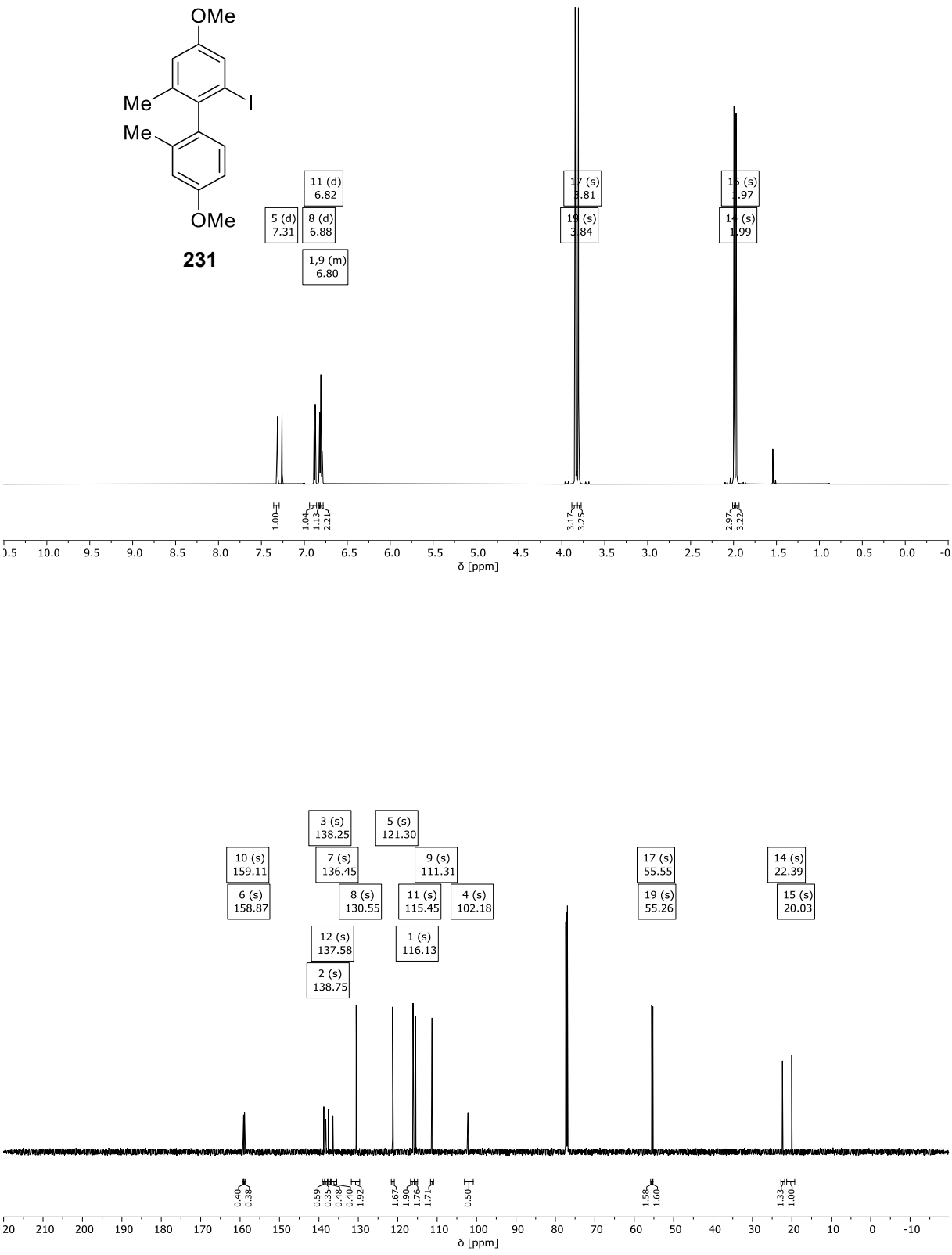

Figure 203: ^{1}H- and ^{13}C-NMR spectra (600 / 151 MHz, $CDCl_3$) of 2-iodo-4,4'-dimethoxy-2',6-dimethyl-1,1'-biphenyl (**231**).

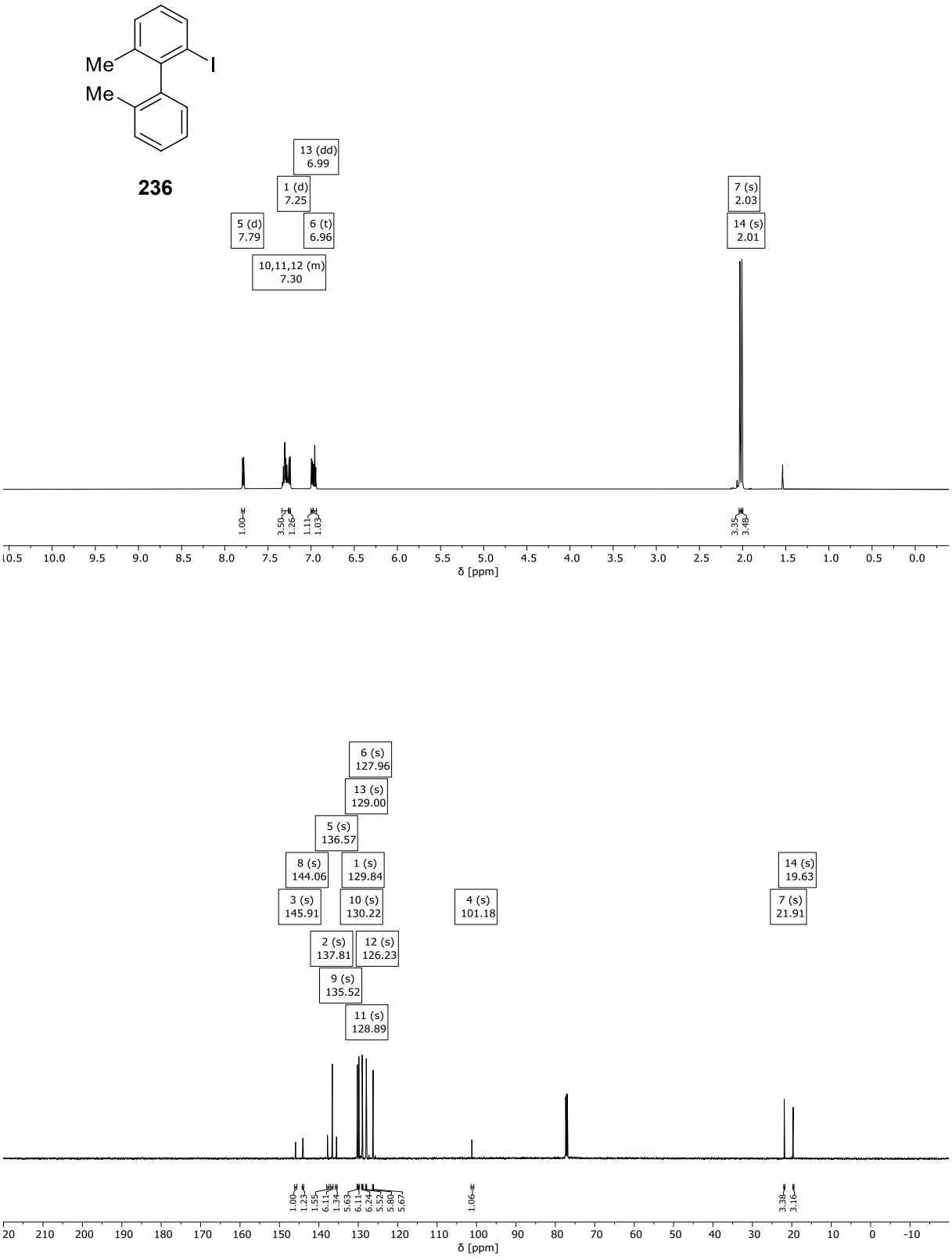

Figure 204: ^{1}H- and ^{13}C-NMR spectra (600 / 151 MHz, $CDCl_3$) of 2-iodo-2',6-dimethyl-1,1'-biphenyl (**236**).

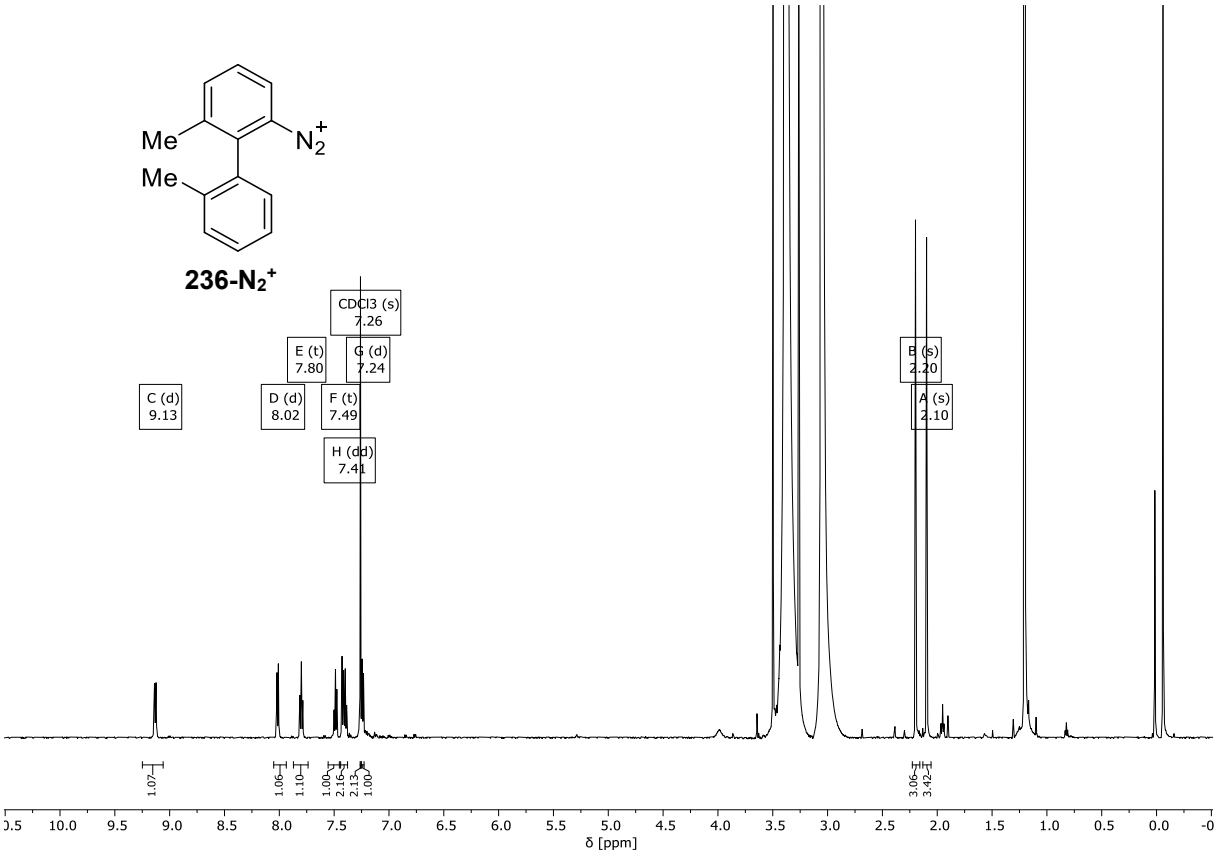

Figure 205: ^{1}H- and ^{13}C-NMR spectra (600 / 151 MHz, $CDCl_3$) of 2',6-dimethyl-[1,1'-biphenyl]-2-diazonium salt (**236-N_2^+**)

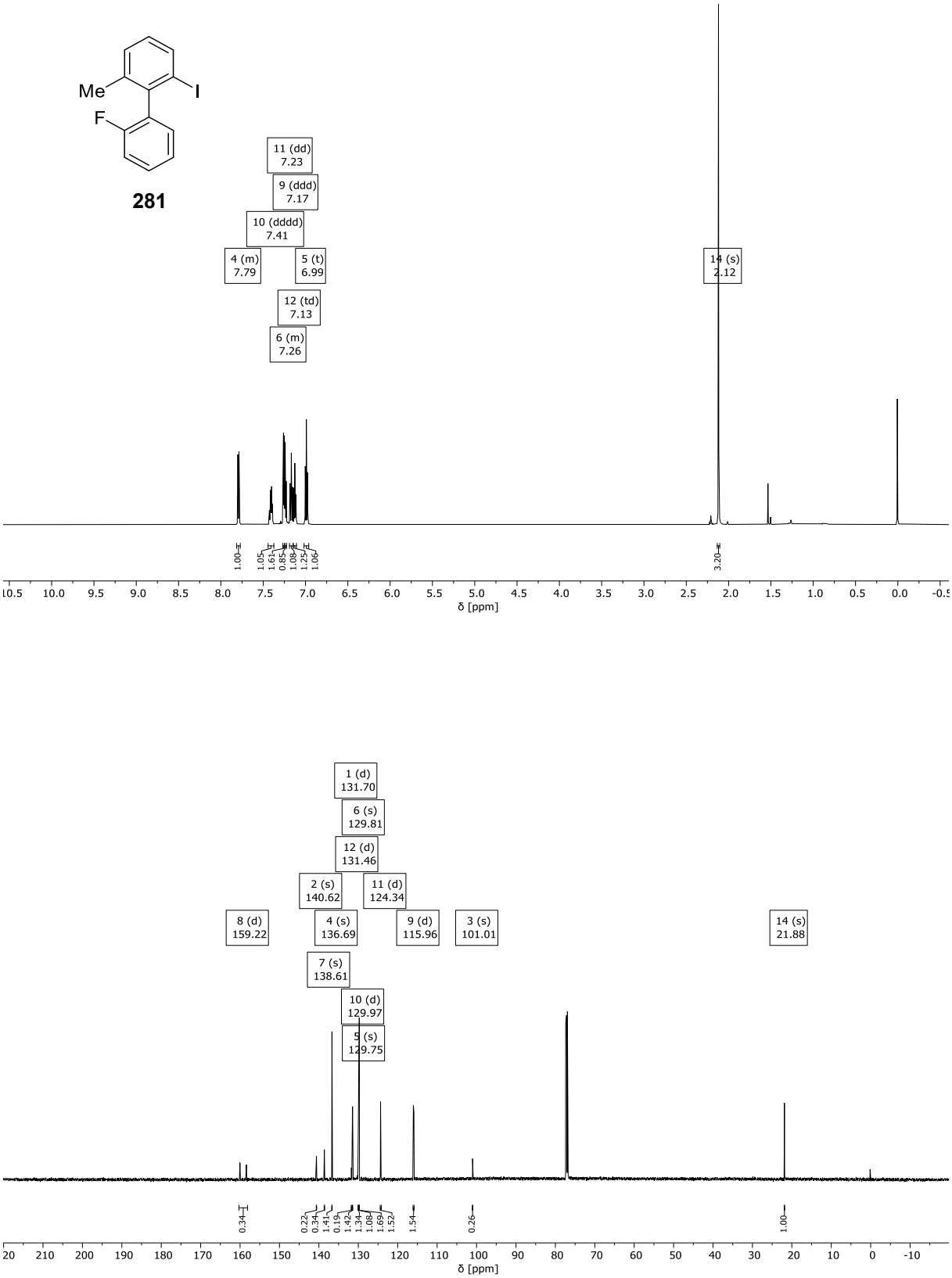

Figure 206: ^{1}H-, ^{13}C-spectra (600 / 151 MHz, $CDCl_3$) of 2'-fluoro-2-iodo-6-methyl-1,1'-biphenyl (**281**).

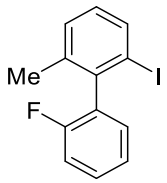

281

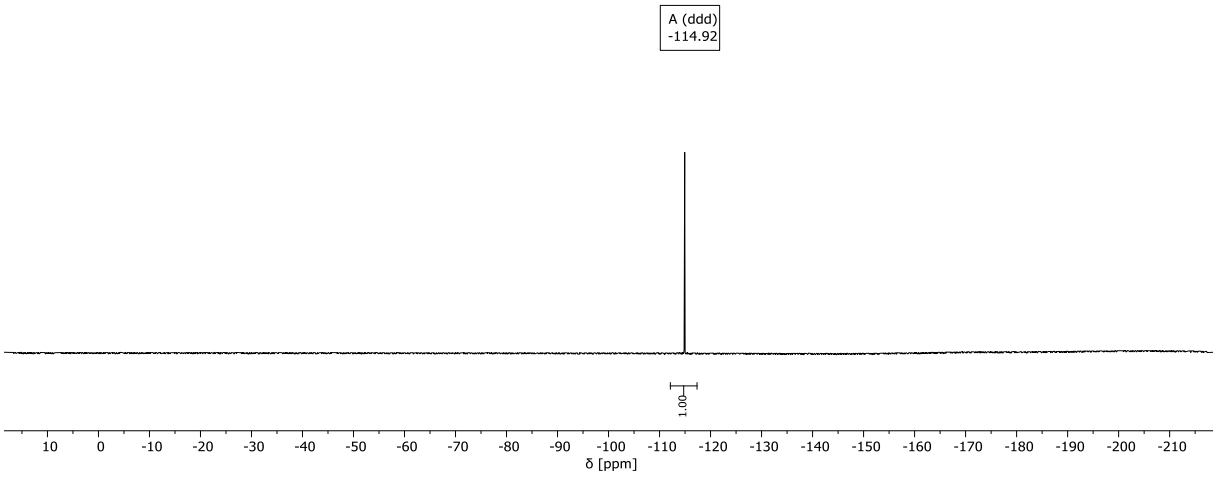

Figure 207: ^{19}F-NMR spectra (282 MHz, $CDCl_3$) of 2'-fluoro-2-iodo-6-methyl-1,1'-biphenyl (**281**).

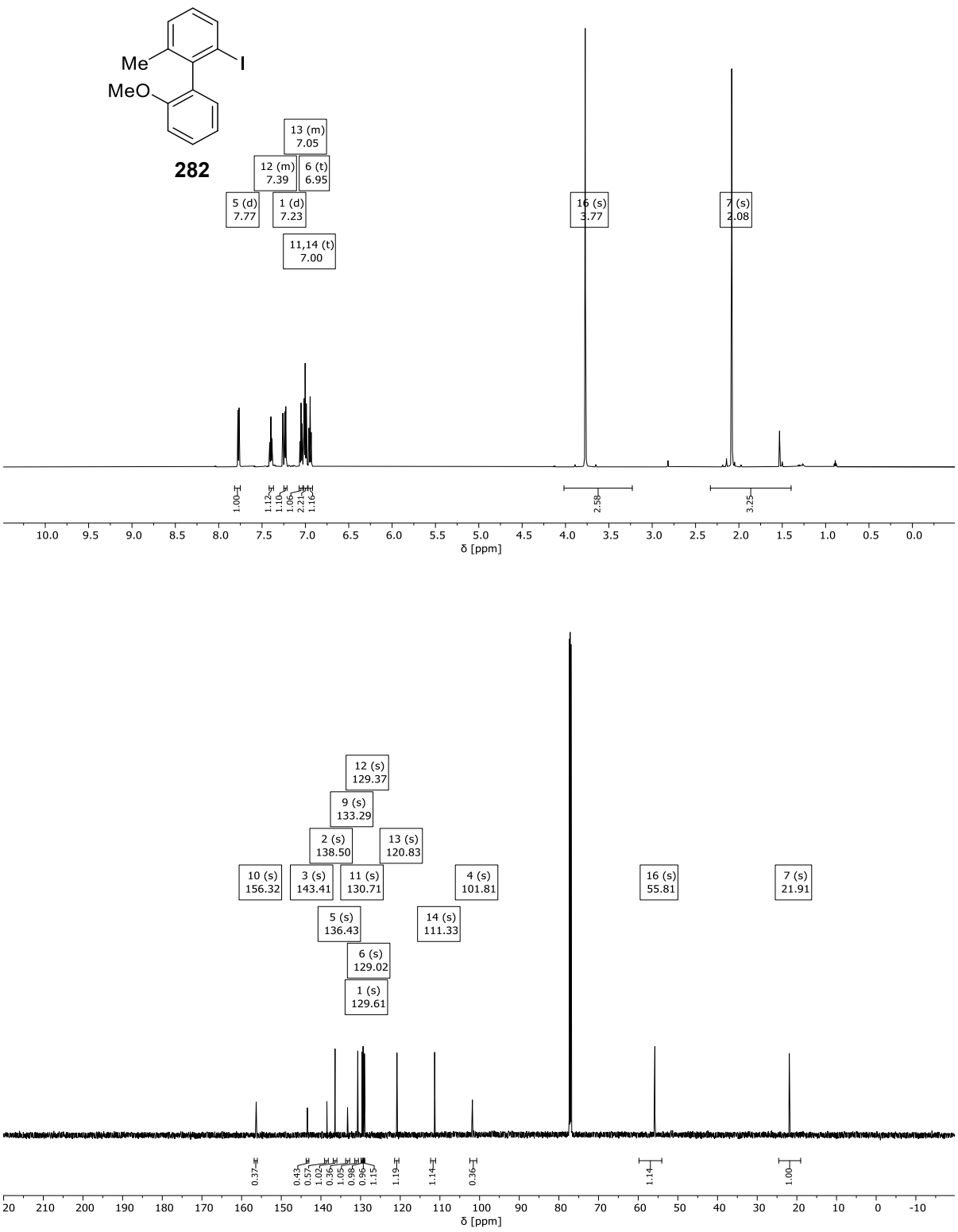

Figure 208: ^{1}H- and ^{13}C-NMR spectra (600 / 151 MHz, $CDCl_3$) of 2-iodo-2'-methoxy-6-methyl-1,1'-biphenyl (**282**).

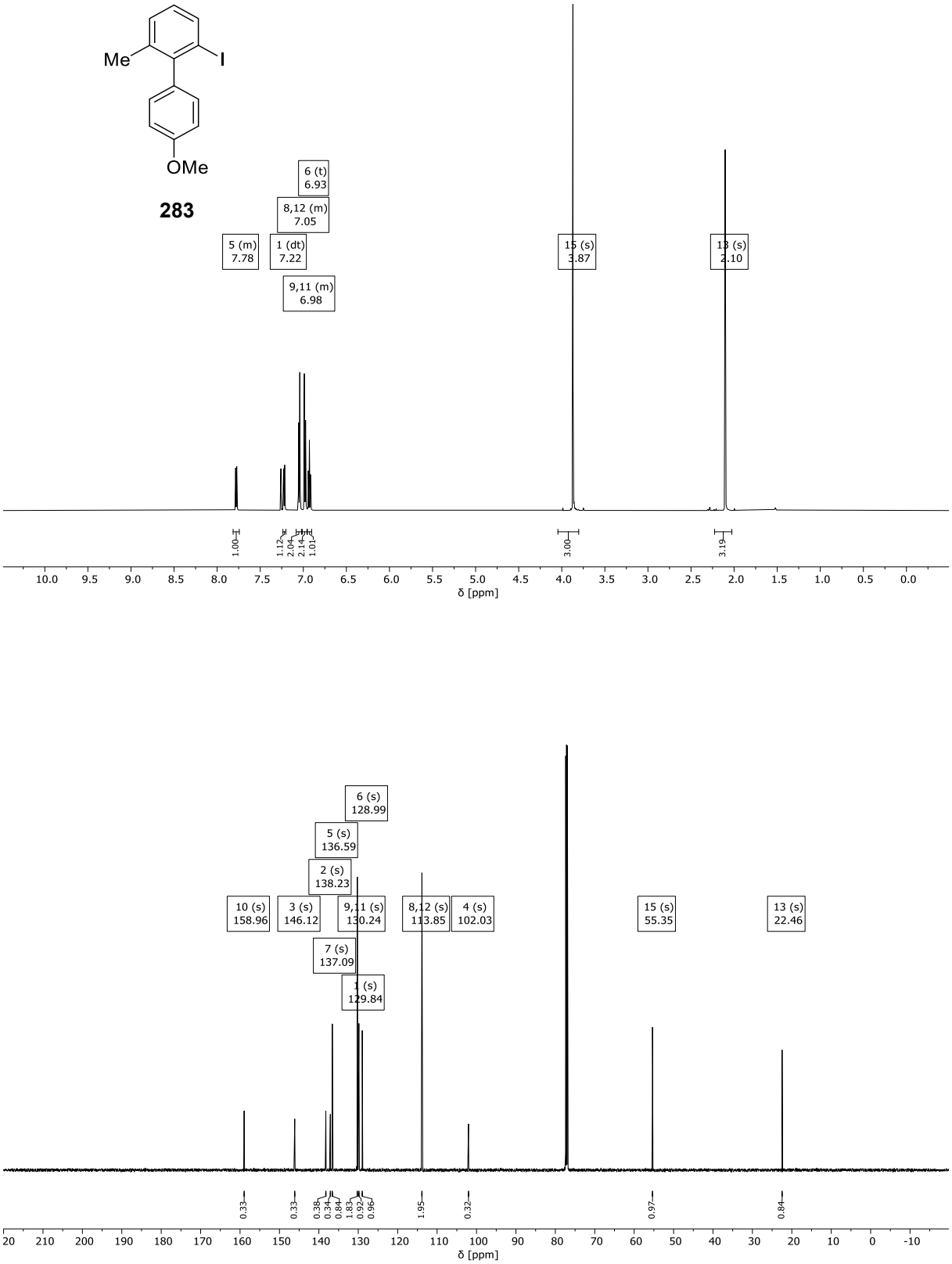

Figure 209: ^{1}H- and ^{13}C-NMR spectra (600 / 151 MHz, $CDCl_3$) of 2-iodo-4'-methoxy-6-methyl-1,1'-biphenyl (**283**).

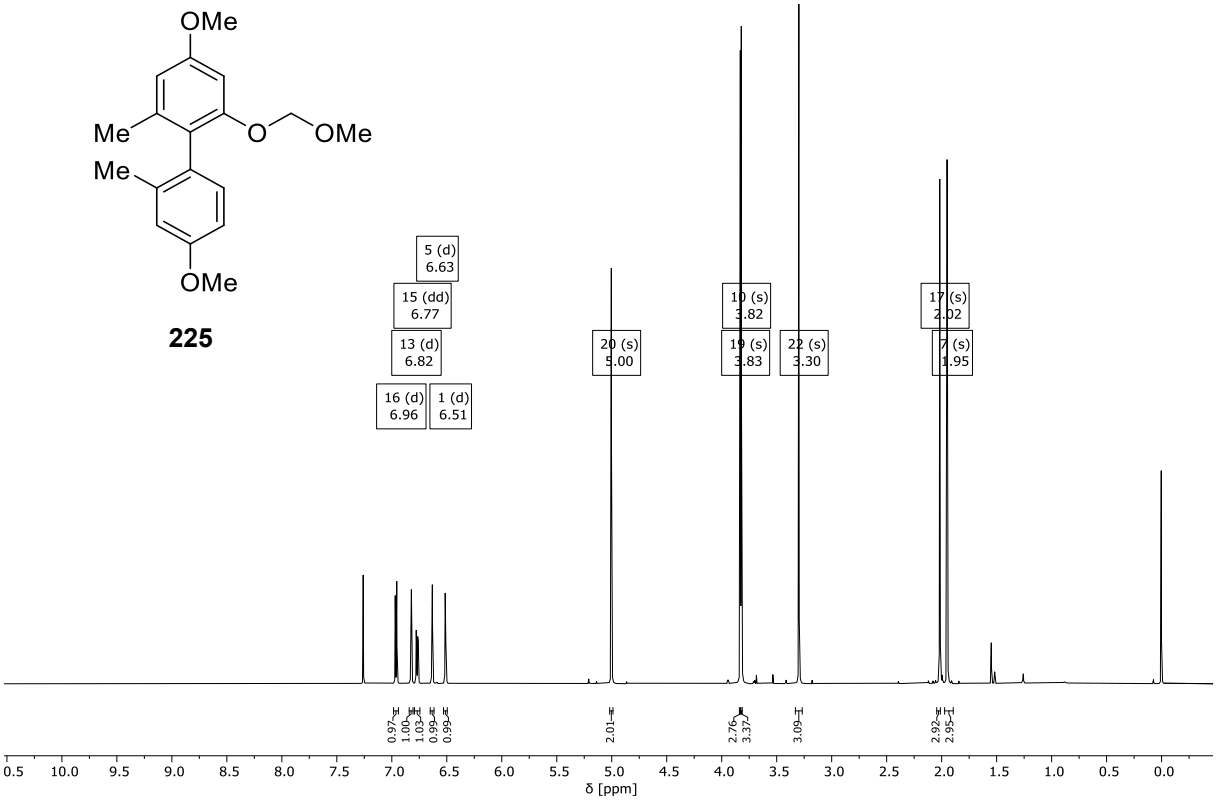

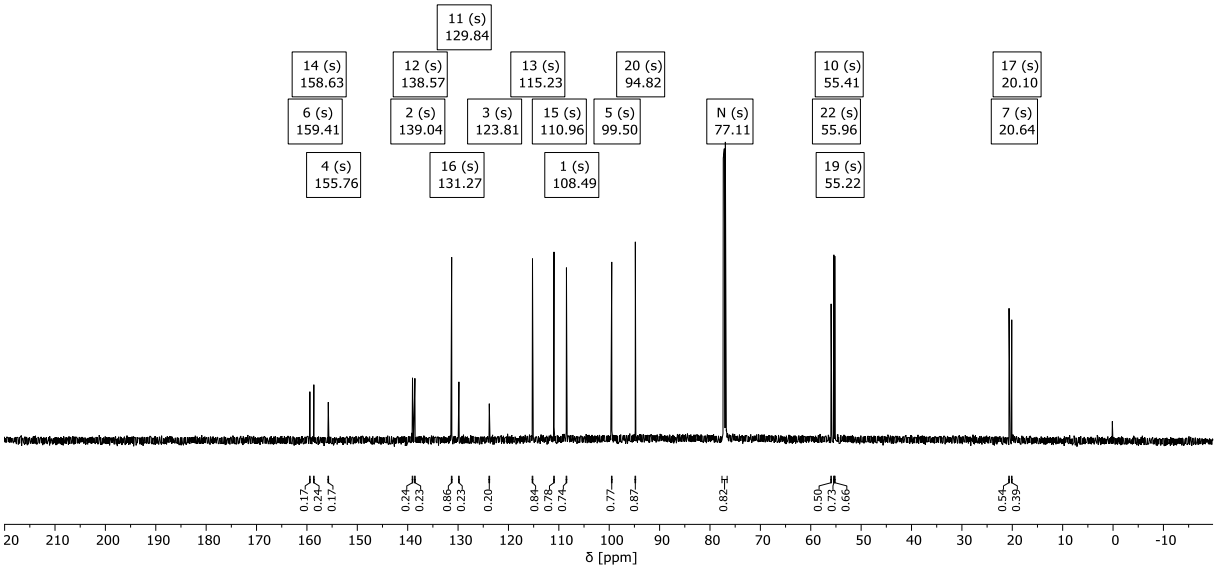

Figure 210: ^{1}H- and ^{13}C-NMR spectra (600 / 151 MHz, $CDCl_3$) of 4,4'-dimethoxy-2-(methoxymethoxy)-2',6-dimethyl-1,1'-biphenyl (**225**).

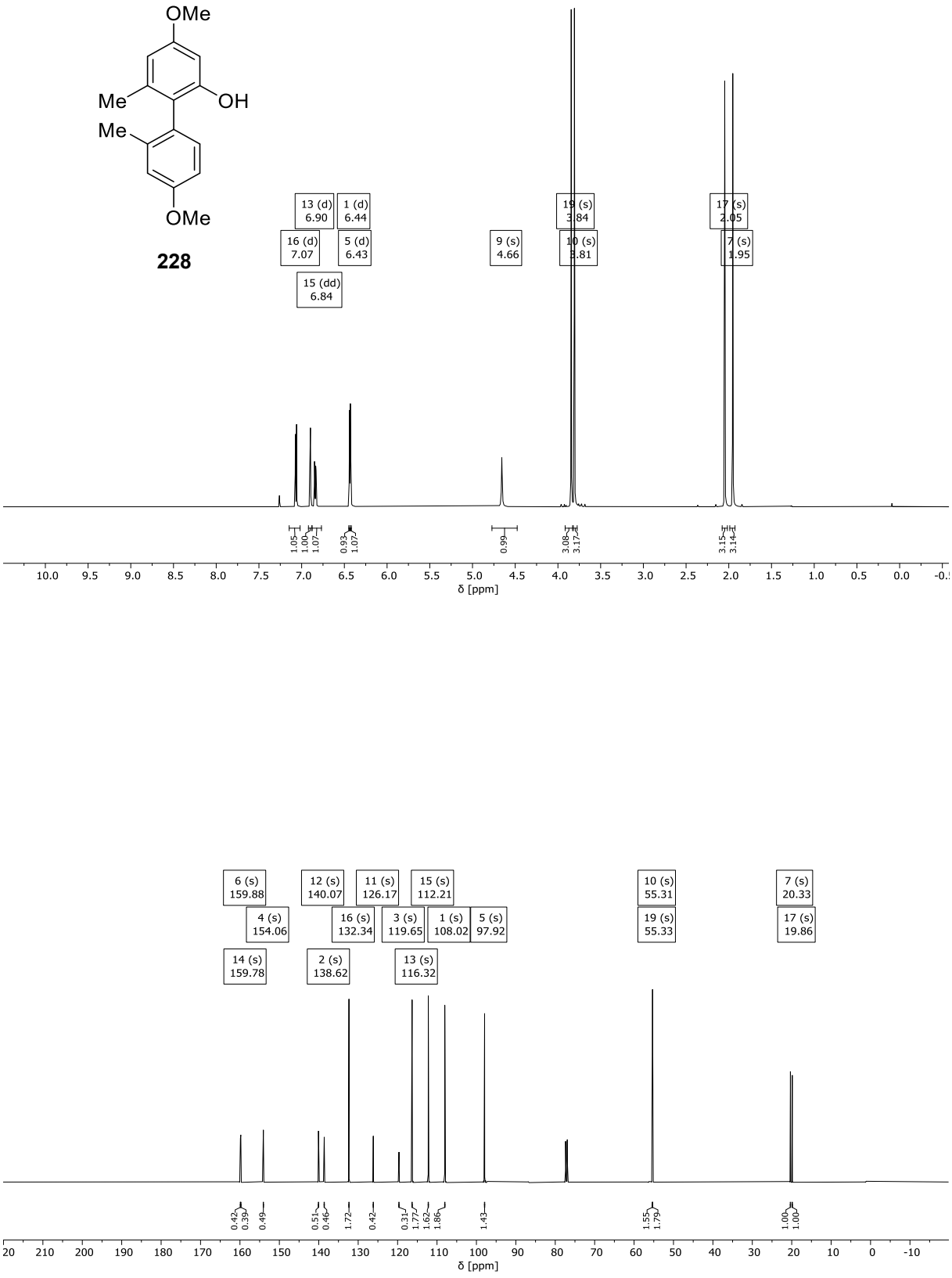

Figure 211: ^{1}H- and ^{13}C-NMR spectra (600 / 151 MHz, $CDCl_3$) of 4,4'-dimethoxy-2',6-dimethyl-[1,1'-biphenyl]-2-ol (**228**).

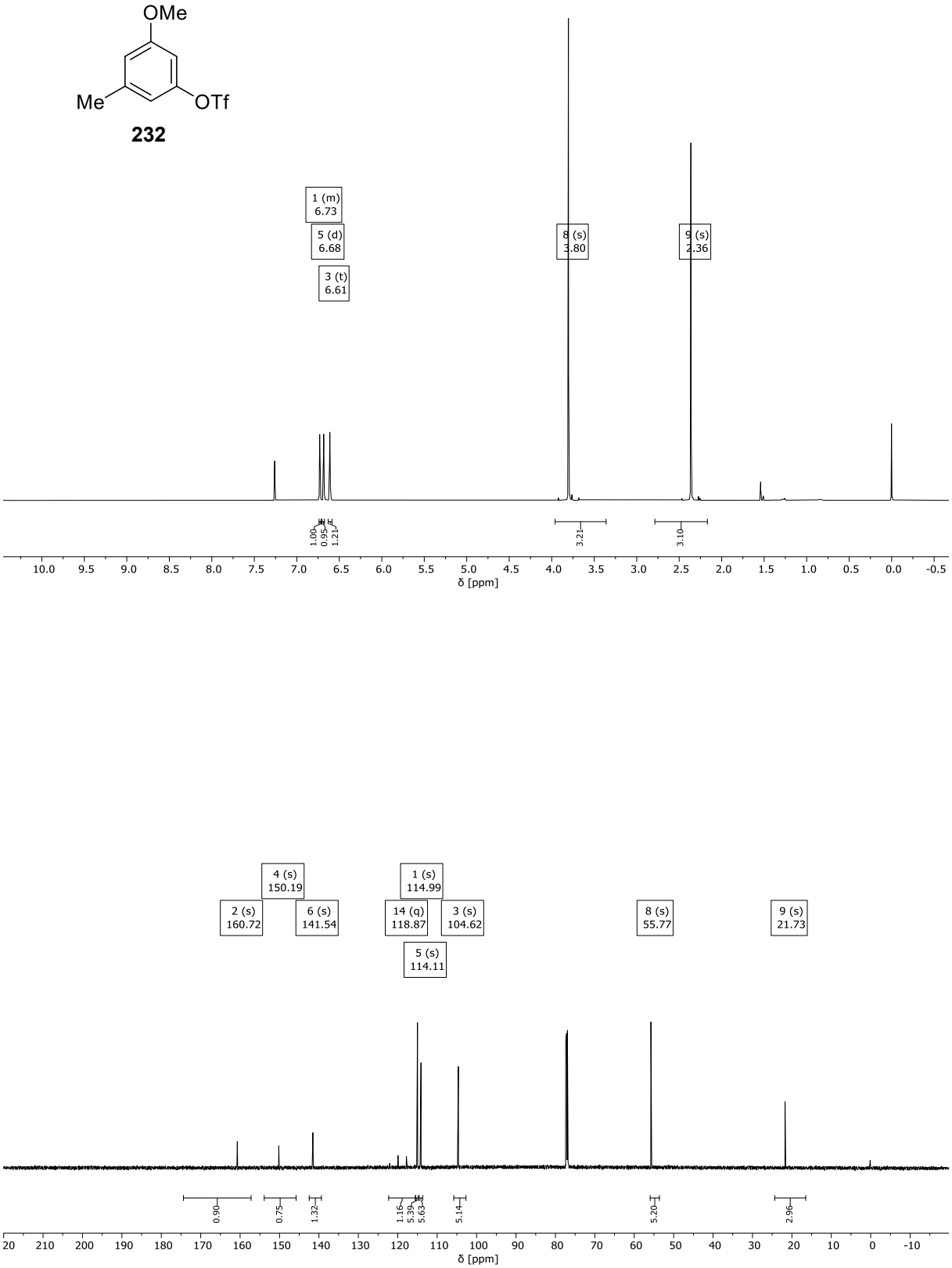

Figure 212: ^{1}H-, ^{13}C-NMR spectra (600 / 151 MHz, $CDCl_3$) of 3-methoxy-5-methylphenyl trifluoromethanesulfonate (**232**).

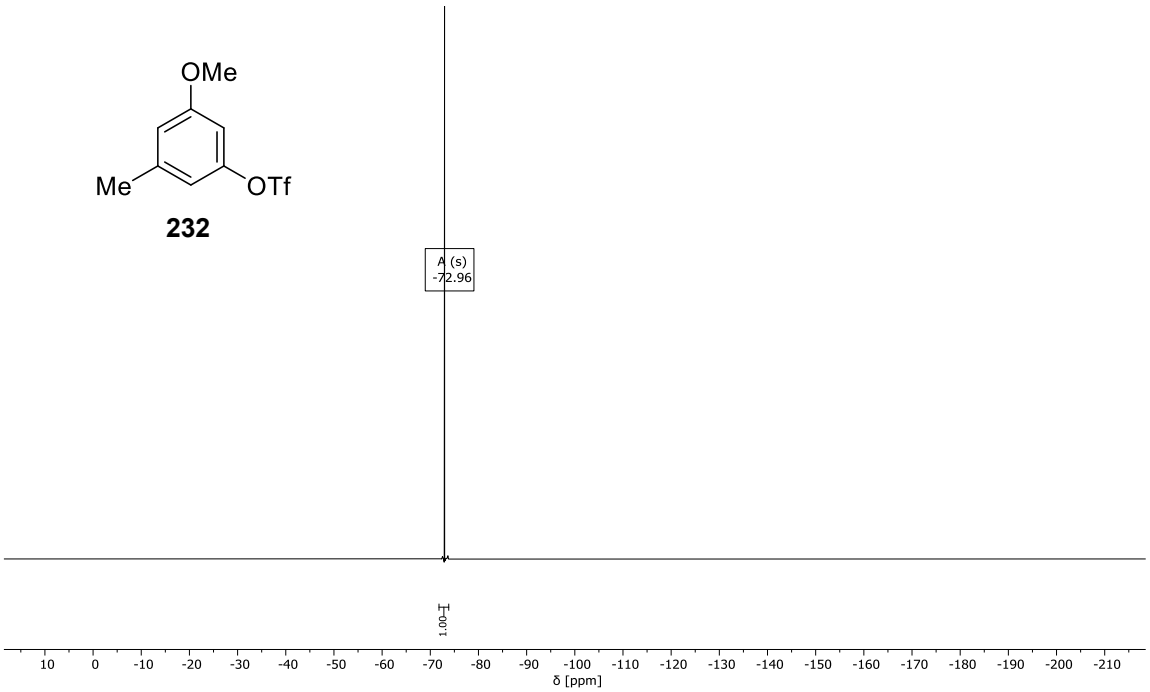

Figure 213: ^{19}F-NMR spectra (282 MHz, $CDCl_3$) of 3-methoxy-5-methylphenyl trifluoromethanesulfonate (**232**).

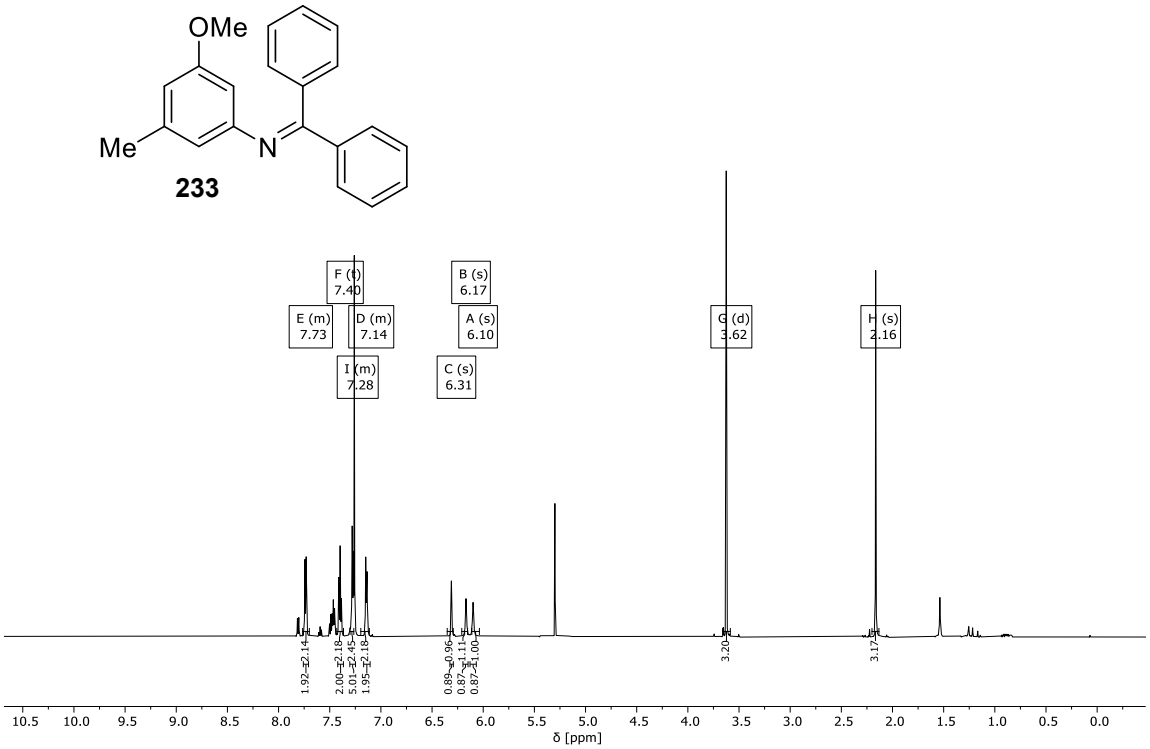

Figure 214: ^{1}H-NMR spectrum (600 MHz, $CDCl_3$) of N-(3-methoxy-5-methylphenyl)-1,1-diphenylmethanimine (**233**).

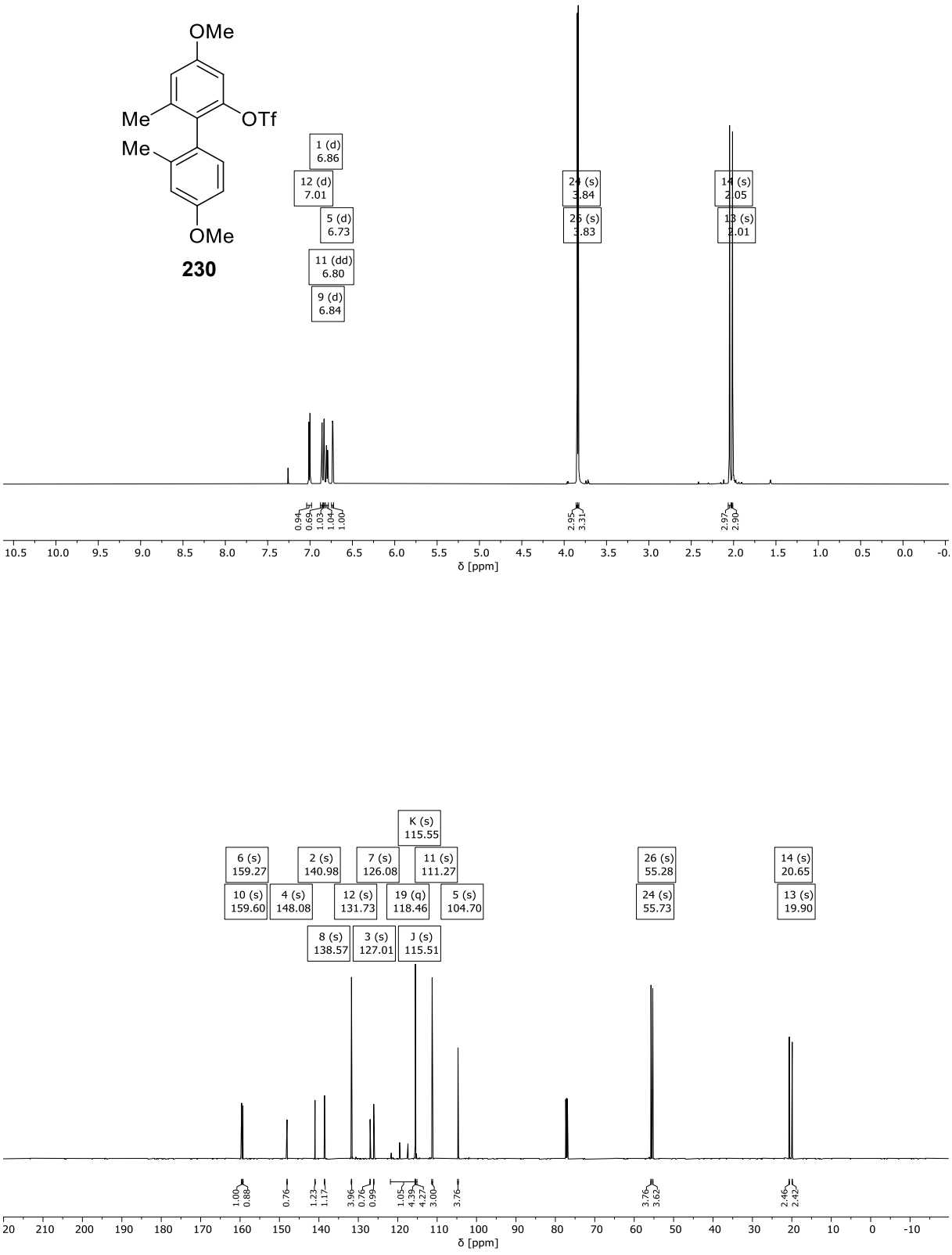

Figure 215: ^{1}H-, ^{13}C-spectra (600 / 151 MHz, $CDCl_3$) of 4,4'-dimethoxy-2',6-dimethyl-[1,1'-biphenyl]-2-yl trifluoromethanesulfonate (**230**).

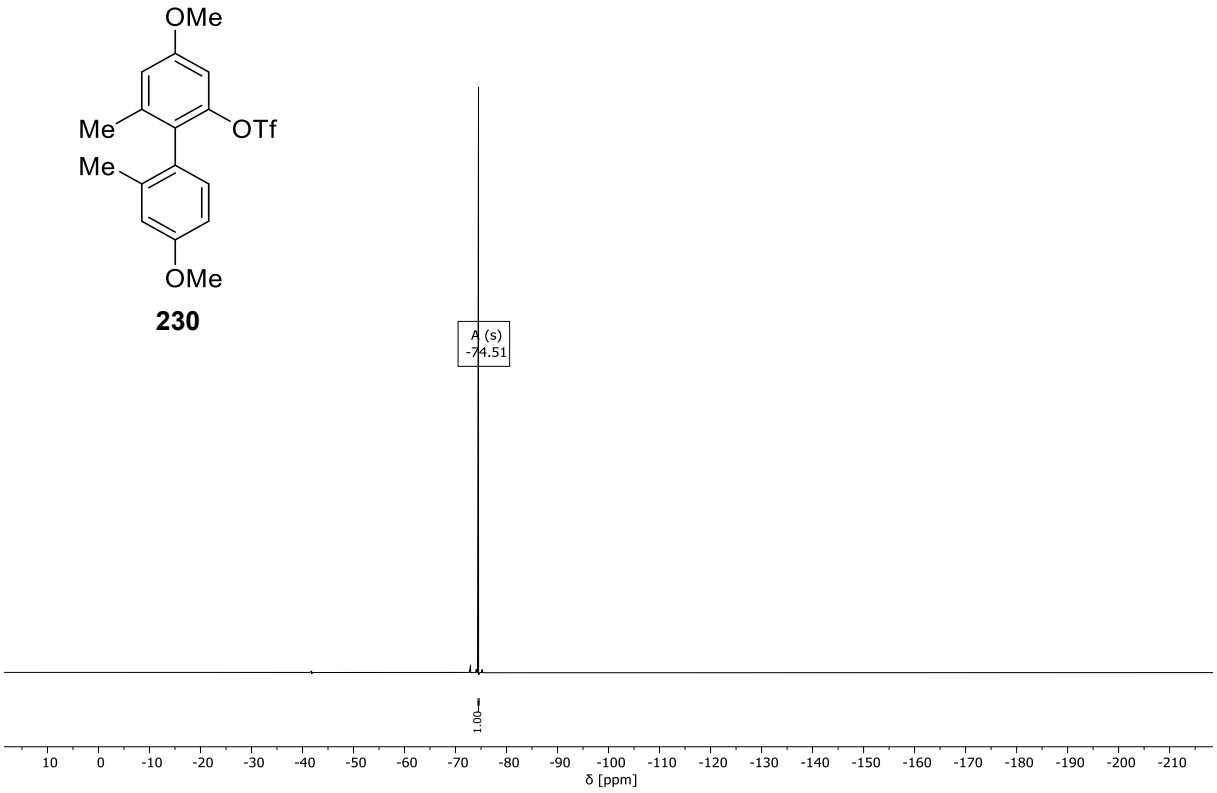

Figure 216: ^{19}F-NMR spectrum (282 MHz, $CDCl_3$) of 4,4'-dimethoxy-2',6-dimethyl-[1,1'-biphenyl]-2-yl trifluoromethanesulfonate (**230**).

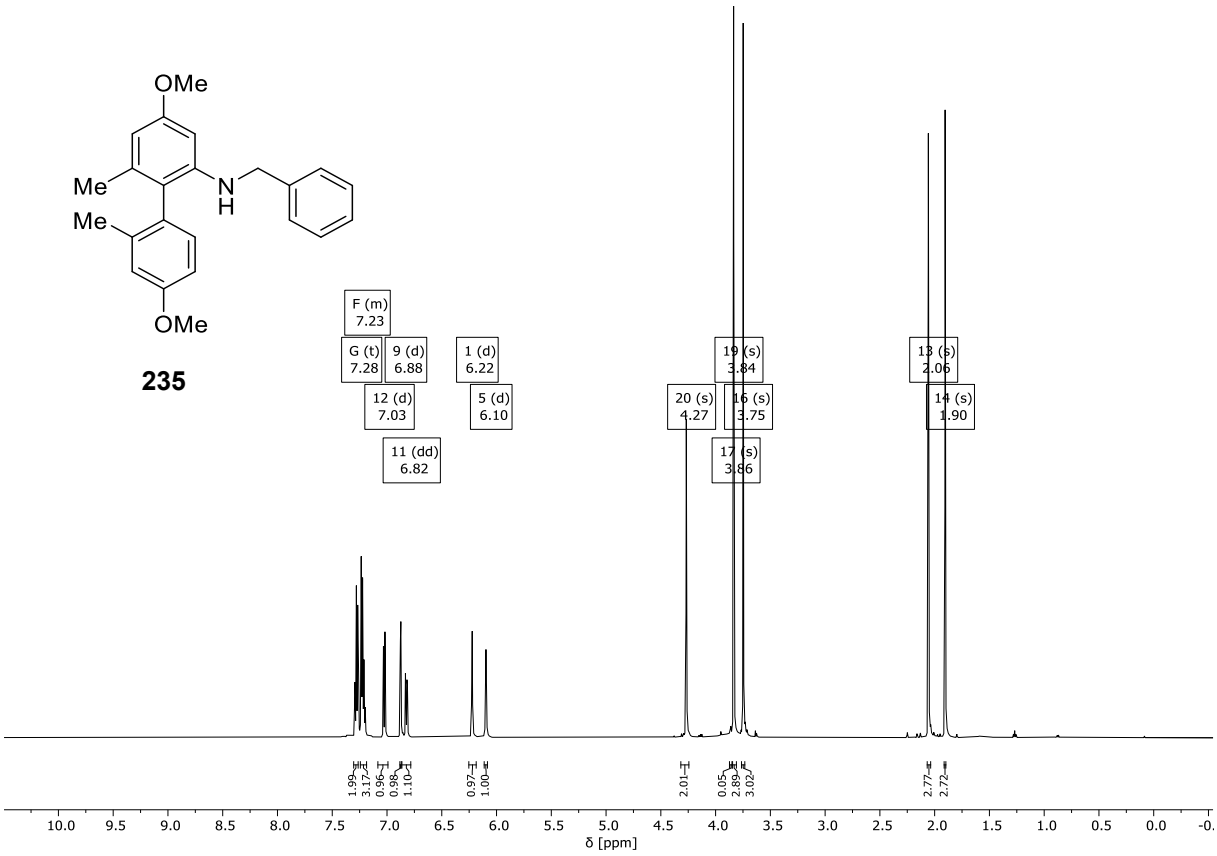

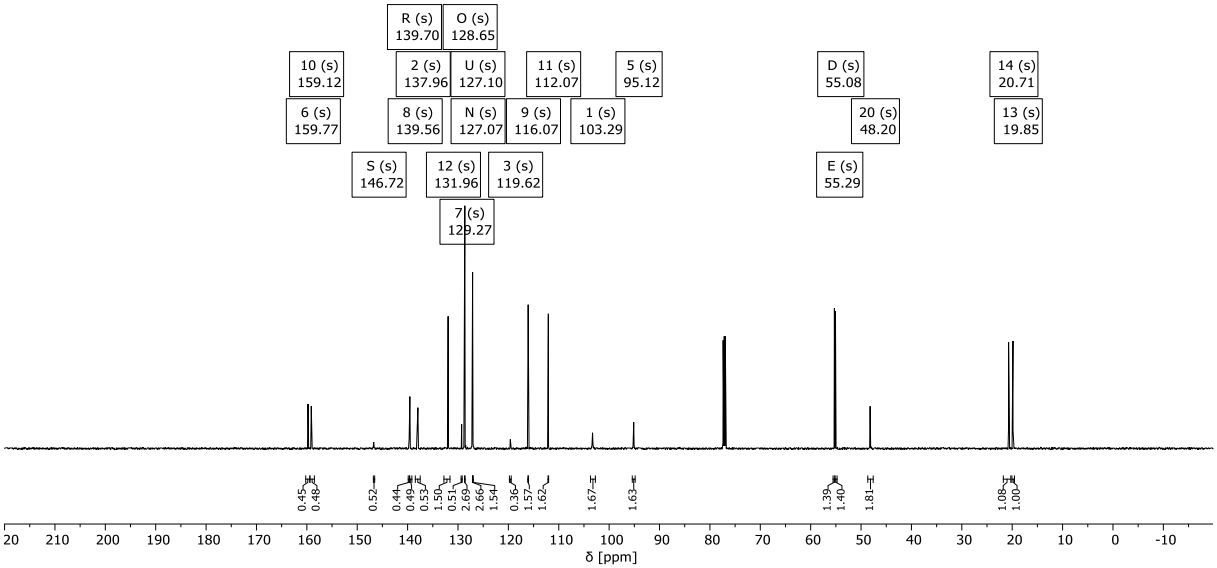

Figure 217: ^{1}H- and ^{13}C-NMR spectra (600 / 151 MHz, $CDCl_3$) of N-benzyl-4,4'-dimethoxy-2',6-dimethyl-[1,1'-biphenyl]-2-amine (**235**).

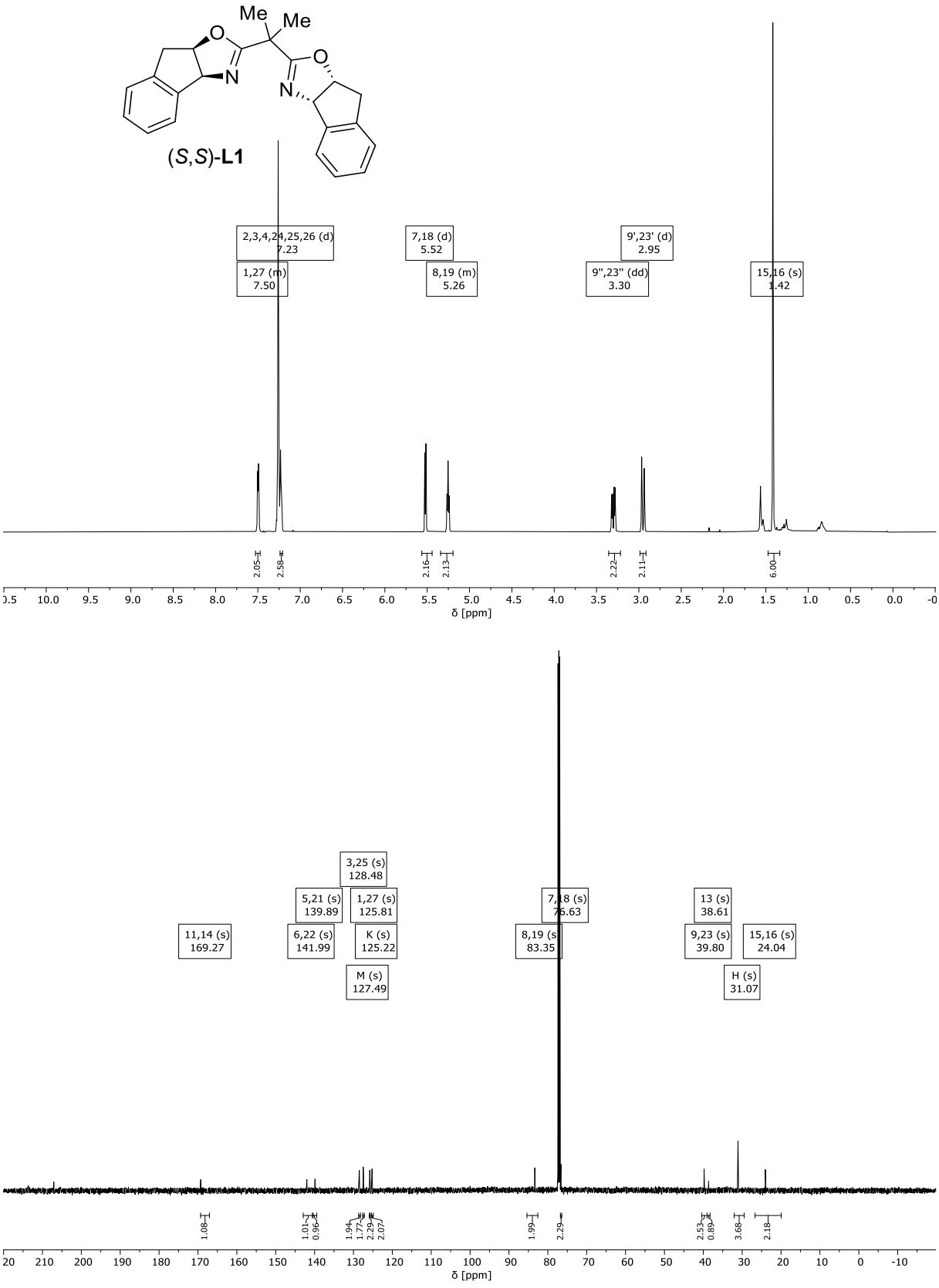

Figure 218: ^{1}H- and ^{13}C-NMR spectra (600 / 151 MHz, $CDCl_3$) of of (3aS,3a'S,8aR,8a'R)-2,2'-(propane-2,2-diyl)bis(3a,8a-dihydro-8H-indeno[1,2-d]oxazole) ((*S*,*S*)-**L1**).

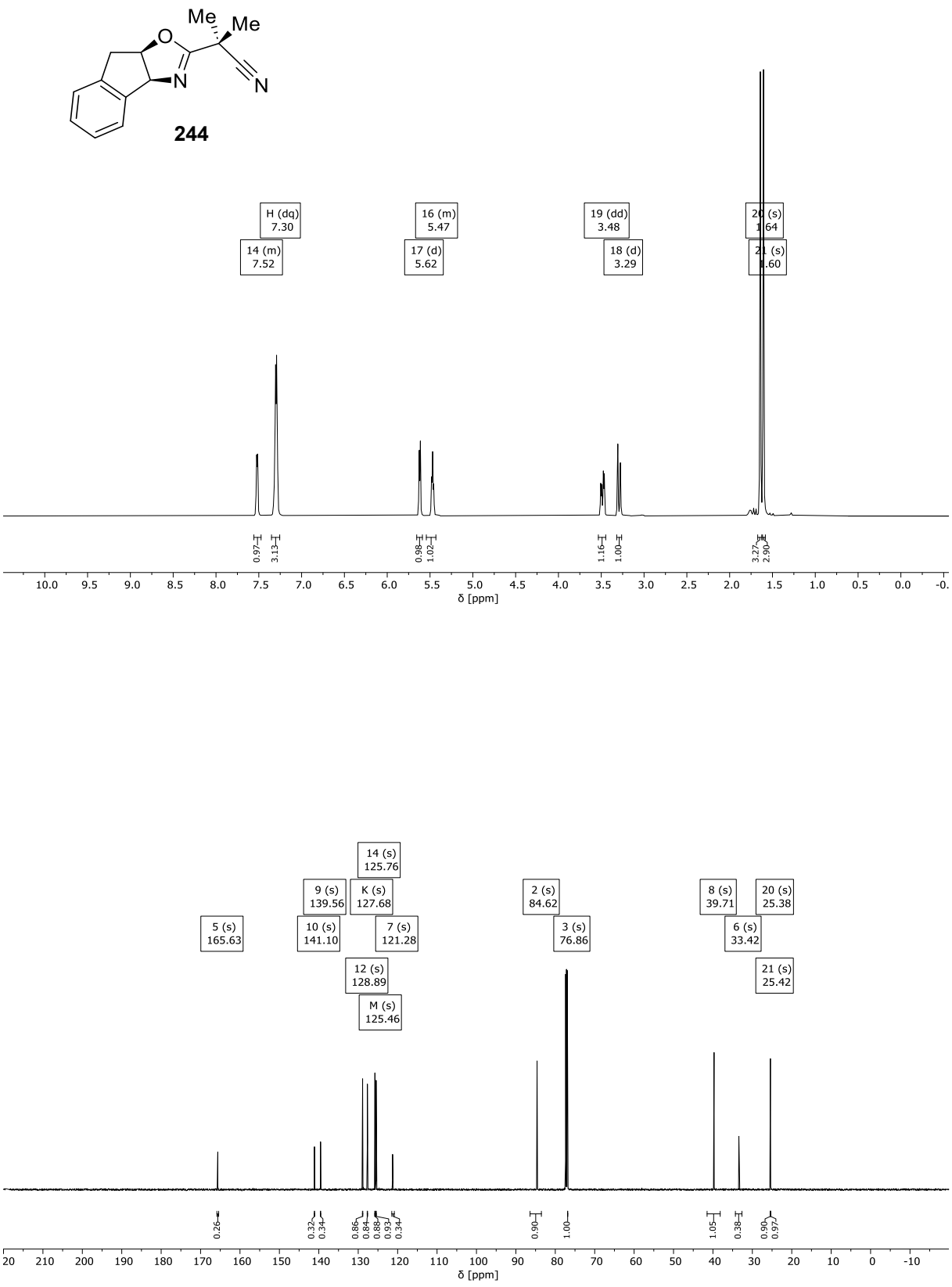

Figure 219: ^{1}H- and ^{13}C-NMR spectra (600 / 151 MHz, $CDCl_3$) of 2-((3aS,8aR)-3a,8a-dihydro-8H-indeno[1,2-d]oxazol-2-yl)-2-methylpropanenitrile (**244**).

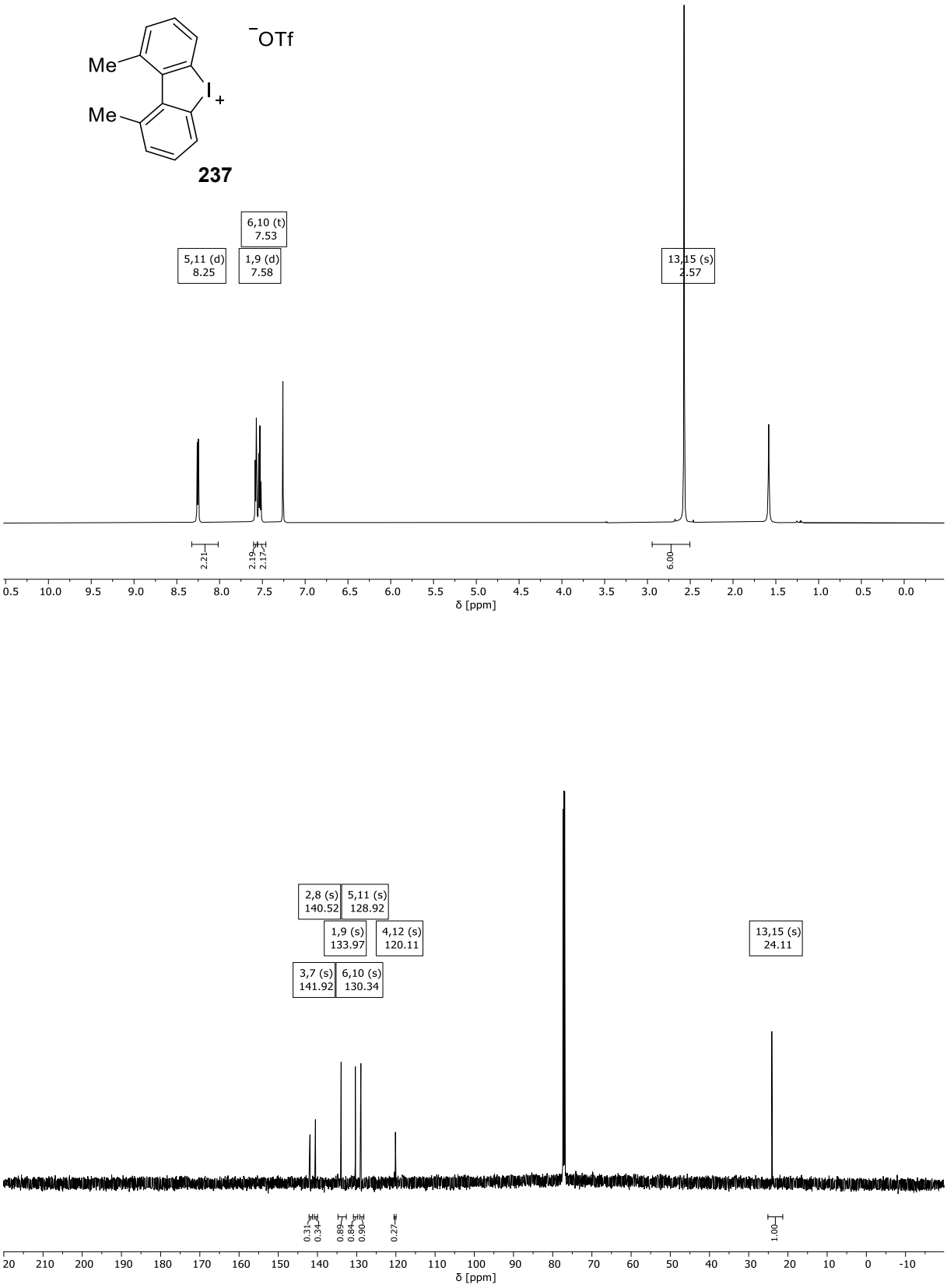

Figure 220: ^{1}H-, ^{13}C-spectra (600 / 151 MHz, $CDCl_3$) of 1,9-dimethyldibenzo[b,d]iodol-5-ium trifluoromethanesulfonate (**237**).

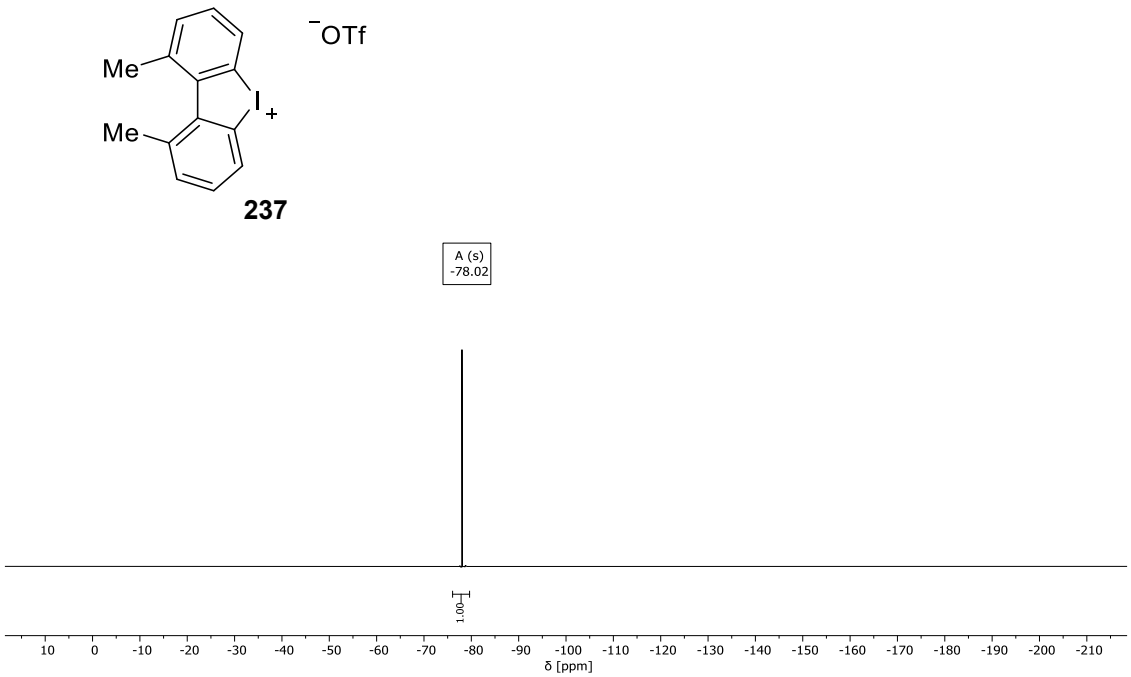

Figure 221: ^{19}F-NMR spectrum (282 MHz, $CDCl_3$) of 1,9-dimethyldibenzo[b,d]iodol-5-ium trifluoromethanesulfonate (**237**).

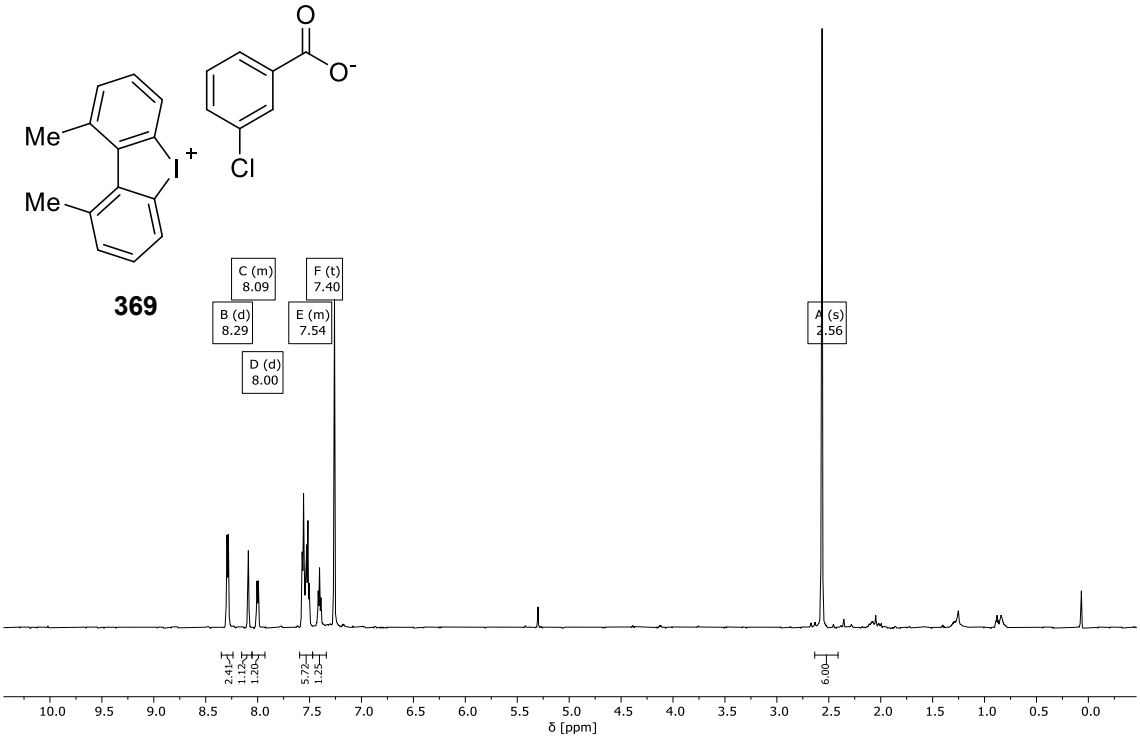

Figure 222: ^{1}H-NMR spectrum (600 MHz, $CDCl_3$) of 1,9-dimethyldibenzo[b,d]iodol-5-ium 3-chlorobenzoate (**369**).

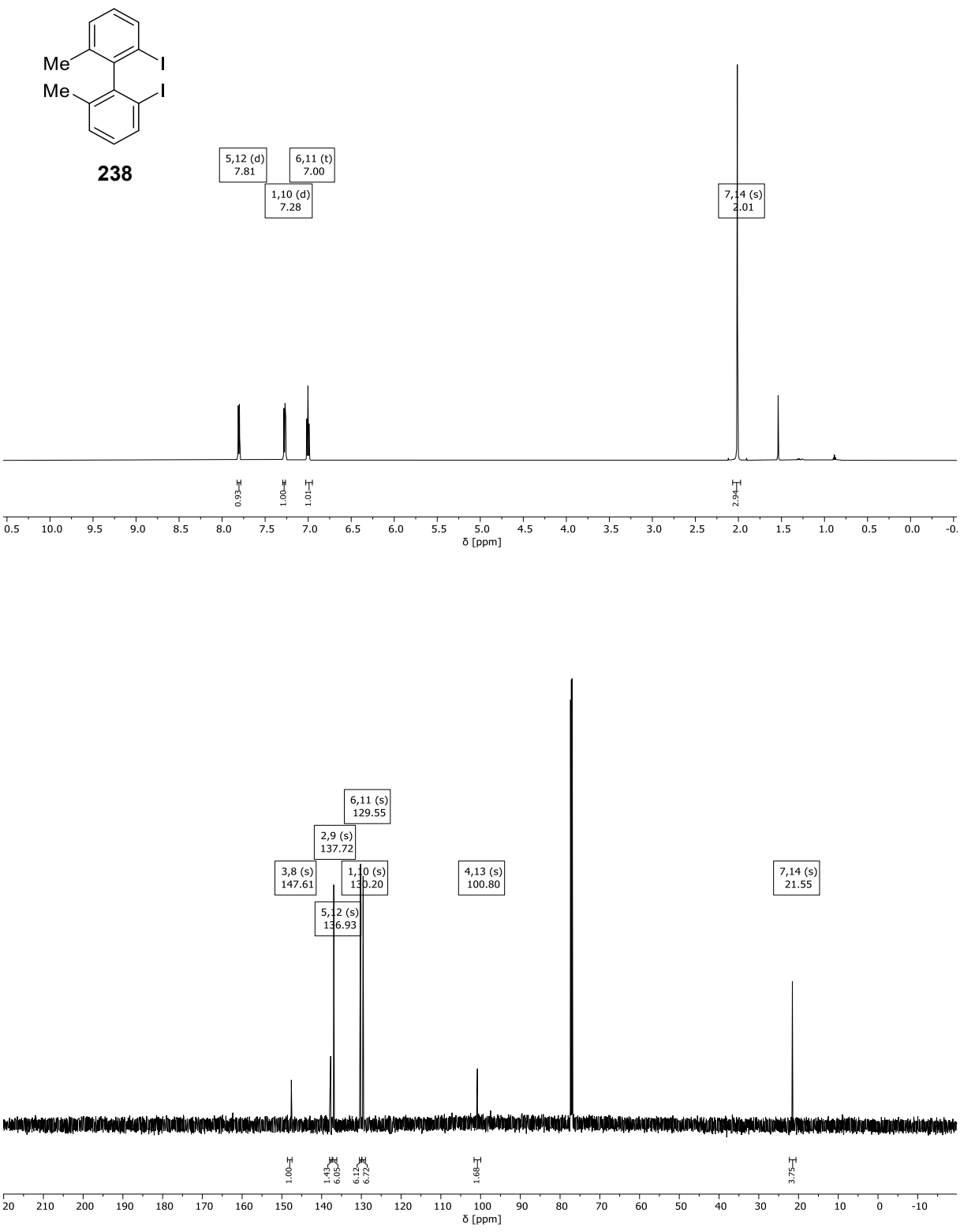

Figure 223: ^{1}H- and ^{13}C-NMR spectra (600 / 151 MHz, $CDCl_3$) of 2,2'-diiodo-6,6'-dimethyl-1,1'-biphenyl (**238**).

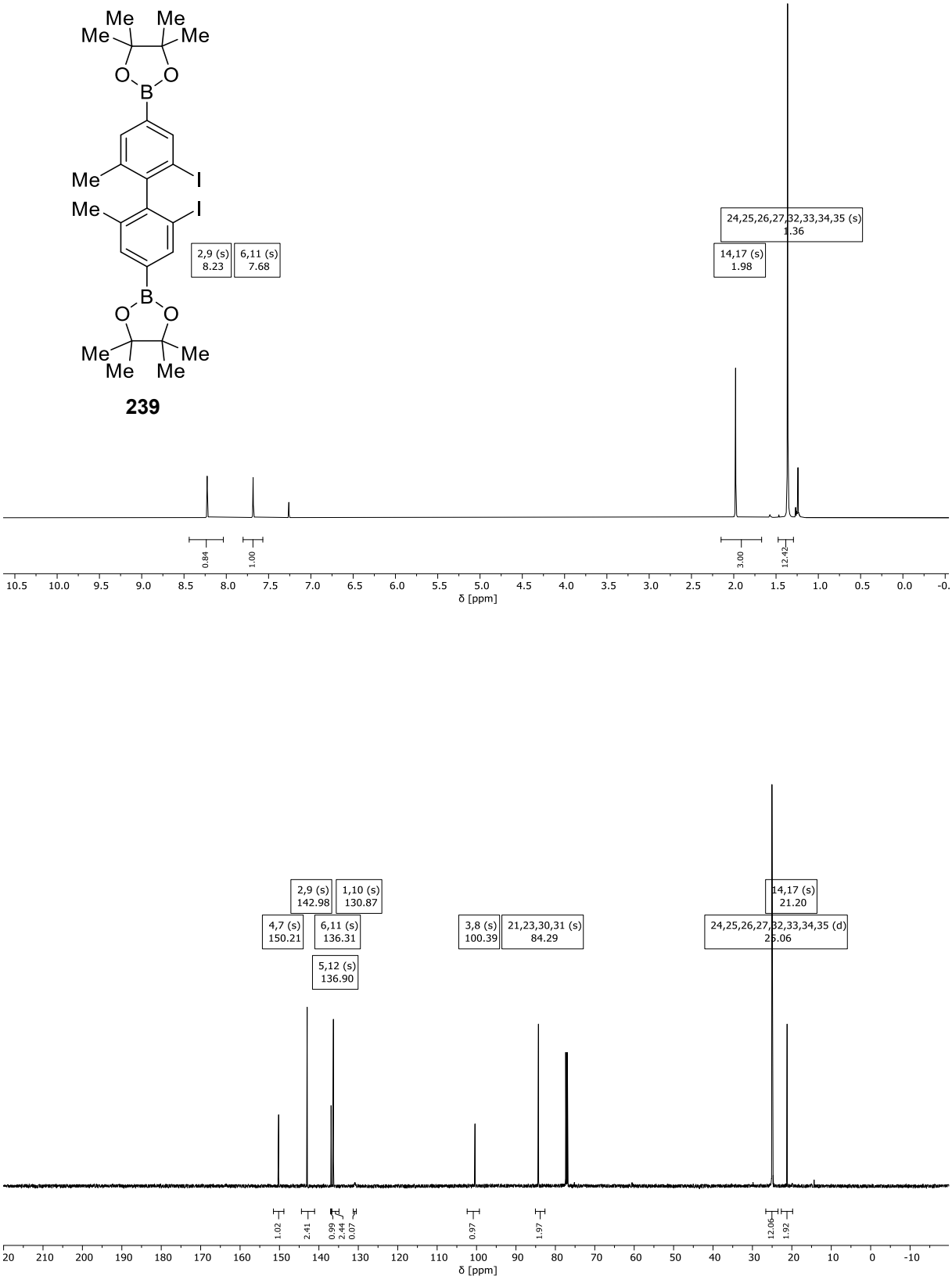

Figure 224: ^{1}H-, ^{13}C- and ^{11}B-NMR spectra (600 / 151 / 96 MHz, $CDCl_3$) of 2,2'-(2,2'-diiodo-6,6'-dimethyl-[1,1'-biphenyl]-4,4'-diyl)bis(4,4,5,5-tetramethyl-1,3,2-dioxaborolane) (**239**).

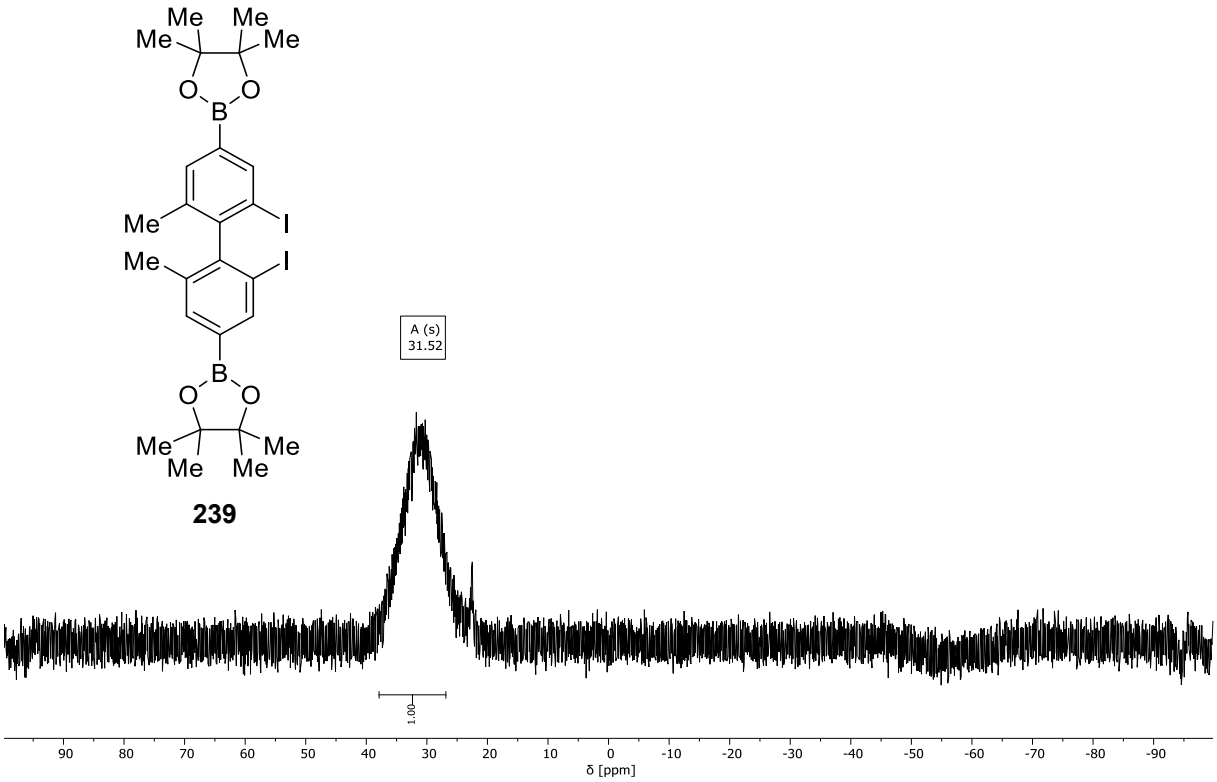

Figure 225: ^{11}B-NMR spectra (96 MHz, $CDCl_3$) of 2,2'-(2,2'-diiodo-6,6'-dimethyl-[1,1'-biphenyl]-4,4'-diyl)bis(4,4,5,5-tetramethyl-1,3,2-dioxaborolane) (**239**).

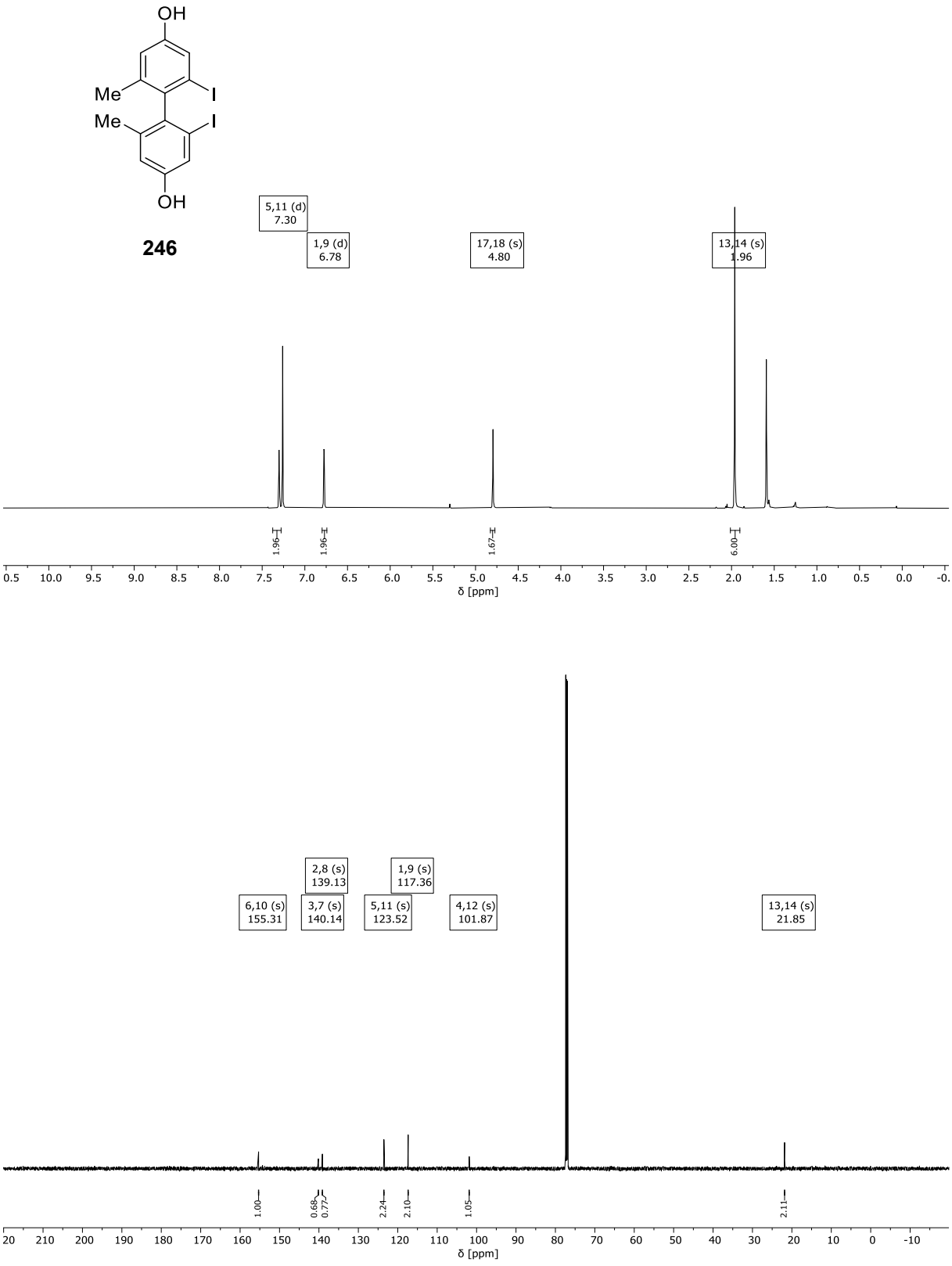

Figure 226: ^{1}H- and ^{13}C-NMR spectra (600 / 151 MHz, $CDCl_3$) of 2,2'-diiodo-6,6'-dimethyl-[1,1'-biphenyl]-4,4'-diol (**246**).

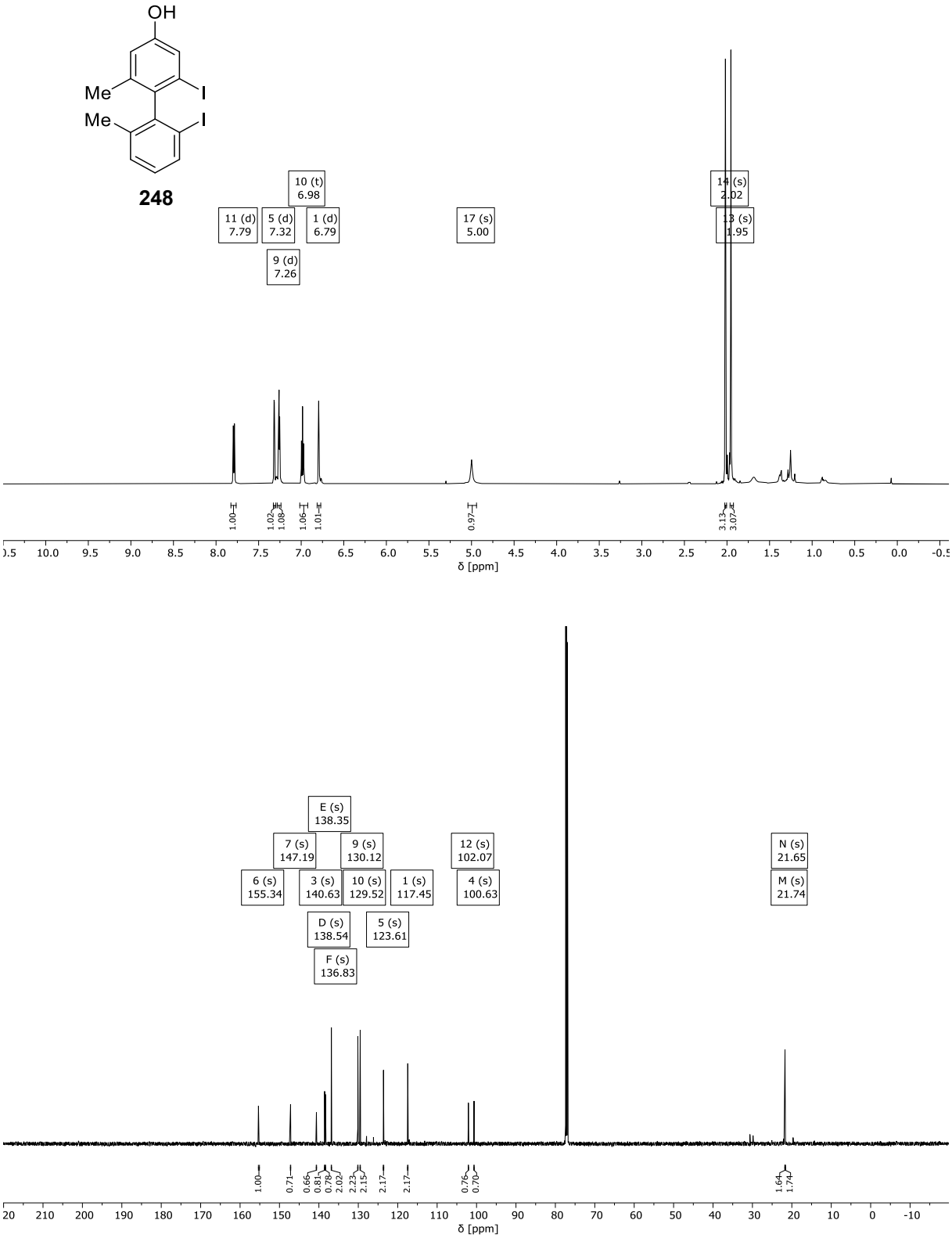

Figure 227: ^{1}H- and ^{13}C-NMR spectra (600 / 151 MHz, $CDCl_3$) of 2,2'-diiodo-6,6'-dimethyl-[1,1'-biphenyl]-4-ol (**248**).

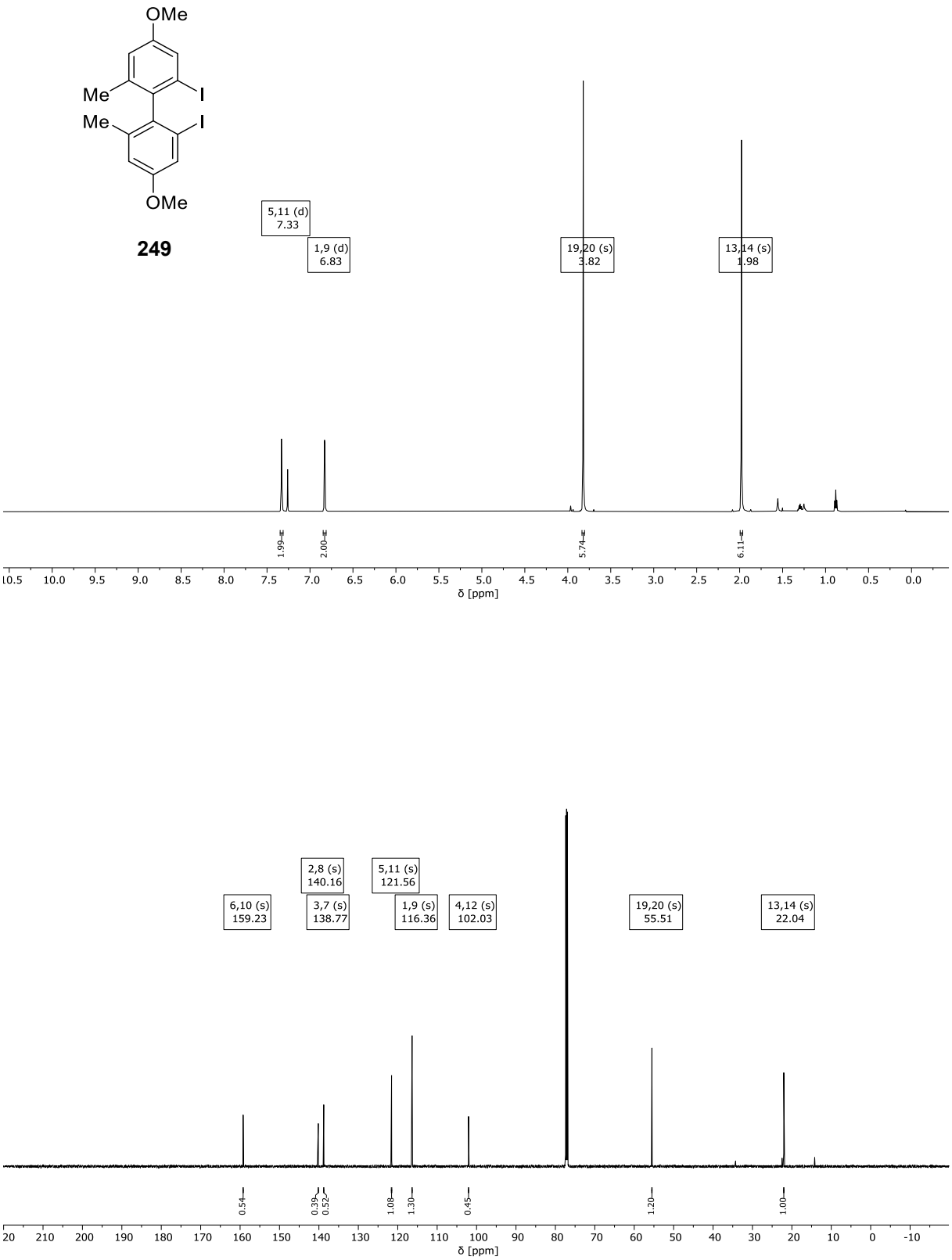

Figure 228: ^{1}H- and ^{13}C-NMR spectra (600 / 151 MHz, $CDCl_3$) of 2,2'-diiodo-4,4'-dimethoxy-6,6'-dimethyl-1,1'-biphenyl (**249**).

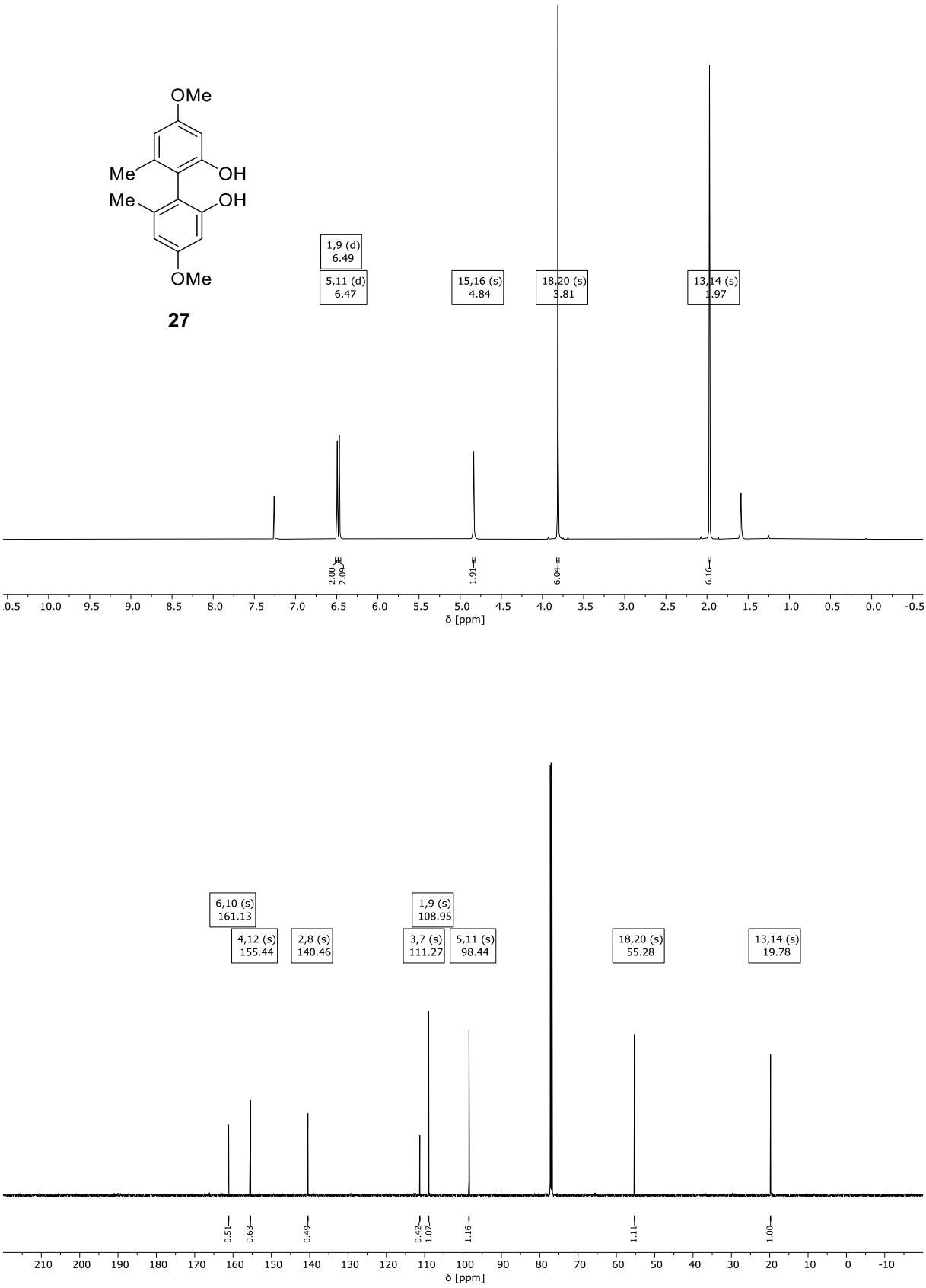

Figure 229: ^{1}H- and ^{13}C-NMR spectra (600 / 151 MHz, $CDCl_3$) of 4,4'-dimethoxy-6,6'-dimethyl-[1,1'-biphenyl]-2,2'-diol (**27**)**.**

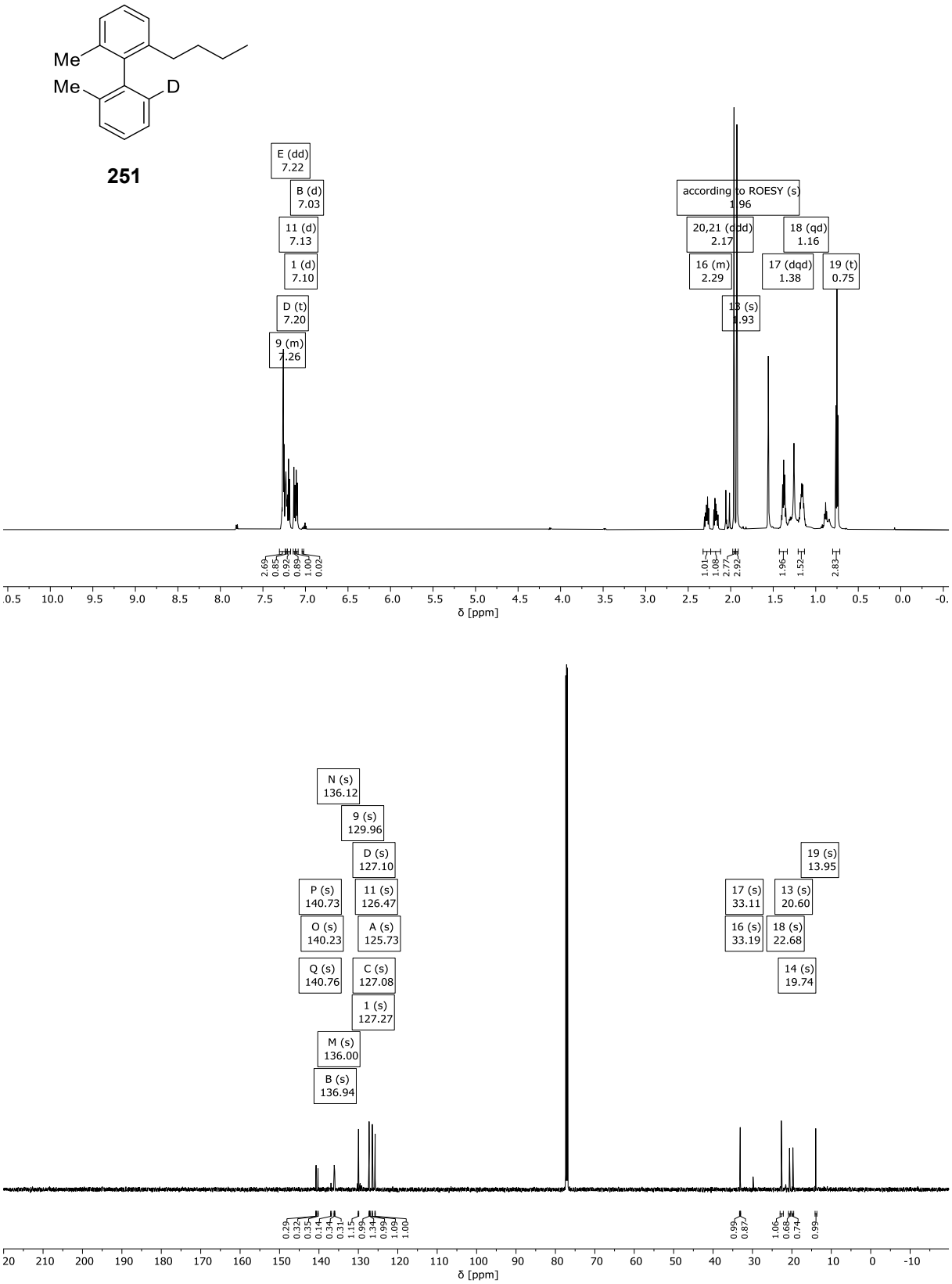

Figure 230: ^{1}H- and ^{13}C-NMR spectra (600 / 151 MHz, $CDCl_3$) of 2-butyl-2',6-dimethyl-1,1'-biphenyl-6'-d (**251**).

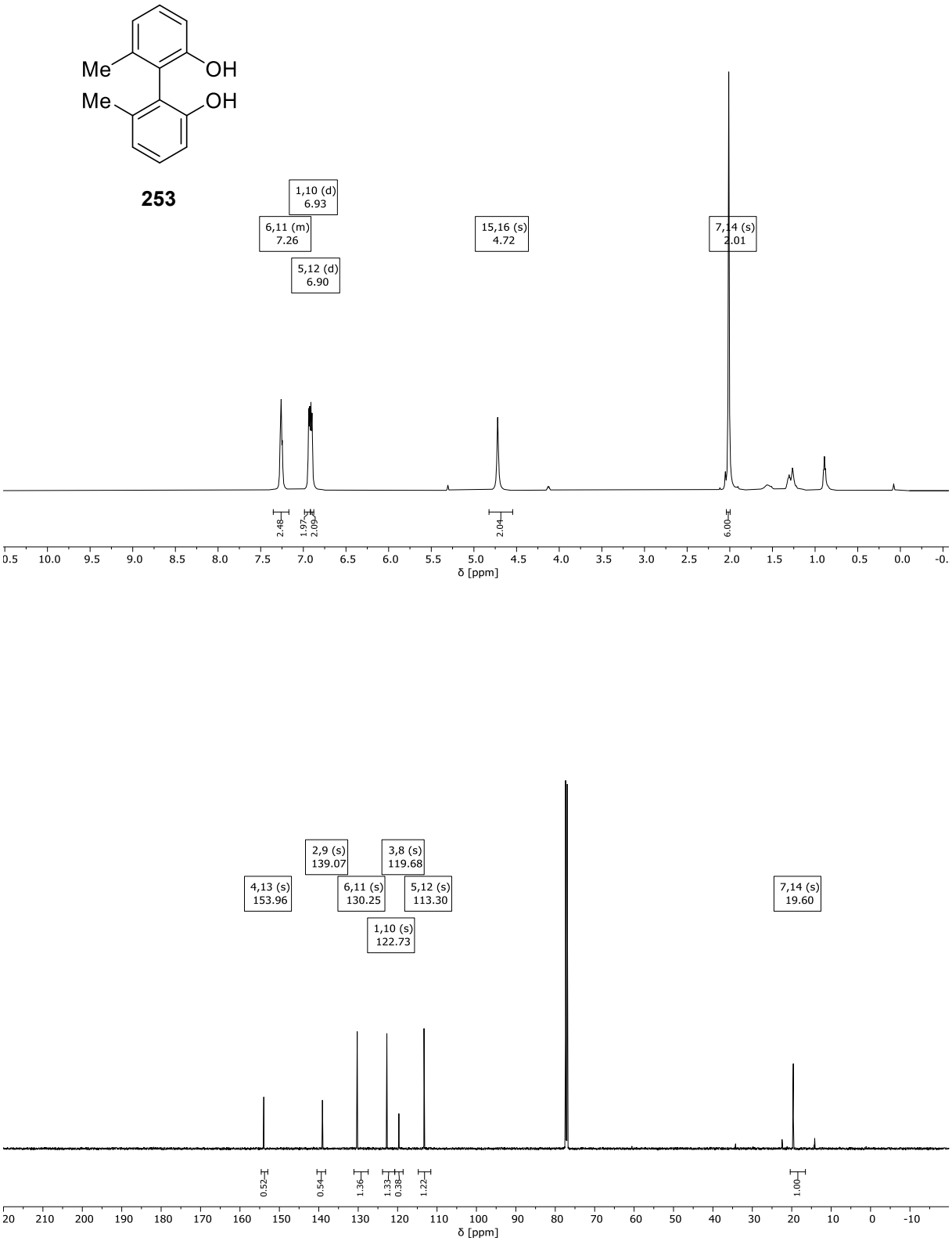

Figure 231: ^{1}H- and ^{13}C-NMR spectra (600 / 151 MHz, $CDCl_3$) of 6,6'-dimethyl-[1,1'-biphenyl]-2,2'-diol (**253**).

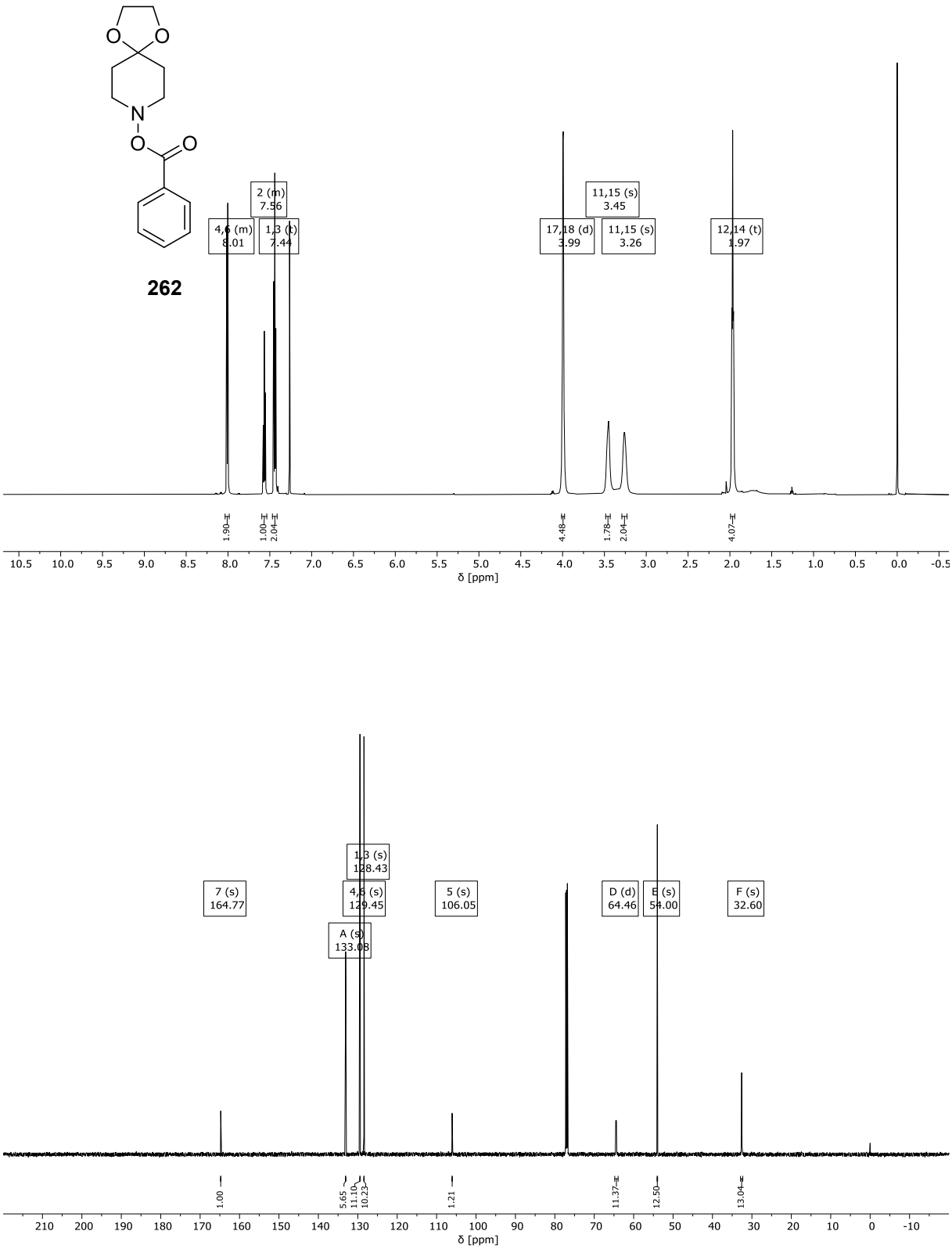

Figure 232: ^{1}H- and ^{13}C-NMR spectra (600 / 151 MHz, $CDCl_3$) of 1,4-dioxa-8-azaspiro[4.5]decan-8-yl benzoate (**262**).

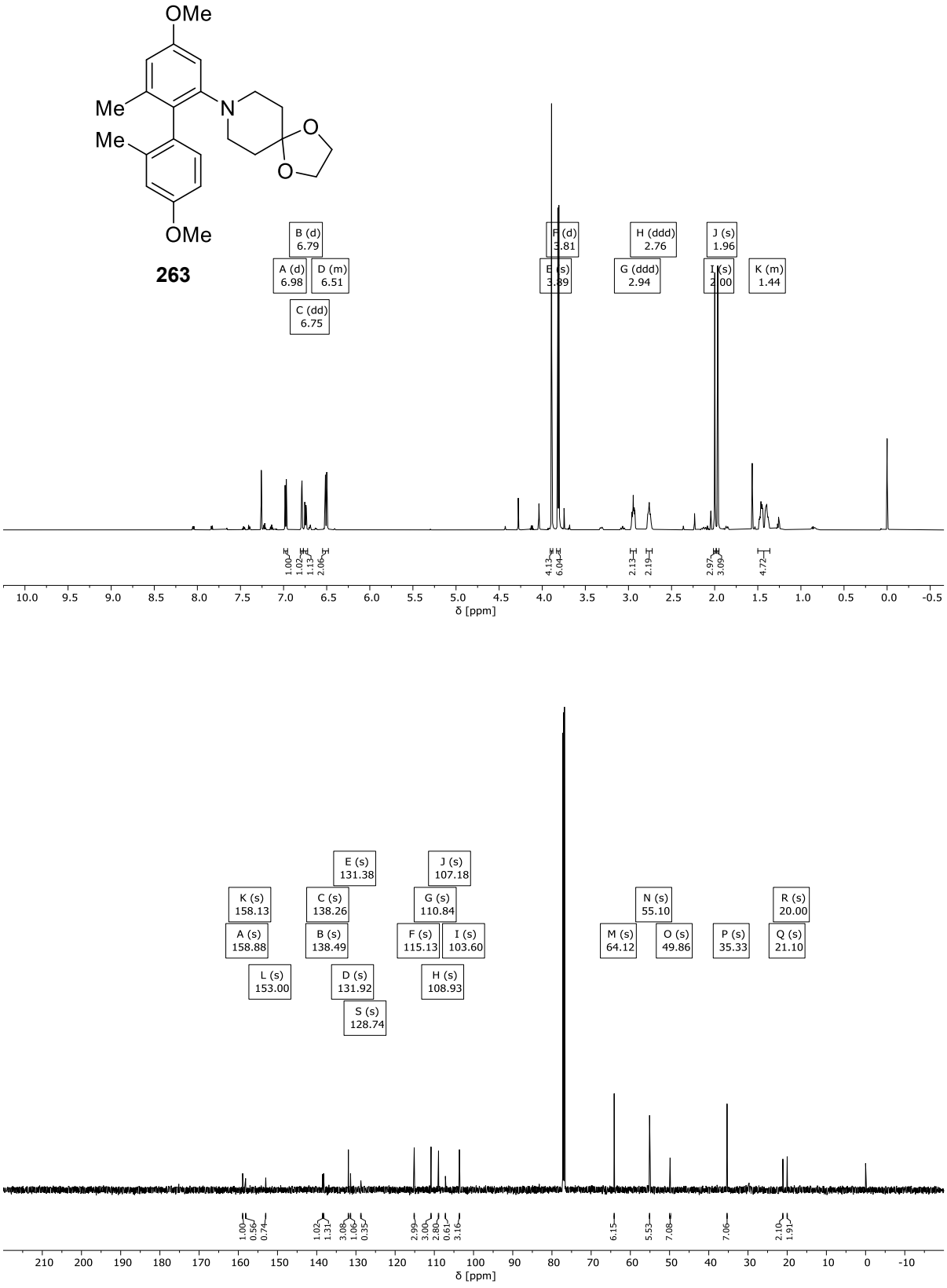

Figure 233: ^{1}H- and ^{13}C-NMR spectra (600 / 151 MHz, $CDCl_3$) of (±)-8-(4,4'-Dimethoxy-2',6-dimethyl-[1,1'-biphenyl]-2-yl)-1,4-dioxa-8-azaspiro[4.5]decan (**263**).

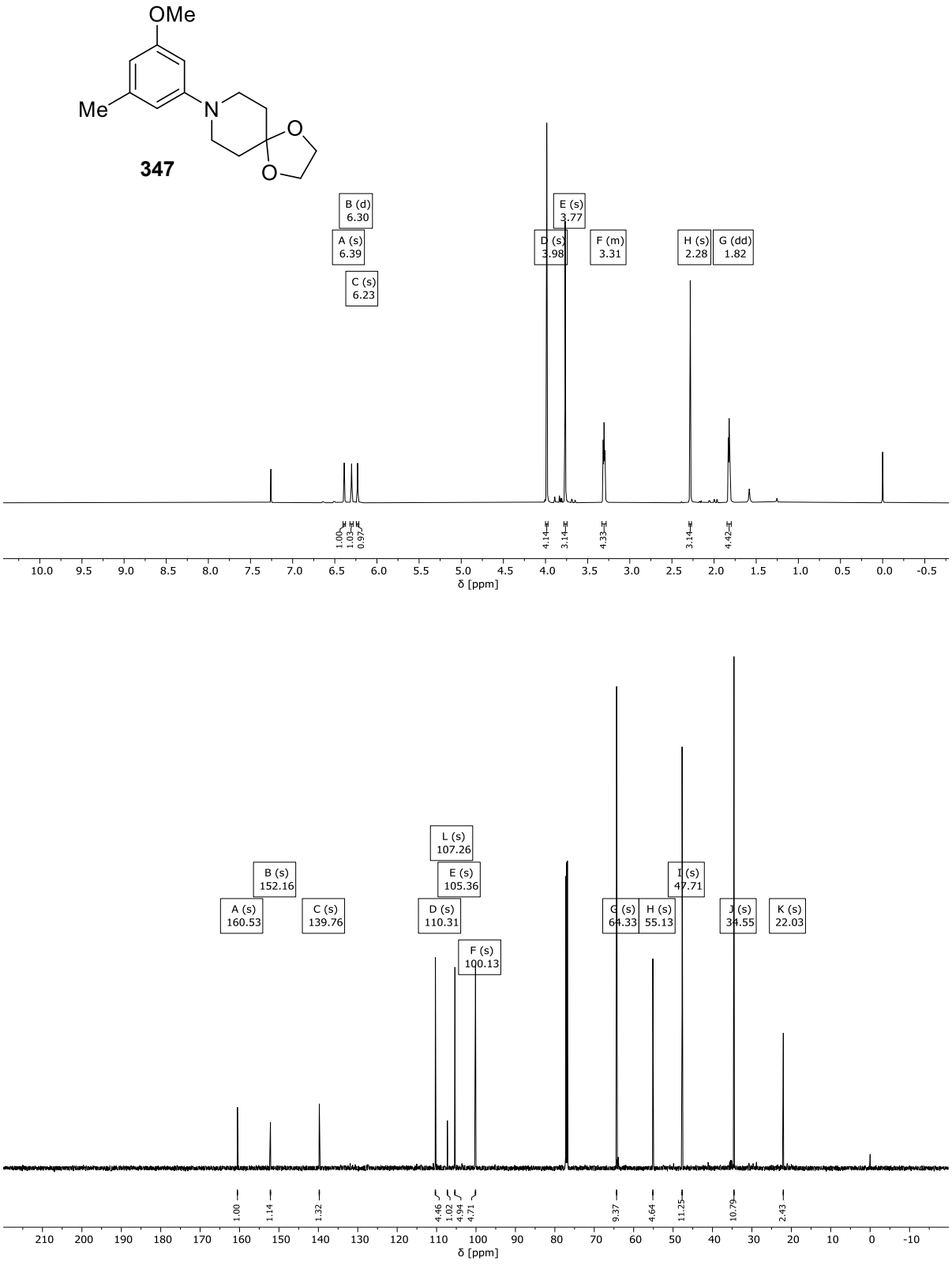

Figure 234: ^{1}H- and ^{13}C-NMR spectra (600 / 151 MHz, $CDCl_3$) of 8-(3-methoxy-5-methylphenyl)-1,4-dioxa-8-azaspiro[4.5]decane (**347**).

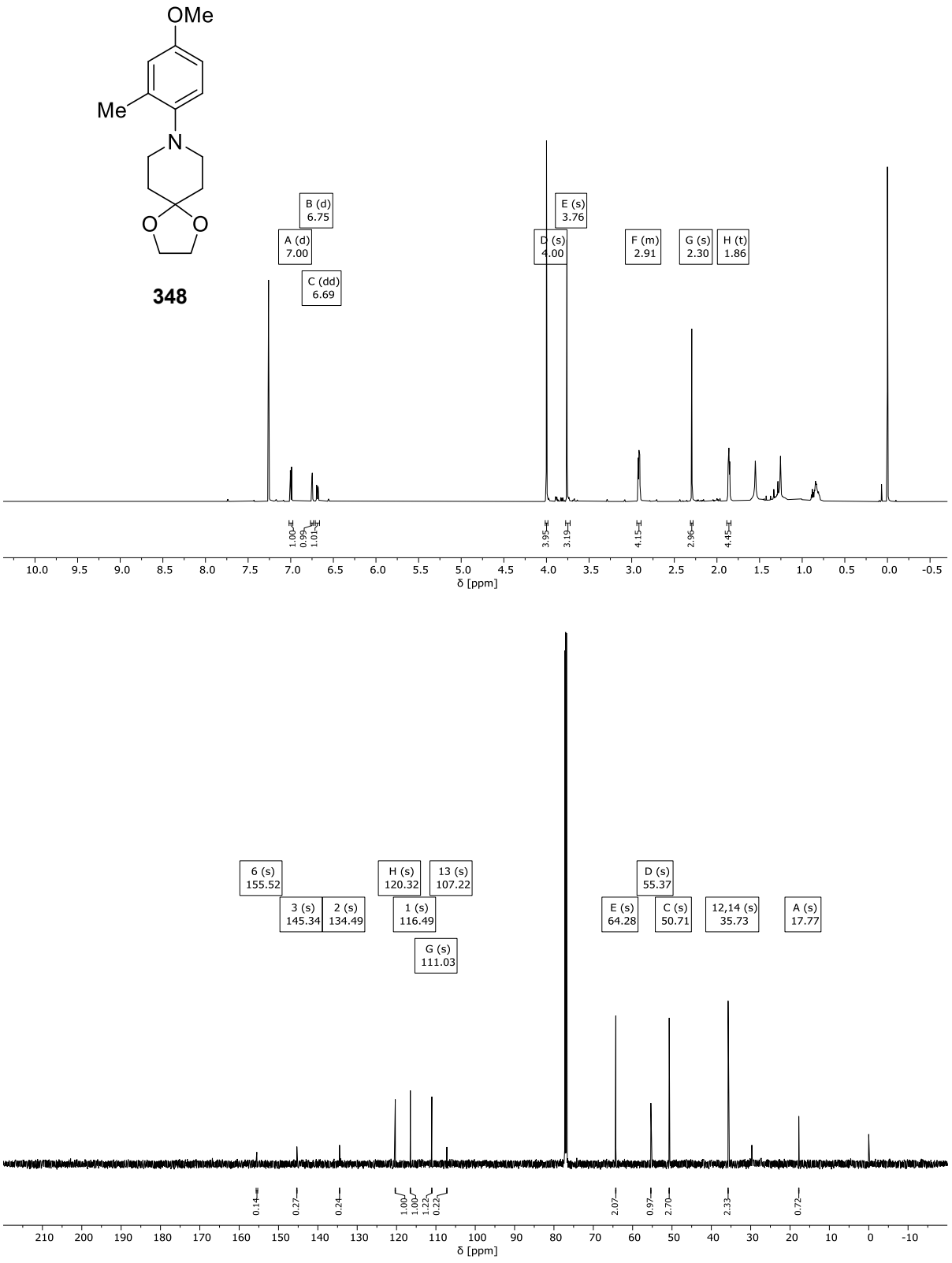

Figure 235: ^{1}H- and ^{13}C-NMR spectra (600 / 151 MHz, $CDCl_3$) of 8-(4-methoxy-2-methylphenyl)-1,4-dioxa-8-azaspiro[4.5]decane (**348**).

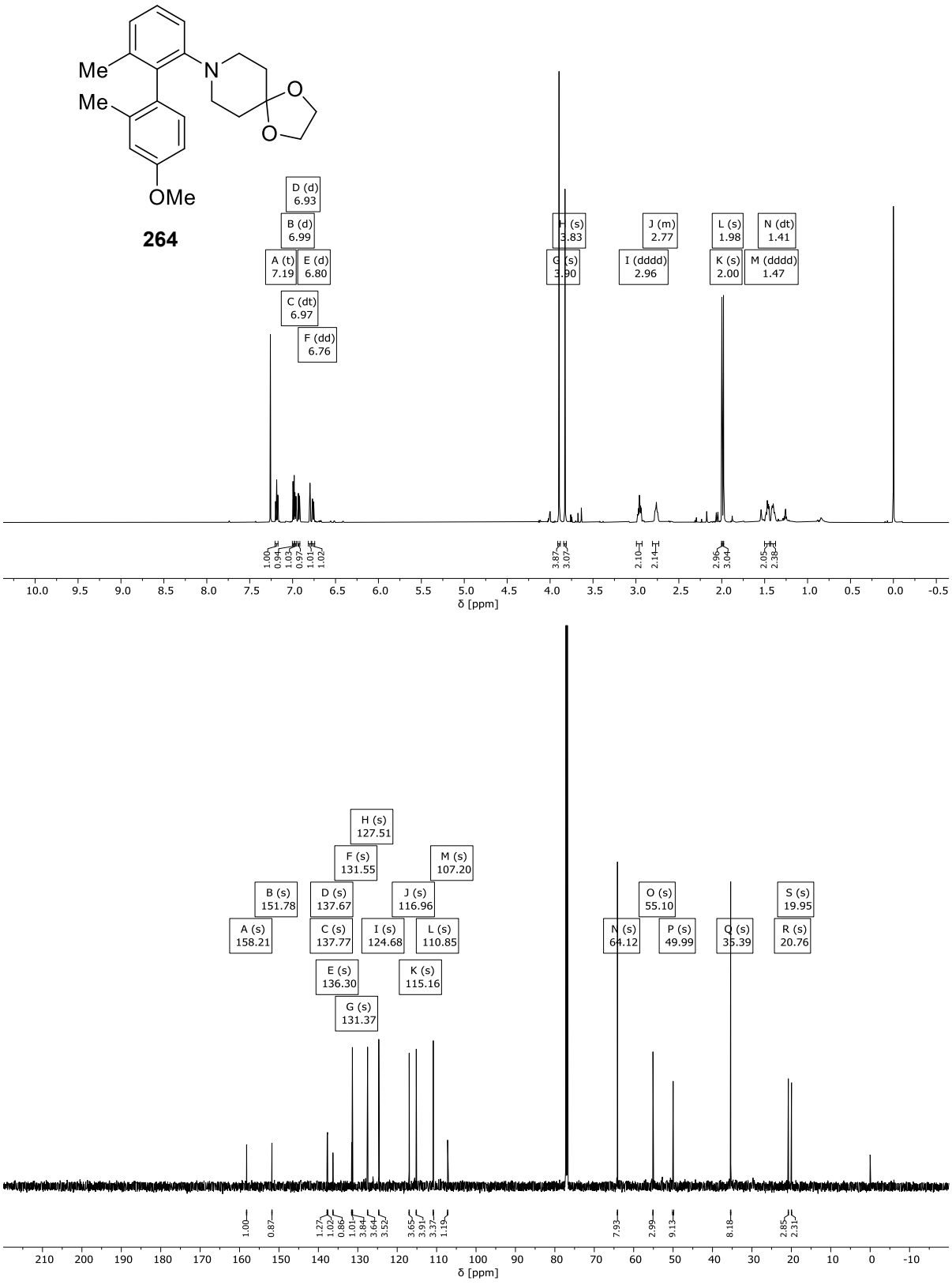

Figure 236: ^{1}H- and ^{13}C-NMR spectra (600 / 151 MHz, $CDCl_3$) of (±)-8-(4'-Methoxy-2',6-dimethyl-[1,1'-biphenyl]-2-yl)-1,4-dioxa-8-azaspiro[4.5]decan (**264**).

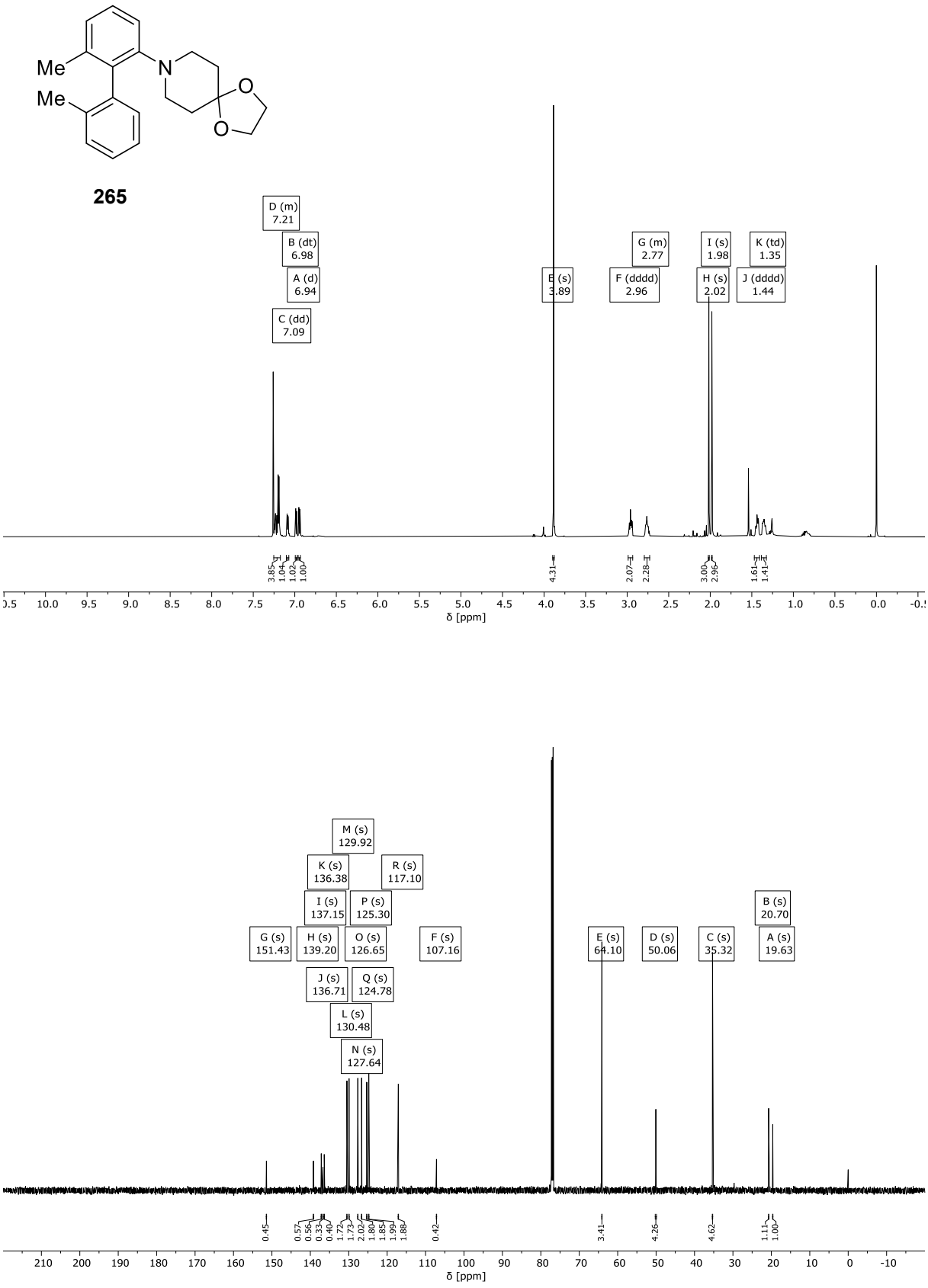

Figure 237: ^{1}H- and ^{13}C-NMR spectra (600 / 151 MHz, $CDCl_3$) of 8-(2',6-dimethyl-[1,1'-biphenyl]-2-yl)-1,4-dioxa-8-azaspiro[4.5]decane (**265**).

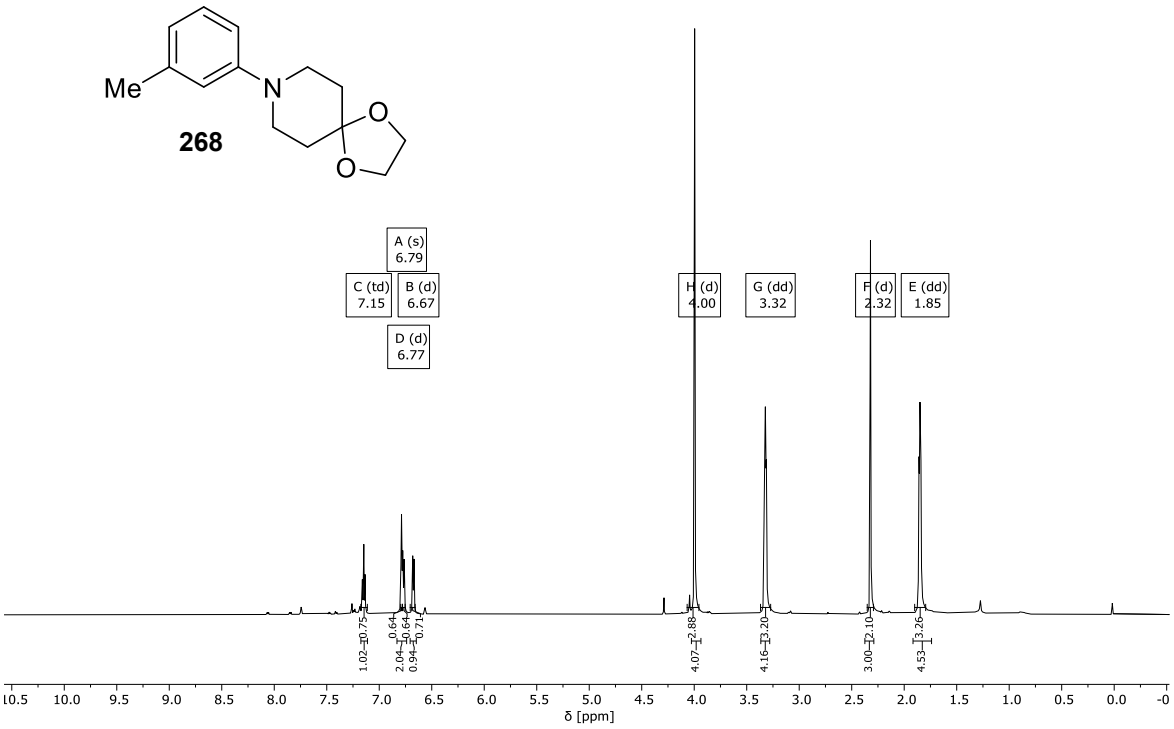

Figure 238: ^{1}H-NMR spectrum (600 MHz, $CDCl_3$) of 8-(*m*-tolyl)-1,4-dioxa-8-azaspiro[4.5]decane (**268**).

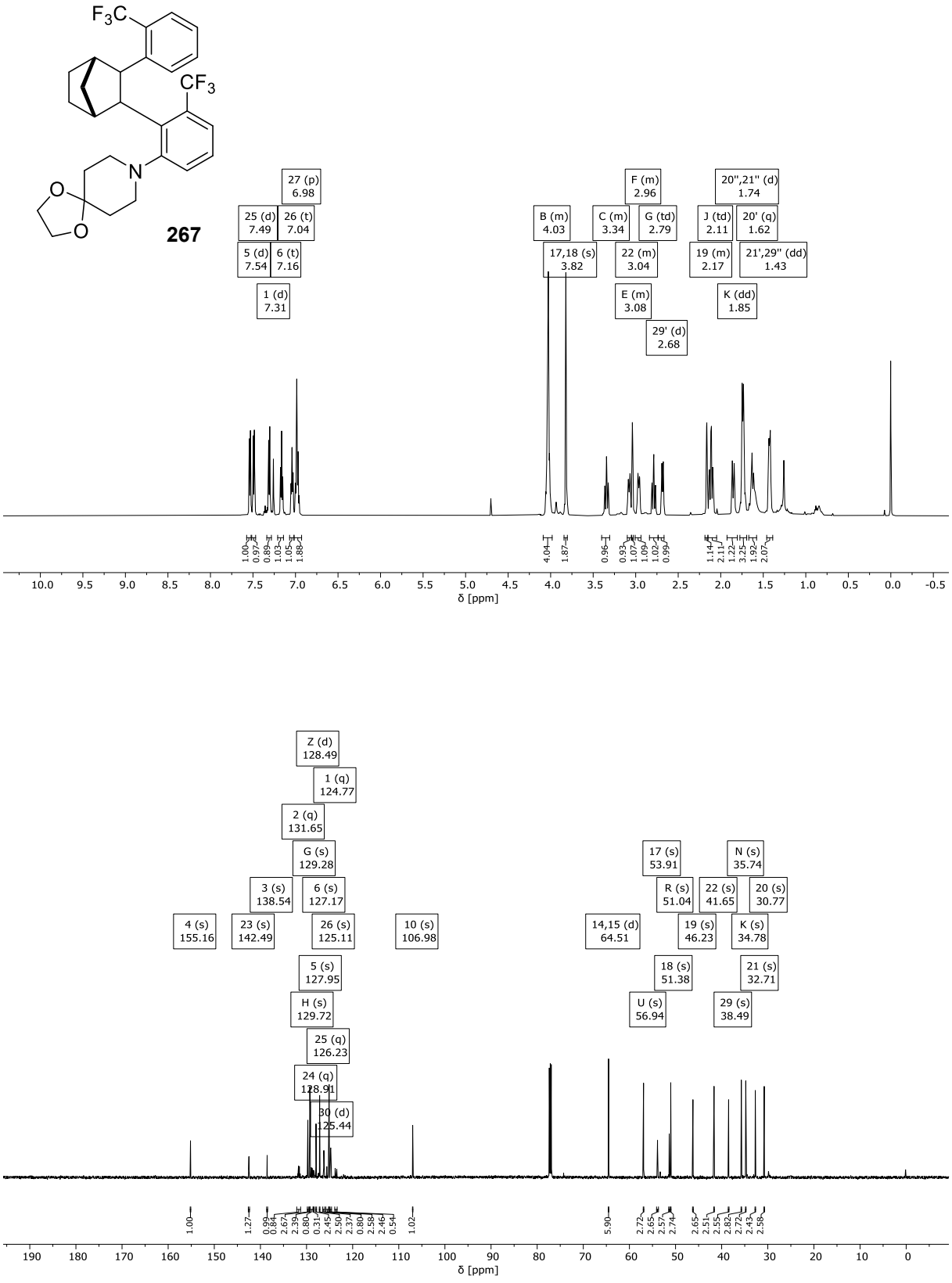

Figure 239: ^{1}H-, ^{13}C-NMR spectra (600 / 151 MHz, $CDCl_3$) of (±)-8-(3-(trifluoromethyl)-2-(3-(2-(trifluoromethyl)phenyl)bicyclo[2.2.1]heptan-2-yl)phenyl)-1,4-dioxa-8-azaspiro[4.5]decane (**267**).

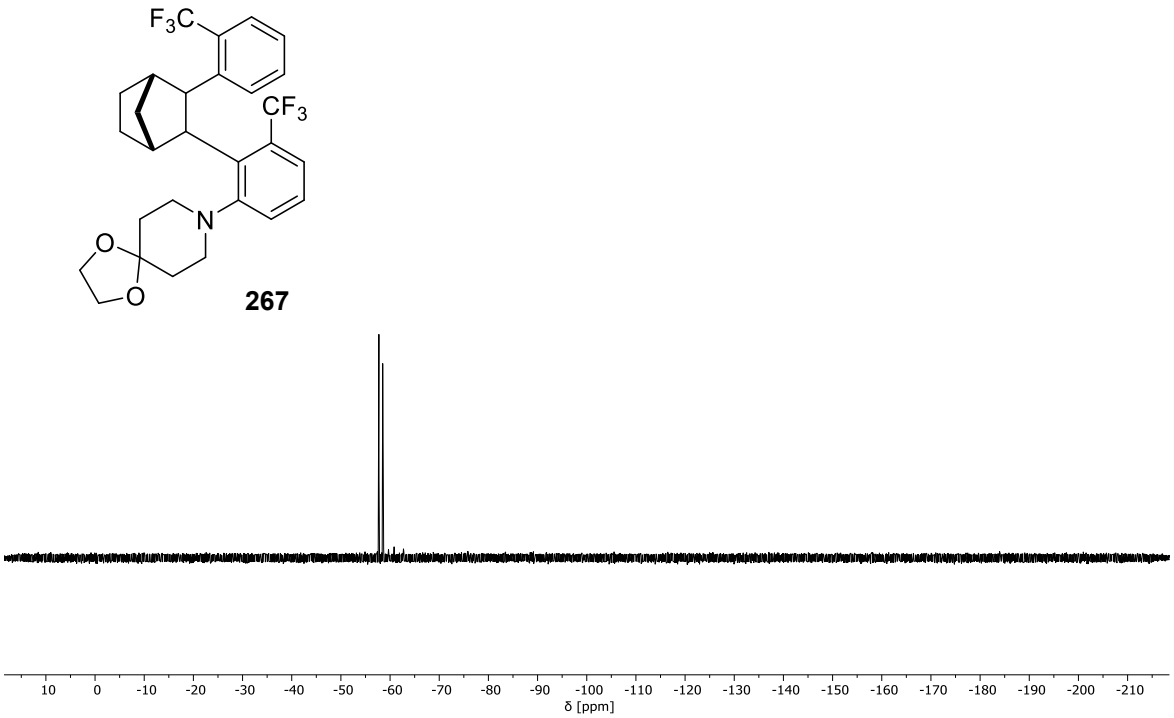

Figure 240: ^{19}F-NMR spectra (282 MHz, $CDCl_3$) of (±)-8-(3-(trifluoromethyl)-2-(3-(2-(trifluoromethyl)phenyl)bicyclo[2.2.1]heptan-2-yl)phenyl)-1,4-dioxa-8-azaspiro[4.5]decane (**267**).

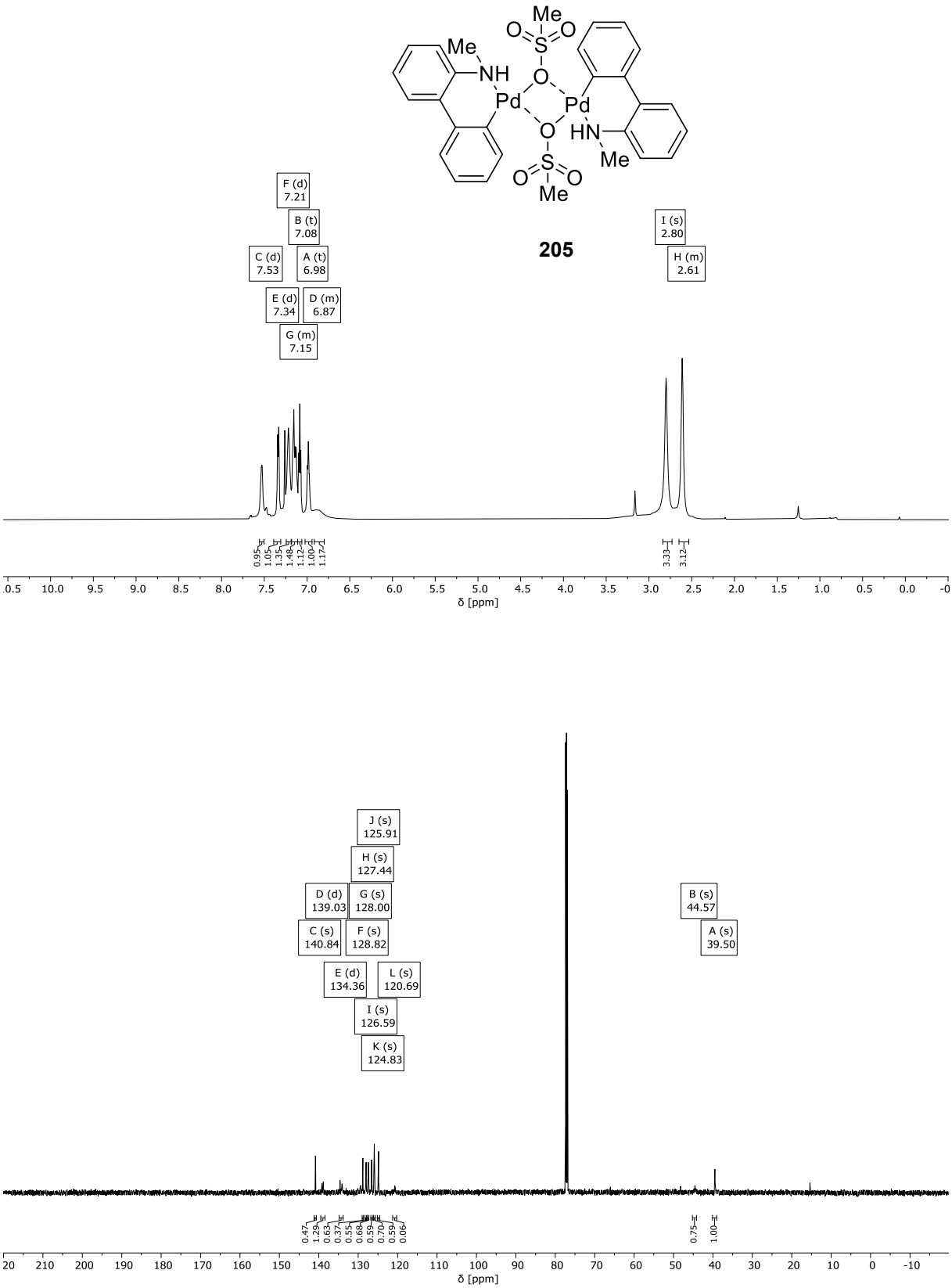

Figure 241: ^{1}H- and ^{13}C-NMR spectra (600 / 151 MHz, $CDCl_3$) of Pd complex **205**.

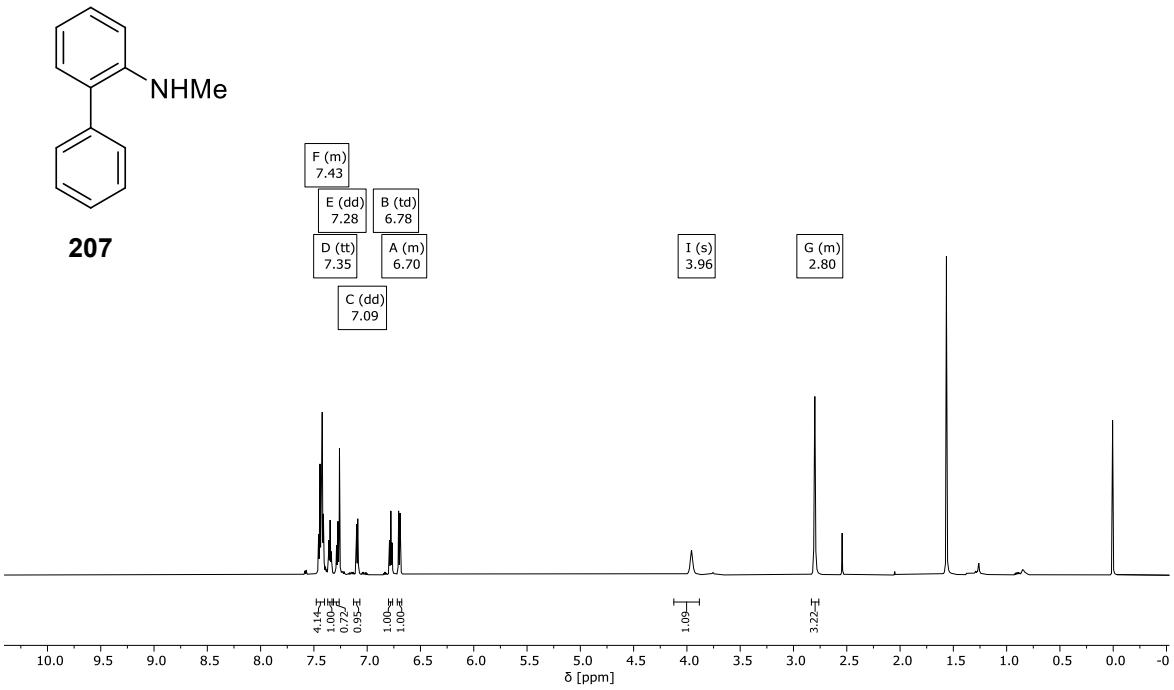

Figure 242: ^{1}H-NMR spectrum (400 MHz, $CDCl_3$) of N-methyl-[1,1'-biphenyl]-2-amine (**207**).

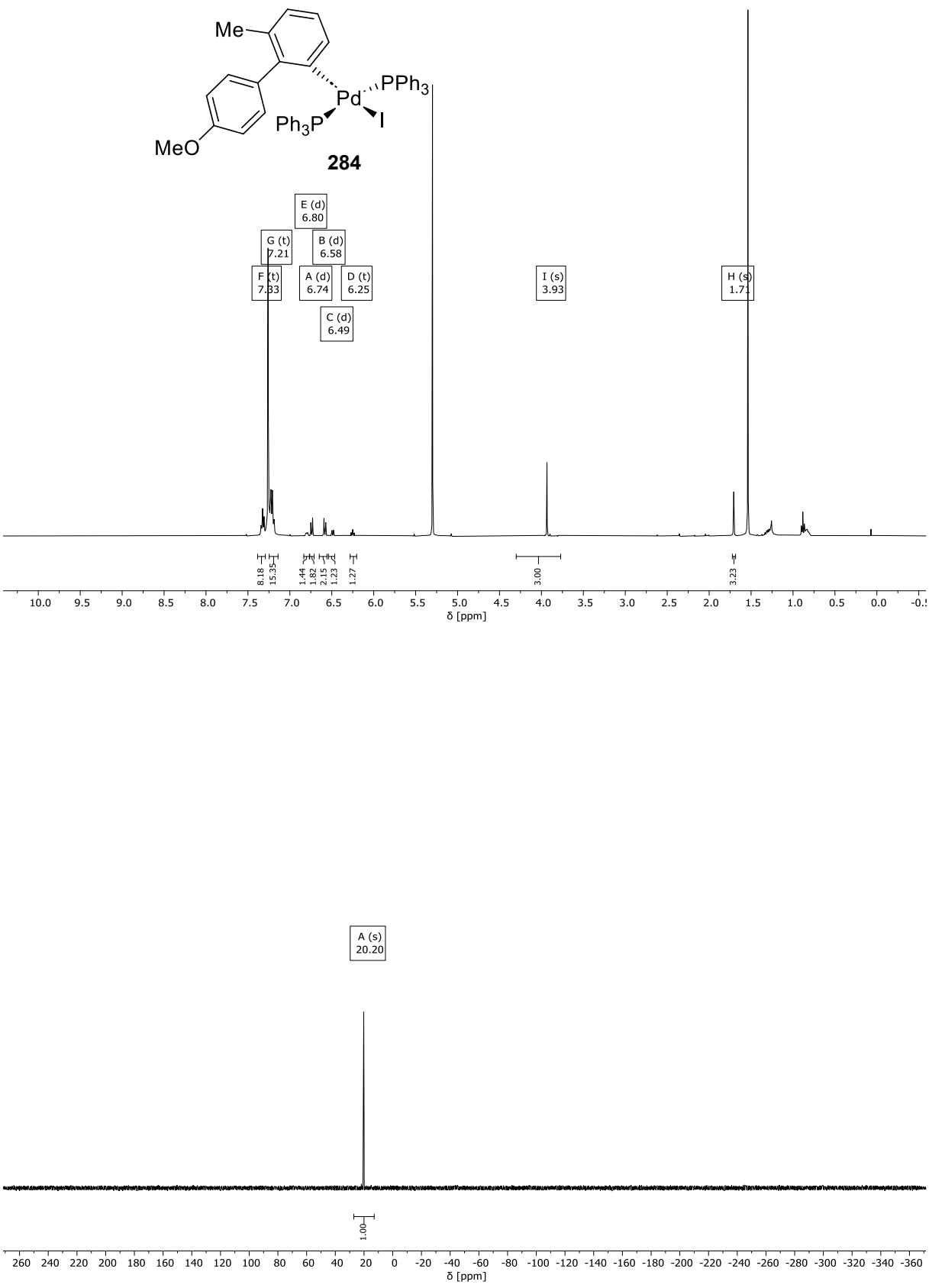

Figure 243: ^{1}H- and ^{31}P-NMR spectra (300 / 122 MHz, $CDCl_3$) of Pd complex **284**.

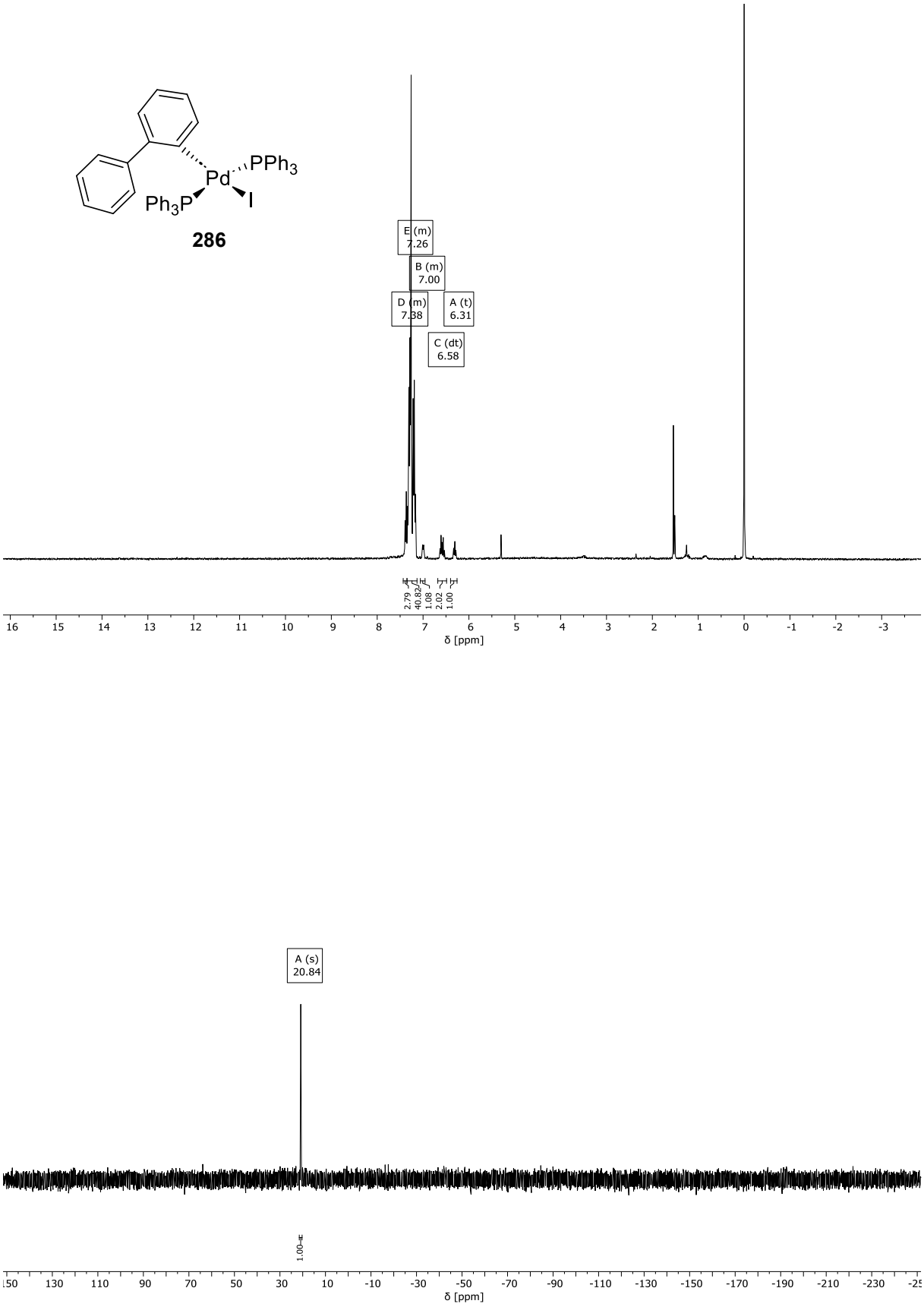

Figure 244: ^{1}H- and ^{31}P-NMR spectra (300 / 122 MHz, $CDCl_3$) of Pd complex **286**.

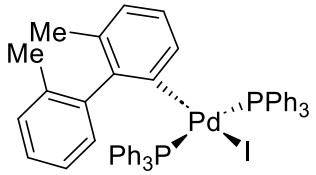

287

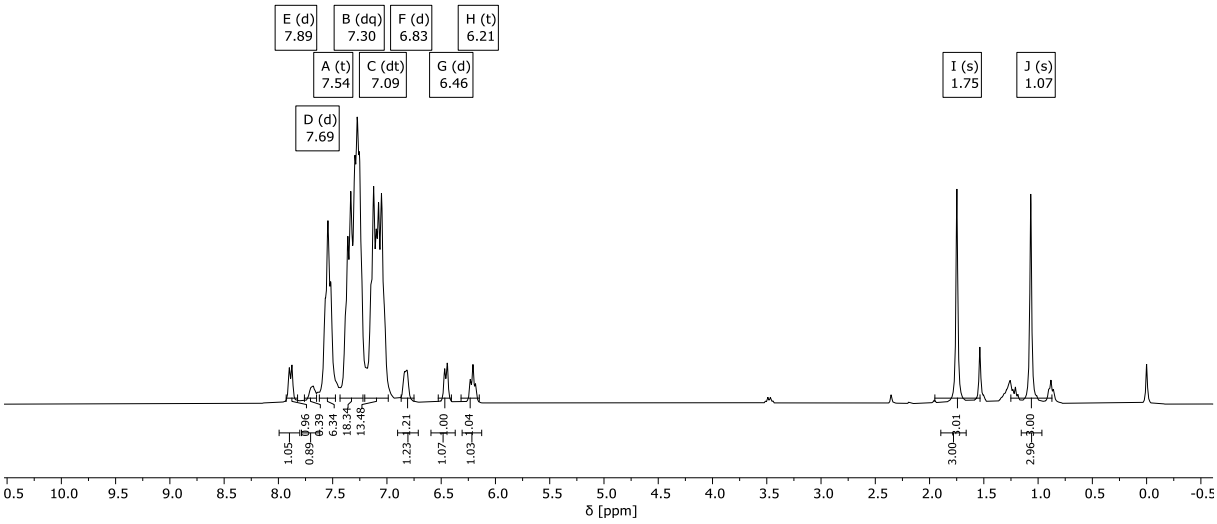

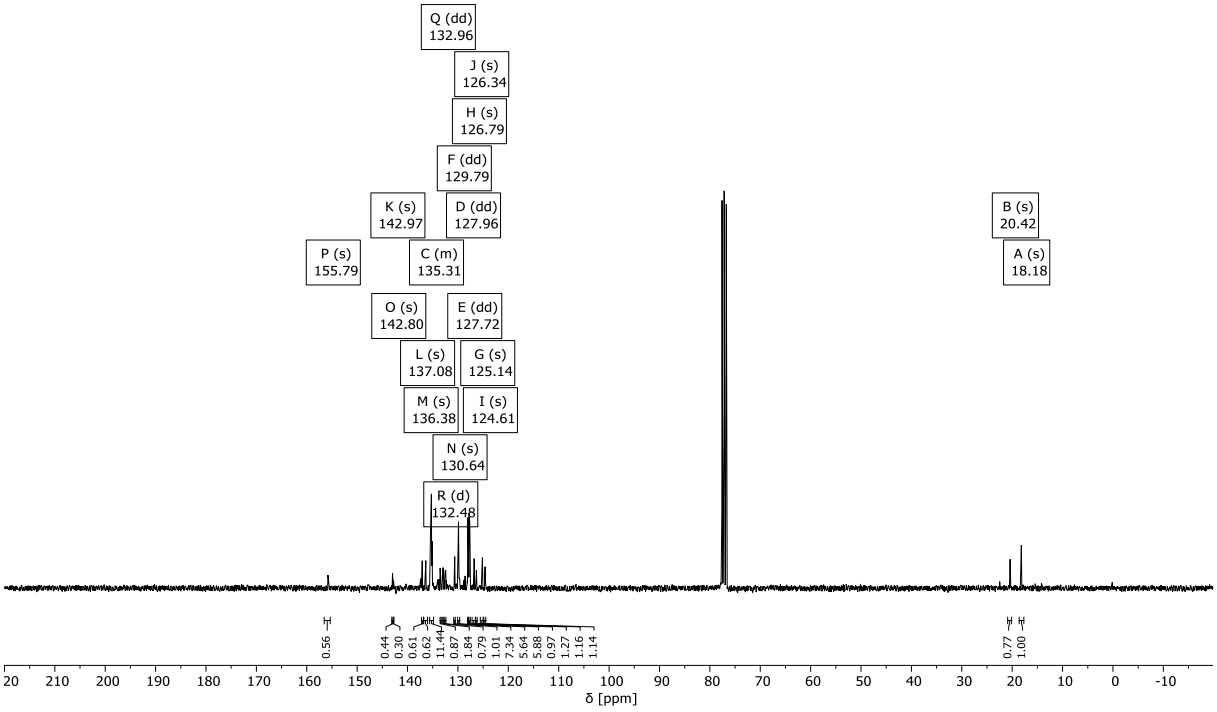

Figure 245: ^{1}H-, ^{13}C-NMR spectra (600 / 151 MHz, $CDCl_3$) of Pd complex **287**.

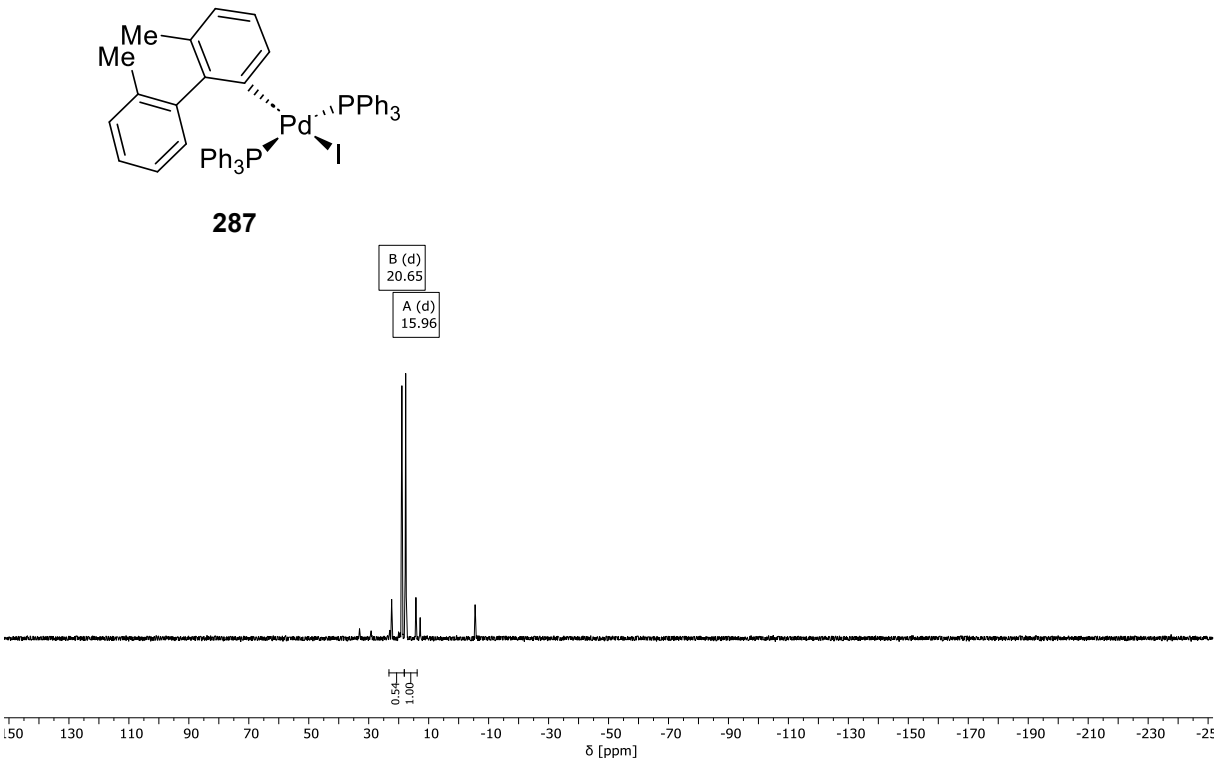

Figure 246: ^{31}P-NMR spectra (121 MHz, $CDCl_3$) of Pd complex **287**.

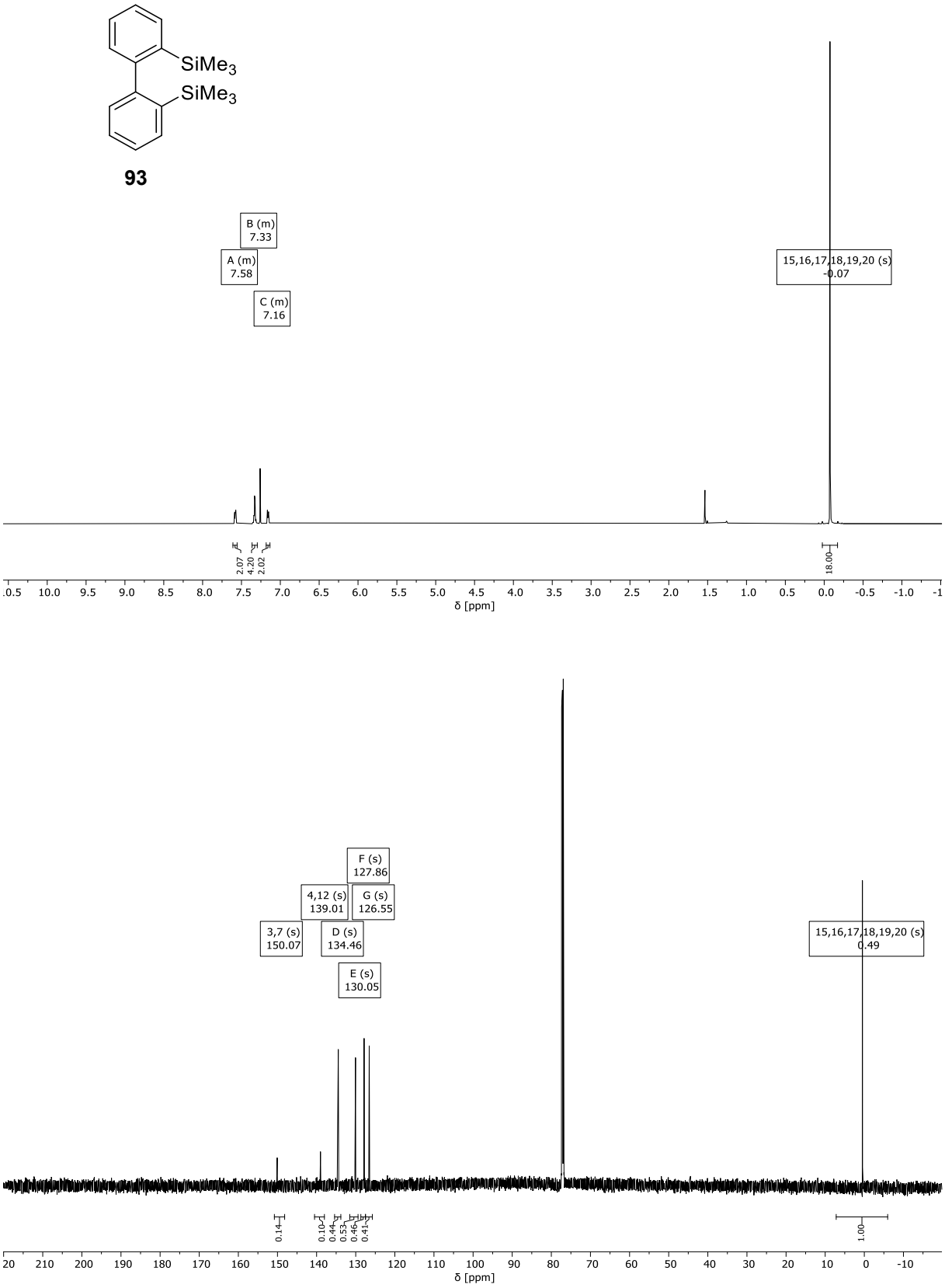

Figure 247: ^{1}H- and ^{13}C-NMR spectra (600 / 151 MHz, $CDCl_3$) of 2,2'-bis(trimethylsilyl)-1,1'-biphenyl (**93**).

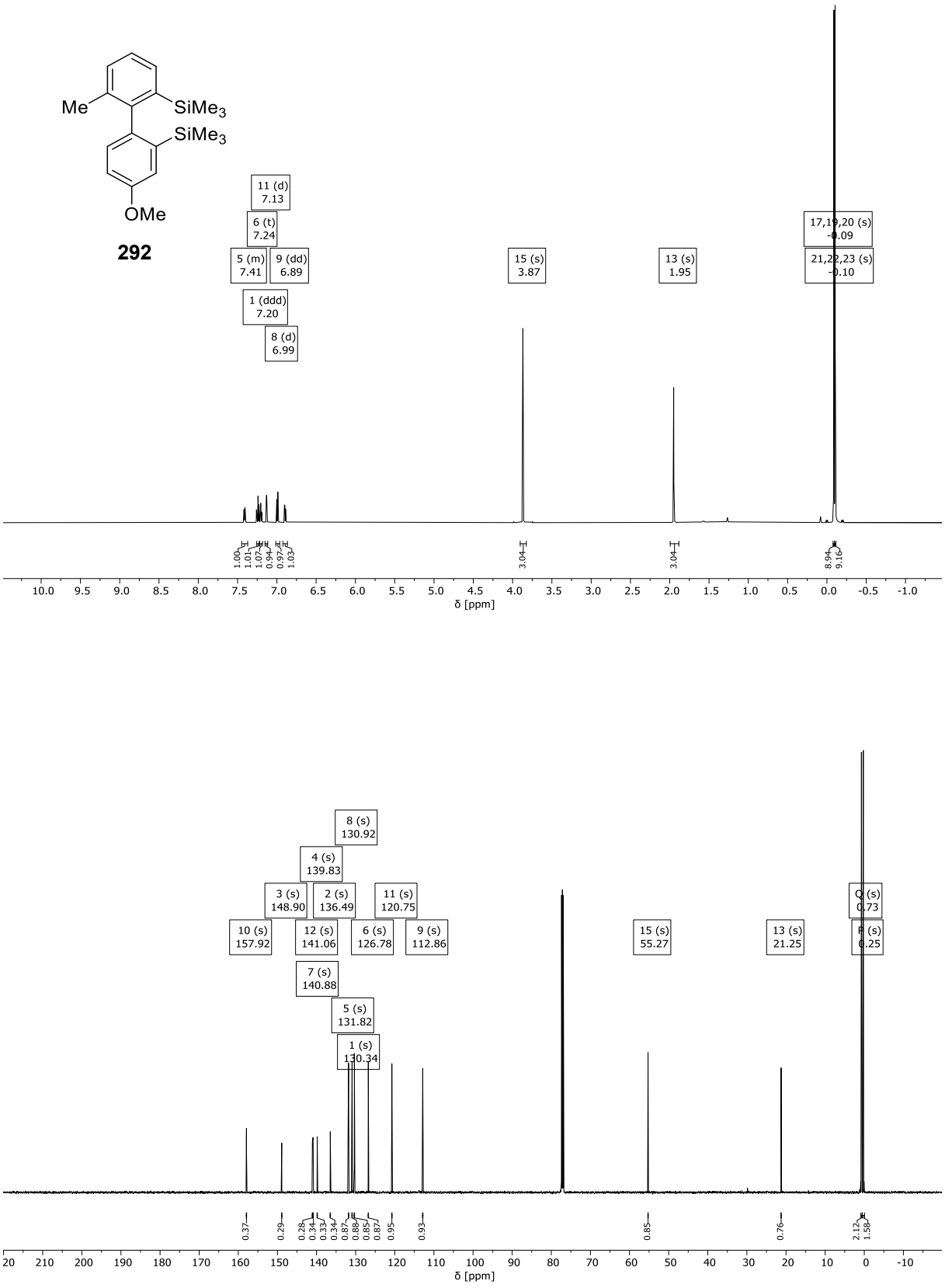

Figure 248: ^{1}H- and ^{13}C-NMR spectra (600 / 151 MHz, $CDCl_3$) of (4-methoxy-6'-methyl-[1,1'-biphenyl]-2,2'-diyl)bis(trimethylsilane) (**292**).

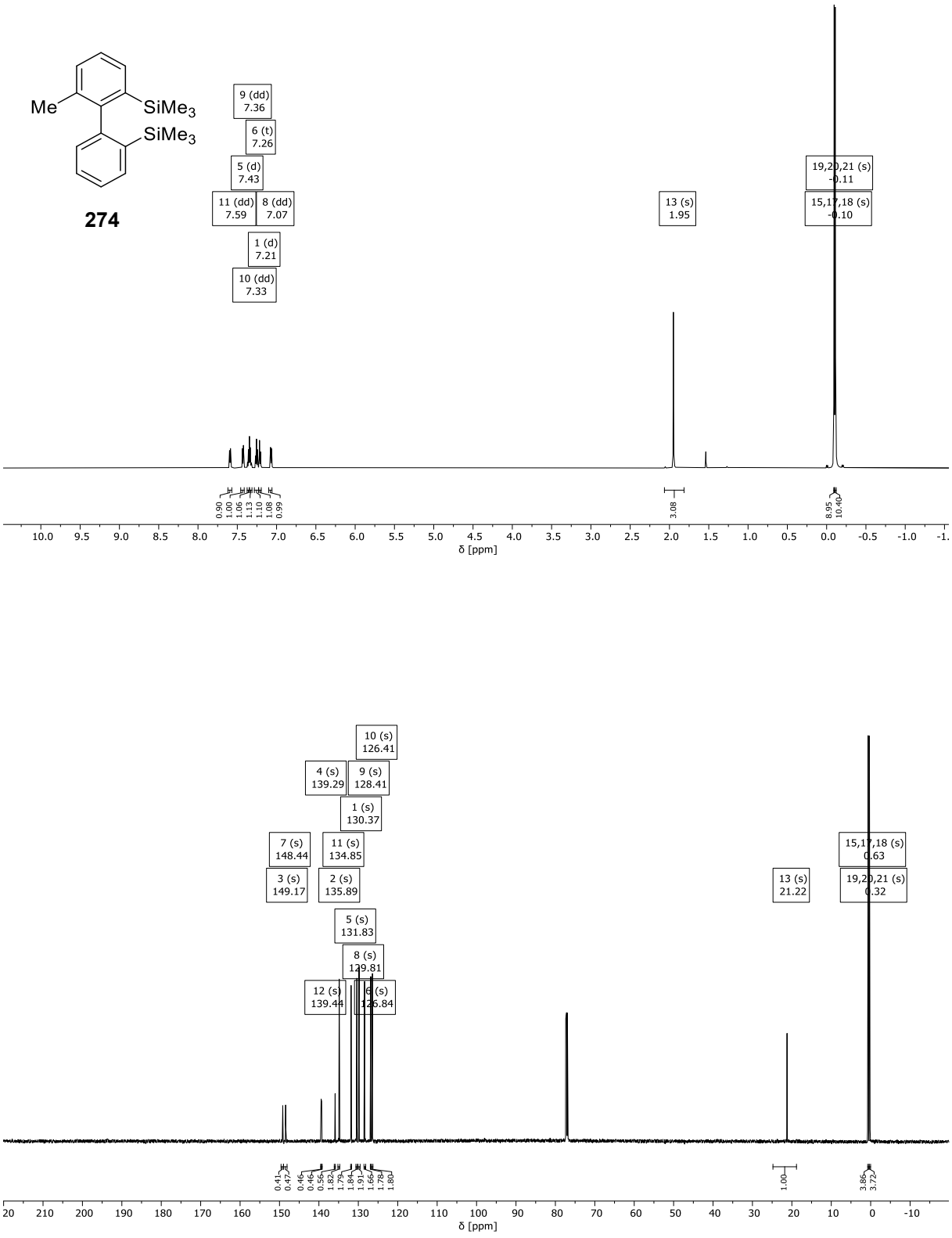

Figure 249: ^{1}H- and ^{13}C-NMR spectra (600 / 151 MHz, $CDCl_3$) of (6-methyl-[1,1'-biphenyl]-2,2'-diyl)bis(trimethylsilane) (**274**).

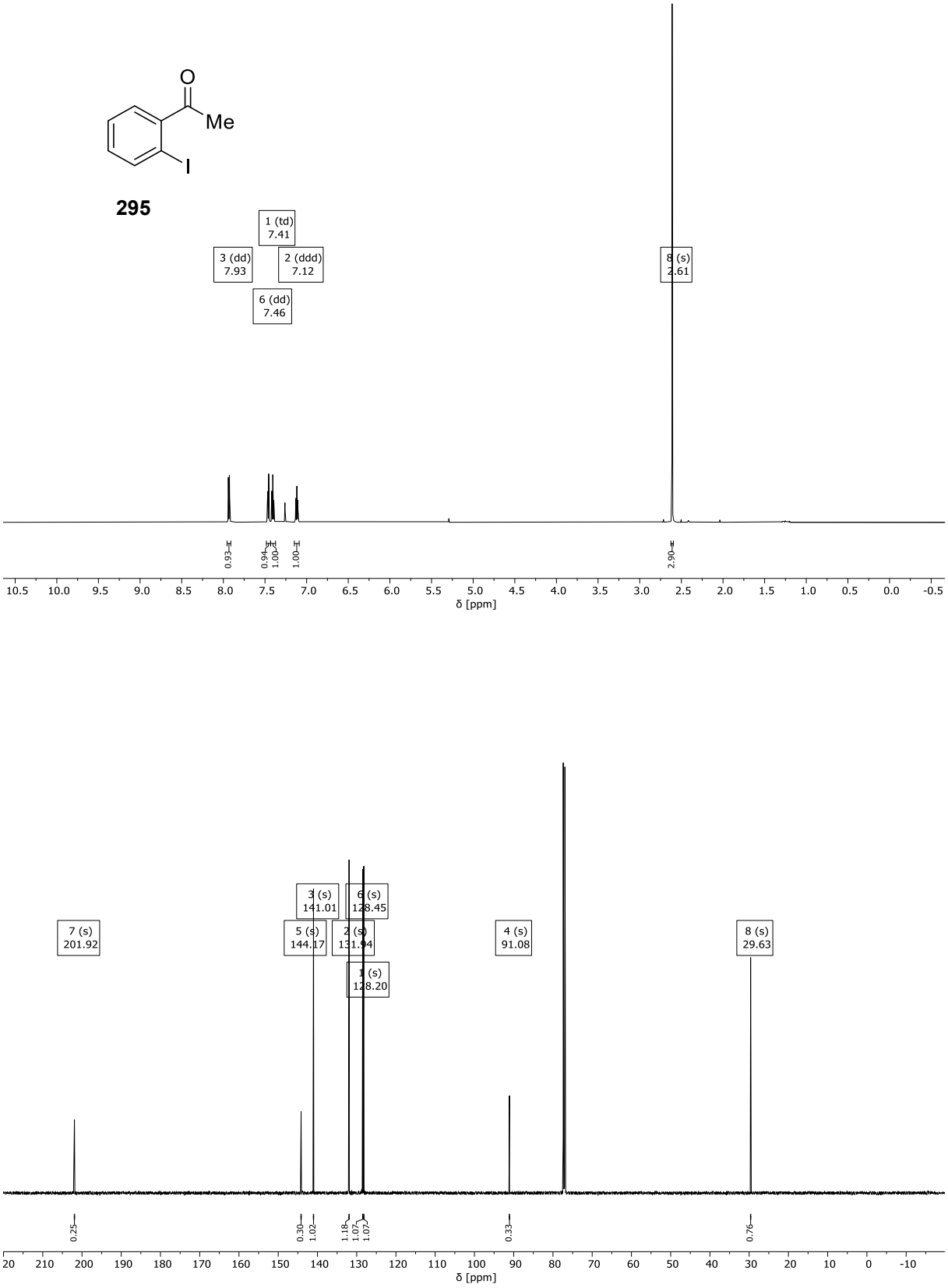

Figure 250: ^{1}H- and ^{13}C-NMR spectra (600 / 151 MHz, $CDCl_3$) of 1-(2-iodophenyl)ethan-1-one (**295**).

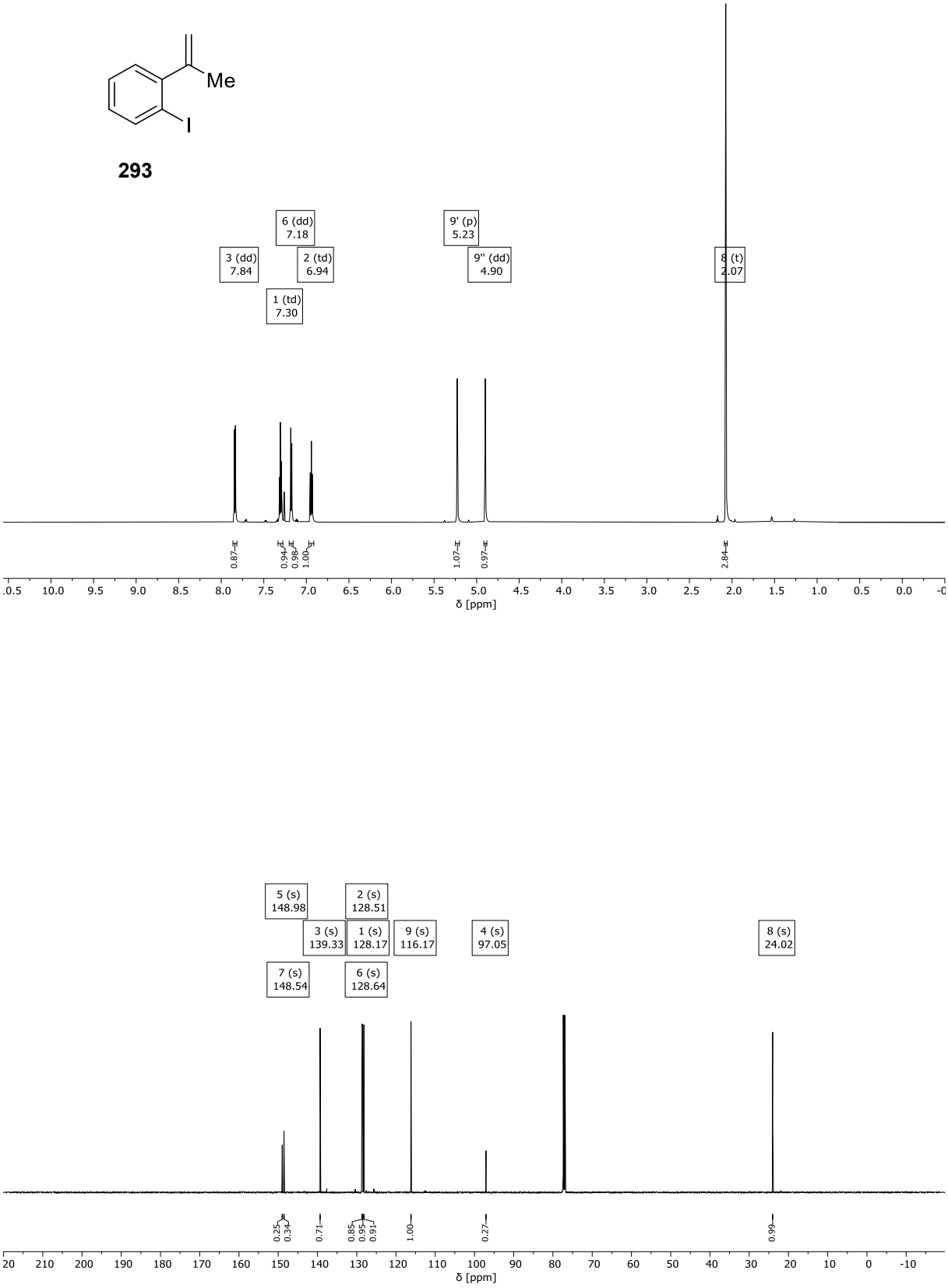

Figure 251: ^{1}H- and ^{13}C-NMR spectra (600 / 151 MHz, $CDCl_3$) of 1-iodo-2-(prop-1-en-2-yl)benzene (**293**).

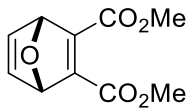

296

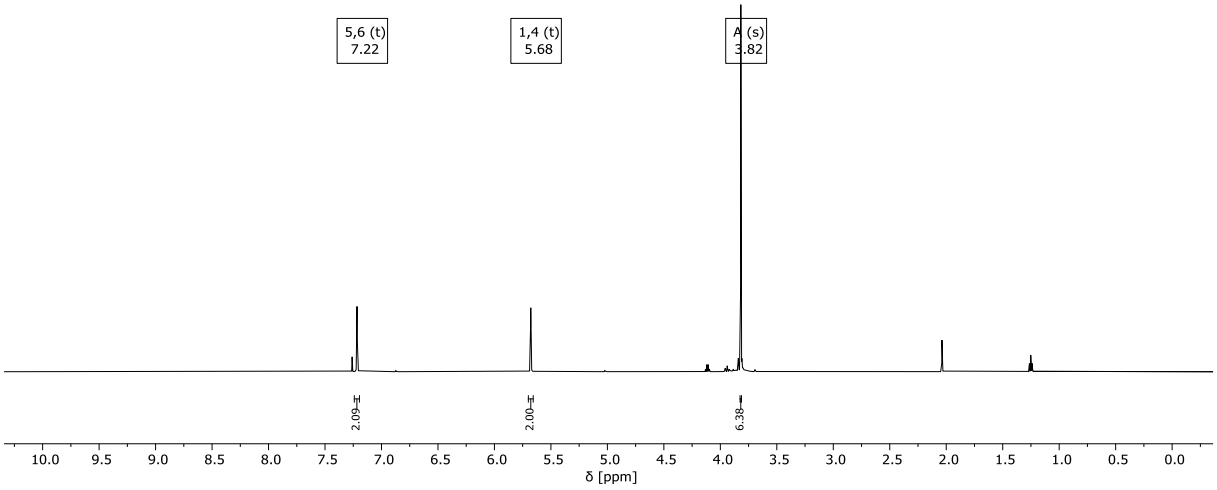

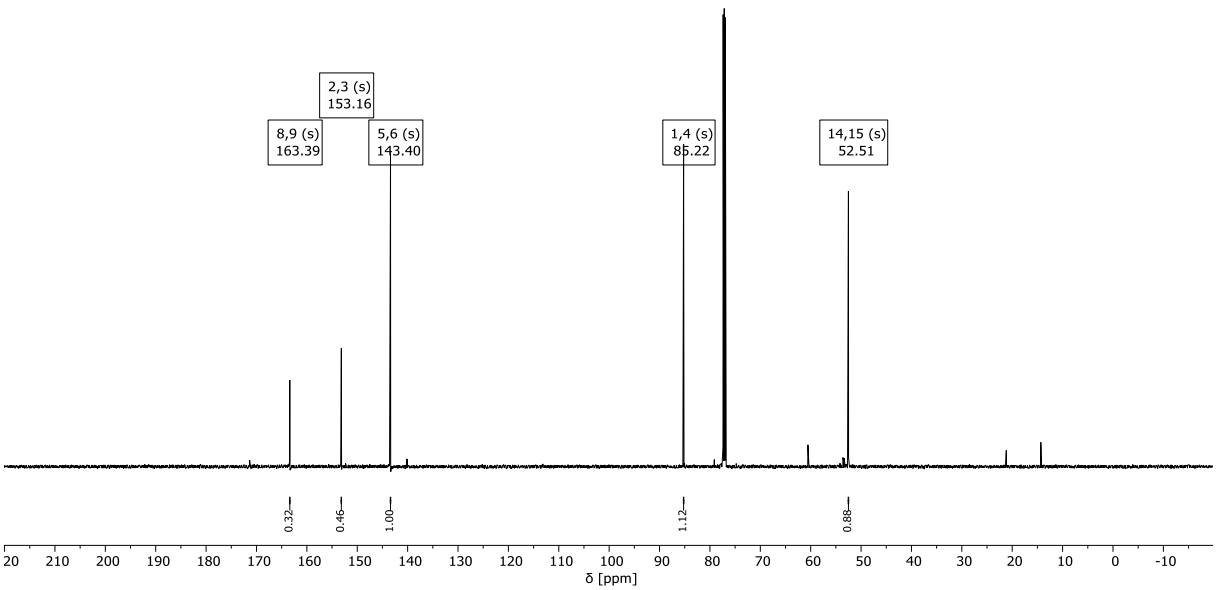

Figure 252: ^{1}H- and ^{13}C-NMR spectra (600 / 151 MHz, $CDCl_3$) of dimethyl (1R,4S)-7-oxabicyclo[2.2.1]hepta-2,5-diene-2,3-dicarboxylate (**296**).

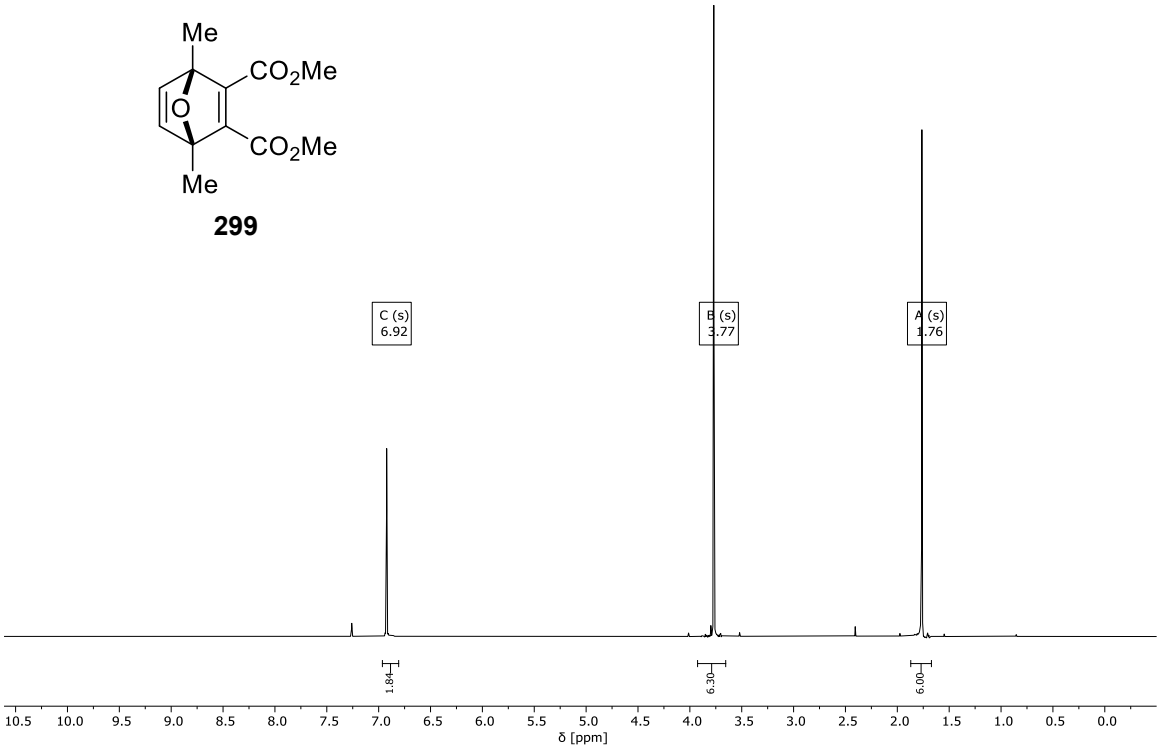

Figure 253: ^{1}H-NMR spectrum (300 MHz, $CDCl_3$) of dimethyl (1R,4S)-1,4-dimethyl-7-oxabicyclo[2.2.1]hepta-2,5-diene-2,3-dicarboxylate (**299**).

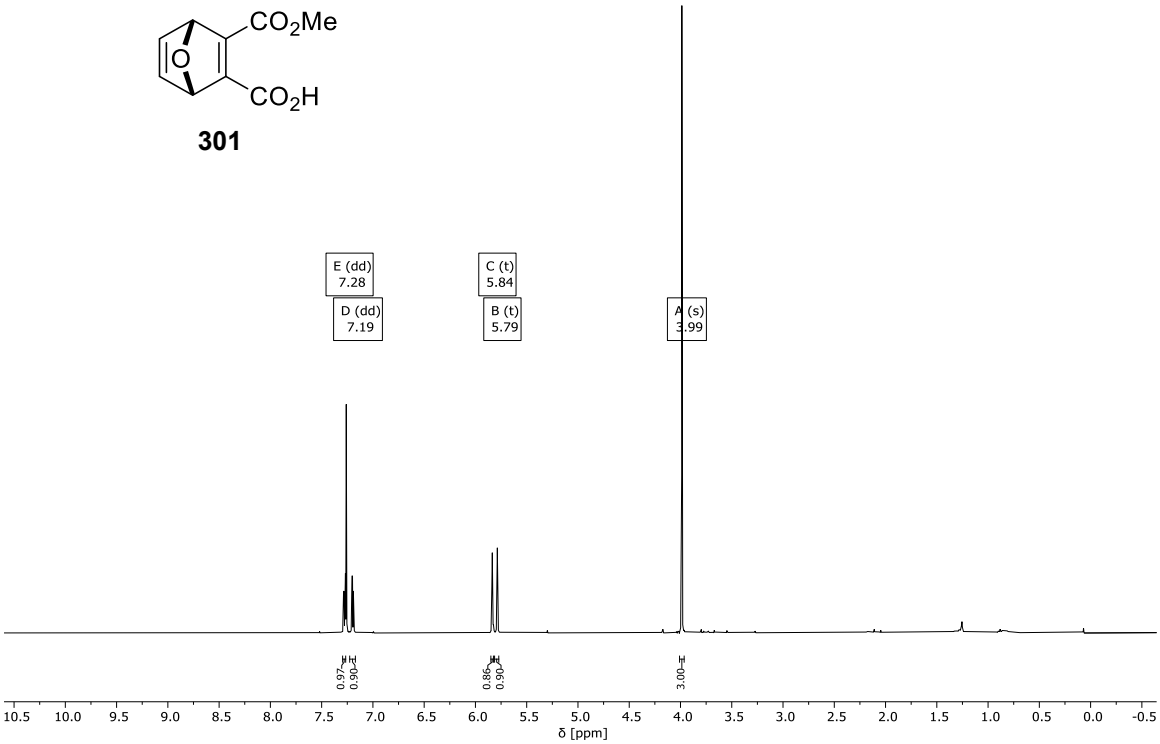

Figure 254: ^{1}H-NMR spectrum (400 MHz, $CDCl_3$) of (1S,4R)-3-(methoxycarbonyl)-7-oxabicyclo[2.2.1]hepta-2,5-diene-2-carboxylic acid (**301**).

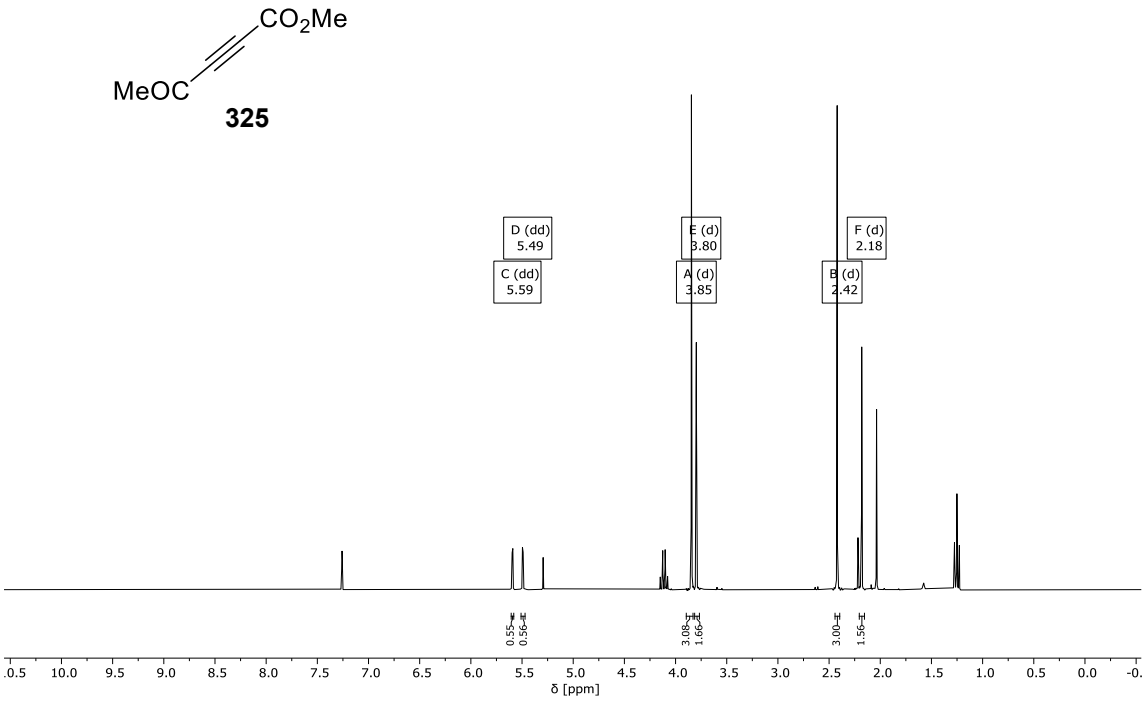

Figure 255: ^{1}H-NMR spectrum (300 MHz, $CDCl_3$) of methyl 4-oxopent-2-ynoate (**325**) (2:1 mixture with side product **326**).

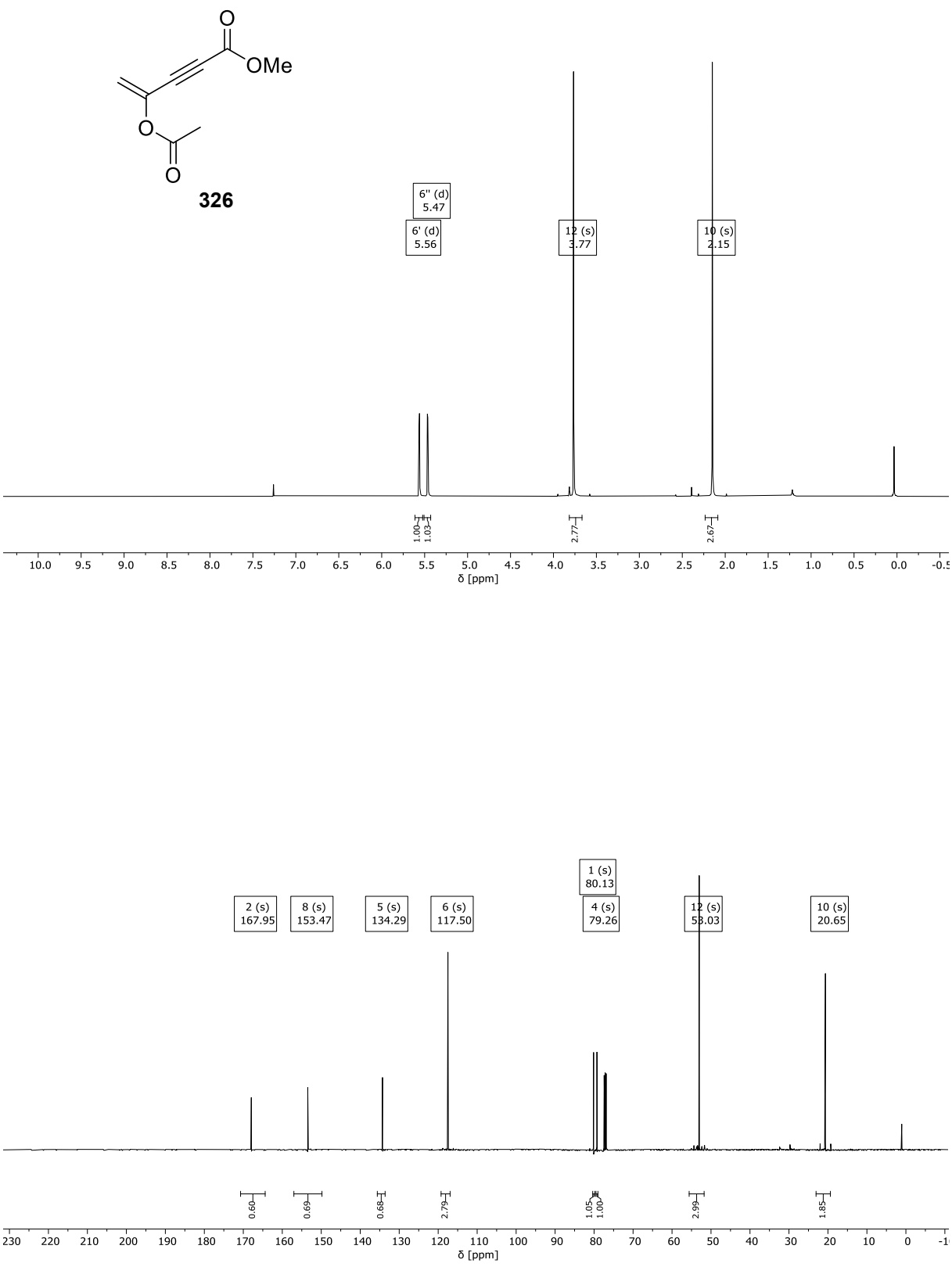

Figure 256 ^{1}H- and ^{13}C-NMR spectra (600 / 151 MHz, $CDCl_3$) of methyl 4-acetoxypent-4-en-2-ynoate (**326**).

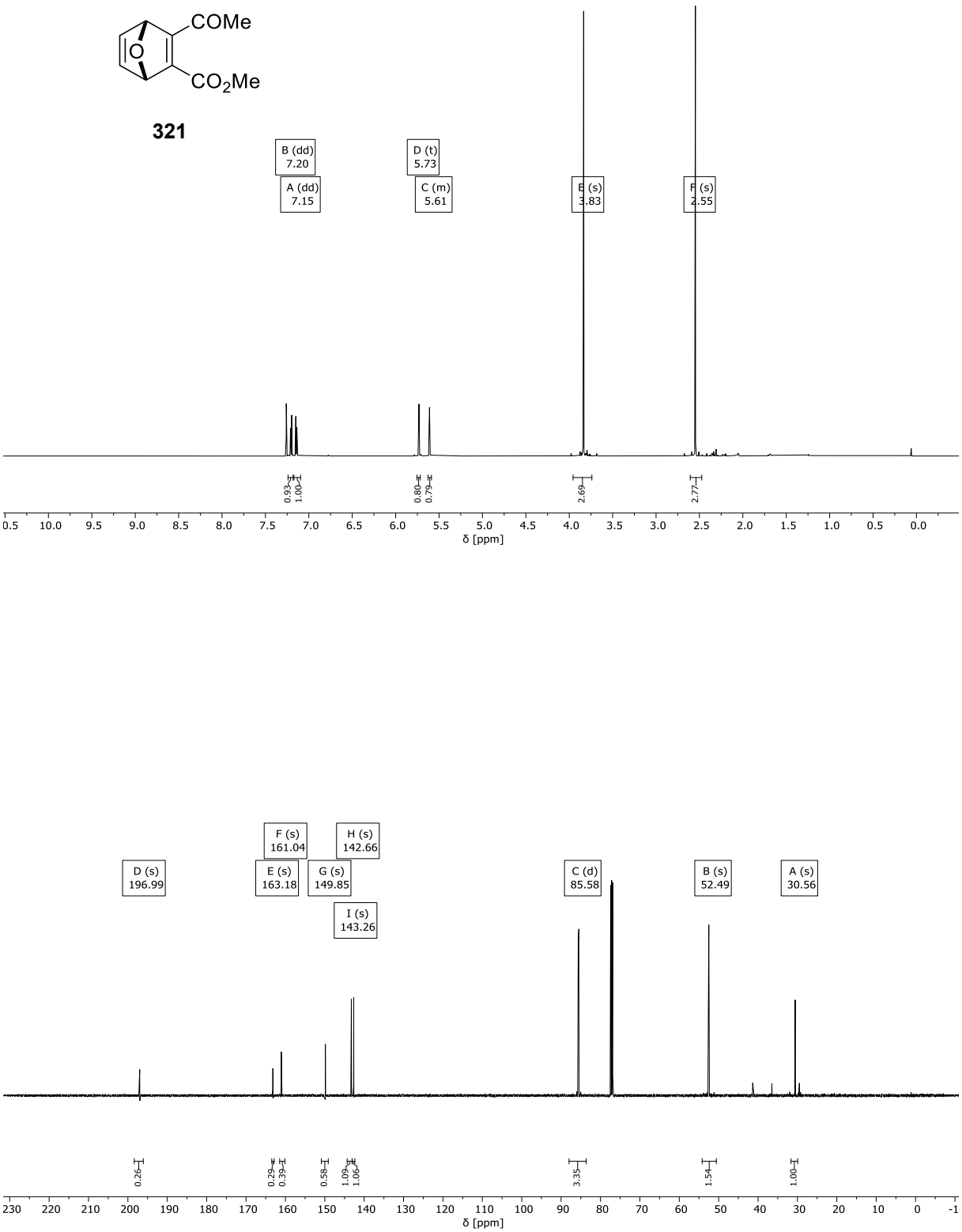

Figure 257: ^{1}H- and ^{13}C-NMR spectra (600 / 151 MHz, $CDCl_3$) of methyl (1S,4R)-3-acetyl-7-oxabicyclo[2.2.1]hepta-2,5-diene-2-carboxylate (**321**).

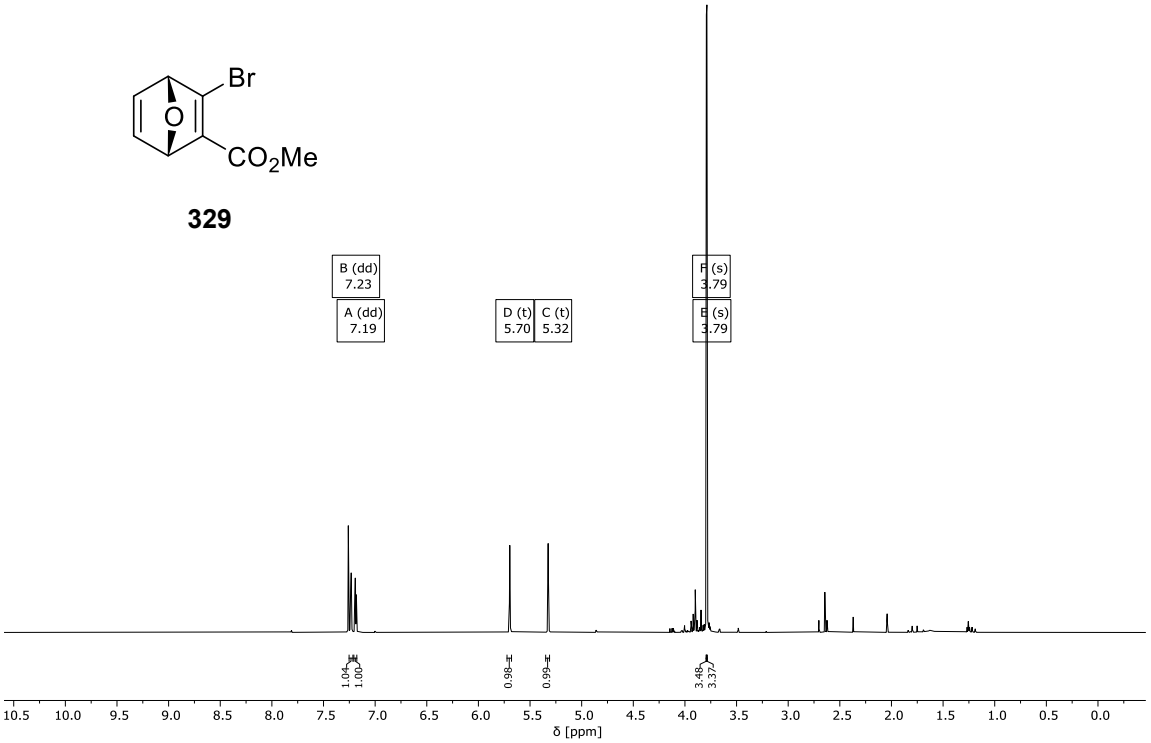

Figure 258: ^{1}H-NMR spectrum (600 MHz, $CDCl_3$) of methyl (1S,4R)-3-bromo-7-oxabicyclo[2.2.1]hepta-2,5-diene-2-carboxylate (**329**).

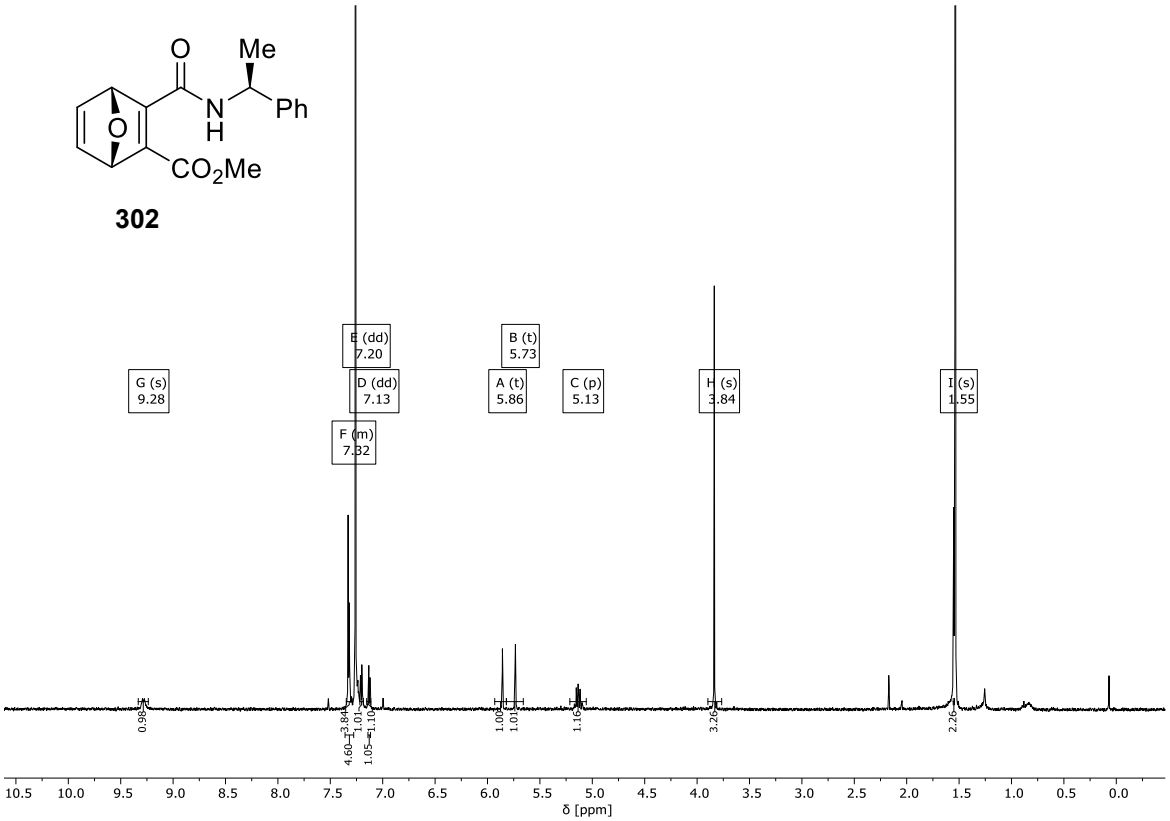

Figure 259: ^{1}H-NMR spectrum (400 MHz, $CDCl_3$) of methyl (1S,4R)-3-(((S)-1-phenylethyl)carbamoyl)-7-oxabicyclo[2.2.1]hepta-2,5-diene-2-carboxylate (**302**).

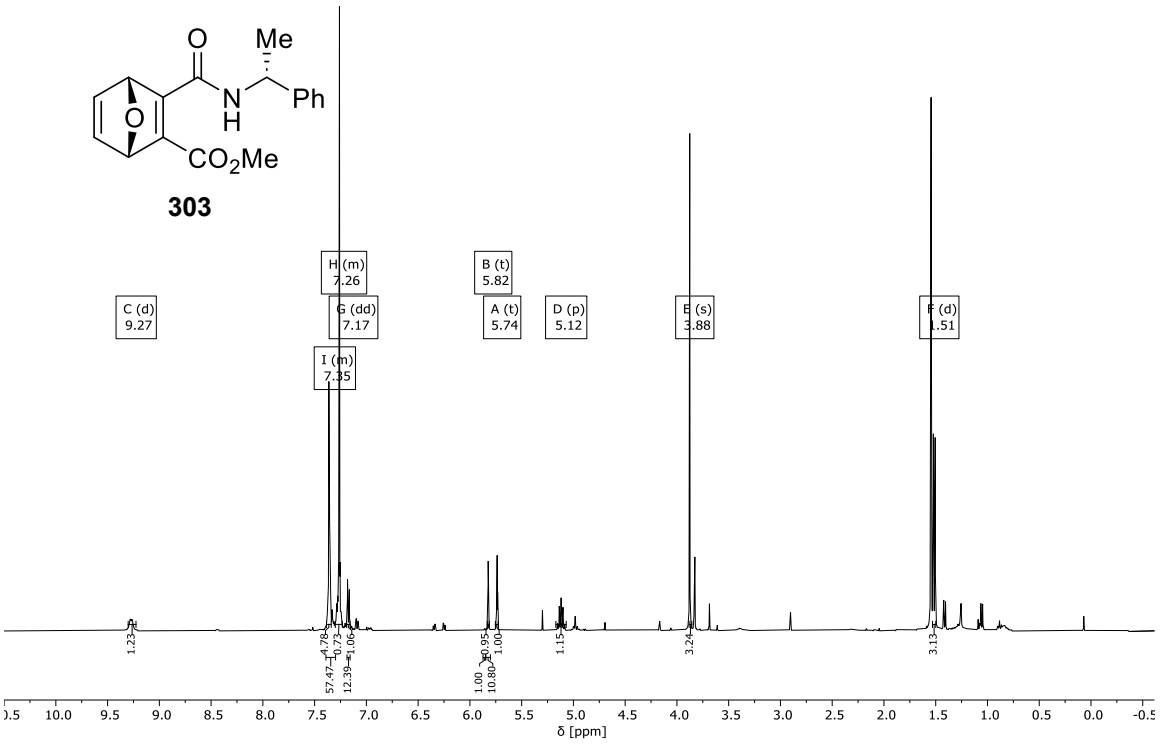

Figure 260: ^{1}H-NMR spectrum (400 MHz, $CDCl_3$) of methyl (1S,4R)-3-(((R)-1-phenylethyl)carbamoyl)-7-oxabicyclo[2.2.1]hepta-2,5-diene-2-carboxylate (**303**).

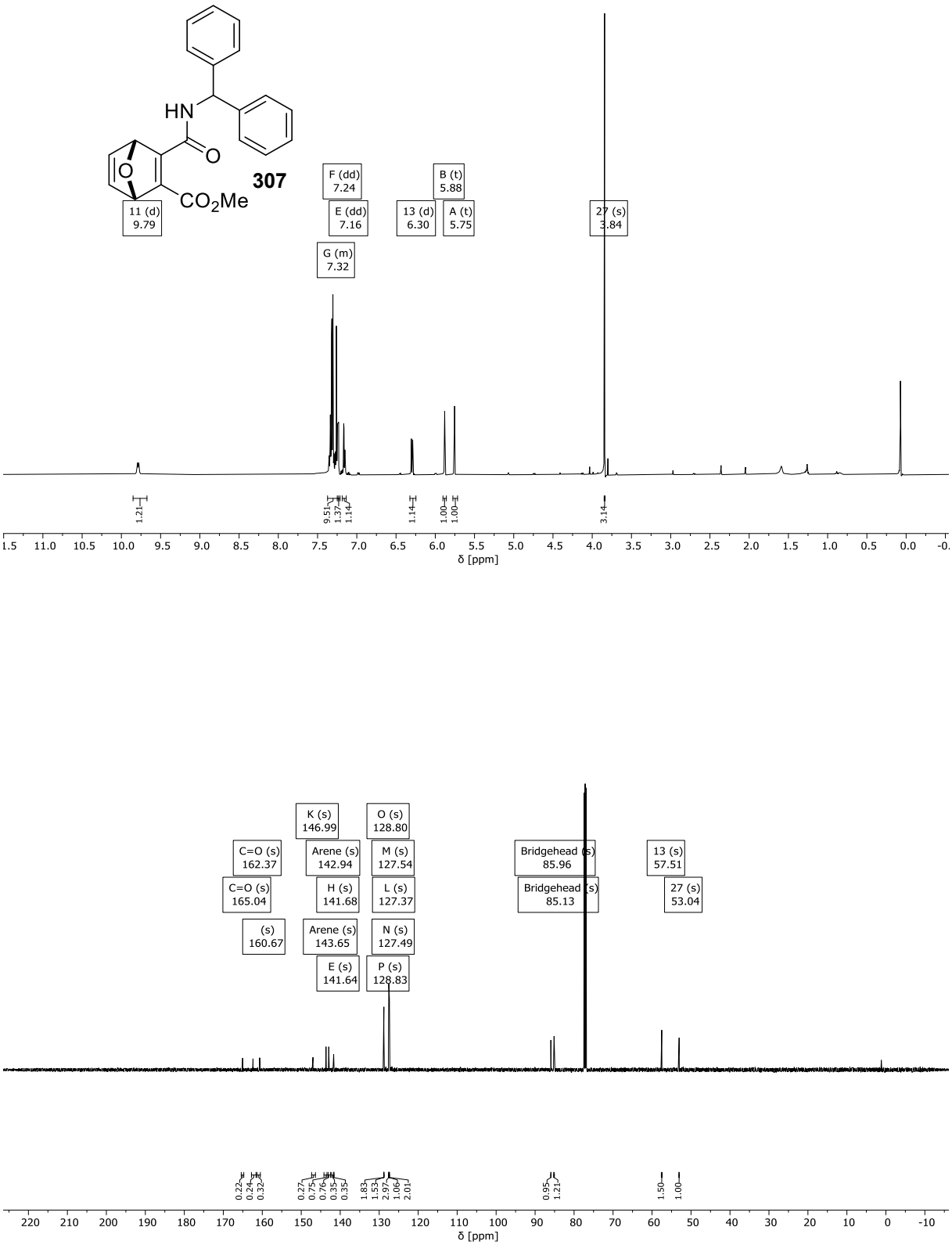

Figure 261: ^{1}H- and ^{13}C-NMR spectra (600 / 151 MHz, $CDCl_3$) of methyl (1R,4S)-3-(benzhydrylcarbamoyl)-7-oxabicyclo[2.2.1]hepta-2,5-diene-2-carboxylate (**307**).

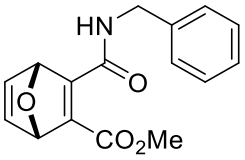

308

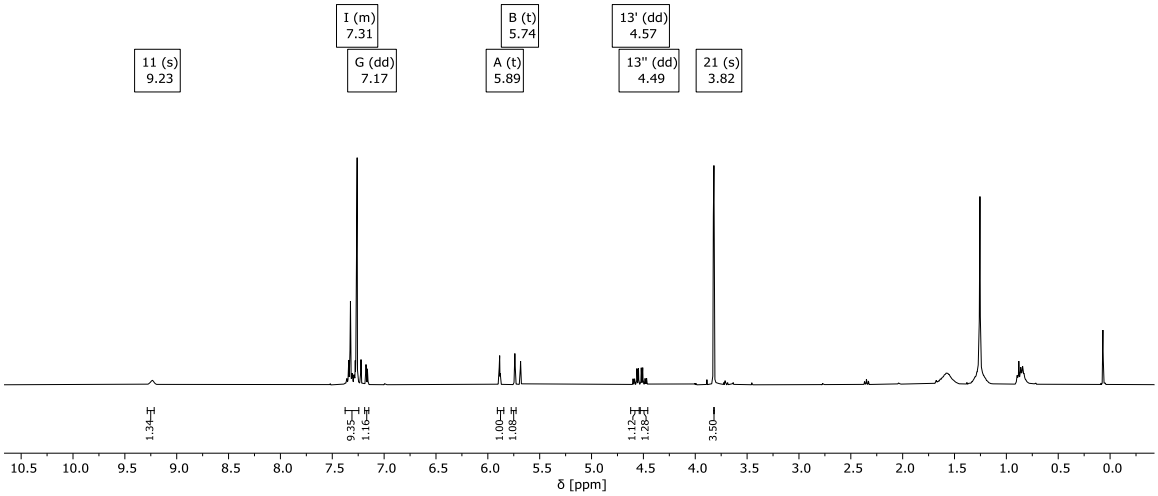

Figure 262: ^{1}H-NMR spectrum (400 MHz, $CDCl_3$) of methyl (1*R*,4*S*)-3-(benzylcarbamoyl)-7-oxabicyclo[2.2.1]hepta-2,5-diene-2-carboxylate (**308**).

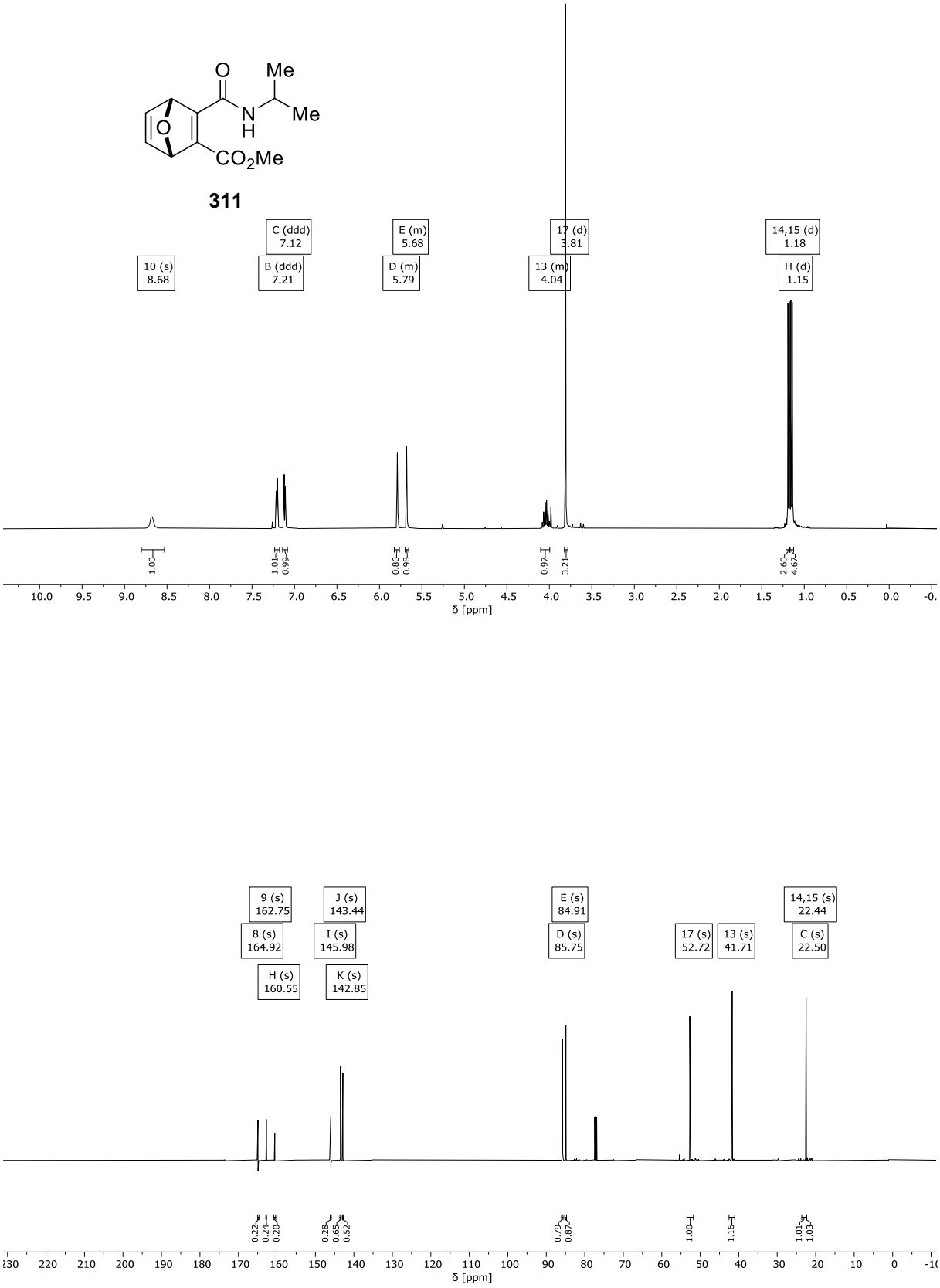

Figure 263: ^{1}H-NMR spectrum (400 MHz, $CDCl_3$) of methyl (1*R*,4*S*)-3-(benzylcarbamoyl)-7-oxabicyclo[2.2.1]hepta-2,5-diene-2-carboxylate (**311**).

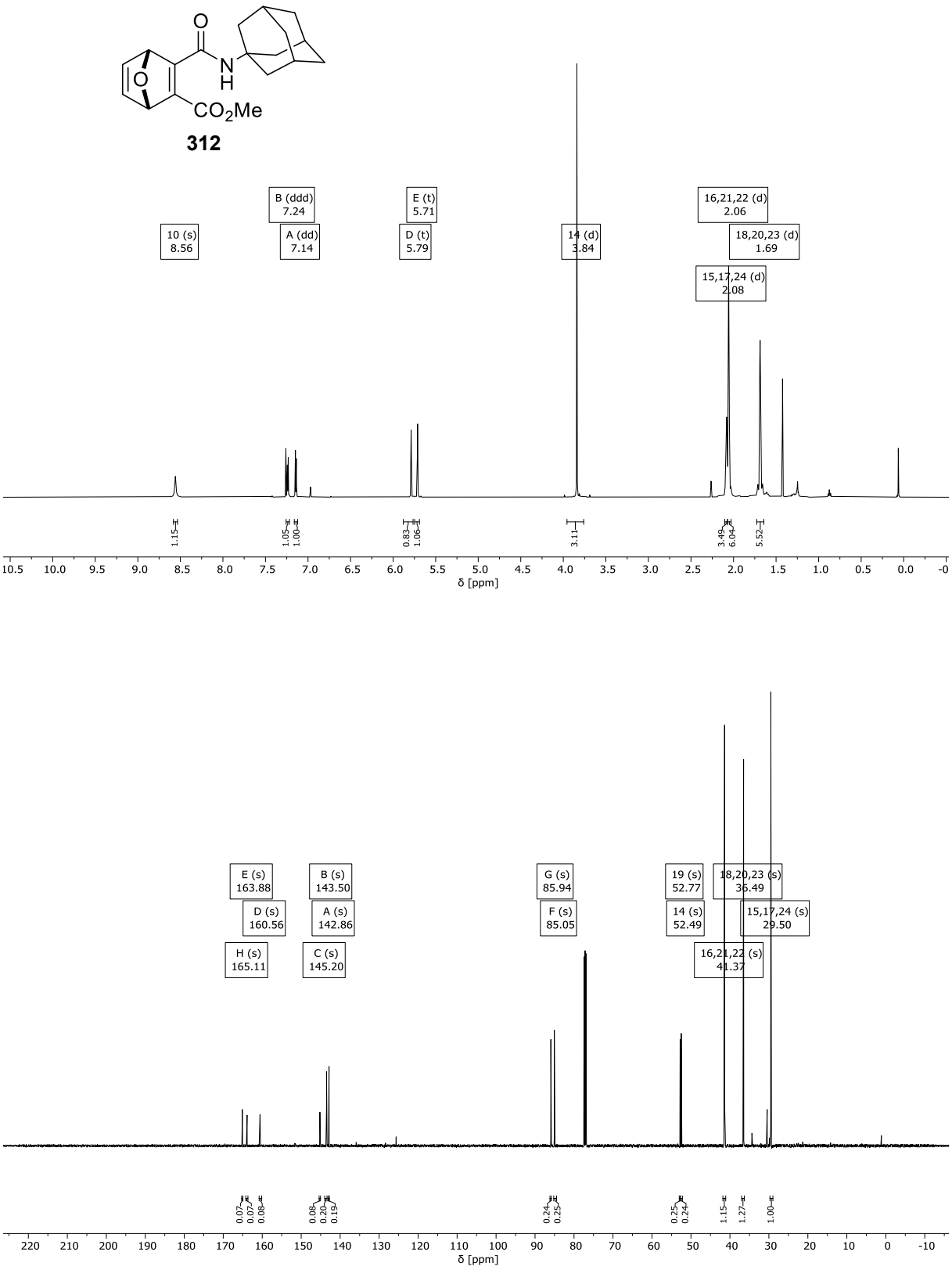

Figure 264: ^{1}H- and ^{13}C-NMR spectra (600 / 151 MHz, $CDCl_3$) of methyl (1R,4S)-3-(((3R,5R,7R)-adamantan-1-yl)carbamoyl)-7-oxabicyclo[2.2.1]hepta-2,5-diene-2-carboxylate (**312**).

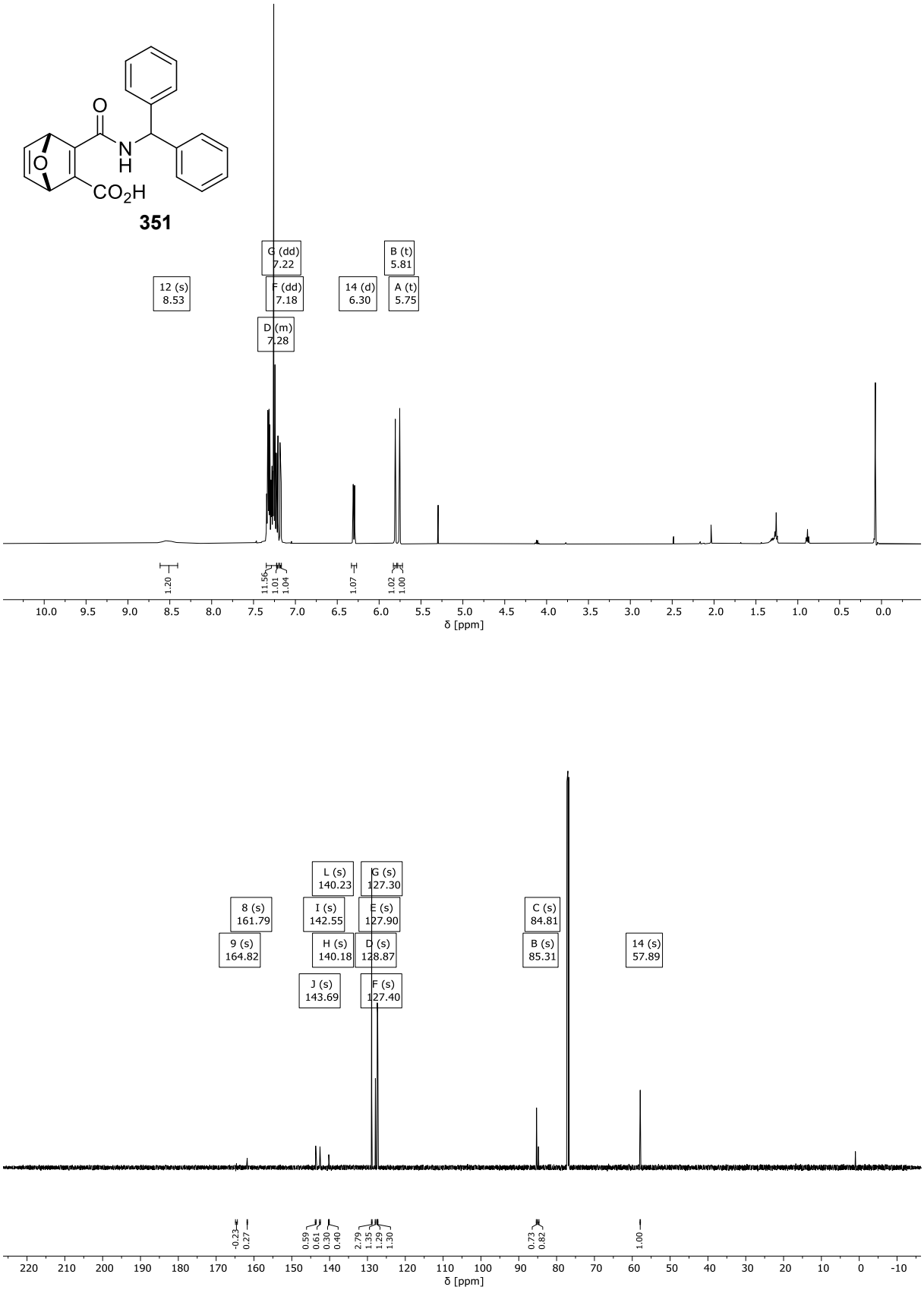

Figure 265: ^{1}H- and ^{13}C-NMR spectra (600 / 151 MHz, $CDCl_3$) of (1S,4R)-3-(benzhydrylcarbamoyl)-7-oxabicyclo[2.2.1]hepta-2,5-diene-2-carboxylic acid (**351**).

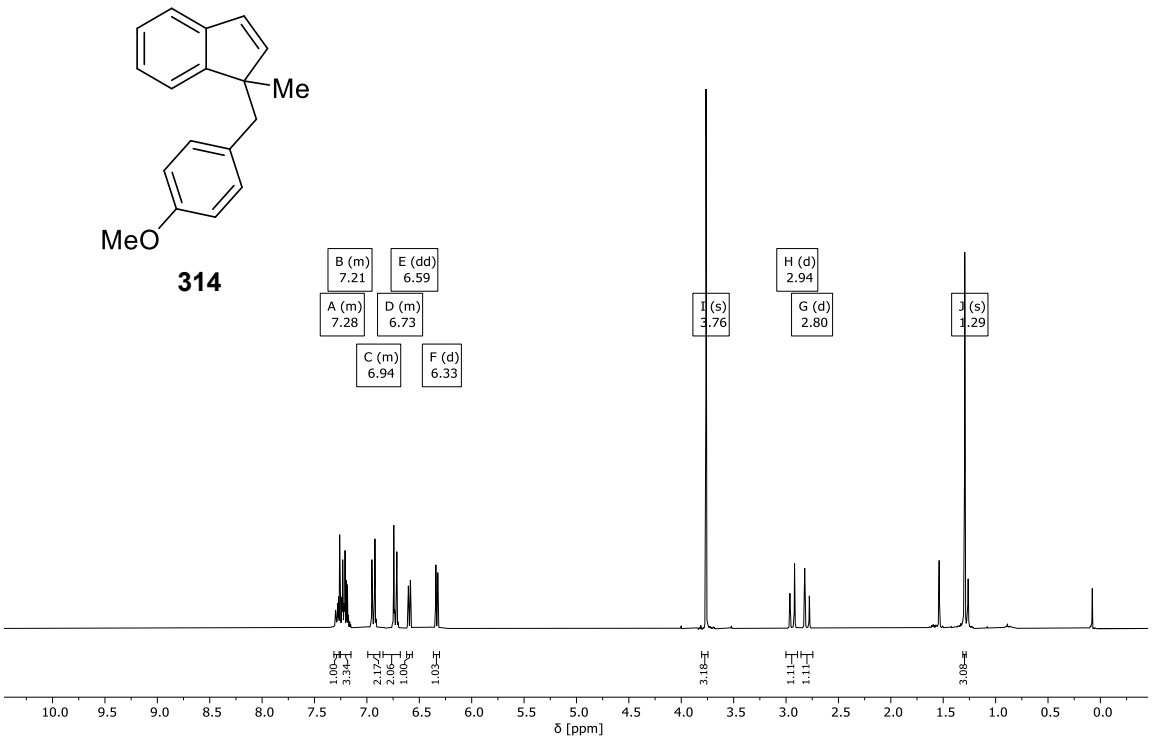

Figure 266: ^{1}H-NMR spectrum (300 MHz, $CDCl_3$) of 1-(4-methoxybenzyl)-1-methyl-1H-indene (**314**).

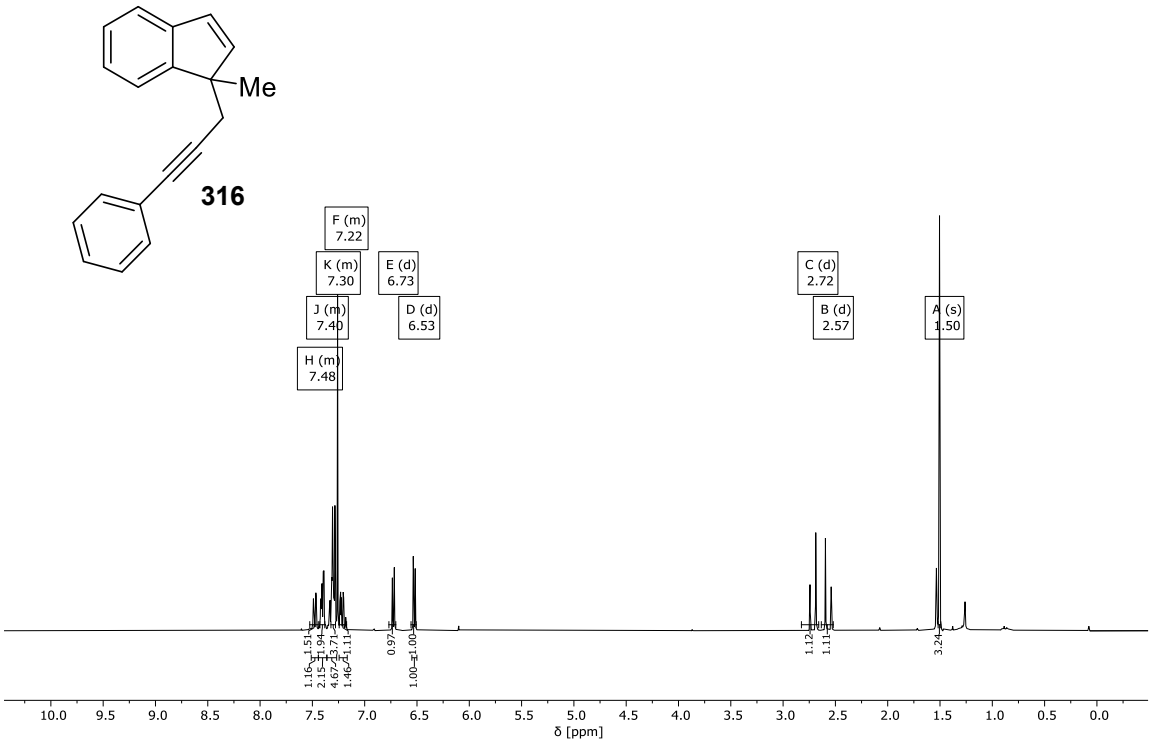

Figure 267: ^{1}H-NMR spectrum (300 MHz, $CDCl_3$) of 1-methyl-1-(3-phenylprop-2-yn-1-yl)-1H-indene (**316**).

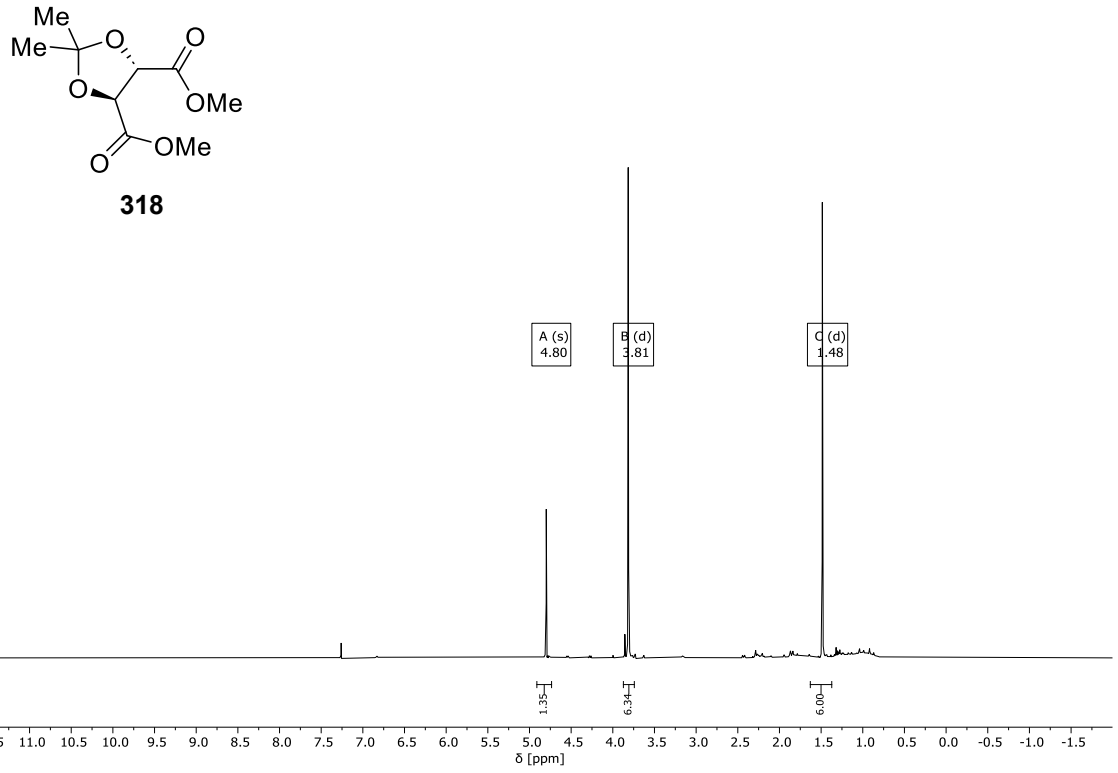

Figure 268: ^{1}H-NMR spectrum (400 MHz, $CDCl_3$) of dimethyl (4S,5S)-2,2-dimethyl-1,3-dioxolane-4,5-dicarboxylate (**318**).

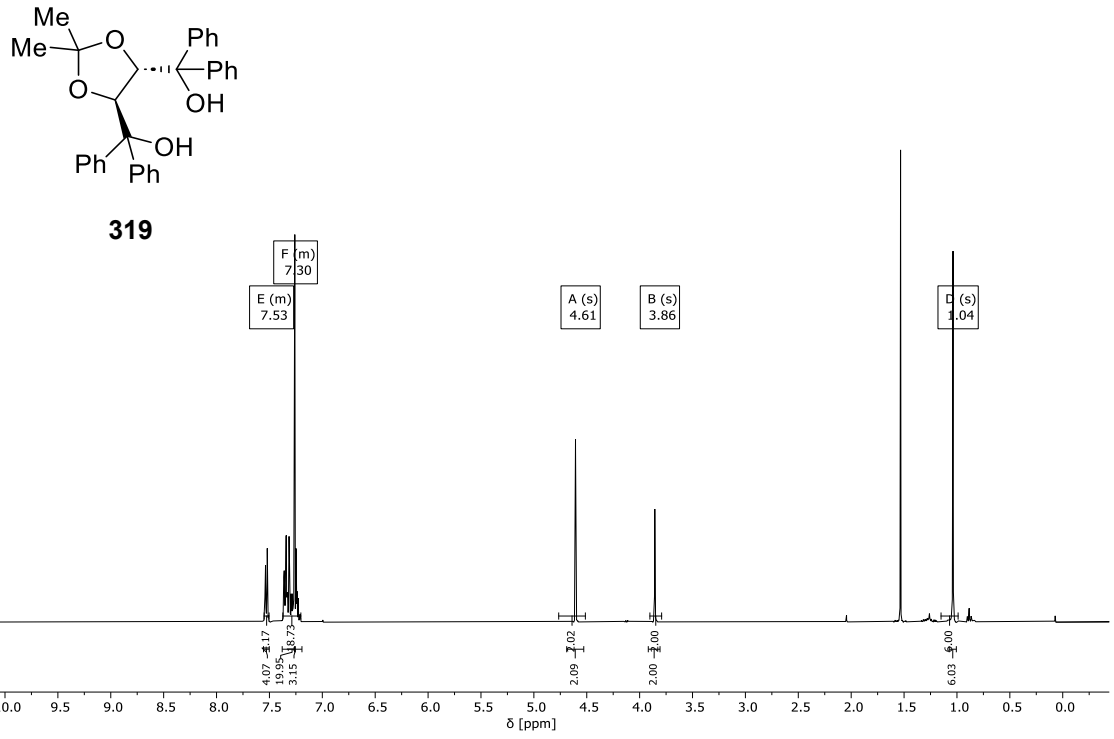

Figure 269: ^{1}H-NMR spectrum (400 MHz, $CDCl_3$) of ((4S,5S)-2,2-dimethyl-1,3-dioxolane-4,5-diyl)bis(diphenylmethanol) (**319**).

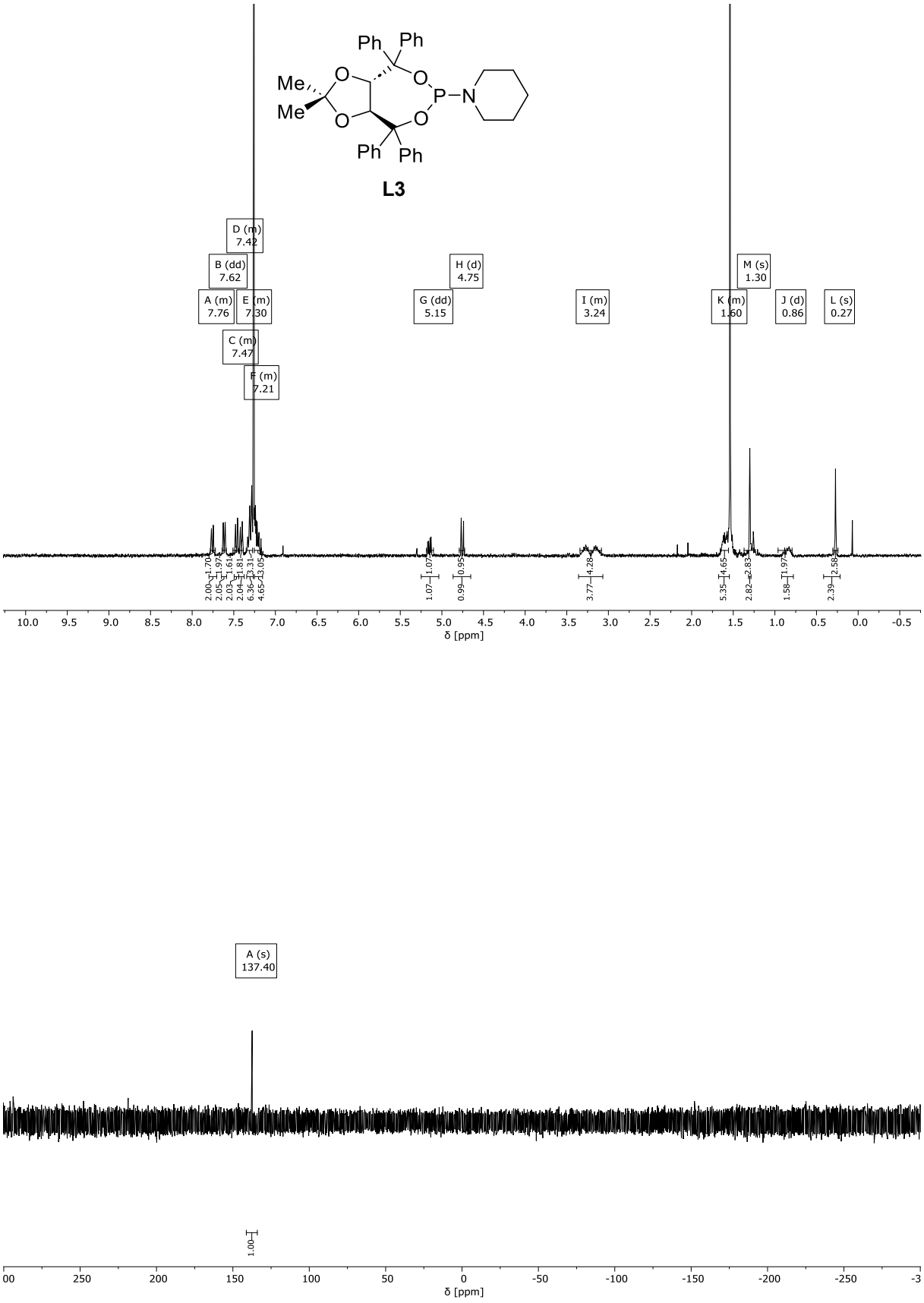

Figure 270: ^{1}H- and ^{31}P-NMR spectra (300 / 121 MHz, $CDCl_3$) of 1-((3aS,8aS)-2,2-dimethyl-4,4,8,8-tetraphenyltetrahydro-[1,3]dioxolo[4,5-e][1,3,2]dioxaphosphepin-6-yl)piperidine **L3**.

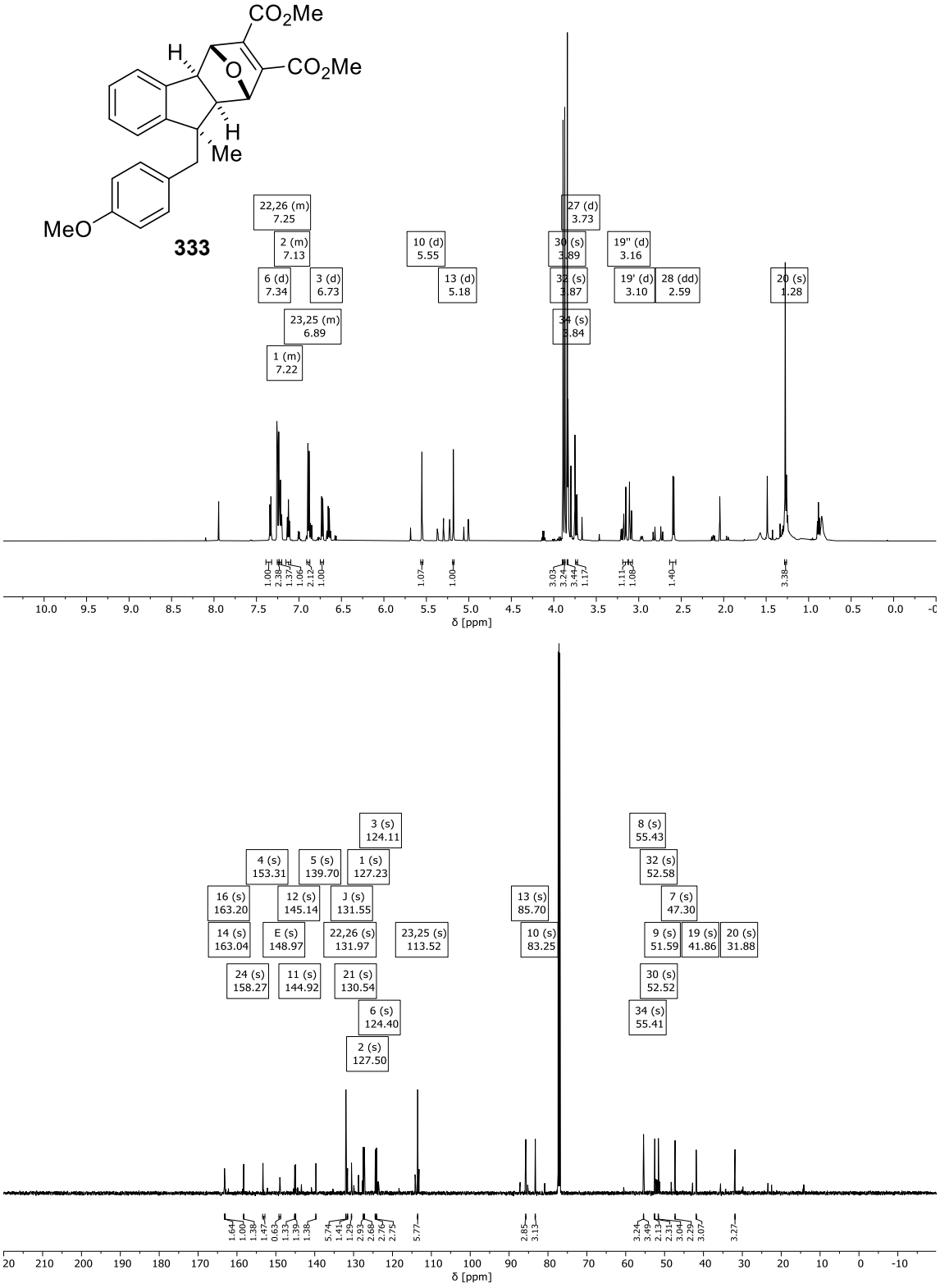

Figure 271: ^{1}H- and ^{13}C-NMR spectra (600 / 151 MHz, $CDCl_3$) of dimethyl (1S,4R,4aS,9R,9aR)-9-(4-methoxybenzyl)-9-methyl-4,4a,9,9a-tetrahydro-1H-1,4-epoxyfluorene-2,3-dicarboxylate **333.**

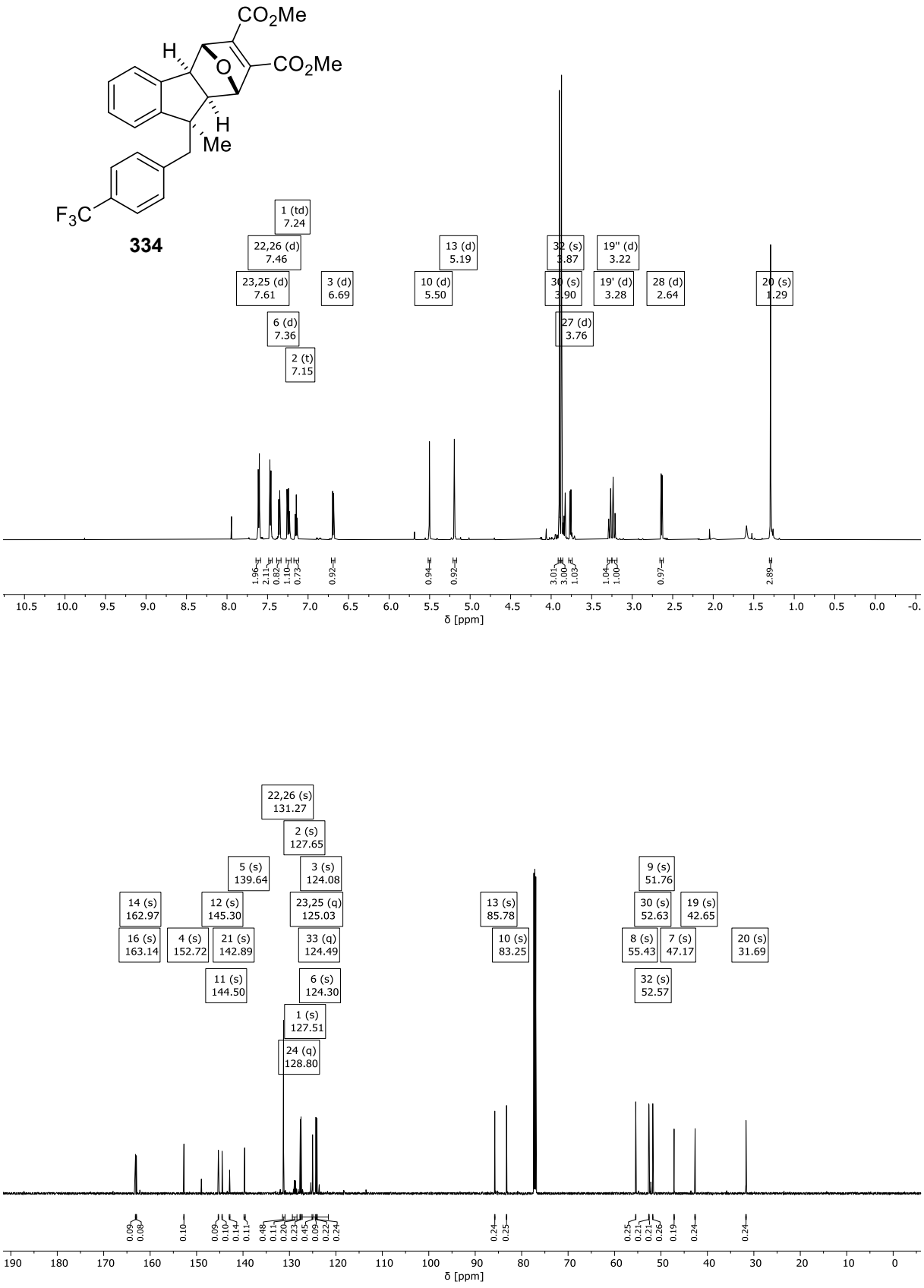

Figure 272: ^{1}H-, ^{13}C-NMR spectra (600 / 151 MHz, $CDCl_3$) of dimethyl (1S,4R,4aS,9R,9aR)-9-methyl-9-(4-(trifluoromethyl)benzyl)-4,4a,9,9a-tetrahydro-1H-1,4-epoxyfluorene-2,3-dicarboxylate (**334**).

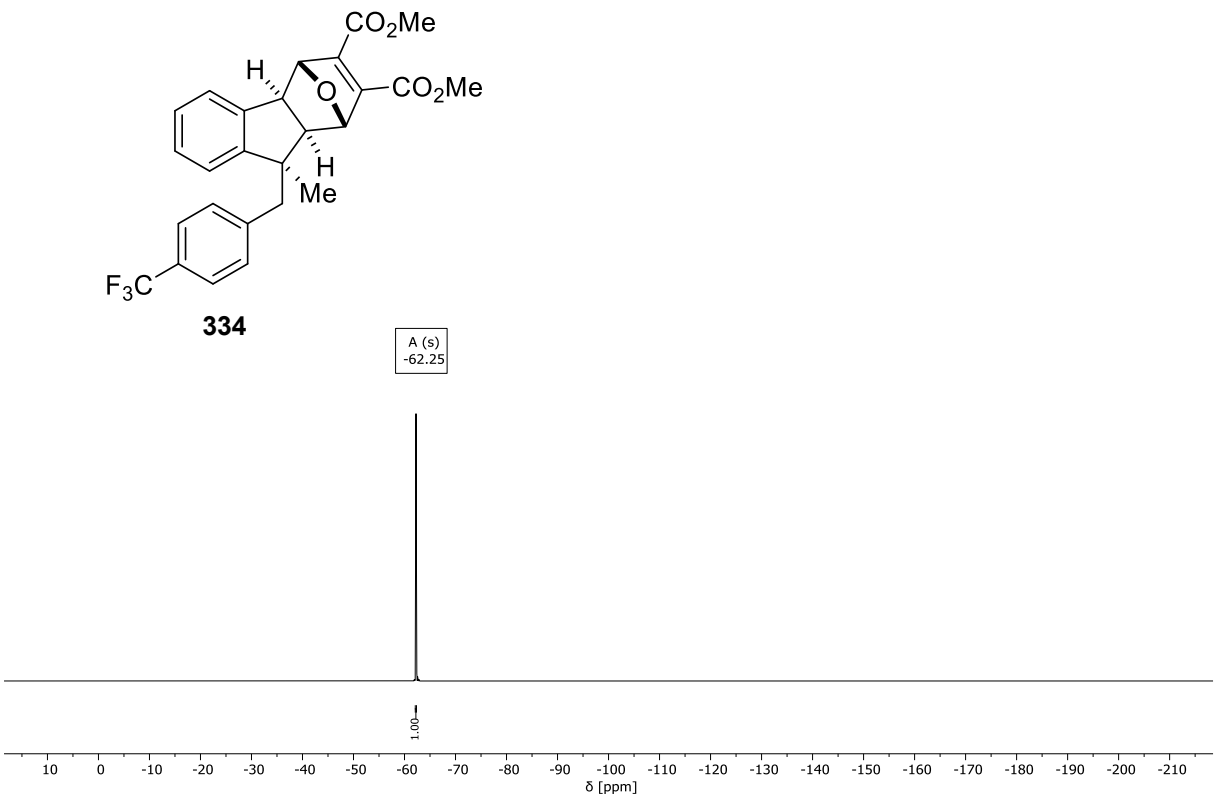

Figure 273: ^{19}F-NMR spectrum (282 MHz, $CDCl_3$) of dimethyl (1S,4R,4aS,9R,9aR)-9-methyl-9-(4-(trifluoromethyl)benzyl)-4,4a,9,9a-tetrahydro-1H-1,4-epoxyfluorene-2,3-dicarboxylate (**334**).

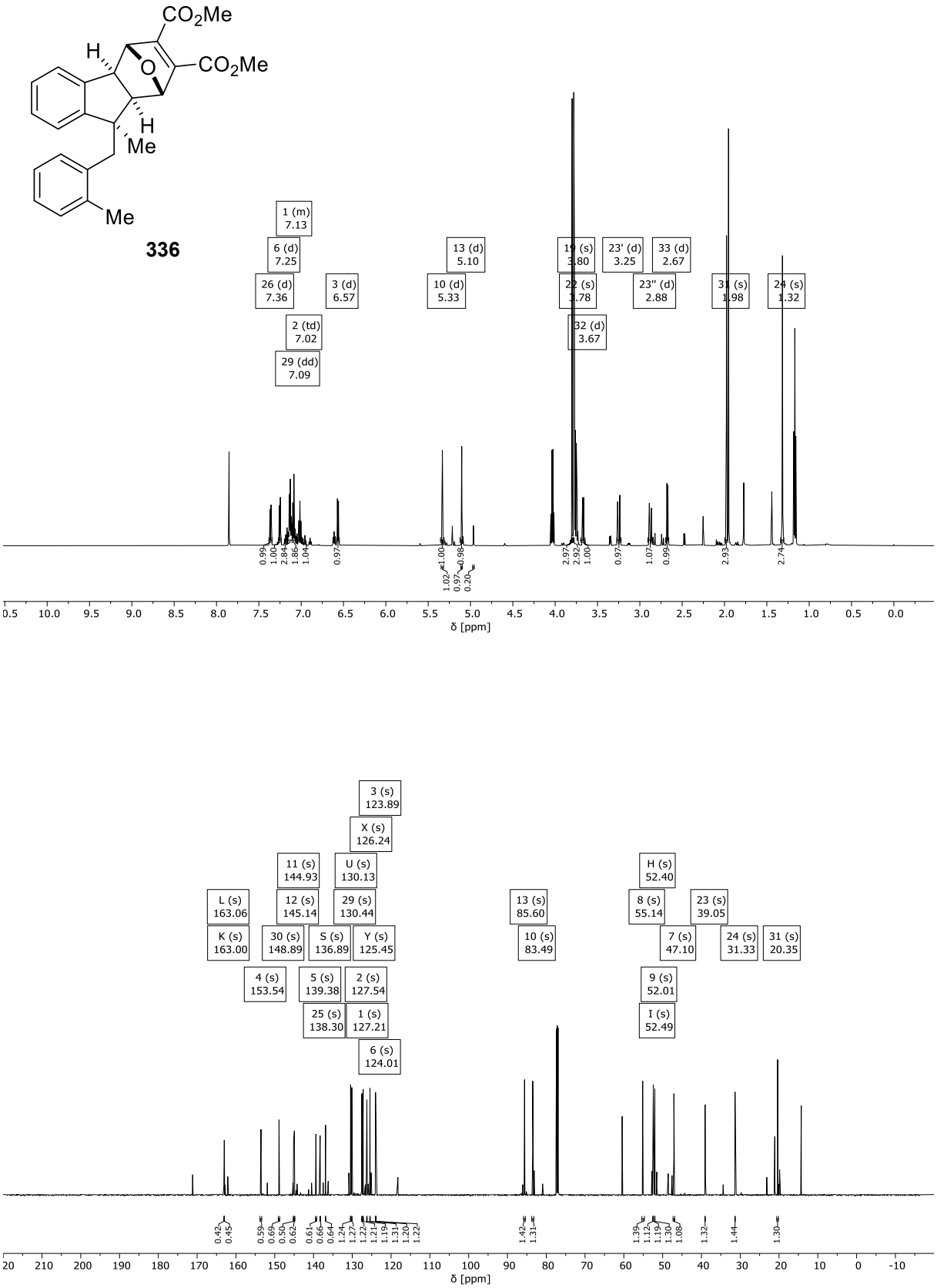

Figure 274: ^{1}H- and ^{13}C-NMR spectra (600 / 151 MHz, $CDCl_3$) of dimethyl (1S,4R,4aS,9R,9aR)-9-methyl-9-(2-methylbenzyl)-4,4a,9,9a-tetrahydro-1H-1,4-epoxyfluorene-2,3-dicarboxylate (**336**).

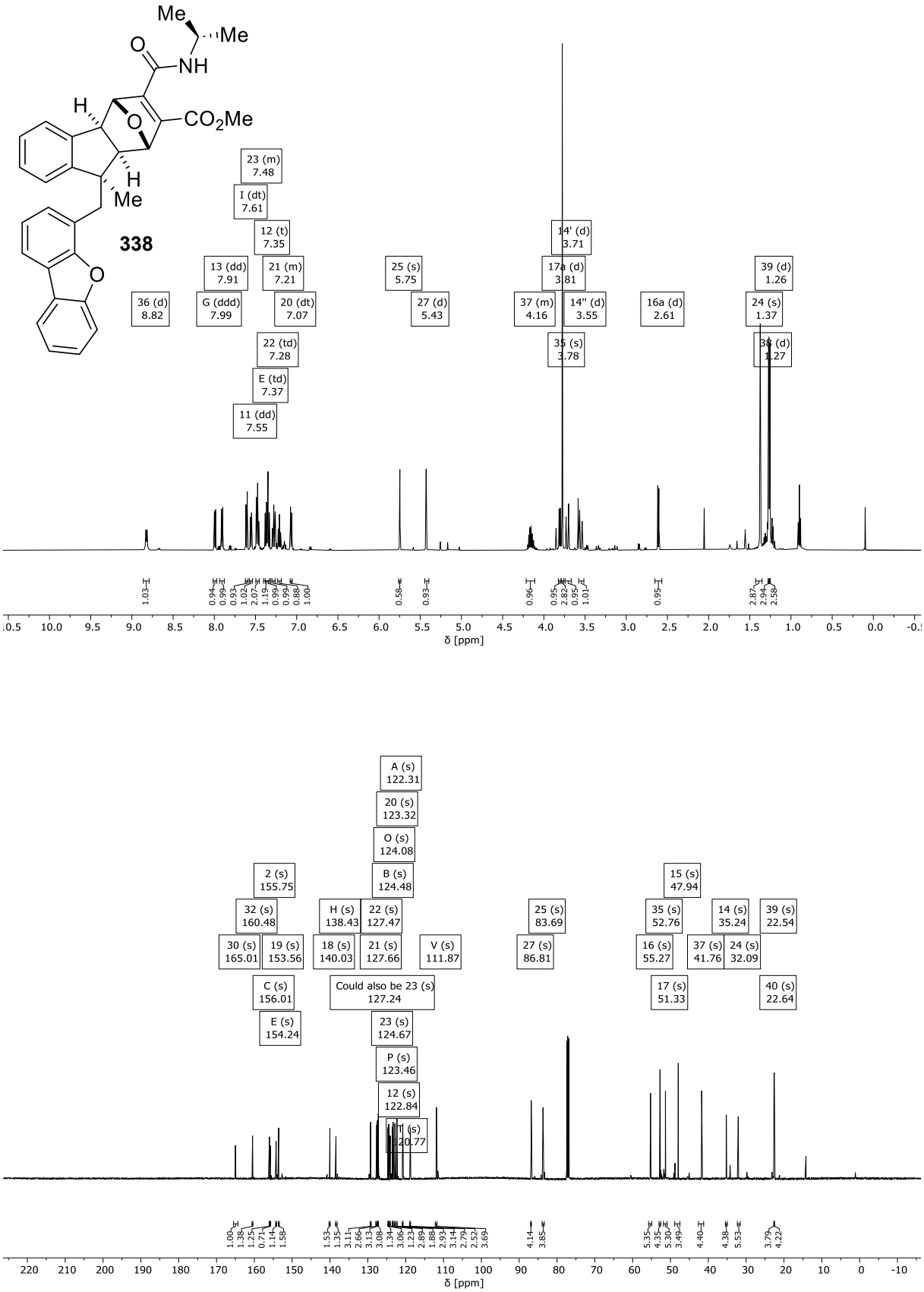

Figure 275: ^{1}H- and ^{13}C-NMR spectra (600 / 151 MHz, $CDCl_3$) of methyl (1S,4R,4aS,9R,9aR)-9-(dibenzo[b,d]furan-4-ylmethyl)-3-(isopropylcarbamoyl)-9-methyl-4,4a,9,9a-tetrahydro-1H-1,4-epoxyfluorene-2-carboxylate (**338**).

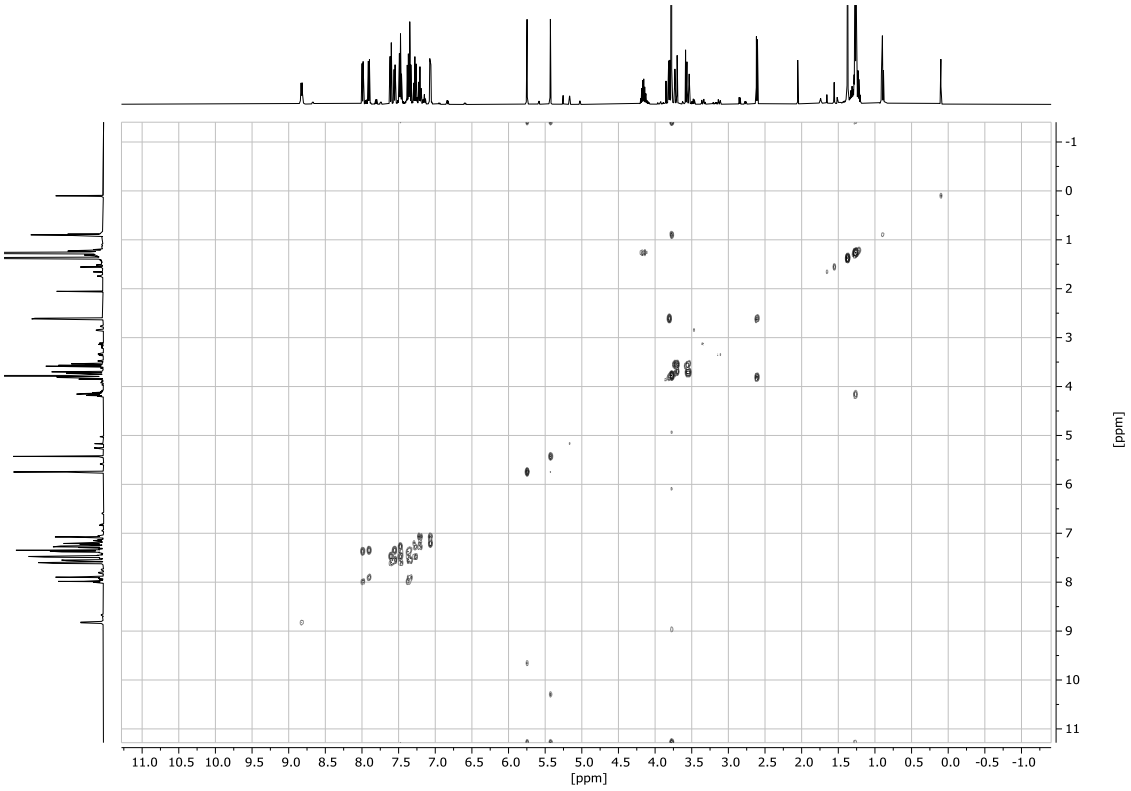

Figure 276: 2D-COSY -NMR spectrum (600 MHz) of methyl (1S,4R,4aS,9R,9aR)-9-(dibenzo[b,d]furan-4-ylmethyl)-3-(isopropylcarbamoyl)-9-methyl-4,4a,9,9a-tetrahydro-1H-1,4-epoxyfluorene-2-carboxylate (**338**).

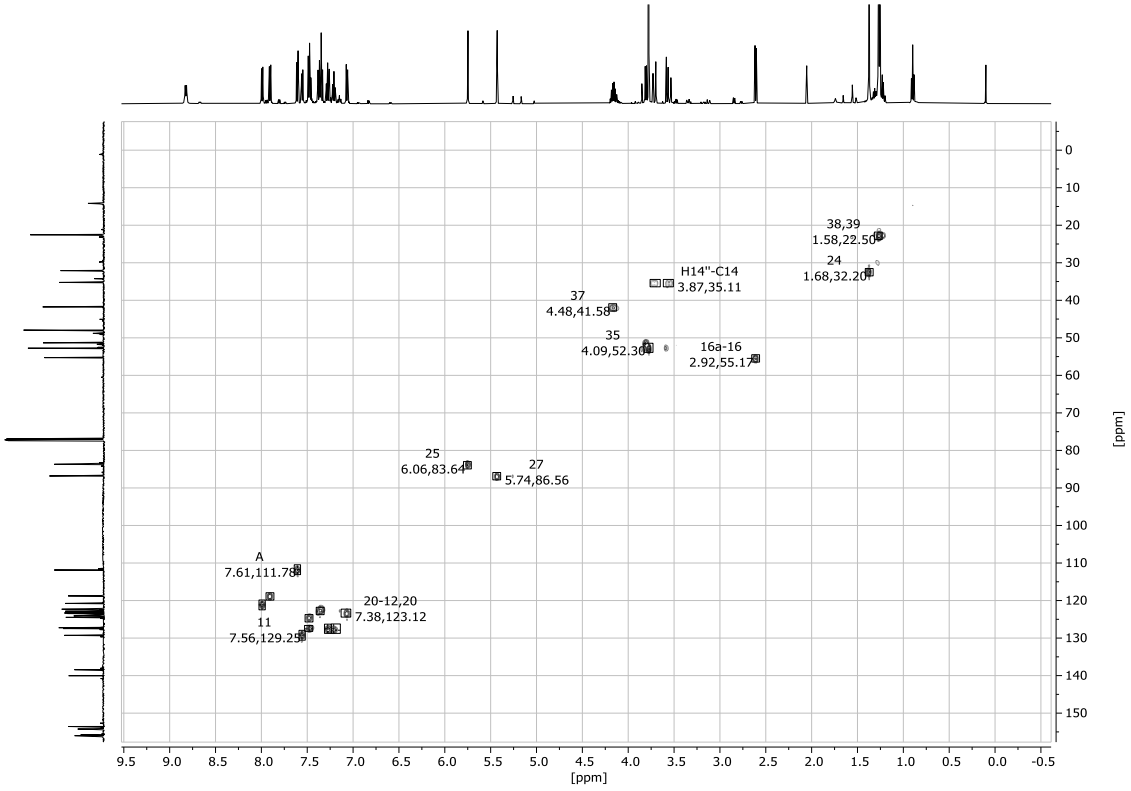

Figure 277: 2D-HSQC-NMR spectrum (600 /151 MHz) of methyl (1S,4R,4aS,9R,9aR)-9-(dibenzo[b,d]furan-4-ylmethyl)-3-(isopropylcarbamoyl)-9-methyl-4,4a,9,9a-tetrahydro-1H-1,4-epoxyfluorene-2-carboxylate (**338**).

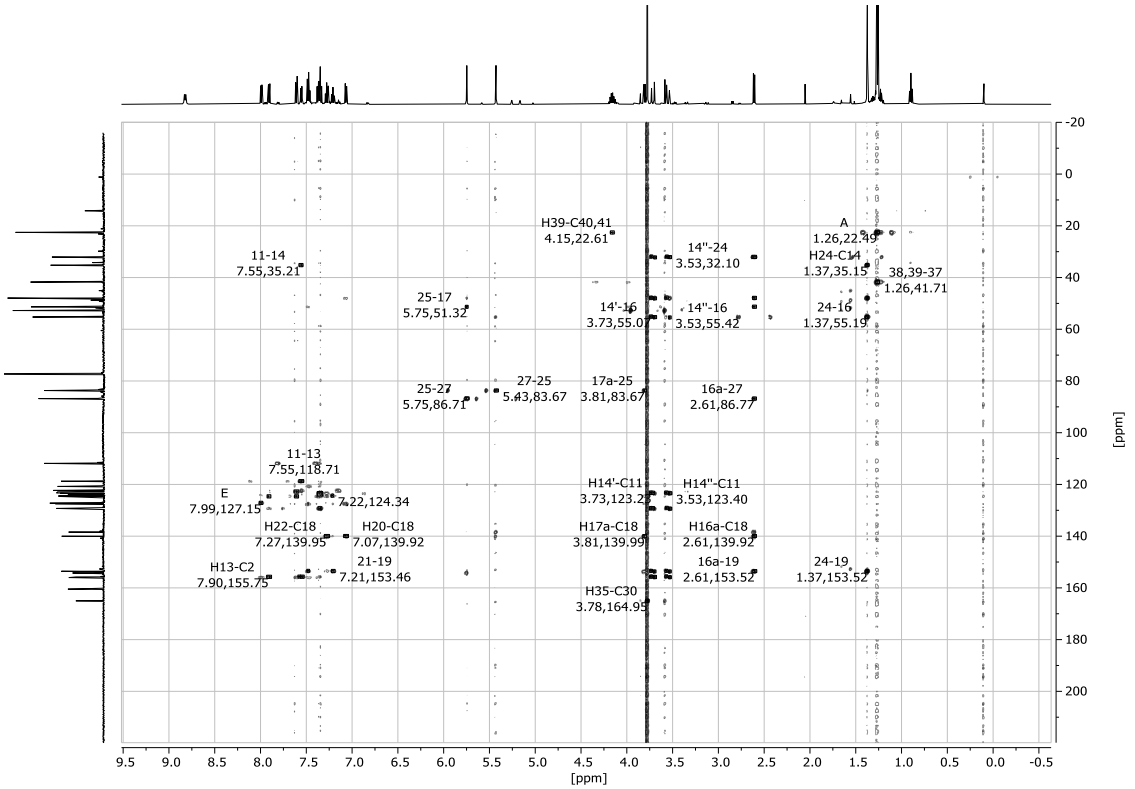

Figure 278: 2D-HMBC-NMR spectrum (600 /151 MHz) of methyl (1S,4R,4aS,9R,9aR)-9-(dibenzo[b,d]furan-4-ylmethyl)-3-(isopropylcarbamoyl)-9-methyl-4,4a,9,9a-tetrahydro-1H-1,4-epoxyfluorene-2-carboxylate (**338**).

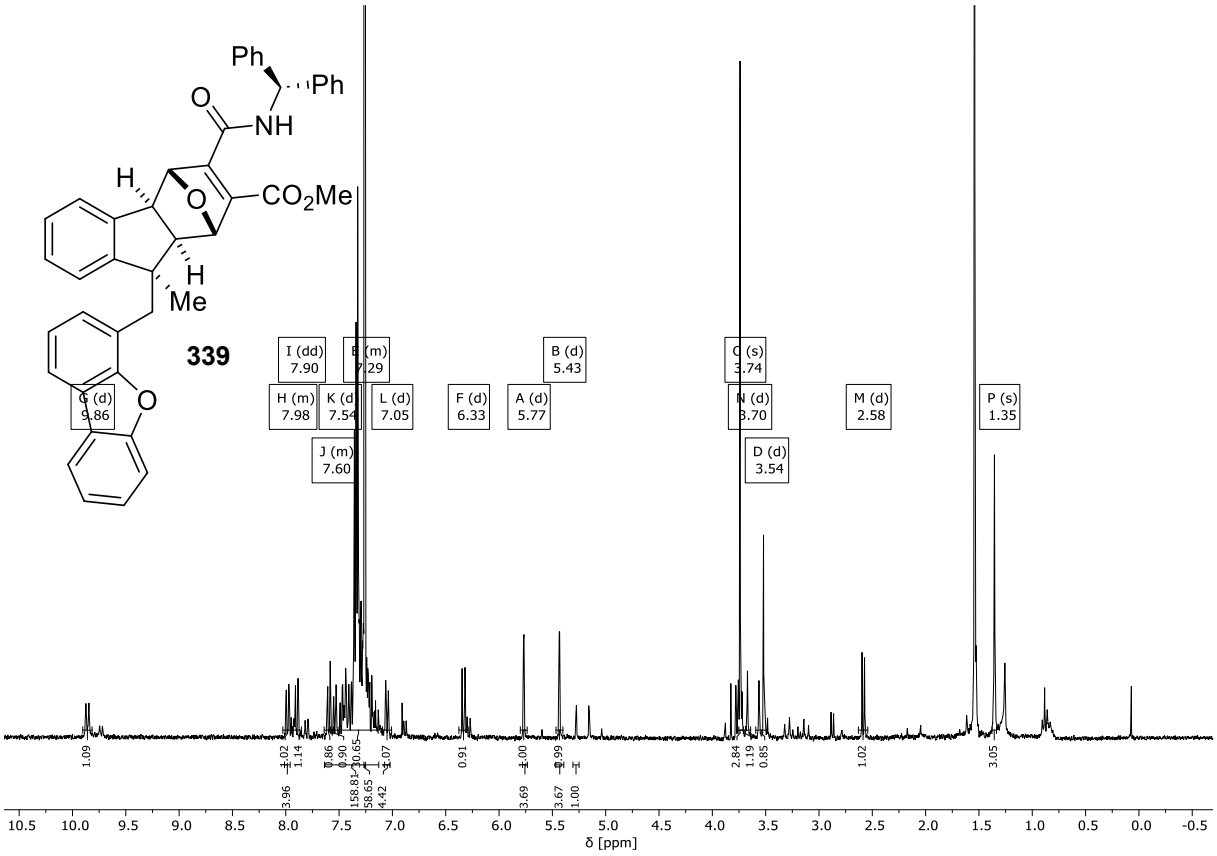

Figure 279: ^{1}H-NMR spectrum (300 MHz, $CDCl_3$) of methyl (1S,4R,4aS,9R,9aR)-3-(benzhydrylcarbamoyl)-9-(dibenzo[b,d]furan-4-ylmethyl)-9-methyl-4,4a,9,9a-tetrahydro-1H-1,4-epoxyfluorene-2-carboxylate (**339**).

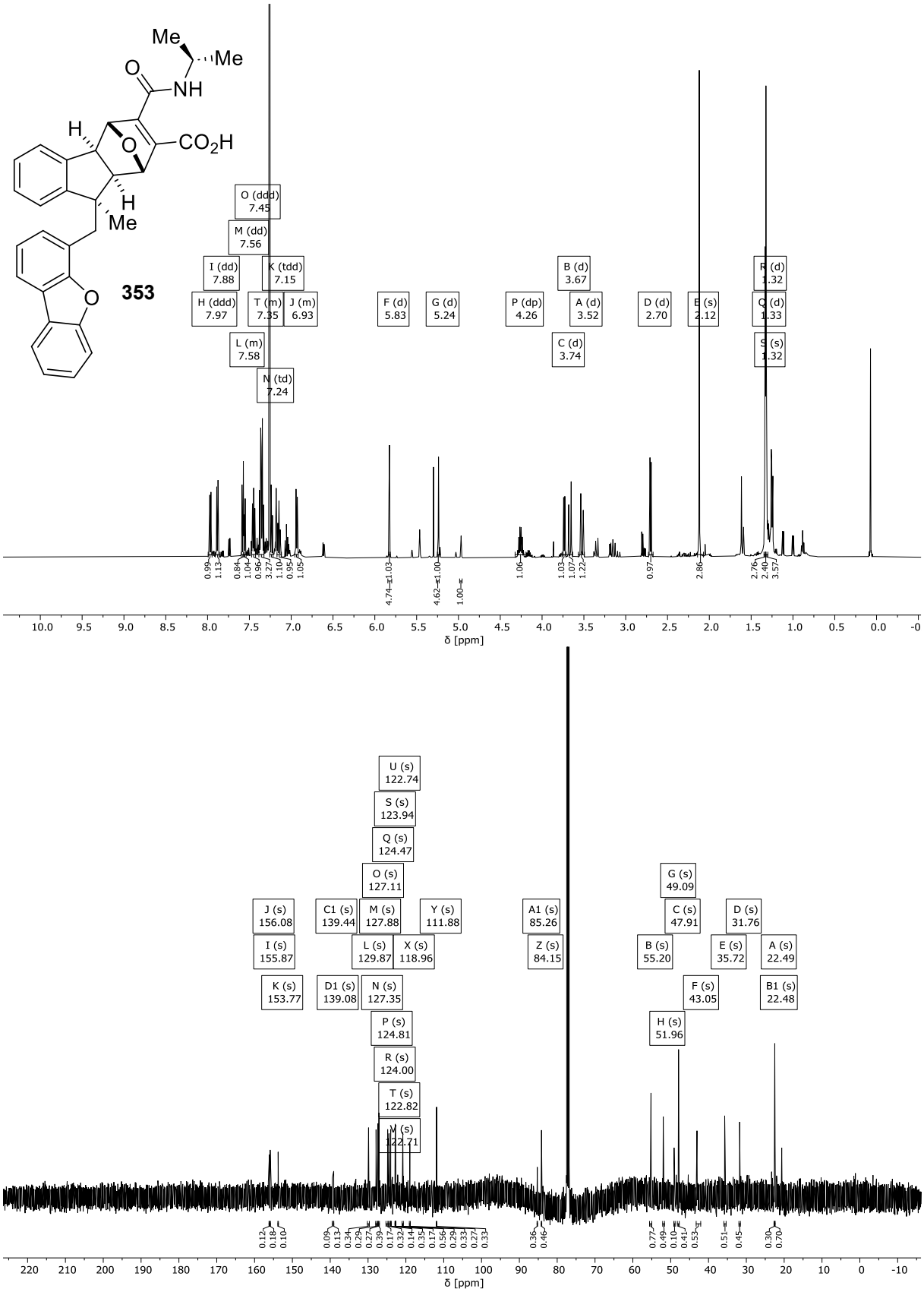

Figure 280: ^{1}H- and ^{13}C-NMR spectra (600 / 151 MHz, $CDCl_3$) of (1S,4R,4aS,9R,9aR)-9-(dibenzo[b,d]furan-4-ylmethyl)-3-(isopropylcarbamoyl)-9-methyl-4,4a,9,9a-tetrahydro-1H-1,4-epoxyfluorene-2-carboxylic acid (**353**).

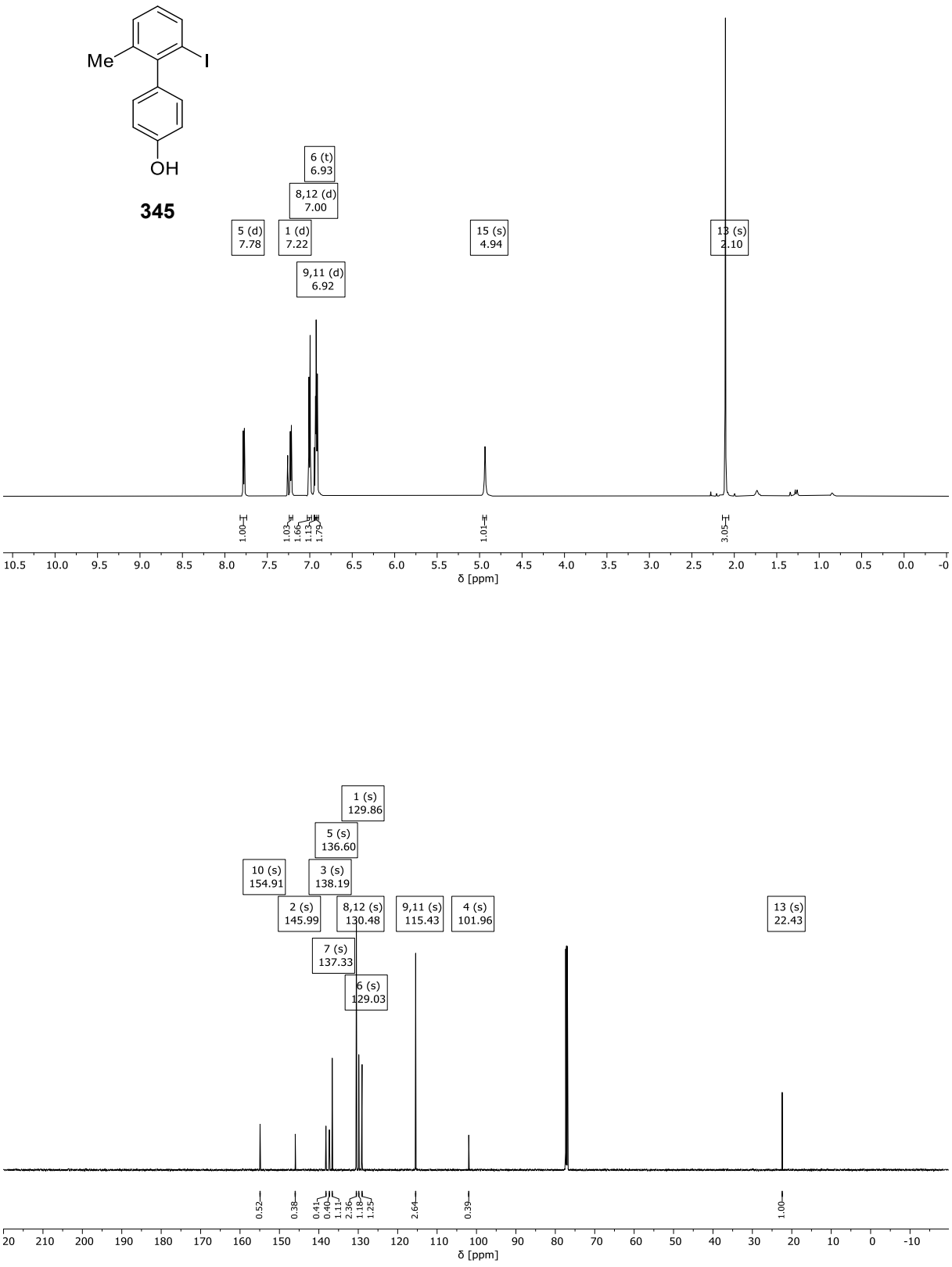

Figure 281: ^{1}H- and ^{13}C-NMR spectra (600 / 151 MHz, $CDCl_3$) of 2'-iodo-6'-methyl-[1,1'-biphenyl]-4-ol (**345).**

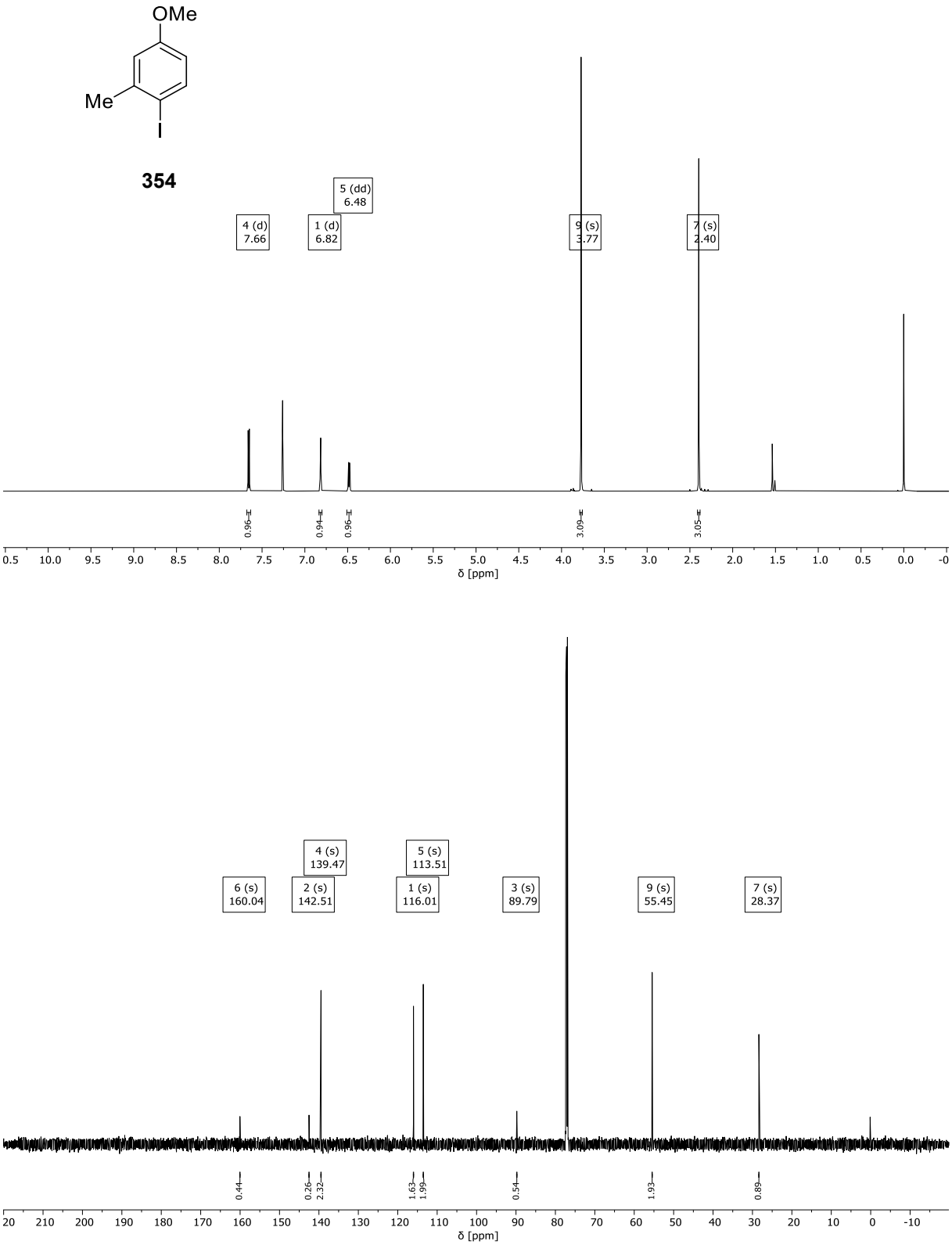

Figure 282: ^{1}H- and ^{13}C-NMR spectra (600 / 151 MHz, $CDCl_3$) of 1-iodo-4-methoxy-2-methylbenzene (**354**).

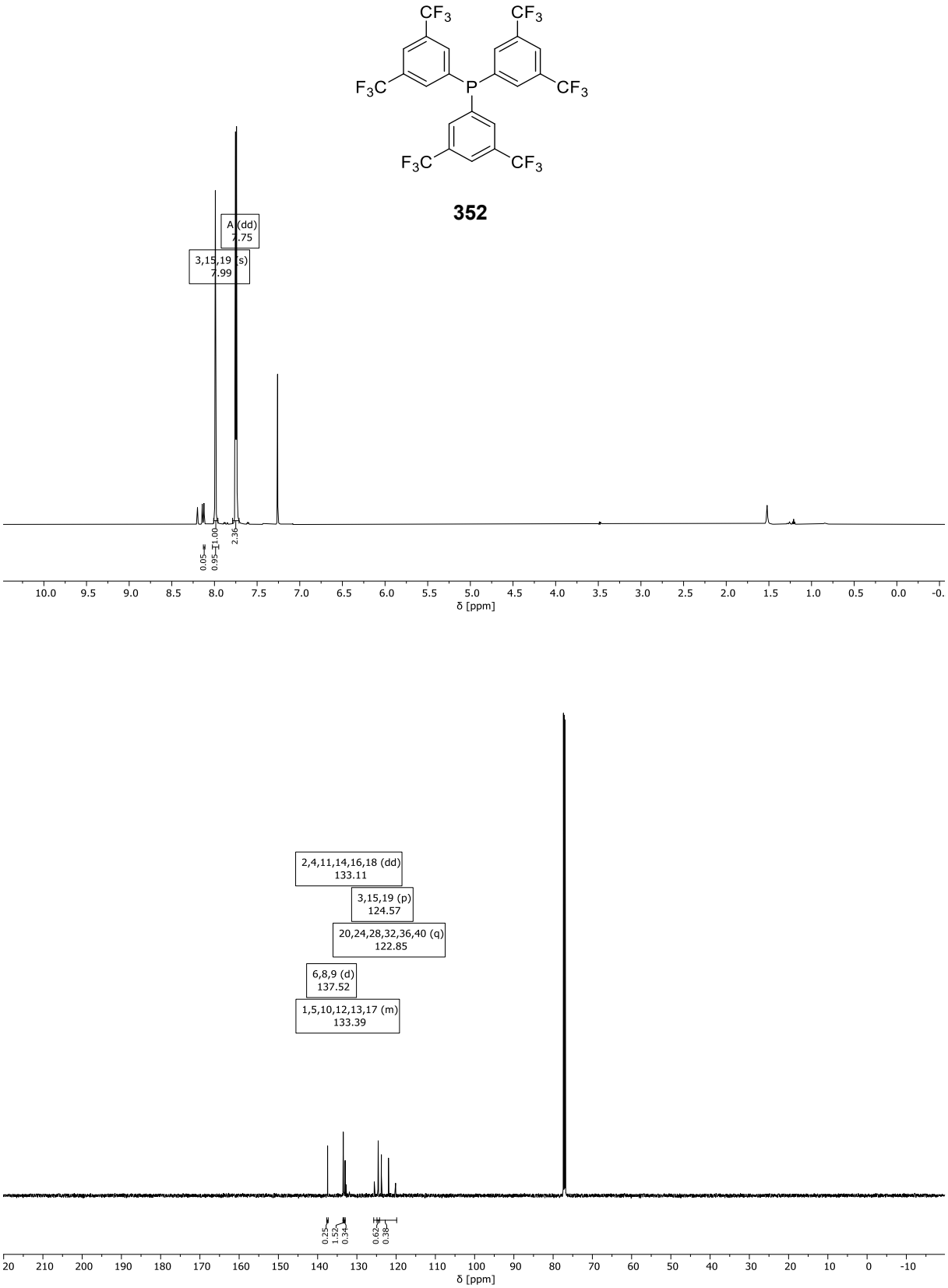

Figure 283: ^{1}H-, ^{13}C-NMR spectra (600 / 151 MHz, $CDCl_3$) of tris(3,5-bis(trifluoromethyl)phenyl)phosphane (**352**).

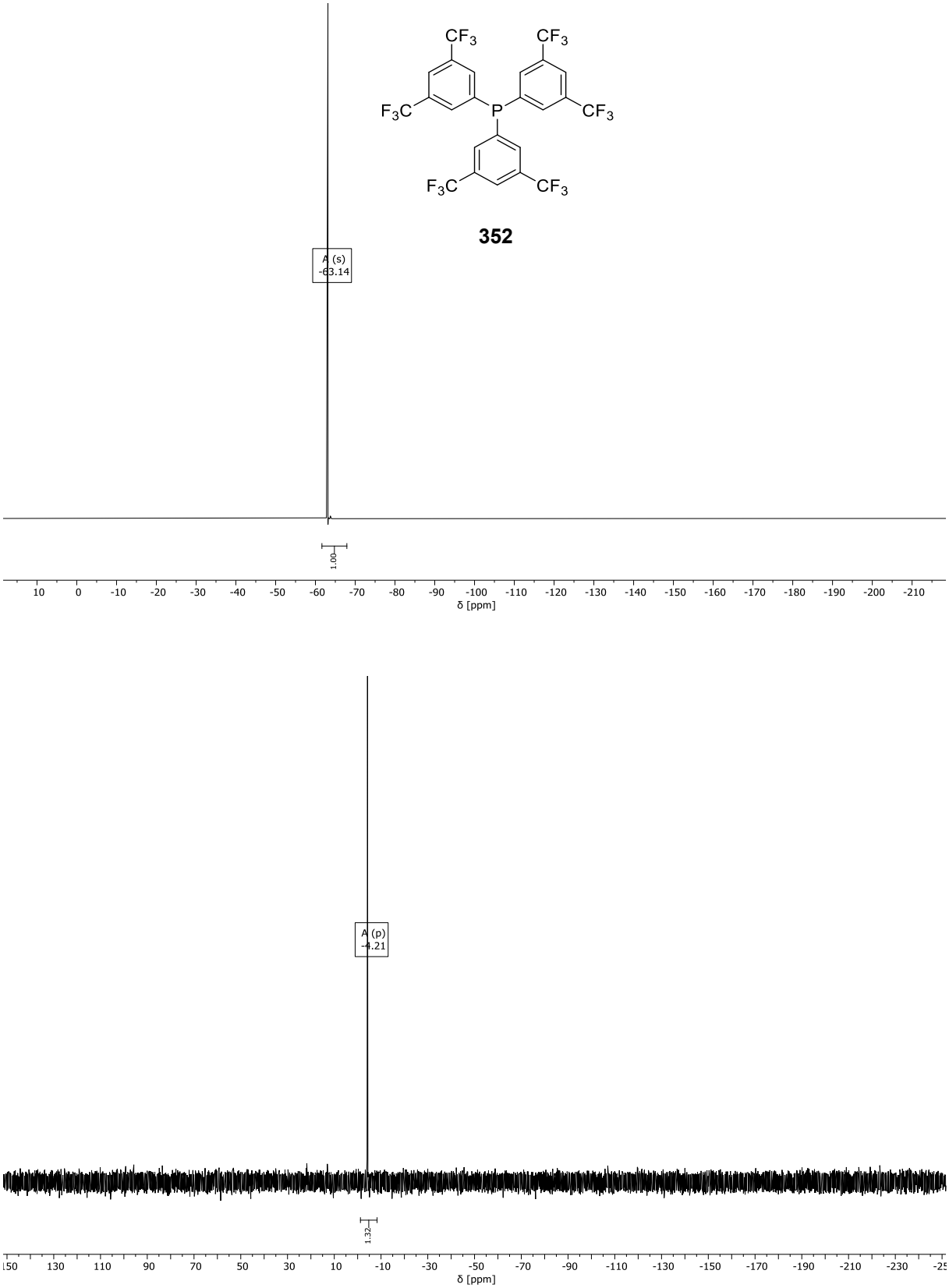

Figure 284: ^{19}F- and ^{31}P-NMR spectra (282 / 122 MHz, $CDCl_3$) of tris(3,5-bis(trifluoromethyl)phenyl)phosphane (**352**).

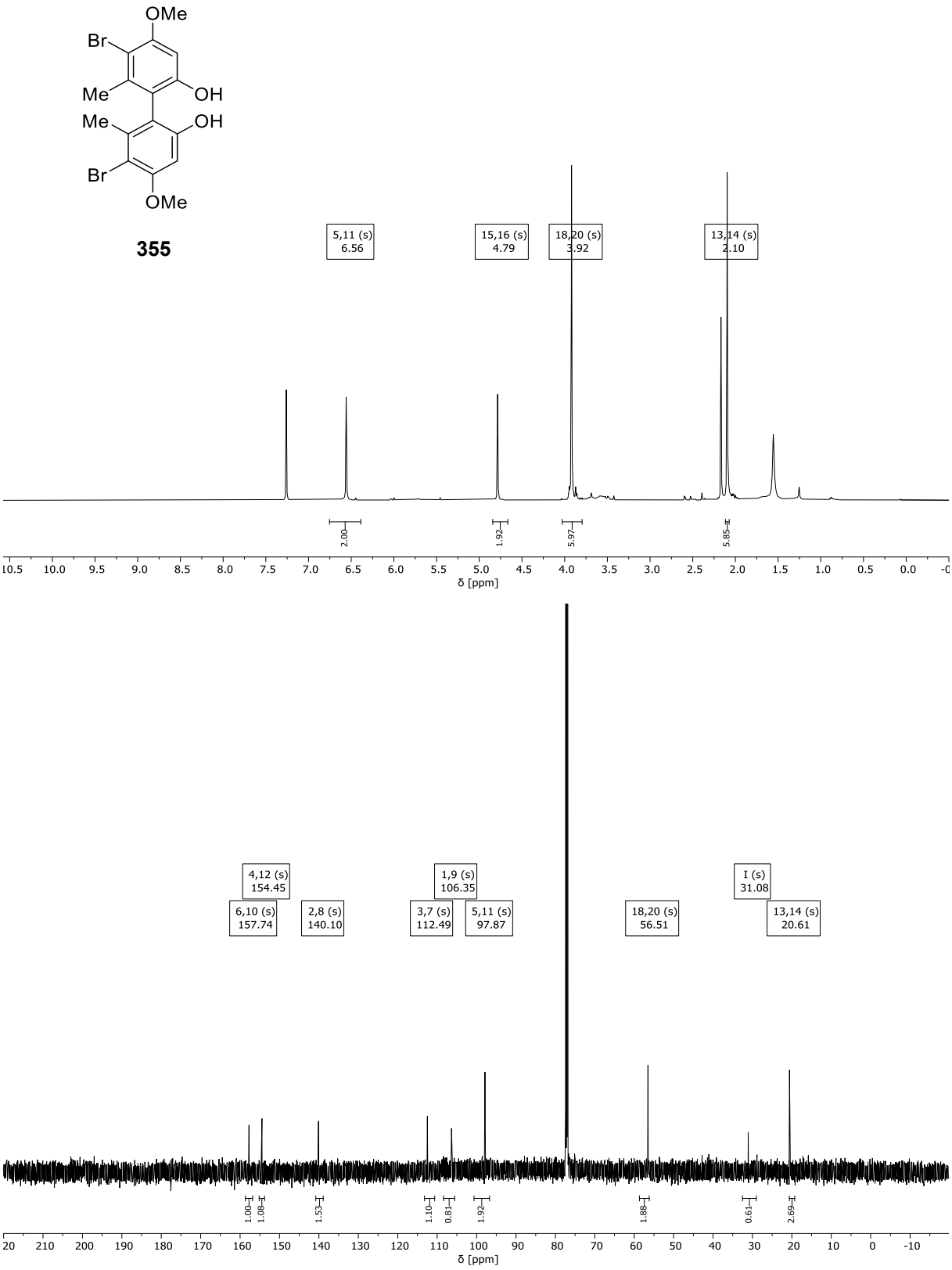

Figure 285: ^{1}H- and ^{13}C-NMR spectra (600 / 151 MHz, $CDCl_3$) of 5,5'-dibromo-4,4'-dimethoxy-6,6'-dimethyl-[1,1'-biphenyl]-2,2'-diol (**355**).

9.2 DFT Geometries and energies

Gibbs* is sum of Final single point energy and G-E(el)

9.2.1 Pd-cycle

(TPSS-D4)

		TPSS D4			wB97M-V	Imaginary fequency
Pd-complex-iPr3P		def2-SVP			def2-TZVPP	
Hartrees (Eh)	Gibbs	G-E(el)	Electronic	**Gibbs ***	Final single point (electronic)	
GS	-2739.63086	0.68532569	-2740.31618	**-2740.44895**	-2741.13427	
TS	-2739.62556	0.68603763	-2740.31159	**-2740.43998**	-2741.12602	69.10i

Atoms						
95		**GS**			**TS**	
C	-0.00810905	-4.42268145	3.60607866	1.58964441	-3.80119314	3.97628548
C	-0.3414634	-3.00326981	4.01904359	0.76170174	-2.53130394	4.02126617
C	0.03465657	-2.58387868	5.31252485	0.85616522	-1.85045331	5.2558514
C	-0.07576328	-1.24992187	5.71687036	0.16748698	-0.67052185	5.53043553
C	-0.54880001	-0.28271444	4.81427517	-0.70817873	-0.17631432	4.56014328
C	-0.95079635	-0.67282329	3.53468031	-0.85610067	-0.83701369	3.33535625
C	-0.90214519	-2.03617756	3.14363706	-0.07582118	-1.9916637	2.99012264
C	-1.33148548	-2.21300478	1.74387954	-0.32303448	-2.3737226	1.55553341
C	-1.98341539	-3.34089589	1.18286619	0.13008152	-3.45910751	0.73594865
C	-2.59671351	-4.44660196	2.0196328	1.1461782	-4.52749707	1.09013655
C	-2.19862153	-3.372823	-0.21276058	-0.38354713	-3.59227217	-0.57357256
C	-1.83352751	-2.29826261	-1.02314191	-1.31313642	-2.71026137	-1.12121087
C	-1.35281045	-1.11206068	-0.43399994	-1.70746405	-1.60874757	-0.35732381
C	-1.14595024	-1.02941211	0.94953385	-1.20392858	-1.42404925	0.93537964
Pd	-1.56690859	0.61627268	2.10429721	-2.01155517	0.08370422	1.98105393
H	0.95103865	-4.7279234	4.06010043	2.02153904	-3.98393186	4.97364891
H	0.08588749	-4.51462962	2.5123522	2.42918553	-3.74050085	3.26676304
H	-0.76727558	-5.15422453	3.93875049	0.98866152	-4.68436578	3.71436405
H	0.46046395	-3.32399641	6.00148591	1.50964141	-2.27825902	6.02494972
H	0.22850291	-0.95857396	6.7286673	0.28670161	-0.16473429	6.49539021
H	-0.62116484	0.76544247	5.12858205	-1.28973651	0.72749062	4.76985208
H	-2.65248537	-4.16820125	3.08343093	0.79511357	-5.20899136	1.88042042
H	-2.04145138	-5.39933243	1.94721533	2.10656652	-4.10042445	1.41415603
H	-3.62473788	-4.64496181	1.66588621	1.34706093	-5.14298808	0.19821136
H	-2.68083721	-4.25379268	-0.65483416	-0.02816676	-4.43563626	-1.17681807
H	-1.97221593	-2.35412067	-2.10972438	-1.69755036	-2.86253913	-2.1362012
H	-1.15836268	-0.25190453	-1.07987638	-2.40565782	-0.88098243	-0.78308669
P	-1.73652509	2.17683594	0.38774572	-2.22139875	1.69441425	0.24812689
P	-3.52694256	1.00038642	3.3394641	-3.72483964	0.86808171	3.42588971
C	-4.85744815	0.13956766	2.39669836	-5.29039747	0.74026851	2.4685825
C	-3.63468226	0.0737766	4.92584221	-4.08138086	-0.26703755	4.83756942
C	-4.14657487	2.68273415	3.72723073	-3.71230557	2.53783569	4.1787421

C	-0.41182218	2.10772009	-0.88940769	-0.87107011	1.61311435	-1.00908179
C	-1.47363336	3.83023284	1.13512334	-1.86793031	3.32383092	1.02663307
C	-3.32281408	2.20591497	-0.5140313	-3.74846084	1.91298311	-0.74055406
C	-4.57854175	-0.43540422	1.1450853	-5.28616398	-0.1315522	1.36219355
C	-6.12718072	-0.05871999	2.97952145	-6.48411213	1.38749399	2.83523811
C	-7.11062888	-0.78407951	2.29701424	-7.65070474	1.18067949	2.08739475
H	-6.33433059	0.32896747	3.98271498	-6.5030655	2.05181371	3.70556459
C	-6.82880268	-1.34117219	1.03912387	-7.63840474	0.31307844	0.9847905
H	-8.09353952	-0.9339716	2.75698444	-8.57658247	1.69176077	2.37287278
C	-3.50120778	1.44735014	-1.68844905	-3.96139819	1.10450717	-1.87760666
C	-4.45355789	2.75341324	0.12570046	-4.81142723	2.71127285	-0.27321006
C	-5.73370183	2.55281026	-0.40167416	-6.04722359	2.71294284	-0.92892701
C	-4.78592388	1.24417883	-2.20864411	-5.19998655	1.10502679	-2.53091902
C	-5.90515295	1.79224434	-1.56673589	-6.24721526	1.90915477	-2.0598614
H	-4.91121084	0.6436647	-3.1161272	-5.34427202	0.47362023	-3.41430254
H	-6.90876219	1.61870149	-1.96859424	-7.21650308	1.90562507	-2.56920114
H	-2.63923292	0.99605896	-2.18804508	-3.1500874	0.47695251	-2.26076613
H	-4.33418693	3.31456748	1.05673276	-4.66973029	3.33570408	0.61212363
H	-6.60209279	2.97563292	0.11399684	-6.86010828	3.33839146	-0.54668028
C	-0.51178649	2.76924726	-2.12783428	-0.95517999	2.26404944	-2.25483561
C	0.74887365	1.37155475	-0.58448186	0.31370505	0.93850824	-0.66014223
C	1.78956321	1.27944684	-1.51654451	1.39247517	0.89869399	-1.55204293
C	0.52822008	2.66685858	-3.06140851	0.12360754	2.2158707	-3.14770818
C	1.6771155	1.9195692	-2.75869574	1.29713967	1.53019691	-2.79980806
H	2.68007892	0.68793734	-1.27853313	2.3047218	0.36087261	-1.27310092
H	2.48308701	1.83215669	-3.49546288	2.13674256	1.48915567	-3.50233019
H	0.79948599	0.83333361	0.36987562	0.37417879	0.42926115	0.30744235
H	-1.40871157	3.34989257	-2.36864422	-1.86628353	2.80398713	-2.5328947
H	0.44050403	3.16806252	-4.03131013	0.04747505	2.71649821	-4.11910366
C	-0.53134204	3.85981883	2.18316343	-1.14120678	3.30299146	2.23312678
C	-2.09874126	5.0199695	0.72928205	-2.19838631	4.55833149	0.43931741
C	-1.79527093	6.22372222	1.38115026	-1.82749917	5.7543363	1.06801641
C	-0.21246805	5.06570773	2.81492093	-0.75729434	4.49821552	2.84995844
C	-0.85184861	6.25000782	2.4182628	-1.10721844	5.72601069	2.271709
H	-2.82509727	5.00643557	-0.08963165	-2.74280871	4.58593638	-0.51044716
H	-0.05638622	2.92072141	2.49987449	-0.87816273	2.33553124	2.68165469
H	0.5273825	5.07884768	3.62251884	-0.19566884	4.46799458	3.7887758
H	-0.61325983	7.194753	2.9180466	-0.81691106	6.66344917	2.75802108
H	-2.29351111	7.14811664	1.07091017	-2.09248991	6.71340117	0.60981733
C	-3.63949211	-1.33511567	4.83474299	-3.64957171	-1.60240186	4.73348349
C	-3.55646367	0.68304213	6.18756745	-4.82917208	0.13214521	5.96195998
C	-3.47215077	-0.10758172	7.34481726	-5.1144119	-0.78751465	6.97993044
C	-3.45848745	-1.50460175	7.24816116	-4.66844313	-2.11370937	6.87747744
C	-3.54853915	-2.11686593	5.9883134	-3.94276823	-2.52045599	5.74925804
H	-3.69311	-1.81723158	3.85395182	-3.06602697	-1.90933832	3.85931348
H	-3.37883232	-2.11830825	8.15194968	-4.88776315	-2.82913658	7.67759888
H	-3.53476867	-3.20847083	5.90213518	-3.59115596	-3.55384141	5.66154388

H	-3.5550533	1.77462159	6.27215041	-5.18409978	1.16437103	6.04828429
H	-3.41219595	0.37423595	8.32676621	-5.68844648	-0.46688264	7.85610972
C	-5.44041156	3.15540563	3.43963582	-4.20018141	3.6555912	3.47309041
C	-3.19095559	3.5736261	4.25706586	-3.01544847	2.75364124	5.38665163
C	-3.52553938	4.90699274	4.51489735	-2.82420497	4.0515731	5.87647565
C	-5.76815869	4.49641745	3.68200901	-4.01123827	4.95120753	3.96551742
C	-4.81534919	5.37279334	4.22135483	-3.32197463	5.15476791	5.16912133
H	-6.77515532	4.85818278	3.44736314	-4.39701081	5.80538484	3.40011193
H	-5.07516854	6.42043161	4.40533372	-3.16942606	6.16906462	5.5524258
H	-6.18489082	2.48050908	3.00757823	-4.73354324	3.50880955	2.53098039
H	-2.17241443	3.21711069	4.44549066	-2.62804357	1.90086223	5.95368537
H	-2.77050446	5.58631497	4.92256231	-2.28457595	4.19851047	6.81831349
C	-5.56022849	-1.17329212	0.47007543	-6.45601126	-0.34888618	0.62699751
H	-7.59549117	-1.92210036	0.51440212	-8.55306167	0.15320032	0.40384885
H	-3.58105872	-0.33106554	0.70980416	-4.35048532	-0.63414765	1.08182354
H	-5.31848973	-1.62385679	-0.49738965	-6.43824214	-1.02475945	-0.23353567

(B97-3c)

		B97-3c		wB97M-V		Imaginary frequency
Pd-complex-iPr3P				def2-TZVPP		
Hartrees (Eh)	Gibbs	G-E(el)	Electronic	**Gibbs ***	Final single point (electronic)	
GS	-2739.86079	0.68096428	-2740.54176	**-2740.47023**	-2741.1512	
TS	-2739.85009	0.68108751	-2740.53117	**-2740.46058**	-2741.14166	82.64i

Atoms						
95		**GS**			**TS**	
C	-0.13151997	-4.83586817	1.64597835	1.64784014	-3.80732241	3.90221879
C	-0.54534696	-3.68467019	2.51556348	0.83464265	-2.54438465	3.95833041
C	0.06175766	-3.56842512	3.77041681	0.98072036	-1.85050268	5.16427732
C	-0.08091672	-2.4330382	4.54362185	0.30740764	-0.68154559	5.44833895
C	-0.82680049	-1.35983834	4.06131192	-0.60053372	-0.20730388	4.5208661
C	-1.47937556	-1.46557791	2.84916453	-0.79418837	-0.87603117	3.32450016
C	-1.39115908	-2.64967206	2.08397597	-0.03967567	-2.02711481	2.96300137
C	-2.06665156	-2.52104917	0.78857858	-0.35203506	-2.43311101	1.55279801
C	-2.71742888	-3.52362054	0.0525395	0.03962619	-3.53402453	0.74212712
C	-3.004248	-4.89129991	0.60127722	1.05383947	-4.59725449	1.05965819
C	-3.25633724	-3.19356539	-1.19483921	-0.53756659	-3.68769859	-0.52296991
C	-3.21853025	-1.90067692	-1.67843833	-1.47054723	-2.81344129	-1.038198
C	-2.71017869	-0.87857212	-0.87957579	-1.80345591	-1.69794646	-0.29354781
C	-2.16559641	-1.17127951	0.35916601	-1.23762163	-1.49423895	0.95333006
Pd	-2.14320624	0.19211658	1.88545743	-1.9771596	0.05002705	1.99717749
H	0.91395363	-5.08029323	1.82870768	2.13811764	-3.96487272	4.85954158
H	-0.23867686	-4.5985761	0.59129539	2.42958155	-3.77706827	3.15090818
H	-0.70658831	-5.74111503	1.83982935	1.03671438	-4.68350377	3.71449322
H	0.70966293	-4.3677788	4.11054526	1.6599186	-2.25332989	5.90420891

H	0.42392706	-2.35803692	5.49937385	0.46033963	-0.17065167	6.39102178
H	-0.86250208	-0.43976648	4.62817485	-1.16884989	0.68504959	4.74178098
H	-2.91241969	-4.9171134	1.68303081	0.74835468	-5.24825957	1.87249838
H	-2.34753167	-5.6590111	0.19275535	2.02390263	-4.18200994	1.30904348
H	-4.02300227	-5.18310989	0.34620286	1.19745624	-5.23093325	0.18823541
H	-3.74588058	-3.96833353	-1.77361052	-0.23644745	-4.53893849	-1.11943221
H	-3.63663231	-1.67012752	-2.65085939	-1.90166373	-2.97977442	-2.01778867
H	-2.77772074	0.1415525	-1.23077877	-2.50382099	-0.98037624	-0.6966408
P	-1.70363767	2.11964386	0.62137757	-2.19378287	1.67553308	0.25466062
P	-3.60872968	0.84477291	3.63921281	-3.69725414	0.86936737	3.44798076
C	-4.78533789	-0.55415434	3.84691692	-5.27508142	0.74745026	2.51784312
C	-3.11738506	1.16008585	5.38432181	-4.08397124	-0.24078277	4.86225201
C	-4.77123547	2.19861869	3.17973725	-3.68582769	2.53490085	4.20144189
C	-0.05502162	1.99882486	-0.1849912	-0.82547908	1.63715754	-0.97375879
C	-1.45012911	3.59537803	1.67489341	-1.89546048	3.32553952	1.00063205
C	-2.81895956	2.71179865	-0.70224827	-3.68982943	1.86009841	-0.77886494
C	-4.85181839	-1.55670494	2.88591552	-5.31814677	-0.14172224	1.44555011
C	-5.67611457	-0.57900254	4.92066531	-6.4377132	1.41727279	2.89105267
C	-6.60065262	-1.60351594	5.03889929	-7.61481967	1.21936743	2.18554475
H	-5.64497594	0.20497523	5.66438924	-6.42711467	2.0952944	3.73274376
C	-6.65409348	-2.60927496	4.08098919	-7.64806128	0.33544147	1.11520019
H	-7.28140952	-1.61776421	5.8798817	-8.51138339	1.7493079	2.47977869
C	-2.37524422	3.12300845	-1.95649273	-3.81698524	1.12127918	-1.9570695
C	-4.1867783	2.70834176	-0.42825826	-4.79215398	2.5843872	-0.32649285
C	-5.09189967	3.14149547	-1.38219296	-5.97823756	2.59248105	-1.04020095
C	-3.28728646	3.54062379	-2.9159851	-5.0081364	1.12342875	-2.66632823
C	-4.64483021	3.55754136	-2.629846	-6.09249719	1.86140086	-2.2136873
H	-2.93385172	3.85221407	-3.89002731	-5.08493482	0.55049082	-3.58109154
H	-5.35328993	3.88371332	-3.38004472	-7.02084564	1.86304005	-2.76925818
H	-1.31999199	3.10731639	-2.18776808	-2.97559504	0.55705696	-2.33374317
H	-4.54069172	2.35797348	0.52984091	-4.72578804	3.14463175	0.59242784
H	-6.14893073	3.13980659	-1.15271527	-6.81989847	3.16047365	-0.6680252
C	0.69100573	3.14400219	-0.46814247	-0.86292527	2.41450128	-2.13076684
C	0.46215209	0.75127112	-0.52264397	0.31729934	0.89730249	-0.68761365
C	1.69486401	0.65286059	-1.15172623	1.40085658	0.92178218	-1.55383266
C	1.92306097	3.04140871	-1.09438184	0.21778591	2.43188402	-2.99726173
C	2.42766498	1.79450939	-1.43960023	1.35261112	1.68319665	-2.71153295
H	2.08566494	-0.32335445	-1.40608611	2.27987034	0.33457389	-1.32426725
H	3.39246775	1.71476602	-1.92347974	2.19614996	1.69735938	-3.38945937
H	-0.10079253	-0.137411	-0.27854207	0.34670366	0.29090564	0.20562388
H	0.3134828	4.1184131	-0.19166962	-1.74028741	3.00278374	-2.36063774
H	2.49321633	3.93646699	-1.30591905	0.17558702	3.03360432	-3.89571448
C	-0.80521457	3.39933987	2.89662108	-1.13891431	3.36493777	2.17072332
C	-1.88189702	4.87099979	1.3277895	-2.29597543	4.52160797	0.41080324
C	-1.6869805	5.93441933	2.19880217	-1.96273343	5.73432453	0.99496282
C	-0.60678886	4.46263159	3.76148306	-0.79523151	4.57724529	2.7446106
C	-1.05465581	5.73311104	3.41749017	-1.21186964	5.76487572	2.16202378

H	-2.39333495	5.02785105	0.38855007	-2.8702926	4.50981609	-0.50478703
H	-0.48374745	2.40406058	3.17770134	-0.82318753	2.43660382	2.63075616
H	-0.11759046	4.29606509	4.71162675	-0.21805614	4.59131557	3.65874298
H	-0.90807153	6.562354	4.09688885	-0.95474453	6.71251334	2.61688028
H	-2.03534434	6.92186655	1.92549383	-2.28426748	6.6582361	0.53205274
C	-2.82819397	0.05640471	6.19300557	-3.64503135	-1.56037695	4.81064001
C	-2.91058071	2.43633213	5.90468276	-4.88894313	0.16868562	5.92410809
C	-2.4293923	2.60580149	7.19465159	-5.22957412	-0.7234141	6.92850238
C	-2.13902202	1.50508873	7.98675136	-4.78043071	-2.03660024	6.87678773
C	-2.34454453	0.22973855	7.47937146	-3.99328765	-2.45277867	5.81345387
H	-2.98683911	-0.94279627	5.81726389	-3.01687141	-1.8778078	3.99128607
H	-1.76252477	1.63909292	8.9922219	-5.04599301	-2.73197881	7.66242157
H	-2.12918435	-0.63937173	8.08674891	-3.6369684	-3.47304889	5.76611386
H	-3.1383028	3.31078707	5.31843488	-5.24614614	1.18780103	5.9731855
H	-2.28797247	3.60670895	7.58129033	-5.84973073	-0.39303864	7.7515301
C	-6.0609481	1.89980105	2.73310299	-4.17533643	3.6469397	3.51759357
C	-4.34951568	3.52860567	3.13422958	-3.01426169	2.73984662	5.40876271
C	-5.19949879	4.52997857	2.69398666	-2.85871093	4.01744229	5.92284016
C	-6.90392501	2.90260853	2.27745937	-4.02314435	4.92229225	4.03446837
C	-6.48144875	4.22351472	2.26325906	-3.36539821	5.11417349	5.24034869
H	-7.89756214	2.64506343	1.93495938	-4.40995938	5.76932732	3.4845338
H	-7.14004461	5.00477275	1.90743113	-3.24236921	6.11111131	5.64213298
H	-6.40990946	0.87913352	2.73313839	-4.68264118	3.51832882	2.57478955
H	-3.34250971	3.79107541	3.40618873	-2.62781681	1.89553212	5.96216498
H	-4.84335663	5.55061757	2.66963056	-2.34264731	4.15402287	6.8640789
C	-5.78244791	-2.57974113	3.00327709	-6.49853061	-0.34958765	0.75158281
H	-7.37534625	-3.41060642	4.17635171	-8.56840221	0.18228284	0.5669043
H	-4.16968279	-1.53781848	2.05005278	-4.41603555	-0.66584262	1.15509568
H	-5.81517391	-3.35510267	2.24983832	-6.51333638	-1.03398583	-0.08543809

(M06-L)

		M06-L			wB97M-V	Imaginary frequency
Pd-complex-iPr3P		def2-SVP			def2-TZVPP	
Hartrees (Eh)	Gibbs	G-E(el)	Electronic	**Gibbs ***	Final single point (electronic)	
GS	-2738.81972	0.69423905	-2739.51396	**-2740.46074**	-2741.15498	
TS	-2738.80578	0.69457537	-2739.50035	**-2740.43998**	-2741.13455	78.35i

Atoms						
95		**GS**			**TS**	
C	0.0928276	-4.83802737	1.63449087	1.37492053	-4.0397584	4.15841933
C	-0.85701015	-3.9851719	2.42533598	0.66224072	-2.71666341	4.13826458
C	-0.88498823	-4.15977905	3.8185025	0.74203999	-2.02632051	5.36151356
C	-1.58741847	-3.29008463	4.63908771	0.15024189	-0.79204549	5.5800268
C	-2.19654578	-2.1579946	4.08513907	-0.61586528	-0.24380944	4.55821943

C	-2.17802555	-1.93433634	2.70818605	-0.74980154	-0.91280865	3.34349057
C	-1.60987133	-2.93017495	1.86111519	-0.06166399	-2.12991861	3.05527484
C	-1.80261237	-2.65075586	0.43063414	-0.25303704	-2.50197866	1.61328152
C	-1.95182251	-3.59847447	-0.60905558	0.16649761	-3.62073617	0.83185728
C	-2.11194621	-5.07279807	-0.37444515	1.0139173	-4.78004614	1.27321802
C	-2.10402016	-3.13161628	-1.92520215	-0.22290295	-3.70015461	-0.51715808
C	-2.17890356	-1.77624865	-2.21021089	-1.00232142	-2.73924961	-1.14047751
C	-2.17561733	-0.85007666	-1.16164899	-1.38794653	-1.62615217	-0.4025171
C	-2.01631339	-1.27230817	0.15634132	-1.00956776	-1.49428566	0.93306243
Pd	-2.4667372	-0.09866899	1.78490758	-1.84888105	0.03662343	1.94995378
H	1.05517909	-4.90950098	2.16314832	1.73605349	-4.24709756	5.17360708
H	0.29643013	-4.4220002	0.63956282	2.25499934	-4.07197439	3.50567058
H	-0.25689578	-5.87252925	1.49596657	0.72868462	-4.87908805	3.88063116
H	-0.31504778	-4.98494767	4.25759767	1.30945702	-2.49289184	6.1714684
H	-1.61984843	-3.45466299	5.72006251	0.26134489	-0.28157134	6.54051145
H	-2.6753183	-1.45365103	4.77090359	-1.12607748	0.71270191	4.71771027
H	-2.37519432	-5.30142972	0.66626624	0.54209874	-5.3935638	2.04910776
H	-1.21294275	-5.6575316	-0.62275855	1.9968043	-4.47386954	1.64731751
H	-2.91764291	-5.4658504	-1.01176684	1.19862178	-5.446554	0.42140736
H	-2.20770895	-3.86338509	-2.73276143	0.10909335	-4.56904599	-1.09211711
H	-2.29792086	-1.43483147	-3.24267202	-1.28969739	-2.84769109	-2.18978603
H	-2.3314281	0.20430482	-1.40346257	-1.98674271	-0.84711595	-0.88446798
P	-1.87920987	1.98107467	0.63668166	-2.18218583	1.74901951	0.17419106
P	-3.75123438	0.85080287	3.64369567	-3.6700797	0.86818973	3.42727496
C	-4.96945276	-0.40478011	4.22181668	-5.24243957	0.72813806	2.48713321
C	-2.90643701	1.41231465	5.17388043	-4.02113666	-0.25681378	4.84119139
C	-4.87927568	2.24438585	3.23051312	-3.69042901	2.53446548	4.17959383
C	-0.19787654	1.92765161	-0.10955224	-0.88579939	1.75716707	-1.13169035
C	-1.64379094	3.41461921	1.76391346	-1.87562445	3.38283564	0.95881541
C	-2.94598255	2.66127144	-0.6880868	-3.73770578	1.94060853	-0.76840988
C	-5.42015417	-1.3572924	3.29764342	-5.26198245	-0.12100431	1.37134407
C	-5.46774826	-0.43633101	5.52927698	-6.43170663	1.35613836	2.88256631
C	-6.40073037	-1.40206856	5.90468143	-7.60612414	1.16188446	2.15823163
H	-5.11634095	0.28547537	6.2710761	-6.44347487	2.00072788	3.76659342
C	-6.85188114	-2.33975439	4.97684706	-7.61178573	0.32302292	1.04329964
H	-6.77294935	-1.42335914	6.93179554	-8.52561505	1.66154665	2.47334312
C	-2.58624882	2.67263494	-2.04260878	-3.96903503	1.1127757	-1.87941373
C	-4.22896688	3.10254579	-0.32783449	-4.78886538	2.751775	-0.31565327
C	-5.11887477	3.56532442	-1.29276776	-6.02455259	2.74726404	-0.95847009
C	-3.48396625	3.12644788	-3.00899697	-5.20416332	1.11080109	-2.52363863
C	-4.74921673	3.57747393	-2.63831992	-6.23730658	1.92847618	-2.06619592
H	-3.18836678	3.12554164	-4.06085246	-5.35796654	0.46491553	-3.39157298
H	-5.44942469	3.93363651	-3.39757258	-7.20683589	1.92459847	-2.57009358
H	-1.59900785	2.31760826	-2.34995614	-3.16747105	0.46903058	-2.25517134
H	-4.53057025	3.0905194	0.72328773	-4.64118897	3.39833582	0.55273374
H	-6.10981629	3.91168122	-0.98857014	-6.82854184	3.38605634	-0.5843544
C	0.33417554	3.07122236	-0.72667001	-1.05654683	2.40058294	-2.36548527

C	0.60049833	0.78473779	0.00715129	0.3482596	1.16280563	-0.8377032
C	1.89856907	0.77810564	-0.50568104	1.3894002	1.20510056	-1.76302877
C	1.62634331	3.05981615	-1.2428892	-0.01551312	2.43566219	-3.29118033
C	2.41083966	1.90966034	-1.13521621	1.20868652	1.83739171	-2.99216716
H	2.51007232	-0.12208647	-0.41070984	2.34421241	0.73183866	-1.52298157
H	3.42646238	1.90111136	-1.53844629	2.02279588	1.86371476	-3.72058084
H	0.19810495	-0.10453644	0.50042171	0.48293897	0.65143207	0.12129824
H	-0.26941838	3.98167751	-0.80147486	-2.01078422	2.87675446	-2.60938597
H	2.02609231	3.95484319	-1.72567644	-0.16164396	2.93632669	-4.25149013
C	-0.9749881	3.15187313	2.96761316	-1.15640437	3.40218435	2.16242508
C	-2.05935037	4.72384599	1.49270954	-2.24914351	4.60066839	0.37335962
C	-1.82904905	5.74040509	2.4200343	-1.93704172	5.80745309	0.99633416
C	-0.74716956	4.16586156	3.89437089	-0.83500992	4.60948788	2.77838283
C	-1.18204052	5.46453931	3.62441213	-1.23228214	5.81384266	2.20063606
H	-2.5780192	4.95344589	0.5577379	-2.78885785	4.60863095	-0.57839914
H	-0.63484555	2.13218788	3.17863192	-0.85034983	2.45394961	2.62277509
H	-0.23729248	3.93670368	4.8337553	-0.28247121	4.60577462	3.72103666
H	-1.0108323	6.26250802	4.35091777	-0.99175039	6.76152992	2.68926584
H	-2.16319626	6.75749196	2.19892312	-2.23951955	6.749989	0.5331181
C	-1.59990511	0.95790819	5.40575604	-3.65538182	-1.60406138	4.71887722
C	-3.49961933	2.26753879	6.11446414	-4.7054341	0.1600888	5.99111351
C	-2.80217742	2.65771576	7.25641206	-4.99407438	-0.74849025	7.00816088
C	-1.50601168	2.19273011	7.47925601	-4.6135483	-2.08434422	6.88383733
C	-0.90723799	1.33915344	6.55319535	-3.95063368	-2.51119741	5.73397201
H	-1.12360263	0.29998118	4.67063443	-3.12259318	-1.93789863	3.82281583
H	-0.96160959	2.49804296	8.37617978	-4.83624923	-2.79391794	7.6844349
H	0.10806025	0.97156383	6.7196813	-3.6509551	-3.5562869	5.62691997
H	-4.51554727	2.63888909	5.95180313	-5.01649467	1.20328318	6.09787504
H	-3.27667752	3.32656953	7.97854642	-5.522599	-0.40917353	7.90245428
C	-6.11059432	1.9741876	2.61163507	-4.24462105	3.63849152	3.51385971
C	-4.50513385	3.58316649	3.41988967	-2.96705348	2.76742615	5.36164591
C	-5.34074621	4.61962705	3.00503627	-2.81708273	4.05819061	5.86435315
C	-6.94286063	3.01181059	2.19776043	-4.09232944	4.92848287	4.01604023
C	-6.56106999	4.33954001	2.39212044	-3.37900742	5.14442577	5.19422052
H	-7.89826402	2.77835162	1.72140638	-4.5314744	5.77155445	3.47676372
H	-7.21475693	5.15372184	2.06975159	-3.25885517	6.15666497	5.5877054
H	-6.42582646	0.93916755	2.45341661	-4.8058666	3.48772888	2.58835496
H	-3.55167061	3.82674026	3.89677156	-2.52720675	1.9260192	5.90584906
H	-5.02799546	5.65493261	3.16394429	-2.25802372	4.21380033	6.79034074
C	-6.3622382	-2.3129322	3.67166452	-6.44005309	-0.32425118	0.65596178
H	-7.5797752	-3.09841623	5.27430545	-8.53375485	0.17309525	0.47567006
H	-5.00357037	-1.36260896	2.28452535	-4.33728609	-0.62231197	1.05720237
H	-6.70126874	-3.0513975	2.94159355	-6.43618072	-0.98229788	-0.21623537

9.2.2 Chiral Acetylene

Oxabicycle **311**

Functional		TPSS D4			wB97M-V
Basis set		def2-SVP			def2-TZVPP
Hartrees (Eh)	Gibbs	G-E(el)	Electronic	**Gibbs ***	Final single point (electronic)
	-821.289685	0.212028	-821.501713	**-821.732951**	-821.944979

Atoms			
32			
O	-0.28436248	2.81359998	0.65652591
C	-0.32903709	1.58517035	0.82490366
N	0.72064241	0.82496753	1.23080557
C	2.04993505	1.40650806	1.42487657
C	-1.61796944	0.88560887	0.57378535
C	-1.99648443	-0.37836091	0.24533168
C	-1.21225621	-1.60527633	0.13164533
O	-1.91703662	-2.57744087	-0.49729841
C	-1.23194142	-3.83404801	-0.65296681
O	-0.06731686	-1.78998099	0.54371701
C	-3.49849925	-0.23703821	-0.14226716
H	-4.10951074	-1.14444669	-0.06222745
C	-3.53904906	0.55412366	-1.47312687
C	-3.15674468	1.7952442	-1.1396976
C	-2.90271845	1.72911842	0.38397469
H	-2.94396601	2.66503109	0.95324957
O	-3.89748179	0.77419628	0.79395666
H	0.61297085	-0.20019808	1.18308415
H	-0.96257254	-4.24661369	0.33325016
H	-0.31205856	-3.69771447	-1.24503851
H	-1.93926799	-4.49342556	-1.17397467
H	-3.76744077	0.13076456	-2.45308039
H	-2.97623164	2.67059502	-1.76568376
C	2.79073883	0.62799855	2.51700777
H	2.2176956	0.63216072	3.45981419
H	3.77990078	1.07847664	2.7072131
H	2.95025156	-0.42330238	2.21341304
C	2.82722743	1.45469555	0.09767054
H	1.87317726	2.44505062	1.75609608
H	2.98131666	0.43606997	-0.30242235
H	3.81616491	1.92436534	0.24377835
H	2.26930466	2.04669879	-0.64668642

9.2.2.1 *i*-Pr$_3$P

Pd-1

Functional		TPSS D4			wB97M-V
Basis set		def2-SVP			def2-TZVPP
Hartrees (Eh)	Gibbs	G-E(el)	Electronic	**Gibbs ***	Final single point (electronic)
cis	-1470.13126	0.37626763	-1470.50753	**-1470.46214**	-1470.8384
trans	-1470.13966	0.3768816	-1470.51654	**-1470.47318**	-1470.85006

Atoms						
51		*cis*			*trans*	
C	-2.19524421	1.60981094	-0.3139234	-1.65168154	-2.07405912	-1.22710422
C	-2.4311021	0.60255073	-1.26100958	-2.04171806	-2.02234279	0.1062287
C	-2.20874979	0.7791587	-2.73989445	-1.67372097	-3.0875017	1.10582258
C	-3.04179342	-0.66312968	-0.76064052	-2.91794747	-0.8819445	0.5049528
C	-4.18781126	-1.34385283	-1.2001662	-4.14389856	-0.94953159	1.18396914
C	-4.54314459	-2.51693553	-0.51892482	-4.85152746	0.24152549	1.39872082
C	-3.74787865	-2.99932618	0.53839189	-4.32072434	1.46233649	0.95188886
C	-2.56451706	-2.34526295	0.92367982	-3.05977474	1.52425889	0.33165796
C	-2.22341037	-1.15493808	0.26778671	-2.33090224	0.34417473	0.11561158
Pd	-0.64402998	0.11477204	0.12541137	-0.46687334	-0.35652635	-0.34150099
I	0.95135973	-1.76990465	1.08144702	1.72582381	-1.93500758	-0.55946981
H	-1.81855127	2.58290609	-0.6436535	-1.00454905	-2.88127874	-1.58501231
H	-2.71378493	1.58535451	0.65136814	-2.16294474	-1.46180694	-1.97813471
H	-3.19422758	0.80593221	-3.2439726	-1.36130869	-2.6385905	2.06344967
H	-1.65437769	-0.07587604	-3.16128967	-0.86412265	-3.73130437	0.72845468
H	-1.67510345	1.71211578	-2.97769859	-2.56354967	-3.71452668	1.3094651
H	-4.79488291	-0.97073504	-2.03327067	-4.55193098	-1.91120998	1.51557247
H	-5.4462602	-3.06426893	-0.81034386	-5.824684	0.21957936	1.90079397
H	-4.05221509	-3.91305375	1.06255285	-4.89348908	2.38598732	1.09620285
P	1.30778802	1.54611552	-0.12064261	0.73187706	1.5818751	0.06516514
C	2.21253059	1.64577103	1.53143012	0.94925912	1.82663977	1.90938101
C	2.52330933	0.68816325	-1.28336626	2.47539074	1.55869997	-0.62374178
C	1.24034726	3.32807591	-0.72665731	-0.13295439	3.13653195	-0.52233961
C	1.21120363	1.80345845	2.69084234	1.81274863	0.69647163	2.49593619
C	3.36479059	2.65580172	1.63002862	-0.40217637	1.91246384	2.63531455
H	2.62475957	0.62140572	1.60189188	1.48082064	2.79183056	2.02379385
H	0.42107877	1.03507439	2.63333198	1.94037302	0.85547675	3.58198532
H	0.73210056	2.79745891	2.69542935	2.81471555	0.64827774	2.03934366
H	1.7378403	1.67939438	3.65450364	1.33073299	-0.28393362	2.33768702
H	4.12937817	2.50693243	0.8507728	-1.03420353	2.73776103	2.26701221
H	3.86588118	2.54131486	2.60875777	-0.22860829	2.07970644	3.7136312
H	3.01178392	3.70025446	1.56685906	-0.97137515	0.97495488	2.51494858
C	0.47890538	4.24484651	0.2464089	-0.73999901	2.95524483	-1.92441849
H	0.41255065	5.26406772	-0.17664305	0.03997647	2.94583359	-2.70344076
H	0.98300338	4.32153705	1.22235446	-1.42653162	3.79240855	-2.1463783

H	-0.54863933	3.88697291	0.4283792	-1.30574584	2.01064797	-1.99363549
C	0.66561665	3.43269091	-2.14794445	0.67969795	4.43552616	-0.40742842
H	2.29453377	3.6628923	-0.76008334	-0.96662919	3.20448767	0.19828056
H	1.23824844	2.83743279	-2.876878	1.47161827	4.48775417	-1.17281626
H	0.6849399	4.48587318	-2.48298207	1.14845325	4.55481518	0.58415857
H	-0.38137347	3.08961992	-2.18416259	0.00994497	5.30024248	-0.56707417
C	1.76387781	-0.01568787	-2.42335788	2.46009484	1.5326433	-2.16010978
H	0.9784539	-0.67512566	-2.0152365	1.75642391	0.77112466	-2.53745348
H	2.46373788	-0.63564777	-3.01263858	3.46671638	1.27170415	-2.53226296
H	1.2895963	0.7047246	-3.11313968	2.18968236	2.51543756	-2.58458463
H	2.92062584	-0.1068585	-0.62359597	2.80824097	0.55685383	-0.29359666
C	3.68980896	1.53238013	-1.81648551	3.45893058	2.60140187	-0.06744096
H	4.27832337	2.00208686	-1.01246211	4.48013687	2.32129687	-0.38470974
H	3.34582107	2.32938701	-2.49908019	3.4595762	2.64104071	1.03467914
H	4.37582573	0.88508827	-2.39311962	3.26344217	3.61620376	-0.44780185
H	-1.92866683	-2.76276042	1.71046991	-2.68396364	2.50250233	0.02012278

Pd-2, *cis*

Functional		TPSS D4			wB97M-V	
Basis set		def2-SVP			def2-TZVPP	
Hartrees (Eh)	Gibbs	G-E(el)	Electronic	**Gibbs ***	Final single point (electronic)	
α	-2291.42266	0.61584354	-2292.038507	**-2292.187117**	-2292.80296	
β	-2291.41869	0.6157095	-2292.034404	**-2292.184251**	-2292.79996	
ΔG	-0.00396881			**-0.00286597**		
kcal/mol				**-1.798396219**		

Atoms						
83		*α*			*β*	
C	-0.94814617	1.76391766	-2.77267096	1.61501488	-0.11999301	4.12782613
C	-0.73827896	2.95108768	-2.15691531	0.44969214	-0.31697227	3.47037052
C	-0.29586518	4.1411497	-2.98642841	-0.60923931	0.75511676	3.4096587
C	-0.92837633	3.16181977	-0.69729854	0.20221658	-1.61276573	2.77076737
C	-1.06648488	4.48847185	-0.21324714	0.50214851	-2.81524758	3.45428909
C	-1.22636081	4.77827383	1.14338584	0.380651	-4.06331216	2.8381802
C	-1.23212494	3.73345726	2.07726998	-0.03886974	-4.13601171	1.50247033
C	-1.08336871	2.4139487	1.63233658	-0.34601509	-2.95935329	0.80630333
C	-0.95041208	2.11819197	0.26516975	-0.25550407	-1.70712896	1.43694011
C	1.08738803	-0.50869048	-0.16815788	0.8405808	0.68722311	-0.67045443
C	1.05918011	0.90354943	-0.21449849	1.26139828	-0.11449714	0.41102148
Pd	-0.9697362	0.04292164	-0.04961136	-0.93419878	-0.16373126	0.18461516
I	-3.6128288	0.56116084	-0.14621047	-3.27003487	-0.95228032	1.27092255
C	1.75650971	1.32678259	1.10073478	2.0589058	-1.25487971	-0.26219015
H	1.54647335	2.32739708	1.49120114	2.17850642	-2.19048131	0.29190903
C	3.23886336	0.9308514	0.88909033	3.34475496	-0.56296959	-0.75545496

C	4.30920192	1.85421602	0.51286742	4.55808514	-0.59699138	0.10587301
O	3.80998728	3.07630225	0.2210549	4.42671444	-0.95987901	1.28409386
C	4.77510335	4.07026567	-0.17235048	5.73276451	-0.21378614	-0.45925887
O	5.51161275	1.59821474	0.45979869	2.9407818	0.19815461	-1.81097383
C	3.23976523	-0.43106161	0.93196518	3.65527947	1.22376712	-2.56771448
C	4.17180031	-1.50541703	0.49852289	4.87191645	1.37190308	-2.65030038
N	5.49699158	-1.22132153	0.50219296	2.77867579	2.0421772	-3.20742865
C	6.48637966	-2.16770782	-0.01855654	1.4189817	-0.05082056	-1.90419
O	3.68014089	-2.59362404	0.1500056	0.95170584	0.10899521	-2.88175896
C	1.7741856	-0.80534759	1.18749431	1.34084781	-1.41886937	-1.49616289
H	1.60050259	-1.77354676	1.66622949	1.80972766	0.81549518	4.66653307
O	1.33042548	0.2910581	1.99614912	2.41177343	-0.87192145	4.12183917
H	-0.77775176	1.65387789	-3.85010739	-0.79827104	1.04781772	2.35545701
H	-1.32635383	0.88964706	-2.22855187	-0.30480193	1.64913916	3.97911803
H	-1.08321149	4.91632494	-3.03359798	-1.57757691	0.38437237	3.78986069
H	-0.07367117	3.83080262	-4.02022166	0.8308906	-2.74814118	4.49703869
H	0.60458382	4.62235465	-2.56161111	0.61453541	-4.97534573	3.39764115
H	-1.06263883	5.31715495	-0.92730527	-0.13889524	-5.10507077	1.0007758
H	-1.34224426	5.81745602	1.46923443	-2.17599272	1.21164683	-1.37389862
H	-1.35225683	3.93840175	3.14692139	-3.65089861	2.08905161	-0.61620146
H	4.19250912	4.97696718	-0.38343465	-1.16333798	2.49200643	-2.33618461
H	5.32362828	3.73605495	-1.0682506	-2.89980055	0.16809918	-2.76178125
H	5.49518716	4.24571485	0.64378455	-4.49110257	2.94010241	-1.57854714
H	5.76371152	-0.23374636	0.64074572	-3.28662288	2.84421395	0.67295518
P	-1.44108165	-2.32869363	-0.0464	-4.25017135	1.21563787	-0.29708676
C	-1.97970682	-2.89794883	1.66300065	-5.43880051	3.21894943	-1.08236156
C	-2.86116745	-2.81262056	-1.17212717	-4.74976435	2.40013187	-2.50561969
C	0.02164075	-3.4704093	-0.41673806	-3.98002199	3.87877383	-1.85455892
C	-3.35263585	-2.36984844	2.09995963	-2.73013034	3.7743172	0.47291617
C	-0.89761595	-2.52903117	2.69148285	-2.68878407	2.20560147	1.34437368
H	-2.04221861	-3.99973312	1.58821004	-4.21393315	3.1159536	1.20843194
H	-4.15202956	-2.63303548	1.38789057	-4.0522256	-0.74989481	-2.33257824
H	-3.34785423	-1.27304977	2.20559382	-3.71839202	-1.50923901	-1.60754773
H	-3.60912428	-2.81795999	3.07776254	-4.44670005	-1.26482672	-3.22811147
H	0.06639488	-3.0208191	2.47534038	-4.88367583	-0.19138622	-1.87200155
H	-1.21278861	-2.84995432	3.70060187	-1.77403841	-0.63737687	-3.43156487
H	-0.73203142	-1.43722603	2.71122996	-3.29995514	0.89767997	-3.49033608
C	0.38852357	-3.4471439	-1.9120984	-1.29484998	-1.31858179	-2.70632232
H	1.42043431	-3.81850914	-2.04052854	-0.99200267	0.0141066	-3.85885735
H	0.33674367	-2.43202698	-2.34303336	-2.18579297	-1.24464845	-4.25753936
H	-0.28382398	-4.09341008	-2.50188323	-1.73508741	2.97960578	-3.67854516
C	-0.06937393	-4.91488506	0.1036724	-2.68888514	3.51758436	-3.56095131
H	0.85830209	-2.99680177	0.12209599	-1.88864987	2.15510632	-4.3936024
H	0.87632586	-5.43445628	-0.13642116	-1.01400314	3.68065135	-4.13952276
H	-0.89072449	-5.48244391	-0.36172804	-0.23760108	1.93919705	-2.56965021
H	-0.19404521	-4.96096035	1.19801083	-0.77136602	3.68293392	-1.44241246
C	-2.7056062	-2.24686077	-2.59347635	-1.6099596	4.39058064	-1.32927897

H	-2.4364695	-1.17809079	-2.55960857	0.07092144	4.23267696	-1.90033072
H	-3.67030231	-2.33136862	-3.12500575	-0.46369257	3.36746471	-0.43032871
H	-1.94823958	-2.79002907	-3.18135155	-0.66874052	-3.02015446	-0.23790237
H	-3.68342212	-2.2384026	-0.70577047	1.53556147	0.2431746	1.40739215
C	-3.23372766	-4.30198616	-1.17031598	0.80278353	1.7773772	-0.63415957
H	-4.20299944	-4.4344523	-1.68519861	6.9540295	-0.09060344	0.34065376
H	-3.34213624	-4.70956456	-0.15058373	7.03719457	1.29980194	0.99455919
H	-2.49047562	-4.91376007	-1.71004396	7.06831491	2.09155516	0.22404049
C	7.77985154	-2.05846509	0.79566182	7.94573416	1.3839812	1.61676071
H	8.22812475	-1.05273493	0.69411989	6.15878908	1.46858623	1.63964788
H	8.52070357	-2.79533929	0.44091938	8.17187278	-0.41002162	-0.53214608
H	7.58687152	-2.24440281	1.86579597	8.0899096	-1.42107394	-0.96587991
C	6.70930767	-1.94200594	-1.52406644	9.09742798	-0.36034464	0.06652881
H	6.03681139	-3.16616805	0.12022242	8.26646836	0.31611779	-1.3609899
H	7.09644793	-0.92435148	-1.71331625	3.37170711	3.1054193	-3.97694007
H	5.7599341	-2.06453666	-2.07199162	4.0212631	2.69043875	-4.76492336
H	7.43726741	-2.67012402	-1.92342625	3.97407435	3.75944923	-3.32518623
H	-1.07446985	1.59792752	2.3623414	2.5288897	3.65798162	-4.41441816
H	1.1407078	1.4962323	-1.12879514	6.8560879	-0.84398563	1.14154941
H	1.27795139	-1.14191581	-1.03631652	5.68801436	0.24184589	-1.38216663

Pd-2, *trans*

Functional		TPSS D4			wB97M-V
Basis set		def2-SVP			def2-TZVPP
Hartrees (Eh)	Gibbs	G-E(el)	Electronic	**Gibbs ***	Final single point (electronic)
α	-2291.42844	0.61685542	-2292.0453	**-2292.19491**	-2292.81177
β	-2291.42914	0.61716169	-2292.0463	**-2292.19556**	-2292.81272
ΔG	0.00070214			**0.00065299**	
kcal/mol				**0.40975213**	

Atoms						
83		*α*			*β*	
C	-0.91413742	-1.12398926	3.42521953	-0.94566586	-0.68100068	3.38148673
C	-0.93396883	-2.40683397	2.99243374	-0.83933732	-2.00245628	3.10737676
C	-0.82360089	-3.51525009	4.02185211	-0.80037591	-2.97794348	4.26733063
C	-1.05840385	-2.80309927	1.56052001	-0.75186565	-2.56224193	1.72847203
C	-1.25742654	-4.17732899	1.26378719	-0.60746833	-3.96786893	1.58473281
C	-1.32815867	-4.6656093	-0.04329513	-0.44807459	-4.58719911	0.3423715
C	-1.15766317	-3.78123601	-1.11535773	-0.41717119	-3.80371737	-0.81682905
C	-0.96423036	-2.4180765	-0.85187639	-0.57841786	-2.41579215	-0.70761567
C	-0.95694383	-1.90374933	0.4589357	-0.76715547	-1.78544703	0.53604676
C	1.27451988	0.71123221	0.7672178	1.06148717	1.15940121	0.52743961
C	1.22186373	-0.68193944	0.77821337	1.21601787	-0.18719341	0.83939758
Pd	-0.87869019	0.1539255	0.56684202	-0.97767662	0.25117182	0.32730605

I	-1.00107602	2.88117782	0.75357516	-1.44431973	2.85507255	-0.44519269
C	1.79649443	-1.08147201	-0.60107541	1.97798952	-0.76456628	-0.37351606
H	1.53912654	-2.07125129	-0.99171991	1.90699723	-1.84211338	-0.55066105
C	3.29847937	-0.71622965	-0.55012579	3.39875746	-0.17551608	-0.26813871
C	4.38167085	-1.68354988	-0.37887934	4.47306574	-1.00071719	0.34784264
O	3.88967441	-2.90564129	-0.06353093	4.14020118	-2.01749518	0.97602236
C	4.87304662	-3.94047996	0.12534909	5.75298067	-0.58017505	0.17965496
O	5.58648336	-1.47114204	-0.50354012	3.24948097	1.13828251	-0.59277836
C	3.32442443	0.64526333	-0.56953612	4.21624005	2.23635944	-0.55463766
C	4.36039624	1.68560024	-0.32041956	5.44089882	2.13469008	-0.49164498
N	5.65115174	1.34763021	-0.57721867	3.58842755	3.43230933	-0.60702176
C	6.7499911	2.27181307	-0.29036008	1.73322521	1.30198159	-0.86071141
O	3.98982154	2.79207745	0.09631416	1.40820226	2.1367402	-1.49023402
C	1.83984237	1.05672925	-0.63005544	1.43700645	0.02344355	-1.44694116
H	1.60949851	2.04908898	-1.03101961	-0.99960648	-0.32730414	4.41741387
O	1.29997107	-0.01732762	-1.42693484	-0.99676011	0.07567937	2.58646962
H	-0.80267524	-0.89421985	4.49112763	-0.87458313	-2.43928491	5.22514939
H	-1.01865891	-0.27283192	2.73611689	0.13577544	-3.56565642	4.27588242
H	-0.65838004	-3.09175402	5.02514544	-1.63612765	-3.70067543	4.21606908
H	0.01041732	-4.20371896	3.79320231	-0.60248255	-4.59643252	2.47879662
H	-1.7449749	-4.12595666	4.06264333	-0.33283982	-5.67465707	0.2865981
H	-1.36166301	-4.88929937	2.08696933	-0.27585126	-4.26234313	-1.80177049
H	-1.49404676	-5.73376307	-0.2190899	-3.30568783	-0.08347712	0.09082125
H	-1.17554488	-4.14234655	-2.14991504	-3.75029891	0.26797936	-1.71204233
H	5.55744281	-3.6716871	0.94676756	-4.23312138	-1.66646313	0.50710761
H	5.46047416	-4.08061408	-0.79695744	-4.25372056	1.23535208	1.06133647
H	4.30299544	-4.8468689	0.36994016	-5.13543228	-0.2085801	-2.17642019
H	5.85706794	0.35088581	-0.74228618	-2.64571801	-0.21339332	-2.66778532
C	7.87011679	2.06546621	-1.31556832	-3.72551999	1.37398385	-1.72020877
H	8.29162894	1.04578599	-1.24026705	-5.20977289	-1.30928722	-2.19548152
H	8.68986474	2.78326258	-1.14082734	-5.3081464	0.14936198	-3.20783551
H	7.49307045	2.208692	-2.34246005	-5.95596057	0.18094582	-1.55327085
C	7.23455419	2.11164825	1.16124913	-2.59407558	-1.31477905	-2.71523945
H	6.31919603	3.28231713	-0.40023136	-1.65887902	0.17270059	-2.3584054
H	8.04522848	2.82852331	1.38208372	-2.85574074	0.15817098	-3.68714664
H	7.61745138	1.08947778	1.33483284	-3.60761872	1.51119963	2.42870371
H	6.40388839	2.30133061	1.8612548	-4.133609	2.35082605	2.91875561
H	-0.81919046	-1.72976332	-1.68849723	-2.55140446	1.80044286	2.30267047
H	1.27295829	-1.32065613	1.66249092	-3.65287357	0.64028421	3.10411934
H	1.39162546	1.3743519	1.62530329	-5.77315769	1.03175834	1.17811753
H	-6.15049898	2.16183922	1.65844969	-4.06736272	2.12731067	0.4350206
C	-5.70431447	1.3094665	1.11401697	-6.21086286	1.92176346	1.66607345
H	-2.6911308	1.29943902	2.91170129	-6.03880308	0.15777744	1.79672323
H	-6.1661158	0.38889166	1.50966387	-6.26538036	0.9226787	0.19861583
H	-5.98848765	1.40954009	0.05245098	-3.83158094	-2.8990527	-0.31855757
C	-3.78452016	1.22114741	2.80021416	-4.63804714	-3.65203689	-0.24721774
C	-4.18216357	1.32436827	1.31962415	-2.90886512	-3.35462262	0.06799907

H	-4.23952583	2.06260113	3.35354545	-3.67734112	-2.67241267	-1.38528221
H	-3.78533987	2.29268713	0.96317152	-5.26629987	-1.38940814	0.22231631
H	-4.13238213	2.82026609	-1.09907117	-4.22324159	-1.997447	2.00701622
H	-4.12550615	0.28406258	3.26735854	-4.65689674	-1.19319015	2.6215113
C	-3.54574221	2.20634416	-1.80209211	-3.20025741	-2.18437699	2.36375952
H	-2.49615658	2.53419207	-1.74161284	-4.82139206	-2.91094853	2.17924326
P	-3.23409075	0.14227019	0.21131251	-0.53975654	-1.80483331	-1.61364832
H	-3.92118195	2.41308442	-2.82161725	1.2566064	-0.63495529	1.83425528
C	-3.68172047	0.70197582	-1.53210425	0.96252325	1.99030369	1.22816173
H	-3.29207878	-2.21990305	-0.10304102	6.87049744	-1.26622534	0.83170075
H	-4.75024927	0.43575303	-1.62878284	7.07962725	-0.7334531	2.26004851
H	-5.15129457	-1.46464409	2.22648129	7.90710741	-1.26919511	2.75830314
C	-4.06228257	-1.55441815	0.3202564	6.16356202	-0.87922045	2.85643498
C	-4.27847248	-1.97567654	1.78396404	7.32377396	0.34422136	2.24239628
C	-2.87585429	-0.10670656	-2.56037038	8.12482274	-1.13737149	-0.03883893
H	-2.9992851	-1.19516419	-2.43167383	8.96781321	-1.68440497	0.41699537
H	-6.15782569	-1.07471897	-0.20711515	8.42563932	-0.07836834	-0.14334185
C	-5.34381159	-1.75444892	-0.50757228	7.94639651	-1.54718885	-1.04749905
H	-1.80074541	0.13076049	-2.4734238	4.44443199	4.58981407	-0.57561152
H	-3.39835553	-1.76592034	2.41077338	5.02386668	4.61053688	0.36219389
H	-4.46928638	-3.0628106	1.82507149	3.77079191	5.45472533	-0.63954687
H	-3.20522048	0.15477361	-3.58229583	5.14379802	4.5689647	-1.42745255
H	-5.17230343	-1.6340922	-1.58968026	6.5664218	-2.32543464	0.90059302
H	-5.70106738	-2.78882513	-0.34941666	5.89288116	0.36729	-0.2045176

TS-1, *cis*

Functional		TPSS D4			wB97M-V	Imaginary frequency
Basis set		def2-SVP			def2-TZVPP	
Hartrees (Eh)	Gibbs	G-E(el)	Electronic	**Gibbs ***	Final single point (electronic)	
α	-2291.42175	0.61656	-2292.03831	**-2292.18577**	-2292.80233	105.57i
β	-2291.41790	0.61615	-2292.03405	**-2292.18335**	-2292.79949	102.22i
ΔG	-0.00385			**-0.00242**		
kcal/mol				**-1.52028**		

Atoms						
83		*α*			*β*	
C	-0.83102934	1.69538952	-2.76821884	1.55966326	-0.05444703	4.17718154
C	-0.69564964	2.90504192	-2.17558803	0.43812894	-0.23718496	3.44434118
C	-0.32345814	4.10527172	-3.02461077	-0.57799319	0.86377276	3.27131276
C	-0.90482918	3.13066548	-0.72191864	0.19578647	-1.55029678	2.77734405
C	-1.15618873	4.44878657	-0.26423549	0.37778333	-2.73676568	3.52429175
C	-1.34801717	4.74823454	1.0862488	0.25122351	-4.00001693	2.93986712
C	-1.26261805	3.72598976	2.04143316	-0.04559747	-4.10476165	1.57340536
C	-0.99152854	2.41797318	1.62451673	-0.22768845	-2.9439593	0.81169495

C	-0.84006945	2.10716228	0.26142764	-0.14761145	-1.67510721	1.4113149
C	1.08269053	-0.46602428	-0.11189624	0.84851065	0.60940673	-0.65789129
C	1.06123085	0.95911019	-0.14059302	1.28576626	-0.23672159	0.40086304
Pd	-0.9636377	0.01490337	-0.01806737	-0.93977304	-0.17839477	0.13906027
I	-3.59794804	0.5972844	-0.14748879	-3.2555319	-1.02483876	1.25105503
C	1.78944543	1.35322347	1.16877656	2.09523947	-1.33706451	-0.32565641
H	1.60185006	2.35235888	1.57394425	2.23652456	-2.28958956	0.19317439
C	3.26041364	0.94104294	0.92691644	3.36431896	-0.60773926	-0.80370619
C	4.33434016	1.85555596	0.54143686	4.5823535	-0.64575458	0.05019191
O	3.84529607	3.08756269	0.27310638	4.46181581	-1.04385187	1.21826235
C	4.81642179	4.07407267	-0.12411706	5.74819643	-0.22810363	-0.50893325
O	5.53271349	1.58650424	0.46390685	2.93898674	0.18135879	-1.82993391
C	3.24466542	-0.42182504	0.95740298	3.63192835	1.24400493	-2.55644638
C	4.15751592	-1.50227493	0.49748906	4.84526619	1.41403146	-2.64232086
N	5.4852754	-1.23081245	0.47934837	2.73757028	2.06824549	-3.1626636
C	6.45741689	-2.18212655	-0.06404946	1.42229461	-0.08477695	-1.91859873
O	3.64889299	-2.58287228	0.15004029	0.94322658	0.09830277	-2.88632896
C	1.78061586	-0.78068796	1.23326697	1.36261917	-1.46741828	-1.55358545
H	1.5997941	-1.75001446	1.70742013	1.75037655	0.89430568	4.69348943
O	1.35942916	0.31451017	2.05733981	2.3231212	-0.83560848	4.26286182
H	-0.64744546	1.57348831	-3.84217879	-0.68889669	1.1228326	2.19650612
H	-1.16248825	0.81091366	-2.20826983	-0.28393702	1.76973072	3.82725988
H	-1.16111367	4.82379447	-3.09509981	-1.58067253	0.53446059	3.59691683
H	-0.06938138	3.79066008	-4.04968374	0.61517571	-2.64594595	4.58968893
H	0.53742719	4.6535941	-2.59971274	0.38974607	-4.90033448	3.54780204
H	-1.22133073	5.26050268	-0.99451388	-0.14436977	-5.08689331	1.09788672
H	-1.55678025	5.77902434	1.39160252	-2.18131917	1.18486216	-1.37524362
H	-1.40420665	3.94107619	3.10632514	-3.65493071	2.05134006	-0.60383627
H	4.24344679	4.99348119	-0.30439055	-1.14784592	2.47508143	-2.29792883
H	5.33816218	3.74901774	-1.03922456	-2.90347822	0.16971652	-2.78359183
H	5.55849763	4.22259635	0.67749761	-4.48411217	2.92608375	-1.55459526
H	5.76405374	-0.24701415	0.62167556	-3.29398424	2.77971963	0.70137717
P	-1.45085522	-2.32310141	-0.02988417	-4.25928731	1.17418857	-0.30455511
C	-2.0006432	-2.90675993	1.66979766	-5.43364318	3.20062756	-1.05964046
C	-2.86294929	-2.79404002	-1.17016418	-4.73895231	2.40664425	-2.49434614
C	0.02157311	-3.44903059	-0.40293143	-3.96520221	3.86689193	-1.80796413
C	-3.3758664	-2.37544043	2.09603531	-2.72410185	3.70610834	0.52298245
C	-0.92514988	-2.54649332	2.70801941	-2.71153443	2.12128553	1.36666332
H	-2.06495137	-4.00801999	1.58762638	-4.22359798	3.05349344	1.23186359
H	-4.17140955	-2.64845012	1.38325516	-4.06265595	-0.74611339	-2.36751765
H	-3.37307835	-1.27711184	2.18707795	-3.73760703	-1.50498514	-1.6377371
H	-3.63692996	-2.81188705	3.07783668	-4.44882684	-1.26078178	-3.26677243
H	0.04265724	-3.02976791	2.48970118	-4.89789072	-0.18541967	-1.91654179
H	-1.24354722	-2.88199696	3.71139669	-1.77959096	-0.63351262	-3.45886566
H	-0.7661218	-1.4541284	2.7428769	-3.29555131	0.9117775	-3.50404018
C	0.40264548	-3.40219388	-1.89400862	-1.306877	-1.32584794	-2.73996073
H	1.43727223	-3.76743601	-2.01716199	-0.99258632	0.01900354	-3.87536064

H	0.3510139	-2.38054527	-2.30901107	-2.19159433	-1.22836284	-4.29372443
H	-0.26130972	-4.04233585	-2.49986824	-1.70473247	3.00245095	-3.63092045
C	-0.06600131	-4.90072861	0.09731841	-2.65368512	3.54736813	-3.50546277
H	0.84943472	-2.97553284	0.14976598	-1.86291132	2.197965	-4.36758801
H	0.8854508	-5.41168292	-0.13831873	-0.97379079	3.70745637	-4.07007843
H	-0.87866666	-5.46671625	-0.38522962	-0.22826105	1.91423587	-2.53619913
H	-0.20388443	-4.96200735	1.18940982	-0.74557976	3.6357058	-1.37020506
C	-2.69677196	-2.21838183	-2.58625049	-1.57393591	4.35309999	-1.24307848
H	-2.43170588	-1.14908164	-2.54266848	0.10840383	4.18427285	-1.80738656
H	-3.65712789	-2.30206988	-3.12571877	-0.44974115	3.28568077	-0.36614538
H	-1.93328628	-2.75587542	-3.17143487	-0.44809185	-3.02405726	-0.2575106
H	-3.6874064	-2.22168942	-0.70493019	1.61055463	0.12048489	1.38245799
C	-3.23511138	-4.28345826	-1.18266419	0.8648465	1.699368	-0.58005478
H	-4.19882117	-4.41230464	-1.70871807	6.97013359	-0.10412735	0.28990767
H	-3.3540038	-4.69857754	-0.16714225	7.04189957	1.27890472	0.96051545
H	-2.48586855	-4.89075372	-1.71919216	7.06448229	2.08035845	0.19977778
C	7.75665962	-2.10785232	0.74519998	7.95065691	1.36401348	1.58226294
H	8.21887886	-1.10690287	0.66028168	6.16311604	1.43226371	1.60898866
H	8.48491899	-2.84847096	0.3725532	8.1896677	-0.40228589	-0.58814285
H	7.56622825	-2.3112812	1.81257924	8.11595245	-1.4088146	-1.03365419
C	6.67679117	-1.93078142	-1.56603387	9.11552083	-0.35156782	0.01004122
H	5.99309789	-3.17589799	0.05837618	8.27700633	0.33432003	-1.40852275
H	7.07995403	-0.91622072	-1.7377268	3.30652323	3.16585657	-3.90166943
H	5.72306614	-2.02632909	-2.11171357	3.97825746	2.78828832	-4.68966189
H	7.39056604	-2.66292721	-1.98321914	3.88009168	3.82360848	-3.22789838
H	-0.90425988	1.61989319	2.36889992	2.45203884	3.70204206	-4.33697465
H	1.18678992	1.53831536	-1.05902678	6.87959237	-0.86836284	1.08120398
H	1.30914773	-1.07312095	-0.99143835	5.69081151	0.25417006	-1.41738119

TS-1, *trans*

Functional		TPSS D4			wB97M-V	Imaginary frequency
Basis set		def2-SVP			def2-TZVPP	
Hartrees (Eh)	Gibbs	G-E(el)	Electronic	**Gibbs ***	Final single point (electronic)	
α	-2291.42288	0.61737	-2292.04025	**-2292.18690**	-2292.80427	205.77i
β	-2291.42273	0.61677	-2292.03949	**-2292.18628**	-2292.80305	216.28i
ΔG	-0.00015			**-0.00062**		
kcal/mol				**-0.39041**		

Atoms						
83		*α*			*β*	
C	-0.86917984	-1.27066141	2.83475942	-0.69459068	-0.70415727	3.18470141
C	-0.88787458	-2.5328758	2.34427123	-0.45993292	-2.00667253	2.89723382
C	-0.74073911	-3.70303648	3.29729685	-0.0820283	-2.95909844	4.0134959
C	-1.05894993	-2.84083285	0.90085777	-0.54853435	-2.5563526	1.52034226

C	-1.52926629	-4.1231511	0.52777907	-0.65102502	-3.95851134	1.34829882
C	-1.68240476	-4.50492153	-0.80838383	-0.67002171	-4.55749731	0.08591556
C	-1.31733636	-3.61325824	-1.82851207	-0.57055275	-3.75686267	-1.06188089
C	-0.82234582	-2.35026839	-1.49045456	-0.45599428	-2.37096943	-0.92469521
C	-0.72323847	-1.92514955	-0.14543923	-0.46105862	-1.74877762	0.34539997
C	1.20598543	0.36815043	0.3036431	0.99420053	0.90311876	0.23731379
C	1.10010054	-1.06560144	0.22593946	1.16086392	-0.49044375	0.5453835
Pd	-0.86796429	0.18978305	0.01704584	-1.00722381	0.29641321	0.11858483
I	-0.86121663	2.85080747	0.27084995	-1.4217168	2.83874767	-0.67553737
C	1.87476161	-1.38677374	-1.07897323	2.05705068	-0.98614448	-0.61761668
H	1.66779957	-2.34824087	-1.56051521	2.06170639	-2.06145727	-0.82204817
C	3.35070146	-1.06592838	-0.77933382	3.42375131	-0.33083504	-0.3648993
C	4.36676389	-2.07187547	-0.47739415	4.45356343	-1.09104835	0.39292524
O	3.79849981	-3.28931681	-0.29197648	4.08925815	-2.10098099	1.01610897
C	4.71294823	-4.36066849	0.00542441	5.72623022	-0.6194528	0.35979012
O	5.58137436	-1.89620443	-0.40096699	3.24192441	0.97854533	-0.69440681
C	3.40667296	0.29552286	-0.72688632	4.14319606	2.12281658	-0.53185262
C	4.4139068	1.28747343	-0.25553469	5.3601728	2.07921394	-0.35795183
N	5.72098747	0.91982021	-0.31500151	3.45923894	3.28463173	-0.6083664
C	6.77583201	1.78999082	0.20903607	1.75463394	1.07769355	-1.09511848
O	4.00860937	2.38361904	0.1548705	1.44652372	1.90252153	-1.74655048
C	1.96215143	0.75098066	-0.98637725	1.55900072	-0.20698421	-1.71278945
H	1.81460416	1.76475286	-1.37316847	-0.58185489	-0.32366133	4.20639859
O	1.50856025	-0.27223835	-1.90078866	-1.01604139	0.00957598	2.41209519
H	-0.70462865	-1.08325317	3.90220846	0.06753338	-2.40878002	4.9560066
H	-1.03319868	-0.39419108	2.18845822	0.84537414	-3.51106061	3.77687104
H	-0.4743021	-3.34909507	4.30594048	-0.87365905	-3.7114551	4.18940128
H	0.03459871	-4.41245473	2.95543864	-0.71754942	-4.59890678	2.2321106
H	-1.6844023	-4.2735573	3.38497679	-0.75107106	-5.64599102	0.00022217
H	-1.798729	-4.83854336	1.31009187	-0.57559295	-4.2080205	-2.05998554
H	-2.06767054	-5.50081869	-1.05066693	-3.38606574	-0.03069996	0.07911609
H	-1.40935364	-3.90075312	-2.88163502	-3.95717871	0.29564782	-1.69178365
H	5.2715951	-4.14157489	0.93031182	-4.28217085	-1.59789791	0.59958519
H	5.43032944	-4.49122712	-0.82152512	-4.2315873	1.32744821	1.0872924
H	4.08812542	-5.25580152	0.12746604	-5.39174679	-0.12676065	-2.04451475
H	5.92804339	-0.07356605	-0.49733988	-2.93696982	-0.26166426	-2.70076923
C	8.056323	1.59011638	-0.60842763	-3.885032	1.3990765	-1.7376837
H	8.42778227	0.55280119	-0.51370025	-5.52001926	-1.22263258	-2.0177573
H	8.85080706	2.26730712	-0.2507962	-5.62396031	0.20477887	-3.07323823
H	7.87606849	1.79650301	-1.67715137	-6.14462028	0.3219311	-1.37708033
C	6.98572378	1.54675771	1.71378948	-2.87827731	-1.36345962	-2.66861256
H	6.400095	2.81953034	0.07593555	-1.93035298	0.14451243	-2.50036834
H	7.76315797	2.22234337	2.11265504	-3.22866184	0.03296018	-3.72554658
H	7.30183355	0.50417167	1.9002155	-3.46381116	1.62581016	2.3864576
H	6.04807786	1.73589729	2.26259192	-3.9295678	2.48655795	2.90046549
H	-0.50733444	-1.66126736	-2.27846119	-2.41620645	1.88936819	2.16434908
H	1.22861422	-1.68355198	1.1187912	-3.46969619	0.77120627	3.08424385

H	1.41034907	0.90709526	1.23297588	-5.73482822	1.14435588	1.3492396
H	-5.97675802	1.4460548	-0.59872994	-4.091431	2.20269889	0.42558529
C	-5.71431062	1.34643189	0.468569	-6.12796483	2.05420134	1.83887805
H	-2.73540875	1.29698127	2.32391974	-5.94217586	0.29616002	2.0242622
H	-6.17490315	2.19631028	1.00516107	-6.31347111	0.99364274	0.42405011
H	-6.18207615	0.42330724	0.85220696	-3.90087648	-2.81640136	-0.25162944
C	-3.82868895	1.2477568	2.19157674	-4.55562039	-3.66681686	0.0141248
C	-4.19655842	1.35462503	0.70271398	-2.86233398	-3.12109144	-0.06383812
H	-4.27119	2.10135585	2.7365443	-4.0130222	-2.63336625	-1.33210425
H	-3.7858191	2.3215857	0.35601655	-5.35113729	-1.36972058	0.42536528
H	-4.12708631	2.84090077	-1.7159666	-4.08406378	-1.90221149	2.09315935
H	-4.20399367	0.3211818	2.65428588	-4.48269714	-1.10632808	2.74194219
C	-3.48337109	2.23533157	-2.37520982	-3.01798221	-2.03439922	2.33319419
H	-2.44166711	2.56134516	-2.22212793	-4.61230063	-2.83875072	2.3508469
P	-3.22488309	0.1697334	-0.38002126	-0.33349905	-1.74683336	-1.81438955
H	-3.77167225	2.45793706	-3.41934824	1.34985093	-0.82977601	1.56709491
C	-3.642033	0.72809838	-2.13041871	1.04203794	1.6887201	0.99796873
H	-3.2292313	-2.18648102	-0.68612085	6.78130337	-1.21569144	1.18200675
H	-4.70785304	0.46759263	-2.26761631	6.80083611	-0.58036751	2.58341914
H	-5.15089212	-1.45382989	1.60166542	7.57969898	-1.04662428	3.21259224
C	-4.02490288	-1.53686884	-0.28286385	5.82527173	-0.7210012	3.07831794
C	-4.26321429	-1.9552902	1.17789555	7.01003968	0.50276959	2.51671222
C	-2.80162469	-0.07570632	-3.13533765	8.12562922	-1.09068943	0.45738836
H	-2.92078329	-1.16507407	-3.00736894	8.92660081	-1.57044617	1.04561243
H	-6.11593151	-1.10546306	-0.84816927	8.39990476	-0.02886137	0.31532083
C	-5.28344593	-1.76897357	-1.13595928	8.08338329	-1.57220506	-0.53429846
H	-1.73097918	0.1677976	-3.01715091	4.24035124	4.48517744	-0.46002985
H	-3.39767115	-1.72936857	1.82000987	4.73891679	4.49672722	0.52320907
H	-4.44001865	-3.04492896	1.2229884	3.52405593	5.31290816	-0.54705023
H	-3.10168943	0.18095361	-4.16772465	5.00663751	4.54008993	-1.25064744
H	-5.0932195	-1.63762752	-2.21377103	6.50654864	-2.27965831	1.28733345
H	-5.6237514	-2.81109678	-0.99044384	5.86719735	0.32404931	-0.03288215

Pd-3, *cis*

Functional		TPSS D4			wB97M-V
Basis set		def2-SVP			def2-TZVPP
Hartrees (Eh)	Gibbs	G-E(el)	Electronic	**Gibbs ***	Final single point (electronic)
α	-2291.476441	0.618559	-2292.095000	**-2292.245405**	-2292.863965
β	-2291.471593	0.618343	-2292.089936	**-2292.241837**	-2292.860179
ΔG	-0.004848			**-0.003568**	
kcal/mol				**-2.239146**	

Atoms		
83	α	β

C	-0.16757292	1.56719471	-2.77409584	1.68292937	-0.33094955	4.34993775
C	-0.28886872	2.78913069	-2.21568232	0.69139071	-0.23529025	3.44420995
C	0.08832702	4.05557296	-2.9500617	-0.00599047	1.06396223	3.111519
C	-0.8312289	2.94639282	-0.83395854	0.17293009	-1.44524463	2.7357916
C	-1.9565865	3.75716788	-0.61932128	-0.62640155	-2.36681754	3.42299519
C	-2.53184421	3.89722364	0.65236341	-1.17260413	-3.48731468	2.77445368
C	-1.98929959	3.21629455	1.74250633	-0.94428965	-3.6878474	1.41365177
C	-0.85593978	2.40889944	1.56329902	-0.14428935	-2.78082271	0.69960525
C	-0.23411022	2.28915714	0.28997469	0.45331752	-1.66654587	1.35123909
C	0.87478176	0.04825153	0.27455314	0.78929287	0.03664502	-0.45485043
C	1.11317935	1.57121464	0.17348522	1.49769872	-0.81646691	0.62104134
Pd	-1.19795718	0.07192088	0.34842205	-1.1571681	-0.45363503	0.06907588
I	-3.85609067	0.5347972	0.21636681	-3.49003682	-1.10985666	1.28040616
C	2.06076685	1.80168448	1.40230063	2.46423777	-1.67832757	-0.26842759
H	2.09955565	2.8224553	1.80288743	2.81240727	-2.61797742	0.17590379
C	3.37850316	1.1452449	1.00057858	3.52425505	-0.70318081	-0.74525055
C	4.51456779	1.86494695	0.42981683	4.78907258	-0.58343088	0.03482087
O	4.19924055	3.16265582	0.19785067	4.84585924	-1.13625237	1.14370618
C	5.25380976	3.96710991	-0.36103682	5.80448627	0.12198407	-0.52973472
O	5.63352097	1.412374	0.18457216	2.88975952	0.04338486	-1.70032998
C	3.13111869	-0.19889338	1.08653329	3.36119856	1.2231963	-2.42554021
C	3.83350311	-1.42788123	0.62207638	4.52214525	1.61490475	-2.52546661
N	5.16170112	-1.32726947	0.37169491	2.33804155	1.86797745	-3.04524666
C	5.93402542	-2.45537073	-0.15048199	1.45765927	-0.50863692	-1.75278966
O	3.18174311	-2.48141119	0.50069522	0.91758494	-0.39149952	-2.69892618
C	1.68699744	-0.30049467	1.56118047	1.68242874	-1.892604	-1.45794688
H	1.41350158	-1.20508148	2.11219632	2.04824347	0.55124581	4.88955899
O	1.55419724	0.87369589	2.37445929	2.16698915	-1.28948357	4.56664377
H	0.22035267	1.43993446	-3.79195229	0.05157958	1.27607548	2.02628934
H	-0.47972395	0.667504	-2.22767898	0.42662365	1.91242472	3.66746114
H	-0.76986825	4.74966676	-3.01271464	-1.08395431	0.98448761	3.34452906
H	0.43498573	3.83908646	-3.9738399	-0.83753875	-2.19123897	4.48242213
H	0.88950979	4.59504387	-2.41010553	-1.79741022	-4.18736857	3.33797051
H	-2.41888063	4.26086763	-1.4743685	-1.39091598	-4.54046015	0.89379851
H	-3.42354049	4.51924823	0.7776684	-2.12655887	1.01240087	-1.35986756
H	-2.44933593	3.29249009	2.73194806	-3.54018415	1.97912725	-0.5981556
H	4.82394131	4.97015925	-0.48643396	-0.92612946	2.21767505	-2.16733708
H	5.57773888	3.55430116	-1.33067045	-2.88138841	0.11198893	-2.82320268
H	6.11864475	3.99276708	0.32224307	-4.25625152	2.95239468	-1.54608812
H	5.57929437	-0.3820029	0.37605606	-3.15556072	2.6365541	0.73749784
P	-1.39988024	-2.1789491	0.12005824	-4.22496698	1.1477268	-0.34581684
C	-1.89307251	-2.99157664	1.73681319	-5.19192262	3.2976485	-1.06975195
C	-2.7396011	-2.67102158	-1.09534843	-4.5273761	2.48454794	-2.50804993
C	0.20430477	-3.03743635	-0.33668219	-3.64632408	3.84840611	-1.75528595
C	-3.33025636	-2.6707302	2.16624826	-2.53464994	3.53601011	0.59571195
C	-0.88293687	-2.61305022	2.83172779	-2.6169942	1.92183138	1.38155123
H	-1.81777821	-4.07830216	1.54143035	-4.07512646	2.94030227	1.2687249

H	-4.07269464	-3.0110487	1.42553687	-4.09482988	-0.74558325	-2.44051361
H	-3.47352747	-1.58642581	2.30814861	-3.81891461	-1.5224262	-1.70810206
H	-3.54523631	-3.18612272	3.12041222	-4.49093065	-1.23587473	-3.34867894
H	0.14514219	-2.92072244	2.57459066	-4.90821204	-0.146696	-1.99876649
H	-1.15357792	-3.11054126	3.78043933	-1.79964417	-0.73086477	-3.51811955
H	-0.88873972	-1.52115333	2.99969941	-3.21531034	0.90885427	-3.51454032
C	0.5943325	-2.78258034	-1.80260348	-1.38966564	-1.4842763	-2.82189088
H	1.66926599	-3.00108006	-1.92615753	-0.96312384	-0.11356681	-3.8889974
H	0.42176085	-1.7355673	-2.10583685	-2.23392652	-1.25947875	-4.3856507
H	0.02946734	-3.43239524	-2.49338401	-1.38183071	2.85349771	-3.4921936
C	0.32392864	-4.53054314	0.01290269	-2.28833969	3.46749907	-3.3737495
H	0.95323146	-2.51678044	0.28248984	-1.57466449	2.10162897	-4.2748191
H	1.35622507	-4.85104747	-0.21399779	-0.58145369	3.51796197	-3.86688385
H	-0.36779108	-5.16249366	-0.56814387	-0.05760966	1.57793231	-2.39441337
H	0.15560175	-4.72481652	1.08467426	-0.45283448	3.28772373	-1.16886873
C	-2.63532378	-1.92509006	-2.43545058	-1.20876499	4.08100504	-1.04021223
H	-2.52989166	-0.83983613	-2.27066933	0.47266758	3.76052614	-1.54273218
H	-3.5648501	-2.08721237	-3.01026163	-0.23889433	2.85938033	-0.17485336
H	-1.79253332	-2.28230604	-3.04934215	0.10374698	-2.96734158	-0.34900485
H	-3.635103	-2.26919759	-0.58566455	2.06504045	-0.23092038	1.35995221
C	-2.90093609	-4.187281	-1.28175137	0.94075174	1.12024479	-0.33929756
H	-3.82690621	-4.38499218	-1.85220331	7.05997564	0.37060328	0.1784216
H	-2.98136218	-4.72622706	-0.32214352	7.09675304	1.81097768	0.71673734
H	-2.0637148	-4.62231342	-1.85384076	7.03979922	2.54108051	-0.11148905
C	7.32304845	-2.4734283	0.49799895	8.03259932	1.99509303	1.27354532
H	7.88832311	-1.55658643	0.24783749	6.24729592	1.9904949	1.39726192
H	7.90555926	-3.33869052	0.13744899	8.25123418	0.05466927	-0.73555189
H	7.24164894	-2.53976271	1.59614173	8.20790448	-0.99039925	-1.08591226
C	5.99904998	-2.40005616	-1.68676006	9.20273696	0.20301166	-0.19569153
H	5.36954531	-3.35690527	0.14343854	8.25787505	0.71650921	-1.6215951
H	6.5051193	-1.47702927	-2.02335981	2.72040204	3.02725958	-3.81033918
H	4.98246251	-2.4175284	-2.11503256	3.46065225	2.74983673	-4.57797341
H	6.55791449	-3.26578485	-2.0842912	3.16017548	3.79301623	-3.15036109
H	-0.38846607	1.91348856	2.4189992	1.79464699	3.39520196	-4.2722788
H	1.60248326	1.86854225	-0.76545756	7.05001244	-0.32796734	1.03234547
H	1.22139784	-0.5175022	-0.60116357	5.59578892	0.64911324	-1.39024266

Pd-3, *trans*

Functional		TPSS D4			wB97M-V
Basis set		def2-SVP			def2-TZVPP
Hartrees (Eh)	Gibbs	G-E(el)	Electronic	**Gibbs ***	Final single point (electronic)
α	-2291.456864	0.618435	-2292.075299	**-2292.223746**	-2292.842180
β	-2291.458393	0.617332	-2292.075725	**-2292.226243**	-2292.843575
ΔG	0.001529			**0.002498**	
kcal/mol				**1.567408**	

Atoms						
83		α			β	
C	-0.00709949	-1.44275649	3.09429864	-0.10574806	-1.3808607	3.64096821
C	-0.09301897	-2.67806202	2.55558515	0.3902532	-2.41542124	2.93606577
C	0.29211275	-3.92099413	3.32565717	1.5696722	-3.24705396	3.38504481
C	-0.60613173	-2.85768391	1.16783604	-0.21676788	-2.78549127	1.6175475
C	-1.6243151	-3.78747784	0.9092459	-1.14641762	-3.82965396	1.53432503
C	-2.18300787	-3.93086001	-0.37340409	-1.71581692	-4.20351397	0.30260668
C	-1.75373919	-3.11023605	-1.41641146	-1.37780465	-3.5149151	-0.86146774
C	-0.70585905	-2.19393997	-1.19997943	-0.42841845	-2.47246584	-0.81418037
C	-0.06598751	-2.10598009	0.07039456	0.19172229	-2.12372265	0.42146303
C	1.08903829	0.09903284	0.04518715	0.99205842	0.15382565	-0.18882017
C	1.2983874	-1.41619102	0.16502566	1.39732513	-1.19389684	0.42102115
Pd	-0.99851838	0.08193343	-0.05970539	-1.05942353	-0.12354344	-0.32708441
I	-0.76629792	2.69586427	-0.04627015	-1.07233231	2.32922936	-1.32038878
C	2.20923145	-1.67551836	-1.09110656	2.51219095	-1.65356256	-0.59629294
H	2.20752689	-2.69855168	-1.48933132	2.71791655	-2.73010163	-0.6312163
C	3.55351592	-1.05915812	-0.72308901	3.67496336	-0.72512208	-0.30262156
C	4.68344076	-1.81863662	-0.19470359	4.6969465	-1.14590862	0.69328017
O	4.31803316	-3.09860654	0.08061271	4.46884635	-2.15016323	1.39063559
C	5.36499394	-3.94110949	0.593838	5.82829834	-0.40110144	0.77753218
O	5.83341174	-1.41972891	-0.01678263	3.29414129	0.47069919	-0.84502177
C	3.34467349	0.29179885	-0.80077876	3.9014008	1.79860028	-0.70201597
C	4.10655725	1.49347266	-0.34922448	5.05820191	2.04586396	-0.36260119
N	5.45490937	1.35520745	-0.2249927	3.00956725	2.76171607	-1.01020495
C	6.28366749	2.45107855	0.27834918	1.90471477	0.22119176	-1.44366736
O	3.48988761	2.54458811	-0.1328351	1.57672408	0.86482891	-2.26720335
C	1.89070025	0.44140568	-1.23890952	2.01414593	-1.1541162	-1.84556346
H	1.61658115	1.36293756	-1.76317911	0.32339075	-1.09414672	4.60871445
O	1.70728594	-0.73497674	-2.05168919	-0.94853586	-0.78973387	3.26597517
H	0.36123726	-1.29015433	4.11568543	1.90162685	-2.95851811	4.39626285
H	-0.31562518	-0.5536527	2.52771469	2.42246073	-3.1226857	2.68993631
H	0.64156765	-3.66894968	4.33992083	1.30995289	-4.3221657	3.38827729
H	1.09461543	-4.47172814	2.80017117	-1.43256676	-4.35942468	2.4493434
H	-0.56085074	-4.61820855	3.41951835	-2.43546657	-5.02820723	0.26765769
H	-2.00999061	-4.39808143	1.7316789	-1.81422738	-3.79913151	-1.824351
H	-2.97226084	-4.67159782	-0.54052525	-3.49017069	-0.03733872	-0.15090987
H	-2.19649934	-3.19841447	-2.41296762	-4.20953251	0.44507091	-1.82332311
H	5.76561548	-3.52727444	1.53404594	-4.62341584	-1.37775225	0.52771505
H	6.18658169	-4.02075721	-0.13724205	-3.85998713	1.44707525	0.96615512
H	4.89812987	-4.92085305	0.76514495	-5.73787497	0.53769158	-1.93418293
H	5.84600008	0.4021436	-0.26377136	-3.58811722	-0.42410086	-2.93229588
C	7.66525808	2.39244722	-0.3821723	-3.78708616	1.46055214	-1.94552489
H	8.18970525	1.4546139	-0.11996239	-6.23560573	-0.43341518	-1.76737548
H	8.29180268	3.23553278	-0.04345169	-6.01099154	0.87334895	-2.95181038

H	7.57639879	2.44224247	-1.48078623	-6.16336699	1.2660919	-1.22540092
C	6.3572053	2.41871028	1.81501091	-3.92910048	-1.47235369	-2.88380397
H	5.76156241	3.37643586	-0.02157224	-2.48638261	-0.41379695	-2.85876759
H	6.95787541	3.26415589	2.19549425	-3.87015866	-0.0234794	-3.92310927
H	6.82137292	1.47793555	2.16338077	-2.83316928	1.54865419	2.10861025
H	5.34380198	2.49320307	2.24352047	-2.94603999	2.51758904	2.62848469
H	-0.25829317	-1.65726598	-2.04275967	-1.80143255	1.48621275	1.72014935
H	1.80164224	-1.72417169	1.0931081	-2.97186858	0.74933391	2.85739684
H	1.37688437	0.70229303	0.91663409	-5.2925323	1.56203928	1.50829807
H	-5.71206147	2.66926583	1.9038879	-3.66424041	2.29096457	0.27759324
C	-5.49767799	1.71596368	1.38621686	-5.40626478	2.5262142	2.03730357
H	-2.18395213	1.33110608	2.47699827	-5.51972678	0.76382336	2.23708435
H	-5.94531471	0.90798768	1.99071791	-6.05689437	1.52692809	0.7156386
H	-6.01457689	1.74382637	0.41167322	-4.79617414	-2.56185919	-0.43476834
C	-3.26823106	1.4896282	2.60426598	-5.39230804	-3.35427297	0.05496929
C	-3.97935081	1.54108926	1.24071707	-3.82530016	-2.99480562	-0.71589278
H	-3.40607807	2.45403629	3.12564663	-5.32365328	-2.27170391	-1.357177
H	-3.56811357	2.42331945	0.71449893	-5.61086912	-0.89603498	0.65727193
H	-4.33028542	2.77617744	-1.31218369	-4.11650124	-1.83349969	1.90609639
H	-3.66900367	0.69556268	3.25512913	-4.15216285	-1.01856139	2.64760679
C	-3.96551766	2.01797594	-2.02488315	-3.07633027	-2.19414572	1.84840157
H	-2.88479345	2.18437477	-2.16702613	-4.74494142	-2.65933636	2.28796319
P	-3.41648014	0.17203599	0.08404789	-0.02580806	-2.05293343	-1.74239694
H	-4.47775903	2.18974584	-2.98970949	1.7976574	-1.10702115	1.43994049
C	-4.25098007	0.58669966	-1.54832755	1.10363741	1.02461249	0.47309965
H	-3.73049663	-2.1681403	-0.00940775	6.83951439	-0.66596455	1.8028252
H	-5.33902564	0.48496519	-1.37581028	6.47939369	0.04617232	3.11837772
H	-4.63334821	-1.15247468	2.74334548	7.22812502	-0.175349	3.89972356
C	-4.27599851	-1.42367883	0.59542794	5.49352995	-0.29471275	3.4766529
C	-3.99734216	-1.75387307	2.07092404	6.44319868	1.14094269	2.97151112
C	-3.81809857	-0.44124019	-2.60651455	8.22041111	-0.26652071	1.27261033
H	-4.05796516	-1.47562446	-2.30626445	9.00082072	-0.49755256	2.01785013
H	-6.39461339	-0.84246123	0.80554662	8.26386652	0.81822245	1.06212696
C	-5.76984443	-1.56957802	0.26206067	8.45530602	-0.80857408	0.34077623
H	-2.72869211	-0.38094992	-2.7777662	3.47087433	4.11911144	-0.89196072
H	-2.94320258	-1.57917058	2.34383435	3.82882426	4.31277053	0.13262079
H	-4.22440269	-2.81795939	2.26501877	2.59942652	4.7436235	-1.12934959
H	-4.33061678	-0.23908129	-3.56471011	4.29536002	4.30402963	-1.60040664
H	-5.9742239	-1.45873006	-0.81573902	6.80401232	-1.75526635	1.97909196
H	-6.10767706	-2.5815259	0.55545731	5.83576525	0.50354937	0.28036504

New-**TS-1** *cis*

		TPSS D4			wB97M-V	Imaginary frequency
Pd-complex-iPr3P		def2-SVP			def2-TZVPP	
Hartrees (Eh)	Gibbs	G-E(el)	Electronic	**Gibbs ***	Final single point (electronic)	

α	-2291.42033	0.61683307	-2292.03716	**-2292.18496**	-2292.80179	126.16i
β	-2291.41888	0.61565846	-2292.03454	**-2292.18386**	-2292.79952	110.92i
ΔG	-0.00145169			**-0.00109996**		
kcal/mol				**-0.6902239**		

Atoms						
83		α			β	
C	-0.8575916	1.52705267	-2.77711967	-0.70145468	2.04188108	-2.70366353
C	-0.66518605	2.76363282	-2.26201495	0.01348351	2.95658502	-2.01153606
C	-0.17265167	3.87827746	-3.16406749	1.11422283	3.7577625	-2.67612321
C	-0.9223856	3.09745674	-0.83705878	-0.2083341	3.20113381	-0.55966041
C	-1.18373707	4.44630684	-0.4884427	-0.12033852	4.5213014	-0.05718445
C	-1.42023163	4.84488151	0.82892673	-0.26355269	4.80592042	1.30248426
C	-1.36891778	3.89596201	1.8597943	-0.46495796	3.7582932	2.2134951
C	-1.08517331	2.56125645	1.55160255	-0.53351469	2.44108743	1.74689093
C	-0.89023163	2.14940125	0.22057912	-0.43734487	2.16018156	0.3719801
C	1.03059643	-0.43053604	0.11923692	0.85297265	-0.75275646	-0.18534355
C	1.00236685	0.98555521	-0.06523415	1.13950497	0.64257268	-0.17005046
Pd	-1.01729372	0.03825745	0.10014725	-1.03839809	0.17054917	-0.02228096
I	-3.65065556	0.60119351	-0.13075031	-3.48862151	1.31450636	0.02196889
C	1.71703659	1.52256059	1.20155952	1.9681346	0.82966692	1.12121172
H	1.52507924	2.56014596	1.49167739	2.00986438	1.83235916	1.55686764
C	3.18980002	1.08841085	1.01962325	3.30997551	0.14882896	0.80114815
C	4.26627405	1.95488325	0.54239945	4.42752009	0.96885694	0.26059388
O	3.77921307	3.1487583	0.1330956	4.15910092	2.09370133	-0.18801414
C	4.75525405	4.08672425	-0.35875204	5.669762	0.42004016	0.29098998
O	5.46546047	1.68091476	0.50658773	3.02971686	-1.18463143	0.81737021
C	3.1735186	-0.26306705	1.19892929	3.84997926	-2.325528	0.41486504
C	4.08549612	-1.38480091	0.85092786	5.0743882	-2.3605857	0.32458465
N	5.41468609	-1.12191821	0.81686455	3.06885231	-3.40435602	0.14612662
C	6.38519632	-2.11904043	0.35924226	1.51833428	-1.25818034	1.11975617
O	3.57361291	-2.49046509	0.59953534	1.15112281	-2.182137	1.57900244
C	1.70748969	-0.59089802	1.50216873	1.35966878	-0.13540602	1.99349594
H	1.52224106	-1.50023299	2.07955156	-0.49830749	1.85459238	-3.76518413
O	1.27741085	0.58827704	2.19309696	-1.52599936	1.49248421	-2.2362402
H	-0.6364931	1.31547357	-3.82991695	2.06934017	3.63900256	-2.13080744
H	-1.27550277	0.71352175	-2.17118826	0.88279391	4.8390003	-2.68358962
H	-0.95783242	4.63821964	-3.33493525	1.25645015	3.43870711	-3.72187604
H	0.12055469	3.47923607	-4.14864697	0.05321615	5.34355817	-0.75891681
H	0.69372496	4.40425935	-2.72231806	-0.20528183	5.84186993	1.65271522
H	-1.22181594	5.20067468	-1.27995245	-0.5669515	3.96233476	3.2850724
H	-1.63662234	5.8953477	1.05042265	-2.05586635	-1.98738354	-0.14690924
H	-1.54543575	4.1896634	2.90036179	-3.56753062	-2.06114965	-1.25428941
H	4.18527862	4.98165834	-0.64228736	-0.88085812	-3.38355281	-0.64761783
H	5.28545615	3.66514389	-1.22852871	-2.672317	-2.55860736	1.53501881
H	5.48967771	4.32002224	0.42955458	-4.26506116	-3.42608941	-1.3365642

H	5.69633898	-0.13014823	0.86860753	-3.32000425	-1.44278888	-2.64007924
P	-1.44063325	-2.30946558	-0.01973284	-4.22682248	-1.35269831	-0.71806986
C	-0.09264606	-3.427401	0.68777759	-3.69201746	-4.14487394	-1.94764599
C	-3.09040053	-2.84135229	0.69259365	-5.25219481	-3.30213262	-1.81842773
C	-1.52722101	-2.83173098	-1.82264921	-4.43524254	-3.87445555	-0.34268674
C	-0.01429603	-4.85618505	0.12304646	-2.80177629	-0.47384688	-2.54972043
C	-0.14558503	-3.4469033	2.22606255	-4.29105494	-1.25711309	-3.13284862
H	0.84397338	-2.92137529	0.39718493	-2.73154517	-2.10427201	-3.29660833
H	0.14712254	-4.86790162	-0.96715146	-3.90662806	-1.79791572	2.03987668
H	-0.91639171	-5.44869367	0.34578156	-3.69046408	-0.72702026	2.18432334
H	0.8486764	-5.37012932	0.58444412	-4.21869804	-2.23044962	3.00842828
H	-0.34034169	-2.44741422	2.65112274	-4.76030297	-1.87553058	1.34650021
H	0.81910993	-3.81072391	2.62308609	-1.52120552	-2.47586551	2.55093198
H	-0.93419268	-4.12684517	2.59036119	-2.95458537	-3.61941949	1.39797003
C	-0.21638401	-2.47807694	-2.54601239	-1.87618332	-2.78878176	3.54929939
H	-0.24989533	-2.85772975	-3.58318847	-1.14047709	-1.4418868	2.62643199
H	0.67106125	-2.9183323	-2.05878088	-0.67813526	-3.13498459	2.27990989
H	-0.07999903	-1.38372956	-2.59105632	-1.2749433	-4.81635781	-0.25199242
C	-2.7368747	-2.23243984	-2.5548852	-2.1994751	-5.15045163	-0.74892159
H	-1.63440735	-3.93269703	-1.80845656	-1.40694676	-4.93116468	0.83634637
H	-3.69427186	-2.54409943	-2.10620325	-0.46578513	-5.50670297	-0.55667518
H	-2.72977419	-2.57209479	-3.60696594	0.03440592	-3.13613964	-0.08347073
H	-2.70957099	-1.13004418	-2.54065291	-0.53150917	-3.29969951	-2.1443003
C	-3.44674887	-4.32329605	0.50526002	-0.35995485	-2.26105147	-2.47629594
H	-3.30349031	-4.66578581	-0.53371169	-1.3382298	-3.72153173	-2.76715223
H	-4.51170582	-4.47387279	0.76046936	0.38617543	-3.88110075	-2.34801607
H	-2.85567207	-4.97679214	1.17000395	-0.66898508	1.61819842	2.45591798
H	-3.77014863	-2.22830327	0.07134056	1.37558068	1.21203065	-1.07062188
C	-3.3012545	-2.37206548	2.14283338	0.91948022	-1.34903085	-1.09893329
H	-4.37925843	-2.41203424	2.38031361	6.82049615	1.08842324	-0.32125721
H	-2.97186841	-1.328055	2.27601246	7.02645274	0.5951931	-1.76373598
H	-2.77391485	-3.01244023	2.8681128	7.22552885	-0.49188457	-1.77999395
C	7.66949778	-2.00869269	1.18833964	7.88250645	1.11112786	-2.23336382
H	8.14835989	-1.02192497	1.04774141	6.12672252	0.79544135	-2.36946791
H	8.39368737	-2.78211725	0.87979638	8.06171064	0.88595484	0.55542115
H	7.45520026	-2.13893555	2.26256826	7.88711019	1.26744982	1.57559074
C	6.63848044	-1.96886093	-1.15086704	8.92774733	1.41851137	0.12606881
H	5.90469112	-3.09630921	0.53792232	8.32484721	-0.18580619	0.62627801
H	7.05396453	-0.97061844	-1.37948873	3.77185763	-4.5934643	-0.26183809
H	5.69632829	-2.09300017	-1.71091234	4.46840782	-4.91500891	0.52965429
H	7.35498916	-2.73163044	-1.50346952	4.34341096	-4.40245779	-1.18494464
H	-1.018127	1.8209963	2.35501948	2.9946132	-5.3510985	-0.4321828
H	1.14687248	1.45837291	-1.04013963	6.55068142	2.15796293	-0.35076159
H	1.29380123	-1.12387183	-0.68347952	5.73370943	-0.5852737	0.50551747

New-**TS-1** *trans*

Appendix

Functional		TPSS D4			wB97M-V	Imaginary frequency
Basis set		def2-SVP			def2-TZVPP	
Hartrees (Eh)	Gibbs	G-E(el)	Electronic	**Gibbs ***	Final single point (electronic)	
α	-2291.42335	0.61716955	-2292.04052	**-2292.18729**	-2292.80446	203.90i
β	-2291.42561	0.61737754	-2292.04299	**-2292.1904**	-2292.80777	207.11i
ΔG	0.00225808			**0.00310335**		
kcal/mol				**1.94735255**		

Atoms						
83		α			β	
C	-0.86917984	-1.27066141	2.83475942	-0.48444954	-1.71373846	2.83063759
C	-0.88787458	-2.5328758	2.34427123	-0.27241425	-2.87147322	2.16087618
C	-0.74073911	-3.70303648	3.29729685	0.17861077	-4.10083377	2.92453322
C	-1.05894993	-2.84083285	0.90085777	-0.46512479	-3.00837076	0.69339679
C	-1.52926629	-4.1231511	0.52777907	-0.67184403	-4.29930711	0.14916553
C	-1.68240476	-4.50492153	-0.80838383	-0.81323951	-4.51872963	-1.22377902
C	-1.31733636	-3.61325824	-1.82851207	-0.69795457	-3.43888767	-2.11181166
C	-0.82234582	-2.35026839	-1.49045456	-0.46806638	-2.15588962	-1.60531392
C	-0.72323847	-1.92514955	-0.14543923	-0.3947569	-1.90968043	-0.21666123
C	1.20598543	0.36815043	0.3036431	1.10842155	0.65602572	0.51900084
C	1.10010054	-1.06560144	0.22593946	1.28921917	-0.73812157	0.24663497
Pd	-0.86796429	0.18978305	0.01704584	-0.90326493	0.08638486	0.26266277
I	-0.86121663	2.85080747	0.27084995	-1.3865716	2.65144196	0.90531299
C	1.87476161	-1.38677374	-1.07897323	2.03046661	-0.72754906	-1.11173086
H	1.66779957	-2.34824087	-1.56051521	2.00048252	-1.64578527	-1.70684107
C	3.35070146	-1.06592838	-0.77933382	3.42705841	-0.16461728	-0.80359428
C	4.36676389	-2.07187547	-0.47739415	4.53796446	-1.11721454	-0.53596686
O	3.79849981	-3.28931681	-0.29197648	4.24550041	-2.30343398	-0.31626362
C	4.71294823	-4.36066849	0.00542441	5.80067803	-0.61895459	-0.5388603
O	5.58137436	-1.89620443	-0.40096699	3.22195531	1.1649772	-0.58942459
C	3.40667296	0.29552286	-0.72688632	4.15439799	2.20222248	-0.13987986
C	4.4139068	1.28747343	-0.25553469	5.38290312	2.13615158	-0.14588244
N	5.72098747	0.91982021	-0.31500151	3.48597278	3.2941959	0.2884627
C	6.77583201	1.78999082	0.20903607	1.69604759	1.35165684	-0.72947351
O	4.00860937	2.38361904	0.1548705	1.31766458	2.34967272	-0.97524779
C	1.96215143	0.75098066	-0.98637725	1.40611674	0.38875886	-1.76173886
H	1.81460416	1.76475286	-1.37316847	-0.29465595	-1.6428921	3.90799492
O	1.50856025	-0.27223835	-1.90078866	-0.86875263	-0.81335341	2.32667157
H	-0.70462865	-1.08325317	3.90220846	0.41991913	-3.84047502	3.96741938
H	-1.03319868	-0.39419108	2.18845822	1.06798541	-4.56378457	2.46042695
H	-0.4743021	-3.34909507	4.30594048	-0.61392271	-4.87207011	2.94954881
H	0.03459871	-4.41245473	2.95543864	-0.73389691	-5.15651929	0.82554087
H	-1.6844023	-4.2735573	3.38497679	-0.98787624	-5.53229677	-1.59916775
H	-1.798729	-4.83854336	1.31009187	-0.77740466	-3.59377394	-3.19343218
H	-2.06767054	-5.50081869	-1.05066693	-3.22707742	-0.34118547	-0.0838768
H	-1.40935364	-3.90075312	-2.88163502	-3.84321196	0.35568808	-1.72125979

H	5.2715951	-4.14157489	0.93031182	-3.68052155	-2.16905884	-0.20759394
H	5.43032944	-4.49122712	-0.82152512	-4.34434048	0.47556088	1.1827164
H	4.08812542	-5.25580152	0.12746604	-2.9425952	-0.13522793	-2.8659209
H	5.92804339	-0.07356605	-0.49733988	-3.9686143	1.88564255	-1.75333084
C	8.056323	1.59011638	-0.60842763	-4.8533234	-0.07540435	-1.85257107
H	8.42778227	0.55280119	-0.51370025	-2.84952744	-1.23410883	-2.88866698
H	8.85080706	2.26730712	-0.2507962	-1.92926946	0.29133016	-2.76427688
H	7.87606849	1.79650301	-1.67715137	-3.3578519	0.19183536	-3.83665902
C	6.98572378	1.54675771	1.71378948	-2.99278225	2.37387073	-1.59677666
H	6.400095	2.81953034	0.07593555	-4.66502683	2.27030428	-0.9900358
H	7.76315797	2.22234337	2.11265504	-4.3576135	2.18958148	-2.74296757
H	7.30183355	0.50417167	1.9002155	-3.89311981	0.23074301	2.63163978
H	6.04807786	1.73589729	2.26259192	-4.08011197	-0.80323996	2.96235242
H	-0.50733444	-1.66126736	-2.27846119	-4.45111051	0.90736768	3.30415226
H	1.22861422	-1.68355198	1.1187912	-2.81986375	0.45416389	2.74788562
H	1.41034907	0.90709526	1.23297588	-5.84466734	0.21466558	0.98293476
H	-5.97675802	1.4460548	-0.59872994	-4.13562678	1.54147621	0.97257386
C	-5.71431062	1.34643189	0.468569	-6.116489	-0.82501002	1.23481348
H	-2.73540875	1.29698127	2.32391974	-6.17253681	0.41338427	-0.05198931
H	-6.17490315	2.19631028	1.00516107	-6.42650294	0.87793913	1.64923296
H	-6.18207615	0.42330724	0.85220696	-3.75067307	-2.8220089	1.18277802
C	-3.82868895	1.2477568	2.19157674	-2.9068564	-2.52417661	1.82439206
C	-4.19655842	1.35462503	0.70271398	-3.71539941	-3.92061565	1.0714336
H	-4.27119	2.10135585	2.7365443	-4.69127935	-2.56761984	1.70222851
H	-3.7858191	2.3215857	0.35601655	-2.79985606	-2.58848578	-0.72316984
H	-4.12708631	2.84090077	-1.7159666	-4.91778715	-2.52397752	-1.04905595
H	-4.20399367	0.3211818	2.65428588	-5.04212735	-3.6228283	-1.05078114
C	-3.48337109	2.23533157	-2.37520982	-4.81854926	-2.20725647	-2.1002048
H	-2.44166711	2.56134516	-2.22212793	-5.84506727	-2.08700561	-0.64225003
P	-3.22488309	0.1697334	-0.38002126	-0.34650771	-1.31383519	-2.29143729
H	-3.77167225	2.45793706	-3.41934824	1.57130855	-1.44643335	1.02905623
C	-3.642033	0.72809838	-2.13041871	1.23804158	1.09482362	1.51201934
H	-3.2292313	-2.18648102	-0.68612085	6.94609464	-1.44530157	-0.15158206
H	-4.70785304	0.46759263	-2.26761631	7.16367841	-1.39088251	1.3708062
H	-5.15089212	-1.45382989	1.60166542	8.01072377	-2.03472397	1.66720161
C	-4.02490288	-1.53686884	-0.28286385	6.26015833	-1.74321075	1.89603762
C	-4.26321429	-1.9552902	1.17789555	7.38153628	-0.357701	1.69724326
C	-2.80162469	-0.07570632	-3.13533765	8.1836926	-1.00922021	-0.94279987
H	-2.92078329	-1.16507407	-3.00736894	9.04706952	-1.6483733	-0.69011263
H	-6.11593151	-1.10546306	-0.84816927	8.45626444	0.03607469	-0.70611708
C	-5.28344593	-1.76897357	-1.13595928	8.0009257	-1.08119385	-2.02838617
H	-1.73097918	0.1677976	-3.01715091	4.30054034	4.38781136	0.75150041
H	-3.39767115	-1.72936857	1.82000987	4.92933227	4.06371735	1.59693894
H	-4.44001865	-3.04492896	1.2229884	3.59336331	5.16780629	1.06332882
H	-3.10168943	0.18095361	-4.16772465	4.95196886	4.74652062	-0.06235769
H	-5.0932195	-1.63762752	-2.21377103	6.66857487	-2.4781959	-0.42472104
H	-5.6237514	-2.81109678	-0.99044384	5.90068626	0.40789555	-0.55345066

9.2.2.2 PPh_3

Pd-1

Functional		TPSS D4			wB97M-V	
Basis set		def2-SVP			def2-TZVPP	
Hartrees (Eh)	Gibbs	G-E(el)	Electronic	**Gibbs ***	Final single point (electronic)	
cis	-1809.344747	0.364786	-1809.709533	**-1809.870560**	-1810.235346	
trans	-1809.349697	0.364529	-1809.714227	**-1809.878259**	-1810.242789	

54		*cis*			*trans*	
C	0.41298351	-2.58686917	-1.12760282	1.81285754	-2.44650383	1.7594853
C	0.5540131	-3.00655251	0.20416019	2.47556954	-2.32658722	0.54411449
C	-0.61095426	-3.47982776	1.03429366	2.46417761	-3.42191663	-0.49057287
C	1.94652723	-3.07863672	0.73603655	3.23980961	-1.06584461	0.29408237
C	2.59704133	-4.12709943	1.40565405	4.56636336	-0.93007436	-0.14266218
C	3.93349463	-3.92768479	1.78127599	5.07954947	0.36481296	-0.30848711
C	4.57530953	-2.70063675	1.5255357	4.26576973	1.48642894	-0.07167831
C	3.89496632	-1.63147052	0.91596464	2.91894381	1.34012457	0.30286976
C	2.57064928	-1.83726061	0.51189071	2.3999945	0.05067961	0.49090348
Pd	0.94403327	-0.75895796	-0.0414893	0.60729808	-0.89166136	0.63451232
I	2.07770763	1.52882695	0.59322056	-1.46882532	-2.58940417	0.5426672
H	-0.58442851	-2.56632322	-1.57895767	1.21797806	-3.33821381	1.98150269
H	1.27045378	-2.62199653	-1.80881437	2.05796615	-1.77916576	2.59337207
H	-0.52877305	-4.57559496	1.17268508	3.44647233	-3.93332883	-0.48733939
H	-1.57675111	-3.26437308	0.55180243	2.31247092	-3.00946897	-1.50194868
H	-0.5936128	-3.02593597	2.03960754	1.67726629	-4.16312842	-0.28087575
H	2.0898947	-5.07576521	1.61670278	5.19237773	-1.80898487	-0.33537243
H	4.48478905	-4.73238897	2.28001925	6.11980018	0.50406963	-0.62203922
H	5.62278406	-2.57210585	1.82321748	4.68372301	2.49221578	-0.19605461
P	-1.13739894	0.35718927	-0.44373182	-0.55241957	0.95742896	-0.02917193
C	-1.6202531	1.51925835	0.89235229	-0.64212989	2.23415064	1.28600304
C	-1.26661487	1.30262374	-2.00946679	0.27978752	1.75517015	-1.45979177
C	-2.5851836	-0.78185221	-0.52698092	-2.29528413	0.81237854	-0.56956876
C	-1.23008127	1.19631551	2.20676464	-1.58075197	3.28399606	1.21159613
C	-2.37323793	2.68189892	0.65644093	0.23392847	2.16180911	2.38484132
C	-2.83247154	-1.50691534	-1.7123028	-3.2727653	0.499033	0.39628586
C	-3.37628654	-1.04123635	0.60843648	-2.6678413	0.97502866	-1.91449348
C	-2.51374551	1.6092104	-2.59327565	0.92429157	0.91571079	-2.38793166
C	-0.08219002	1.74063268	-2.63116478	0.29950671	3.14767856	-1.65020708
H	4.38593361	-0.66335155	0.77478127	2.29976521	2.23402585	0.43165164
C	-1.61388762	2.01395941	3.27627437	-1.62138085	4.26053475	2.21445847
C	-2.74210473	3.50626739	1.72827531	0.18821344	3.14092286	3.38610268
C	-2.36929501	3.17137441	3.03762964	-0.73534369	4.19219832	3.30040953
H	-0.60432762	0.31418296	2.38280246	-2.28836694	3.32572941	0.3770911

H	-1.30428185	1.75744921	4.29472512	-2.35284825	5.07321465	2.15194022
H	-2.6593286	2.95481315	-0.36366398	0.94071171	1.32685481	2.44700607
H	-3.31939077	4.41726813	1.53744519	0.87126699	3.07582619	4.2394256
H	-2.6571745	3.81972431	3.87211255	-0.77345467	4.95401829	4.08637979
C	-3.84102099	-2.47754898	-1.75468574	-4.61273361	0.37396166	0.01807808
C	-4.38321414	-2.01566254	0.56303668	-4.01216464	0.83619204	-2.28904545
C	-4.61528124	-2.74018213	-0.61438489	-4.98439599	0.53980117	-1.32514847
H	-2.24180386	-1.29960242	-2.61143163	-2.98259215	0.35126359	1.44104245
H	-3.20599556	-0.47891152	1.53173994	-1.91183123	1.21220828	-2.66903264
H	-4.99171332	-2.20526318	1.45373437	-4.29774669	0.96365381	-3.33857126
H	-5.40245127	-3.50071434	-0.64727845	-6.03383484	0.43326024	-1.6199354
H	-4.02397665	-3.02920759	-2.68303026	-5.3680916	0.13124554	0.77251985
C	-0.14568839	2.48399061	-3.8175492	0.96126521	3.69307082	-2.75911518
C	-2.57063959	2.35092051	-3.77988423	1.57388077	1.46295754	-3.49979939
C	-1.38691611	2.79026498	-4.39236573	1.59670748	2.85327216	-3.68462537
H	0.88462767	1.50553467	-2.17283635	-0.18279884	3.81016929	-0.92508905
H	0.78060541	2.82206287	-4.2936061	0.98432448	4.77942332	-2.8961387
H	-3.43935304	1.2589208	-2.12456031	0.93037151	-0.16670129	-2.21666493
H	-3.54209239	2.58550388	-4.22819242	2.07676937	0.80358241	-4.21466358
H	-1.43398951	3.36879443	-5.32127794	2.11708572	3.28327263	-4.54709149

Pd-2, *cis*

Functional		TPSS D4			wB97M-V	
Basis set		def2-SVP			def2-TZVPP	
Hartrees (Eh)	Gibbs	G-E(el)	Electronic	**Gibbs ***	Final single point (electronic)	
α	-2630.638310	0.602955	-2631.241265	**-2631.597018**	-2632.199973	
β	-2630.635313	0.603084	-2631.238397	**-2631.595208**	-2632.198291	
ΔG	-0.002997			**-0.001811**		
kcal/mol				**-1.136120**		

Atoms						
86		*α*			*β*	
C	-1.17024541	-1.74463217	3.22188041	-0.37576654	-1.86538341	2.96612574
C	-0.44878385	-2.85220625	2.93306685	0.82094804	-2.42339952	2.67242206
C	0.43085473	-3.49456292	3.98563922	2.003932	-2.29256312	3.60853018
C	-0.48278488	-3.4865779	1.58748915	1.04976756	-3.16934399	1.40211407
C	-0.36601297	-4.89459882	1.47732679	1.80709015	-4.36571736	1.42350236
C	-0.36527102	-5.53822494	0.23777212	2.08018826	-5.08002372	0.2545002
C	-0.46494336	-4.77739229	-0.93637865	1.61154787	-4.59840544	-0.9765932
C	-0.56750324	-3.38249766	-0.85325429	0.87128088	-3.40924943	-1.02326912
C	-0.58013447	-2.73213199	0.39200129	0.58634845	-2.69612301	0.15223283
C	1.23187873	0.21195389	0.42963743	0.93022162	0.74316111	-0.25806252
C	1.37123542	-1.16189716	0.68730385	1.58727902	-0.32118252	0.3799132
Pd	-0.74768681	-0.6516018	0.36492169	-0.47989174	-0.91763831	-0.04896082

I	-3.28151992	-1.21617301	-0.275027	-2.52403489	-2.57831758	-0.43777523
C	2.05555127	-1.70699785	-0.58788072	2.62180107	-0.78999165	-0.66924106
H	1.95542393	-2.77619198	-0.7996915	3.00967743	-1.80930705	-0.58164259
C	3.48521421	-1.11424596	-0.57361917	3.65178673	0.3536911	-0.71227945
O	4.35169339	-3.07851835	0.29914365	4.85682777	0.26987195	0.15631336
O	5.85152392	-1.49360768	-0.30536948	4.83497001	-0.53344194	1.10200612
C	3.31767841	0.2106312	-0.84676005	5.8974235	1.09003905	-0.13883633
C	4.17787196	1.42593139	-0.82494063	3.01260983	1.37179446	-1.35392931
N	5.51897999	1.23128295	-0.87612434	3.43168382	2.75972168	-1.5405228
O	3.63036792	2.54069665	-0.77441935	4.58277385	3.19005459	-1.49867934
C	1.79622683	0.37120121	-1.00959521	2.36609522	3.56215045	-1.78163698
H	1.45306813	1.21753384	-1.61371962	1.59985844	0.80820082	-1.65364116
O	1.4477558	-0.89002877	-1.59945564	1.03676014	1.25898802	-2.47783395
H	-1.10682657	-1.26983795	4.20848923	1.91224808	-0.56492249	-1.89681796
H	-1.87535708	-1.3208472	2.49721691	-0.51959892	-1.29971769	3.89534129
H	0.48390138	-2.86862801	4.89161651	-1.24635413	-2.00029585	2.31454668
H	1.45656471	-3.66154213	3.60601639	2.31504768	-3.27770951	4.00331032
H	0.04141301	-4.48500159	4.28724715	1.761642	-1.64803767	4.47016094
H	-0.29029311	-5.49562129	2.38982801	2.88291699	-1.87632016	3.08007629
H	-0.28831355	-6.62975658	0.18786993	2.17823156	-4.74426772	2.3820992
H	-0.46718729	-5.26579997	-1.91749968	2.65993366	-6.00804412	0.30354184
P	-1.37433766	1.67150366	0.21745992	1.81952411	-5.14589119	-1.90297205
C	-1.272026	2.22100967	-1.5260167	-1.9916769	0.91713421	-0.24371433
C	-3.06921113	2.07032111	0.80024984	-3.8142074	0.70317138	-0.23968163
C	-0.36977079	2.9317389	1.12495337	-1.82153428	2.14695228	1.11213832
C	-1.23077082	1.24245866	-2.5375632	-1.63850599	1.77221331	-1.8235841
C	-1.22585184	3.5866963	-1.87450484	-4.39393696	0.13550887	0.91264105
C	-0.75774396	3.37743448	2.40452399	-4.63446332	1.10716381	-1.30511378
C	0.85614721	3.38262308	0.59177216	-1.707222	0.96529375	-2.98087576
C	-3.92162881	2.93557885	0.09679978	-1.19795038	3.10210631	-1.93026383
C	-3.50177382	1.50242559	2.01519058	-2.56762712	3.34292033	1.11509621
H	-0.64114829	-2.7907567	-1.77075707	-1.01642915	1.82815066	2.22150707
H	1.51749392	-1.60831631	1.67276754	0.51726208	-3.03001861	-1.985886
H	1.31156136	1.00517146	1.175468	1.77461623	-0.41362259	1.45111868
C	-1.14992013	1.6266234	-3.88239722	0.58337906	1.65496796	0.23414325
C	-1.14759104	3.96436836	-3.22052149	7.06783864	1.18172556	0.73770619
C	-1.10994532	2.98524308	-4.22521584	6.83312383	2.22111911	1.84761711
H	-1.2583806	0.1827166	-2.26198694	5.94973063	1.94456212	2.44734034
H	-1.11425099	0.85900291	-4.66216666	6.66571879	3.22336305	1.41295008
H	-1.23819879	4.35217832	-1.09185288	7.70649592	2.27562114	2.52137275
H	-1.11043762	5.02633806	-3.48555841	8.31341171	1.48348063	-0.1020446
H	-1.04327869	3.283984	-5.27690899	8.46304575	0.71029883	-0.87454965
C	0.06323162	4.24995431	3.13131577	9.21104569	1.51621566	0.53887065
C	1.67831308	4.24768778	1.32455576	8.22132115	2.46361895	-0.60580725
C	1.28417442	4.68531962	2.59668713	2.67350612	4.95424517	-1.97698248
H	-1.7100522	3.05312167	2.83344203	3.1871084	5.36169078	-1.09080478
H	1.19844315	3.06163885	-0.39457353	1.70635325	5.45106068	-2.13181754

H	2.63246458	4.55834497	0.88850341	3.32530347	5.08150927	-2.85701369
H	1.92523516	5.36330902	3.17051557	7.16091727	0.18711575	1.20721685
H	-0.25780717	4.59147721	4.12131827	5.71523103	1.8494577	-0.81146594
C	-4.76155666	1.82084772	2.53230421	-5.78054681	-0.01472876	0.99827637
C	-5.19100959	3.23824828	0.60997055	-6.02560188	0.94427471	-1.21803582
C	-5.61035699	2.68861014	1.82840529	-6.59948422	0.38571445	-0.06951274
H	-2.85704352	0.79272773	2.54379351	-3.75597833	-0.19387325	1.73930107
H	-5.0897729	1.37242081	3.4757028	-6.22337464	-0.45935146	1.89547354
H	-3.60655916	3.35993328	-0.86064795	-4.1941427	1.54817349	-2.2041015
H	-5.85563838	3.90419074	0.04936719	-6.65981194	1.25829041	-2.05392149
H	-6.60307843	2.92630205	2.22520009	-7.68537628	0.25856251	-0.00494544
C	4.68350232	-1.86574782	-0.19716861	-1.36268119	1.49581651	-4.22888116
C	6.46609447	2.34476306	-0.80863536	-0.84588775	3.62473408	-3.18395815
H	5.86507647	0.26144155	-0.79665135	-0.93004492	2.8278953	-4.33297245
C	7.59885848	2.12184701	-1.81804085	-2.01365117	-0.08402369	-2.89174495
H	8.1714656	1.20762697	-1.57502787	-1.11272797	3.72839248	-1.03719927
H	8.30043332	2.97368684	-1.80404777	-0.50291955	4.66193331	-3.26062168
H	7.19725144	2.01659849	-2.84003799	-0.65233042	3.23990823	-5.30884105
C	6.98179868	2.52843449	0.62903019	-1.41906925	0.86357123	-5.12094492
H	5.88314512	3.23839656	-1.09007802	-0.93217629	2.70987531	3.30836748
H	7.67737395	3.38428939	0.68643274	-2.47341874	4.22535331	2.19757392
H	7.51747776	1.62416278	0.97083411	-1.65265751	3.9117747	3.29302672
H	6.14080942	2.71729252	1.31739258	-0.4778142	0.87250665	2.23721204
C	5.45441469	-3.91447306	0.6991381	-0.30819116	2.45119981	4.17024312
H	4.9985185	-4.83487186	1.08769381	-3.23555141	3.57200019	0.27775279
H	6.05296386	-3.41098211	1.47587787	-3.0522844	5.15511316	2.19413528
H	6.10096882	-4.13049024	-0.16724902	-1.58723142	4.60106132	4.14166488

Pd-2, *trans*

Functional		TPSS D4			wB97M-V	
Basis set		def2-SVP			def2-TZVPP	
Hartrees (Eh)	Gibbs	G-E(el)	Electronic	**Gibbs ***	Final single point (electronic)	
α	-2630.646769	0.604749	-2631.251518	**-2631.605152**	-2632.209901	
β	-2630.641040	0.603130	-2631.244170	**-2631.599276**	-2632.202406	
ΔG	-0.005729			**-0.005876**		
kcal/mol				**-3.687246**		

Atoms						
86		*α*			*β*	
C	1.08622454	1.59706556	2.60169839	0.67274413	-3.11596373	2.64950906
C	1.32466551	2.72536292	1.89043106	-0.54215181	-3.06748737	2.06865503
C	1.96677576	3.89900332	2.60252371	-1.81486449	-2.8472325	2.84558048
C	0.99685454	2.8920964	0.44774908	-0.66114664	-3.30274782	0.58968566
C	1.17450801	4.17064789	-0.13909556	-0.9688057	-4.60020695	0.12949634

C	0.92055249	4.42032156	-1.49046978	-1.02321679	-4.89199745	-1.23883775
C	0.47749467	3.37933938	-2.31319663	-0.73689759	-3.88517191	-2.17054394
C	0.28620699	2.1041793	-1.75992338	-0.43933097	-2.58567543	-1.72996084
C	0.53332857	1.847292	-0.40009401	-0.44416603	-2.27919734	-0.36094112
C	-1.84970343	-0.47044164	0.7606645	1.8316453	-0.23481737	1.1848588
C	-1.69631918	0.90271091	0.55940358	1.82928187	-0.72401648	-0.13348664
Pd	0.24891844	-0.12594941	0.11672227	-0.23671615	-0.44177739	0.49908253
I	0.29897026	-2.83219632	0.33187373	-0.96514318	0.99776058	2.70339866
C	-2.48207009	1.17267976	-0.74552196	2.1987601	0.51071089	-0.99049081
H	-2.2205903	2.06763481	-1.31930777	1.90606473	0.5056749	-2.04613449
C	-3.97191946	0.98046624	-0.37941025	3.68383815	0.77142231	-0.70029376
C	-4.92044392	2.07383989	-0.17111934	4.69627344	0.28048753	-1.67447537
O	-4.28109501	3.2679663	-0.15370091	4.31815673	-0.48201838	-2.57835979
C	-5.12193493	4.42035452	0.03985057	5.9738752	0.71028457	-1.51431051
O	-6.13939654	1.97827249	-0.03802392	3.70047089	1.25114186	0.57686058
C	-4.10848168	-0.36060159	-0.18327247	4.83118142	1.55758303	1.45425266
C	-5.15269081	-1.23433176	0.41916595	6.00778553	1.6895129	1.11869447
N	-6.43729164	-0.79544197	0.36050324	4.42334051	1.69839914	2.73545469
C	-7.52108024	-1.53019453	1.01628915	2.22080382	1.25627106	1.01926002
O	-4.79467752	-2.30226241	0.93601057	1.92281015	1.94457587	1.81728291
C	-2.70067879	-0.93383969	-0.44417509	1.58267437	1.57479177	-0.23706994
H	-2.63102908	-1.98944512	-0.72635782	0.79338604	-2.96488462	3.72887081
O	-2.23748722	-0.03921627	-1.47645507	1.57798241	-3.30325184	2.06027118
H	1.36573062	1.53811712	3.66004878	-1.61500632	-2.77294355	3.92658781
H	0.61504446	0.70833122	2.15804774	-2.52926669	-3.67096821	2.66265607
H	2.21862844	3.62880489	3.64039156	-2.3060363	-1.91297546	2.52398037
H	1.29264068	4.77506626	2.63518099	-1.15145566	-5.38784047	0.86972151
H	2.892737	4.21641592	2.09037677	-1.26153599	-5.90705552	-1.57449203
H	1.52351304	4.99885064	0.48256093	-0.74116437	-4.10190747	-3.24446958
H	1.07648388	5.42551881	-1.89638644	-2.33412185	-0.05117637	-0.42154207
H	0.28241013	3.54848298	-3.378239	-3.64105151	-1.09523405	0.28671902
H	-5.87149919	4.48524663	-0.76595977	-2.88632424	1.69544991	-0.32170025
H	-4.44524785	5.28522316	0.01787873	-2.41093789	-0.23947147	-2.24900967
H	-5.64436585	4.35417633	1.00847001	-3.76382664	-2.43543591	-0.13641031
H	-6.59109161	0.18416837	0.07736701	-4.39399776	-0.63781089	1.3873554
P	2.49423005	-0.2883989	-0.49487387	-1.35393598	0.34592467	-2.97377932
C	2.62698291	-0.83091211	-2.23633453	-3.480157	-0.83213125	-2.93967207
C	3.52193353	1.24028623	-0.45690175	-1.91250161	2.70729673	-0.23847287
C	3.46650136	-1.45395478	0.53563296	-4.24136347	2.03459434	-0.48892461
C	3.86156444	-0.79538979	-2.91730316	-0.21455675	-1.81462391	-2.47020948
C	1.47112754	-1.26272118	-2.91210488	2.05370387	-1.73990422	-0.46196486
C	4.35235716	-2.39733013	-0.00947843	2.0148856	-0.79975114	2.10021463
C	3.29878957	-1.38184658	1.93230391	7.05385234	0.22212416	-2.37413547
C	4.20765833	1.61329024	0.71366964	7.63476475	-1.09396472	-1.82827173
C	3.5544504	2.09532414	-1.57578263	8.06968984	-0.94163947	-0.82378915
C	-8.81907085	-1.33864072	0.2248387	8.42764416	-1.47566636	-2.49580054
H	-9.12250689	-0.27519527	0.21527343	6.84248252	-1.85778202	-1.75898772

H	-9.63841148	-1.91908456	0.68254501	8.11403358	1.31717623	-2.53221239
H	-8.69552411	-1.67210879	-0.81954119	8.91699431	0.97990715	-3.20974322
C	-7.65485196	-1.10528583	2.48919903	8.57471401	1.56396257	-1.55768053
H	-7.2156134	-2.59076244	0.9899884	7.66955625	2.23764414	-2.94749885
H	-7.8990816	-0.02994087	2.56453563	5.45784794	2.00378715	3.68950563
H	-6.70899466	-1.2909021	3.0248968	6.21676265	1.20422613	3.69805309
H	-8.45514901	-1.67917764	2.98928273	4.95016813	2.07439849	4.66070913
H	-0.06578585	1.29071792	-2.40362719	5.94609542	2.9572896	3.42911822
H	-1.53865388	1.66423725	1.32683887	6.58135455	0.01074586	-3.34951522
H	-1.83932282	-1.01196325	1.70822502	6.20107559	1.21467419	-0.64285868
C	4.25533875	3.30436289	-1.52032879	-4.66340319	-3.29173594	0.50905709
C	4.93401495	3.67404166	-0.35055154	-5.28716998	-1.50449282	2.0299613
C	4.91269236	2.82302089	0.76274768	-5.42866276	-2.82825095	1.5891138
H	5.45014373	3.09735781	1.67673662	-3.14780248	-2.81515119	-0.95712423
H	4.20074382	0.95794727	1.5881882	-4.75273289	-4.33004105	0.17327245
H	3.02193443	1.82053948	-2.48940257	-4.26071909	0.38485306	1.75244576
H	4.26448006	3.9629836	-2.39484209	-5.86777698	-1.14402373	2.88542224
H	5.483081	4.6208757	-0.30885679	-6.12782345	-3.50242518	2.09531063
C	3.93738267	-1.20674515	-4.25345533	-1.35509625	0.31886674	-4.37190704
C	2.78263794	-1.64320682	-4.9212111	-3.47480588	-0.86418994	-4.34203163
C	1.551611	-1.66611328	-4.25168572	-2.41409335	-0.29511481	-5.05937091
H	0.64706622	-1.99986561	-4.77034488	-0.52730432	0.81772165	-2.42949746
H	0.51324318	-1.28362089	-2.38040499	-4.31932761	-1.26626415	-2.38849399
H	4.89941394	-1.1817162	-4.77628093	-4.30845595	-1.33393882	-4.8749765
H	2.84377826	-1.96088945	-5.96770633	-2.41385817	-0.32402595	-6.15409966
H	4.7592884	-0.43228684	-2.40624234	-0.52711108	0.77280175	-4.92639837
C	5.07458892	-3.2492258	0.83776022	-4.62275014	3.38205488	-0.53240289
C	4.03269231	-2.22372087	2.77385178	-2.299145	4.05139854	-0.30140706
C	4.92247934	-3.16077821	2.22771272	-3.65305879	4.39073573	-0.43690029
H	4.46283077	-2.48950221	-1.09331473	-4.99868175	1.2495236	-0.58381612
H	5.75358252	-3.99159817	0.40500858	-5.68025693	3.64329909	-0.64659405
H	2.57256766	-0.67957905	2.35463563	-0.85773333	2.43921584	-0.11794493
H	3.89356451	-2.16235461	3.85824837	-1.53845133	4.83575753	-0.23152062
H	5.48642444	-3.83067345	2.88544713	-3.95391945	5.44337102	-0.47235209

TS-1, *cis*

Functional		TPSS D4			wB97M-V	Imaginary frequency
Basis set		def2-SVP			def2-TZVPP	
Hartrees (Eh)	Gibbs	G-E(el)	Electronic	**Gibbs ***	Final single point (electronic)	
α	-2630.634005	0.604100	-2631.238105	**-2631.591516**	-2632.195616	198.11i
β	-2630.629596	0.603990	-2631.233587	**-2631.589538**	-2632.193529	208.52i
ΔG	-0.004409			**-0.001977**		
kcal/mol				**-1.240799**		

Atoms						
86		α			β	
C	-0.60942812	-1.57810318	3.32856053	-0.01549128	-1.55182107	3.1437704
C	-0.14286174	-2.81111474	3.02296674	1.08830904	-2.25318367	2.8034424
C	0.58343948	-3.63229447	4.06981311	2.33854112	-2.25383585	3.65706391
C	-0.32102359	-3.42044956	1.67999524	1.14700379	-3.0453263	1.54271075
C	-0.46590241	-4.82408318	1.56661334	1.62728922	-4.37344693	1.57144598
C	-0.62057909	-5.45306641	0.32931188	1.72861275	-5.13943938	0.40737883
C	-0.60686481	-4.68770107	-0.84682026	1.38104203	-4.57514082	-0.83000995
C	-0.43498393	-3.30308457	-0.76721117	0.93264039	-3.25248993	-0.88876232
C	-0.30783548	-2.66009314	0.47968438	0.78925544	-2.49320082	0.28927076
C	1.21427264	0.0810656	0.38483193	0.97156003	0.60513727	-0.19323409
C	1.37857582	-1.33502071	0.56069174	1.69360794	-0.55565927	0.25625509
Pd	-0.76745947	-0.58334945	0.39023376	-0.53567083	-0.84816035	0.01779549
I	-3.30579719	-1.38061787	0.01530693	-2.49822931	-2.67241318	0.07671581
C	2.0798282	-1.76617467	-0.751067	2.66714798	-0.83643184	-0.91570599
H	2.02123334	-2.82318306	-1.02849556	3.08603308	-1.84433942	-0.98969778
C	3.48555318	-1.1347608	-0.7011191	3.66411344	0.32858745	-0.86547454
O	4.39340105	-3.12352837	0.06780268	4.91138463	0.17269864	-0.07057019
O	5.85858235	-1.46963417	-0.42478822	4.9566172	-0.745456	0.76394312
C	3.27892415	0.19829397	-0.90600127	5.91511948	1.05706944	-0.30100757
C	4.11731672	1.42828606	-0.84177427	2.9617543	1.40130226	-1.32798705
N	5.4619425	1.26020726	-0.87298726	3.3361791	2.81576464	-1.34275265
O	3.55565362	2.53580612	-0.78143873	4.47704618	3.27263646	-1.31397763
C	1.7557141	0.32622287	-1.04995171	2.23821166	3.60784716	-1.40098736
H	1.38084216	1.19024928	-1.60908073	1.54723206	0.84806895	-1.6110886
O	1.42822101	-0.91356879	-1.7014495	0.9355291	1.38202467	-2.34449267
H	-0.43204154	-1.13417817	4.31538221	1.85869272	-0.48184703	-2.04522076
H	-1.21277481	-1.00120113	2.61321299	-0.04190293	-0.95359132	4.06325847
H	0.79076221	-3.02778016	4.9678563	-0.92840535	-1.60248016	2.53833235
H	1.537781	-4.0324035	3.68047422	2.58692871	-3.27503016	4.00078073
H	-0.0205485	-4.50251533	4.3881362	2.21531937	-1.61461606	4.54710578
H	-0.47918802	-5.43168214	2.47703704	3.21081209	-1.89922572	3.0749884
H	-0.75039467	-6.53949077	0.28222995	1.90828534	-4.8152998	2.53357729
H	-0.73280945	-5.16586055	-1.82432349	2.08598746	-6.17309131	0.4631446
P	-1.41732375	1.66144438	0.21922041	1.45892886	-5.1639183	-1.7505102
C	-1.27962013	2.18984039	-1.5282958	-2.03693654	0.90751728	-0.27304009
C	-3.11838063	2.09935204	0.74726576	-3.85510444	0.67060182	-0.34397429
C	-0.40078659	2.88444015	1.15536749	-1.92067537	2.16636962	1.0602968
C	-1.39435068	1.20068997	-2.52467839	-1.63279044	1.75375493	-1.84576217
C	-1.08162629	3.53516631	-1.89855567	-4.48215917	0.14810022	0.8052184
C	-0.83092144	3.36777962	2.40742756	-4.62875713	1.01028207	-1.46593916
C	0.86597197	3.27401949	0.67405878	-1.64531394	0.94484949	-3.00323259
C	-3.90509984	3.00967489	0.02331638	-1.20654922	3.08908892	-1.93829274
C	-3.61950037	1.53729044	1.93807356	-2.71178311	3.33309122	1.02895469
H	-0.41396504	-2.70202919	-1.68136507	-1.09771019	1.91653445	2.17305757
H	1.66829944	-1.75862796	1.52513963	0.6803377	-2.80190461	-1.85320117

H	1.41932443	0.80109993	1.1831521	2.04129724	-0.64903529	1.28647671
C	-1.31107532	1.55572055	-3.87689932	0.80432387	1.47165249	0.45446174
C	-0.99588208	3.88298807	-3.25273685	7.11889315	1.07611531	0.53409445
C	-1.1103321	2.89466837	-4.24210808	6.8965508	1.94630531	1.78353516
H	-1.54702735	0.15633545	-2.22902303	6.04957045	1.55540082	2.37193231
H	-1.39822254	0.78115499	-4.64573025	6.67571227	2.99041115	1.49616285
H	-0.98530372	4.30667697	-1.12796711	7.79494744	1.94501218	2.42592725
H	-0.83623285	4.92886362	-3.53565356	8.31578191	1.53607294	-0.30457381
H	-1.03825143	3.16958442	-5.29993775	8.45676458	0.87894395	-1.17933407
C	-0.00874888	4.217291	3.15982116	9.23894148	1.51765274	0.29955616
C	1.68619578	4.12047177	1.43057508	8.16946151	2.57037611	-0.66754005
C	1.25211948	4.59483063	2.67633449	2.49442394	5.02368041	-1.41404901
H	-1.81532389	3.08950914	2.79457635	3.07128275	5.31760979	-0.5219689
H	1.2440893	2.92887475	-0.29056035	1.5058244	5.50241054	-1.41567202
H	2.66791592	4.39047225	1.02957342	3.06558048	5.29989584	-2.31580433
H	1.89224856	5.25800903	3.26829001	7.266605	0.03192776	0.86006532
H	-0.36099162	4.58801712	4.12849952	5.68331152	1.88893771	-0.86300772
C	-4.88199591	1.90884492	2.41273459	-5.86966059	-0.02026661	0.83038062
C	-5.17788617	3.3641639	0.49273682	-6.01983872	0.82890293	-1.43852687
C	-5.66461457	2.8209609	1.68897686	-6.64086903	0.31518648	-0.29314494
H	-3.0276073	0.79411417	2.48164839	-3.88213027	-0.12790822	1.67769623
H	-5.26473636	1.46627617	3.33813412	-6.34914032	-0.42924481	1.72564316
H	-3.53313908	3.43384014	-0.91394963	-4.15271667	1.41909089	-2.36190585
H	-5.7906701	4.0662334	-0.08265158	-6.61690764	1.09411578	-2.31755977
H	-6.65939318	3.09923319	2.05316667	-7.72677589	0.17352957	-0.27475699
C	4.69856224	-1.87515504	-0.35468714	-1.25965943	1.47724956	-4.23825355
C	6.37822643	2.39791536	-0.7756038	-0.8107324	3.61417936	-3.1779991
H	5.82989632	0.29675373	-0.81217461	-0.83998951	2.81455688	-4.32789179
C	7.64658022	2.09764812	-1.58134386	-1.93616575	-0.10925452	-2.92435341
H	8.17974719	1.22333552	-1.16449297	-1.16071086	3.71502809	-1.04239784
H	8.33482343	2.9594966	-1.55154744	-0.47346704	4.65412178	-3.24253319
H	7.40091699	1.88296828	-2.63525821	-0.527186	3.22773093	-5.29257303
C	6.67531527	2.73447978	0.69631584	-1.27102271	0.84253191	-5.13021014
H	5.83950938	3.25203697	-1.22225069	-1.04067684	2.83635419	3.22980198
H	7.33231459	3.61942729	0.76733908	-2.64521619	4.25391208	2.08103214
H	7.17837583	1.88740476	1.19688223	-1.80675594	4.00859386	3.1805827
H	5.73772682	2.95432005	1.23390318	-0.52232601	0.98432315	2.21539128
C	5.51457837	-3.95044181	0.43433322	-0.4024571	2.63021979	4.0955006
H	5.08088962	-4.90625743	0.75737757	-3.39020595	3.50957948	0.18722551
H	6.08507814	-3.47926064	1.25144357	-3.25929888	5.16031424	2.05059766
H	6.18116913	-4.09257699	-0.4320567	-1.76373513	4.72738464	4.00590908

TS-1, *trans*

Functional	TPSS D4	wB97M-V	Imaginary frequency
Basis set	def2-SVP	def2-TZVPP	

Appendix

Hartrees (Eh)	Gibbs	G-E(el)	Electronic	**Gibbs ***	Final single point (electronic)	
α	-2630.636974	0.604993	-2631.241967	**-2631.592322**	-2632.197315	206.03i
β	-2630.632132	0.603535	-2631.235666	**-2631.590923**	-2632.194457	218.69i
ΔG	-0.004842			**-0.001400**		
kcal/mol				**-0.878465**		

Atoms						
86		α			β	
C	0.70253649	1.45941158	2.50055457	1.08854061	-3.92455852	1.57234625
C	0.83641377	2.63168431	1.83458284	0.10899627	-3.05006698	1.25373975
C	1.15120544	3.88699794	2.62226142	-0.72061782	-2.35719683	2.30358131
C	0.72289869	2.75208664	0.3596758	-0.17110868	-2.78776684	-0.19166077
C	1.1416483	3.95321822	-0.25996858	-0.51132945	-3.87886505	-1.01681815
C	1.08509004	4.14032996	-1.64314975	-0.68834448	-3.73011343	-2.39848614
C	0.60307404	3.11261219	-2.46451217	-0.47638022	-2.47740235	-2.98925021
C	0.13849064	1.9300277	-1.8807265	-0.10501783	-1.38929053	-2.19022146
C	0.17759171	1.73209418	-0.48196334	-0.00126148	-1.50634102	-0.79185193
C	-1.76901295	-0.37224457	0.44936561	1.69485438	0.37538637	0.93514474
C	-1.59594192	1.04746649	0.21668339	1.77622842	-0.68110252	-0.03462955
Pd	0.25300494	-0.35801038	-0.06093045	-0.31765833	0.25304435	0.36584213
I	0.24244526	-3.00305211	0.14297365	-0.78942969	1.97232913	2.35889049
C	-2.52986623	1.2924989	-1.00049334	2.46079634	0.00584384	-1.23815911
H	-2.33864391	2.18628887	-1.6037362	2.333718	-0.45735443	-2.2217989
C	-3.96156835	1.10663685	-0.46757897	3.90955741	0.24196936	-0.78588882
C	-4.86151351	2.20618798	-0.12663757	4.94817442	-0.75233055	-1.17066249
O	-4.20413703	3.39211094	-0.15227475	4.57116471	-1.84017936	-1.63411593
C	-4.99967287	4.54888204	0.16601885	6.24582573	-0.40117989	-0.98279301
O	-6.05892076	2.12549856	0.14260358	3.82681556	1.26014821	0.11576153
C	-4.08564467	-0.23697151	-0.2676252	4.85660094	1.84310736	0.97963241
C	-5.06724488	-1.10384382	0.4436748	6.07433519	1.71630775	0.85915112
N	-6.34466963	-0.64854307	0.53284705	4.29579575	2.58108328	1.96190231
C	-7.35878824	-1.38450659	1.29086151	2.32081855	1.58498881	0.20272894
O	-4.67045848	-2.18274745	0.90523213	2.02843531	2.58468202	0.54168285
C	-2.72333199	-0.81581394	-0.67806095	1.9164478	1.33214868	-1.16054698
H	-2.68846743	-1.86870559	-0.97718442	1.32575697	-4.15528815	2.61811499
O	-2.34680979	0.08326357	-1.74380962	1.68292971	-4.42601344	0.79949264
H	0.77678145	1.42276689	3.59356479	-0.33556699	-2.55627245	3.31702209
H	0.5341864	0.50533344	1.97632261	-1.77009356	-2.6961534	2.24677442
H	1.12687619	3.68060196	3.7040309	-0.74254484	-1.25982007	2.14081962
H	0.43587933	4.70086505	2.40519164	-0.64598289	-4.85879103	-0.54652937
H	2.16060365	4.26342401	2.372265	-0.96907911	-4.59310831	-3.01148942
H	1.54378778	4.75959391	0.35754119	-0.59531228	-2.33902443	-4.06907355
H	1.43172839	5.08348711	-2.07801304	-2.56349219	0.31015552	-0.36098082
H	0.57072585	3.23309921	-3.55282569	-3.43290016	-1.09103398	0.41359867
H	-5.83628958	4.64502923	-0.54547316	-3.61595388	1.78630708	-0.05173757
H	-4.31726017	5.40607687	0.0880653	-2.82824643	0.1932562	-2.17783673

H	-5.40812971	4.46336253	1.18657001	-3.40532304	-2.37113338	-0.17262392
H	-6.51684327	0.33647417	0.28110116	-3.95849051	-0.93230824	1.71322691
P	2.54434606	-0.39314226	-0.58879772	-1.98041928	0.98083948	-2.98087219
C	2.82187576	-0.89308988	-2.32868255	-3.87490016	-0.52738144	-2.7775751
C	3.45746793	1.20089244	-0.44212439	-3.02406365	3.05987572	-0.13454569
C	3.5327608	-1.52966844	0.46387327	-5.00929463	1.67547532	0.10781031
C	4.08269011	-0.77814675	-2.95165152	0.09035989	-0.42456821	-2.66345914
C	1.72910848	-1.3882008	-3.06456003	2.0605832	-1.69557288	0.25195233
C	4.56834061	-2.3398352	-0.03077945	1.8480591	0.22504186	2.00711613
C	3.20914496	-1.58162547	1.83407395	7.33271057	-1.35360575	-1.22032407
C	3.89829141	1.62908436	0.82591501	7.56882399	-2.2312572	0.02141596
C	3.64322435	2.04626756	-1.55134049	7.86866035	-1.61151468	0.88593906
C	-8.735577	-1.15215738	0.65959937	8.36709404	-2.97019724	-0.1700512
H	-9.01895765	-0.0844135	0.71154298	6.64620508	-2.77701776	0.28015804
H	-9.5070745	-1.73241577	1.19415981	8.5896607	-0.59361833	-1.65635148
H	-8.73831952	-1.45949112	-0.39999759	9.40848389	-1.29952879	-1.87718397
C	-7.31334213	-0.9993192	2.77990156	8.93618549	0.08713172	-0.85680629
H	-7.07815876	-2.44861921	1.20204368	8.39231044	0.0069664	-2.56058197
H	-7.52984371	0.07654786	2.91101931	5.21365667	3.20557449	2.87936416
H	-6.31459452	-1.21337979	3.19534358	5.82073134	2.44073631	3.3910313
H	-8.05922593	-1.57682792	3.3544183	4.58560768	3.75214644	3.59530152
H	-0.28887643	1.1426366	-2.50959835	5.88489643	3.89159696	2.33704226
H	-1.59290391	1.74789121	1.05803069	6.98203373	-2.00475634	-2.04017806
H	-1.88877439	-0.80179272	1.44893319	6.42999476	0.45349643	-0.43446305
C	4.27574688	3.28665657	-1.39786028	-3.93779459	-3.46952012	0.51580728
C	4.71459506	3.70558851	-0.13577493	-4.49158838	-2.03345026	2.39303296
C	4.52030519	2.87352049	0.97702331	-4.48886722	-3.30306972	1.79398593
H	4.86368396	3.1894477	1.96802709	-2.95728581	-2.51616187	-1.15953878
H	3.76201123	0.98526838	1.69927862	-3.91119212	-4.4607537	0.05116932
H	3.28835268	1.74044702	-2.53880037	-3.93069806	0.05016694	2.19602084
H	4.4156884	3.93177299	-2.27168671	-4.90126152	-1.90113075	3.39988425
H	5.20800631	4.67634075	-0.01769448	-4.90443233	-4.16339329	2.32928767
C	4.2456515	-1.16648874	-4.28699716	-2.15961024	1.02493345	-4.36808633
C	3.15273102	-1.66472971	-5.01312686	-4.04398739	-0.49201325	-4.1686642
C	1.89612671	-1.77221206	-4.40200869	-3.18562846	0.27794614	-4.96622417
H	1.03959495	-2.15705601	-4.96505419	-1.17188664	1.55351171	-2.51026456
H	0.75124773	-1.47737012	-2.57789901	-4.56372504	-1.11335606	-2.16184886
H	5.22778037	-1.07659384	-4.76349715	-4.85682265	-1.06321433	-4.62997187
H	3.28251189	-1.96529204	-6.0584577	-3.3216788	0.30328211	-6.05268572
H	4.93338748	-0.36962253	-2.39629907	-1.49318052	1.63822883	-4.98380228
C	5.28562912	-3.17261295	0.83919558	-5.79783916	2.82926944	0.20996598
C	3.93805592	-2.40098558	2.70268741	-3.81776816	4.20990404	-0.04621654
C	4.97909988	-3.19888236	2.20634486	-5.2036838	4.09712452	0.13415288
H	4.80435232	-2.34319657	-1.09830729	-5.48170301	0.68883144	0.14985768
H	6.08357041	-3.80918893	0.44214529	-6.88100907	2.7356541	0.34323588
H	2.36350342	-0.99798083	2.21238642	-1.94025848	3.14720944	-0.25671014
H	3.67570106	-2.43474687	3.76524036	-3.34829995	5.19733148	-0.10575574

H	5.54011514	-3.8530417	2.88227868	-5.82195559	4.99777801	0.21386594

Pd-3, *cis*

Functional		TPSS D4			wB97M-V	
Basis set		def2-SVP			def2-TZVPP	
Hartrees (Eh)	Gibbs	G-E(el)	Electronic	**Gibbs ***	Final single point (electronic)	
α	-2630.683653	0.605892	-2631.289546	**-2631.645914**	-2632.251806	
β	-2630.679600	0.606073	-2631.285673	**-2631.644252**	-2632.250325	
ΔG	-0.004053			**-0.001662**		
kcal/mol				**-1.042764**		

Atoms						
86		α			β	
C	0.13404583	-0.93949769	3.16065558	0.87662224	-1.5303731	3.52032563
C	0.10439377	-2.27901172	3.00707329	1.72810206	-2.27141312	2.78490715
C	0.54301244	-3.22495794	4.10263963	3.19000611	-2.45838614	3.12067317
C	-0.38361491	-2.90885278	1.74184337	1.22386368	-2.97802096	1.56385698
C	-1.47236727	-3.79234646	1.78565965	0.65038922	-4.25106837	1.66795959
C	-1.97949408	-4.39993868	0.62493284	0.14895406	-4.91769371	0.53738626
C	-1.40082099	-4.12442968	-0.61110323	0.19921108	-4.30662506	-0.71546341
C	-0.29445912	-3.25709677	-0.68916819	0.76382121	-3.02650809	-0.84793735
C	0.25459389	-2.66518117	0.48045752	1.31677971	-2.35933704	0.2812702
C	1.14996303	-0.41694929	-0.04569957	1.04635228	0.05396463	-0.30243721
C	1.54381924	-1.84260395	0.39584265	2.05799629	-1.03528789	0.11120023
Pd	-0.87625003	-0.74057099	-0.37410344	-0.68837385	-1.06203861	-0.00538062
I	-3.40958887	-1.30115774	-1.14158666	-2.70904995	-2.62100727	0.80753536
C	2.47966182	-2.25557602	-0.78666318	3.04344751	-1.0132484	-1.11515514
H	2.61373082	-3.33238021	-0.94925734	3.63884712	-1.92060121	-1.27213652
C	3.7408914	-1.4158929	-0.60896033	3.78504381	0.30087049	-0.9505405
O	4.77576089	-3.1825393	0.48166686	5.03505306	0.33443217	-0.14455335
O	6.03251344	-1.33185216	0.1577322	5.31660846	-0.65055948	0.55840286
C	3.37804494	-0.15590667	-1.00452869	5.80035736	1.45424498	-0.23121083
C	4.04334429	1.18109596	-1.03670375	2.86608976	1.24903734	-1.3075132
N	5.35098364	1.22515872	-0.67808812	2.90123759	2.6917293	-1.04791221
O	3.39356916	2.17370937	-1.40719396	3.90147824	3.40136244	-0.97091252
C	1.91043525	-0.28272613	-1.40119793	1.64879737	3.17917162	-0.87058618
H	1.53649783	0.45067478	-2.12456465	1.60422138	0.46598707	-1.69449366
O	1.85963727	-1.62478822	-1.92001761	0.9254177	0.93290814	-2.4139629
H	0.48762426	-0.48052745	4.09173599	2.16657958	-0.74227128	-2.21890608
H	-0.20514179	-0.26861876	2.36346662	1.2123071	-1.01031219	4.4265828
H	0.86056668	-2.67695687	5.00502671	-0.18004622	-1.44335309	3.23910728
H	1.38197325	-3.85857122	3.75777764	3.41692093	-3.5333497	3.25028055
H	-0.27380092	-3.91540604	4.38349992	3.45997429	-1.92676054	4.04862533
H	-1.95535964	-3.98983649	2.74872928	3.84188313	-2.0933325	2.30383459

H	-2.84533268	-5.06556017	0.69403337	0.57537182	-4.71742726	2.65540305
H	-1.80566002	-4.56315745	-1.52689124	-0.30658913	-5.90638451	0.6497177
P	-1.38118746	1.44439029	-0.17344579	-0.21521988	-4.80814256	-1.59491384
C	-1.41171726	2.33738384	-1.77062903	-1.92022926	0.77700481	-0.3404746
C	-2.99412084	1.73995403	0.64552752	-3.75350539	0.73310048	-0.27451318
C	-0.23174731	2.4343285	0.86355397	-1.56523216	2.14798948	0.82859503
C	-1.61803659	1.60372707	-2.95374087	-1.55692289	1.38019849	-2.03419605
C	-1.24966204	3.73676243	-1.833957	-4.35923239	0.54519233	0.9840384
C	-0.51707684	2.70650913	2.21625306	-4.5534311	0.88037746	-1.4197656
C	0.99851247	2.85330167	0.31956941	-1.59384655	0.40708558	-3.05627998
C	-3.8176483	2.81866028	0.28568661	-1.17233794	2.69406383	-2.34499045
C	-3.37084659	0.89203676	1.70515145	-2.23406507	3.38348312	0.70719834
H	0.19318042	-3.08208758	-1.65182308	-0.68060734	1.94248976	1.90198896
H	2.0713722	-1.87567426	1.36136779	0.86676197	-2.56089017	-1.83307766
H	1.36715344	0.37836362	0.68003291	2.58761605	-0.78947636	1.04058854
C	-1.66868841	2.26514299	-4.18748489	1.02208467	0.92131574	0.37050886
C	-1.30125786	4.39113146	-3.07093242	6.96768057	1.64934989	0.63069998
C	-1.51117733	3.65681059	-4.24788844	6.55479614	2.31557433	1.9550498
H	-1.75073164	0.51765535	-2.89439722	5.8159434	1.68796592	2.48132422
H	-1.8295669	1.68791412	-5.10383142	6.10487709	3.30749956	1.76731528
H	-1.07263043	4.3117559	-0.91939811	7.42973773	2.44935576	2.61569653
H	-1.17242515	5.47778962	-3.1156455	8.03721549	2.44554495	-0.12476106
H	-1.5461381	4.17155446	-5.21410566	8.32161784	1.93089782	-1.05812363
C	0.41384602	3.39321813	3.00724089	8.94041926	2.56595633	0.49785567
C	1.92314228	3.54243578	1.11401781	7.66839502	3.45530942	-0.38443442
C	1.63414324	3.81460973	2.45893835	1.55595696	4.57182362	-0.52055931
H	-1.47033733	2.39088555	2.65021739	2.25297132	4.80604239	0.29962471
H	1.26169866	2.64340129	-0.72057322	0.51548017	4.72894679	-0.20484798
H	2.87067262	3.85261843	0.6635401	1.80319007	5.2001503	-1.39277118
H	2.35760846	4.35443483	3.07969657	7.34029812	0.63454143	0.85285603
H	0.17835106	3.60554744	4.05572432	5.38206554	2.27314111	-0.6954483
C	-4.5527306	1.13858773	2.41166006	-5.75215094	0.5160735	1.09146392
C	-5.01031276	3.04973404	0.98550232	-5.95126963	0.83964589	-1.30643678
C	-5.3759488	2.2163387	2.05088965	-6.55113149	0.65844239	-0.05409192
H	-2.74625863	0.0274102	1.95535127	-3.73833277	0.41402714	1.87548074
H	-4.8423215	0.47419399	3.23242285	-6.21670304	0.36634405	2.07147147
H	-3.54123488	3.46896542	-0.54951982	-4.09163064	1.02926176	-2.40009727
H	-5.65733128	3.8831787	0.69191642	-6.56982716	0.95236991	-2.20315718
H	-6.30917958	2.39882919	2.59444008	-7.64251822	0.62561548	0.03163437
C	4.95768156	-1.91861049	0.02696841	-1.26052467	0.75181519	-4.37028373
C	6.11536677	2.47177101	-0.67609941	-0.82263691	3.03166454	-3.66092732
H	5.80183789	0.35012455	-0.36288921	-0.8672125	2.06529054	-4.67400666
C	7.45281625	2.26360727	-1.39904478	-1.85634214	-0.62756417	-2.80549528
H	8.069118	1.50755462	-0.87838746	-1.12148283	3.45101646	-1.55994392
H	8.02664922	3.20610682	-1.43035651	-0.50725946	4.05489834	-3.89130757
H	7.28771874	1.92076108	-2.43443606	-0.58749285	2.33081747	-5.69887206
C	6.29994206	2.98742458	0.76165658	-1.28805543	-0.01050892	-5.15552572

H	5.49615539	3.19260075	-1.23655915	-0.42837959	2.97559247	2.81555771
H	6.8391631	3.95134857	0.7634334	-1.97391733	4.41612401	1.61675184
H	6.88166232	2.26674071	1.36494473	-1.06305433	4.21629377	2.66655099
H	5.32125562	3.13396408	1.24917744	-0.20883086	0.9622603	2.02904524
C	5.91642833	-3.78081242	1.12418153	0.25922574	2.8045994	3.65042737
H	5.58260058	-4.77540426	1.44963461	-2.9756925	3.52835011	-0.08562464
H	6.23547233	-3.17051375	1.9850499	-2.49518406	5.3741029	1.51579181
H	6.7560089	-3.86164929	0.41414122	-0.86607795	5.02280605	3.38094708

Pd-3, *trans*

Functional		TPSS D4			wB97M-V	
Basis set		def2-SVP			def2-TZVPP	
Hartrees (Eh)	Gibbs	G-E(el)	Electronic	**Gibbs ***	Final single point (electronic)	
α	-2630.671355	0.607183	-2631.278538	**-2631.632130**	-2632.239313	
β	-2630.675919	0.605993	-2631.281911	**-2631.637983**	-2632.243975	
ΔG	0.004564			**0.005853**		
kcal/mol				**3.672480**		

Atoms						
86		α			β	
C	-0.02761766	1.07751968	2.86727083	1.54538546	-4.26065201	1.58492167
C	0.22019763	2.34313445	2.46914264	0.88413309	-3.10220061	1.39511559
C	0.2116275	3.50661831	3.43612545	0.71818452	-2.06748868	2.48670775
C	0.5333294	2.66621863	1.04439618	0.23029824	-2.80944165	0.08427002
C	1.71284232	3.36264483	0.73362817	-0.83203705	-3.6032459	-0.36305887
C	2.04837006	3.70270385	-0.58738613	-1.47448212	-3.34983117	-1.59034905
C	1.21796096	3.31266373	-1.63538746	-1.07507817	-2.27444648	-2.37705499
C	0.02836236	2.61153086	-1.36498148	0.0118824	-1.46838875	-1.96704101
C	-0.36615245	2.32638072	-0.0235271	0.70119664	-1.74610404	-0.75119801
C	-1.74899936	0.28144152	-0.03782197	1.68761398	0.43155722	-0.09913994
C	-1.77674601	1.79333593	0.25311767	2.01581658	-1.03321053	-0.43908451
Pd	0.24422251	0.14337235	-0.64178946	-0.37456007	0.41026531	-0.36774922
I	0.01515265	-2.44551907	-0.29890146	-0.38578653	2.76091424	0.76592125
C	-2.85249244	2.2570349	-0.78737463	2.94138518	-0.83757238	-1.69765321
H	-2.8224587	3.3140145	-1.08264718	3.01990005	-1.69670001	-2.37471777
C	-4.17278207	1.71267666	-0.24931786	4.23412078	-0.27981549	-1.12807394
C	-5.12265902	2.49819927	0.53492273	5.33861738	-1.21693516	-0.78394942
O	-4.60389852	3.71508872	0.84334494	5.10725947	-2.43645455	-0.80210649
C	-5.46485001	4.57619424	1.6097877	6.54396594	-0.67002649	-0.47514794
O	-6.25443117	2.16719043	0.88619192	3.93154594	1.01546359	-0.81387736
C	-4.11871881	0.36763301	-0.49802982	4.7051372	2.00712863	-0.05851384
C	-4.92268514	-0.81681438	-0.07348195	5.91627246	1.98894561	0.15793758
N	-6.19771639	-0.57992636	0.33639938	3.90134667	2.9964515	0.38339957
C	-7.04880485	-1.66689128	0.82240622	2.46206618	1.19578472	-1.20605717

O	-4.40817717	-1.9412563	-0.13544615	2.1188826	2.20865643	-1.44369357
C	-2.77766118	0.15058713	-1.19194664	2.36333576	0.31326249	-2.33832073
H	-2.68937563	-0.72755855	-1.83999978	2.01872321	-4.49557638	2.54583488
O	-2.61368545	1.39098177	-1.90815321	1.65213209	-4.99494213	0.77895747
H	-0.25417216	0.85019332	3.91604136	1.36005077	-2.29001465	3.35481967
H	0.00699306	0.23522532	2.16506942	-0.33303974	-2.04426814	2.82959677
H	-0.00710331	3.17193262	4.46335096	0.9447778	-1.05021516	2.12289856
H	-0.5470799	4.25439591	3.13774669	-1.16721875	-4.4339972	0.26495373
H	1.18486214	4.0316406	3.44169658	-2.29439104	-3.99735498	-1.91389852
H	2.39481658	3.63914629	1.54476382	-1.57312899	-2.06471459	-3.32819778
H	2.97716944	4.24390553	-0.79056862	-2.7457449	0.32281627	-0.67050286
H	1.47843039	3.55543191	-2.66923671	-3.41945302	-1.26891637	-0.05703773
H	-6.3896959	4.79119521	1.04922192	-3.81694917	1.56585101	0.16315148
H	-4.88785504	5.49572364	1.77888991	-3.30579436	0.51297164	-2.40961194
H	-5.73257858	4.09850432	2.56673995	-4.32802176	-2.08390102	-0.75292349
H	-6.48018095	0.39904668	0.49607247	-2.94422638	-1.68416722	1.20310021
P	2.5819603	-0.18251554	-1.11392903	-2.34037116	0.67628596	-3.41928182
C	2.96176237	-1.25964064	-2.55201289	-4.67402182	0.58185088	-2.74424187
C	3.79447735	1.17567599	-1.43292527	-3.79140673	2.88503492	-0.33392625
C	3.27116815	-1.00783584	0.37281628	-4.6078652	1.2661265	1.28522664
C	4.29774104	-1.55447061	-2.89449138	0.45045313	-0.73628835	-2.65392981
C	1.9169096	-1.7384171	-3.36151241	2.55491969	-1.58340866	0.3467707
C	3.92685839	-2.24962582	0.34893738	1.93265122	0.76355673	0.91849465
C	3.03627797	-0.37106515	1.60826815	7.6607607	-1.50069424	-0.02339997
C	4.67760138	1.66880431	-0.45667508	7.60716717	-1.70047593	1.5015824
C	3.79942473	1.75912739	-2.71666516	7.6868537	-0.73022573	2.02481848
C	-8.51519692	-1.33443318	0.52774711	8.43528273	-2.34801085	1.84093886
H	-8.82991984	-0.42320097	1.06971831	6.6545776	-2.17756363	1.7868769
H	-9.17085952	-2.16188587	0.84898087	8.9822584	-0.88413439	-0.49415248
H	-8.66982245	-1.16469863	-0.55152038	9.83313927	-1.51944833	-0.19351495
C	-6.78812622	-1.9421285	2.31375487	9.13319615	0.11655321	-0.04816129
H	-6.74260969	-2.56167971	0.25214484	8.99591676	-0.77792481	-1.59224655
H	-7.02569338	-1.05075397	2.92272408	4.53366364	4.03136484	1.15696465
H	-5.72860579	-2.20530544	2.46855548	5.04236873	3.59660055	2.03302785
H	-7.41019562	-2.78271962	2.66976393	3.7203372	4.70125204	1.46609311
H	-0.66772608	2.37394053	-2.17449659	5.2754977	4.56709753	0.5416033
H	-2.07628121	2.0429375	1.28206016	7.51063846	-2.48272338	-0.5049418
H	-1.93836143	-0.38984234	0.80929206	6.57988496	0.35099851	-0.33072071
C	4.66524365	2.81637277	-3.01491098	-4.76156477	-3.29260574	-0.19024768
C	5.540555	3.30895154	-2.03340547	-3.38844242	-2.88477367	1.76899883
C	5.54531034	2.7296974	-0.75747769	-4.29687174	-3.69384096	1.07046388
H	6.23358861	3.09837362	0.01090768	-4.68574122	-1.78711657	-1.7430929
H	4.69990423	1.21804389	0.53960632	-5.46447584	-3.92580066	-0.7424385
H	3.12391064	1.37528074	-3.48904262	-2.21334222	-1.05996496	1.72978865
H	4.66139106	3.25564222	-4.01839819	-3.01352256	-3.19632363	2.74969069
H	6.22141487	4.13438281	-2.26703642	-4.63890569	-4.63849846	1.50647059
C	4.57914549	-2.34072351	-4.01781376	-2.73281906	0.86558407	-4.75186834

C	3.53108022	-2.82360195	-4.8173216	-5.06426821	0.76185052	-4.07670601
C	2.20307187	-2.51651223	-4.49213086	-4.0943415	0.89747508	-5.08275738
H	1.38307307	-2.88582632	-5.11673816	-1.27938396	0.67238002	-3.148384
H	0.88085772	-1.50641914	-3.09540355	-5.43193284	0.51486452	-1.95638615
H	5.61860374	-2.57201187	-4.27429033	-6.12866969	0.80905324	-4.33061246
H	3.75285782	-3.43550757	-5.69842316	-4.402628	1.04484685	-6.12337653
H	5.11710618	-1.15788839	-2.28525406	-1.97295488	0.99663163	-5.5294097
C	4.36088279	-2.83502523	1.54648443	-5.3685692	2.27199278	1.89906492
C	3.48029476	-0.95381285	2.80028404	-4.5584851	3.88252548	0.27647659
C	4.14465831	-2.18899734	2.77132221	-5.34681606	3.57953551	1.39674968
H	4.07900731	-2.77279145	-0.59923361	-4.63899475	0.24672991	1.68095729
H	4.86157445	-3.80878296	1.52077385	-5.98424978	2.02743702	2.77137499
H	2.48169332	0.57325311	1.63819756	-3.17146612	3.12925941	-1.20222598
H	3.28826778	-0.45041417	3.75380737	-4.53195956	4.90351438	-0.11863225
H	4.48076813	-2.65428237	3.70412281	-5.94273469	4.36296753	1.8771295

New-**TS-1** *cis*

Functional		TPSS D4			wB97M-V	Imaginary frequency
Basis set		def2-SVP			def2-TZVPP	
Hartrees (Eh)	Gibbs	G-E(el)	Electronic	Gibbs *	Final single point (electronic)	
α	-2291.42335	0.61716955	-2292.04052	**-2292.18729**	-2292.80446	196.38i
β	-2291.42561	0.61737754	-2292.04299	**-2292.1904**	-2292.80777	190.76i
ΔG	0.00225808			**0.00310335**		
kcal/mol				**1.94735255**		

Atoms						
86		*α*			*β*	
C	-0.35617927	-1.69112097	3.2092467	-0.0259451	-2.1077113	2.90800322
C	0.10726861	-2.91606015	2.86788276	0.76597103	-3.08413114	2.40804893
C	0.89271533	-3.73765103	3.87088927	1.76417025	-3.80041589	3.29380563
C	-0.12839829	-3.5156748	1.52959698	0.70527606	-3.49530081	0.98187481
C	-0.23430314	-4.92219677	1.40671497	0.93210115	-4.84656493	0.62858857
C	-0.43488273	-5.54335288	0.17209909	0.9125775	-5.27403879	-0.70068502
C	-0.50881953	-4.76614531	-0.99391352	0.69264214	-4.34437201	-1.72834836
C	-0.37951945	-3.37735894	-0.90661025	0.49339717	-2.99801432	-1.41007078
C	-0.20692826	-2.74330063	0.33919469	0.478262	-2.57110304	-0.06909629
C	1.22184749	0.05061932	0.19736466	1.19095937	0.4695464	0.39253947
C	1.43960737	-1.36205907	0.33928575	1.73014638	-0.85939349	0.28424129
Pd	-0.73374064	-0.68120255	0.30223242	-0.51862355	-0.70635741	0.13450174
I	-3.25943548	-1.55514886	0.03623571	-2.78654079	-2.13321682	-0.24112617
C	2.07906124	-1.7504781	-1.01649117	2.50293332	-0.81330801	-1.05300169
H	2.03701158	-2.80427346	-1.30882592	2.70026553	-1.76677183	-1.55203618
C	3.46592109	-1.07676572	-1.03125892	3.72029099	0.07289499	-0.76421182
O	4.47363139	-3.04555802	-0.33943227	4.99259936	-0.58558613	-0.35829605

O	5.8593486	-1.34116177	-0.88716494	4.93684395	-1.77077456	0.00572385
C	3.20843969	0.25239047	-1.20010888	6.12791233	0.1557912	-0.40468625
C	4.01067391	1.50679183	-1.15059853	3.2166836	1.33721182	-0.68720012
N	5.35601013	1.38334164	-1.26371741	3.89784509	2.58366008	-0.33418603
O	3.41765975	2.59238391	-1.02634157	5.11440203	2.76799252	-0.31504318
C	1.67620002	0.33513738	-1.26004052	3.01630085	3.56420458	-0.03645733
H	1.24547494	1.19602758	-1.78283434	1.69456511	1.16382178	-0.89597818
O	1.351829	-0.90333669	-1.91523071	1.13774721	2.03243019	-1.26576761
H	-0.133972	-1.25544966	4.1906138	1.6795205	0.07119351	-1.83306955
H	-0.9999323	-1.11219382	2.53117503	0.05795712	-1.789003	3.95388512
H	0.31479005	-4.61814561	4.20852207	-0.80372025	-1.63440805	2.29327122
H	1.13485381	-3.13893697	4.76406409	2.77518055	-3.78790906	2.84671654
H	1.83249343	-4.12161113	3.43301668	1.4886208	-4.86243531	3.43248792
H	-0.17811987	-5.53958403	2.30877966	1.80855581	-3.33556018	4.29228853
H	-0.53145562	-6.63296231	0.11915942	1.11073163	-5.57972368	1.42148452
H	-0.67074262	-5.23818125	-1.96908869	1.07630536	-6.33083593	-0.93602281
P	-1.46343394	1.54533732	0.1896401	0.67554835	-4.66496933	-2.77563666
C	-1.42344013	2.09761888	-1.55538316	-1.89487935	1.15832335	0.0132713
C	-3.15347472	1.91552467	0.79919021	-3.19162059	1.38720513	1.29399916
C	-0.449817	2.79307223	1.09605534	-1.1144861	2.83201115	0.08647924
C	-1.553804	1.1157393	-2.55710658	-2.70077082	1.15800425	-1.63169785
C	-1.28332016	3.45215314	-1.91821016	-3.42181273	0.39737313	2.26507568
C	-0.84796012	3.25697415	2.36599039	-3.92205823	2.59332481	1.34357728
C	0.78505791	3.22520291	0.57014115	-1.89592996	0.78295515	-2.72684213
C	-3.57722607	1.32307381	2.00523838	-4.046995	1.49927122	-1.83696227
C	-4.00765433	2.80017106	0.12142216	-0.60560294	3.27048866	1.32597368
H	-0.42911387	-2.76628819	-1.81300845	-1.03289058	3.68301073	-1.03001802
H	1.80075005	-1.79018592	1.27736737	0.32705212	-2.26760638	-2.20861439
H	1.44762576	0.76448349	0.99563503	2.15388955	-1.38404255	1.1425611
C	-1.54433255	1.48713577	-3.9074238	1.16643841	1.02088401	1.3382238
C	-1.27125536	3.81634974	-3.27078858	7.40000341	-0.37189457	0.09530082
C	-1.40168963	2.83542087	-4.26546642	7.51023287	-0.1778185	1.6177884
H	-1.65882411	0.06388943	-2.26728694	6.6771488	-0.69087817	2.12645704
H	-1.64289777	0.71820457	-4.68050243	7.47738177	0.89601669	1.87726948
H	-1.1741242	4.21826657	-1.14399818	8.45895782	-0.59809334	1.99605606
H	-1.15658201	4.86948761	-3.54856651	8.55615642	0.27937789	-0.67020283
H	-1.38716278	3.12358572	-5.32213524	8.45841093	0.10288193	-1.75484715
C	-0.02516483	4.12797205	3.09263984	9.52188552	-0.1350364	-0.33394751
C	1.60621105	4.09294047	1.3010916	8.57804988	1.3713941	-0.49709285
C	1.2046018	4.54690077	2.56521992	3.60623722	4.83159827	0.30867191
H	-1.80844944	2.94665405	2.78710343	4.252072	4.7224396	1.19535447
H	1.13767085	2.89827059	-0.41037996	2.76142021	5.4998265	0.51542125
H	2.56320163	4.39592572	0.86542445	4.21394219	5.20858396	-0.53019418
H	1.84557555	5.22660976	3.13717286	7.37299283	-1.45596903	-0.11233766
H	-0.35258388	4.48284536	4.07585372	6.0169643	1.17289647	-0.53532074
C	-5.2712811	3.09793461	0.65134529	-4.38425392	0.60309888	3.26283502
C	-4.83089209	1.63819616	2.5401378	-4.89231144	2.78827337	2.3338913

C	-5.68160965	2.52401127	1.86184033	-5.12523307	1.79214744	3.29436006
H	-3.69530475	3.24742904	-0.82676921	-2.8589429	-0.53934029	2.22442655
H	-5.93717124	3.77982539	0.1118207	-4.55689931	-0.17438247	4.01420688
H	-2.9311847	0.59999525	2.51302405	-3.72255117	3.38575764	0.61448954
H	-5.15313538	1.17188233	3.47682319	-5.46167738	3.72351604	2.36031301
H	-6.66954698	2.75795177	2.27276273	-5.88099518	1.94782451	4.07181841
C	4.7177774	-1.78339036	-0.76054549	-2.4323674	0.77803522	-4.01924234
C	6.24264763	2.54509392	-1.17896071	-4.58160738	1.47855497	-3.13262289
H	5.75569069	0.43082512	-1.24683068	-3.77637136	1.12550064	-4.22408497
C	7.42609934	2.3566654	-2.13424881	-0.85800513	0.47012565	-2.55914014
H	8.03055897	1.47631053	-1.84728369	-4.68583364	1.75494555	-0.98700256
H	8.08527533	3.24130656	-2.11001765	-5.63615276	1.73074417	-3.28689139
H	7.07476484	2.21148635	-3.16991172	-4.19956887	1.10725812	-5.23411409
C	6.68380609	2.78525375	0.27540143	-1.80350525	0.48361132	-4.86596602
H	5.63091494	3.40518262	-1.50217214	-0.46919381	4.96187365	-0.90226518
H	7.32227583	3.68369807	0.34519839	-0.05106761	4.54799557	1.45177845
H	7.25729068	1.92138915	0.65764377	0.00875586	5.40134952	0.33839225
H	5.80216187	2.93454888	0.9211182	-1.42752996	3.35409283	-1.99620174
C	5.6374398	-3.84107363	-0.0430428	-0.42288479	5.62202823	-1.77501471
H	5.25108888	-4.81452512	0.28734833	-0.6743209	2.61658943	2.20296231
H	6.2341175	-3.36272745	0.75087275	0.32448282	4.88421406	2.42428336
H	6.26272034	-3.95004569	-0.94432093	0.42116198	6.41115195	0.44082716

New-**TS-1** *trans*

Functional		TPSS D4			wB97M-V	Imaginary frequency
Basis set		def2-SVP			def2-TZVPP	
Hartrees (Eh)	Gibbs	G-E(el)	Electronic	Gibbs *	Final single point (electronic)	
α	-2630.63709	0.60469358	-2631.24178	**-2631.59283**	-2632.19752	205.11i
β	-2630.63732	0.6047189	-2631.24204	**-2631.5929**	-2632.19762	213.61i
ΔG	0.00023407			**7.084E-05**		
kcal/mol				**0.04445228**		

Atoms						
86		*α*			*β*	
C	0.34327732	1.84805612	2.4227651	-0.04923409	-1.76188869	2.71184924
C	0.43273158	2.95305058	1.64374929	0.17343366	-2.85916722	1.94916432
C	0.55021796	4.30820753	2.31084702	0.5739059	-4.15714484	2.62203631
C	0.44563143	2.90995801	0.16054091	0.02727587	-2.87314191	0.47155677
C	0.82626523	4.07204174	-0.55149334	-0.19084411	-4.11021443	-0.18017735
C	0.8794583	4.11007836	-1.94679513	-0.31640534	-4.21107977	-1.56679605
C	0.54759319	2.96692169	-2.68623703	-0.18669865	-3.06265702	-2.35919834
C	0.12031045	1.8168672	-2.01538719	0.06567771	-1.83198095	-1.74714417
C	0.05389457	1.76716085	-0.6044067	0.14896332	-1.70915247	-0.34402339
C	-1.8214108	-0.38485612	0.36913437	1.70495314	0.7329924	0.67463772

C	-1.71622748	1.02181735	0.04038207	1.85045437	-0.62723064	0.23510682
Pd	0.23290842	-0.26203204	0.02555918	-0.3044673	0.24928994	0.33326913
I	0.37948398	-2.86733369	0.50504835	-0.81907652	2.74004864	1.1255995
C	-2.56886112	1.11608503	-1.25524328	2.58343826	-0.47147316	-1.11796943
H	-2.38538296	1.97532912	-1.90883874	2.52516032	-1.3098472	-1.81924643
C	-4.02334641	0.87256425	-0.81612581	3.99603308	0.01503919	-0.76245727
C	-5.01634244	1.92949102	-0.63802563	5.08757483	-0.98868833	-0.64096956
O	-4.43589372	3.15293114	-0.71158948	4.77054663	-2.18622006	-0.56612154
C	-5.32943076	4.27202054	-0.56504213	6.36214097	-0.52157614	-0.61647445
O	-6.22461762	1.78645668	-0.45827022	3.82885006	1.31322091	-0.38548168
C	-4.07950498	-0.45847203	-0.52283439	4.79416048	2.26454768	0.17219169
C	-5.06021145	-1.33670488	0.1753156	6.02020219	2.16902709	0.13910282
N	-6.36670963	-0.96514511	0.12813386	4.16016754	3.31296071	0.73937595
C	-7.39335027	-1.71503338	0.85478991	2.3087415	1.55669542	-0.48488379
O	-4.63661533	-2.34982846	0.74864982	1.95579246	2.58654545	-0.60525079
C	-2.65570212	-0.97198282	-0.78714712	1.98390349	0.7321048	-1.62427942
H	-2.53342511	-2.03905903	-1.00110397	0.10610469	-1.7920355	3.79681227
O	-2.25569001	-0.12908145	-1.88897731	-0.40718281	-0.81005588	2.28631311
H	0.31630899	1.93307098	3.51528324	0.79108807	-3.9892993	3.68906824
H	0.31667735	0.83240933	1.9978783	1.46373819	-4.60650983	2.14575453
H	-0.21471751	5.01601649	1.94303584	-0.23914942	-4.9051277	2.56168905
H	1.53866747	4.76240766	2.11100843	-0.28532317	-5.01772126	0.42165851
H	0.43963992	4.21153724	3.40258258	-0.50737577	-5.18610025	-2.02641352
H	1.11140656	4.96813867	0.00451031	-0.27111127	-3.12134869	-3.44973033
H	1.19309077	5.02856715	-2.45358316	-2.55586204	-0.1657245	-0.28094052
H	0.6018536	2.97144517	-3.78031858	-2.74696032	0.3322762	-2.03711667
H	-6.10196678	4.24888416	-1.35119566	-3.05951917	-1.9287851	-0.17692545
H	-4.69902668	5.16651619	-0.66012781	-3.96741258	0.74090882	0.48337203
H	-5.82284854	4.24170888	0.42044837	-1.665924	0.94259353	-2.6978361
H	-6.57924194	-0.01485476	-0.2113029	-3.98114469	0.18987904	-2.7034647
P	2.56791888	-0.16406257	-0.25995539	-4.1379582	2.09524768	0.12599752
C	3.09246486	-0.83246851	-1.88303467	-4.85189865	0.16026367	1.41000414
C	3.33990224	1.50808628	-0.20928831	-3.39574142	-2.70999651	-1.29582809
C	3.51084637	-1.08337175	1.02265484	-3.05190704	-2.52827024	1.10031122
C	4.40089274	-0.65381949	-2.38034977	0.20615729	-0.94318638	-2.36758963
C	2.15089422	-1.53963577	-2.65377938	2.12517751	-1.42754468	0.92594973
C	4.67767045	-1.81530593	0.74615234	1.84638752	1.04730887	1.71252611
C	3.02142835	-1.03557319	2.34252178	7.49769046	-1.41497617	-0.37945462
C	3.62828799	2.10007373	1.03640485	7.78904001	-1.53274837	1.1267816
C	3.56215764	2.2473862	-1.38581461	8.05012125	-0.54656086	1.55194816
C	-8.72184391	-1.62625316	0.0966206	8.63162919	-2.22325077	1.30872717
H	-9.07560273	-0.57987194	0.04114847	6.90251906	-1.92045262	1.65611933
H	-9.49860238	-2.21827607	0.61023705	8.71000317	-0.9291641	-1.18133694
H	-8.61343461	-2.00942442	-0.93231065	9.56213517	-1.6171903	-1.04572472
C	-7.50325809	-1.22252551	2.30847193	9.02986591	0.07516223	-0.8466587
H	-7.03743315	-2.76004651	0.8720112	8.47190043	-0.87513789	-2.25718586
H	-8.25631685	-1.81024872	2.86291375	5.00889446	4.31958618	1.32265668

H	-7.80118566	-0.15858817	2.33872574	5.6301071	3.87934375	2.1199009
H	-6.53250606	-1.33286135	2.81978613	4.32658344	5.07755572	1.72971603
H	-0.19592402	0.9374049	-2.58521764	5.66837944	4.75324671	0.5529918
H	-1.81386652	1.77920421	0.82477356	7.17412695	-2.40351793	-0.7488672
H	-1.99193293	-0.74812359	1.3873381	6.488011	0.49617663	-0.50319385
C	4.08383482	3.54526727	-1.31752981	-1.80658897	1.37854366	-4.02309321
C	4.37187368	4.12752232	-0.0767911	-4.11573233	0.62067494	-4.02823115
C	4.13839383	3.40172439	1.10081888	-3.02717248	1.21104876	-4.69064274
H	4.36463943	3.84606308	2.07608923	-0.72084024	1.08928353	-2.1599382
H	3.46243527	1.53969578	1.96074048	-0.96049398	1.85546744	-4.52866376
H	3.32591092	1.81104126	-2.35989878	-4.83885075	-0.24351484	-2.17802542
H	4.2559498	4.10653423	-2.24204847	-5.07548797	0.50595804	-4.54343232
H	4.77940649	5.14299397	-0.0260348	-3.13764407	1.55190017	-5.72580637
C	4.76101149	-1.18813722	-3.62351372	-5.17331541	2.84904713	0.68959304
C	3.81886137	-1.89874706	-4.38324783	-5.88491159	0.92165834	1.97461311
C	2.5151149	-2.07025689	-3.89874149	-6.04684511	2.26720586	1.61911619
H	1.77507836	-2.62055176	-4.48892852	-3.464189	2.5575881	-0.60006805
H	1.13608104	-1.67927232	-2.26521389	-4.75417845	-0.89333201	1.6837846
H	5.77928354	-1.04677892	-4.00143834	-6.56926438	0.4540667	2.6906773
H	4.10253149	-2.31465996	-5.35608944	-6.8553087	2.85965262	2.06082498
H	5.13426576	-0.08275791	-1.8015184	-5.29305802	3.89887378	0.40221172
C	5.35611766	-2.47319132	1.78133921	-3.4231191	-3.86789609	1.25863352
C	3.70985875	-1.67955303	3.37648624	-3.75770757	-4.05463709	-1.13466599
C	4.87977207	-2.40055388	3.09735363	-3.78300691	-4.63365693	0.14032381
H	5.04964022	-1.89316428	-0.27895843	-2.72921512	-1.95171528	1.97261538
H	6.25863588	-3.05078306	1.55449368	-3.41639456	-4.31714867	2.25745585
H	2.08319473	-0.51190587	2.55185561	-3.36706446	-2.27350584	-2.29777669
H	3.31830857	-1.63696996	4.39820478	-4.01538779	-4.65268715	-2.01527031
H	5.41142607	-2.91806251	3.90303396	-4.06925347	-5.68386149	0.26187465

10 Compound list

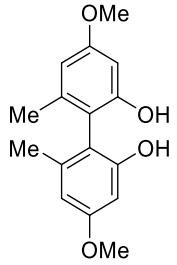		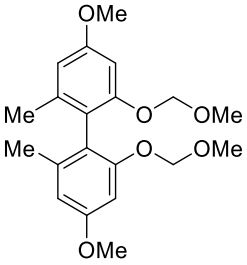		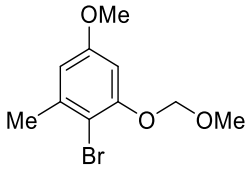		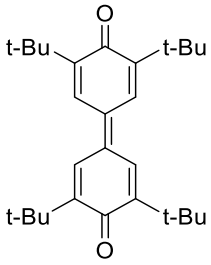	
MKL0031	**27**	MKL0024	**28**	MKL0023	**29**	MKL0022	**30**
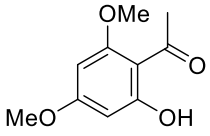		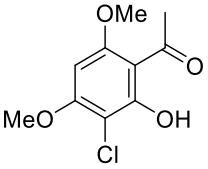		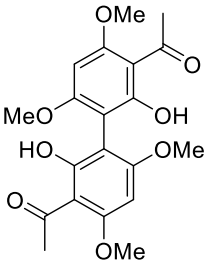		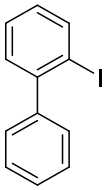	
MKL0070	**47**	MKL0143 B	**48**	MKL0078	**49**	MKL0057	**92**
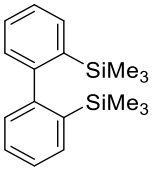		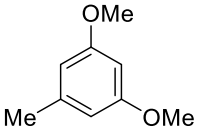		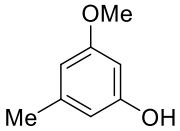		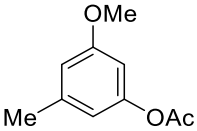	
MKL0125	**93**	MKL0017	**123**	MKL0018	**124**	MKL0019	**125**
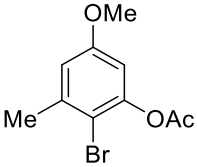		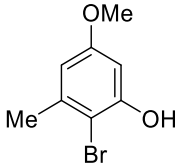		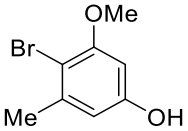		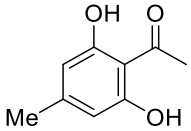	
MKL0020	**126**	MKL0021	**128**	MKL0021 B	**129**	MKL0007	**131**
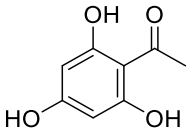		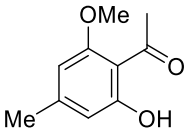		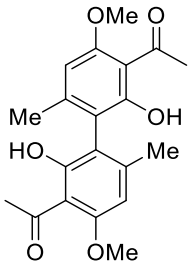			
MKL0067	**132**	MKL0008	**133**	MKL0033	**134**		
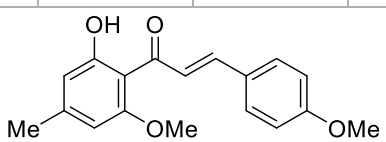				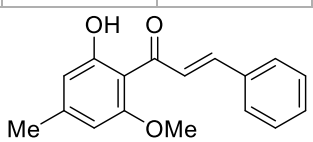			
MKL0116		**135**		MKL0004a		**136**	

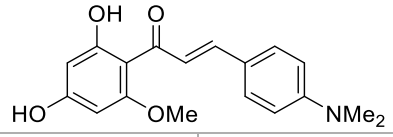		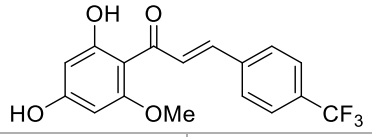	
MKL0010	**137**	MKL0013	**138**
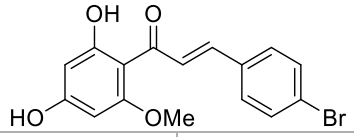		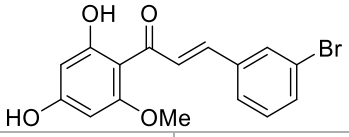	
MKL0006	**139**	MKL0065	**140**
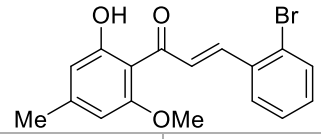		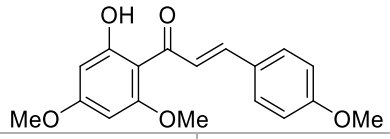	
MKL0066	**141**	MKL0115	**142**
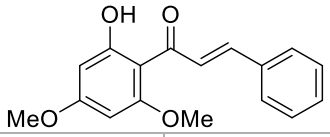		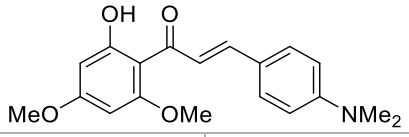	
MKL0077	**143**	MKL0076	**144**
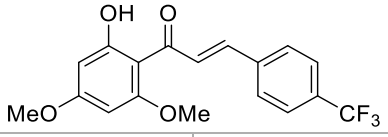		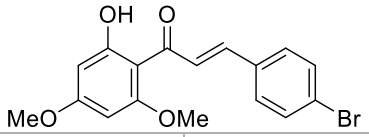	
MKL0071	**145**	MKL0072	**146**
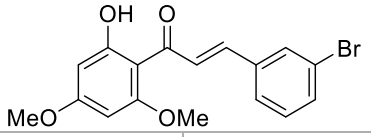		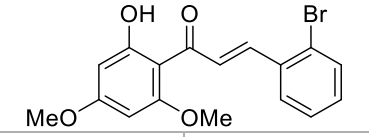	
MKL0074	**147**	MKL0075	**148**
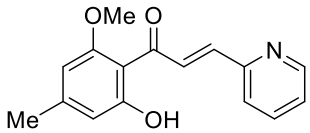		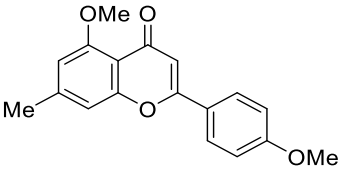	
MKL0005	**149**	MKL0122	**150**
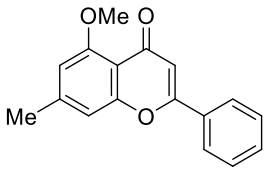		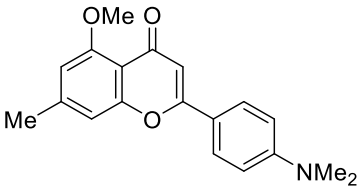	
MKL0004b	**151**	MKL0011	**152**
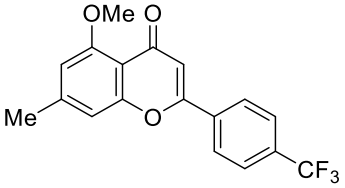		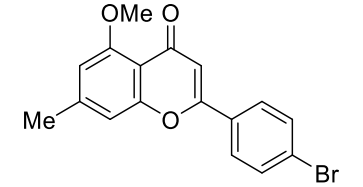	
MKL0015	**153**	MKL0014	**154**

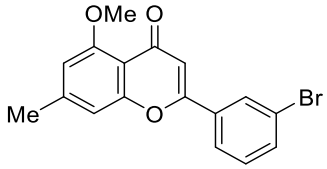		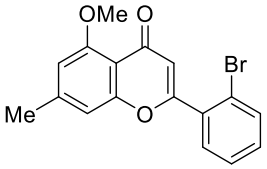	
MKL0083	**155**	MKL0084	**156**
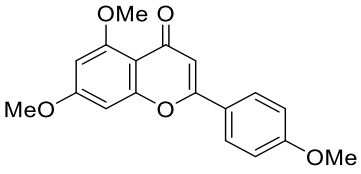		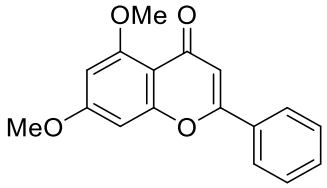	
MKL0121	**157**	MKL0110	**158**
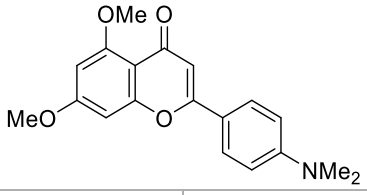		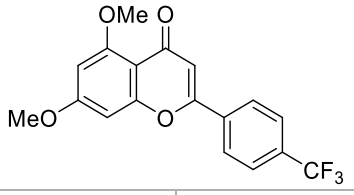	
MKL0109	**159**	MKL0108	**160**
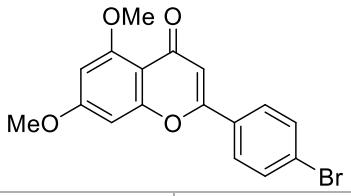		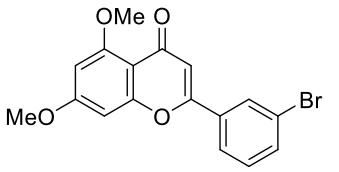	
MKL0080	**161**	MKL0081	**162**
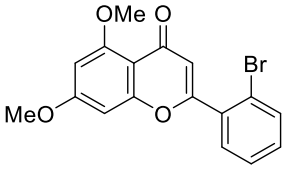			
MKL0082	**163**		
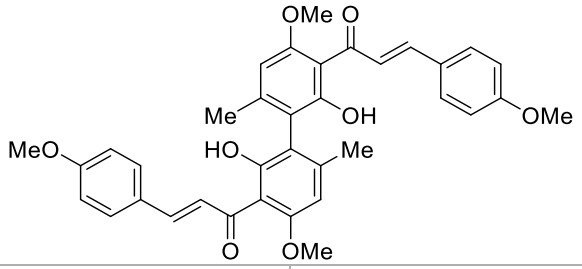		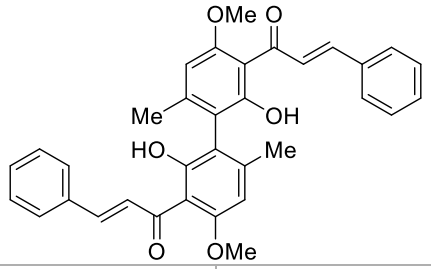	
MKL0118	**165**	MKL0037	**166**
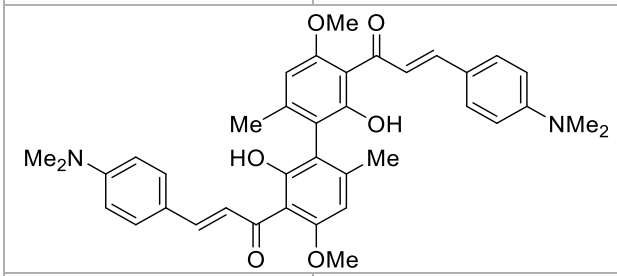		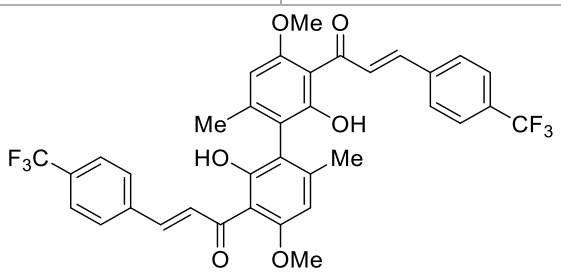	
MKL0039	**167**	MKL0043	**168**

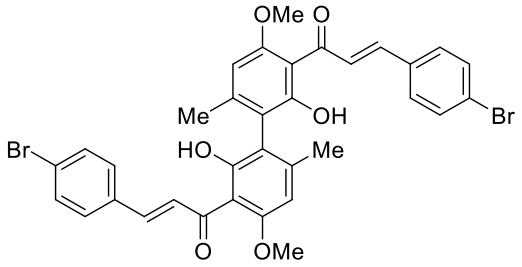		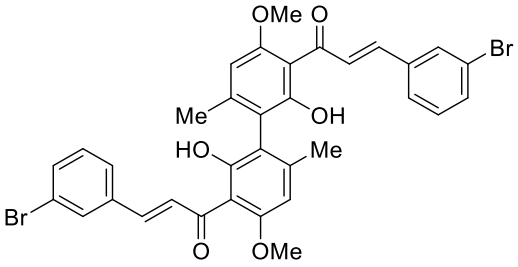	
MKL0044	**169**	MKL0068	**170**
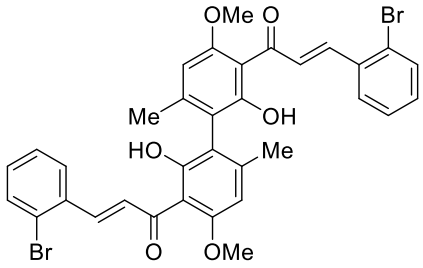		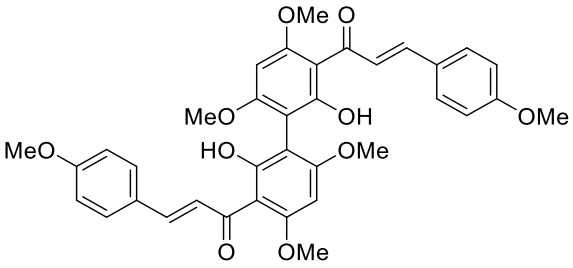	
MKL0069	**171**	MKL0117	**172**
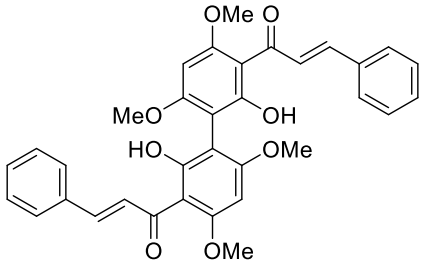		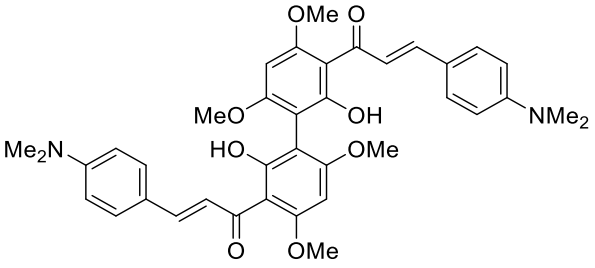	
MKL0085	**173**	MKL0090	**174**
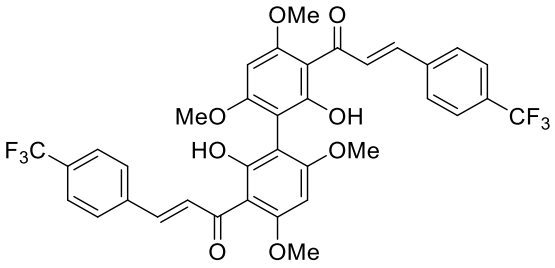		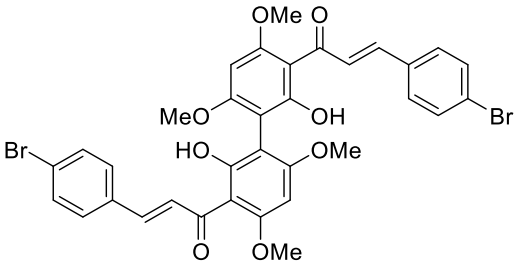	
MKL0089	**175**	MKL0086	**176**
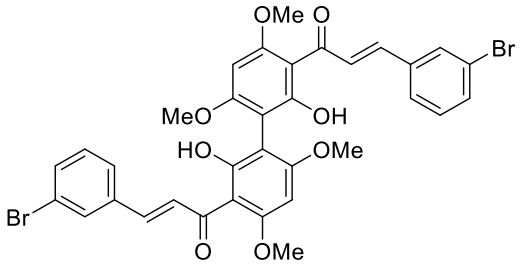		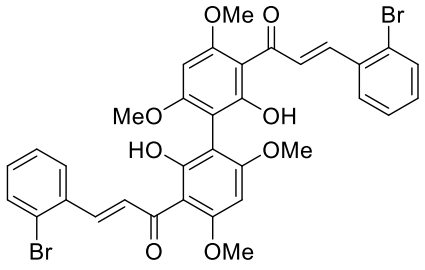	
MKL0087	**177**	MKL0088	**178**

Compound list

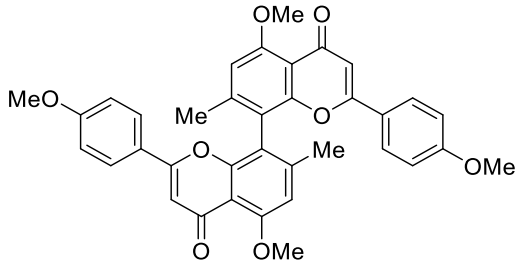		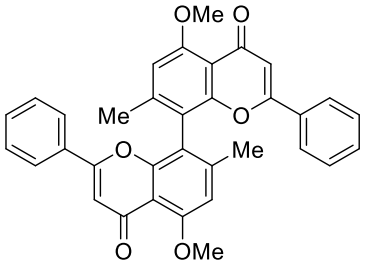	
MKL0124	**179**	MKL0107	**180**
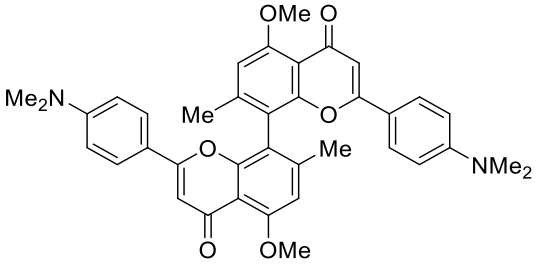		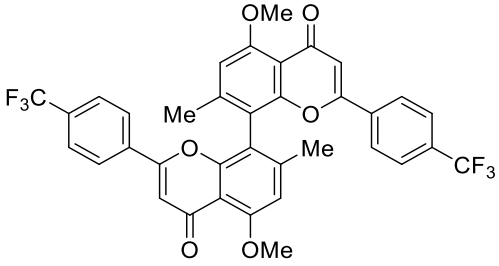	
MKL0073	**181**	MKL0104	**182**
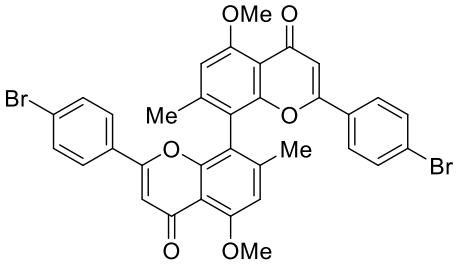		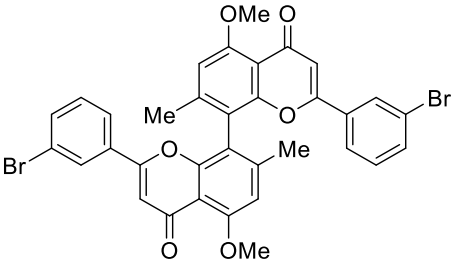	
MKL0079	**183**	MKL0105	**184**
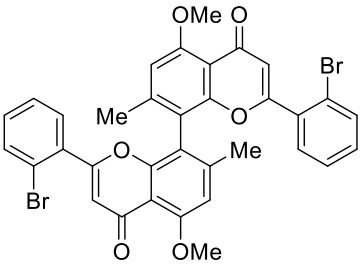		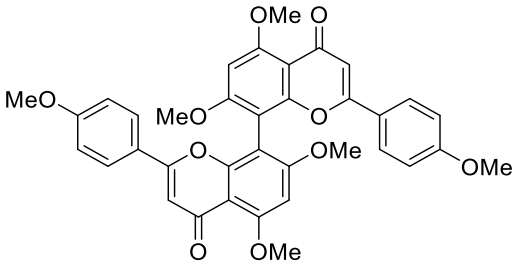	
MKL0106	**185**	MKL0123	**186**
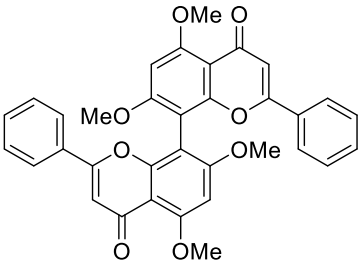		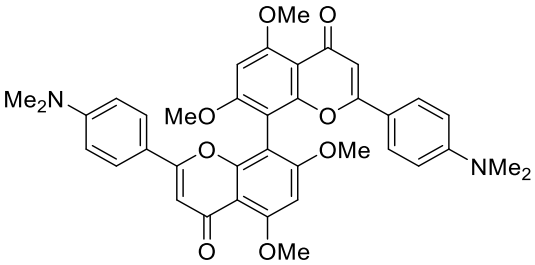	
MKL0103	**187**	MKL0102	**188**

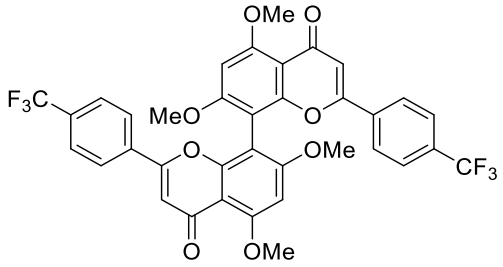		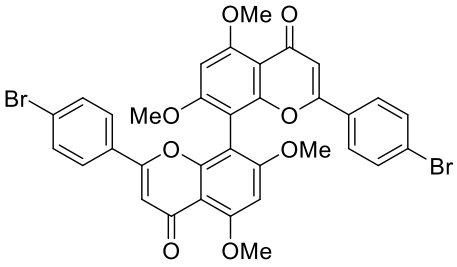	
MKL0100	**189**	MKL0099	**190**
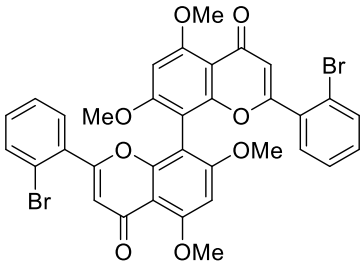		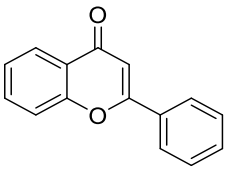	
MKL0098	**192**	MKL0001	**194**
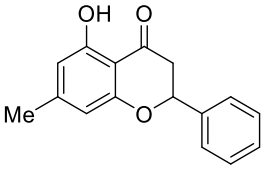		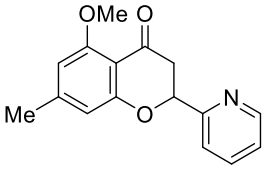	
MKL0009sp	**196**	MKL0030sp	**164**
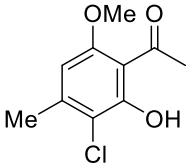	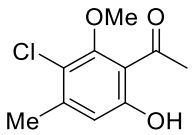	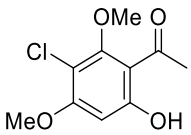	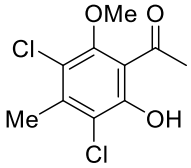
MKL0141 B	**198**	MKL0141 A	**199**	MKL0143 A	**200**	MKL0150	**201**
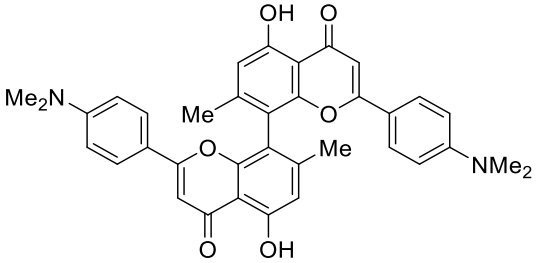		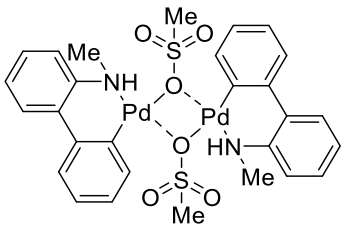	
MKL0154	**204**	MKL0034	**205**
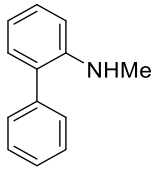		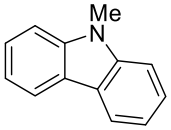	
MKL0032	**207**	MKL111sp CarbazoleG4	**208**

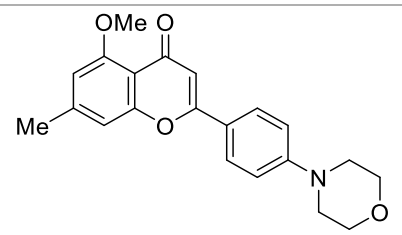		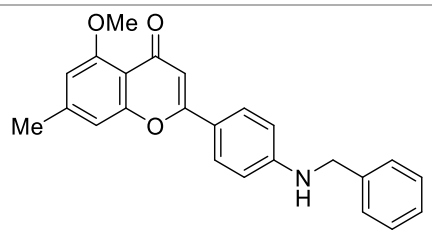	
MKL_DGR009	**210**	MKL_DGR010	**211**
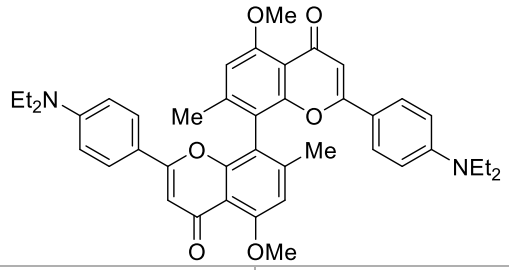		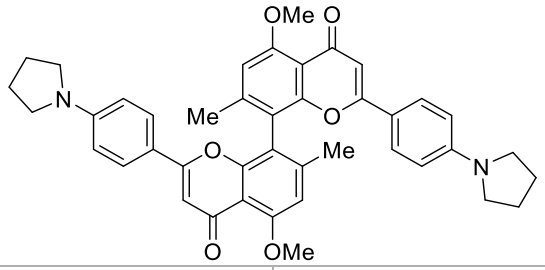	
MKL_DGR019	**212**	MKL_DGR017	**213**
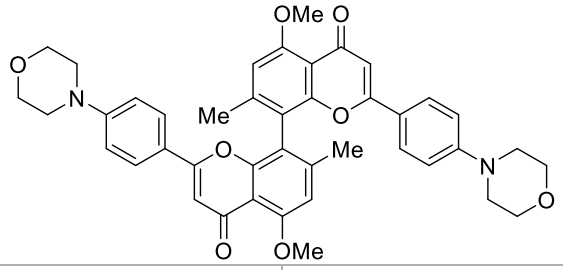		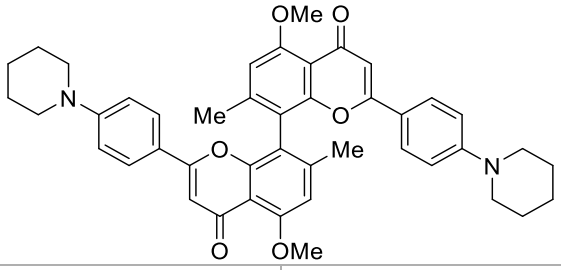	
MKL_DGR013	**214**	MKL_DGR018	**215**
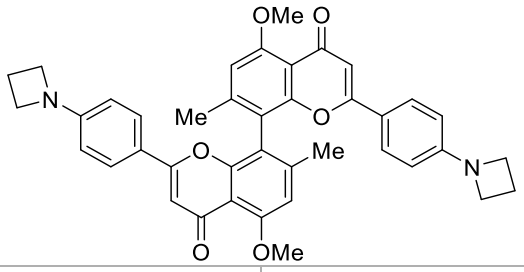		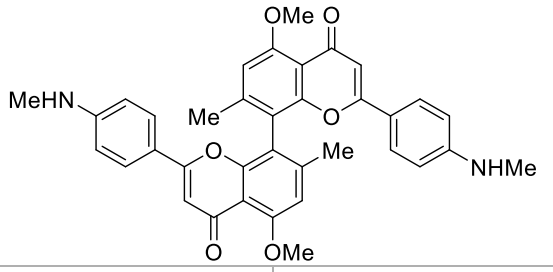	
MKL0192	**216**	MKL0193	**217**
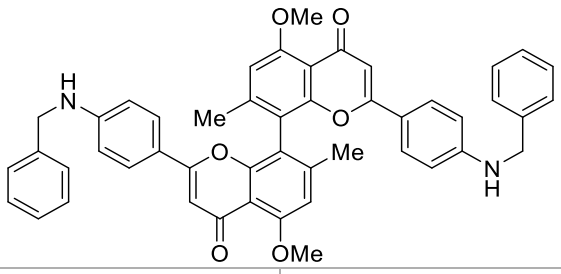		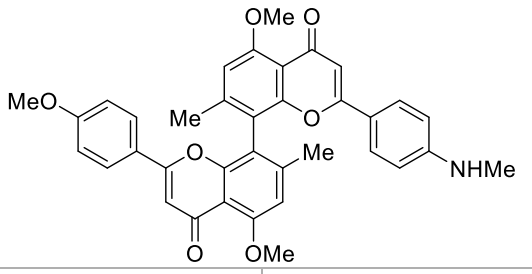	
MKL_DGR014	**218**	MKL0193sp	**219**
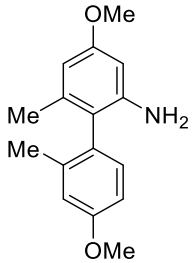		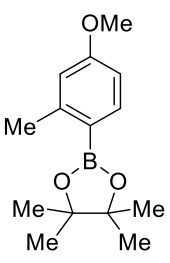	
MKL0055	**221**	MKL0040	**222**
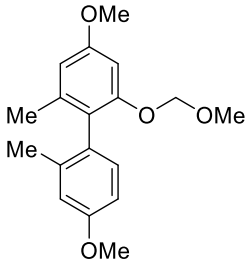		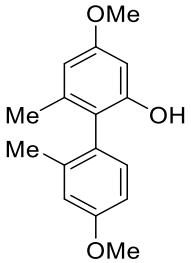	
MKL0046	**225**	MKL0047	**228**

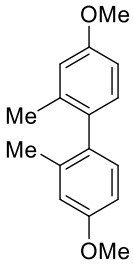		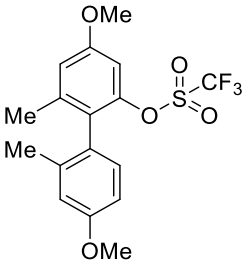		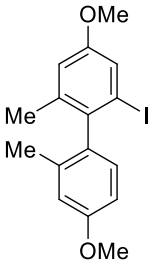		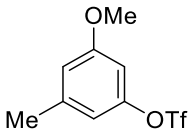	
MKL0047sp	**229**	MKL0050	**230**	MKL0058	**231**	MKL0016	**232**
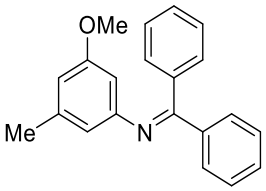		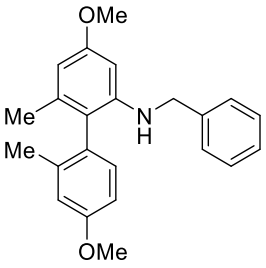		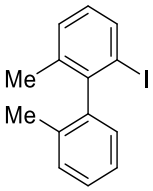		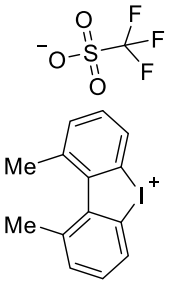	
MKL0025	**233**	MKL0054	**235**	MKL0097	**236**	MKL0113	**237**
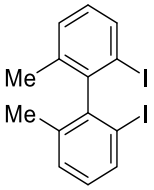		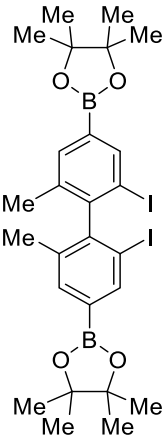		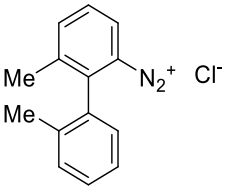		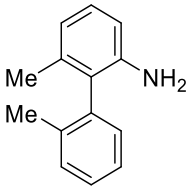	
MKL0132	**238**	MKL0135	**239**	MKL0097 N_2^+	**236-N2+**	MKL0095	**241**
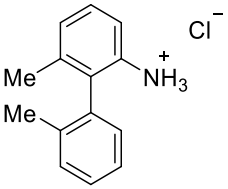							
MKL0095HCl		**241·HCl**					
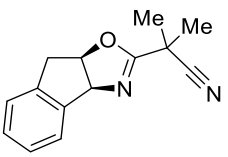				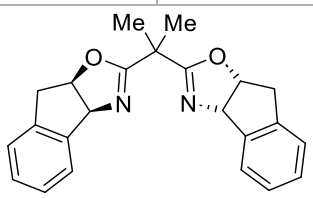			
MKL0091Bsp		**244**		MKL0091B		**L1**	

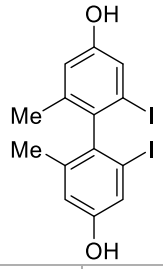		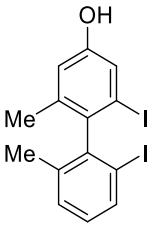		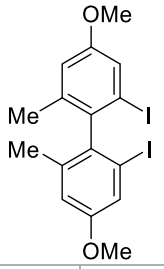		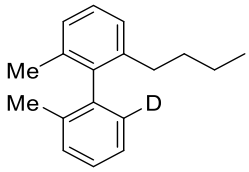	
MKL0184	**246**	MKL0184sp	**248**	MKL0186	**249**	MKL0188	**252**
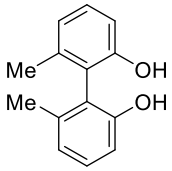		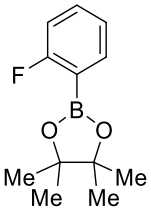		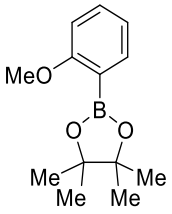		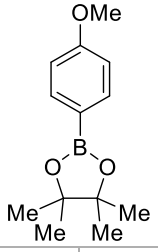	
MKL187	**253**	MKL0151	**258**	MKL0137	**259**	MSC010	**260**
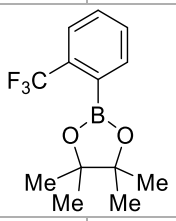		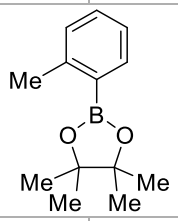		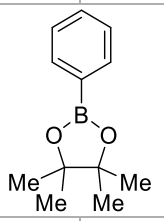			
MKL0144	**257**	MKL0093	**256**	MKL0131	**261**		
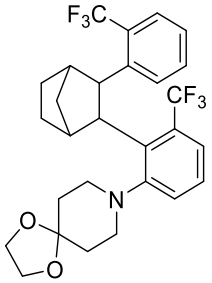		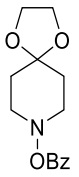		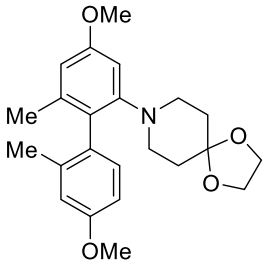		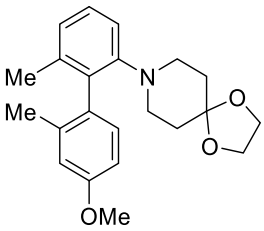	
MKL0146sp	**267**	MKL0048	**262**	MKL0051	**263**	MKL-MSC050	**264**
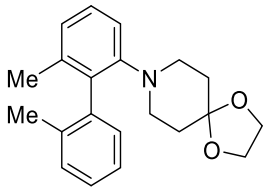				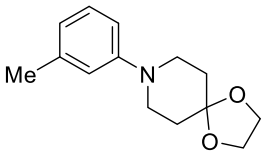			
MKL0111		**265**		MKL0111sp1		**268**	
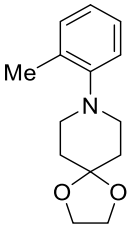		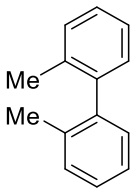		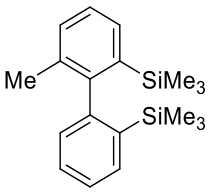		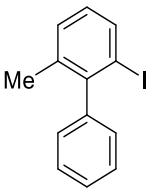	
MKL0111sp2	**269**	MKL0097sp	**270**	MKL0133	**274**	MKL0130	**275**

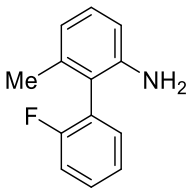		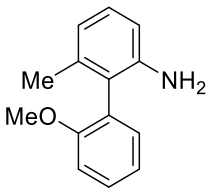		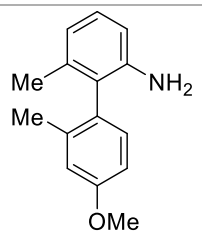		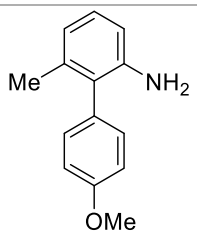	
MKL0152	**276**	MKL0138	**277**	MKL0094	**278**	MKL0159	**279**
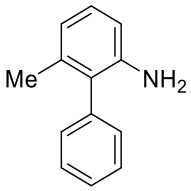		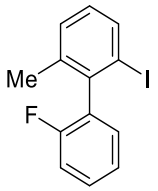		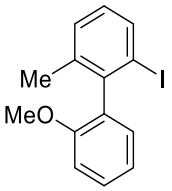		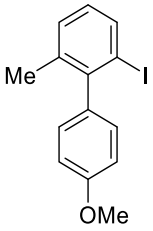	
MKL0129	**280**	MKL0157	**281**	MKL0139	**282**	MKL0161	**283**
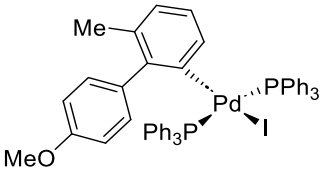				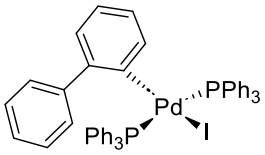			
CAN_MKL042sp		**285**		MKL0114sp		**288**	
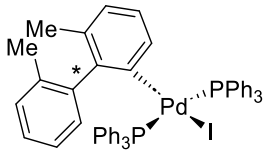						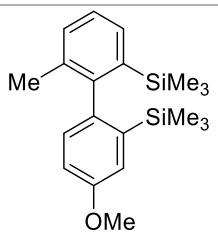	
MKL0112sp		**289**				MKL0164	**292**
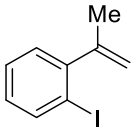		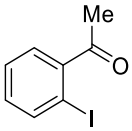		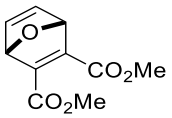		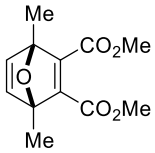	
CAN-MKL002 MKL0165	**293**	CAN-MKL001 MKL0160	**295**	CAN-MKL003 MKL0163	**296**	CAN-MKL053	**299**
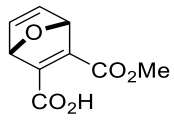		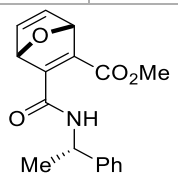		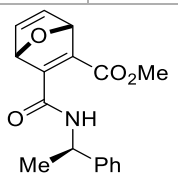		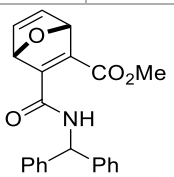	
CAN-MKL010 MKL0179	**301**	CAN-MKL014	**302**	CAN-MKL014A	**303**	CAN-MKL040	**307**

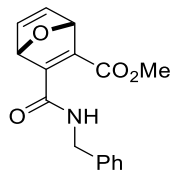		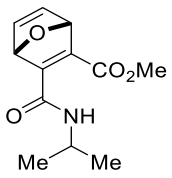		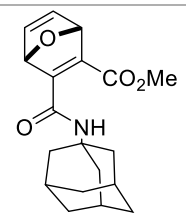		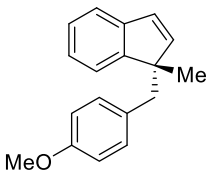	
CAN-MKL012	**308**	CAN-MKL035	**311**	CAN-MKL048	**312**	CAN-MKL016	**314**
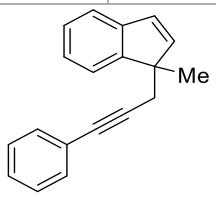		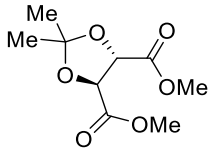		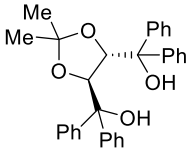			
CAN-MKL041	**316**	CAN-MKL017	**318**	CAN-MKL019	**319**		
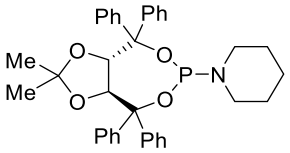				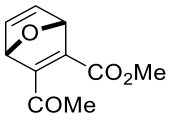		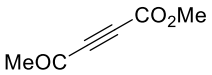	
CAN-MKL023		**L3**		CAN-MKL038	**321**	CAN-MKL028	**325**
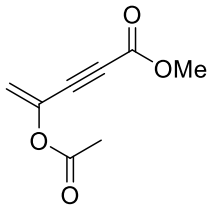		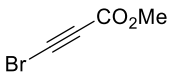		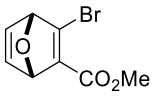			
CAN-MKL028sp	**326**	MKL0162	**328**	MKL0166	**329**		
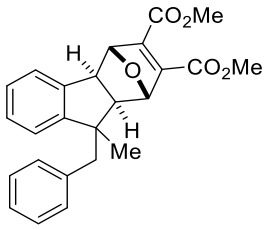				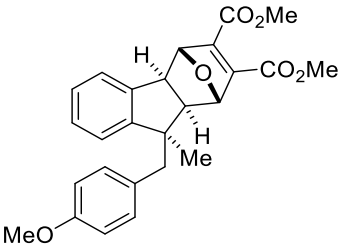			
CAN-MKL062		**332**		MKL0169		**333**	
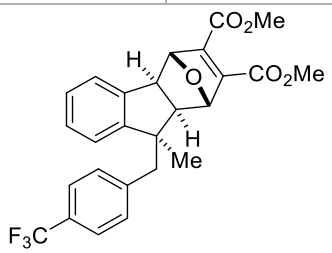				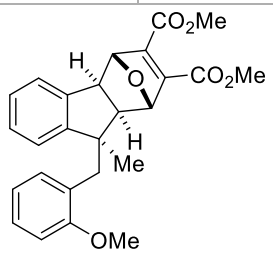			
MKL0170		**334**		MKL0177		**335**	

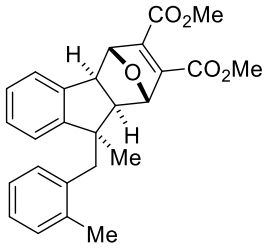		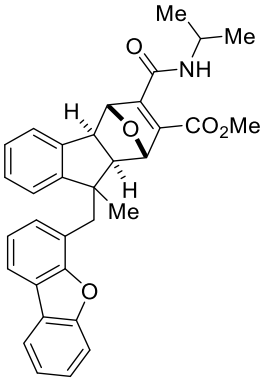	
MKL0178	**336**	CAN-MKL039	**338**
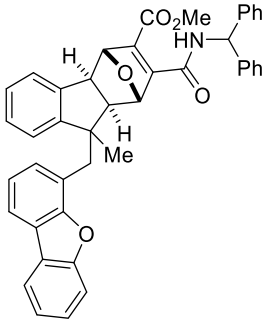		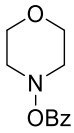	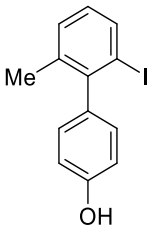
CAN-MKL044	**339**	MKL-MSC019	**342**	MKL0173	**345**
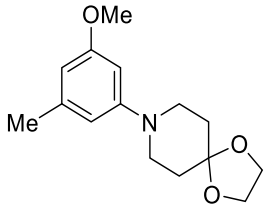		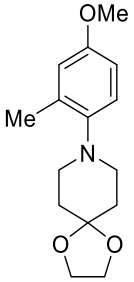	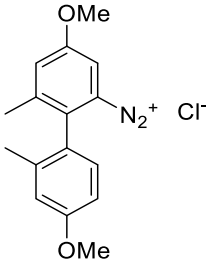
MKL0051 MKL-MSC038sp1	**347**	MKL0051 MKL-MSC38sp2	**348**	MKL058-N_2^+	**349**
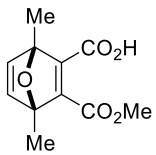	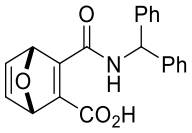	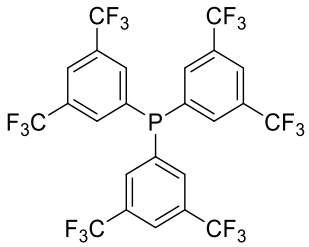			
CAN-MKL054	**353**	CAN-MKL055	**351**	MKL0168	**352**

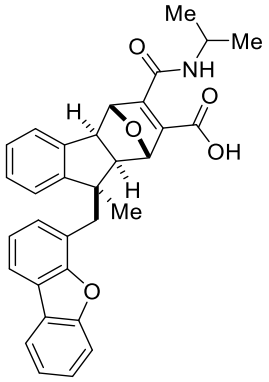		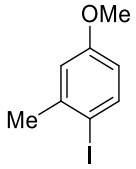		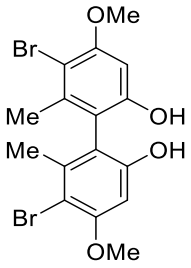	
CAN-MKL058	**353**	MKL0049	**354**	MKL0155	**355**

11 Danksagung

Zuallererst möchte ich mich bei Prof. Dr. Jörg Pietruszka bedanken. Vielen Dank, dass du mir über die Jahre Vertrauen entgegengebracht hast. Möge das das Ausprobieren neuer Reaktionen oder das Starten verschiedener Projekte sein, ich weiß die Freiheit in der Gestaltung der Promotion wirklich zu schätzen. Zusätzlich hast du mir die Möglichkeit gegeben mich in einem Auslandsaufenthalt zu beweisen. Ich weiß, dass das nicht selbstverständlich ist und bin froh dich als Betreuer gehabt zu haben. Ich habe viel für meinen weiteren Weg gelernt und nehme viel, sowohl fachlich als auch persönlich aus dieser Zeit mir.

Weiterhin möchte ich Prof. Dr. Thomas J. J. Müller für die Übernahme des Zweitgutachtens und für die ersten Eindrücke der organischen Chemie im Studium, die (offenkundig) einen nachhaltigen Eindruck hinterlassen haben, bedanken.

Additionally, I want to thank Prof. Dr. Mark Lautens for accommodating me in his working group for a research stay. It was truly an amazing time that I had at the institute, I learned a lot and will cherish the stay in Toronto for a long time!

Ich möchte mich bei allen Leuten, die während meiner Zeit im IBOC waren, bedanken, sei es Kollegen oder kurzfristige Aufenthalte, durch jede Interaktion konnte ich als Mensch wachsen und mich weiterentwickeln. Danke speziell auch Birgit Henßen und Vera Ophoven für die Unterstützung im Labor und Thomas Classen für seine Bemühungen um das Institut. Besonders möchte ich den Mitgliedern von Labor 2004, speziell der sogenannten ‘alten Garde’, danken. Danke Marvin, Teresa, Benedikt, Max, Ruth und Julian dafür, dass wir zusammen Spaß haben konnten, den Laboralltag überwinden konnten und doch so produktiv auf wissenschaftlicher sowie menschlicher Ebene zusammenarbeiten konnten.

Ich möchte mich weiterhin bei meinen Kooperationspartnern bedanken. Danke und grazie, Lena, Flaminia, Céline für die unkomplizierte und zuverlässige Zusammenarbeit. Besonderer Dank gilt auch Dr. Martina Holz für ihre hervorragende Koordinationstätigkeit im GRK2158, aber auch für die vielen schönen persönlichen Gespräche.

Einen besonderen Dank möchte ich Marvin Mantel, Fabian Hogenkamp, Hannah Braß und Totti Lamerz aussprechen, dafür, dass ihr euch durch meine frühen Versionen der Arbeit durchgewurschtelt habt und mir konstruktives Feedback gegeben habt.

Besonderer Dank gilt ebenfalls Team Biaryl. Teil eines Teams gewesen zu sein war wissenschaftlich einfach unglaublich bereichernd, zusätzlich haben sich dadurch Freundschaften gebildet, die hoffentlich noch lange halten werden!

Die Liste folgender Personen ist ohne bestimmte Reihenfolge kompiliert. Ich möchte mich bei Max für die schöne Zeit im Labor und die Unterstützung und Kohl-laboration bei verschiedenen Projekten bedanken, du bist ein echtes Original. Danke auch an dich Daniel, dass es so unkompliziert war mit dir zu arbeiten. Bei Ruth möchte ich mich für die superschöne Zeit zusammen im Labor bedanken. Danke dafür, dass ich dir immer meine schlechten Witze erzählen konnte und danke für das gemeinsame Lachen. Bei Sebastian möchte ich mich auch ganz recht herzlich für das Einstellen verschiedener Bildschirmschoner bedanken und für den vielen Spaß und die anregenden wissenschaftlichen Diskussionen, den wir zusammen haben konnten und wünsche ihm, dass ihm jemand Erika aus Wirsing nachbaut. Bei Lisa möchte ich mich für die schöne Freundschaft bedanken, danke, dass wir so viel Spaß während der relativ kurzen Überlappung im IBOC haben konnten (UwU). Weiterhin möchte ich Hannah danken, dafür, dass wir so ehrliche Unterhaltungen führen können und auch wenn wir uns mal länger nicht sehen, jede Unterhaltung genauso unbeschwert ist wie immer. Auch danke dafür, wenn du mal meine Kummerbox warst! „Dein Zahnarzt ist mein Flugzeug nur in schlimm“ – Hannah U. C. Braß, 2023. Danke Fabi dafür, dass du einfach immer freundlich bist, danke Marc dafür, dass du auch nach so vielen Jahren noch den Kontakt hältst, danke Alex für die vielen Memes, danke Teresa für den Quatsch im Labor, danke Mona (Winnewupp) für die Pickups und dass du so ne coole Kegelrobbe bist, Marvin fürs Teller wegziehen, mulțumesc, Diana, pentru toate conversațiile pe care le-am avut în bucătărie și pentru a juca Terraria, köszönöm, Krisztián, a magyar leckéket. Danke auch an Siggi für die vielen Gelegenheiten Sushi essen gehen zu können.

I also want to thank all members of the Lautens Group and especially Xavier for the warm welcome and interesting discussions and insights into palladium catalysis. I was able to learn a lot of new techniques and had a great time in Toronto because of you!

Zusätzlich möchte ich ganz besonders noch Julian Greb danken. Danke, dass du mich in der Bachelorarbeit so gut unterwiesen hast, es hat immer unglaublich viel Spaß gemacht mit dir über Chemie zu sprechen und neue Dinge von dir zu lernen! Manchmal denke ich an die Schichtarbeit während Corona 2020 und die damit verbundenen Autofahrten, in denen wir uns so viel unterhalten konnten. Einfach Danke!

Ich möchte zusätzlich noch all meinen Freunden danken, die mich vielleicht auch nur indirekt durch emotionalen Support beim Anfertigen dieser Arbeit unterstützt haben. Speziell sind hier Christian, Mira, Marco, Philipp, Dragana und Saskia zu erwähnen, ich habe mich immer sehr gefreut euch auf meinen Ausflügen in die Uni zu sehen und mit euch zu quatschen!

Auch noch ein großes Dankeschön geht an die "Honeybees", Emilia, René, Fabi und Luke für den starken Zusammenhalt seit einer halben Ewigkeit.

Ich möchte meiner Familie danken. Danke Anneli, Julius, Heike, Bernward, E-Lou, Nico, Ole, Golda, Ivo, Ruby und natürlich den 100 weiteren Verwandten die ich nicht alle benennen kann für die freundliche Unterstützung und das aufrichtige Interesse an meiner Arbeit.

Last but certainly not least möchte ich meiner Freundin Charlotte ‘Totti’ Lamerz aka Tox danken. Vielen Dank für die liebe Unterstützung all die Jahre. Danke dafür, dass du immer freundlich bist und immer ein offenes Ohr hast. Ohne dich wäre ich als Mensch jetzt nicht da, wo ich bin. Danke einfach für alles!

12 Erklärung

Ich versichere an Eides statt, dass die Dissertation von mir selbständig und ohne unzulässige fremde Hilfe unter Beachtung der „Grundsätze zur Sicherung guter wissenschaftlicher Praxis an der Heinrich-Heine-Universität Düsseldorf“ erstellt worden ist. Die vorliegende Dissertation wurde ausschließlich an der Mathematisch-Naturwissenschaftlichen Fakultät der Heinrich-Heine-Universität Düsseldorf vorgelegt. Es wurde zuvor kein weiterer Promotionsversuch unternommen.

Moritz Klischan

Band 35
Ammoniumylide in der asymmetrischen Organokatalyse
L. Öhler (2019), V, 377 pp
ISBN: 978-3-95806-407-2

Band 36
Enantioselektive Totalsynthese von Altersolanolen
B. Mechsner (2019), I, V, 311 pp
ISBN: 978-3-95806-412-6

Band 37
Glycosynthases — tuning glycosidase activity towards glycoside diversification and synthesis
M. R. Hayes (2019), VI, 225 pp
ISBN: 978-3-95806-441-6

Band 38
**Chemoenzymatische Synthesemethoden –
Zugang zur duftenden Welt der Chemie und darüber hinaus**
C. Kumru (2019), V, 338 pp
ISBN: 978-3-95806-446-1

Band 39
Oxidoreduktasen für die Bereitstellung von Schlüsselbausteinen der Natur- und Wirkstoffsynthese
R. Krug (2020), 216 pp
ISBN: 978-3-95806-454-6

Band 40
Die farbenfrohe Welt der Prodiginine - Neue Enzyme für die Synthese bioaktiver Naturstoffderivate
H. U. C. Braß (2021), IX, 349 pp
ISBN: 978-3-95806-523-9

Band 41
Oxidoreduktasen: Von neuen Biokatalysatoren bis zum fertigen Naturstoff
D. Dickmann (2021), 274 pp
ISBN: 978-3-95806-573-4

Band 42
**Chemie ohne Grenzen –
Biokatalysatoren und Bororganyle als wertvolle Hilfsmittel für die zielmolekülorientierte, enantioselektive Synthese**
M. R. Mantel (2021), 487 pp
ISBN: 978-3-95806-585-7

Band 43
Über tetraolbasierte Allylboronsäureester und deren Potential in der stereoselektiven Synthese
P. Ullrich (2022), xii, 324 pp
ISBN: 978-3-95806-618-2

Band 44
Design, Synthese und Charakterisierung neuartiger *photocaged compounds* – Optimierte Werkzeuge zur Etablierung wellenlängenselektiver Genexpression
F. Hogenkamp (2022), V, 456 pp
ISBN: 978-3-95806-637-3

Band 45
Charakterisierung von Methyltransferasen zur enantioselektiven Synthese von Hexahydropyrrolo[2,3-*b*]indol basierten Naturstoffen
P. Schneider (2023), x, 315 pp
ISBN: 978-3-95806-690-8

Band 46
Untersuchungen zu enzymatischen Halogenierungsreaktionen in der organischen Synthese
A. V. Fejzagić (2023), XI, 264 pp
ISBN: 978-3-95806-728-8

Band 47
Biochemische Charakterisierung von modularen dirigierenden Proteinen
N. Huwa (2024), X, 235 pp
ISBN: 978-3-95806-745-5

Band 48
Immobilisierte Enzyme und Kofaktor-Regenerierung in der kontinuierlichen Durchflusssynthese
B. Baumer (2024), XVIII, 231 pp
ISBN: 978-3-95806-783-7

Band 49
Biaryl-based natural products as structural motif for pharmaceutically relevant compounds
M. K. T. Klischan (2025), V, 657 pp
ISBN: 978-3-95806-801-8

Bioorganische Chemie an der Heinrich-Heine-Universität Düsseldorf im Forschungszentrum Jülich

Herausgegeben von Jörg Pietruszka

Band 49
ISBN 978-3-95806-801-8